Proceedings of the Third International Conference on the Peaceful Uses of Atomic Energy

Held in Geneva
31 August–9 September 1964

Volume 2

Reactor Physics

MULTILINGUAL EDITION
ÉDITION MULTILINGUE
МНОГОЯЗЫЧНОЕ ИЗДАНИЕ
EDICIÓN PLURILINGÜE

UNITED NATIONS
New York
1965

EXPLANATORY NOTE

The Proceedings of the Third International Conference on the Peaceful Uses of Atomic Energy comprise a single, multilingual publication of sixteen volumes. This form was prescribed by the General Assembly of the United Nations in approving the Conference budget.

Papers accepted for consideration at the Conference are accordingly printed herein only in the original language of submission, each being followed by its abstract in the other three languages of the Conference.*

The budgetary arrangements for the Conference required also that Governments provide abstracts and papers in two of the Conference languages. One of the three abstracts following each paper is, therefore, in a translation provided by the Government concerned. The abstracts were translated into the other two languages either by the Division of Language Services, International Atomic Energy Agency (IAEA) in Vienna, or, with its assistance, through the intermediary of the national atomic energy authorities in London, Paris, Moscow and Madrid.

The Foreword by the Secretary-General of the United Nations, the Preface by the Director General of IAEA, and this Explanatory Note, together with the records of discussion at each of the six scientific general sessions and thirty-six technical sessions of the Conference, are published in all four languages. All other material, which is largely of a formal nature and is confined to Volumes 1 and 16, is published in the language of submission or delivery, followed in the case of French, Russian and Spanish originals by the English translation.

Governments whose national tongue is not one of the four Conference languages were consulted as to their preference for the language in which their papers should appear in these Proceedings.

The Table of Contents in each volume gives the titles of papers in the original language, or language of choice, followed in the case of French, Russian and Spanish titles by the English translation.

Starting from the 992 abstracts submitted by Governments, specialized agencies and IAEA, the Scientific Secretariat, working under the guidance of the United Nations Scientific Advisory Committee, finally chose 747 papers for inclusion in the Programme of the Conference; of these, 358 were selected for oral presentation at the 42 working sessions.

In arranging the programme, the Scientific Secretariat aimed at achieving a balanced schedule, providing for the oral presentation of as many papers as possible at each session while still leaving adequate time for discussion of the material presented. Two afternoons were left entirely free, to enable informal groups to discuss matters arising out of discussions at the formal sessions of the Conference. No records were taken of such informal meetings.

Wherever possible, the author, or authors, of papers were consulted during the Conference by members of the Scientific Secretariat, who acted as secretaries of session, or by the team of editors made available for the purpose by IAEA,** to ensure maximum accuracy.

The records of discussion at the various sessions, based on notes taken in the meetings by IAEA records officers,** and checked where necessary against the sound recordings made of all sessions, were prepared by the Division of Language Services of IAEA in English, and subsequently translated into French, Russian and Spanish through the intermediary of the atomic energy authorities in the three countries concerned (see third paragraph of the present note).

The editing of the English, French and Spanish papers was carried out at the United Nations Office at Geneva under United Nations supervision by a team of editors, whose services, also, were made available by the atomic energy authorities of their respective countries, with some help from outside consultants. The editing of the Russian papers was done in Moscow in similar circumstances. The following served as editors: Mr. A. de Calmès, Dr. C. E. Granados, Mr. D. H. Hill, Mr. V. F. Kalinin, Cand. Tech. Sc., Dr. R. Lapage, Mr. E. T. Marles, Dr. J. D. C. Mole, Mr. C. Ségot, Mr. J. J. Stobbs, Mr. C. R. Symons and Mr. J. Williamson.

The task of printing this large collection of scientific information has been shared by printers in

* The languages of the Conference were English, French, Russian and Spanish.

** The names of the scientific secretaries, editors and records officers will be found in the list of the Conference Secretariat in Annex 1, Volume 1, of this series.

Belgium, Canada, France, Switzerland, the Union of Soviet Socialist Republics and the United Kingdom.

Full titles of the sixteen volumes of these Proceedings, together with the sessions covered by each volume, are as follows:

Volume No.		Sessions included
1	Progress in Atomic Energy	A, B, 1.6, C, H
2	Reactor Physics	3.1
3	Reactor Studies and Performance	3.2, 3.3
4	Reactor Control	3.4, 3.5
5	Nuclear Reactors — I. Gas-cooled and Water-cooled Reactors	1.1, 1.2, 1.3
6	Nuclear Reactors — II. Fast Reactors and Advanced Concepts	1.4, 1.5, 1.7
7	Research and Testing Reactors	D, 1.9, 1.8
8	Reactor Engineering and Equipment	1.10, 1.11, 3.7
9	Reactor Materials	2.8, 2.9, 2.4
10	Nuclear Fuels — I. Fabrication and Reprocessing	2.3, 2.6, 2.7
11	Nuclear Fuels — II. Types and Economics	2.5, 2.1, 2.2
12	Nuclear Fuels — III. Raw Materials	2.11, 2.12, 2.10
13	Nuclear Safety	3.9, 3.8 3.6
14	Environmental Aspects of Atomic Energy and Waste Management	3.10, 3.11
15	Special Aspects of Nuclear Energy and Isotope Applications	E, 4.1, F, G, 4.2
16	List of Papers and Indexes	

NOTE EXPLICATIVE

Les Actes de la troisième Conférence internationale sur l'utilisation de l'énergie atomique à des fins pacifiques sont publiés ici sous la forme d'une édition unique, multilingue, en seize volumes. Cette présentation a été décidée par l'Assemblée générale lorsqu'elle a approuvé le budget de la Conférence.

En conséquence, les mémoires qui ont été acceptés pour la Conférence sont reproduits ici dans la langue originale dans laquelle ils ont été soumis et sont suivis d'un résumé dans les trois autres langues de la Conférence *.

Aux termes des dispositions budgétaires prises en vue de la Conférence, les gouvernements devaient fournir les résumés et les mémoires dans deux des langues de la Conférence. Ainsi, sur les trois résumés qui suivent chaque mémoire, un est une traduction fournie par le gouvernement intéressé. La traduction des résumés dans les deux autres langues a été faite soit par la Division des services linguistiques de l'Agence internationale de l'énergie atomique (AIEA), à Vienne, soit avec son concours, par les soins des organismes nationaux compétents en matière d'énergie atomique à Londres, Paris, Moscou et Madrid.

L'avant-propos du Secrétaire général de l'Organisation des Nations Unies, la préface du Directeur général de l'AIEA et la présente note explicative, ainsi que les comptes rendus de chacune des six séances scientifiques générales et des trente-six séances techniques de la Conférence, sont publiés dans les quatre langues. Tous les autres textes, qui pour la plupart sont d'un caractère non technique et figurent dans les volumes 1 et 16, sont publiés dans la langue dans laquelle ils ont été présentés par écrit ou oralement et sont suivis, lorsque cette langue est l'espagnol, le français ou le russe, d'une traduction en anglais.

Les gouvernements des pays dont la langue officielle n'est pas l'une des quatre langues utilisées à la Conférence ont été consultés pour savoir dans quelle langue ils préféraient voir paraître leurs mémoires.

La table des matières de chaque volume donne les titres des mémoires dans la langue originale ou dans la langue choisie; ces indications sont suivies, pour les titres en espagnol, en français et en russe, de la traduction en anglais.

Sur les 992 résumés présentés par les gouvernements, les institutions spécialisées et l'AIEA, le Secrétariat scientifique, travaillant sous la direction du Comité consultatif scientifique des Nations Unies, en a finalement retenu 747 pour les inscrire au programme de la Conférence; sur ce nombre, 358 ont été présentés oralement aux 42 séances de travail.

En établissant le programme de la Conférence, le Secrétariat scientifique a cherché à réaliser un équilibre: il s'est efforcé de ménager un temps suffisant pour la présentation du plus grand nombre possible de mémoires tout en laissant du temps pour leur discussion. Deux après-midi avaient été laissés entièrement libres afin de permettre aux participants d'organiser des réunions non officielles et de discuter en petits groupes des questions qui se posaient à la suite des séances officielles de la Conférence. Ces réunions n'ont pas fait l'objet de comptes rendus.

Toutes les fois que cela a été possible, l'auteur ou les auteurs des mémoires ont été consultés pendant la Conférence par les membres du Secrétariat scientifique, qui ont assuré le secrétariat des séances, ou par l'équipe d'« éditeurs » que l'AIEA ** avait mis à cet effet à la disposition de la Conférence, afin d'assurer l'exactitude la plus grande.

Les comptes rendus des discussions aux réunions, établis d'après les notes prises en séance par les rédacteurs de comptes rendus de l'AIEA** et comparés toutes les fois qu'il le fallait avec les enregistrements sonores, ont été rédigés en anglais par la Division des services linguistiques de l'AIEA, puis traduits en espagnol, en français et en russe par les soins des organismes compétents en matière d'énergie atomique des trois pays intéressés (voir le troisième alinéa de la présente note).

Les mémoires rédigés en anglais, en espagnol et en français ont été mis au point pour l'impression à l'Office européen des Nations Unies à Genève, sous le contrôle de l'ONU, par une équipe de rédac-

* Les langues de la Conférence étaient l'anglais, l'espagnol, le français et le russe.

** On trouvera les noms des secrétaires scientifiques, des « éditeurs » et des rédacteurs de comptes rendus dans la liste des membres du secrétariat de la Conférence à l'annexe 1 du volume 1.

teurs mis à la disposition de la Conférence par les organismes compétents en matière d'énergie atomiques des pays intéressés, avec l'aide de quelques consultants extérieurs. La mise au point définitive des mémoires rédigés en russe a été faite à Moscou dans les mêmes conditions. Voici les noms des rédacteurs qui ont assuré la mise au point des mémoires: M. A. de Calmès, M. C. E. Granados, M. D. H. Hill, M. V. F. Kalinin, M^lle R. Lapage, M. E. T. Marles, M^lle J. D. C. Mole, M. C. Ségot, M. J. J. Stobbs, M. C. R. Symons et M. J. Williamson.

Des entreprises de Belgique, du Canada, de France, du Royaume-Uni, de Suisse et de l'Union des Républiques socialistes soviétiques se sont partagé la tâche que représentait l'impression de cette masse importante de documents scientifiques.

Les titres complets des seize volumes des Actes de la Conférence, ainsi que les numéros des séances sur lesquelles porte chaque volume, figurent ci-après:

ПОЯСНИТЕЛЬНАЯ ЗАПИСКА

Труды третьей Международной конференции по использованию атомной энергии в мирных целях представляют собой единое многоязычное издание из шестнадцати томов. Такая форма была предусмотрена Генеральной Ассамблеей Организации Объединенных Наций при одобрении ею бюджета Конференции.

Принятые к рассмотрению Конференцией доклады соответственно опубликованы здесь лишь на языке оригинала; при этом каждый доклад сопровождается аннотацией на других трех языках Конференции*.

Бюджетные постановления в отношении проведения Конференции также предусматривали, что правительства представят аннотации и доклады на двух языках Конференции. Поэтому одна из трех аннотаций, сопровождающих каждый доклад, является переводом, представленным соответствующим правительством. Аннотации были переведены на другие два языка либо Отделом переводов Международного агентства по атомной энергии (МАГАТЭ) в Вене, либо с его помощью при сотрудничестве национальных органов, ведающих вопросами атомной энергии, в Лондоне, Париже, Москве и Мадриде.

Введение и предисловие Генерального Секретаря Организации Объединенных Наций и Генерального директора МАГАТЭ, соответственно, и настоящая пояснительная записка, наряду с протоколами каждого из шести научных пленарных заседаний и тридцати шести секционных заседаний Конференции, публикуются на всех четырех языках. Все другие материалы, которые по своему характеру в основном относятся к числу официальных и содержатся в томах 1 и 16, публикуются на языке оригинала; и когда речь идет о французских, русских и испанских оригиналах, то к ним приложен английский перевод.

С правительствами стран, язык которых не относится к числу четырех языков Конференции, были проведены консультации по поводу того, на каком языке было бы желательно, по их мнению, опубликовать в настоящих трудах представленные ими доклады.

В содержании каждого тома указаны заглавия докладов на языке оригинала либо на другом избранном языке, и в том случае, когда речь идет о французских, русских и испанских заглавиях, их сопровождает английский перевод.

Из 992 аннотаций, представленных правительствами, специализированными учреждениями, а также МАГАТЭ, Ученый секретариат, работая под руководством Научного консультативного комитета Организации Объединенных Наций, в итоге отобрал 747 докладов для включения их в программу Конференции; из них 358 были отобраны для представления в устной форме на 42 рабочих заседаниях.

При составлении программы Ученый секретариат ставил целью добиться сбалансированного расписания, которое дало бы возможность представить в устной форме максимальное количество докладов на каждом заседании при обеспечении достаточного времени для проведения дискуссии по поводу представленного материала. В двух случаях имеющееся во второй половине дня время оставили нераспределенным, с тем чтобы дать возможность неофициальным группам обсудить вопросы, возникшие в ходе дискуссии на официальных заседаниях Конференции. На таких неофициальных заседаниях протоколы не составлялись.

По мере возможности, с автором или авторами докладов консультировались в ходе Конференции члены Ученого секретариата, которые выполняли функции секретарей заседаний, либо такие консультации проводились группой редакторов, которые были выделены МАГАТЭ** для этой цели, с тем чтобы обеспечить максимальную точность.

* Языками Конференции являлись: английский, французский, русский и испанский.

** Фамилии ученых секретарей, редакторов и протоколистов приведены в перечне сотрудников секретариата Конференции в приложении 1-ом к тому 1-му настоящей серии.

Протоколы дискуссии на различных заседаниях, составленные на основе записей, сделанных в ходе заседаний протоколистами МАГАТЭ*, и проверенные, по мере необходимости, путем сравнения со звуковой записью, которая велась на всех заседаниях, были подготовлены Отделом переводов МАГАТЭ на английском языке и впоследствии переведены на французский, русский и испанский языки при сотрудничестве национальных органов, ведающих вопросами атомной энергии, в трех заинтересованных странах (смотри третий абзац пояснительной записки).

Работа по редактированию документов на английском, французском и испанском языках была проведена в Европейском отделении Организации Объединенных Наций, в Женеве, под руководством Организации Объединенных Наций группой редакторов, услуги которых были также предоставлены по линии органов, ведающих вопросами атомной энергии в соответствующих странах, с использованием в некоторой степени помощи приглашенных со стороны консультантов. Русские документы редактировались в Москве в таких же условиях. Нижеследующие лица осуществляли работу в качестве редакторов: д-р К. Э. Гранадос, кандидат технических наук В. Ф. Калинин, г-н А. де Кальмэс, д-р Р. Лепейдж, г-н Э. Т. Марлз, д-р Дж. Д. К. Моул, г-н Ч. Р. Саймонс, г-н Дж. Дж. Стобз, г-н Ш. Сэго, г-н Дж. Уильямсон, г-н Д. Х. Хилл.

В выполнении задачи по печатанию этой обширной научной информации принимали участие типографии в Бельгии, Канаде, Соединенном Королевстве, Союзе Советских Социалистических Республик, Франции и Швейцарии.

Ниже приводятся полные заглавия шестнадцати томов настоящих Трудов, а также указывается, какие сессии охватываются каждым томом:

* Фамилии ученых секретарей, редакторов и протоколистов приведены в перечне сотрудников секретариата Конференции в приложении 1-ом к тому 1-му настоящей серии.

Номер Тома		Заседания, включенные в том
1	Прогресс в работах по атомной энергии	A, B, 1.6, C, H
2	Физика реакторов	3.1
3	Изучение реакторов и их характеристики	3.2, 3.3
4	Регулирование реакторов	3.4, 3.5
5	Ядерные реакторы — I. Реакторы с водяным и газовым охлаждением	1.1, 1.2, 1.3
6	Ядерные реакторы — II. Реакторы на быстрых нейтронах и усовершенствованные реакторы	1.4, 1.5, 1.7
7	Исследовательские и испытательные реакторы	D, 1.9, 1.8
8	Технология и оборудование реакторов	1.10, 1.11. 3.7
9	Реакторные материалы	2.8, 2.9, 2.4
10	Ядерное топливо — I. Изготовление и переработка	2.3, 2.6, 2.7
11	Ядерное топливо — II. Типы и экономика	2.5, 2.1, 2.2
12	Ядерное топливо — III. Сырьевые материалы	2.11, 2.12, 2.10
13	Ядерная безопасность	3.9, 3.8, 3.6
14	Исследование окружающей среды и удаление радиоактивных отходов	3.10, 3.11
15	Специальные аспекты применения ядерной энергии и изотопов	E, 4.1, F, G, 4.2
16	Список докладов и указатели	

NOTA EXPLICATIVA

Las Actas de la tercera Conferencia Internacional sobre la Utilización de la Energía Atómica con Fines Pacíficos están constituidas por una publicación única y plurilingüe compuesta de dieciséis volúmenes, en conformidad con lo dispuesto por la Asamblea General de las Naciones Unidas al aprobar el presupuesto de la Conferencia.

Por consiguiente, las memorias aceptadas para ser examinadas en la Conferencia sólo figuran impresas en el idioma original en que se presentaron, y cada una de ellas va seguida de un resumen de la misma en los otros tres idiomas de la Conferencia *.

En los arreglos presupuestarios para la Conferencia se dispuso también que los gobiernos tenían asimismo que presentar resúmenes y memorias en dos de los idiomas de la Conferencia. En consecuencia, uno de los tres resúmenes que siguen a cada memoria es una traducción facilitada por el gobierno interesado. Los resúmenes fueron traducidos a los otros dos idiomas, ya por la División de Idiomas del Organismo Internacional de Energía Atómica (OIEA) de Viena, o, con su asistencia, por conducto de las autoridades nacionales de energía atómica de Londres, París, Moscú y Madrid.

La introducción del Secretario General de las Naciones Unidas, el prefacio del Director General del OIEA y la presente nota explicativa, junto con las actas de los debates celebrados en cada una de las seis sesiones científicas generales y las treinta y seis sesiones técnicas de la Conferencia, se publican en los cuatro idiomas. El resto del material, que reviste en su mayoría un carácter oficial y está contenido exclusivamente en los volúmenes 1 y 16, se publica en el idioma en que fue presentado o entregado, seguido para los originales en español, francés y ruso, de la traducción en inglés.

Se consultó a los gobiernos cuyo idioma nacional no es uno de los cuatro idiomas de la Conferencia para saber en cuál de ellos preferían que se publicaran sus memorias en estas Actas.

El índice de cada volumen contiene los títulos de las memorias en el idioma original, o en el idioma elegido, seguidos, cuando se trata de títulos en español, francés y ruso, de la traducción en inglés.

De los 992 resúmenes presentados por gobiernos, organismos especializados y el OIEA, la Secretaría Científica, bajo la dirección del Comité Científico Consultivo de las Naciones Unidas, escogió por último 747 memorias que debían ser incluidas en el programa de la Conferencia; de éstas, 358 fueron seleccionadas para ser presentadas oralmente en las 42 sesiones de trabajo.

Al preparar el programa de actividades, la Secretaría Científica trató de conseguir un justo equilibrio, y así se previó la presentación oral del mayor número posible de memorias en cada sesión, pero dejando todavía tiempo suficiente para examinar la información presentada. Se dejaron dos tardes totalmente libres, a fin de que los grupos oficiosos pudieran examinar las cuestiones que surgieran en las sesiones oficiales de la Conferencia. No se levantó acta de tales reuniones.

Siempre que fue posible, el autor, o los autores, de las memorias fueron consultados en el curso de la Conferencia por miembros de la Secretaría Científica, que actuaron de secretarios de sesión, o por un grupo de editores facilitado a dicho efecto por el OIEA**, a fin de asegurar la máxima exactitud.

Las actas de los debates celebrados en las diversas sesiones, basadas en notas tomadas en las reuniones por redactores de actas del OIEA**, y verificadas siempre que fue necesario mediante las grabaciones efectuadas en todas las sesiones, fueron preparadas por la División de Idiomas del Organismo Internacional de Energía Atómica (OIEA) en inglés, y traducidas después al español, el francés y el ruso por conducto de las autoridades de energía atómica de los tres países interesados (véase el tercer párrafo de la presente nota).

La preparación para la publicación del texto de los documentos en español, francés e inglés se efectuó en la Oficina de Ginebra de las Naciones Unidas, bajo la fiscalización de las Naciones Unidas, por un equipo de editores cuyos servicios fueron también proporcionados por las autoridades de energía atómica de sus respectivos países, con alguna ayuda de consultores del exterior. La preparación para la publicación de los documentos en ruso se efectuó en Moscú en circunstancias análogas. Actuaron de editores las personas siguientes: Sr. A. de Calmès, Dr. C. E. Granados, Sr. D. H. Hill,

* Los idiomas de la Conferencia fueron el español, el francés, el inglés y el ruso.

** Los nombres de los secretarios científicos, editores y redactores de actas figuran en la lista de la Secretaría de la Conferencia, en el anexo 1, volumen 1, de esta serie.

Sr. V. F. Kalinin, Dra. R. Lapage, Sr. E. T. Marles, Dra. J. D. C. Mole, Sr. C. Ségot, Sr. J. J. Stobbs, Sr. C. R. Symons y Sr. J. Williamson.

En la impresión de esta gran recopilación de información científica han participado impresores de Bélgica, el Canadá, Francia, el Reino Unido, Suiza y la Unión de Repúblicas Socialistas Soviéticas.

Los títulos completos de los dieciséis volúmenes de estas Actas, junto con las sesiones comprendidas en cada volumen, son los siguientes:

TABLE OF CONTENTS

Volume 2

Session 3.1

NEW DEVELOPMENTS IN REACTOR PHYSICS

LIST OF PAPERS

Studies of resonance absorption and the Doppler phenomenon for fast and thermal reactors

By J. Codd, J. E. Beardwood, D. C. Leslie and H. M. Sumner*

Before 1960 most work on neutron resonance absorption and its temperature dependence concerned thermal reactors. Since then, increasing effort has been devoted to the resonance problems of future dilute fast reactors, especially because of the important safety advantage provided by a sufficiently large prompt negative Doppler temperature coefficient [1]. For thermal reactors, the basic theoretical problem is to calculate the resonance absorption integral of the fertile material for a $1/E$ flux spectrum, including detailed treatment of the core lattice structure. In dilute fast reactors, however, the spectrum is not initially known and must be calculated, normally by multigroup theory. The problem is then to determine effective multigroup constants for the fissile and fertile materials which allow for self-shielding and Doppler broadening of resonances. Core heterogeneity effects must be taken into account, although in some types of power reactor they are estimated to be small. Most of the Doppler effect comes from the energy region below 10 keV [2], which is also the main region of interest in the thermal reactor problem.

In Part I of this paper we describe some theoretical investigations concerning dilute fast reactor systems. Two specific problems are first discussed: the mutual shielding by resonances of the fissile and fertile materials: and the effect on the calculated fissile material Doppler coefficient when multilevel resonance theory is used instead of the customary single level theory. A new numerical method for treating the resonance region is outlined, and results of a preliminary test calculation are given.

Part II deals with the calculation of resonance integrals for thermal reactors. The use of equivalence theorems, which enable a heterogeneous lattice to be treated by consideration of a fictitious homogeneous system, is explained, and an improved form of the standard equivalence theorem is stated. The application of equivalence theorems to treat regular arrays and liquid-filled clusters of rods is discussed. Calculated values of the ^{238}U resonance integral and its temperature dependence are then compared with experimental data on UO_2 rods, and air-filled and D_2O-filled clusters, and also with Monte Carlo calculations. Finally, calculations of the shielding effect of ^{238}U resonances upon the resonance reaction rates of ^{235}U and ^{239}Pu in thermal reactor fuel are compared with experimental measurements.

* UK Atomic Energy Authority, AEE Winfrith.

PART I. FAST REACTOR INVESTIGATIONS

^{238}U–^{239}Pu resonance overlapping

The calculation of resonance absorption and Doppler coefficients in dilute fast reactors is normally based on the use of effective cross sections, which allow for resonance self-shielding and Doppler broadening. These cross sections are evaluated as a function of energy and then averaged over an assumed spectrum, to give group constants for use in multigroup theory calculations of critical size, etc. It has been customary to evaluate effective cross sections for the fissile and fertile materials separately, thus neglecting the possibility of mutual shielding of resonances of these materials. This assumption has recently been examined by several authors [3–7]. Numerical calculations for a typical infinite homogeneous core medium [3–4], showed that the absorption in a single ^{239}Pu resonance, and its Doppler temperature change, vary strongly with separation from a nearby ^{238}U resonance. In particular, the Doppler change becomes negative over a certain range of separations. This behaviour is due to the perturbation of the flux spectrum by the ^{238}U resonance. In the unresolved region one can estimate the net effect of the resonance overlapping by averaging over all relative separations of resonances, assuming the two sequences to be randomly distributed with respect to each other, as well as over the Porter-Thomas distributions of widths.

As an example we consider a typical core medium, composed of an infinite homogeneous mixture of ^{239}Pu and ^{238}U in atomic ratio 1/7, with total non-resonant scattering cross sections 400 barns per ^{239}Pu atom. The fractional Doppler change in the ^{239}Pu absorptions, $\Delta A/A$, for temperature rise 300 to 600 °K, was calculated both with and without ^{238}U resonance overlapping. The calculation was based upon an analytical expression for the absorption due to Rowlands [7], and brief details are given in [4]. The results at several energy values are shown in Table 1. It will be seen that the Doppler effect is reduced by ^{238}U resonance overlapping, and becomes negative just above 2 keV. This is explained by the change in the fine structure flux spectrum when the ^{238}U resonances

Table 1. Fractional Doppler changes in ^{238}U and ^{239}Pu absorption between 300 and 600°K, for a dilute fast reactor

Energy (keV)	^{238}U (no overlap)	^{239}Pu (no overlap)	^{239}Pu (overlap)
0.2	0.151	0.050	0.041
0.5	0.152	0.031	0.021
1.0	0.134	0.019	0.008
2.0	0.108	0.011	0.001
5.0	0.071	0.005	−0.002
10.0	0.046	0.002	−0.002
50.0	0.013	0.0005	−0.0003

broaden. Qualitatively similar results were obtained by Hwang [5]. The presence of ^{239}Pu resonances was estimated to have a negligible effect on the ^{238}U Doppler change [4].

The effect of ^{238}U resonance overlapping on the Doppler temperature coefficient of a large bare reactor was investigated very approximately in reference [4]. Using the same method, it has been estimated that the changes in $\Delta A/A$ due to overlapping shown in Table 1 would increase the magnitude of the overall negative Doppler coefficient by the order of 10%.

For the purpose of detailed multigroup theory calculations of the Doppler coefficient it is necessary to work with effective cross sections. In this connection Rowlands [7] has investigated analytically the problem of overlapping of two independent sequences of resonances. For each sequence he derives a narrow resonance (NR) flux weighting spectrum, which has been averaged over the position and sizes of the other sequence. This spectrum is then used to obtain effective cross sections, defined as the average reaction rate for any given process, per absorber nucleus, divided by the average true flux, i.e., the flux with dips at the resonance positions of both sequences. It is found that the effective cross sections are given approximately by the same mathematical expression as if the presence of the second sequence were ignored. However, the total non-resonant scattering cross sections per atom, which appears as a variable, is increased by a factor which does depend slightly on the properties of the second sequence.

Although the effective cross sections are thus approximately unaffected by the presence of a second resonance sequence, this is not so for the reaction rates and flux spectrum themselves. In particular, the reaction rate for one sequence is reduced by a factor which accounts for overlapping and depends approximately on the properties of the second sequence only. In Part II, this result is discussed in relation to a thermal reactor problem. The Doppler coefficient for the type of dilute fast reactor under consideration is determined primarily by the temperature dependence of the reaction rates. It will therefore be affected by resonance overlapping as shown in the above example. This overlapping is included in the effective cross sections obtained by Rowlands.

While further investigation of the resonance overlapping problem is required, including comparison of the various treatments now available, the important conclusions from the work so far done, is that there is no indication of an adverse effect on the Doppler coefficient of dilute fast reactors.

Multilevel interference

Some exploratory calculations have been made to assess the effect of using multilevel theory instead of single level theory, which is assumed in most fast reactor resonance absorption and Doppler investigations. Multilevel theory introduces the characteristic asymmetry in the shape of a fission resonance due to interference from neighbouring levels, and this is observed in the resolved region. For simplicity the calculations were made for a pair of average resonances separated by the mean level spacing. The cross sections were calculated using Vogt's formulation of multilevel theory, with an approximate method of inverting the level matrix involved. The value of a certain multilevel parameter occurring in the theory was chosen to give maximum interference effect between the two resonances. Attention was confined to the $J=4$ and $J=1$ sequences of uranium-235 and plutonium-239 resonances, respectively, and mean resonance parameters were assumed. In particular the mean level spacings were taken to be 1 eV and 3 eV respectively.

Two cases were investigated corresponding to a dilute fast reactor with plutonium–uranium oxide fuel, and a sample of uranium-235 as might be used in a Doppler measurement by the oscillator technique. Let d_m and d_s denote the Doppler reactivity change from a narrow energy group for temperature rise 300 to 600°K, according to multilevel and single level theory. The following table gives the calculated ratio d_m/d_s at three energy values in the Doppler region.*

Energy (keV)	Reactor (^{239}Pu)	Sample (^{235}U)
0.2	1.006	1.12
0.5	1.007	0.91
1.0	1.010	0.81

The results suggest that multilevel theory corrections may be negligible in the case of a dilute fast reactor, but are more important for a concentrated sample of fissile material. The greater effect in the latter case is due partly to the much stronger resonance self-shielding (small scattering cross section per atom), and partly to the smaller mean spacing of uranium-235 resonances.

In general, multilevel interference depends on resonance parameters and spacings of several neighbouring resonances, and a complete treatment for the unresolved region would require an averaging over the appropriate statistical distribution of parameters. It should, therefore, be emphasised that the above results are intended to be illustrative only.

* P. J. Collins, private communication.

A numerical method for fast reactor resonance problems

The attempt to refine conventional methods to deal with the specific resonance problems of dilute fast reactors leads to considerable mathematical and computational difficulties. There is much to be gained by adopting a purely numerical approach which will allow automatically for resonance overlapping, Porter-Thomas fluctuations of resonance widths, multilevel interference, core heterogeneity, etc. A method along these lines has been developed by Brissenden and Durston [8], suitable for large digital computers.

The basis of the scheme is to produce a library of Doppler-broadened cross sections for each of the mani fissile and fertile isotopes at several temperatures, and tabulated at suitably fine energy intervals on magnetic tape (they will be actual, not "effective", cross sections). In the resolved region, known resonance parameters are used. For the unresolved region a Fortran code RESP has been prepared which selects widths and spacings for both s and p wave levels by random sampling from appropriate statistical distributions, the mean values being provided as input data. A code GENEX uses the output from RESP to compute cross sections according to an approximate form of multilevel theory and also Doppler-broadens them. The cross sections are tabulated at about 150000 energy points between zero energy and 20 keV. The interval of tabulation has been chosen to suit all isotopes of current interest.

A third computer programme SDR2 uses the cross-sections to calculate the detailed infinite medium neutron flux spectrum over the above energy range. A step-by-step method is used to solve the slowing-down transport equation, assuming either a constant $1/E$ source or an arbitrary, numerically prescribed, source, above 20 keV. The solution refers to a two region cell, using the collision probability technique. The cross sections of coolant and structural materials present in either cell region can include a limited number of resonances, so that for example the 2.85 keV resonance in sodium coolant can be taken into account. The flux and cross sections are then processed to give 47-group averaged cross sections for use in standard multigroup calculations, as well as detailed information on reaction rates.

A preliminary test of the new method has been made and the results are shown in Fig. 1. They refer to a homogeneous mixture of carbon and ^{238}U in atomic proportions 30:1, and temperature 300°K. 44-group averaged capture cross sections for ^{238}U, covering the total energy range 30 eV to 20 keV, are plotted against energy. For the unresolved region above 1.8 keV, the s and p wave strength functions were taken to be 1.0 and 2.3×10^{-4}, respectively, and a chi-squared distribution with one degree of freedom was assumed for the neutron widths. The mean capture width and s wave level spacing were taken to be 0.025 eV and 18.3 eV, respectively.

For comparison, results obtained by a conventional method of calculating effective cross sections are also

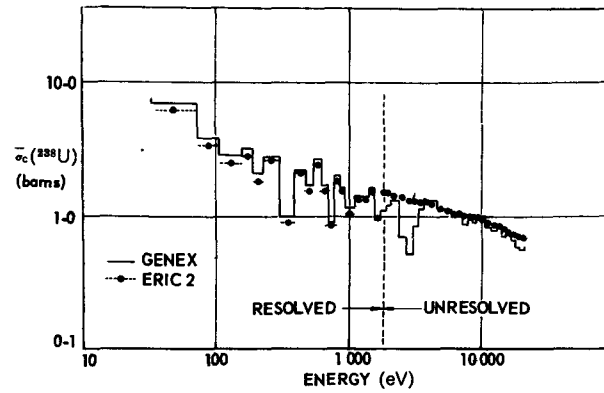

Figure 1. Group capture cross sections for ^{238}U at 300°K in a 30/1 carbon/^{238}U mixture

shown in Fig. 1. They were computed by means of the ERIC code as described below, assuming a $1/E$ flux weighting spectrum. The agreement between the two methods is in general satisfactory, although certain discrepancies will be observed. The ERIC group cross sections in the resolved region are higher than the GENEX values, since they are defined with respect to the unperturbed flux spectrum, instead of the actual spectrum as in GENEX. The low GENEX values at the beginning of the unresolved region are due to the omission of p wave resonances below 4 keV in this particular test. The new method is at present in the testing stage, and various checks on the numerical methods and data remain to be completed.

PART II. THERMAL REACTOR INVESTIGATIONS

Calculation of resonance integrals

The resonance integral I is defined as the total resonance reaction rate per absorber nucleus, in a fuel element which is placed in an isotropic uniform neutron flux with $1/E$ energy-dependence. In the simple case of a two-region problem with all slowing-down by narrow resonance scatterers, the Chernick-Vernon collision probability formulation [9] gives

$$I = \int \{(P_{00}\sigma_p/\sigma_0) + (1 - P_{00})\}\sigma_a \, dE/E \qquad (1)$$

Here P_{00} is the probability that a neutron which has just made a collision in the fuel region will also make its next collision in this region, while σ_0, σ_p and σ_a, are the total, potential scattering, and absorption cross sections of the fuel per resonant absorber nucleus.

In the method of Nordheim [10], equation (1) is integrated numerically, using tabulated values of P_{00}. An alternative method is to use a suitable rational approximation for P_{00}, which converts the problem into the simpler one of evaluating I for an infinite homogeneous medium. For example, the use of the Wigner rational approximation [11], for a simple convex fuel rod gives

$$I = F(\sigma_p + \sigma_e) \qquad (2)$$

where F denotes the resonance integral for an infinite homogeneous medium, and $\sigma_e = 1/N\bar{l}$ where N is the number of resonant absorber nuclei per unit volume,

and $\bar{l}$ is the mean chord of the rod: this is the standard equivalence theorem. This theorem gives resonance integrals which are typically 10% too low. Bell [12] suggested the improved form

$$I = F(\sigma_p + a\sigma_e) \qquad (3)$$

but indicated no method of determining the factor a other than by comparison of known homogeneous and heterogeneous resonance integrals. It has been shown, however, that a can be calculated theoretically by using improved rational approximations for P_{00} [13]. Analysis based upon the approximation proposed independently by Carlvik [14] and Fukai (unpublished):

$$P_{00} = 2x/(x+2) - x/(x+3) \qquad (4)$$

with $x = \sigma_0/\sigma_e$, showed that $a = 1.16$ should be a good value for systems of practical interest. It can be shown that the improved equivalence theorem (3) is valid under the assumptions of the intermediate resonance theory of Goldstein and Cohen [15], which is used in the calculations to be described. This theory is an improvement over the conventional narrow resonance (NR) and infinite absorber mass (IM) approximations.

The application of the equivalence theorem (3) to the case of regular arrays and liquid-filled clusters of rods is also investigated in [13]. The basic problem is to determine the geometric quantity $\bar{\mathscr{l}}$, from which σ_e is obtained. $\bar{\mathscr{l}}$ is defined generally in terms of P_{00} in the limiting case of large total fuel cross section Σ_0,

$$P_{00} = 1 - 1/\Sigma_0 \bar{\mathscr{l}} + \ldots \qquad (5)$$

For a simple convex body, $\bar{\mathscr{l}}$ is the mean chord, equal to $4V/S$, where V and S denote the volume and surface. For complex bodies, it is customary to work with the effective surface S_{eff}, defined by $\bar{\mathscr{l}} = 4V/S_{eff}$, where $\bar{\mathscr{l}}$ is given by equation (5). The problem of a regular lattice is treated in [13] by considering a cylindricalized cell, composed of a fuel rod surrounded by an annular moderator region. The isotropic scatter boundary condition of Askew and Brissenden [16] is used on the outer surfaces of the cell. The required collision probabilities for the cell are obtained using the method of Bonalumi [17]. As an example, Fig. 2 shows the

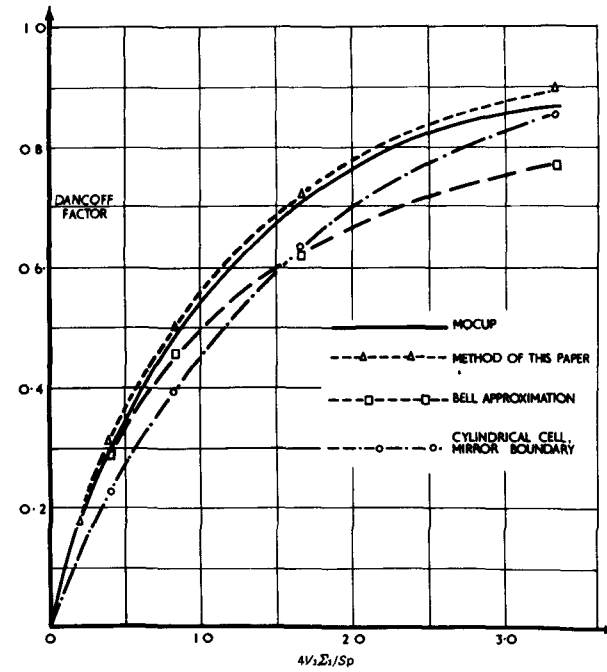

Figure 2. Variation of Dancoff factor with $4V_1\Sigma_1/Sp$ for a square pin cell with $V_1V_0=1$

calculated variation of the Dancoff factor (S_{eff}/S) with the moderator total cross section Σ_1 for a two-region cell with V (moderator) $= V$ (fuel). The results are in excellent agreement with Monte Carlo calculations made with the MOCUP code [18] for the actual square geometry, and which may be regarded as essentially exact. The use of a cylindricalized cell with a mirror boundary condition is obviously unsatisfactory. The Bell approximation, as might be expected, is adequate when Σ_1 is small, but not otherwise.

In order to apply the equivalence theorem (3), one must be able to calculate the resonance integral for an infinite homogeneous medium. A FORTRAN computer code ERIC [19] has been used for this purpose. In the resolved region the calculation is based on the intermediate resonance theory of reference [15]. In the unresolved region up to 10 keV, the narrow resonance approximation is assumed, and the resonance integral is calculated by averaging over the Porter-

Table 2. ^{238}U resonance integral for UO_2 fuel over energy range 4 eV to 10 keV, calculated by the ERIC code

σ_e (barns)	T(°K) 300	500	700	900	1300	1700	2100
5	9.064	9.395	9.654	9.871	10.232	10.532	10.794
10	10.814	11.203	11.512	11.774	12.215	12.589	12.918
15	12.261	12.708	13.065	13.371	13.892	14.337	14.732
20	13.528	14.030	14.436	14.786	15.385	15.900	16.359
25	14.672	15.228	15.681	16.074	16.750	17.334	17.855
30	15.723	16.334	16.832	17.266	18.018	18.669	19.251
35	16.702	17.364	17.909	18.385	19.210	19.926	20.568
45	18.490	19.256	19.890	20.448	21.417	22.259	23.014
55	20.109	20.975	21.697	22.333	23.441	24.403	25.267

Uranium and oxygen scattering is treated by the intermediate resonance theory.

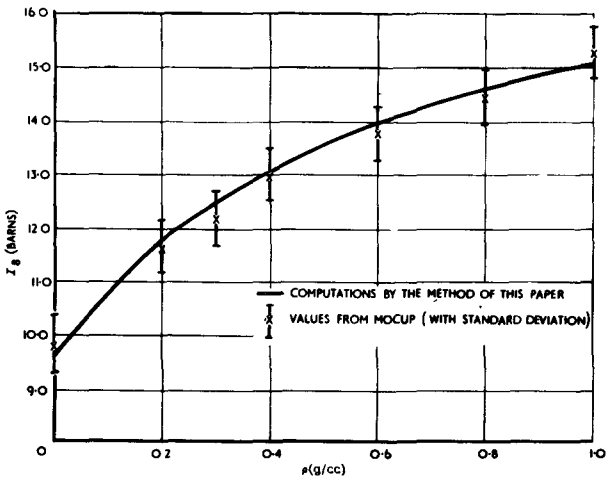

Figure 3. Variation of the ^{238}U resonance integral I_8 for the SGHW prototype with coolant density

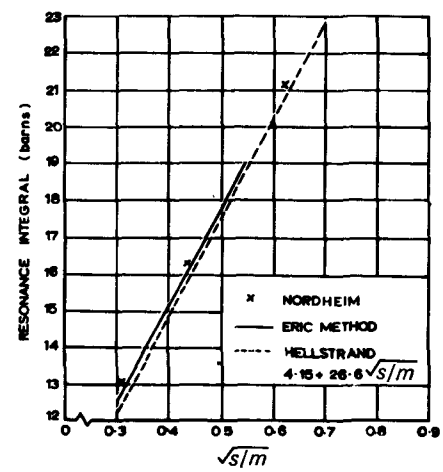

Figure 4. ^{238}U resonance integral for oxide rods at 300°K

Thomas distributions of resonance widths. Both s and p wave resonance sequences are included. For fast reactor work, the code will calculate effective cross sections. Some computed values of the ^{238}U resonance integral I_8 for uranium oxide are given in Table 2, as a function of temperature and excess scattering cross section σ_e. Table 3 includes some similar data for ^{235}U. For the calculations in the section below, however, it was convenient to use the self-shielding factor, defined as the ratio of the resonance absorption integral to its value for infinite dilution, and it is this factor which is tabulated. The calculated resonance absorption integral for infinite dilution is 304 barns, and the ratio of the capture to fission integrals is 0.9.

For the problems investigated in the next section, calculations have also been made by the Monte Carlo method, using the MOCUP code [18]. This code tracks neutrons from the starting energy, 10 keV down to 4 eV, in the actual lattice geometry, and computes the total resonance absorption. From this quantity, the resonance integral can be obtained. A correction for resonance absorption above 10 keV has been applied to both the ERIC and MOCUP results, obtained by a separate Monte Carlo calculation.

The use of equivalence theorems, in conjunction with tabulated data obtained from the ERIC code, provides a relatively rapid method of calculating resonance integrals for practical fuel elements. A comparison of this method with Monte Carlo calculations, for the H_2O-filled uranium oxide rod cluster of the Steam Generating Heavy Water Reactor prototype [20], is shown in Fig. 3. The agreement gives strong support to the ERIC calculation of the ^{238}U resonance integral, and to the methods of reference [13].

Table 3. ^{235}U self-shielding factor R_5 against temperature T and excess scattering cross section, σ_e

σ_e (barns)	T(°K) 300	900	1500
100	0.507	0.554	0.580
300	0.669	0.715	0.739
1000	0.828	0.861	0.877
10000	0.974	0.980	0.983

COMPARISONS WITH EXPERIMENT

^{238}U resonance integrals

Calculations have been made by the ERIC and MOCUP (Monte Carlo) codes for comparison with the measured ^{238}U resonance integrals of Hellstrand [21], for single uranium oxide rods, and air-filled and D_2O-filled clusters. Such a comparison requires corrections to be made for several factors, including the effective energy range of the experimental measurements, and deviations from the $1/E$ spectrum. The magnitude of these corrections has been carefully estimated using Monte Carlo methods to simulate the experimental situation [22]. In the ERIC calculations, the factor a in equation (3) was taken equal to 1.16. The geometric quantity $\bar{\mathscr{F}}$, which determines σ_e, was taken as the diameter for solid rods, and was calculated by the methods of reference [13] for the D_2O clusters. For the air-filled clusters, $\bar{\mathscr{F}}$ was obtained using the simple rubber band model.

The ERIC results and experimental data for single oxide rods are shown in Fig. 4 as a function of $(S/M)^{\frac{1}{2}}$, where S/M is the surface-to-mass ratio. Values calculated by Nordheim [10], using the numerical integration method referred to in the first section of Part II, are also included. The agreement between theory and experiment is good.

The ERIC results for some oxide rods and air-filled clusters are shown together in Table 4. The agreement with experiment is again good, except that the ERIC results for the 27 rod cluster lies just outside the experimental error. An account of the calculations for these systems, including also a comparison with the Monte Carlo results, is included in reference [23].

ERIC and MOCUP calculations of the ^{238}U resonance integral for two D_2O-filled clusters of oxide rods are compared with experiment in Table 5. The agreement is close for the 7 rod cluster, but the calculated values for the 19 rod cluster are rather higher than the experimental figure.

Table 4. ^{238}U resonance integrals (I_8) for single rods of UO_2 and air-filled clusters. Comparison of Hellstrand's measurements with ERIC calculations

Number of rods	Rod radius (cm)	S_{eff}/M (cm^2/g)	I_8 (Hellstrand) (barns)	I_8 (ERIC) (barns)
1	0.59	0.323	19.4	19.1
1	0.78	0.249	17.4	17.3
7	0.74	0.126	13.8±0.3	13.8
19	0.74	0.085	12.1±0.3	12.1
27	0.59	0.086	11.8±0.3	12.3

Table 5. ^{238}U resonance integrals (I_8) for D_2O-filled clusters of UO_2 rods. Comparison of Hellstrand's measurements with ERIC and MOCUP calculations

Number of rods	S_{eff}/M (cm^2/g)	I_8 (Hellstrand) (barns)	I_8 (MOCUP) (barns)	I_8 (ERIC) (barns)
7	0.14	14.5±0.3	14.6±0.3	14.4
19	0.11	12.8±0.3	13.2±0.4	13.2

Experimental measurements of the temperature-dependence of the ^{238}U resonance integral have been analysed on the assumption that

$$I(T) = I(T_0)\ \{1 + \beta(T^{\frac{1}{2}} - T_0^{\frac{1}{2}})\}, \qquad (6)$$

where T is the absolute temperature, and T_0 is equal to 239°K. Calculations using the resonance integral data in Table 2 showed that over the temperature range 300 to 900°K, the coefficient β for uranium oxide fuel could be expressed approximately as a linear function of the surface-to-mass ratio S/M, namely

$$\beta = 0.0057 + 0.0053\ S/M \qquad (7)$$

for S/M in the range 0.1 to 0.5 cm^2/g.

The relation (7) is shown in Fig. 5, and is in good agreement with the measurements of Hellstrand *et al.* [24] for uranium oxide rods of various sizes.

Shielding of ^{235}U by ^{238}U resonances

Experiments have been carried out at Winfrith to measure the shielding effect of ^{238}U resonances on the

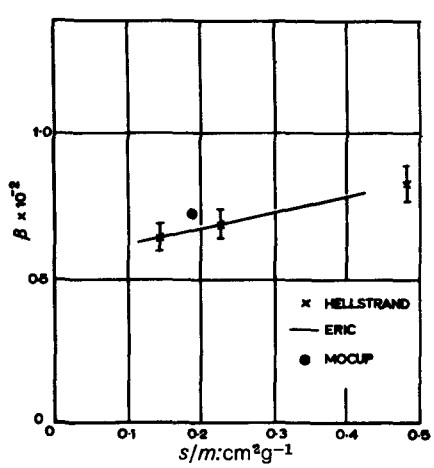

Figure 5. The Doppler coefficient β vs. S/M for UO_2

^{235}U and ^{239}Pu reaction rates in thermal reactor fuel [25]. The epi-cadmium reaction rates in small ^{235}U and ^{239}Pu samples were measured at the centres of a 1.2 in. diameter natural uranium bar and a similar copper bar, placed in a uranium–graphite sub-critical assembly. Since the non-resonant part of the uranium absorption cross section is approximately the same as the copper absorption cross section between 0.5 and 100 eV, the difference in observed reaction rates is mainly due to the shielding by uranium resonances. In the case of the ^{235}U sample, one has to consider ^{235}U self-shielding as well as shielding by ^{238}U resonances. Further measurements were made with similar uranium bars of varying ^{235}U enrichment, and extrapolation of the results to zero enrichment enabled the shielding effect of the ^{238}U resonances to be estimated separately.

Calculations were made by both the Monte Carlo and ERIC methods for comparison with the experimental results. The Monte Carlo code MOCUP allows automatically for resonance overlapping. The ERIC code was modified to deal approximately with the problem. In the resolved region, pairs of neighbouring ^{235}U and ^{238}U resonances were selected, and the ^{235}U reaction rate was calculated assuming a smooth $(1/E)$ variation of the collision density through both resonances. In the unresolved region, the calculations were made by a statistical averaging method, as used in some of the fast reactor studies. The following are preliminary estimates of the ^{238}U shielding factor, i.e., the ratio of the resonance reaction rates in the fissile samples, with and without ^{238}U present:

	^{235}U	^{239}Pu
Experiment	0.91±0.3	0.91±0.03
MOCUP	0.896±0.024	0.91
ERIC	0.886	—

It is interesting to note that ^{238}U shielding effect is nearly the same for both fissile isotopes. This result is consistent with the theory of Rowlands [7] for a mixture of two resonance absorbing materials. As

noted earlier, he finds that the reaction rate in one material is reduced by a factor which depends, in the first approximation, on the properties of the second material only. The theory was developed, however, to treat the unresolved region in dilute fast reactors, and further work is necessary to test its accuracy in thermal reactor conditions.

The implication of the observed ^{238}U shielding effect is discussed in reference [25]. It is concluded that it would be unlikely to affect significantly the reactivity of thermal reactors with fuel of low ^{235}U enrichment, but might require small corrections to be made to the results of activation experiments.

CONCLUDING REMARKS

Comparisons with experiment and Monte Carlo calculations have shown that ^{238}U resonance integrals for complex thermal reactor lattices, as well as the shielding effect of ^{238}U on ^{235}U and ^{239}Pu resonance reaction rates, can be reliably predicted by relatively straightforward calculations for a homogeneous medium, provided accurate equivalence theorems are used to define the properties of this medium.

In the case of dilute fast reactors, there is a need for experimental data, especially on fissile material Doppler effects, to check the methods of calculation which have been developed.

REFERENCES

1. Smith, R. D., *et al.*, *Fast Reactor Physics Including Results from UK Zero Power Reactors*, P/166, Vol. 6, these Proceedings.
2. Greebler, P., and Hutchins, B. A., Proceedings of the Seminar on the Physics of Fast and Intermediate Reactors, Vol. 3, p. 121, IAEA, Vienna (1962).
3. Codd, J., and Collins, P. J., UKAEA report AEEW-M427 (1964).
4. Codd, J., and Collins, P. J., Proceedings of the Conference on Breeding Economics and Safety in Large Fast Power Reactors, USAEC report ANL 6792 (October 1963).
5. Hwang, R. N., *ibid.*
6. Froelich, R., Ott, K., and Schmidt, J. J., *ibid.*
7. Rowlands, J. L., UKAEA report AEEW-M398 (1963).
8. Brissenden, R. J., and Durston, C., UKAEA report AEEW-M429 (1963).
9. Chernick, J., and Vernon, R., Nuclear Sci. Eng., *4*, 649 (1958).
10. Nordheim, L., USAEC report GA-2527 (1961).
11. Dresner, L., *Resonance Absorption in Nuclear Reactors*, Pergamon Press (1960).
12. Bell, G. I., USAEC report LA-2322 (1959).
13. Leslie, D. C., Hill, J. G., and Jonsson, A., UKAEA report AEEW-R353 (1964).
14. Carlvik, I., AB Atomenergi report RFR-174 (1962).
15. Goldstein, R., and Cohen, E. R., Nuclear Sci. Eng., *13*, 132 (1962).
16. Askew, J. R., and Brissenden, R. J., UKAEA report AEEW-R161 (1963).
17. Bonalumi, R., Energia Nuclear, *8*, 326 (1961).
18. Bannister, G., Basher, J. C., and Pull, I. C., UKAEA report AEEW-R243 (1964).
19. Sumner, H. M., UKAEA reports AEEW-M304 (1963), and AEEW-R323 (1964).
20. Campbell, C. G., *et al.*, *Reactor Physics Studies for Steam Generating Heavy Water Reactors*, P/174, Vol. 3, these Proceedings.
21. Hellstrand, E. J., Appl. Phys., *28*, 1493 (1957).
22. Beardwood, J. E., and Tyror, J. G., UKAEA report AEEW-R247 (1964).
23. Beardwood, J. E., and Sumner, H. M., UKAEA report AEEW-R345 (1964).
24. Hellstrand, E., Blomberg, P., and Horner, S., Nuclear Sci. Eng., *8*, 497 (1960).
25. Askew, J. R., and Sanders, J. E., UKAEA report AEEW-M415 (1963).

ABSTRACT—RÉSUMÉ—АННОТАЦИЯ—RESUMEN

A/172 Royaume-Uni

Etudes de l'absorption par résonance et du phénomène de Doppler pour les réacteurs rapides et thermiques

par J. Codd *et al.*

La première partie du mémoire décrit certains travaux de recherche concernant l'absorption par résonance et le degré dont elle dépend de la température dans les réacteurs rapides à combustible dilué. On examine deux problèmes particuliers en se référant spécialement au coefficient de température de Doppler: le chevauchement des résonances des constituants fissile et fertile du combustible, et les conséquences de l'emploi de la théorie de résonance à niveaux multiples au lieu de l'habituelle théorie à simple niveau. On décrit ensuite une nouvelle méthode numérique pour la zone d'énergie de résonance des réacteurs rapides à combustible dilué. Cette méthode tient compte automatiquement du chevauchement des résonances et de la théorie à niveaux multiples aussi bien que de l'hétérogénéité du cœur, et elle permet de calculer le spectre détaillé des énergies de neutrons comprises entre 20 keV et les énergies thermiques. Certains résultats d'un essai préliminaire de la méthode effectué sur un mélange homogène d'uranium 238 et de carbone sont comparés aux calculs faits selon une méthode classique.

La deuxième partie traite des calculs relatifs aux intégrales de résonance pour les réacteurs thermiques hétérogènes. On y explique l'emploi des théorèmes d'équivalence, qui permettent d'appliquer à un système hétérogène les résultats obtenus pour un milieu homogène. De là découle une forme améliorée du théorème d'équivalence usuel pour les barreaux

isolés de combustible solide. On discute de l'application des théorèmes d'équivalence à des réseaux réguliers ou des grappes de barreaux de combustible, en introduisant le concept de « surface efficace ». On décrit ensuite dans ses grandes lignes une méthode servant à calculer ce paramètre pour des réseaux ou grappes remplis de liquide. Les valeurs calculées de l'intégrale de résonance et sa variation avec la température sont ensuite comparées aux données expérimentales sur les barreaux et les grappes de UO_2, ainsi qu'aux résultats obtenus avec la méthode de Monte-Carlo.

On étudie ensuite l'intégrale de résonance dans le cas des isotopes fissiles lorsqu'ils sont mélangés à l'uranium 238, en considérant particulièrement l'effet du chevauchement des résonances. Les résultats numériques sont comparés aux vitesses de réaction relatives mesurées pour des échantillons fissiles dans des barreaux d'uranium et de cuivre irradiés dans un réseau de graphite avec combustible uranium.

более совершенная форма стандартной эквивалентной теоремы для изолированных твердых тепловыделяющих стержней. Обсуждается применение эквивалентных теорем для расчета правильных систем или ограниченных сборок тепловыделяющих элементов, вводится понятие «эффективная поверхность». Описан метод расчета этого параметра для систем с жидким заполнением и сборок. Расчетные значения резонансного интеграла и его зависимость от температуры сравниваются с эксплуатационными результатами для стержней и сборок из двуокиси урана, а также с данными, полученными по методу Монте-Карло.

Проведены исследования резонансного интеграла для смеси делящихся изотопов и U^{238} с учетом эффекта наложения резонансов. Результаты, полученные численными методами, сравниваются с измерениями относительных скоростей реакции для образцов делящегося материала в урановых и медных блоках, облученных в уран-графитовой решетке.

A/172 Соединенное Королевство

Исследование резонансного поглощения и допплеровского эффекта в реакторах на тепловых и быстрых нейтронах

Дж. Кодд *et al.*

Первый раздел доклада посвящен описанию некоторых исследований резонансного поглощения и его зависимости от температуры в реакторах на быстрых нейтронах с разбавленным топливом. Обсуждаются две специальные проблемы, касающиеся допплеровского температурного коэффициента: наложения резонансов делящихся материалов, состав вторичного ядерного топлива и последствия использования резонансной теории с многими уровнями вместо обычной резонансной теории с одним уровнем. Описан новый численный метод обработки применительно к области резонансной энергии для реакторов на быстрых нейтронах с разбавленным топливом. Этот метод автоматически подходит для случая наложения резонансов, теории с многими уровнями, а также для гетерогенной активной зоны. Метод позволяет вычислять с достаточной точностью энергетический спектр нейтронов в интервале от тепловой энергии до 20 *кэв*. Приводится сравнение предварительных результатов, полученных этим методом, для гомогенной смеси U^{238} и графита с результатами расчетов обычным методом.

Во втором разделе доклада даются расчеты резонансных интегралов для гетерогенных реакторов на тепловых нейтронах. Объясняется использование эквивалентных теорем, позволяющих применять данные для гомогенной среды к расчету гетерогенных систем. Определена

A/172 Reino Unido

Estudios de absorción de resonancia y efecto Doppler en reactores rápidos y térmicos

por J. Codd *et al.*

La primera parte del documento describe algunas investigaciones sobre absorción de resonancia y su dependencia de la temperatura, en reactores rápidos diluidos. Se tratan dos problemas particulares con especial referencia al coeficiente de temperatura Doppler: la superposición de resonancias de los componentes fisibles y fértiles del combustible, y las consecuencias de utilizar la teoría de resonancia de muchos niveles en lugar de la teoría habituel de un solo nivel. Se describe un nuevo método numérico para tratar la región de energía de resonancia de reactores rápidos diluidos. Este método tiene en cuenta automaticamente la superposición de resonancias y la teoría de muchos niveles así como la heterogeneidad del núcleo, y permite calcular el espectro detallado de energía de neutrones entre 20 keV y energías térmicas. Se comparan algunos resultados de una prueba preliminar del método, para una mezcla homogénea de uranio-238 y carbono, con cálculos hechos usando un método convencional.

La segunda parte aborda los cálculos de las integrales de resonancia en reactores térmicos heterogéneos. Se expone el uso de los teoremas de equivalencia, que permiten aplicar a un sistema heterogéneo los resultados obtenidos para un medio homogéneo. Se deduce una forma perfeccionada del teorema normal de equivalencia, para barras aisladas de combustible sólido. Se discute la aplicación de los teoremas de equivalencia a sistemas regulares o haces finitos de

barras de combustible, introduciendo el concepto de «superficie efectiva». Se esboza un método para calcular este parámetro para sistemas con carga líquida o haces de barras. Se comparan después los valores calculados de la integral de resonancia y su dependencia de la temperatura, con datos experimentales de barras y haces de UO_2, y también con resultados obtenidos por el método de Monte Carlo.

Se hace un estudio de la integral de resonancia para núclidos fisibles mezclados con uranio-238, con particular atención al efecto de superposición de resonancias. Los resultados numéricos se comparan con medidas de las velocidades relativas de reacción de muestras fisibles en barras de uranio y cobre, que fueron irradiadas en una red de grafito con combustible de uranio.

Neutron thermalization and reactor applications

By J. R. Beyster,* N. Corngold,** H. C. Honeck,** G. D. Joanou* and D. E. Parks*

The design of thermal reactors has often been based on approximate treatment of the nuclear physics and on extensive experimental tests of critical and exponential assemblies to determine or adjust reactor parameters. Recently, however, it has become important to improve our understanding of the physical phenomena occurring in reactors in order to develop reliable computational procedures for optimizing reactor design. These procedures require detailed knowledge of all relevant neutron cross sections, and reliable methods of predicting thermal reactor neutron spectra. The demand for cross sections of sufficient accuracy for reactor analysis is being answered by careful measurement [1]. However, the problem of predicting thermal reactor spectra under all spatial and temperature conditions likely to be encountered in a physical system requires in addition an understanding of thermal neutron scattering. A great deal of progress has been made in the last few years in developing this understanding. It is the primary purpose of this paper to describe these advances and their significance from the standpoint of reactor technology.

Underlying the earliest descriptions of thermal neutron scattering and spectra was the fact that the first reactors were very well thermalized ($\xi\Sigma_s/\Sigma_a \gg 1$). As a consequence, it was useful and expedient to consider a Maxwellian distribution of thermal neutrons at a temperature T_n differing only slightly from the actual temperature of the moderator [2];

$$T_n = T\left[1 + A\frac{\Sigma_a(kT)}{\xi\Sigma_s}\right] \qquad (1)$$

One could presumably determine the value of the dimensionless coefficient A by measuring the activation of $1/v$-foils by neutrons belonging to the spectrum under investigation. This description of the spectrum is of little use for $\Sigma_a(kT)/\xi\Sigma_s \gtrsim 0.1$, or when the spectrum is appreciably influenced by resonance absorbers. Also, there is the difficulty caused by the absence of a well-defined transition energy above which slowing-down theory is valid and below which the spectrum is Maxwellian [3]. This latter difficulty is overcome in the Wilkins [4] and Wigner-Wilkins [5] theories of thermal neutron scattering in which the moderator is considered to be an ideal gas consisting of heavy nuclei or protons respectively. However, detailed theoretical and experimental studies of neutron thermalization have shown that these simple models are not usually adequate for reactor design calculations, and scattering cross sections which embody the characteristic crystalline and molecular properties of the moderator are necessary. Subsequent sections of this paper discuss theoretical procedures for calculating these scattering cross sections, the experimental tests performed to assess the adequacy of the procedures, and the sensitivity of typical reactor calculations to the scattering description.

THEORY

The general theory of neutron thermalization by chemically bound systems is based on the Fermi pseudo-potential approximation [6,7,8,9]. For thermalization studies, the fundamental cross section of interest is the differential cross section $\sigma(E_0,E,\theta)$ for energy transfer from an initial energy E_0 to a final energy E through an angle θ in the laboratory system. For an isotropic moderator at temperature T consisting of a single atomic species of atomic mass M, this cross section can be expressed in the form [10];

$$\sigma(E_0,E,\theta) = \frac{1}{4\pi T}\sqrt{\left(\frac{E}{E_0}\right)}\,e^{-\frac{\beta}{2}}\sigma_b S(\alpha,\beta)$$
$$= \frac{1}{4\pi T}\sqrt{\left(\frac{E}{E_0}\right)}e^{-\frac{\beta}{2}}[\sigma_b S_s(\alpha,\beta) + \sigma_c S_d(\alpha,\beta)] \qquad (2)$$

where σ_b is the bound atom cross section, σ_c is the bound coherent cross section, $\alpha = (E_0 + E - 2\sqrt{(E_0E)}\cos\theta)/MT$, $\beta = (E_0 - E)/T$, ($\hbar = k =$ neutron mass $= 1$). $S(\alpha,\beta)$, the scattering law is a function of only the two variables α and β. The self part $S_s(\alpha,\beta)$ represents the scattering of a neutron by a single atom in the interatomic force field of all its neighbours while the distinct part $S_d(\alpha,\beta)$ represents the effects of interference between neutron waves scattered from different atoms. Several physical and mathematical approximations are generally introduced to reduce the problem of calculating $\sigma(E_0,E,\theta)$ to a tractable form. The first approximation considered is that of neglecting interference effects in the inelastic scattering of neutrons. Marshall and Stuart [11] and Butler [12] have made calculations which show that interference effects are generally a small part of the inelastic scattering. Thus, it is expected that interference phenomena in inelastic scattering will have a small effect on most neutron spectra. For elastic scattering the interference effects

* General Atomic.
** Brookhaven National Laboratory.

Table 1. Characteristics of some scattering kernel codes

Allowed form of $\rho(\beta)$

Code name	Installation	Computer	Continuous	Delta function	Diffusive motion	Anisotropy	Moderators
ROBESPIERRE	GA	7090	No	Yes	No	No	H_2O, D_2O, CH_2
GAKER	BNL-GA	7090	No	Yes	No	No	H_2O, D_2O, CH_2
KERNEL PAM	KAPL	S-2000	No	Yes	No	No	H_2O, D_2O, CH_2
SUMMIT	GA	7090	Yes	No	No	Yes	Graphite
SUMMIT II	GA	7090 7044	Yes	No	No	No	ZrH, CH_2, C_6H_6 C, Be, BeO
LEAP PIXIE	Winfrith	7090	Yes	Yes	Yes	No	C, D_2O, BeO, Be, H_2O
GASKET	GA	7090 7044	Yes	Yes	Yes	No	All moderators

are dominant except for hydrogenous moderators. These considerations result in the incoherent approximation for inelastic scattering in which for solids $S_d(\alpha,\beta)$ is replaced by its elastic part, $S_d^{el}(\alpha,\beta)$, which is easily calculated. S_d^{el} in the latter case gives rise to the well-known Bragg peaks in the scattering cross section. The Bragg effects are unimportant for most reactor spectral calculations but must be considered in the interpretation of the decay of a thermalized pulse in a finite medium.

$S_s(\alpha,\beta)$ which depends rather sensitively on moderator atomic motion, has a significant effect on thermal reactor spectra. Fortunately, this effect is not so pronounced as to require a completely detailed description of moderator atomic motions. Most calculations of $S_s(\alpha,\beta)$ for moderators have as their basis [10];

$$S_s(\alpha,\beta)=\frac{1}{2\pi}\int_{-\infty}^{+\infty} I(\alpha,\tau)\, e^{i\beta\tau}d\tau \qquad (3)$$

with $I(\alpha,\tau)$ given by the Gaussian approximation;

$$I(\alpha,\tau)=\exp\left\{-\alpha\int_{-\infty}^{+\infty}\frac{\rho(\beta)}{\beta\sinh(\beta/2)}\times[\cosh(\beta/2)-\cos\beta\tau]\,d\beta\right\} \qquad (4)$$

The entire dependence of the neutron scattering on the motion of moderator atoms is contained in $\rho(\beta)$ or equivalently $\rho(\omega)$, where $\omega=T\beta/\hbar$. In the case of a harmonically vibrating solid, $\rho(\omega)$ is identical with the frequency distribution or density of modes of lattice vibrations. For other systems such as liquids, the interpretation of $\rho(\omega)$ as a density of modes is not a rigorous interpretation. The form (4) of the Gaussian approximation is verified by many of the exactly soluble physical models; (*a*) the ideal gas (as a limiting case), (*b*) a system of isotropic Einstein oscillators, (*c*) a simple cubic crystal with one atom per unit cell and (*d*) the diffusing atom model of a monatomic liquid.

In a real physical system, there are always effects which cannot be rigorously accounted for within the framework of the Gaussian approximation. Among these effects are the anharmonic vibrations in solids and molecules, the free or hindered rotations of a semi-rigid molecule, and the anisotropic but harmonic vibrations of atoms in a polycrsytalline material. Although the corrections to the Gaussian approximation are expected to have a rather small effect on neutron spectra, detailed calculations of the magnitude of these effects exist only for the cases of anisotropic motion of the atoms in carbon [13] and water [14].

The results given below show that with a physically realistic $\rho(\omega)$, the $S_s(\alpha,\beta)$ calculated on the basis of the Gaussian approximation leads to agreement between many theoretical and experimental reactor design quantities. The same agreement cannot generally be obtained by rigorous application of the free gas or heavy gas models. Many of the codes that have been developed for calculating scattering law or scattering kernels are listed in Table 1.

EXPERIMENTAL COMPARISONS

The frequency distribution $\rho(\omega)$ for many of the common moderators has been obtained as a result of studies of double differential neutron scattering, lattice dynamics, Raman and infrared spectroscopy and specific heat (see section immediately below). Other experiments of a more integral nature help establish the adequacy for reactor design of these frequency spectra and the scattering cross sections derived therefrom (see section on integral data comparisons).

Determination of $\rho(\omega)$

Here we discuss some of the techniques for measuring the frequency distribution $\rho(\omega)$. Although the complete determination of $\rho(\omega)$ usually depends on theoretical considerations using data from more than one type of experiment, this discussion is limited to techniques of neutron spectroscopy. One method of determining $\rho(\omega)$ is to measure the one phonon incoherent scattering [15] cross section which is directly proportional to the frequency spectrum for crystals having simple cubic symmetry. This procedure is not generally useful since only vanadium, hydrogen, and certain special alloys scatter almost completely incoherently. A more efficacious technique is to measure the dispersion relations [16] $\vec{\omega}(k)$ versus $\vec{k}$ where $\vec{k}$ is the phonon wave vector, by observing the one phonon

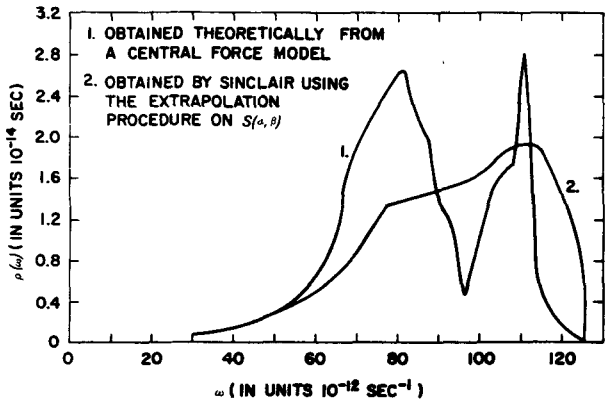

Figure 1. Frequency spectrum of beryllium

coherent scattering of monoenergetic neutrons in a crystal symmetry direction. From this the force constants in a particular model for the atomic binding in the lattice can be calculated to determine $\rho(\omega)$ [17]. The frequency spectrum of beryllium [18] determined by this procedure is shown in Fig. 1. A frequently used method of determining $\rho(\omega)$ utilizes the scattering law $S(\alpha,\beta)$ [10] measurements. The limit $\alpha\to 0$ of $S_s(\alpha,\beta)$ is proportional to $\rho(\beta)$ and this serves as a basis for determining $\rho(\beta)$ by extrapolating measured values of $S(\alpha,\beta)/\alpha$ toward $\alpha=0$ for fixed β. A significant difficulty sometimes arises, however, since $S(\alpha,\beta)\simeq S_s(\alpha,\beta)$ only for large values of α, whereas the extrapolation often must proceed from small values where interference effects are at a maximum. In addition, measurements of $S(\alpha,\beta)$ often do not have sufficient accuracy. In Fig. 1 the frequency distribution derived from the extrapolation technique [19] is compared with $\rho(\omega)$ determined from accurately measured dispersion relations. In Fig. 2 two frequency distributions for graphite, which are currently used in reactor analysis are shown; (*a*) an approximate theoretical calculation of $\rho(\omega)$ of Yoshimori and Kitano [20,13] and (*b*) $\rho(\omega)$ derived from the scattering law [19]. It would appear that significant discrepancies exist between various determinations of frequency distributions. Proposed frequency spectra exist for most of the other common moderators including H_2O [22], D_2O [12], BeO [19], CH_2 [19], ZrH [21] and many other materials [23].

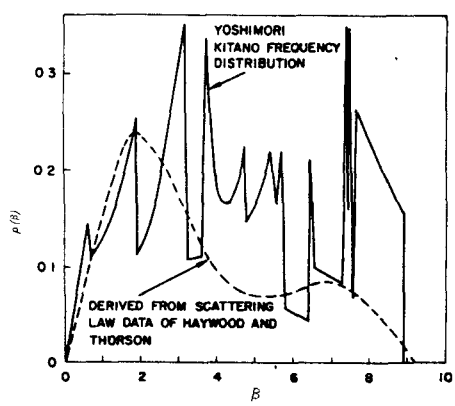

Figure 2. Lattice frequency spectra for graphite

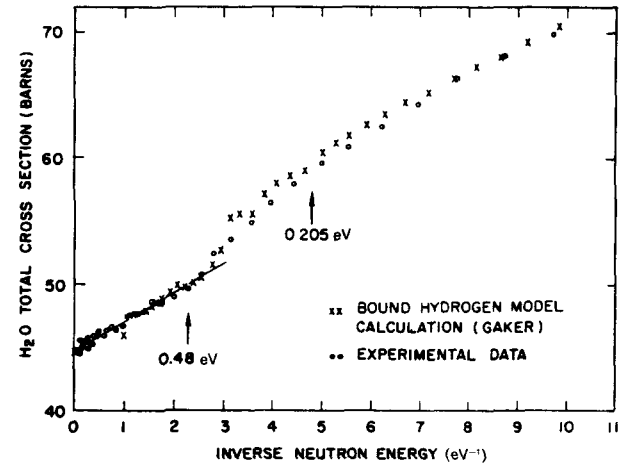

Figure 3. Variation of H_2O total cross section with inverse neutron energy

Although some of the frequency spectra are not accurately determined, they are known well enough for many reactor design calculations. For example, typical reactor spectra [18] calculated by using the two different frequency spectra proposed for the beryllium lattice in Fig. 1 differ in shape by about 10%.

Integral data comparisons

From the standpoint of reactor design it appears that only certain important properties of a moderator need to be predicted reasonably accurately. These include, for example, the total neutron cross section, the transport cross section or differential scattering cross sections, infinite medium or scalar neutron flux spectra, and/or M_2 (the second energy moment). These quantities mainly depend on the P_0 and P_1 scattering matrices. Calculations at several laboratories have indicated that higher order scattering has little effect on the thermal neutron spectra and transport.

Spectral and cross-section comparisons

The total cross-section experiment for some of the common moderators has been performed with sufficient accuracy over the required energy range to provide a meaningful test of the scattering description. In Fig. 3, a recently measured total cross section of water [14] can be seen to agree quite well with the predictions of the bound hydrogen atom model for water. Similar results are available for other common moderators.

An integral experiment which is usually quite sensitive to the P_0 energy transfer cross sections is the quasi-infinite medium neutron spectrum measurement. Experimental results are compared with calculations using the neutron diffusion equation;

$$(\Sigma(E)+DB^2)\phi(E)=\int_0^{E_m}\phi(E')\Sigma_s(E'\to E)\mathrm{d}E'+S(E)$$

where D is the diffusion constant, B^2 is the local buckling and is purposely made as small as possible, $S(E)$ the epithermal source contribution and E_m an

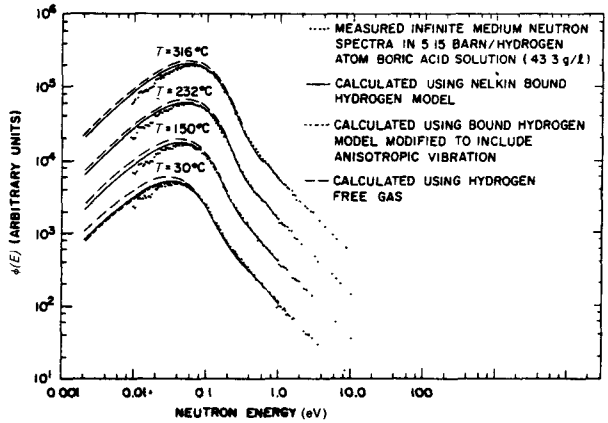

Figure 4. Infinite-medium neutron spectra in borated water as a function of moderator temperature

upper energy limit in the slowing down energy region. Results from a typical series of temperature dependent spectral experiments [14] in H_2O are compared with calculations in Fig. 4. Similar comparisons included those made for water with various resonance absorbers [24,25], graphite poisoned with $1/v$ and resonance absorbers [26,27] and D_2O [14,26], CH_2 [24,28], BeO, C_6H_6, and ZrH [14], all poisoned with $1/v$ absorber. The effect of resonance absorption in the energy region 0.07 to 0.5 eV on neutron spectra affords a most stringent test of the scattering model. It is apparent from the studies of infinite medium spectra that scattering kernels based on the current state of our knowledge of $\rho(\omega)$ can be utilized to make predictions with reasonable accuracy.

Several techniques have been used to test the transport properties of scattering kernels including measurements of angular flux $\phi(E,x,\mu)$ in a finite one-dimensional medium, of differential scattering cross sections, and of spectra in reactor lattices. Figure 5 shows a well-defined experimental geometry and the angular flux spectral results for this thin $1/v$ poisoned water slab. These spectra were calculated [14] using the S_n method of solving the neutron transport equation (GAPLSN). The P_0 and P_1 scattering matrices and epithermal source terms were necessary for the

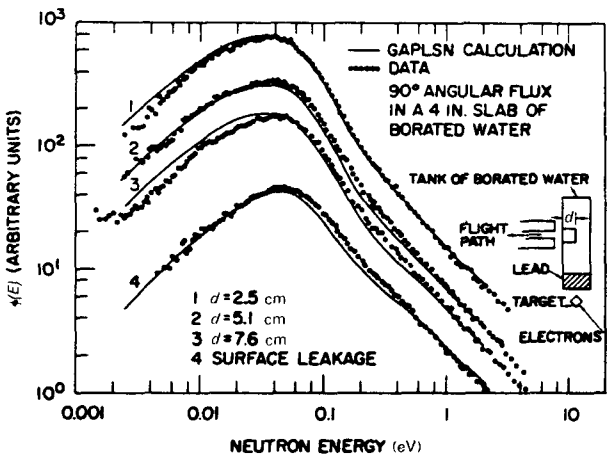

Figure 5. 90° angular flux in a 4 in slab of borated water

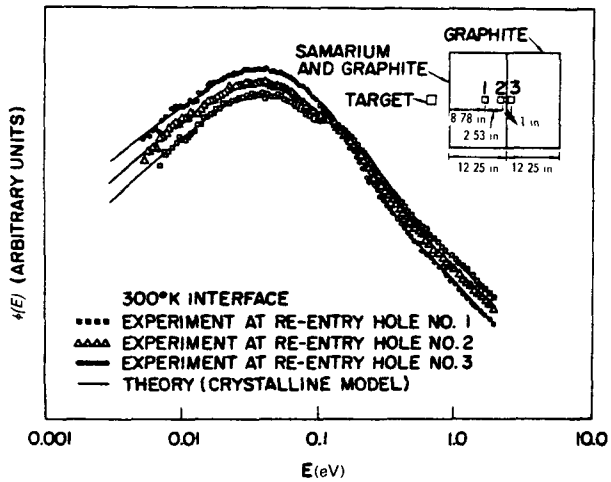

Figure 6. Thermal spectra measured in interface assembly

solution of the problem and the bound hydrogen kernel for water was used. Completely satisfactory agreement has not been attained as yet on this one-dimensional problem possibly because of the difficulty of creating a perfect one-dimensional configuration. In addition Fig. 6 shows results for a one-dimensional graphite interface problem [29]. Measurements were not made in the direction of the flux gradient as in the previous case. It appears from the space dependent experiments conducted to date that angular flux spectra measured in the direction of large flux gradients are the most difficult to predict, and these cases are often of great concern to the reactor designer.

Another method of testing the angular portion of the scattering kernel is to measure $\sigma(E,\mu)$ [30] the scattering angular distribution. Recent results for water [14] are compared with theory based on the bound hydrogen model in Fig. 7. The experimental results, from which multigroup diffusion constants can be derived for reactor analysis, agree well with theory except at forward angles above a few tenths eV neutron energy.

Thermal neutron spectrum experiments in reactor lattices [31–34] yield results which are generally quite sensitive to the neutron transport. This experiment, however, is difficult to perform under clean experimental conditions because beam extraction can perturb the flux in the lattice. Interpretation is difficult since a highly directional flux is obtained which is not simply related to the scalar flux [35]. Recent work in large D_2O lattices [34] has overcome some of these difficulties by using a scatterer to extract a beam. The experimental problem still remains in small H_2O lattices.

Transient phenomena

Typical reactor spectra may be characterized by their "slowing-down" and "thermal" components, while the spectra obtained in most pulsed and exponential experiments lack the slowing-down component. These experiments are nevertheless useful in

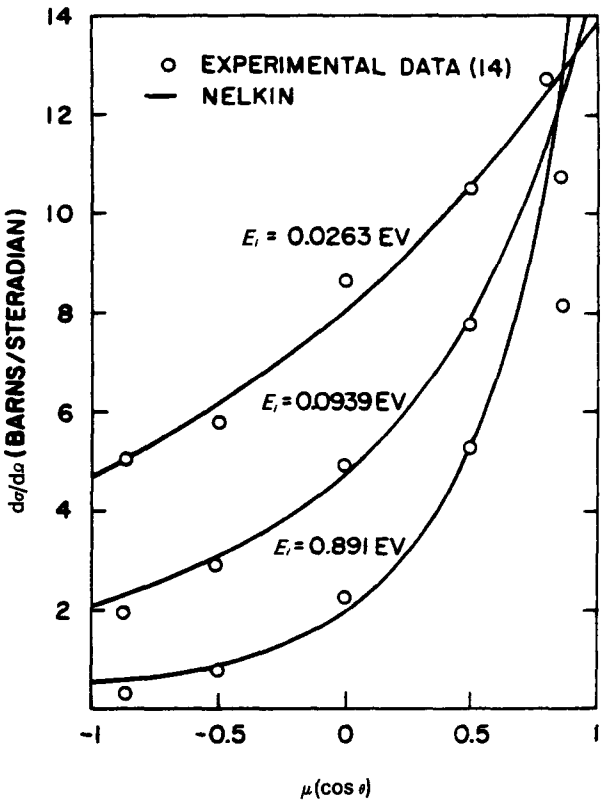

Figure 7. Measurements and calculations of the differential cross section of water

testing models for scattering kernels, and in providing averaged diffusion parameters for use in few-group theories. The analysis of the pulsed neutron source experiment [36] in a subcritical medium is based upon the representation;

$$N(\vec{r},\vec{v},t) \sim \Sigma_k N_k(\vec{r},\vec{v})\, e^{\omega_k t} \tag{5}$$

which, for a system that is not too small, gives a scalar flux;

$$\lim_{t \downarrow \infty} \int d\vec{\Omega} N(\vec{r},\vec{v},t) \sim U_0(\vec{r})\, \Sigma_k N_k(v^2)\, e^{-\lambda_k t} \to U_0(\vec{r}) \times N_0(v^2) e^{-\lambda_0 t} \tag{6}$$

With $1/v$ absorption, measurements of the variation of λ_0 with buckling (B^2) give the Maxwellian average of $v\lambda_{tr}(v)$ and the cooling coefficient, C (which is related to the inelastic part of the scattering kernel). Discrepancies between theory and experiment are most apparent at large B^2 (small samples). In H_2O, measurements of C range from 2900 to 4800 cm^4/sec, in graphite from 12 to 41 $\times$ 10^5 cm^4/sec, and in beryllium from 1 to 4 $\times$ 10^5 cm^4/sec. There are two difficulties which have to be overcome. First, in the case of the coherent, crystalline, and relatively heavy moderators, it is not clear that the experimenter has been observing the asymptotic mode [36]. Second, the smallest samples considered have bucklings such that $B\langle\lambda_{tr}\rangle$ lies in the range 0.1 to 1.0. Thus, the data that are most important in determining C are subject to large (and, at present, undetermined) transport corrections. Indeed, one finds curves of λ_0 versus B^2 which are different for water samples having different shapes ("square" and "flat"), yet are characterized by the same bucklings [24,37,38]. This difficulty will be aggravated in the case of coherent moderator materials where $\langle\lambda_{tr}\rangle$ increases as the sample size decreases.

Recent theoretical analysis of the pulsed source experiment has indicated additional difficulties [39–41]. The λ_k are eigenvalues of the unbounded scattering operator;

$$S\, N_k(v^2) = \int dv' [v'\, \Sigma_s(v',v) - v\, \Sigma_s(v,v')] N_k(v'^2) \tag{7}$$

whose spectrum appears to consist of a set of discrete points, and a continuous set bounded from below by $(v\Sigma_s)_{min}$. When the space-distribution is proportional to exp $(i\, B\cdot r)$ one sees [42] that λ_0 must be less than $v(\Sigma_s + \Sigma_a)_{min}$, and that for sufficiently large B^2 no fundamental mode exists. Nevertheless several experiments performed on crystalline materials give results which violate this limit. While it is possible that a rigorous transport treatment of the Boltzmann equation will undo this contradiction, it is apparent that the experiments should be repeated and verified.

Some measurements and calculations of λ_1 for H_2O have been reported [36]. Though data are few, calculations have been refined considerably [41,42] and show that simple M_2 expressions for λ and C [36] can be in error by as much as an order of magnitude. It is also likely that a discrete λ_1 will not be observed in the common crystalline moderators [43].

The analysis of the thermal neutron diffusion-length experiment gives similar results. Here;

$$N(\vec{r},\vec{v}) = \Sigma_j\, e^{-\vec{\kappa}_j\cdot\vec{r}} F_j(\vec{v}), \tag{8}$$

where the F_j are eigenfunctions of an operator closely related to equation (6). Again the spectrum of eigenvalues contains a discrete and a continuous portion, the latter setting in at $\kappa = (\Sigma_s + \Sigma_a)_{min}$ [42,44]. In a $1/v$ system, the expansion of κ_0 in powers of $v\Sigma_a$ again yields $\langle v\lambda_{tr}\rangle$ and C. Since the experiments are always carried out in "large" geometry, the difficulties associated with transport boundary conditions are avoided. The most successful experiments to date have been those performed in H_2O [45].

In another group of experiments [46,47], transients are induced by spatial discontinuities—in temperature and composition. The distributions are far from asymptotic, and an analysis via Eq. (8) appears unwise. It is based instead upon an expansion in terms of non-orthogonal energy modes which have Maxwellian shape, but different characteristic temperatures. Among the results are "rethermalization cross sections", which characterize the spatial relaxation of the neutron spectrum.

There are unanswered questions connected with much that we have sketched here, and, these issues will be pursued in the future. There is also promise at present of direct practical applications of pulsed neutron techniques in the analysis of multiplying assemblies [14,48–50].

Table 2. Characteristics of some thermalization codes

Code name	Installation	Computer	Language	Angular representation	Geometry	Energy representation	Scattering kernels	Anisotropic scattering
MARC	BAPL	S-2000	TAC	Monte Carlo	Slab, Hexagonal lattice	Monte Carlo	Arbitrary	P_1
TRAM	KAPL	S-2000	TAC	Monte Carlo	Arbitrary	Monte Carlo	Arbitrary	P_3
CASINO	SRL	704	FORTRAN	Monte Carlo	Hexagonal lattice	Monte Carlo	Brown-St. John	$P\infty$
WDSN	Winfrith	7090	FORTRAN	DSN	Cylinder	Multigroup	Arbitrary	No
GAPLSN	GA	7090	FLOCO	DSN	Slab, cylinder, sphere	Multigroup	Arbitrary	$P\infty$
THERMOS	BNL	7090	FORTRAN	Int. Trans.	Slab, cylinder	Multigroup	Arbitrary	No
TET	DTMB	7090	FORTRAN	Disc. Ords.	Slab	Multigroup	Arbitrary	P_3
SLOP-1	BAPL	704	SAP	P_1, P_3, DP_1	Slab, cylinder, sphere	Multigroup	Arbitrary	P_3
ULCER	AI	7090	FORTRAN	P_1	Slab, cylinder, sphere	Multigroup	Arbitrary	P_1
SWAKRUM	KAPL	704	FORTRAN, SAP	P_1, P_3, DP_1	Slab	Few modes	Arbitrary	P_3
SPECTROX	Winfrith	Mercury		Amouyal's Method	Cylindrical cell	Diff. Eq.	Generalized heavy gas	No
KATE-1	BAPL	S-2000	TAC	Infinite medium		Diff. Eq.	H. gas	No
TEMPEST-II	AI	7090	FORTRAN	Infinite medium		Diff. Eq.	H gas or heavy gas	No
GATHER-II	GA	7090	FORTRAN	Infinite medium Fourier transform		Multigroup	Arbitrary	P_1
QUICKIE	AI	7090	FORTRAN	Infinite medium		Multigroup	Arbitrary	P_1
GAZE-II	GA	7090 7044	FORTRAN		Slab, cylinder, sphere	Multigroup	Arbitrary	No
GAMBLE	GA	7090 7044	FORTRAN		x, y r, z	Multigroup	Arbitrary	No
S-X	HAPO	7090	FLOCO	$(P_1)SN$	Slab, cylinder, sphere	Multigroup	Arbitrary	P_1

THERMAL REACTOR CALCULATIONS

A variety of techniques (Table 2) have been used to compute thermal neutron spectra in reactors [51]. These methods include diffusion theory combined with a heavy gas kernel, multigroup transport theory with crystal or bound atom kernels [52, 53], and Monte Carlo methods [54]. The diffusion theory methods are most applicable to large media with smoothly varying properties (an homogenized reactor), while the transport theory methods are needed for small highly absorbing regions with sharp material discontinuities (reactor cells), or when angular distributions are important (strong flux gradients).

The principal approach is the multigroup method in which the energy region below a cutoff (usually around 1–2 eV) is divided into groups. If many groups are used, and 30–50 is common, the spacing of the groups is not critical (except when resonance absorbers are present) and it is a good approximation to evaluate all quantities at the center of the group rather than averaging over the group. If few-groups are used, it is generally necessary to first compute a many-group spectrum and average the kernels and cross sections over the few-groups. The resulting few-group kernels are applicable only to the class of problems determined by the weighting spectra. Next the kernels $\Sigma_s(E' \to E, \mu)$ must be evaluated for the selected energy mesh. Most applications require the Legendre components of the kernel $\Sigma_{sn}(E' \to E)$. A variety of computer codes have been written to compute the Legendre component scattering matrices [51]. Examples of typical reactor calculations which show the sensitivity of the results to scattering models are given in the next two sections.

H_2O, D_2O, and CH_2 lattice calculations

Many of the same techniques have been used to compute thermal spectra in light and heavy water lattices and polyethylene lattices. The kernels most frequently used are the Nelkin kernel [22, 55, 56], the free gas kernel[51] and the Brown-St. John kernel [57]. The methods used to solve the transport equation include Monte Carlo [54, 58], S_n [59], and integral transport methods [36, 51]. We will consider the lattice parameter ξ (disadvantage factor), f (thermal utilization), η (neutrons produced per neutron absorbed in the fuel), L^2 (thermal migration area) and reaction rates.

Let us characterize the scattering kernel by its transport cross section and M_2 (essentially the zeroth and second energy transfer moments of the kernel), and discuss the sensitivity of the lattice parameters to them for a typical lattice [51]. The lattice is composed of $\frac{1}{8}$ in uranium plates (1.25% enriched) in light water. Measurements and calculations of the disadvantage factors and average moderator velocity have been made as a function of water to uranium ratio W/U for this lattice. The slopes of the ξ curves are determined by the energy variation of the transport cross section; the level is determined by both the transport cross section and by M_2. In this example the ξ predicted by

Table 3. Effects of crystalline binding and nuclide concentration on thermal[a] cross sections

Moderator temperature, °K	300			1200			1200	
Carbon to ^{235}U ratio	4000			4000			∞	
Carbon to Pu ratio	∞			∞			2000	
Scattering Model	Crystal	Free gas	Heavy gas	Crystal	Free gas	Heavy gas	Crystal	Heavy gas
	σ (barns)	% Diff.	% Diff.	σ (barns)	% Diff.	% Diff.	σ (barns)	% Diff.
^{235}U Absorption	321	+14	+17	227	+ 1.0	+1.5	99.3	−8.7
^{239}Pu Absorption	940	−1.0	+1.7	1340	−0.22	+0.22	489	−8.8
^{240}Pu Absorption	1100	+11	+5	982	+0.11	+1.6	1940	+64
^{135}Xe Absorption	1540000	+7.4	+11	800000	+1.8	+2.0	187000	−22
^{149}Sm Absorption	41800	−3.6	+1.1	25300	+1.1	+0.75	6680	−22
$(1/v)^b$ Absorption	0.515	+11	+14	0.374	+0.86	+1.2	0.210	−6.4

a The cross sections are averaged over a group from zero to 2.38 eV.
b The $(1/v)$ represents a nuclide whose 2200 m/s absorption cross section is unity and varies inversely with velocity.

the hydrogen gas kernel is 5% lower at $W/U=4$ than predicted by the Nelkin kernel resulting in an 0.7% overestimate of f. The value of η depends mainly on M_2 and the W/U ratio. For these lattices, a 20% change in M_2 results in a 0.25% change in η at $W/U=1$, and a 0.6% change at $W/U=4$. Thus, the parameters η and f tend to be insensitive to the scattering kernel since they are ratios of reaction rates and the absorption and fission cross sections are nearly proportional to $1/v$. If resonance absorbers (i.e., plutonium) are used, the sensitivity will be considerably greater. Reaction rates and L^2 are more sensitive to the kernel than η and f. For the above example, a 20% change in M_2 would result in a 5.6% change in a $1/v$ reaction rate and L^2 at $W/U=1$, and a 2.8% change at $W/U=4$. These changes are significant for operating reactors since plutonium build-up and control worth are directly related to the above sensitivity to reaction rate and L^2 [60]. From H_2O, D_2O, and CH_2 lattice physics investigations it appears that better agreement between experiment and theory is generally obtained using bound atom scattering cross sections.

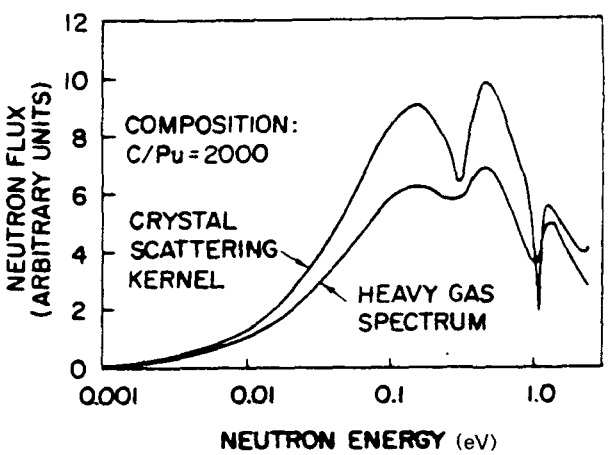

Figure 8. Thermal flux spectra in graphite at 1200°K

Crystalline moderators

The Wilkins heavy gas model [4], the free gas model [5], and the Parks kernel [13] for polycrystalline graphite have been extensively used in the calculation of thermal neutron spectra and reaction rates in graphite reactors. The use of the heavy gas model or the free gas model can lead to large uncertainties in reaction rates, power distributions, temperature coefficients, etc. For example, the value of M_2 predicted for a free gas of mass 12 is 2.809 as compared to an M_2 of 0.9784 predicted by the crystalline model. Figure 8 shows the spectrum predictions based on two physical models for a graphite-plutonium composition similar to that produced in a Calder Hall reactor. Table 3 shows the significant variations that one can expect to find between calculated average cross sections using both realistic (crystal) and non-realistic (free or heavy gas) scattering models. Suich [61] has shown for the BNL graphite research reactor that the Parks graphite kernel was found to yield the same η as a free gas of mass 21.4, while in order to predict f, a mass of 28.8 was needed. In addition, in order to predict $\frac{1}{\eta}\frac{d\eta}{dt}$, a mass of 32.4 was needed compared to a mass of 46.1 for $\frac{1}{f}\frac{df}{dt}$. Thus, typical calculations for the graphite lattices reported here are more sensitive to the approximations underlying the scattering kernel than are results for many water, heavy water and polyethylene lattices. Much less analysis has been done for representative Be and BeO moderated reactors but it is clear that in most cases, these systems should be somewhat less sensitive than graphite to the degree of physical exactness incorporated into the scattering kernel.

REFERENCES

1. U.S. Atomic Energy Comm. reports WASH-1044 and WASH-1047, AEC Nuclear Cross Sections Advisory Group Compilations.
2. Cohen, E. R., U.S. Atomic Energy Comm. report NAA-SR-1127 (1955); Coveyou, R. R., J. Nuclear Energy, *2*, 153 (1956).
3. Corngold, N., Annals of Physics, *6*, 368 (1959).
4. Wilkins, J. E., U.S. Atomic Energy Comm. report CP-2481 (1944).
5. Wigner, E. P., and Wilkins, J. E., U.S. Atomic Energy Comm. report AECD-2275 (1944).
6. Fermi, E., Ricerca Sci., VII, *2*, 13 (1936).
7. van Hove, L., Phys. Rev., *95* (1954).
8. Wick, G. C., Phys. Rev., *94*, 1228 (1954).
9. Placzek, G., Phys. Rev., *87*, 371 (1952).
10. Egelstaff, P. A., and Schofield, P., Nuclear Sci. Eng., *12*, 260 (1962).
11. Marshall, W., and Stuart, R., Proceedings of Symposium on Inelastic Scattering of Neutrons, IAEA, Vienna (1960).
12. Butler, D., Proc. Phys. Soc., *81*, 276 and 294 (1963).
13. Wikner, N. F., Joanou, G. D., and Parks, D. E., U.S. Atomic Energy Comm. report GA-4169 (1963).
14. Young, J. A., *et al.*, U.S. Atomic Energy Comm. report GA-4659 (1964).
15. van Hove, L., Phys. Rev., *93*, 1207 (1954).
16. Brockhouse, B. N., Proceedings of Symposium on Inelastic Scattering of Neutrons, IAEA, Vienna (1960).
17. Schmunk, R. E., Brugger, R. M., Randolph, P. D., and Strong, K. A., Phys. Rev., *128*, 562 (1962).
18. Young, J. A., Trans. American Nuclear Society (1963) and U.S. Atomic Energy Comm. report GA-4638 (1963).
19. Proceedings of the Symposium on Inelastic Scattering of Neutrons in Solids and Liquids, Chalk River, Canada (1962).
20. Yoshimori, A., and Kitano, Y., J. Phys. Soc. Japan, *11*, 352 (1956).
21. Woods, A. D. B., Brockhouse, B. N., Sakamoto, M., and Sinclair, R. N., Proceedings of Symposium on Inelastic Scattering of Neutrons, IAEA, Vienna (1960).
22. Nelkin, M. S., Phys. Rev., *110*, 741 (1960).
23. Maradudin, A. A., *et al.*, *Theory of Lattice Dynamics in the Harmonic Approximation*, edited by Seitz, F., and Turnbull, D. B. I., Academic Press Inc., New York (1963).
24. Beyster, J. R., *et al.*, U.S. Atomic Energy Comm. report GA-2544 (1961).
25. Poole, M. J., IAEA Symposium on Critical Experiments, Paper SM 42/18, Amsterdam (1963).
26. Sinclair, R. N., and Goode, P. D., U.K. Atomic Energy Authority report AERE PR/NP-5.
27. Parks, D. E., Beyster, J. R., and Wikner, N. F., Nuclear Sci. Eng., 13(4) (1962).
28. Bach, D. R., Bunch, S. I., Roessner, J. R., and Slovacek, R. E., Trans. American Nuclear Society, *3*, 490 (1960).
29. Bardes, R. G., Houghton, G. H., Parks, D. E., and Beyster, J. R., U.S. Atomic Energy Comm. report GA-4812 (1963).
30. Reinsch, V. L., and Springer, T., Z. Naturforsch., *16a*, 112–116 (1961).
31. Barclay, F. R., Coates, M. S., *et al.*, Proc. BNL Conference on Neutron Scattering, *2*, 359 (1962).
32. Campbell, C., Proceedings of the Second International Conference on the Peaceful Uses of Atomic Energy, P/10, Vol. 16, p. 233, United Nations (1958).
33. Mostovoi, V. I., Proc. BNL Conference on Neutron Scattering, *2*, 411 (1962).
34. Johansson, E., Jonsson, E., *et al.*, Aktiebolaget Atomenergi, AE-123 (1963).
35. Honeck, H. C., and Takahashi, Nuclear Sci. Eng., *15*, 115 (1963).
36. U.S. Atomic Energy Comm. report BNL-719, Vols. 3 and 4 (1962), Proc. BNL Thermalization Conference.
37. Hall, R. S., *et al.*, Proc. Phys. Soc., *79*, 257 (1962).
38. Kuchle, M., Nukleonik, *2*, 131 (1960).
39. Corngold, N., Michael, P., and Wollman, W., Nuclear Sci. Eng., *15*, 13 (1963).
40. Koppel, J. U., *ibid.*, *16*, 101 (1963).
41. Ohanian, M., and Daitch, P., *ibid.* (to be published).
42. Corngold, N., and Michael, P., *ibid.* (to be published).
43. Corngold, N., and Shapiro, C., unpublished manuscript.
44. Maiorov, L., U.S. Atomic Energy Comm. report BNL-719, p. 1375 (1962) Proc. BNL Thermalization Conference.
45. Koppel, J. U., *ibid.*, p. 1012.
46. Bennett, R. A., *ibid.*, p. 838.
47. Feiner, F., *et al.*, *ibid.*, p. 900.
48. Beckurts, K. H., Nucl. Instr. and Meth., *11*, 144 (1961).
49. Garelis, E., and Russell, J. L., Nuclear Sci. Eng., *16*, 263–270 (1963).
50. Slovacek, R., *et al.*, Trans. American Nuclear Society, *6*, 298 (1963).
51. Honeck, H. C., *A Review of the Methods for Computing Thermal Neutron Spectra*, U.S. Atomic Energy Comm. report BNL-821 (1963).
52. Gelbard, E., IAEA Symposium on Critical Experiments, Amsterdam (1963).
53. Leslie, D. C., U.S. Atomic Energy Comm. report BNL-719, Vol. 2, p. 592 (1962), Proc. BNL Thermalization Conference.
54. Brown, H. D., J. Nuclear Energy, *8*, 177 (1959).
55. Honeck, H. C., Trans. American Nuclear Society, *5*, 47 (1962).
56. Goldman, D. T., and Federighi, Nuclear Sci. Eng., *16*, 165 (1963).
57. Brown, H. D., and St. John, D., U.S. Atomic Energy Comm. report DP-33 (1954).
58. Pfeiffer, R., and Stone, W., U.S. Atomic Energy Comm. report KAPL-M-RPG-1 (1962).
59. Hinman, G. W., U.S. Atomic Energy Comm. report GAMD-3425 (1962).
60. Peterson, G. T., Aline, P., and McWhorter, R. J., IAEA Symposium on Critical Experiments, Amsterdam (1963).
61. Suich, J., Nuclear Sci. Eng. (in the press).

ABSTRACT—RÉSUMÉ—АННОТАЦИЯ—RESUMEN

A/258 Etats-Unis d'Amérique

Thermalisation des neutrons et applications aux réacteurs

par J. R. Beyster et *al.*

La description physique de la thermalisation et du transport des neutrons au-dessous de quelques électron-volts est très importante pour la conception des réacteurs thermiques avancés. Cette description, exprimée en sections efficaces de diffusion aux basses énergies, peut être combinée avec les données voulues concernant les sections efficaces de fission, d'absorption et de transport rapide pour le calcul des spectres de neutrons des réacteurs et de leur performance. Les nombreuses méthodes numériques spéciales qui existent actuellement dans ce but permettent de calculer d'une manière assez précise les paramètres d'un réacteur, à condition que les sections efficaces fondamentales soient connues. Cependant, ce n'est qu'au cours des dernières années que le traitement des sections efficaces de diffusion des neutrons aux basses énergies (thermalisation) a pu être entrepris de façon autre qu'élémentaire, cela à cause des complications introduites par la structure du réseau modérateur et les liaisons chimiques.

On a entrepris aux Etats-Unis d'importantes études pour obtenir des matrices de diffusion d'une précision suffisante pour les modérateurs habituels H_2O, D_2O, $(CH_2)_n$, C_6H_6, C, Be et ZrH_x. La procédure utilisée a consisté à lier le modèle théorique de diffusion aux propriétés physiques et chimiques connues du modérateur, c'est-à-dire variation de la chaleur spécifique en fonction de la température, spectres de fréquences de vibration et de rotation, constantes élastiques, relations de dispersion, sections efficaces totales pour les neutrons, etc. Un autre procédé consistait à utiliser les valeurs expérimentales de $S(\alpha,\beta)$ pour en déduire la distribution en fréquence des phonons. L'utilisation directe de $S(\alpha,\beta)$ dans les calculs des réacteurs n'est pas possible faute de données expérimentales dans tout le domaine des variables α,β et de la température.

On a étudié expérimentalement la validité et les limites des matrices théoriques de diffusion pour ces modérateurs, en mesurant les spectres à l'état stationnaire, les distributions de flux dans l'espace et le comportement en fonction du temps dans les conditions expérimentales applicables à l'analyse des réacteurs. La vérification des matrices théoriques de diffusion représente pour l'analyse des réacteurs un travail considérable car il faut mesurer les spectres thermiques et d'autres paramètres des réacteurs dans un domaine étendu de températures ($<60°K$ à $>1\,000°K$), d'absorption et de flux spatiaux. L'étude des spectres de neutrons dans des géométries « propres » s'approchant d'un milieu infini constitue l'une des vérifications les plus simples et les plus convenables des matrices de diffusion. De nombreuses études de ce genre ont été faites aux Etats-Unis aux températures ambiantes pour les modérateurs habituels. On a démontré que les matrices de diffusion fondées sur la connaissance de la structure moléculaire ou cristalline de ces modérateurs permettent de prédire les spectres de neutrons avec une précision très supérieure à celle que l'on obtenait avec les descriptions de la diffusion d'atomes libres ou avec d'autres méthodes arbitraires. On a fait un grand nombre d'expériences avec des spectres en fonction de la température, et, là encore, les descriptions plus précises de la diffusion commencent à fournir la précision qu'exige actuellement l'analyse des réacteurs. De plus, ces mesures, qui établissent en fait la validité de la composante isotrope inélastique de la matrice de diffusion, servent de base pour améliorer encore le modèle et ajuster les modèles de diffusion.

Les spectres de flux angulaires (spectres en milieux finis) ont été particulièrement difficiles à étudier expérimentalement sans ambiguïté. Ces mesures fournissent une vérification importante des composantes isotrope et anisotrope de la matrice de diffusion. Les résultats expérimentaux mettent en évidence quelques divergences notables dans la théorie, dans les conditions limites analogues à celles des réseaux de réacteur réels. D'autres études expérimentales ayant pour but de vérifier les matrices de diffusion thermique du point de vue de la conception du réacteur comprennent la mesure de la longueur de diffusion thermique par des méthodes d'absorption pulsées ou continues, les distributions de flux thermique aux discontinuités d'espace et de température, et les études de spectres en fonction du temps.

Des méthodes numériques généralement applicables au calcul des matrices de diffusion thermique sont élaborées aux Etats-Unis et vérifiées par les méthodes expérimentales décrites ci-dessus. Ces méthodes souples sont conçues de manière à tenir compte des besoins particuliers des utilisateurs; par exemple, le choix du modérateur, la maille d'énergie, la température du modérateur et la structure cristalline.

A/258 США

Термализация нейтронов и применение реакторов

Дж. Р. Бейстер *et al.*

При расчетах усовершенствованных реакторов на тепловых нейтронах очень важным является физическое описание замедления и переноса нейтронов ниже нескольких электронвольт. Это описание, выраженное через сечения рассеяния нейтронов низких энергий, для расчета спектров нейтронов в реакторах и реактив-

ных характеристик может быть скомбинировано с необходимыми данными о сечениях деления, поглощения и переноса быстрых нейтронов. Если исходные данные о сечениях известны, то с помощью целого ряда разработанных в настоящее время численных методов можно внести в расчетные параметры реактора довольно существенные уточнения. Однако учет рассеяния нейтронов низких энергий (термализация) лишь в последние годы стал производиться не самым элементарным образом, а более строго, так как до последнего времени сложность учета кристаллического строения замедлителя и химической связи не могла быть преодолена.

В Соединенных Штатах был выполнен ряд работ по определению с необходимой точностью ядер интегралов, описывающих рассеяние нейтронов для обычных замедлителей — H_2O, D_2O, $(CH_2)_n$, C_6H_6, C, Be и ZrH_x. Процедура их определения заключалась в установлении соответствия теоретической модели рассеяния и известных физических и химических свойств замедлителя, то есть температурной зависимости теплоемкости спектрам частот колебаний и вращений постоянным упругости, дисперсионным соотношениям, полным нейтронным сечениям и т. д. Другой способ состоял в определении спектра собственных колебаний из экспериментально определенного закона рассеяния $S(\alpha, \beta)$. Прямое приложение закона рассеяния $S(\alpha, \beta)$ к реакторным расчетам было невыполнимым, так как не было экспериментальных данных по всему диапазону величин переменных α, β и температуры.

Степень точности теоретических ядер интегральных членов, описывающих рассеяние, была изучена путем сравнения с результатами измерений установившихся спектров, пространственных распределений, нейтронного потока и его временного поведения для указанных выше замедлителей. Опыты велись в условиях, допускающих расчет с помощью обычных реакторных методов. С точки зрения реакторной физики получение подтверждения теоретических данных о рассеянии тепловых нейтронов представляется довольно сложным, так как спектры тепловых нейтронов и другие параметры реакторов должны быть измерены в широких диапазонах изменения температуры (от < 60 до $> 1000°$ K) поглощения и пространственных распределений нейтронного потока. Исследование нейтронных потоков в несложных геометрических формах в условиях, приближающихся к условиям бесконечной среды, является одним из самых простых и подходящих методов проверки теоретических законов рассеяния.

В Соединенных Штатах эти исследования выполнены при обычных температурах для обычных замедлителей. Показано, что теоретические законы рассеяния, построенные на представлениях о молекулярной или кристаллической структуре замедлителей, дают реакторщику-расчетчику возможность предсказывать спектры нейтронов с гораздо большей точностью, чем это было возможно ранее при использовании модели свободных атомов или различных других нестрогих рецептов. Было проведено много опытов по изучению зависимости спектров от температуры и было опять показано, что для обеспечения нужной для расчетов современных реакторов точности необходимо хорошее знание законов рассеяния. Кроме того, эти измерения, позволяющие проверить точность описания лишь изотропных компонентов неупругого рассеяния, служат основанием для дальнейшего усовершенствования моделей.

Точные измерения угловых распределений нейтронных потоков (спектры в конечных средах) особенно трудны. Однако эти измерения дают возможность проверить как изотропные, так и анизотропные компоненты рассеяния. Опытные данные указывают на существенную неточность теории, использующей граничные условия, подобные тем, которые используются при расчетах реакторных решеток. Другие экспериментальные исследования, которые предназначены для проверки точности законов рассеяния тепловых нейтронов с точки зрения проектирования реакторов, заключались в следующем: измерение длин диффузии тепловых нейтронов с помощью импульсной техники или методом непрерывного поглощения; распределение тепловых потоков в окрестностях разрывов пространственной или температурной непрерывности и изучение спектров во времени.

В Соединенных Штатах разрабатываются и проверяются экспериментально указанными выше способами численные методы расчета законов рассеяния, предназначенные для широкого использования. Эти методы построены так, чтобы предусмотреть различные возможности, которые могут понадобиться проектантам, как, например, выбор замедлителя, распределение энергетических групп, температура замедлителя и его кристаллическая структура.

A/258 Estados Unidos de América

Termalización de neutrones y aplicación a la física de reactores

por J. R. Beyster *et al.*

La descripción física de la termalización y transporte de neutrones con energías de unos pocos electrón-voltios es muy importante en diseños previos de reactores térmicos. Esta descripción, expresada en función de secciones eficaces de dispersión de baja energía, puede combinarse con los datos necesarios de fisión, absorción y sección eficaz de transporte de

neutrones rápidos para calcular rendimientos y espectros de neutrones de reactores. Los diversos métodos numéricos especiales, de los que se dispone actualmente para efectuar esta labor, permiten incorporar simplificaciones relativamente grandes en los cálculos de parámetros que intervienen en el proyecto del reactor con tal que sean conocidos los datos básicos de secciones eficaces. No obstante, únicamente en los últimos años se ha considerado el tratamiento de secciones eficaces de dispersión de neutrones de baja energía (termalización) de una manera no elemental a causa de las complicaciones introducidas por la estructura reticular y la ligadura química del moderador.

En los Estados Unidos se han realizado trabajos prolongados para desarrollar núcleos de dispersión de la exactitud requerida para los moderadores usuales, H_2O, D_2O, $(CH_2)_n$, C_6H_6, C, Be y ZrH_x, empleados en los reactores. El procedimiento empleado ha sido relacionar el modelo teórico de dispersión con las propiedades físicas y químicas conocidas del moderador; es decir, variación del calor específico con la temperatura, espectros de frecuencias de vibración y de rotación, constantes elásticas, relaciones de dispersión, secciones eficaces totales de neutrones, etc. Otro método consiste en emplear $S(\alpha,\beta)$, determinada experimentalmente, para deducir una distribución de frecuencias de fonones. No ha resultado práctico emplear directamente $S(\alpha,\beta)$ en cálculos de reactores debido a que los datos experimentales no están disponibles para la totalidad de valores de las variables α,β y temperatura. La adecuación y las limitaciones de los núcleos teóricos de dispersión han sido estudiadas experimentalmente para los moderadores antes citados mediante medidas de espectros estacionarios, distribuciones espaciales de flujo y comportamiento del mismo en función del tiempo bajo condiciones experimentales pertinentes para el análisis de reactores. La comprobación de los núcleos teóricos de dispersión, desde el punto de vista del analista de reactores, representa una empresa bastante ardua puesto que los espectros térmicos y otros parámetros deben ser medidos para comparaciones teóricas sobre una amplia zona de temperaturas (menores de 60 °K hasta mayores de 1 000 °K), absorción y flujos espaciales. Una investigación de espectros de neutrones en geometrías limpias, próximas a las de un medio infinito, constituye una de las pruebas más sencillas y más apropiadas de núcleos de dispersión térmica. En los Estados Unidos estos estudios se han realizado en gran escala a temperatura ambiente para los moderadores corrientes empleados en los reactores. Se ha demostrado que los núcleos de dispersión basados en un conocimiento de la estructura molecular o cristalina de los moderadores precitados, permiten al analista de reactores predecir espectros de neutrones con una precisión mucho mayor que la que es posible con las descripciones anteriores de la dispersión por átomos libres o diversas reglas arbitrarias. Se han realizado muchas medidas de espectros en función de la temperatura y, por otra parte, las descripciones de la dispersión más realistas han empezado a proporcionar la precisión requerida por los análisis actuales de reactores. Además, estas medidas, que establecen esencialmente la validez de la componente inelástica isotrópica del núcleo de dispersión, sirven de base para perfeccionamientos y ajustes adicionales de los modelos de dispersión.

Ha sido extremadamente difícil estudiar experimentalmente y sin ambigüedad el flujo espectral angular (espectros en medios finitos). Estas medidas dan una prueba importante lo mismo de las componentes isotrópicas que de las anisotrópicas del núcleo de dispersión. Los resultados experimentales muestran algunas discrepancias significativas con la teoría bajo condiciones de contorno parecidas a las de los reticulados existentes en el reactor. Otras investigaciones experimentales que sirven para probar núcleos de dispersión térmica desde el punto de vista de diseño del reactor, son las medidas de longitudes de difusión térmica mediante técnicas pulsadas o continuas de absorción, distribuciones de flujo térmico en discontinuidades de espacio y de temperatura y estudios espectrales en función del tiempo.

En los Estados Unidos se han desarrollado técnicas numéricas aplicables, en general, al cálculo de núcleos de dispersión térmica y que se han probado mediante los métodos experimentales mencionados. Estos métodos flexibles son proyectados para incorporar muchas provisiones exigidas por los usuarios; por ejemplo, la elección del moderador, su temperatura, reticulado de energía y estructura cristalina.

Developments in neutron transport theory

By G. I. Bell, B. G. Carlson and K. D. Lathrop*

NEW APPROACHES TO NEUTRON TRANSPORT THEORY

Neutron Transport Theory conventionally starts from the linear Boltzmann equation or the associated integral equations for the expected neutron flux. We shall begin, however, by summarizing some recent theoretical efforts which broaden the base of neutron transport theory by taking different starting points.

Most fundamental has been the work of Osborn and Yip [1] in attempting to derive a neutron transport theory from the principles of quantum mechanics. Starting from the quantum mechanical Liouville equation for the density matrix, they have used the coarse grained phase space of Ono [2], together with the formalism of quantum field theory for treating the variable number of particles. After some approximations (of somewhat uncertain significance) a Boltzmann equation is derived for a singlet neutron density. Quantum mechanical neutron-nucleus interaction terms are present and these are shown to reduce to the description in terms of conventional cross sections for several cases. The procedure is not limited to the expected value or singlet neutron distribution function, but equations for the time development of higher order distribution functions are derived and transport fluctuation problems may thus be formulated.

Less ambitious is work [3] on a stochastic generalization of the Boltzmann equation. Consider as a simple example, one velocity neutron multiplication in a medium with isotropic scattering. Let $p_n(\vec{x},\vec{\Omega},t;\, R,t_f)$ be the probability that a neutron at $\vec{x}$, with direction $\vec{\Omega}$, at time t will lead to exactly n neutrons in the region R of $(\vec{x},\vec{\Omega})$ space at time t_f. Then the probability generating function

$$G(z,\vec{x},\vec{\Omega}t;R,t_f)\equiv 1-\Gamma=\sum_{n=o}^{\infty} p_n z^n \qquad (1)$$

will satisfy a non-linear integro-differential equation [3,4].

$$\vec{\Omega}.\mathrm{grad}_x\Gamma+\frac{1}{v}\frac{\partial\Gamma}{\mathrm{d}t}=\sigma\Gamma-c\sigma\int\Gamma\frac{\mathrm{d}\vec{\Omega}}{4\pi}+\sum_{j=2}^{J}(-1)^j\frac{\chi_j\sigma}{j!}\left[\Gamma\frac{\mathrm{d}\vec{\Omega}}{4\pi}\right]^j \qquad (2)$$

where $\sigma(\vec{x})$ is the total cross section, $c(\vec{x})$ the mean number of emerging neutrons per collision, $\chi_2/2!$ the mean number of neutron pairs, $\chi_3/3!$ the mean number of triplets, etc. This equation is to be solved backwards in time from the final condition (at $t=t_f$) $\Gamma=1-z$ if $(\vec{x},\vec{\Omega})\in R$, $\Gamma=0$ otherwise, and subject to boundary conditions of zero outgoing Γ.

Equations for the moments of the probability distribution can be obtained by differentiating Eq. (2) with respect to z and then setting $z=1$. Direct solutions are also possible and we note some general properties of Γ. For Γ small, the linearized Eq. (2) is just the adjoint to the Boltzmann equation for the neutron density, and this result holds for the energy dependent problem. (The first moment of the distribution satisfies the same equation.) Note that for R suitably small (and t_f-t bounded), Γ is approximately $1-z)p_1$, which is small.

For a supercritical system, Eq. (2) will have time independent solutions with Γ equal to the probability of obtaining a persisting chain reaction from the initial neutron. We have found such solutions for the energy dependent problem with S_n techniques. The non-linear terms in Eq. (2) appear as absorptions.

This method is readily generalized to allow for more general final states, energy dependence, delayed neutrons, and sources. One may thus study a variety of correlation-fluctuation problems.

Finally we refer to the method of invariant imbedding which has been formulated by Bellman, Kalaba and Wing for neutron transport problems [5].

The method amounts to a systematic use of invariance principles similar to those introduced by Ambarzumian and so effectively employed by Chandrasekhar in radiative transfer. One considers not merely, for example, a slab with a particular thickness of interest, but a whole class of slabs with different thicknesses in which the particular slab problem is *imbedded*, and one asks how the emergent neutron flux changes as the thickness is varied. In this manner one formulates non-linear integrodifferential equations for the emergent flux, say, involving derivatives with respect to the variable dimension. These equations are, however, subject to conditions at only a single boundary (dimension $=0$) as contrasted with the conventional Boltzmann approach which involves conditions at two boundaries. Thus one can solve starting at the single boundary. On the other hand, the equations are non-linear and they do not readily give fluxes at interior points.

* Los Alamos Scientific Laboratory, Los Alamos, New Mexico.

We are not aware of applications of invariant imbedding *per se* to any realistic neutron transport problems. On the other hand, systematic use has been made of invariance principles, in analytical work by Mullikin [6], as well as in numerical work, for example in [7]. Also, such methods are not restricted to expected value problems.

ANALYSIS OF THE LINEAR BOLTZMANN EQUATION

Mathematical analysis of the linear Boltzmann equation and associated integral equations is of fundamental importance in neutron transport theory. We summarize significant progress in three areas.

Spectrum of the Time Dependent Boltzmann Operator

Consider the time-dependent Boltzmann equation for the expected neutron flux, $\psi(\vec{x},\vec{v},t)$: $d\psi/dt = B\psi$ where B is of the form:

$$B\psi = -\vec{\Omega}.\nabla\psi - \sigma(\vec{x},\vec{v})\psi + \int K(\vec{x},\vec{v},\vec{v}')\,\psi(\vec{x},\vec{v}',t)\,d\vec{v}' \quad (3)$$

and ψ satisfies boundary conditions of no neutrons coming into the region of interest. The spectrum of the operator B has been analyzed for several cases and in particular the eigenvalues λ_i, for which $\lambda_i\psi_i = B\psi_i$ have been sought. For physical operators, K, it has been generally assumed that there exists at least one eigenvalue and that the eigenvalue of largest real part, λ_0, will have an everywhere non-negative eigenfunction, ψ_0, which the solutions will approach at late times for rather general initial conditions on ψ. The existence of an infinite number of such eigenvalues and a complete set of eigenfunctions has been frequently postulated [8] but never proved.

Wing and Lehner, however, showed [9, 10] that this postulate does not hold for the one velocity problem in slab geometry. They proved that the point spectrum of B is a non-empty *finite* set of real numbers, having $\lambda_i > -\sigma v$. In addition B has a continuous spectrum consisting of all λ for which $Re(\lambda) < -\sigma v$. These results were extended by Pimbley [11] to the multigroup problem in slab geometry with the added assumption that the matrix of transfer cross sections must be symmetrizable by a diagonal matrix. This assumption should be satisfied for thermalization kernels, but not for criticality problems.

For bounded geometries, and neutron velocities > 0, it has been proved by Jörgens [12] that B has at least one eigenvalue provided that K is positive for all $\vec{x}$, $\vec{v}$, and $\vec{v}'$, in suitable sub-regions of $\vec{x}$, $\vec{v}$ space. This condition should be satisfied for both criticality and thermalization problems. Jörgens also derived an asymptotic expansion for ψ at late times which, while slightly more general than a simple exponential dependence on time, is not inconsistent with the simple behaviour.

Nelkin [13], discussing the limit as neutron velocities approach zero, has conjectured that there may exist no eigenvalues for sufficiently small bounded regions. For the one-velocity problem in a sphere, Van Norton [14] has found that B has a countable infinity of real eigenvalues accumulating at $-\infty$; however he did not prove anything regarding completeness of the eigenfunctions.

We thus conclude that a dominant eigenvalue, λ_0, of the Boltzmann operator generally seems to exist while a complete set of discrete eigenfunctions does not exist for slab geometry and may not exist for bounded geometry.

Methods using singular integral equations

In recent years, new methods for the exact solution of simple neutron transport problems have been developed using the theory of singular integral equations [15]. Consider, for example, the monoenergetic Boltzmann equation in a plane, infinite, isotropically scattering medium

$$\mu\frac{\partial\psi}{\partial x} + \psi = \frac{1}{2}c\int_{-1}^{1}\psi(x,\mu')d\mu' \quad (4)$$

A solution may be written in terms of two familiar [8] discrete eigenfunctions

$$\psi_{0\pm}(x,\mu) = \frac{1}{2}c\nu_0 e^{\mp x/\nu_0}/(\nu_0 \mp \mu)\;1 - c\nu_0\tanh^{-1}(1/\nu_0) = 0 \quad (5)$$

and, in addition the singular eigenfunctions

$$\psi_\nu(x,\mu) = e^{-x/\nu}\left[\lambda(\nu)\delta(\mu-\nu) + \frac{1}{2}c\nu P\left(\frac{1}{\nu-\mu}\right)\right]\lambda(\nu) = 1 - c\nu\tanh^{-1}\nu \quad (6)$$

with ν real and $-1 \leq \nu \leq 1$. As originally noted by Van Kampen [16], such singular eigenfunctions can be interpreted as distributions in the sense of L. Schwartz, all physical observables involving integrals over the singular eigenfunctions. Case [17] first postulated that a general solution to Eq. (4) may be written as

$$\psi(x,\mu) = a_{0+}\psi_{0+}(x,\mu) + a_{0-}\psi_{0-}(x,\mu) + \int_{-1}^{1}A(\nu)\psi_\nu(x,\mu)d\nu \quad (7)$$

with the expansion coefficients $a_{0\pm}$ and $A(\nu)$ to be determined by boundary or other conditions on $\psi(x,\mu)$. Using the theory of singular integral equations [15], he showed that, for suitable ψ, solutions for $A(\nu)$ exist and are unique. Hence the eigenfunctions are called complete. Case also proved orthogonality relations for determining expansion coefficients and gave partial range completeness theorems (useful for boundary conditions for, say, $\mu < 0$) thereby establishing all the necessary machinery for eigenfunction expansion solutions. The application of the machinery leads easily to angular Green's functions for homogeneous infinite and half-space media and solutions of the plane albedo and Milne problems [17]. In these cases the expansion coefficients, $A(\nu)$, can be found in closed form. An independent treatment for $c = 1$ was

given at about the same time by Van Kampen [18], and the singular eigenfunctions were also developed by Wigner [19]. They were recognized but not used by Davison in Ref. [8], page 268.

Extensions of the eigenfunction expansion technique have been numerous. The criticality problem for a finite slab was formulated by Mitsis[20] and Zelazny [21]. In this problem $A(\nu)$ cannot be found in closed form but the singular integral equation determining A may be reduced, by standard methods [15] to an inhomogeneous Fredholm equation which can be solved by iteration. Mitsis found that the zeroth order iterate, corresponding to the contributions from the discrete eigenfunctions, gave the diffusion theory result for the critical thickness, $t_0 = \pi|\nu_0| - 2\ z_0$, where z_0 is the Milne problem extrapolation distance. As is seen below, the first correction term is unimportant except for thin slabs.

Table 1. Slab critical thicknesses (mean free path) [20]

c	1.01	1.10	1.30	1.60	2.00
t^a (zeroth approx.)	16.69	4.24	1.878[a]	1.030	0.634
t_1 (first approx.)	16.69	4.24	1.875[a]	1.022	0.621

[a] Different numbers, which are in error, appeared here in Ref. [20]. Results by Leonard (private communication) have been substituted.

Mika, *et al.* [22,23], extended the method to include anisotropic scattering (as represented by finite Legendre polynomial expansions) in monoenergetic, plane geometry problems. In such problems the analysis is complicated only by the possibility of additional discrete eigenvalues, some of which, for particular values of scattering parameters, may even be imbedded in the continuum, corresponding to the physically unlikely situation of diffusion lengths shorter than a mean free path. An interesting question is whether the possible extra eigenvalues are physically meaningful or whether they are introduced by finite polynomial expansions.

In energy dependent problems, extensions of the method to two group and multigroup models for isotropically scattering plane media have been made by Zelazny and Kuznell [24,25]. Again, additional discrete eigenvalues are possible; and, if the total cross section is not constant, the continuum is more complicated (for the g^{th} group, singularities are due to $\sigma_g\nu - \mu$ terms). Continuous energy dependence has been considered in the time-dependent infinite medium thermalization problem analyzed by Corngold [26] and Koppel [27] and in steady-state space and energy dependent problems studied by Ferziger and Leonard [28,29]. In the latter problems, if the total cross section is constant in energy and a symmetrizable energy transfer kernel is expanded in terms of energy eigenfunctions, Eq. (4) is obtained with c modified by the j^{th} energy eigenvalue for ψ corresponding to the coefficient of the j^{th} energy eigenfunction [28]. For energy dependent cross sections, results are also possible [29,30]. For example, in the case of the heavy gas model in a $1/v$ absorbing infinite medium, diffusion theory is found to predict accurate diffusion lengths only for small absorption *and* only for the first energy mode. The implication is that, in energy dependent problems, asymptotic reactor theory is possibly less accurate and the use of an extrapolation distance less meaningful than in monoenergetic problems [29].

Mitsis [31] in an attempt to extend methods using eigenfunction expansion to general geometries, found elementary solutions (in the form of Eqs. (5) and (6)) of the three-dimensional integro-differential transport equation and formed a general solution by superposition of elementary solutions. Although the superposition solution, subjected to the applicable symmetries, yielded the neutron distribution in spherical and infinite cylindrical geometry, no completeness could be shown primarily because superposition destroys the singular nature of the elementary solutions so useful in plane geometry. In addition, no general procedure for finding the expansion coefficients was determined, and the approach failed to produce those solutions singular at the origin in curved geometries [31]. In one dimensional geometries these difficulties were overcome by a new approach developed by Leonard and Mullikin [32,33] and extended by Mitsis [31]. By defining a suitable transform pair a singular integral equation for the neutron density is obtained directly and there is no need to prove the existence of a complete set of eigenfunctions. To illustrate, consider Eq. (4) for a slab of width $2b$ with $\psi(b,-\mu) = \psi(-b,\mu) = 0\ (\mu > 0)$. With the neutron density defined as

$$\rho(x) = \int_{-1}^{1} \psi(x,\mu)\mathrm{d}\mu = \int_{0}^{1} [\psi(x,\mu) + \psi(x,-\mu)]\mathrm{d}\mu \qquad (8)$$

integration of Eq. (4) gives $(\mu > 0)$

$$\psi(x,\mu) = \frac{c}{2\mu}\int_{-b}^{x} \rho(y) e^{-(x-y)/\mu}\mathrm{d}y,$$

$$\psi(x,-\mu) = \frac{c}{2\mu}\int_{x}^{b} \rho(y) e^{-(y-x)/\mu}\,\mathrm{d}y. \qquad (9)$$

Eqs. (8) and (9) form a transform pair including boundary conditions. Inserting (8) in (9) and integrating over y gives a non-singular integral equation $(\mu > 0)$:

$$\psi(x,\mu) = \frac{c}{2}\int_{-1}^{1} \frac{\nu\psi(x,\nu) - \mu\psi(x,\mu)}{\nu - \mu}\,\mathrm{d}\nu$$

$$+ \frac{c}{2}\int_{0}^{1} \frac{\mu\psi(x,\mu) + \nu\psi(x,-\nu) - \nu e^{-(b+x)/\mu}\psi(b,\nu)}{\nu + \mu}\,\mathrm{d}\nu \qquad (10)$$

which can be written as a singular integral equation by collecting terms involving $\psi(x,\mu)$:

$$\lambda(\mu)\psi(x,\mu) = \frac{c}{2}P\int_{-1}^{1} \frac{\nu\psi(x,\nu)\mathrm{d}\nu}{\nu - \mu}$$

$$- \frac{c}{2}e^{-(b+x)/\mu}\int_{0}^{1} \frac{\nu\psi(b,\nu)\mathrm{d}\nu}{\nu + \mu} \quad \mu > 0 \qquad (11)$$

For $x=b$ Eq. (11) is an equation for $\psi(b,\mu)$ adjoint in the singular part to the expansion coefficient equation obtained by the method of Case [31,32]. Once $\psi(b,\mu)$ is known, $\psi(x,\mu)$ is determined by Eq. (11), and, in addition, there is a side condition, the criticality equation, obtained by demanding that the right hand side vanish at those $\mu=\nu_0$ for which $\lambda(\nu_0)=0$. The above treatment is easily extended to spherical geometry since $r\rho(r)$ (with, however, $r\rho(r)$ an odd function) satisfies the same equation as $\rho(x)$ [8]. Mitsis also showed that, in spherical geometry, a pseudo-distribution, $\phi(r,\mu)$,

$$1/r\int_{-1}^{1}\phi(r,\mu)\mathrm{d}\mu=\int_{-1}^{1}\psi(r,\mu)\mathrm{d}\mu \qquad (12)$$

satisfies Eq. (4) while in infinite cylindrical geometry a similar pseudo density transform satisfies an equation that also is amenable to eigenfunction expansion analysis [31].

In addition to the lack of geometric generality, the methods discussed above are restricted by the variation of the eigenvalue spectrum from problem to problem. For example, for the case of $1/r$ cross section dependence in spherical geometry, Aamodt [34] reports an infinite set of discrete eigenvalues and no continuum. Nevertheless, the methods of singular integral equations have significantly broadened the class of transport problems which can be solved exactly. The utility of the exact solutions for complex practical calculations is questionable, but solutions of simple problems are particularly valuable as calibration standards for approximate solutions, both analytic and numerical.

Variational methods

Variational methods for estimating eigenvalues of the Boltzmann operator [8], or flux weighted averages [8,35] are familiar in neutron transport theory. Because the general Boltzmann operator is nonself-adjoint, such variational expressions involve integrals of bilinear combinations of the neutron flux and its adjoint. Moreover the functionals are not upper or lower bounds to the exact results. Thus to obtain *reliable* eigenvalues from variational methods one must use rather good trial functions for flux and adjoint.

Of course, in some special cases (one velocity theory with isotropic scattering [8], or thermalization in an infinite medium, to mention two examples) the equations may be rendered self-adjoint and extremum principles may be used. Mowery and Murray [36], however, have suggested that even for self-adjoint problems, there are advantages to be gained by not using the same flux trial function everywhere in the functional but in using two independent trial functions as in a nonself-adjoint problem.

Some new approaches to transport problems have used a variational functional as a Lagrangian. Thus, if we formally consider equations for the flux ψ and its adjoint ψ^*, $H\psi=f$ and $H^*\psi^*=g^*$, the functional

$$F(\psi^*\psi)=(g^*,\psi)+(\psi^*,f)-(\psi^*,H\psi) \qquad (13)$$

may be interpreted as a Lagrangian of the system. If the functional F is stationary for small independent variations of ψ and ψ^*, then $H\psi=f$ and $H^*\psi^*=g$ must be satisfied. If approximate trial functions are used in the Lagrangian, then by requiring the functional to be stationary, we may derive equations for the trial functions. Selengut [37] developed this method and applied it to such problems as the reduction of two-dimensional diffusion problems to coupled one-dimensional problems and the derivation of multigroup constants which are weighted by both flux and adjoint.

An interesting application of the Lagrangian method to the one-velocity Boltzmann equation in plane geometry, including boundary terms and weight functions in the functional, has been made by Pomraning and Clark [38]. To obtain a self-adjoint operator for the problem, they have considered the equation obtained by differentiating the Boltzmann equation with respect to space. It is shown that the corresponding Lagrangian leads to an independence of even and odd (in angle) parts of the flux, and thus to a failure of neutron conservation. By using the self-adjoint formulation for only the even (or odd) part and the original Boltzmann equation for the other part, the nonself-adjointness is separated from the Boltzmann equation. However, an extremum variational principle is still not obtained for $c>1$.

Variational calculations for flux weighted averages usually have errors of second order in trial function errors. Kostin [39] has developed methods with higher order errors. If, for example, we seek the weighted average, $W=(w,\psi)$, where $H\psi=f$, then introducing the exact Green's operator $G=H^{-1}$ and n approximate operators $G_i=G-\delta G_i$, the functional

$$W_n=(w,G[I-\prod_{i=1}^{n}(I-HG_i)]f) \qquad (14)$$

has an error proportional to $\prod_{i=1}^{n}\delta G_i$. The exact G is not required for evaluating W_n. W_2 equals our previous functional, Eq. (13), if we identify $w=g^+$, $G_1{}^+g^+=\psi^+$, and $G_2f=\psi$. Kostin has considered further generalizations and their relation to previous variational methods.

We thus see that variational methods have continued to provide an orderly approach to the approximate solution of many problems in neutron transport theory.

NUMERICAL METHODS

The main methods for numerically solving the transport equation are based on two well-known traditions in neutron transport theory: "discrete ordinates" and "spherical harmonics", traditions which had their beginnings about twenty years ago. Davison and Sykes [8] discuss the initial work in these fields and give the main analytic results of this and subsequent efforts.

Discrete ordinates and the S_n method

According to the first tradition the neutron flux $\psi = \psi(\vec{R},t,\vec{\Omega},v)$ is given a discrete representation $\psi_m(\vec{R},t,v)$, $m = 1,2,\ldots,M$, with respect to the variable $\vec{\Omega}$. In other words the neutrons are divided among a finite number of beams (discrete rays) having intensities ψ_m in the directions $\vec{\Omega}_m$ and corresponding weights w_m. The discrete theory may then be stated in terms of neutron balance equations involving ψ_m, one equation for each ray. The directions $\vec{\Omega}_m$ may be pictured as points on a unit sphere, points specified by number triplets (μ_m,η_m,ξ_m) of direction cosines. The weights may be interpreted as surface areas about the points, covering the $\vec{\Omega}$ domain and so measured that $\Sigma_m w_m = 1.0$. For simple geometries, that is, slabs and spheres of dimensionality $d = 1$, the components of $\vec{\Omega}$ reduce to μ ($-1 \leq \mu \leq 1$).

A general formulation of the discrete ordinate method in numerical work is the S_n method. (The original approach [40,41], which used an explicit representation of the angular distribution, has been superseded by the much more general method outlined below.) Here one selects M discrete directions, $M = 2^d n(n+2)/8$, where n is the order of approximation, $n = 2,4,6,\ldots$, and d is the number of components of $\vec{R}$. These are reduced to $M = n$ directions in the simple geometries where additional symmetry allows the grouping of direction points. The points selected may be arranged in triangular fashion on each octant of the unit sphere. In general the points may be chosen according to the user's preferences or requirements, following certain basic though not very restrictive rules. Thus the discrete methods known as P_{n-1} and Double-$P_{\frac{1}{2}n-1}$, n even, are included as special cases [7].

Once a quadrature scheme (set of ψ_m) is chosen a discrete ray balance equation must be formulated and numerically solved. Recent important advances have been made in these directions [7]. First, it is emphasized that analytic transport equations are statements of neutron balance and that a numerical approach should preserve this balance identically for a mesh cell and not just in the limit of a vanishingly small cell. Second, the frame of reference of $\vec{\Omega}$ is usually locally aligned with the intersecting co-ordinate surface in the $\vec{R}$-space. It follows then, in geometries with curvature, that neutrons in the process of streaming will usually find their $\vec{\Omega}$ co-ordinates changing. The transport formulation must therefore provide a mechanism for ray-to-ray transfer of neutrons which are streaming. Direct application of difference methods to the analytical transport equation provides this mechanism but does not guarantee neutron balance. Direct differencing may, of course, distort the physical model and lead to inaccurate or meaningless results. A formulation which handles ray-to-ray transfers, guarantees neutron balance in a finite cell, and decouples the angular quadrature scheme from the spatial quadrature scheme is outlined below.

The formulation is illustrated in the stationary case assuming two components for $\vec{R}$, the multigroup treatment for v, and a general anisotropic source. In terms of N, where N denotes the local average of ψ over a cell volume or a cell face, the neutron balance equation is written with four pairs of "loss-gain" terms

$$\begin{aligned}\mu_m(A_{i+1,j+\frac{1}{2}}N_{g,m,i+1,j+\frac{1}{2}} - A_{i,j+\frac{1}{2}}N_{g,m,i,j+\frac{1}{2}}) \\ + \eta_m(B_{i+\frac{1}{2},j+1}N_{g,m,i+\frac{1}{2},j+1} - B_{i+\frac{1}{2},j}N_{g,m,i+\frac{1}{2},j}) \\ + (\alpha_{m+\frac{1}{2},i+\frac{1}{2},j+\frac{1}{2}}N_{g,m+\frac{1}{2},i+\frac{1}{2},j+\frac{1}{2}} \\ - \alpha_{m-\frac{1}{2},i+\frac{1}{2},j+\frac{1}{2}}N_{g,m-\frac{1}{2},i+\frac{1}{2},j+\frac{1}{2}})/w_m \\ + V_{i+\frac{1}{2},j+\frac{1}{2}}\sigma_{g,i+\frac{1}{2},j+\frac{1}{2}}N_{g,m,i+\frac{1}{2},j+\frac{1}{2}} \\ = V_{i+\frac{1}{2},j+\frac{1}{2}}S_{g,m,i+\frac{1}{2},j+\frac{1}{2}} \quad (15)\end{aligned}$$

or, omitting the centered subscripts ($i+\frac{1}{2}$, $j+\frac{1}{2}$, g, and m), as

$$\begin{aligned}\mu(A_{i+1}N_{i+1} - A_iN_i) + \eta(B_{j+1}N_{j+1} - B_jN_j) \\ + (\alpha_{m+\frac{1}{2}}N_{m+\frac{1}{2}} - \alpha_{m-\frac{1}{2}}N_{m-\frac{1}{2}})/w + V\sigma N = VS \quad (16)\end{aligned}$$

In Eq. (16) geometry enters through the area elements A and B and the volume element V so that the term $\mu A_i N_i w$ can be interpreted as a gain due to flow across the cell face of area A_i while $V\sigma N w$ is a loss in the cell due to neutron-nuclei collisions, etc. For cylindrical (r,z) geometry, for example, $A_i = 2\pi r_i \Delta z$, $B = B_j = B_{j+1} = \pi(r_{i+1}^2 - r_i^2)$ and $V = B\Delta z$. The direction variable enters through the weights w and the cosines (μ,η,ξ) where $\mu^2 + \eta^2 + \xi^2 = 1.0$ in orthogonal frames. The coefficients α handle the ray-to-ray transfer. Arguing for isotropic ψ that all N's should be equal, that $V\sigma N = VS$, and that the flow terms should vanish leads to (since $B_{j+1} = B_j$)

$$\alpha_{m+\frac{1}{2}} - \alpha_{m-\frac{1}{2}} = w\mu(A_{i+1} - A_i) \quad (17)$$

Requiring that one ray receives no neutrons ($\alpha_{\frac{1}{2}} = 0$) and that Eq. (17) conserve neutrons ($\Sigma_m w\mu = 0$) determines the α.

The preceding is readily extended to more than one curvature and more than two dimensions, and time-dependent problems can normally be reduced to sequences of stationary ones [7].

To solve Eq. (16) numerically one may make assumptions based on the continuous property of the flux ψ, thereby defining what are called "diamond" difference schemes, the simplest of these being

$$2N = N_{i+1} + N_i = N_{j+1} + N_j = N_{m+\frac{1}{2}} + N_{m-\frac{1}{2}} \quad (18)$$

which together with Eq. (16) gives a system of four equations in the seven N's. Three of the N's can be assumed known from results for neighbouring cells for which the calculations have already been done (or else from boundary conditions), and hence one may solve for the remaining four N's.

The evaluation of N involves, besides the known N's and coefficients, the source term S which is implicit since in general it depends on quantities not yet calculated. It may also entail boundary conditions which depend on such quantities. One resolves this in the customary way by introducing iterative procedures.

Hence, in the calculation of S, one uses "previous values" whenever current values are lacking. By previous values we mean data from a previous iteration; initially these would be trial values.

The most efficient evaluation is obtained by solving Eq. (16) for N using Eq. (18) to eliminate unknown subscripted Ns. The algorithms which produce true solutions of Eq. (16) are well established [7] and S_n methods have been applied to a great variety of practical problems in diverse geometries.

Spherical harmonics and other polynomial methods

According to the second tradition ψ is approximated by polynomials in μ with coefficients a_m, $m = 1, 2, \ldots, M$, depending on $\vec{R},t$, and v. In the basic approach, called spherical harmonics, ψ is expanded in a truncated Legendre series.

Recently, expansions in orthogonal polynomials other than Legendre have been examined, mostly in quest of improvements in accuracy for fixed M and for better convergence with increasing M (in cases where $M = n$). Aspelund [42] and Conkie [43] developed the basic formalism (and solutions in some cases) in connection with expansions of ψ using Tchebycheff polynomials. Encouraging results were obtained in comparisons with spherical harmonics in simple test problems. It was noted however that the Tchebycheff method had some analytical shortcomings, that it could not, for example, be applied to spheres with the effectiveness of the Legendre method. Yabushita [44] confirmed the findings in [43] and made some further contributions to the Tchebycheff case.

Mika and Zelazny [45] and Pomraning and Clark [46] examined, in a similar vein, the use of Gegenbauer and Jacobi polynomials. It was observed in [46] that polynomial expansions do not conserve neutrons except in the Legendre case where the polynomials are orthogonal with uniform weight function over the μ-interval $(-1,1)$: $W(\mu) \equiv 1.0$. This difficulty was resolved in an acceptable way be replacing the first equation of the expansion by the group balance equation (the first equation in the Legendre set).

By removing the restriction to orthogonal polynomials on the interval $(-1,1)$ further variety has been introduced. The method of Yvon [8,47] implies two Legendre polynomials, one for each of the μ-intervals $(-1,0)$ and $(0,1)$. This method has proved particularly valuable in treating problems with plane geometry. Bareiss [48] extended this idea to approximation by two or more polynomials. In the first S_n method [40] ψ was represented by connected line segments. Bengston [49], following Yvon's example of allowing a discontinuity at $\mu = 0$, converted S_n to Double-$S_{\frac{1}{2}n}$. Simple step function representations have also been considered.

The polynomial method may be based on quite arbitrary (piecewise polynomial) representations of ψ with coefficients a_{lm} and on certain "moment" transformations θ_{lm} of the transport equation. This can be done consistently with all the methods discussed above and serves therefore to unify and extend these methods. It also provides a means for improving accuracy for fixed M in that, as in S_n, representation and transformation are decoupled. In this general form the polynomial method is referred to as the moment, or M_n, method [50].

The operators θ_{lm} are applied to the representation of ψ as well as the transport equation. The first step yields linear equations for the moments $\psi_{lm}(\vec{R},t,v)$ of ψ in terms of the coefficients a_{lm} and, by inversion, equations for a_{lm} in terms of the ψ_{lm}. The second step results in a set of differential equations similar to but simpler than the spherical harmonics equations. In the cylindrical case with $d = 1$, for example, from which one can readily generalize to higher d, the moment operators are given by:

$$\theta_{lm} \equiv \frac{1}{\pi} \int_{-1}^{1} d\mu \int_{0}^{\frac{1}{2}\pi} d\omega W(\xi,\mu)\xi^l \mu^m \qquad (19)$$

where $l = 0,2, \ldots$, $m = 1,2, \ldots$, subject to $l + m < n$, and where $\xi^2 = (1-\mu^2)\cos^2\omega$. Normally one would choose $W \equiv 1.0$ since it is more convenient to regard weight assignment as a part of the representation. For the simple geometries (slabs and spheres with $d = 1$). Equation (19) reduces to $\theta_{lm} = \theta_m = \frac{1}{2}\int d\mu W(\mu)\mu^m$.

The number of moments in M_n equals, by construction, the number of discrete rays in S_n. The "terminal" moments ψ_{lm}, $l + m = n$, l, m and n even, can be expressed in terms of the lower order $(l + m < n)$ moments. The resulting equations are called the terminating conditions. By using these conditions the M_n equations may be solved by methods which very closely parallel those of S_n [50].

Integral transport theory

A different approach to numerical solution may be made starting from the integral equation for neutron transport [8]. The integral equation is approximated for solution by introducing a discrete space-velocity mesh and evaluating the kernel, numerically or otherwise, to obtain coefficients connecting the values of the neutron flux at the mesh points. Such methods have been used in special cases for many years; frequently in combination with other methods such as diffusion theory or Monte Carlo. The advantage of the integral formulation is that for isotropic scattering the angular flux need not be computed. The disadvantage is that, except in simple cases, a rather complicated kernel must be evaluated, although only once (if dimensions and cross sections are not being varied) in a given problem.

Honeck [51] has developed integral theory for accurately solving the thermal utilization problem in cylindrical or plane cell geometry. The discrete approximation to the integral equation leads to a set of coupled linear equations for the flux values which are efficiently solved by scaling and over-relaxation techniques.

Kopp [52] has given an interesting iterative method for solving the integral equation by alternating between first a diffusion theory calculation and second an integral theory solution for a *purely absorbing* medium which generates not only a correction to the diffusion theory but also a new source for a further diffusion calculation. The iterative procedure was found to converge rapidly for a test case in plane geometry.

Treatment of anisotropic sources

The source term in a transport problem (for example S in Eq. (16)) will in general be anisotropic. In particular, in a multigroup calculation, neutron scattering will usually lead to an anisotropic source in every group. In each method discussed above, a spherical harmonics expansion may be used to represent the angular dependence of the anisotropic source. Linear anisotropy may be conveniently treated in any of the methods, although in integral theory the advantage of calculating only the scalar flux is lost. If higher terms in the expansion are necessary to represent the anisotropy, the source term becomes complicated especially for cylindrical geometry and for $d > 1$. At some degree of complexity, direct use of group averaged differential cross sections may become economical. Step functions have been found to be accurate for representing such cross sections [53].

Attempts have been made to estimate requirements for anisotropic scattering representations. The diagonal transport correction is frequently found to be sufficiently accurate [51,54] and permits an isotropic type solution. Seldom is more than a quadratic scattering representation required [54,55]. Even for photon transport four or five terms of a spherical harmonics expansion seem to suffice [55,56], and we have found good agreement between Monte Carlo and S_n calculations in problems of photon penetration and heating in slabs and spheres by using a P_3 scattering representation. For fast neutron scattering, also, a few term expansion is sufficient for scattering anisotropy although flux anisotropy may require much higher order quadrature [55,57]. In sum, source anisotropies can now be handled by existing numerical transport methods.

REFERENCES

1. Osborn, R. K., and Yip, S., *Foundations of Neutron Transport Theory*, to be published as an A.N.S. monograph.
2. Ono, S., Prog. Theor. Phys. (Japan), *12*, 113 (1954).
3. Bell, G., to be published.
4. Pal, L., Acta. Physica Hung., *14*, 345 (1962).
5. Bellman, R., Kalaba, R., and Wing, G. M., J. Math. Phys., *1*, 280 (1961), and in other papers referred to therein.
6. Mullikin, T. W., J. of Math. Anal. and Appl., *3*, 441 (1961), and reference [32].
7. Carlson, B. G., *Numerical Formulation and Solution of Neutron Transport Problems*, Los Alamos Report LA-2996 (1964).
8. Davison, B., and Sykes, J. B., *Neutron Transport Theory*, Oxford (1957).
9. Lehner, J., and Wing, G. M., Comm. Pure Appl. Math., *8*, 217 (1955).
10. Lehner, J., and Wing, G. M., Duke Math. J., *23*, 125 (1956).
11. Pimbley, G. H., J. Math. Mech., *8*, 837 (1959).
12. Jörgens, K., Comm. Pure Appl. Math., *11*, 219 (1958).
13. Nelkin, M., *Asymptotic Solutions of the Transport Equation for Thermal Neutrons*, General Atomic Report GA-3298 (1962).
14. Van Norton, R., Comm. Pure Appl. Math., *15*, 149 (1962).
15. Muskhelishvilli, N. I., *Singular Integral Equations*, Noordhoff, Groningen (1953).
16. Van Kampen, N. G., Physica, *21*, 949 (1955).
17. Case, K. M., Annals of Physics, *9*, 1 (1960).
18. Van Kampen, N. G., Proc. Koninkl. Nederl. Akad. van Wetenschappen, *63B*, 93 (1960).
19. Wigner, E. P., Proc. Symp. Appl. Math., Am. Math. Soc. XI, 89 (1961).
20. Mitsis, G. J., Argonne Report ANL-6459 (1961) and Nucl. Sci. Eng., *17*, 55 (1963).
21. Zelazny, R., J. Math. Phys., *2*, 538 (1961).
22. Mika, J. R., Nucl. Sci. Eng., *11*, 415 (1961). See [33] for direct singular integral equation approach.
23. Zelazny, R., Kuznell, A., and Mika, J., Annals of Physics, *16*, 69 (1961).
24. Zelazny, R., and Kuznell, A., Annals of Physics, *16*, 81 (1961).
25. Zelazny, R., and Kuznell, A., *Multigroup Neutron Transport Theory, Physics of Fast and Intermediate Reactors II*, IAEA, Vienna, 51 (1962).
26. Corngold, N., Michael, P., and Wollmann, W., Nucl. Sci. Eng., *15*, 13 (1963).
27. Koppel, J. U., Nucl. Sci. Eng., *16*, 101 (1963).
28. Ferziger, J. H., and Leonard, A., Annals of Physics, *22*, 192 (1963).
29. Leonard, A., and Ferziger, J. H., *Energy Dependent Neutron Transport Theory: II*, to be published.
30. Bednarz, R. J., and Mika, J. R., J. of Math. Phys., *4*, 1285 (1963).
31. Mitsis, G. J., *Transport Solutions to the Monoenergetic Critical Problems*, Argonne Report ANL-6787 (1963).
32. Leonard, A., and Mullikin, T. W., *Solutions to the Criticality Problems for Spheres and Slabs*, Rand Report RM-3256-PR (1962) and earlier reports referred to therein.
33. Leonard, A., and Mullikin, T. W., *A Spectral Analysis of the Anisotropic Neutron Transport Kernel in Slab Geometry with Applications*, Rand Report RM-3807-PR (1963).
34. Aamodt, R. E., *Three Soluble Problems in Linear Transport Theory*, Thesis, Michigan University, Ann Arbor, Report NP-12458 (1962).
35. Francis, N. C., Stewart, J. C., Bohl, L. S., and Kreiger, T. J., Proceedings of the Second International Conference on the Peaceful Uses of Atomic Energy, P/627, Vol. 16, p. 517, United Nations (1958).
36. Mowery, A. C., Jr., and Murray, R. L., Nucl. Sci. Eng., *14*, 401 (1962).
37. Selengut, D. S., *Variational Analysis of Multi-Dimensional Systems*, Hanford Quarterly Report, HW-59126, Richland, Washington: HAPO (1958).
38. Pomraning, G. C., and Clark, M., Jn., Nucl. Sci. Eng., *16*, 147 (1963).
39. Kostin, M. D., and Brooks, H., *Generalized Variational Method*, Trans. Am. Nucl. Soc., *5*, 1, 41 (1962), and Kostin, M. D., thesis, Harvard University (1963).

40. Carlson, B. G., *Solution of the Transport Equation by S_n Approximations*, Los Alamos Reports LA-1599 (1953), and LA-1891 (1955).

41. Carlson, B. G., and Bell, G., Proceedings of the Second International Conference on the Peaceful Uses of Atomic Energy, P/2386, Vol. 16, p. 535, United Nations (1958).

42. Aspelund, O., Proceedings of the Second International Conference on the Peaceful Uses of Atomic Energy, P/573, Vol. 16, p. 530, United Nations (1958).

43. Conkie, W. R., Nucl. Sci. Eng., *6*, 260 (1959).

44. Yabushita, S., J. Math. Phys., *2*, 543 (1961).

45. Mika, J., and Zelazny, R., Bull. Acad. Polon. Sci. Ser., *8*, 59 (1960).

46. Pomraning, G. C., and Clark, M., Jr., Nucl. Sci. Eng., *17*, 8 (1963).

47. Kourganoff, V., *Basic Methods in Transfer Problems*, 101, Oxford (1952).

48. Bareiss, E. H., Proceedings of the Second International Conference on the Peaceful Uses of Atomic Energy, P/639, Vol. 16, p. 503, United Nations (1958).

49. Bengston, J., *Approximate Solutions of the Neutron Transport Equation Assuming a Discontinuity in the Angular Density*, Lawrence Radiation Lab. Report UCRL-4691 (1956).

50. Carlson, B. G., *The Methods of Moments Applied to Transport Theory*, Los Alamos Report LA-3060 (1964).

51. Honeck, H. C., Nucl. Sci. Eng., *18*, 49 (1964).

52. Kopp, H. J., Nucl. Sci. Eng., *17*, 65 (1963).

53. Lathrop, K. D., *Anisotropic Scattering in the Transport Equation*, Los Alamos Report LAMS-2873 (1963).

54. Joanou, G. D., and Halim Kazi, A., *The Validity of the Transport Approximation in Fast-Reactor Calculations*, Trans. Am. Nucl. Soc., *6*, 17 (1961).

55. Lathrop, K. D., *Anisotropic Scattering Approximations in the Boltzmann Transport Equation*, Los Alamos Report LA-3051 (1964).

56. Lanning, W. D., *A Fortran Program to Solve the P-3 Gamma Ray Equations in Slab Geometry*, Westinghouse Report WAPD-TM-356 (1963).

57. Francis, N. C., Brooks, E. J., and Watson, R. A., *The Diffusion of Fast Neutrons with Strong Forward Scattering*, Trans. Am. Nucl. Soc., *6*, 2, 283 (1963).

ABSTRACT—RÉSUMÉ—АННОТАЦИЯ—RESUMEN

A/261 Etats-Unis d'Amérique

Evolution de la théorie du transport des neutrons

par G. I. Bell et *al.*

Les études récemment entreprises en vue d'élargir la théorie du transport des neutrons et des photons comprennent: *a*) l'établissement systématique d'une équation de transport à partir du formalisme de la théorie quantique des champs à l'aide de distributions de densités brutes; *b*) l'utilisation de fonctions génératrices de probabilités ainsi que d'équations de première collision pour formuler une théorie stochastique du transport des neutrons et notamment des écarts arbitraires par rapport à la moyenne; *c*) l'utilisation de méthodes d'imprégnation invariante dans lesquelles les équations de Boltzmann ou les équations de transport courantes avec des conditions à deux limites sont remplacées par des équations non linéaires avec des conditions à une seule limite.

Les auteurs examinent les améliorations récentes apportées à l'analyse classique de l'équation de transport et des intégrales linéaires connexes. Ils étudient les propriétés du spectre des valeurs propres de l'opérateur de transport et exposent la méthode de développement des solutions générales en fonction d'un ensemble complet de valeurs propres. Ils exposent de la même façon la généralisation de la méthode de développement des valeurs propres: d'une géométrie plane à une géométrie courbe, de lois de diffusion isotrope à des lois de diffusion plus générales et des problèmes monoénergétiques à des problèmes qui sont fonction de l'énergie. Ils indiquent les limitations et les développements possibles de la méthode.

Les auteurs donnent un apercu de l'évolution récente des méthodes de la théorie intégrale et des méthodes variationnelles, notamment des méthodes donnant un résultat avec une erreur d'ordre supérieur dans la fonction d'essai. La partie analytique du mémoire s'achève par l'étude de quelques-unes des modifications et simplifications utiles de l'équation de transport, en particulier de son terme source.

La deuxième partie du mémoire porte sur les méthodes numériques. Les auteurs étudient d'abord la méthode multigroupes généralisée des ordonnées discrètes, en commençant par établir des équations intégrales dénommées équations d'équilibre dans une maille de cellule. A cet égard, ils examinent diverses simplifications, en particulier la théorie de la diffusion.

Ils étudient ensuite l'application de modèles de différences à l'équation d'équilibre, puis décrivent les règles d'évaluation des formules de récursion qui en découlent. Les principaux problèmes qui se posent dans ce cas tiennent au contrôle des erreurs, au traitement des termes sources implicites et des conditions aux limites et à la convergence des processus d'itération à plusieurs niveaux. On examine brièvement la question des itérations internes et externes et des itérations des valeurs propres, ainsi que celle de l'essai de convergence connexe.

Au sujet de l'équation de diffusion, les auteurs notent les méthodes permettant de réduire les itérations internes ou de s'en passer. A cet égard, la méthode de réflexion, liée au principe d'imprégnation invariante, est étendue aux problèmes à plusieurs dimensions. Les auteurs indiquent les perfectionnements apportés aux méthodes utilisées pour résoudre la forme du deuxième ordre de l'équation de diffusion et l'application de ces méthodes à l'équation de transport. Ils présentent quelques comparaisons numériques de diverses méthodes utilisées pour résoudre ces équations.

Enfin, les auteurs résument les perfectionnements apportés aux méthodes numériques non discrètes, aux calculs de Monte-Carlo et, au sujet de ces derniers, aux méthodes déterministes.

A/261 США

Успехи в развитии теории переноса нейтронов

Дж. Белл *et al.*

Последние работы в области усовершенствования теоретической базы теории переноса нейтронов и фотонов были направлены на (1) строгий вывод транспортного уравнения, исходя из формализма теории квантованных полей, с помощью крупнозернистых распределений плотности; (2) употребление функций вероятности рождения, а также уравнений первых соударений для формулировки стохастической теории переноса нейтронов, включающей произвольные отклонения от среднего эффективного значения, и (3) употребление инвариантного метода «внедрения», где обычные уравнения переноса или уравнение Больцмана с краевыми условиями для двух границ заменяются нелинейными уравнениями с краевыми условиями на одной границе.

Рассматриваются последние усовершенствования в области классического анализа транспортного уравнения и связанных с ним линейных интегральных уравнений. Дается обзор свойств спектра собственных значений транспортных операторов и описываются способы разложения общих решений в ряд по полному набору собственных функций. Обсуждаются вопросы распространения метода разложения в ряд по собственным функциям не только на случай плоской, но и на случай сложной криволинейной геометрии; не только для изотропного, но и для более общего закона рассеяния; не только для односкоростных задач, но и для случаев, когда существенна зависимость от энергии. Обсуждаются факторы, ограничивающие возможности метода, и факторы, потенциально расширяющие эти возможности.

Подытожены успехи в области развития интегральной теории и вариационных методов (включая методы, которые дают результат с ошибкой высокого порядка в ошибке пробной функции). Аналитическая часть этого доклада заканчивается обзором некоторых пригодных преобразований и упрощений транспортного уравнения и, в частности, члена, содержащего источник.

Во второй части доклада рассматриваются численные методы. Сначала обсуждается обобщенный многогрупповой метод дискретных ординат (начиная с формулировки интегральных уравнений, называемых уравнениями баланса для сеточных ячеек). В этом же контексте обсуждаются различные упрощения, в частности, диффузионное приближение.

Затем обсуждается применение конечноразностных методов к уравнениям баланса и описываются правила для оценки результата рекуррентных формул. Здесь самым важным является: контроль ошибок, применение неявных членов источников и граничных условий, сходимость многогрупповых итерационных процессов. Кратко рассмотрены процессы внутренних и внешних итераций, итераций собственных значений, а также соответствующие методы проверки сходимости.

Указаны методы, которые дают возможность при решении диффузионного уравнения уменьшать число внутренних итераций или вообще обходиться без них. Метод отражения, связанный с методом инвариантного «внедрения», применяется к решению многомерных задач. Обсуждаются успехи в технике решения диффузионного уравнения второго порядка и распространение этих методов к решению транспортных задач. Приводятся результаты сравнения численных результатов, полученных различными методами.

В заключение рассматриваются успехи в области применения недискретных численных методов, метода Монте-Карло и при сочетании последних с детерминическими методами.

A/261 Estados Unidos de América

Progresos en la teoría de transporte neutrónico

por G. I. Bell *et al.*

Entre los esfuerzos hechos recientemente a fin de ensanchar la base teórica del transporte de neutrones y fotones se cuentan: *a*) la deducción sistemática de una ecuación de transporte partiendo del formalismo de la teoría cuántica de campos por medio de distribuciones groseras de la densidad; *b*) utilización de funciones generatrices de probabilidad junto con ecuaciones de primer choque a fin de formular una teoría estocástica de transporte neutrónico que incluya desviaciones arbitrarias del valor medio, y *c*) métodos de engaste invariante en los que se sustituyen las ecuaciones usuales de Boltzmann o de transporte, con condiciones en dos límites, por ecuaciones no lineales con condiciones en un solo límite.

Se consideran ciertos avances recientes en el análisis clásico de la ecuación de transporte y de las ecuaciones integrales lineales relacionadas con ella. Se revisan las propiedades del espectro de valores propios del operador de transporte y se esboza el método de desarrollo de soluciones generales en función de un conjunto de funciones propias. Se bosqueja la extensión del método de desarrollo en funciones propias desde geometrías planas a curvas, de leyes de dispersión

isótropas a otras más generales y de problemas monoenergéticos a problemas en que varía la energía. Se señalan las limitaciones del método y sus posibles extensiones.

Se resumen los recientes avances en teoría integral y métodos variacionales incluyendo métodos que proporcionan un resultado con un error de orden elevado en el error de la función de ajuste. La parte analítica del trabajo concluye con una revisión de algunas de las transformaciones y simplificaciones útiles de la ecuación de transporte, en particular de su término fuente.

La segunda parte del trabajo trata de métodos numéricos. Se discute en primer lugar el método de multigroup con ordenadas discretas generalizadas, empezando por formular las ecuaciones integrales, llamadas ecuaciones de balance en la red de la celda. En este esquema se consideran diversas simplificaciones, en particular la teoría de difusión.

A continuación se discute la aplicación de esquemas de diferencias a la ecuación de balance y luego se describen las fórmulas de recurrencia que resultan. En este caso las preocupaciones mayores son: el control de los errores, el tratamiento de los términos fuente implícitos y de las condiciones en los límites y la convergencia de los procesos iterativos de niveles múltiples. Se examina brevemente la cuestión de las iteraciones interna, externa y de valores propios, así como la prueba de convergencia correspondiente.

Respecto a la ecuación de difusión, se señalan métodos que minimizan las iteraciones internas o bien permiten despreciarlas. En este caso se extiende a problemas multidimensionales el método de reflexión que está ligado al concepto de engaste invariante. Se señalan avances en las técnicas de resolver la ecuación de difusión en su forma de segundo orden y la extensión de esta técnica al caso de transporte. Se presentan algunas comparaciones numéricas entre distintos métodos de resolución.

Por último, se resumen los progresos en técnicas numéricas no discretas, métodos de Monte Carlo y de combinación de este último con métodos determinísticos.

Developments in resonance absorption

By J. Chernick and M. M. Levine*

The subject of the resonance absorption of neutrons in reactors has continued to challenge investigators since the 1958 Geneva Conference. Our review of this work will be limited to that published in the United States although it would be remiss not to call attention to the widespread and fine research work carried out abroad during the past few years. The review will also be limited to developments in resonance absorption for thermal reactors. Developments in resonance absorption for fast reactors will be considered in a companion paper entitled *Physics of Fast Reactors* by Avery *et al.***

In the United States, progress in the field has continued along the lines outlined in the review paper by Sampson and Chernick [1]. In particular, the integral equation approach to a quantitative theory discussed at the Second Geneva Conference [2] has fulfilled its early promise. Indeed for certain now classical problems, such as the resolved resonance integral of ordinary uranium metal rods, there is little to choose between simple calculations such as those of Vernon [3] or Drawbaugh [4], Nordheim's method for the direct solution of the integral equation [5], or Levine's Monte Carlo calculations [6]. Other problems exhibit greater sensitivity to the calculational model. In many cases, crucial experimental data are still lacking. Thus, the lack of an adequate representation of the low level resonance structure of fissionable nuclides [7] continues to hold up accurate calculations of the resonance absorption of neutrons in highly enriched fuels. The present concerted effort in major European laboratories as well as in the United States to improve the accuracy of neutron cross-section measurements bodes well for the early elimination of outstanding discrepancies such as those still existing for low energy ^{235}U and ^{232}Th resonances.

Although the modern theory of resonance absorption is in harmony with Wigner's original concepts as well as those of Gurevich and Pomeranchouk of the USSR, new concepts and tools have been developed which generalize and transcend the earlier work. A new language is emerging based on these concepts which include the method of "collision" or "escape" probabilities for reactor lattices, the "uniform" or "flat" flux approximation for subregions of a lattice, "equivalence theorems" between lattices and between mixtures and lattices, the narrow resonance (NR) approximation, and the infinite mass absorber (IA or IM) or wide resonance (WR) approximation. These concepts will be reviewed since they are necessary to the understanding of recent improvements such as the intermediate resonance (IR) formulation of Goldstein and Cohen [8].

The papers reviewed here are generally concerned either with refinements of the basic theoretical methods or with extensions of calculational tools to more novel or complex problems or with integral experiments designed to test or improve aspects of the theory. It is clear that considerable progress has been made since 1958 in all these important areas of a field which was once felt to be too complex ever to emerge from a state of semi-empiricism.

THE METHOD OF COLLISION PROBABILITIES

The collision probability method of solving neutron transport problems is becoming increasingly popular although the basic concept is old. Consider a lump of purely absorbing and fissioning material. If η is the average neutron multiplication per absorption and P_0 is the average probability that a neutron will make a collision during its flight through the lump, then $\eta P_0 = 1$ is the condition for criticality. The complement $1 - P_0$ of the average collision probability is called the *escape probability* of the lump. In general, P_0 is a complex average over neutron energy and spatial distribution but the assumption of uniform or *flat flux* and isotropic scattering reduces the problem to simple geometrical considerations [9]. The restriction on scattering may be lifted for a heavy scatterer where the resulting neutron energy degradation may be neglected (the *infinite mass* approximation). In this case, the condition for criticality becomes $\eta P_0 \sigma_a / (\sigma_t - \sigma_s P_0) = 1$.

One of the early uses of the collision probability method was in one-group calculations of the fast fission factor of widely separated or *isolated* uranium lumps in a reactor lattice [10]. These restrictions were relaxed by Chernick and Mozer [11,12] who systematically used the detailed collision probabilities $P_{ij}(E)$ for neutrons uniformly produced in subvolume V_i of a lattice at energy E which make their first collision in subvolume V_j. A number of recent papers have been devoted to the improvement of such calculations.

* Brookhaven National Laboratory, Upton, N.Y.
** Vol. 6, these Proceedings.

Another early use of the collision probability method was in the solution of Peierls' integral equation for monoenergetic neutrons [11]. The great superiority of the method over spherical harmonics approximations for thin slabs [13] is shown in Table 1, which compares calculated flux disadvantage factors for a non-absorbing moderator. The convergence of the P_n method is poor for small values of d_0/λ_0 and d_1/λ_1, the widths of the fuel and moderator slabs in mean free paths, even for values of the fuel absorption probability p_a as low as 0.1. The poor showing of the standard spherical harmonics method is one reason for the popularity of the collision probability method, in addition to the latter's clear physical appeal.

The collision probability method becomes inaccurate when the dimensions of the volume elements are chosen to be large compared to a mean free path. Corngold has developed an integral transport method [14] which reduces to the flat flux collision probability method in lowest-order approximation. Fukai [15] has shown that Corngold's second-moment approximation yields results that are generally better than P_5 calculations even for thick slabs. A comparison of calculated flux disadvantage factors with exact values is given in Table 2.

One of the most popular methods of treating the diffusion of monoenergetic neutrons in large lattice cells remains that of Amouyal, Benoist, and Horowitz [16], who skilfully blended collision probability methods for the fuel with elementary diffusion theory for the moderator. However, the inadequacy of one-group diffusion theory is becoming apparent as adequate knowledge of neutron thermalization has become available. The first attempt at multigroup collision probability methods for treating neutron thermalization problems was that of Takahashi [17]. The work of Honeck and Kaplan [18] resulted in the general multigroup, multiregion integral transport code THERMOS. Honeck's recent review [19] of disadvantage factors for uranium-water lattices shows that both his theoretical calculations and experimental measurements at the Bettis and Brookhaven Laboratories have become so accurate that systematic differences of only a few per cent can be detected.

Table 1. Flux disadvantage factors for thin slab lattices

d_0/λ_0	d_1/λ_1	P_a	P_3	P_5	Collision prob.
0.50	0.50	0.10	1.024	1.033	1.049
		0.50	1.121	1.166	1.244
	1.00	0.10	1.035	1.044	1.055
		0.50	1.174	1.222	1.272
1.00	0.50	0.10	1.069	1.088	1.109
		0.50	1.339	1.431	1.533
	1.00	0.10	1.087	1.103	1.113
		0.50	1.428	1.507	1.556

Table 2. Flux disadvantage factors for thick slab lattices

d_0/λ_0	d_1/λ_1	P_a	P_3	P_5	Corngold	Exact
2	2	0.10	1.2784	1.2897	1.2935	1.2937
		0.50	2.3331	2.3905	2.4149	2.4161
	5	0.10	1.4200	1.4250	1.4266	1.4269
		0.50	3.0499	3.0757	3.0873	3.0894
5	2	0.10	1.9776	1.9926	1.9959	1.9986
		0.50	5.0944	5.2015	5.2304	5.2544
	5	0.10	2.3045	2.3094	2.3098	2.3117
		0.50	6.8010	6.8471	6.8526	6.8737

In studies of the resonance absorption of neutrons, simple flat flux collision probabilities have been shown to be generally adequate even for relatively large fuel and moderator dimensions. The reason is that almost all resonances are narrow compared to neutron energy losses and are generally well separated so that the asymptotic flux distribution is recovered between resonances. Thus neutrons effectively make only one collision within a resonance. Of these which slow down into a resonance trap within the fuel, the fraction P_0 collide within a fuel lump. Of those which slow down within the moderator, the fraction $1-P_1$ escape into a lump if P_1 is the corresponding collision probability for the moderator. Thus under the *narrow resonance* (NR) approximation for both the fuel and moderator the resonance integral, in terms of collision probabilities, becomes [20];

$$I(\mathrm{NR}) = \int \left[\sigma_p P_0 + \frac{\Sigma_1 V_1}{N_0 V_0}(1-P_1)\right] p_a \frac{dE}{E} \qquad (1)$$

where σ_p is the ordinary potential scattering cross section of the fuel and p_a is the absorption probability per fuel collision.

The narrow resonance approximation fails for important low energy resonances of heavy absorbers. In these cases accurate estimates of resonance integral may generally be obtained by use of the *infinite mass* (IM or IA) or *wide resonance* (WR) approximation for the fuel. The corresponding resonance integral is then;

$$I(\mathrm{NRIM}) = \int \frac{\Sigma_1 V_1}{N_0 V_0} \frac{(1-P_1)}{1-P_0 p_s} p_a \frac{dE}{E} \qquad (2)$$

where p_s is the scattering probability and the factor $(1-P_0 p_s)^{-1}$ represents the increase in absorption rate due to repeated collisions in the fuel without energy loss. The popular abbreviations NR and NRIA were first applied to the above formulae by Spinney, who studied their range of validity for individual resonances [21].

Under the flat flux approximation, a general reciprocity theorem exists [9,22,23] between the collision probabilities $P_0(E)$ and $P_1(E)$:

$$(1-P_0)\Sigma_0 l_0 = (1-P_1)\Sigma_1 l_1 \qquad (3)$$

where $l_0 = 4V_0/S$ and $l_1 = 4V_1/S$ are mean chord lengths in the fuel and moderator respectively. Eq. (3) makes it possible to restrict consideration to fuel collision probabilities $P_0(E)$ for reactor lattices. For widely spaced fuel lumps or for slab lattices the geometrical problems are then relatively simple. Other geometries such as closely packed lattices of single fuel rods or clusters of fuel rods are more complex. Dancoff and Ginsburg [24] were the first to consider

Table 3. Dancoff factors (1—c) for black rod lattices

Lattice	Rod diam. (in)	v_1/v_0	Fukai	Sauer	Monte Carlo
Square	0.25	0.273	—	0.202	0.2005±0.0005
		0.6	0.358	0.378	0.372 ±0.001
		1	0.531	0.524	0.521 ±0.002
		3	0.815	0.819	0.826 ±0.006
	0.60	0.273	—	0.358	0.362 ±0.001
		0.6	0.591	0.615	0.609 ±0.003
		1	0.764	0.764	0.778 ±0.005
		3	0.959	0.955	0.976 ±0.009
Hexagon	0.25	1	0.534	0.534	0.526 ±0.002
		3	0.828	0.821	0.821 ±0.006
	0.60	1	0.765	0.784	0.783 ±0.005
		3	0.962	0.956	0.960 ±0.011

the reduction in the effective surface of a black lump due to the shadowing effect of surrounding lumps. Improved analytical methods of obtaining Dancoff corrections for rodded lattices have been discussed by Carlvik and Pershagen [25], Thie [26], Fukai [27], Velarde [28], Sauer [29], Bonalumi [30] and others. The formulas of Fukai and Sauer for solid rod lattices in water are compared with results of Monte Carlo calculations in Table 3. The method of Sauer is based on an approximate chord length distribution whose logarithmic moment must be matched to that of the exact chord length distribution. Other more approximate formulae are discussed by Fukai [27] who has now developed an IBM 7090 code which yields exact Dancoff corrections for rod lattices (personal communication). Methods of calculating collision probabilities for fuel clusters have not been as well explored [25, 31].

For widely spaced lattices;

$$1-P_0=\lambda_0\, G/l_0 \tag{4}$$

where G is the fraction of the neutrons entering a lump which make a collision in crossing the lump. Wigner's well-known rational approximation for the penetrability factor G is given by:

$$G_W=\frac{1}{1+\lambda_0/l_0} \tag{5}$$

The use of the latter approximation greatly simplifies the calculation of resonance integrals [32, 33].

Another useful approximation [22, 34] connects the fuel escape probability for a lattice with that of an isolated lump;

$$(1-P_0)_{\text{(lattice)}}\cong(1-P_0)_{\text{(lump)}}\,\frac{(1-C)}{1-C(1-G)} \tag{6}$$

where C is the exact Dancoff correction for black fuel lumps summed over all neighbouring lumps. While the simplicity of the rational approximation is lost, Nordheim [35] recommends the use of (6) in improving the accuracy of numerical solutions.

EQUIVALENCE THEOREMS

The variety of reactor lattices is so great that equivalence relations between different systems are useful even when they are not wholly exact. Creutz *et al.* [36] were the first to suggest a relationship between the resonance integrals of fuel lumps composed of mixtures of uranium and light elements and the potential scattering cross section of the lump per uranium atom. Later, Dresner attempted to correlate resonance integrals of similar lumps containing uranium or thorium with available experimental data [31, 37].

A significant advance was made by Bakshi [38] in 1957 when he examined the error incurred in the use of Wigner's rational approximation in Eq. (1). Under the rational approximation, the resonance integrals of widely spaced lumps become identical with that of homogeneous mixtures, the quantity $1/N_0 l_0$ of the lump playing the same role as the potential scattering cross section of the moderator per absorbing atom in mixtures. Bakshi then examined the necessary conditions for equivalence between the resonance integrals of lattices and of isolated lumps. In addition to the reciprocity condition (3), he found that the escape probability for the fuel lump had to be identical with that of an isolated lump of larger size at all neutron energies. Again, it was clear that this could not be rigorously true. However, in the black lump limit the condition for equivalence becomes;

$$l_{0\,\text{(lattice)}}=\frac{l_{0\,\text{(lump)}}}{1-C} \tag{7}$$

where C is the exact Dancoff correction.

With the above equivalence relation [38], one can view a fuel lump (or lattice of fuel lumps) as having an effective macroscopic cross section proportional to its surface, in addition to its ordinary potential scattering cross section. One then obtains the general equivalence "theorem":

"Systems having equal effective potential scattering have equal resonance integrals without distinction between homogeneous and heterogeneous systems."

Bakshi's equivalence theorems were based on Eqs. (1) and (2), which involve extreme assumptions regarding neutron energy degradation. The principle was extended to higher order in energy degradation by Chernick and Vernon. The concepts were further refined and generalized by Nordheim [35], Dresner [31] and Goldstein and Brooks [39].

The Wigner approximation, Eq. (5), goes to the correct limits for large and small l_0 but it is not exact for any intermediate value. The modified rational approximation;

$$(1-P_0)=\frac{1}{1+al_0/\lambda_0} \tag{8}$$

is an improvement for practical reactor lattices. This leads to the equivalence reaction between lattices and single lumps;

$$l_{0\,\text{(lattice)}}=l_{0\,\text{(single lump)}}[1+(a-1)C]/[1-C] \tag{9}$$

which reduces to Bakshi's Eq. (7) for $a=1$. Levine [6] found that the value $a=1.1$ brings the lattice resonance integrals into good agreement with single lump results for rod lattices. Aisu and Minton [40] have

Table 4. Escape probabilities for absorbing slabs in water

Water Slab Width Σ_0/l_0	0.50 in		0.25 in		0.125 in	
	Eq. (7)	Exact	Eq. (7)	Exact	Eq. (7)	Exact
0.5	0.689	0.691	0.649	0.652	0.574	0.566
1.0	0.541	0.537	0.493	0.490	0.409	0.395
1.5	0.443	0.443	0.395	0.390	0.312	0.301
2.0	0.374	0.371	0.326	0.322	0.250	0.241
3.0	0.2803	0.2791	0.239	0.238	0.176	0.171
4.0	0.2216	0.2206	0.1857	0.1838	0.134	0.132
6.0	0.1534	0.1528	0.1266	0.1260	0.0898	0.0893
8.0	0.1162	0.1159	0.0954	0.0952	0.0674	0.0673

verified this result for rod lattices by single energy calculations but indicate that Eq. (7) remains superior for slab lattices.

Introduction of Eq. (8) into Eqs. (1) and (2) leads to a modification of Bakshi's equivalence principle for homogeneous mixtures and lumps of different materials. The effective potential scattering cross section per absorber atom becomes;

$$\sigma^* = \sigma_p/a_1 + S_{eff}/4NV. \tag{10}$$

When a_1 is unity this yields the original equivalence relation. However, Levine found that $a_1 = 1.27$ gives good correspondence between rods of ^{238}U metal, oxide, and carbide.

The adequacy of the equivalence relation (7) is shown for slab lattices in Table 4. In general, the agreement is excellent except for relatively transparent absorbers in thin water slabs. Table 5 compares the approximations (6) and (7) and Monte Carlo calculations for a hexagonal lattice of absorbing rods in an equal volume of water [35]. Eq. (6) is an improvement for thin, transparent rods, but the simple equivalence relation (7) appears to be superior for strongly absorbing lumps. The relatively large percentage error in Eq. (9) for large optical thicknesses does not appear to influence the resonance capture rate very much, however, due to the saturation of this rate for very black lumps. No detailed comparison of the relative accuracy of calculated resonance integrals have, however, been carried out. A number of simpler but less accurate equivalence theorems for lattices have also been proposed.

THE INTEGRAL EQUATION METHOD

The difficulties in the way of the solution of resonance absorption problems based on the rigorous Boltzmann equation led Chernick [1, 11] to suggest the use of the coupled integral equations;

$$F_0(E) = [1 - P_1(E)] \sum_i \int_E^{E/\alpha_i} \frac{\Sigma_{si}}{\Sigma_{t_1}} \frac{F_1(E')dE'}{(1-\alpha_i)E'}$$

$$+ P_0(E) \sum_j \int_E^{E/\alpha_j} \frac{\Sigma_{sj}}{\Sigma_{t_0}} \frac{F_0(E')dE'}{(1-\alpha_j)E'},$$

$$F_1(E) = P_1(E) \sum_i \int_E^{E/\alpha_i} \frac{\Sigma_{si}}{\Sigma_{t_1}} \frac{F_1(E')dE'}{(1-\alpha_i)E'}$$

$$+ [1 - P_0(E)] \sum_j \int_E^{E/\alpha_j} \frac{\Sigma_{sj}}{\Sigma_{t_0}} \frac{F_0(E')dE'}{(1-\alpha_j)E'} \tag{11}$$

Here F denotes the average collision density, P the average collision probability in the region indicated by its subscript. The Eq. (11) are specialized to a two-region lattice consisting of fuel lumps (subscript 0) and moderator (subscript 1). The flat flux approximation is generally used in calculations of average collision probabilities but any error incurred could be eliminated by further subdivision of the lattice.

The system (11) reduces to the single integral equation;

$$F_0(E) = \frac{(1-P_1)}{\xi E} + P_0 \sum_j \int_E^{E/\alpha_j} \frac{\Sigma_{sj} F_0(E')dE'}{\Sigma_{t_0}(1-\alpha_j)E'} \tag{12}$$

under the NR approximation.

Equation (12) or its parallel form for homogeneous mixtures has been the starting point of most recent investigations of resonance absorption. Under extreme assumptions for neutron energy degradation in fuel collisions [20] it yields the simple NR formula (1) or the NRIM formula (2). Improved formulations have been suggested by Spinney [21], Chernick and Vernon [33], Bell [23], Spinrad [2], Hasegawa [41], Rothenstein [22], Goldstein and Cohen [8], Gast [42] and Goldstein and Brooks [39], and some of these authors have also considered starting points more general than (12). Numerical methods of solving the integral equation have been developed by Nordheim and Kuncir [5], by Kelber [43] and by Kier [44].

Recent studies of resonance flux disadvantage factors include those of Dresner [31], Hayes, Luming and Zweifel [45], Vaughan [46], Takahashi and Corngold [47] and Iijima [48]. That Equation (12) leads to formula (2) in the infinite mass limit is a defect of the model, since it is known that p depends exponentially rather than linearly on the resonance integral for pure

Table 5. Escape probabilities for a hexagonal lattice of absorbing rods in an equal volume of water

Rod diam. Σ_0/l_0	0.60 in			0.25 in		
	Eq. (6)	Eq. (7)	Monte Carlo	Eq. (6)	Eq. (7)	Monte Carlo
0.5	0.689	0.706	0.691±0.004	0.571	0.614	0.572±0.004
1.0	0.520	0.535	0.522±0.004	0.393	0.427	0.397±0.003
1.5	0.416	0.430	0.422±0.003	0.298	0.319	0.304±0.003
2.0	0.335	0.344	0.346±0.003	0.239	0.251	0.248±0.002
3.0	0.244	0.248	0.250±0.002	0.169	0.174	0.173±0.002
4.0	0.189	0.192	0.194±0.002	0.130	0.132	0.133±0.002
6.0	0.130	0.130	0.133±0.002	0.088	0.089	0.088±0.002
8.0	0.098	0.098	0.100±0.002	—	—	—

hydrogen moderation. There is therefore a correction of order $(1-P)^2$ for mixtures [33] or for lattices under the flat flux approximation [22]. Iijima's results indicate that the latter correction may require modification for low energy resonances in thick lumps, widely separated by a medium mass moderator. In particular he finds that the 6.7 eV resonance in ^{238}U produces a deficiency of resonance neutrons but only within a mean free path of a uranium slab in an infinite graphite moderator. While the effect on resonance integrals is not large it is worth further study. Rothenstein [49] compared Monte Carlo results for the 6.7 eV resonance in a standard graphite lattice with calculations based on the solution of (11) by successive approximation. He obtained good agreement despite the use of flat flux collision probabilities for both fuel and moderator.

Both Rothenstein and Iijima also studied the question of flux recovery between resonances. Their results again confirm the general adequacy of this assumption for heavy absorbers. For fissionable nuclides, or for admixed absorbers with close resonances, this question is only now beginning to get the attention it deserves [43,44], in part because of the importance of these problems in fast reactors. The statistics of neutron resonance parameters is another area of importance to both thermal and fast reactors. As shown by Codd and Collins [50], statistical fluctuations in neutron and fission widths are important to the determination of Doppler coefficients of fast reactors. Figure 1 shows the importance of ^{239}Pu level spacing on the problem of overlap with ^{238}U resonances at 1 keV [51]. Unfortunately the necessary data on reaction widths, spacings, spin assignments, etc., are not yet sufficiently numerous or accurate. A review of theoretical and experimental progress in this direction has been carried out by Garrison [52].

Second-order approximations to the solution of Eq. (12) are discussed in a general and elegant manner by Dresner [31] and a hierarchy of successive approximations is considered by Bell [23]. The work of Goldstein and Cohen [8] on the homogeneous integral equation and of Goldstein and Brooks [39] on its equivalent heterogeneous equation yields the intermediate resonance (IR) formula as an interpolation

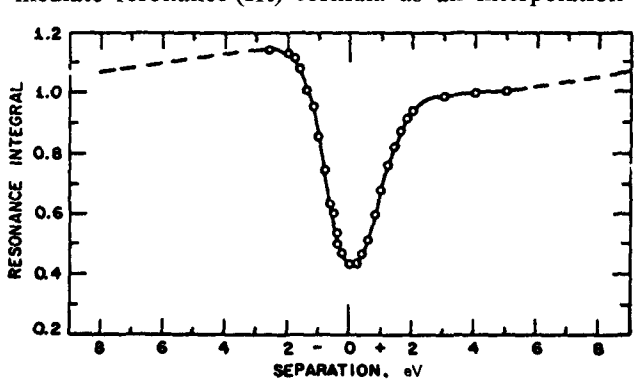

Figure 1. Plutonium-239 resonance integral versus separation of plutonium-239 resonance from a uranium-238 level at 1000 eV, temperature =300°K, normalized to 1 barn at s=5 eV

Table 6. Effect of temperature variation of interpolation parameter μ on intermediate resonance integral $I\mu$; $I\mu=(I\,[\mathrm{NRIM}]+\mu I\,[\mathrm{NR}])/(1+\mu)$. (1:1 uranium-238–H mixtures)

Resonance Energy (eV)	Temp. T (°K)	$\mu(T)$	$I\mu$ (barns)	$I\mu(0)$
6.68	0	0.0510	4.06	4.06
	900	0.0476	4.20	4.20
21	0	0.262	1.80	1.80
	900	0.237	1.90	1.90
103	0	0.554	0.402	0.402
	900	0.588	0.445	0.448
192	0	1.57	0.172	0.172
	900	1.74	0.191	0.195
209	0	3.01	0.107	0.107
	900	2.93	0.146	0.146

device between the NR and NRIM formulas. The major limitation of the work, its restriction to 0°K, has been largely removed by McKay and Pollard [53], who give examples which indicate that the interpolation formula is insensitive to temperature (Table 6).

Rothenstein and Chernik [54] have shown that the NR and NRIM formulae are not suitable for calculations of the resonance absorption of neutrons in prominent resonances of medium mass absorbers. These wide resonances are characterized by strong scattering, natural line shape, and little Doppler broadening. Interference between potential and resonance scattering is important here and occasionally in other cases [55]. Methods of attack on the problem have thus far included numerical integration, Monte Carlo calculations, and the IR formula [39], all of which yield consonant results.

Lane, Nordheim and Sampson have considered resonance absorption in moderators with randomly distributed absorber grains. The Dancoff correction C is readily derived in this case [56]. Figure 2 shows the improvement in Doppler coefficient with increase in grain diameter d for ThO_2 grains in graphite. Nordheim [5] has also calculated the exact moderating effect of the oxygen in UO_2 lumps and finds that it gives a noticeable correction to the resonance integrals of thick rods.

MONTE CARLO METHODS

The present generation of high speed digital computers has broadened the applicability of the Monte

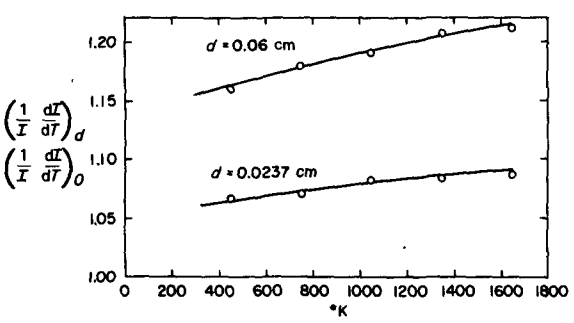

Figure 2. Dependence of Doppler effect on grain diameter D.

Carlo method. It is now being used widely as an experimental tool for testing resonance absorption models and, in a few laboratories, as a production tool for design calculations.

The limitation of the original REP code [57] to a single resonance absorber has been lifted. The REPETITIOUS code [58] permits one Doppler broadened absorber and one unbroadened fissile isotope. Code RECAP [59] prepares a tabulation of cross sections versus energy which may include up to five Doppler broadened absorbers. Burnup code RBU [60,61] has a Monte Carlo option. A present defect of the codes is the lack of adequate multilevel representation of fission cross sections.

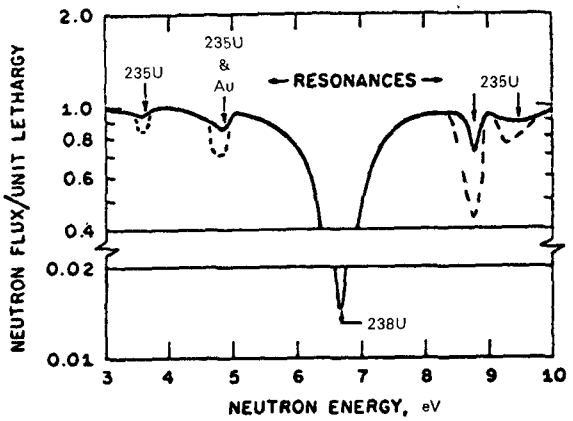

Figure 3. Resonance interference effects. Flux versus energy for H:U=1, enrichment=1%, Au abundance 10^{-6}

The ability to handle more than one resonance absorber makes it possible to investigate such problems as resonance overlap. An example is the Monte Carlo study by Foell, Grimesey and Tong [62] on the effect of overlap in mixtures involving combinations of gold, indium oxide, and lead oxide. Some effects of overlap involving ^{238}U, ^{235}U, and gold obtained by Kelber [51] from an analytic rather than a Monte Carlo approach are shown in Fig. 3.

A series of Monte Carlo calculations with large numbers of histories and high precision has been reported by Levine [6] for ^{238}U resonance absorption. The results for metal and oxide rods are compared in Fig. 4 with the results of Vernon [3] and Drawbaugh [4] based on the NR *v.* NRIM approximation and of Nordheim [5] based on numerical integration of Eq. (12). All these methods are based on the flat flux approximation and show good agreement with Monte Carlo results except for very thick rods (small $\sqrt{(S/M)}$) where the flat flux approximation becomes inapplicable.

The metal and oxide results for the resolved resonances of ^{238}U are combined in Fig. 5 with the aid of the equivalence relation based on the independent variable σ^* of Eq. (10). Similar results were obtained for the unresolved resonances below 30 keV.

Above 30 keV, deviations from the idealized $p/\xi E$ spectrum occur in a lattice because of the localized fission sources and nonconstant scattering cross sections. Rief [63] developed the Monte Carlo code MOCCA to study absorption processes in this region.

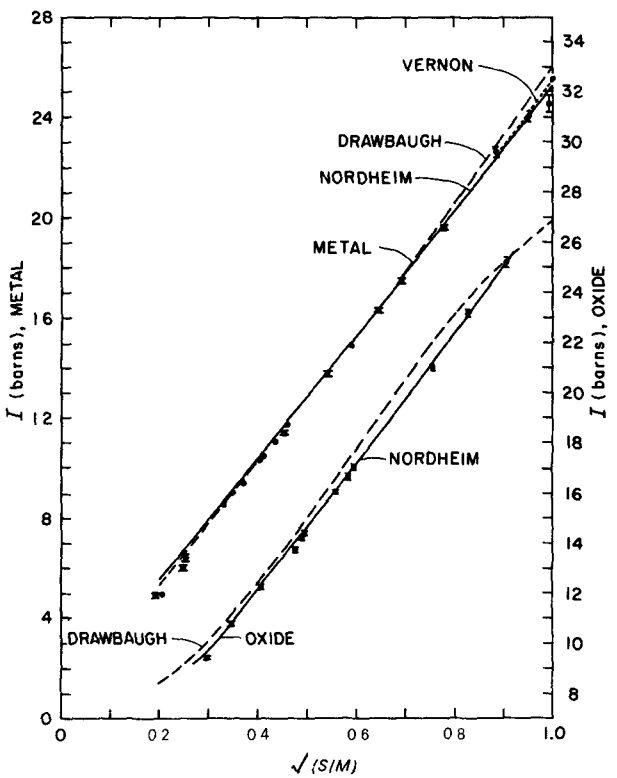

Figure 4. Calculated uranium-238 metal and oxide resonance integrals versus $\sqrt{(S/M)}$

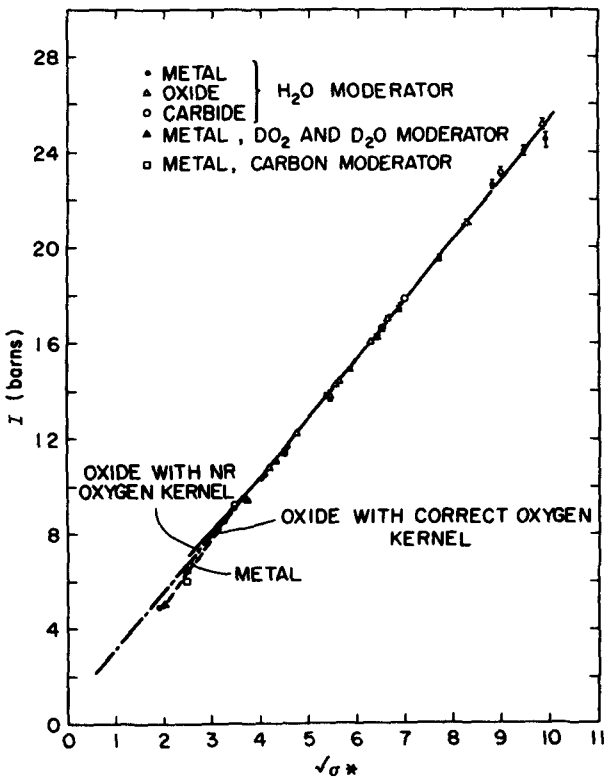

Figure 5. Calculated uranium-238 resonance integral versus generalized scattering per atom

The code has now been extended to lower energies as well. MOCCA studies of ^{238}U capture in typical lattices above 30 keV [6] yield resonance integrals of 1 to 2 or more barns as compared to the naive value of 0.8 barns for a $1/E$ spectrum.

Smith, Hardy and Klein [64] have compared measured resonance activation as a function of position in a uranium rod with results of Monte Carlo calculations. The excellent agreement is another verification both of the adequacy of the Monte Carlo method and of the resonance parameters used for ^{238}U.

RESONANCE INTEGRAL MEASUREMENTS

Measurements of resonance integrals of lumped absorbers by activation or reactivity techniques require several normalization and correction factors. Some of these depend on the measurement technique such as fission product activity in activation measurements or scattering and energy degradation in reactivity measurements. Corrections common to both types of measurement include the amount of absorption below the lowest resonance and the shape of the spectrum in which the measurement is made.

The smooth cross section contribution to the resonance integral has been subtracted from all measured values to be quoted here. The correction is relatively simple and accurate for ^{238}U since its cross section is small and closely $1/v$. On the other hand ^{232}Th has a larger smooth cross section which is non-$1/v$. A number of authors have estimated resonance parameters for a single negative energy level which can account for the low energy behaviour of thorium [65, 68]. We follow Weitman here who places the resonance at -5 eV [68]. Other estimates differ by a few tenths of a barn for the energy interval between 0.4 and 20 eV.

For purposes of comparison of experiments with each other and with calculations, it is customary to reduce measurements to a $1/E$ spectrum. These corrections are difficult since the spectra in which the measurements are made are not accurately known and approximate calculations are relied upon for their estimation. On the other hand, the reactor physicist is finding [6,69] that resonance integrals measured by activation are by themselves inadequate for the treatment of reactor lattices. Both the experimentalist and theorist are beginning to give these problems the attention they deserve.

Recent measurements of resonance integrals of uranium and uranium oxide rods are given in Table 7, while Table 8 lists the corresponding results for thorium. The resonance integrals have been corrected for smooth capture above the low energy cutoff and correspond to an idealized $1/E$ spectrum up to 10 MeV. The data are also plotted to Figs. 6 and 7, except for that of Moore, Pattenden and Tattersall because of uncertainties in their spectrum [68].

It is of interest to compare these recent results for ^{238}U with those included in Dresner's review [31]. The average value of $2.82 + 26.9\sqrt{(S/M)}$ shows a smaller volume term and a larger surface term than the average resonance integral listed by Dresner. The resonance integrals in lattices obtained by lattice reactivity measurements tend to rise more rapidly with $\sqrt{(S/M)}$ than those obtained by activation analysis, again indicating the fundamental difference between these resonance integrals. The agreement with calculations (Fig. 4) is excellent.

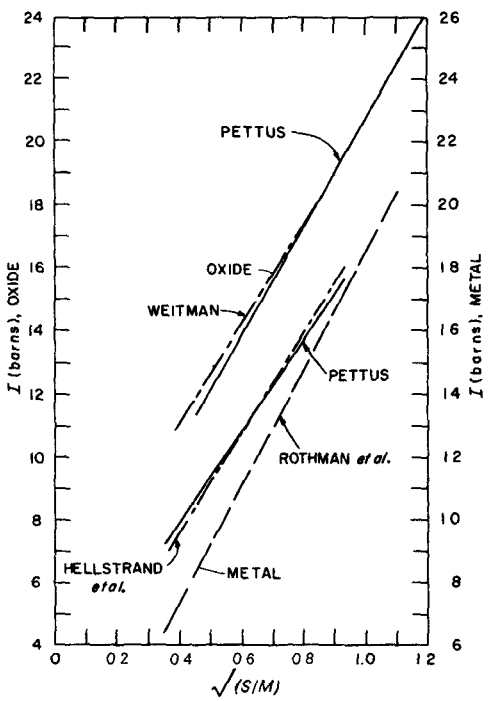

Figure 6. Measured thorium-232 metal and oxide resonance integrals versus $\sqrt{(S/M)}$

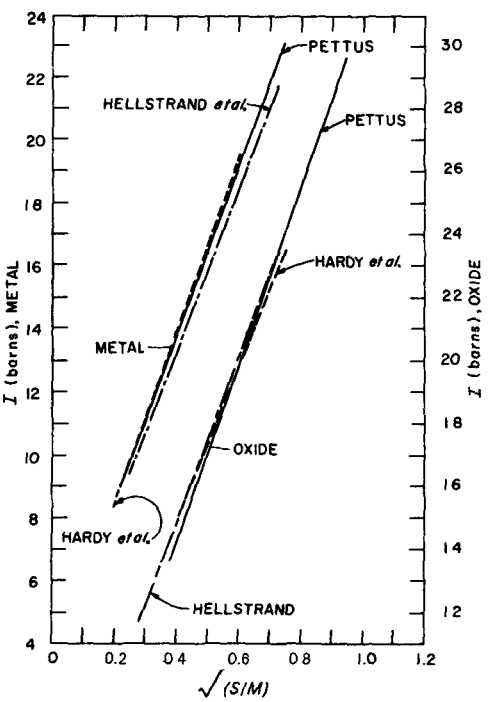

Figure 7. Measured uranium-238 metal and oxide resonance integrals versus $\sqrt{(S/M)}$

Table 7. Resonance integrals of uranium-238

Author	I (barns)	$\sqrt{(S/M)}$
	Metal	
Pettus [87]	$(2.8\pm0.5)+(27.1\pm0.9)\sqrt{(S/M)}$	0.25–0.75
Hardy *et al.* [88]	$2.71+27.8\sqrt{(S/M)}$ $\pm0{\cdot}6$	0.20–0.60
Hellstrand *et al.* [89]	$2.95+25.8\sqrt{(S/M)}$ $\pm5\%$	0.25–0.73
Moore *et al.* [90]	$2.42+28.7\sqrt{(S/M)}$ $\pm6\%$	0.26–0.63
	Oxide	
Pettus [87]	$(3.0\pm0.4)+(28.0\pm0.6)\sqrt{(S/M)}$	0.38–0.95
Hardy *et al.* [88]	$4.89+24.8\sqrt{(S/M)}$ ±0.6	0.40–0.75
Hellstrand *et al.* [89]	$4.15+26.6\sqrt{(S/M)}$ $\pm5\%$	0.28–0.84
Moore *et al.* [90]	$4.57+29.1\sqrt{(S/M)}$ $\pm6\%$	0.39–0.81

Table 8. Resonance integrals of thorium-232

Author	I (barns)	$\sqrt{(S/M)}$
	Metal	
Pettus [92]	$3.91+14.81\sqrt{(S/M)}$ $\pm5\%$	0.36–0.93
Hellstrand *et al.* [73]	$3.25+15.9\sqrt{(S/M)}$ $\pm5.5\%$	0.39–0.84
Rothman *et al.* [93]	$(1.5\pm1.3)+(17.2\pm2.1)\sqrt{(S/M)}$	0.37–0.93
Moore *et al.* [90]	$2.54+20.1\sqrt{(S/M)}$ $\pm7\%$	0.35–1.10
	Oxide	
Pettus [92]	$3.41+17.32\sqrt{(S/M)}$ $\pm5\%$	0.46–1.19
Weitman [68]	$4.9+15.5\sqrt{(S/M)}$ $\pm5\%$	0.50–1.00
Moore *et al.* [90]	$2.79+21.2\sqrt{(S/M)}$ $\pm7\%$	0.38–0.81

The average resonance integral for thorium is $2.89+16.0\sqrt{(S/M)}$ which may be compared with Nordheim's calculated value of $1.4+16.1\sqrt{(S/M)}$ [70] and Sehgal's estimate of $2.9+14.6\sqrt{(S/M)}$ [71]. Nordheim's calculations were based on a value of Γ_γ of 34 mV while Sehgal's was based on a value of Γ_γ of 24 mV. Recent measurements by Palevsky *et al.* [72] indicate that $\Gamma_\gamma \approx 30$ mV. In results reported earlier [73] Hellstrand and Weitman overcorrected for the smooth cross section of thorium and Nordheim [70] arbitrarily reduced his volume term by 1.9 barns to get agreement with their work. Restoration of the 1.9 barns would improve the agreement with experiment.

Doppler coefficients

Almost all recent work verifies the near linearity of resonance integrals with the square root of the absolute temperature. It is therefore convenient to express the temperature coefficient as

$$\beta = \frac{1}{I(T_0)} \frac{\mathrm{d}\, I(T)}{\mathrm{d}\, T^{\frac{1}{2}}} \qquad (13)$$

where β is observed to increase with S/M. Earlier work on the temperature dependence of resonance integrals has been reviewed by Pearce [74]. Therefore only recent results are quoted here.

Table 9 lists β values for uranium and uranium oxide rods. The results of calculations by Nordheim [5], Arnold and Dannels [75] and Vernon [76] are also shown. The Monte Carlo calculations of Arnold and Dannels include resonances only up to 5530 eV. Inclusion of higher energy resonances might improve the agreement between their results and the others.

For thorium, Pettus has measured a value of $\beta = 0.016$ for an oxide rod with $S/M = 0.66$. Measurements of the Doppler effect for thorium dispersed in graphite were reported by Bardes *et al.* [77]. A recent declassified report [78] is of interest since it shows the effect of temperature through the phase transitions of uranium.

Dilute resonance integrals

Estimates of the dilute resonance integral of ^{238}U have not changed appreciably from the value of 268 barns given by Chernick and Vernon [33]. The measured values (Table 10) are not sufficiently accurate to contradict this result. It appears that the 280 barn value chosen by experimenters for normalization of lump measurements is somewhat high. For thorium,

Table 9. Doppler coefficients of uranium-238

Author	$\beta\,(10^{-4})/\sqrt{°K}$	T_{max} (°C)	S/M
		Metal	
Pettus [87]	$48+64\ S/M$	600	0.11–0.25
Hellstrand *et al.* [94]	$51+50\ S/M$	600	0.08–0.28
Palowich *et al.* [95]	53 ± 3	580	0.22
Nordheim calc. [5]	$51+47\ S/M$	600	0.1 –1.0
Vernon calc. [76]	$51+53\ S/M$	800	0.05–0.5
Smith [78]	54 ± 5	970	0.059
		Oxide	
Pettus [87]	$61+47\ S/M$	1000	0.21–0.45
Hellstrand *et al.* [94]	$58+50\ S/M$	750	0.15–0.48
Palowitch *et al.*]95]	69 ± 6	950	0.38
Spano [96]	61	500	0.29
Nordheim calc. [5]	$58+56\ S/M$	600	0.2 –1.0
Arnold *et al.* calc. [75]	$69.6-2.62/(S/M)$	2800	0.15–0.6

Table 10. Dilute resonance integrals

Author	$I(^{238}U)$	$I(^{232}Th)$
Sampson [97]	265	80.5
Tattersall *et al.* [98]	285 ± 25	106 ± 10
Macklin *et al.* [99]	281 ± 20	67 ± 5
Johnston *et al.* [100]		85 ± 5
Tiren [67]		83 ± 6

estimates of resonance integrals range from 83 barns [67] to 89 barns [33]. The large variation reflects the present uncertainty in resonance parameters. The recent measurements of thorium resonance parameters by Palevsky [72] and by Haddad [79] may improve these estimates.

Other measurements

Recent measurements include the dilute resonance integral of ^{240}Pu by Nichols [80], of resonance integrals and interference between resonances of ^{115}In, gold and ^{185}Ru by Brown, Connolly and Foell [81] and of mixtures of thorium oxide and ^{238}U oxides by Foell and Connolly [82]. Some experimental results pertinent to equivalence relations between uranium lattices have been obtained by Hardy, Klein and Smith [83]. In water lattices the standard cadmium ratio technique [84] of measuring resonance absorption has become increasingly unsatisfactory as accurate calculations have become available [85]. Changes in technique discussed by Price [86] have greatly improved the accuracy of these measurements.

REFERENCES

1. Sampson, J. B., and Chernik, J., *Physics and Mathematics*, Chap. 6, Progress in Nuclear Energy Series I, Pergamon Press, London and New York (1958).
2. Spinrad, B., Chernik, J., and Corngold, N., Proceedings of the Second International Conference on the Peaceful Uses of Atomic Energy, P/1847, Vol. 16, p. 191, United Nations (1958).
3. Vernon, A. R., Nuclear Sci. Eng., *7*, 252 (1960).
4. Drawbaugh, D., US Atomic Energy Comm. report CEND-104 (1960).
5. Nordheim, L. W., Nuclear Sci. Eng., *12*, 457 (1962), and US Atomic Energy Comm. reports GA-2525 and GA-2527 (1961).
6. Levine, M. M., Nuclear Sci. Eng., *16*, 271 (1963).
7. Adler, D. B., and Adler, F. T., Trans. American Nuclear Society, *5*, (1), 53 (1962), and *5* (2), 407 (1962), and *6* (1), 37 (1963).
8. Goldstein, R., and Cohen, E. R., Nuclear Sci. Eng., *13*, 132 (1962).
9. Case, K. M., Placzek, G., and Dehoffman, F., *Introduction to the Theory of Neutron Diffusion*, US Govt. Printing Office, Washington, D.C. (1953).
10. Weinberg, A. M., and Wigner, E. P., *The Physical Theory of Neutron Chain Reactors*, Chap. 20, University of Chicago Press, Chicago, Illinois (1958).
11. Chernick, J., Proceedings of the First International Conference on the Peaceful Uses of Atomic Energy, P/603, Vol. 5, p. 215, United Nations (1955).
12. Argonne National Laboratory, *Reactor Physics Constants*, ANL-5800, Section 3.6, 2nd ed., US Government Printing Office, Washington, D.C. (1963).
13. Chernick, J., US Atomic Energy Comm. report BNL-622, p. 31 (1960).
14. Corngold, N., J. Nuclear Energy, *4*, 293 (1957) and US Atomic Energy Comm. report BNL-445 (1956).
15. Fukai, Y., Nuclear Sci. Eng., *13*, 345 (1962).
16. Amouyal, A., Benoist, P., and Horowitz, J., J. Nuclear Energy, *6*, 79 (1957).
17. Takahashi, H., Nuclear Sci. Eng., *5*, 338 (1959).
18. Honeck, H., and Kaplan, I., *ibid.*, *8*, 203 (1960).
19. Honeck, H., *ibid.*, *18*, 49 (1964).
20. Chernick, J., US Atomic Energy Comm. report BNL-433, p. 119 (1956), Proceedings of a Brookhaven Conference.
21. Spinney, K. T., *ibid.*, p. 103.
22. Rothenstein, W., Nuclear Sci. Eng., *7*, 162 (1960) and US Atomic Energy Comm. report BNL-563 (1959).
23. Bell, G. I., US Atomic Energy Comm. report LA-2322 (1959).
24. Dancoff, S. M., and Ginsburg, M., US Atomic Energy Comm. report CP-2157 (1944).
25. Carlvik, I., and Pershagen, B., US Atomic Energy Comm. report AE-16 (1959).
26. Thie, J. A., Nuclear Sci. Eng., *5*, 75 (1959).
27. Fukai, Y., *ibid.*, *9*, 370 (1961).
28. Velarde, G., *ibid.*, *15*, 99 (1963).
29. Sauer, A., *ibid.*, *16*, 329 (1963).
30. Bonalumi, R., Energia Nucleare, *8*, 326 /1961).
31. Dresner, L., *Resonance Absorption in Nuclear Reactors*, Pergamon Press, Oxford (1960).
32. Wigner, E. P., Creutz, E., Jupnik, H., and Snyder, T., J. Appl. Phys., *26*, 260 (1955).
33. Chernick, J., and Vernon, R., Nuclear Sci. Eng., *4*, 649 (1958).
34. Bell, G. I., *ibid.*, *5*, 138 (1959).
35. Nordheim, L. W., Proc. Symposia Applied Math., Vol. *11*, p. 58, Amer. Math. Soc., Providence (1961) and US Atomic Energy Comm. Report GA-638 (Rev.) (1959).
36. Creutz, E., Jupnik, H., Snyder, T., and Wigner, E. P., J. Appl. Phys., *26*, 257 (1955).
37. Dresner, L., Nuclear Sci. Eng., *1*, 501 (1956).
38. Bakshi, P., US Atomic Energy Comm. report BNL-4381 (1959).
39. Goldstein, R., and Brooks, H., Nuclear Sci. Eng. (to be published).
40. Aisu, H., and Minton, G. H., Nuclear Sci. Eng. (to be published).
41. Hasegawa, K., US Atomic Energy Comm. report ORNL-2705 (1959).
42. Gast, P., Nuclear Sci. Eng. (to be published).
43. Kelber, C. N., US Atomic Energy Comm. report ANL-6709 (1963).
44. Kier, P. H., Sc.D. Thesis, Massachusetts Institute of Technology (November 1963).
45. Hayes, W. T., Luming, M., and Zweifel, P. F., Trans. American Nuclear Society, *3* (2), 366 (1960).
46. Vaughan, E. U., *ibid.*, *4*, (2), 275 (1961).
47. Takahashi, H., and Corngold, N., *ibid.*, *3* (1), 230 (1960).
48. Iijima, S., Nuclear Sci. Eng., *17*, 42 (1963).
49. Rothenstein, W., *ibid.*, *8*, 122 (1960) and US Atomic Energy Comm. report BNL-4497 (1959).
50. Codd, J., and Collins, P. J., EAES Symposium on Advances in Reactor Theory, Part II, Paper III, p. 3, Karlsruhe (April 1963).

51. Kelber, C. N., Trans. American Nuclear Society, *6* (2), 273 (1963).
52. Garrison, J., US Atomic Energy Comm. report BNL-7402 (1964).
53. McKay, M. H., and Pollard, J. P., Nuclear Sci. Eng., *16*, 243 (1963).
54. Rothenstein, W., and Chernick, J., *ibid.*, *7*, 454 (1960).
55. Bell, G. I., *ibid.*, *9*, 409 (1961).
56. Lane, R. K., Nordheim, L. W., and Sampson, J. B., *ibid.*, *14*, 390 (1962).
57. Richtmyer, R. D., van Norton, R., and Wolfe, A., Proceedings of the Second International Conference on the Peaceful Uses of Atomic Energy, P/2489, Vol. 16, p. 180, United Nations (1958).
58. Davidson, P., *et al.*, US Atomic Energy Comm. report WCAP-1434 (1961).
59. Candelore, N. R., and Gast, R. C., US Atomic Energy Comm. report WAPD-TM-407 (1963)
60. Triplett, J. R., Merrill, E. T., and Burr, J. R., US Atomic Energy Comm. report HW-70049 (1961).
61. Fillmore, F. L., *Nuclear Performance of Power Reactor Cores*, San Francisco, California TID-7672, p. 157 (September 1963).
62. Foell, W. K., Grimesey, R. A., and Tong, S., Trans. American Nuclear Society, *6*, (2) 272 (1963).
63. Rief, H., US Atomic Energy Comm. report BNL-647 (1961).
64. Smith, G., Hardy, J. Jr., and Klein, D., Nuclear Sci. Eng., *8*, 449 (1960).
65. Seth, K. K., Hughes, D. J., Zimmerman, R. L., and Garth, R. C., Phys. Rev., *110*, 692 (1958).
66. Cooper, G. S., Garrison, J. D., and Hines, W. A., Trans. American Nuclear Society, *4* (2), 271 (1961).
67. Tiren, L. I., and Jenkins, J. M., UK Atomic Energy Authority report AEEW-R-1963 (1962).
68. Weitman, J., Nuclear Sci. Eng., *18*, 246 (1964).
69. Chernick, J., Honeck, H. C., Michael, P., Moore, S. P., and Srikantiah, G., *ibid.*, *13*, 205 (1962).
70. Nordheim, L. W., US Atomic Energy Comm. report GA-3973 (1963).
71. Sehgal, B., Trans. American Nuclear Society, *6* (1), 41 (1963).
72. Palevsky, H., Chrien, R. E., Haddad, E., and Lopez, W. M., Bull. Amer. Phys. Soc., Ser. 2, *9* (1), 20 (1964).
73. Hellstrand, E., and Weitman, J., Nuclear Sci. Eng., *9*, 507 (1961).
74. Pearce, R. M., J. Nuclear Energy, A *13*, 150 (1961).
75. Arnold, W. H., and Dannels, R. A., Trans. American Nuclear Society, *3* (1), 229 (1960).
76. Vernon, R., EAES Symposium on Advances in Reactor Theory, Part II, paper III, p. 4, Karlsruhe (April 1963).
77. Bardes, R., Brown, J., Pound, D., and Sampson, J., Trans. American Nuclear Society, *4* (2), 275 (1961).
78. Smith, R. I., US Atomic Energy Comm. report HW-71112 and Nuclear Sci. Eng. (to be published).
79. Haddad, E., Froehner, F., Friesenhahn, S. J., and Lopez, W. M., Bull. Amer. Phys. Soc., Ser. 2, *9* (1), 31 (1964).
80. Nichols, P. F., Nuclear Sci. Eng., *17*, 144 (1963).
81. Brown, H. L., Connolly, T. J., and Foell, W. K., Trans. American Nuclear Society, *5* (2), 375 (1961).
82. Foell, W. K., and Connolly, T. J. (to be presented at Annual Meeting of the American Nuclear Society, June 1964).
83. Hardy, J. Jr., Klein, D., and Smith, G. G., Nuclear Sci. Eng., *14*, 366 (1962).
84. Kouts, H., Sher, R., Brown, J. R., Klein, D., Stein, S., Hellens, R. L., Arnold, H., Ball, R. M., and Davison, P. W., Proceedings of the Second International Conference on the Peaceful Uses of Atomic Energy, P/1841, Vol. 12, p. 446, United Nations (1958).
85. Hellens, R. L., and Honeck, H. C., IAEA Conference on Light Water Lattices, Vienna (June 1962).
86. Price, G. L., IAEA Symposium on Exponential and Critical Experiments, Paper SM 42/27, Amsterdam (September 1963).
87. Pettus, W. G., US Atomic Energy Comm. report BAW-1244 (1962).
88. Hardy, J., Smith, G. G., and Klein, D., Nuclear Sci. Eng., *14*, 358 (1962).
89. Hellstrand, E., and Lundgren, C., *ibid.*, *12*, 435 (1962).
90. Moore, P. G. F., Pattenden, S. K., and Tattersall, R. B., UK Atomic Energy Authority report AEEW R57 (1961).
91. Hellstrand, E., J. Appl. Phys., *28*, 1493 (1957).
92. Pettus, W. G., US Atomic Energy Comm. report BAW-1286 (1963).
93. Rothman, A. B., and Ward, C. E., Nuclear Sci. Eng., *12*, 293 (1962).
94. Hellstrand, E., Blomberg, P., and Horner, S., *ibid.*, *8*, 497 (1960).
95. Palowitch, B. L., and Frantz, F. S., *ibid.*, *15*, 146 (1963).
96. Spano, A. H., *ibid.* (to be published about April 1964).
97. Sampson, J. B., US Atomic Energy Comm. report GA-3069 (1962).
98. Tattersall, R. B., Rose, H., Pattenden, S. K., and Jowitt, D., J. Nuclear Energy, *12A*, 32 (1960).
99. Macklin, R. L., and Pomerance, H. S., *ibid.*, *2*, 243 (1956).
100. Johnston, F. J., Halperin, J., and Stoughton, R. V., *ibid.*, *11A*, 95 (1960).

ABSTRACT—RÉSUMÉ—АННОТАЦИЯ—RESUMEN

A/262 Etats-Unis d'Amérique

Evolution de la théorie et des calculs de l'absorption par résonance

par J. Chernick et M. M. Levine

On a beaucoup amélioré depuis 1958 les méthodes analytiques de calcul de l'absorption par résonance des neutrons dans les réacteurs. Ces progrès sont dus notamment à d'importants travaux sur les corrections du deuxième ordre, aux formules de Goldstein et Cohen pour la résonance intermédiaire et au code numérique de Nordheim pour la solution directe d'une fonction intégrale de l'énergie.

L'étroite analogie entre les intégrales concernant les ensembles homogènes et hétérogènes a conduit à une série de théorèmes d'équivalence qui sont, dans l'ensemble, de plus en plus précis. Pour les réseaux très compacts, le facteur de correction de Dancoff est important. Dans les déterminations relatives aux réseaux de barreaux, les améliorations sont l'œuvre de plusieurs chercheurs, et on a trouvé des relations d'équivalence améliorées pour différents barreaux comprenant de l'uranium dans l'eau ordinaire et barreaux d'uranium métallique dans l'eau lourde et le graphite.

A mesure qu'on se rendait mieux compte de la précision de ces méthodes théoriques, on mettait au point des expériences intégrales plus précises pour vérifier les différents aspects de la théorie, et il en est résulté une augmentation notable de la précision de ces expériences intégrales. On a pu également améliorer de façon considérable les mesures expérimentales des coefficients Doppler. L'importance des coefficients Doppler pour la sûreté des grands réacteurs à neutrons rapides a suscité un vif intérêt pour leur mesure et pour l'obtention de données plus précises sur la résonance neutronique dans la région statistique.

Les modèles actuels de calculatrices numériques à très grande vitesse ont développé l'utilisation des méthodes de Monte Carlo. On a éliminé un grand nombre des limitations imposées par le premier programme REP, notamment celles qui portaient sur le nombre d'absorbeurs par résonance et sur les données géométriques. Toutefois, on n'a pas encore résolu la difficulté due au fait que l'on ne dispose pas d'une représentation satisfaisante des effets d'interférence à plusieurs niveaux dans le domaine des résonances rapprochées des matières fissiles. On espère que les efforts concertés tentés actuellement pour mesurer la structure de la résonance aux faibles énergies et les méthodes améliorées d'ajustement des courbes permettront certains progrès dans ce domaine. Le code Monte Carlo MOCCA a permis d'étudier avec une bonne précision la capture par résonance aux hautes énergies. D'autres études ont expliqué les différences qui existent entre la capture par résonance dans un spectre $1/E$ et celles d'un réseau de réacteur réel.

L'absorption par résonance dans les réseaux à eau a été étudiée de manière approfondie, et les résultats des calculs ont permis d'améliorer la précision avec laquelle les propriétés nucléaires d'un réseau peuvent être prévues. D'autres modérateurs font actuellement l'objet d'études similaires. On n'a pas encore bien vérifié si certaines méthodes simples pouvaient être appliquées aux grappes de barreaux.

A/262 США

Успехи в теории резонансного поглощения

Дж. Черник, М. М. Левин

С 1958 года аналитические методы расчета резонансного поглощения нейтронов в ядерных реакторах получили существенное развитие. В этой связи следует отметить большую работу по вычислению поправок второго порядка, формулы Гольдстейна и Коэна для промежуточных резонансов и вычислительную программу Нордхейма для прямого решения интегрального уравнения, зависящего от энергии.

Аналогия между интегральными уравнениями для гомогенных и гетерогенных систем привела к ряду все более точных теорем эквивалентности. Для плотных решеток весьма существенна поправка Данкова. Уточнение этой поправки для стержневых решеток было сделано несколькими авторами, причем были разработаны уточненные соотношения эквивалентности для ряда решеток из урансодержащих стержней в воде и металлических урановых стержней в тяжелой воде и в графите.

По мере выявления точности теоретических методов разрабатывались и более точные интегральные опыты для изучения разных сторон теории. Значительные усовершенствования были достигнуты в экспериментальных измерениях допплеровских коэффициентов. Важность допплеровских коэффициентов для обеспечения безопасности больших реакторов на быстрых нейтронах возбудила значительный интерес к их измерению и получению уточненных данных о нейтронных резонансных параметрах в статистической области.

Появление быстродействующих счетно-решающих цифровых машин открыло в последнее время возможность широкого использования метода Монте-Карло. Многие из ограничений, имевших место в первой программе такого рода — программе REP, до известной степени сняты, в том числе ограничение количества ре-

зонансных поглотителей и ограничения, связанные с расчетом геометрии. Одним из оставшихся затруднений является отсутствие метода правильного описания интерференционных эффектов между уровнями для случая близкорасположенных резонансов в делящихся материалах. Однако и в этой области ожидается успех как благодаря усилиям, направленным на измерение резонансной структуры в области низких энергий, так и благодаря усовершенствованию методов описания экспериментальных данных аналитическими формами. В области высоких энергий возможность рассмотрения резонансного поглощения с удовлетворительной точностью открылась с появлением программы расчета методом Монте-Карло МОССА. Другие исследования позволили выявить причины различия между резонансным захватом на фермиевском спектре и захватом в реакторной решетке.

Резонансное поглощение в водяных решетках было тщательно изучено, и результаты этих расчетов помогли увеличить точность расчета ядерных свойств таких решеток. Подобные исследования продолжаются для других замедлителей. Применимость простых методов при решении задач для случая ансамблей стержней до сих пор еще не проверена.

A/262 Estados Unidos de América

Progresos acerca de absorción de resonancia

por J. Chernick y M. M. Levine

Desde 1958 se han perfeccionado notablemente los métodos analíticos para el cálculo de la absorción de resonancia de neutrones en los reactores. Los progresos realizados incluyen extenso trabajo sobre correcciones de segundo orden, las fórmulas para resonancias intermedias de Goldstein y Cohen y el programa de cálculo numérico de Nordheim para la solución directa de una ecuación integral con dependencia respecto de la energía.

La estrecha analogía entre las ecuaciones integrales para sistemas homogéneos y heterogéneos ha conducido a una serie de teoremas de equivalencia cada vez más restrictivos. En redes compactas llega a ser importante la corrección de Dancoff. Varios autores han hecho progresos en su determinación para el caso de redes de barras y han obtenido relaciones de equivalencia más convenientes para una serie de redes de barras que llevan uranio, en agua, y de barras de uranio metálico, en D_2O y grafito.

A medida que se ha difundido la precisión que dan los métodos teóricos; se han diseñado experimentos integrales más precisos para comprobar diferentes aspectos de la teoría que han supuesto importantes progresos en la precisión de estos resultados experimentales. Se ha alcanzado un notable progreso también en las medidas experimentales de coeficientes Doppler. La importancia de los coeficientes Doppler en la seguridad de grandes reactores rápidos ha estimulado un interés considerable en su medida y en la obtención de mejores datos para las resonancias de neutrones en la región estadística.

La disponibilidad de calculadoras digiatles de alta velocidad han ampliado el uso de los métodos de Monte Carlo. Muchas de las limitaciones del primitivo programa REP han desaparecido, incluyendo limitaciones en el número de absorbentes de resonancia y en las rutinas geométricas. Todavía persiste la dificultad de no disponer de una representación adecuada de los efectos de interferencia entre multiniveles en las resonancias apiñadas de los materiales fisibles. Se esperan progresos del actual esfuerzo combinado tanto en medidas de la estructura de las resonancias de baja energía como en mejores métodos de ajuste de curvas experimentales. El programa de Monte Carlo, MOCCA, perfeccionado, ha hecho posible investigar capturas de resonancia de alta energía con una buena precisión. Otros estudios han aclarado las diferencias entra la captura de resonancia en un espectro $1/E$ y la que aparece en los reactores reales.

Se ha estudiado detalladamente la absorción de resonancias en redes en agua. Los resultados de estos cálculos han ayudado a mejorar la precisión con la cual pueden predecirse las propiedades nucleares de estas redes. Están en marcha estudios análogos para otros moderadores. Todavía no se ha comprobado adecuadamente la bondad de métodos sencillos para tratar con haces de barras.

Влияние резонансной структуры сечений на распространение и замедление нейтронов в средах и резонансные эффекты на делящихся элементах

Л. П. Абагян, Н. О. Базазянц, И. И. Бондаренко, А. Г. Гусейнов, А. А. Лукьянов, У. М. Маханов, В. И. Мелентьев, М. Н. Николаев, В. В. Орлов, Н. С. Работнов, А. П. Суворов, Л. Н. Усачев, В. В. Филиппов

Важность учета резонансной структуры сечений и особенно сечения U^{238} была понята в самых первых работах по теории цепной реакции на тепловых нейтронах. Соответствующая теория применительно к расчету тепловых реакторов разрабатывалась многими авторами [1-6] В 1957 г. И. И. Бондаренко обратил внимание на необходимость учета резонансных эффектов при изучении физики реакторов на быстрых нейтронах. Впоследствии это было подтверждено результатами макроскопических экспериментов [7,8] и их расчетом.

В настоящем докладе дается обобщенная формулировка основных результатов работ по изучению физических эффектов, связанных с резонансной структурой сечений, и методов их учета при реакторных расчетах. Часть этих результатов была опубликована ранее [7-15] и использовалась при составлении системы многогрупповых констант [16] для расчета быстрых и промежуточных реакторов и защиты. Вопросы, связанные с теоретическим и экспериментальным изучением резонансного захвата в гетерогенных тепловых реакторах, здесь не рассматриваются.

УЧЕТ РЕЗОНАНСНОЙ СТРУКТУРЫ СЕЧЕНИЙ ПРИ РАСЧЕТАХ ЯДЕРНЫХ РЕАКТОРОВ

В энергетическом спектре нейтронов, формирующемся при их распространении в веществе, можно выделить две характерные особенности. Во-первых, нейтронный поток испытывает резкие резонансные изменения, соответствующие резонансной структуре сечений, которые образуют как бы «микроструктуру» спектра. Во-вторых, поглощение, диффузия нейтронов и наличие источников приводят к более или менее плавному изменению среднего потока нейтронов, к его отклонению от спектра Ферми.

Определение пространственно-энергетических распределений нейтронов в средах при плавно изменяющихся сечениях может быть выполнено различными известными методами. Что же касается расчета «микроструктуры» нейтронного спектра, то точное решение этой задачи требует прежде всего знания детального хода нейтронных сечений во всей энергетической области, представляющей интерес для реакторных задач, и поэтому в настоящее время невозможно.

К счастью, конечной целью расчетов почти всегда является определение характеристик, усредненных по большому числу резонансов (иногда, правда, требуется детальное знание нейтронного потока в окрестностях нескольких первых сильных резонансов, однако число таких резонансов невелико и их индивидуальный учет не представляет особых трудностей). Для решения этих задач достаточно знать поток нейтронов $\vec{\varphi}(\vec{r}, u, \vec{\Omega})$, усредненный по резонансным особенностям. При этом для определения средних чисел процессов, происходящих в среде, необходимо использовать сечения, усредненные с весом нейтронного потока:

$$\bar{\Sigma}_x = \frac{\int_{\Delta u} \Sigma_x(u)\,\varphi(\vec{r}, u, \vec{\Omega})\,du}{\int_{\Delta u} \varphi(\vec{r}, u, \vec{\Omega})\,du} \qquad (1)$$

(индекс x означает тип реакции — деление, захват и пр.). Определенные таким образом средние сечения оказываются, вообще говоря, зависящими от направления и координат, и, что самое главное, для их определения необходимо знать форму нейтронного спектра $\varphi(\vec{r}, u, \vec{\Omega})$, которая заранее неизвестна.

Однако если диффузия и (или) интервал усреднения настолько малы, что

$$\left| D \frac{\nabla^2 \varphi}{\varphi} \right| \ll \Sigma_a + \frac{\xi \Sigma_s}{\Delta u} \qquad (2)$$

(но в то же время Δu достаточно велико, чтобы усреднение приводило к сглаживанию сечений), $\varphi(\vec{r}, u, \vec{\Omega})$ для одномерной геометрии может быть представлено в виде

$$\varphi(\vec{r}, u, \vec{\Omega}) = \frac{1}{4\pi} \sum_l (2l+1) \bar{\varphi}_l(u, \vec{r}) \Phi_l(u) P_l(\mu), \qquad (3)$$

где $\bar{\varphi}_l$ — плавная функция u, а $\Phi_l(u) = \frac{\varphi_l(u, \vec{r})}{\bar{\varphi}_l(u, \vec{r})}$ описывают микроструктуру спектров сферических гармоник и определяются только сечениями среды. Отметим, что, хотя условие (2) является по существу условием применимости диффузионного приближения, усредненные с этим условием сечения могут использоваться и в более высоких приближениях.

Условие (2) обычно может быть выполнено, если рассматриваются области, достаточно удаленные от границ раздела сред и от концентрированных источников нейтронов. Для описания распространения нейтронов в этих областях могут быть использованы заранее составленные усредненные константы. Задача более точного нахождения распределений нейтронных потоков вблизи границ требует при этом специального рассмотрения (так же как и задача определения потоков в средах с глубокими интерференционными провалами в сечении, для которых условие (2) также не может быть выполнено).

Ограничимся рассмотрением широкого круга реакторных задач, в которых условие (3) может быть выполнено.

Кинетическое уравнение в l-представлении. Система уравнений для моментов $\varphi_l(x, u)$ имеет вид (для простоты рассмотрим плоско-параллельную задачу)

$$\left.\begin{aligned} &\varphi_0 \Sigma + \frac{\partial \varphi_1}{\partial x} = Q_0(x, u) + \sum_i \int \varphi_0(x, u') \times \\ &\quad \times \Sigma^i_{S0}(u' \to u)\, du' + \int \varphi_0(x, u') \times \\ &\quad \times \Sigma_{in0}(u' \to u)\, du', \\ &\varphi_l \Sigma + \frac{1}{2l+1} \left\{ (l+1) \frac{\partial \varphi_{l+1}}{\partial x} + l \frac{\partial \varphi_{l-1}}{\partial x} \right\} = \\ &\quad = \sum_i \int \varphi_l(x, u') \Sigma^i_{Sl}(u' \to u)\, du' + \\ &\quad + \int \varphi_l(x, u') \Sigma_{inl}(u' \to u)\, du'. \end{aligned}\right\} \qquad (4)$$

Здесь $l = 1, 2, \ldots$; Σ — полное сечение; Σ^i_{Sl} и Σ_{inl} l-е гармоники сечения упругого рассеяния на i-м компоненте среды и сечения неупругого рассеяния.

Поскольку $\partial \varphi_1 / \partial x$ по предположению мало, а Q_0 и интегралы в правой части уравнения для φ_0 являются плавными функциями энергий, то в пределах малого интервала усреднения мы можем принять спектр потока нейтронов $\varphi_0 = \psi/\Sigma\,(u) \sim 1/\Sigma\,(u)$, где ψ — плотность столкновений.

Аналогичные рассуждения приводят к

$$\varphi_l(u) \approx \sum_{n=0}^{l} \frac{a_{l-n}}{\Sigma^{n+1}(u)}, \qquad (5)$$

где коэффициенты a_{l-n} определяются (с точностью до постоянной) рекуррентной формулой

$$a_{l-n} = \frac{1}{1 - \left\langle \frac{\Sigma_{sf_l}}{\Sigma} \right\rangle} \sum_{n=0}^{l-1} \left\langle \frac{\Sigma_{sf_l}}{\Sigma^{n+2}} \right\rangle a_{l-n-1}. \qquad (6)$$

Здесь

$$\Sigma_{sf_l} = \sum_i \int \Sigma^i_{Sl}(u' \to u)\, du'.$$

Усредняя уравнения (4), получим систему уравнений для $\bar{\varphi}_l(x, u)$:

$$\left.\begin{aligned} &\bar{\varphi}_0 \bar{\Sigma}_0 + \frac{\partial \bar{\varphi}_1}{\partial x} = Q_0 + \sum_i \int \bar{\varphi}_0(x, u') \times \\ &\quad \times \bar{\Sigma}^i_{S0}(u' \to u)\, du' + \\ &\quad + \int \bar{\varphi}_0(x, u') \bar{\Sigma}_{in0}(u' \to u)\, du', \\ &\bar{\varphi}_l \bar{\Sigma}_l + \frac{1}{2l+1} \left\{ (l+1) \frac{\partial \bar{\varphi}_{l+1}}{\partial x} + l \frac{\partial \bar{\varphi}_{l-1}}{\partial x} \right\} = \\ &\quad = \sum_i \int \bar{\varphi}_l(x, u') \bar{\Sigma}^i_{Sl}(u' \to u)\, du' + \\ &\quad + \int \bar{\varphi}_l(x, u') \bar{\Sigma}_{inl}(u' \to u)\, du', \end{aligned}\right\} \qquad (7)$$

где усредненные сечения определяются формулами

$$\left.\begin{aligned} &\bar{\Sigma}_l = \frac{\langle \varphi_l \Sigma \rangle}{\langle \varphi_l \rangle}; \quad \bar{\Sigma}^i_{Sl}(u' \to u) = \\ &\quad = \frac{\langle \Sigma^i_{Sl}(u' \to u) \varphi_l(u') \rangle}{\langle \varphi_l(u') \rangle}, \\ &\bar{\Sigma}_x = \frac{\left\langle \frac{\Sigma_x}{\Sigma} \right\rangle}{\left\langle \frac{1}{\Sigma} \right\rangle}; \quad \bar{\Sigma}_{in_l}(u' \to u) = \\ &\quad = \frac{\langle \Sigma_{inl}(u' \to u) \varphi_l(u') \rangle}{\langle \varphi_l(u') \rangle}, \end{aligned}\right\} \qquad (8)$$

а $\varphi_l(u)$ — формулой (5).

Кроме условия (2), изложенный метод усреднения основывается на ряде предположений.

1. Пренебрегается изменением плотности столкновений в интервале усреднения Δu за счет плачековских осцилляций спектра за каж-

дым из резонансов. Эти осцилляции приводят к изменениям микроструктуры спектра нейтронов, в частности к отклонению $\varphi_0(u)$ от $1/\Sigma(u)$, что не трудно учесть в рамках изложенного метода усреднения. Однако влияние этого эффекта едва ли может оказаться существенным в области энергий, где применим статистический подход к учету резонансной структуры сечений. Действительно, вклад каждого отдельного резонанса в плотность столкновений мал, а учет распределения расстояний между уровнями и сравнительно быстрое изменение с энергией отношения этого расстояния к потере энергии нейтрона при рассеянии приводят к сглаживанию плотности столкновений. Этот эффект может оказаться заметным лишь для нескольких низколежащих резонансов, требующих индивидуального рассмотрения.

2. Предполагается, что резонансы можно считать узкими по сравнению с потерей энергии нейтронов при рассеянии. Как правило, это условие не выполняется лишь для нескольких первых резонансов, которые, как отмечалось, следует рассматривать отдельно.

3. Для определения спектра $\varphi_l(u)$ в интервале Δu в интегральных членах уравнений (4) полагалось $\int \bar{\varphi}_l(u')\,\overline{\Sigma}_{Sl}(u'\to u)\,du' \approx \approx \langle\varphi_l\Sigma_S f_l\rangle$, что может заметно нарушаться при больших потерях энергии (рассеяние на водороде, неупругое рассеяние). Более точный учет спектра $\varphi_l(u)$ при усреднении сечений может быть выполнен с помощью последовательных приближений.

Приближение Грюлинга — Гертцеля. Часто встречаются системы, в которых анизотропия нейтронного потока велика лишь в области высоких энергий, где замедление в основном определяется неупругим рассеянием. При этом для учета упругого замедления можно воспользоваться приближением Грюлинга — Гертцеля, которое приводит к уравнениям:

$$\begin{aligned}
&\frac{\partial}{\partial u}\left\{\left[\bar{\xi}\overline{\Sigma}_S\left(1-\frac{\partial\bar{\gamma}}{\partial u}\right)+\bar{\gamma}(\overline{\Sigma}_a+\overline{\Sigma}_{in}+\overline{\Sigma}_f)\right]\bar{\varphi}_0-\right.\\
&\left.-\bar{\gamma}\left[-\frac{\partial\bar{\varphi}_1}{\partial x}+Q_0+\int\bar{\varphi}_0\overline{\Sigma_{in}f_{in0}}\,du'\right]\right\}+\\
&+\bar{\varphi}_0(\overline{\Sigma}_a+\overline{\Sigma}_{in}+\overline{\Sigma}_f)=\\
&=Q_0-\frac{\partial\bar{\varphi}_1}{\partial x}+\int\bar{\varphi}_0\overline{\Sigma_{in}f_{in0}}\,du',\\
&\bar{\varphi}_1[\overline{\Sigma}_1-\overline{\Sigma_S f_1}]+\frac{1}{3}\left[\frac{\partial\bar{\varphi}_0}{\partial x}+2\frac{\partial\bar{\varphi}_2}{\partial x}\right]=\\
&=\int\bar{\varphi}_1\overline{\Sigma_{in}f_{in1}}\,du'-\frac{\partial}{\partial u}(\bar{\varphi}_1\bar{\chi}_{11}\overline{\Sigma}_S),\\
&\bar{\varphi}_l[\overline{\Sigma}_l-\overline{\Sigma_S f_l}]+\frac{1}{2l+1}\left[l\frac{\partial\bar{\varphi}_{l-1}}{\partial x}+(l+1)\frac{\partial\bar{\varphi}_{l+1}}{\partial x}\right]=\\
&=\int\bar{\varphi}_l\overline{\Sigma_{in}f_{inl}}\,du'.
\end{aligned}\qquad(9)$$

Замедление нейтронов при упругом рассеянии на легких ядрах может быть при необходимости рассмотрено в системе (9) так же, как неупругое рассеяние.

Если обозначить моменты функции рассеяния $f(\mu_0, u, u'\to u)$ через

$$\chi_{ln}(u)=\int(u'\to u)^n\,du'\int P_l(\mu)\,f(\mu,u,u'\to u)\,d\vec{\Omega},\qquad(10)$$

то коэффициенты уравнения (9), используя формулы усреднения (8), можно записать в виде

$$\left.\begin{aligned}
&\bar{\xi}=\frac{\left\langle\frac{\sum_i\chi^i_{01}\Sigma^i_S}{\Sigma}\right\rangle}{\left\langle\frac{\Sigma_S}{\Sigma}\right\rangle},\quad\bar{\gamma}=\frac{\left\langle\frac{\sum_i\chi^i_{02}\Sigma^i_S}{\Sigma}\right\rangle}{4\left\langle\frac{\sum_i\chi^i_{01}\Sigma^i_S}{\Sigma}\right\rangle},\\
&\bar{\chi}_{11}=\frac{\left\langle\varphi_1\sum_i\chi^i_{11}\Sigma^i_S\right\rangle}{\langle\Sigma_S\varphi_1\rangle},\quad\overline{\Sigma_S f_l}=\frac{\left\langle\varphi_l\sum_i\chi^i_{l0}\Sigma^i_S\right\rangle}{\langle\varphi_l\rangle}.
\end{aligned}\right\}\qquad(11)$$

Моменты χ_{ln} можно найти из следующих формул:
для водорода

$$\chi_{01}=1,\ \chi_{02}=2,\ \chi_{10}=\frac{2}{3},\ \chi_{11}=\frac{4}{9};\qquad(12)$$

для ядер с $A\gg 1$

$$\chi_{01}=\frac{2}{A}[1-\chi_{10}(u)],$$

$$\chi_{02}=\frac{16}{3A^2}\left[1-\frac{2}{3}\chi_{10}(u)+\frac{1}{2}\chi_{20}(u)\right],$$

$$\chi_{11}=-\frac{2}{3A}[1-3\chi_{10}(u)+2\chi_{20}(u)],$$

где χ_{10} и χ_{20} — моменты измеряемого в опытах по рассеянию углового распределения нейтронов.

Поскольку усредненные таким образом сечения и поток нейтронов являются достаточно плавно изменяющимися функциями энергии, то переход к некоторому конечно-разностному представлению (например, к многогрупповому) может быть осуществлен методами, разработанными для случая плавных сечений [17]. В нашу задачу не входит рассмотрение этих методов.

Кинетическое уравнение Больтцмана. Наряду с решением задачи переноса в представлении сферических гармоник в практических расчетах получили распространение методы прямого численного решения кинетического уравнения Больтцмана (S_n-метод [27], метод Владимирова [28] и др.). Поэтому представляется целесообразным записать такое уравнение для усредненного по резонансам потока нейтронов $\bar{\varphi}(x, u, \mu)$.

Для этого мы можем воспользоваться результатами, полученными выше, «свернув» си-

стему (7). Умножив l-е уравнение этой системы на $P_l(\mu)(2l+1)/4\pi$ и суммируя уравнения, получим

$$\sum_{l=0}^{\infty} \frac{2l+1}{4\pi} \bar{\Sigma}_l \bar{\varphi}_l P_l(\mu) + \mu \frac{\partial \bar{\varphi}}{\partial x} =$$

$$= \frac{1}{4\pi} Q + \sum_i \int \bar{\varphi}(x, u', \mu') \bar{\Sigma}_S^i(u' \to u, \mu_0)\, du'\, d\bar{\Omega}' +$$

$$+ \int \varphi(x, u', \mu')\, \bar{\Sigma}_{in}(u' \to u, \mu_0)\, du'\, d\bar{\Omega}', \quad (13)$$

где

$$\bar{\Sigma}_S^i(u' \to u, \mu_0) = \sum_{l=0}^{\infty} \frac{2l+1}{4\pi} \bar{\Sigma}_{Sl}^i(u' \to u) P_l(\mu_0)$$

и аналогично $\bar{\Sigma}_{in}$. Сумма в левой части полученного уравнения может быть представлена следующим образом. Пусть при $l \to \infty$ $\bar{\Sigma}_l \to \Sigma_\infty$. Тогда эта сумма есть

$$\sum_{l=0}^{\infty} \frac{2l+1}{4\pi} (\bar{\Sigma}_l - \Sigma_\infty) \bar{\varphi}_l P_l(\mu) +$$

$$+ \Sigma_\infty \sum_{l=0}^{\infty} \frac{2l+1}{4\pi} \bar{\varphi}_l P_l(\mu) = \int \bar{\varphi}(x, \mu', u) \times$$

$$\times \Sigma'(u, \mu_0)\, d\bar{\Omega}' + \Sigma_\infty \bar{\varphi}(x, u, \mu), \quad (14)$$

где

$$\Sigma'(u, \mu_0) = \sum_{l=0}^{\infty} \frac{2l+1}{4\pi} (\bar{\Sigma}_l - \Sigma_\infty) P_l(\mu_0).$$

Таким образом, эффект резонансной структуры полного сечения оказался эквивалентным некоторому дополнительному упругому рассеянию нейтронов с сечением $[-\Sigma'(u, \mu_0)]$ одновременно с перенормировкой полного сечения: $\Sigma \to \Sigma_\infty$. Заметим, что

$$\Sigma_\infty = \lim_{l\to\infty} \bar{\Sigma}_l = \lim_{l\to\infty} \frac{\langle \Sigma \varphi_l \rangle}{\langle \varphi_l \rangle}.$$

Например, при изотропном упругом рассеянии на ядрах $\varphi_l \sim \frac{1}{\Sigma^{l+1}}$ и $\Sigma_\infty = \lim_{l\to\infty} \frac{\left\langle \frac{1}{\Sigma^l} \right\rangle}{\left\langle \frac{1}{\Sigma^{l+1}} \right\rangle} =$ $= \Sigma_{\min}$, где $\Sigma_{\min}$—минимальное сечение в интервале усреднения.

Усреднение микроскопических сечений отдельных элементов. Для проведения массовых расчетов реакторных систем весьма желательно иметь систему заранее составленных усредненных сечений отдельных элементов, используемых в реакторостроении, с тем чтобы на основе этой системы могли вычисляться макроскопические сечения для любых реакторных систем. В связи с этим встает вопрос, как следует усреднять микроскопические сечения элементов для того, чтобы получить правильные средние значения макроскопических характеристик среды, состоящей из смеси этих элементов. Эта задача может быть решена строго лишь в случае, когда в каждом интервале усреднения лишь одна из компонент смеси обладает резонансной структурой сечений. В этом случае средние значения макроскопических сечений среды (8) будут получены правильно, если величины $\langle 1/\Sigma^n \rangle$, $\langle \Sigma_{Sl}(u' \to u)/\Sigma^n \rangle / \langle 1/\Sigma^n \rangle$ и т. п. вычислять следующим образом:

$$\left\langle \frac{1}{\Sigma^n} \right\rangle^{-\frac{1}{n}} = \sum_i N_i \langle \sigma^i \rangle_n,$$

$$\frac{\left\langle \frac{\Sigma_{Sl}(u' \to u)}{\Sigma^n} \right\rangle}{\left\langle \frac{1}{\Sigma^n} \right\rangle} = \sum_i N_i \langle \sigma_{Sl}^i(u' \to u) \rangle_n, \quad (15)$$

где

$$\langle \sigma^i \rangle_n = \left\langle \frac{1}{(\sigma^i + \tilde{\sigma})^n} \right\rangle^{-\frac{1}{n}} - \tilde{\sigma};$$

$$\langle \sigma_{Sl}^i(u' \to u) \rangle_n = \frac{\left\langle \frac{\sigma_{Sl}(u' \to u)}{(\sigma^i + \tilde{\sigma})^n} \right\rangle}{\left\langle \frac{1}{(\sigma^i + \tilde{\sigma})^n} \right\rangle}; \quad (16)$$

N_i— плотность ядер i-й компоненты смеси; $\tilde{\sigma}$ — полное сечение всех остальных компонентов смеси, приходящееся на одно ядро рассматриваемого элемента.

В случае, когда смесь содержит несколько элементов с флуктуирующими сечениями, результаты усреднения макроскопических сечений зависят от взаимного положения резонансов этих элементов. В этом случае средние сечения среды могут быть представлены через усредненные сечения отдельных элементов лишь приближенно. Погрешность этого приближения оказывается наименьшей, если при усреднении микроскопических сечений каждого элемента по формулам (16) под $\tilde{\sigma}$ понимать среднее полное сечение всех остальных компонент среды, приходящееся на одно ядро рассматриваемого элемента. Конкретные расчеты показывают, что эта погрешность, как правило, меньше, чем ошибки, связанные с неточностью экспериментальных данных.

Задание результатов усреднения сечений отдельных элементов в зависимости от «сечения разбавления» $\tilde{\sigma}$ позволит вычислить макроскопические константы в любой среде, состоящей из этих элементов [16].

Метод подгрупп. В изложенной выше методике учета резонансной структуры сечений предполагалось, что структура нейтронного спектра в среде постоянна. Несмотря на то что это приближение имеет, как отмечалось, широкую область применимости, существуют случаи, когда структура нейтронного спектра, а стало быть и усредненные сечения (8) существенно зависят от координат. Такая ситуация имеет место во всех случаях, когда в нейтронный поток значительный вклад дают нейтроны,

не испытавшие ни одного столкновения (иногда несколько столкновений) с ядрами рассматриваемой среды (вблизи источников или границы раздела сред, в средах, имеющих глубокие интерференционные провалы в сечении).

В этих случаях информация о структуре сечений, содержащаяся в зависимостях усредненных сечений (16) от величины «сечения разбавления» $\tilde{\sigma}$, оказывается, строго говоря, недостаточной. Для введения более полной информации, необходимой для решения отмеченных задач, может быть использован так называемый метод подгрупп [14], описание которого будет более наглядным, если предположить, что плавная энергетическая зависимость нейтронного потока описывается многогрупповым методом.

Рассмотрим группу нейтронов, энергии которых лежат в интервале ΔE. Разобьем эту группу на несколько подгрупп, объединяя в каждую из них те нейтроны, для которых величина полного сечения лежит в небольших интервалах $(\Delta\sigma)_k$. Припишем теперь всем нейтронам каждой подгруппы одинаковые — средние — значения полного сечения, сечений реакций и дифференциальных сечений рассеяния. Если интервалы $(\Delta\sigma)_k$ достаточно малы, то полные сечения будут близки к истинным. В известной степени это будет иметь место и для парциальных сечений, поскольку между ними и полным сечением существует определенная корреляция.

Распространение рассматриваемой группы в протяженной среде с малым градиентом может быть описано обычными методами с использованием констант (16), вычисление которых производится усреднением по подгруппам. Если же структура спектра в среде не постоянна (и, следовательно, соотношение между долями подгрупп зависит от координат), то следует производить расчет распространения каждой подгруппы отдельно.

Для этого должны быть заданы дополнительно сечения переходов из одной подгруппы в другую за счет упругого и неупругого рассеяния и деления. Вычисление сечений перехода, обусловленных двумя последними процессами, не представляет принципиальных трудностей, поскольку происходящее при этих процессах изменение энергии нейтронов значительно превосходит расстояние между резонансами.

Что же касается сечений перехода в результате упругого замедления, то при его вычислении необходимо принимать во внимание соотношение между потерей энергии при рассеянии и расстоянием между уровнями. В области разрешенных уровней сечения перехода могут быть получены из имеющихся данных о детальном ходе сечений. В более высокой области энергий для этой цели необходимо привлекать статистическое рассмотрение, основанное на данных о средних резонансных параметрах. Наконец, при еще больших энергиях, где потеря энергии при упругом рассеянии превышает расстояние между уровнями, вероятности упругих переходов становятся пропорциональными долям тех подгрупп, в которые осуществляется переход.

Переходы нейтронов из каждой подгруппы могут осуществляться в любую подгруппу данной группы, что существенно усложняет расчет. Процедура расчета пространственно-энергетического распределения нейтронов должна заключаться в последовательном решении взаимосвязанных систем уравнений для подгрупп методами, аналогичными тем, которые используются при решении задач о термализации нейтронов.

Следует, однако, отметить, что число подгрупп, на которые следует разбивать группы, может быть небольшим. Например, для вычисления усредненных параметров P_1- или P_3-приближений достаточно разбиения на две или соответственно на три подгруппы.

РАСЧЕТ УСРЕДНЕННЫХ СЕЧЕНИЙ

Как было показано выше, для определения среднегрупповых параметров среды необходимо знание различным образом усредненных сечений (15). Определение этих величин из экспериментальных данных об энергетической зависимости сечений возможно лишь в области низких энергий, где структура сечений изучена достаточно подробно. При этом следует отметить, что величина таких параметров, как $\langle 1/\sigma^n \rangle$, определяется в основном теми энергетическими областями, в которых полное сечение мало и поэтому, как правило, измеряется с низкой точностью.

В связи с этим возникает задача о восстановлении формы кривой энергетической зависимости сечений по имеющимся экспериментальным данным, полученным с плохим разрешением, на основании теоретических представлений о структуре сечений.

Структура сечений в области изолированных резонансов. Строгое решение этой задачи возможно лишь в области изолированных уровней. Как известно, энергетическая зависимость сечений в окрестности изолированного уровня определяется формулами Брейта — Вигнера:

$$\sigma = \frac{\sigma_0}{1+x^2}(\cos 2\varphi_l - x \sin 2\varphi_l) + \sigma_p = \sigma_r + \sigma_p, \tag{17а}$$

$$\sigma_x = \frac{\sigma_0}{1+x^2}\frac{\Gamma_x}{\Gamma}, \tag{17б}$$

$$d\sigma_S = \lambda\!\!\!^{-2} d\Omega \sum_L P_L(\mu)\left[B_L^{nn} + \sum_j \frac{B_L(j) - A_L(j) - xI_L(j)}{2(2I+1)(1+x^2)}\right] = \frac{1}{4\pi} d\Omega \sum_L P_L(\mu) \times \times (f_{Lp}\sigma_p + f_{Lr}\sigma_{Sr})(2L+1), \tag{17в}$$

где

$$\sigma_0 = 4\pi\lambda^2 \left[\frac{2J+1}{2(2I+1)}\right] \frac{\Gamma_n}{\Gamma}; \quad x = \frac{2(E_0-E)}{\Gamma};$$

Γ_n и Γ — нейтронная и полная ширина резонанса; Γ_x — ширина по отношению к реакции x; E_0 — резонансная энергия; λ — длина волны нейтрона; φ_l — фаза потенциального рассеяния, имеющая тот же момент и четность, что и резонансный уровень; σ_r — формально определенное «сечение реакции». B_L^{nn} описывает вклад потенциального рассеяния в L-ю гармонику сечения рассеяния

$$B_L^{nn} = \sum_{l_1 l_0} (2l_1+1)(2l_0+1)(l_1 0 l_0 0 \mid L0)^2 \times \\ \times \sin\varphi_{l_1} \sin\varphi_{l_0} \cos(\varphi_{l_1} - \varphi_{l_0}). \quad (18а)$$

Коэффициенты B_L, A_L, I_L определяются резонансными параметрами и фазами потенциального рассеяния, интерферирующими с резонансом:

$$B_L = Z^2(lJlJ \mid jL) \frac{\Gamma_n^2}{\Gamma^2}, \quad (18б)$$

$$A_L = 2(2J+1) \sum_{l'} (2l'+1)(l'0l0 \mid L0)^2 \times \\ \times \frac{\Gamma_n}{\Gamma} \sin\varphi_{l'} \sin(2\varphi_l - \varphi_{l'}), \quad (18в)$$

$$I_L = 2(2J+1) \sum_{l'} (2l'+1)(l'0l0 \mid L0)^2 \times \\ \times \frac{\Gamma_n}{\Gamma} \sin\varphi_{l'} \cos(2\varphi_l - \varphi_{l'}), \quad (18г)$$

$(l'0l0 \mid L0)$ и $Z(lJlJ \mid jL)$ — коэффициенты Клебша — Жордана и Блатта — Биденхорна, протабулированные в работе [18].

Написанные выше формулы предполагают, что резонанс образуется нейтронами лишь с одним орбитальным моментом l. Предполагается также, что ядра неподвижны. При учете теплового движения ядер формулы для сечения (17а, б) принимают вид [5,18]

$$\sigma = \sigma_p + \sigma_0 \sqrt{\frac{\pi}{4}} \operatorname{Re}\left[\omega\left(\xi\frac{x}{2} + i\frac{\xi}{2}\right) \times \right. \\ \left. \times \exp(2i\varphi_l)\right], \quad (19а)$$

$$\sigma_x = \sigma_0 \sqrt{\frac{\pi}{4}} \frac{\Gamma_x}{\Gamma} \operatorname{Re}\left[\omega\left(\xi\frac{x}{2} + i\frac{\xi}{2}\right)\right] \equiv \\ \equiv \sigma_0 \frac{\Gamma_x}{\Gamma} \psi(\xi, x), \quad (19б)$$

где $\xi = \Gamma/\Delta$; $\Delta = 2\sqrt{kTE_0/A}$ — допплеровская ширина уровня; ω — интеграл вероятностей от комплексного аргумента, для которого существуют подробные таблицы [19].

Для перехода от формул (19) к формулам (17) необходимым является условие $\xi \gg 1$. В противном случае допплеровское уширение существенно влияет на форму резонанса.

Учет допплеровского уширения уровней при рассмотрении анизотропии рассеяния не представляет большого интереса, так как в тех случаях, когда этот эффект играет заметную роль, рассеивающие резонансы с высокими орбитальными моментами, как правило, нельзя считать изолированными.

Усреднение сечений в области разрешенных изолированных резонансов. В этой области энергий сечения (16), усредненные по резонансам, могут быть выражены через резонансные параметры и вычислены.

Метод вычисления средних сечений, необходимых для выполнения расчетов в диффузионном приближении, был подробно рассмотрен в работах [12, 15]. Здесь мы приведем более общие формулы, позволяющие вычислять также и сечения, требующиеся для более высоких приближений. Вывод этих формул аналогичен изложенному в цитированных работах и поэтому здесь опускается.

$$\left\langle \frac{1}{(\sigma+\tilde{\sigma})^n} \right\rangle = \left[\frac{1}{\sigma_p+\tilde{\sigma}}\right]^n \sum_{m=0}^{n} (-1)^m C_n^m I_{r,m}, \quad (20а)$$

$$\left\langle \frac{\sigma_s f_L}{(\sigma+\tilde{\sigma})^n} \right\rangle = \sigma_p f_{Lp} \left\langle \frac{1}{(\sigma+\tilde{\sigma})^n} \right\rangle + J_{Ln}. \quad (20б)$$

Здесь

$$I_{r,m} = \left\langle \left[\frac{\sigma_x}{\sigma+\tilde{\sigma}}\right]^m \right\rangle; \quad (21а)$$

$$J_{Ln} = \left\langle \frac{\sigma_{Sr} f_{Lr}}{(\sigma+\tilde{\sigma})^n} \right\rangle. \quad (21б)$$

Определим также

$$I_x = \left\langle \frac{\sigma_x}{\sigma+\tilde{\sigma}} \right\rangle. \quad (21в)$$

Подстановка в формулы (21) выражений (17) или (19) для сечений приводит к следующему:

$$I_{r,m} = \frac{1}{\Delta u} \sum_k \frac{\Gamma_k}{2E_{0k}} \eta_m(\xi_k, \alpha_k, \varphi_k) \times \\ \times \alpha_k^m \int_{-\infty}^{+\infty} \left[\frac{\cos 2\varphi_k - x\sin 2\varphi_k}{1+x^2-x\alpha_k\sin 2\varphi_k + \alpha_k\cos 2\varphi_k}\right]^m dx, \quad (22а)$$

$$J_{Ln} = \frac{4\pi\lambda^2}{\Delta u (2L+1)(\sigma_p+\tilde{\sigma})^n} \sum_k \frac{\Gamma_k}{2E_{0k}} \times \\ \times \int_{-\infty}^{+\infty} \frac{(\gamma_L - x\beta_L)(1+x^2)^{n-1}\,dx}{(1+x^2-x\alpha_k\sin 2\varphi_k + \alpha_k\cos 2\varphi_k)^n}. \quad (23а)$$

В частности,

$$I_{r,1} = \frac{\pi}{\Delta u} \sum_k \frac{\Gamma_k}{2E_{0k}} \alpha_k \times \\ \times \frac{\eta_1(\xi_k, \alpha_k, \varphi_k)\left[\cos 2\varphi_k - \frac{\alpha_k}{2}\sin^2 2\varphi_k\right]}{[(1-\alpha_k\sin^2\varphi_k)(1+\alpha_k\cos^2\varphi_k)]^{1/2}}, \quad (22б)$$

$$I_{r,2} = \frac{\pi}{2\Delta u} \sum_k \frac{\Gamma_k}{2E_{0k}} \alpha_k^2 \times \\ \times \frac{\eta_2(\xi_k, \alpha_k, \varphi_k)}{[(1-\alpha_k\sin^2\varphi_k)(1+\alpha_k\cos^2\varphi_k)]^{3/2}}, \quad (22в)$$

$$J_{L,1}=\frac{4\pi^2\lambda^2}{\Delta u\,(2L+1)\,(\sigma_p+\widetilde{\sigma})}\sum_k\frac{\Gamma_k}{2E_{0k}}\times$$

$$\times\frac{\gamma_{Lk}-\beta_{Lk}\dfrac{\alpha_k}{2}\sin 2\varphi_k}{[(1-\alpha_k\sin^2\varphi_k)\,(1+\alpha_k\cos^2\varphi_k)]^{1/2}}, \quad (23б)$$

$$J_{L,2}=\frac{\pi^2\lambda^2}{2\Delta u\,(2L+1)\,(\sigma_p+\widetilde{\sigma})^2}\sum_k\frac{\Gamma_k}{2E_{0k}}\times$$

$$\times\frac{2\gamma_{Lk}\,(2+\alpha_k\cos 2\varphi_k)}{[(1-\alpha_k\sin^2\varphi_k)\,(1+\alpha_k\cos^2\varphi_k)]^{3/2}}- \quad (23в)$$

$$-\frac{\beta_{Lk}\,\alpha_{Lk}\sin 2\varphi_k(4+3\alpha_k\cos 2\varphi_k-\dfrac{\alpha_k^2}{2}\sin^2 2\varphi_k)}{[(1-\alpha_k\sin^2\varphi_k)\,(1+\alpha_k\cos^2\varphi_k)]^{3/2}},$$

$$I_x=\frac{1}{\Delta u}\sum_k\frac{\pi}{2}\frac{\Gamma_{xk}}{2E_{0k}}\alpha_k\times$$

$$\times\frac{\eta_1'(\xi_k,\alpha_k,\varphi_k)}{[(1-\alpha_k\sin^2\varphi_k)\,(1-\alpha_k\cos^2\varphi_k)]^{1/2}}. \quad (24)$$

Суммирование здесь ведется по всем уровням k в интервале усреднения Δu

$$\alpha_k=\frac{\sigma_{0k}}{\sigma_p+\widetilde{\sigma}},\ \gamma_L=\sum_j\frac{B_L-A_L}{2(2I+1)},\ \beta_L=\sum_j\frac{I_L}{2(2I+1)}.$$

Функции η_1' и η_m определены таким образом, что в отсутствие допплеровского уширения резонансов они равны единице. Для $m=1,2$ эти функции вычислялись в ряде работ [4, 5, 9] в предположении отсутствия эффекта интерференции резонансного и потенциального рассеяния ($\varphi=0$). При этом $\eta_1'=\eta_1$. Расчет этих функций при $\varphi\neq 0$ также не представляет особых трудностей.

Область неразрешенных изолированных резонансов. В области энергий, где резонансы не разрешены, но их еще можно считать изолированными, при вычислении интегральных величин (21) могут быть использованы средние параметры резонансов.

Так как сечения при данной энергии представляют собой суммы сечений для каждого из возможных значений полного момента J и четности π, то средние интегральные характеристики можно записать в виде суммы по отдельным моментам

$$I_{r,m}=\sum_\nu I_{r,m}^\nu,\ J_{L,n}^\nu=\sum_\nu J_{L,n}^\nu,\ I_x=\sum_\nu I_x^\nu, \quad (25)$$

где $\nu=J_i\pi$. Величины $I_{r,m}^\nu$, $J_{L,m}^\nu$ и I_x^ν могут быть выражены следующим образом:

$$I_{r,m}^\nu=\frac{1}{2}\frac{\Gamma_\nu}{D_\nu}\bar{\alpha}_\nu^m\eta_m(\bar{\xi}_\nu,\bar{\alpha}_\nu,\varphi_\nu)f_m(\bar{\xi}_\nu,\bar{\alpha}_\nu,\varphi_\nu)\times$$

$$\times\int_{-\infty}^{+\infty}\left[\frac{\cos 2\varphi_\nu-x\sin 2\varphi_\nu}{1+x^2-x\bar{\alpha}_\nu\sin 2\varphi_\nu+\bar{\alpha}_\nu\cos 2\varphi_\nu}\right]^m dx, \quad (26)$$

$$J_{L,n}^\nu=\frac{4\pi\lambda^2}{(2L+1)\,(\sigma_p+\widetilde{\sigma})^n}\frac{\Gamma_\nu}{2D}\zeta(\bar{\alpha}_\nu,\bar{\gamma}_{L\nu},\bar{\beta}_{L\nu},\varphi_\nu)\times$$

$$\times\int_{-\infty}^{+\infty}\frac{(\bar{\gamma}_{L\nu}-x\bar{\beta}_{L\nu})\,(x^2+1)^{n-1}\,dx}{(1+x^2-x\bar{\alpha}_\nu\sin 2\varphi_\nu+\bar{\alpha}_\nu\cos 2\varphi_\nu)^n}. \quad (27)$$

$$I_x^\nu=\frac{\pi}{2}\frac{\overline{\Gamma_{x\nu}}}{D_\nu}\bar{\alpha}_\nu\frac{\eta_1'(\bar{\xi}_\nu,\bar{\alpha}_\nu,\varphi_\nu)\,\chi_1'(\bar{\alpha}_\nu,\bar{\xi}_\nu,\varphi_\nu)}{[(1-\bar{\alpha}_\nu\sin^2\varphi_\nu)\,(1+\bar{\alpha}_\nu\cos^2\varphi_\nu)]^{1/2}}, \quad (28)$$

где

$$\alpha_\nu=4\pi\lambda^2\frac{2J+1}{2(2I+1)}\frac{\bar{\Gamma}_{n\nu}}{\bar{\Gamma}_\nu}\frac{1}{(\sigma_p+\widetilde{\sigma}+\sum\limits_{\nu'\neq 0}\bar{\sigma}_{r\nu'})}. \quad (29)$$

Сумма в знаменателе последнего выражения введена для учета наложения резонансов с различными спинами и четностями. $\bar{D}_\nu$ — среднее расстояние между уровнями со спином J и четностью π.

Все значения параметров вычисляются при средней энергии интервала усреднения. Функции χ', χ_m и $\zeta_{L,s}$ учитывают зависимость вычисляемых величин от флуктуаций парциальных ширин. Эти флуктуации описываются распределением Портера — Томаса [20], и указанные функции могут быть получены численным расчетом. Результаты вычислений некоторых из этих функций приведены в работах [12, 21]. Некоторые другие аспекты учета влияния флуктуаций парциальных ширин на величины средних сечений будут рассмотрены ниже.

Область резонансных уровней, частично перекрывающихся за счет допплеровского уширения. Расчет усредненных сечений в области частично перекрывающихся интерферирующих резонансов в настоящее время невозможен из-за отсутствия удовлетворительного теоретического представления структуры сечений для этой области энергий. Оценки эффектов самоэкранировки могут быть выполнены лишь для случая, когда перекрывание резонансов наступает за счет их допплеровского уширения ($\Delta\sim\bar{D}$, но $\Gamma\ll\bar{D}$).

Для этого случая разработан метод вычисления усредненных сечений, основанный на представлении их в виде разности собственно среднего сечения и некоторой поправки на эффект самоэкранирования, имеющей вид дисперсии

$$\left.\begin{aligned}\frac{\left\langle\frac{\sigma_x}{\sigma}\right\rangle}{\left\langle\frac{1}{\sigma}\right\rangle}&=\bar{\sigma}_x-\frac{1}{\bar{\sigma}}(\overline{\sigma_x\sigma}-\bar{\sigma}_x\bar{\sigma}),\\ \left\langle\frac{1}{\sigma^n}\right\rangle&=\frac{1}{\bar{\sigma}^n}+\frac{1}{2}n(n+1)\frac{\overline{\sigma^2}-\bar{\sigma}^2}{\bar{\sigma}^{n+2}}.\end{aligned}\right\} \quad (30)$$

Если для вычисления поправки использовать предположение о большой допплеровской ширине резонансов и считать уровни эквидистантными, то

$$\left.\begin{aligned}\overline{\sigma_x\sigma}-\bar{\sigma}_x\bar{\sigma}&=\sum_\nu\bar{\sigma}_{x\nu}\bar{\sigma}_{r\nu}\times\\ &\times\left[2\exp\left(-\frac{2\pi^2}{b_\nu^2}\right)+\left(\frac{b_\nu}{\sqrt{2\pi}}\right)\frac{\Phi_x^\nu}{S_x}\right],\\ \overline{\sigma^2}-\bar{\sigma}^2&=\sum_\nu\bar{\sigma}_{r\nu}^2\times\\ &\times\left[2\exp\left(-\frac{2\pi^2}{b_\nu^2}\right)+\left(\frac{b_\nu}{\sqrt{2\pi}}\right)\Phi^\nu\right],\end{aligned}\right\} \quad (31)$$

где $\nu = J_i л$; $b_\nu = \bar{D}_\nu/\Delta$; функции Φ_x^ν, Φ^ν и S_x [10,12,21] учитывают влияние распределения приведенных ширин на величину сечения.

Влияние интерференции резонансного и потенциального рассеяний на резонансную самоэкранировку сечений. Интерференция между резонансным и потенциальным рассеянием приводит к сильному изменению формы резонансной линии. Максимум резонанса сдвигается по отношению к резонансной энергии на величину $E_{max} - E_0 = (\Gamma/2)\operatorname{tg}\varphi_l$, величина сечения в максимуме становится равной $\sigma_{max} = \sigma_0 + \sigma_{min}$, где $\sigma_{min} = \sigma_p - \sigma_0 \sin^2\varphi_l$ достигается при энергии $E_{min} = E_0 - (\Gamma/2)\operatorname{ctg}\varphi_l$. В случае четно-четных ядер, для которых S-нейтроны образуют состояния лишь с одним полным моментом $J = 1/2$, величина сечения в минимуме равна $\sigma_p(1 - \Gamma_n/\Gamma)$ и в случае, когда ширины неупругих процессов малы, может быть весьма малой. Так, например, полное сечение железа в интерференционном минимуме резонанса Fe^{56} при $E_0 = 29$ *кэв* равно примерно 0,2 *барн* и практически целиком определяется примесью других изотопов железа.

Ясно, что при вычислении величин $\langle 1/\sigma_n \rangle$ и т. п. наличие этих минимумов сказывается определяющим образом. Однако этот эффект может оказывать существенное влияние и на величину эффективного резонансного интеграла поглощения (рис. 1).

Особенно существенным может быть учет интерференции резонансного и потенциального

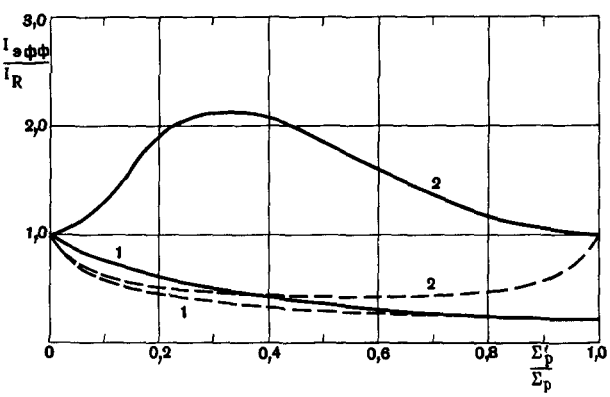

Рис. 1. Зависимость резонансного интеграла поглощения для уровня Fe^{56} при 26 *кэв* от разбавления естественной смеси изотопов железа разбавителем с большей потерей энергии при упругом рассеянии и сечением $\tilde{\Sigma} = \Sigma_p^1 - \Sigma_p$. Пунктирные кривые вычислены без учета флуктуаций плотности столкновений. При учете сплошных кривых эти флуктуации принимались во внимание:
1 — без учета интерференции резонансного и потенциального рассеяния; *2* — с учетом интерференции

решения при вычислении температурной зависимости эффективного резонансного интеграла (табл. 1).

Таблица 1. Температурная зависимость резонансного интеграла поглощения (в барнах) для уровня U^{238} при 663 *эв* ($\tilde{\sigma}=0$)

φ	Температура, °K		
	0	300	900
Равно нулю	0,011	0,012	0,014
Не равно нулю	0,027	0,024	0,021

Аналогичный эффект имеет место и для других высоколежащих уровней U^{238}, обладающих большой нейтронной шириной.

Эффект интерференции резонансного и потенциального рассеяния может быть весьма существен и в области частично перекрывающихся уровней (рис. 2).

Вследствие эффекта интерференции условие $\Gamma < D$ еще не дает оснований считать, что в сечениях не проявляется резонансная структура. Сечения станут плавными лишь тогда, когда откроется большое число каналов для распада составного ядра.

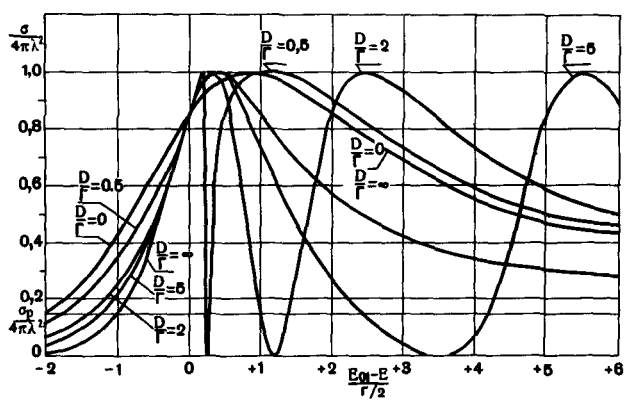

Рис. 2. Поведение сечения в окрестности двух близколежащих S-резонансов четно-четного ядра в предположении, что $\Gamma_n = \Gamma$ и в потенциальном сечении присутствует только S-волна

Учет непостоянства плотности столкновений. Как отмечалось выше, плачековские осцилляции плотности столкновений в случае узких резонансов слабо сказываются на результатах усреднения сечений. Они, однако, должны приниматься во внимание при рассмотрении резонансов, ширина которых сравнима с потерей энергии на ядрах того же элемента, но существенно меньше, чем потеря энергии при рассеянии на ядрах других компонент смеси. Энергетическая зависимость плотности столкновений в этом случае должна находиться путем решения интегрального уравнения

$$\Psi(u) = \sum_i \int_{u-r_i}^{u} \Psi(u') \frac{\Sigma_S^i(u' \to u)}{\Sigma(u')} du'. \quad (32)$$

В ряде случаев учет непостоянства плотности столкновений может приводить к существенному изменению результатов усреднения.

В качестве примера можно привести зависимость эффективного резонансного интеграла поглощения от разбавления для уровня Fe^{56} при 29 *кэв*, приведенную на рис. 1. Изменение этой зависимости по сравнению со случаем постоянства плотности столкновений обусловлено возникновением всплеска плотности столкновений в области интерференционного минимума, где отношение Σ_c/Σ резко возрастает. Другим примером может служить энергетическая зависимость плотности столкновений в области первого резонанса U^{238} при 6,7 *эв*, вычисленная в работе [11] методом Монте-Карло.

Влияние резонансной самоэкранировки на усредненные параметры анизотропии рассеяния. Использование формул (22) для вычисления усредненных значений параметров анизотропии рассеяния требует знания спинов резонансных уровней, образуемых при захвате нейтронов с высоким орбитальным моментом, и фаз потенциального рассеяния.

ВЛИЯНИЕ ФЛУКТУАЦИЙ ПАРЦИАЛЬНЫХ ШИРИН НА СРЕДНИЕ СЕЧЕНИЯ ДЕЛЯЩИХСЯ ЭЛЕМЕНТОВ

Рассмотрим влияние флуктуаций нейтронной и делительной ширин на различные средние величины, характеризующие отношение вероятностей деления и радиационного захвата при поглощении нейтрона. Поставлено несколько экспериментов по измерению величин, характеризующих это отношение. Измеряются или сечения радиационного захвата σ_γ и деления σ_f, или среднее число вторичных нейтронов на один захваченный нейтрон $\eta = \dfrac{\bar{\nu}\sigma_f}{\sigma_f + \sigma_\gamma}$ ($\bar{\nu}$ — число вторичных нейтронов на одно деление), или отношение числа захватов к числу делений σ_γ/σ_f. Непосредственное усреднение этих величин по энергии дает следующие средние характеристики отношения радиационного захвата к делению: 1) $\alpha = \bar{\sigma}_\gamma/\bar{\sigma}_f$; 2) $\alpha_\eta = \bar{\nu}/\bar{\eta} - 1$, где $\bar{\eta} = \bar{\nu}\left(\overline{\dfrac{\sigma_f}{\sigma_\gamma + \sigma_f}}\right)$; 3) $\langle\alpha\rangle = \left(\overline{\dfrac{\sigma_\gamma}{\sigma_f}}\right)$. И, наконец, используют величину, которую можно получить лишь в результате анализа сечений радиационного захвата и деления в резонансной области $\bar{\alpha} = \bar{\Gamma}_\gamma/\bar{\Gamma}_f$. Заметим, что все эти величины разные. Наиболее важна для реакторных расчетов величина α. Чтобы показать количественно, как сильно могут различаться эти величины, рассмотрим систему изолированных, неперекрывающихся уровней с одинаковым спином и учтем статистические флуктуации нейтронных и делительных ширин в соответствии с работами Бете [29], Олексы [31], Лэйна и Линна [21], Портера и Томаса [20]. В дальнейшем будем операцию усреднения по флуктуациям Γ_f и Γ_n обозначать скобками $\langle\ldots\rangle$. Тогда (считая, что Γ_γ не

Таблица 2. Влияние резонансной самоэкранировки на средние характеристики рассеяния нейтронов ядрами кислорода

Без учета самоэкранировки				Среда	Коэффициенты самоэкранировки			
ΔE	$\bar{\Sigma}_S$	$\dfrac{\overline{\xi\Sigma_S}}{\bar{\Sigma}_S}$	$\dfrac{\overline{\mu\Sigma_S}}{\bar{\Sigma}_S}$		$\dfrac{\overline{(\Sigma_S/\Sigma_{tot})}}{\bar{\Sigma}_S\overline{(1/\Sigma_{tot})}}$	$\dfrac{\overline{(\xi\Sigma_S/\Sigma_{tot})}}{\overline{\xi\Sigma_S}\,\overline{(1/\Sigma_{tot})}}$	$\dfrac{\overline{(\Sigma_S/\Sigma^2_{tot})}}{\bar{\Sigma}_S\overline{(1/\Sigma^2_{tot})}}$	$\dfrac{\overline{(\mu\Sigma_S/\Sigma^2_{tot})}\,\bar{\Sigma}_S}{\overline{\mu\Sigma_S}\,\overline{(\Sigma_S/\Sigma^2_{tot})}}$
0,2—0,4	3,80	0,134	—0,14	0	0,975 0,994 0,995	0,968 0,987 0,993	0,960 0,976 0,992	0,910 0,933 0,950
0,4—0,8	5,60	0,086	0,23	0	0,774 0,850 0,908	0,788 0,832 0,900	0,678 0,767 0,837	1,100 1,060 1,050
0,8—1,4	4,30	0,110	0,08	0	0,900 0,960 1,000	0,860 0,935 0,975	0,858 0,930 1,000	1,075 1,250 1,110
1,4—2,5	1,75	0,100	0,12	0	0,720 0,980 0,992	0,684 0,980 0,992	0,372 0,937 0,950	2,120 0,995 0,995

В настоящее время имеющаяся по этому поводу информация весьма ограничена. Более или менее надежные и полные сведения есть лишь для первых уровней наиболее легких ядер. Расчеты, выполненные для этих ядер, показывают, что влияние резонансной самоэкранировки на форму усредненных угловых распределений может оказывать заметное влияние на распространение и замедление нейтронов. В качестве примера могут быть приведены результаты вычисления усредненных характеристик сечения рассеяния кислорода (табл. 2). Усреднение производилось в групповых интервалах, принятых в работе [16], на основании результатов измерений угловых распределений, выполненных Лангсдорфом и др. [22].

Результаты вычислений относятся как к чистому кислороду, так и к кислороду, содержащемуся в двуокиси урана и в воде. Флуктуации плотности столкновений во внимание не принимались.

флуктуирует) получаем

$$\left.\begin{aligned} \alpha &= \Gamma_\gamma \frac{\left\langle \frac{\Gamma_n}{\Gamma_\gamma+\Gamma_f+\Gamma_n} \right\rangle}{\left\langle \frac{\Gamma_f\Gamma_n}{\Gamma_\gamma+\Gamma_f+\Gamma_n} \right\rangle}, \quad \langle\alpha\rangle = \Gamma_\gamma \left\langle \frac{1}{\Gamma_f} \right\rangle, \\ \alpha_\eta &= \Gamma_\gamma \left\langle \frac{1}{\Gamma_f+\Gamma_n} \right\rangle \text{ и } \bar{\alpha} = \frac{\Gamma_\gamma}{\langle\Gamma_f\rangle}. \end{aligned}\right\} \quad (33)$$

Используя явный вид χ^2-распределений с числом степеней свободы ν для делительной ширины и с одной степенью свободы для нейтронной, легко показать, что

$$\langle\alpha\rangle > \alpha_\eta > \alpha > \bar{\alpha}. \quad (34)$$

При постоянной средней делительной и радиационной ширинах с увеличением энергии только из-за роста нейтронной ширины α уменьшается, приближаясь к $\bar{\alpha}$ еще до того, как начинает играть роль поглощение P-нейтронов.

В действительности при взаимодействии S-нейтронов с ядром, имеющим спин I, образуются уровни компаунд-ядра со спинами $J = I \pm \frac{1}{2}$ и статистическими весами, пропорциональными $2J + 1$. Поэтому усреднения сечений или ширин нужно проводить отдельно для каждой системы уровней, которая характеризуется собственным средним значением делительной и приведенной нейтронной ширин и, вообще говоря, своим числом каналов деления, формулы (30) соответственно модифицируются, однако система неравенств (31) продолжает выполняться. Интерференция между уровнями и перекрытие резонансов с хорошей точностью не меняют средней площади под резонансами и поэтому не влияют на величину α, то есть не нарушают неравенства $\alpha > \bar{\alpha}$, которое должно выполняться строго. Соответствующие расчеты для Pu^{239} с учетом существования двух подсистем резонансов подтверждают это (рис. 3). Значения использованных в расчете параметров приведены в подписи к рис. 3.

Для U^{233} $\bar{\alpha} = 0{,}15$, а $\alpha = 0{,}35$ [31]. Расчетные значения α равны 0,27 и 0,34 для ν, равных 2 и 3 соответственно, если использовать средние делительные ширины для двух подсистем резонансов, приведенные в работе [32].

Однако на U^{235}, начиная примерно с 7 *эв*, неравенство (34) для наблюдаемых величин нарушается: для 30 резонансов выше этой энергии $\bar{\alpha} = 1{,}4$, а $\alpha = 1{,}2$ [33, 34, 39]. Это противоречие можно устранить, если сделать предположение о частичном пропуске резонансов с малыми Γ_n^0 и большими Γ_f. Формулы, полученные в работе [35] для количественных оценок последствий такого пропуска, объясняют и другие аномалии в резонансной структуре U^{235} в рассматриваемой области энергий — наличие в сечении деления фона $\sim \frac{30\ барн}{\sqrt{E}}$, резкое отличие при малых Γ_n^0 наблюдаемого распределения приведенных нейтронных ширин от одноканального χ^2-распределения, а также малое наблюдаемое значение средней делительной

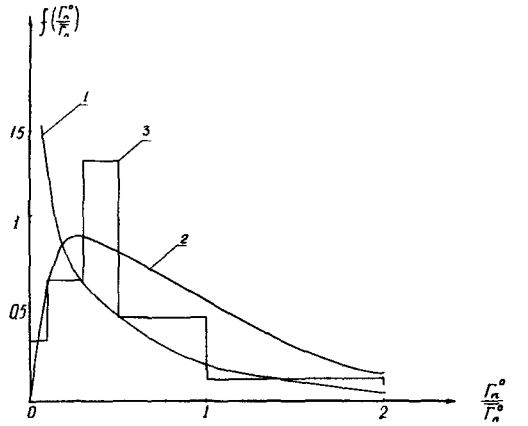

Рис. 3. Сравнение расчетных и экспериментальных значений α для ядра Pu^{239}. Средние значения резонансных параметров взяты из работ[33,38] и равны $\bar{\Gamma}_f^0 = 40$ *мв*; $\bar{\Gamma}_f^1 = 160$ *мв*, $\bar{\Gamma}_n^0 = 0{,}6$ *мв*; экспериментальное распределение делительных ширин соответствует $\nu \simeq 1$ для обеих систем резонансов[35]; экспериментальные значения α согласуются с таким предположением в пределах, обусловленных статистической неопределенностью резонансных параметров

ширины резонансов с 11 по 40 ($\Gamma_{f(11-40)} = 29$ *мв*) по сравнению с аналогичной величиной для первых десяти уровней $\Gamma_{f(1-10)} = 78$ *мв* (рис. 4). Получаемое с учетом пропуска уровней истинное значение $\bar{\alpha}$ равно примерно 0,85, что удовлетворяет неравенству (34), и в предположении, что $\nu = 3$, дает $\alpha\,(0{,}85) = 1{,}15$, которое удовлетворительно согласуется с экспериментом.

Если такое предположение справедливо, то оно означает также, что действительные значения среднего расстояния между уровнями и средней приведенной нейтронной шириной примерно в 1,5—2 раза меньше наблюдаемых значений.

Для величины $\langle\alpha\rangle$ при $\nu = 1{,}2$ интегралы, содержащиеся в выражениях (33), расходятся. Фактически это, конечно, означает, что при столь широких распределениях делительных ширин, когда очень малые значения Γ_f имеют заметную вероятность, величина $\langle\alpha\rangle$ будет принимать некое случайное значение, значительно превышающее $\bar{\alpha}$, α и α_η. При $\nu > 2$ интегралы сходятся, и для ν, равного 3 и 4, получаются значения $\langle\alpha\rangle$, равные $3\bar{\alpha}$ и $2\bar{\alpha}$ соответственно. Однако на величину $\langle\alpha\rangle$ сильно влияют перекрытие и интерференция резонансов, значительно ее понижая. Приближение изолированных резонансов лучше всего подходит к Pu^{239}, и у этого ядра действительно $\langle\alpha\rangle \sim 2{,}5 \gg \bar{\alpha} \approx \approx 0{,}4$, как и следует ожидать для $\nu = 1$; у U^{233} $\langle\alpha\rangle \sim 0{,}35 \sim \alpha > \bar{\alpha} = 0{,}15$. Сильнее

всего интерференция и перекрытие у U^{235}, и у него $\langle\alpha\rangle$ близко к $\bar{\alpha}$.

Из сказанного также вытекает, что при относительных измерениях σ_γ/σ_f будет наблюдаться следующее: пока энергетическое разрешение лучше, чем среднее расстояние между уровнями, величина σ_γ/σ_f в каждой точке будет примерно совпадать с Γ_γ/Γ_f соответствующего

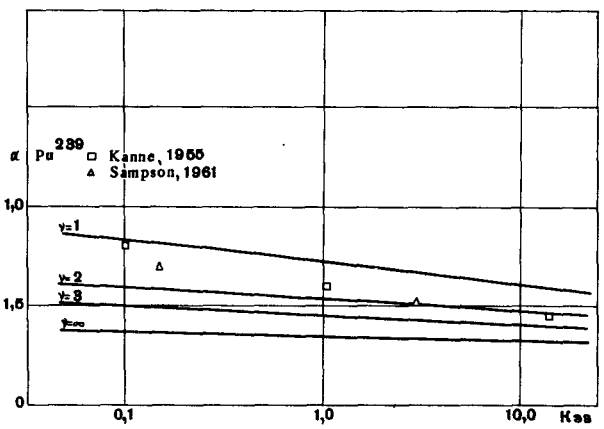

Рис. 4. Экспериментальная гистограмма (*3*) статистического распределения приведенных нейтронных ширин резонансов 11—40 ядра U^{235} сравнивается с одноканальным χ^2-распределением (*1*) и распределением, рассчитанным согласно результатам работы[35] с учетом пропуска слабых резонансов (*2*)

резонанса и испытывать колебания, отвечающие резонансной структуре сечений. Среднее значение этой величины по промежутку, включающему много резонансов, будет совпадать с $\langle\alpha\rangle$. С продвижением по энергетической оси разрешение селектора падает, и когда оно становится значительно хуже среднего расстояния между уровнями, то начинают автоматически усредняться сечения в числителе и в знаменателе и происходит «превращение» $\langle\alpha\rangle$ в α — среднее значение измеряемой величины заметно падает, хотя ни с какой ядерно-физической причиной это не связано. Поэтому представляют большой интерес результаты относительных измерений σ_γ/σ_f с плохим энергетическим разрешением (порядка энергетического интервала группы), но с хорошей статистикой, которые прямо дают α для соответствующей группы.

В 26-групповой системе констант, которая опубликована в работе [16], расчет коэффициентов блокировки деления f_f и завхата f_c для Pu^{239} проводился по средним параметрам, взятым из работы [36]. Кроме того, так же как и в работе [37], предполагалось, что делительная ширина подчиняется трехканальному распределению. Поскольку средние параметры резонансов Pu^{239}, полученные в [33], и одноканальное распределение делительных ширин, по-видимому, лучше описывают экспериментальные данные, то они и были использованы для расчетов коэффициентов блокировки, приведенных в табл. 3. В области энергий до 1 *кэв* расчет производился в приближении узких резонансов и при предположении, что уровни с одинаковыми J не перекрываются. Учет распределения ширин Γ_n и Γ_f, производился так же, как в работе [37]. Температурная зависимость сечений деления и захвата определялась с помощью функций, рассчитанных авторами работ [9].

Коэффициенты блокировки в энергетической области выше нескольких килоэлектронвольт, где резонансы начинают перекрываться за счет допплеровского уширения, рассчитывались по методике, изложенной в работе [10]. В приводимой таблице f_f и f_c отражен тот факт, что в этой области энергий σ_f блокируется сильнее, чем σ_γ, и, следовательно, α ухудшается с увеличением блокировки.

В области 12—14 групп коэффициенты блокировки интерполировались. В группах ниже 18-й f_f и f_c не пересчитывались.

Надо отметить, что расчеты эффекта Допплера в быстром окисном реакторе объемом 2000 *л* с коэффициентами блокировки, приведенными в табл. 3, дали результаты, очень близкие к результатам, полученным на основании коэффициентов блокировок, приведенных в работе [16].

ЭКСПЕРИМЕНТАЛЬНОЕ ОПРЕДЕЛЕНИЕ УСРЕДНЕННЫХ СЕЧЕНИЙ

Вычисление усредненных сечений по формулам для изолированных резонансов возможно лишь в сравнительно узкой области энергий, где можно пренебречь влиянием эффекта интерференции между уровнями с одинаковым моментом и четностью и где влияние резонансов, образуемых нейтронами с высокими орбитальными моментами (для которых средние резонансные параметры обычно известны плохо), не слишком велико. При более высоких энергиях расчет средних характеристик, зависящих от структуры сечений, становится ненадежным. В связи с этим встает вопрос об экспериментальном определении этих характеристик.

В работах [7, 12, 13] был предложен метод измерения параметров структуры полных сечений, позволяющий получить такие характеристики, как $\langle 1/\Sigma^n\rangle$, путем анализа кривых пропускания пучка нейтронов через исследуемое вещество. Тот же принцип может быть использован и для измерения всех других характеристик, необходимых для описания распространения нейтронов в средах в условиях, когда флуктуации плотности столкновений не сказываются заметным образом на результатах усреднения.

Таблица 3. Коэффициенты блокировки сечений деления и радиационного захвата Pu^{239}

E	t	T, °K	f_f				f_c			
			$\tilde{\sigma}=10^3$	$\tilde{\sigma}=10^2$	$\tilde{\sigma}=10$	$\tilde{\sigma}=0$	$\tilde{\sigma}=10^3$	$\tilde{\sigma}=10^2$	$\tilde{\sigma}=10$	$\tilde{\sigma}=0$
21,5—46,5 *кэв*	10	300	1,00	0,99	0,97	0,94	1,00	1,00	0,98	0,96
		900	1,00	1,00	0,98	0,97	1,00	1,00	0,99	0,98
		2100	1,00	1,00	0,99	0,98	1,00	1,00	0,99	0,99
10,0—21,5 *кэв*	11	300	1,00	0,98	0,93	0,88	1,00	0,99	0,95	0,91
		900	1,00	0,99	0,97	0,93	1,00	1,00	0,98	0,95
		2100	1,00	0,99	0,98	0,95	1,00	1,00	0,99	0,97
4,65—10,0 *кэв*	12	300	1,00	0,96	0,87	0,80	1,00	0,96	0,87	0,80
		900	1,00	0,98	0,93	0,87	1,00	0,98	0,94	0,88
		2100	1,00	0,99	0,95	0,91	1,00	0,99	0,96	0,92
2,15—4,65 *кэв*	13	300	0,99	0,92	0,79	0,69	0,99	0,92	0,77	0,67
		900	1,00	0,96	0,87	0,79	1,00	0,96	0,87	0,78
		2100	1,00	0,98	0,91	0,88	1,00	0,98	0,91	0,87
1,00—2,15 *кэв*	14	300	0,98	0,88	0,67	0,56	0,98	0,87	0,62	0,51
		900	0,99	0,92	0,78	0,69	0,99	0,91	0,76	0,66
		2100	1,00	0,95	0,86	0,82	1,00	0,95	0,84	0,79
465—1000 *эв*	15	300	0,97	0,80	0,53	0,42	0,96	0,76	0,46	0,36
		900	0,98	0,86	0,64	0,53	0,97	0,82	0,58	0,47
		2100	0,99	0,90	0,77	0,71	0,99	0,89	0,72	0,64
215—465 *эв*	16	300	0,93	0,70	0,41	0,30	0,91	0,62	0,33	0,24
		900	0,96	0,78	0,50	0,38	0,94	0,72	0,42	0,31
		2100	0,98	0,83	0,58	0,52	0,96	0,80	0,53	0,45
100—215 *эв*	17	300	0,91	0,63	0,34	0,25	0,89	0,58	0,28	0,20
		900	0,94	0,69	0,41	0,32	0,92	0,64	0,34	0,26
		2100	0,97	0,75	0,49	0,39	0,95	0,70	0,41	0,32
46,5—100 *эв*	18	300	0,78	0,50	0,37	0,34	0,75	0,44	0,30	0,27
		900	0,83	0,59	0,45	0,42	0,80	0,52	0,38	0,35
		2100	0,87	0,66	0,54	0,52	0,85	0,61	0,47	0,44

Методика измерений. Методика таких измерений заключается в следующем. Коллимированный пучок нейтронов со спектром $f(E)$, лежащим в интервале ΔE около энергии E, падает на образец из исследуемого вещества толщиной t. Если соблюдены условия «хорошей» геометрии, то детектор с эффективностью $\varepsilon(E)$, расположенный за образцом, будет регистрировать лишь те нейтроны, которые прошли через образец без взаимодействия. В этом случае зависимость $N(t)$ скорости счета детектора от толщины образца может быть описана функцией пропускания

$$T(t)=\frac{N(t)}{N(0)}=\frac{\int_{\Delta E} f(E)\,\varepsilon(E)\,e^{-N\sigma(E)\,t}\,dE}{\int_{\Delta E} f(E)\,\varepsilon(E)\,dE}, \quad (35)$$

где N — плотность ядер в образце.

Введя функцию $P(\sigma)$ распределения полного сечения образца для нейтронов падающего пучка, можно переписать это выражение следующим образом:

$$T(t)=\frac{\int \varepsilon[E(\sigma)]\,p(\sigma)\,e^{-N\sigma t}\,d\sigma}{\int \varepsilon[E(\sigma)]\,p(\sigma)\,d\sigma}. \quad (36)$$

Здесь $E(\sigma)$ — функция, обратная $\sigma(E)$, интегрирование ведется по всему интервалу изменения σ. (Здесь и далее принимаем для простоты, что $f(E)=1$ в интервале ΔE и нулю вне этого интервала.)

Если интервал ΔE не слишком велик, не представляет труда выбрать детектор с эффективностью, постоянной в пределах этого интервала. Наряду с этим представляет интерес случай, когда детектор регистрирует какой-либо процесс, происходящий в тонком слое того же вещества, из которого изготовлен образец. В этом случае энергетическая чувствительность детектора будет пропорциональна сечению этого процесса и, стало быть, скоррелирована с полным сечением. Допустим, что наряду с детектором, обладающим постоянной чувствительностью, мы располагаем набором детекторов, регистрирующих все интересующие нас реакции в исследуемом веществе, а также гармоники углового распределения рассеянных нейтронов. Функции пропускания, измеренные с помощью этих детекторов, будут иметь вид

$$T(t)=\int p(\sigma)\,e^{-N\sigma t}\,d\sigma,$$

$$T_x(t)=\int \sigma_x[E(\sigma)]\,p(\sigma)\,e^{-N\sigma t}\,d\sigma, \quad (37)$$

$$T_{SL}(t)=\int \sigma_S[E(\sigma)]\,f_L[E(\sigma)]\,p(\sigma)\,e^{-N\sigma t}\,d\sigma.$$

Представим теперь приближенно $P(\sigma)$ в виде суммы δ-функций

$$p(\sigma)=\sum_{i=1}^{m} a_i \delta(\sigma-\bar{\sigma}_i),$$

что соответствует представлению энергетической зависимости полного сечения в интервале ΔE ступенчатой кривой. В этом случае функции пропускания (37) могут быть выражены в виде суммы экспонент

$$\left.\begin{aligned} T(t)&=\sum_{i=1}^{m} a_i e^{-N\bar{\sigma}_i t},\\ T_c(t)&=\sum_{i=1}^{m} b_i e^{-N\bar{\sigma}_i t},\\ T_{SL}(t)&=\sum_{i=1}^{m} c_{iL} e^{-N\bar{\sigma}_i t}, \end{aligned}\right\} \qquad (38)$$

где

$$b_i=a_i\frac{\overline{\sigma_{ci}}}{\bar{\sigma}_c};\quad c_{iL}=a_i\frac{\overline{(\sigma_S f_L)_i}}{\overline{(\sigma_S f_L)_i}}; \qquad (39)$$

$\bar{\sigma}_x$ и $\overline{(\sigma_S f_L)}$ — сечение реакции типа x и n-я гармоника упругого рассеяния, усредненные по спектру нейтронов в пучке; $\overline{\sigma_{xi}}$ и $\overline{(\sigma_s f_L)_i}$ — те же величины, усредненные по спектру той доли a_i нейтронов пучка, для которых полное сечение равно в среднем $\bar{\sigma}_i$.

Эти величины, как нетрудно видеть, представляют собой те самые параметры, которые фигурировали в методе подгрупп. Для их определения необходимо располагать набором функций пропускания (37), измеренных до достаточно больших толщин. Представление этих функций в форме (38) может быть осуществлено путем их совместного анализа методом наименьших квадратов, с помощью которого можно также определить максимальное число экспонент в разложениях.

Средние сечения могут быть измерены с помощью тех же детекторов обычными методами.

Значения параметров (15) связаны с характеристиками подгрупп простыми соотношениями:

$$\left.\begin{aligned} \left\langle\frac{1}{(\sigma+\tilde{\sigma})^n}\right\rangle&=\sum_{i=1}^{m} a_i\left(\frac{1}{\bar{\sigma}_i+\tilde{\sigma}}\right)^n,\\ \left\langle\frac{\sigma_x}{(\sigma+\tilde{\sigma})}\right\rangle&=\sum_{i=1}^{m} b_i\frac{1}{\bar{\sigma}_i+\tilde{\sigma}},\\ \left\langle\frac{\sigma_S f_L}{(\sigma+\tilde{\sigma})^n}\right\rangle&=\sum_{i=1}^{m} c_{iL}\left(\frac{1}{\bar{\sigma}_i+\tilde{\sigma}}\right)^n. \end{aligned}\right\} \qquad (40)$$

Эти величины можно определить и непосредственно из кривых пропускания с помощью соотношений типа

$$\left\langle\frac{\sigma_S f_L}{(\sigma+\tilde{\sigma})^n}\right\rangle=\frac{N^n}{n!}\overline{\sigma_S f_L}\int_0^\infty T_{SL}(t)\,e^{-N\bar{\sigma}t}t^{n-1}dt, \qquad (41)$$

которые полезны также для оценки максимальной степени n, при которой величины $\langle\langle 1/(\sigma+\tilde{\sigma})^n\rangle\rangle$ имеют еще разумную точность.

Измерения характеристик структуры полных сечений. Изложенная методика требует использования достаточно интенсивных пучков нейтронов и детекторов высокой эффективности. Поэтому до настоящего времени она использовалась главным образом для измерений характеристик структуры полных сечений. В килоэлектронвольтной области энергий в этих измерениях в качестве источника нейтронов использовалась тритиевая мишень электростатического генератора, облучаемая протонами. В области энергий 0,3—3 *Мэв* измерения производились под углом 0° к направлению протонного пучка. В области 10—300 *кэв* использовались нейтроны, вылетающие под углом 120°. Начаты также измерения характеристик структуры полных сечений тяжелых ядер в электронвольтной области энергий. Эти измерения производятся методом времени пролета на реакторе ИБР [23].

Детекторами нейтронов во всех экспериментах служили батареи пропорциональных счетчиков с $B^{10}F_3$. Результаты большинства измерений в области 0,3—3 *Мэв* были опубликованы в работах [13,14]. Некоторые новые данные приводятся на рис. 5—11. Данные, полученные методом времени пролета, приводятся для групповых интервалов, используемых в работе [16].

Измерение резонансной самоэкранировки углового распределения быстрых нейтронов, рассеянных ядрами железа. Это измерение является пока единственным измерением резонансной самоэкранировки парциальных сечений, выполненным по изложенной методике. Выбор железа в качестве исследуемого веществе был обусловлен тем, что среди элементов со средним атомным весом оно обладает наиболее ярко выраженной структурой сечений в мегаэлектронвольтной области энергий. С другой стороны, изучение железа представляло интерес и с практической точки зрения как наиболее широко используемого конструкционного и защитного материала. Источником нейтронов в этом эксперименте служил пучок нейтронов, выходящий из активной зоны реактора БР-5 [24]. Жесткая часть спектра нейтронов этого пучка весьма близка к соответствующей части нейтронов деления [25]. Детектором служила многослойная ионизационная камера деления с Th^{232}, имеющая эффективный порог чувствительности $\sim 1{,}5$ *Мэв*.

С помощью этой камеры измерялась как функция пропускания нейтронов через образцы

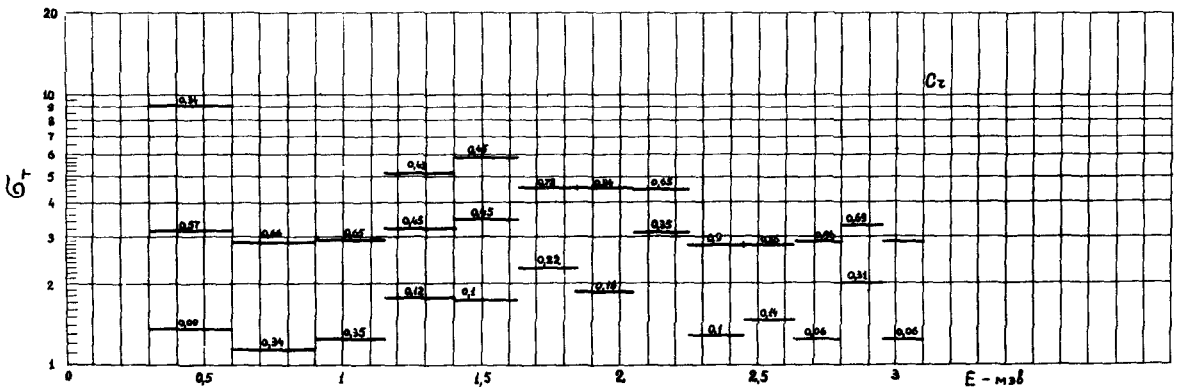

Рис. 5. Структура полного сечения $_{24}Cr$

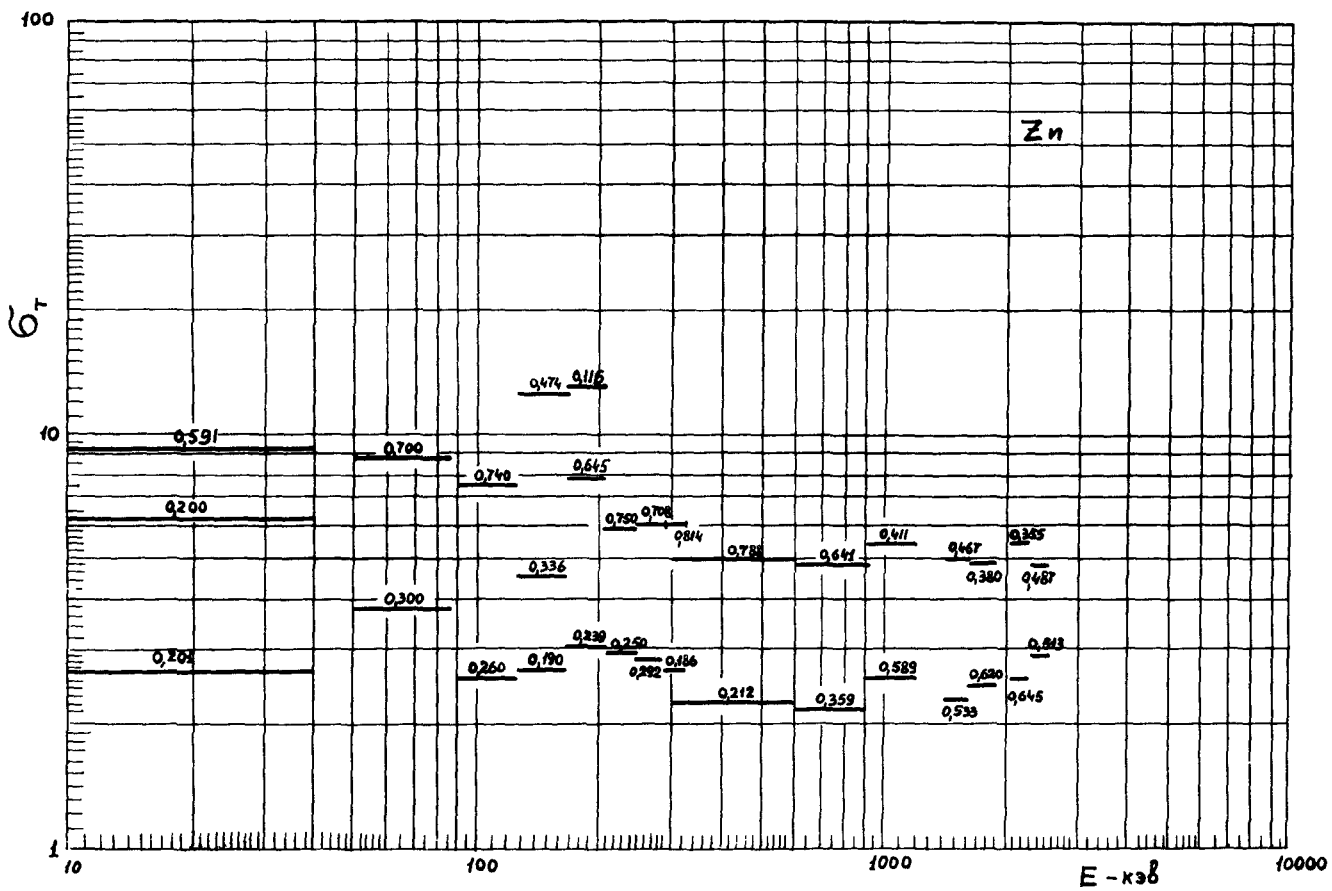

Рис. 6. Структура полного сечения $_{30}Zn$

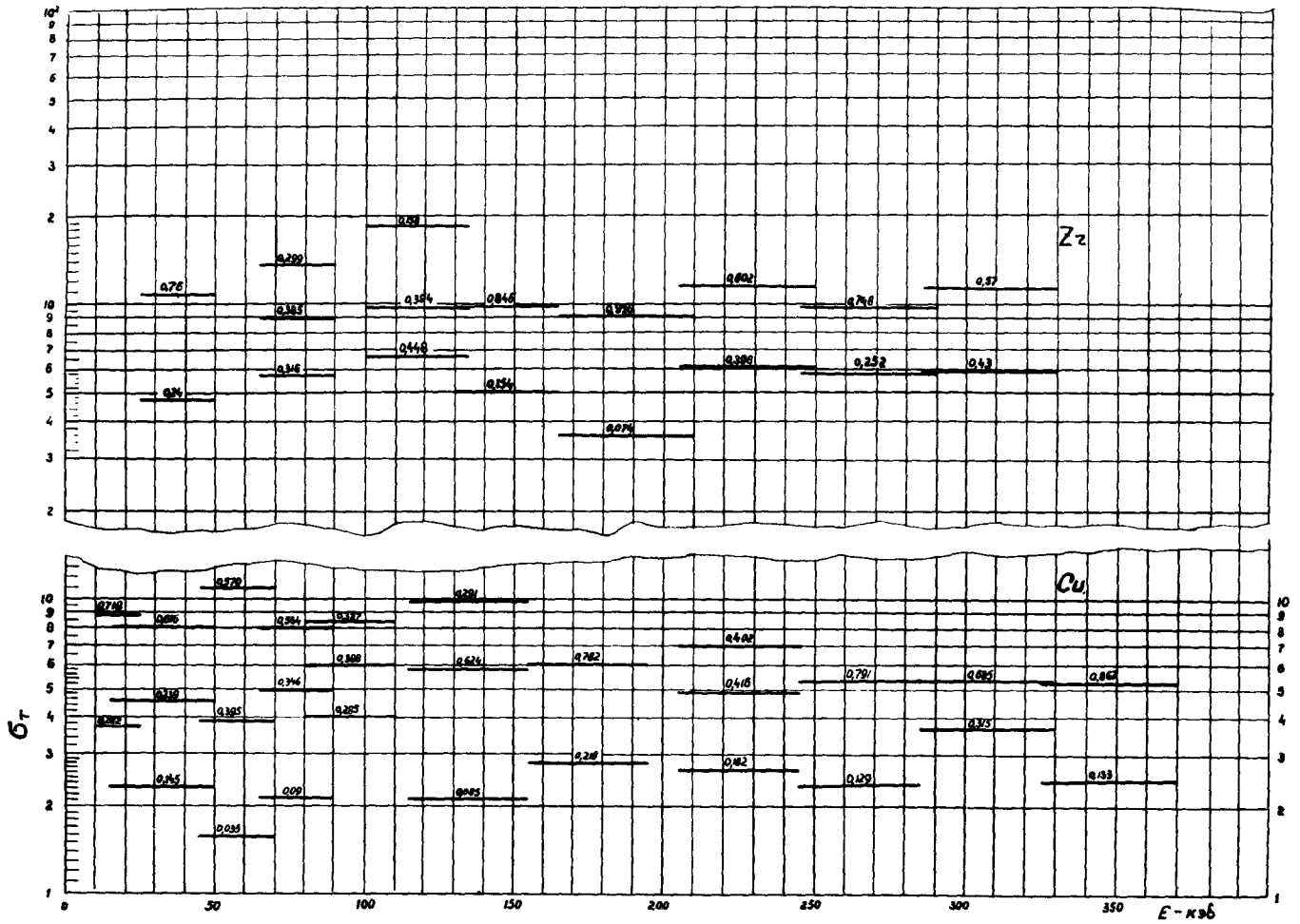

Рис. 7. Структура полного сечения $_{40}$Zr и $_{29}$Cu

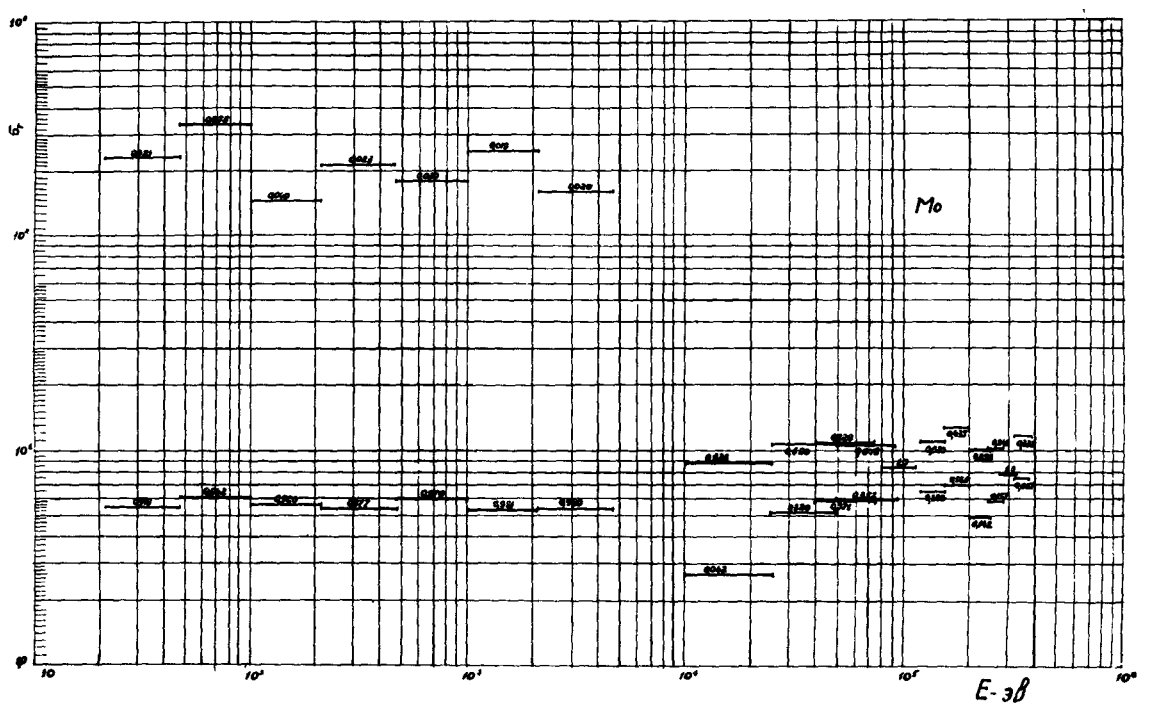

Рис. 8. Структура полного сечения $_{42}$Mo

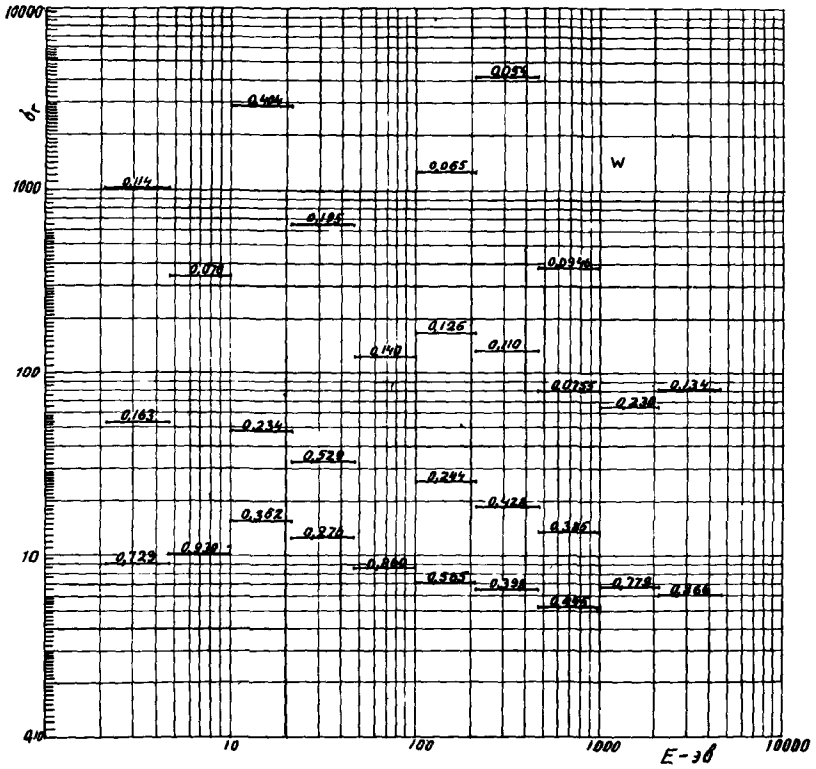

Рис. 9. Структура полного сечения $_{74}$W

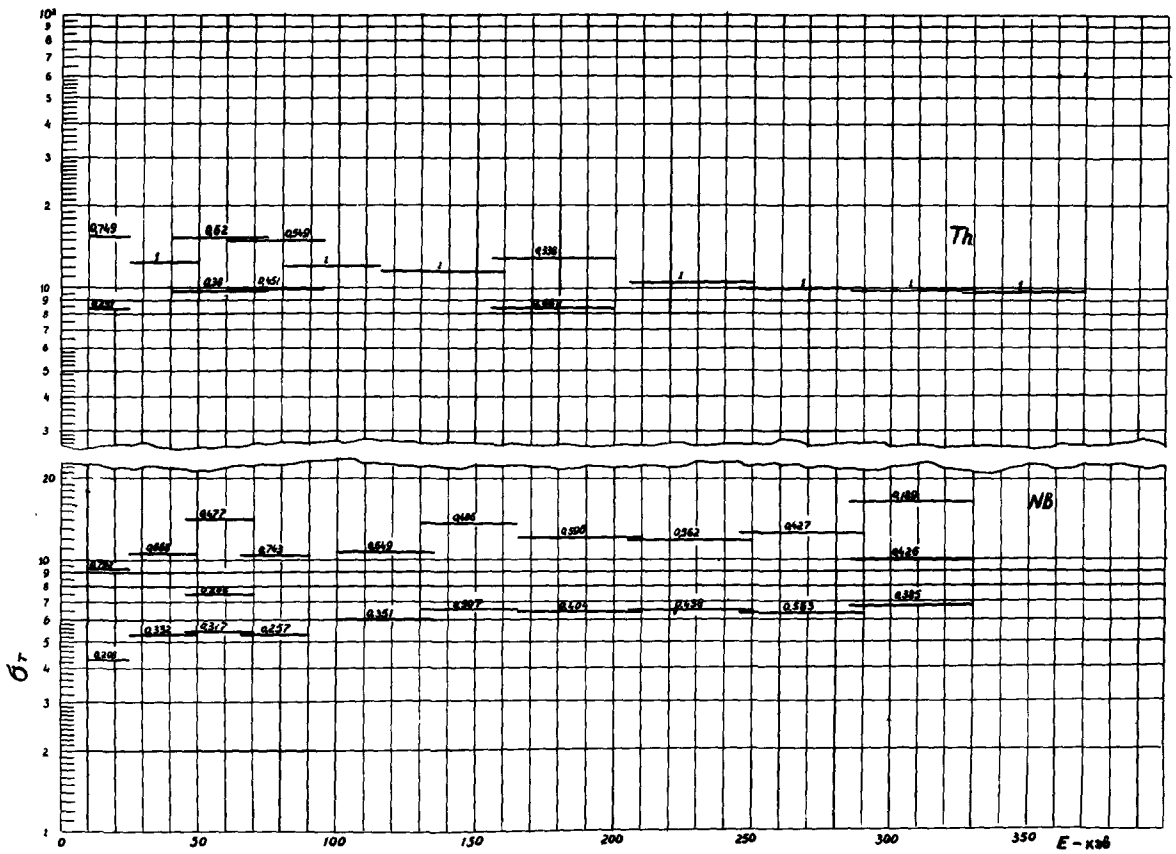

Рис. 10. Структура полного сечения $_{41}$Nb и $_{90}$Th

железа различной толщины, так и угловые распределения нейтронов, прошедших через образец и рассеявшихся на тонком рассеивателе, помещенном в пучок за образцом.

Путем совместного анализа кривых пропускания $T(t)$ и $T_{SL}(t)$, полученных в этом эксперименте, удалось разбить нейтроны регистрируемой части пучка на две подгруппы с характеристиками, приведенными в табл. 4.

Таблица 4. Сечения железа для двух подгрупп нейтронов деления, способных делить Th^{232}

i	a_i	$\tilde{\sigma}_i$	σ_{Si}	$(\overline{\sigma_S f_1})_i$	$(\overline{\sigma_S f_2})_i$	$(\overline{\sigma_S f_3})_i$
1	0,59	2,24	1,95	0,58	0,565	0,325
2	0,41	4,60	3,44	1,80	1,12	0,815

Полученные данные позволили проиллюстрировать влияние точности учета резонансной самоэкранировки при решении задачи на прохождение нейтронов через толстый слой вещества. Так, например, асимптотическая длина релаксации быстрых нейтронов ($E > 1{,}5$ *Мэв*) в железе, рассчитанная по одногрупповым константам (16) в P_4-приближении [26], оказалась равной 7,95 *см*. При расчете же этой величины методом подгрупп ее значение было найдено равным 8,40 *см*.

ЛИТЕРАТУРА

1. I. I. Gurevich and I. J. Pomeranchouk. The theory of resonance absorption in heterogeneous systems, Proceedings of the International Conference on the Peaceful Uses of Atomic Energy, Geneva, 1955, P/649, Vol. V, United Nations, New York, 1956.

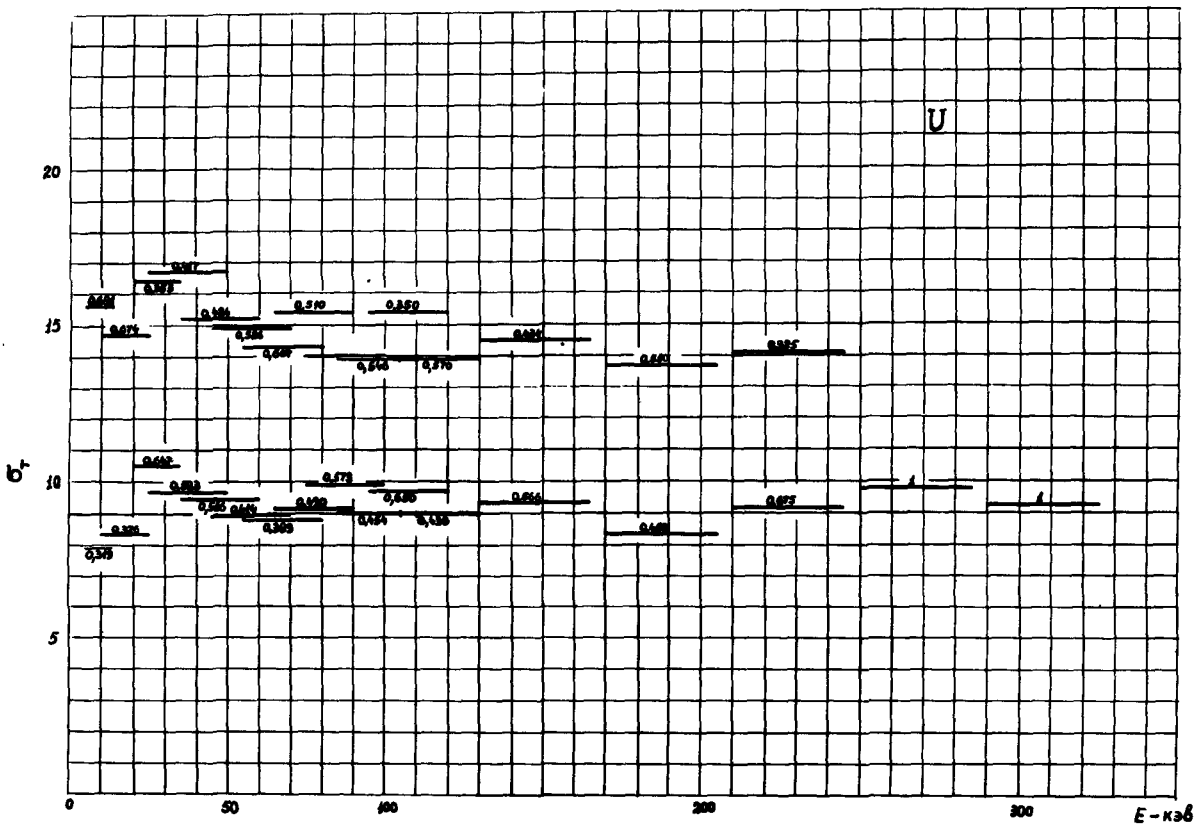

Рис. 11. Структура полного сечения $_{92}V$

Приведенные данные не могут быть объяснены плавными изменениями сечений железа, имеющими место в исследуемой области энергий; хотя этот эффект и имел место, различие в характеристиках подгрупп обусловлено в основном наличием резонансной структуры сечений. Данные табл. 4 свидетельствуют, в частности, о том, что анизотропия упругого рассеяния нейтронов в области энергии порядка 3—4 *Мэв* обусловлена в основном резонансным рассеянием.

2. E. Wigner, E. Creutz, H. Jupnik and I. Snyder. J. Appl. Phys., *26*, 92 and 260 (1955).
3. А. П. Рудик. В сб. «Теория ядерных реакторов на тепловых нейтронах». Изд. 2. М., Госатомиздат, 1961.
4. В. В. Орлов, Т. В. Голашвили, А. И. Васкин. В сб. «Нейтронная физика». М., Госатомиздат, 1961, стр. 116.
5. Л. Дреснер. Резонансное поглощение в ядерных реакторах. М., Госатомиздат, 1962.
6. Вейнберг и Вигнер. Физическая теория ядерных реакторов, гл. 9. М., ИЛ, 1961.

7. А. И. Лейпунский и др. Труды Второй международной конференции по мирному использованию атомной энергии, Женева, 1958. Доклад советских ученых, P/2038. М., Атомиздат, 1959.
8. М. Н. Николаев, В. В. Филиппов и И. И. Бондаренко. Доклад № 85 в сб. Physics of fast and intermediate reactors, IAEA, Vienna, 1962.
9. И. В. Гордеев, В. В. Орлов, Т. Х. Седельников. Атомная энергия, *9*, 252 (1957).
10. А. А. Лукьянов, В. В. Орлов. Атомная энергия, *10*, 262 (1961).
11. Г. И. Марчук, Ф. Ф. Михайлус. Атомная энергия, *4*, 220 (1958).
12. А. А. Лукьянов, В. В. Орлов. В сб. «Нейтронная физика». М., Госатомиздат, 1961, стр. 105.
13. М. Н. Николаев, В. В. Филиппов, И. И. Бондаренко. Атомная энергия, *11*, 445 (1961).
14. М. Н. Николаев, В. В. Филиппов. Атомная энергия, *15*, 493 (1963).
15. А. А. Лукьянов. Влияние резонансной структуры сечений на поглощение, замедление и диффузию нейтронов в средах, Диссертация (1963).
16. Л. П. Абагян, Н. О. Базазянц, И. И. Бондаренко, М. Н. Николаев. Групповые константы для расчета ядерных реакторов. М., Госатомиздат, 1964.
17. Г. И. Марчук. Методы расчета ядерных реакторов. М., Госатомиздат, 1964.
18. А. М. Балдин, В. И. Гольданский и И. Л. Розенталь. Кинематика ядерных реакций. М., Физматгиз, 1959.
19. В. Н. Фадеева и М. В. Терентьев. Таблицы значений интеграла вероятностей от комплексного аргумента. М., Физматгиз, 1956.
20. C. Porter and R. Thomas. Phys. Rev., *104*, 483 (1956).
21. A. Lane and J. Lynn. Proc. Phys. Soc., *A-70*, 557 (1957).
22. R. O. Lane, Jr., A. Langsdorf, J. E. Monahan. Ann. Phys., *12*, 135 (1961).
23. Г. Е. Блохин и др. Доклад № 81 в сб. «Physics of fast and intermediate reactors». IAEA, Vienna, 1962, p. 399.
24. А. И. Лейпунский и др. Труды Второй международной конференции по мирному использованию атомной энергии, Женева, 1958. Доклады советских ученых, P/2129. М., Атомиздат, 1959.
25. А. И. Лейпунский и др. Доклад № 80 в сб. «Physics of fast and intermediate reactors». IAEA, Vienna, 1962, p. 315.
26. Д. А. Бродер, С. А. Куркин, А. А. Кутузов, В. В. Левин, В. В. Орлов. Труды Второй международной конференции по мирному использованию атомной энергии, Женева, 1958. Доклады советских ученых. М., Атомиздат, 1959.
27. Б. Карлсон, Дж. Белл. В сб. «Физика ядерных реакторов». М., Атомиздат, 1959, стр. 408.
28. В. С. Владимиров. В сб. «Вычислительная математика», № 3 (1958).
29. Н. Бете. В сб. «Успехи в области ядерной энергии». М., ИЛ, 1958, стр. 119.
30. S. Oleksa, J. Nulc. Energy, *5*, 16 (1957).
31. M. L. Yeater, R. W. Hochkenbury, R. R. Fuldwood, Nucl. Sci. and Eng., *9*, 105 (1961).
32. C. Reich, M. Moore. Phys. Rev., *118*, 718 (1960.
33. К. П. Игнатьев, И. В. Кирпичников, С. И. Сухоручкин. Атомная энергия, *16*, 110 (1964).
34. F. D. Brooks. Proceeding of the Symposium on neutron timeof-flight methods. Session II, Saclay, 1961, p. 131.
35. Л. Н. Усачев, В. А. Павлинчку, Работнов. Атомная энергия, в печати.
36. Н. О. Базазянц, И. В. Гордеев. Атомная энергия, *13*, 321 (1962).
37. P. Greebler, R. A. Hutchins. Physics of fast and intermediate reactors, vol. III, IAEA, Vienna, 1962, p. 121.
38. И. В. Гордеев, Д. А. Кардашев, А. В. Малышев. Ядерно-физические константы. М., Госатомиздат, 1963.
39. G. de Saussure, L. W. Weston et al. Nucl. Sci. Abstract, *18*, 151 (1024) (1964).

ABSTRACT—RÉSUMÉ—АННОТАЦИЯ—RESUMEN

A/357 USSR

Influence of cross-section resonance structure on neutron diffusion and moderation, and resonance effects on fissionable nuclei

By L. P. Abagyan *et al.*

The method of taking into account the resonance structure of neutron cross section in the reactor theory is considered. These effects are shown to be of considerable, and sometimes of major, importance for the determination of neutron space energy distributions even for fast reactors. The method is developed to take into account the resonance structure in multi-group reactor calculation for P_n and S_n approximations.

The theory for evaluation of resonance structure parameters is described for different energy ranges. For isolated levels this theory is rigorous, but only qualitative estimates of the effects in question can be made for partially overlapping resonances. It is also shown that, because of the interference between potential and resonance scattering, the cross-section fluctuations in the region of overlapping resonances are strong enough for resonance self-shielding to be quite significant in this energy range.

Theoretical conclusions need experimental proof. In this paper some methods are described for measuring parameters of resonance structure of cross sections which affect the neutron diffusion in media. These methods do not require high energy resolution and can be applied at any neutron energy, including the region of overlapping levels. The experimental results obtained by these methods are summarized and compared with the theory.

The mean values and statistical distributions of fission width are important characteristics of the resonance structure. Some theoretical conceptions on fission-channel scheme were used to make a reasonable choice of these characteristics. The Bohr-Wheeler

formula for average fission widths was used to analyse experimental data for reactions (d,pf), (n,f) and (γ,f). These data are found to be in agreement with the concept of fission channels proposed by A. Bohr, negative parity channels being 0.6–0.8 MeV above the first positive parity channel. In this case, the Bohr-Wheeler formula is shown to describe quantitatively the fission widths of neutron resonance of ^{233}U, ^{235}U and ^{242}Pu. One must assume ^{239}Pu having the ground state of negative parity to explain the sharp disagreement between theory and experiment for this nucleus.

Experimental distributions of fission and reduced neutron widths of neutron resonances were analysed. The existence of two sub-systems of resonances with different spins and possible omission of weak levels were taken into account. Resulting numbers of fission channels are $N=1$ for ^{239}Pu, $N\approx 2$ for ^{235}U and $N\gtrsim 3$ for ^{233}U.

The dependence of $\bar{\alpha}=\bar{\sigma}_\gamma/\bar{\sigma}_t$ on energy for s neutrons was calculated ($\alpha=\bar{\Gamma}_\gamma/\bar{\Gamma}_t$ was taken to be constant). Always $\bar{\alpha}>\alpha$, the difference between the two values being especially large at neutron energy $E_n\sim 100$ eV. With an increase in neutron energy, when the contribution of neutron width increases and fluctuations of the total width decrease, the value of $\bar{\alpha}$ approaches α, i.e., diminishes even before neutron p-wave becomes significant. The maximum effect of this kind is expected for ^{239}Pu—the nucleus with the most broad distribution of fission widths and with the greatest reduced neutron width.

These results were also used for calculating temperature effect for ^{239}Pu.

A/357 URSS

Influence de la structure de résonance des sections efficaces sur la diffusion et le ralentissement des neutrons dans divers milieux et effets de résonance avec les éléments fissiles

par L. P. Abagyan *et al.*

Les auteurs examinent l'importance que revêt la structure de résonance des sections efficaces pour le calcul des réacteurs nucléaires. Ils montrent que, même pour les réacteurs à neutrons rapides, elle joue un rôle essentiel et détermine parfois la distribution spatiale des neutrons selon leur énergie.

Ils ont élaboré des méthodes permettant de tenir compte de la structure de résonance des sections efficaces pour les calculs multigroupes de réacteurs par approximations P_n et S_n.

Ils exposent une théorie qui permet de calculer les paramètres indispensables de la structure des sections efficaces pour différents intervalles d'énergie. Pour des niveaux isolés, la théorie est d'une application rigoureuse. Par contre, dans le cas de niveaux se recouvrant partiellement, elle ne permet qu'une évaluation qualitative des effets.

Les auteurs signalent également que, par suite de l'interférence de la diffusion résonnante et de la dispersion potentielle, la section efficace accuse d'assez fortes fluctuations dans la région du chevauchement des résonances, ce qui peut provoquer une notable autoprotection de résonance des sections dans ce domaine d'énergie.

Pour cette raison, les conclusions auxquelles aboutit la théorie nécessitent une vérification expérimentale. Le mémoire expose comment on peut procéder à cette vérification. On y décrit les méthodes permettant de trouver expérimentalement les paramètres de la structure des sections efficaces qui déterminent l'influence de celle-ci sur la diffusion des neutrons. Ces méthodes n'exigent pas un grand pouvoir de résolution en énergie et peuvent donc être utilisées dans toute la gamme d'énergies, y compris dans la région des chevauchements.

Les auteurs récapitulent les résultats obtenus expérimentalement à l'aide de ces méthodes et les comparent aux résultats des calculs.

Pour tenir compte des effets de résonance sur les noyaux fissiles, il importe surtout de connaître les valeurs et les distributions statistiques des largeurs de fission. Pour faire un choix judicieux entre ces valeurs, les auteurs ont utilisé, en plus des données expérimentales immédiates, certaines conceptions théoriques de la structure des voies de fission. Ils ont analysé les données expérimentales obtenues sur les réactions (d,pf), (γ,f) et (n,f) en appliquant la formule de Bohr-Wheeler pour les largeurs de fission moyennes. Toutes les données expérimentales indiquées concordent avec la structure des voies de fission proposée par A. Bohr. On a constaté, à ce propos, que les voies de fission de parité négative se trouvent à 0,6–0,8 MeV plus haut que les premières voies de parité positive. Lorsque les voies de fission sont disposées de la sorte, la formule de Bohr-Wheeler décrit quantitativement les largeurs de fission moyennes à la résonance neutronique pour les noyaux de ^{233}U, ^{235}U et ^{241}Pu. Pour expliquer l'écart sensible dans le cas de ^{239}Pu, il faut supposer que l'état fondamental de ce noyau présente une parité négative.

Les auteurs ont analysé les données expérimentales sur la distribution des largeurs réduites de neutrons et des largeurs de fission aux résonances neutroniques, en prenant en considération l'existence de deux systèmes secondaires de résonance comportant des spins différents et l'omission éventuelle des résonances faibles. Les voies de fission ainsi déterminées ont les valeurs suivantes: $N=1$ pour ^{239}Pu, $N\approx 2$ pour ^{235}U et $N\gtrsim 3$ pour ^{233}U.

On a calculé la dépendance énergétique de $\bar{\alpha}=\bar{\sigma}_\gamma/\bar{\sigma}_t$ pour les neutrons s lorsque $\alpha=\bar{\Gamma}_\gamma/\bar{\Gamma}_f$ est constant. $\bar{\alpha}$ est toujours plus grand que α, cette différence étant particulièrement sensible dans la zone d'épirésonance proprement dite. Avec l'augmentation de l'énergie, c'est-à-dire lorsque la contribution de la largeur neutronique s'accroît et que les variations de la largeur

totale s'affaiblissent, la valeur de $\bar{\alpha}$ s'approche de celle de α; en d'autres termes, α diminue avant que la contribution des neutrons p ne devienne substantielle. Cet effet est particulièrement marqué dans les noyaux où la distribution des largeurs de fission est la plus étendue et où la largeur réduite de neutrons atteint sa valeur maximale, c'est-à-dire dans les noyaux de ^{239}Pu.

Les valeurs obtenues pour les voies de fission ont été utilisées pour calculer l'effet de la température sur ^{239}Pu.

A/357 URSS

Influencia de la estructura resonante de las secciones eficaces sobre la distribución y moderación de los neutrones en los medios y efectos resonantes en los elementos fisionables

por L. P. Abagyan *et al.*

Se examinó la cuestión de cómo tener en cuenta la estructura resonante de las secciones eficaces en el cálculo de los reactores nucleares. Se demuestra que, incluso en el caso de los reactores rápidos, es muy importante tener en cuenta la estructura resonante de las secciones eficaces y que puede incluso determinar el carácter de la distribución energética y espacial de los neutrones.

Se ha desarrollado un método para tener en cuenta la estructura resonante de las secciones eficaces en los cálculos de reactores con varios grupos de neutrones en las aproximaciones P_n y S_n.

Se expone una teoría que permite calcular los parámetros de la estructura de las secciones eficaces necesarios en diferentes dominios energéticos. Esta teoría es rigurosa en el caso de niveles aislados. Sin embargo, cuando los niveles en parte se solapan, la teoría puede dar sólo una estimación cualitativa de los efectos considerados.

Se demuestra, a la vez, que, como consecuencia de la interferencia de la dispersión potencial y de la resonante, la sección eficaz fluctúa bastante fuertemente en el dominio de las resonancias que se solapan parcialmente, por lo cual el autoblindaje resonante de las secciones eficaces puede ser muy importante en este intervalo energético.

En estas condiciones, las consecuencias de la teoría requieren una comprobación experimental. En el informe se expone un método para llevarlo a cabo, como también un método de determinación experimental de los parámetros de estructura de las secciones eficaces que determinan la influencia de ésta sobre la distribución de los neutrones en los medios. Este último método no exige una elevada resolución energética, y por esto puede utilizarse en todo intervalo de energías, en particular también en el dominio de niveles que se solapan.

Se pasa revista a los datos experimentales obtenidos con dicho método. Los resultados del experimento se comparan con los valores calculados.

Para tener en cuenta los efectos de resonancia en los núcleos fisionables es importante, en particular, conocer los valores y las distribuciones estadísticas de las anchuras de fisión. Para escoger justificadamente los valores de dichas magnitudes, se utilizan en el informe, además de datos experimentales directos, modelos teóricos de la estructura de los canales de fisión. Se analizaron resultados de experimentos sobre las reacciones (d,pf), (γ,f) y (n,f) partiendo de la fórmula de Bohr-Wheeler para la anchura media de fisión. Todos estos datos experimentales concuerdan con la estructura de los canales de fisión propuesta por A. Bohr. Los canales de fisión de paridad negativa se encuentran de 0,6 a 0,8 MeV por encima de los primeros canales de paridad positiva. Para esta disposición de los canales de fisión, la fórmula de Bohr-Wheeler reproduce cuantitativamente las anchuras medias de fisión de las resonancias neutrónicas de los núcleos ^{233}U, ^{235}U y ^{241}Pu. Para explicar la marcada divergencia en el caso del ^{239}Pu es necesario suponer que el estado fundamental de este núcleo es de paridad negativa.

Se analizaron los datos experimentales sobre distribuciones de las anchuras neutrónicas reducidas y de fisión de las resonancias de los elementos fisionables, teniendo en cuenta la existencia de dos subsistemas de resonancias con diferentes spins y la posible omisión de resonancias débiles. Se obtuvieron los siguientes números de canales de fisión: $N=1$ para el ^{239}Pu; $N\approx 2$ para el ^{235}U; y $N\gtrsim 3$ para el ^{233}U.

Se calculó teóricamente la dependencia energética de $\alpha=\bar{\sigma}_\gamma/\bar{\sigma}_f$ para neutrones-s y valor constante de $\alpha=\bar{\Gamma}_\gamma/\bar{\Gamma}_f$. La magnitud $\bar{\alpha}$ es siempre mayor que α e, inmediatamente por encima de la región de resonancias, difieren mucho entre sí. A medida que aumenta la energía, cuando la contribución de la anchura neutrónica aumenta y la fluctuación de la anchura total disminuye, el valor $\bar{\alpha}$ se acerca a α, es decir, va decreciendo hasta que la contribución de los neutrones-p llega a ser considerable. Este efecto se manifiesta sobre todo en un núcleo que presenta la más amplia distribución de anchuras de fisión y la máxima anchura neutrónica reducida: el ^{239}Pu.

Los valores obtenidos para los canales de fisión se utilizaron para el cálculo del efecto de temperatura en el ^{239}Pu.

Методы решения уравнения переноса в неоднородных и ограниченных средах

С. М. Ермаков, Б. А. Ефименко, В. Г. Золотухин, Ф. Ф. Михайлус, Ш. С. Николайшвили, В. П. Поливанский

В настоящее время метод Монте-Карло является основным методом решения задач переноса излучения в неоднородных (конечных или бесконечных) средах в условиях энергетической зависимости сечений и неизотропности процессов рассеяния. Основное преимущество метода Монте-Карло перед обычными численными методами — приспособленность к многомерным проблемам — ярко проявляется в задачах теории переноса.

Действительно, решение общего кинетического уравнения для дифференциального потока $\Phi(\vec{r}, \vec{\Omega}, E)$, зависящего в общем случае от шести переменных, является пока безнадежно трудной задачей. Во многих случаях, когда требуется вычисление функционалов определенного типа, эта проблема многомерности не облегчается и теорией сопряженных функций, поскольку размерность задачи остается все еще слишком высокой.

В то же время метод Монте-Карло в зависимости от характера той информации, которую нужно получить, может быть сравнительно просто модифицирован с целью автоматического исключения ряда переменных. В данном докладе развиты два варианта метода: а) применительно к задаче вычисления дифференциального потока $\Phi(\vec{r}, \vec{\Omega}, E)$ для некоторого ограниченного набора координат, направлений и энергий и б) применительно к задаче нахождения функционалов определенного типа.

Во многих случаях, когда рассматриваемые поля излучений обладают высокой степенью симметрии, целесообразно пользоваться конечно-разностными методами. Так, например, численное решение задачи об угловых и спектральных распределениях излучения на различных расстояниях от точечного изотропного источника является более эффективным по сравнению с таким широко известным методом, как метод моментов. Область применения конечно-разностных методов может быть значительно расширена, если воспользоваться аппаратом сопряженных уравнений. Последнее справедливо в тех случаях, когда искомые функционалы зависят от меньшего числа независимых переменных по сравнению с функцией, описывающей пространственно-энергетические и угловые распределения излучения.

КОНЕЧНО-РАЗНОСТНЫЕ МЕТОДЫ

Плоскопараллельные задачи. Решение многих задач о прохождении γ-квантов через вещество сводится к отысканию функции $N(z, \mu, \lambda)$, удовлетворяющей уравнению [1]

$$\mu \frac{\partial N}{\partial z} + \Sigma N = F + f, \tag{1}$$

где

$$F = \int_0^{2\pi} d\alpha \int_{-1}^{+1} G(\xi, \lambda_1) N(z, \mu^1, \lambda_1) d\mu'; \tag{2}$$

$$\xi = \mu\mu' + \sqrt{1-\mu^2}\sqrt{1-\mu'^2}\cos\alpha; \quad \lambda_1 = \lambda - 1 + \xi$$

при дополнительных условиях

$$\left.\begin{aligned} N(0, \mu, \lambda) &= \chi(\mu, \lambda), & \mu > 0; \\ N(a, \mu, \lambda) &= 0, & \mu < 0. \end{aligned}\right\} \tag{3}$$

Функция f, χ, Σ и G предполагаются известными. Для приближенного решения уравнения (1) разобьем интервал $[0 \leqslant z \leqslant a]$ на n частей, интервал $[-1 \leqslant \mu \leqslant 1]$ на m частей, а вдоль оси λ отложим точки $\lambda_0, \lambda_1, \lambda_2, \ldots, \lambda_p, \ldots$ λ_0 — наименьшая длина волны первичных γ-квантов. Узлы разбиения интервалов $[0 \leqslant z \leqslant a]$ и $[-1 \leqslant \mu \leqslant 1]$ обозначим соответственно через z_k, $k = 0,1, \ldots, n$, и μ_ν, $\nu = 0,1, \ldots, m$, $z = 0$, $z_n = a$, $\mu_0 = 1$, $\mu_m = -1$. Приближенные значения функции $N(z, \mu, \lambda)$ в точке $(z_k, \mu_\nu, \lambda_p)$ будем обозначать через $N^p_{\nu k}$. Аналогичные обозначения будем применять и для других функций.

Вернемся к уравнению (1) и положим в нем $\mu = \mu_\nu$ и $\lambda = \lambda_p$. Тогда будем иметь

$$\mu_\nu \frac{dN^p_\nu}{dz} + \Sigma^p N^p_\nu = F^p_\nu + f^p_\nu. \tag{4}$$

Обозначения не требуют пояснений. Функция F^p_ν определяется интегралом (2) при $\mu = \mu_\nu$ и $\lambda = \lambda_p$.

Если допустить временно, что правая часть уравнения (4) известна, то задача сводится к интегрированию обыкновенного дифференциального уравнения первого порядка. Интегрируя его по z в пределах (z_k, z_{k+1})

и используя квадратную формулу трапеций, получим приближенно *

$$\mu_\nu (N^p_{\nu k+1} - N^p_{\nu k}) + \frac{\Sigma^p \Delta z_k}{2} (N^p_{\nu k+1} + N^p_{\nu k}) =$$

$$= \frac{\Delta z_k}{2} (F^p_{\nu k+1} + F^p_{\nu k} + f^p_{\nu k+1} + f^p_{\nu k}), \qquad (5)$$

$\Delta z_k = z_{k+1} - z_k$, $k = 0, 1, \ldots, n-1$. К последней системе следует присоединить дополнительные условия, вытекающие из граничных условий (3)

$$\left.\begin{aligned} N^p_{\nu 0} &= \chi(\mu_\nu, \lambda_p), & \mu_\nu > 0; \\ N^p_{\nu n} &= 0, & \mu_\nu < 0. \end{aligned}\right\} \qquad (6)$$

После этого система (5) решается в направлении возрастающих k, если $\mu_\nu > 0$, и в противоположном направлении при $\mu_\nu < 0$ **.

Переходя к приближенному вычислению функции $F(z, \mu, \lambda)$, стоящей в правой части уравнения (4), заметим предварительно, что ее выражение (2), представляющее собой общепринятую запись интеграла рассеяния, не годится для наших целей. Предлагаемый нами метод основан на другом представлении этого интеграла, которое получается путем замены переменных интегрирования и имеет вид

$$F(z, \mu, \lambda) = \int_0^{2\pi} d\alpha \int_{-1}^{+1} G(\xi, \lambda) N(z, \mu', \lambda_1) d\xi, \qquad (7)$$

где

$$\mu' = \mu\xi + \sqrt{1-\mu^2}\sqrt{1-\xi^2}\cos\alpha. \qquad (8)$$

Положив здесь $\mu = \mu_\nu$ и $\lambda = \lambda_p$, получим

$$F^p_\nu = \int_0^{2\pi} d\alpha \int_{-1}^{+1} G(\xi, \lambda_p - 1 + \xi) N(z, \mu', \lambda_p - 1 + \xi) d\xi, \qquad (9)$$

где μ' вычисляется по формуле (8) при $\mu = \mu_\nu$. Для вычисления внутреннего интеграла можно построить квадратную формулу с узлами ξ_{pq}, определяемыми из условий

$$\lambda_p - 1 + \xi_{pq} = \lambda_q, \quad q = p-s, \quad p-(s-1), \ldots, p. \qquad (10)$$

Тогда интеграл (9) запишется приближенно в виде

$$F^p_\nu = \pi A_{pq} N^p_\nu + \sum_{q=p-s}^{p-1} A_{pq} \int_0^\pi N(z, \mu^\nu_{pq}, \lambda_{p-q})\, d\alpha; \qquad (11)$$

$$\mu^\nu_{pq} = \mu_\nu \xi_{pq} + \sqrt{1-\mu^2_\nu}\sqrt{1-\xi^2_{pq}}\cos\alpha. \qquad (12)$$

Предположим теперь, что значения функции $N(z, \mu, \lambda)$ при $\lambda = \lambda_q < \lambda_p$ уже найдены. Тогда, подставляя соотношение (11) в уравнение (4) и перенося член $\pi A_{p_0} N^p_\nu$ в левую часть, получим

$$\mu \frac{\partial N^p_\nu}{\partial z} + (\Sigma^p - \pi A_{p_0}) N^p_\nu = \sum_{q=1}^{mp} A_{pq} \int_0^\pi N(z, \mu^\nu_{pq}, \lambda_{p-q})\, d\alpha. \qquad (13)$$

Правая часть последнего уравнения содержит известные функции, и задача решается методом, уже описанным выше. Остается вычислить интегралы

$$J^\nu_{pq} = \int_0^\pi N(z, \mu, \lambda_{p-q})\, d\alpha \qquad (14)$$

при $\mu = \mu^\nu_{pq}$ (см. формулу (12)). С этой целью разделим интервал $(-1 \leqslant \mu \leqslant +1)$ на две части $(-1, 0)$ и $(0, +1)$ и на каждой из них положим приближенно

$$N(z, \mu, \lambda_p) = \begin{cases} \sum_{s=0}^{r_1} a_{sp}(z)\mu^s, & \mu > 0; \\ \sum_{s=0}^{r_2} b_{sp}(z)\mu^s, & \mu < 0. \end{cases} \qquad (15)$$

Здесь r_1 и r_2 — некоторые постоянные, а коэффициенты a_{sp} и b_{sp} могут быть найдены различными способами, например методом наименьших квадратов.

Подставляя выражения (15) в формулу (14), приходим к интегралам, вычисление которых не представляет особых трудностей. Таким образом, нахождение пространственного и углового распределений γ-квантов при каждом новом значении энергетической переменной сводится к решению обыкновенного дифференциального уравнения (13) с известной правой частью, определенной на предыдущих этапах вычислений. При этом отпадает необходимость в применении метода последовательных приближений, обычно используемого при конечно-разностном решении многоскоростных кинетических уравнений [2, 3]. Отметим также, что описанный метод без существенных изменений может быть использован для решения задач переноса нейтронов в легких замедлителях.

Сферически-симметричные задачи. В этом случае задача сводится к решению уравнения [2]

$$\mu \frac{\partial N}{\partial r} + \frac{1-\mu^2}{r} \frac{\partial N}{\partial \mu} + \Sigma N = F + f \qquad (16)$$

с граничным условием

$$N(a, \mu, \lambda) = \chi(\mu, \lambda), \quad \mu < 0. \qquad (17)$$

В уравнении (16) интеграл рассеяния F определяется по той же формуле, что и в случае плоско-параллельных задач (с той разницей, что переменная z заменена переменной r).

Следовательно, задача сводится к дифференциальному уравнению (16) с известной правой частью, которое можно решить конечно-разностными методами, описанными в работах [3, 4].

---

* Предполагается, что Σ не зависит от z. Это ограничение несущественно.

** Разбиение интервала $[-1 \leqslant \mu \leqslant 1]$ таково, что ни один из узлов μ_ν не попадает на точку $\mu = 0$.

МЕТОДЫ МОНТЕ-КАРЛО

Расчет дифференциального потока $\Phi(\vec{r}, \vec{\Omega}, E)$. Известно, что метод прямого моделирования движения частицы в веществе оказался пригодным для сравнительно узкого класса задач. Был разработан ряд модификаций метода для повышения его статистической эффективности.

Одной из таких модификаций метода применительно к проблеме переноса излучения является метод локального вычисления потока. В первоначальной формулировке метода [5, 6] использован тот факт, что рассеянная часть дифференциального потока $\Phi_s(\vec{r}, \vec{\Omega}, E)$ в фиксированной точке пространства $\vec{r}^* = (x^*, y^*, z^*)$ равна среднему значению случайной величины

$$\xi = \sum_{n=1}^{\infty} W_n \frac{e^{-\tau(\vec{r}_n, \vec{r}^*, E'_n)}}{\varrho_n^2} f_s(\vec{r}_n, E_{n-1}, \vec{\Omega}_{n-1}\cdot\vec{\Omega}'_n) \times$$

$$\times \Delta(\vec{\Omega}'_n, \vec{\Omega}) \Delta(E'_n, E);$$

$$\varrho_n = |\vec{r}_n - \vec{r}^*|; \quad \vec{\Omega}'_n = \frac{\vec{r}^* - \vec{r}_n}{\varrho_n}, \qquad (18)$$

где $\vec{r}_n$, $\vec{\Omega}_n$, E_n — соответственно радиус-вектор точки n-го рассеяния частиц, направление и энергия после рассеяния; $f_s(\vec{r}_n, E_{n-1}, \vec{\Omega}_{n-1}\vec{\Omega}'_n)$ — функция рассеяния, то есть рассчитанная на единицу телесного угла вероятность частице, имевшей до рассеяния энергию E_{n-1} и направление $\vec{\Omega}_{n-1}$, рассеяться в направлении $\vec{\Omega}'_n$ (при этом ее энергия есть $E'_n = \varphi(E_{n-1}, \vec{\Omega}_{n-1}\cdot\vec{\Omega}'_n)$. В формуле (18) W_n есть «вес» n-го рассеяния, $\tau(\vec{r}_n, \vec{r}^*, E'_n)$ — оптическое расстояние между точками $\vec{r}_n$ и $\vec{r}^*$ для частиц с энергией E'_n, $\Delta(x'_n, x)$ — характеристическая функция интервала Δx около x.

Каждая отдельная реализация процесса блуждания частицы («история») доставляет выборочные значения координат частицы в фазовом пространстве $Q = (\vec{r}, \vec{\Omega}, E)$, по которым вычисляется соответствующее значение случайной величины ξ. Согласно теореме Хинчина [7] имеет место сходимость по вероятности среднеарифметического из N «историй» к точному значению потока при $N \to \infty$. Вследствие того что высшие моменты случайной величины ξ и, в частности, дисперсия не существуют, эта сходимость весьма медленная. Другим недостатком метода является необходимость просмотра очень большого количества «историй» для получения надежных сведений об угловом и энергетическом распределении потока.

Калос [8] предложил модификацию описанного метода, имеющую конечную дисперсию для полного потока

$$\Phi_s(\vec{r}) = \int\int \Phi(\vec{r}^*, \vec{\Omega}, E)\, d\vec{\Omega}\, dE.$$

Этот метод основан на включении множителя $1/\varrho_n^2$, обусловливающего расходимость дисперсии ξ, в переходную вероятность марковской цепи положений частицы в фазовом пространстве и, следовательно, изменяющего характер выборки.

Можно предложить вариант метода Монте-Карло, дающий конечную дисперсию для полного потока и не изменяющий характер выборки. Другой полезной особенностью метода является возможность получения энергетического распределения $\Phi_s(\vec{r}^*, \vec{\Omega}^*, E)$ для выделенного фиксированного направления $\vec{\Omega}^*$.

В описанном выше методе оценка потока основана на представлении его в виде суммы вкладов нерассеянного излучения, источниками которого являются отдельные точки рассеяния блуждающей частицы. Легко показать, что аналогичное представление имеет место, если суммировать вклады однократно рассеянного излучения, так что

$$\Phi_s(\vec{r}^*, \vec{\Omega}^*, E) = \Phi^{(1)}(\vec{r}^*, \vec{\Omega}^*, E) + \mathrm{MO} \sum_{n=1}^{\infty} \xi_n;$$

$$\xi_n = \frac{W_n e^{-\tau(\vec{r}_n, \vec{r}'_n, E'_n) - \tau(\vec{r}'_n, \vec{r}^*, E)}}{x_n^2} \Sigma_s(\vec{r}'_n, E'_n) \times$$

$$\times f_s\left(\vec{r}_n, E_{n-1}, \frac{\vec{\Omega}_{n-1}\cdot\vec{x}_n}{x_n}\right) f_s\left(\vec{r}'_n, E'_n, \frac{\vec{\Omega}^*\cdot\vec{x}_n}{x_n}\right) \frac{1}{\frac{dE}{dt_n}}, \qquad (19)$$

где

$$\vec{x}_n = \vec{R}_n - \vec{\Omega}^* \cdot t_n; \quad \vec{R}_n = \vec{r}^* - \vec{r}_n;$$

$$\vec{r}'_n = \vec{r}_n + \vec{x}_n = \vec{r}^* - \vec{\Omega}^* t_n;$$

$$E'_n = \varphi\left(\vec{r}_n, E_{n-1}, \frac{\vec{\Omega}_{n-1}\cdot\vec{x}_n}{x_n}\right);$$

$$E = \varphi\left(\vec{r}'_n, E'_n, \frac{\vec{\Omega}^*\cdot\vec{x}_n}{x_n}\right).$$

В формуле (19) $\Phi^{(1)}(\vec{r}^*, \vec{\Omega}^*, E)$ есть вклад однократно рассеянного излучения, МО — символ математического ожидания.

Можно показать, что оценка, вытекающая из формулы (19), имеет конечную дисперсию для полного потока. Дисперсия дифференциального потока Φ_s не существует, однако устраняется трудность, связанная с малостью фазового объема в пространстве направлений.

В качестве примера рассмотрим случай однородной бесконечной среды с изотропным рассеянием. Для изотропного источника формула (19) приводит к следующему результату:

$$\Phi_s(r) = \mathrm{MO} \sum_{n=1}^{\infty} \left(\frac{\Sigma_s}{\Sigma_t}\right)^n F(R_{n-1}),$$

где

$$F(R)=\frac{2\Sigma_t}{4\pi R}\sum_{k=0}^{\infty}\frac{1}{(2k+1)}E_{2(k+1)}(R\Sigma_t);$$

$$R_n=|\vec{r}_n-\vec{R}_0|;\quad |R_0|=r;\quad E_j(x)=\int_1^{\infty}\frac{e^{-xt}}{t^j}dt.$$

В табл. 1 приведены результаты 10 выборок по 200 «историй» в каждой для случая $\Sigma_s/\Sigma_t = 0{,}75$, $r\Sigma_t = 1$, полученные двумя описанными выше методами.

Другой способ повышения эффективности метода локального вычисления потока основы-

Таблица 1

Номер выборки	Поток по (18)	Поток по (19)
1	0,0678	0,0656
2	0,0689	0,0660
3	0,0624	0,0634
4	0,0843	0,0721
5	0,0596	0,0637
6	0,0688	0,0628
7	0,0842	0,0689
8	0,0746	0,0660
9	0,0896	0,0761
10	0,0567	0,0615
Среднее	0,0709	0,0666
Точное значение	0,0665	

вается на том факте, что случайные величины

$$\xi'=\xi\Psi_1(\vec{r}^*)\ \text{и}\ \xi''=\xi\Psi_2(\vec{S}^*)$$

обладают конечной дисперсией, если $\vec{r}^*$ и $\vec{S}^*$ случайные векторы с невырожденными в D и соответственно S распределениями. Здесь Ψ_1 и Ψ_2 произвольные суммируемые с квадратом в D (на S соответственно) функции, D — область трехмерного пространства переменных x^*, y^*, z^*, а S^* — участок поверхности в том же пространстве.

Это обстоятельство позволяет, выбирая в качестве функции Ψ_1 ортонормированные с весом в D функции, вычислять коэффициенты Фурье функции потока.

Если весовая функция $p(\vec{r}^*)$ выбрана удачно, то восстановление функции потока по ее коэффициентам Фурье осуществляется с достаточно высокой точностью. Те же соображения справедливы относительно вычисления потока на поверхности S.

Вычисления производятся следующим образом. В начале каждой «истории» частицы случайным образом в D выбирается положение детектора $\vec{r}^*$. Вычисляется величина $\xi(\vec{r}^*)$. Далее можно домножить $\xi(\vec{r}^*)$ на $\Psi_i(\vec{r}^*)$ и на $p(\vec{r}^*)$. Если $\vec{r}^*$ — вектор, распределенный равномерно в D, то МО $\xi(\vec{r}^*)\varphi_i(\vec{r}^*)p(\vec{r}^*)$ есть коэффициент Фурье функции потока, $\varphi_i(\vec{r}^*)$ ортонормированные в D с весом $p(\vec{r}^*)$ функции ($i = 0,1, \ldots, n$).

Такой способ вычисления коэффициентов Фурье, однако, не является наилучшим, так как МО $\xi(\vec{r}^*)\varphi_i(\vec{r}^*)p(\vec{r}^*)$ может быть малой величиной, а дисперсия $D\{\xi(\vec{r}^*)\varphi_i(\vec{r}^*)p(\vec{r}^*)\}$ может оказаться значительной. В этих случаях полезным оказывается следующее обобщение теорем 1 и 2 работы [9] (далее мы будем пользоваться обозначениями этой работы). Пусть $f(Q)$ — суммируемая с квадратом с весом $p(Q)$ ($p(Q) \geqslant 0$) в D функция ($Q \in D$).

Рассмотрим обобщенный интерполяционный многочлен $p(Q) = c_0\varphi_0(Q) + c_1\varphi_1(Q) + \ldots + c_n\varphi_n(Q)$, константы c_i ($i = 0,1, \ldots, n$) определяются из условий $p(Q_j) = f(Q_j)$, где Q_j — некоторые фиксированные точки области D. Справедлива следующая теорема.

Теорема 1. Если точки Q_j выбираются в области D случайно с плотностью вероятности $w_n(Q_0, Q_1, \ldots, Q_n)$

$$w_n=\frac{1}{(n+1)!}\left[\det\|\varphi_0(Q_m)\sqrt{p(Q_m)}, \ldots, \varphi_n(Q_m)\sqrt{p(Q_m)}\|_0^n\right]^2,$$

то

$$\text{МО}\,c_i=\int_D p(Q)f(Q)\varphi_i(Q)\,dQ,\quad i=0, 1, \ldots, n.$$

При тех же предположениях справедлива

Теорема 2. Дисперсия случайной величины c_i равна

$$\int_D p(Q)\left[f(Q)-\sum_{i=0}^{n}\text{МО}\,c_i\varphi_i(Q)\right]^2 dQ.$$

Ниже в табл. 2 приводятся результаты расчета численного спектра γ-квантов в воздухе по методу локального вычисления потока.

В табл. 3 те же величины получены при помощи линейного алгебраического интерполирования по случайным точкам. Весовая функция в данном случае не вводилась.

Таблица 2

Номер группы	Номер выборки			
	1	2	3	4
1	1,580	0,925	0,737	0,808
2	1,039	1,162	1,123	0,975
3	0,450	0,296	0,342	0,496
4	0,826	0,303	0,104	0,228
5	0,123	0,105	0,214	0,149
6	0,138	0,594	0,376	0,129
7	0,053	0,145	0,110	0,112
8	0,073	0,208	0,164	0,022
Интегральный поток	4,832	3,322	4,107	2,917

В таблицах приведены четыре группы данных. Каждая группа получена в результате 1000 испытаний.

Источник γ-квантов — точечный изотропный моноэнергетический $E_0 = 1{,}25$ *Мэв*. Расстояние от источника до детектора равно 30 *м*. Интервал энергий от 0 до 1,25 *Мэв* разбит на 8 равных групп. Если приведенное в табл. 2 и 3 число умножить на 10^{-9}, то мы получим количество γ-квантов в 1 *сек/см*^{2}, попавших в данную энергетическую группу.

Таблица 3

Номер группы	Номер выборки			
	1	2	3	4
1	1,006	0,864	0,678	0,827
2	1,463	1,359	0,910	1,322
3	0,335	0,437	0,753	0,173
4	0,301	0,127	0,117	0,292
5	0,461	0,415	0,289	0,576
6	0,398	0,095	0,281	0,356
7	0,192	0,050	0,694	0,000
8	0,000	0,417	0,087	0,460
Интегральный поток	3,986	3,763	3,809	4,006

РАСЧЕТ ФУНКЦИОНАЛОВ ОТ ДИФФЕРЕНЦИАЛЬНОГО ПОТОКА

1. В неоднородных задачах теории переноса нейтронов метод Монте-Карло часто применяется для вычисления функционалов f от дифференциального потока $\Phi(\vec{r}, \vec{\Omega}, E)$ в пространственно-энергетической области $\Delta E \cdot \Delta v$

$$f = \int d\vec{\Omega}_0 \int\limits_{\Delta E_0} dE_0 \int\limits_{\Delta v_0} dr_0 S(\vec{r}_0, \vec{\Omega}_0, E) \times \int d\Omega \int\limits_{\Delta E} dE \int\limits_{\Delta v} d\vec{r}\, f(\vec{r}, \vec{\Omega}, E) \times \Phi(\vec{r}_0, E_0, \vec{\Omega}_0; \vec{r}, \vec{\Omega}, E), \quad (20)$$

где $\Phi(r, \vec{\Omega}, \vec{E}; r_0, \vec{\Omega}_0, E_0)$ — функция Грина соответствующего уравнения переноса. Как правило, области определения источника $S(\vec{r}_0, \vec{\Omega}_0, E)$ и функции $f(\vec{r}, \vec{\Omega}, E)$ сильно отличаются, поэтому повышение статистической эффективности достигается, когда выборку начальных координат «истории» осуществляют[10] в соответствии с функцией ценности относительно функционала f. Точное отыскание функции ценности — задача не менее сложная, чем исходная, поэтому при оценке функционала f естественно попытаться конструировать такую функцию ценности. Если такая функция $\widetilde{Q}(\vec{r}_0, \vec{\Omega}_0, E_0)$ построена, то функционал f можно переписать в виде [1]

$$f = \int d\Omega_0 \int\limits_{\Delta E_0} dE_0 \int d\vec{r}_0 \widetilde{S}(\vec{r}_0, \vec{\Omega}_0, E_0) R(\vec{r}_0, \vec{\Omega}_0, E_0) \times \times \int d\vec{\Omega} \int dE \int dr f(\vec{r}, \vec{\Omega}, E) \Phi(\vec{\Omega}, \vec{r}, E; \vec{\Omega}_0, r_0, E_0), \quad (21)$$

где

$$\widetilde{S}(\vec{r}_0, \vec{\Omega}_0, E_0) = \frac{S(\vec{r}_0, \vec{\Omega}_0, E_0)\widetilde{Q}(\vec{r}_0, \vec{\Omega}_0, E_0)}{\int d\vec{\Omega}_0 \int dE_0 \int d\vec{r}_0 S(\vec{r}_0, \vec{\Omega}_0, E_0)\widetilde{Q}(r_0, \Omega_0, E_0)};$$

$$R(\vec{r}_0, \vec{\Omega}_0, E_0) = \frac{\int d\vec{\Omega} \int dE \int d\vec{r} S \cdot Q}{\widetilde{Q}(\vec{r}_0, \vec{\Omega}_0, E_0)}$$

и выбор начальных координат «истории» осуществлять в соответствии с плотностью $\widetilde{S}$ и начальным весом R.

При определении параметров разрешенных нейтронных уровней по результатам измерений радиационного захвата возникает необходимость вычисления функционалов вида (20), которые представляют в этом случае среднюю скорость поглощения в плоском образце толщиной H нейтронов от плоского источника с заданным спектром $S(E_0)$ в интервале энергий ΔE_0, целиком заключающем рассматриваемый резонанс [11, 12, 13]. В этой задаче метод Монте-Карло применяется для оценки средней скорости поглощения нейтронов, испытавших рассеяние P_s, которое имеет вид

$$P_s = \int\limits_{\Delta E_0} dE_0 S(E_0) \int\limits_{-1}^{+1} d\mu \int\limits_{\Delta E} dE \int\limits_{0}^{H} \times dz\, \Sigma_\gamma(E) \Phi_s(z, \mu, E, E_0), \quad (22)$$

где $\Phi_s(z, \mu, E, E_0)$ — поток нейтронов после однократного рассеяния. Для оценки функционала (22) использование функции ценности весьма существенно, так как область определения источника ΔE_0 всегда значительно превосходит область, где функция ценности

$$Q(E_0) = \int\limits_{-1}^{+1} d\mu \int\limits_{\Delta E} dE \int\limits_{0}^{H} dz\, \Sigma_\gamma(E) \Phi_s(z, \mu, E, E_0)$$

отлична от нуля.

Для построения приближенной функции $\widetilde{Q}(E_0)$ выберем следующую модель переноса нейтронов. Будем считать, что нейтроны распространяются в образце эффективной толщины H^* без столкновения, но на границе некоторая доля нейтронов P отражается с изменением энергии на величину средней логарифмической потери ξ, Тогда приближенная функция ценности запишется следующим образом:

$$\widetilde{Q}(E_0) = \sum_{n=0}^{\infty} P_{n+1} \varrho^n \prod_{l=0}^{n} S_l, \quad (23)$$

где

$$P_k = \frac{\sigma_\gamma(E_k)}{\sigma_t(E_k)}\left(1 - e^{-H^*\Sigma_t(E_k)}\right);$$

$$S_k = \frac{\sigma_s(E_k)}{\sigma_t(E_k)}\left(1 - e^{-H\Sigma(E_k)}\right);$$

$$E_k = E_0 e^{-k\xi}.$$

В методе существенной выборки начальных координат всегда используется нормированная функция ценности, поэтому отклонения значений параметров H^* и P от H и 1 соответственно не оказывают большого влияния на эффективность применения приближенной функции. Основная черта этой функции — смещение максимума относительно резонансной энергии — передается достаточно хорошо введением в выражение (23) средней логарифмической потери ξ. При реализации метода Монте-Карло для оценки функционалов типа (22) важно, что введение способа существенной выборки по функции ценности (23) не препятствует применению метода подобных траекторий для одновременного коррелированного расчета широкого набора толщин образцов.

Этот способ улучшения статистической эффективности оказался весьма полезным также в задаче расчета резонансного поглощения в плоском слоистом активационном детекторе [14]. С помощью одной приближенной функции ценности для образца промежуточной толщины удается провести вычисления активационного поглощения на отдельном уровне во внутреннем слое детектора одновременно для широкого набора толщин фильтров. Такие расчеты были проведены для некоторых активируемых изотопов с целью получить оптимальные толщины образцов для измерения спектров нейтронов внутри реактора.

2. Другой способ увеличения статистической эффективности метода Монте-Карло при оценке функционалов (20) в случае, когда его область $\Delta E \cdot \Delta v$ определения существенно меньше области определения плотности потока $\varphi(\vec{r}, \vec{\Omega}, E)$, основан на получении некоторой информации о функции ценности в процессе блужданий и использовании ее для выбора дальнейшей судьбы нейтрона. Это способ ветвлений.

Если в процессе блужданий нейтрон имеет перед очередным столкновением координаты $(\vec{r}_n, \vec{\Omega}_n, E_n)$, не принадлежащие области определения функционала, то вероятность внести вклад в этот функционал после столкновения равна соответствующей части G_f объема единичного гиперкуба. Выбирая случайно и равномерно точку ϱ из этой части гиперкуба, мы получаем при каждом столкновении вклад в функционал f и одну из ветвей для дальнейшей судьбы нейтрона. Вторая ветвь, обеспечивающая компенсацию смещения такой выборки, соответствует случайной точке из области гиперкуба, дополнительной к G_f. Выбор между этими двумя ветвями осуществляется случайным образом в соответствии с их весами G_f и $1 - G_f$.

Применение способа ветвлений оказалось весьма полезным при вычислении методом Монте-Карло функции влияния для моноэнергетического изотропного источника, расположенного на поверхности блока в бесконечной цилиндрической решетке. Эта функция, являющаяся аналогом функции Плачека в гомогенной среде, представляет интерес в задачах резонансного поглощения в гетерогенных средах.

В этой задаче в качестве функционала f рассматривалась следующая величина:

$$f = \int d\vec{\Omega} \int\limits_{v_{бл}} d\vec{r} \int dE \Sigma_t(\vec{r}, E)\, \Phi(\vec{r}, \vec{\Omega}, E),$$

представляющая среднюю плотность столкновений в блоке в интервале энергий $E_i \leqslant E \leqslant E_{i+1}$.

Определение границ многомерной области G_f и выбор случайной точки из этой области, как правило, представляют весьма трудную задачу, поэтому желательно организовывать ветвления по одной из переменных.

В рассматриваемом случае область, обеспечивающая вклад в функционал f, определяется условием

$$|\sin\varphi_{n+1}| \leqslant \frac{R_{бл}}{|r|} \equiv A,$$

где φ_{n+1} — азимутальный угол направления скорости нейтронов после рассеяния, а $R_{бл}$ — радиус блока. Ветвление осуществляется по одной переменной — μ_0 — косинусу угла рассеяния в системе инерции. Тогда можно получить следующие соотношения для весов ветвей:

$$G_1 = \frac{1}{2}\left|\mu_0^{(1)} - \mu_0^{(2)}\right|; \quad G_2 = 1 - G_1,$$

где

$$\mu_0^{(1,2)} = \frac{\eta_{1,2}\sqrt{(M^2+1)\varkappa_{1,2}^2 \sin^2\theta + M^2\eta_{1,2}^2} - \varkappa_{1,2}^2 \sin^2\theta}{M(\sin^2\theta\,\varkappa_{1,2}^2 + \eta_{1,2}^2)},$$

а

$$\eta_{1,2} = A\xi' \pm \sqrt{1+A^2}\,\eta';$$

$$\varkappa_{1,2} = A\cos\varphi \mp \sqrt{1-A^2}\sin\varphi;$$

$$\xi' = \sin\alpha\sin\varphi_n + \cos\alpha\cos\varphi_n\cos\theta_n;$$

$$\eta' = \sin\alpha\cos\varphi_n - \cos\alpha\sin\varphi_n\cos\theta_n;$$

M — масса ядра.

Вычисления гетерогенной функции Плачека показали значительное увеличение статистической эффективности метода Монте-Карло за счет применения способа ветвлений, особенно в случае очень тонких блоков.

ЛИТЕРАТУРА

1. У. Фано, Л. Спенсер и М. Бергер. Перенос гамма-излучения. М., Госатомиздат, 1963.
2. Г. И. Марчук. Теория и методы расчета ядерных реакторов. М., Госатомиздат, 1961.
3. Б. Карлсон. Численное решение задач кинетической теории нейтронов. В сб. «Теория ядерных реакторов». Под ред. Г. Биркхофа и Е. Вигнера. М., Госатомиздат, 1963.
4. Ш. С. Николайшвили. Односкоростная задача об угловых распределениях нейтронов, испускаемых точечным изотропным источником, помещенным в центре сферы. В сб. «Теория и методы расчета реакторов». М., Госатомиздат, 1961.
5. R. E. Lynch, W. P. Johnson, T. W. Beniot, C. D. Zerby. ORNL-2292, vol. 1-A.
6. В. Г. Золотухин, С. М. Ермаков. Применение метода Монте-Карло для расчета защиты от ядерных излучений. В сб. «Вопросы физики защиты реакторов». Под ред. Д. Л. Бродера и др. М., Госатомиздат, 1963.
7. Б. В. Гнеденко, А. Н. Колмогоров. Предельные теоремы для сумм независимых случайных величин. М., Гостехиздат, 1948.
8. M. H. Kalos. Nucl. Sci. and Eng., *16*, No. 1, 111 (1963).
9. С. М. Ермаков. Журнал вычислительной математики и математической физики, *3*, № 1, 186 (1963).
10. Г. И. Марчук, В. В. Орлов. К теории сопряженных функций. В сб. «Нейтронная физика». Под ред. Г. И. Марчука. М., Госатомиздат, 1961.
11. Д. Зелигер, Н. Илиеску, Ким Хи Сан, Д. Лонго, Л. Б. Пикельнер и Э. И. Шарапов. ОИЯИ Р-1218, Дубна (1963).
12. J. Kennett, L. M. Bollinger. Nucl. Phys., *42*, 249 (1959).
13. E. R. Rae, E. R. Collins, B. B. Kinsey, J. E. Lynn, E. R. Wiblin. Nucl. Phys., *5*, 89 (1958).
14. М. Н. Николаев. Атомная энергия, *11*, 522 (1963).

ABSTRACT—RÉSUMÉ—АННОТАЦИЯ—RESUMEN

A/363 USSR

Methods of solution of transport equation in inhomogeneous and finite media

By S. M. Ermakov *et al.*

The paper consists of three parts. The first part is devoted to finite-difference methods of solution of plane-parallel and spherical-symmetric γ-quanta and neutron transport problems in hydrogenous media. In the second part some methods for the improvement of the statistical efficiency of Monte Carlo methods for the case of radiation transport problems in inhomogeneous and finite media are considered. The third part is devoted to the Monte Carlo study of the neutron penetration through the resonance absorber slab.

1. To formulate a finite-difference method of solution of the integro-differential transport equation it is necessary to consider separately two problems: (*a*) a finite-difference representation of the differential part of the equation and the solution of the system obtained; (*b*) an approximate estimate of the scattering integral occurring in the equation.

In the case of plane-parallel problems, the formulation of part (*a*) is not difficult. When the spherically-symmetric problems are investigated, the method similar to the Carlson's S_n-method can be used. The difficulties due to singularities of the equation at the origin are avoided by means of the Vladimirov's characteristics method.

For the formulation of part (*b*) both for the plane-parallel and spherically-symmetric problems, the scattering integral is written down as a double integral along the surface of unit sphere and then evaluated using the simplest quadrature formula so constructed that the main features of the scattering kernel and the relatively weak dependence of the directional distributions on the energy are taken into account.

In practice the energy interval is divided into subintervals and in each of them the spectral distribution is represented by a linear function of energy with coefficients depending on directional and spatial coordinates. At each fixed value of energy the integro-differential equation is considered to be a differential equation with a known right side. An appropriate choice of the quadrature formula for the approximate calculation of the scattering integral makes the use of iterative procedures unnecessary.

A range of applications of the methods described can be extended appreciably by means of the adjoint function theory.

2. In the second part of the paper, problems of calculating differential angular and energy distributions of the radiation at a fixed point in space (local flux calculation method) are examined. This method, proposed by Zerby and collaborators, has an infinite standard deviation which considerably reduces its efficiency. A modification of the local flux calculation method is proposed which will have a finite standard deviation for the total flux or dose rate at a point fixed in space.

Calculation of Fourier coefficients of the flux function in terms of space variables also ensures finiteness of the standard deviation. In this case the slow convergence of Fourier series may be improved by the choice of a weighting function which takes into account the singularity of the integrand. An application of the local flux calculation method to the problem of penetration of radiation over a small surface element is also discussed in the paper.

The mathematical aspects of the problem arising as a result of the application of random quadrature formulae of higher accuracy are discussed. New quadrature formulae and evaluation of their errors, and examples of the calculation for one-velocity problems with an isotropic scattering are given.

3. A transfer of neutrons in a resonance absorber

slab is considered. For this purpose the Monte Carlo method using importance sampling of initial energies of neutrons proved to be very effective. A specially constructed function is used as an adjoint function. This approach makes it possible to perform neutron absorption and penetration calculations for a wide range of sample thicknesses.

A/363 URSS

Méthodes pour la solution des équations de transport dans des milieux non homogènes et finis

par S. M. Ermakov *et al.*

Le mémoire se compose de trois parties. La première est consacrée à l'application des méthodes aux différences finies à la solution des problèmes plan-parallèle et des problèmes de symétrie sphérique que pose le transport des photons et des neutrons dans des milieux hydrogénés. La deuxième traite de plusieurs procédés permettant d'augmenter l'efficacité statistique des méthodes de Monte-Carlo pour l'étude des problèmes de transport dans des milieux non homogènes et finis. La troisième partie est consacrée à l'étude, par une méthode de Monte-Carlo, du problème de la pénétration des neutrons dans une plaque d'absorption par résonance.

1. Pour formuler une méthode aux différences finies permettant de résoudre l'équation de transport intégro-différentielle, il faut étudier les deux problèmes suivants: *a*) représentation aux différences finies de la partie différentielle de l'équation et solution du système obtenu; *b*) calcul approché de l'intégrale de diffusion.

En ce qui concerne les problèmes plan-parallèle, le point *a*) ne présente aucune difficulté. Lorsque l'on étudie les problèmes de symétrie sphérique, on peut faire appel à une méthode analogue à la méthode S_n de Carlson. Pour éviter les difficultés dues aux singularités de l'équation au centre, on a recours à la méthode des caractéristiques de Vladimirov. On utilise cette même méthode pour passer de l'intensité du rayonnement émis dans une direction proche de la direction orientée vers le centre à l'intensité du rayonnement émis dans le sens opposé.

Pour ce qui est du point *b*), tant pour les problèmes plan-parallèle que pour ceux de symétrie sphérique, on écrit l'intégrale de diffusion sous la forme d'une intégrale double le long de la surface d'une sphère unitaire, pour la calculer ensuite à l'aide de formules de quadrature les plus simples. En établissant ces formules, on tient compte des particularités du noyau de diffusion et du fait que les fonctions de distribution angulaire varient relativement peu selon l'énergie.

En pratique, l'intervalle des énergies est subdivisé en sous-intervalles, et dans chacun de ceux-ci la distribution spectrale est représentée par une fonction linéaire de l'énergie dont les coefficients dépendent des coordonnées angulaires et spatiales. Pour une valeur donnée de l'énergie, l'équation intégro-différentielle est considérée comme étant une équation différentielle dont le membre de droite serait connu. Le choix d'une formule de quadrature appropriée pour le calcul approximatif de l'intégrale de diffusion permet d'éviter l'emploi d'une méthode d'itération. Le champ d'application des méthodes décrites peut être sensiblement élargi au moyen de la théorie des fonctions conjuguées.

2. Dans la deuxième partie du mémoire, les auteurs examinent les problèmes que pose le calcul de la distribution différentielle angulaire et énergétique du rayonnement en un point fixe de l'espace (méthode du calcul local du flux). Sous la forme proposée par Zerby et ses collaborateurs, cette méthode a une dispersion infinie, ce qui réduit sensiblement son efficacité. Les auteurs proposent une variante de la méthode de calcul du flux, qui a une dispersion finie pour la totalité du flux ou la dose en un point fixe de l'espace.

Le caractère fini de la dispersion est également assuré par le calcul des coefficients de Fourier de la fonction de flux suivant les variables spatiales. Dans ce cas, on peut éviter la convergence lente de la série de Fourier en choisissant une fonction de pondération qui tienne compte de la singularité de l'intégrande.

Les auteurs examinent également l'application de la méthode du calcul local du flux pour résoudre le problème du passage du rayonnement par une petite zone de la surface.

Ils étudient les aspects mathématiques d'un problème ayant trait à l'application de formules de quadrature stochastiques de grande précision. Ils indiquent de nouvelles formules de quadrature et évaluent leur degré de précision. Ils donnent à titre d'exemple la solution de problèmes à une vitesse avec diffusion isotrope.

3. Les auteurs étudient le problème du transport des neutrons dans une plaque d'absorption par résonance. La méthode de Monte-Carlo avec sélection judicieuse des énergies neutroniques initiales à partir du spectre de la source s'est révélée particulièrement efficace à cet effet. Comme fonction d'efficacité, on choisit une courbe spécialement construite qui permet de calculer l'absorption et le transport des neutrons pour des échantillons d'épaisseur très variée.

A/363 URSS

Métodos de resolución de la ecuación del transporte en medios no homogéneos y limitados

por S. M. Ermakov *et al.*

El documento consta de tres partes. La primera parte está dedicada a los métodos de diferencias finitas para la resolución de los problemas de transporte de cuantos gamma y de neutrones en medios hidrogenados con simetría plano-paralela y esférica.

En la segunda, se consideran algunos procedimientos para aumentar la eficacia estadística de los métodos de Monte Carlo en su aplicación a los problemas de transporte de la radiación en medios no homogéneos y limitados. La tercera parte está dedicada a la resolución con el método de Monte Carlo del problema del paso de los neutrones a través de una capa de absorbente que presenta resonancias.

1. Al formular el método de diferencias finitas para la resolución de la ecuación integrodiferencial del transporte hay que considerar por separado los dos problemas siguientes: *a*) representación de la parte diferencial de la ecuación mediante diferencias finitas y resolución del sistema así obtenido; *b*) cálculo aproximado de la integral de dispersión.

En el caso de simetría plano-paralela, la formulación de la primera parte del método no presenta dificultad. Para resolver el caso de simetría esférica, se utiliza un método análogo al método S_n de Carlson. Para soslayar las dificultades ligadas a las singularidades de la ecuación en el centro, se aplica el método de las características de Vladimirov. Este mismo método se emplea para pasar de las intensidades de la radiación en una dirección próxima a la radial hacia el centro a la intensidad en el sentido opuesto.

Para formular la segunda parte del método, tanto en el caso de simetría plano-paralela como en el de simetría esférica, la integral de dispersión se escribe como integral doble extendida a la superficie de la esfera de radio unidad y se calcula luego con ayuda de fórmulas de cuadratura muy simples. Al hacerlo se tiene en cuenta el comportamiento singular de la indicatriz de dispersión y se aprovecha la circunstancia de que las distribuciones angulares dependen relativamente poco de la energía.

En la realización práctica de los cálculos se subdivide el intervalo energético considerado en intervalos parciales y en cada uno de ellos la distribución espectral se representa mediante una función lineal de la energía con coeficientes que dependen de las variables angulares y espaciales. Para cada valor fijado de la energía, la ecuación integrodiferencial se considera como ecuación diferencial con segundo miembro conocido. Eligiendo convenientemente la fórmula de cuadratura para el cálculo aproximado de la integral de dispersión se puede evitar acudir al método de aproximaciones sucesivas.

El área de problemas a los que es aplicable este algoritmo se puede ampliar considerablemente si se introducen las funciones adjuntas.

2. En la segunda parte del documento se estudian los problemas del cálculo de la distribución angular y energética diferencial de la radiación en un punto fijo del espacio (método del cálculo local del flujo). Este método, en la forma propuesta por Tserb *et al.*, presenta una dispersión infinita, lo que restringe considerablemente su eficacia. Se propone una modificación del método del cálculo local del flujo, con dispersión finita para el flujo total o la dosis en un punto fijo del espacio.

Se consigue también una dispersión finita mediante el cálculo de los coeficientes de Fourier del flujo con relación a las variables espaciales. La lenta convergencia de la serie de Fourier se puede superar eligiendo una función de peso que tenga en cuenta la singularidad de la función subintegral.

En el informe se examina también la aplicación del método del cálculo local del flujo cuando se trata de resolver el problema del paso de la radiación a través de una pequeña porción de superficie.

Se examinan los aspectos matemáticos del problema asociados con la aplicación de fórmulas de cuadratura de alta precisión. Se presentan nuevas fórmulas de cuadratura y se da una estimación del error. Se ofrecen ejemplos del cálculo para el caso de partículas monoenergéticas y dispersión isótropa.

3. Se estudia la resolución del problema del transporte de neutrones en una lámina plana de absorbente con resonancias. Para la resolución de este problema resultó muy eficaz el método de Monte Carlo con una selección considerable de las energías iniciales de los neutrones del espectro de la fuente. Como función importancia se elige una función construída de manera especial y que permite calcular la absorción y el transporte de neutrones para una amplia gama de espesores.

Analytical methods in energy dependent transport theory

By H. Hejtmanek*

SECTION 1

We shall consider the Boltzmann equation of the following form:

$$l(v)\mu\frac{\partial\psi}{\partial x}+\psi=\iint_{\mathscr{R}}\mathrm{d}v'\mathrm{d}\mu'\ K(v',\mu'\to v,\mu)\psi(x,v',\mu') \tag{1}$$

where ψ is the collision density of neutrons and $l(v)=\Sigma^{-1}(v)$ is the total mean free path. The kernel gives the number of secondary neutrons per one collision. The two dimensional domain $\mathscr{R}$ consists of all points (v,μ) with $0\leq v\leq v_{\max}$ and $-1\leq\mu\leq+1$. We shall separate the space variable by the initial substitution:

$$\psi(x,v,\mu)=\exp\left(-\frac{x}{z}\right)\phi z(v,\mu) \tag{2}$$

where the separational constant z is an arbitrary complex number to be determined later. We get the singular integral equation

$$\left(1-\frac{l(v)\mu}{z}\right)\phi z=\iint_{\mathscr{R}}\mathrm{d}v'\mathrm{d}\mu'\ K(v',\mu'\to v,\mu)\phi z(v',\mu') \tag{3}$$

SECTION 2

The intervals $[0,v_{\max})$ and $[-1,+1]$ are divided into sub-intervals

$$I_i=(v_{i-1},v_i)\qquad 0=v_0<v_1<\ldots<v_M=v_{\max}$$

$$J_j=(\mu_{j-1},\mu_j)\qquad -1=\mu_0<\mu_1<\ldots<\mu_N=+1$$

The mean free path and the kernel have the form of step functions:

$$l(v)=\sum_{i=1}^{M}l_i\chi_i(v) \tag{4}$$

$$K(v',\mu'\to v,\mu)=\sum_{i,j,k,l,}K(i,j\to m,n)\chi_i(v')\chi(\mu')\chi_m(v)\chi_n(\mu')$$

where $\chi_i(v)$ and $\chi_j(\mu)$ are characteristic functions of the intervals I_i and J_i respectively. We define

$$\Phi_{ij}(z)=\int_{I_i}\mathrm{d}v P\int_{J_i}\mathrm{d}\mu\ \phi z(v,\mu) \tag{5}$$

Equation (3) can now be rearranged and solved

$$\phi_z(v,\mu)=\left[\Sigma K(i,j\to m,n)\frac{z\Phi ij(z)}{z-l_m\mu}+\lambda(z,v)\delta(z-l_m\mu)\right]\times\chi_m(v)\chi_n(\mu) \tag{6}$$

We apply the operation

$$\int_{I_r}\mathrm{d}v P\int_{J_s}\mathrm{d}\mu$$

to both sides of Eq. (6) and get a system of linear equations for the $\Phi_{ij}(z)$

$$\Phi_{rs}=\Sigma K(i,j\to m,n)\Phi_{ij}\int_{I_r}\mathrm{d}v\ P\int_{J_s}\mathrm{d}\mu\frac{z}{z-l_r\mu}\chi_m(v)\chi_n(\mu)+\int_{I_r}\mathrm{d}v P\int_{J_s}\mathrm{d}\mu\lambda(z,v)\delta(z-l_r\mu) \tag{7}$$

$$g_{rs}=\int_{I_r}\mathrm{d}v P\int_{J_s}\mathrm{d}\mu\frac{z}{z-l_r\mu}$$

$$\lambda_{rs}=\int_{I_r}\mathrm{d}v P\int_{J_s}\mathrm{d}\mu\ \lambda(z,v)\delta(z-l_r\mu) \tag{8}$$

In Eq. (7) the summation over (m,n) can be carried out, so we get

$$\Phi_{rs}=g_{rs}(z)\sum_{i,j}K(i,j\to r,s)\Phi_{ij}+\lambda_{rs}(z) \tag{9}$$

or in matrix notation

$$(E-A(z))\vec{\phi}=\vec{\lambda}(z) \tag{10}$$

SECTION 3

We assume $l_i>0$ and $\max l_i=1$ for all $i=1,\ldots M$, so the step function $\mu=z/l(v)$ in the (v,μ) plane is completely outside the domain $\mathscr{R}$ for z real and $|z|>1$. The functions $g_{mn}(z)$ are sectionally holomorphic in the whole analytic plane cut by the real interval $S_{mn}=[l_m\mu_{n-1},l_m\mu_n]$

$$g_{mn}(z)=m(I_m)\ P\int_{l_m\mu_{n-1}}^{l_m\mu_n}\frac{z}{z-\mu}\mathrm{d}\mu \tag{11}$$

We compute $g_{mn}(z)$ and distinguish the two cases

$$z\notin S_{mn}\ g_{mn}(z)=m(I_m)z\ \ln\left(+\frac{z-l_m\mu_{n-1}}{z-l_m\mu_n}\right) \tag{12}$$

and

$$z\epsilon S_{mn}{}^0\ g_{mn}(z)=m(I_m)z\ \ln\left(-\frac{z-l_m\mu_{n-1}}{z-l_m\mu_n}\right) \tag{13}$$

g_{mn} has no zeros $z\notin S_{mn}$. If $z\epsilon S_{mn}{}^0$ there are at most two in $z=0$, if $0\epsilon S_{mn}{}^0$, and $z=\frac{1}{2}(l_m\mu_{n-1}+l_m\mu_n)$. We define the open set S by

$$S=[-1,+1]-\sum_{m=1,n=0}^{M,N}l_m\mu_n \tag{14}$$

This set is simply the open interval $(-1,+1)$ perforated by the points $l_m\mu_n$. The determinant of the linear transformation in Eq. (9)

* Atominstitut der Österreichischen Hochschulen, Vienna.

$$D(z) = \det |E - A(z)| \tag{15}$$

contains products of the $g_{mn}(z)$. These products are sectionally holomorphic in the analytic plane cut by the set S. To prove this statement we have to show that near the point $l_m\mu_n$ the product is $\sigma(|z - l_m\mu_n|^{-\gamma})$ $0 \leq \gamma < 1$. This is true because $g_{mn} = \sigma(|z - l_m\mu_n|^{-\epsilon})$ for all $\epsilon > 0$. Then the product is $\sigma(|z - l_m\mu_n|^{-(\epsilon_1 + \ldots + \epsilon_T)})$ with ϵ_T so small that $\epsilon_1 + \ldots + \epsilon_T < 1$. $D(z)$ is a sectionally holomorphic function in the analytic plane cut by S. For all $z \notin [-1, +1]$ the functions $\lambda_{mn}(z)$ vanish, for $z \in S$ we get

$$\lambda_{mn}(z) = \int_{I_m} \lambda(z,\nu) \mathrm{d}\nu P \int_{J_n} \delta(z - l_m\mu) \mathrm{d}\mu$$

$$= \lambda_m(z) \times \begin{cases} 1 \text{ if } z \Sigma_m \epsilon J_n \\ 0 \text{ otherwise} \end{cases} \tag{16}$$

SECTION 4

The system of linear equations (9) whose coefficients depend on the complex parameter z becomes homogeneous for

$$z \notin [-1, +1] \; [E - A(z)]\vec{\phi} = 0$$

It has a non-trivial solution if and only if

$$D(z_\sigma) = 0 \tag{17}$$

The number of zeros in the cut plane is finite, the solutions span a linear manifold in the $M.N$ dimensional space whose dimension depends on the rank of the matrix $E - A(z)$. For $z \epsilon S$ $\vec{\lambda}(z) \neq 0$, so the system becomes unhomogeneous and can be solved for $\vec{\phi}$

$$\vec{\phi} = [E - A(z)]^{-1}\vec{\lambda}(z) \tag{18}$$

$\vec{\phi} = \vec{\phi}(z)$ $z \epsilon S$ describes a curve in the $M.N$ dimensional space, except at the points where $\det |E - A(z)| = 0$, but these are of finite number. The solution of Eq. (3) has the form

$$\phi_z(\nu,\mu) = \sum_{m,n} \left[\frac{\phi_{mn}(z) - \lambda_{mn}(z)}{g_{mn}(z)} P \frac{z}{z - l_m\mu} + \lambda(z,\nu)\delta(z - l_m\mu) \right] \chi_m(\nu)\chi_n(\mu)$$

for $z = z_\sigma \notin [-1, +1]$ and $z \epsilon S$. (19)

SECTION 5

The adjoint equation has a solution similar to Eq. (6)

$$\hat{\phi}_z(\nu,\mu) = \sum \left[K(m,n \to i,j) \frac{z\hat{\Phi}_{ij}(z)}{z - l_m\mu} + \hat{\lambda}(z,\nu)\delta(z - l_m\mu) \right] \times \chi_m(\nu)\chi_n(\mu) \tag{20}$$

the $\hat{\Phi}_{ij}$ being solutions of the system of linear equations

$$\hat{\Phi}_{rs} = g_{rs}(z) \sum_{i,j} K(r,s \to i,j) \hat{\Phi}_{ij} + \hat{\lambda}_{rs}(z) \tag{21}$$

The determinant of the adjoint equation equals (15). This follows from the identity

$$\det |\delta_{ik} - a_i b_{ik}| = \det |\delta_{ik} - a_k b_{ki}| \tag{22}$$

so we have

$$\hat{D}(z) = D(z) \tag{23}$$

The orthogonality relation has the form

$$\int_0^{\nu_{\max}} \mathrm{d}\nu \, P \int_{-1}^{+1} \mathrm{d}\mu \; l(\nu)\mu\phi_z(\nu,\mu)\phi_w(\nu,\mu) = 0 \tag{24}$$

if $z \neq w$.

SECTION 6

To prove the completeness of (19) we follow an idea of Bednarz and Mika [1]. We have to show that every step function $\psi(\nu,\mu)$ can be represented uniquely by the system (19) with certain coefficients A

$$\psi(\nu,\mu) = \sum_\sigma A_\sigma \phi_\sigma(\nu,\mu) + P \int_{-1}^{+1} A(z)\phi_z(\nu,\mu)\mathrm{d}z \tag{25}$$

We have for $I_m \times J_n$

$$\psi_{mn} = \sum_\sigma A_\sigma B_{mn}(z_\sigma) \frac{z_\sigma}{z_\sigma - l_m\mu} + P \int_{-1}^{+1} A(z) B_{mn}(z) \frac{z}{z - l_m\mu} \mathrm{d}z + \lambda(l_m\mu,\nu) A(l_m\mu) \tag{26}$$

with

$$B_{mn}(z) = \frac{\Phi_{mn}(z) - \lambda_{mn}(z)}{g_{mn}(z)} \tag{27}$$

The left side of Eq. (26) is independent of ν, so is the right side. We can choose $\lambda(z,\nu)$, a step function in ν.

$$\lambda(z,\nu) = \Sigma \lambda_i(z)\chi_i(\nu) \tag{28}$$

The function

$$\tilde{\psi}_{mn}(\mu) = \psi_{mn} - \sum_\sigma A_\sigma B_{mn}(z_\sigma) \frac{z_\sigma}{z_\sigma - l_m\mu} \tag{29}$$

can be written in the form

$$\tilde{\psi}_{mn}(\mu) = \lambda_m(l_m\mu) \; A(l_m\mu) + P \int_{-1}^{+1} A(z) \; B_{mn}(z) \frac{z}{z - l_m\mu} \, dz \tag{30}$$

The system of singular integral equations has a simultaneous solution $A(z)$ for a proper choice of $\lambda m(z)$.

SECTION 7

If the kernel in the Boltzmann equation is real, then

$$\overline{D(z)} = D(\bar{z}) \tag{31}$$

so with an eigenvalue z_σ, $\bar{z}_\sigma$ is an eigenvalue too. A necessary condition for criticality of a slab would be the existence of a positive and symmetric solution of (1). This is true if at least one eigenvalue is purely imaginary.

SECTION 8

The time dependent Boltzmann equation can be reduced by a Laplace transform to equation (1) with a parameter

$$l(v)\mu\frac{\partial\psi}{\partial x}+\lambda\psi=\iint_{\mathscr{R}}\mathrm{d}v'\mathrm{d}\mu' K(v',\mu'\to v,\mu)\psi(x,v,\mu') \quad (32)$$

This has been done by Wing [2] in the energy independent case. To find the eigenvalue λ we can use the method proposed above. So we can solve the initial value problem of a slab and the equivalent problem of finding the critical length [3].

SECTION 9

If $K(v',\mu'\to v,\mu)$ is a continuous function, it is possible to give a proof of existence of solutions to (1) by the limiting process

$$\max_i (v_i - v_{i-1})\to 0$$
$$\max_i (\mu_i - \mu_{i-1})\to 0$$

REFERENCES

1. Bednarz, R., and Mika, J., Institut of Nuclear Research (Poland) Report No. 385/IX.
2. Wing, G. M., *An Introduction to Transport Theory*, John Wiley and Sons (1962).
3. Hejtmanek, H., to be published.

ABSTRACT—RÉSUMÉ—АННОТАЦИЯ—RESUMEN

A/401 Autriche

Méthodes analytiques dans la théorie du transport en fonction de l'énergie

par H. Hejtmanek

La densité des neutrons en fonction du temps dans un espace de configuration à six dimensions est d'une importance fondamentale pour le calcul des différents paramètres et fonctions décrivant un réacteur. Il faut obtenir la solution de l'équation de Boltzmann avec les conditions aux limites et les valeurs initiales particulières déterminées par le réacteur que l'on considère. L'opérateur de choc du côté droit de l'équation ne dépend que des propriétés de choc et de transport du milieu du réacteur. Celles-ci sont elles-mêmes fonctions de l'espace et du temps:

$$\iint_{\mathscr{R}}\mathrm{d}v'\mathrm{d}\mu'\ K(v',\mu'\to v,\mu)-\left(1-\frac{l(v)\mu}{z}\right)$$

Il existe un grand nombre de méthodes approximatives qui rendent le calcul numérique possible avec une exactitude et une sûreté plus ou moins grandes. Il n'y a qu'un petit nombre de publications (1958, G. M. Wing) qui traitent de l'existence et de la structure des solutions. Elles donnent, en employant l'analyse avec variables réelles et variables complexes, des solutions rigoureuses et complètes de l'équation de Boltzmann indépendante de l'énergie et prouvent que quelques-unes des idées communément acceptées que l'on peut trouver dans les manuels de la théorie des réacteurs sont fausses. Dans l'équation de Boltzmann fonction de l'énergie, ou dans les équations que l'on en déduit, les opérateurs ne sont pas auto-adjoints. Ces opérateurs sont plus généraux que les observables employées habituellement en mécanique quantique. Ce fait complique la solution du problème. A l'aide de la théorie des opérateurs linéaires dans l'espace de Hilbert, deux cas principaux sont traités en détail: *a*) le spectre énergétique stationnaire dans un réacteur infini; *b*) la densité des neutrons en fonction du temps dans un réacteur-plaque.

Les modèles sur lesquels les calculs sont fondés sont très réalistes. Ils ne reposent sur aucune approximation mathématique. On peut donc espérer en tirer de bonnes méthodes d'approximation et déterminer le degré d'exactitude, ce qui n'est pas possible avec les autres méthodes.

A/401 Австрия

Аналитические методы в теории переноса, учитывающей зависимость от энергии

Г. Хейтманек

Зависящая от времени плотность нейтронов в шестимерном конфигурационном пространстве имеет важнейшее значение для расчета различных параметров и функций, характеризующих реакторы. Она определяется как решение уравнения Больцмана со специальными граничными и начальными условиями, которые определяются для каждого рассматриваемого реактора. Оператор столкновений в правой части уравнения зависит только от тех свойств реакторной среды, которые определяют характер столкновений и перенос нейтронов. Эти свойства также могут зависеть от пространства и времени:

$$\int\int dv'd\mu' K(v',\mu'\to v,\mu)-\left(1-\frac{l(v)\mu}{z}\right).$$

Для решения этой задачи имеются различные приближенные методы. Они позволяют сделать численные расчеты с большей или меньшей точностью и надежностью. Однако вопросы существования и структуры решений

рассматривались лишь в небольшом числе работ (Дж. М. Уинг, 1958 год). В этой работе были получены полные и строгие решения зависящего от энергии уравнения Больцмана и показано, что некоторые данные, приводимые в учебниках по теории реакторов, являются ошибочными. Операторы, появляющиеся в зависящем от энергии уравнении Больцмана или в полученных из него уравнениях, не являются самосопряженными. Эти операторы являются более общими, чем обычно используемые в квантовой механике. Это усложняет решение проблемы. В настоящей работе с помощью теории линейных операторов в гильбертовом пространстве подробно рассматриваются две основные задачи:

1) нахождение стационарного спектра нейтронов в неограниченном реакторе и

2) определение временной зависимости плотности нейтронов в плоском реакторе.

Основные модели расчета являются весьма реалистичными. Не делается никаких математических приближений. Можно ожидать таким образом, что предлагаемый путь решения может, в отличие от всех других методов, привести к хорошим приближенным методам, степень точности которых может быть сколь угодно высока.

A/401 Austria

Métodos analíticos en la teoría del transporte dependiente de la energía

por H. Hejtmanek

La densidad neutrónica dependiente del tiempo en el espacio hexadimensional de las configuraciones es de importancia fundamental para el cálculo de los diversos parámetros y funciones que describen un reactor. Es solución de la ecuación de Boltzmann con valores iniciales y condiciones de contorno determinados por el reactor que se considere. El operador de colisión que aparece en el segundo miembro de la ecuación depende sólo de las propiedades de colisión y de transporte del medio que constituye el reactor. También puede depender de las variables espaciales y del tiempo:

$$\iint_{\mathscr{R}} d\nu' d\mu' \cdot K(\nu', \mu' \to \nu, \mu) - \left(1 - \frac{l(\nu)\mu}{z}\right)$$

Hay diversos métodos aproximados que hacen posible el cálculo numérico, con más o menos precisión y seguridad. Sólo hay unos pocos artículos (1958, G. M. Wing) referentes a la existencia y estructura de las soluciones. Utilizando el análisis real y el complejo, proporcionan soluciones rigurosas y completas de la ecuación de Boltzmann independiente de la energía y prueban que ciertos lugares comunes que aparecen en los textos de teoría de reactores son falsos. Los operadores que aparecen en la ecuación de Boltzmann dependiente de la energía, o en las ecuaciones que de ella se deducen, no son autoadjuntos. Estos operadores son más generales que los observables usualmente empleados en mecánica cuántica. Esto complica la solución del problema. Utilizando la teoría de operadores lineales en el espacio de Hilbert, se tratan con detalle dos ejemplos importantes: *a*) El espectro neutrónico estacionario de un reactor ilimitado; *b*) La dependencia temporal de la densidad neutrónica en un reactor laminar.

Los modelos fundamentales del cálculo son bastante realistas. No se hacen aproximaciones matemáticas. Por eso se puede esperar que, a diferencia de los demás métodos, se puedan deducir sistemas de aproximación con el grado de precisión que se desee.

An approach to the solution of the two-group neutron diffusion equations in XY geometry

By T. Toivanen*

Most calculations in reactor theory are made under the assumption of spatial separability of the neutron flux distribution. In small fully reflected reactors this assumption introduces considerable errors, and it becomes necessary to treat the reactor two- or three-dimensionally. When the geometry of the reactor involves the distribution of material in two or three dimensions, an exact analytic solution is not available for group diffusion equations. Purely numerical calculations based on finite difference techniques are time consuming and expensive. The importance of analytic methods for solving two- and three-dimensional problems is reflected by the large number of investigations which have been devoted to the subject.

The purpose of this paper is to develop a new semi-analytic technique for treating reactors in which the outer reflector can be considered as infinite in extent. We deal with two-dimensional two-group diffusion equations. The particular reactor configuration investigated consists of a rectangular core fully reflected by a homogeneous infinite reflector. The discussion begins with the introduction of Green's functions for the reflector region and the formulation of the problem as a system of two-dimensional integral equations. In the next section the double Hankel transformation is applied in order to transform the set of integral equations into a more tractable set. We approach the solution in transform space by approximating the integral operators in the transformed equations by degenerate ones enabling us to reduce the problem to that of solving a finite system of linear algebraic equations. The solution in co-ordinate space is then found by an inverse Hankel transformation.

The method is not perfectly general. The utilization of the double Hankel transformation requires a symmetrical distribution of the reflector material. The method is capable of generating both the eigenvalues and the two-dimensional fluxes.

Integral equation formulation of the problem

The new technique developed is applied to a reactor geometry involving a rectangular core with dimensions $2a$ and $2b$. The core is completely reflected by an infinite homogeneous reflector, so that the reactor occupies the entire two-dimensional Euclidean space R_2.

Let G denote the interface between core and reflector and $\bar{G}$ its topological complement in space R_2. In the two-group diffusion approximation, the spatial neutron flux distribution in region $\bar{G}$ is described by the group equations [1]

$$\mathscr{D}_f(x,y)\nabla^2\phi_f(x,y) - \Sigma_f(x,y)\phi_f(x,y) + \frac{k(x,y)}{p(x,y)}\Sigma_a(x,y)\phi_s(x,y) = 0 \quad (1)$$

$$\mathscr{D}_s(x,y)\nabla^2\phi_s(x,y) - \Sigma_a(x,y)\phi_s(x,y) + p(x,y)\Sigma_f(x,y)\phi_f(x,y) = 0 \quad (2)$$

Here the subscripts f and s refer to the fast and thermal groups, respectively. The following symbols of conventional reactor theory are used:

$\phi_i(x,y)$ = neutron flux of group i, i = s,f
$\mathscr{D}_i(x,y)$ = diffusion coefficient of group i
$\Sigma_a(x,y)$ = absorption cross section for thermal neutrons
$\Sigma_f(x,y)$ = fast removal cross section
$k(x,y)$ = infinite multiplication factor
$p(x,y)$ = resonance escape probability

All of the material parameters are constant in the core and reflector regions. At the core reflector interface they have a finite discontinuity.

Let us denote by $L^2(R_2)$ the space of Lebesgue square integrable functions defined on R_2. Then the functions possessing continuous derivatives up to the second order on $\bar{G}$, being finite and non-negative, and satisfying the familiar boundary conditions of diffusion theory at G, define a linear manifold D in space $L^2(R_2)$. Acceptable solutions of Eqs. (1) and (2) belong to the class D.

For problems where the classical method of separation of variables fails, the use of Green's functions and integral equations techniques offers a powerful alternative approach. Rearranging the terms in Eqs. (1) and (2) we obtain

$$\left(-\nabla^2 + \frac{1}{L_f^2}\right)\phi_f(x,y) = \frac{k(x,y)}{p(x,y)}\frac{\Sigma_a(x,y)}{\mathscr{D}_f(x,y)}\phi_s(x,y) + \left[\frac{\Sigma_{fr}}{\mathscr{D}_{fr}} - \frac{\Sigma_f(x,y)}{\mathscr{D}_f(x,y)}\right]\phi_f(x,y), \quad (3)$$

* Institute of Technical Physics, Institute of Technology, Helsinki.

$$\left(-\nabla^2+\frac{1}{L_s^2}\right)\phi_r(x,y)-\frac{\Sigma_{tr}}{\mathscr{D}_{sr}}\phi_f(x,y)$$
$$=\left[p(x,y)\frac{\Sigma_f(x,y)}{\mathscr{D}_s(x,y)}-\frac{\Sigma_{tr}}{\mathscr{D}_{sr}}\right]\phi_f(x,y)$$
$$+\left[\frac{\Sigma_{ar}}{\mathscr{D}_{sr}}-\frac{\Sigma_a(x,y)}{\mathscr{D}_s(x,y)}\right]\phi_s(x,y) \quad (4)$$

where the reflector constants are indicated by the subscript r. Note that the right-hand sides of Eqs. (3) and (4) vanish outside the core. The quantities

$$L_t^2=\frac{\Sigma_{tr}}{\mathscr{D}_{tr}} \text{ and } L_s^2=\frac{\Sigma_{as}}{\mathscr{D}_{sr}}$$

are the slowing-down area and the diffusion area of the reflector, respectively. Let us now introduce two-dimensional infinite region Green's functions for the differential operators appearing on the left-hand side of Eqs. (3) and (4)

$$\left(-\nabla^2+\frac{1}{L_i^2}\right)\mathscr{G}_i(x,y,x_0,y_0)$$
$$=\delta(x-x_0)\,\delta(y-y_0),\ i=\text{s,f} \quad (5)$$

Eq. (3) is now converted into an integral equation as follows. Multiplying Eq. (3) by $G_f(x,y,x_0,y_0)$, Eq. (5) with $i=$f by $\phi_f(x,y)$, subtracting, and integrating over the region $\bar{G}$ we obtain

$$\phi_f(x,y)=\iint_{\bar{G}}[\mathscr{G}_f(x,y,x_0,y_0)\nabla^2\phi_f(x_0,y_0)$$
$$-\phi_f(x_0,y_0)\nabla^2\mathscr{G}_f(x,y,x_0,y_0)]\,dx_0,dy_0$$
$$+\left(\frac{\Sigma_{tr}}{\mathscr{D}_{tr}}-\frac{\Sigma_{tc}}{\mathscr{D}_{tc}}\right)\int_{-a}^{a}\int_{-b}^{b}\phi_f(x_0,y_0)\mathscr{G}_f(x,y,x_0,y_0)\,dx_0,dy_0$$
$$+\frac{k}{p}\frac{\Sigma_{ac}}{\mathscr{D}_{tc}}\int_{-a}^{a}\int_{-b}^{b}\phi_s(x_0,y_0)\mathscr{G}_f(x,y,x_0,y_0)\,dx_0,dy_0 \quad (6)$$

where the subscript c stands for the core region. Since the Laplacians in the first integral on the right-hand side of Eq. (6) act on different manifolds of the space $L^2(R_2)$ the corresponding differential operators are non-self-adjoint, and the integral over the region $\bar{G}$ does not vanish. The former Laplacian acts on the manifold D while the domain of the latter is restricted to functions which are continuous and have continuous first derivatives in (x,y) space except at the point $x=x_0$, $y=y_0$. Bearing in mind the discontinuity of the first partial derivatives of the fluxes at G, and integrating by parts twice, we arrive at the result

$$\phi_f(x,y)=\int_{-a}^{a}\mathscr{G}_f(x,y,x_0,b)\frac{\partial}{\partial y_0}[\phi_f(x_0,b-0)$$
$$-\phi_f(x_0,b+0)]\,dx_0+\int_{-a}^{a}\mathscr{G}_f(x,y,x_0,-b)\frac{\partial}{\partial y_0}\cdot$$
$$\times[\phi_f(x_0,-b-0)-\phi_f(x_0,-b+0)]\,dx_0$$
$$+\int_{-b}^{b}\mathscr{G}_f(x,y,a,y_0)\frac{\partial}{\partial x_0}[\phi_f(a-0,y_0)-\phi_f(a+0,y_0)]dy_0$$
$$+\int_{-b}^{b}\mathscr{G}_f(x,y,-a,y_0)\frac{\partial}{\partial x_0}[\phi_f(-a-0,y_0)$$
$$-\phi_f(-a+0,y_0)]\,dy_0+\left(\frac{\Sigma_{tr}}{\mathscr{D}_{tr}}-\frac{\Sigma_{tc}}{\mathscr{D}_{tc}}\right)$$
$$\times\int_{-a}^{a}\int_{-b}^{b}\phi_s(x_0,y_0)\mathscr{G}_f(x,y,x_0,y_0)\,dx_0dy_0$$
$$+\frac{k}{p}\frac{\Sigma_{ac}}{\mathscr{D}_{tc}}\int_{-a}^{a}\int_{-b}^{b}\phi_s(x_0,y_0)\mathscr{G}_f(x,y,x_0,y_0)\,dx_0dy_0. \quad (7)$$

The integral equation describing diffusion in the thermal group may be derived from Eq. (4) in a similar fashion. The result is

$$\phi_s(x,y)-\frac{\Sigma_{tr}}{\mathscr{D}_{sr}}\int_{-\infty}^{\infty}\int_{-\infty}^{\infty}\mathscr{G}_s(x,y,x_0,y_0)\phi_f(x_0,y_0)\,dx_0dy_0$$
$$=\int_{-a}^{a}\mathscr{G}_s(x,y,x_0,b)\frac{\partial}{\partial y_0}[\phi_s(x_0,b-0)-\phi_s(x_0,b+0)]\,dx_0$$
$$+\int_{-a}^{a}\mathscr{G}_s(x,y,x_0,-b)\frac{\partial}{\partial y_0}[\phi_s(x_0,-b+0)$$
$$-\phi_s(x_0,-b+0)]\,dx_0+\int_{-b}^{b}\mathscr{G}_s(x,y,a,y_0)\frac{\partial}{\partial x_0}$$
$$\times[\phi_s(a-0,y_0)-\phi_s(a+0,y_0)]\,dy_0$$
$$+\int_{-b}^{b}\mathscr{G}_s(x,y,-a,y_0)\frac{\partial}{\partial x_0}[\phi_s(-a-0,y_0)$$
$$-\phi_s(-a+0,y_0)\,dy_0+\left(p\frac{\Sigma_{tc}}{\mathscr{D}_{sc}}-\frac{\Sigma_{tr}}{\mathscr{D}_{sr}}\right)$$
$$\int_{-a}^{a}\int_{-b}^{b}\mathscr{G}_s(x,y,x_0,y_0)\phi_f(x_0,y_0)\,dx_0dy_0$$
$$+\left(\frac{\Sigma_{ar}}{\mathscr{D}_{sr}}-\frac{\Sigma_{ac}}{\mathscr{D}_{sc}}\right)\int_{-a}^{a}\int_{-b}^{b}\mathscr{G}_s(x,y,x_0,y_0)\phi_s(x_0,y_0)\,dx_0dy_0. \quad (8)$$

Eqs. (7) and (8) represent our problem in an integral equation formulation. We still need an additional relation between the left-hand and right-hand derivatives of the fluxes at G. This relation is provided by the continuity of currents conditions

$$\mathscr{D}_{ic}\frac{\partial}{\partial x}\phi_i(\pm a-0,y)$$
$$=\mathscr{D}_{ir}\frac{\partial}{\partial x}\phi_i(\pm a+0,y),\ -b\leq y\leq b,$$
$$\mathscr{D}_{ic}\frac{\partial}{\partial y}\phi_i(x,\pm b-0)$$
$$=\mathscr{D}_{ir}\frac{\partial}{\partial y}\phi_i(x,\pm b+0),\ -a\leq x\leq a. \quad (9)$$

The formulation of the problem is now complete.

The method of solution

The solutions of Eqs. (7) and (8) will be sought in the Hilbert space $L^2(R_2)$ by expanding the fluxes in terms of the eigenfunctions of a two-dimensional Laplacian operator. Because the flux distributions are symmetrical we may restrict the domain of the Laplacian to the functions defined over the quarter

reactor $0 \leq x < \infty$, $0 \leq y < \infty$. The spectral representation thus assumes the form

$$\psi_i(B_x,B_y) = \int_0^\infty \int_0^\infty (xy)^{\frac{1}{2}}]_{-\frac{1}{2}}(B_x x)]_{-\frac{1}{2}} \times (B_y y)\phi_i(x,y)\, dx dy, \quad (10)$$

$$\phi_i(x,y) = \int_0^\infty \int_0^\infty (xy)^{\frac{1}{2}}]_{-\frac{1}{2}}(B_x x)]_{-\frac{1}{2}} \times (B_y y)\psi_i(B_x,B_y)\, dB_x dB_y, \quad (11)$$

Eqs. (10) and (11) represent the familiar formulae for the double Hankel transform of a function of two variables. The symmetric and unitary integral operator defined by (10) maps the fluxes $\phi_i(x,y)$ into the images $\psi_i(B_x,B_y)$. With the aid of this mapping we may transform Eqs. (7) and (8) from (x,y) space into (B_x,B_y) space. For this purpose the eigenfunction expansion (11) is substituted into (7) and (8) and the resulting equations are multiplied by

$$(xy)^{\frac{1}{2}}]_{-\frac{1}{2}}(B_{0x}x)]_{-\frac{1}{2}}(B_{0y}y)$$

and then integrated over the quarter reactor. The problem of finding eigenfunction expansions for the derivatives of the fluxes at the core reflector interface requires special consideration. Differentiating under the integral sign with respect to x in (11) we find that

$$\frac{\partial \phi_i(x,y)}{\partial x} = -\int_0^\infty \int_0^\infty xy^{\frac{1}{2}}B_x^{\frac{3}{2}}B_y^{\frac{1}{2}}]_{\frac{1}{2}}(B_x x)]_{-\frac{1}{2}}(B_y y)\psi_i(B_x,B_y)\, dB_x dB_y.$$

When $0 \leq y \leq b$, and x approaches a, where the derivative is discontinuous, the integral is equal to one-half the sum of the right-hand and left-hand derivatives

$$\tfrac{1}{2}\left[\frac{\partial \phi_i(a-0,y)}{\partial x} + \frac{\partial \phi_i(a+0,y)}{\partial x}\right] = -\int_0^\infty \int_0^\infty ay^{\frac{1}{2}}B_x^{\frac{3}{2}}B_y^{\frac{1}{2}}]_{\frac{1}{2}}(B_x a)]_{-\frac{1}{2}}(B_y y)\psi_i(B_x,B_y)\, dB_x dB_y. \quad (12)$$

Taking into account the continuity of currents conditions (9) Eq. (12) becomes

$$\frac{\partial \phi_i(a-0,y)}{\partial x} - \frac{\partial \phi_i(a+0,y)}{\partial x} = d_i \int_0^\infty \int_0^\infty ay^{\frac{1}{2}}B_x^{\frac{3}{2}}B_y^{\frac{1}{2}}]_{\frac{1}{2}}(B_x a)]_{-\frac{1}{2}}(B_y y)\psi_i(B_x B_y)\, dB_x dB_y, \quad (13)$$

where d_i is the abbreviation

$$d_i = 2.\frac{\mathscr{D}_{ic} - \mathscr{D}_{ir}}{\mathscr{D}_{ic} + \mathscr{D}_{ir}}, \quad i = \text{s,f}.$$

Eq. (13) gives the required expansion for derivatives with respect to x. Derivatives with respect to y are treated similarly.

The transformation procedure described above results in a new system of integral equations for the transformed fluxes $\psi_f(B_x,B_y)$ and $\psi_s(B_x,B_y)$. In transform space Eqs. (7) and (8) take the form

$$\begin{aligned}\psi_f(B_x,B_y) = \mathscr{G}_f(B_x,B_y)\{ &- d_f \int_0^\infty \int_0^\infty (B_x,B_{0x})^{\frac{1}{2}}(B_y,B_{0y})^{\frac{1}{2}} \times B_{0x}K_x(B_x,B_{0x})L_y(B_y,B_{0y})\psi_f(B_{0x},B_{0y})\, dB_{0x}dB_{0y} \\ &\times d_f \int_0^\infty \int_0^\infty (B_x B_{0x})^{\frac{1}{2}}(B_y B_{0y})^{\frac{1}{2}}B_{0y}K_y(B_y,B_{0y})L_x \times (B_x,B_{0x})\psi_f(B_{0x},B_{0y})\, dB_{0x}dB_{0y} \\ &+ \left(\frac{\Sigma_{fr}}{\mathscr{D}_{fr}} - \frac{\Sigma_{fc}}{\mathscr{D}_{fc}}\right) \int_0^\infty \int_0^\infty (B_x B_{0x})^{\frac{1}{2}}(B_y B_{0y})^{\frac{1}{2}}L_x(B_x,B_{0x}) \times L_y(B_y,B_{0y})\psi_f(B_{0x},B_{0y})\, dB_{0x}dB_{0y} \\ &+ \frac{k}{p}\frac{\Sigma_{ac}}{\mathscr{D}_{fc}} \int_0^\infty \int_0^\infty (B_x B_{0x})^{\frac{1}{2}}(B_y B_{0y})^{\frac{1}{2}}L_x(B_x,B_{0x}) \times L_y(B_y,B_{0y})\psi_s(B_{0x},B_{0y})\, dB_{0x}dB_{0y}\}, \end{aligned} \quad (14)$$

$$\begin{aligned}\psi_s(B_x,B_y) = \mathscr{G}_s(B_x,B_y)\Big\{&\frac{\Sigma_{fr}}{\mathscr{D}_{sr}}\psi_f(B_x,B_y) \\ &- d_s \int_0^\infty \int_0^\infty (B_x B_{0x})^{\frac{1}{2}}(B_y B_{0y})^{\frac{1}{2}}B_{0x}K_x(B_x,B_{0x}) \times L_y(B_y,B_{0y})\psi_s(B_{0x},B_{0y})\, dB_{0x}dB_{0y} \\ &- d_s \int_0^\infty \int_0^\infty (B_x B_{0x})^{\frac{1}{2}}(B_y B_{0y})^{\frac{1}{2}}B_{0y}K_y(B_y,B_{0y}) \times L_x(B_x,B_{0x})\psi_s(B_{0x},B_{0y})\, dB_{0x}dB_{0y} \\ &+ \left(\frac{\Sigma_{ar}}{\mathscr{D}_{sr}} - \frac{\Sigma_{ac}}{\mathscr{D}_{sc}}\right) \int_0^\infty \int_0^\infty (B_x B_{0x})^{\frac{1}{2}}(B_y B_{0y})^{\frac{1}{2}}L_x(B_x,B_{0x}) \times L_y(B_y,B_{0y})\psi_s(B_{0x},B_{0y})\, dB_{0x}dB_{0y} \\ &+ \left(\frac{p\Sigma_{fc}}{\mathscr{D}_{sc}} - \frac{\Sigma_{fr}}{\mathscr{D}_{sr}}\right) \int_0^\infty \int_0^\infty (B_x B_{0x})^{\frac{1}{2}}(B_y B_{0y})^{\frac{1}{2}}L_x(B_x,B_{0x}) \times L_y(B_y,B_{0y})\psi_f(B_{0x},B_{0y})\, dB_{0x}dB_{0y}\Big\}, \end{aligned} \quad (15)$$

where

$$\mathscr{G}_i(B_x,B_y) = \left(B_x^2 + B_y^2 + \frac{1}{L_i^2}\right)^{-1}, \quad i = \text{s,f}$$

is the Hankel transform of the Green's function (5), where the symmetric kernels $L_x(B_x,B_{0x})$ and $L_y(B_y,B_{0y})$ are defined by the integrals

$$L_x(B_x,B_{0x}) = \int_0^a]_{-\frac{1}{2}}(B_x x_0)]_{-\frac{1}{2}}(B_{0x}x_0)x_0\, dx_0,$$

$$L_y(B_y,B_{0y}) = \int_0^b]_{-\frac{1}{2}}(B_y y_0)]_{-\frac{1}{2}}(B_{0y}y_0)y_0\, dy_0, \quad (16)$$

and where $K_x(B_x,B_{0x})$ and $K_y(B_y,B_{0y})$ denote the degenerate kernels

$$K_x(B_x,B_{0x}) = a]_1(B_{0x}a)]_{-\frac{1}{2}}(B_x a),$$

$$K_y(B_y,B_{0y}) = b]_1(B_{0y}b)]_{-\frac{1}{2}}(B_y b). \quad (17)$$

Let us now consider the self-adjoint integral operator L defined by

$$L\psi_i = \int_0^\infty \int_0^\infty (B_x B_{0x})^{\frac{1}{2}}(B_y B_{0y})^{\frac{1}{2}}L_x(B_x,B_{0x})L_y(B_y,B_{0y}) \times \psi_i(B_{0x},B_{0y})\, dB_{0x}dB_{0y}.$$

With the aid of the addition theorems for Bessel functions we can find the bilinear series

$$L_x(B_x,B_{0x}) = \frac{1}{B_xB_{0x}} \times \sum_{k=0}^{\infty} 2(2k+\tfrac{1}{2})]_{2k+\frac{1}{2}}(B_xa)]_{2k+\frac{1}{2}}(B_{0x}a),$$

$$L_y(B_y,B_{0y}) = \frac{1}{B_yB_{0y}} \times \sum_{l=0}^{\infty} 2(2l+\tfrac{1}{2})]_{2l+\frac{1}{2}}(B_yb)]_{2l+\frac{1}{2}}(B_{0y}b) \quad (18)$$

for the kernels $L_x(B_x,B_{0x})$ and $L_y(B_y,B_{0y})$. For the case when the kernels (16) contain Bessel functions of zero order the reader will find a detailed derivation of the series (18) in Ref. [2]. By employing the series (18) we may observe the following properties of the operator L. The kernel of the integral operator L is quadratically integrable over the basic square, symmetric, and consequently a Hilbert-Schmidt kernel. The eigenfunctions of L form an orthogonal set, and, according to the Hilbert-Schmidt theorem, the values of the operator L may be expanded in an absolutely and uniformly converging Fourier series

$$L\psi_i = \sum_{k,l=0}^{\infty} 4(2k+\tfrac{1}{2})(2l+\tfrac{1}{2})c_{k,}{}^{t}{}_{l}(B_xB_y)^{-\frac{1}{2}}]_{2k+\frac{1}{2}} \times (B_xa)]_{2l+\frac{1}{2}}(B_yb) \quad (19)$$

in terms of this set. The expansion coefficients $c_{k,}{}^{t}{}_{l}$ are defined by

$$c_{k,}{}^{t}{}_{l} = \int_0^{\infty}\int_0^{\infty} (B_{0x}B_{0y})^{-\frac{1}{2}}]_{2k+\frac{1}{2}}(B_{0x}a)]_{2l+\frac{1}{2}}(B_{0y}b) \times \psi_i(B_{0x},B_{0y})\, dB_{0x}dB_{0y}. \quad (20)$$

The Hilbert-Schmidt series (19) forms the basic result for further development of the theory. We replace the integral operator L by a degenerate operator by truncating the series (19) after the first N^2 terms. Then only degenerate operators appear in Eqs. (14) and (15). Defining two additional sets as scalars,

$$x_{0,}{}^{t}{}_{l} = \int_0^{\infty}\int_0^{\infty} (B_{0x}B_{0y})^{-\frac{1}{2}}B_{0x}{}^{2}]_{\frac{1}{2}}(B_{0x}a)]_{2l+\frac{1}{2}}(B_{0y}b) \times \psi_i(B_{0x},B_{0y})\, dB_{0x}dB_{0y} \quad (21)$$

and

$$y_{k,}{}^{t}{}_{0} = \int_0^{\infty}\int_0^{\infty} (B_{0x}B_{0y})^{-\frac{1}{2}}B_{0y}{}^{2}]_{2k+\frac{1}{2}}(B_{0x}a)]_{\frac{1}{2}}(B_{0y}b) \times \psi_i(B_{0x},B_{0y})\, dB_{0x}dB_{0y} \quad (22)$$

we can immediately write down an Nth order approximation to the solution in transform space

$$(B_xB_y)^{\frac{1}{2}}\psi_f(B_x,B_y) = \mathscr{G}_f(B_x,B_y)\{-d_faB_x]_{-\frac{1}{2}}(B_xa)\sum_{l=0}^{N} 2(2l+\tfrac{1}{2}) \times x_{0,}{}^{t}{}_{l}]_{2l+\frac{1}{2}}(B_yb) - d_fbB_y]_{-\frac{1}{2}}(B_yb)\sum_{k=0}^{N} 2(2k+\tfrac{1}{2})y_{k,}{}^{t}{}_{0}]_{2k+\frac{1}{2}}(B_xa)$$

$$+\left(\frac{\Sigma_{\mathrm{tr}}}{\mathscr{D}_{\mathrm{tr}}}-\frac{\Sigma_{\mathrm{tc}}}{\mathscr{D}_{\mathrm{tc}}}\right)\sum_{k,l=0}^{N} 4(2k+\tfrac{1}{2})(2l+\tfrac{1}{2})c_{k,}{}^{t}{}_{l}]_{2k+\frac{1}{2}} + (B_xa)]_{2l+\frac{1}{2}}(B_yb) + \frac{k}{p}\frac{\Sigma_{\mathrm{ac}}}{\mathscr{D}_{\mathrm{tc}}}\sum_{k,l=0}^{N} 4(2k+\tfrac{1}{2})(2l+\tfrac{1}{2})c_{k,}{}^{s}{}_{l}]_{2k+\frac{1}{2}} \times (B_xa)]_{2l+\frac{1}{2}}(B_yb)\Big\}, \quad (23)$$

$$(B_xB_y)^{\frac{1}{2}}\psi_s(B_x,B_y) = \mathscr{G}_s(B_x,B_y)\Big\{\frac{\Sigma_{\mathrm{tv}}}{\mathscr{D}_{\mathrm{sr}}}(B_xB_y)^{\frac{1}{2}}\psi_t(B_x,B_y) - d_saB_x]_{-\frac{1}{2}}(B_xa)\sum_{l=0}^{N} 2(2l+\tfrac{1}{2})x_{0,}{}^{s}{}_{l}]_{2l+\frac{1}{2}}(B_yb) - d_sbB_y]_{-\frac{1}{2}}(B_yb)\sum_{k=0}^{N} 2(2k+\tfrac{1}{2})Y_{k,}{}^{s}{}_{0}]_{2k+\frac{1}{2}}(B_xa)$$

$$+\left(\frac{\Sigma_{\mathrm{ar}}}{\mathscr{D}_{\mathrm{sr}}}-\frac{\Sigma_{\mathrm{ac}}}{\mathscr{D}_{\mathrm{sc}}}\right)\sum_{k,l=0}^{N} 4(2k+\tfrac{1}{2})(2l+\tfrac{1}{2})c_{k,}{}^{s}{}_{l}]_{2k+\frac{1}{2}} \times (B_xa)]_{2l+\frac{1}{2}}(B_yb) + \left(p\frac{\Sigma_{\mathrm{tc}}}{\mathscr{D}_{\mathrm{sc}}}-\frac{\Sigma_{\mathrm{tr}}}{\mathscr{D}_{\mathrm{sr}}}\right)\sum_{k,l=0}^{N} 4(2k+\tfrac{1}{2})(2l+\tfrac{1}{2})c_{k,}{}^{t}{}_{l}]_{2k+\frac{1}{2}} \times (B_xa)]_{2l+\frac{1}{2}}(B_yb)\Big\}. \quad (24)$$

The solution contains $2N^2+4N$ unknown coefficients $c_{k,}{}^{t}{}_{l}$, $c_{k,}{}^{s}{}_{l}$, $x_{0,}{}^{t}{}_{l}$, $x_{0,}{}^{s}{}_{l}$, $y_{k,}{}^{t}{}_{0}$ and $y_{k,}{}^{s}{}_{0}$, $k,l=0,1,2,\ldots,N$, which are determined by substituting Eqs. (23) and (24) into (20), (21), and (22). We notice that the 4N coefficients $x_{0,}{}^{t}{}_{l}$, $x_{0,}{}^{s}{}_{l}$, $y_{k,}{}^{t}{}_{0}$, and $y_{k,}{}^{s}{}_{0}$ arise from the discontinuity of the diffusion coefficients at the core reflector interface. For the sake of simplicity we now make the additional assumption that the diffusion coefficients in both groups are space independent. Then $d_t=d_s=0$ and the remaining coefficients $c_{k,}{}^{t}{}_{l}$ and $c_{k,}{}^{s}{}_{l}$ satisfy the set of homogeneous linear algebraic equations

$$c_{k,}{}^{t}{}_{l} = \sum_{m,n=0}^{N} 4(2m+\tfrac{1}{2})(2n+\tfrac{1}{2})\left[\left(\frac{\Sigma_{\mathrm{tr}}}{\mathscr{D}_{\mathrm{tr}}}-\frac{\Sigma_{\mathrm{tc}}}{\mathscr{D}_{\mathrm{tc}}}\right)c_{m,}{}^{t}{}_{n} + \frac{k}{p}\frac{\Sigma_{\mathrm{ac}}}{\mathscr{D}_{\mathrm{tc}}}c_{m,}{}^{s}{}_{n}\right]\int_0^{\infty}\int_0^{\infty}]_{2k+\frac{1}{2}}(B_xa)]_{2l+\frac{1}{2}}(B_yb)]_{2m+\frac{1}{2}} \times (B_xa)]_{2n+\frac{1}{2}}(B_yb)\,\mathscr{G}_t(B_x,B_y)\frac{dB_xdB_y}{B_xB_y}, \quad (25)$$

$$c_{k,}{}^{s}{}_{l} = \sum_{m,n=0}^{N} 4(2m+\tfrac{1}{2})(2n+\tfrac{1}{2}) \times \int_0^{\infty}\int_0^{\infty}]_{2k+\frac{1}{2}}(B_xa)]_{2l+\frac{1}{2}}(B_yb)]_{2m+\frac{1}{2}}(B_xa)]_{2n+\frac{1}{2}}(B_yb) \times \mathscr{G}_s(B_x,B_y) \times \Big\{c_{m,}{}^{s}{}_{n}\left[\frac{\Sigma_{\mathrm{ar}}}{\mathscr{D}_{\mathrm{sr}}}-\frac{\Sigma_{\mathrm{ac}}}{\mathscr{D}_{\mathrm{sc}}}+\frac{k}{p}\frac{\Sigma_{\mathrm{ac}}}{\mathscr{D}_{\mathrm{tc}}}\frac{\Sigma_{\mathrm{tr}}}{\mathscr{D}_{\mathrm{sr}}}\mathscr{G}_t(B_x,B_y)\right] + c_{m,}{}^{t}{}_{n}\left[p\frac{\Sigma_{\mathrm{tc}}}{\mathscr{D}_{\mathrm{tc}}}-\frac{\Sigma_{\mathrm{tr}}}{\mathscr{D}_{\mathrm{sr}}}+\frac{\Sigma_{\mathrm{tr}}}{\mathscr{D}_{\mathrm{sr}}}\left(\frac{\Sigma_{\mathrm{tr}}}{\mathscr{D}_{\mathrm{tr}}}-\frac{\Sigma_{\mathrm{tc}}}{\mathscr{D}_{\mathrm{tc}}}\right) \times \mathscr{G}_t(B_x,B_y)\right]\Big\}\frac{dB_xdB_y}{B_xB_y}. \quad (26)$$

In order that Eqs. (25) and (26) possess a nontrivial solution, the determinant of coefficients must vanish. The roots of this determinant give the Nth order approximation to the eigenvalues of the problem. Eqs. (25) and (26) must be solved for $N=1,2,\ldots$, until the required accuracy is achieved. The rate of convergence depends on the size of the core. When the dimensions of the core decrease the rate of convergence increases, so that a large leakage implies rapid convergence.

After the coefficients $c_{k,}{}^{f}{}_{l}$ and $c_{k,}{}^{s}{}_{l}$ have been found from (25) to (26), they are inserted in Eqs. (23) and (24) yielding an Nth order approximation to the transformed fluxes. Finally, the flux distributions in (x,y) space,

$$\phi_f(x,y)=\sum_{k,l=0}^{N}4(2k+\tfrac{1}{2})(2l+\tfrac{1}{2})\times\left[\left(\frac{\Sigma_{fr}}{\mathscr{D}_{fr}}-\frac{\Sigma_{fc}}{\mathscr{D}_{fc}}\right)c_{k,}{}^{f}{}_{l}+\frac{k}{p}\frac{\Sigma_{ac}}{\mathscr{D}_{fc}}c_{k,}{}^{s}{}_{l}\right]\times\int_0^\infty\int_0^\infty(xy)^{\frac{1}{2}}]_{-\frac{1}{2}}(B_xx)]_{-\frac{1}{2}}(B_yy)]_{2k+\frac{1}{2}}(B_xa)]_{2l+\frac{1}{2}}(B_yb)\times\mathscr{G}_f(B_x,B_y)\,dB_xdB_y,$$

and

$$\phi_s(x,y)=\sum_{k,l=0}^{N}4(2k+\tfrac{1}{2})(2l+\tfrac{1}{2})\times\int_0^\infty\int_0^\infty(xy)^{\frac{1}{2}}]_{-\frac{1}{2}}(B_xx)]_{-\frac{1}{2}}(B_yy)]_{2k+\frac{1}{2}}(B_xa)_{2l+\frac{1}{2}}(B_yb)\times\mathscr{G}_s(B_x,B_y)$$

$$\times\left\{c_{k,}{}^{s}{}_{l}\left[\frac{\Sigma_{ar}}{\mathscr{D}_{sr}}-\frac{\Sigma_{ac}}{\mathscr{D}_{sc}}+\frac{k}{p}\frac{\Sigma_{ac}}{\mathscr{D}_{fc}}\mathscr{G}_f(B_x,B_y)\right]+c_{k,}{}^{f}{}_{l}\left[p\frac{\Sigma_{fc}}{\mathscr{D}_{sc}}-\frac{\Sigma_{sr}}{\mathscr{D}_{sr}}+\frac{\Sigma_{fr}}{\mathscr{D}_{sr}}\left(\frac{\Sigma_{fr}}{\mathscr{D}_{fr}}-\frac{\Sigma_{fc}}{\mathscr{D}_{fc}}\right)\times\mathscr{G}_f(B_x,B_y)\right]\right\}dB_xdB_y,$$

result from applying the inverse transformation (11) to both sides of Eqs. (23) and (24).

Summary

The integral equation technique described above has been previously applied to the investigation of a one-dimensional three region three-group problem [2]. In the present paper we have pointed out how the method can be formally extended to the two-dimensional reactor configuration. Further extensions to completely reflected cylindrical reactors in which the fluxes are independent of the azimuthal angle, and to three-dimensional rectangular parallelepipeds, are obvious. Extension to the investigation of time-dependent problems by Laplace transformation is also possible.

REFERENCES

1. Weinberg, A., and Wigner, P., *The Physical Theory of Neutron Chain Reactors*, Univ. of Chicago Press, Chicago (1958).
2. Toivanen, T., Nuclear Sci. and Eng., *16*, pp. 185–186 (1963).

ABSTRACT—RÉSUMÉ—АННОТАЦИЯ—RESUMEN

A/410 Finlande

Une méthode de résolution des équations de diffusion à deux groupes de neutrons dans une géométrie XY

par T. Toivanen

On expose une nouvelle technique semi-analytique pour trouver les valeurs propres et les flux à deux groupes dans un cœur de réacteur rectangulaire entouré par un réflecteur homogène infini. La méthode de résolution est une extension de la technique antérieurement développée pour les problèmes à une dimension. Par l'introduction des fonctions de Green pour la région infinie du réflecteur, les équations de diffusion à groupes ainsi que les conditions de limite correspondantes sont converties en un système d'équations intégrales à deux dimensions. Pour résoudre ces équations, on utilise la transformation double de Hankel. Dans les équations de deuxième ordre de Fredholm, transformées selon Hankel, les opérateurs d'intégration peuvent être représentés approximativement par des opérateurs dégénérés, et le problème se réduit à la solution de systèmes infinis d'équations algébriques linéaires. Par la résolution du système fini tronqué correspondant, une solution approximative est construite dans l'espace de transformation. Pour ce qui est de la solution correspondante dans l'espace des coordonnées, elle est obtenue par l'application de la transformation inverse de Hankel. La méthode ne se limite pas aux problèmes à deux dimensions. Les problèmes contenant des configurations de réacteur plus complexes, par exemple un bloc rectangulaire totalement réfléchi ou bien un cœur cylindrique fini avec des réflecteurs aussi bien radiaux qu'axiaux, peuvent également être traités par cette méthode.

A/410 Финляндия

Подход к решению двухгрупповых уравнений нейтронной диффузии в xy-геометрии

Т. Тойванен

Описывается новый полуаналитический метод для нахождения собственных значений и двухгрупповых потоков в двумерной прямо-

угольной зоне реактора, окруженной бесконечным гомогенным отражателем. Этот метод решения представляет собой расширение метода, предварительно разработанного для одномерных задач. Путем применения функций Грина для зоны бесконечного отражателя групповые уравнения диффузии и соответствующие граничные условия превращаются в систему двумерных интегральных уравнений. При решении этих уравнений применяется двойное преобразование Ханкеля. После преобразования Ханкеля интегральные операторы в уравнениях Фредгольма второго рода могут быть приближенно заменены на вырожденные, благодаря чему проблема сводится к решению бесконечных систем линейных алгебраических уравнений. Путем решения соответствующим образом обрезанной конечной системы строится приближенное решение в преобразованном пространстве. Соответствующее решение в пространстве обычных координат находят затем путем обратного преобразования Ханкеля. Применение этого метода не ограничено двумерными задачами. Проблемы, связанные с более сложными конфигурациями реактора, например проблема трехмерного реактора с прямоугольной активной зоной и отражателем или конечной цилиндрической активной зоной с радиальными и с аксиальными торцовыми отражателями, также поддаются обработке этим методом.

A/410 Finlandia

Un método de resolución de las ecuaciones de difusión para dos grupos de neutrones en geometria XY

por T. Toivanen

Se describe una técnica nueva, semianalítica, para determinar los valores propios y los flujos, en teoría de dos grupos, de un reactor bidimensional formado por un núcleo rectangular rodeado de un reflector homogéneo e infinito. El método de resolución es una generalización de la técnica desarrollada anteriormente para problemas unidimensionales. Introduciendo las funciones de Green correspondientes a la región infinita de reflector, se convierten las ecuaciones de difusión para dos grupos, juntamente con las condiciones de contorno, en un sistema de ecuaciones integrales. Para resolver estas ecuaciones se aplica la transformación doble de Hankel. En las ecuaciones de Fredholm de segunda especie resultantes de aplicar la transformación Hankel, se pueden aproximar los núcleos integrales por núcleos degenerados, y el problema se reduce a la resolución de un sistema de infinitas ecuaciones algebraicas lineales. Resolviendo el correspondiente problema finito truncado, se obtiene una solución aproximada en espacio transformado. La solución correspondiente en el espacio de las coordenadas se halla aplicando la transformación inversa de Hankel. El método no está limitado a problemas bidimensionales. Se pueden tratar, también, con este método problemas que implican configuraciones más complejas de reactores, p.e. un núcleo tridimensional paralelepipédico completamente reflejado o un núcleo cilíndrico, finito, con reflectores axil y radial.

Eigenfunction expansion method in neutron transport theory

By R. Zelazny*

The present paper considers a most general case of the Boltzmann equation with an anisotropic energy dependent kernel and an energy dependent total cross section (mean free path) for neutron transport problems in plane geometry. This form of the Boltzmann equation covers all physically possible situations. Following the approach of the author applied for heavy gas moderators and the approach of R. Bednarz and J. Mika the basic concepts of the eigenfunction expansion method are presented. The sectionally holomorphic integral operator is introduced, which permits reduction of the singular integral equation, appearing in the proof of the completeness theorem, to the Riemann-Hilbert problem. The solubility conditions determine the discrete part of the eigenfunction expansion.

Having proved the completeness theorem the albedo and critical problem for a slab is formulated and reduced to a singular integral equation completely identical with the integral equation of the completeness theorem. Thus a procedure similar to that of the reduction to the Riemann-Hilbert problem can be applied. The solubility conditions determine the discrete part of the expansion (asymptotic solution). In the case of the critical problem these conditions take the form of the system of homogeneous algebraic equations with respect to constants of the discrete part of the expansion. A necessary and sufficient condition for the existence of nontrivial solutions is the vanishing of the characteristic determinant, which in this case is an exact critical condition for the critical thickness of the slab.

In this way was founded a general scheme for treating the general case of space-energy dependent neutron transport problems in plane geometry.

Introduction

The eigenfunction expansion method originated in plasma oscillations, N. G. Van Kampen [1] noticed that continuous eigenfunctions (modes) of the Boltzmann equation need not necessarily be functions in the usual sense. The integration applied to a continuous eigenvalue (over the whole continuous spectrum) permits the continuous eigenfunctions to be distributions. This concept was transferred into the one-velocity, isotropic neutron transport problems by K. M. Case [2]. Similar concepts were introduced independently by P. Lafore and J. P. Millot [3], but without the mathematical exactness and completeness theorem of Case. Thus he should be considered as the founder of this method in neutron transport. His ideas were the starting point for the author in considerations of the critical problem for a slab [4]—first nonclassical problem, reduced to the Fredholm type integral equation with an exact critical condition. Paper [4] showed the great possibilities of the method. Simple, hand-made calculations based on Neumann's iteration procedure permit the calculation of the critical thickness of the slab with very high accuracy [5]. Analogously many basic plane problems such as the albedo problem for a slab, critical multilayer problems and the asymptotic reactor theory can be formulated and solved [6,7,8]. With the next step it appeared that not only the one-velocity Boltzmann equation with isotropic scattering of neutrons can be dealt along this method. First, the limitation of the isotropic scattering was removed from the theory [9,10], and the method was then applied to the multigroup neutron problems with isotropic scattering [11,12]. Afterwards, the method was extended to thermalization problems in heavy gas [13, 14] and then applied to the general case of anisotropic, energy dependent Boltzmann equation by R. Bednarz and J. Mika [15]. These were the main steps towards the full application of the eigenfunction method in plane problems of neutron transport theory. The only limitation was that the integral equations occurring in space-energy dependent problems were solved originally only in the full range of continuous eigenvalue spectrum by appropriate reduction to the Riemann-Hilbert problem. This was strictly connected with a knowledge, in an explicit form, of the sectionally holomorphic operator, with a cut over the whole interval $(-1,1)$, being the continuous spectrum of the eigenvalue of the Boltzmann equation. The above operator permitted this reduction in an explicit form. Except for the completeness theorem, all other problems such as Milne's problem and the slab problems required (according to contemporary views) that this reduction be carried out over the partial range of this spectrum. The difficulty did not seem to be overcome by the usual methods of approach. Recently, K. Fuchs and S. Collatz [16] have shown for the isotropic,

* Institute of Nuclear Research, Swierk, Poland.

energy dependent kernel a new way of dealing with the critical problem for a slab. This method has been extended to the general case of anisotropic, and the energy dependent kernel and has been presented in this paper in application to albedo and the critical problem for a slab. It seems that this is the most satisfactory method for applying the eigenfunction method for the solution of all basic problems in the plane neutron transport theory with an arbitrary scattering law of neutrons. Of course, there is still much interesting work to be done but the principal ideas of the method have been firmly founded.

Even before this programme was completed many authors (see for example [17]) had considered this method as very perspicacious and attractive from the practical and gnoseological point of view.

This paper presents the solution to the Boltzmann equation with an anisotropic, energy dependent kernel and energy dependent total cross-section. This case contains in principle all possible physical situations (only slight modifications are to be introduced for slowing down problems, which do not change the presented, basic mathematical scheme). The next two sections are devoted to the definition of eigenvalues and eigenfunctions of the Boltzmann equation and to the proof of the completeness theorem. They are based on the paper [15] with minor modifications by the author. The last section is concerned with the solution of the albedo and the critical problem for a slab.

Eigenvalues and eigenfunctions in the case of an energy and angle dependent kernel

The most general form of the stationary Boltzmann equation in plane geometry is as follows:

$$l(E)\mu(\partial\tilde{\psi}/\partial x)+\tilde{\psi}(x,\mu,E) = \int_{E_0}^{E_1} dE' \int_{-1}^{1} d\mu \tilde{K}(\mu,E;\mu',E')\tilde{\psi}(x,\mu,E') \quad (1)$$

where $\tilde{\psi}(x,\mu,E)$ is the collision density of neutrons, $l(E)$ is the total mean free path of neutrons and μ is the cosine of the angle between the neutron velocity and the x axis. The kernel $\tilde{K}(\mu,E;\mu',E')$ gives the number of secondary neutrons, characterized by the cosine μ of their velocity and their energy E, induced by one collision of the neutron of the energy E' and the cosine μ'. The specification of this kernel, of the limits of energy integration and of the mean free path dependence on energy, allows for a complete formulation of the problem. In principle, all interesting, stationary cases of neutron transport problems in plane geometry are described by this equation.

Following [15], let us introduce new variables

$$\nu=\mu l(E), \quad \nu'=\mu' l(E'), \quad (2)$$

which enable us to rewrite Eq. (1) in the form:

$$\nu(\partial\psi/\partial x)+\psi(x,\nu,E) = \int_{E_0}^{E'} dE' \int_{-l(E)}^{l(E)} d\nu' K(\nu,E;\nu',E')\psi(x,\nu',E') \quad (3)$$

The function $\psi(x,\nu,E)$ and the kernel $K(\nu,E;\nu',E')$ are connected with the former $\psi(x,\mu,E)$ and $K(\nu,E;\nu',E')$ in a trivial way.

We shall use also the following notation:

$$E\epsilon M(\nu) \text{ if } l(E)\geq|\nu| \text{ for } \nu\epsilon(-1,1) \quad (4)$$

For $\nu\notin(-1,1)$ the set $M(\nu)$ is empty.

This convention gives us the alternative form of Eq. (3):

$$\nu(\partial\psi/\partial x)+\psi(x,\nu,E) = \int_{-1}^{1} d\nu' \int_{M(\nu')} dE' K(\nu,E;\nu',E')\psi(x,\nu',E') \quad (5)$$

where $E\epsilon M(\nu)$.

To solve this equation we use the Ansatz of K. M. Case [2]

$$\psi(x,\nu,E)=\exp(-x/t)\phi(t,\nu,E) \quad (6)$$

where t is an arbitrary complex number (eigenvalue) and $\phi(t,\nu,E)$ is a corresponding eigenfunction which are to be determined in due course. The Ansatz (6) introduced to Eq. (5) gives the following equation for ϕ and t:

$$(t-\nu)\phi(t,\nu,E) = t\int_{-1}^{1} d\nu' \int_{M(\nu')} dE' K(\nu',E;\nu'E')\phi(t,\nu'E') \quad (7)$$

Denoting

$$\int_{-1}^{1} d\nu' \int_{M(\nu')} dE' K(\nu,E;\nu',E')\phi(t,\nu',E') \equiv H(t,\nu,E) \quad (8)$$

we may write Eq. (7) in a simpler form and solve it explicitly:

$$\phi(t,\nu,E)=tH(t,\nu,E)/(t-\nu)+\lambda(\nu,E)\delta(\nu-t) \quad (9)$$

where $\lambda(\bar{\nu},E)$ is an arbitrary function. This function can be connected with $H(t,\bar{\nu},E)$ if we use the relation (8). Substitution of Eq. (8) gives:

$$H(t,\nu,E)+\left[t\int_{-1}^{1} d\nu'/(\nu-t)\right]\int_{M(\nu')} dE' K(\nu,E;\nu',E')H (t,\nu',E')=\int_{M(t)} dE' K(\nu,E,t,E')\lambda(t,E') \quad (10)$$

It is convenient to introduce here an integral operator $\Omega_{\nu,E}(z)$ defined as follows:

$$\Omega_{\nu,E}(z)f(z,\nu,E)\equiv\phi(z,\nu,E)+z\int_{-1}^{1} d\nu'/(\nu'-z) \int_{M(\nu')} dE' K(\nu,E;\nu',E')\phi(z,\nu',E') \quad (11)$$

Assuming that the kernel $K(\nu,E;\nu',E')$ has the property that integrated with respect to E' with any function $f(z,\nu',E')$ which is sectionally holomorphic with respect to z with a cut $(-1,1)$ and of the H^* class with respect to ν', it gives a function which is again sectionally holomorphic with respect to z, we may say that the operator $\Omega_{\nu,E}(z)$ is a sectionally holomorphic operator with a cut $(-1,1)$ in the z plane.

Using the Plemelj formulae [18] we can calculate the boundary values of $\Omega_{v,E}(z)$ on both sides acting on a cut on arbitrary function $f(z,\nu,E)$ (possibly with the same cut):

$$\Omega^{\pm}{}_{\nu,E}(s)f^{\pm}(s,\nu,E) = P\Omega_{\nu,E}(s)f^{\pm}(s,\nu,E) \pm i\pi s\omega_{\nu,E}(s,\nu)f^{\pm}(s,\nu,E) \quad (12)$$

where P denotes the Cauchy principal value integration and $+$ and $-$ denote the upper and lower boundary limits on the cut $(-1,1)$, respectively. The newly introduced operator $\omega_{\nu,E}(s,\nu)$ is defined below

$$\omega_{\nu,E}(s,\nu)f^{\pm}(s,\nu,E) \equiv \int_{M(s)} \mathrm{d}E' K(\nu,E;s,E')f^{\pm}(s,s,E') \quad (13)$$

Eq. (10) can now be rewritten in the form:

$$P\Omega_{\nu,E}(t)H(t,\nu,E) = \omega_{\nu,E}(t,\nu)\lambda(t,E') \quad (14)$$

For any $t\epsilon(-1,1)$ Eq. (14) relates $\lambda(t,E')$ with the function $H(t,\nu,E)$. One must remember only that in this case the integration entering in the definition of $P\Omega_{\nu,E}(t)$ is understood in the Cauchy principal value sense. In this way we have a continuous part of the eigenvalue spectrum. The corresponding eigenfunctions are given by Eq. (9) with function λ fulfilling the relation (14). Function $H(t,\nu,E)$ remains arbitrary.
For $t\epsilon(-1,1)$ the right hand side of Eq. (14) vanishes ($M(t)$ is then empty) and we thus obtain an equation for the discrete part of the eigenvalue spectrum and corresponding functions:

$$\Omega_{\nu,E}(L_i)H(L_i,\nu,E) = 0 \quad (i=1,\ldots N) \quad (15)$$

Assuming (for the sake of simplicity) that L_i are the simple roots of the Eq. (15) the multiple roots must be treated in a way described in [19], the corresponding eigenfunctions will be

$$\phi(L_i,\nu,E) = L_iH(L_i,\nu,E)/(L_i-\nu) \quad (16)$$

It may also happen that Eq. (15) is satisfied by some values $L_k(k=N+1,\ldots M)$ lying on the cut (-1.1). This means that strictly speaking the following equations are satisfied:

$$\Omega^{\pm}{}_{\nu,}E(Lk)H^{\pm}(Lk,\nu,E) = 0 \quad (k=N+1,\ldots M) \quad (17)$$

Let it be noted from the definition that the operator $\Omega_{\nu,E}(z)$ has the following properties:

$$[\Omega_{\nu,E}(z)]^* = \Omega_{\nu,E}(z^*), \quad \Omega^{+}{}_{\nu,E}(s) = [\Omega^{-}{}_{\nu,E}(s)]^* \quad (18)$$

where * denotes the complex cojugation. Thus are derived:

(*a*) L_k are common roots of the pair of Eq. (17)
(*b*) $H^{+}(L_k,\nu,E) = [H^{-}(L_k,\nu,E)]^*$

It should be proved that these discrete eigenfunctions are bounded. No completely satisfactory proof has been given up to now. In this way we have found the full set of eigenfunctions and corresponding eigenfunctions. These functions are orthogonal to the similar set of eigenfunctions of the adjoint Eq. (15). It is important to prove the completeness theorem for this set of eigenfunctions.

Completeness theorem

To claim that any solution of Boltzmann Eq. (1) can be presented as a superposition of expressions (6) it must be proved that the set of eigenfunctions is complete. In other words one must show that any function $\psi(\nu,E)$ can, in a unique way, be expanded in terms of these eigenfunctions:

$$\psi(\nu,E) = \int_{-1}^{1} s\mathrm{d}sH(s,\nu,E)/(s-\nu) + \lambda(\nu,E) + \sum_{i=1}^{M} A_iL_iH(L_i,\nu,E)/(L_i-\nu) \quad (19)$$

It means that functions $H(s,\nu,E)$, $\lambda(\nu,E)$ and constants A_i should be uniquely determined by $\psi(\nu,E)$. Multiplying Eq. (19) by $K(p,E;\nu,E')$ and integrating over $M(\nu)$, we can apply relation (14) and get

$$\psi(\nu,p,E) = \int_{M(\nu)} \mathrm{d}E'K(p,E;\nu,E') \int_{-1}^{1} s\mathrm{d}sH(s,\nu,E')/(s-\nu) + H(\nu,p,E) + \nu\int_{-1}^{1} \mathrm{d}\nu'/(\nu'-\nu) \int_{M(\nu')} \mathrm{d}E'K(p,E;\nu',E')H(\nu,\nu',E') \quad (20)$$

where

$$\psi(\nu,p,E) = \int_{M(\nu)} \mathrm{d}E'K(p,E;\nu,E')[\psi(\nu,E') - \sum_{i=1}^{M} A_iL_iH(L_i,\nu,E')]/(L_i-\nu) \quad (21)$$

As usual let us define a sectionally holomorphic function

$$N(z,\nu,E) \equiv 1/2\pi i\int_{-1}^{1} s\mathrm{d}sH(s,\nu,E)/(s-z) \quad (22)$$

Using this function and the definition of the $\Omega_{\nu,E}(z)$ operator and the Plemelj formulae, Eq. (20) can be rewritten in the form of the Riemann-Hilbert problem

$$\omega\Omega^{+}{}_{p,E}(\nu)N^{+}(\nu,p,E) - F^{+}(\nu,p,E) = \Omega^{-}{}_{p,E}(\nu)N^{-}(\nu,p,E) - F^{-}(\nu,p,E) \quad (23)$$

where

$$F(z,p,E) \equiv 1/2\pi i\int_{-1}^{1} \nu\mathrm{d}\nu\psi(\nu,p,E)/(\nu-z) \quad (24)$$

Using the properties of all entering functions for $z\to\infty$ and the Liouville theorem we can conclude that

$$\Omega_{\nu,E}(z)N(z,\nu,E) = F(z,\nu,E) \quad (25)$$

This is an integral equation for a sectionally holomorphic function $N(z,\nu,E)$. The condition of the solubility of this equation can be formulated in two different but equivalent ways. There are some points in z plane where the homogeneous part of Eq. (25) vanishes. They are the discrete eigenvalues defined by (15) and (17). In these points the right hand side of Eq. (25) must vanish

$$F(L_k,\nu,E) = 0 \quad (k=1,\ldots M) \quad (26)$$

These are conditions which allow us to determine the discrete part of the expansion (19). It can be proved that this point of view complies with the requirements of the orthogonality of $F(z,\nu,E)$ with the solutions to the homogeneous, adjoint integral equations. The same result can be obtained using the orthogonal set of eigenfunctions of the adjoint operator $\Omega_{\nu,E}(z)$, mentioned towards the end of the last section. Thus the whole problem is now reduced to the solution of Eq. (25). Having determined $N(z,\nu,E)$ we can easily find function $H(s,\nu,E)$ by using the Plemelj formulae and the function $\lambda(\nu,E)$ from Eq. (19). The completeness theorem is in principle proved.

The critical and albedo problem for a slab

One of the most important applications of the presented general scheme of eigenfunction expansion method is the critical and albedo problem for a slab. Up to now it has been considered that such problems are connected with singular integral equations over a partial range with respect to s. This fact has considerably restricted the practical solutions of the space-energetical problems. Using the ideas of K. Fuchs and S. Collatz [16], which they formulated for the isotropic energy dependent kernel, one can prove also that in the general case the critical and albedo problem can be dealt with in such a way as to avoid singular integral equations over the partial range.

Let us consider the slab of the thickness $2x_0$, irradiated by two independent beams of neutrons, characterized by distributions $f+(\nu,E)$ and $f-(\nu,E)$ on the right and left surface, respectively.

The general solution of the Boltzmann equation can be written on the basis of previous considerations in the form:

$$\psi(x,\nu,E)=\sum_{i=1}^{M} A_iL_iH(L_i,\nu,E)/(L_i-\nu)[\exp(-x/L_i)] + \int_{-1}^{1} s\,\mathrm{d}s H(s,\nu,E)[\exp(-x/s)]/(s-\nu) + \lambda(\nu,E)\exp(-x/\nu) \quad (27)$$

The coefficients of this expansion should be determined from the boundary conditions:

$$\psi(x_0,\nu,E)=f_+(\nu,E), \quad \nu<0$$
$$\psi(-x_0,\nu,E)=f_-(\nu,E), \quad \nu>0 \quad (28)$$

and the relation (10) between the function $\lambda(\nu,E)$ and $H(s,\nu,E)$. In contrast to the procedure characteristic for the presented proof of the completeness theorem let us determine the function $\lambda(\nu,E)$ from the boundary condition (28).

$$\nu<0,\ \lambda(\nu,E)=\exp(x_0/\nu)f_+(\nu,E) - \sum_{i=1}^{M} A_iL_iH(L_i,\nu,E)\exp[-x_0(1/L_i-1/\nu)]/(L_i-\nu) - \int_{-1}^{1} s\,\mathrm{d}s H(s,\nu,E)\exp[-x_0(1/s-1/\nu)]/(s-\nu)$$

$$\nu>0,\ \lambda(\nu,E)=\exp(x_0/\nu)f(\nu,E) - \sum_{i=1}^{M} A_iL_iH(L_i,\nu,E)\exp[+x_0(1/L_i-1/\nu)]/-(L_i-\nu) - s\,\mathrm{d}s H(s,\nu,E)\exp[+x_0(1/s-1/\nu)]/(s-\nu)$$

Combining these two formulae we can write:

$$\lambda(\nu,E)=\exp(-x_0/|\nu|)f_{-\mathrm{sgn}\nu}(\nu,E) - \int_{-1}^{1} s\,\mathrm{d}s H(s,\nu,E)\exp[x_0\mathrm{sgn}\nu(1/L_i-1/\nu)]/(s-\nu) - \sum_{i=1}^{M} A_iL_iH(L_i,\nu,E)\exp[x_0\mathrm{sgn}\nu(1/L_i-1/\nu)]/(L_i-\nu) \quad (29)$$

and introduce it into the relation (10):

$$H(t,\nu,E) + t\int_{-1}^{1}\mathrm{d}\nu'/(\nu'-t)\int_{M(\nu')}\mathrm{d}E'K(\nu,E;\nu',E')H(t,\nu,E) = \int_{M(t)}\mathrm{d}E'K(\nu,E;t,E')[f_{-\mathrm{sgn}\nu}(t,E')\exp(-x_0/|\nu|) - \int_{-1}^{1} s\,\mathrm{d}s H(s,t,E')\exp[x_0\mathrm{sgn}t(1/s-1/t)]/(s-t) - \sum_{i=1}^{M} A_iL_iH(L_i,t,E)\exp[x_0\mathrm{sgn}t(1/L_i-1/t)]/(L_i-t) \quad (30)$$

Eq. (30) can be rewritten in the form:

$$H(t,\nu,E) + t\int_{-1}^{1}(\mathrm{d}\nu'/\nu'-t)\int_{M(\nu')}\mathrm{d}E'K(\nu,E;\nu',E')H(t,\nu',E') + \int_{M(t)}\mathrm{d}E'K(\nu,E;t,E')\int_{-1}^{1}\nu'\mathrm{d}\nu'H(\nu',t,E') \exp[x_0\mathrm{sgn}t(1/\nu'-1/t)]/(\nu'-t)=F(t,\nu,E) \quad (31)$$

where

$$F(t,\nu,E)\equiv\int_{M(t)}\mathrm{d}E'K(\nu,E;t,E')\{f_{-\mathrm{sgn}t}(t,E')\exp(-x_0/|t|) - \sum_{i=1}^{M} A_iL_iH(L_i,t,E)\exp[x_0\mathrm{sgn}t(1/L_i-1/t)/(L_i-t)]\} \quad (32)$$

Introducing a new unknown function $h(t,\nu,E)$ by the relation

$$h(t,\nu,E)=\exp(-x_0/|t|)H(t,\nu,E) \quad (33)$$

Eq. (31) takes ultimately the form:

$$h(t,\nu,E) + t\int_{-1}^{1}\mathrm{d}\nu'/(\nu'-t)\int_{M(\nu')}\mathrm{d}E'K(\nu,E;\nu',E')h(t,\nu',E') + \int_{M(t)}\mathrm{d}E'K(\nu,E;t,E')\int_{-1}^{1}\nu'\mathrm{d}\nu'h(\nu',t,E')/(\nu'-t) = F(t,\nu,E)\exp(-x_0/|t|) \quad (34)$$

Let us observe that Eq. (34) is completely identical in form with Eq. (20). This means that the same procedure of reduction can be applied to the Riemann-Hilbert problem. This gives the integral equation

$$\Omega_{\nu,E}(z)n(z,\nu,E) = f(z,\nu,E) \quad (35)$$

where

$$n(z,\nu,E) \equiv 1/2\pi i \int_{-1}^{1} s\,ds h(s,\nu,E)/(s-z) \quad (36)$$

$$f(z,\nu,E) \equiv 1/2\pi i \int_{-1}^{1} s\,ds F(s,\nu,E)\exp(-x_0/|s|)/(s-z) \quad (37)$$

As previously the solubility conditions have the form:

$$1/2\pi i \int_{-1}^{1} s\,ds F(s,\nu,E)\exp(-x_0/|s|)/(s-L_i) = 0 \quad (i=1,\ldots M) \quad (38)$$

In the case of the albedo problem they permit the determination of all constants A_i in terms of f_+ and f_-. In the case of a critical problem for a slab $f_+ = f_- \equiv 0$ and we get from (38) a system of homogeneous algebraic equations for A_i. The necessary and sufficient condition for the existence of nontrivial solutions is the vanishing of the characteristic determinant. It is the exact critical condition for the determination of the critical thickness x_0.

In conclusion we may claim that space-energy dependent problems can be dealt with by means of the eigenfunction expansion method. There are now open ways for specification of the energy transfer kernels, examination of the discrete eigenvalues and eigenfunctions and numerical calculations of all plane problems with a practical interest.

REFERENCES

1. van Kampen, N. G., Physica, *21*, 949 (1955).
2. Case, K. M., Ann. Phys. (N.Y.), *9*, 1 (1960).
3. Lafore, P., and Millot, J. P., Rept CEA No. 1072.
4. Zelazny, R., J. Math. Phys., *2*, 538 (1961).
5. Mitsis, G. J., Nuclear Sci. Eng., *17*, 55 (1963).
6. Zelazny, R., and Kuszell, A., Physica, *27*, 597 (1961).
7. Kuszell, A., Acta Phys. Pol., *20*, 567 (1961).
8. Mika, J., Nukleonika, *7*, 361 (1962).
9. Zelazny, R., Kuszell, A., and Mika, J., Ann. Phys. (N.Y.), *16*, 69 (1961).
10. Mika, J., Nuclear Sci. Eng., *11*, 415 (1961).
11. Zelazny, R., and Kuszell, A., Ann. Phys. (N.Y.), *16*, 81 (1961).
12. Zelazny, R., and Kuszell, A., Physics of Fast and Intermediate Reactors III, Vienna (1962).
13. Zelazny, R., Proc. Neutron Thermalization Conf., BNL (1962).
14. Ferzinger, J. H., and Leonard, A., Ann. Phys. (N.Y.), *22*, 192 (1963).
15. Bednarz, R., and Mika, J., J. Math. Phys., *4*, 1285 (1963).
16. Fuchs, K., and Collatz, S., private communication.
17. Dresner, L., and Weinberg, A. M., Rev. Mod. Phys., *34*, 747 (1962).
18. Muskhelishvili, N. J., *Singular Integral Equations*, Nordhoff (1952).
19. Zelazny, R., Ann. Phys. (N.Y.), *19*, 177 (1962).

ABSTRACT—RÉSUMÉ—АННОТАЦИЯ—RESUMEN

A/498 Pologne

Développement en fonctions propres dans la théorie du transport des neutrons

par R. Żelazny

Le mémoire traite de la recherche d'une solution générale de l'équation cinétique de Boltzmann, au moyen du développement en fonctions propres, qui ouvre de nouvelles perspectives très vastes dans la théorie du transport des neutrons.

La méthode est fondée sur l'équation de Boltzmann à une seule vitesse, avec diffusion isotrope des neutrons dans une géométrie arbitraire.

L'auteur introduit le concept fondamental de la fonction propre et de la valeur propre de cette équation, et en étudie les propriétés. Puis, il établit une solution générale de l'équation de Boltzmann et formule le problème aux limites. Il donne des exemples de problèmes dont les propriétés de symétrie sont différentes et commente les études faites sur ce sujet par différentes autres méthodes. Les problèmes à symétrie sphérique sont spécialement évoqués.

L'auteur étend ensuite cette méthode pour tenir compte de la diffusion anisotrope des neutrons, des noyaux qui sont fonction de l'énergie et des problèmes qui sont fonction du temps dans une géométrie plane. Il examine les valeurs propres et les fonctions propres correspondantes et démontre sommairement que ces fonctions propres constituent un système complet. Il étudie la possibilité d'appliquer cette méthode à divers problèmes de criticité et de spectre dans la théorie des réacteurs.

L'auteur s'attache plus particulièrement au problème de la réduction des équations intégrales singulières à celles de Fredholm, ainsi qu'aux conditions supplémentaires auxquelles leurs solutions doivent satisfaire. Ces conditions, qui sont étroitement liées aux indices des équations intégrales singulières, jouent le rôle le plus important dans la physique de la théorie.

A/498 Польша

Метод собственных функций в теории переноса нейтронов

Р. Желязны

Этот доклад посвящен проблеме общего решения кинетического уравнения Больцмана при помощи метода собственных функций, который открывает новые и широкие перспективы в теории переноса нейтронов.

Метод формулируется на основе односкоростного уравнения Больцмана с изотропным рассеянием нейтронов, но для произвольной геометрии.

Введено фундаментальное понятие собственной функции и собственного числа этого уравнения и обсуждены их свойства. Сконструировано затем общее решение уравнения Больцмана и сформулирована проблема граничных значений.

Рассмотрены некоторые задачи с различными свойствами симметрии. Критически рассмотрены и комментированы другие работы в этом направлении, основанные на различных подходах. В особенности это относится к проблемам сферической симметрии.

Для плоской геометрии этот подход расширяется в дальнейшем на задачи с анизотропным рассеянием нейтронов, на ядра, зависящие от энергии, и задачи, зависящие от времени. Обсуждены собственные значения и соответствующие собственные функции для этих случаев и намечены доказательства теорем о полноте. Сформулированы и оценены возможные применения этого метода к расчету критических и спектральных характеристик реакторов.

Особое внимание уделено вопросам регуляризации сингулярных интегральных уравнений до уравнений типа Фредгольма и добавочным условиям, которые должны быть выполнены при их решении. Эти условия тесно связаны с сингулярностью интегральных уравнений и играют важнейшую роль в теории.

A/498 Polonia

El método de desarrollo en funciones propias en la teoría del transporte de neutrones

por R. Żelazny

El objeto de la presente memoria es la solución general de la ecuación del transporte de Boltzmann obtenida siguiendo el método de desarrollo en serie de funciones propias, método que abre nuevas y amplias perspectivas en la teoría del transporte de neutrones.

Se describe este método para el caso de la ecuación de Boltzmann correspondiente a neutrones monoenergéticos y dispersión isotropa, en cualquier geometría.

Se introduce el concepto fundamental de función propia y valor propio de dicha ecuación y se discuten sus propiedades. Se construye luego la solución general de la ecuación de Boltzmann y se formula el problema de contorno. Se presentan algunos problemas con diferentes propiedades de simetría.

Este procedimiento se generaliza después a problemas en los que la dispersión neutrónica es anisótropa, a aquellos en los que los núcleos integrales dependen de la energía y a problemas en que aparece la variable tiempo, en el caso de simetría plana.

Se estudian los valores propios y las correspondientes funciones propias para estos casos y se esbozan las demostraciones de los teoremas relativos al carácter completo. Se examinan y formulan posibles aplicaciones de este método a las cuestiones de criticidad y de espectro neutrónico en la teoría de reactores. Particular atención se dedica a las cuestiones de regularización de las ecuaciones integrales singulares hasta reducirlas a ecuaciones de Fredholm, y a las condiciones suplementarias que deben cumplir sus soluciones. Estas condiciones están íntimamente ligadas con los índices de las ecuaciones integrales singulares y representan un papel muy importante en la teoría.

Some iterative methods for the construction of solutions of neutron transport equations

By I. Marek*

In this paper, the iterative methods of the type "source iterations" are given for the approximate construction of solutions of neutron transport equations, namely for the solution of eigenvalue problems. The purpose of our considerations is not to solve a particular problem with the given operators—for example, to determine the critical parameters of a nuclear reactor —but to consider the neutron transport equations in the general form. We assume that the operators, which occur in the mentioned equations, have only some general properties. These properties are characteristic of a comparatively extensive class of neutron transport problems. As showed by G. Birkhoff, such a general property in a determined sense is the positivity of some operators, which characterize the given problem. Therefore we write the neutron transport equations in the symbolical form in which the individual models of the description of the neutron transport are not distinguished. We pay particular attention to continuous models and we mention the problem of reducing corresponding equations into a system of algebraic linear equations.

On the basis of the general properties of neutron transport equations:

(*a*) we give the conditions for the convergence of iterative methods for the construction of solutions of these equations;

(*b*) we give a method for the transfer of eigenvalue problems to a system of inhomogeneous problems;

(*c*) for the construction of solutions of inhomogeneous equations, we give also an iterative method which converges more rapidly than the usual method of successive approximations. This method is particularly suitable for cases where it is necessary to solve both those problems with the external sources and the corresponding eigenvalue problems.

NOTATION AND FORMULATION OF THE PROBLEMS

The time-independent neutron transport equations can be symbolically written in the following form

$$Lx = Bx + \lambda Cx + s \tag{1}$$

$$Lx = Bx + \lambda \,.\, Cx \tag{2}$$

where the operator L describes the diffusion and absorption, B the scattering, C the fission. The vector x denotes either the neutron flux or the density of neutrons, s the external sources. The form of the operators L,B,C depends on the one hand on the model of the neutron transport and on the other hand on the domain $\mathscr{G}$ in which the above-mentioned nuclear processes are observed. The domain $\mathscr{G}$ is assumed to be bounded. This assumption is not essential [6] [12]. Further properties of the domain $\mathscr{G}$, namely the smoothness of its boundary, will not be explicitly described. We refer the reader to papers in which the problem of the existence of the Eq. (1) and (2) is considered [8,13] [15 Birkhoff p. 132, Habetler and Martino, p. 145] [24–26]. The assumptions about the operators L,B,C and their domains $\mathscr{D}(L)$, $\mathscr{D}(B)$, $\mathscr{D}(C)$, namely, the validity of the inclusions

$$\mathscr{D}(L) \subset \mathscr{D}(B) \subset \mathscr{D}(C)$$

and the existence of the bounded inverse operator $(L-B)^{-1}$ are fulfilled in the type of problem which is considered in our contribution.

The convergence of the following iterative processes depends on one essential property—namely, the existence of a characteristic value λ of Eq. (2), for which the inequality $|\lambda| > \lambda_0$ holds for every characteristic value λ of Eq. (2) different from λ_0. The existence of such a characteristic value λ_0 is a consequence of the positivity (in the sense which is separately determined in any individual case) of the operator $(L-B)^{-1}C$ or of the operator $C(L-B)^{-1}$ (see [8], the positivity of the components in the usual sense; [13], absolute positivity and compactness; [15] Birkhoff, the uniform positivity).

Besides Eqs. (1), (2) we shall consider also the corresponding adjoint equations

$$L^*x^* = B^*x^* + \bar{\lambda}C^*x^* + s^*, \text{ and} \tag{3}$$

$$L^*x^* = B^*x^* + \bar{\lambda}C^*x^*, \tag{4}$$

where L^*, B^*, C^* are the adjoint operators to the operators L,B,C. The existence of L^*, B^*, C^* is evident in certain neutron transport problems and therefore we shall assume that they exist. With the help of the iterations with the adjoint operators L^*, B^*, C^* we get a special iterative process, which is in a certain sense optimal. The physical meaning of Eqs. (3) and (4)

* Mathematical Institute of Charles University, Prague.

was studied by L. N. Usačev [22]. See also [10], p. 46.

The iterative methods presented here can be used for the construction of solutions of neutron transport equations investigated in any arbitrary geometry. For the solution of inhomogeneous equations the best methods are those given by R. S. Varga in his excellent book [23], as is well known. Therefore, here we shall examine the methods of solution of eigenvalue problems and the transformation of such problems into inhomogeneous problems.

ITERATIVE METHODS OF THE TYPE "SOURCE ITERATION"

Let X be some Banach space elements whose vector functions are defined on $\mathscr{R} = \mathscr{G} \times \Omega$ where Ω denotes a set having a compact closure in Euclidean space. With the symbol K we denote the cone of the non-negative vector functions of X. Let X' be the adjoint space of continuous linear forms on X and let $[X]$ be the space of bounded linear transformations into itself. The norm in $[X]$ is usually defined as

$$\|A\| = \sup_{\|x\|=1} \|Ax\|.$$

Let us assume that

(*a*) Equation (2) has one and only one solution $x_0, \|x_0\| = 1$ which is positive in $\mathscr{R}$;

(*b*) the solution x_0 corresponds to the positive characteristic value λ_0;

(*c*) the value $\mu_0 = \lambda_0^{-1}$ is the simple pole of the resolvent $R(\lambda,T) = (\lambda I - T)^{-1}$* and the dominant point of the spectrum $\sigma(T)$ of the operator T, where T denotes one of the operators $(L-B)^{-1}C$, or $C(L-B)^{-1}$

Note. The point $\mu_0 \in \sigma(T)$ is called the dominant point of the spectrum $\sigma(T)$ of the operator $T \in [x]$, if the inequality

$$|\lambda| < |\mu_0| \tag{5}$$

holds for $\lambda \in \sigma(T)$, $\lambda \neq \mu_0$.

Evidently from the assumption (*c*) follows the validity of the inequality $|\lambda| > \lambda_0$ for every characteristic value of Eq. (2).

It has already been noted that the assumptions (*a*) to (*c*) are fulfilled for neutron transport problems—for full particulars see Refs. [8, 13] [15] Birkhoff, Habetler, Martino [24–26]. It follows from the assumptions (*a*) to (*c*) that in the norm of the space $[X]$ the following relation holds,

$$\mu_0^{-n} T^n \to B_1$$

where

$$B_1 = \frac{1}{2\pi i} \int_{\Gamma_0} R(\lambda_1 T)\, d\lambda,$$

and where Γ_0 denotes the boundary of the circle $C_0 = \{\lambda \mid |\lambda - \mu_0| \leq \rho_0\}$ for which $C_0 \cap \sigma(T) = \{\mu_0\}$, see [11]. The proof of the convergence of the iterative methods presented here is based simply on this fact.

* I denotes the identity operator.

Let $\{y_n'\}$, $\{z_n'\}$ be sequences of such functionals that there exists a functional y' where

$$y_n'(x) \to y'(x),\ z_n'(x) \to y'(x) \text{ for every } x \in X \tag{6}$$

and $y_n'(\lambda x) = \lambda y_n'(x)$, $z_n'(\lambda x) = \lambda z_n'(x)$

for $x \in X$ and $\lambda > 0$. (7)

Further let C_1, C_2 be constants independent of $x \in X$, $y \in X$, n, such that

$$\begin{aligned} |y_n'(x) - y_n'(y)| &\leq C_1 \|x - y\|, \\ |z_n'(x) - z_n'(y)| &\leq C_2 \|x - y\| \end{aligned} \tag{8}$$

for $x \in X$, $y \in X$, $n = 1, 2, \ldots$

Let us assume that the inequalities

$$y_n'(x) \geq 0,\ z_n'(x) \geq 0 \tag{9}$$

hold for $x \in K$, and let

$$y'(B_1 x^{(0)}) \neq 0 \tag{10}$$

where $x^{(0)} \in K$, $B_1 x^{(0)} \neq 0$ is some suitable element.

We introduce an operator C_1 as

$$C_1 = \frac{1}{2\pi i} \int_{\Gamma_0'} R(\lambda, T^*)\, d\lambda$$

where Γ_0' denotes the boundary of the circle $C_0' = \{\lambda \mid |\lambda - \mu_0| \leq \rho_0'\}$, $C_0' \cap \sigma(T^*) = \{\mu_0\}$.

Let the sequences $\{y_n\}$, $\{z_n\}$, $y_n \in X, z_n \in X$, converge weakly to a vector $y \in x$, i.e., the relations

$$\langle y_n, x' \rangle \to \langle y, x' \rangle,\ \langle z_n, x' \rangle \to \langle y, x' \rangle \tag{11}$$

hold for every $x' \in X'$. Here the expression $\langle u, v' \rangle$ denotes the value of the form $v' \in X'$ at the element $u \in X$.

Further,

$$\langle y, C_1 x^{*(0)} \rangle > 0 \tag{12}$$

where $x^{*(0)} \in X'$ is a non-negative form, i.e., $x^{*(0)}(x) \geq 0$ if $x \in K$.

The iterations of the type "source iteration" can be defined with the help of the formulae

$$v^{(n)} = Cu_{(n)},\ Lu^{(n+1)} = Bu^{(n+1)} + v^{(n)}, \tag{13}$$

$$u_{(n+1)} = \lambda_{(n)} u^{(n+1)},\ u_{(0)} = x^{(0)},$$

$$\lambda_{(n)} = \frac{y_n'(u_{(n)})}{z_n'(u^{(n+1)})} \tag{14}$$

$$\begin{aligned} &L^* u_{(n)}{}^* = B^* u_{(n)}{}^* + v^{*(n)},\ u^{*(n+1)} = C^* u_{(n)}{}^*, \\ &v^{*(n+1)} = \lambda_{(n)}{}^* u^{*(n+1)},\ v^{*(0)} = x^{*(0)}, \end{aligned} \tag{15}$$

$$\lambda_{(n)}{}^* = \frac{\langle y_n, v^{*(n)} \rangle}{\langle z_n, u^{*(n+1)} \rangle} \tag{16}$$

for $T = (L-B)^{-1}C$ and hence also for $T^* = C^*(L^* - B^*)^{-1}$;

Similarly

$$\begin{aligned} &u^{(n+1)} = Cu_{(n)},\ Lu_{(n)} = Bu_{(n)} + v^{(n)}, \\ &v^{(n+1)} = \lambda_{(n)} u^{(n+1)},\ v^{(0)} = x^{(0)}, \end{aligned} \tag{17}$$

$$\lambda_{(n)} = \frac{y_n'(v^{(n)})}{z_n'(u^{(n+1)})} \tag{18}$$

$$v^{*(n)} = C^* u_{(n)}{}^*, \; L^* u^{*(n+1)} = B^* u^{*(n+1)} + v^{*(n)},$$
$$u_{(n+1)}{}^* = \lambda_{(n)}{}^* u^{*(n+1)}, \; u_{(0)}{}^* = x^{*(0)}, \tag{19}$$

$$\lambda_{(n)}{}^* = \frac{\langle y_n, u_{(n)}{}^* \rangle}{\langle z_n, u^{*(n+1)} \rangle} \tag{20}$$

for $T = C(L-B)^{-1}$ and hence also for $T^* = (L^* - -B^*)^{-1} C^*$.

Theorem 1. If the conditions (6) to (12) are fulfilled, then

$$\lambda_{(n)} \to \lambda_0, \; \lambda_{(n)}{}^* \to \lambda_0$$

and in the norm of the space X

$$u_{(n)} \to u_0, \; v^{*(n)} \to v_0{}^*;$$
$$v^{(n)} \to v_0, \; u_{(n)}{}^* \to u_0{}^*,$$

where $u_0 = c_3 B_1 x^{(0)}$, $v_0{}^* = c_4 C_1 x^{*(0)}$, $v_0 = c_5 B_1 x^{(0)}$, $u_0{}^* = c_6 C_1 x^{*(0)}$ and where c_3, c_4, c_5, c_6 are positive constants. Thus $u_0, v_0, u_0{}^*, v_0{}^*$ are eigenvectors of Eqs. (2) and (4) corresponding to the characteristic value λ_0. Moreover we get the estimates

$$|\lambda_{(n)} - \lambda_0| \leq c_7 q^n, \; |\lambda_{(n)}{}^* - \lambda_0| \leq c_8 q^n,$$
$$\|u_{(n)} - u_0\| \leq c_9 q^n, \; \|v^{*(n)} - v_0{}^*\| \leq c_{10} q^n,$$
$$\|v^{(n)} - v_0\| \leq c_{11} q^n, \; \|u_{(n)}{}^* - u_0{}^*\| \leq c_{12} q^n,$$

where $q = \lambda_0 \mu$ and where μ denotes the radius of the circle C_2 with the centre at the origin in the interior of which there lies the set $\sigma(T) - \{\mu_0\}$. Thus $q < 1$ and the rapidity of the convergence of the sequences (13) to (20) is equal to the rapidity of the convergence of the geometric sequence $\{q^n\}$ to zero.

The particular choice of the functionals y_n', z_n' or the vectors y_n, z_n gives some well-known iterative processes and also some new iterative methods.

As examples we give some iterative processes which belong to the type described above. Explicitly only the elements $\lambda_{(n)}, \lambda_{(n)}{}^*$ will be shown because the characterization of the given process can be made according to these elements. We assume that $T = (L-B)^{-1}C$, because the case $T = C(L-B)^{-1}$ can be investigated analogously.

(*A*) Let $X = C(\mathscr{R})$ be the Banach space of vector functions which are continuous on $\overline{\mathscr{R}}$. Let $x^{(0)} \in X$ be a non-negative function such that there exist points $r_{01}, \ldots, r_{0p}$, for which $x^{(0)}(r_{0j}) > 0$ if $j = 1, \ldots, p$. Then we put

$$z_n'(x) = y_n'(x) = y'(x) = \sum_{j=1}^{P} \xi_j x^{(0)}(r_{0j}),$$

where ξ_j is equal either to 0 or 1 and moreover

$$\sum_{j=1}^{P} \xi_j > 0.$$

We get the well-known iterative method

$$\lambda_{(n)} = \frac{\sum_{j=1}^{P} \xi_j u_{(n)}(r_{0j})}{\sum_{j=1}^{P} \xi_j u^{(n+1)}(r_0)_j}$$

Particularly, if $\xi_j = 0$ for $j > 1$, we get

$$\lambda_{(n)} = \frac{u_{(n)}(r_{01})}{u^{(n+1)}(r_{01})}$$

(See Ref. [10], p. 47, and [30]).

The adjoint iterative process can be obtained by putting $z_n = y_n = x^{(0)}$. Then

$$\lambda_{(n)}{}^* = \frac{\int_{\mathscr{R}} x^{(0)}(t) \, dv^{*(n)}(t)}{\int_{\mathscr{R}} x^{(0)}(t) \, du^{*(n+1)}(t)}$$

(*B*) Let X be a Banach space of vector functions defined on $\mathscr{R}$. Let $A \in [X]$, $AK \subset K$, $AB_1 x^{(0)} \neq 0$. Let us put

$$z_n'(x) = y_n'(x) = y'(x) = \|Ax\|.$$

Thus

$$\lambda_{(n)} = \frac{\|Au_{(n)}\|}{\|Au^{(n+1)}\|}$$

and we get the well-known Kellogg's iterative method (see Ref. [9] [16], p. 260 and [11]).

(*C*) Let X be a Hilbert space of vector functions defined on $\mathscr{R}$. The inner product in X we denote (x,y) where $x \in X, y \in X$. It is known that in that case the continuous linear form on X can be expressed as $\langle y, x' \rangle = (y, x)$ where $x' \in X', x \in X$; thus $X' = X$.

Let us put $z_n' = y_n' = v^{*(p)}$, where p is a fixed index. We get the following iterative process

$$\lambda_{(n)} = \frac{(u_{(n)}, v^{*(p)})}{(u^{(n+1)}, v^{*(p)})}.$$ See [10], p. 71.

If we put $z_n' = y_n' = v^{*(n)}$, $z_n = y_n = u_{(n)}$, we get the iterative processes for which

$$\lambda_{(n)} = \frac{(u_{(n)}, v^{*(n)})}{(u^{(n+1)}, v^{*(n)})}, \; \lambda_{(n)}{}^* = \frac{(u_{(n)}) \, v^{*(n)})}{(u_{(n)}, u^{*(n+1)})}$$

Evidently

$$\lambda_{(n)} = \lambda_{(n)}{}^* = \frac{(T^{2n} x^{(0)}, x^{*(0)})}{(T^{2n+1} x^{(0)}, x^{*(0)})} \tag{21}$$

This process is optimal in the following sense. If we find the minimal value of the function

$$\xi_n(\nu) = (\nu u^{(n+1)} - u_{(n)}, \nu u^{*(n+1)} - v^{*(n)})$$

we get the argument $\nu_n = \lambda_{(n)}$, where $\lambda_{(n)}$ is defined in Eq. (21), for which the function ξ_n comes into a minimal value [14].

APPLICATIONS OF THE ITERATIVE METHODS

With the help of the mentioned iterative methods, the original eigenvalue problem can be transferred to a sequence of inhomogeneous problems. Then we must solve equations of the type

$$Lu - Bu = v \tag{22}$$

Solutions of these equations can be found approximately particularly with the help of iterations. The Eq. (22) must still be transferred to systems of linear

algebraic equations for the continuous model. This arrangement depends on the form of the operators L,B,C, i.e., it depends on the model in which the neutron transport is investigated.

For the discretization of equations of the neutron motion the Carlson's S_n-method (see Ref. [4] [15, Carlson, p. 243] [17, p. 164]) and the P_n-method of the spherical harmonics (see for example Ref. [17, p. 142] [10, p. 290]) are used. The method of characteristics is used for the case of spherically symmetric domains (see Ref. [10, p. 365] [17, p. 118] [27]).

For the discretizations of diffusion equations the net-methods are used. Of special importance is the question of the convergence and the stability in the case with discontinuous functions (see Ref. [18–21] [10, p. 139] [31]).

Iterative methods are also the basis for the construction of solutions of neutron transport equations with the help of Monte Carlo methods (see Ref. [5,7] [15, Richtmayer, p. 215] [28]).

As R. S. Varga shows in his book [23], the over relaxation methods and the Chebyshev semi-iterative methods are fully satisfactory for the solution of the Eqs. (1), (3), and (22) when the operators $(L-B)^{-1}$, $(L-B)^{-1}C$ are finite-dimensional. For the solution of Eqs. (1) and (3) we give also one iterative method. This method is advantageous particularly if the knowledge of the minimal characteristic value of Eq. (2) is needed. This iterative method makes use of some approximations of the value λ_0. The rapidity of the convergence of this process is greater than the rapidity of the convergence of the usual successive approximations. The approximative solutions of Eqs. (1) and (3) can be found with the help of Neuman's series, i.e., in the form

$$z_{n+1} = \frac{\lambda_{(n)}}{\lambda_{(n)} - \lambda} w_{n+1} + \sum_{k=0}^{n} w_k, \tag{23}$$

$$z_n^{*}{}_{+1} = \frac{\lambda_{(n)}^{*}}{\lambda_{(n)}^{*} - \bar{\lambda}} w_n^{*}{}_{+1} + \sum_{k=0}^{n} w_k^{*}, \tag{24}$$

where $\lambda_{(n)}$, $\lambda_{(n)}^{*}$ are defined by Eqs. (14) and (16), $w_0 = (L-B)^{-1}s$, $w_0^{*} = T^{*}s^{*}$ if $T = (L-B)^{-1}C$; if $T = C(L-B)^{-1}$, then $\lambda_{(n)}$, $\lambda_{(n)}^{*}$ are defined by (18) and (20), $w_0 = Ts$, $w_0^{*} = (L^{*}-B^{*})^{-1}s^{*}$ and in both cases $w_k = (\lambda T)^k w_0$, $w_k^{*} = (\bar{\lambda} T^{*})^k w_0^{*}$.

Theorem 2. Assume $|\lambda| < \lambda_0$. Then there exists one and only one solution x of Eq. (1) and one and only one solution x^{*} of Eq. (3). The sequences (23) and (24) converge to these solutions x, x^{*}: $z_n \to x$, $z_n^{*} \to x^{*}$ and the following estimates hold,

$$\|z_n - x\| \leq c_{13}\alpha^n, \|z_n^{*} - x^{*}\| \leq c_{14}\alpha^n,$$

where $\alpha = |\lambda\nu|$, $\lambda_0^{-1} > \nu > \mu$ and where μ denotes the radius of the circle C containing the set $\sigma(T) - \{\mu_0\}$.

Note. Evidently the improvement of the convergence according to usual successive approximations will be the greater the smaller is the value $\lambda_0\mu$.

REFERENCES

1. Birkhoff, G., Trans. Amer. Math. Soc., *85*, 219 (1957).
2. Birkhoff, G., Proc. Mat. Acad. Sci. USA, *45*, 557 (1959).
3. Birkhoff, G., and Varga, R. S. Rep. WAPD-166 (1957); J. Soc. Industr. Appl. Math. *6*, 354 (1958).
4. Carlson, B. G., Rep. LA-1891 (1955).
5. Curtiss, J. H., J. Math. and Phys., 32, *4*, 209–232 (1954).
6. Feix, M., Nicourd, P., and Valentin, S., Comptes rendus Acad. Sci., 244 (1957).
7. Gatesoup, M., and Guilland, J., Publs. Inst. Statist. Univ. Paris, *10*, N4, 243 (1961).
8. Habetler, G. J., and Martino, M. A., Rep. KAPL-1896 (1958).
9. Kellogg, O. D., Math. Ann., *86*, 14 (1922).
10. Marčuk, G. I., *Numerical methods of nuclear reactors.* Moscow (1958).
11. Marek, I., Czech. Math. Journ., *12* 536 (1962).
12. Marek, I., Aplikace matematiky, *8*, 102 (1963).
13. Marek, I., Aplikace matematiky, *8*, 442 (1963).
14. Marek, I., Comment. Math. Univ. Carol. 4, *2*, 53 (1963).
15. Proc. of Symposia in Appl. Math. Vol. *XI. Nuclear reactor theory*, Amer. Math. Soc. (1961) Russian translation. Moscow (1962).
16. Riesz, F., and Nagy, B. S., *Leçons d'analyse fonctionelle.* Russian translation, Moscow (1954).
17. Richtmayer, R. D., *Difference methods for initial value problems*, Russian translation, Moscow (1960).
18. Tikhonov, A. N., and Samarski, A. A., Dok. Akad. Nauk USSR, 108, *N3*, 393 (1956); 122, *N3* 188 (1958); 122 *N4*, 562 (1958); 124, *N3*, 529 (1959); 124, *N4*, 779 (1959); 131, *N3*, 514 (1960); 131, *N6*, 1264 (1960).
19. Tikhonov, A. N., and Samarski, A. A., J. Num. Math. and Math. Phys. I, *N1*, 5 (1961).
20. Tikhonov, A. N., and Samarski, A. A., J. Num. Math. and Math. Phys. I, *N3*, 425 (1961).
21. Tikhonov, A. N., and Samarski, A. A., J. Num. Math. and Math. Phys. II, *N5*, 784 (1961).
22. Usačev, L. N., Compendium on reactor construction and theory, Moscow (1955).
23. Varga, R. S., *Matrix iterative analysis.* Prentise Hall (1962).
24. Varga, R. S., and Martino, M. A., Proceedings of the Second International Conference on the Peaceful Uses of Atomic Energy, P/1541, Vol. 16, p. 570, United Nations (1958).
25. Vladimirov, V. S., Izv. Akad. Nauk USSR ser. matem., *21*, 3 (1957).
26. Vladimirov, V. S., Izv. Akad. Nauk USSR, ser. matem., *21*, 681 (1957).
27. Vladimirov, V. S., Vyčisl. Matěmatika, *3*, 3 (1958).
28. Vladimirov, V. S., Těorija verojatn., *1* (1956).
29. Vladimirov, V. S., Prikl. matem. i mech. XIX, *N3* (1955).
30. Weilandt, H., Math. Zeitschr., *50*, 93–141 (1944).
31. Young, D. M., Trans. Amer. Math. Soc., *76*, 92 (1954).

ABSTRACT—RÉSUMÉ—АННОТАЦИЯ—RESUMEN

A/632 Tchécoslovaquie

Méthodes d'itération pour la résolution d'équations du transport des neutrons

par I. Marek

Dans un problème indépendant du temps, les équations du transport des neutrons peuvent être mises sous la forme

$$Lx = Bx + \lambda Cx + s \tag{1}$$

où les opérateurs L,B,C et les vecteurs x,s ont la signification suivante: l'opérateur L représente la diffusion et l'absorption, B la dispersion, C la fission; le vecteur x le nombre volumique de neutrons ou le flux de neutrons, et s les sources extérieures. Soit l'équation (1) qui exprime le transport des neutrons dans un domaine limité $\mathscr{R}$. La forme des opérateurs L,B,C dépend de l'approximation à laquelle se rapporte le transport des neutrons (voir G. J. Habetler, M. A. Martino, G. Birkhoff, G. I. Marčuk, I. Marek, R. S. Varga, V. S. Vladimirov). Dans les travaux qu'ils ont publiés, ces auteurs ont prouvé entre autres que l'équation

$$Lx = Bx + \lambda Cx \tag{2}$$

a une solution x_0 qui est positive dans $\mathscr{R}$. Cette solution correspond à la valeur caractéristique positive λ_0 pour laquelle l'inégalité $|\lambda| > \lambda_0$ est satisfaite pour chacune des différentes valeurs caractéristiques λ de l'équation (2). En outre, cette équation n'a dans $\mathscr{R}$ d'autre solution non négative que cx_0, où c représente une constante positive. Cela découle des propriétés des opérateurs $(L-B)^{-1}C, C(L-B)^{-1}$. On peut facilement prouver que la valeur $\mu_0 = \lambda_0^{-1}$ est la valeur propre dominante de l'opérateur T, T représentant un des opérateurs $(L-B)^{-1}C, C(L-B)^{-1}$.

Il est possible, au moyen de méthodes d'itération, d'établir les éléments propres de l'équation (2) et les solutions de l'équation (1). Le mémoire a pour objet de présenter un processus général d'itération et de prouver sa convergence.

Soit X un espace de Banach de fonctions de vecteurs dans $\mathscr{R}$ et y_n', z_n', y' des fonctionnelles continues dans lesquelles

$$y_n'(x) \to y'(x), z_n'(x) \to y'(x)$$

pour toutes les valeurs de $x \in X$ et

$$y_n'(\lambda x) = \lambda y_n'(x),\ z_n'(\lambda x) = \lambda z_n'(x)$$

pour toutes les valeurs de $x \in X$ et $\lambda > 0$.

Soit les relations $y_n'(x) \geqslant 0$, $z_n'(x) \geqslant 0$ qui s'appliquent à tous les vecteurs non négatifs $x \in X$; d'où $y'(x) \geqslant 0$ s'applique à tous les vecteurs. Soit en outre $y'(x_0) > 0$, où x_0 est le vecteur propre positif de l'équation (2).

On pose $x_{n+1} = \mu_n^{-1} T x_{(n)}$
où $x_{(0)}$ est un vecteur positif. Soit, en outre,

$$\mu_n = \frac{z_n'(Tx_{(n)})}{y_n'(x_{(n)})}$$

Théorème 1. Les séries $\{\mu_n\}$, $\{x_{(n)}\}$ sont convergentes

$$\mu_n \to \lambda_0^{-1},\ x_{(n)} \to cx_0,$$

où $Lx_0 = Bx_0 + \lambda_0 Cx_0$ et c est une constante positive.

On peut, pour construire des solutions de l'équation (1), utiliser les formules suivantes:

$$z_n + 1 = \frac{\lambda_{(n)}}{\lambda_{(n)} - \lambda} \mathscr{W}_{n+1} + \sum_{k=0}^{n} \mathscr{W}_k$$

où $s_{(n)} = \mu_n^{-1}$, $\mathscr{W}_k = (\lambda T)^k \mathscr{W}_0$ et $\mathscr{W}_0 = (L-B)^{-1}s$ lorsque $T = (L-B)^{-1}C$ et $\mathscr{W}_0 = C(L-B)^{-1}$ lorsque $T = C(L-B)^{-1}$

Théorème 2. Soit l'inégalité $|\lambda| < \lambda_0$, qui est satisfaite. Il existe alors une solution z et une seule de l'équation (1) où s est un élément arbitraire dans X. En outre, dans la norme de X, $z_{n+1} \to z$ est conservée. La rapidité de la convergence est plus grande que dans la méthode courante des approximations successives.

A l'aide de fonctionnelles spéciales y_n', z_n', les auteurs sont parvenus à quelques méthodes d'itération connues, d'une part, et à des processus d'itération non encore utilisés, d'autre part.

A/632 Чехословакия

Некоторые итерационные методы построения решений уравнений переноса нейтронов

И. Марек

Уравнения переноса нейтронов в стационарном случае можно записать в виде

$$Lx = Bx - \lambda Cx + s, \tag{1}$$

где операторы L, B, C и векторы x, s имеют следующее значение: оператор L обозначает диффузию и поглощение, B — рассеяние, C — деление; вектор x обозначает плотность нейтронов или нейтронный поток, s — внешние источники. Мы предполагаем, что уравнение (1) описывает перенос нейтронов в данной ограниченной области $\mathscr{R}$. Вид операторов L, B, C зависит от приближения, в котором рассматривается перенос нейтронов (Биргофф, Хабетлер, Мартино, Марчук, Марек, Варга, Владимиров и другие). В работах этих авторов кроме других результатов доказано, что уравнение

$$Lx = Bx + \lambda Cx \tag{2}$$

обладает положительным в области $\mathscr{R}$ решением x_0. Это решение отвечает положительному характеристическому значению λ_0, для которого имеет место неравенство $|\lambda| > \lambda_0$ для каждого другого характеристического значения λ уравнения (2). Более того, это уравнение не имеет в области $\mathscr{R}$ других неотрицательных решений, кроме Cx_0, где C — положительная константа. Этот факт является следствием свойств операторов $(L - B)^{-1}C$ и $C(L - B)^{-1}$. Можно легко убедиться в том, что $\mu_0 = \lambda_0^{-1}$ является доминантным собственным значением оператора T, где T один из операторов $(L - B)^{-1}C$ или $C(L - B)^{-1}$.

Для приближенного построения собственных элементов уравнения (2) и решений уравнения (1) выгодными являются итерационные методы. Наша цель — привести некоторую общую итеративную схему и доказать ее сходимость.

Пусть x — некоторое банахово пространство вектор-функций на $\mathscr{R}$. Пусть $\{y_n'\}$, $\{z_n'\}$, y' — последовательности непрерывных функционалов, таких, что

$$y_n'(x) \to y'(x), \quad z_n'(x) \to y'(x)$$

для $x \in X$ и

$$y_n'(\lambda x) = \lambda y_n'(x), \quad z_n'(\lambda x) = \lambda z_n'(x)$$

для $x \in X$, $\lambda > 0$.

Пусть для неотрицательных векторов $x \in X$ выполняются соотношения $y_n'(x) \geqslant 0$, $z_n'(x) \geqslant 0$, так что для таких x $y'(x) \geqslant 0$. Кроме того, пусть $y'(x_0) > 0$ для положительного собственного вектора x_0 уравнения (2).

Положим, что $x_{(n+1)} = \mu_n^{-1} T x_{(n)}$, где x_0 — вектор положительный в $\mathfrak{A}$ и

$$\mu_n = \frac{z'(Tx_{(n)})}{y_n'(x_{(n)})}.$$

Т е о р е м а 1. Последовательности $\{\mu_n\}$, $\{x_{(n)}\}$ сходятся:

$$\mu_n \to \lambda_0^{-1}, \quad x_{(n)} \to cx_0,$$

где

$$Lx_0 = Bx_0 + \lambda_0 cx_0$$

и c — положительная постоянная.

Для приближенного построения решений уравнения (1) мы можем потом использовать формулу

$$z_{n+1} = \frac{\lambda_{(n)}}{\lambda_{(n)} - \lambda} W_{n+1} + \sum_{k=0}^{n} W_k,$$

где

$$\lambda_{(n)} = \mu_n^{-1}, \quad W_k = (\lambda T)^k W_0 \text{ и } W_0 = (L - B)\, s^{-1},$$

если

$$T = (h - B)^{-1}C \text{ или } W_0 = C(L - B)^{-1}$$

если $T = C\ (L - B)^{-1}$.

Т е о р е м а 2. Если $|\lambda| < \lambda_0$, то существует одно и только одно решение z уравнения (1), где s — произвольный элемент из пространства x, причем в норме X $z_{n+1} \to z$. При этом скорость сходимости больше, чем у обычных последовательных приближений.

Специальным выбором функционалов y_n', z_n' мы можем получить некоторые известные итерационные схемы и даже некоторые новые, пока не использованные итерационные методы.

A/632 Checoslovaquia

Algunos métodos iterativos para la construcción de soluciones de las ecuaciones del transporte de neutrones

por I. Marek

La ecuación del transporte de neutrones se escribe, para el estado estacionario

$$Lx = Bx + \lambda Cx + s \tag{1}$$

donde los operadores L, B y C y los vectores x, s tienen el significado siguiente: el operador L representa la difusión y la absorción, el B, la dispersión, el C, la fisión; el vector x representa la densidad neutrónica o el flujo neutrónico, y s, las fuentes exteriores. Supongamos que la ecuación (1) describe el transporte de neutrones en un volumen finito dado $\mathscr{R}$. La forma de los operadores L, B y C depende de la aproximación en que se considere el transporte de neutrones (véase G. J. Habetler, M. A. Martino, G. Birkhoff, G. I. Marchuk, I. Marek, R. S. Varga, V. S. Vladimirov). En trabajos de estos autores se demuestra, entre otros resultados, que la ecuación

$$Lx = Bx + \lambda Cx \tag{2}$$

tiene una solución x_0 que es positiva en $\mathscr{R}$. Esta solución corresponde a un valor propio positivo λ_0 tal que, para cualquier otro valor propio λ de la ecuación (2), se tiene $|\lambda| > \lambda_0$. Además, esta ecuación no tiene ninguna solución no negativa en $\mathscr{R}$ diferente de la cx_0, donde c es una constante positiva. Esta hecho es consecuencia de las propiedades de los operadores $(L - B)^{-1}C$ y $C(L - B)^{-1}$. Es fácil demostrar que el valor $\mu_0 = \lambda_0^{-1}$ es el valor propio dominante del operador T, donde T es uno de los operadores $(L - B)^{-1}C$, $C(L - B)^{-1}$.

Para construir los elementos propios de la ecuación (2) y las soluciones de la ecuación (1), existen métodos iterativos adecuados. Nuestro propósito es presentar un esquema iterativo general y probar su convergencia.

Sea X el espacio de Banach de las funciones-vector en $\mathscr{R}$. Sean y_n', z_n', y' funcionales continuas tales que

$$y_n'(x) \to y'(x), \quad z_n'(x) \to y'(x)$$

para $x \in X$ y

$$y_n'(\lambda x) = \lambda y_n'(x), \quad z_n'(\lambda x) = \lambda z_n'(x)$$

para $x \in X$ y $\lambda > 0$.

Supongamos que se cumplen las relaciones $y_n'(x) \geqslant 0$, $z_n'(x) \geqslant 0$ para todo vector no negativo $x \in X$. Para estos vectores se tiene, pues, $y'(x) \geqslant 0$. Además, sea $y'(x_0) > 0$ para el vector propio positivo, x_0, de la ecuación (2).

Hagamos $x_{(n+1)} = \mu_n^{-1} T x_{(n)}$

donde $x_{(0)}$ es un vector positivo. Sea, además.

$$\mu_n = \frac{z_n'(Tx_{(n)})}{y_n'(x_{(n)})}$$

Teorema 1. Las sucesiones $\{\mu_n\}$, $\{x_{(n)}\}$ son convergentes, $\mu_n \to \lambda_0^{-1}$, $x_{(n)} \to cx_0$,
donde $Lx_0 = Bx_0 + \lambda_0 Cx_0$ y c es una constante positiva.

Para construir soluciones de la ecuación (1), se pueden emplear las fórmulas siguientes:

$$z_{n+1} = \frac{\lambda_{(n)}}{\lambda_{(n)} - \lambda} \mathscr{W}_{n+1} + \sum_{k=0}^{n} \mathscr{W}_k,$$

donde $\lambda_{(n)} = \mu_n^{-1}$, $\mathscr{W}_k = (\lambda T)^k \mathscr{W}_0$ y $\mathscr{W}_0 = (L-B)^{-1}s$, si $T = (L-B)^{-1}C$, y $\mathscr{W}_0 = C(L-B)^{-1}s$, si $T = C(L-B)^{-1}$.

Teorema 2. Supongamos que se cumple la desigualdad $|\lambda| < \lambda_0$. Existe una solución y solo una, z, de la ecuación (1), donde s es un elemento arbitrario de X. Además $z_{n+1} \to z$ en norma-X. La convergencia es más rápida que en el método ordinario de aproximaciones sucesivas.

Utilizando funcionales especiales para y_n', z_n' se obtienen, de una parte, algunos métodos iterativos conocidos, y, de otra, procesos iterativos no empleados hasta ahora.

Analytical treatment of neutron thermalization in two-medium Wigner-Seitz cells of cylindrical symmetry

By H. Küsters*

The practical calculation of neutron thermalization problems relies almost exclusively on numerical methods [1–3]. An analytical representation of the neutron spectrum in the moderator of a heterogeneous reactor in diffusion and heavy gas approximation was obtained by Kunze [4] by idealizing the fuel rods to line absorbers with an effective absorption as in the monoenergetic theory of Meetz [5]. However, this method gives no information about the spectra in the fuel rods which are of primary importance for quantitative calculation of heterogeneous systems.

The object of this paper is to obtain analytically the energy and space dependent neutron distribution in a two-medium Wigner-Seitz cell of cylindrical symmetry. With regard to its scattering properties, the moderator is treated as a monatomic gas. The energy loss of scattered neutrons in the fuel is neglected. In the numerical evaluation of the method the parameters important in thermalization problems for heterogeneous reactors are discussed. The influence of anisotropic scattering of neutrons in the moderator is shown by comparing with the spectra for isotropic scattering. Finally, the amount the spectra calculated in P_1 approximation may deviate from exact solutions is estimated.

BASIC EQUATIONS AND SCATTERING KERNELS

Let us consider an infinitely long unit cell. The space dependence of the neutron distribution is then characterized by the distance r from the axis of symmetry. The transport equation is given by:

$$\frac{1}{\Sigma_0}\vec{\Omega}\nabla\psi(r,\epsilon,\vec{\Omega})+\sigma_t(\epsilon)\psi(r,\epsilon,\vec{\Omega}) = \int_0^\infty d\epsilon' \int_{4\pi} d\Omega'\, \sigma_s(\epsilon'\to\epsilon,\vec{\Omega}\to\vec{\Omega})\psi(r,\epsilon',\vec{\Omega}') \quad (1)$$

where Σ_0 is the constant scattering cross section for high neutron energies, $\sigma_t(\epsilon)=\Sigma_t(\epsilon)/\Sigma_0, \epsilon = E/KT$ (T = moderator temperature) and $\sigma_s(\epsilon'\to\epsilon,\vec{\Omega}'\to\vec{\Omega})$ is the macroscopic transfer cross section divided by Σ_0. One has to solve (1) in each medium under the following boundary conditions;

$$\psi_M(R,\epsilon,\vec{\Omega})=\psi_M(R,\epsilon,-\vec{\Omega}) \quad (2.1)$$

$$\psi_M(\rho,\epsilon,\vec{\Omega})=\psi_U(\rho,\epsilon,\vec{\Omega}) \quad (2.2)$$

$$\psi_U(r,\epsilon,\vec{\Omega}) \text{ regular for } r\to 0 \quad (2.3)$$

$$\psi(r,\epsilon,\vec{\Omega})\sim 1/\epsilon \text{ for } \epsilon\to\infty \quad (2.4)$$

R being the radius of the unit cell, ρ the radius of the fuel rod, and M and U characterize the moderator or fuel zone, respectively.

In a stationary thermal reactor a space independent $1/\epsilon$ spectrum appears above the thermal energy region [6]. Therefore, one can describe the thermalization region with the homogeneous equation (1) and condition (2.4). For solving the problem we expand the flux $\psi(r,\epsilon,\vec{\Omega})$ and the transfer cross section in spherical harmonics;

$$\psi(r,\epsilon,\vec{\Omega})=\sum_{lm}\phi_{lm}(r,\epsilon)\,Y_{lm}(\vec{\Omega}) \quad (3)$$

$$\sigma_s(\epsilon'\to\epsilon,\vec{\Omega}'\to\vec{\Omega})=\sum_l \frac{2l+1}{4\pi}K_l(\epsilon',\epsilon)P_l(\vec{\Omega}\,.\,\vec{\Omega}') \quad (4)$$

$Y_{lm}(\vec{\Omega})$ are the spherical harmonics, normalized to one and $P_l(\vec{\Omega}.\vec{\Omega}')$ are the Legendre polynomials. Taking into account the symmetry properties of the problem, one obtains in P_1-approximation (for the general formulation in higher P_L-approximation see [7]);

$$\sigma_t(\epsilon)\phi_{00})r,\epsilon)-\frac{2}{\Sigma_0\sqrt{6}}\left(\frac{\partial}{\partial r}+\frac{1}{r}\right)\phi_{11}(r,\epsilon) = \int_0^\infty K_0(\epsilon',\epsilon)\phi_{00}(r,\epsilon')\,d\epsilon'-\frac{1}{\Sigma_0\sqrt{6}}\frac{\partial\phi_{00}(r,\epsilon)}{\partial r} + \sigma_t(\epsilon)\phi_{11}(r,\epsilon)=\int_0^\infty K_1(\epsilon',\epsilon)\phi_{11}(r,\epsilon')\,d\epsilon' \quad (5)$$

In the fuel zone Eq. (4) can be replaced by;

$$\sigma_s U(\epsilon'\to\epsilon,\vec{\Omega}'\vec{\Omega})=\frac{1}{4\pi}\delta(\epsilon'-\epsilon) \quad (6)$$

where $\delta(\epsilon'-\epsilon)$ is the delta function. The system (5) has to be modified correspondingly. The scattering kernels for the moderator are given in the monatomic gas model by (M is the mass of the scattering medium, the neutron mass is set equal to one);

$$K_0(\epsilon',\epsilon)=\frac{b^2}{2\epsilon'}(F_1+F_2) \quad (7)$$

* Kernforschungszentrum, Karlsruhe.

$$K_1(\epsilon',\epsilon)=\frac{b^2}{2\epsilon'}\sqrt{\left(\frac{M}{\epsilon\epsilon'}\right)}\{(\epsilon b-\epsilon' a-\sqrt{M})F_1 + (\epsilon' b-\epsilon a-\sqrt{M})F_2+\frac{2}{\sqrt{\pi}}[(\sqrt{\epsilon}+\sqrt{\epsilon'})E_1 \pm(\sqrt{\epsilon'}-\sqrt{\epsilon})E_2]\} \quad (8)$$

where

$$b=\tfrac{1}{2}\left(\sqrt{M}+\frac{1}{\sqrt{M}}\right);\ a=\tfrac{1}{2}\left(\sqrt{M}-\frac{1}{\sqrt{M}}\right);$$
$$E_1=\mathrm{e}^{-(b\sqrt{\epsilon}-a\sqrt{\epsilon'})^2}\ E_2=\mathrm{e}^{-(b\sqrt{\epsilon}+a\sqrt{\epsilon'})^2};$$
$$F_1=\mathrm{Erf}(b\sqrt{\epsilon}-a\sqrt{\epsilon'})\mp(\mathrm{Erf}b\sqrt{\epsilon}+a\sqrt{\epsilon'})$$
$$F_2=\mathrm{e}^{-(\epsilon-\epsilon')}\,[\mathrm{Erf}(b\sqrt{\epsilon'}-a\sqrt{\epsilon}) \pm \mathrm{Erf}(b\sqrt{\epsilon'}+a\sqrt{\epsilon})];\ \mathrm{Erf}\,(x)=\frac{2}{\sqrt{\pi}}\cdot\int_0^x \mathrm{e}^{-t^2}\,\mathrm{d}t \quad (9)$$

The upper sign is to be taken for $\epsilon'<\epsilon$ (scattering up), the lower sign for $\epsilon'>\epsilon$ (slowing down). For the total scattering cross section in the moderator one obtains:

$$\sigma_s^{\mathrm{M}}(\epsilon)=\left(1+\frac{1}{2\epsilon M}\right)\mathrm{Erf}\,(\sqrt{(\epsilon)}M)+\frac{\mathrm{e}^{-\epsilon M}}{\sqrt{\pi}\sqrt{\epsilon M}}. \quad (10)$$

In solving the system (5) we notice that for high energies $\epsilon\gg 1$ the neutron mostly loses energy in a collision with a moderator atom, while for $\epsilon\approx 1$ the neutron may take up energy. These two energy regions are naturally not separated physically, however, one can use the different character of the moderating and equilibrating processes in the choice of the method of solution (epithermal solution or thermal solution, respectively). As a consequence of the strong absorption, hardening and depression of the spectra will result in the fuel, but apart from these effects, the whole character of the solution in the moderator is transferred to the spectrum in the fuel, so that the mathematical treatment is the same for both media.

EPITHERMAL SOLUTIONS

We suppose a $1/\sqrt{\epsilon}$ absorption in the moderator and the fuel zone, then solve the system (5) in the epithermal region $\epsilon\gg 1$ by;

$$\phi_{lm}^{\mathrm{epi}}(r,\epsilon)=\frac{c}{\epsilon}\delta_{l0}+\frac{A_{lm}(r)}{\epsilon^{3/2}}+\frac{B_{lm}(r)}{\epsilon^2}+\ldots \quad (11)$$

Equation (11) contains the condition (2.4) that the $1/\epsilon$ part of the flux is space independent for high energies and $\delta_{ll'}$ is Kronecker's symbol.

It is customary to neglect the temperature motion of the moderator atoms for epithermal energies $\epsilon\gtrsim 16$ and to take the simple expressions of the kernels (7) and (8) for $T=0$. The application of this method to the infinite medium case, however, has shown [7] that the discontinuity of the scattering kernels ($T=300\,^\circ$K in the thermal region, $T=0$ in the epithermal region) may produce considerable errors in the spectrum. Therefore, all integrals of the right-hand side in (5) have to be evaluated with the asymptotic expansion of the temperature dependent kernels. Then one has to calculate integrals of the form;

$$I_n(\epsilon)=\int_{-\sqrt{\frac{\epsilon}{M}}}^{\infty}\frac{\mathrm{e}^{-y^2}}{(y+b\sqrt{\epsilon})^{n'}}\,\mathrm{d}y$$

One obtains an excellent approximation by replacing the integrand by a Gaussian of the same value and same curvature at the maximum. This results in;

$$I_n(\epsilon)\approx\frac{\sqrt{\pi}}{(b\sqrt{\epsilon})n}\left(1+\frac{n(n+1)}{4b^2\epsilon}\right) \quad (12)$$

With (12) all integrals can be evaluated analytically [7]. If one inserts (11) into (5) an unhomogeneous set of differential equations for the functions $A_{lm}(r)$ and $B_{lm}(r)$ will result for every power in $1/\sqrt{\epsilon}$ (the term 1ϵ satisfies (5) identically). The special solution of the unhomogeneous system in the moderator zone is identical with the solution for the infinite medium; the general solution of the homogeneous system leads to an eigenvalue problem and is given by the modified Bessel functions of the second kind. For instance, one easily obtains;

$$A_{00}(r)=-\frac{c\sigma_{\mathrm{a}}^{\mathrm{M}}}{1-\alpha_1{}^0}+B_1I_0(\kappa_1 r)+C_1K_0(\kappa_1 r),\ \text{with}$$
$$\sigma_{\mathrm{a}}^{\mathrm{M}}=\Sigma_{\mathrm{a}}^{\mathrm{M}}(\epsilon=1)/\Sigma_{0\mathrm{M}},\ \alpha_n{}^0$$
$$=\frac{2}{n+2}\,\frac{1-\sqrt{\alpha}^{n+2}}{1-\alpha},\ \alpha=\left(\frac{M-1}{M+1}\right)^2, \quad (13)$$
$$\kappa_1=\Sigma_{0\mathrm{M}}\sqrt{3(1-\alpha_1{}^0)(1-\alpha_1{}^1)},\ \alpha_1{}^1$$
$$=b^2\sqrt{M}\left[\frac{b}{2}(1-\sqrt{\alpha^3})-a(1-\alpha)\right] \quad (14)$$

The determination of the other space dependent functions is analogous [7]. In the fuel zone one obtains, instead of (13), in P_1-approximation;

$$A_{00}{}^{\mathrm{U}}(r)=A_{\mathrm{U}}+\tfrac{3}{4}\,c\sigma_{\mathrm{a}}{}^{\mathrm{U}}(\Sigma_{0\mathrm{U}}r)^2 \quad (15)$$

The functions $B_{lm}{}^{\mathrm{U}}(r)$ contain further powers in r. Bessel functions appear for the first time in P_3-approximation in the epithermal solution for the fuel medium [7]. The free constants A_{U},B_1,C_1 in (13) and (15) (and also the constants in $B_{lm}(r)$) are determined by the boundary conditions (2). The result is;

$${}^{\mathrm{M}}\phi_{lm}{}^{\mathrm{epi}}(r,\epsilon)=\phi_{\mathrm{M}}(\epsilon)\delta_{l0}+\sum_{j=1}^{H}(B_jI_m(\kappa_j r) + (-1)^m C_jK_m(\kappa_j r))\chi_{lm}{}^j(\epsilon)$$
$${}^{\mathrm{U}}\phi_{lm}{}^{\mathrm{epi}}(r,\epsilon)=\phi_{\mathrm{U}}(\epsilon)\delta_{l0}+\sum_{j=1}^{H}(\Sigma_{0\mathrm{U}}r)^{2m-\frac{1}{2}}\psi_{lm}{}^j(\epsilon) \quad (16)$$

where $\phi_{\mathrm{M}}(\epsilon)$ and $\phi_{\mathrm{U}}(\epsilon)$, respectively, are the space independent parts of the solutions, for instance;

$$\phi_{\mathrm{M}}(\epsilon)=\frac{c}{\epsilon}-\frac{c\sigma_{\mathrm{a}}^{\mathrm{M}}}{1-\alpha_1{}^0}\frac{1}{\epsilon^{3/2}} + \left[\frac{(\sigma_{\mathrm{a}}^{\mathrm{M}})^2}{1-\alpha_1{}^0)\ (1-\alpha_2{}^0)}+\frac{2M-1}{M}\right]\frac{1}{\epsilon^2}\mp\ldots \quad (17)$$

H determines the number of positive eigenvalues ν_j in the epithermal region ($\kappa_j=\Sigma_0\nu_j$), for an expansion up to $1/\epsilon^{n/2}$ one obtains $H=n-2$ in P_1-approximation.

$\chi_{lm}{}^{j}(\epsilon)$ or $\psi_{lm}{}^{j}(\epsilon)$ are the energy dependent parts of the solutions coupled to the corresponding Bessel function or r-powers, respectively. For instance, the quantity $\chi_{00}{}^{1}(\epsilon)$ is given by;

$$\chi_{00}{}^{1}(\epsilon)=\frac{1}{\epsilon^{3/2}}+\frac{b_{00}{}^{(1)}}{\epsilon^{2}}+\ldots,$$

where $b_{00}{}^{(1)}$ is a known constant. The term $(2M-1)/M$ in (17) results from the temperature dependence of the scattering kernel and is important for weak absorption.

THERMAL SOLUTIONS

We extrapolate the complete epithermal solution continuously to $\epsilon=0$ by multiplying by a damping function which is unity in the epithermal region and vanishes with a sufficiently high power for low energies;

$$\phi_{lm}{}^{*}(r,\epsilon)=g_{\lambda}(\epsilon)\phi_{lm}{}^{\mathrm{epi}}(r,\epsilon) \tag{18}$$

$$g_{\lambda}(\epsilon)=\mathrm{e}^{-\epsilon}\left(\mathrm{e}^{\epsilon}-\sum_{k=0}^{\lambda}\frac{\epsilon^{k}}{k!}\right) \tag{19}$$

$g_{\lambda}(\epsilon)$ has the required properties;

$$g_{\lambda}(\epsilon)=\begin{cases}1 & \text{for } \epsilon\gg 1\\ \epsilon^{\lambda+1} & \text{for } \epsilon\to 0\end{cases} \tag{20}$$

λ must be large enough so that the last term considered in the asymptotic expansion becomes regular for $\epsilon=0$ by multiplying with (19).

Now, the difference of the true spectrum and this extrapolated solution has to be determined;

$$\Delta\phi_{lm}(r,\epsilon)=\phi_{lm}(r,\epsilon)-\phi_{lm}{}^{*}(r,\epsilon) \tag{21}$$

Insertion of (21) into (5) gives an unhomogeneous system for $\Delta\phi_{lm}(r,\epsilon)$. If we abbreviate the system (5) by $B\phi_{lm}(r,\epsilon)=0$, the result is;

$$B\Delta\phi_{lm}(r,\epsilon)=-B\phi_{lm}{}^{*}(r,\epsilon)=Q_{lm}(r,\epsilon) \tag{22}$$

For $\epsilon\gg 1$ the quantities $\phi_{lm}{}^{*}(r,\epsilon)=\phi_{lm}{}^{\mathrm{epi}}(r,\epsilon)$ solve the system approximately and the unhomogeneity $Q_{lm}(r,\epsilon)$ vanishes correspondingly. We look for a solution of (22) by an expansion of the difference spectrum and the unhomogeneity in a system of orthonormal functions;

$$\Delta\phi_{lm}(r,\epsilon)=\sum_{p} T_{lm}{}^{p}(r)\omega_{p}(\epsilon) \tag{23}$$

$$Q_{lm}(r,\epsilon)=\sum_{p} q_{lm}{}^{p}(r)\ \omega_{p}(\epsilon), \text{ with}$$

$$\int_{0}^{\infty}\omega_{p}^{+}(\epsilon)\omega_{p'}(\epsilon)\,\mathrm{d}\epsilon=\delta_{pp'} \tag{24}$$

The basis $\omega_{p}(\epsilon)$ has to obey the following conditions;

(*a*) The principle of detailed balance for the scattering kernels has to be guaranteed for representation in this system.

(*b*) The adjoint functions $\omega_{p}^{+}(\epsilon)$ must decay exponentially, otherwise divergent integrals may arise.

From the first condition it follows for unsymmetrized kernels that;

$$\omega_{p}(\epsilon)=\epsilon\mathrm{e}^{-\epsilon}\omega_{p}^{+}(\epsilon) \tag{25}$$

Condition (*b*) results, if one considers the expansion of the unhomogeneity in (23);

$$q_{lm}{}^{p}(r)=\int_{0}^{\infty}\omega_{p}^{+}(\epsilon)Q_{lm}(r,\epsilon)\,\mathrm{d}\epsilon \tag{26}$$

If one has found the exact epithermal solution, then $Q_{lm}(r,\epsilon)$ is zero for $\epsilon\gg 1$ and all the moments (26) can be determined. As one can find the epithermal solution only approximately (for instance in equation (11) up to the power $1/\epsilon^{n}$), however, it follows that;

$$Q_{lm}(r,\epsilon)=\theta\left(\frac{1}{\epsilon^{n+\frac{1}{2}}}\right)$$

If the adjoint functions $\omega_{p}^{+}(\epsilon)$ are only polynomials of the order p in ϵ (with Eq. (25) the Laguerre polynomials result, see [7]), these polynomials cannot be used for $p>n-1/2$, because the integration in (26) has to be carried out up to infinity. For the description of the thermal energy region at least four basis functions are necessary, therefore n is $>7/2$. Now, the determination of the epithermal solution for higher n values is tedious and unnecessary on physical grounds. On the other hand, one cannot choose n very large anyway, because the asymptotic expansion is semi-convergent. Moreover, the application of Laguerre polynomials shows that, because of weighting with ϵ^{p}, the thermal spectrum is very sensitive on the accuracy of the epithermal solution [4].

These considerations led to the introduction of an exponentially decaying term in the adjoint functions. Thus, all difficulties are removed and the interesting energy region can be treated without any cut-off. Both the thermal and epithermal solutions join continuously. For the adjoint functions we put;

$$\omega_{p}^{+}(\epsilon)=\mathrm{e}^{-s_{p}\epsilon}P_{p}(\epsilon), \tag{27}$$

where $P_{p}(\epsilon)$ is a polynomial of the order p in ϵ. With

$$S_{p}=p/8. \tag{28}$$

A highly optimal basis system results for thermalization problems after orthonormalization, showing good convergence in the infinite medium case [7] even for relatively strong absorption parameters ($\Delta=1$, [8]).

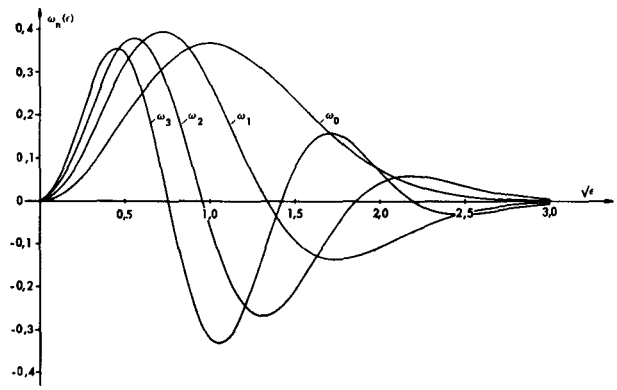

Figure 1. The basis functions $\omega_{n}(\epsilon)=\epsilon\mathrm{e}^{-(1+Sn)\epsilon}P_{n}(\epsilon)$ for $S_{n}=n/8$

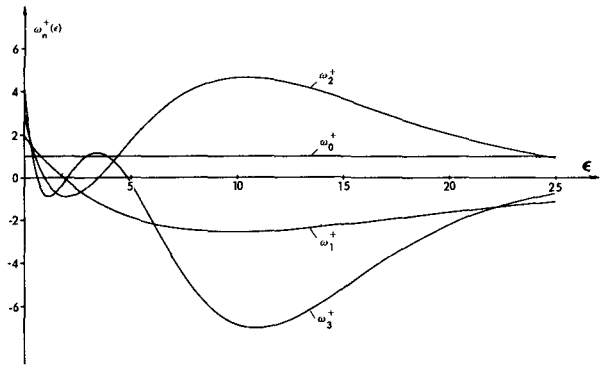

Figure 2. The adjoint functions $\omega_n^+(\epsilon) = e^{-S_n\epsilon}P_n(\epsilon)$ for $S_n = n/8$

It is important that the Maxwellian distribution $\epsilon e^{-\epsilon}$ be the first term of an expansion into this system. This is guaranteed by (28). In Figs. 1 and 2 the first four basis functions and the adjoints are shown.

The unhomogeneous system (22) then can be solved without any difficulty. First, one determines the moments $q_{lm}{}^p(r)$ and obtains the special solution of the unhomogeneous equation with a formulation corresponding to the form of the unhomogeneity. For instance one finds in the moderator medium (cf. (16));

$$q_{00}{}^p(r) = \int_0^\infty \omega_p+(\epsilon)\{\int_0^\infty K_0(\epsilon',\epsilon)g_\lambda(\epsilon')\phi_M(\epsilon')\,d\epsilon - \sigma_t{}^M(\epsilon)g_\lambda(\epsilon)\phi_M(\epsilon)\}\,d\epsilon + \sum_{j=1}^{H}(B_jI_0(\kappa_j r)+C_jK_0(\kappa_j r)) \times \int_0^\infty \omega_p+(\epsilon)\{\int_0^\infty K_0(\epsilon',\epsilon)g_\lambda(\epsilon')\chi_{00}{}^j(\epsilon')\,d\epsilon' + g_\lambda(\epsilon)\left[\frac{2\nu j}{\sqrt{6}}\chi_{11}{}^j(\epsilon) - \sigma_t{}^M(\epsilon)\chi_{00}{}^j(\epsilon)\right]\}\,d\epsilon. \quad (29)$$

The following formulation is tried for the special solution $\widehat{\Delta\phi}_{lm}{}^M$;

$$\widehat{\Delta\phi}_{lm}{}^M(r,\epsilon) = \delta_{10}\sum_{p=0}^{N}\gamma_p{}^M\omega_p(\epsilon) + \sum_{j=1}^{H}(B_jI_m(\kappa_j r) + (-1)^m C_jK_m(\kappa_j r))\sum_{p=0}^{N}\tau_{lm}{}^{jp}\omega_p(\epsilon) \quad (30)$$

where N is the number of basis functions taken into account. Then the space dependence on both sides of Eq. (22) is described by the same Bessel functions. The resulting system has to be satisfied for every r. One obtains from the equations for the energy variable, by multiplying this system with $\omega_p^+(\epsilon)$ and integrating, an unhomogeneous set of equations for $\gamma_p{}^M$ and $\tau_{lm}{}^{pj}$ in (30).

The particular solutions of the homogeneous equation (22) are the Bessel functions $I_m(\Lambda r)$ and $K_m(\Lambda r)$, where $\Lambda = \Sigma_0\mu$ and μ is an eigenvalue for the thermal region. As for epithermal energies one obtains an eigenvalue problem, when the number of positive eigenvalues is equal to the number of basis functions which have been taken into account. The general solution $\widetilde{\Delta\phi}$ of the homogeneous system is obtained by superposition of all possible eigenvectors $\vec{R}_{lm}{}^j$;

$$\widetilde{\Delta\phi}_{lm}{}^M(r,\epsilon) = \sum_{j=0}^{N}(B_H{}^{jM}I_m(\Lambda_M{}^j r) + (-1)^m C_H{}^{jM}K_m(\Lambda_M{}^j r))\sum_{p=0}^{N}R_{lm}{}^{jp}\omega_p(\epsilon) \quad (31)$$

In the fuel medium the method of solution is quite analogous, but because of (2.3) one has to take into account only Bessel functions $I_m(\Lambda r)$. The free constants $B_H{}^{jM}, C_H{}^{jM}$ and the corresponding constants in the fuel are again determined by the conditions (2.1) and (2.2). The detailed equations are found in [7].

RESULTS AND CONCLUSIONS

The method has been applied to a unit cell containing natural uranium and a heavy water moderator ($R = 9.5$ cm, $\rho = 1.6$ cm). The calculations are done with the following cross sections (40 °C moderator temperature);

$$\Sigma_{aU}(\epsilon = 1) = 0.347\ \text{cm}^{-1},\ \Sigma_a{}^M(\epsilon = 1) = 7.74 \times 10^{-5}\ \text{cm}^{-1},\ \Sigma_{0U} = 0.387\ \text{cm}^{-1}.$$

Accuracy of the method

The expansion of the epithermal neutron distribution was terminated at $1/\epsilon^2$. In the thermal region five basis functions have been considered.

As an examination of the calculation method and of the approximations in the epithermal and thermal region we use the integral neutron balance equation for the unit cell, which is quite independent of the special method one has chosen to solve the problem. One obtains for $1/\sqrt{\epsilon}$ absorption;

$$V_U \cdot \Sigma_a{}^U(\epsilon = 1)\int_0^\infty \phi_U(\epsilon)\frac{d\epsilon}{\sqrt{\epsilon}} + V_M\Sigma_a{}^M(\epsilon = 1)\int_0^\infty \bar{\phi}_M(\epsilon)\frac{d\epsilon}{\sqrt{\epsilon}} = V_M c(\xi\Sigma_{0M}) \quad (32)$$

where $\bar{\phi}(\epsilon)$ is the spatially averaged spectrum of the appropriate medium ($\phi(r,\epsilon) = \phi_{00}(r,\epsilon)$), c is the normalization constant for the $1/\epsilon$ part, V_U and V_M, respectively, are the volumes of the fuel and the moderator and ξ is the mean logarithmic energy loss per collision. The right-hand side of (32) counts the number of neutrons which enter the region of thermalization per unit time.

The integral expression (32) also allows a differential interpretation. At first, the absorption rate in the moderator (A_M) in (32) is very small for the systems considered here ($A_M \approx 0.01\ A_U$), so that (32) is mainly a test on A_U. The main contribution to the integrals in (32) arises from energies of around $\epsilon \approx 1$. (the thermal spectrum decreases about a factor of 100 from $\epsilon \approx 1$ to $\epsilon = 10$). The region around $\epsilon \approx 1$ must have been calculated correctly, if (32) is satisfied. By this method a correct thermal spectrum is obtained only if the epithermal solution is correct, because the asymptotic solution is the source in the equation for the thermal spectrum. Therefore, Eq. (32) is a test for the average fuel spectrum, too, especially on the ratio of the maximum value near $\epsilon = 1$ to a representative value at

epithermal energies. Because of the strong coupling of the solutions at the fuel/moderator interface, the average spectrum in the moderator is also tested indirectly by (32). The error in the balance equation is about 0.1% for all interesting cases.

Important parameters for thermalization problems in heterogeneous systems

If one treats the moderator as a monatomic gas, the question arises what mass M one has to choose in the scattering kernels (7) and (8). Spectra in infinite media are not very sensitive to the mass, if $\Sigma_a(\epsilon=1)/\xi\Sigma_0$ is taken to be constant [7,8]. This quotient is also the important quantity for spectrum calculations in heterogeneous systems, for it follows from (32) and the above discussion that because of the weak absorption in the moderator the average fuel spectrum is practically fixed by the product $\xi\Sigma_{0M}$ (apart from geometry and normalization constants). $\xi\Sigma_{0M}$ is known for the system considered, e.g., $\xi\Sigma_{0M}=0.178$ cm^{-1} for D_2O. The way of selecting the individual factors ξ or Σ_{0M} should be without great influence on the average fuel spectrum, however. The spectrum in the moderator only may show a relatively major change, but only within the limit of the balance (Eq. 32). In Fig. 3 the spectra for $M=2$ and $M=8$ with $\xi\Sigma_{0M}=0.178$ cm^{-1} are compared. With the same normalization c only a difference of about 1% results in the average fuel spectra for $\epsilon=1$. The flux depression $\bar{\phi}_M(\epsilon)/\bar{\phi}_U(\epsilon)$ increases with increasing mass (decreasing mean free path in the moderator), while the average fuel spectrum is nearly unchanged. If one takes for Σ_{0M} the scattering cross section for D_2O ($\Sigma_{0M}=0.353$ cm^{-1}), the effective mass $M=3.26$ results from $\xi\Sigma_{0M}=0.178$. The average spectra in the fuel for $M=2$, $M=3.26$ and $M=3.6$ (Sachs-Teller mass) are indistinguishable within the limit of drawing accuracy. In particular, it is to be pointed out that the scattering of neutrons with oxygen is not to be considered separately, because this is included in the slowing down power $\xi\Sigma_{0M}$. A change in the scattering cross section Σ_{0U} of uranium of about 10% has a negligible influence on the fuel spectra.

Influence of anisotropic scattering in the moderator

An idea of this effect is also conveyed by the balance equation. As the right-hand side of (32) is independent of the anisotropic scattering, only a more thermalized spectrum in the moderator can result in the case of isotropic scattering ($\approx 5\%$). The calculation gives a difference of less than 0.1% in $\bar{\phi}_U(\epsilon)$.

Comparison with the results obtained by Kunze

In Fig. 4 the solutions obtained by Kunze in the heavy gas approximation in the centre of the moderator and at the fuel boundary (broken lines) are compared with the results of this paper. It is seen that towards the centre of the fuel rod appreciable hardening and depression result as a consequence of the strong absorption. The maximum values of the spectra

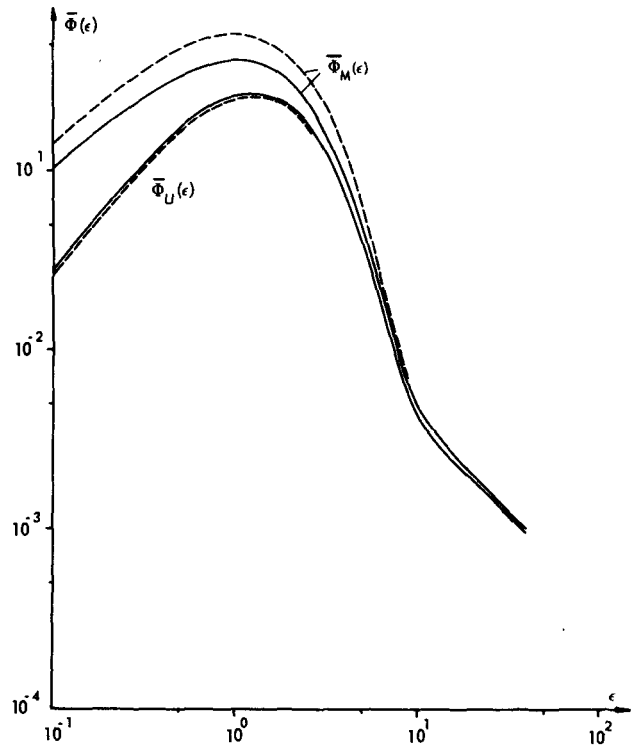

Figure 3. Spatially averaged spectra in a unit cell of natural uranium ($\rho=1.6$ cm) and D_2O (R = 9.5 cm) for different masses of the moderator; $M=8$ (broken lines) and $M=2$. The slowing down power in both cases is $\xi\Sigma_0=0.178$ cm^{-1}

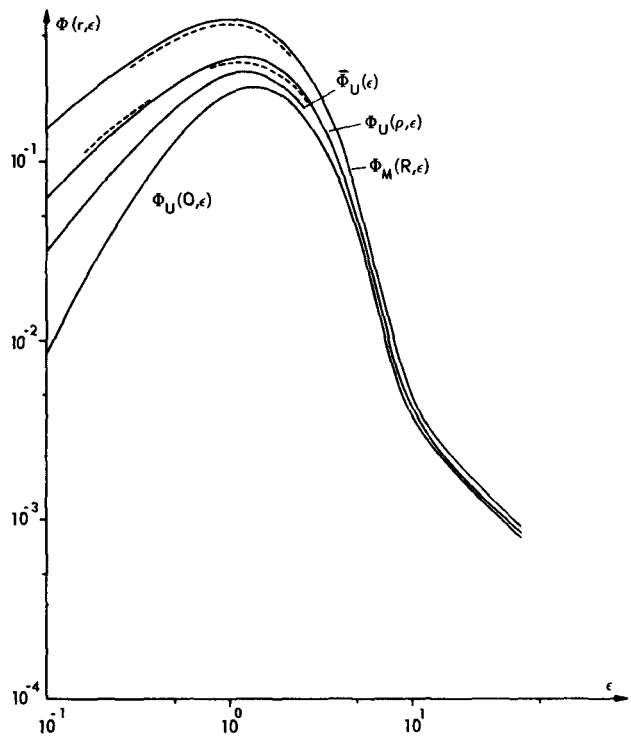

Figure 4. Comparison of the spectra obtained by Kunze [4] in the centre of the moderator and at the fuel boundary (broken lines) with the results of this paper. $\xi\Sigma_0=0.233$ cm^{-1}

are for energies $\epsilon = 1$ (cell boundary), $\epsilon = 1.2$ (fuel boundary), $\epsilon = 1.24$ (average spectrum in the fuel) and $\epsilon = 1.35$ (rod centre).

Influence of higher spherical harmonics

If one looks for the spatial distribution of neutrons in the Wigner-Seitz cell for different energies ϵ, the ratio $\phi_M(R)/\phi_U(r=0)$ increases with decreasing energy as a consequence of the strong absorption in the fuel. Now, it is known from cell calculations [9, 10] that the P_1-approximation underestimates the flux depression. As the error increases with increasing absorption in the fuel, it is to be expected that in higher P_L-approximations hardening of the spectra in the fuel will result in comparison with the P_1-approximation, in addition to an increase in flux depression. In the P_5-approximation, the depression, for the geometries considered here, is larger by about 15% than in the P_1-approximation ($\epsilon \approx 1$). In varying the mass of the moderator from $M = 2$ to $M = 8$, we have found a higher flux depression ($\approx 25\%$, cf. Fig. 3), where the average spectrum in the fuel practically did not change. As the balance Eq. (32) with the right-hand side unchanged has to be satisfied, too, by the exact solution, one can expect that major deviations from the average spectra in the fuel calculated here in P_1-approximation will not appear. The remaining uncertainty in the value of the flux depression can be eliminated sufficiently well by averaging the absorption cross sections with the calculated average spectra in the fuel and the moderator and then determining the flux depression in the unit cell monoenergetically with high accuracy (f-calculations).

ACKNOWLEDGEMENTS

The author wishes to express his appreciation to Dr. K. Ott, Dr. W. Häfele and Dipl. Phys. E. Kiefhaber for valuable discussions.

REFERENCES

1. Honeck, H. C., Nuclear Sci. Eng., *8*, 193 (1960).
2. Högberg, T., J. Nuclear Energy, *12*, 145 (1960).
3. Leslie, D. C., United Kingdom Atomic Energy report AEEW-M-211 (1963).
4. Kunze, H., Nuclear Sci. Eng., *15*, 1 (1963).
5. Meetz, K., Proceedings of the Second International Conference on the Peaceful Uses of Atomic Energy, P/968, Vol. 16, p. 611, United Nations (1958).
6. Häfele, W., Nukleonik, *1*, 197 (1959).
7. Küsters, H., Dissertation Karlsruhe (1964) (to be published in Nukleonik).
8. Hurwitz, H., Nelkin, M. S., and Habetler, H. J., Nuclear Sci. Eng., *1*, 280 (1956).
9. Küsters, H., Report KFK-15, Karlsruhe (1959).
10. Küsters, H., and Ott, K., Nukleonik, *4*, 91 (1962).

ABSTRACT—RÉSUMÉ—АННОТАЦИЯ—RESUMEN

A/643 République fédérale d'Allemagne

Traitement analytique de la thermalisation neutronique dans des cellules Wigner-Seitz à deux milieux de symétrie cylindrique

par H. Küsters

Il s'agit d'une méthode analytique qui donne la solution du problème de la thermalisation dans l'espace et l'énergie dans une cellule cylindrique de Wigner-Seitz. Cette cellule contient une barre de combustible de longueur infinie au milieu d'un modérateur qui est traité comme un gaz monoatomique.

Pour les deux milieux, l'équation de Boltzmann est résolue par développement de la distribution des neutrons et de la section efficace de diffusion de transfert en harmoniques sphériques. Il en résulte, pour les coefficients du développement dépendant de l'énergie et de l'espace, un système d'équations intégro-différentielles. Ce système est d'abord résolu pour les énergies des neutrons épithermiques ($\epsilon \gtrsim 16kT$). Dans cette zone le comportement énergétique du spectre est décrit par une série en puissances de $1/\sqrt{\epsilon}$, si l'on considère que l'absorption est en $1/\sqrt{\epsilon}$. On s'aperçoit que le modèle de ralentissement ne peut être utilisé si la température du modérateur est zéro. Pour cette raison toutes les intégrales de diffusion furent évaluées par voie analytique utilisant la représentation asymptotique de la section efficace différentielle.

Cette méthode nous fournit un système d'équations différentielles inhomogènes dont la solution est donnée par des fonctions de Bessel modifiées du type 2. Quant aux calculs du combustible et du modérateur, les constantes libres sont déterminées par les conditions aux limites de la cellule.

La solution épithermique est extrapolée à l'énergie zéro par multiplication par une fonction d'amortissement qui disparaît avec une puissance suffisamment élevée pour $\epsilon \to 0$. La différence entre le vrai spectre et cette fonction artificielle est ensuite développée en série de fonctions orthonormales ayant un comportement asymptotique exponentiel. Il en résulte une équation inhomogène pour le spectre désignant cette différence. En opérant avec le noyau de diffusion non symétrique, les fonctions de base doivent obéir à une condition définie garantissant le bilan détaillé de la représentation du noyau dans ce système. D'autre part les fonctions adjointes doivent inclure un facteur exponentiel pour éviter que les coefficients du développement de l'inhomogénéité ne deviennent infinis.

Le calcul général pour obtenir le spectre de différence s'effectue ensuite sans autres complications. La solution homogène des équations inhomogènes pour le modérateur ainsi que pour le combustible pose un problème de valeur propre.

Cette méthode fut d'abord appliquée au cas d'un milieu infini dans le but de considérer des questions de convergence et de consistance. A titre d'épreuve, le

bilan intégral des neutrons fut calculé. En utilisant quatre fonctions de base et un développement asymptotique jusqu'à $1/\epsilon^4$, le résultat est très supérieur à un pour cent. Les calculs pour la cellule effectués à l'approximation P_1 contribuent également à un bilan supérieur à un pour cent avec un développement épithermique jusqu'à $1/\epsilon^2$. La corrélation entre les spectres et la masse du modérateur est étudiée ainsi que l'influence d'une diffusion anisotrope. Il devient évident que le spectre moyen dans le combustible s'écarte sensiblement du spectre à la surface de l'élément.

La formulation mathématique est effectuée jusqu'à une approximation en P_3; les calculs numériques s'arrêtent cependant en P_1.

A/643 ФРГ

Аналитическая обработка данных по термализации нейтронов в ячейках Вигнера-Зейтца с цилиндрической симметрией, состоящих из двух сред

X. Кюстерс

В докладе представлен аналитический метод решения проблемы термализации с пространственно-энергетической зависимостью для цилиндрической ячейки Вигнера-Зейтца, содержащей бесконечно длинный тепловыделяющий элемент, окруженный замедлителем, который рассматривается как одноатомный газ. Потеря энергии в процессе рассеяния нейтронов на ядрах топлива пренебрежимо мала.

Решается уравнение Больцмана в двух средах путем разложения на сферические гармоники пространственно-энергетического распределения нейтронов и сечения рассеяния. Система сопряженных интегро-дифференциальных уравнений является результатом разложения коэффициентов, зависящих от пространства и энергии. Эта система сначала решается для нейтронов эпитепловых энергий ($\varepsilon \geqslant 16\ kT$). В этой области система может описывать энергетические распределения спектра с помощью степенного ряда $1/\sqrt{\varepsilon}$, если рассматривается только поглощение типа $1/\sqrt{\varepsilon}$. В этой области энергий система не может иметь дело с ядром замедления при нулевой температуре замедлителя. Поэтому все интегралы рассеяния оценивались аналитически с асимптотическим представлением скорректированного ядра замедления.

Указанная методика приводит к системе неоднородных дифференциальных уравнений, которые могут быть решены с помощью модифицированных функций Бесселя второго рода. Свободные константы для топлива и замедлителя определяются из граничных условий ячейки.

Решение для эпитепловой области экстраполируется к нулевой энергии путем умножения на функцию «затухания», которая довольно быстро стремится к нулю при ε, стремящемся к нулю. Затем разница между действительным спектром и вычисленной функцией разлагается в систему ортогональных функций, имеющих экспоненциальный асимптотический характер. Эта разница выражается неоднородным уравнением. Для случая с несимметризированным ядром рассеяния основные функции должны удовлетворять определенному условию, которое уравновешивает ядро, представленное в этой системе. С другой стороны, сопряженные функции должны содержать экспоненциальный член, так как в противном случае разложение коэффициентов может привести к бесконечности.

Приводится общий расчет разницы между действительными и расчетными спектрами. Однородное решение неоднородных уравнений как для замедлителя, так и для топлива приводит к задаче о собственных значениях.

Этот метод был впервые применен для случая бесконечной среды при решении задачи о сходимости и непротиворечивости. Для проверки был вычислен баланс интегрального потока нейтронов. Результаты, имеющие точность выше одного процента, получены с помощью четырех основных функций и асимптотического разложения до члена $1/\varepsilon^4$. Расчеты ячейки, сделанные в P_1-приближении, дают баланс с точностью выше одного процента при эпитепловом разложении до члена $1/\varepsilon^2$. Исследовалась зависимость спектра от массы замедлителя, а также влияние анизотропного рассеяния. Оказалось, что усредненный спектр в топливе заметно отличается от спектра на границе топлива.

Математическое представление выполнено в P_3-приближении, однако численные расчеты сделаны только в P_1-приближении.

A/643 República Federal de Alemania

Tratamiento analítico de la termalización de neutrones en las células Wigner-Seitz de dos medios con simetría cilíndrica

por H. Küsters

Se presenta un método analítico para la solución del problema de termalización en el espacio geométrico y de energías para una célula de Wigner-Seitz, que contiene un elemento combustible infinitamente largo, rodeado de un moderador, considerado como un gas monoatómico. Se desprecian las pérdidas de energía de los neutrones dispersados en el combustible.

Se resuelve la ecuación de Boltzmann en los dos medios, desarrollando la distribución de neutrones y la sección eficaz de transferencia de difusión en

armónicos esféricos. Se obtiene para los coeficientes del desarrollo, que dependan tanto del espacio como de la energía, un sistema de ecuaciones íntegro-diferenciales. Este sistema se resuelve primero para las energías epitérmicas de los neutrones ($\epsilon \gtrsim 16kT$). En esta región puede describirse el comportamiento energético del espectro mediante una serie de potencias de $1/\sqrt{\epsilon}$, si sólo se considera la absorción $1/\sqrt{\epsilon}$. En esta región no puede considerarse el núcleo de la moderación para la temperatura cero del moderador. Por consiguiente, todas las integrales de dispersión han sido calculadas analíticamente, con la representación asintótica del núcleo correcto.

Este procedimiento conduce a un sistema de ecuaciones diferenciales inhomogéneas que puede resolverse mediante funciones modificadas de Bessel de segunda especie. Las constantes indeterminadas, correspondientes a las soluciones en los medios combustible y moderador, se fijan mediante las condiciones en los límites de la célula.

La solución epitérmica se extrapola a las energías cero mediante la multiplicación por la función « de amortiguamiento » que se anula con una potencia suficientemente elevada para $\epsilon \to 0$. A continuación se desarrolla la diferencia entre el espectro real y esta función artificial en un sistema de funciones ortonormales, con comportamiento asintótico exponencial. Como resultado, se obtiene para este espectro diferencial una ecuación inhomogénea. Si se considera el núcleo de dispersión no simétrico, las funciones de base deben obedecer a una cierta condición que asegure el equilibrio microscópico de la representación del núcleo en este sistema. Por otra parte, las funciones adjuntas también deben incluir un factor exponencial, puesto que en el caso contrario los coeficientes del desarrollo de la inhomogeneidad puedan resultar infinitos.

El cálculo general que conduce al espectro diferencial no presenta dificultad. La solución homogénea de la ecuación inhomogénea, tanto en el medio combustible como en el moderador, conduce a un problema de valores propios.

Este método ha sido aplicado primero al caso de un medio infinito para el estudio de la cuestión de la convergencia y de la consistencia. Como verificación se ha calculado el equilibrio integral de neutrones. Se ha obtenido una precisión mucho mejor que el uno por ciento con cuatro funciones de base y un desarrollo asintótico hasta $1/\epsilon^4$. Los cálculos de las células, realizados en una aproximación P_1 consistente, reproducen también el equilibrio mejor que al uno por ciento, con un desarrollo epitérmico hasta $1/\epsilon^2$. Se ha estudiado la correlación entre el espectro y la masa del moderador, como también la influencia de la dispersión anisotrópica. Se observa que el espectro medio del combustible difiere apreciablemente del correspondiente a los límites del mismo.

Se ha llevado a cabo la formulación matemática hasta la aproximación en P_3, pero los cálculos numéricos se han limitado a la aproximación en P_1.

L'optimisation du coefficient initial de régénération d'un réacteur nucléaire: un problème de la théorie des jeux

par I. I. Purica*

Un des problèmes actuels dans le domaine de la physique des réacteurs nucléaires est de trouver le meilleur moyen d'utiliser la quantité disponible de noyaux fertiles d'uranium 238 et de thorium 232. Dans ce but, on emploie les réacteurs nucléaires régénérateurs soit à neutrons thermiques, avec uranium 233 – thorium 232, soit à neutrons rapides, avec plutonium 239 – uranium 238.

Le problème spécifique pour de tels réacteurs est d'obtenir le plus grand nombre de noyaux fissiles par capture de neutrons dans le matériel fertile, tout en perdant le moins possible de noyaux fissiles nécessaires à la masse critique et au fonctionnement, à une puissance donnée, du réacteur.

Or cela dépend, entre autres, de la distribution spatiale initiale du matériel fertile et fissile dans le réacteur et de la quantité de matériel fertile utilisée.

On démontre ici que le problème de trouver la distribution optimale se réduit à un problème de la théorie des jeux à deux matrices, à somme non nulle.

Prenons par exemple un réacteur à plutonium – uranium 238, et supposons qu'on emploie dans ce réacteur une quantité donnée de noyaux d'uranium U et qu'on dispose d'une quantité de noyaux de plutonium P plus grande que celle P_c nécessaire pour la masse critique.

Le volume total V du réacteur est divisé en q volumes $V_i = \gamma_i V (i = 1,2, \ldots q)$.

Chaque volume V_i contient un nombre $U_i = \mu_i U$ de noyaux d'uranium 238 et un nombre $P_i = \xi_i P_c$ de noyaux de plutonium. Ainsi la structure géométrique et matérielle du réacteur est caractérisée par les distributions γ_i, μ_i, ξ_i, nombres purs satisfaisant les relations:

$$\sum_{i=1}^{q} \gamma_i = \sum_{i=1}^{q} \mu_i = \sum_{i=1}^{q} \xi_i = 1.\ \gamma_i > 0;\ \mu_i > 0;\ \xi_i > 0 \qquad (1)$$

avec

$$\mu_i U + \xi_i P_c \leq \gamma_i V N, \qquad (2)$$

condition restrictive due à la limitation de la densité totale, N, des noyaux dans un volume donné, pour les motifs physiques connus.

Pour un volume minimal, la relation (2) se réduit à une égalité, et:

$$V_p + V_u = V \text{ et } V_p = P_c/N \text{ et } V_u = U/N$$

Pour une distribution supposée connue (μ_i, ξ_i) et pour une quantité γ donnée, ces relations déterminent γ_i si P_c est connu par la condition de criticité du réacteur, condition plus ou moins complexe, fonction du modèle de réacteur employé.

Limitons-nous au modèle à un groupe de neutrons, où le flux $\phi_i(\vec{r})$ satisfait la relation connue:

$$\nabla^2 \phi_i(\vec{r}) + B_i^2 \phi_i(\vec{r}) = 0 \qquad (3)$$

Les valeurs propres B_i^2 sont déterminées par les sections efficaces macroscopiques moyennes de diffusion, d'absorption et de fission de l'uranium et du plutonium, pour le spectre d'énergie des neutrons dans le réacteur, à l'aide de:

$$B_i^2 = \frac{B_p^2 \xi_i^2 \epsilon^2 + \left(B_p^2 \frac{D_u}{D_p} + B_u^2 \frac{D_p}{D_u} \right) \xi_i \mu_i \epsilon + B_u^2 \mu_i^2}{(\mu_i + \xi_i \epsilon)^2} \qquad (4)$$

où B_p^2, D_p, B_u^2, D_u sont les laplaciens et les coefficients de diffusion respectivement pour le plutonium et l'uranium à la densité maximale N, et

$$\epsilon = P_c/U = V_p/V_u \text{ pour la densité } N.$$

L'équation (3) s'applique à chaque volume V_i avec des conditions de continuité du flux et du courant de neutrons sur les surfaces de séparation des volumes, et avec la condition que le flux soit fini et qu'il s'annule à la surface extérieure extrapolée du réacteur.

On obtient ainsi un système homogène à $2q$ équations algébriques, dont la condition de compatibilité détermine la valeur ϵ pour une distribution (μ_i, ξ_i) donnée, et par suite la valeur de P_c nécessaire au fonctionnement du réacteur. Ainsi, le réacteur est complètement déterminé par les conditions ci-dessus, si l'on donne la quantité d'uranium U et la distribution (μ_i, ξ_i).

La quantité de noyaux d'uranium se transformant en plutonium par capture neutronique et avec une section efficace microscopique σ_u^{cp}, dans l'unité de temps et pour chaque noyau d'uranium présent dans le réacteur, sera:

$$K_1 = \frac{1}{U} \sum_{i=1}^{q} \int_{Vi} \sigma_u^{cp} N_i^u \phi_i(\vec{r}) \mathrm{d}V = \sigma_u^{cp} \sum_{i=1}^{q} \mu_i \phi_i \qquad (5)$$

* Institut de physique atomique, Bucarest.

où la valeur moyenne du flux neutronique dans le volume V_i est:

$$\bar{\phi}_i = \frac{1}{V_i} \int_{Vi} \vec{\phi_i}(\vec{r}) \mathrm{d}V$$

De même, le nombre de noyaux de plutonium qui disparaissent par fission et par capture non fissile, pour chaque noyau d'uranium, pendant le fonctionnement du réacteur est:

$$K_2 = \frac{1}{U} \sum_{i=1}^{q} \int_{Vi} \sigma_p{}^a N_i{}^p \phi_i(\vec{r}) \mathrm{d}V = \sigma_p{}^a \epsilon \sum_{i=1}^{q} \xi_i \bar{\phi}_i \quad (6)$$

Les flux neutroniques $\bar{\phi}_i$ dépendent de la distribution μ_i, ξ_i et de ϵ. Pour chaque couple de distributions (μ^k,ξ^l) avec $\mu^k \equiv \{\mu_i{}^k\}$; $\xi^l \equiv \{\xi_i{}^l\}$ et, pour une valeur U donnée, nous aurons un couple de valeur (K_1,K_2) bien déterminée. Pour un nombre fini de couples (μ^k,ξ^l); $(k,l = 1,2, \ldots m,n)$, on a pour K_1 et K_2 des valeurs qui forment des matrices d'indice (k,l).

Notre problème se réduit au calcul des distributions μ et ξ pour lesquelles K_1 est maximal et K_2 minimal.

Le rapport $K_1/K_2 = R$, comme le coefficient de reproduction d'un réacteur nucléaire régénérateur.

Sous cette forme, on peut aisément interpréter notre problème à l'aide de la théorie des jeux. Supposons, par exemple, deux joueurs, l'un possédant la quantité d'uranium U, qu'il distribue suivant μ^k, tandis que l'autre distribue la quantité de plutonium P_c suivant ξ^l. Le gain du premier est donné par les termes de la matrice $K_1(k,l)$ et la perte du deuxième par ceux de $K_2(k,l)$. Le premier est donc intéressé à choisir telle distribution μ^k qui réalise un maximum pour $K_1(\mu^k,\xi^l)$ quelle que soit la distribution ξ^l choisie par le deuxième, et le deuxième choisira la distribution donnant un minimum $K_2(k,l)$ pour n'importe quelle distribution μ^k choisie par le premier.

Ainsi, nous avons affaire à un jeu Γ (K_1,K_2) bimatriciel, à somme non nulle.

Or, il arrive en général qu'on ne trouve pas une paire de distributions satisfaisant à la fois les deux conditions, c'est-à-dire qu'on ne trouve pas toujours une solution d'équilibre du jeu dans l'ensemble des stratégies pures (μ^k,ξ^l).

Il est connu que, dans ce cas, la solution est donnée par des stratégies complexes représentées par des vecteurs $\vec{X} = (x_k)$; $\vec{Y} = (y_l)$, dont les composantes sont les fréquences d'utilisation des stratégies pures μ^k,ξ^l et satisfont $\sum_{k=1}^{m} x_k = \sum_{l=1}^{n} y_e = 1$.

Les solutions des équations:

$$\vec{X} \,.\, K_1(k,l) \,.\, \vec{Y}^* \geqslant K_1(k, .) \vec{Y}^*; \; (k = 1,2, \ldots m)$$

$$\vec{X} \,.\, K_2(k,l) \; \vec{Y}^* \geqslant \vec{X} \,.\, K_2(\,.\,,l); \; (l = 1,2, \ldots n)$$

donnent les conditions d'équilibre de notre jeu.

Ici $\vec{Y}^*$ représente le transposé du vecteur $\vec{Y}$, $K_1(k, .)$ la k-ième ligne de la matrice $K_1(k,l)$, et $K_2(\,.\,,l)$ la l-ième colonne de la matrice $K_2(k,l)$.

Les solutions d'équilibre du jeu bimatriciel ont été données par Vorobief en 1958 [1].

Le problème d'optimisation du coefficient de reproduction par la distribution spatiale du matériel fertile et fissile dans un réacteur nucléaire se réduit donc à un problème étudié et résolu dans la théorie des jeux. Les calculs nécessaires pour résoudre ce problème, même pour des cas simplifiés, nécessitent l'emploi de calculateurs électroniques.

BIBLIOGRAPHIE

1. Teoria Veroiatnesti i ieo Primenenie, Vol. 3, nº. 3 (1958).

ABSTRACT—RÉSUMÉ—АННОТАЦИЯ—RESUMEN

A/674 Romania

Optimization of the initial conversion ratio of a nuclear reactor considered as a games theory problem

By I. I. Purica

It is shown that the problem of obtaining a maximum initial conversion ratio (by non-homogeneous spatial distribution of the fissile material), together with minimum fuel consumption, has the structure of a two-matrix game with a non-zero sum.

The volume of the reactor is regarded as being divided into q separate, indeterminate volumes, each containing $U_i = \mu_i U$ fertile nuclei and $P_i = \xi_i P_c$ fissile nuclei, where U is the total number of fertile nuclei and P_c is the number of fissile nuclei necessary for critical mass.

These conditions of maximum density and criticality make it possible to determine the geometrical structure and the value of P_c for a given U and a given distribution (μ_i,ξ_i).

The number of fissile nuclei produced in a reactor in unit time is

$$K_1 = \sigma_u{}^{cp} \sum_{i=1}^{q} \mu_i \bar{\phi}_i$$

and the number of fissile nuclei disappearing is

$$K_2 = \sigma_p{}^a \epsilon \sum_{i=1}^{q} \xi_i \bar{\phi}_i$$

where $\sigma_u{}^{cp}$ is the cross section of the process leading to the appearance of a fissile nucleus, $\sigma_p{}^a$ the cross section of the process leading to the disappearance of a fissile nucleus, $\bar{\phi}_i$ the mean neutron flux in the region i, and $\epsilon = P_c/U$.

The gain K_1 and the loss K_2 of fuel are functions of the distribution (μ_i,ξ_i) adopted and of U.

The ratio K_1/K_2 is the breeding ratio of a breeder reactor.

Let us assume two players, one possessing U fertile nuclei and adopting the distribution $\mu_i{}^k$, the other adopting the distribution $\xi_i{}^e$ of P_c fissile nuclei.

The gain of the first is given by the terms of the matrix K_1 ($\mu_i{}^k$,$\xi_i{}^e$) and the loss of the second is given by those of the matrix K_2 ($\mu_i{}^k$,$\xi_i{}^e$). The first is therefore interested in choosing the $\mu_i{}^k$ distribution which makes K_1 a maximum for any $\mu_i{}^e$ distribution chosen by the second. The second will choose the $\xi^e{}_i$ distribution making K_2 a minimum for any $\mu_i{}^k$ distribution chosen by the first.

The problem thus corresponds to the structure of a two-matrix game with a non-zero sum $\Gamma(K_1,K_2)$.

For fast neutron breeder and two-region thermal reactors, an analysis is made of the information that can be obtained by studying the strategy of the game.

A/674 Румыния

Оптимизация начального коэффициента воспроизводства ядерного реактора как задача теории игр

И. И. Пурика

Показано, что задача получения максимального начального коэффициента воспроизводства (путем негомогенного пространственного распределения делящегося материала) одновременно с минимальным расходом горючего имеет структуру биматричной игры с ненулевой суммой.

Для этой цели объем реактора разделяется на q отдельных недетерминированных объемов. Каждый из них содержит $U_i = \mu_i U$ ядер сырьевого и $p_i = \xi_i p_c$ ядер делящегося материала (U — полное число ядер сырьевого материала, p_c — количество делящихся ядер, необходимое для достижения критичности).

Условия максимальной плотности и критичности дают возможность определения геометрической структуры и величины p_c для данных U и распределения (μ_i, ξ_i).

Количество делящихся ядер, производимое в реакторе в единицу времени, определяется выражением

$$k_1 = \sigma_U^{\text{ср}} \sum_{i=1}^{q} \mu_i \overline{\psi}_i ,$$

а количество исчезающих делящихся ядер определяется выражением

$$k_2 = \sigma_p^a \varepsilon \sum_{i=1}^{q} \xi_i \overline{\psi}_i ,$$

где $\sigma_U^{\text{ср}}$ — эффективное сечение процесса, который ведет к появлению одного делящегося ядра; σ_p^a — эффективное сечение процесса, ведущего к исчезновению одного делящегося ядра; $\overline{\Phi}_i$ — средний поток в области i и $\varepsilon = p_c/U$.

Выигрыш k_1 и потеря k_2 горючего — функции от распределения (μ_i, ξ_i) и от U.

Отношение k_1/k_2 — коэффициент воспроизводства реактора-бриддера.

Пусть есть два игрока — один имеет количество сырьевых ядер U и реализует распределение μ_i^k, другой реализует распределение ξ_i^l всех p_c делящихся ядер. Выигрыш первого дается членами матрицы k_1 (μ_i^k, ξ_i^l), потеря второго — членами матрицы k_2 (μ_i^k, ξ_i^l). Следовательно, первый должен выбрать такое распределение μ_i^k, которое сделает k_1 максимальным для любого распределения ξ^l, выбранного вторым. Второй выбирает распределение ξ_i^l, которое сделает k_2 минимальным для любого распределения μ_i^k, выбранного первым.

Задача, таким образом, имеет структуру одной биматричной игры с ненулевой суммой Γ (k_1, k_2).

Для реакторов-бриддеров на быстрых нейтронах и для реакторов на тепловых нейтронах с двумя зонами делается анализ информации, которую можно получить путем изучения стратегии игры. Расчеты были произведены в P_1-приближении.

A/674 Rumania

La optimización del coeficiente inicial de regeneración de un reactor nuclear como problema de la teoría de juegos

por I. I. Purica

Se demuestra que la estructura del problema de obtener un coeficiente inicial de regeneración máximo (mediante una distribución espacial no homogénea del material fisionable) junto a la obtención simultánea de un consumo mínimo de combustible, es la de un juego bimatricial de suma no nula.

Se considera para ello el volumen del reactor dividido en q volúmenes distintos, indeterminados, que contienen cada uno $U_i = \mu_i U$ núcleos fértiles y $P_i = \xi_i P_c$ núcleos fisibles, siendo U el número total de núcleos fértiles y P_c la cantidad necesaria de núcleos fisibles para conseguir una masa crítica.

Las condiciones de densidad máxima y criticidad permiten determinar la estructura geométrica y P_c, para un U y una distribución (μ_i,ξ_i) dadas.

El total de núcleos fisibles producidos en el reactor por unidad de tiempo es:

$$K_1 = \sigma_u^{\text{ср}} \sum_{i=1}^{q} \mu_i \phi_i$$

y el total de núcleos fisibles que desaparecen:

$$K_2 = \sigma_p{}^{a} \epsilon \sum_{i=1}^{q} \xi_i \bar{\phi}_i$$

donde, $\sigma_u{}^{cp}$ es la sección eficaz del proceso que conduce a la aparición de un núcleo fisible, $\sigma_p{}^{a}$ la sección eficaz del proceso que conduce a la desaparición de un núcleo fisible, $\bar{\phi}_i$ el flujo neutrónico medio en la región i, y $\epsilon = P_c/U$.

La ganancia K_1 y la pérdida K_2 de combustible son funciones de la distribución μ_i, ξ_i adoptada y de U.

La relación K_1/K_2 es el coeficiente de reproducción de un reactor nuclear regenerador.

Supongamos dos jugadores, uno que posee un total U de núcleos fértiles y que efectúa la distribución $\mu_i{}^k$, y otro que efectúa la distribución $\xi_i{}^l$ de P_c núcleos fisionables.

Las ganancias del primero están dadas por los términos de la matriz $K_1(\mu_i{}^k,\xi_i{}^l)$ y las pérdidas del segundo por las de la matriz $K_2(\mu_i{}^k,\xi_i{}^l)$. El primero está interesado en elegir una distribución $\mu_i{}^k$ tal que haga K_1 máximo, cualquiera que sea la distribución $\xi_i{}^l$ elegida por el segundo. El segundo eligirá una distribución $\xi_i{}^l$ que haga a K_2 mínimo para cualquier distribución $\mu_i{}^k$ elegida por el primero.

El problema requiere, por lo tanto, la estructura de un juego bimatricial, de suma no nula $\Gamma(K_1,K_2)$.

Se hace un análisis de las informaciones que se pueden obtener a partir del estudio de las estrategias del juego para los reactores regeneradores de neutrones rápidos y los reactores térmicos de dos zonas.

Détermination, par la méthode de la caractéristique de fréquence, de la déformation du spectre des neutrons thermiques dans les milieux hétérogènes*

par I. Purica, N. Seferian et E. Răcătăianu**

CONSIDÉRATIONS THÉORIQUES***

Le problème de la déformation du spectre neutronique a fait l'objet de nombreuses études à cause de l'importance qu'il présente pour les réacteurs thermiques.

Si pour les milieux homogènes on dispose maintenant d'une grande quantité cohérente de données expérimentales et d'analyses théoriques de ces données, pour les milieux hétérogènes les résultats existants ne sont pas satisfaisants.

Nous nous proposons ici d'apporter quelques contributions concernant la déformation du spectre neutronique dans les milieux hétérogènes. Dans ce but nous avons employé la méthode de la caractéristique de fréquence exposée dans nos communications antérieures.

Par la méthode de la caractéristique de fréquence, on mesure l'amplitude de l'oscillation du flux neutronique pour différentes fréquences. C'est la transformée de Fourier de la caractéristique d'impulsion qui est déterminée couramment par la méthode de la source pulsée. On obtient ainsi les valeurs propres avec toutes les informations qu'elles peuvent fournir.

Les conditions d'applicabilité et les relations qui existent entre cette méthode, d'une part, et la méthode de la source pulsée et l'étude de la propagation des ondes neutroniques, d'autre part, ont été analysées par nous dans [1], et quelques résultats expérimentaux ont été exposés dans [2].

Nous employons comme source de neutrons un faisceau neutronique qui provient d'une colonne thermique, donc ayant un spectre de Maxwell; le bruit neutronique provenant d'autres sources est éliminé par la manière dont on mesure l'amplitude des oscillations.

C'est pour ces motifs que nous avons considéré cette méthode comme indiquée pour l'étude de la déformation du spectre des neutrons thermiques dans les milieux hétérogènes.

Pour interpréter les résultats expérimentaux, nous avons utilisé un modèle qui sera brièvement exposé ici.

Le problème du spectre neutronique dans un réacteur a été abordé en suivant une conception utilisée dans l'étude des milieux modérateurs [2], [3], [4]. La variation avec l'énergie du flux est décomposée dans un système de fonctions bi-orthonormales $\mathscr{L}_n(E/E_0)$, $\mathscr{L}_n{}^+(E/E_0)$ construit avec les polynômes de Laguerre $L_n^{(1)}$ pondérés sur une fonction qui représente une distribution maxwellienne du flux $(E/E_0)\,e^{-(E/E_0)}$.

Lorsqu'on considère un flux $\phi^0(\vec{r},E,t)$ dans le modérateur et un flux $\phi^1(\vec{r},E,t)$ dans les barres combustibles, on peut tenir compte de la différence des spectres respectifs, en considérant:

$$\begin{aligned}\phi^0(\vec{r},E,t) &= \sum_n \psi_n{}^0(\vec{r},t)\mathscr{L}_n(E/E_0)\\ \phi^1(\vec{r},E,t) &= \sum_n \psi_n{}^1(\vec{r},t)\mathscr{L}_n(E/E_0)\end{aligned} \tag{1}$$

Si nous nous limitons aux deux premiers termes du développement en série (1), on peut approcher une distribution maxwellienne déformée par une autre distribution maxwellienne $\mathscr{M}(E/E_m)=\mathscr{L}_0(E/E_m)$ dont l'énergie la plus probable est différente de E_0.

Ainsi les flux $\phi^{0,1}(\vec{r},E)$ peuvent être représentés par:

$$\begin{aligned}\phi^{0,1}(\vec{r},E) &= \psi_{\mathscr{M}}{}^{0,(1)}(\vec{r})\mathscr{M}(E/E_{m_0};(m_1))\\ &= \psi_0{}^{0,(1)}(\vec{r})\mathscr{L}_0(E/E_0)+\psi_1{}^{0,(1)}(\vec{r})\mathscr{L}_1(E/E_0)\end{aligned} \tag{2}$$

Le système de fonctions bi-orthonormales $\mathscr{L}_k,\mathscr{L}_k\dagger$ est défini par:

$$\mathscr{L}_k(E/E_0)=\frac{L_k^{(1)}(E/E_0)}{\sqrt{k!(k+1)!}}\cdot\frac{E}{E_0}\cdot e^{-E/E_0}$$

$$\mathscr{L}_k\dagger(E/E_0)=\frac{L_n^{(1)}(E/E_0)}{\sqrt{k!(k+1)!}}$$

De cette définition résultent immédiatement les relations suivantes:

$$\begin{aligned}\mathscr{M}(E/E_{m_0,m_1}) &= \mathscr{L}_0(E/E_{m_0,m_1})=\frac{E_{m_0,m_1}}{E_0}\mathscr{L}_0(E/E_0)\\ &+\sqrt{2}\frac{E_{m_0,m_1}}{E_0}\left(1-\frac{E_{m_0,m_1}}{E_0}\right)\mathscr{L}_1(E/E_0)\end{aligned} \tag{3}$$

* Travail effectué par contrat de recherche n° 229/RB AIEA-Vienne.

** Institut de physique atomique, Bucarest.

*** Par I. Purica.

De la comparaison des relations (2) et (3) résulte:

$$\psi_0^{0,1}(\vec{r}) = \frac{E_{m_0,m_1}}{E_0}\psi_{\mathcal{M}}{}^{0,1}(\vec{r}) \tag{4}$$

$$\psi_1^{0,1}(\vec{r}) = \sqrt{2}\,\frac{E_{m_0,m_1}}{E_0}\left(1 - \frac{E_{m_0,m_1}}{E_0}\right)\psi_{\mathcal{M}}{}^{0,1}(\vec{r})$$

et donc:

$$E_{m_0,m_1} = E_0\left[1 - \frac{1}{\sqrt{2}}\psi_1^{0,1}(\vec{r})/\psi_0^{0,1}(\vec{r})\right] \tag{5}$$

On peut définir ainsi un spectre Maxwell caractérisé par E_m si l'on connaît le rapport $\psi_1(\vec{r})/\psi_0(\vec{r})$.

Or, ce rapport dépend en général de la position spatiale.

La distribution spatiale du flux neutronique peut être exprimée par une série dans la base des fonctions propres $\chi_p(\vec{r})$ orthonormées du laplacien avec les conditions aux limites convenables.

Dans ce cas, pour chaque harmonique $\chi_n(\vec{r})_t$, la valeur de l'énergie E_{mn} est fonction seulement des caractéristiques nucléaires du milieu.

Lorsque le flux $\phi(\vec{r},E,t)$ est une fonction périodique de pulsation:

$$\phi(\vec{r},E,t) = \mathrm{Re}\,\phi\,(\vec{r},E)\mathrm{e}^{j\omega t}$$

l'énergie E_{mn} est une valeur complexe qui pour $\omega = 0$ devient l'énergie correspondante de la vitesse la plus probable de la distribution Maxwell pour l'harmonique spatial, n, dans une distribution spatiale stationnaire.

Une source de neutrons thermiques, modulée sinusoïdalement, excite dans un réseau multiplicateur ou non multiplicateur tous les harmoniques spatiaux. Pour les réseaux multiplicateurs, lorsque la condition de criticité est satisfaite, la distribution spatiale et énergétique des neutrons est donnée par la fondamentale seule, pour une source d'intensité nulle. La condition de criticité, pour une structure géométrique de la cellule et une structure nucléaire donnée, dépend seulement de la valeur du laplacien $B_g{}^2$.

On peut donc obtenir des informations sur le spectre des neutrons thermiques dans un réseau multiplicateur en étudiant le spectre de la fondamentale dans un milieu non multiplicateur ayant la même structure géométrique et les mêmes sections d'absorption et de diffusion, à la condition que la source soit thermique. Or, ces conditions peuvent être réalisées en utilisant la méthode de la caractéristique de fréquence.

La formule (5) montre que, pour la fondamentale spatiale, le spectre des neutrons est caractérisé soit par ψ_1/ψ_0 soit par E_m. La connaissance des facteurs qui déterminent ϕ_n permettra donc le calcul de E_m, et ces facteurs peuvent être déterminés par l'étude de λ_n.

L'équation qui résulte de la condition de conservation du nombre des neutrons dans un milieu fini, parallélépipédique, hétérogène, dont les hétérogénéités sont des barres disposées dans un réseau quadratique et pour un régime oscillant à une pulsation ω, est:

$$\int_V \mathrm{d}\vec{r}\,\frac{j\omega}{v}\,\phi^0(\vec{r},E) = \int_V \mathrm{d}\vec{r}H^0\phi^0 - \frac{s_1}{s_0}\sum_{k,j}\int_{V'_{kj}} \mathrm{d}r\Sigma^1{}_a(E)\phi^1(\vec{r},E) + \int_V \mathrm{d}rS(\vec{r},E) \tag{6}$$

où l'opérateur H^0 est:

$$H^0 = D^0(E)\nabla^2 - \Sigma_0{}^0(E) - J^0(E',E)$$

$$J^0(E',E) = \int_0^\infty \mathrm{d}E'[\Sigma_s{}^0(E\to E') - \Sigma_s{}^0(E'\to E)\,.\,\delta(E',E)]$$

et la source $S(\vec{r},E)$ contient les termes de la source de fission $S^{\mathrm{F}}(\vec{r},E)$ et de la source extérieure $S^{\mathrm{ex}}(\vec{r},E)$.

La variation avec le temps du flux $\phi^0(\vec{r},E,t)$ et de la source extérieure est donnée par:

$$\phi^0(\vec{r},E,t) = \mathrm{Re}\phi^0(\vec{r},E)\mathrm{e}^{j\omega t};\ S^{\mathrm{ex}}(\vec{r},E,t) = \mathrm{Re}\,S^{\mathrm{ex}}(\vec{r},E)\mathrm{e}^{-j\omega t}$$

V'_{kj} est le volume de la barre cylindrique dont l'axe est situé en (x_k,y_j,z).

Pour des pulsations ω relativement petites, on peut considérer le flux $\phi^1(\vec{r},E)$ comme solution de l'équation de diffusion des neutrons dans la barre (x_k,y_j,z), d'une symétrie cylindrique, avec une distribution maxwellienne et avec la condition:

$$\phi^1(R_1,E) \approx \phi^0(x_k,y_j,z,E) \tag{7}$$

Après avoir homogénéisé par:

$$\sum_{k,j} \to \frac{1}{S_c}\int_{-a}^{+a}\mathrm{d}x_k\int_{-b}^{+b}\mathrm{d}y_j \tag{8}$$

si on utilise la relation (4), le terme qui donne l'absorption dans les barres fait ainsi que l'équation (6) devient une équation différentielle qui contient seulement le flux dans le modérateur.

Cette équation différentielle peut être réduite, par les méthodes connues, à un système d'équations algébriques:

$$\sum_k\left[\frac{j\omega}{v_0}\left(\frac{v_0}{v}\right)_{jk} - \mathrm{H}_{jk,\xi\eta\zeta}{}^0 + \frac{S_c}{S_0}\sum_{jk}{}^1 Q_\zeta{}^1\right]\psi_{k\xi\eta\zeta}{}^0 - \frac{S_c}{S_0}\Sigma_{j1}{}^1 Q_\zeta{}^1\,\sqrt{2}\,\frac{E_{m_1}-E_{m_0}}{E_0}\psi_{01\xi\eta\zeta}{}^0 = S_{j1\xi\eta\zeta}{}^{\mathrm{ex}} + S_{j1\xi\eta\zeta}{}^{\mathrm{F}} \tag{9}$$

avec

$$\mathrm{H}_{jk,\xi\eta\zeta}{}^0 = D_{jk}{}^0\,B_{\xi\eta\zeta}{}^2 - \Sigma_{jk}{}^0 - j_{jk}{}^0$$

Les indices k,j se rapportent aux coefficients de la décomposition en série par rapport aux $\mathscr{L}_k(E/E_0)$, et les indices ξ,η,ζ aux coefficients de la décomposition en série des harmoniques spatiaux $\chi_\xi(x).\chi_n(y)\chi_\zeta(z)_1$, où s_c est la surface de la cellule et s_0 celle du modérateur, Q_ζ est le coefficient d'écran de la barre, différent pour différents harmoniques spatiaux ζ, à cause de la hauteur finie des barres.

Considérons $D^0(E)$ constant et $\Sigma_a(E)=\Sigma_{a_0}(v_0/v)$; alors:

$$D_{jk}{}^0 = D\delta_{jk}; \Sigma_{jk}{}^0 = \Sigma_{a0}\left(\frac{v_0}{v}\right)_{jk} = \Sigma_{a0} w_{jk} \quad (10)$$

et

$$\left(-\frac{v_0}{v}\right)_{jk} = \int d\left(\frac{E}{E_0}\right)\mathscr{L}_j{}^+(E/E_0)\frac{v_0}{v(E)}\mathscr{L}_k(E/E_0) = w_{jk}$$

La source extérieure est une source ponctuelle avec une distribution maxwellienne, telle que:

$$s_j{}^{ex}{}_{,\xi\eta\zeta} = \begin{cases} s_0{}^{ex}{}_{,\xi\eta\zeta}; & j=0 \\ 0 & ; j\neq 0 \end{cases} \quad (11)$$

La source de fission peut être calculée en négligeant le temps de ralentissement par rapport au temps de diffusion, utilisant le deuxième théorème des réacteurs nucléaires et prenant pour les noyaux de ralentissement:

$$\mathscr{K}(B_{\xi\eta\zeta}{}^2{}_{,E}) = p e^{-\mathscr{T}(E)B_{\xi\eta\zeta}{}^2}\delta(E-E_r) \quad (12)$$

où p est la probabilité d'éviter l'absorption de résonance, $\mathscr{T}(E)$ l'âge Fermi jusqu' à l'énergie E, et où $\delta(E-E_r)$ spécifie que nous considérons les neutrons de fission thermalisés comme une source de neutrons ayant l'énergie E_r.

Finalement on obtient:

$$s_0{}^F{}_{,\xi\eta\zeta} = \frac{s_1}{s_0} Q\zeta^1 r \Sigma_{f0}{}^1 p \,.\, e^{-\mathscr{T}(E_r)B_{\xi\eta\zeta}{}^2}\Big[W_{00}\psi_0{}^0{}_{,\xi\eta\zeta} + W_{01}\psi_1{}^0{}_{,\xi\eta\zeta} - \sqrt{2}\, W_{01}\frac{E_{m_1}-E_{m_0}}{E_0}\psi_{01}{}^0{}_{,\xi\eta\zeta}\Big] \quad (13)$$

$$\times\, s_1{}^F{}_{,\xi\eta\zeta} = s_0{}^F{}_{,\xi\eta\zeta}\left(2-\frac{E_r}{E_0}\right)$$

L'introduction de (13) dans (9) conduit à un système d'équations algébriques qui permettent la détermination de $\psi_0{}^0$, $\psi_1{}^0$ pour la fondamentale spatiale $(\xi,\eta,\zeta)=(1,1,1)$.

Lorsque la criticité est réalisée, pour $B_{111}{}^2 = B_{cr.}{}^2$, $s_0{}^{ex}=0$; $\omega=0$ vu la condition de compatibilité du système d'équations (9), on peut exprimer le rapport qui caractérise le spectre par:

$$\frac{\psi_1{}^0}{\psi_0{}^0} = -\frac{W_{10}}{W_{11}} \cdot \frac{\bar\Sigma_0 v_0\left(1-\frac{W_{11}}{W_{10}}f_0\sqrt{2}\frac{E_{m_1}-E_{m_0}}{E_0}\right) - \frac{W_{00}}{W_{10}}k\phi\bar\Sigma_0 e^{-\mathscr{T}(E_r)B_{cr}{}^2}\epsilon_r\left(1-\frac{W_{01}}{W_{00}}\sqrt{2}\frac{E_{m_1}-E_{m_0}}{E_0}\right)}{\bar\Sigma_0 v_0 + \frac{D^0 r_0}{W_{11}}B_{cr}{}^2 + \frac{M_2}{4W_{11}} - \frac{W_{01}}{W_{11}}k\phi\bar\Sigma_0\epsilon_r e^{-\mathscr{T}(E_r)B_{cr}{}^2}} \quad (14)$$

Les définitions pour $\bar\Sigma_0, f_0, k_\infty, \epsilon_r$ sont les suivantes:

$\bar\Sigma_0$ est la section d'absorption totale homogénéisée, sans tenir compte de la différence spectrale entre la barre et le modérateur

$$\Sigma_0 = \Sigma_{a0}{}^0 + \frac{s_1}{s_0}\, Q\zeta^1\Sigma_{a0}{}^1$$

f_0 est le facteur d'utilisation des neutrons thermiques, k_∞ le coefficient de multiplication dans un milieu infini:

$$\epsilon_r = 2 - \frac{E_r}{E_0}$$

Nous avons explicité la différence entre les énergies E_{m_1}, E_{m_0} caractérisant la distribution Maxwell équivalente pour les barres et pour le modérateur, celle-ci étant directement accessible à l'expérience. D'ailleurs, $(E_{m_1}-E_{m_0})/E_0$ pourrait être calculé si nécessaire.

Les éléments qui déterminent $\psi_1{}^0/\psi_0{}^0$, donc E_{m_0}, sont susceptibles d'être mesurés par l'étude des valeurs propres λ du système d'équations (9).

Etant donné le manque de place pour l'étude expérimentale présentée dans ce mémoire, nous nous limiterons aux milieux hétérogènes non multiplicateurs pour $k_\infty=0$. La plus petite valeur propre λ_0 peut être mise sous la forme habituelle:

$$\lambda_0 = \bar\Sigma_0 v_0 + D_0 B^2 - \bar C_0 B^4$$

Mais, dans ce cas, les valeurs $\bar\Sigma_0, \bar D_0, \bar C_0$ sont données par:

$$\begin{aligned} \bar\Sigma_0 &= \bar\Sigma_{a_0} v_0 - \frac{W_{01}}{W_{00}} v_0\theta \\ \bar D_0 &= \left[1 - 4\frac{W_{01}}{W_{00}{}^2}(W_{00}W_{11} - 2W_{01}{}^2)\frac{\theta}{M_2{}^0}\right]\frac{V_0}{W_{00}} \cdot D^0 \\ \bar C_0 &= \left[1 - 8\frac{W_{01}}{W_{00}{}^2} W_{00}W_{11} - W_{01}{}^2)\frac{\theta}{M_2{}^0}\right] \times \frac{W_{01}{}^2}{W_{00}{}^3} \cdot \frac{4(D^0)^2 v_0}{M_2} \end{aligned} \quad (15)$$

où

$$\theta = \frac{s_1}{s_0} Q\zeta^1\Sigma_{a0}{}^1\sqrt{2}\frac{E_{m_1}-E_{m_0}}{E_0}$$

Pour $E_{m_1}=E_{m_0}$ les formules se réduisent à celle calculée par Pourohit [3]. On a considéré le rapport $4\theta/M_2{}^0 \ll 1$.

La variation de $\Sigma_{a_0}{}^1$ permettra la détermination de $Q\zeta^1(E_{m_1}-E_{m_0})/E_0$ comme fonction de $\Sigma_{a_0}{}^1$, section d'absorption dans les barres. Si les caractéristiques nucléaires des barres utilisées pour réaliser un milieu non multiplicateur sont les mêmes que celles des barres combustibles, on a un moyen de séparer l'influence sur le spectre Maxwell équivalent, dans le modérateur et dans les barres, due à l'absorption dans les barres, de l'influence produite par la thermalisation du spectre de fission, caractérisée dans notre modèle théorique par le facteur $\epsilon_r = 2 - E_r/E_0$.

RÉSULTATS EXPÉRIMENTAUX

Les vérifications expérimentales des possibilités offertes par la méthode de la caractéristique de fréquence pour déterminer la déformation du spectre

maxwellien des neutrons thermiques dans les milieux hétérogènes ont été faites avec le réseau de l'ensemble sous-critique à uranium enrichi et graphite de l'Institut de physique atomique de Bucarest.

Dans la première étape nous avons vérifié la possibilité de déterminer par la mesure de $\lambda_0(B^2)$ les facteurs $\bar{\Sigma}, \bar{D}_0, \bar{C}_0$, et la variation de ces valeurs avec la section d'absorption dans les barres; nous avons déterminé ainsi la différence de température $T_{m_1} - T_{m_0}/k = E_{m_1} - E_{m_0}$ du spectre Maxwell équivalent des neutrons dans les barres et le modérateur.

La température absolue du spectre des neutrons dans les barres a été déterminée par une comparaison de l'effet produit sur λ_0 par un absorbant dont la section effective suit la loi « $1/v$», le bore, et l'effet produit par le cadmium.

On a modifié le laplacien B^2 dans le domaine $10^{-2}-10^{-3}$ cm^{-2} en conservant une hauteur constante du prisme en graphite.

On a utilisé comme source de neutrons thermiques le faisceau axial de la colonne thermique du réacteur VVR-S. Le faisceau a été modulé sinusoïdalement à l'aide d'un disque en cadmium et diffusé par une cible située à l'intérieur de l'ensemble sous-critique. Le flux neutronique a été mesuré par un scintillateur à bore et un photomultiplicateur. Le schéma électronique utilisé permet la mesure simultanée de la valeur moyenne, de l'amplitude de l'oscillation et de la phase. Une description plus détaillée du système de mesure et les caractéristiques géométriques du réseau ont été données en [2].

Pour contrôler l'exactitude des valeurs déterminées par la méthode de la caractéristique de fréquence, nous avons vérifié l'indépendance de l'efficacité spectrale du détecteur, l'influence des harmoniques spatiaux supérieurs, et nous avons constamment fait un test spécifique de la méthode et du schéma d'analyse harmonique utilisé.

La source que nous avons utilisée peut être représentée par l'expression analytique:

$$S(\vec{r},E,t) = \mathrm{Re}\ S_0\delta(\vec{r}-\vec{r}_s)M_s(E)[1+a\ e^{j\omega t}]$$

$\vec{r}_s$ étant le vecteur de position de la cible, a le degré de modulation, ω la pulsation, $M(E)$ la distribution énergétique supposée isotrope.

On peut démontrer que le rapport entre le carré de l'amplitude mesurée $A^2(\omega)$ pour $\omega = 0$ et le carré de la valeur moyenne mesurée doit être, en première approximation, indépendant du spectre de la source et de l'efficacité du détecteur:

$$k_s = \frac{A^2(0)}{(\bar{N})^2} = 4\frac{a^2}{\pi^2}$$

pour $a = 1$, on devrait obtenir $k_s = 0{,}4083$.

Pour une cible en graphite nous avons obtenu $k_c = 0{,}431 + 0{,}0027$, et pour une cible en paraffine $k_p = 0{,}455 + 0{,}0009$.

La différence entre k_c et k_p, qui est très petite, semble être due à la différence entre les spectres après leur diffusion sur les cibles respectives.

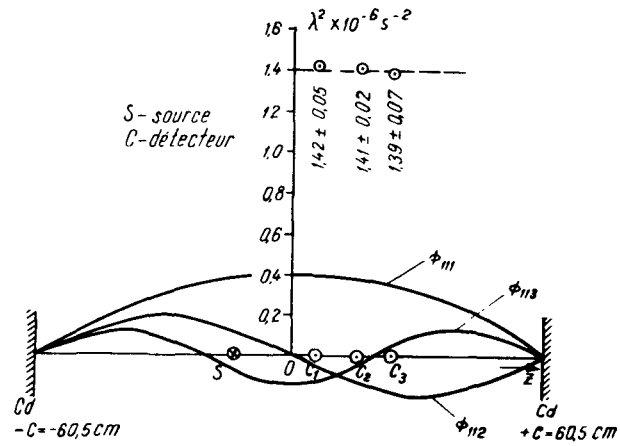

Figure 1

L'influence des harmoniques supérieurs a été étudiée en plaçant la source et le détecteur dans différentes positions qui favorisent l'influence de l'harmonique deux ou trois.

Parce que la variation du carré de l'amplitude avec ω^2 est une hyperbole:

$$A_{\xi\eta\zeta}{}^2(\omega^2) = \frac{\gamma_{\xi\eta\zeta}}{\omega^2 + \lambda_0{}^2{}_{,\xi\eta\zeta}}$$

on peut utiliser les propriétés des hyperboles pour séparer les harmoniques supérieurs.

Dans la figure 1, on peut voir les valeurs de λ_0 pour la fondamentale séparée des caractéristiques de fréquences $A^2(\omega)$, pour trois positions du détecteur caractérisées par un puissant harmonique d'ordre deux et trois sur l'axe vertical du prisme. Même dans cette situation, nous avons obtenu λ_0 avec une précision de 2–5 %.

L'indépendance de la valeur λ de l'efficacité du détecteur au spectre des neutrons enregistré a été vérifiée en utilisant deux scintillateurs de caractéristiques différentes, dont le rapport des impulsions enregistrées a été:

- —dans la colonne thermique: $(k_1/k_2) = 1{,}71$;
- —pour la configuration avec $B_g{}^2 = 2{,}9 \cdot 10^{-3}$ cm^{-2} (noté par C_5) de l'ensemble sans uranium: $(k_1/k_2) = 24{,}04$;
- —pour la même configuration avec des barres d'uranium $(k_1/k_2) = 16{,}40$.

Ces valeurs dénotent une grande différence de l'efficacité des scintillateurs dans différents spectres des neutrons.

Malgré les grandes variations de l'efficacité des scintillateurs, les valeurs de λ_0 mesurées avec eux concordent dans la limite des erreurs expérimentales.

La pulsation ω a été maintenue constante pour chaque point de la caractéristique de fréquence par la stabilisation de la vitesse du moteur avec une précision déterminée par expérience de 2–0,4 %. Les erreurs statistiques ont été de l'ordre de 1 %, et on a utilisé un nombre de 25–35 points pour chaque courbe $A^2(\omega)$.

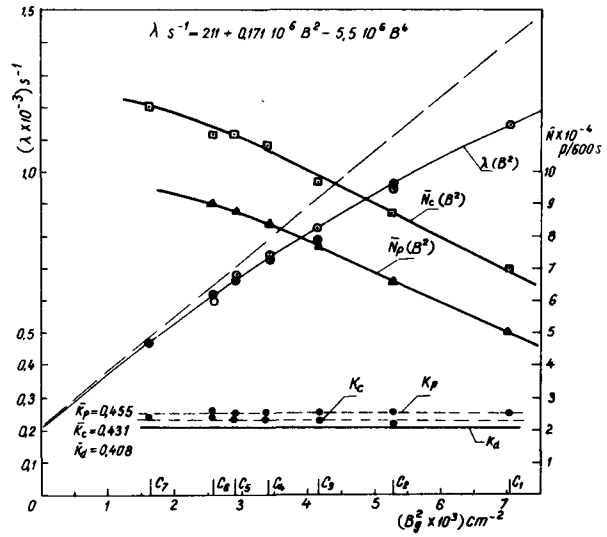

Figure 2

La vérification de la variation de $\bar{\Sigma}_0, \bar{D}_0$ et $\bar{C}_0$ avec la variation de la section efficace d'absorption dans les barres a été faite en utilisant des solutions d'acide borique et de sulfate de cadmium, à des concentrations différentes.

On a utilisé sept configurations de géométries différentes. Nous avons considéré ce nombre suffisant, étant donné que notre intention n'était pas d'obtenir la précision maximale.

Dans les figures 2 et 3, on voit la variation de λ avec B_g^2 pour des barres en tubes d'aluminium, d'un diamètre intérieur de 1,3 cm et d'un diamètre extérieur de 1,5 cm, remplies avec de l'eau et avec du diphényle.

Quoique la valeur moyenne du flux neutronique soit très différente pour la cible en graphite, par rapport à celle en paraffine, les valeurs de λ_0 sont concordantes.

L'approximation par une parabole, utilisant la méthode des moindres carrés, donne:

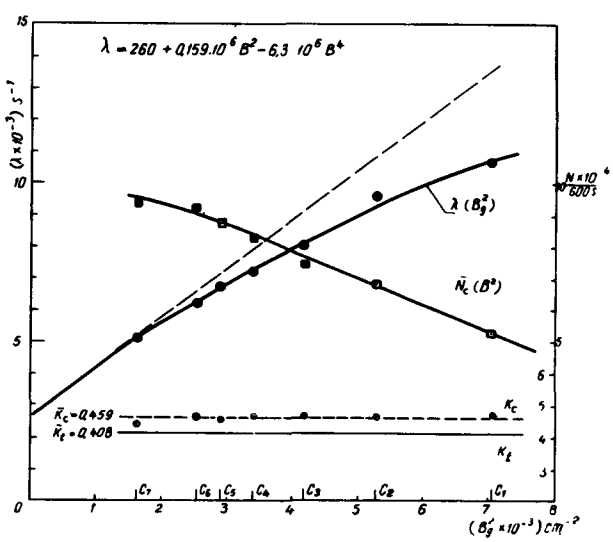

Figure 3

$$\lambda_{H_2O} = 211 \pm 11 + (171 \pm 6) \cdot 10^3 B^2 - (5{,}5 \pm 0{,}5) \cdot 10^6 B^4$$

$$\lambda_{D_t} = 260 \pm 5 + (159 \pm 2{,}7) \cdot 10^3 B^2 - (6{,}3 \pm 0{,}22) \cdot 10^6 B^4$$

La valeur du facteur de refroidissement C se situe dans le domaine des valeurs obtenues pour le graphite par la méthode de la source pulsée ($2{,}5 \leqslant C \leqslant 5$).

Le coefficient de diffusion est beaucoup plus affecté par la diffusion dans les barres. Pour le graphite pur, à 1,6 g/cm³, la valeur est $D_0 = 208.10^3$ s^{-1} cm^2.

L'empoisonnement des barres par du bore et du cadmium conduit à la modification de λ_0. Pour quelques configurations, la variation de λ_0, avec la section efficace à 0,0253 eV pour le bore et le cadmium, a été représentée dans la figure 4.

Dans la même figure, on peut voir la variation de réactivité produite dans le réacteur VVR-S par les mêmes barres contenant des concentrations différentes de bore et de cadmium. Pour le domaine $\Sigma_{B(Cd)}{}^1 = 0{,}0 - 0{,}25$ cm^{-1} la variation est presque linéaire, ce qui montre que le coefficient $Q\zeta^1$ est constant. Lorsque $\Sigma_{B(Cd)}{}^1$ varie dans ce domaine, les calculs effectués donnent une variation de 0,999 jusqu'à 0,90 − 0,92, selon la température du spectre neutronique.

A partir des courbes, telles que celles représentées dans la figure 4, pour différentes configurations géométriques, on peut déterminer la variation de $\bar{\Sigma}_0$, $\bar{D}_0$, et $\bar{C}_0$ en fonction de la section d'absorption dans les barres.

Dans la figure 5, sont représentées les courbes obtenues avec les erreurs les plus probables.

La variation est dans le sens prévu par les formules (15).

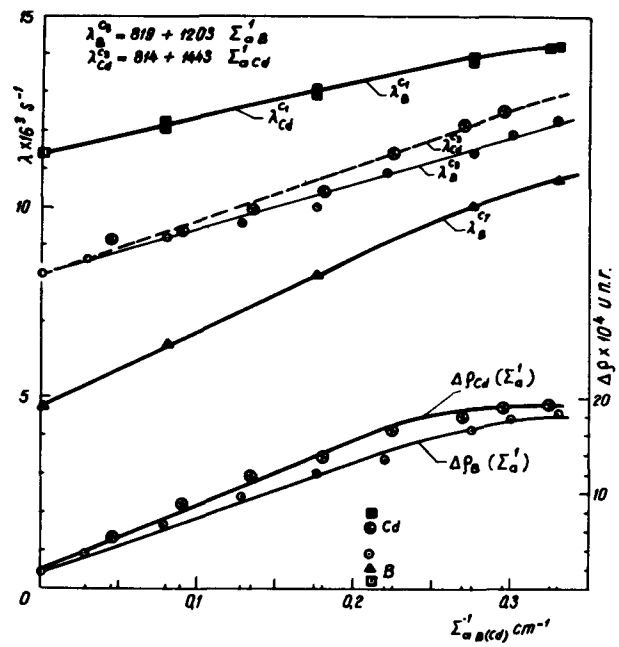

Figure 4

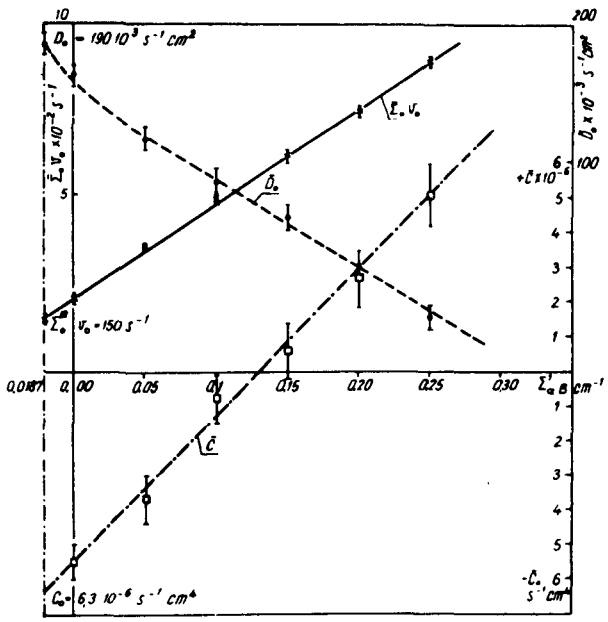

Figure 5

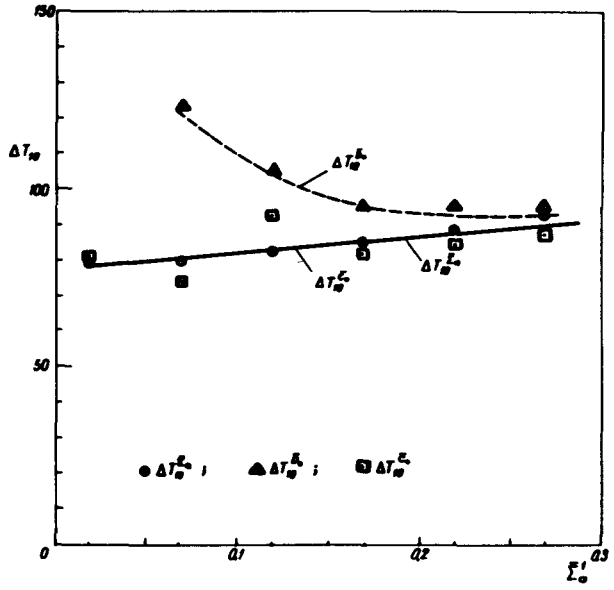

Figure 6

On a déduit de $\bar{\Sigma}_0(\Sigma_B{}^1)$ la valeur de $(E_{m_1} - E_{m_0})/E_0$ en employant pour $Q_\xi{}^1$ la valeur calculée, qui concorde d'ailleurs avec celle mesurée par le coefficient du danger.

Avec la différence de température ainsi obtenue, on a déduit de $\bar{C}_0$ la valeur de $M_2{}^0$, qui a été 0,0215, en bon accord avec les résultats obtenus pour le graphite avec la méthode de la source pulsée, mais presque trois fois plus petite que la valeur calculée par Kothari.

Avec cette valeur pour $M_2{}^0$ on a calculé la différence entre la température dans les barres et dans le modérateur à l'aide des formules (15).

Les résultats sont représentés dans la figure 6, où

$$\Delta T_{10} = 293\ (E_{m_1} - E_{m_0})/E_0 \quad (°C)$$

La différence de température croît lentement avec la section d'absorption dans les barres, ce qui signifie que l'effet de la croissance de la section d'absorption dans les barres se ressent fortement sur le spectre dans le modérateur.

Cela s'explique par la présence d'eau dans les barres que nous avons utilisées.

Dans ce cas, les neutrons thermiques qui ont pénétré dans les barres ont une probabilité de retourner dans le modérateur plus petite que celle des neutrons plus rapides se trouvant dans les barres.

La valeur de la différence de température déduite de la variation de $\bar{D}_0$ tend vers les valeurs déduites de $\bar{\Sigma}_0$ et $\bar{C}_0$ lorsque $\Sigma_{a_0}{}^1$ est grande par rapport à la section d'absorption de l'eau. Pour les petites valeurs de $\Sigma_{a_0}{}^1$ la formule (15) n'est valable que dans une première approximation. Des études plus détaillées sont en cours.

En conclusion, nous pouvons affirmer que la méthode de la caractéristique de fréquence représente un moyen puissant pour l'étude de la déformation du spectre des neutrons thermiques dans les milieux hétérogènes, multiplicateurs ou non.

Les résultats expérimentaux confirment le modèle théorique que nous avons employé, exposé dans la première partie.

REMERCIEMENTS

Nous tenons à remercier ici le professeur Horia Hulubei, académicien, pour ses conseils, ainsi que l'équipe qui travaille à l'ensemble sous-critique de l'Institut de physique atomique de Bucarest, spécialement les collègues I. Guiglea et Marcu, pour l'aide apportée à l'accomplissement de la partie expérimentale et aux calculs.

BIBLIOGRAPHIE

1. Purica, I. I., *Sur l'étude du comportement des neutrons thermiques dans les milieux finis avec la méthode de la caractéristique de fréquence*, avril 1963, IFA, 35 FR, Conf. int. sur la physique et la technique des réacteurs nucléaires de recherche, Prague (1963).
2. Purica, I. I., Seferian, N., Răcătăianu, E., *Etude d'un ensemble sous-critique par la méthode de la caractéristique de fréquence*, Exponential and Critical Experiments, vol. III, 71–86, AIEA, Vienne (1964).
3. Pourohit, S. N., Nuclear Science Eng., 9, 157 (1961).
4. Kazarnovsky, M. V., Stepanov, A. V., et Chapiro, F. L., *Thermalisation et diffusion des neutrons dans les milieux lourds*, Actes de la deuxième Conférence internationale sur l'utilisation de l'énergie atomique à des fins pacifiques, P/2148, vol. 7, p. 654, Nations Unies (1958).

ABSTRACT—RÉSUMÉ—АННОТАЦИЯ—RESUMEN

A/675 Romania

Determination of thermal neutron spectrum deformations in heterogeneous media by frequency response method

By I. Purica *et al.*

The paper analyses the possibilities offered by the frequency characteristic method for determining the deformation of the thermal neutron spectrum in a multiplying lattice. Use is made of the P_1L_2 approximation.

The theoretical results are compared with experiments carried out on an enriched uranium-graphite subcritical assembly. Separation of the effect of absorption in the uranium on deformation of the neutron spectrum is achieved by substituting suitable absorbing and diffusing substances for uranium.

A/675 Румыния

Определение искажений спектра тепловых нейтронов в размножающей решетке методом частотной характеристики

И. Пурика *et al.*

Анализируются возможности метода частотной характеристики для измерения отклонения от максвелловского распределения спектра тепловых нейтронов в размножающей решетке в рамках P_1L_2-приближения.

Теоретические результаты сравниваются с экспериментальными данными, полученными для подкритической решетки с естественным ураном и графитом. Выделение эффекта поглощения нейтронов в урановых стержнях, приводящего к деформации спектра, сделано путем замены урана материалами, обладающими одинаковыми с ним поглощающими или диффузионными свойствами.

A/675 Rumania

Determinación de la deformación del espectro de neutrones térmicos en un medio multiplicador por el método de la característica de frecuencia

por I. Purica *et al.*

Los autores analizan las posibilidades ofrecidas por el método de la característica de frecuencia para determinar la deformación del espectro de neutrones térmicos en un medio multiplicador, utilizando la aproximacion P_1L_2.

Los resultados teóricos se comparan con los obtenidos de un experimento subcrítico a base de uranio enriquecido y grafito. El efecto de absorción en el uranio sobre la deformación del espectro neutrónico se ha separado sustituyéndole por absorbentes y dispersores adecuados.

Penetration of neutrons in cylindrical air ducts in diffusing media

By A. Etemad and J. M. Pictet*

The study of the neutron penetration in channels within a diffusing medium is of great importance in the physics of reactors, particularly in the subject of reactor shielding.

The streaming of neutrons along the channels is a source of difficulty since it diminishes the efficiency of the reflector or that of the shielding.

The problem of the propagation of neutrons in media pierced by channels does not easily lend itself to rigorous theoretical treatment, due to the geometric complexities. The simplified methods [1], [2], [3] that one normally uses to calculate neutron fluxes in these configurations give poor results. Alternatively, very good results may be obtained by the use of the Monte Carlo method, but the computations are usually very prolix, and the cost prohibitive.

The present study sets out a tentative theory of channels, which yields sufficiently exact results after only a reasonable amount of computation. This theory has been applied to the case of channels within light water.

An experimental study was undertaken in order to verify the precision of the theoretical predictions. The comparison of the theoretical and experimental results exhibits a very satisfactory agreement.

Definition of the problem and general considerations

Let us consider a semi-infinite diffusing medium, bounded by a surface or volume source, and containing parallel cylindrical channels whose axes are perpendicular to the plane separating the source and the diffusing medium (Fig. 1).

The problem is to compute the neutron flux in the channels and in the diffusing medium surrounding the channels.

The neutron flux Φ_i at a given energy, at a point P inside a channel, can be considered to be made up of three components (Fig. 1), they are:

(a) The direct component Φ_a made up of neutrons which penetrate the channel from its mouth and travel directly to the point P.

(b) The reflected component Φ_b made up of neutrons which penetrate the channel from its mouth and arrive at the point P after having been reflected by the material medium surrounding the channel.

(c) The leakage component Φ_c comprising the neutrons which arrive at the point P without having passed through the channel mouth; these neutrons enter the channel via its lateral walls.

In the diffusing medium the component Φ_a does not exist and the neutron flux is made up of the components Φ_b and Φ_c, analogous to those which have just been defined for the interior of the channel.

We will suggest, below, a calculation method in which the neutron flux is treated by transport theory within the channels and by diffusion theory within the diffusing medium; these theories are coupled by a reasonable choice for the angular distribution of neutrons entering the channel.

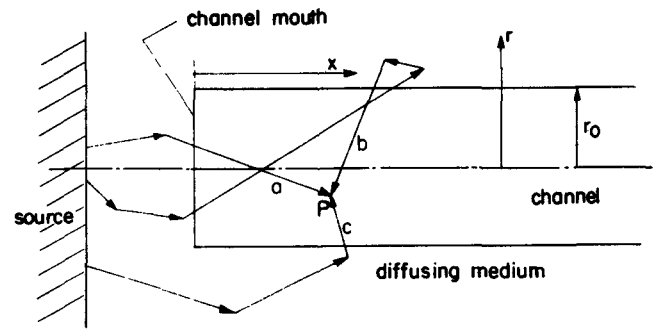

Figure 1. Layout of a channel in a diffusing medium

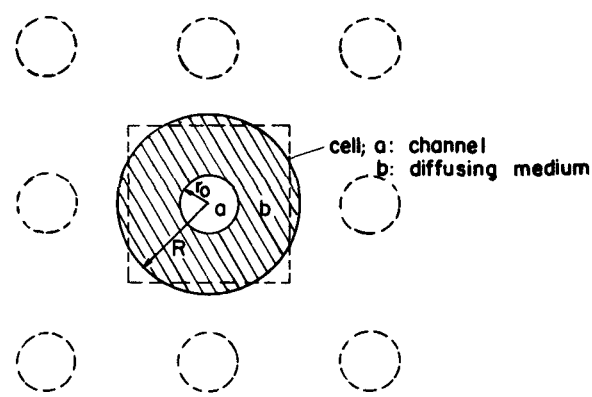

Figure 2. Layout of a cell considered in a lattice of channels

* Swiss Federal Institute for Reactor Research, Würenlingen, Switzerland.

In a lattice of channels we define a cylindrical cell of radius R, made up of a channel of radius r_0 and a certain quantity of moderator around it (Fig. 2); this quantity of moderator being chosen so as to conserve the moderator: channels volume ratio. In laying down proper boundary conditions on the external surface of this cell, one may take into account the influence of the other cells. It is precisely this isolated channel which is the subject of our study.

In order to simplify the notation we shall use, in the calculations, dimensions scaled to the channel radius r_0 taken as unity; un-scaled dimensions appear as "over-lined" letters.

The determination of the flux in the diffusing medium

The diffusion equation and boundary conditions

In the case of cylindrical symmetry the diffusion equation for group "i" may be written as,

$$\frac{\partial^2\Phi_i}{\partial r^2}+\frac{1}{r}\frac{\partial\Phi_i}{\partial r}+\frac{\partial^2\Phi_i}{\partial x^2}-\lambda_i^2\Phi_i=S_i \qquad (1)$$

where λ_i is the reciprocal of the relaxation length for the neutrons, and Φ_i and S_i are respectively the flux and the source at the point (x,r).

The flux $\Phi_i(x,r)$ is subject to the following boundary conditions:

$$\Phi_{0i}{}^0\text{: given} \qquad (2)$$

$$\lim_{x\to\infty}\Phi_i(x,r)=0 \qquad (3)$$

$$J_{ri}(x,R)=-D_i\frac{\partial\Phi_i}{\partial r}\bigg|r=R=0 \qquad (4)$$

$$j_{ri}^{+}(x)=Q_i(x)+\int_0^L j_{ri}^{-}(x')\,.\,F(x,x')\,.\,dx' \qquad (5)$$

where

$\Phi_{0i}{}^0$ = the flux at the point $x=0$ when there is no channel,

$J_{ri}(x,R)$ = net radial neutron current at the point with abscissa x on the external surface of the cell,

D_i = the diffusion coefficient,

$j_{ri}(x)$ = radial neutron current at the point with abscissa x on the lateral wall of the channel (the sign $(+)$ designates the current entering the diffusing medium, and the sign $(-)$ that entering the channel),

$Q_i(x)$ = neutron current entering the diffusing medium at the point with abscissa x on the lateral wall of the channel and coming directly from the channel mouth,

$F(x,x')$ = neutron current entering the diffusing medium at the point with abscissa x on the lateral wall of the channel and coming from a zone of the wall, of unit length, situated on the abscissa x' and emitting one neutron per second and per unit surface,

L = length of the channel.

The boundary condition (5) sets up the neutron book keeping at a point with abscissa x on the wall of the channel. It is of great importance since it allows one to take correct account of the neutron penetration in the channel.

The determination of the functions $Q(x)$ and $F(x,x')$

According to the theory of neutron transport in a void, the neutron current $J_{\vec{n}}(M)$ arising from a surface S and crossing a unit surface normal to a unit vector at the point M is given by,

$$J_{\vec{n}}(M)=\int_S \vec{n}\,.\,\frac{\vec{\rho}}{\rho}\,.\,j(N)\,.\,f(\mu)\,.\,\frac{1}{\rho^2}\,.\,dS \qquad (6)$$

where

$j(N)$ = total current leaving the source at the point N,

$\vec{\rho}$ = $\vec{NM}$ and $\rho=\overline{NM}$,

$f(\mu)$ = the angular distribution of the neutrons emitted by the source,

μ = $\cos\theta$; θ being the angle between the direction of emission and the normal to the surface.

In the relation (6) it is assumed that the angular distribution depends only on the angle θ.

Rewriting relation (6) for the case of the configuration of Fig. 3 we have

$$Q_i(x)=\iint\cos\phi\,.\,j_{0i}^{+}\,.\,f(\mu)\,.\,\frac{1}{\rho^2}\,.\,\delta\,.\,d\gamma\,.\,d\delta, \qquad (7)$$

where j_{0i}^{+} is the current entering the channel via its mouth. We assume that the current j_{0i}^{+} is constant over the whole surface formed by the mouth of the channel.

If $f(\mu)$ is given by Fermi's law of angular distribution [4], we have,

$$f(\mu)=\frac{\mu+\sqrt{3}\mu^2}{\pi\left(1+\frac{2}{\sqrt{3}}\right)}. \qquad (8)$$

Substituting (8) into (7) and integrating [5] one obtains,

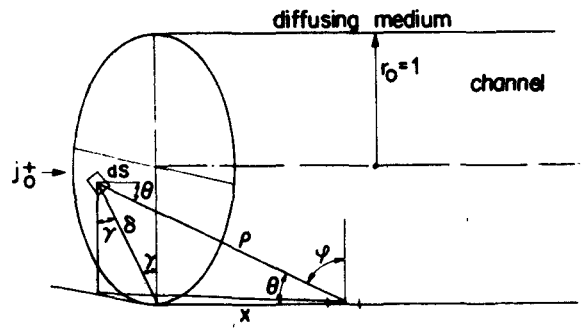

Figure 3. Configuration considered for the calculation of $Q(x)$

$$Q_i(x)=\frac{j_{0i}^{+}}{1+\frac{2}{\sqrt{3}}}\left\{\tfrac{1}{2}\left[\frac{x^2+2}{\sqrt{(x^2+4)}}-x\right]+\frac{\sqrt{(x^2+4)}}{\pi\sqrt{3}}\,.\,H(x)\right\} \quad (9)$$

with

$$H(x)=(2-k^2)\,.\,E(k)-2(1-k^2)\,.\,K(k) \quad (10)$$

where,

$$k=\frac{2}{\sqrt{(x^2+4)}}. \quad (11)$$

$K(k)$ and $E(k)$ are complete elliptic integrals of the first and second type respectively.

The function $F(x,x')$ is obtained in a similar fashion by writing out equation (6) in the case of the configuration of Fig. 4; we thus obtain,

$$F(x,x')=2\int_0^{\pi}\cos\gamma\,.f(\mu)\,.\frac{1}{\rho^2}\,.\,\mathrm{d}\beta\,. \quad (12)$$

Assuming that the angular distribution of neutrons emitted by the lateral wall of the channel follows a linear law in the cosine of the emission angle, one obtains

$$f(\mu)=\frac{\mu}{\pi}. \quad (13)$$

Introducing (13) into (12) and integrating [5] we get,

$$F(x,x')=F(|x-x'|)=\tfrac{1}{2}\left\{1-\frac{|x-x'|\,[(x-x')^2+6]}{[(x-x')^2+4]^{3/2}}\right\}. \quad (14)$$

The solution of the diffusion equation

On account of the complexity of the boundary condition (5) on the wall of the channel, the analytical solution of Eq. (1) is attended by considerable mathematical difficulties; a numerical approach is equally ruled out as it involves extremely lengthy calculations.

In order to avoid this difficulty we may let ourselves be guided by physical considerations in order to arrive at an approximate expression for $\Phi(x,r)$.

Since the void in the channel offers no obstacle to the axial penetration of neutrons, we may suppose that in the diffusing medium and near the channel, the axial flux variation is sufficiently small to justify the neglect of its second derivative with respect to x in Eq. (1). On the other hand, at some distance from the channel, the radial variation of the flux becomes negligible, leaving only the second derivative with respect to x alone in the equation. With these considerations in mind we may replace Eq. (1) by two equations, each involving only one variable:

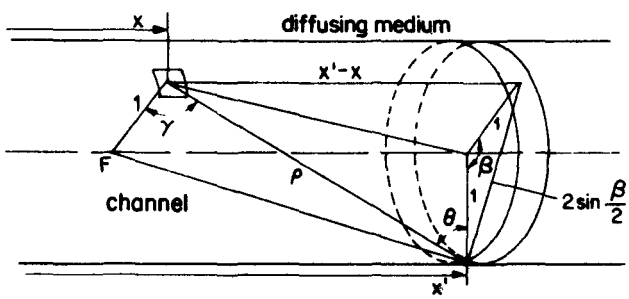

Figure 4. Configuration considered for the calculation of F(x,x')

$$\frac{\mathrm{d}^2\Phi_i^{\mathrm{p}}}{\mathrm{d}x^2}-\lambda_i^2\Phi_i^{\mathrm{p}}=S_i^{\mathrm{p}} \quad (15)$$

$$\frac{\mathrm{d}^2\Phi_i^{\mathrm{c}}}{\mathrm{d}r^2}+\frac{1}{r}\frac{\mathrm{d}\Phi_i^{\mathrm{c}}}{\mathrm{d}r}-\lambda_i^2\Phi_i^{\mathrm{c}}=S_i^{\mathrm{c}} \quad (16)$$

with

$$\Phi_i=\Phi_i^{\mathrm{p}}+\Phi_i^{\mathrm{c}}. \quad (17)$$

The source term S_i is considered as the result of the superposition of two sources S_i^{p} and S_i^{c} by virtue of the same reasoning as led us to consider the solution of Eq. (1) as the superposition of the solutions of Eqs. (15) and (16). In fact the source is, apart from a constant factor, the solution of an equation of the type (1) applied to neutrons of the preceding group $(i-1)$.

The solutions of the Eqs. (15) and (16) may be written:

$$\Phi_i^{\mathrm{p}}=E_i\,\mathrm{e}^{\lambda_i x}+F_i\,\mathrm{e}^{-\lambda_i x}+S_i'^{\mathrm{p}} \quad (18)$$

$$\Phi_i^{\mathrm{c}}=A_iI_0(\lambda_i r)+B_iK_0(\lambda_i r)+S_i'^{\mathrm{c}} \quad (19)$$

The constants E_i and F_i can be found with the help of the boundary conditions (2) and (3); condition (4) allows A_i to be expressed as a function of B_i ($A_i=\alpha_iB_i$); finally condition (5) shows that A_i and B_i should be considered as functions of x.

The expression for the flux $\Phi_i(x,r)$ hence becomes:

$$\Phi_i(x,r)=M_i\,.\,\mathrm{e}^{-\lambda_i x}+S_i'^{\mathrm{p}}(x)\,.\,N_i(x,r,R)\,.\,B_i(x)+S_i'^{\mathrm{c}}(x,r) \quad (20)$$

with

$$M_i=\Phi_{0i}^{0}-S_i'^{\mathrm{p}}(0) \quad (21)$$

$$N_i(x,r,R)=\alpha_i(x,R)I_0(\lambda_i r)+K_0(\lambda_i r). \quad (22)$$

In order to find $B_i(x)$ we use the boundary condition (5). The currents $j_{ri}^{+}(x)$ and $j_{ri}^{-}(x)$ are expressed as follows:

$$j_{ri}^{+}(x)=\frac{\Phi_i(x,r=1)}{4}\mp\frac{D_i}{2}\left.\frac{\partial\Phi_i(x,r)}{\partial r}\right|r=1 \quad (23)$$

Substituting relation (20) into (23) and introducing the result into (5) one obtains an integral equation for $B_i(x)$ of the following general form:

$$B_i(x)=G_i(x)+\beta_i\int_0^{L}B_i(x')\,.\,F(x,x')\mathrm{d}x'. \quad (24)$$

Under certain conditions an approximate solution of this equation may be derived analytically. However, a numerical treatment by means of a digital computer is frequently simpler and speedier.

Now, knowing $B_i(x)$, Eq. (20) allows us to find $\Phi_i(x,r)$.

We may compute the reflected and leakage components separately by applying the superposition

principle which follows from the linearity of the diffusion law (obtained solution) and that of the integral operator (boundary condition (5)).

Since the reflected component is, by definition, independent of the first two terms of the second part of Eq. (20), we may write,

$$\Phi_{bi}(x,r) = N_{bi}(x,r,R) \,.\, B_{bi}(x) + S_{bi}{}'^{c}(x,r) \qquad (25)$$

$$\Phi_{ci}(x,r) = M_i \, e^{-\lambda_i x} + S_i{}'^{p}(x) + N_{ci}(x,r,R) \,.\, B_{ci}(x) + S_{ci}{}'^{c}(x,r). \qquad (26)$$

Eq. (24) hence resolves itself into two similar equations for $B_{bi}(x)$ and $B_{ci}(x)$ respectively.

The computation of the flux inside the channel

The wall of the channel forms a source emitting neutrons towards the interior of the channel. The flux within the channel is hence obtained by integrating the source intensity (neutron current leaving the diffusion medium) over the surface of the wall of the channel.

In the void the neutron flux $\Phi(M)$ at a point M, originating from a surface source S, is given by,

$$\Phi(M) = \int_S j(N) \,.\, f(\mu) \,.\, \frac{1}{\rho^2} \,.\, dS. \qquad (27)$$

Writing out this relation in the case of the configuration of Fig. 5 one obtains,

$$\Phi_i(z) = j_{0i}^{+} \int_0^1 f_1(\mu) \,.\, \frac{1}{\rho_1{}^2} \,.\, 2\pi r \,.\, dr + \int_0^L j_{ri}^{-}(x) \,.\, f_2(\mu) \,.\, \frac{1}{\rho_2{}^2} \,.\, 2\pi \,.\, dx \qquad (28)$$

where $\Phi_i(z)$ is the flux on the channel axis.

Assuming a Fermi angular distribution for neutrons coming from the mouth of the channel, and a cosine distribution for neutrons originating from the channel wall, we find:

$$\Phi_i(z) = \Phi_{ai}(z) + \int_0^L j_{ri}^{-}(x) \,.\, H(x,r) \,.\, dx \qquad (29)$$

with,

$$\Phi_{ai}(z) = \frac{2 j_{0j}^{+}}{1 + \frac{2}{\sqrt{3}}} \left[1 + \frac{\sqrt{3}}{2} - \frac{1}{\left(1 + \frac{1}{z^2}\right)^{1/2}} - \frac{\sqrt{3}/2}{1 + \frac{1}{z^2}} \right] \qquad (30)$$

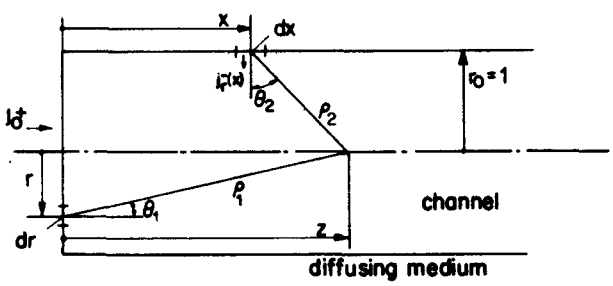

Figure 5. Configuration considered for the calculation of the flux on the channel axis

$$H(x,z) = 2\,[(z-x)^2 + 1]^{-3/2} \qquad (31)$$

Note that Φ_{ai} is the direct contribution to the flux and the integral in the second part of relation (29) gives us the reflected Φ_{bi} and leakage Φ_{ci} contributions, if one replaces j_{ri}^{-} by j_{rbi}^{-} and j_{rci}^{-} respectively.

It remains to indicate how j_{0i}^{+} may be determined. It is clear that the direct and reflected components of the flux in the channel are proportional to j_{0i}^{+}, whereas the leakage component is independent of j_{0i}^{+}. The total flux at the channel mouth may therefore be expressed by the following symbolic relation:

$$\Phi_{0i} = p_i j_{0i}^{+} + q_i j_{0i}^{+} + s_i = (p_i + q_i) j_{0i}^{+} + s_i. \qquad (32)$$

Similar reasoning allows us to express the current leaving the channel j_{0i}^{-} by the following relation:

$$j_{0i}^{-} = u_i j_{0i}^{+} + v_i. \qquad (33)$$

According to diffusion theory we may write:

$$j_{0i}^{+} + j_{0i}^{-} = \tfrac{1}{2} \Phi_0. \qquad (34)$$

The three relations (32), (33) and (34) yield:

$$j_{0i}^{+} = \frac{\frac{1}{2} s_i - v_i}{1 + u_i - \frac{1}{2}(p_i + q_i)}. \qquad (35)$$

The computation of j_{0i}^{+} by means of relation (35) is handicapped by the difficulty of determining the difference between two nearly equal quantities. It is possible, at the price of a small sacrifice in accuracy, to obtain j_{0i}^{+} in a very simple manner. We assume that the current j_{0i}^{+} is equal to the current j_{0i}^{0+} at the same position the channel being absent. Knowing the flux distribution in the diffusing medium without a channel, one may find j_{0i}^{0+} and hence j_{0i}^{+} quite easily.

Application of the method

The choice of a problem

We have used the above method to calculate the thermal neutron flux in the case of channels surrounded by light water.

Two principal reasons have influenced this choice. The first is that in light water sufficiently far from sources, the neutron spectrum attains an equilibrium value, and the thermal neutrons follow the same attenuation law as the fast neutrons. This equilibrium allows us to introduce an important simplification in the calculation of the thermal neutron flux, which consists in considering only one group (thermal), provided that group constants which take proper account of the effect of fast neutrons are employed. The second reason is that the experimental study of the thermal neutron flux in the case of channels surrounded by water can be effected relatively simply in the pool of a swimming pool reactor.

In the equilibrium hypothesis, the expressions for fluxes Φ_b and Φ_c in the water surrounding the channel are written:

$$\Phi_b(x,r) = B_b(x) \left[\frac{K_1(\lambda R)}{I_1(\lambda R)} I_0(\lambda r) + K_0(\lambda r) \right] \qquad (36)$$

$$\Phi_c(x,r) = e^{-\lambda x} + B_c(x)\left[\frac{K_1(\lambda R)}{I_1(\lambda R)} I_0(\lambda r) + K_0(\lambda r)\right] \quad (37)$$

where λ represents the reciprocal of the slowing down length of fast neutrons. These fluxes are normalized with respect to the value of the flux at the position of the channel mouth, the channel being considered absent.

The expressions (36) and (37) are valid in the case of a lattice of parallel channels and for a cell of radius R. In order to obtain the corresponding relations for an isolated channel, one lets the pitch of the lattice tend to infinity; the ratio $K_1(\lambda R)/I_1(\lambda R)$ then tends to zero and the terms in $I_0(\lambda r)$ disappear.

The functions of $B_b(x)$ and $B_c(x)$ are fixed by the following equations valid on the wall of the channel:

$$a_1 B_b(x) = Q(x) + a_2 \int_0^L B_b(x') \,.\, F(x,x') \,.\, dx' \quad (38)$$

$$a_1 B_c(x) = P(x) + a_2 \int_0^L B_c(x') \,.\, F(x,x') \,.\, dx' \quad (39)$$

where $Q(x)$ is given by equation (9), and where,

$$P(x) = \tfrac{1}{4}\left[-e^{-\lambda x} + \int_0^L e^{-\lambda x'} \,.\, F(x,x') \,.\, dx'\right] \quad (40)$$

$$a_1, a_2 = \tfrac{1}{4}\left\{\frac{K_1(\lambda R)}{I_1(\lambda R)}[I_0(\lambda r_0) \mp 2\lambda D I_1(\lambda r_0)] + K_0(\lambda r_0) \pm 2\lambda D K_1(\lambda r_0)\right\} \quad (41)$$

D standing for the thermal neutron diffusion coefficient.

Numerical computation

Case of a single channel

Our study has been applied to two channels of different dimensions, that is:

Channel 1: 5.9 cm in diameter by 170 cm in length;
Channel 2: 12.5 cm in diameter by 250 cm in length.

The value of λ was taken as the reciprocal of the square root of the Fermi age of fission neutrons to thermal energy. From [6] we have $\bar{\tau} = 33$ cm^2; which gives us $\bar{\lambda} = 0.174$ cm^{-1}. For the diffusion coefficient we have taken $\bar{D} = 0.16$ cm [7].

The results of the computations, relating to the thermal flux on the wall as well as inside the channel, are displayed in Figs. 6 and 7 for channel 1 and in Figs. 8 and 9 for channel 2. Note that in Figs. 7 and 9 the fluxes within the channel are scaled to the value of the flux at the channel mouth.

Case of a lattice of channels

We have considered a regular lattice consisting of channels of 6 cm in diameter and 60 cm long. The thermal neutron flux was calculated on the channel wall for varying lattice pitches as follows:

Case	Lattice pitch	Cell radius (R)
1	20 cm	11.28 cm
2	15 cm	8.46 cm
3	12 cm	6.77 cm

The results of the calculations are set out in Figs. 10 and 11.

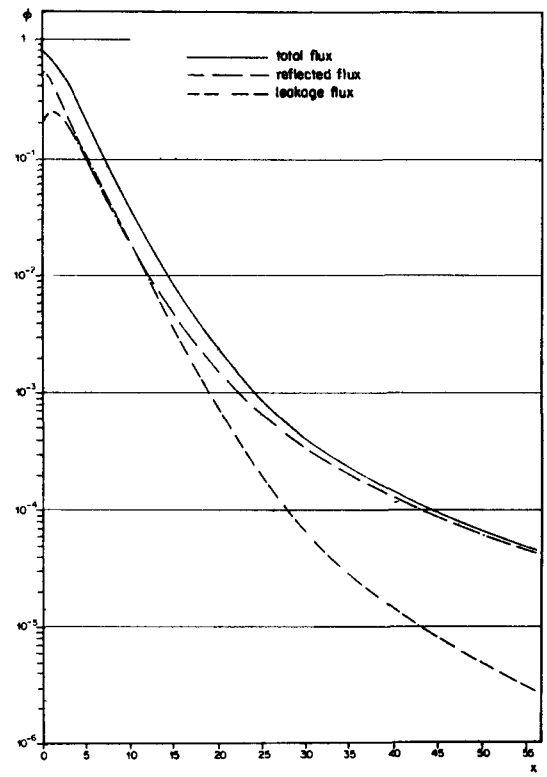

Figure 6. Distribution of thermal flux on the wall of channel 1

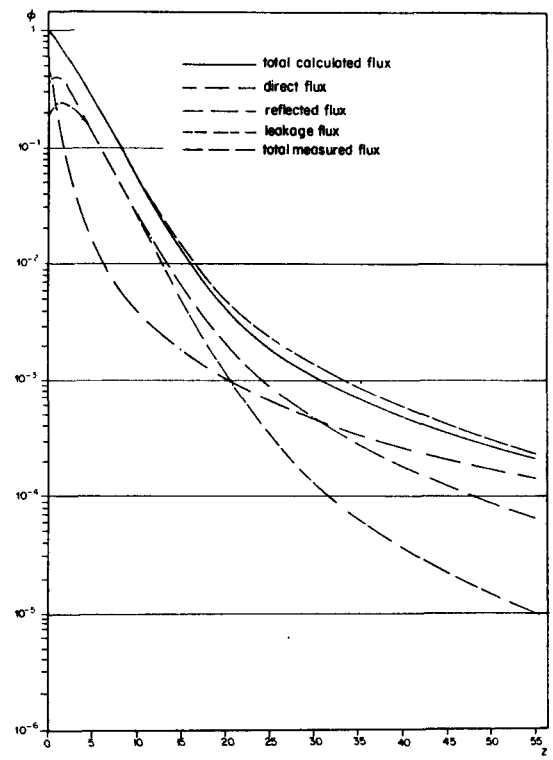

Figure 7. Distribution of thermal flux on the axis of channel 1

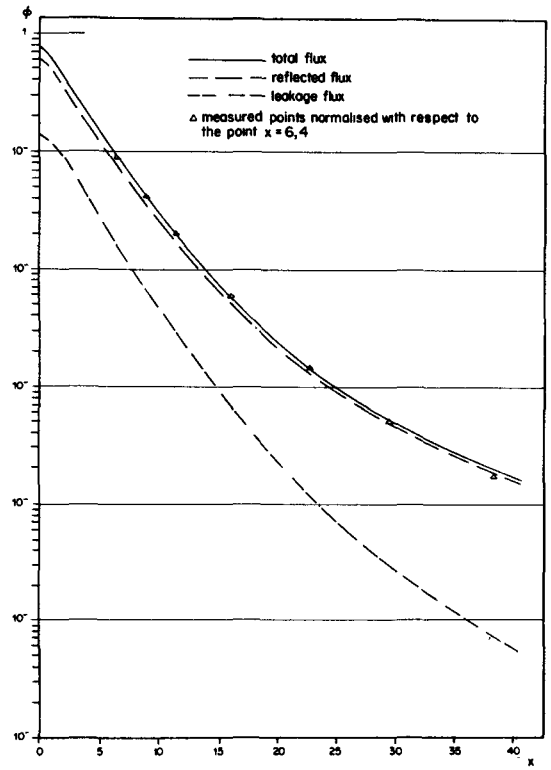

Figure 8. Distribution of thermal flux on the wall of channel 2

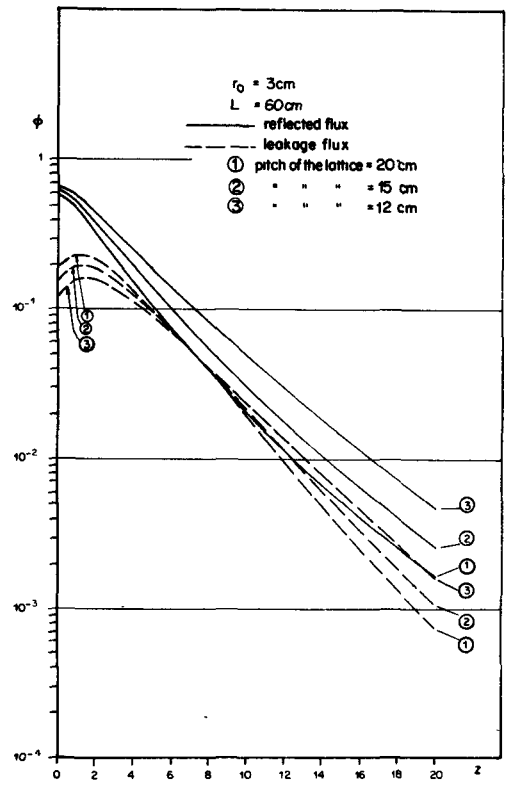

Figure 10. Distribution of thermal flux (reflected and leakage) on the wall of a channel within a lattice of channels

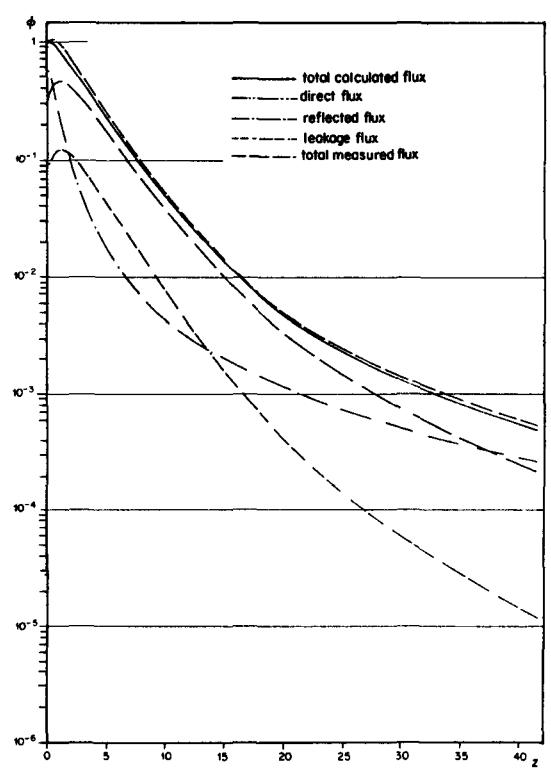

Figure 9. Distribution of thermal flux on the axis of channel 2

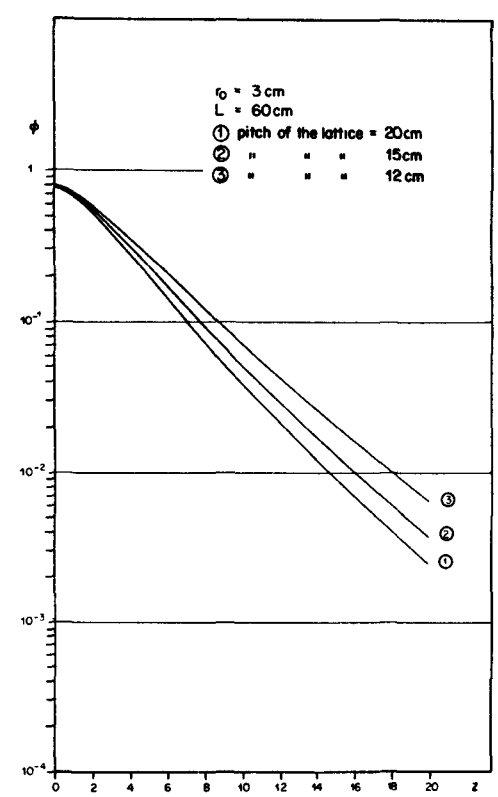

Figure 11. Distribution of thermal flux on the wall of a channel within a lattice of channels

The experimental study

The experimental study relating to channels 1 and 2 were performed in the pool of the swimming pool reactor SAPHIR [8] in order to check the accuracy of the results of the calculations for the single channel case. The reactor core was used as the neutron source. The channel mouth was placed 15 cm from the surface of the core; at this distance the equilibrium between the fast and thermal neutron fluxes is practically attained [9].

The thermal flux was measured by means of Dysprosium detectors inside the channel and by means of a BF_3 counter outside the channel. The totality of measurements performed is described in detail in reference [5].

We have on Figs. 7 and 9 given the thermal fluxes measured within channels 1 and 2; these fluxes are scaled to the value of the flux at the channel mouth. The thermal flux measured on the wall of channel 2 is indicated in Fig. 8. No measurements have been performed as yet upon a lattice of channels.

CONCLUSIONS

Figs. 7, 8 and 9 allow us to make a direct comparison between theoretical and experimental results. This comparison shows a very good agreement between calculated and measured fluxes. The discrepancies are, actually, very small; the maximum discrepancy does not exceed 22% for the flux in channel 1 and 14% for the flux in channel 2. This agreement shows that the suggested method provides very satisfactory results in cases which we have been able to check so far. Furthermore, the necessary computations for the use of this method are not overlong and remain within acceptable limits.

ACKNOWLEDGEMENTS

We wish to thank Professor B. Vittoz, of the Ecole Polytechnique of Lausanne University, and Dr. R. Meier, Head of the Physics Division in our Institute, for their support enabling this work to be carried out, and for the suggestions which they have made. We thank Dr. J. Patry and Mr. G. Burnand, Mr. H. W. Jungen and Mr. J. Keller who, by programming and carrying out machine computations, have greatly helped us. Our thanks are equally due to Mr. H. Winkler and the personnel of the SAPHIR reactor for having eased the work during experiments.

REFERENCES

1. *Formulaire sur le calcul de la protection des réacteurs*, Report C. E. A., No. 2253 (1963).
2. Blizard, E. P., Reactor Handbook, Vol. III, Part B, Shielding, New York (1962).
3. Piercey, C. C., *The Transmission of Thermal Neutrons Along Air Filled Ducts in Water*, AEEW-R-70 (1962).
4. Fermi, E., *Sul moto dei neutroni nelle sostanze idrogenate*, La Ricerca Scientifica VII-2, 13 (1936).
5. Etemad, A., *Etude de la pénétration des neutrons thermiques dans des canaux cylindriques vides traversant un milieu hydrogène*, EIR-Bericht No. 60 (1963).
6. Weinberg, A. M., and Wigner, E. P., *The Physical Theory of Neutron Chain Reactors*, The University of Chicago Press (1958).
7. Price, B. T., Horton, C. C., and Spinney, K. T., *Radiation Shielding*, Pergamon Press (1957).
8. Alder, F., *et al.*, *Description of the Swiss Research Reactors*, RAG-Bericht No. 2 (1957).
9. Pictet, J. M., and Etemad, A., *Bulk Shielding Studies at the Reactor SAPHIR*, EIR-Bericht No. 27 (1962).

ABSTRACT—RÉSUMÉ—АННОТАЦИЯ—RESUMEN

A/688 Suisse

Etude de la pénétration des neutrons dans des canaux cylindriques vides traversant un milieu diffusant

par A. Etemad et J. M. Pictet

Ce mémoire constitue une tentative pour trouver une solution intermédiaire entre, d'une part, les méthodes simples d'évaluation du flux de neutrons thermiques dans des canaux cylindriques droits fournissant généralement des résultats médiocres et, d'autre part, des calculs de Monte-Carlo d'une longueur prohibitive.

Une méthode est élaborée pour la détermination du flux de neutrons thermiques dans un canal dû aux neutrons de toutes énergies émis par une source plane perpendiculaire à l'axe du canal.

Le flux thermique dans le canal est formé de trois composantes: *a*) composante directe; *b*) composante réfléchie; *c*) composante diffusée.

La détermination de la première composante ne présente pas de difficulté. Le problème principal consiste à déterminer les deux autres composantes.

La méthode proposée est basée sur l'application de la théorie du transport à l'intérieur du canal et de la théorie de la diffusion à deux groupes dans le milieu entourant le canal. La liaison entre ces deux théories se fait au moyen d'un choix raisonnable de distributions angulaires pour les neutrons entrant dans le canal.

On suppose qu'il y a équilibre entre les flux rapide et thermique dans le voisinage du canal, ce qui implique la présence d'une quantité suffisante d'hydrogène dans le milieu matériel. Cette hypothèse d'équilibre introduit une simplification importante dans la

méthode en permettant d'effectuer les calculs pour le groupe thermique seulement.

La condition aux limites sur la paroi du canal est satisfaite en établissant un bilan exact des neutrons à chaque point, compte tenu de la réflection multiple des neutrons par le milieu matériel entourant le canal. Cela nous conduit à une équation intégrale de Fredholm dont la résolution constitue la partie la plus importante des calculs numériques.

A titre d'exemple, la méthode est appliquée au cas de canaux entourés par de l'eau.

Afin de vérifier la validité de cette méthode, des mesures du flux thermique sont effectuées au moyen de feuilles de dysprosium, dans des tubes de plexiglas hermétiquement fermés et immergés dans l'eau du bassin du réacteur piscine SAPHIR en utilisant le cœur du réacteur comme source de neutrons.

La comparaison entre les flux calculé et mesuré dans deux canaux de dimensions différentes montre que les résultats théoriques sont en très bon accord avec les résultats expérimentaux. L'écart relatif maximal est de 14% pour un canal de 250 cm de long et de 12,5 cm de diamètre et de 22% pour un canal de 170 cm de long et de 5,9 cm de diamètre. L'atténuation maximale du flux thermique dans ces canaux est respectivement 6.10^{-4} et 2.10^{-4}.

A/688 Швейцария

Проникновение тепловых нейтронов в цилиндрические каналы, проходящие через водородную среду

А. Этемад, Ж. М. Пиктет

Работа представляет собой попытку найти промежуточное решение, с одной стороны, между простыми методами оценки потока тепловых нейтронов в прямых цилиндрических каналах, которые обычно дают посредственные результаты, и расчетами по методу Монте-Карло, с другой стороны, отличающимися непозволительной длительностью.

Разработан метод для определения потока тепловых нейтронов в канале, обусловленного нейтронами различных энергий, испускаемыми плоским источником, перпендикулярным к оси канала.

Тепловой поток в канале образуется тремя составляющими: *а*) прямой составляющей; *b*) составляющей отражения; *с*) составляющей рассеяния.

Определение первой составляющей не представляет затруднений. Основная проблема заключается в определении двух других составляющих. Предложенный метод основан на применении теории переноса внутри канала и двухгрупповой теории рассеяния в среде, окружающей канал. Связь между этими двумя теориями осуществляется с помощью разумного выбора угловых распределений для нейтронов, попадающих в канал.

Допускают, что вблизи канала существует равновесие между потоками быстрых и тепловых нейтронов, что предполагает наличие достаточного количества водорода в среде вещества. Эта гипотеза равновесия вводит важное упрощение в метод, позволяя производить вычисления только для группы тепловых нейтронов.

Граничные условия на стенке канала удовлетворяются путем установления точного нейтронного баланса в каждой точке с учетом множественного отражения нейтронов в среде вещества, окружающего канал. Это приводит к интегральному уравнению Фредхольма, решение которого составляет наиболее важную часть числовых расчетов.

Например, этот метод применим в случае каналов, окруженных водой.

С целью проверки правильности этого метода проводились измерения потока тепловых нейтронов с помощью диспрозиевой фольги в герметически закрытых трубках из плексигласа, которые погружались в воду бассейна погружного реактора SAPHIR, при этом в качестве источника нейтронов использовалась активная зона реактора.

Сравнение потока, вычисленного и измеренного в двух каналах различного размера, показывает, что теоретические результаты очень хорошо согласуются с экспериментальными. Максимальное относительное отклонение составляло 14% для канала длиной 250 *см* и диаметром 12,5 *см* и 22% для канала длиной 170 *см* и диаметром 5,9 *см*.

Максимальное ослабление потока тепловых нейтронов в этих каналах составляет соответственно $6 \cdot 10^{-4}$ и $2 \cdot 10^{-4}$

A/688 Suiza

Penetración de neutrones en canales cilíndricos que atraviesan medios difusores

por A. Etemad y J. M. Pictet

El presente trabajo constituye un intento de encontrar una solución intermedia entre los métodos simples de evaluación del flujo de neutrones térmicos en canales cilíndricos rectos que, en general, dan resultados mediocres, y los cálculos según el método de Monte Carlo que son excesivamente largos.

Se ha estudiado un método para determinar el flujo de neutrones térmicos en un canal, formado por neutrones de todas las energías emitidos por una fuente plana perpendicular al eje del canal.

El flujo térmico en el canal está formado por tres componentes: *a*) componente directa; *b*) componente reflejada; (*c*) componente dispersa.

La determinación de la primera componente no

ofrece dificultad alguna; el problema principal consiste en determinar las otras dos.

El método propuesto se basa en la aplicación de la teoría del transporte en el interior del canal y de la teoría de la difusión de dos grupos en el medio que rodea el canal. Ambas teorías se combinan convenientemente mediante una elección razonable de distribuciones angulares para los neutrones que penetran en el canal.

Se supone que el flujo rápido y el flujo térmico en la proximidad del canal se encuentran en equilibrio, lo que a su vez supone la presencia de una cantidad suficiente de hidrógeno en el medio material. Esta hipótesis de equilibrio introduce una importante simplificación en el método porque permite efectuar los cálculos para el grupo térmico solamente.

La condición de contorno en la pared del canal se satisface estableciendo un balance exacto de los neutrones en cada punto, teniendo en cuenta la reflexión múltiple de los neutrones debida al medio material que envuelve el canal. Esto conduce a una ecuación integral de Fredholm cuya solución constituye la parte más importante de los cálculos numéricos.

A título de ejemplo, los autores aplican el método al case de canales rodeados de agua.

Para verificar la validez de este método, se midió el flujo térmico mediante láminas de disprosio en tubos de plexiglás herméticamente cerrados y sumergidos en el agua de la piscina del reactor SAPHIR, utilizando el núcleo del reactor como fuente neutrónica.

De la comparación entre el flujo calculado y el flujo medido en dos canales de diferentes dimensiones se deduce que los resultados teóricos concuerdan muy satisfactoriamente con los resultados experimentales. La máxima discrepancia relativa es de 14 por ciento para un canal de 250 cm de largo por 12,5 cm de diámetro y de 22 por ciento para un canal de 170 cm de largo por 5,9 cm de diámetro. La atenuación máxima del flujo térmico en dichos canales es de 6×10^{-4} y 2×10^{-4}, respectivamente.

An analytical method for neutron thermalization calculations in heterogeneous reactors

By J. Pop-Jordanov*

It is well known that the use of the diffusion approximation for studying neutron thermalization in heterogeneous reactors may result in considerable errors [1]. On the other hand, more exact numerical methods are rather laborious and require the use of large digital computers. In this paper, the use of the diffusion approximation in absorbing media has been avoided, but the treatment remained analytical, thus simplifying practical calculations.

Theory

Neutron distribution in the moderator

If a moderator is assumed to be without absorption, the heavy gas model in the diffusion approximation gives [1,2]:

$$E\frac{\partial^2\psi(\vec{r},E)}{\partial E^2}+(2-E)\frac{\partial\psi(\vec{r},E)}{\partial E}+l^2{}_0\triangle\psi(\vec{r},E)=0 \quad (1)$$

where

$$\psi(\vec{r},E)=\frac{N(\vec{r},E)}{m(E)}=\frac{\sqrt{\Pi}}{2}\frac{1}{\sqrt{E}}e^{+E}N(\vec{r},E), \quad (2)$$

$l_0=1/(\Sigma_{s1}\sqrt{(3\xi)}$, $N(\vec{r},E)$ —the number of neutrons with energy E at point $\vec{r}$, E —neutron energy in units kT_0, T_0 —temperature of the medium, Σ_{s1} —macroscopic scattering cross section of moderator, ξ —mean logarithmic energy loss per collision of moderator.

The solution of equation (1) for cylindrical symmetry can be sought for as a product of a function depending on r and a function depending on E. Including the particular solution for $n=0$, one gets

$$\psi(r,E)=f(r)+\sum_{n=1}^{\infty}L_n{}^{(1)}(E)\,[c_nK_0(\sqrt{(n)}r/l_0)+c'_nI_0\,(\sqrt{(n)}r/l_0)] \quad (3)$$

where $f(r)$ is the solution of the equation $\triangle f=0$, $L_n{}^{(1)}$ —n^{th} order Laguerre polynomial of the first class, and I_0 and K_0 modified Bessel functions of the first and second kind, of zero order.

In deriving equation (1) it is implicitly assumed that $\xi\neq 0$. With $\xi=0$, one obtains the one-velocity equation instead of equation (1) which is physically natural. On the other hand, $\xi=0$ mathematically corresponds to $n=0$. Taking this into account we shall use for the member $f(r)$ the solution of the complete one-velocity diffusion equation.* The density of neutron sources will be supposed to be Maxwellian with temperature T_0.

The above interpretation of the member $f(r)$ makes it also possible to satisfy the reflective boundary condition at the outer boundary of the cell, which applying the orthogonality of the Laguerre polynomials gives

$$\left[\frac{df(r)}{dr}\right]_{r=R}=0 \quad (4)$$

and

$$c'_n=c_n\frac{K_1(\sqrt{n}\,R/l_0)}{I_1(\sqrt{n}\,R/l_0)},\quad n>0 \quad (5)$$

The use of Maxwellian density of neutron sources and the reflective boundary condition makes the method non-applicable to tightly packed lattices.

The asymptotic case $R\to\infty$ can also be treated [3]. Then one obtains.

$$\psi(r,E)=f(r)+\sum_{n=1}^{\infty}c_nL_n{}^{(1)}(E)K_0\,(\sqrt{(n)}r/l_0)$$

It is evident that at sufficient distances from the fuel, where $r\gg l_0$, the energy distribution of neutron density becomes Maxwellian with $f(r)$ representing the spatial distribution of neutrons in that region. Practically, the asymptotic expression can be applied when $R\gg l_0$.

The boundary condition on the fuel surface

Inside the fuel and on its surface the diffusion approximation may result in large errors. Therefore, we assume that on the fuel surface there is a boundary condition for every neutron energy, which can be determined without using the diffusion approximation

Applying the neutron balance method [4] to the case of a grey cylinder with absorption probability $\Gamma_0=1-\frac{j_+}{j_-}$ (where j_- is the current of incident neutrons and j_+ the current of neutrons scattered out or passed

* Boris Kidrič Institute of Nuclear Sciences, Beograd-Vinča Yugoslavia.

* A further improvement seems to be possible by taking for the zero order member $f(r)$ a non-diffusional solution of the one-velocity equation (for instance in P_3 approximation). Such a procedure seems to be physically reasonable, but yet more rigorous mathematical evidence is necessary.

through without scattering), we obtain the boundary condition on the fuel surface:

$$\lambda=\lambda_0+\frac{4}{3}\left(\frac{1}{\Gamma_0}-1\right)$$

where λ_0 is the boundary condition for a black cylinder. Connecting Γ_0 with escape probability P_0 [5,6] we get:

$$\lambda=\lambda_0+\frac{4}{3}\left[\frac{Q(E)}{\bar{l}_0\Sigma_{a0}(E)}-\frac{1}{2}\right]$$

$\bar{l}_0$ is the mean chord of the volume of the fuel being equal to 2ρ for a cylinder, and $Q(E)=P_0^{-1}(E)-\Sigma_{a0}(E)\bar{l}_0/2$.

Thus, the dependence of λ on neutron energy is expressed through the dependence of P_0 or Q on fuel cross sections. To determine $P_0(E)$ or $Q(E)$ one can use not only the formulae from [5,6], but also any sufficiently exact solution of the one-velocity equation.

The application of the boundary condition $\lambda(E)$

Taking into account the dependence on energy, we have

$$\Sigma_{sl}\left[\frac{N(r,E)}{\frac{\partial N(r,E)}{\partial r}}\right]_{r=\rho}=\lambda(E) \tag{6}$$

Using the expressions (2), (3) and (5) after certain transformations, one gets

$$\sum_{n=0}^{\infty} a_n L_n^{(1)}(E)\lambda^{-1}(E)=1-\sum_{n=1}^{\infty} a_n L_n^{(1)}(E)\, z^{-1}{}_n \tag{7}$$

where

$$a_0=\frac{\Sigma_{sl}f(\rho)}{f'(\rho)} \tag{8}$$

$$a_n=\frac{\Sigma_{sl}}{f'(\rho)}c_n K_0(\sqrt{(n)}\rho/l_0)\,[1+\triangle_n]$$

$$Z_n^{-1}=\sqrt{(3n\xi)}\frac{K_1}{K_0}(\sqrt{(n)}\rho/l_0)\left[\frac{1-\theta_n}{1+\triangle_n}\right]$$

$$\triangle_n=\frac{K_1}{I_1}(\sqrt{(n)}R/l_0)\frac{I_0}{K_0}(\sqrt{(n)}\rho/l_0)$$

$$\theta_n=\frac{K_1}{I_1}(\sqrt{(n)}R/l_0)\frac{I_1}{K_1}(\sqrt{(n)}\rho/l_0)$$

Evidently, in the asymptotic case $R\to\infty$, $\triangle_n$ and θ_n tend to zero.

By integrating Eqs. (7) in energy and using the orthogonality of the Laguerre polynomials, an infinite system of algebraic equations is obtained:

$$\sum_{n=0}^{\infty} a_n\gamma_{nm}=\delta_{0m}-(1-\delta_{0m})\,(m+1)\,Z_m^{-1}\,a_m \tag{9}$$

where

$$\gamma_{nm}=\int_0^{\infty} E e^{-E}L_n^{(1)}(E)L_m^{(1)}(E)\lambda^{-1}(E)\mathrm{d}E$$

The solution of this system gives the coefficients a_n.

All the interesting parameters will later be expressed in terms of a_n.

Fuel disadvantage factor

By definition one has

$$F_f=\frac{\int_0^{\infty}N(\rho,E)\mathrm{d}E}{\int_0^{\infty}N(E)\mathrm{d}E} \tag{10}$$

where the bar means the mean value over the fuel region.

In determining $N(\rho,E)$ we shall assume the distribution of neutrons going in and coming out of the fuel to be isotropic, and in $N(E)$ we shall neglect the slowing down in the fuel. Taking into account the connexion between j_+/j_- and Γ_0, one gets:

$$F_f=\frac{\int_0^{\infty}2(j_-+j_+)\frac{1}{v}\mathrm{d}E}{\int_0^{\infty}(j_--j_+)\frac{S_0}{V_0v\Sigma_{a0}}\mathrm{d}E}=\frac{\int_0^{\infty}j_-\left(1-\frac{\Gamma_0}{2}\right)\frac{1}{v}\mathrm{d}E}{\int_0^{\infty}\frac{1}{\bar{l}_0\Sigma_{a0}}j_-\Gamma_0\frac{1}{v}\mathrm{d}E} \tag{11}$$

On the other hand, connecting $j_-\Gamma_0$ with the distribution in the moderator and using expressions (3) and (6), after some transformations, one obtains

$$j_-\Gamma_0=\frac{v}{3\Sigma_{tr}}\left[\frac{2}{\sqrt{\pi}}\sqrt{E}\,e^{-E}\frac{f'(\rho)}{\lambda(E)}\sum_{n=0}^{\infty}a_nL_n^{(1)}(E)\right] \tag{12}$$

Substituting (12) in (11) one gets

$$F_f=\frac{\sum_{n=0}^{\infty}a_ng_n}{\sum_{n=0}^{\infty}a_nh_n} \tag{13}$$

where

$$g_n=\int_0^{\infty}\phi_n(E)Q(E)\mathrm{d}E,\quad h_n=\int_0^{\infty}\phi_n(E)\mathrm{d}E$$

$$\rho_n(E)=\sqrt{E}\,e^{-E}L_n^{(1)}(E)\lambda^{-1}(E)\,\Sigma^{-1}{}_{a0}(E)$$

The coefficients a_n are determined by Eqs. (9).

Moderator disadvantage factor

By definition one has

$$F_m=\frac{\frac{1}{Vl}\int N(r)\,\mathrm{d}V}{N(\rho)} \tag{14}$$

where integration is spread over the moderator volume V_1.

To determine $N(r)$ expression (3) multiplied by $m(E)$ has to be integrated over the energy. The result is

$$N(r)=f(r)+\sum_{n=1}^{\infty}a_nc_n\left[K_0(\sqrt{(n)}r/l_0)+\frac{K_1}{I_1}(\sqrt{(n)}R/l_0)I_0(\sqrt{(n)}r/l_0)\right] \tag{15}$$

where

$$a_n = \frac{2}{\sqrt{\pi}} \int_0^\infty \sqrt{E}\, e^{-E} L_n^{(1)}(E)\, dE = \frac{1}{\sqrt{\pi}} \frac{\Gamma\left(n+\frac{1}{2}\right)}{n!}$$

Substituting (15) in (14), after integration one gets

$$F_m = \frac{\frac{\bar{f}(r)}{f(\rho)} + \frac{2\rho}{R^2-\rho^2} \frac{l_0}{\sqrt{3\xi}} \frac{1}{a_0} \sum_{n=1}^{\infty} \frac{a_n a_n}{nZ_n}}{1 + \frac{1}{a_0} \sum_{n=1}^{\infty} a_n a_n} \qquad (16)$$

where $\bar{f}(r)$ designates the mean value over the moderator region in the cell.

Mean neutron energy and neutron temperature

By definition one has

$$\bar{E}(r) = \frac{\int_0^\infty E\, N(r,E)\, dE}{\int_0^\infty N(r,E)\, dE}$$

Introducing here expression (3) multiplied by $m(E)$ and integrating, one gets the mean neutron energy at any point of the moderator. For $r=\rho$ this formula gives the mean energy of neutrons on the fuel surface

$$\bar{E}(\rho) = \frac{3}{2} \frac{1 - \frac{1}{a_0} \sum_{n=1}^{\infty} \frac{1}{2n-1} a_n a_n}{1 + \frac{1}{a_0} \sum_{n=1}^{\infty} a_n a_n} \qquad (17)$$

The mean energy over the whole moderator can be obtained from the expression

$$\bar{E} = \frac{\int_\rho^R r\, dr \int_0^\infty E\, N(r,E)\, dE}{\int_\rho^R r\, dr \int_0^\infty N(r,E)\, dE}$$

The integration over E and r gives

$$\bar{E} = \frac{3}{2} \frac{\frac{\bar{f}(r)}{f(\rho)} - \frac{2\rho}{R^2-\rho^2} \frac{l_0}{\sqrt{(3\xi)}} \frac{1}{a_0} \sum_{n=1}^{\infty} \frac{1}{2n-1} \frac{a_n a_n}{nZ_n}}{\frac{\bar{f}(r)}{f(\rho)} + \frac{2\rho}{R^2-\rho^2} \frac{l_0}{\sqrt{(3\xi)}} \frac{1}{a_0} \sum_{n=1}^{\infty} \frac{a_n a_n}{nZ_n}} \qquad (18)$$

The neutron temperature may be defined as:

$$T_n = \frac{2}{3} \bar{E} T_0 \qquad (19)$$

($\bar{E}$ is expressed in units of kT_0).

Introducing here the above expressions one can get the corresponding neutron temperature.

Results of calculation

Comparison with other methods

For comparison we took two typical cells with natural uranium for which calculations and experiments have already been made [7], case D-2: a heavy water lattice with pitch 9.2 cm and radius of the fuel rod 1.27 cm; case C-1: a graphite lattice with pitch 19 cm and radius of the fuel rod 2.13 cm.

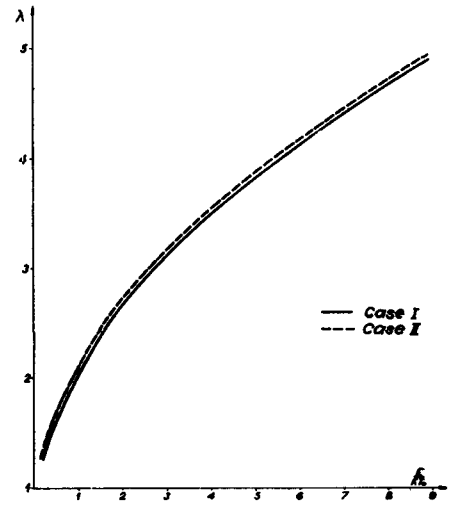

Figure 1. The dependence of the boundary condition $\lambda(E)$ on energy (heavy water lattice D-2)

Case I: P_0 calculated using the formula from [5]; Case II: P_0 calculated using the numerical results from [8]

Calculations for the heavy water system were made in two ways: in the first case for the probability P_0 we used the formula from [5] and in the second case the results of the numerical solution of the one-velocity integral transport equation from [8]. Figure 1 shows the dependence of the boundary condition $\lambda(E)$ on energy in both cases. As can be seen deviation from the constant is considerable. On the other hand both cases give quite close results.

The dependence of the cross sections on energy was calculated from the experimental data [9]. The mean logarithmic energy loss for heavy water was calculated according to the formula for mixture and the effect of chemical bond was taken into account by using the same effective mass of deuterium as that in [7]

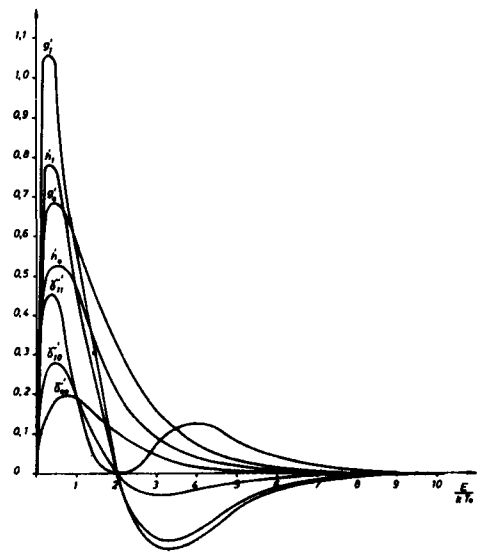

Figure 2. The integrand curves of the zero and first orders (heavy water lattice D-2)

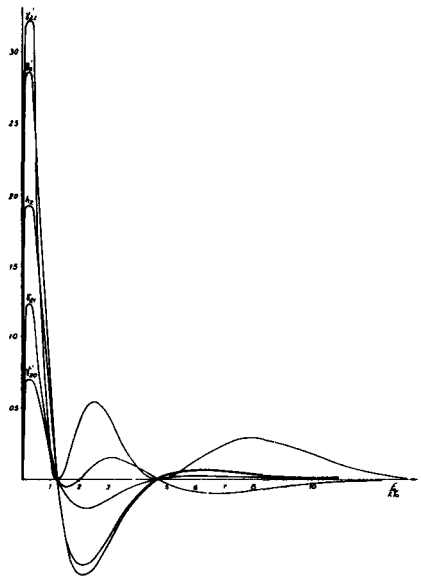

Figure 3. The integrand curves of the second order (heavy water lattice D-2)

($M_D = 3.595$). Coefficients γ_{nm}, g_n and h_n were determined by numerical integration. The integrand curves for the heavy water system are given in Fig. 2. It can be seen that the integrals converge rapidly. Similar graphs have been obtained for the graphite system too.

The results of calculating factors F_f and F_m are shown in Tables 1 and 2, together with results obtained in [7]. For comparison calculations were made according to the equations in [1] (where thermalization was taken into account by the diffusion method) and

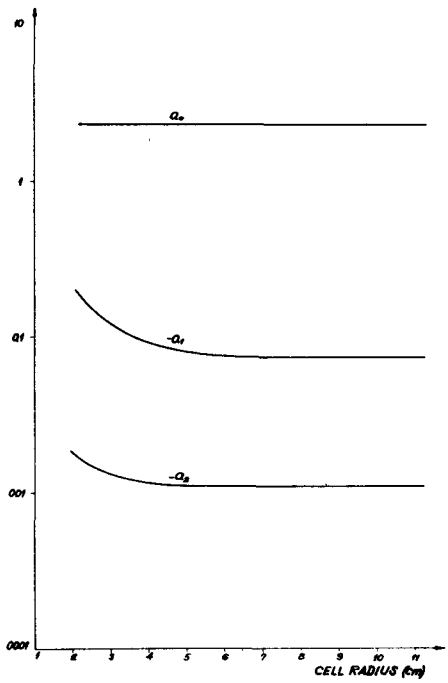

Figure 4. Coefficients a_n for heavy water cells containing a natural uranium 1.27 cm radius fuel rod

Table 1. Fuel and moderator disadvantage factors for the heavy water lattice D-2

One velocity						
	Diffusion theory (P_1)		ABH method [5]		Transport theory [8]	
v m/s	2200	2500	2200	2500	2200	2500
F_f	1.161	1.138	1.224	1.193	1.252	1.218

Including thermalization						
	Galanin's diffusion theory method [1]	Proposed method		Honeck's numerical method [7]		Experiment [7]
		Case I	Case II	$v^* = 3$	$v^* = 4$	
F_f	1.152	1.197	1.210	1.214	1.210	1.198 ±2.5%
F_m		1.349	1.350	1.376	1.371	1.347

according to the one-velocity theory, in diffusion approximation (P_1), according to [5], and according to the numerical solution of the integral transport equation [8]. The one-velocity calculations were made for two mean neutron velocities (2200 and 2500 m/s) so that the effect of choosing the mean velocity could be seen.

Convergency of the method

The above results were obtained with only two members of the series, i.e. $a_n = 0$ for $n \geqslant 2$. To check the convergency of the method directly, we calculated the case D-2 taking into account the third member of the series too. The obtained integrand curves of the second order are shown in Fig. 3 while the results for the coefficients a_n are given in Fig. 4.

As can be seen the coefficients a_n decrease with increasing n which leads to rapid convergency. The result of this is a slight change of the factors F_f, F_m and $T_n(\rho)$. Calculations with three members of the series gives $F_f = 1.198$, $F_m = 1.352$ and $T_n(\rho) = 313\,°\mathrm{K}$, whereas calculations with two members have given 1.197, 1.349 and 310 °K, respectively.

Theoretically, this convergency is contributed by the rapid decrease of the Bessel functions K_0 and K_1 with increasing argument which in our case is proportional to $\sqrt{n}$.

Table 2. Fuel disadvantage factor for the graphite lattice C-1

	One-velocity diffusion theory (P_1)		One-velocity ABH method [5]		Including thermalization			Experiment [7]
	$v = 2200$ m/s	$v = 2500$ m/s	$v = 2200$ m/s	$v = 2500$ m/s	Proposed method	Honeck's numerical method [7] $v^* = 3$	corr.	
F_f	1.418	1.357	1.436	1.366	1.393	1.410	1.369	1.380

Table 3. Fuel, moderator and cell disadvantage factors for the RB lattices

	Lattice pitch (cm)	Proposed method	Experiment [10]
F_f	8.0	1.1907	1.185
	11.3	1.1911	1.185
	15.7	1.1913	1.185
F_m	8.0	1.323	1.288
	11.3	1.397	1.402
	15.7	1.465	1.482
δ	8.0	1.575	1.526
	11.3	1.664	1.661
	15.7	1.745	1.756

Application to the RB reactor

In practice the fuel element cladding is fairly thin and the effects of thermalization in it may be neglected. Thus, although in principle there is no obstacle for the proposed method to be applied to systems with a large number of media, in practice it is sufficient to take the influence of the cladding only in the one-velocity member $f(r)$.

This procedure was used for theoretical analysis of the experiments on the Yugoslav RB reactor (heavy water cells with 1.25 cm radius natural uranium rods in 0.1 cm thick aluminium cladding). Table 3 shows the results of calculating the disadvantage factors for different lattice pitches together with some preliminary experimental values.

CONCLUSION

The proposed method for the calculation of neutron thermalization in heterogeneous reactors is more accurate, but not much more laborious than the diffusion theory methods.

The convergency of the method is satisfactory.

The limitations of the method are: small absorption in the moderator, negligible moderation in the fuel and a sufficiently large lattice pitch. The method is applicable to heavy water and graphite systems, but not to light water systems.

By applying the proposed method formulae have been developed for the determination of thermal utilization and neutron temperature. However, since the method does not imply $1/v$ cross section dependence, it can also be used for the study of long-term reactivity changes.

ACKNOWLEDGEMENT

The author is indebted to A. D. Galanin for his valuable suggestions and to N. Raišić for useful discussions.

REFERENCES

1. Galanin, A. D., Sbornik, Neitronaia fizika, Gosatomizdat, Moskva, pp. 46–55 (1961).
2. Hurwitz, H., Nelkin, M. S., and Habatler, G. I., Nucl. Sci. Eng., *1*, 280 (1956).
3. Pop-Jordanov, J. P., ITEF No. 133, Moskva (January 1963).
4. Bat, G. A., and Zareckij, D. F., Atomnaia Energiia, *4*, 510–519 (1958).
5. Amouyal, A., Benoist, P., and Horowitz, J., J. Nucl. Energy, *6*, 79 (1957).
6. Galanin, A. D., Sbornik, Neitronaia fizika, Gosatomizdat, Moskva, pp. 125–142 (1961).
7. Honeck, H. C., Nucl. Sci. Eng., *8*, 193–209 (1960).
8. Bogdanova, T. D., Kronrod, A. S., and Filler, F. M., ITEF No. 129, Moskva (January 1963).
9. Hughes, L. J., and Schwartz, R. B., *Neutron Cross Sections*, BNL 325 (1958).
10. Takač, S., to be published in Bull. Boris Kidrič Inst. Nucl. Sci.

ABSTRACT—RÉSUMÉ—АННОТАЦИЯ—RESUMEN

A/705 Yougoslavie

Méthode analytique de calcul de la thermalisation des neutrons dans les réacteurs hétérogènes

par J. Pop-Jordanov

Il est bien connu que l'emploi de l'approximation de la diffusion pour l'étude de la thermalisation des neutrons dans les réacteurs hétérogènes peut être une source de fortes erreurs. D'autre part, l'emploi de méthodes précises non fondées sur la diffusion, qui sont numériques et assez complexes, exige l'utilisation de grandes calculatrices numériques. La méthode décrite dans le mémoire, tout en étant analytique, ne comporte pas l'approximation de la diffusion. Cette manière de procéder a permis de mieux comprendre la physique du phénomène et de faciliter les calculs expérimentaux.

Le ralentisseur est étudié sur la base du modèle à gaz lourd; on ne tient pas compte du ralentissement dans le combustible et on admet que la distribution angulaire des neutrons à la surface extérieure du combustible est isotrope. Le facteur non maxwellien de distribution dans le modérateur est exprimé comme étant la somme d'une solution exacte à une seule vitesse et d'une série de polynômes de Laguerre multipliée par les fonctions de Bessel. On a déterminé à la surface du combustible une condition aux limites variables selon l'énergie par la méthode du bilan neutronique sans employer l'approximation de diffusion, et on a rapproché la formule obtenue des proba-

bilités de fuite correspondantes dont la dépendance par rapport à l'énergie est déterminée à partir des données de base sur les sections efficaces. Les conséquences de l'emploi de diverses probabilités de fuite ont été étudiées. On a établi des formules explicites pour calculer les facteurs de «désavantage» du combustible et du ralentisseur, l'énergie moyenne des neutrons et leur température. La concordance des développements s'est révélée satisfaisante. On a adapté la méthode pour des calculs expérimentaux à diverses températures et avec des éléments combustibles cylindriques, y compris les gainages.

Pour vérifier la méthode, on a fait des calculs sur des cellules eau lourde-graphite, à la fois par la méthode de diffusion et par des méthodes plus exactes en tenant compte de la thermalisation et aussi sans en tenir compte. Les résultats obtenus avec la méthode proposée se sont révélés beaucoup plus exacts que ceux obtenus par les méthodes de diffusion, et ils concordent bien avec les résultats calculés et expérimentaux de Honeck. Enfin, on a utilisé la méthode pour procéder à l'analyse théorique d'expériences avec le réacteur yougoslave RB.

A/705 Югославия

Аналитический метод вычисления термализации нейтронов в гетерогенных реакторах

Й. Поп-Йорданов

Известно, что применение диффузионного приближения к изучению термализации нейтронов в гетерогенных реакторах может привести к заметным погрешностям. С другой стороны, более точные недиффузионные методы, которые являются численными и слишком громоздкими, требуют применения больших цифровых вычислительных машин. В настоящей работе отказались от применения диффузионного приближения по отношению к поглощающей среде, причем пользовались аналитическим методом. Такой подход обеспечил как более ясную физическую картину явления, так и более простой способ для практических вычислений.

Замедлитель рассматривался по модели тяжелого газа, замедление в блоке не учитывалось и предполагалось, что угловое распределение нейтронов на границе блока изотропно. Немаксвелловский фактор распределения в замедлителе выражен суммой точного решения односкоростной задачи и ряда из произведений полиномов Лагерра на функции Бесселя. Зависящее от энергии граничное условие на поверхности блока определено, исходя из условия баланса нейтронов, то есть без использования диффузионного приближения, и результат связан с соответствующими вероятностями выхода, энергетическая зависимость которых определяется из основных данных по сечениям. Исследованы эффекты использования различных вероятностей выхода. Выведены формулы для вычисления коэффициента экранировки, коэффициента проигрыша для замедлителя, средней энергии нейтронов и нейтронной температуры. Сходимость разложений оказалась удовлетворительной. Метод приспособлен для практических вычислений с различными температурами и различными цилиндрическими блоками, в том числе и с оболочками.

Чтобы проверить метод, произведены вычисления для случаев тяжеловодных и графитовых ячеек с учетом и без учета термализации как в диффузионном приближении, так и более точными методами. Установлено, что предложенный метод дает результаты заметно точнее, чем диффузионная теория. Эти результаты хорошо совпадают с данными численных расчетов и экспериментальными результатами Гонека. Затем метод был применен к теоретическому анализу экспериментов на югославском реакторе RB.

A/705 Yugoslavia

Un método analítico para cálculos de termalización de neutrones en reactores heterogéneos

por J. Pop-Jordanov

Es bien sabido que el empleo de la aproximación de difusión para el estudio de la termalización en reactores heterogéneos puede conducir a errores considerables. Por otra parte, métodos exactos, al margen de la teoría de difusión, que son métodos numéricos y más bien laboriosos, requieren el uso de grandes calculadoras digitales. En este informe se ha evitado el empleo de la aproximación de difusión en medios absorbentes, pero el tratamiento matemático sigue siendo analítico. Esto permite un conocimiento más claro de la física del fenómeno y una simplificación de los cálculos prácticos.

En el moderador se aplica el modelo de gas pesado, y se desprecia la moderación en el combustible; la distribución angular de los neutrones en la superficie de éste se supone isotropa. El factor no-maxwelliano de distribución en el moderador se expresa como suma de una solución exacta para un grupo de energía y una serie de polinomios de Laguerre multiplicados por funciones de Bessel. Se ha determinado una condición de contorno, dependiente de la energía, en la superficie del combustible por el método del balance neutrónico, sin emplear la aproximación de la difusión, y la fórmula resultante se ha ligado con las correspondientes probabilidades de escape, cuya dependencia energética se determina a partir de las secciones eficaces básicas. Se ha estudiado qué efectos resultan de utilizar diferentes probabilidades de escape y se han deducido fórmulas explícitas para calcular factores de «desventaja» del combustible y del moderador, la energía media neutrónica y la temperatura de los neutrones.

La convergencia de los desarrollos es satisfactoria. Se ha adaptado el método a cálculos prácticos con distintas temperaturas y diferentes elementos combustibles, incluyendo las vainas, cilíndricos.

Para contrastar el método, se calcularon celdas de agua pesada y de grafito utilizando la aproximación de la difusión y otros métodos más exactos, teniendo en cuenta la termalización y sin considerarla. Los resultados del método propuesto son mucho más precisos que los de los métodos de difusión y concuerdan mejor con los resultados numéricos y experimentales de Honeck. Finalmente, se ha utilizado el método para el análisis teórico de los experimentos realizados en el reactor yugoslavo RB.

One-velocity neutron diffusion calculations based on a two-group reactor model

By S. Bingulac, L. Radanović, B. Lazarević and M. Mataušek*

Many processes in reactor physics are described by the energy dependent neutron diffusion equations which for many practical purposes can often be reduced to one-dimensional two-group equations. Though such two-group models are satisfactory from the standpoint of accuracy, they require rather extensive computations which are usually iterative and involve the use of digital computers. In many applications, however, and particularly in dynamic analyses [1], where the studies are performed on analogue computers, it is preferable to avoid iterative calculations. The usual practice in such situations is to resort to one group models, which allow the solution to be expressed analytically. However, the loss in accuracy is rather great particularly when several media of different properties are involved.

This paper describes a procedure by which the solution of the two-group neutron diffusion equations can be expressed analytically in the form which, from the computational standpoint, is as simple as the one-group model, but retains the accuracy of the two-group treatment. In describing the procedure, the case of a multi-region nuclear reactor of cylindrical geometry is treated, but the method applied and the results obtained are of more general application.

Another approach in approximate solution of diffusion equations, suggested by Galanin [2] is applicable only in special ideal cases.

STATEMENT OF THE PROBLEM

The one-dimensional, two-group approximation of the radial flux distribution in a multi-region nuclear reactor [3] results in the following set of diffusion equations in vector notation:

$$\begin{Vmatrix} \nabla^2 - a_{11}^i & a_{12}^i \\ a_{21}^i & \nabla^2 - a_{22}^i \end{Vmatrix} \cdot \begin{Vmatrix} F^i(r) \\ N^i(r) \end{Vmatrix} = \|A^i\| \overrightarrow{Q^i(r)} = 0 \qquad (1)$$

which describe the fast and thermal flux $F^i(r)$, $N^i(r)$ in the ith region, defined by the interval:

$$R_{i-1} \leqslant r < R_i \quad i = 1,2, \ldots I \qquad (2)$$

I being the number of reactor regions.

Coefficients a_{nm}^i of the matrix $\|A^i\|$ are determined by the material and geometrical constants of the ith reactor region.**

The solution $\overrightarrow{Q^i(r)}$ of Eq. (1) is subject to the following conditions:

(a) at the centre of the reactor $r = R_0 = 0$

$$\frac{\mathrm{d}}{\mathrm{d}r} \overrightarrow{Q^1(0)} = \frac{\mathrm{d}}{\mathrm{d}r} \overrightarrow{Q_0^1} = 0 \qquad (3)$$

(b) at the extrapolated boundary of the reactor; $r = R_I$

$$\vec{Q}^I(R_I) = \overrightarrow{Q_I^I} = 0$$

(c) at the interface between any two regions; $r = R_i$

$$\begin{Vmatrix} D^i \end{Vmatrix} \frac{\mathrm{d}}{\mathrm{d}r} \vec{Q}_i^i = \begin{Vmatrix} D^{i+1} \end{Vmatrix} \frac{\mathrm{d}}{\mathrm{d}r} \vec{Q}_i^{i+1}$$

$$\vec{Q}_i^i = \vec{Q}_i^{i+1}$$

where $\vec{Q}_i^{i+1} = \vec{Q}^{i+1}(R_i)$, and

$$\begin{Vmatrix} D^i \end{Vmatrix} = \begin{Vmatrix} D_f^i & 0 \\ 0 & D_n^i \end{Vmatrix}$$

D_f^i and D_n^i being diffusion coefficients for the fast and thermal group in the region i.

The problem thus formulated requires iterative adjustment of two parameters to satisfy the boundary conditions. In most cases these two parameters are:

(a) ratio of the fast and thermal flux at the centre of the reactor; $q_0 = F_0^1 / N_0^1$, and

(b) the thickness of one of the regions; i.e. $r = R_k$, between regions k and $k+1$.

The usual procedure in solving such a problem consists of representing the solution of the two mutually coupled Eqs. (1) as a linear combination of solutions of homogeneous equations in the form:

$$\overrightarrow{Q^i(r)} = \|B^i\| \overrightarrow{W^i(r)} = \begin{Vmatrix} b_{11}^i & b_{12}^i \\ b_{21}^i & b_{22}^i \end{Vmatrix} \cdot \begin{Vmatrix} X^i(r) \\ Y^i(r) \end{Vmatrix} \qquad (4)$$

where for cylindrical geometry $X^i(r)$ and $Y^i(r)$, coordinates of vector $\overrightarrow{W^i(r)}$, are solutions of [3]:

$$(a) \quad \frac{\mathrm{d}^2}{\mathrm{d}r^2} X^i(r) + \frac{1}{r} \cdot \frac{\mathrm{d}X^i(r)}{\mathrm{d}r} + \mu_i^2 i X^i(r) = 0$$

$$(b) \quad \frac{\mathrm{d}^2}{\mathrm{d}r^2} Y^i(r) + \frac{1}{r} \cdot \frac{\mathrm{d}Y^i(r)}{\mathrm{d}r} - \nu_i^2 Y^i(r) = 0 \qquad (5)$$

* Boris Kidrič Institute of Nuclear Sciences, Beograd-Vinča.

** See Appendix.

while the initial and boundary conditions (3) take the form:

$$(a)\ \text{at } r=R_0\text{: } \frac{\mathrm{d}}{\mathrm{d}r}\overrightarrow{W_0{}^1}=0$$

$$(b)\ \text{at } r=R_I\text{: } \overrightarrow{W_I{}^I}=0$$

$$(c)\ \text{at } r=R_i\text{: } \overrightarrow{W_1{}^{i+1}}=\|G^i\|\cdot\overrightarrow{W_i{}^i}$$

$$\frac{\mathrm{d}}{\mathrm{d}r}\overrightarrow{W_i{}^{i+1}}=\|H^i\|\cdot\frac{\mathrm{d}}{\mathrm{d}r}\overrightarrow{W_i{}^i} \qquad (6)$$

where $\|G^i\|=\|B^{i+1}\|^{-1}\cdot\|Bi\|$, and

$$\|H^i\|=[\|D^{i+1}\|\cdot\|B^{i+1}\|]^{-1}\cdot\|D^i\|\cdot\|B^i\|$$

The formulae for calculating elements $b^i{}_{nm}$ of the matrix $\|B^i\|$ are given in the Appendix.

Appropriate values of initial conditions for Eq. (5) are then sought by iterative adjustment of the two variable parameters using a digital computer [4].

TRANSFORMATION INTO RICCATI EQUATIONS

To avoid iterative computation it is necessary to formulate the problem in such a way that the two variable parameters can be determined separately. This suggests the use of first order equations with appropriate conditions that can be satisfied by adjusting one parameter. Since in most practical cases the nature of the diffusion process is such that there is always one point in the reactor where either the flux or its derivative is zero, we may try the substitution:

$$U^i(r)=\frac{\mathrm{d}X^i(r)}{\mathrm{d}r}\cdot\frac{1}{X^i(r)}$$

$$V^i(r)=\frac{\mathrm{d}Y^i(r)}{\mathrm{d}r}\cdot\frac{1}{Y^i(r)} \qquad (7)$$

which will eliminate the initial ratio of the fast and thermal flux as a variable parameter.

Introducing substitution (7) into Eqs. (5) one obtains [5]:

$$(a)\quad \frac{\mathrm{d}U^i(r)}{\mathrm{d}r}+[U^i(r)]^2+\frac{U^i(r)}{r}+\mu_i{}^2=0$$

$$(b)\quad \frac{\mathrm{d}V^i(r)}{\mathrm{d}r}+[V^i(r)]^2+\frac{V^i(r)}{r}-\nu_i{}^2=0 \qquad (8)$$

Using substitution (7) and designating $Y_i{}^i/X_i{}^i$ by $Z_i{}^i$, boundary and initial conditions (6) become:

(a) at $r=R_0=0$: $U^1(0)=U_0{}^1=0$; $V_0{}^1=0$

(b) at $r=R_I$: $[U_I{}^I]^{-1}=0$; $[V_I{}^I]^{-1}=0$

$$(c)\ \text{at } r=R_i\text{: } U_i{}^{i+1}=\frac{h_{11}{}^iU_i{}^i+h_{12}{}^iV_i{}^iZ_i{}^i}{g_{11}{}^i+g_{12}{}^iZ_i{}^i}$$

$$V_i{}^{i+1}=\frac{h_{21}{}^iU_i{}^i+h_{22}{}^iV_i{}^iZ_i{}^i}{g_{21}{}^i+g_{22}{}^iZ_i{}^i} \qquad (9)$$

The original Bessel Eqs. (5) are thus transformed into Riccati Eqs. (8) which are of the first order.

EXHIBITED PROPERTIES OF RICCATI EQUATIONS

As can be seen from Eqs. (9) the initial values of $U^i(r)$ and $V^i(r)$ at the centre of the reactor do not depend on the initial values $F_0{}^1$ and $N_0{}^1$. As a result, $U^i(r)$ and $V^i(r)$ are independent of the parameter q_0, and the original problem of iterative adjustment of two parameters has now been reduced to finding only the critical radius R_k. As a further consequence of Eqs. (9) the values of $U^i(r)$ and $V^i(r)$ are completely specified both at the centre of the reactor and at the extrapolated boundary.

Another valuable property [5] exhibited by Eq. (8b) is that its solutions can be represented by the following asymptotic expression:

$$V_j{}^i=\nu_i\,[-(2R_j\nu_i)^{-1}+(-1)^{(i+j)}\times\sqrt{1+(2R_j\nu_i)^{-2}}] \qquad (10)$$

which follows from the fact that the value of $V^i(r)$ at one end of the reactor region is independent of the initial value at the other end if the thickness of the region is sufficiently large. In other words, values $V_j{}^i$ are dependent only on the coefficient ν_i and corresponding radius R_j.

As will be seen later, it is now possible by solving Eqs. (8), starting both from the centre ($i=1$) and from the extrapolated boundary ($i=\mathrm{I}$) and using conditions in Eq. (9c), to reduce the total number of regions to only two, and find the critical radius R_k which will satisfy conditions in Eqs. (9).

DERIVATION OF THE ANALYTICAL EXPRESSION FOR THE FLUX EQUATION

Owing to the previous transformations it is possible to determine the critical radius and the coefficients

$$Z_j{}^i,\ V_j{}^i \text{ and } U_j{}^i \qquad (11)$$

for all regions and radii.

Taking into account that the values of function $Y^i(r)$ and its derivatives $\mathrm{d}Y^i(r)/\mathrm{d}r$ at both boundaries $r=R_j$ of each region can be expressed as

$$Y_j{}^i=X_j{}^iZ_j{}^i$$

$$\frac{\mathrm{d}}{\mathrm{d}r}Y_j{}^i=X_j{}^iV_j{}^iZ_j{}^i \qquad (12)$$

where $j=i-1$ and i for the left and right boundary, respectively, and that the values $X_j{}^i=X^i(R_j)$ may be obtained by solving the one-group diffusion equation:

$$\frac{\mathrm{d}^2X^i(r)}{\mathrm{d}r^2}+\frac{1}{r}\frac{\mathrm{d}X^i(r)}{\mathrm{d}r}+X^i(r)\cdot\mu_i{}^2=0 \qquad (13)$$

with known ratio of initial conditions:

$$\frac{\mathrm{d}X_j{}^i}{\mathrm{d}r}\cdot\frac{1}{X_j{}^i}=U_j{}^i, \qquad (14)$$

it remains only to determine the function $Y^i(r)$ within the boundaries of each region.

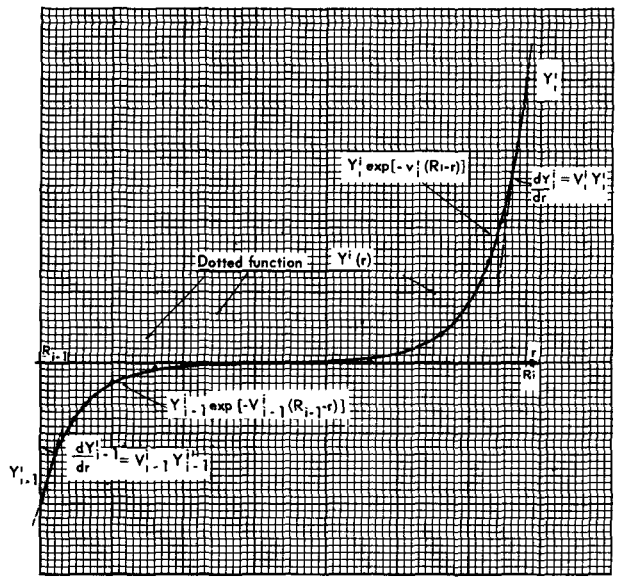

Figure 1. Typical form of function $Y^i(r)$ with two corresponding exponential functions

From Eq. (4) the thermal flux is given as:

$$N^i(r) = b_{21}{}^i X^i(r) + b_{22}{}^i Y^i(r) \tag{15}$$

A typical form of the function $Y^i(r)$ obtained by solving Eq. (8*b*) on an analogue computer is shown in Fig. 1. Taking into account Fig. 1 and using the exact values $Y_j{}^i$ and $\mathrm{d}Y_j{}^i/\mathrm{d}r$, the functions $Y^i(r)$ may be approximated by two exponential functions in the following way:

$$Y^i(r) \approx X^i{}_{i-1} Z^i{}_{i-1} \exp\left[-V^i{}_{i-1}(R_{i-1} - r)\right] + X_i{}^i Z_i{}^i \exp\left[-V_i{}^i(R_i - r)\right] \tag{16}$$

For comparison, these two exponential functions are also represented in Fig. 1.

Due to the fact that boundary values $Y_j{}^i$ are maximum and that these values are known exactly with their derivatives at these points, errors due to approximation are negligible. Thus, using Eqs. (12) and (15) the thermal flux distribution can be expressed as:

$$N^i(r) = b_{21}{}^i X^i(r) + b_{22}{}^i X_i{}^i Z_i{}^i \exp\left[-V_i{}^i(R_i - r)\right] + b_{22}{}^i X^i{}_{i-1} Z^i{}_{i-1} \exp\left[-V^i{}_{i-1}(R_{i-1} - r)\right] \tag{17}$$

NORMALIZATION OF RICCATI EQUATIONS

Instead of determining coefficients

$$Z_j{}^i,\ V_j{}^i \text{ and } U_j{}^i \tag{18}$$

by solving Riccati Eqs. (8) for each particular set of reactor parameters, it is possible to use a series of curves which represent the solutions of normalized Riccati equations, obtained once and for all [6].

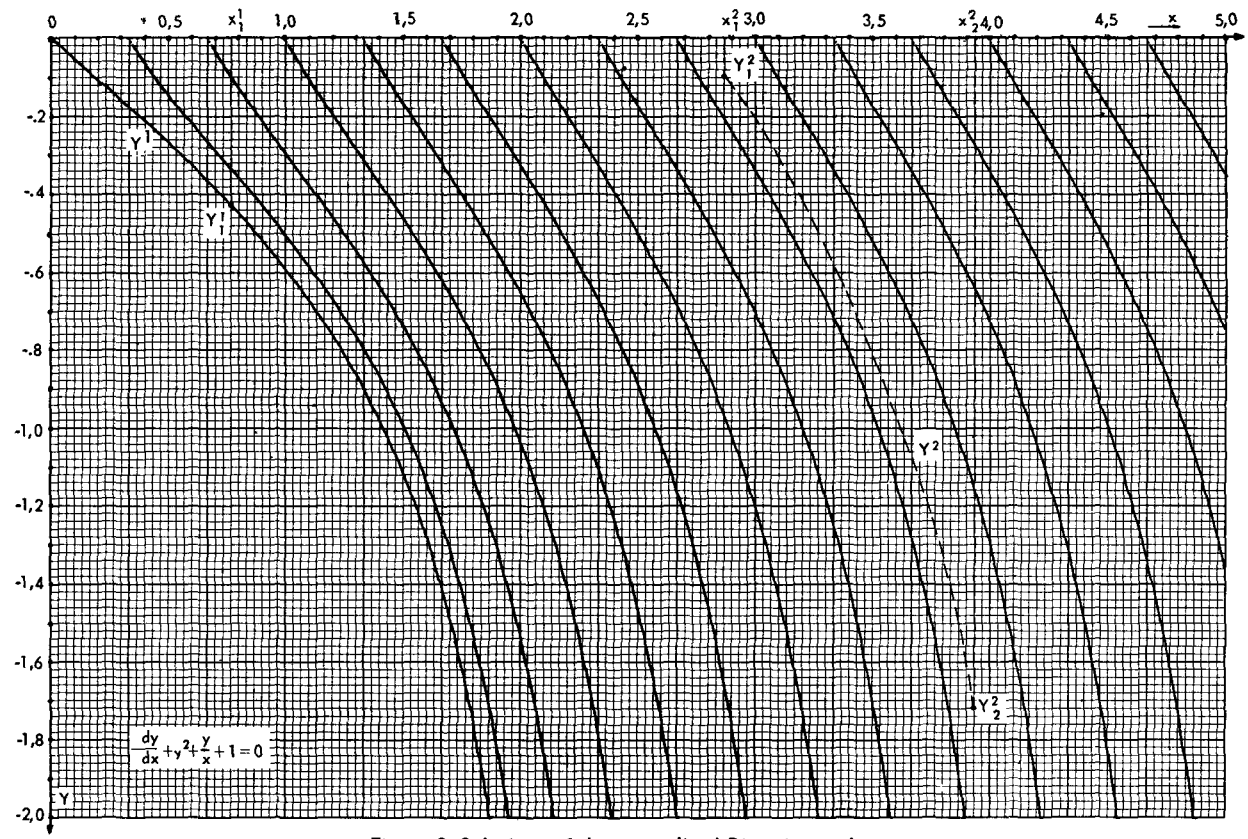

Figure 2. Solutions of the normalized Riccati equation

$$\frac{\mathrm{d}y}{\mathrm{d}x} + y^2 + \frac{y}{x} + 1 = 0$$ for different initial conditions

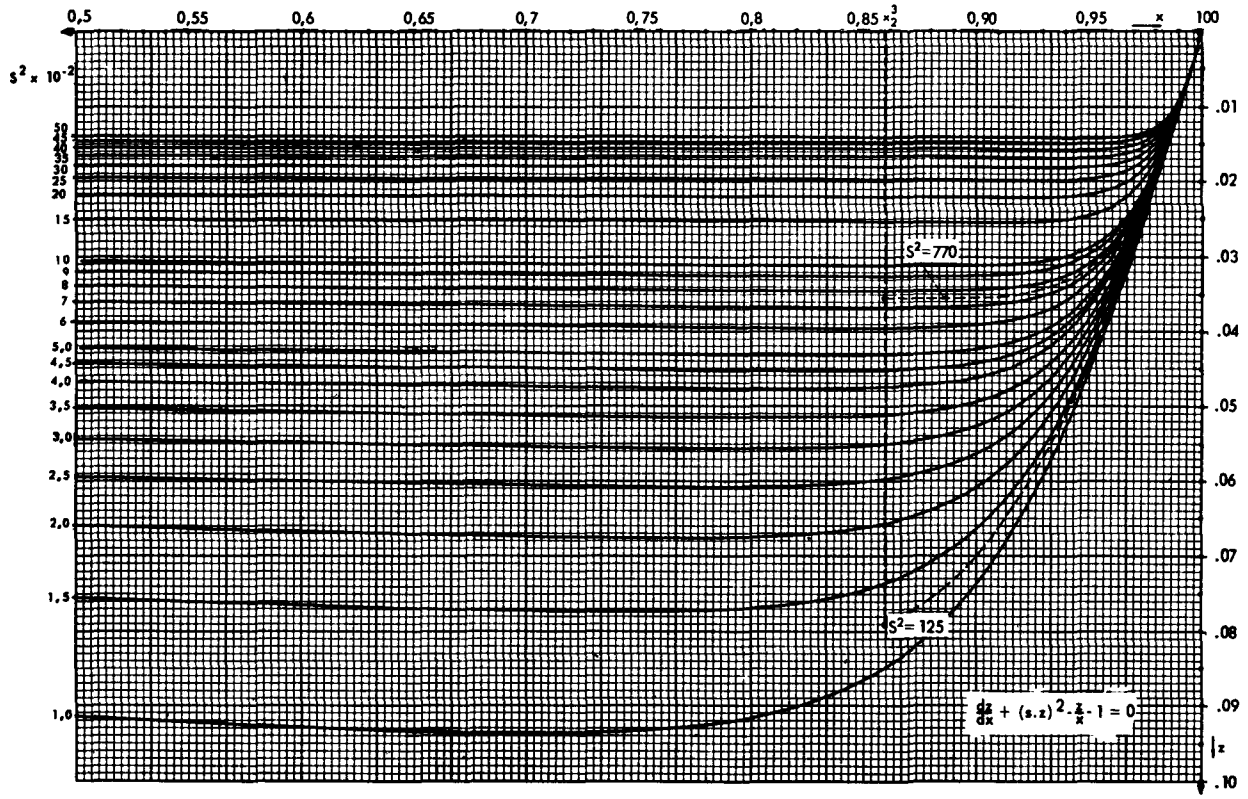

Figure 3. Solutions of the normalized Riccati equation

$\frac{dz}{dx} + (s \cdot z)^2 - \frac{z}{x} - 1 = 0$, for various s. (Initial conditions: $x = 1$, $z = 0$)

To normalize Eq. (8*a*) we introduce the substitutions:

$$U^i(r) = y^i(x) \cdot \mu_i \text{ and } r = \frac{x}{\mu_i} \tag{19}$$

and obtain:

$$\frac{dy^i(x)}{dx} + [y^i(x)]^2 + \frac{y^i(x)}{x} + 1 = 0 \tag{20}$$

The solutions $y^i(x)$ for different values of $y_j{}^i = y^i(x_j{}^i)$ and $x_j{}^i = R_j \cdot \mu_i$, obtained on an analogue computer are shown in Fig. 2. Figure 3 represents the solutions $z(x)$ of the normalized equation

$$\frac{dz(x)}{dx} + [s \cdot z(x)]^2 - z(x)/x - 1 = 0 \tag{21}$$

for various s, which are necessary for $i = I$ (last region).

In deriving Eq. (21) we used substitutions:

$$z(x) = \frac{1}{R_I U^I(r)},\ z(x) = \frac{1}{R_I V^I(r)},\ x = \frac{r}{R_I} \tag{22}$$

The procedure of determining coefficients (18) using Figs. 2 and 3 is explained in the given example.

CONCLUSION

As has been shown, all coefficients appearing in Eq. (17) may be easily determined from material and geometrical constants of the given reactor using simple formulae and the family of curves shown in Figs. 2 and 3. Since these formulae and curves are derived from a two-group reactor model, the accuracy attainable with Eq. (17) approaches that of the two-group treatment.

On the other hand, since, in addition to the two exponential functions, Eq. (17) contains only the function $X^i(r)$ which is a solution of the one-group reactor model, it can be concluded that the simplicity of analytical treatment of Eq. (17) is compatible with one-group approximation.

EXAMPLE

To illustrate the practical application of this procedure consider a gas-cooled power reactor with two active zones and one reflector. Values of the material constants for all regions are given in Table 1:*

Table 1

	$i=1$	$i=2$	$i=3$
$\Sigma_f{}^i \cdot 10^3$	2.5058	2.9158	2.9112
$\Sigma_n{}^i \cdot 10^3$	5.3793	3.6946	0.3561
$D_f{}^i$	1.7042	1.5253	1.15596
$D_n{}^i$	1.3651	1.2123	0.9119
$k_\infty{}^i$	1.0282	1.0815	0.0000

* Symbols used are the same as in Ref. [3].

The geometrical constants are:

axial buckling $\alpha_z^2 = 0.2486 \cdot 10^{-4}$

The radius between the first and second region $r = R_1$ is unknown.

Other radii are: $R_2 = 472$ cm

$R_3 = 550$ cm

Matrices $\|a_{nm}{}^i\|$ from Eq. (1) may be found using given material and geometrical constants of the reactor. These matrices are:

Table 2

	$i=1$		$i=2$		$i=3$	
$10^{+3}\|a_{nm}{}^i\|$	−1.495	3.241	−1.912	2.618	−2.543	0.000
	1.841	−3.932	2.403	−3.096	3.193	−0.415

Matrices $\|B^i\|$ which transform diffusion equations into the Bessel equations, Eq. (4), are:

Table 3

	$i=1$		$i=2$		$i=3$	
$\|B^i\|$	1.000	1.000	1.000	1.000	0.000	1.000
	0.462	1.223	0.765	1.201	1.000	1.523

Arguments of Bessel functions (3) become:

Table 4

	$i=1$	$i=2$	$i=3$
$\mu_i^2 \cdot 10^{+3}$	0.00495	0.06915	−2.54238
$\nu_i^2 \cdot 10^{+3}$	5.46615	5.08442	0.41537

Matrices $\|G^i\|$ and $\|H^i\|$ which define conditions at the interface between any two regions may be determined using Eqs. (4) and (6). These matrices are:

Table 5

	$i=1$		$i=2$	
$\|G^i\|$	0.8457	−0.0113	1.0000	1.0000
	0.1536	1.1132	2.2659	0.2993
$\|H^i\|$	0.9475	−0.0193	1.3193	1.3193
	0.1698	1.1367	2.9952	0.3854

From Fig. 3, which gives the values of $U^I{}_{I-1}$ and $V^I{}_{I-1}$, we may for $x_2{}^3 = R_2/R_3 = 0.861$, determine:

(*a*) $s^2 = R_3{}^2\mu_3{}^2 = 125$

$$z = (U_2{}^3 \cdot R_3)^{-1} = 3.5 \cdot 10^{-2}$$

(*b*) $s^2 = R_3{}^2\nu_3{}^2 = 770$

$$z = (V_2{}^3 \cdot R_3)^{-1} = 7.91 \cdot 10^{-2} \quad (23)$$

From Eq. (10): $V_2{}^2 = 0.07024$

Knowing $U_2{}^3$; $V_2{}^3$ and $V_2{}^2$ using Eq. (9*c*), which represent a system of two algebraic equations with two unknowns, we find:

$$Z_2{}^2 = -0.2273$$
$$U_2{}^2 = \quad 0.01423 \quad (24)$$

According to Eq. (10) for $300\text{ cm} \leq r = R_1 < 350$ cm we have:

$$V_1{}^1 = \quad 0.07191 \pm 1.2 \cdot 10^{-3}$$
$$V_1{}^2 = -0.07152 \pm 1.2 \cdot 10^{-3} \quad (25)$$

Value $y_2{}^2 = U_2{}^2\mu_2 = 1.71$ defines one end point of the solution $y^i(x^i)$, which corresponds to $x_2{}^2 = 3.92$ ($i = 2$ and $r = R_2$). Also, $U_0{}^1 = 0$ and $r = R_0$, Eq. (9*a*), defines one end point $(y_0{}^1; x_0{}^1 = 0; 0)$ for the first region ($i = 1$).

Other end points $(y_1{}^1, x_1{}^1)$ and $(y_1{}^2, x_1{}^2)$ of these functions have to satisfy the following conditions:

(*a*) $R_1 = x_1{}^1/\mu_1 = x_1{}^2/\mu_2$, and

$$(b)\quad U_1{}^1 = \frac{g_{11}{}^1}{h_{11}{}^1} U_1{}^2 + \frac{g_{21}{}^1 h_{12}{}^1}{g_{22}{}^1 h_{11}{}^1} \cdot V_1{}^1 \left[1 - \frac{h_{22}{}^1 V_1{}^1}{g_{22}{}^1 V_1{}^2}\right]^{-1} \quad (26)$$

Condition (26*b*) is derived eliminating $Z_1{}^1$ from Eq. (9*c*) and taking into account the relations:

$$\frac{h_{12}{}^1 h_{21}{}^1}{h_{11}{}^1 h_{22}{}^1} \ll 1 \quad \frac{g_{12}{}^1 g_{21}{}^1}{g_{11}{}^1 g_{22}{}^1} \ll 1$$

Using calculated $V_1{}^1$ and $V_1{}^2$ and curves in Fig. 2 from conditions (26) we get

$$U_1{}^1 = y_1{}^1\mu_1 = -0.915 \cdot 10^{-3}$$
$$U_1{}^2 = y_1{}^2\mu_2 = -0.847 \cdot 10^{-3} \quad (27)$$

and consequently the critical radius is

$$r = R_1 = \frac{x_1{}^1}{\mu_1} = \frac{x_1{}^2}{\mu_2} = 343 \text{ cm}.$$

From Eq. (9*c*) we may now determine

$$Z_1{}^1 = -0.113525$$

Using Eq. (6*c*) it may be shown that the ratio $Z_1{}^2 = Y_1{}^2/X_1{}^2$ is as follows:

$$Z_1{}^2 = \frac{g_{21}{}^1 + g_{22}{}^1 Z_1{}^1}{g_{11}{}^1 + g_{12}{}^1 Z_1{}^1} = 0.0468 \quad (28)$$

Finally, according to Eq. (17) and curves 2 and 3, the thermal flux distribution through active regions may be approximated with the expression:

$$N^i(r) = \begin{cases} N^1(r) & \text{for } R_0 \leq r < R_1 \\ N^2(r) & \text{for } R_1 \leq r < R_2 \end{cases} \quad (29)$$

where $N^i(r)$ is given with Eq. (15).

It should be pointed out that the radial distribution of fast flux $F^i(r)$ may also be similarly obtained, if required. Figure 4 represents thermal and fast flux distributions, obtained by the proposed method.

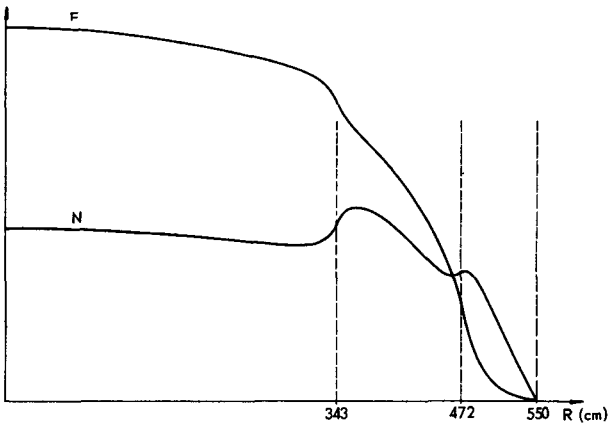

Figure 4. Thermal and fast flux distribution obtained by the proposed method

As has been explained earlier all constants

$$Z_j^i,\ U_j^i,\ V_j^i,\ b_{nm}^i \qquad \begin{matrix} i=1,\ 2,\ \ldots\ I. \\ j=1-1,\ i. \\ n,\ m=1,\ 2. \end{matrix}$$

may be easily determined using the obtained family of curves and the set of formulae derived in the paper and appendix.

APPENDIX

Review of the formulae which are used in the determination of the coefficients a_{nm}^i, b_{nm}^i, μ_i, ν_i, g_{nm}^i and h_{nm}^i.

$$\frac{b_{21}^i}{b_{11}^i} = \frac{1}{2a_{12}^i}\left[a_{11}^i - a_{22}^i + \sqrt{[(a_{11}^i - a_{22}^i)^2 + 4a_{12}^i\, a_{21}^i]}\ \right]$$

$$\frac{b_{22}^i}{b_{12}^i} = \frac{1}{2a_{12}^i}\left[a_{11}^i - a_{22}^i - \sqrt{[(a_{11}^i - a_{22}^i)^2 + 4a_{12}^i\, a_{21}^i]}\ \right]$$

Two of four b_{nm}^i may be chosen arbitrarily.

$$\mu_i^2 = a_{11}^i - a_{12}^i \frac{b_{21}^i}{b_{11}^i} = a_{22}^i - a_{21}^i \frac{b_{11}^i}{b_{21}^i}$$

$$\nu_i^2 = a_{11}^i - a_{12}^i \frac{b_{22}^i}{b_{12}^i} = a_{22}^i - a_{21}^i \frac{b_{12}^i}{b_{22}^i}$$

$$\|G^i\| = \|g_{nm}^i\| = \frac{1}{|B^{i+1}|}\begin{Vmatrix} b_{11}^i b_{22}^{i+1} - b_{21}^i b_{12}^{i+1} & b_{12}^i b_{22}^{i+1} - b_{22}^i b_{12}^{i+1} \\ b_{21}^i b_{11}^{i+1} - b_{11}^i b_{21}^{i+1} & b_{22}^i b_{11}^{i+1} - b_{12}^i b_{21}^{i+1} \end{Vmatrix}$$

$$\|H^i\| = \|h_{nm}^i\| = \frac{1}{|B^{i+1}|}\begin{Vmatrix} p_f^i b_{11}^i b_{22}^{i+1} - p_n^i b_{21}^i b_{12}^{i+1} & p_f^i b_{12}^i b_{22}^{i+1} - p_n^i b_{22}^i b_{12}^{i+1} \\ p_n^i b_{21}^i b_{11}^{i+1} - p_f^i b_{11}^i b_{21}^{i+1} & p_n^i b_{22}^i b_{11}^{i+1} - p_f^i b_{12}^i b_{21}^{i+1} \end{Vmatrix}$$

where $p_f^i = D_f^i / D_f^{i+1}$, $p_n^i = D_n^i / D_n^{i+1}$, and

$$|B^i| = \det \|B^i\| = b_{22}^i b_{11}^i - b_{12}^i b_{21}^i.$$

$$a_{11}^i = \frac{\Sigma_f^i}{D_f^i} + \alpha z^2 \qquad a_{12}^i = \frac{\Sigma_n^i}{D_f^i} \cdot k_\infty^i$$

$$a_{21}^i = \frac{\Sigma_f^i}{D_n^i} \qquad a_{22}^i = \frac{\Sigma_n^i}{D_n^i} + \alpha z^2$$

REFERENCES

1. Radanović, L., Bingulac, S., Lazarević, B., and Mataušek, M., *Two channel method for reactor heat transfer analysis*, Boris Kidrič Institute of Nuclear Sciences, Report No. 3.09, Beograd (1963).
2. Galanin, A., *Theory of nuclear reactors* (in Russian), Atomizdat, Moskva, 150 (1959).
3. Glasstone, S., and Edlund, M. C., *The elements of nuclear reactor theory*, Van Nostrand, Princeton, USA (1955).
4. Amouyal, A., Bacher, P., *et al.*, Rififi, *Méthode de calcul analytique de la condition critique et des flux d'une pile à régions variées en théorie à deux groupes*, Report CEA, No. 1398, Saclay (1960).
5. Radanović, L., Bingulac, S., Lazarević, B., and Mataušek, M., *An analogue computer method for solving flux distribution problems in multiregion nuclear reactors*, Report *VIII*, Nuclear Congress, Rome (1963).
6. Radanović, L., Bingulac, S., Lazarević, B., and Mataušek, M., in Proc. of ETAN Conf., Zagreb (in Serbocroatian), ETAN, Beograd, 283 (1963).

ABSTRACT—RÉSUMÉ—АННОТАЦИЯ—RESUMEN

A/706 Yougoslavie

Calculs de la diffusion de neutrons à une seule vitesse à partir d'un modèle à deux groupes

par S. Bingulac *et al.*

Quand on évalue les dimensions critiques et les distributions de flux dans des réacteurs nucléaires à plusieurs régions, il est avantageux de disposer d'une méthode qui conserve la simplicité de calcul du traitement à un groupe tout en s'approchant de la précision que l'on peut obtenir avec un modèle à deux groupes. De telles représentations analytiques simples, suffisamment précises, sont très importantes dans les études de dynamique pour lesquelles il faut obtenir simultanément la solution de l'équation de flux et de la fonction d'importance sur un calculateur analogique.

Le mémoire décrit une procédure permettant de représenter la distribution de flux par une expression de la forme:

$$\phi^i(r) = \phi^i{}_1(r) + Z^i{}_i \phi^i{}_1(R_i) \exp\left[-V^i{}_i(R_i - r)\right] + Z^i{}_{i-1}\phi^i{}_1(R_{i-1}) \exp\left[-V^i{}_{i-1}(R_{i-1} - r)\right]$$

où $\phi^i{}_1(r)$ est la solution de l'équation de diffusion à un groupe dans la $i$ème région du réacteur, définie par l'intervalle: $R_{i-1} \leqslant r < R_i$, tandis que $Z^i{}_i$, $Z^i{}_{i-1}$, $V^i{}_{i-1}$ et $V^i{}_i$ sont des constantes.

A chaque interface entre deux régions, la fonction $\phi_1{}^i(r)$ doit satisfaire à une condition limite définie par:

$$\lim_{r \to R_i} \frac{d\phi^i{}_1(r)}{dr} \cdot \frac{1}{\phi^i{}_1(r)} = U^i{}_i$$

Pour cette expression un utilise un modèle unidimensionnel à deux groupes, adapté à l'utilisation d'un calculateur analogique. Les équations de diffusion à deux groupes sont transformées en équations de Riccati avec les conditions initiales et les conditions aux limites correspondantes. En utilisant les propriétés de la solution des équations de Riccati, on réduit à deux régions seulement le réacteur à plusieurs régions, avec un ensemble simple d'équations pour déterminer les dimensions critiques et les coefficients:

$$Z^i{}_i,\ Z^i{}_{i-1},\ V^i{}_i,\ V^i{}_{i-1},\ U_i{}^i$$

pour toutes les régions.

On peut résoudre une fois pour toutes l'ensemble normalisé de ces équations, ce qui donne une famille de courbes dont on peut déduire les dimensions critiques et les coefficients pour différents paramètres de réacteurs.

On peut utiliser cette méthode pour des géométries sphériques et cylindriques, ainsi que pour toute disposition des zones actives et des réflecteurs. On discute à l'aide d'exemples concrets l'application pratique et la précision de ce procédé.

A/706 Югославия

Односкоростное вычисление диффузии нейтронов, основанное на двухгрупповой модели реактора

С. Бингулаи *et al.*

При определении критических размеров и распределения потока у многозонных ядерных реакторов полезно располагать методом, который в отношении точности приближается к двухгрупповой трактовке, а с точки зрения вычисления сохраняет свойства одногруппового метода. Такой достаточно точный, но аналитически несложный метод удобен, в частности, для динамических анализов на моделирующих устройствах, которые часто требуют одновременного определения распределения нейтронного потока и его сопряженной функции.

В настоящей работе предлагается метод, с помощью которого распределение нейтронного потока можно представить в форме

$$\varphi^i(r) = \varphi^i_1(r) + Z^i_i \varphi^i_1(R_i) \exp\left[-V^i_i(R_i - r)\right] + Z^i_{i-1}\varphi^i_1(R_{i-1}) \exp\left]-V^i_{i-1}(R_{i-1} - r)\right],$$

где $\varphi^i_1(r)$ является решением одногруппового диффузионного уравнения в зоне i, определенной интервалом $R_{i-1} \leqslant r < R_i$; Z^i_i, Z^i_{i-1} и V_{i-1} — постоянные.

На границе между двумя соседними зонами функции $\varphi^i_1(r)$ должны удовлетворять следующим граничным условиям:

$$\lim_{\to R_i} \frac{d\varphi^i_1(r)}{dr} \frac{1}{\varphi^i_1(r)} = U^i_i.$$

При определении выражения для потока использована одномерная двухгрупповая модель реактора, приспособленная для моделирующего устройства. Двухгрупповые диффузионные уравнения преобразовались в дифференциальные уравнения Риккати с соответствующими начальными и граничными условиями. Благодаря обнаруженным свойствам уравнения Риккати многозонный реактор сводится к реактору лишь с двумя эквивалентными зонами и несложной системе уравнений, решение которой определяет критические размеры и коэффициенты

$$Z^i_i,\ Z^i_{i-1},\ V^i_i,\ V^i_{i-1},\ U^i_i$$

для всех зон реактора.

Путем перенормировки этой системы уравнений получается семейство кривых, из которых легко можно определить коэффициенты и критические размеры для различных значений реакторных параметров.

Изложенный метод можно применить как

к сферической, так и к цилиндрической геометрии. Порядок активных зон и отражателей может быть произвольным. Практическое применение и точность метода продемонстрированы на специфическом примере.

A/706 Yugoslavia

Cálculos de difusión neutrónica a una velocidad, basados en un modelo de reactor de dos grupos

por S. Bingulac *et al.*

Al evaluar las dimensiones críticas y distribuciones de flujo en reactores de varias regiones, es ventajoso el empleo de métodos que poseen las ventajas de la simplicidad de cálculo del tratamiento en un grupo, y cuya precisión se aproxime a la lograda con el modelo en dos grupos. Estas ecuaciones de flujo, analíticamente simples pero suficientemente precisas, son particularmente importantes en estados dinámicos en los que se requiere la obtención simultánea de la solución de la ecuación de flujo y su adjunta, por medio de una calculadora analógica.

El artículo describe un procedimiento que permite representar la distribución de flujo, mediante una expresión de la forma,

$$\phi^i(r) = \phi^i{}_1(r) + Z^i{}_i \phi^i{}_1(R_i) \exp\left[-V^i{}_i(R_i - r)\right] + Z^i{}_{i-1} \phi^i{}_1(R_{i-1}) \exp\left[-V^i{}_{i-1}(R_{i-1} - r)\right]$$

donde $\phi^i{}_1(r)$ es la solución de la ecuación de difusión de un grupo en la i-ésima región del reactor, definida por el intervalo: $R_{i-1} \leqslant r < R_i$ mientras que $Z^i{}_i$, $Z^i{}_{i-1}$, $V^i{}_i$ y $V^i{}_{i-1}$ son constantes.

En cada interfase entre dos regiones, la función $\Phi^i{}_1(r)$ debe satisfacer una condición de contorno definida por,

$$\lim_{r \to R_i} \frac{\mathrm{d}\phi^i{}_1(r)}{\mathrm{d}r} \cdot \frac{1}{\phi^i{}_1(r)} = U^i{}_i$$

Para la deducción de esta expresión, se utiliza un modelo de reactor monodimensional en dos grupos, adaptado a la resolución con una calculadora analógica. Las ecuaciones de difusión de dos grupos se transforman en ecuaciones de Riccati, con las condiciones iniciales y de contorno asociadas. Las propiedades de las ecuaciones de Riccati permiten la reducción del reactor en varias regiones a otro de solo dos regiones, lo que únicamente precisa un sistema de ecuaciones simple, que determinan las condiciones críticas y los coeficientes,

$$Z^i{}_i,\ Z^i{}_{i-1},\ V^i{}_i,\ V^i{}_{i-1},\ U^i{}_i$$

para todas las regiones.

Este sistema de ecuaciones normalizado puede resolverse una vez por todas, con lo que se obtiene una familia de curvas que permiten la determinación fácil de las dimensiones críticas y de los coeficientes, para varios parámetros del reactor.

Este procedimiento es aplicable a geometrías esférica y cilíndrica, y a cualquier disposición de regiones activas y reflectores. Se discute en ejemplos específicos la aplicación práctica y la precisión del método.

Angular leakage spectrum of thermal neutrons

By R. Kladnik*

The determination of the stationary angular and energy distribution of thermal neutrons on the boundary of a finite medium is one of the important problems which have not yet been solved in the theory of thermal neutron experiments. So far this problem has been dealt with within the framework of a diffusion or P_1 approximation [1].

The diffusion theory, corrected for the transport mean free path, can describe the space, and energy, variation of the thermal neutron flux in regions within the homogeneous medium which are several mean free paths away from the boundaries or localized absorbers and sources. However, no reliable results of the diffusion theory for the angular behaviour of the neutron flux are available especially for the boundary regions where the angular dependency of the neutron flux becomes important. The reason for this is the inadequacy of the diffusion theory to properly take into account the boundary conditions. Some improvements are gained by applying the spherical harmonics method (P_N). However, because of the poor convergency, the P_N method in the high-order approximation must be used and this requirement makes the P_N method too cumbersome.

If we want to obtain approximate expressions for the linear extrapolation distance and for the angular distribution of the leakage spectrum of thermal neutrons we have to apply some other method. We shall use the eigenfunction expansion method in connexion with the variational method. The application of the variational method to the neutron transport problems of this kind has already been described by several authors [2–5].

In order to demonstrate the basic properties of the angular distribution of the thermal neutron flux on the boundary of the medium, we shall take the simplest geometry: the semi-infinite medium is on the left side surrounded by vacuum. The medium may absorb neutrons; however, it contains no neutron sources. Neutrons are supplied to the medium from the infinity; there are no neutrons entering the medium at the boundary surface $x=0$.

The neutron flux $\phi(x,E,\mu)$ (x is the spatial coordinate, E the neutron energy, and μ the cosine of an angle between the neutron velocity vector and the positive x-axis; μ is positive for the in-going directions), is a solution of the well-known stationary integro-differential transport equation. We seek the solutions of this equation satisfying boundary conditions associated with our problem. Because of the non re-entrant boundary surface at $x=0$, we require

$$\phi(0,E,\mu)=0 \tag{1}$$

for all in-going directions, i.e. for $\mu>0$.

Using the above boundary condition, we can integrate the integro-differential form of the transport equation and we obtain an integral transport equation which we shall solve approximately by using the variational method.

The problem of a finite medium can formally be made equivalent to an infinite medium problem providing fictitious negative sources are introduced on the boundary surface $x=0$ [6]. Our problem is then equivalent to the infinite medium problem with positive neutron sources at the infinity ($x\to\infty$) and with fictitious negative sources on the boundary surface ($x=0$).

THE EIGENFUNCTION EXPANSION

It is hoped that neutron transport problems can be solved with the aid of certain eigenfunctions which form a complete set. These eigenfunctions may be searched for with an Ansatz form as [5]:

$$\phi(x,E,\mu)\to M(E)g(E,\mu)e^{-\kappa x} \tag{2}$$

where $M(E)$ represents the Maxwellian flux distribution and where κ and $g(E,\mu)$ are the eigenvalue and the eigenfunction, respectively, of the following homogeneous integral equation:

$$[\Sigma(E)-\kappa\mu]g(E,\mu)=\int_0^\infty\int_{-1}^{1}\Sigma(E,\mu\to E',\mu')g(E',\mu')\mathrm{d}E'\mathrm{d}\mu' \tag{3}$$

This eigenequation is obtained from the integro-differential transport equation if the detailed balance condition for the differential scattering probability $\Sigma(E,\mu\to E',\mu')$ is used.

The eigensolutions κ_i and $g^{(i)}(E,\mu)$ of the above eigenequation may be either discrete or continuous and it is hoped that they form a complete set of orthogonal functions. If so, then the neutron flux $\phi(x,E,\mu)$, being a solution of the transport equation, can be written as:

$$\phi(x,E,\mu)=M(E)\sum_i C_i g^{(i)}(E,\mu)e^{-\kappa_i x} \tag{4}$$

* J. Stefan, Nuclear Institute, Ljubljana.

where, for the continuous part of the set of eigenfunctions, the summation sign must be replaced by an integration sign. The constants C_i depend upon the distribution of sources; they represent contributions of the particular eigensolutions in the spectrum of the neutron sources.

It follows from the nature of the eigenequation (3) that, for each eigensolution $\kappa_i, g^{(i)}(E,\mu)$ with the positive real part of κ_i, also a pair $-\kappa_i, g^{(i)}(E,\mu)$ is a solution of the same eigenequation. The general form of the neutron flux $\phi(x,E,\mu)$, Eq. (4), can then be written as:

$$\phi(x,E,\mu) = M(E)\sum_j \{C_j g^{(j)}(E,\mu)e^{-\kappa_j x} + F_j g^{(j)}(E,-\mu)e^{\kappa_j x}\}; \quad (5)$$

the index j runs over the eigensolutions with the positive real part of κ_j only. The constants C_j represent contributions of the sources from the left side of the system (C_j values are negative in our case, since we have fictitious negative sources on the boundary surface $x=0$), whereas the constants F_j represent contributions of the neutron sources from the right-hand side ($F_j > 0$).

According to the geometry of our problem, regions with sufficiently large x are far away from neutron sources of any kind. For such regions, in the development, Eq. (5), terms with the smallest real part of κ_j will be predominant. We shall call this solution the asymptotic solution ϕ_{as}:

$$\phi_{as}(x,E,\mu) = M(E)[C_1 g(E,\mu)e^{-\kappa x} + F_1 g(E,-\mu)e^{\kappa x}] \quad (6)$$

Here, κ represents the lowest real eigenvalue of Eq. (3), and $g(E,\mu)$ is the corresponding non-negative eigenfunction. The inverse of κ is known as the diffusion length.

The asymptotic solution (6) may be written in a more convenient form by replacing the constants C_1 and F_1 with new constants C and X_0, defined by:

$$C_1 = -(C/2\kappa)e^{-\kappa x_0} \text{ and } F_1 = (C/2\kappa)e^{\kappa x_0} \quad (7)$$

We then have:

$$\phi_{as}(x,E,\mu) = C.M(E)\left[g_1(E,\mu)\frac{1}{\kappa}\sinh\kappa(x+x_0) - g_2(E,\mu)\cosh\kappa(x+x_0)\right] \quad (8)$$

where

$$2g_1(E,\mu) = g(E,\mu) + g(E,-\mu)$$
$$2\kappa g_2(E,\mu) = g(E,\mu) - g(E,-\mu) \quad (9)$$

The constant C depends on the intensity of the neutron sources at the infinity, whereas the parameter x_0—the extrapolated end-point—reflects the conditions on the boundary of the medium. The quantity x_0 is connected with the linear extrapolation distance q through the equation:

$$q = (1/\kappa)\tanh\kappa x_0 \quad (10)$$

The asymptotic flux $\phi_{as}(x,E,\mu)$ cannot describe the distribution of neutrons in regions near the boundary. Due to the vicinity of the fictitious negative sources, higher eigensolutions must be added. The expression for the neutron flux in the vicinity of the boundary can then be written as:

$$\phi(x,E,\mu) = \phi_{as}(x,E,\mu) + M(E)\sum_{j=2} C_j g^{(j)}(E,\mu)e^{-\kappa_j x}$$

where the constants C_j are negative. Write $C_j = -C.C_j''$.

Then we have

$$\phi(x,E,\mu) = C.M(E)\left[g_1(E,\mu)\frac{1}{\kappa}\sinh\kappa x - g_2(E,\mu)\cosh\kappa x + q(x,E,\mu)\right] \quad (11)$$

where

$$q(x,E,\mu) = q.[g_1(E,\mu)\cosh\kappa x - \kappa g_2(E,\mu)\sinh\kappa x] - \sum_{j=2} C''_j g^{(j)}(E,\mu)e^{-\kappa_j x} \quad (12)$$

The first term on the right-hand side of Eq. (12) represents the asymptotic form of the function $q(x,E,\mu)$. The deviation of the function $q(x,E,\mu)$ from its asymptotic form is described by the higher eigensolutions $\kappa_j g^{(j)}(E,\mu)$. Unfortunately, these functions are not yet known and we have to use appropriate approximations.

With the aid of the above eigenfunctions $g(E,\mu)$ we can formulate an integral form of the boundary condition which turns out to be very useful. To obtain this integral boundary condition we construct an integral $K^{(i)}(x)$ of the following form:

$$K^{(i)}(x) = \int_0^\infty \int_{-1}^1 \phi(x,E,\mu)g^{(i)}(E,\mu)\mu dE d\mu \quad (13)$$

Multiplying the integro-differential form of the transport equation by $g^{(i)}(E,\mu)dEd\mu$, integrating over E and μ, and by taking into account the eigenequation (3), we find that $K^{(i)}(x)$ is a solution of the first-order differential equation:

$$\frac{d}{dx}K^{(i)}(x) = -\kappa_i K^{(i)}(x)$$

Hence

$$K^{(i)}(x) = \int_0^\infty \int_{-1}^1 \phi(x,E,\mu)g^{(i)}(E,\mu)\mu dE d\mu = \text{const.}e^{-\kappa_i x} \quad (14)$$

This equation is valid for all eigensolutions of Eq. (3).

Suppose that the development (4) for the neutron flux is justified. The above condition (14) then gives:

$$\sum_j C_j e^{-\kappa_j x}\int_0^\infty \int_{-1}^1 M(E)g^{(i)}(E,\mu)g^{(j)}(E,\mu)\mu dE d\mu = \text{const.}e^{-\kappa_i x}$$

This equation will be satisfied for all $x \geqq 0$ only if the

eigensolutions $g^{(i)}(E,\mu)$ constitute a set of orthogonal functions with

$$\int_0^\infty \int_{-1}^1 M(E)g^{(i)}(E,\mu)g^{(j)}(E,\mu)\mu dE d\mu = N_i \theta_{ij} \quad (15)$$

The value of the constant in Eq. (14) is then equal to $C_i N_i$.

Since Eq. (15) actually represents the orthogonality condition for the eigenfunctions $g^{(i)}(E,\mu)$, [7], we can conclude that the development (4) is correct.

We shall use Eq. (14) for the lowest eigensolution pair $[\kappa, g(E,\mu)]$ and $[-\kappa, g(E,\mu)]$:

$$\int_0^\infty \int_{-1}^1 \phi(x,E,\mu)g(E,\mu)\mu dE d\mu = C_1 N_1 e^{-\kappa x} \quad (16)$$

$$\int_0^\infty \int_{-1}^1 \phi(x,E,\mu)g(E,-\mu)\mu dE d\mu = -F_1 N_1 e^{\kappa x} \quad (17)$$

with

$$N_1 = \int_0^\infty \int_{-1}^1 M(E)g^2(E,\mu)\mu dE d\mu = 2\kappa . a_{12}$$

where a_{12} is one of the double integrals of the following form:

$$a_{ik} = 2\int_0^\infty \int_0^1 M(E)g_i(E,\mu)g_k(E,\mu)\mu dE d\mu;\ i,k = 1,2 \quad (18)$$

In the above derivation we have used the definition (9) for the functions $g_1(E,\mu)$ and $g_2(E,\mu)$. If we use expressions (7) for the constants C_1 and F_1 and if we then subtract Eq. (17) from Eq. (16) we arrive at the equation:

$$\int_0^\infty \int_{-1}^1 \phi(x,E,\mu)g_2(E,\mu)\mu dE d\mu = C a_{12}(1/\kappa)\sinh\kappa(x+x_0) \quad (19)$$

We shall need this equation in order to obtain explicit expression for the linear extrapolation distance q. If we write Eq. (19) for $x=0$ and make use of the boundary condition (1) we obtain:

$$(1/\kappa)\sinh\kappa x_0 = (1/Ca_{12})\int_0^\infty \int_0^1 \phi(0,E,-\mu)g_2(E,\mu)\mu dE d\mu$$

In the next step we replace $\phi(0,E,-\mu)$ by Eq. (11) and use the definition (10) for q; we obtain the final expression for q equal to:

$$q = \frac{a_{22}}{2a_{12}} + \frac{1}{a_{12}}\int_0^\infty \int_0^1 M(E)q(0,E,-\mu)g_2(E,\mu)\mu dE d\mu \quad (20)$$

The integrals a_{12} and a_{22} are defined by Eq. (18). If the function $q(0,E,-\mu)$ were known, the above expression would give us the linear extrapolation distance. We cannot determine $q(x,E,\mu)$ from the expression (12) since the higher eigenfunctions $g^{(j)}(E,\mu)$ are not known. Hence, we have to find approximate expressions for the function $q(0,E,-\mu)$, for instance, by solving the integral equation for the function $q(x,E,\mu)$.

The integral equation for $q(x,E,\mu)$ is obtained directly from the integral transport equation if Eq. (11) is used for $\phi(x,E,\mu)$. We have:

$$q(x,E,\mu) = \epsilon(\mu)g_2(E,\mu)e^{-x\Sigma(E)/\mu} + \mathcal{K}\{q(x,E,\mu)\} \quad (21)$$

with $\epsilon(\mu)=1$ for $\mu>0$, and $=0$ for $\mu<0$. The operator $\mathcal{K}\{q\}$ is the well-known integral transport operator [5].

We shall solve the above unhomogeneous integral equation approximately using the variational method.

THE VARIATIONAL METHOD

The variational method has, for this purpose, been introduced by Nelkin [4] for the case of a non-absorbing medium with isotropic scattering. The method has then been generalized by Kuščer and the author [5] in order to include the effects of the absorption and the anisotropic scattering. See reference [5] for the details.

One constructs a functional $I\{q\}$ which attains its stationary value when the function q is a solution of the integral equation (21). It turns out that the stationary value of the functional $I\{q\}$ is proportional to the double integral on the right-hand side of Eq. (20). Since the error of the stationary functional is of the second order in magnitude, we can, in this way, obtain a fairly good estimate for the linear extrapolation distance q.

The problem is how to find the form of the trial function $\tilde{q}$. The trial function must reflect the physical situation as much as possible, and simultaneously it must be of such form that the integral equation (3) can be used and that the integration over x can be carried out analytically. The best form of the trial function $\tilde{q}$ would be given by Eq. (12), i.e.

$$\tilde{q}(x,E,\mu) = A_1[g_1(E,\mu)\cosh\kappa x - \kappa g_2(E,\mu)\sinh\kappa x] - \sum_{j=2} A_j g^{(j)}(E,\mu)e^{-\kappa_j x} \quad (22)$$

where A_j $(j=1,2,\ldots)$ are the variational parameters whose optimized values are calculated from the following system of algebraic equations,

$$\frac{\partial}{\partial A_j} I\{\tilde{q}\} = 0,\ j = 1,2\ldots \quad (23)$$

Since the higher eigensolutions $g^{(j)}(E,\mu)$ with κ_j are not known, we have to use a more simple trial function, e.g.,

$$\tilde{q}(x,E,\mu) \approx A_1[g_1(E,\mu)\cosh\kappa x - g_2(E,\mu)\sinh\kappa x] - [A_2 g_1(E,\mu) + A_3 g_2(E,\mu)]e^{-x/l_0} \quad (24)$$

The constant l_0 is an arbitrary length; it represents some sort of an average decay length of the higher eigenfunction contributions to the flux distribution in the vicinity of the boundary. We shall be changing l_0 to obtain better results.

Using the above trial function (24) we can calculate the parameters A_1, A_2, and A_3 from the system of algebraic equations (23). We obtain the following results:

$$A_1 = \frac{a_0a_3a_6 + a_1a_4a_6 - a_2a_3a_5}{(a_1+a_3)a_6 - a_2a_3}$$

$$A_2 = \frac{a_3(a_0 - a_5) + a_1(a_4 - a_5)}{(a_1+a_3)a_6 - a_2a_3}$$

$$A_3 = \frac{a_0a_6 - a_2a_5 + a_4(a_2 - a_6)}{(a_1+a_3)a_6 - a_2a_3} \qquad (25)$$

with

$a_0 = \alpha_{12}/\alpha_{11}$

$a_1 = (\beta_{12} + l_0(\beta_{11} - \alpha_{11}))/\alpha_{11}$

$a_2 = (\beta_{11} + l_0\kappa^2(\beta_{12} - \alpha_{12}))/\alpha_{11}$

$a_3 = l_0 + a_4$

$a_4 = (\beta_{22} + l_0(\beta_{12} - \alpha_{12}))/(\beta_{12} + l_0(\beta_{11} - \alpha_{11}))$

$a_5 = (\beta_{12} + l_0\kappa^2(\beta_{22} - \alpha_{22}))/(\beta_{11} + l_0\kappa^2(\beta_{12} - \alpha_{12}))$

$a_6 = 1 + l_0\kappa^2 a_5,$

where

$$\beta_{ik} = 2\int_0^\infty \int_0^1 M(E)\frac{g_i(E,\mu)g_k(E,\mu)}{1+\mu/l_0\Sigma(E)}\mu \mathrm{d}E\mathrm{d}\mu \qquad (26)$$

The stationary value of the chosen functional can also be expressed in terms of the variational parameters A_j. We then obtain the final form of the linear extrapolation distance q equal to [5]:

$$2q = \frac{\alpha_{22}}{\alpha_{12}} + A_1 - \frac{\alpha_{11}}{\alpha_{12}}(A_2a_2a_5 - A_3a_1a_4) \qquad (27)$$

Once q is known, the extrapolation end-point x_0 can be obtained from Eq. (10).

The variational trial function (24) is too crude to be used as $q(x,E,\mu)$ in the expression for the angular leakage flux (11). We gain some improvement by iterating the integral Eq. (21), using the variational trial function as a first trial. The first iteration can be carried out analytically. We obtain the following result, for $x=0$ and $\mu<0$:

$$q(0,E,-\mu) = A_1g_1(E,\mu) - \left[1+\frac{\mu}{l_0\Sigma(E)}\right]^{-1} \cdot \left[A_2\langle g_1(E,\mu) - \frac{\mu\kappa^2}{\Sigma(E)}g_2(E,\mu)\rangle + A_3\langle\frac{\mu}{\Sigma(E)}g_1(E,\mu) - g_2(E,\mu)\rangle\right], \mu>0 \qquad (28)$$

The angular and the energy distribution of the neutrons leaking into the vacuum is then given by:

$$\phi(0,E,-\mu) = N.M(E)[g_2(E,\mu) + q(0,E,-\mu)],\ \mu>0 \qquad (29)$$

APPLICATION TO THE MONOKINETIC CASE

The situation is especially simple in the case of a monokinetic transport theory with isotropic scattering and no absorption. There we have: $\Sigma(E)\to\Sigma_s(E)\to\Sigma_s$, where Σ_s is the high-energy limit of the macroscopic scattering cross section. $g_1(E,\mu)\to 1$, $g_2(E,\mu)\to\mu/\Sigma_s$, [7]. The calculation of the variational constants (25), the linear extrapolation distance q (27), and the angular distribution of the leaking neutrons (29) is then relatively simple. We shall be changing the value of the arbitrary constant l_0 in order to get the best agreement with the exact values for q and the angular distribution [2,6].

The results for q (27) for different values of the arbitrary constant l_0 show that the best agreement ($\approx 0.005\,\%$) with the exact value $0.71045/\Sigma_s$ is obtained with l_0 equal to about $1/3\Sigma_s$, indicating that the contribution of the higher eigenfunctions to the flux distribution near the boundary decays with the average decay length equal to about one-third of the total mean free path. A similar conclusion can be drawn from the comparison of the results for the angular distribution. In Table 1 the results for the angular distribution of leaking neutrons (29) are compared with the exact values [2] for two cases: $l_0\Sigma_s = 1.0$ and $l_0\Sigma_s = 0.3$. All angular distributions are normalized to the unit integral of the angular distribution on the boundary surface. The error for the second case is, in the average, more than 10 times smaller than for the first case. Our method with $l_0\Sigma_s = 0.3$ gives the angular distribution accurate to about $0.05\,\%$ for all angles of leakage, with the exception at $\mu = 0$, where the error sharply increases up to about $3\,\%$. With $l_0\Sigma_s = 1.0$, the corresponding average error is about $0.5\,\%$, except for those angles approaching $\pi/2$.

LEAKAGE FROM MONATOMIC GASEOUS MODERATORS

We have first to determine the functions $g_1(E,\mu)$ and $g_2(E,\mu)$ which are the even and the odd part, respectively, of the lowest eigensolution $g(E,\mu)$. In Ref. [7] a semi-analytical method for solving the eigenequation (3) is presented. On the basis of this method, we have written a FORTRAN programme which gives numerical values for the extrapolation distances x_0 and q, together with the angular and energy distributions of the leakage neutron flux for different atomic mass numbers of a monatomic gaseous moderator with different absorption probabilities. The scattering cross section is supposed to be independent of the relative velocity between the neutron and the scattering

Table 1. The variational solution for the monokinetic leakage flux $\phi(0,-\mu)$ compared to the exact values of the leakage flux $\phi_{ex}(0,-\mu)$, [2]

μ	$\phi_{ex}(0,-\mu)$	$\frac{1-\phi(0,-\mu)/\phi_{ex}(0,-\mu)}{l_0\Sigma_s = 1.0}$ in %	$l_0\Sigma_s = 0.3$
0.0 . . .	0.5000	−8.6	−2.6
0.1 . . .	0.6236	−2.1	−0.05
0.2 . . .	0.7251	−0.61	+0.03
0.3 . . .	0.8212	+0.01	0.01
0.4 . . .	0.9146	0.28	0.01
0.5 . . .	1.0064	0.42	0.01
0.6 . . .	1.0971	0.47	0.03
0.7 . . .	1.1870	0.52	0.03
0.8 . . .	1.2764	0.51	0.05
0.9 . . .	1.3653	0.46	0.05
1.0 . . .	1.4539	0.45	0.06

nucleus. Furthermore, the $1/v$-dependence of the absorption cross section is assumed. The probability for absorption is measured by the parameter γ, defined as the ratio of the average absorption cross-section ($\bar{\Sigma}_a$) to the high-energy limit of the total cross-section (Σ_s):

$$\gamma = \bar{\Sigma}_a / \Sigma_s$$

The absorption cross section is averaged over the Maxwellian flux distribution: $\bar{\Sigma}_a = \sqrt{\pi}\Sigma_a(kT_m)/2$, where T_m is the temperature of the moderator. We were able to run the programme only for one case, with $l_0\Sigma_s = 1.0$.

DISCUSSION

In a previous paper [7], we have shown that the calculated values for the diffusion length L and the diffusion coefficient D of a monatomic gaseous moderator agree fairly well with the measured values for L and D for a light water moderator if one takes an effective mass number $A = 1.9$ and $\Sigma_s \approx 2.5$ cm^{-1}. We obtain $\Sigma_s q = 0.819$ in this case, or, $q = 0.819 \times 0.40$ cm $= 0.33$ cm. This result is about 6% lower than the experimental value. The difference is probably due to the improper choice of the arbitrary length l_0.

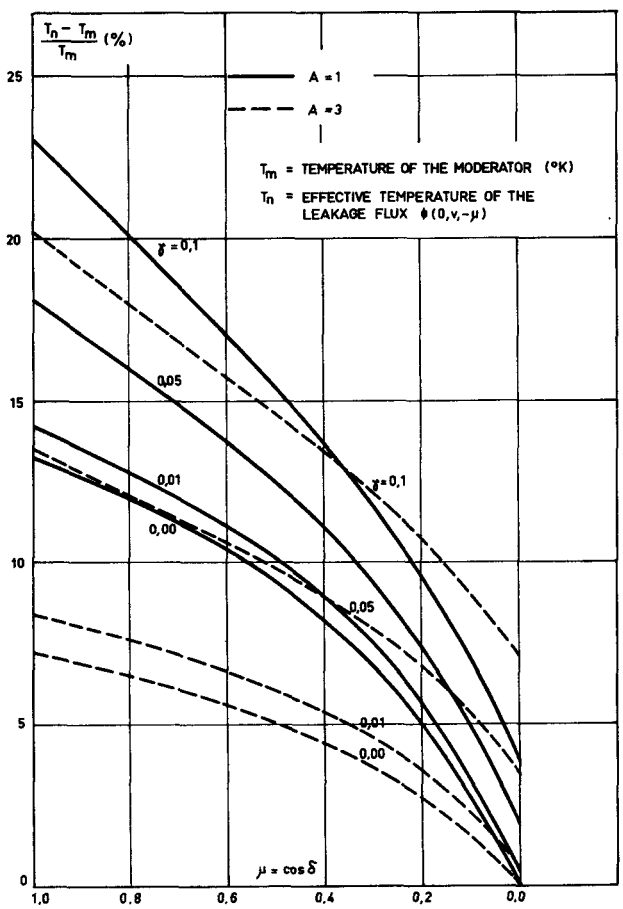

Figure 1. The effective temperature of the leakage flux as a function of the angle of leakage. T_m is the moderator temperature

Numerical results for the angular leakage flux (29) indicate the energy distribution of the emerging neutrons to be approximately of Maxwellian shape but at a temperature higher than the moderator temperature (the diffusion hardening effect of the boundary). We define the effective temperature of the neutron energy distribution (T_n) with the aid of the average energy which we write as $3kT_n/2$.

In Fig. 1 the effective temperature of the leaking neutrons is given as a function of the emerging angle for the atomic masses $A = 1$ and 3 at different absorption probabilities (γ). The temperature is higher in the directions perpendicular to the boundary surface than in the grazing directions. This variation of the effective temperature is less distinct in heavier moderators. The angular variation of the effective temperature is probably not large enough to be measurable with reliable precision.

In non-absorbing media the temperature of emerging neutrons is higher than the moderator temperature for two reasons: first, in the vicinity of the boundary, faster neutrons have more chance to escape than slower neutrons because $\Sigma_s(E)$ is a decreasing function in energy. Second, the scattering of slow neutrons is more isotropic than for fast neutrons. Hence, if E is small, the flow of neutrons towards the boundary is

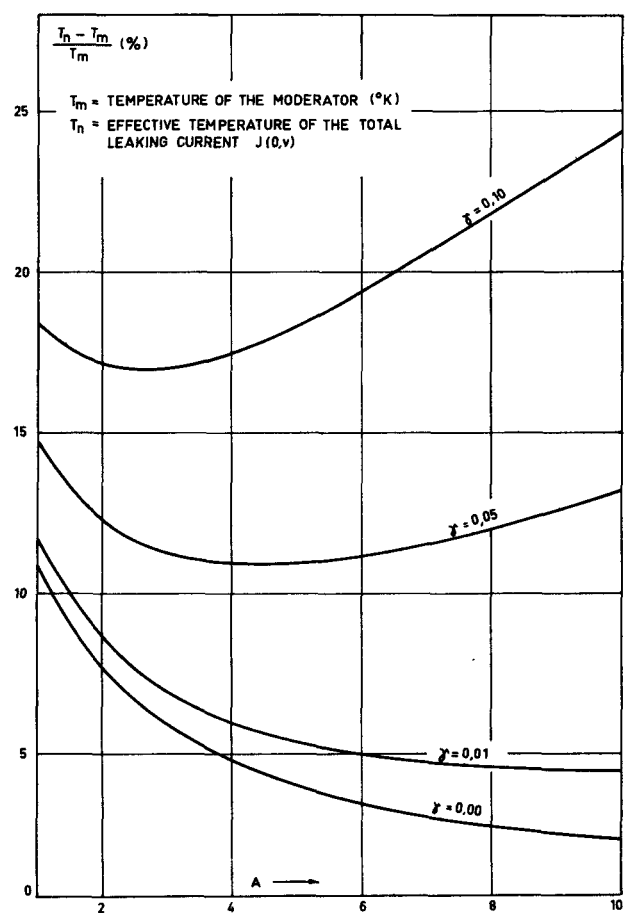

Figure 2. The effective temperature of the net leaking current as a function of the atomic mass number of a monatomic gaseous moderator

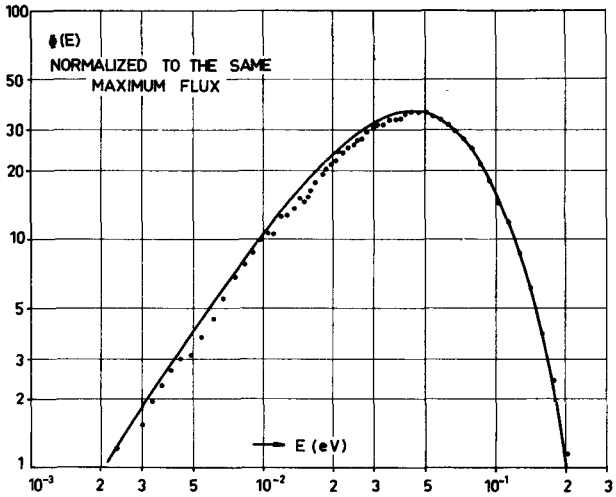

Figure 3. The calculated spectrum of the leakage flux for the monatomic gaseous hydrogen compared to the measured spectrum for water (8). Solid curve—calculated spectrum with A=1 and γ=0.0. Dots—measured spectrum from a 15 cm cube of water. Both spectra refer to the direction perpendicular to the surface of the moderator

scattered around more diffusely than for larger energies. On the other hand, the difference in the scattering properties of fast and slow neutrons is less pronounced in heavier moderators. The curve for $\gamma = 0.0$ (non-absorbing media) in Fig. 2 is therefore a regularly decreasing curve.

In absorbing media, the hardening effect on the spectrum is increased because of the preferential absorption of slow neutrons. For light nuclei, the absorption effect on the spectrum hardening is not so large because the scattering probability is still appreciable. However, since the absorption effect is proportional to A and since the diffusion hardening regularly decreases with increasing A, then, for heavier nuclei the absorption effect becomes dominant and the curves with $\gamma > 0$ (Fig. 2) turn upward. The turning point moves to lower A if the absorption strength of the medium is higher.

In Fig. 3 the calculated spectrum of the leakage flux (for the direction perpendicular to the surface of the moderator) is compared to the measured spectrum [8]. The time-of-flight spectrum was measured from a water cube with the edge equal to 15 cm. A good agreement is obtained if the monatomic gas with $A = 1$ and no absorption is used, whereas the effective mass number ($A = 1.9$ for the water hydrogen) gives much softer spectrum (compare the effective temperatures of $A = 1$ and $A = 1.9$ in Fig. 2)than the experiment. It is astonishing that the free-gas spectrum with $A = 1$ agrees with the measurements so well. Actually, the free-hydrogen spectrum should be harder than the measured spectrum. The reason for the above agreement is probably due to the improper choice of the parameter l_0. Smaller l_0 gives a harder spectrum.

ACKNOWLEDGEMENTS

The author would like to express his sincere thanks to Dr. M. Čopič for many fruitful discussions and to Dr. R. G. Taecker, Director of the IINSE, Argonne, Ill., for his interest in this problem. The numerical part of this work was done while the author was with the IINSE. Thanks also to the teaching staff for their help.

REFERENCES

1. Conkie, W. R., Nuclear Sci. and Eng., *7*, 295 (1960).
2. Kourganoff, V., *Basic methods in transfer problems*, Oxford Univ. Press, London (1952).
3. Ptycina, N. V., in *Nekotoryje matematičeskije zadači nejtronnoj fiziki* (*Some mathematical problems of neutron physics*), ed. Kuzbecov, E. S., Izd. Moskovsk. Univ., Moscow (1960).
4. Nelkin, M., Nuclear Sci. and Eng., *7*, 552 (1960).
5. Kladnik, R., and Kuščer, I., Nuclear Sci. and Eng., *13*, 149 (1962).
6. Case, K. M., *et al.*, in *Introduction to the theory of neutron diffusion*, Vol. I, Los Alamos Publication (1953).
7. Kladnik, R., Nuclear Sci. and Eng., *17*, 185 (1963).
8. Beckurts, K. H., and Reichardt, W., Proc. of the Symposium on Neutron Time-of-Flight Methods, Saclay, France, 239 (1961).

ABSTRACT—RÉSUMÉ—АННОТАЦИЯ—RESUMEN

A/708 Yougoslavie

Spectre angulaire de fuite des neutrons thermiques

par R. Kladnik

L'auteur fait un bref exposé de la méthode de variation et d'itération appliquée à l'équation intégrale du transport pour des neutrons thermiques dans un milieu semi-infini absorbant et sans sources. Cette méthode est utilisée pour obtenir une expression explicite de la longueur d'extrapolation linéaire et de la distribution du flux des neutrons thermiques en fonction de la solution relative au milieu infini.

On considère, à titre d'exemple, un ralentisseur classique à gaz monoatomique pour lequel la solution en milieu infini a déjà été obtenue semi-analytiquement. On suppose que la section efficace d'absorption suit la loi $1/v$. On a résolu la partie numérique du problème à l'aide d'une calculatrice numérique IBM 704.

On présente les résultats numériques relatifs à la distance d'extrapolation linéaire pour différentes masses atomiques et diverses probabilités d'absorption du milieu. La température effective des neutrons de fuite est aussi étudiée en fonction de la masse atomique, de l'absorption du milieu, ainsi que pour différentes directions de fuite des neutrons.

Les résultats théoriques sont comparés aux valeurs expérimentales.

A/708 Югославия

Угловой спектор утечки тепловых нейтронов

Р. Кладник *et al.*

Дается краткое описание вариационно-итерационного метода решения интегрального уравнения переноса для тепловых нейтронов в полубесконечной поглощающей среде без источников. Этот метод используется для получения точных выражений длины линейной экстраполяции и потока утечки тепловых нейтронов через соответствующие решения для бесконечной среды.

В качестве примера был выбран обычный одноатомный газообразный замедлитель, для которого решение для бесконечной среды уже было получено ранее полуаналитическим способом. Предполагается, что сечение поглощения подчиняется закону $1/v$. Численная сторона проблемы была разрешена на электронно-вычислительной машине IBM-704.

Приводятся численные результаты длины экстраполяции для различных значений атомных масс и для нескольких значений вероятности поглощения в рассматриваемой среде. Обсуждается также вопрос эффективной температуры нейтронов утечки в зависимости от атомной массы, поглощения в среде и для различных направлений утечки нейтронов.

Производится сравнение теоретических результатов с экспериментальными данными.

A/708 Yugoslavia

Espectro angular de los neutrones térmicos que escapan de un medio

por R. Kladnik

El autor expone brevemente el método de variación e iteración aplicado a la ecuación integral del transporte para los neutrones térmicos en un medio absorbente semiinfinito y sin fuentes. Este método se emplea con miras a obtener una expresión explícita para la longitud de extrapolación lineal y la distribución de los neutrones térmicos que escapan del medio, en función de la solución hallada para el respectivo medio infinito.

A título de ejemplo, considera un moderador clásico de gas monoatómico, para el cual ya se había obtenido por un procedimiento semianalítico la solución correspondiente al caso del medio infinito. Se supone que la sección eficaz de absorción obedece a la ley $1/v$. Para resolver la parte numérica del problema, se recurrió a una calculadora IBM 704.

En la memoria se presentan los resultados numéricos obtenidos para la longitud de extrapolación lineal para distintas masas atómicas y para diferentes probabilidades de absorción del medio. Asimismo, se examina la temperatura efectiva de los neutrones que escapan como función de la masa atómica, la absorción del medio y de su dirección de escape.

Los datos teóricos se comparan con los resultados experimentales.

Generalization of the Fermi Age Theory and its application to the calculation of resonance escape probability

By G. Rakavy and J. J. Wagschal*

The essential step in Fermi's Age Theory is to connect the slowing down density $q(u)$ with the flux $\phi(u)$ by the approximate expression

$$q(u) = \xi_1 \sigma_s(u) \phi(u) \tag{1}$$

$\sigma_s(u)$ being the scattering cross section at lethargy u and ξ_1 a constant. The exact connexion is given by the double integral,

$$q(u) = \int_0^{-\ln(1-\alpha)} dv \int_{u-v}^{u} du' \, \sigma(u',v) \, \phi(u'), \quad \alpha = 4A/(A+1)^2 \tag{2}$$

where $\sigma(u,v) = \frac{1}{\alpha} \sigma_s(u) \, e^{-v}$ is the cross section to scatter a neutron from lethargy u to lethargy $u+v$. Expanding $\sigma(u',v) \, \phi(u')$ as a series in $(u'-u)$ and integrating with respect to v one obtains:

$$q(u) = -\int dv \sum_{n=0}^{\infty} \frac{(-v)^{n+1}}{(n+1)!} \frac{d^n}{du^n} [\sigma(u,v) \, \phi(u)]$$

$$= \sum_{n=0} \xi_{n+1} \frac{d^n}{du^n} F(u). \tag{3}$$

$$\xi_n = -\frac{1}{\alpha} \int_0^{-\ln(1-\alpha)} dv \quad (-v)^n \, e^{-v}/n! \approx$$

$$- \frac{(-\alpha)^n}{(n+1)!} \text{(for } \alpha \ll 1), \; F(u) = \sigma_s(u) \, \phi(u)$$

The accuracy of approximating this series by its first term, which is Fermi's expression for the slowing down density, depends on the specific case. In some problems, the use of two terms is essential to obtain reasonable accuracy.

A very simple case in which the convergence of the series, Eq. (3), may easily be checked is that of constant ratio of absorption to scattering cross sections. In this case, the flux far from the source behaves like a single exponential, $\phi \sim e^{-\lambda u}$, where λ is a solution of the transcendental equation [1]:

$$1 + \frac{\sigma_a}{\sigma_s} = \frac{e^{\alpha\lambda} - 1}{\alpha\lambda} \, (\alpha \ll 1) \tag{4}$$

Truncating the series, Eq. (3), at the N^{th} term is equivalent in this case to truncating the series expansion of e^{λ} at the same number of terms.

Considering now the slowing down of a pulse of neutrons through a resonance, the time dependence of the pulse is described by the equation:

$$\frac{1}{v} \frac{\partial \phi}{\partial t} + \frac{\partial q}{\partial u} + \sigma_a \, \phi = 0 \tag{5}$$

If Fermi's approximation, Eq. (1), is used for $q(u)$, this equation describes the motion of a pulse upwards in lethargy as if it were rigid. The location of the pulse moves with 'velocity' $\frac{du}{dt} = \xi_1 \sigma_s v$. The resonance escape probability obtained by this approximation is

$$\frac{q}{q_0} = \exp \left[-\int_{u_0}^{u} du' \, \sigma_a(u') / \xi_1 \sigma_s(u') \right] \tag{6}$$

which, as is well known, is too low.

Using two terms in the expansion of $q(u)$ induces a dispersion of the pulse and helps it to tunnel through narrow resonances. The result for the resonance escape probability is much improved in this approximation.

$$\text{Inserting } q = \xi_1 F + \xi_2 \frac{\partial F}{\partial u} \tag{7}$$

into Eq. (5), we have:

$$\frac{1}{v\sigma_s} \frac{\partial F}{\partial t} + \xi_1 \frac{\partial F}{\partial u} + \xi_2 \frac{\partial^2 F}{\partial u^2} + \frac{\sigma_a}{\sigma_s} F = 0 \tag{8}$$

In the special case $v\sigma_s = \text{constant}$, $\frac{\sigma_a}{\sigma_s} = \text{constant}$, a solution to this equation may easily be given. To simplify somewhat the expressions, we also assume $\alpha \ll 1$ (i.e. $A \gg 1$). We obtain:

$$\frac{\partial F}{\partial \tau} = \frac{2}{3} \frac{\partial^2 F}{\partial x^2} - \frac{\partial F}{\partial x} - \frac{\sigma_a}{\sigma_s} F.$$

$$F = (8\pi\tau/3)^{-\frac{1}{2}} \exp \left[-(X - X_0 - \tau)^2/(8\tau/3) \right] \cdot$$

$$\exp \left(-\sigma_a \tau / \sigma_s \right) \tag{9}$$

where $X = u/\frac{1}{2}\alpha$, and $\tau = \sigma_s v t$

It may be observed that, contrary to the result of Fermi's theory, the pulse is dispersed very fast until it becomes a few times broader than α. If the pulse passes

* Hebrew University of Jerusalem, Israel.

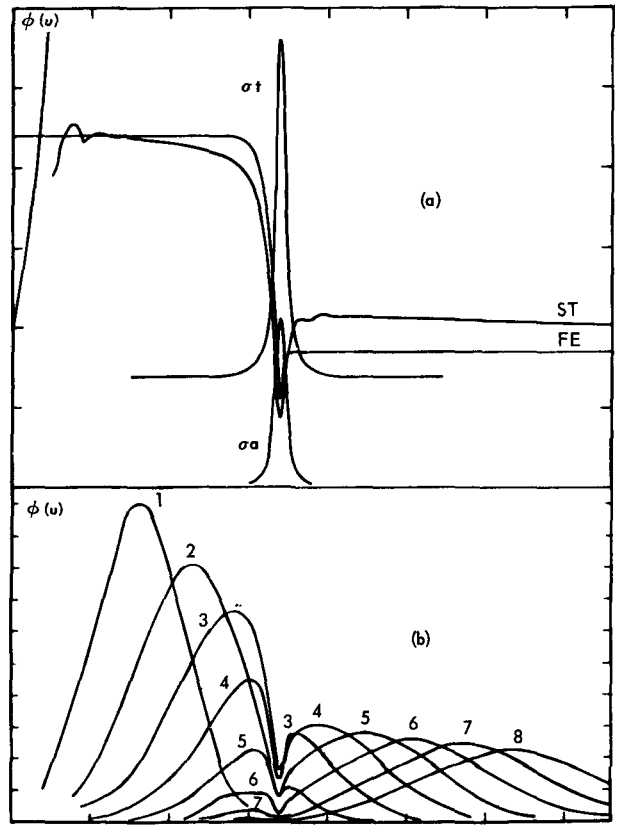

Figure 1(a). Stationary flux and Fermi's approximation
The stationary flux distribution of neutrons emanating from a source at a distance eight times the maximum lethargy gain from a resonance
ST is the flux as given by exact calculation
FE as given by Fermi's approximation, Eq. (6)

Figure 1(b). Flux as a function of lethargy at equal time intervals
The flux distribution of a pulse of neutrons emitted from the source at equal time intervals after emission. The cross sections are the same as indicated in (a)

a resonance with a width of the order of α, it is quite strongly dispersed and leaks through the resonance, reducing thereby the absorption and increasing the resonance escape probability. In Fig. 1 the behaviour of such a pulse leaking through a resonance is illustrated. Using the two term approximation, Eq. (8), the exact behaviour of the pulse is very well described.

Table 1. Calculations of resonance escape probabilities

Method of calculation	q/q_0	% Error	Equation
Numerical solution of the integral Eq.	0.457	—	—
Time dependent – 2 terms	0.452	−1.1	Eq. (8)
Goertzel–Greuling [2]	0.450	−1.53	Eq. (10), $f=2/3$
Time dependent – 1 term (Fermi)	0.389	−14.8	Eq. (10), $f=0$
Wigner's N. R. Formula [3]	0.473	+3.4	Eq. (10), $f=1$

This time dependent picture may explain why the Goertzel Greuling approximation for the resonance escape probability [2] is far superior to Fermi's expression, Eq. (6). Goertzel Greuling's formula

$$\frac{q}{q_0} = \exp\left[-\int du'\, \sigma_a(u')/\xi_1\, (\sigma_s + f\sigma_a)\right] \text{ where } f \approx \frac{2}{3} \quad (10)$$

may be obtained by using the two term approximation, Eq. (7), for the slowing down density. The derivative F' in the second term of Eq. (7) is further approximated by $F' = -\sigma_a\, \phi(u)/\xi_1$, as obtained in Fermi's theory.

As an example, the resonance escape probability for a fictitious resonance with the following properties $\alpha E_r/\Gamma = 3.14$, $\Gamma_\gamma/\Gamma_n = 1$, $(\sigma_s)_{max}/(\sigma_s)_{background} = 2.5$ was calculated. The interference between resonance and potential scattering was omitted. The results presented (Table 1) clearly illustrate the improvement obtained by including the second term in the expansion for the slowing down density. Consequently, diffusion or transport calculations using Fermi's expression, Eq. (1), for the slowing down density may considerably be improved by applying Eq. (9).

REFERENCES

1. Weinberg, A. M., and Wigner, E. P., *The physical theory of chain reactors*, University Press, Chicago, 298 (1958).
2. Goertzel, G., and Greuling, E., Nuclear Sci. Eng., 7, 69 (1960).
3. Dresner, L., *Resonance absorption in nuclear reactors*, Pergamon Press, Oxford, 15 (1960).

ABSTRACT—RÉSUMÉ—АННОТАЦИЯ—RESUMEN

A/827 Israël

Généralisation de la théorie de l'âge de Fermi et son application au calcul du facteur antitrappe

par G. Rakavy et J. J. Wagschal

Une généralisation de la théorie de l'âge de Fermi est obtenue en remplaçant l'expression $\xi\Sigma\phi(u)$ — la densité de ralentissement — par l'expression différentielle

$$q(u)=\sigma_1(u)\phi(u)+\frac{\mathrm{d}}{\mathrm{d}u}[\sigma_2(u)\phi(u)]+\frac{\mathrm{d}^2}{\mathrm{d}u^2}[\sigma_3(u)\phi(u)]+\ldots \quad (1)$$

Les coefficients $\sigma_n(u)$ sont définis par la formule

$$\sigma_n(u)=\frac{1}{n!}\int(-v)^n\,\sigma(u,v)\mathrm{d}v \quad (2)$$

$\sigma(u,v)\mathrm{d}v$ est la section efficace, pour un neutron ayant une léthargie u, de gagner une quantité de léthargie dans l'intervalle v, $v+\mathrm{d}v$.

Cette expression pour la densité de ralentissement q s'obtient après une intégration par termes du développement en série de l'expression exacte pour q. Le premier terme dans (1) est exactement l'expression de Fermi pour la densité de ralentissement. Les termes suivants donnent la dispersion des neutrons dans l'espace de léthargie pendant le ralentissement.

L'expression différentielle (1) pour la densité de ralentissement peut s'appliquer aussi aux calculs du transport et de la diffusion. Les auteurs présentent des résultats des calculs du facteur antitrappe obtenus par l'expression (1) en coupant la série après assez peu de termes. Une comparaison est faite avec des méthodes différentes de calcul du facteur antitrappe.

A/827 Израиль

Обобщение фермиевской теории возраста и ее применение к расчетам вероятности избежания резонансного захвата

Г. Ракави, Дж. Дж. Вагшал

Обобщение фермиевской теории возраста было достигнуто путем замены выражения $\xi\Sigma\varphi(u)$ — плотности замедления — на дифференциальное выражение:

$$q(u)=\sigma_1(u)\,\varphi(u)+\frac{d}{du}[\sigma_2(u)\,\varphi(u)]+\frac{d^2}{du^2}[\sigma_3(u)\,\varphi(u)]+\ldots \quad (1)$$

Коэффициенты $\sigma_n(u)$ определяются выражением

$$\sigma_n(u)=\frac{1}{n!}\int^{n}(-v)^n\sigma(u,\,v)\,dv, \quad (2)$$

где $\sigma(u,\,v)\,dv$ — эффективное сечение при летаргии u для прироста летаргии в интервале v, $v+dv$.

Выражение для плотности замедления q получается путем разложения плотности соударений в точном выражении для q в ряд и интегрирования член за членом. Первый член в уравнении (1) — это фермиевское выражение для плотности замедления. Другие члены описывают рассеяние нейтронов в пространстве летаргии в течение времени замедления.

Дифференциальное выражение (1) для плотности замедления может быть применено в расчетах диффузии или переноса. В докладе представлены результаты вычисления вероятности избежания резонансного захвата, полученные путем усечения уравнения (1) после нескольких членов. Результаты сравниваются с полученными другими методами расчета вероятности избежания резонансного захвата.

A/827 Israel

Generalización de la teoría de la edad de Fermi y su aplicación al cálculo de la probabilidad de escape a la resonancia

por G. Rakavy y J. J. Wagschal

Se obtiene una generalización de la teoría de la edad de Fermi sustituyendo la expresión $\xi\Sigma\phi(u)$ (densidad de moderación) por la expresión diferencial

$$q(u)=\sigma_1(u)\,\phi(u)+\frac{\mathrm{d}}{\mathrm{d}u}[\sigma_2(u)\,\phi(u)]+\frac{\mathrm{d}^2}{\mathrm{d}u^2}[\sigma_3(u)\phi(u)]+\ldots \quad (1)$$

Los coeficientes $\sigma_n(u)$ se definen por

$$\sigma_n(u)=\frac{1}{n!}\int(-v)^n\,\sigma(u,v)\,\mathrm{d}v \quad (2)$$

siendo $\sigma\,(u,v)$ la sección eficaz de una ganancia de letargia en el intervalo v, $v+\mathrm{d}v$ para neutrones de letargia u.

La expresión (1) de la densidad de moderación q, se obtiene por una integración término a término del desarrollo en serie de la densidad de colisión en la expresión exacta de q. El primer término de (1) es la

notación de Fermi para la densidad de moderación. Los términos siguientes expresan la dispersión de neutrones en el espacio de letargia durante la moderación.

La expresión diferencial (1) para la densidad de moderación puede aplicarse en los cálculos de difusión y de transporte. Presentamos resultados de cálculo de la probabilidad de escape a la resonancia obtenidos mediante la expresión (1), limitando la serie a unos pocos términos. Se hace una comparación con otros métodos de cálculo de la probabilidad de escape a la resonancia.

Thermalisation et spectres de neutrons

par M. Cadilhac, J.-L. Soulé et O. Tretiakoff*

MODÈLES SIMPLES DE THERMALISATION

Depuis plusieurs années, divers auteurs ont montré que le remplacement des lois exactes de thermalisation par certains modèles synthétiques simplifiait beaucoup le calcul des spectres de neutrons dans le domaine des énergies inférieures à quelques électron-volts et facilitait la discussion des propriétés physiques de ces spectres, tout en respectant celles de ces propriétés qui sont importantes en physique des réacteurs.

Modèle primaire

La première tentative en ce sens est due à J. Horowitz (1959, non publié), qui a remarqué qu'un opérateur de thermalisation dépend d'une fonction arbitraire si on lui impose d'être différentiel du second ordre, car il est alors, en vertu de la propriété du bilan détaillé, nécessairement de la forme:

$$\Theta = \xi\,\Sigma_s(\infty)\frac{d}{dy}f(y)\left(y\frac{d}{dy}+y-1\right)$$

avec $f(\infty)=1$ ($y=\dfrac{E}{kT}$, énergie réduite). On obtient ainsi un modèle qui conserve la simplicité du modèle de Wilkins (gaz lourd) correspondant à $f(y)=1$, mais permet, grâce à cette fonction $f(y)$, de rendre compte, pour l'essentiel, de l'influence sur les spectres de la structure du modérateur. Ce modèle de « gaz lourd généralisé » a été étudié et utilisé par divers auteurs [1,2,3], et il a été proposé, dans le cas du graphite, un ajustement de la fonction $f(y)$ d'après un spectre d'origine expérimentale [4].

Ce modèle, que nous appellerons « primaire », présente toutefois un inconvénient:

Si Θ est un opérateur différentiel, la thermalisation des neutrons est traitée de façon continue, sans que l'on puisse tenir compte des transferts finis d'énergie que ces neutrons subissent en réalité; les spectres calculés deviennent par suite incorrects pour de fortes résonances d'absorption.

Modèle secondaire

Pour cette raison l'un des auteurs a proposé [5,6] un modèle « secondaire », plus général, qui fait intervenir deux fonctions arbitraires de l'énergie, et dans lequel Θ est un opérateur intégral. Ce modèle conduit à des calculs de spectres aussi simples que le modèle primaire. Il comporte comme cas particulier le modèle de Wigner-Wilkins (hydrogène gazeux monoatomique). Une présentation unifiée des modèles primaire et secondaire est possible grâce à une formulation appropriée que nous allons rappeler.

Le flux $\Phi(y)$ et la densité de ralentissement $q(y)$ sont liés, d'une façon tout à fait générale, et indépendamment de la loi d'absorption, par la relation:

$$\frac{dq(y)}{dy}=\Theta\Phi(y)$$

à laquelle on peut donner la forme

$$\frac{d}{dy}\frac{\Phi(y)}{\Phi_M(y)}=Jq(y)$$

en tenant compte de $q(0)=0$, et en tirant parti du fait que lorsque $q(y)$ s'annule, $\Phi(y)$ doit être proportionnel au flux d'équilibre de Maxwell $\Phi_M(y)$. J est un opérateur auto-adjoint, d'après le théorème du bilan détaillé. Le modèle simple que nous avons proposé consiste à prendre J sous la forme d'un opérateur différentiel du second ordre auto-adjoint:

$$J=j(y)-\frac{d}{dy}k(y)\frac{d}{dy}$$

ce qui introduit deux fonctions $j(y)$ et $k(y)$.

Si $k(y)=0$, J est en fait un opérateur multiplicatif:

$$J=j(y)$$

et on retrouve sans peine le modèle primaire, avec

$$\frac{1}{f(y)}=\xi\Sigma_s(\infty)yj(y)\Phi_M(y)$$

Si $k(y)\neq 0$ (modèle secondaire), on peut voir que $\Phi_M(y')\Sigma_s(y'\to y)$ est une fonction de Green, du type $u(y<)v(y>)$. On voit ainsi que l'hydrogène gazeux monoatomique est un cas particulier du modèle. On a dans ce cas:

$$J=\left(1-\frac{d}{dy}\right)\frac{1}{\Sigma_s(y)\Phi_M(y)}\left(1+\frac{d}{dy}\right)$$

A haute énergie ($y\gg 1$), le raccordement avec la théorie classique du ralentissement impose aux fonctions $j(y)$ et $k(y)$ un comportement tel que les fonctions:

$$G(y)=\xi\Sigma_s(\infty)\ yj(y)\Phi_M(y)$$

$$H(y)=\xi\Sigma_s(\infty)\ k(y)\Phi_M(y)$$

* Commissariat à l'énergie atomique. Avec la collaboration de J. P. de Brion, M. Livolant et D. Pillard.

aient des limites finies lorsque $y \to \infty$, avec $G(\infty) = 1$. Le modèle dégénère alors, et la relation entre $\Phi(y)$ et $q(y)$ prend la forme:

$$\Phi(y) = \frac{1}{\xi \Sigma_s(\infty)} \left[G(y) \frac{q(y)}{y} - H(y) \frac{dq(y)}{dy} \right]$$

On retrouve les modèles simples connus en théorie du ralentissement [7]:

a) Le modèle de ralentissement continu de Fermi ($H(y) = 0$) correspond au modèle primaire;

b) Les modèles de Wigner et de Goertzel-Greuling ($H(y) \neq 0$) généralisant l'hydrogène gazeux correspondent au modèle secondaire.

SPECTRES EN MILIEU HOMOGÈNE

Détermination du spectre

La détermination du spectre d'équilibre $\Phi(y)$ en présence d'une source permanente de densité $S(y)$, d'une source d'énergie infinie d'intensité Q et d'une absorption $\Sigma_a(y)$, doit s'effectuer à partir de la relation de thermalisation:

$$\frac{d}{dy} \frac{\Phi(y)}{\Phi_M(y)} = j(y) q(y) - \frac{d}{dy} \left[k(y) \frac{dq(y)}{dy} \right] \qquad (1)$$

et de l'équation du bilan:

$$\frac{d}{dy} q(y) = \Sigma_a(y) \Phi(y) - S(y) \quad \begin{matrix} q(0) = 0 \\ q(\infty) = Q \end{matrix} \qquad (2)$$

Par substitution de (2) dans (1) et regroupement, on obtient:

$$\frac{d}{dy} \left[\left(\frac{1 + k \Phi_M \Sigma_a}{\Phi_M} \right) \Phi - kS \right] = jq \qquad (3)$$

Les équations (2) et (3) constituent un système différentiel du premier ordre pour les inconnues $\Phi(y)$ et $q(y)$. Il est d'ailleurs commode de substituer à Φ une inconnue auxiliaire égale à $(1 + k\Phi_M \Sigma_a)\, \Phi - k \Phi_M S$.

La solution particulière à déterminer est fixée par les conditions $q(0) = 0$ et $q(\infty) = Q$. Il s'agit donc d'un problème aux limites. On peut cependant le résoudre par une méthode à pas successifs en partant de l'origine; il suffit d'effectuer les calculs avec deux valeurs initiales différentes de $\frac{\Phi(y)}{y}$, et de déterminer *a posteriori* la combinaison qui fournit la bonne valeur de $q(\infty)$. Si S est nul (mais non Q), un seul calcul suffit, avec une simple règle de trois *a posteriori*.

Des précautions sont à prendre en raison des singularités des coefficients pour $y \to 0$ et $y \to \infty$.

Cas d'une absorption faible

Les cas où l'absorption est faible devant la modération étant d'une grande importance pratique, on est conduit à s'intéresser particulièrement au problème suivant: pour une source entièrement localisée à l'infini, et pour une forme donnée de la loi d'absorption, trouver le développement du flux en puissances successives de l'intensité de l'absorption.

On posera donc:

$$S(y) = 0, \frac{Q}{\xi \Sigma_s(\infty)} = 1, \frac{\Sigma_a(y)}{\xi \Sigma_s(\infty)} = r \alpha(y), \; r = \frac{\Sigma_a(1)}{\xi \Sigma_s(\infty)}.$$

Dans ces conditions, le flux peut s'écrire:

$$\Phi(y) = \frac{1}{r} \Phi_0(y) + \Phi_1(y) + r \Phi_2(y) + \ldots$$

où Φ_0 est un flux maxwellien normalisé par la condition:
$\int_0^\infty \alpha(y)\, \Phi_0(y)\, dy = 1$ et où Φ_1, Φ_2, ... sont déterminés de proche en proche par les conditions:

$$n = 1, 2, \ldots \quad \frac{1}{\xi \Sigma_s(\infty)} \Theta \Phi_n = \alpha(y)\, \Phi_{n-1}(y)$$

$$\int_0^\infty \alpha(y)\, \Phi_n(y) dy = 0$$

Ainsi, la détermination de chaque Φ_n est celle d'un flux en présence d'une source, sans absorption. Le flux Φ_1 se comporte toujours comme $1/y$ pour $y \to \infty$. Les flux Φ_1, Φ_2, ... sont des caractéristiques de la loi $\alpha(y)$ et du modérateur. Ceux qui sont relatifs à $\alpha(y) = \frac{1}{\sqrt{y}}$ ont une importance particulière.

La fonction G_0

On sait en effet que la fonction Φ_1 correspondant à une « loi en $1/v$ » est la caractéristique fondamentale d'un modérateur [8]. Or, dans un modèle secondaire, Φ_1 dépend à la fois de G et de H. On peut remplacer la fonction G dans la présentation de ce modèle par une fonction G_0 qui détermine entièrement Φ_1. Considérons en effet l'identité entre opérateurs:

$$J = j - \frac{d}{dy} k \frac{d}{dy} = j_0 - \frac{1}{q_0} \frac{d}{dy} k q_0^2 \frac{d}{dy} \frac{1}{q_0}$$

avec

$$j_0 = j - \frac{1}{q_0} (k q'_0)'$$

et prenons

$$q_0(y) = \frac{2}{\sqrt{\pi}} \int_0^y \sqrt{y' e^{-y'}}\, dy'$$

On a alors:

$$\frac{d}{dy} \frac{\Phi_1(y)}{\Phi_M(y)} = J q_0 = j_0 q_0$$

ce qui montre bien que Φ_1 ne dépend que de j_0, ou encore de

$$G_0(y) = \xi \Sigma_s(\infty) y j_0(y) \Phi_M(y) = G(y) - \frac{y^2 e^{-y}}{\int_0^y \sqrt{y'}\, e^{-y'} dy'} \frac{d}{dy} \left[\frac{H(y)}{\sqrt{y}} \right]$$

Remarquons que G et G_0 ont le même développement asymptotique.

Influence de G_0 et H sur les spectres

Lorsque l'absorption est faible et proche d'une loi en $1/v$, la partie non maxwellienne du spectre ne dépend pratiquement que de G_0; en outre, on peut dire qu'en gros, dans la zone épithermique, le spectre est le produit par G_0 du spectre qui régnerait dans le gaz lourd.

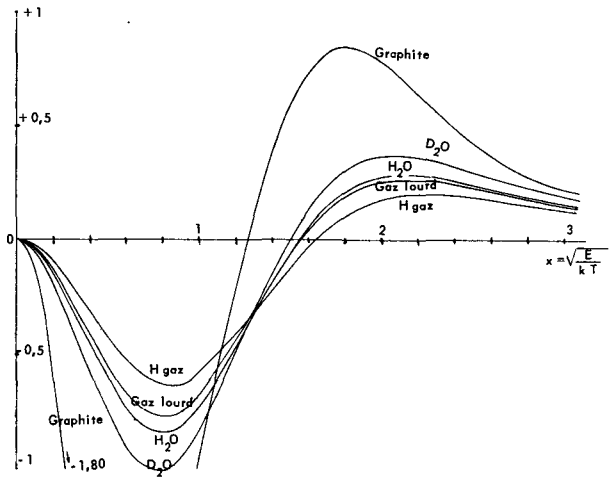

Figure 1. Flux Φ_1 des modérateurs usuels (à 20 °C)

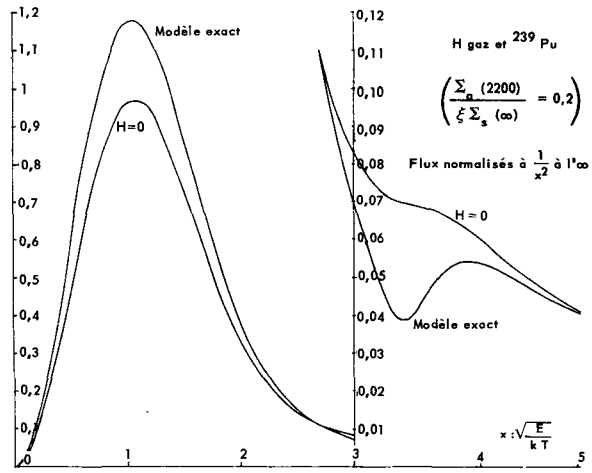

Figure 2. Influence de la fonction H

Ce fait est illustré par les figures 1 et 3, où l'on peut comparer les Φ_1 et les G_0 de différents modérateurs.

Le rôle de H se manifeste lorsque l'intensité de l'absorption croît, en particulier quand la loi d'absorption présente des résonances marquées. C'est en effet cette fonction qui traduit la possibilité plus ou moins grande offerte aux neutrons de franchir les résonances par un petit nombre de diffusions.

Pour voir clairement l'influence de H sur les flux, on doit comparer des modèles ayant même G_0. En particulier, on peut associer à un modèle secondaire le modèle primaire défini par $G=G_0$, $H=0$.

L'influence de H est illustrée quantitativement par la figure 2, où l'on montre le flux obtenu en présence de ^{239}Pu et d'un modérateur « hydrogène gazeux » selon qu'on conserve ou qu'on annule la fonction H.

REPRÉSENTATION DES MODÉRATEURS USUELS

Principe de l'ajustement

Pour chaque modérateur usuel (et à chaque température), on doit déterminer la paire de fonctions G_0, H (ou G, H) qui représente correctement les propriétés modératrices du milieu; autrement dit, on doit effectuer un ajustement. Ce qu'on désire en pratique, c'est évidemment que les flux qu'on sera amené à calculer avec ce modèle soient suffisamment exacts; en fait, ces flux sont ceux qui correspondent à une certaine famille de lois d'absorption. Plus précisément, il est possible de respecter exactement deux flux (outre Φ_M en l'absence d'absorption) puisqu'on dispose de deux fonctions arbitraires. Etant donné l'importance des lois d'absorption en $1/v$, il paraît naturel d'ajuster le modèle de façon à respecter les Φ_1 et Φ_2 relatifs à cette loi. On définit ainsi un procédé canonique d'ajustement permettant d'effectuer de façon systématique les comparaisons entre modérateurs et les tests de validité.

Ajustement sur les moments

Si le modérateur réel est assez voisin d'un modèle secondaire, on peut ajuster sans inconvénient sur deux flux presque quelconques. Dans le cas contraire, un tel ajustement peut servir de première approximation à l'ajustement définitif. Or l'ajustement sur Φ_1 et Φ_2 présente l'inconvénient d'obliger à calculer les sections différentielles du modèle réel (pour la détermination de Φ_1 et Φ_2). Il est donc intéressant d'étudier des ajustements qui évitent ces calculs longs et délicats. Dans le cas où le modèle physique qui représente correctement le modérateur est de type « normal » ou gaussien (ce qui est maintenant admis pour tous les modérateurs usuels) on sait calculer directement les « moments » $\int_0^\infty \Sigma(y\to y')\ (y'^n - y^n)\mathrm{d}y'$ pour n entier et tout y [9]. On peut donner une justification particulière au procédé d'ajustement qui consiste à respecter les deux premiers moments du modèle physique [ou, plus précisément, ces moments multipliés par un même facteur — toujours très voisin de l'unité — choisi de façon que $\xi\Sigma_s(\infty)$ soit conservé]. En particulier, on peut montrer que le G_0 ainsi obtenu possède un développement asymptotique à l'infini dont les trois premiers termes sont identiques à ceux du G_0 ajusté sur Φ_1.

Lorsque le spectre de liaison des atomes du modérateur est relativement étalé (cas du graphite) on constate que cet ajustement est excellent. Par contre, dans le cas de l'eau ou de l'eau lourde les liaisons intramoléculaires se traduisent sur G_0 par des oscillations qui doivent être éliminées de l'ajustement définitif.

Résultats

Dans les figures 3 et 4, on présente les fonctions G_0 et H obtenues à la température ordinaire pour les modérateurs suivants: graphite, eau lourde, eau légère, en prenant comme référence les modèles physiques définis ci-dessous.

Graphite: modèle d'Egelstaff, rectifié par Wikner *et al.* [10]. Selon ce modèle, le spectre de vibration est isotrope, et la densité est continue de 0 à 2550 °K (d'abord proportionnelle à ω^2 jusqu'à 30 °K, puis proportionnelle à ω jusqu'à 300 °K, et constante pour le reste).

Eau légère: modèle de Nelkin [11], où l'on a substitué les données expérimentales de Haywood et Thorson [12] en ce qui concerne les liaisons intermoléculaires.

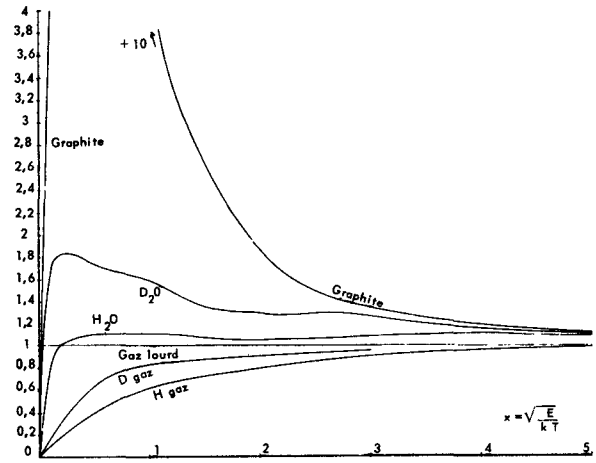

Figure 3. Fonction G_0 des modérateurs usuels (à 20 °C)

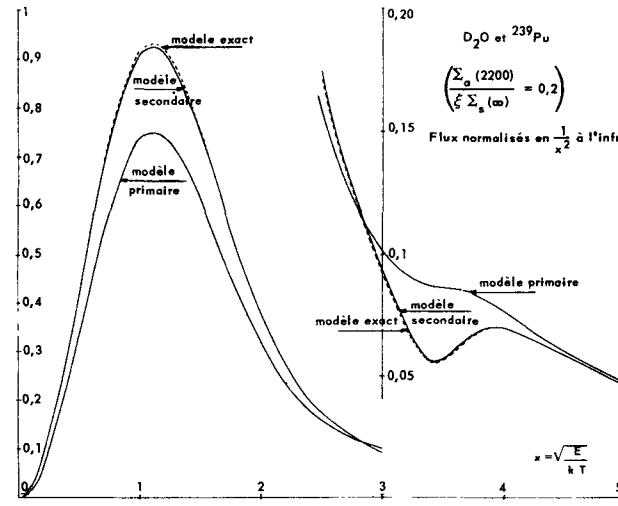

Figure 5. Test du modèle secondaire

Eau lourde: modèle de Butler [13] modifié de même (l'oxygène est pris en compte, mais non les interférences).

En fait, dans chacun de ces trois cas il subsiste quelque incertitude sur le poids à attribuer aux « modes optiques » (liaisons fortes), et nous avons été amenés à envisager plusieurs modèles pour les comparaisons avec l'expérience [14].

On donne à titre d'exemple dans les figures 5 et 6 des spectres obtenus respectivement avec le modèle exact (section différentielle) ou les modèles secondaire puis primaire correspondants.

TRAITEMENT HÉTÉROGÈNE DE LA CELLULE

Le calcul du spectre est avant tout un moyen d'évaluer correctement le bilan de neutrons; on peut en général décomposer la cellule en un petit nombre de régions physiquement homogènes dans lesquelles on a besoin de connaître les spectres moyens $\Phi(y)$. Dans de nombreux cas on se limitera à deux régions: l'une englobant le combustible, l'autre le modérateur.

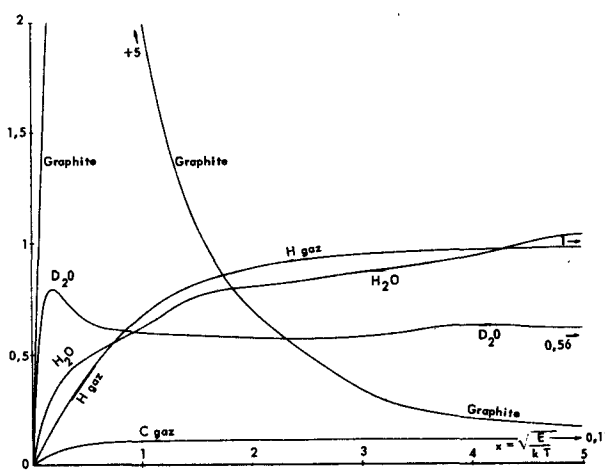

Figure 4. Fonction H des modérateurs usuels (à 20 °C)

La conservation des neutrons à chaque énergie permet d'écrire de façon rigoureuse:

$$\Theta_u \Phi_u(y) = \Sigma_u(y)\Phi_u(y) - I(y)$$
$$\Theta_m \Phi_m(y) = \Sigma_m(y)\Phi_m(y) + \frac{V_u}{V_m} I(y) \qquad (4)$$

Θ_u et Θ_m étant les opérateurs de thermalisation qui représentent respectivement les propriétés du combustible et du modérateur, $I(y)$ étant le courant net de neutrons du modérateur vers le combustible (par unité de volume de combustible).

Absence de ralentissement dans le combustible ($\Theta_u = 0$)

Dans ce cas particulier, une généralisation de la méthode Amoyual-Benoist-Horowitz permet d'obtenir $\Phi_u(y)$ et $\Phi_m(y)$ par l'intermédiaire du calcul de la distribution du spectre dans le modérateur de la cellule.

Rappelons qu'en théorie monocinétique cette méthode [15] consiste à prendre pour $\Phi(r)$ dans le

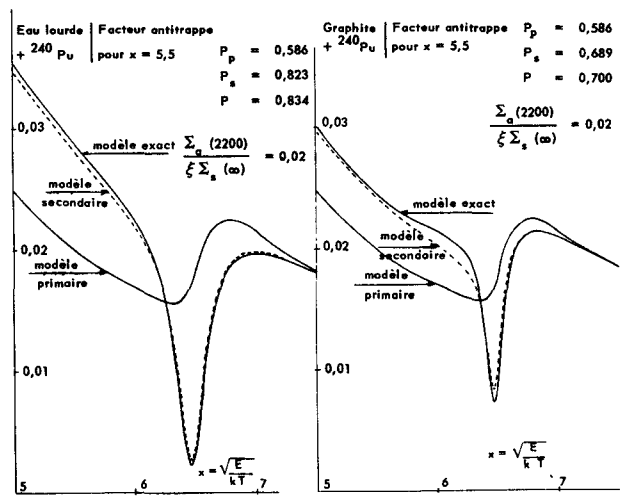

Figure 6. Test du modèle secondaire

modérateur la solution de l'équation de diffusion avec source uniforme:

$$D\triangle\Phi(r)+S=0$$

les conditions aux limites étant $\frac{d\Phi}{dr}(\bar{b})=0$ (périphérie de la cellule) et $\lambda\frac{d\Phi}{dr}(c)=\Phi(c)$, la longueur d'extrapolation λ tenant compte des effets de transport au voisinage du combustible (calcul choc par choc).

L'équation précédente se généralise sous la forme:

$$D(y)\triangle\Phi(r,y)+\Theta\Phi(r,y)-\Sigma_m(y)\Phi(r,y)=0$$

Les conditions aux limites spatiales deviennent $\frac{d\phi}{dr}(b,y)=0$ et $\lambda(y)\frac{d\phi}{dr}(c,y)=\Phi(c,y)$; la longueur d'extrapolation $\lambda(y)$ est maintenant calculée par la méthode A.B.H. pour chaque énergie.

Si l'on adopte pour Θ le modèle secondaire, on obtient les équations:

$$\frac{d}{dy}q(r,y)=-D\triangle\Phi(r,y)+\Sigma_m(y)\Phi(r,y)$$

$$y\Phi_M(y)\frac{d}{dy}\frac{1}{\Phi_M(y)}\left[\Phi(r,y)+\frac{H(y)}{\xi\Sigma_s(\infty)}\frac{d}{dy}q(r,y)\right]=\frac{G(y)}{\xi\Sigma_s(\infty)}q(r,y)$$

les conditions aux limites pour $q(r,y)$ étant:

$$q(r,0)=0 \quad q(r,\infty)=Q=\text{constante}$$

La solution peut être obtenue [8, 16] en utilisant pour $\Phi(r,y)$ le développement

$$\Phi(r,y)=\Sigma\psi_i(y)\Phi_i(r,y)$$

les $\Phi_i(r,y)$ étant les fonctions propres de l'opérateur $\triangle$ ($\triangle\Phi_i+B_i^2(y)\Phi_i=0$) vérifiant chacune les conditions aux limites en $r=\bar{b}$ et $r=c$.

Les termes successifs de cette série décroissent asymptotiquement comme $1/B_i^4$ et sa convergence est uniforme en y.

Compte tenu du bilan dans le combustible:

$$V_u\Sigma_u(y)\Phi_u(y)=-D\int_{V_m}\triangle\Phi(r,y)d\vec{r}$$

le calcul précédent donne le spectre moyen dans le combustible et le courant $I(y)=\Sigma_u(y)\Phi_u(y)$.

La convergence de la méthode est illustrée par la figure 7, qui représente les fonctions $h(y)=\Phi_u(y)/\Phi_m(y)$ obtenues en limitant le développement de $\Phi(r,y)$ à K termes ($K=1,2,5$) dans un exemple caractéristique.

L'approximation du premier ordre est suffisante lorsque la loi d'absorption du combustible ne présente pas de résonances accentuées.

On remarquera que cette approximation équivaut à la relation:

$$I(y)=\gamma(y)[\Phi_m(y)-\Phi_u(y)] \qquad (5)$$

où $\gamma(y)=\Sigma_u(y)\frac{h(y)}{1-h(y)}$ est relié directement à la longueur d'extrapolation $\lambda(y)$.

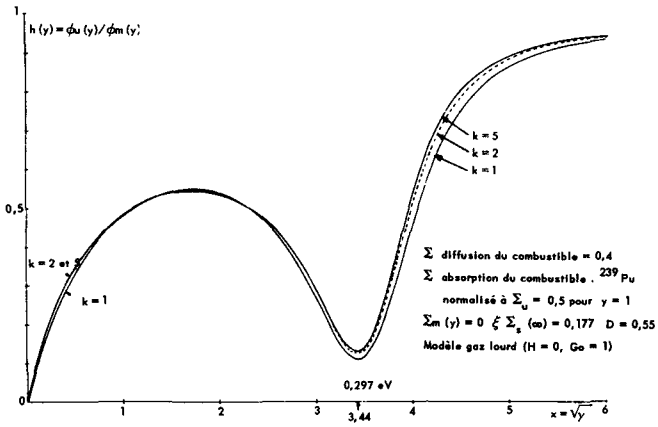

Figure 7. Cellule cylindrique c = 1, b = 8

Cette relation, qui ramène formellement la résolution du système (4) à un problème du type homogène, est couramment utilisée en pratique.

Ralentissement dans le combustible

Lorsque le combustible contribue aux phénomènes de thermalisation, on peut caractériser ses propriétés par un opérateur Θ_u. Si l'on utilise pour Θ_u et Θ_m le modèle secondaire, le système à résoudre s'écrit:

$$y\Phi_M\frac{d}{dy}\frac{1}{\Phi_M}\left[\Phi_u+\frac{H_u(y)}{\xi\Sigma_s(\infty)_u}\frac{dq_u}{dy}\right]=\frac{G_u(y)}{\xi\Sigma_s(\infty)_u}q_u$$

$$y\Phi_M\frac{d}{dy}\frac{1}{\Phi_M}\left[\Phi_m+\frac{H_m(y)}{\xi\Sigma_s(\infty)_m}\frac{dq_m}{dy}\right]=\frac{G_m(y)}{\xi\Sigma_s(\infty_m)}q_m$$

$$\frac{dq_u}{dy}=\Sigma_u(y)\Phi_u-I(y)\,.\,\frac{dq_m}{dy}=\Sigma_m(y)\Phi_m+\frac{V_u}{V_m}I(y)$$

Les conditions aux limites du problème sont maintenant:

$$q_u(0)=q_m(0)=0 \qquad \frac{q_u(\infty)}{\xi\Sigma_s(\infty)_u}=\frac{q_m(\infty)}{\xi\Sigma_s(\infty)_m}=Q$$

On complète en pratique ces équations par la relation (5), dont l'utilisation a été étudiée par D. C. Leslie [17].

Elles se transposent aisément au cas où le combustible et le modérateur sont à des températures différentes.

APPLICATIONS

L'emploi des sections efficaces effectives (Westcott, 1958) présente l'intérêt de mettre en évidence dans le calcul du bilan de neutrons en milieu hétérogène des grandeurs dont certaines sont directement accessibles à l'expérience:

Distribution spatiale de la densité de neutrons (taux de réaction d'un détecteur en $1/v$) par les mesures de structures fines (manganèse).

Sections efficaces effectives pour différents phénomènes en un même point, par la mesure d'indices de spectre (rapport de deux $\hat{\sigma}$ dans le spectre étudié, normalisé à l'unité dans un spectre maxwellien de référence).

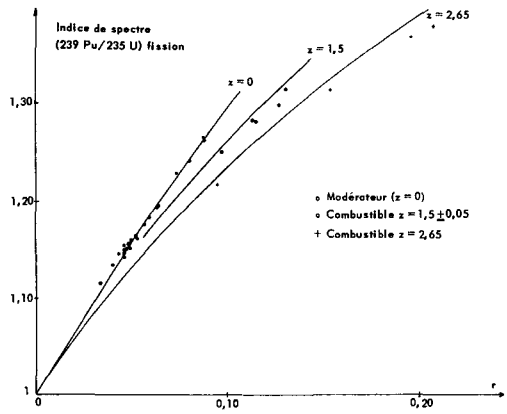

Figure 8. Indices de spectre, réseaux U métal-graphite

Le formalisme correspondant est employé systématiquement dans un code faisant appel aux modèles et aux méthodes décrits dans cette communication. Le calcul du spectre et des principales sections efficaces effectives demande de quelques secondes à une minute (IBM 7094) suivant la complexité du problème et le volume des résultats. Différentes variantes de ce code sont adaptées à chaque problème particulier: interprétation détaillée d'expériences (structures fines, indices de spectre, mesure des propriétés de milieux multiplicateurs), association avec les codes de calcul de réseaux.

On peut éviter le recours à la machine lorsque certaines conditions sont réunies: pas d'effets de rethermalisation, absorption du combustible voisine de la loi en $1/v$. Pour un modérateur donné, les sections efficaces effectives couramment utilisées sont alors tabulées en fonction de trois paramètres: T (température), r (intensité de la source à l'infini rapportée à la densité de neutrons) et Z (paramètre caractérisant l'hétérogénéité du réseau) [8]. On peut comparer dans la figure 8 les valeurs de l'indice de spectre $^{239}Pu/^{235}U$ (fission) tirées de ces tables avec les valeurs expérimentales correspondantes pour un réseau type uranium naturel–graphite.

On trouvera, dans d'autres mémoires présentés par le CEA à cette conférence, les exemples d'utilisation les plus importants.

BIBLIOGRAPHIE

1. Schaefer, G. W., Allsopp, K., *Chemical binding effects in the generalized heavy free gas approximation*, BNL 719, *2*, pp. 614–655 (1962).
2. Corngold, N., *The phase integral method in neutron thermalization*, BNL 719, *4*, pp. 1075–1102 (1962).
3. Pitcher, H. H. W., *The generalized heavy free gas thermalization operator*, AEEW-M-350 (1963).
4. Leslie, D. C., *Calculation of thermal spectra in lattice cells*, BNL 719, *2*, pp. 592–609 (1962).
5. Cadilhac, M., Horowitz, J., Soulé, J.-L., Tretiakoff, O., *Some mathematical and physical remarks on neutron thermalization in infinite homogeneous systems*, BNL 719, *2*, pp. 439–463 (1962).
6. Cadilhac, M., *Méthodes théoriques pour l'étude de la thermalisation des neutrons dans les milieux absorbants infinis et homogènes*, Rapport CEA 2368 (1964).
7. Dresner, L., *Resonance absorption in nuclear reactors*, Pergamon Press (1960).
8. Horowitz, J., Tretiakoff, O., *Effective cross-sections for thermal reactors*, EANDC (E), 14 (1960).
9. Soulé, J.-L., Pillard, D., *Les moments de transfert d'énergie en thermalisation*, Rapport CEA 2472 (1964).
10. Wikner, N. F., Joanou, G. D., Parks, D. E., *Neutron thermalization in graphite*, GA-4169 (1963).
11. Nelkin, M., *The scattering of slow neutrons by water*, Phys. Rev., *119*, p. 791 (1960).
12. Haywood, B. C., Thorson, I. M., *The scattering law for light and heavy water at 20°C and 150°C*, BNL 719, *1*, pp. 26–53 (1962).
13. Butler, D., *The scattering of slow neutrons by heavy water, I and II*, Proc. Phys. Soc., *81*, pp. 276–299 (1963).
14. Soulé, J.-L., *Modèles simples pour les thermaliseurs usuels*, Rapport CEA 2473 (1964).
15. Amouyal, A., Benoist, P., Horowitz, J., *Nouvelle méthode de détermination du facteur d'utilisation thermique d'une cellule*, J. Nucl. Energ., *6*, pp. 79–98 (1957).
16. Tretiakoff, O., de Brion, J.-P., Mougey, J., Naudet, R., *Thermalisation en milieu hétérogène*, Rapport CEA 2474 (1964).
17. Leslie, D. C., *The "Spectrox" method for thermal spectra in lattice cells*, React. Sc. and Techn., *17*, pp. 293–306 (1963).
18. Cogne, F., Journet, J., *Mesures fines dans des réseaux à graphite*, Rapport CEA 2479 (1964).

ABSTRACT—RÉSUMÉ—АННОТАЦИЯ—RESUMEN

A/73 France

Neutron thermalization and spectra

By M. Cadilhac *et al.*

The investigation of the neutron spectra in thermal reactors is of increasing importance because of the part played in them by plutonium. It has been remarked that, whatever the absorption law, the scattering law in the moderator affects the spectrum only through certain over-all properties. It would thus seem possible to develop a simplified representation of this effect which would lead to a clear understanding of the phenomena, reducing at the same time the volume of numerical calculations required.

The "synthetic" model employed by the authors presents the advantage of reducing the determination of the spectra in a homogeneous medium to the resolution of a second order differential equation, like the Wigner-Wilkins model (monatomic gaseous hydrogen) and the "generalized heavy gas" model of J. Horowitz, which, incidentally, are both special cases. The model is, on the other hand, sufficiently general to allow a correct treatment of the situations met with in practice and in particular the important case where the presence of plutonium introduces absorption resonances at low energy. Actually, the chemical or crystalline bonds of the moderator are introduced into the proposed model through two energy functions. These functions have been adjusted for the usual moderators (graphite, heavy water, light water) by means of known theoretical scattering laws.

In a heterogeneous medium, the most important factor is the mean spectrum in the fuel of one cell, obtained by a generalization of the Amouyal-Benoist-Horowitz method. The proposed model lends itself particularly well to such calculations and also allows the effects of rethermalization (for instance when the cooling system and the moderator are at different temperatures) to be treated.

Finally, some examples are given of practical applications: codes for spectra and effective cross-section computations (publication of tables), codes for the treatment of the neutron balance in a lattice or for the interpretation of experiments (spectral indices, critical experiments on plutonium, diffusion parameters).

A/73 Франция

Термализация и спектры нейтронов

М. Кадилак *et al.*

Исследование спектров нейтронов, преобладающих в реакторах на тепловых нейтронах, приобретает все большее значение в связи с применением плутония. Установлено, что на спектр нейтронов независимо от характера поглощения влияют только определенные общие закономерности диффузии замедлителя. Следовательно, a priori возможно составить упрощенное выражение этого явления, которое дает отчетливое представление о процессе в целом и уменьшит объем необходимых расчетов.

«Синтетическая» модель, принятая авторами, дает возможность свести определение спектров нейтронов в гомогенной среде к решению дифференциального уравнения второго порядка, подобно модели Вигнера — Уилкинса (атомарный газообразный водород) и модели Горовица, которые, впрочем, обе имеют отношение к специальным случаям. Вместе с тем модель имеет слишком общий характер, чтобы ее можно было использовать для точных практических расчетов, особенно если присутствие плутония вызывает появление резонансов поглощения при низких энергиях. В практических условиях химические и кристаллические связи замедлителя осложняют предложенную модель за счет двух функций энергий. Эти функции уточнены для обычных замедлителей (графит, тяжелая и обычная вода) на основе известных теоретических законов диффузии.

В гетерогенной среде прежде всего должен быть известен средний спектр нейтронов в топливе ячейки, что позволяет создать общий метод Амуйаль — Бенуа — Горовица. Предлагаемая модель особенно применима для этих расчетов, позволяя одновременно учитывать эффекты ретермализации (когда, например, теплоноситель имеет температуру, отличную от температуры замедлителя).

В заключение приведены примеры практического использования модели: формулы, расчеты спектров нейтронов, расчет эффективных сечений при составлении таблиц, решение проблем нейтронного баланса в активной зоне, объяснение результатов экспериментов (индексы спектров, критические опыты с плутонием, параметры диффузии).

A/73 Francia

Termalización y espectros de neutrones

por M. Cadilhac *et al.*

El estudio de los espectros de neutrones que reinan en los reactores térmicos ha tomado una importancia creciente debido al papel que en ello desempeña el plutonio. Cualquiera que sea, por otra parte, la ley de absorción, se comprueba que la ley de difusión del moderador solo actúa sobre el espectro a través de

ciertas propiedades globales. Es, pues, posible, *a priori*, establecer una representación simplificada de esta acción, que conduzca a una comprensión clara de los fenómenos, reduciendo el volumen de los cálculos numéricos necesarios.

El modelo « sintético » adoptado por los autores presenta la ventaja de reducir la determinación de los espectros en medio homogéneo a la resolución de una ecuación diferencial de segundo orden, como el modelo de Wigner-Wilkins (hidrógeno gaseoso monoatómico) y el modelo de « gas pesado generalizado » de J. Horowitz, que son, por otra parte, el uno y el otro, casos particulares de aquél. Pero, además, este modelo es bastante general para permitir tratar correctamente las situaciones halladas en la práctica, y en particular el caso importante en que la presencia de plutonio hace aparecer resonancias de absorción de baja energía. Los enlaces químicos o cristalinos del moderador intèrvienen, en efecto, en el modelo propuesto por intermedio de dos funciones de la energía. Estas funciones han sido ajustadas, para los moderadores usuales (grafito, agua pesada, agua ligera), a partir de leyes teóricas de difusión conocidas.

En medio heterogéneo importa ante todo conocer bien el espectro medio en el combustible de una celda, lo que permite una generalización del método de Amouyal-Benoist-Horowitz. El modelo presentado se presta particularmente bien a estos cálculos, y permite tratar igualmente los efectos de retermalización (cuando, por ejemplo, el refrigerante está a temperatura diferente de la del moderador).

Se dan, finalmente, ejemplos de utilización práctica: códigos que permiten calcular los espectros, las secciones eficaces efectivas (publicación de tablas), tratamiento de problemas de balance neutrónico en una red, o interpretación de experiencias (índices de espectro, experiencias críticas con plutonio, parámetros de difusión).

Perfectionnements dans les méthodes de calcul neutronique des réacteurs thermiques

par R. Naudet, A. Amouyal et P. Benoist *

Le présent mémoire rassemble un certain nombre de théories nouvelles et de méthodes de calcul relatives aux réseaux à neutrons thermiques mises au point au CEA. L'étude de la thermalisation des neutrons fait l'objet d'un mémoire séparé [11]: les progrès réalisés en France dans ce domaine constituent certainement la nouveauté essentielle dans les méthodes de calcul. Mais d'autres problèmes existent en dehors de celui-là, ou en constituent des applications particulières.

CALCUL DES COEFFICIENTS DE DIFFUSION DANS LES RÉSEAUX COMPORTANT DES CAVITÉS

Les études théoriques réalisées à Saclay sur le transport des neutrons ont permis d'établir des expressions simples des coefficients de diffusion, applicables en particulier lorsque les réseaux comportent des cavités. On trouvera un exposé général dans [1]; une publication partielle avait été donnée antérieurement dans [2]. Rappelons que la première théorie sur ce sujet avait été publiée en 1949 par Behrens [3]; on a reconnu depuis assez longtemps déjà ses insuffisances, qui proviennent d'hypothèses de base trop schématiques.

Le calcul des fuites dans un réacteur hétérogène de dimensions finies se présente en théorie d'une manière extrêmement compliquée. En particulier, dès que les fuites ne sont pas infiniment petites le coefficient de diffusion ne dépend pas uniquement des propriétés intrinsèques du milieu mais aussi de ses dimensions. Pour une pile suffisamment grande, cependant, on peut négliger cette correction, ce qui conduit dans le cas d'un milieu homogène à la représentation classique de l'aire de diffusion par le sixième du carré moyen de la distance franchie en ligne droite de la source à l'absorption. Mais on peut démontrer que cette représentation n'est plus exacte en toute rigueur dans un réseau (comme l'avait admis en particulier Behrens): il apparaît dans l'expression du coefficient de diffusion un terme supplémentaire, qui ne tend vers zéro qu'avec l'absorption. Enfin d'autres difficultés proviennent du fait qu'on n'a pas le droit à priori de négliger le couplage entre groupes d'énergie.

P. Benoist a présenté une formulation très générale du calcul des fuites de neutrons, qui permet de ne négliger au départ aucun des phénomènes mentionnés ci-dessus, et par suite d'en apprécier l'incidence dans chaque cas. On montre d'ailleurs que, dans la plupart des applications pratiques, les diverses corrections indiquées peuvent être négligées sans erreur grave.

Le problème le plus important dans le cas d'un réseau consiste à savoir définir un milieu homogène équivalent du point de vue de la migration des neutrons. Chaque milieu i constitutif de la cellule peut alors être caractérisé par un libre parcours de transport λ_i (qui peut être éventuellement infini: c'est le cas du vide); on cherche à obtenir une moyenne pondérée de ces λ_i.

Pour donner une idée simple de la forme des expressions auxquelles on est conduit, supposons un instant que l'on puisse négliger les corrélations angulaires entre parcours successifs. On peut alors démontrer que la moyenne du libre parcours pour un neutron né dans le milieu i est $\Sigma_j P_{ij}\lambda_i$, où P_{ij} est la probabilité pour ce neutron d'avoir sa première collision dans le milieu j. La moyenne du libre parcours pour la cellule s'obtient en pondérant les expressions précédentes par les volumes et les flux. On remarque que si tous les milieux sont grands par rapport aux libres parcours, $\Sigma_j P_{ij}\lambda_j \neq \lambda_i$, et on retrouve la règle élémentaire de pondération; au contraire, si un des λ_j devient infini, les produits $P_{ij}\lambda_j$ restent finis: il n'y a donc aucune difficulté à supposer qu'un des milieux de la cellule est constitué par du vide.

Cependant les propriétés de diffusion du milieu ne sont pas isotropes en général (même si le choc est isotrope): il faut donc définir un coefficient de diffusion D_k dans une direction donnée; on est amené pour cela à substituer aux P_{ij} des probabilités « orientées » $P_{ij,k}$ dont le calcul fait intervenir le cosinus de l'angle entre la direction du neutron et la direction considérée k. En particulier si c est l'indice relatif à un milieu vide, les expressions $P_{cc,k}\lambda_c$ font intervenir des grandeurs caractérisant la géométrie de la cavité (rapport du carré moyen des cordes de direction donnée au carré de la moyenne de ces cordes): on retrouve le terme de transport de Behrens. La formulation indiquée est cependant déjà beaucoup plus générale, puisqu'elle permet de tenir compte correctement des différences de libre parcours et de flux dans la cellule (on voit apparaître par exemple un terme nouveau qui traduit la transparence de l'élément combustible).

* Commissariat à l'énergie atomique.

En réalité l'insuffisance la plus grave de la théorie de Behrens, aussi bien que de l'approche qui précède, est le fait de négliger les corrélations angulaires entre parcours successifs (on voit bien en particulier que si un neutron vient de traverser une cavité, il a plus de chance de parcourir une grande distance lors de son parcours suivant s'il est diffusé vers l'arrière que s'il est diffusé vers l'avant). Or il est possible de déduire de la formulation très générale de la référence [1], dans le cas où on admet seulement les hypothèses faites plus haut, une expression qui a la même forme que celle qui vient d'être donnée mais qui la généralise largement*:

$$D_j = \frac{\bar{\lambda}_k}{3} = \frac{1}{3}\frac{\sum_{ij} V_i \phi_i P^*_{ij,k} \lambda_j}{\sum_i V_i \phi_i}$$

avec

$$P^*_{ij,k} = P_{ij,k} + \sum_{l=1}^{\infty} P^{(l)}_{ij,k}$$

les termes d'ordre l faisant intervenir les corrélations angulaires entre des parcours séparés par l collisions.

Dans le cas d'un réseau usuel à deux dimensions, ces corrélations n'existent que pour le coefficient de diffusion radial. Pour calculer pratiquement les $P^*_{ij,r}$, plusieurs méthodes ont été proposées. Dans la référence [2] on calculait les premiers termes du développement en l; cette méthode a l'inconvénient de converger lentement. Une nouvelle méthode dite « intégrale », qui calcule globalement l'ensemble des termes de corrélation angulaire, a alors été étudiée.

On est ramené en fait à résoudre l'équation de transport pour une source anisotrope particulière, proportionnelle au cosinus de l'angle de la direction d'émission avec la direction k, et pouvant être considérée comme uniforme dans chaque milieu i. Il est commode de définir alors un certain mode fictif de naissance et de capture des neutrons: les $P^*_{ij,k}$ seront regardés comme des probabilités pour un neutron né « fictivement » dans i d'être capturé « fictivement » dans j; on peut de même définir des probabilités de sortie « fictive » d'un milieu; ces nouvelles définitions sont justifiées par l'existence d'une relation de conservation des neutrons « fictifs » en tout point analogue à celle qui régit les neutrons réels (elle traduit physiquement la conservation des quantités de mouvement dans la direction k). Ainsi formulé le problème devient analogue formellement à celui du facteur d'utilisation thermique, et on est amené alors à un mode de raisonnement très voisin de celui développé dans la référence [9]. Moyennant des hypothèses raisonnables sur les distributions angulaires d'entrée dans chaque milieu, on peut traiter séparément les différents milieux, et, de même que dans [9] on « ajustait » une longueur d'extrapolation sur celle du corps noir, de même ici on « ajuste » un terme sur le cas particulier d'une cellule à canal vide. Pour ce problème du canal vide, Carter [5] et Leslie [4] ont obtenu une formule simple et précise, mais qui s'appuie sur une interpolation assez arbitraire; on a établi une formule d'une précision comparable et qui ne nécessite pas d'interpolation. En définitive les $P^*_{ij,r}$ s'expriment simplement en fonction des $P_{ij,r}$.

Pour les géométries usuelles de cellule, en symétrie cylindrique, les fonctions $P_{ij,z}$ et $P_{ij,r}$ ont été tabulées ou tracées sous forme d'abaques (l'une d'entre elles n'est autre que la fonction Q_k de Behrens). En outre un programme de calcul est en cours d'écriture pour le cas complexe d'une cellule comportant une grappe de barres de configuration quelconque dans un canal cylindrique, à partir de formules établies sans approximation dans [1]. Ces fonctions $P_{ij,k}$ ont l'avantage de pouvoir également servir au calcul de ϵ, f et p.

Enfin une méthode variationnelle a été programmée qui est précise, mais extrêmement lourde: elle a été utilisée pour apprécier la validité des calculs précédents. On trouve ainsi que la méthode intégrale conduit, pour des cellules de type courant, à un écart ne dépassant pas 2 à 3 millièmes sur le coefficient de diffusion radial; l'ancienne formule [2] limitée à $l=2$ conduit à un écart de l'ordre de 1 à 3% sur le coefficient radial pour des cellules normales, cet écart croissant très vite avec les dimensions du canal; la formule de Behrens conduit, tant pour le coefficient axial que pour le coefficient radial, à des écarts beaucoup plus considérables.

On donne dans [1] un certain nombre de corrections, facilement utilisables, permettant de rendre compte des effets envisagés au début: correction dépendant du laplacien, qui peut affecter fortement le coefficient axial pour des piles de faible hauteur; correction liée à l'absorption, qui n'affecte que le coefficient radial (sans action sur l'aire de migration, elle apparaît dans le calcul séparé des coefficients thermique et rapide). On a étudié également les effets d'interaction de canal à canal qui s'introduisent dans des réseaux à pas serré.

Une autre application intéressante de la théorie est la suivante: on peut montrer que le flux réel n'est pas séparable en un produit du flux macroscopique et de la structure fine, mais qu'il s'ajoute à ce produit un terme supplémentaire proportionnel au produit du gradient du flux macroscopique par une fonction périodique antisymétrique à l'échelle d'une cellule. L'intensité C de cette composante antisymétrique est proportionnelle à la quantité:

$$\frac{D_r}{\frac{1}{z}\lambda_m} - \frac{\phi_m}{\phi_t}$$

où λ_m est le libre parcours et ϕ_m le flux moyen ordinaire dans le modérateur, et ϕ_t le flux moyen dans toute la cellule. La mesure de la quantité C, même avec une précision limitée, détermine alors le coefficient radial D_r avec une précision bien meilleure.

Par exemple on a fait la mesure dans AQUILON 2 pour des grappes de 19 crayons d'UO_2 enrichis à 3,5% gainés d'aluminium de ϕ_e 9,5 mm, placés dans des tubes de gaz ϕ_e 80 mm dans un réseau de pas carré

* Bien qu'obtenue à partir d'un formalisme différent, l'expression obtenue par Leslie [4] est équivalente.

170 mm: deux dispositions ont été étudiées, une disposition serrée avec les crayons jointifs, et une autre où les crayons sont espacés de 6 mm entre gaines. Deux méthodes différentes ont été utilisées pour la détermination de C. Les valeurs de $\frac{D_r}{\frac{1}{z}\lambda_m}$ obtenues pour les neutrons thermiques sont les suivantes:

	Expérience structure fine	Expérience macroscopique	Nouvelle formule	Behrens
Grappe écartée .	1.207±0,02	1.205±0,02	1.207	1.076
Grappe serrée .	1.196±0,02	1.196±0,02	1.217	1.237

(la formule de Behrens donne un résultat trop faible dans le premier cas, parce qu'elle ne tient pas compte de la « transparence » de la grappe, qui est alors très grande; dans le second cas, le fait de négliger les corrélations angulaires devient prédominant; s'il s'agissait d'un barreau encore plus opaque, la formule de Behrens donnerait de ce fait un résultat nettement trop fort).

RÉPARTITION DES DENSITÉS NEUTRONIQUES DANS LES DIFFÉRENTS MILIEUX CONSTITUANT UNE CELLULE

Le spectre variant en tout point, il est nécessaire en théorie de tenir compte simultanément de la diffusion et de la thermalisation des neutrons pour obtenir leur répartition dans la cellule. D'où, dans plusieurs laboratoires, la mise au point de codes de transport à un très grand nombre de groupes de vitesses. A Saclay, en particulier, de tels codes existent. Les calculs numériques sont extrêmement lourds. Toutefois, les recherches sur la thermalisation en milieu hétérogène [13] ont montré qu'une solution de base — qui constitue d'ailleurs une approximation suffisante dans la plupart des cas pratiques — consiste à prendre en considération la répartition des densités partielles à chaque vitesse, obtenue en théorie monocinétique avec des sources uniformes et les sections efficaces correspondant à cette vitesse. Dans ces conditions la résolution du problème monocinétique conserve tout son intérêt.

Calculs à une vitesse

Extension de la méthode des doubles harmoniques sphériques

J. Yvon avait présenté en 1955 une méthode dite « double P_n », qui a été utilisée avec succès depuis de nombreuses années en géométrie plane [7]. Son extension aux géométries sphérique et cylindrique infinie comportait une difficulté due au fait que le produit de la masse de Dirac $\delta(\mu)$ et de la fonction échelon unité $U(\mu)$ n'est défini qu'à une constante multiplicative près: $U(\mu)\delta(\mu) = \lambda\delta(\mu)$ où λ est une constante arbitraire.

A. Amouyal a montré que la vitesse de convergence des développements associés à la valeur $\lambda = 1$ (singularité orientée vers l'extérieur) est relativement satisfaisante, ce qui nous a incités à écrire une série de programmes utilisant ce type de méthode.

Les résultats numériques, par comparaison avec la méthode P_n ordinaire ou avec les méthodes type S_n [8], montrent que double P_1 est meilleur que P_5 ou S_4, et que double P_2 est meilleur que S_8.

Généralisation de la méthode « ABH »

La résolution de l'équation du transport, même en se bornant à une vitesse et en utilisant les calculs numériques les plus appropriés (par exemple double P_n), reste tout de même assez lourde. On est donc amené à rechercher des méthodes simplifiées permettant d'atteindre des résultats suffisamment corrects avec des moyens de calcul beaucoup moins lourds. Celle décrite dans la référence [10] répond à cet objet.

Les auteurs de la référence [9] avaient proposé une méthode très simple, qui est connue parfois sous le nom d'« ABH ». De nombreuses vérifications numériques par comparaison avec la résolution des équations du transport ont justifié sa validité: toutefois elle ne s'appliquait qu'au cas où la cellule, supposée cylindrique, comporte uniquement un barreau de combustible et du modérateur, avec éventuellement une gaine d'air entre les deux. Dans les cas pratiques on est souvent amené à considérer un certain nombre de milieux supplémentaires: réfrigérant, tube de guidage, isolement thermique, tube de force. La méthode exposée dans [10] est une généralisation qui permet de traiter un nombre quelconque de milieux concentriques.

On utilise la méthode choc par choc, comme on le faisait déjà pour le combustible, pour le traitement des différents milieux, à l'exception du dernier (modérateur), qui peut être traité comme auparavant par une théorie de diffusion avec condition ajustée sur la surface interne. Les mêmes hypothèses simplificatrices sont admises (isotropie des densités angulaires entrante et sortante à chaque frontière — probabilité de sortie après un ou plusieurs chocs obtenue en remplaçant la source de premier choc par sa moyenne dans ce milieu).

Dans les cas rencontrés en pratique, la limitation de précision introduite par ces hypothèses est la plupart du temps négligeable.

La méthode présente l'avantage d'être standard quel que soit le nombre de milieux et de ne pas exiger un traitement particulier des milieux vides. Elle peut fournir également un calcul approché des densités dans une barre combustible devenue hétérogène par suite de l'irradiation: il suffit de la décomposer en plusieurs zones homogènes concentriques. La méthode a fait l'objet d'un code pour calculateur IBM 7094; le temps de calcul est extrêmement court, compris dans les cas usuels entre une fraction de seconde et quelques secondes.

Prise en compte de la thermalisation

Considérons le rapport des densités moyennes dans deux milieux, par exemple le combustible et le modérateur. Pour utiliser l'hypothèse mentionnée plus haut, il faut connaître pour toute vitesse v le rapport $h(v)$ des densités partielles calculées en monocinétique à cette vitesse; alors si $n(v)$ est le spectre moyen dans le modérateur, normalisé à l'unité, le rapport des densités totales est $h = \int_0^\infty h(v)n(v)\mathrm{d}v$. Cette intégration est effectuée automatiquement en même temps que le calcul du spectre.

Soit h_M la valeur de h pour une vitesse moyenne, par exemple la vitesse la plus probable du spectre de Maxwell à la température du modérateur. $\bar{h}$ sera en général différent de h_M, et il le sera davantage si la loi de capture du combustible est compliquée (par exemple, barreau contenant une forte proportion de plutonium). L'exemple suivant montre comment varie $\bar{h}$ par rapport à h_M, pour des réseaux à eau lourde formés de barres d'uranium naturel ϕ 44 en fonction du pas:

Pas (en mm)	$1/h_M$	$1/\bar{h}$
130	2299	2157
170	2490	2427
210	2651	2636
250	2791	2806
290	2913	2950

Dans le cas où la cellule comporte un certain nombre de milieux entre combustible et modérateur, on peut gagner du temps de calcul en n'effectuant le calcul détaillé pour la généralisation de la méthode ABH mentionnée ci-dessus que pour une vitesse moyenne, et en définissant les variations $h(v)$ par un traitement plus élémentaire des tubes; il suffit de recaler ces fonctions sur les valeurs h_M. C'est ce qui est fait en particulier dans le code pratique de calcul des réseaux à eau lourde.

COMPÉTITION ENTRE FUITES ET CAPTURES DANS LE DOMAINE THERMIQUE

Le calcul de l'aire de migration des neutrons se formule simplement dans deux cas limites: celui du ralentissement pur, dans lequel on néglige la vitesse des noyaux diffusants et où il n'y a pas de captures, et celui de la diffusion thermique, dans lequel les neutrons sont supposés en équilibre dans un milieu de capture faible et uniforme. Dans un réacteur thermique, on peut à la rigueur utiliser ces deux schémas au début et à la fin de la vie du neutron, mais il faut bien aussi considérer une zone de transition où les phénomènes sont visiblement beaucoup plus complexes. Comment effectuer le raccordement, et comment dépend-il de la répartition des captures?

On voit bien par exemple que la forme de la loi de capture joue un rôle important: si le combustible est formé essentiellement de plutonium, une fraction notable des neutrons disparaissent au voisinage de 0,3 eV, avant d'atteindre le domaine thermique, et leur migration est donc plus courte. Les théories élémentaires nous laissent désarmés devant ce problème, car on ne sait pas comment définir la section de capture moyenne qui intervient dans l'aire de diffusion.

Deux méthodes différentes ont été étudiées à Saclay pour résoudre ce problème [14]. Elles sont complémentaires et s'éclairent mutuellement; elles reposent en définitive sur le même formalisme, et on montre qu'on peut les ramener l'une à l'autre. Dans la première méthode on suit le neutron au cours de ses chocs successifs, et on s'intéresse en particulier à la manière dont varie sa probabilité de capture; dans la seconde, on considère globalement le spectre, en écrivant à chaque vitesse le bilan des neutrons qui arrivent et disparaissent. La première méthode donne lieu à des interprétations intéressantes qui permettent une meilleure compréhension des phénomènes physiques; la seconde donne lieu à des calculs plus commodes.

Dans le premier cas on écrit:

$$M^2 = \sum_{N=1}^{\infty} L^2(N)\Omega(N)G(N)$$

avec

$$L^2(N) = \sum_{n=1}^{N} l^2(n) \quad G(N) = \prod_{n=1}^{N-1} [1 - \Omega(n)]$$

$\Omega(N)$ étant la probabilité pour un neutron qui a subi $N-1$ chocs d'être capturé lors du choc suivant, et $l^2(N)$ étant l'accroissement de M^2 dû à ce choc supplémentaire. Le calcul des quantités $\Omega(N)$ et $l^2(N)$ nécessite la connaissance des spectres partiels constitués par les neutrons qui ont subi un nombre donné de chocs: on est donc amené à utiliser directement les sections de diffusion différentielle, et à reconstituer le spectre total par générations successives; on n'a d'ailleurs besoin de le faire que pour un nombre restreint de chocs. Cette manière de raisonner permet en particulier d'interpréter très facilement les effets liés à l'intensité et à la distribution de la loi de captures ou aux caractéristiques géométriques de la cellule.

On peut obtenir les mêmes résultats si les échanges d'énergie provoqués par le modérateur sont définis globalement au moyen d'un opérateur « synthétique »: désignant par $n(v)$ la densité partielle pour les neutrons de vitesse v, et par H l'opérateur en question, on écrit: $\mathrm{H}n(v) = n(v)v.\ [\Sigma_a(v) + D(v)B^2]$. En faisant l'intégration de chacun de ces deux termes sur le spectre d'équilibre, on obtient les proportions relatives de neutrons disparaissant soit par absorption, soit par fuites. Les nouvelles théories de thermalisation développées à Saclay [12] permettent précisément de faire appel à des opérateurs qui se prêtent à des calculs commodes.

Pour montrer comment on peut interpréter les résultats, prenons un exemple très simple: supposons que le milieu soit homogène, que B^2 soit extrêmement petit, que D soit indépendant de la vitesse, et que l'absorption soit en $1/v$. La proportion relative de fuites aux captures est le produit de B^2 par:

$$M^2 = \frac{D}{\Sigma_a(v_0)} \int n(v) \frac{v}{v_0} \mathrm{d}v$$

Décomposons $n(v)$, qui est supposée normalisée, en deux termes: $n(v) = M(v) + E(v)$, $M(v)$ étant une maxwellienne normalisée (ce qui implique $\int_0^\infty E(v)\mathrm{d}v = 0$). Le premier terme fournit l'aire de diffusion classique $L^2 = \frac{D}{\Sigma_a(v_0)} \sqrt{\frac{4T}{\Pi T_0}}$. Le second terme divergerait si on poursuivait l'intégration jusqu'à l'infini; mais on remarque que si v_1 et v_2 sont tous deux très grands, compte tenu de la forme asymptotique du spectre, la contribution de l'intervalle (v_1, v_2) est $\frac{D}{\xi \Sigma_s} \mathrm{Log} \left(\frac{v_1}{v_2}\right)^2$: on retrouve la forme élémentaire de l'aire de ralentissement τ. Conservant pour v_1 une vitesse arbitraire suffisament grande, utilisons maintenant cette expression pour définir v_2, en écrivant qu'elle est égale au deuxième terme de l'intégrale ci-dessus jusqu'à v_1. Tout se passe comme si on pouvait juxtaposer les deux processus élémentaires évoqués au début, avec une borne définie par v_2.

Voici, à titre d'exemple, les valeurs de $E^* = \frac{S_2^2}{2}$, en fonction de $\tau = \frac{\Sigma_a(S_0)}{\xi \Sigma_s} \sqrt{\frac{T_0}{T}}$, d'une part pour le modèle « gaz infiniment lourd », d'autre part pour un modèle de thermalisation représentant le graphite:

τ	E^* gaz lourd (en kT)	E^* graphite
0,01	5,3	1,6
0,05	6,0	2,1
0,10	6,8	2,8
0,15	7,7	3,5
0,20	8,7	4,6

On remarque que la borne équivalente n'est pas kT, mais une valeur un peu plus élevée, et que τ devient un peu plus court lorsque la capture moyenne du milieu augmente. D'autre part l'utilisation du modèle graphite au lieu de celui du gaz lourd provoque un allongement de τ, parce que le ralentissement est moins efficace au voisinage de l'énergie thermique à cause des liaisons cristallines.

Le cas élémentaire qui vient d'être présenté peut être généralisé. Il n'y a aucune difficulté à utiliser un $D(v)$ variable qu'on peut recaler sur les valeurs expérimentales des mesures de l'âge, ou de l'aire de diffusion thermique. Si la capture n'est pas en $1/v$ on est amené à remplacer dans l'expression L^2 la section de capture à 2200 m par la section effective au sens de Westcott; en outre la position de v_2 est modifiée par suite de la déformation de spectre par effet de « self-shielding ». De même dans le cas d'un milieu hétérogène, on est amené à utiliser des rapports de densité entre les différents milieux tels qu le $\bar{h}$ défini au paragraphe précédent et dont le calcul — on l'a vu — fait intervenir lui-même le spectre de neutrons.

Enfin lorsque B^2 n'est pas infiniment petit, c'est-à-dire que les fuites interviennent de manière notable dans la disparition des neutrons, cet effet est tout naturellement pris en compte par l'équation d'équilibre écrite plus haut, et réagit bien entendu sur le spectre.

ÉTABLISSEMENT DU BILAN DE NEUTRONS

Comme on a pu s'en rendre compte dans les paragraphes précédents, plutôt que de recourir à des méthodes multigroupes qui sont non seulement très lourdes, mais posent le problème du choix des constantes numériques, on préfère, grâce à l'emploi de méthodes synthétiques, faire en sorte qu'on puisse intégrer de manière continue les phénomènes sur tout le domaine d'énergie.

Pratiquement on est amené à distinguer deux domaines, séparés par une énergie de l'ordre de quelques eV, qui n'a d'ailleurs pas besoin d'être fixée avec précision. Dans le domaine inférieur, le bilan est obtenu à chaque vitesse en écrivant que la résultante de transferts d'énergie (obtenue grâce à l'opérateur de thermalisation) compense exactement les neutrons qui disparaissent soit par absorption dans les différents milieux [chacun avec sa loi de capture propre $\Sigma(v)$ et sa densité neutronique moyenne $h(v)$], soit par fuites. Il suffit ensuite d'intégrer ces divers événements sur le spectre d'équilibre pour obtenir le bilan des fissions, des absorptions parasites et des fuites. Ces opérations sont particulièrement commodes puisqu'on est conduit à un système d'équations différentielles; un calcul de réseau ne demande que quelques secondes sur IBM 7094.

Dans le domaine supérieur on peut en principe procéder de même; le spectre moyen est beaucoup plus simple, le ralentissement n'étant qu'une forme dégénérée de la thermalisation; en revanche les problèmes d'hétérogénéité s'y posent de manière plus aiguë, d'une part à cause de la localisation des sources dans les barres d'uranium, d'autre part à cause des très fortes résonances de l'uranium-238, qui donnent lieu à des effets de « self-shielding » complexes.

Il reste donc à dire quelques mots sur les problèmes posés par l'uranium-238 dans le domaine du ralentissement.

CALCUL DU FACTEUR ANTITRAPPE

Dès leur naissance, les neutrons sont capturés dans l'uranium-238. La relative petitesse de la section de capture aux hautes énergies est compensée par une présence beaucoup plus fréquente des neutrons dans l'uranium. Avant même qu'ils aient quitté le barreau qui leur a donné naissance, une fraction non négligeable est absorbée (par exemple 1,5 % dans le cas d'un barreau de 44 mm de diamètre); il est facile d'incorporer ce calcul dans celui de ϵ comme l'a montré B.I. Spinrad il y a longtemps. Mais il est bien évident qu'après leur première sortie du barreau les neutrons y retournent fréquemment et restent relativement groupés autour de lui; ce n'est qu'aux énergies assez

basses, et à condition que le pas du réseau ne soit pas trop grand, qu'on peut considérer leur densité comme uniforme.

C'est dire que même si le spectre moyen est en dE/E, on n'a pas du tout une loi de cette forme dans le combustible. Cela est particulièrement vrai dans les réseaux à eau lourde, où la distance entre barres est très souvent largement supérieure à l'aire de ralentissement. Or la contribution relative des résonances situées à énergie élevée dans l'intégrale effective, si elle est très faible en milieu infiniment dilué, n'est pas du tout négligeable dans des barreaux compacts; en effet, le « self-shielding » s'applique très inégalement et atténue surtout les grandes résonances situées à basse énergie.

Il faut donc séparer les effets dus à la géométrie du barreau et ceux dus à la géométrie de la cellule, en introduisant le spectre dans le barreau et en l'intégrant sur la section de capture.

Le calcul est rendu difficile pour les raisons suivantes. D'une part la décomposition de l'intégrale de résonance effective en fonction de l'énergie est délicate, particulièrement dans le domaine compris entre 1 et 30 keV, qui est celui où on ne connaît qu'une distribution statistique des paramètres de résonance: or, c'est ce domaine précisément qui intervient le plus dans l'effet indiqué. D'autre part la répartition spatiale des neutrons à une énergie donnée ne peut être calculée simplement; elle est en particulier fortement perturbée par la présence de l'uranium, dont les propriétés de ralentissement sont très différentes de celles du modérateur.

Les études faites à Saclay sur ce sujet [15] ont porté sur les deux points. En ce qui concerne le premier, une nouvelle présentation de la méthode « NR » a permis de traiter correctement les fluctuations dans la zone statistique, et d'ajuster le mieux possible le raccordement de la courbe de capture pour chaque géométrie de barreau, d'une part avec la zone des résonances résolues, d'autre part avec la zone rapide.

En ce qui concerne le second, on a étudié le ralentissement des neutrons dans le réseau par la méthode de Monte Carlo. Lorsqu'on réduit les barres d'uranium à de simples sources filiformes, on retrouve des distributions spatiales à chaque énergie qui sont analogues à celles qui peuvent être prédites à partir de méthodes analytiques telles que celles des moments [16] (la théorie de l'âge étant bien entendu très incorrecte). La méthode de Monte Carlo n'est donc pas absolument nécessaire dans ce cas, sauf cependant aux énergies élevées, c'est-à-dire pour les neutrons qui ont subi très peu de chocs; par contre elle est pratiquement indispensable pour apprécier les perturbations apportées par l'uranium (on peut ensuite en déduire des facteurs correctifs semi-empiriques). On a pu également étudier de manière fine l'effet d'ombre des résonances les unes sur les autres, c'est-à-dire l'atténuation de la densité du fait des captures qui ne se fait évidemment pas de façon uniforme dans la cellule.

On peut traduire les résultats par la valeur ΔI_{eff} qu'il faut ajouter à l'intégrale de résonance effective définie dans un spectre en dE/E, pour que la formule élémentaire du facteur antitrappe donne le résultat correct. Voici à titre d'exemple les valeurs de ΔI_{eff} calculées pour des barres d'uranium de 2 cm de rayon, en fonction de la quantité de modérateur associée:

Vm (cm²)	200	300	400	500	600	700	800	900
ΔI_{eff} (barns)	0,08	0,41	0,89	1,51	2,24	3,04	3,87	4,81

BIBLIOGRAPHIE

1. Benoist, P., *Théorie du coefficient de diffusion des neutrons dans un réseau comportant des cavités*, Rapport CEA 2278 (1963).
2. Benoist, P., *Formulation générale et calcul pratique du coefficient de diffusion*, Rapport CEA 1354 (1959), Reactor Science, *13*, 97 (1961).
3. Behrens, D. J., Proc. Phys. Soc., 62, *10*, 358 A (1959).
4. Leslie, D. C., *The weighting of diffusion coefficients in cell calculations*, Reactor Science and Technology, *26*, 1 (1962).
5. Carter, C., Reactor Science and Technology, *15*, 76 (1961), et *15*, 113 (1961).
6. Benoist, P., et Palmedo, P. F., *Interaction du flux macroscopique et de la structure fine dans les piles hétérogènes* — SM 42/66 AIEA — Amsterdam (1963).
7. Yvon, J., *La diffusion macroscopique des neutrons — Une méthode d'approximation*, J. Nuclear Energy — part I, *4*, 305–318 (1957).
8. Carlson, B. G., et Bell, G. I., Actes de la Deuxième Conférence internationale sur l'utilisation de l'énergie atomique à des fins pacifiques, P/2386, Vol. 7, Nations Unies (1958).
9. Amouyal, A., Benoist P., et Horowitz, J., *Nouvelle méthode de détermination du facteur d'utilisation thermique d'une cellule*, J. Nuclear Energy, *6*, 79 (1957).
10. Amouyal, A., Benoist, P., et Guionnet, C., *Calcul du facteur d'utilisation thermique dans une cellule formée d'un nombre quelconque de milieux concentriques*, Rapport CEA 1967 (1961).
11. Cadilhac, M., Soulé, J. L., et Tretiakoff, O., *Thermalisation et spectres de neutrons*. Voir, dans le présent volume, mémoire P/73.
12. Cadilhac, M., *Méthodes théoriques pour l'étude de la thermalisation des neutrons*, Rapport CEA 2268 (1964).
13. Tretiakoff, O., de Brion, J. P., Mougey, J., et Naudet, R., *Thermalisation en milieu hétérogène*, Rapport CEA 2474 (1964).
14. Naudet, R., *Etude de la migration des neutrons dans un milieu multiplicateur suivant l'intensité et la distribution des captures*, Rapport CEA 2476 (1964).
15. Mougey, J., et Naudet, R., *Calcul du facteur antitrappe dans les réseaux à eau lourde*, Rapport CEA 2475 (1964).
16. Goldstein, H., Certaine, J., Nucl. Sc. Eng., *10*, 16–23 (1961).

ABSTRACT—RÉSUMÉ—АННОТАЦИЯ—RESUMEN

A/74 France

Improvements in methods of neutron calculation for thermal reactors

By R. Naudet *et al.*

A number of new theories and calculation methods for thermal neutron lattices are reported in this paper. Recent achievements in thermalization theory represent the main improvement in reactor physics: this work is described in a separate paper. But there are many other problems, and the target is eventually to obtain a better understanding of the over-all neutron balance. Among the topics discussed are the following:

Calculation of diffusion coefficients in lattices with cavities;

Distribution of neutron densities in the different media forming a cell;

Competition of leakage and absorption in the thermal range;

Establishment of the neutron balance;

Calculation of the resonance escape probability.

A/74 Франция

Усовершенствование методов нейтронного расчета реакторов на тепловых нейтронах

Р. Нодэ *et al.*

Настоящий доклад посвящен определенной группе новых разработанных в Комиссариате по атомной энергии теорий и методов расчета активных зон реакторов на тепловых нейтронах. Теория термализации является темой отдельного сообщения: успехи, достигнутые во Франции в этой области, несомненно, представляют существенный вклад в методы расчета. Дан обзор других проблем, развивающих и дополняющих теорию термализации. Достижения в этих различных областях обеспечивают в настоящее время значительно лучшее понимание нейтронного баланса в реакторах на тепловых нейтронах. Последовательно освещены следующие проблемы:

— расчет коэффициента использования тепловых нейтронов в объеме, образованном концентрическими средами, по монокинетической теории с учетом термализации;
— установление зависимости между утечкой нейтронов в области замедления и утечкой нейтронов в области тепловых нейтронов;
— коэффициенты диффузии в размножающей среде, включающей полости;
— спектр нейтронов при замедлении и расчет вероятности избежания резонансного захвата;
— определение баланса нейтронов;
— специальные проблемы: применение методов гетерогенного расчета, трактовка уравнения переноса по двойному коду Pn, тонкозернистая структура топлива и т. д.

В этих областях достигнуты важные усовершенствования, которые уже используются для практических расчетов решетки.

A/74 Francia

Perfeccionamientos en los métodos de cálculo neutrónico de reactores térmicos

por R. Naudet *et al.*

La comunicación presente reune un cierto número de teorías nuevas y de métodos de cálculo, relativos a redes de neutrones térmicos, puestos a punto en el CEA. La teoría de la termalización es objeto de una comunicación separada: los progresos realizados en Francia en este dominio constituyen ciertamente la novedad esencial en los métodos de cálculo, pero otros problemas se entrelazan con él y le completan. A ellos se les pasa revista en este trabajo. Los progresos realizados en estos diferentes dominios permiten ahora una comprensión mucho mejor del balance neutrónico en los reactores térmicos. Se exponen sucesivamente los problemas siguientes:

Cálculo de los coeficientes de difusión en redes con huecos;

Repartición de las densidades neutrónicas en los distintos medios que forman una celda;

Competición entre fugas y capturas en la región térmica;

Balance neutrónico;

Cálculo de la probabilidad de escape a la resonancia.

Evaluation, storage and processing of nuclear data for reactor calculations

By J. S. Story,* M. F. James,* W. M. M. Kerr,** K. Parker,** I. C. Pull,* and P. Schofield.***

Through the use of large computers reactor calculations are nowadays much more detailed and precise than was possible in the early years of the atomic energy industry. Safety problems and the increasing complexity of advanced reactors have stimulated this advance, and it is being supported by large measurement programmes to provide nuclear reaction data of improved accuracy and extent [1]. However, preparation of the derived quantities needed for reactor calculations can be most laborious. To attack this task in a systematic way scientists in the UKAEA are building up a computer data library on punched cards and magnetic tape of all needed nuclear cross sections, with versatile processing programmes to generate the derived quantities required.

Part 1 of the paper describes this work. At the time of writing the library contains differential neutron cross-section data in the range 1 meV to 15 MeV for 39 materials, including angular distributions from scattering collisions and neutron spectra from non-elastic reactions. Some gamma ray cross sections are also available. Complete and detailed differential cross sections are obtained from experimental measurements, interpreted and extended as necessary with the help of nuclear theory. We refer to these as "evaluated data", and have outlined some of the practical aspects of evaluation.

A variety of computer programmes is associated with the data library: these include programmes for assembling the library, programmes for converting parametric to tabular data, and the processing programmes GALAXY and DICE, for preparing the derived quantities needed in reactor calculations.

The data are stored in form of binary-coded decimals, and the associated computer programmes are written in Fortran, so that they can be used with different computers.**** This is important because we believe there is great need for international collaboration and exchange of evaluated nuclear cross section data.

Part 2 summarizes work on the evaluation of data on thermal neutron scattering laws: several of the points made in general terms in part 1 are aptly illustrated by this example. The differential cross section cannot be measured over the whole range of initial and final energies and scattering angles at all the temperatures required. So it is necessary to lean heavily on theory in correlating and extrapolating the measurements. The adequacy of scattering laws generated in this way may be tested by appeal to measurements of neutron spectra in moderating assemblies.

PART ONE
1. THE PROCESS AND PROBLEMS OF EVALUATION

A data file***** for a single nuclide, however accurate and comprehensive, is of little value alone. The first phase of the work, if it is to be of general use for reactor calculation, is to establish a preliminary library for all the more important materials. This itself is quite a large undertaking. All cross sections needed must be represented over the full energy range, although it may not be necessary to attempt the same degree of accuracy for all the materials, nor for all the different cross sections or different parts of the energy range.

Having produced the preliminary library, the tasks remain of improving it and extending it to include data for other materials of interest, and of revising the data from time to time in the light of new information. The last is a continuing and exacting task, though on average the data for a single nuclide may be revised only once in every few years. In view of the large and increasing rate at which new experimental data are being produced it is desirable to mechanize the tasks of evaluation as much as is practicable.

In deciding the order in which new evaluations should be undertaken one needs to know about the status of new measurements, and their importance in reactor calculations. Evaluators in the UKAEA have been helped in this task by regular contacts with data measurers and with reactor physicists. The general procedure followed in evaluating data may be outlined:

* UKAEA, Atomic Energy Establishment, Winfrith.
** UKAEA, Atomic Weapons Research Establishment, Aldermaston.
*** UKAEA, Atomic Energy Research Establishment, Harwell.

**** These features differ from those of the earlier Aldermaston data system described by Parker [2].

***** We use this term to denote a complete set of evaluated neutron (or photon) cross section data for a single material. A data library consists of data files for a number of materials.

(*a*) The literature must be searched for relevant references. The Brookhaven reports BNL 325 and BNL 400 [3–5], Howerton's compilations [6], and Nuclear Science Abstracts are obvious starting points. However these generally provide little information about new measurements in progress, which are often of the greatest interest for reactor calculations. There is a great need for a much more complete and up-to-date reference index than is available at the time of writing; see section 6, item (*b*).

(*b*) The references must be studied and the data compared; discussion with data measurers can sometimes shed light on discrepancies. They should be compared with theoretical predictions and any gaps in the data made good by recourse to theory. For this stage of the work, it is very desirable to have the experimental data in tables or on punched cards; the graphical presentations usually available are rarely satisfactory.

(*c*) A set of preferred values is prepared on punched cards, and these must be carefully checked. This would be an arduous task but it can mostly be done mechanically with the help of a programme such as CHECK which is described in section 4. To aid checking it is worth while to include some otherwise redundant information; for example we record the total cross section as well as the partial cross sections; energy values are repeated with each cross section.

(*d*) Finally the details of the evaluation, and the justifications for the choices that have been made, should be described in a report. It is often not worth while to perfect all parts of a new evaluation, especially if it is known that new experimental data will soon be available: it is therefore very important that all known shortcomings of the evaluation should be frankly reported, as a guide to users and to help in future revisions.

2. THE DATA LIBRARY

The library contains basic microscopic neutron and photon cross-section data over energy ranges of about 1 meV to 15 MeV for neutrons, and 10 keV to 20 MeV for photons. The data include the number of secondaries from a collision and their distributions in energy and direction. The information currently contained in the library is described in the references cited in the appendix. Neutron cross-section data are available for H, D, T, ^{3}He, ^{4}He, Be, B, ^{10}B, C, N, O, F, Na, Al, Si, Cl, Ca, Cr, Fe, Ni, Cu, Zr, Cd, ^{135}Xe, Au, Pb, Th, ^{233}U, ^{235}U, ^{236}U, ^{238}U, ^{237}Np, ^{239}Pu, ^{240}Pu, ^{241}Pu, H_2O, D_2O, and BeO. Photon cross sections are available for H, Be, C, N, O, Al, Fe, Pb, U, and Pu. Most of the data were evaluated at AWRE Aldermaston and AEE Winfrith, but other evaluations have been used for some materials.

All data are represented on IBM punched cards in a standard format which allows six pieces of information and a label on each card. The working medium is high density magnetic tape containing the same information as the corresponding cards, in BCD mode (binary-coded decimals). BCD mode is convenient for the Fortran programmes associated with the library, and facilitates transmission of the data between different laboratories with different computers.

A full description of the format may be found in reference [7]. It is sufficiently flexible to allow inclusion of many different kinds of reaction data, in point-by-point tabulations or in parametric forms. Three dimensional arrays may be included, such as the scattering law $S(\alpha,\beta)$ considered as a function of temperature. Data are first classified among thirteen general classes which include cross sections for neutrons and photons; angular distributions and energy spectra of secondaries; neutron resonance parameters; statistical parameters for the unresolved resonance range; and thermal scattering laws. There is next a particular classification by reactions so that, for example, neutron elastic scattering is distinguished from the (n,2n) reaction.

Every complete set of data in the library is organized into several sections each preceded by a short "heading section", which is an index to the nature and number of the data following it. The format is designed to facilitate checking through the inclusion of some redundant information on heading cards and data cards; for example see sections 1 and 4. A complete set of data for a particular material is labelled with a "nuclide identification number". When a revised set of data is prepared for the same material a new identification number is assigned and both sets are stored in the library, so that reactor physicists may continue to use the older compilation if they wish.

3. CONVERSION OF PARAMETRIC TO TABULAR DATA

Some of the cross sections in the data library are obtained most naturally by calculation from parametric forms whose parameters are determined from the experimental data. Examples are: (*a*) the thermal neutron scattering law derived from the frequency function $p(\beta)$ (see part 2 of this paper); (*b*) resonance parameters, which may be derived from the measurements even when the instrumental broadening is not accurately known; (*c*) the parameters of statistical distributions of resonance widths and spacings, which can be used to convey not only the average cross sections but also their probable fluctuations. In each of these examples the parametric forms have physical significance and may be used to correlate the results of a number of separate experiments.

Use of parametric forms can yield a great saving of storage space in the data library. Thus, to represent the cross sections in the resolved resonance region accurately requires at least ten tabular points per resonance for each cross section and for each temperature, whereas five or six parameters would suffice to convey all the information needed.

At the time of writing all the data in the library are in point value tabulations, to suit the processing programmes GALAXY and DICE (see section 5) which currently accept data only in this form. For the future we envisage the use of a master data library containing

tabular and parametric data as may be most convenient. Special computer programmes would be used to generate secondary data libraries containing only point tabulations for specified temperatures.

Several such programmes are alrady in use. The uses of the programmes LEAP [9] and PIXSE [10] are described in part 2 of this paper. The programme GENEX [11] is used to calculate Doppler broadened cross sections from resonance parameters input in the library format; a subsidiary programme RESP is used to sample for resonance parameters in the unresolved region using statistical data.

Further programmes to make use of resonance parameter data are being developed. One of these will use the multilevel Breit-Wigner approximation and will calculate penetrabilities and shift factors for neutrons with orbital angular momenta $l \leq 5$, and for charged particle emissions. Another programme performs similar calculations for $l=0$, using the more accurate formulae of Reich and Moore [12] for non-fissile nuclides. For fissile nuclides a programme using the formulae of Vogt [13] is already available.

4. ANCILLARY COMPUTER PROGRAMMES

Production of the data library is simplified by using a number of ancillary computer programmes. Current versions of these programmes operate on one or both of the IBM 7090 or IBM 7030 (STRETCH) computers, or on the IBM 1401: but most of them are written in Fortran so that they can readily be adapted for other computers of similar calibre.

NDTP. The preparation of magnetic tapes from punched cards is accomplished by using the IBM 1401 programme NDTP described by Webster [14]. This writes data on tape, copies tapes, modifies specific records (cards), rearranges the ordering of data on tape and provides a printed listing of the contents of a tape.

CHECK. Before any part of a data library is put into use it is essential to check the accuracy of representation and the self-consistency of the data. Large numbers of punched cards are used in preparing the library and a number of punching errors must be expected. Most of the tedium of checking can be avoided by using the IBM 7030 programme CHECK [15] which applies a great variety of logical and arithmetical tests. For example, the sum of partial cross sections is compared with the total cross section at each energy point; the energy points are checked for monotonic increase. Our experience has been that for each data file an average of three CHECK runs are needed to locate and remove errors; the average number of errors has been about 5 per 1000 cards (less than 0.1% of the units of information). CHECK can of course only detect inconsistencies in the data and format discrepancies.

NDF PRINT [16] is an IBM 7030 programme for preparing an annotated listing of data in the library in an easy-to-read form. The programme output is on magnetic tapes from which prints are obtained as required by use of an IBM 1401.

GROD [17] is a programme used with the IBM 7030 computer and an associated SC 4020 high speed microfilm recorder to obtain a graphic representation of data presented in tabular form in the library format.

REFORM [18] is an IBM 7030/7090 programme which accepts data prepared in a simplified format for ease of punching, and reproduces them on magnetic tape in the standard format of the data library.

SPLICE [19] is an IBM 7090 Fortran programme used to join a new set of low energy data to an existing set. It deletes the original data up to the junction, and revises the heading cards and the sequential numbering above it.

These last two programmes are less general than might be desired, but have nevertheless proved very useful, because they simplify and reduce the amount of card punching needed in developing the data library.

5. PROCESSING PROGRAMMES

Processing programmes are used to prepare the derived quantities needed for reactor calculations from the basic nuclear data stored in the cross section library. RESP and GENEX (see section 4) and PIXSE (see part 2) are processing programmes developed for specialized purposes. GALAXY and DICE described below have been designed in conjunction with the library, to satisfy rather general requirements.

GALAXY

Introduction

The function of the processing programme GALAXY is to produce group averaged cross sections for use in neutronics programmes, for instance, those based on S_n and diffusion approximations to neutron transport theory. The programme uses for input basic neutron cross-section data in the library format, together with control information provided by the user. The group-averaged data produced by the output scheme are printed. In addition special forms of the output will be available for direct input to some of the standard multigroup programmes, including STRAINT, an S_n code in spherical or slab geometry [20]; Winfrith DSN, a one-dimensional S_n code in cylindrical geometry [21]; and CRAM, a two-dimensional diffusion theory code [22].

GALAXY is at present written in Fortran II language and requires an IBM 7090 computer with twelve tape units (including the system tapes). It was decided to make GALAXY as general as possible so that it could be used to produce input data for many different varieties of multigroup calculation, although of course special requirements may arise which cannot be satisfied by it. The programme specification and strategy have been designed with this end in view. Some restrictions have been imposed, most of which are of minor importance and can easily be relaxed; the only restriction to be noted here concerns the output scheme which is at present limited to a maximum of 40 groups.

Strategy

Control data must be provided for each of a number of mixtures in turn, and must include proportions of constituent materials, effective temperature, and details of the weighting spectra to be used (see below). For each mixture several quantities are calculated which are the same for every component of the mixture; namely, the group widths in energy and lethargy units, and the group-averaged weighted mean energy, inverse velocity, and the energy corresponding to the weighted mean lethargy. If the total cross section of the mixture is required for spectrum weighting in the narrow resonance approximation it is calculated at each of the aggregate of energy points at which the cross sections of the constituent materials are given. An option is available to form the weighted mean of the inverse transport cross section.

The programme goes on to calculate group-averaged cross sections for specified reactions and energy groups, for each constituent material in turn. Any reaction for which data are provided in the library format may be processed in this way. In addition the group-averaged energy release cross section is calculated. For any neutron producing reaction the group-to-group transfer cross section may be expressed as a sum of Legendre polynomials in the cosine of the angle of deflection (laboratory frame of reference): up to six moments of this expansion can be calculated. At the time of writing routines exist which calculate these moments for the following reactions: elastic scattering by a static nucleus, thermal neutron scattering in accordance with a scattering law of the form $S(\alpha,\beta)$ (defined in part 2 of this paper), inelastic scattering to discrete levels and to a continuum, (n, 2n), (n, 3n) and (n, fission).

Weighting spectra

Six basic energy spectra are available for weighting purposes when forming the group averages. These basic spectra are: (*a*)E^{-x}, with $x \geqslant 0$, where E is the neutron energy; (*b*) an arbitrary Maxwellian distribution; (*c*) any arbitrary continuous spectrum given in tabular form; and the further three spectra obtained from these by dividing by the total cross section of the mixture. This allows for self-shielding effects in the narrow resonance approximation.

Any linear combinations of these six basic spectra may be used, and the spectrum may vary from group to group and from mixture to mixture. Different spectra may be specified for weighting the quantities (such as the group mean energy) which are the same for every constituent of a mixture, and for weighting the cross sections. Fission spectra needed for weighting purposes can be presented in tabular form.

The output scheme

Following execution by the main section of GALAXY the processed data described above are available, for each specified mixture, on a magnetic tape. These are the group-averaged data for each reaction separately, no combination having been effected: in particular the group transfer matrices have dimensions $G(G+2)$ to allow for transfers above and below the range of interest, where G is the total number of groups.

This magnetic tape could be used as input to a suitably prepared neutronics programme, either directly or after suitable processing. However GALAXY contains an additional output stage which provides the following general facilities:

Mixing. The group-averaged cross sections for a mixture may be formed by linear combination of the cross sections for its constituents.

Condensing. The computed data may be reduced to fewer groups, using a specified spectrum.

Combining. Certain combinations of group-averaged data may be formed. For instance, all neutron capture cross sections may be added, $(n,\gamma)+(n,p)+(n,\alpha)+$ etc. Similarly, all non-fission group-to-group transfer cross sections may be combined.

Substitution. This facility will allow the user to replace some of the GALAXY generated quantities with specified alternative values, but it is not available at the time of writing.

Present status and future work

The programme is in use, although a few minor faults have yet to be eliminated. It is briefly described in Ref. [23] which gives operating instructions. Future work may include an improved treatment of cross sections in the resonance region, using resonance parameters for input. It is also hoped to develop a fundamental mode calculation within GALAXY, and to use the derived spectrum as a weighting function.

DICE

DICE [24] converts the nuclear data in the library into forms which are more convenient for use in Monte Carlo calculations and assists in consulting these data when required by the tracking programme. It is written in S1 language (an adaption of Fortran II) for use with the IBM 7030 (STRETCH) computer. The four main parts of DICE are:

A programme MOULD which accepts neutron cross-section data in the library format, converts them to forms suitable for Monte Carlo calculations, and stores them on a library tape. Printed listings of the converted data are obtained.

A routine ABSYNTH which, on being informed on the compositions of the various materials, abstracts the relevant sets of data from the MOULD library tape and synthesizes the data table in core storage in convenient forms.

A subroutine CR which, at each collision in the Monte Carlo calculation, consults the data table provided by ABSYNTH and calculates the properties of emergent neutrons.

A subroutine EGMV which extracts the mean-free-path of a neutron from the data table, so that the

Monte Carlo tracking programme can determine the material in which the next collision occurs.
MOULD is used only to add new sets of data to the MOULD library tape. CR and EGMV are embedded in the Monte Carlo tracking programme which uses ABSYNTH at the outset. An important feature of DICE is that it is independent of geometry, so that tracking programmes in one or two dimensions use DICE with equal facility.

The fundamental feature of DICE is the standardization of the conversion process for all data sets. The ABSYNTH data table is provided with a reference system based on a hierarchical arrangement of six levels of consultation. At each level a smaller and smaller region of the data table is isolated in response to random sampling or otherwise, until a complete specification of the properties of a neutron emerging from a collision has been attained.

Since different regions of the physical system which is being studied may be of different materials, the tracking programme first specifies a material and isolates the relevant block of data: for multi-component materials a second operation specifies the particular component involved in a given collision, and a subset of the block already isolated is identified. This subset contains all the information required for every possible neutron reaction with the specified component material. The next step is to select one of the allowed reactions. If this reaction results in the emission of secondary neutrons the incident neutron energy is used to isolate a particular energy range within which are given the multiplicity, energy distribution, and directional distribution of these secondary neutrons. The appropriate distributions are selected for each secondary neutron, and so the outcome of each collision is completely determined.

Another version of DICE, suitable for weighted tracking, is available also.

6. HOPES FOR INTERNATIONAL COLLABORATION

To prepare a complete set of evaluated cross sections for a single nucleus, over the full energy range, is a time-consuming process. To prepare a library of data for all the nuclei of interest in reactor physics, and to keep it up to date in the light of new measurements is a task beyond the capacity of a small group. Existing evaluation groups, working independently, have all had to treat some parts of the work in less detail than is desirable. Widespread international collaboration in this field is an urgent necessity if full value is to be obtained from the money invested in experimental work.

For this reason members of the UKAEA evaluation groups have participated actively in the work of Compilation Study Groups set up by the European American Nuclear Data Committee; we have benefited from the informal collaboration which ensued, and have made copies of the UKAEA data library available to other laboratories on a reciprocal basis. Some practical measures to promote the necessary collaboration are described below:

(*a*) The exchange and use of data files prepared in different laboratories would be simplified by agreement on a common format to be used internationally for storage of evaluated data on punched cards or magnetic tape. Several evaluation groups have already agreed to make use of the UKAEA format for this purpose as it is the most complete and flexible one published at the time of writing.

(*b*) Every evaluation group needs a complete and up-to-date bibliographical reference index, but it is becoming increasingly difficult for each small group to undertake a sufficiently complete literature search and an adequate degree of cross-referencing. To overcome these difficulties several prominent evaluation groups have agreed to collaborate in maintaining the automated reference index system CINDA devised by Goldstein [25].

(*c*) A list of existing compilations of evaluated cross section data has been prepared by Parker [26]. Unfortunately it is often difficult to ascertain the status of a compilation. This emphasizes the importance of an adequate write-up of any new compilation; it is especially important that any shortcomings should be faithfully reported.

Evaluation work need not be confined to the larger laboratories; however, access to a good library is necessary, and contact with theoretical nuclear physicists and experimental workers is important.

PART TWO

7. EVALUATION OF DATA ON THE THERMAL NEUTRON SCATTERING LAW

Prediction of reactor parameters in advanced thermal reactor systems requires more detailed knowledge of the slow neutron spectra than can be deduced from a limited series of reaction rate measurements on zero energy assemblies. This is particularly true for reactors in which the fuel or moderator composition changes during lifetime (for instance during high burn-up where plutonium is produced and burnt, and in spectral shift reactors); and in reactors in which there are moderating materials at very different temperatures (as in the Steam Generating Heavy Water reactor—SGHW).

It is necessary to be able to do multigroup neutronics calculations of the distributions of thermal neutrons in reactor systems, and there is a need for evaluation of cross sections for energy transfer between neutrons and moderating atoms. Since it is not practicable to measure partial differential cross sections $\sigma(E \rightarrow E', \theta)$ over the complete range of incident neutron energies E, final energies E', and angles θ, at all temperatures required, it is necessary to rely heavily on theoretical methods of extrapolation and interpolation of the experimental results. The adequacy of the cross sections produced is most convincingly checked by comparing measured spectra in simple geometrical arrangements with theoretical predictions based on the calculated data. Thus the production of scattering data

to be used in reactor calculations involves the three stages of (*a*) measurement, (*b*) calculation and processing, (*c*) assessment.

Measurement

The measurement of scattering cross sections in the thermal region is described by Batchelor, Egelstaff, Ferguson and Rae [1]. The results are presented in the form of a "scattering law" $S(\alpha,\beta)$ which is related to $\sigma(E\rightarrow E', \theta)$. For a moderator with a single nuclear species of mass A times the neutron mass,

$$\sigma(E\rightarrow E', \theta) = \sigma_b(4\pi kT)^{-1}\sqrt{E'/E}\,\exp(-\beta/2)\,S(\alpha,\beta),$$

where σ_b is the bound atom cross section, and kT is the temperature in energy units. The dimensionless variables α and β represent the square of the momentum transfer, and the energy transfer between the neutron and moderator:

$$\alpha = (AkT)^{-1}[E + E' - 2\sqrt{EE'}\cos\theta];\ \beta = (E'-E)/kT$$

When more than one species is present, it is conventional to express $\sigma(E\rightarrow E',\theta)$ in the same form with σ_b referring to the dominant scatterer (e.g., protons in hydrogenous material).

The general theory of the scattering law has been presented elsewhere [27,28]. In general $S(\alpha,\beta)$ consists of the sum of a number of terms: a "self" term for each nuclear species and "interference" terms both for interference scattering from one nuclear species and between different species.

Calculation and processing

At present the extrapolation of the experimental measurements is based on the "incoherent Gaussian" approximation. The nature of this approximation is described in Ref. [28], and it is thought to be sufficiently accurate to describe the thermalization properties of most moderators, though some correction is needed to evaluate the total cross section from it in coherent scatterers. Within this approximation, $S(\alpha,\beta)$ is expressed in terms of a normalized frequency function $\rho(\beta)$, which, however, may be rather strongly temperature dependent.

A related function $p(\beta)$, given by

$$p(\beta) = \tfrac{1}{2}\beta\,\rho(\beta)\,\mathrm{cosech}(\beta/2),$$

may be obtained from the experimental measurements [28] for a range of values of β, but for very small and very large values of β information about $\rho(\beta)$ must be obtained from other sources (e.g., infra-red absorption for large β).

Two computer programmes are now available for the computation of $S(\alpha,\beta)$ from a given $p(\beta)$, and for the computation of cross sections for reactor calculations from $S(\alpha,\beta)$. Both programmes exist in versions for the IBM 7090 and IBM 7030 (STRETCH) computers.

The programme LEAP [9] calculates $S(\alpha,\beta)$, given $p(\beta)$ in numerical form, using the methods described in Ref. [28]. In addition to dealing with continuous distributions of $p(\beta)$, the programme can also admit δ-functions in the distribution, to represent for example, internal molecular vibrations in the scatterer. The running time of the programme depends very much on the form of $p(\beta)$ and the mass of the scatterer, but as an example, a scattering law for water with ninety values of α and ninety of β takes about 25 minutes on the IBM 7090, or 10 minutes on STRETCH.

The programme PIXSE [10] is a flexible processing programme to calculate either "point" or "group" scattering matrices to be used in transport calculations. The output of the IBM 7090 and STRETCH versions may be used directly in the transport theory programmes Winfrith DSN [21] and STRAINT [20] respectively.

The input to PIXSE is either a tabular set of values of $S(\alpha,\beta)$ (the output from LEAP), or parameters specifying one of two possible analytical forms of $S(\alpha,\beta)$—the monoatomic gas or a "width model" [29] which corresponds to a one parameter representation of $p(\beta)$. PIXSE computes: (*a*) the isotropic component and angular moments of the microscopic cross sections $\sigma(E\rightarrow E',\theta)$ and (*b*) group-averaged cross sections $\sigma_{gg'}$, with any desired group structure and with any specified weighting spectrum within each group. In addition to cross sections within the thermal region, PIXSE calculates the source of neutrons in each group due to scattering from above the thermal region, and the loss of neutrons by upscatter out of the thermal region. A forty-group calculation from a tabulation of $S(\alpha,\beta)$ takes between 4 and 20 minutes.

Assessment

In order to assess the adequacy of the scattering laws obtained by the combination of experiment and theory outlined above, a large programme of measurements of thermal neutron spectra has been carried out at Harwell. As well as measurements in homogeneous systems, experiments have been performed in systems in which there are spatial variations of the spectrum. A review of the experimental programme has been given recently by Poole *et al.* [30]. A more detailed assessment of scattering laws on the basis of these experiments is in preparation.

One of the aims of this work is to see to what extent simplified models of the scattering law, such as the width model, are capable of producing adequate prediction of reactor parameters. It is now well established that in many cases reactor parameters are insensitive to details of the neutron spectrum [31–33] provided the variation of total cross section with energy is given correctly. A width model for water has been used with some success in predicting reaction rates in the SGHW lattice [34]. However, such models cannot be used with complete confidence for all purposes until they have been shown to give agreement with measured energy distributions in a wide variety of experimental conditions.

ACKNOWLEDGEMENTS

The evaluation and compilation of data, and the development of the format for the data libraries, of the processing programmes GALAXY and DICE, and of the various ancillary programmes, would have been impossible without the co-operation of many people. The authors would like to thank all who have helped and to take this opportunity of acknowledging in particular the contributions of B. E. Blythe, B. A. Brett, D. Bryden, M. J. Clements, D. M. Jarman, Miss S. M. Miller, Miss I. J. Nicol, J. B. Parker, E. D. Pendlebury, D. Sams, R. D. Wade, and D. V. J. Williams, at Aldermaston; and of Mrs. E. P. Barrington, V. J. Bell, L. W. Blott, K. Gregson, D. C. King, T. P. Moorhead, M. F. J. Peacock, A. L. Pope, L. H. Underhill, and Miss D. A. Welford, at Winfrith.

APPENDIX

Key references to the data available in the library

A brief account of the data in the library, or references to it may be found in [8]. More detailed reports are available for some materials, namely:

Be	Parker, K., AWRE 0-27/60 (1960)
C	Parker, K., AWRE 0-71/60 (1960)
Na	Moorhead, T. P., AEEW-R254 (1963)
Zr	Hemmings, P. J., AHSB(S)R62 (1963)
^{135}Xe	Sumner, H. M., AEEW-R116 (1962)
^{235}U	Parker, K., AWRE 0-82/63 (1963)
^{238}U	Parker, K., AWRE 0-79/63 (1963)

Reference [35] gives a summary of data for many of the materials, but is now partially obsolete. Finally, Ref. [36] gives the photon cross sections for H, C, N, O, Al, Fe, Pb, U, and Pu.

REFERENCES

1. Batchelor, R., Egelstaff, P. A., Ferguson, A. T. G., and Rae, E. R., *Neutron interactions with reactor materials* (1964).
2. Parker, K., Proc. IAEA Symposium of the physics of fast and intermediate reactors, Vol. *1*, 207 (1962).
3. Hughes, D. J., and Schwartz, R. B., BNL 325 (2nd edition 1958).
4. Hughes, D. J., Magurno, B. A., and Brussel, M. K., Supplement No. 1 to BNL 325 (2nd edition) (1960).
5. Goldberg, M. D., May, V. M., and Stehn, J. R., BNL 400 (2nd edition 1962).
6. Howerton, R. J., UCRL 5351 (1958), UCRL 5226 (revised 1959), and UCRL 5573 (1961).
7. Parker, K., AWRE 0-70/63 (1963).
8. Barrington, E. P., Pope A. L., and Story, J. S, AEEW-R351 (1964).
9. McLatchie, R. C. F., AERE, private communication (1963).
10. Macdougall, J. D., AEEW-M318 (1963).
11. Brissenden, R. G., and Durston, C., AEEW-M429 (1964).
12. Reich, C. W., and Moore, M. S., Phys. Rev., *111*, 929 (1958).
    Moore, M. S., and Reich, C. W., Phys. Rev., *118*, 718 (1960).
13. Vogt, E., Phys. Rev., *112*, p. 203 (1958), and *118*, 724 (1960).
14. Webster, R. J., AWRE 0-71/63 (1963).
15. Blott, L. W., and Parker, K., AEEW-M347 (1964).
16. Jarman, D. M., Parker, K., and Pendlebury, E. D., AWRE 0-4/64 (1964).
17. King, D. C., AEEW-M426 (1964).
18. Blott, L. W., AEEW (1963); see appendix A of reference [7].
19. Blott, L. W., AEEW (1963), private communication.
20. Wade, R. D., AWRE 0-12/63 (1963).
21. Francescon, S., AEEW-R 273 (1963).
22. Hassitt, A., UKAEA, TRG 229 R (1962).
23. Bell, V. J., Blott, L. W., Kerr, W. M. M., Parker, K., Pull, I. C., Wade, R. D., and Williams, D. V. J., AEEW-M422 (1964).
24. Kerr, W. M. M., AWRE (1963) private communication.
25. Goldstein, H., and Pomeroy, D., NDA 2-80 (1958).
26. Parker, K., EANDC (UK) 26 (1963).
27. Egelstaff, P. A., Nucl. Sci. Eng., *12*, 250 (1962).
28. Egelstaff, P. A., and Schofield, P., Nucl. Sci. Eng., *12*, 260 (1962).
29. Egelstaff, P. A., AERE NP/Gen. 29 (1962).
30. Poole, M. J., Schofield, P., and Sinclair, R. N., Proc. IAEA symposium on critical and exponential experiments (1963).
31. Macdougall, J. D., BNL 719 (C-32), *1*, 121 (1962).
32. Honeck, H., IAEA report of the panel on light water lattices, 233 (1962).
33. Wikner, N. F., Joanou, G. D., and Parks, D. E., private communication.
34. Leslie, D. C., and Terry, M. J., AEEW-R250 (1963).
35. Buckingham, B. R. S., Parker, K., and Pendlebury, E. D., AWRE 0-28/60 (1961).
36. Buckingham, B. R. S., and Pendlebury, E. D., AWRE 0-65/60 (1960).

ABSTRACT—RÉSUMÉ—АННОТАЦИЯ—RESUMEN

A/168 Royaume-Uni

Evaluation, stockage et utilisation des données nucléaires pour les calculs des réacteurs

par J. S. Story *et al.*

Grâce à l'utilisation des machines à calculer perfectionnées, les calculs des réacteurs sont maintenant beaucoup plus précis et plus détaillés qu'ils ne pouvaient l'être au début de l'industrie atomique. Ces progrès ont été favorisés par les mesures des sections efficaces vis-à-vis des neutrons, qui ont été améliorées tant en nombre qu'en précision. Cependant, la préparation des valeurs dérivant de ces sections efficaces et nécessaires pour le calcul des réacteurs peut être extrêmement laborieuse. Pour surmonter cette difficulté d'une manière systématique, les chercheurs de l'UKAEA sont en train d'établir une collection de valeurs, sous forme de cartes perforées et rubans magnétiques, portant sur la gamme complète des sections efficaces fondamentales nécessaires — cela avec des programmes de traitement souples pour obtenir les valeurs déduites des sections efficaces.

La première partie du mémoire décrit ce travail. On discute la manière d'évaluer les sections efficaces de la collection. Pour que celle-ci soit facilement utilisable pour les calculs des réacteurs, elle doit contenir une gamme complète de données relatives aux matériaux les plus importants. Ainsi, la première étape de ce travail est-elle une entreprise d'assez grande envergure; elle est maintenant achevée en ce qui concerne la collection de données de l'UKAEA. A l'heure actuelle, cette collection comprend les sections efficaces neutroniques dans la gamme de 1 meV à 15 MeV pour 39 éléments, y compris les distributions angulaires et énergétiques des neutrons secondaires. Certaines sections efficaces pour les photons dans la gamme de 10 keV à 20 MeV sont également disponibles.

La présentation utilisée dans la collection est très souple et permet de représenter les données à la fois sous forme de tableaux et de manière paramétrique. Cette dernière solution est très avantageuse dans certaines parties de la gamme énergétique, si l'on dispose de programmes de calcul pour l'interprétation. De tels programmes sont actuellement utilisés et d'autres en préparation. Les données étant très nombreuses, un utilise plusieurs programmes auxiliaires afin de mécaniser les travaux tels que la vérification, la modification et l'impression de la collection.

Les principaux « programmes de traitement » mis au point pour l'emploi avec la collection sont: GALAXY, qui donne des sections efficaces multigroupes, et DICE, qui prépare les données pour les calculs par la méthode Monte-Carlo et facilite l'étude des données obtenues.

L'extension de la collection et sa mise à jour à la lumière de nouvelles mesures est une tâche continue, qui deviendra vraisemblablement de plus en plus difficile et urgente avec l'augmentation croissante du nombre des nouvelles données expérimentales. Une collaboration internationale est nécessaire pour tirer pleinement parti des travaux expérimentaux. Une certaine collaboration non officielle est déjà amorcée.

La deuxième partie décrit les travaux effectués sur l'évaluation des données relatives à la loi de diffusion des neutrons thermiques; cet exemple sert à illustrer plusieurs problèmes exposés d'une façon générale dans la première partie. La section efficace différentielle de diffusion ne peut être mesurée dans toute la gamme des énergies et angles de diffusion initiaux et finaux ainsi qu'à toutes les températures voulues. Aussi est-il nécessaire de recourir beaucoup à la théorie pour interpréter et extrapoler les mesures. On vérifie la validité des lois de diffusion ainsi obtenues en faisant appel aux mesures des spectres neutroniques dans des ensembles modérateurs.

A/168 Соединенное Королевство

Оценка, сбор и обработка ядерных констант для расчета реакторов

Дж. С. Стори *et al.*

Благодаря использованию крупных современных вычислительных машин значительно повысилась точность расчетов реактора по сравнению с точностью в первые годы создания атомной промышленности. Этот прогресс стал возможен также благодаря наличию большого количества экспериментальных данных по нейтронным сечениям, измеренным с более высокой точностью. Однако определение производных величин, необходимых для реакторных расчетов, остается все еще чрезвычайно трудоемким процессом. Для преодоления этой трудности сотрудники Управления по атомной энергии Великобритании занимаются систематическим комплектованием библиотеки ядерных констант, регистрируемых на перфокартах и магнитных лентах. Регистрируется полный диапазон необходимых ядерных сечений и ведется разносторонняя обработка данных для получения производных величин.

Первая часть доклада посвящена описанию этих работ. Обсуждается процесс оценки сечений, включаемых в библиотеку ядерных констант. Чтобы быть полезной для расчетов реактора, библиотека должна содержать полный комплект данных по наиболее важным материалам. В начальной стадии сбор констант представлял большие трудности, но в последнее время эту функцию выполняет библиотека ядерных констант Управления по атомной

энергии Великобритании. В настоящее время библиотека располагает данными по нейтронным сечениям в интервале энергий от 1 до 15 *Мэв* для 39 материалов, включая угловое и энергетическое распределение вторичных нейтронов. Имеются также некоторые сечения для фотонов в интервале от 10 *кэв* до 20 *Мэв*.

Формат библиотеки очень гибкий, он позволяет давать как параметрическое, так и табличное представление констант. Последнее обстоятельство является важным для некоторых энергетических областей в случае, если вычислительные программы пригодны для их интерпретации. Некоторые из этих программ используются уже в настоящее время, другие находятся в стадии разработки. Поскольку ядерных констант очень много, то в библиотеке используются некоторые вспомогательные программы для механизации таких работ, как сверка, корректировка и печатание библиотеки.

Основными программами по обработке констант, составленными для общего пользования библиотекой, являются GALAXY, которая дает многогрупповые сечения, и DICE, которая готовит данные для расчетов по методу Монте-Карло и для вспомогательных расчетов производных величин.

Проводится работа по расширению библиотеки и поддержанию ее на современном уровне в свете новых измерений. Такая работа становится все более необходимой по мере роста количества новых экспериментальных результатов. Для наиболее полного сбора экспериментальных данных необходима организация международного сотрудничества в этой области. Некоторое неофициальное сотрудничество уже начато.

Во второй части доклада суммируется работа по оценке констант, полученных из закона рассеяния тепловых нейтронов; некоторые точки основных уровней, приведенных в первой части, иллюстрируются примерами. Дифференциальные сечения рассеяния не могут быть измерены в диапазоне от начальной до конечной энергии и для всех углов рассеяния при требуемых значениях температуры. Поэтому необходимо использовать теоретические результаты для интерпретации и экстраполяции экспериментальных данных. Пригодность законов рассеяния, полученных таким образом, определяется на основе измерений спектра нейтронов в замедляющих сборках.

A/168 Reino Unido

Evaluación, archivo y tratamiento de datos nucleares para el cálculo de reactores

por J. S. Story *et al.*

Debido al uso de grandes calculadoras, los cálculos del reactor son hoy día mucho más precisos que en los primeros tiempos de la industria de la energía nuclear. Colaboran eficazmente en este desarrollo el elevado número y la mayor precisión de las medidas de secciones eficaces. Sin embargo, la preparación de las magnitudes que de ellas se deducen necesarias en los cálculos puede ser extraordinariamente laboriosa. Para vencer esta dificultad se está trabajando sistemáticamente en la UKAEA para preparar una colección de datos en fichas perforadas y en cinta magnética del total de secciones eficaces nucleares básicas, que junto con el uso de programas versátiles de tratamiento de datos han de suministrar las magnitudes derivadas que se precisen.

La primera parte de la presente memoria describe este trabajo. Se discute el proceso de evaluación de las secciones eficaces que se incluirán en el catálogo. Para que una colección de datos sea útil en los cálculos de reactores ha de contener toda una serie de ellos para los materiales más importantes. Por lo tanto, la etapa inicial de su preparación es una empresa de gran envergadura, que ya ha sido terminada en lo que a la colección de datos de la UKAEA se refiere. En la actualidad, consta de secciones eficaces neutrónicas en el intervalo 1 meV – 15 MeV para 39 materiales, incluyendo distribuciones angulares y energéticas de neutrones secundarios. También están incluidas algunas secciones eficaces de rayos gamma en el intervalo 10 keV – 20 MeV.

El formato de la collección es muy flexible, pudiendo incluirse en ella los datos bien en tablas, bien en forma paramétrica. Esta última forma tiene considerables ventajas en algunas regiones del espectro energético si se dispone de programas para su interpretación, algunos de los cuales ya están en uso y otros se están desarrollando. Debido a la gran cantidad de datos se usan varios programas auxiliares para automatizar trabajos de comprobación, modificación e impresión.

Los principales programas de tratamiento de datos desarrollados para uso general son: GALAXY, que proporciona secciones eficaces para varios grupos, y DICE, que prepara datos para cálculos de Monte Carlo y los organiza para facilitar su consulta.

El aumentar la colección de datos y mantenerla al día es una labor continua que se hará probablemente más precisa y urgente conforme aumente la cantidad de nuevos datos experimentales. Para obtener pleno rendimiento del trabajo experimental se hace precisa la colaboración internacional. De manera no oficial existe ya cierta colaboración.

En la parte 2.ª se resume la evaluación de datos sobre la ley de dispersión de neutrones térmicos; varios puntos examinados en términos generales en la parte 1.ª se ilustran mediante este ejemplo. La sección eficaz de dispersión diferencial no puede medirse en todos los intervalos de energías iniciales y finales de ángulos de dispersión, ni para todas las temperaturas requeridas. Por lo tanto, es preciso interpolar y extrapolar las medidas con ayuda de modelos teóricos. Las leyes de dispersión obtenidas de esta forma se comprueban recurriendo a medidas de espectros neutrónicos en conjuntos moderadores.

Calculation of reactor power and temperature distribution in three spatial dimensions

By A. B. Whiteley,* R. Prescott,* J. J. Syrett,** J. Walsh,*** A. N. Buckler,**** J. G. Tyror,**** and H. E. Wrigley*****

This paper describes the development of a large scale computer programme SKIP [1] to calculate reactor flux and temperature distributions in three spatial dimensions. The major section of this work is a diffusion theory calculation for up to five neutron energy groups with explicit reactivity feed-back from associated equations defining material temperatures and xenon-135 concentration. Ancillary programmes to calculate absorber constants (Section 4) and detailed local flux distributions (Section 5) have also been developed.

This work, which is a joint CEGB/UKAEA enterprise, was undertaken for the following reasons:

(*a*) *CEGB reasons*: The safe and economic operation of current and future CEGB power reactors requires detailed knowledge of reactor power and temperature distributions, often on a channel by channel basis. Absorber loading studies and studies of start-up conditions when the flux and hence temperature distributions are distorted by partially inserted absorbers thus require a large flexible computer programme.

(*b*) *UKAEA reasons*: Primarily for design problems and general studies of a wide range of reactor types including water moderated and fast reactors.

(*c*) *Development potential*: The present steady state calculation has also been conceived as the starting point for elaborate three dimensional kinetic and burn-up programmes. Experience with other advanced computer programmes [2, 3] and developments in the computer field led to the belief that the project was both necessary and feasible.

1. GENERAL PRINCIPLES OF SKIP PROGRAMME

Explicit reactivity feed-back from temperatures and xenon

The group diffusion equations are solved in a non-linear form, i.e., the coefficients are functions of material temperatures and xenon-135 concentration which in turn are functions of the neutron flux distribution. In practice the equations are solved in a quasi-linear manner with periodic recalculation of temperatures and xenon concentration and consequent modification of the diffusion equation coefficients.

Few group diffusion equations

Up to five neutron energy groups are allowed with a general scatter matrix between the groups. This feature permits wider application of the programme than a more conventional two group model. However, advantage may be taken of simpler scatter schemes, particularly when down-scatter only is present, i.e., neutrons scatter from higher to lower energy groups only.

Restrictions on mesh size

Considerations of computation time and programme organisation within the computer led to the maximum number of finite difference mesh points being limited to ~15000 with cartesian mesh geometry.

Heat transfer

The heat transfer equations solved by the first version of the programme apply to a civil gas-cooled graphite-moderated reactor. The solution of these equations forms a self contained sub-routine with the minimum of linkage with the main programme. Thus it will be relatively straightforward to replace this section by another describing the thermal aspects of a different reactor type.

2. MAJOR PROBLEMS

Method of representing discrete absorbers

The representation of discrete absorbers presents a problem in any diffusion programme. In the SKIP approach there arises the additional problem of representing an absorber which lies neither at a mesh intersection nor at the centre of a mesh area. This difficulty arises from the fact that the number of mesh points is often insufficient for an individual channel representation. The approach adopted and the method of obtaining numerical values for the absorber properties are discussed more fully in Section 4.

* *Computing* Branch, Research and Development Department, CEGB, London.
** Reactor Physics Section, Research and Development Department, CEGB, London.
*** Department of Mathematics, Manchester University.
**** Reactor Development Laboratory, UKAEA, Windscale.
***** Atomic Energy Establishment, UKAEA, Winfrith.

Combination of heterogeneous and homogeneous methods

In order to study small areas of the reactor on a channel by channel basis, it is necessary to develop fine structure calculations using the diffusion solution to give the background macroscopic flux. This is done by taking an array of homogeneous fluxes covering the area in question. Second-order surfaces are then fitted to these fluxes from which the boundary conditions for the fine structure calculations are derived (see Section 5).

Numerical Analysis and Programming

The major problem in the field of numerical analysis was the choice of method of iterating through the non-linear flux equations. Point, block, and alternating direction iterative schemes were considered but the final choice was for a point successive over-relaxation scheme as the techniques were well established and convergence was reasonably assured in the non-linear situation. Convergence is accelerated by applying Chebychev extrapolation to the sources and the finite difference equations are set up by the method of Varga [4] (see Section 6).

A programme of the size and complexity of SKIP is only practicable with computers of the class of the IBM 7090. Many of the programming problems are specific to the particular machine characteristics and great use has been made of the overlapping input/output facilities of the 7090. Much of the programme has been written in FORTRAN but certain sections have had to be written in machine language for greater efficiency.

3. DESCRIPTION OF THE BASIC DIFFUSION PROGRAMME

Neutronics equations

The basic form of the few group diffusion equations are given in Eqs. (1), (2), (3) in Appendix 1. It will be noted that the effect of both fixed and movable absorbers are included as local additions to the macroscopic absorption cross-sections.

It is implicitly assumed that the few group data can be calculated without detailed knowledge of the local neutron energy spectrum, i.e., there is effective separability of spectrum and spatial effects. Spatial variation of nuclear properties is allowed for by defining geometrical regions within the core in which particular sets of properties exist and up to 100 sets of data may be used in two group cases. Fission and absorption cross-sections are allowed a linear temperature dependence, Eq. (6), whilst the group multiplication constants are allowed a more elaborate temperature dependence involving both mean moderator and mean fuel temperatures as shown in Eq. (5) of Appendix 1.

Nuclear data in a form suitable for the SKIP programme must be obtained from independent lattice calculations. A number of methods are in existence ranging from the two-group correlated approach developed for the UK civil gas-cooled graphite-moderated reactors [5] to an elaborate scheme based on a 40 energy group transport theory calculation [6].

Fixed source terms may be included either as a uniformly distributed source or as discrete line or point sources. Thus sub-critical flux distributions may be calculated if desired.

The external boundary conditions are general in form, i.e., there may be coupling between the energy groups via the boundary conditions. This enables reflector effects to be represented by the boundary conditions and eliminates the need for extending the finite difference mesh into the reflector region with a resulting saving in the number of mesh points at which the flux equation must be solved.

The xenon concentration at each point is calculated directly from Eq. (4) of Appendix 1 and is recalculated periodically as the flux iterations proceed. Other fission product poisons are not calculated explicitly and must be included in the nuclear data.

Heat transfer model

The present heat transfer model is based on a typical UK civil gas-cooled reactor. The fuel, coolant channel and moderator are divided into concentric regions in each of which the mean material temperature is calculated. These regions are distributed two in the fuel, one in the can, one in the coolant and up to ten in the moderator. In addition, temperatures are calculated at the centre and surface of the fuel, and at the channel surface of the moderator. Thus, at any axial point in the channel, up to 17 temperatures may be calculated.

Mean moderator and mean fuel temperatures at each point are derived by suitably averaging the appropriate regional temperatures and it is these mean temperatures which modify the nuclear properties and hence the coefficients in the diffusion equations. A limited amount of spatial variation of heat transfer data is permitted to allow different fuel elements or channel properties to be represented in different parts of the core. Some temperature dependence of thermal properties (e.g., thermal conductivities) is also allowed.

Criticality and normalisation options

The solution of the steady state diffusion equations in an eigenvalue problem and this means in general that some parameter must be altered to obtain a critical state. Three alternative methods are available:

(*a*) Alter the penetration of a group of absorbers (control rods)

(*b*) Apply a constant multiplying factor to the group multiplication constants K_j at every point

(*c*) Change the absorption cross-section equally at every point.

The programme must also normalise the absolute flux level to satisfy some desired thermal criterion. Again, a number of alternative options are available and these include reactor power, coolant outlet temperature, maximum can temperature and maximum fuel temperature.

Data and output edit facilities

The programme demands a large volume of input data and a single case can produce up to 300000 numbers as output. It is therefore essential that extensive edit facilities are available to display both input data and output for easy checking and assimilation. Two types of output format are available; one in which selected variables on a given horizontal plane are printed out in plans corresponding to the reactor geometry, the other printing out the axial distribution of neutron flux, xenon concentration and material temperatures in any selected channel.

4. REPRESENTATION OF ABSORBERS

A new method of absorber representation in finite difference codes has been developed to permit the absorbers to be positioned at any point within a mesh region [7]. The method is based on the expansion of the flux surrounding the absorber into radial harmonics retaining up to second order terms. The finite difference estimates of neutron currents into, and absorption within, the region containing the rod(s) are then corrected using this analytical expansion.

Outline of method

The two-group fluxes at any point (r,θ) in a region containing R absorbers is expressed as:

$$\phi_f = uZ_1 - vZ_2 \quad \phi_{th} = Z_1 + Z_2$$

$$Z_1 = \sum_{n=0}^{2} J_n(\beta r)\,[A_n \cos n\theta + B_n \sin n\theta] + \sum_{i=1}^{R} G_i Y_0(\beta r'_i)$$

$$Z_2 = \sum_{n=0}^{2} I_n(\gamma r)\,[C_n \cos n\theta + E_n \sin n\theta] + \sum_{i=1}^{R} H_i K_0(\gamma r'_i)$$

where u,v and β,γ are the conventional two-group coupling coefficients and bucklings respectively.

The arbitrary coefficients are determined by equating the analytical fluxes with the finite difference fluxes at the four corners of the surrounding region and from the extrapolation length boundary conditions at the surface of the absorber channels. In order to maintain the symmetry of the finite difference equations, it is convenient to introduce the corrections in the form of four pseudo-absorption cross-sections for the four quadrants of the mesh region. For the jth quadrant, we have for each group:

$$\phi_j \mu_j = \frac{4}{H} 2\left\{J_{j-1} - J_{j-} - D\,[2\phi_j - (\phi_{j-1} + \phi_{j+1})] + \sum_{i=1}^{R} S_j A_1\right\}$$

where S_j is the fraction of the rod surface in the jth quadrant. The currents J are obtained by integration over the boundary in question and the rod absorption(s) A from $A = 2\pi a D\phi(a)/\lambda$ where a is the rod radius and λ the extrapolation length into the control rod.

In order to simplify the computation of the neutron current integrals, the Bessel functions have been expanded into expressions which can be integrated analytically and two alternative expansions have been investigated.

Comparison of method with analytical solution

Comparisons have been made between the method outlined above used in conjunction with a specially written two dimensional finite difference programme and an analytical solution based on the methods of Codd and Rennie [8]. The comparisons were made for an array of 52 control rods distributed over a typical magnox reactor. These comparisons show that reactivity held by the rods and neutron flux can both be predicted to within 2% of the values obtained analytically. Simple "smearing" of the rods over the mesh region on the other hand gave errors in the order of 40% in the reactivity held by them.

The methods described above are exploratory and do not cover all situations likely to arise in practice. Thus in two dimensional calculations the methods refer to interstitial rather than in-channel absorbers. For three dimensional calculations, it is suggested that a series of two dimensional calculations are performed to obtain correction factors as a function of axial height in the rodded zone, with the use of conventional finite difference equations in the region beneath the rods. Near the rod tip, some empirical joining function $f(\theta)$ for rods penetrating a fraction θ into the mesh volume should be applied to the correction factors.

5. HETEROGENEOUS STUDIES

The solution of the homogeneous neutron diffusion equations using a coarse finite difference mesh provides a broad macroscopic picture of the reactor power distributions. For many operational purposes it is desirable however to obtain more accurate channel-to-channel solutions—especially near channel vacancies, absorbers or other lattice singularities.

In SKIP we endeavour to meet this requirement by having the ability to superimpose a solution of the heterogeneous neutron flux equations upon the macroscopic solution. The coarse-mesh finite difference solution for the reactor is used to provide a boundary condition on a special sub-region of the reactor which is then treated using heterogeneous methods. Routines are available for investigating small two and three dimensional sub-regions in this way but they are limited to two neutron energy groups.

The basic heterogeneous method

Group diffusion theory with two energy groups is used in the special region and the fuel channels are represented by a series of line sources of fast neutrons, sinks of thermal neutrons and thermal dipoles to allow for neutron streaming in the channels. The solutions

for the fast and thermal fluxes are:

$$\psi(\vec{r}) = \sum_k K_{Fk} P_k$$

$$\phi(\vec{r}) = \sum_k \left\{ K_{FMk} P_k - K_{Mk}\sigma_k + K_{Dk} \frac{\vec{B}_k(\vec{r}-\vec{r}_k)}{\vec{r}-\vec{r}_k} \right\}$$

where

P_k = fast source strength of the channel at $\vec{r}_k$

σ_k = thermal sink strength of the channel at $\vec{r}_k$

$\vec{B}_k$ = dipole strength of the channel at $\vec{r}_k$

and the K_k are the diffusion theory kernels giving flux distributions around sources at $\vec{r}_k$.

In order to determine the unknowns P_k, σ_k and $\vec{B}_k$, we require three equations for each channel. Neutron balance considerations in the channel for each group give two equations relating the mean fluxes and flux gradients at the channel wall through the known neutron absorption, production and slowing down properties inside the channel. Considerations of dipole strength give a third relation; it has been shown by Carter and Jarvis [9] that a void acts as a polarized medium with the dipole strength related to the thermal flux gradient in it by

$$\vec{B}_k = -2\pi D_M b_k (\nabla\phi)_k$$

where b_k is a term depending upon the geometry of the channel. It is assumed that the effect of the dipoles may be ignored in calculating the flux gradient.

Combination of homogeneous and heterogeneous methods

The work on combining the two approaches was performed by C. Sheffield and J. L. Bear (then of the English Electric Company Limited) under a UKAEA contract. The source-sink and homogeneous solutions are matched on the boundaries of the special region. This is done separately for fast and thermal groups using bounding conditions of the form:

$$\psi_i - \mu_{Fj}\left[\frac{\mathrm{d}\psi}{\mathrm{d}n}\right] = 0 \text{ and } \phi_j - \mu_{Mj}\left[\frac{\mathrm{d}\phi}{\mathrm{d}n}\right] = 0$$

where μ_F, μ_M are extrapolation lengths derived from quadratic surfaces obtained from the homogeneous solution, and $\mathrm{d}/\mathrm{d}n$ is the derivative normal to the boundary of the special region.

In order that the heterogeneous calculation should satisfy these boundary conditions, the special region is surrounded by fast and thermal images in the fuel channels immediately outside the special region. (In order that boundary conditions derived from the homogeneous, macroscopic flux may be applied to the heterogeneous, microscopic flux it is necessary that the boundary of the special region should lie mid-way between fuel channels.)

The complete set of all boundary conditions may be conveniently written in matrix form and the resulting eigenvalue equation is:

$$(F^* - XT^*)\,\vec{V} = 0$$

where $\vec{V}$ is the eigenvector of unknown source-sinks and F^*, T^* are matrices of those coefficients which do and do not contain the fuel multiplication factor on which the eigenvalue X operates. This final system of equations is solved by iterating for X and $\vec{V}$ on the matrix $(T^*)^{-1}F^*$ and the fluxes $\psi(\vec{r})$, $\phi(\vec{r})$ obtained from the expressions above.

6. NUMERICAL AND PROGRAMMING TECHNIQUES

The finite difference form of the neutron diffusion equations may be expressed in matrix notation as:

$$A\vec{\phi} = \frac{1}{\lambda} B\vec{\phi}$$

where $\vec{\phi}$ is a vector whose elements are the flux values at mesh points and λ is the largest eigenvalue of the matrix $A^{-1}B$. and is initially unknown. The problem is non-linear as the elements of A and B depend on $\vec{\phi}$.

This equation is solved iteratively as follows:

$$A\vec{\phi}^* = B\vec{\phi}^{(n)}$$

Following which $\lambda^{(n+1)}$ is estimated and

$$\vec{\phi}^{(n+1)} = \frac{1}{\lambda^{(n+1)}}\vec{\phi}^*$$

Initially every iteration, and later less frequently the auxiliary equations are solved and the matrix coefficients recalculated. The flux is scaled at the same time to give the required power level.

The convergence of the iterative process is accelerated by Chebychev extrapolation, application of which is delayed until the shift in eigenvalue spectrum, which results from the recalculation of matrix coefficients, is small.

The equations for $\vec{\phi}^*$ at each stage of the iterative procedure above are themselves solved iteratively because of the large number of zero elements in the matrix A. The method used is point successive over-relaxation (SOR). No thorough analysis of the problem was possible due to its non-linear nature and this method was chosen as the one most likely to prove satisfactory. More sophisticated methods may prove less efficient in non-linear cases where the finite difference coefficients have to be recomputed frequently. The optimum acceleration parameters for the point SOR method are estimated by the programme once the major effect of the non-linearities has been taken into account.

The programme is written for an IBM 7090 computer with 12 magnetic tape units. Tape is used as a backing store and as an input-output medium. The majority of the programme is in the FORTRAN II language, but certain sections are written in IBM machine code. For example, a machine coded routine is used for reading and writing tape in parallel with calculation in the computer, as this is not possible with FORTRAN II.

7. KINETIC EXTENSION OF STEADY STATE PROGRAMME

The need to carry out reactor kinetic studies in three spatial dimensions is discussed in another paper presented at this Conference [10] and the existing three dimensional reactor kinetic programmes STAB/STABLE [3, 11] are also described. The main limitation of these programmes is the restricted number of mesh points leading to a poor physical representation of the reactor and in some cases to poor numerical accuracy. The representation of control absorbers is also restrictive. A new three dimensional kinetic programme based on the SKIP steady state programme is being developed which will, it is hoped, overcome all these objections although at the expense of computing time (say $\frac{1}{4}$–$\frac{1}{2}$ hour per time step on the IBM 7090). The numerical techniques to be employed are similar to those used in the STAB/STABLE programmes, i.e., fully implicit integration in time and semi-analytic treatment of delayed neutrons.

8. COMPARISON WITH OTHER METHODS OF CALCULATION

A number of other three dimensional diffusion theory computer codes are now in existence but these are straightforward finite difference solutions of the diffusion equation requiring a fine mesh size to predict with reasonable accuracy the neutron flux around absorbers. Furthermore, these other codes do not allow implicitly for the reactivity feedback effects of xenon and temperature on the flux distribution and reactivity. The effect of temperature is of particular importance in a gas-cooled graphite moderated reactor where the moderator and fuel temperatures can vary by over 200 °C across the reactor core, with a significant effect on the flux distribution and on the reactivity taken up by partly inserted control rods.

Fully heterogeneous computer codes also exist for representing an entire reactor, but limitations in machine size and speed restrict these to a two dimensional simulation of only a few hundred channels. However, at the UKAEA Reactor Development Laboratory at Windscale, theoretical development of the solution of heterogeneous problems by finite difference methods is in progress [12] and it is hoped that this will enable much larger three dimensional heterogeneous problems to be solved in a time comparable with that required for a finite difference diffusion theory solution of the same problem treated homogeneously.

The SKIP programme has so far only been run on test cases with about 2000 mesh points but extrapolation from these results gives a computation time of $1\frac{1}{2}$ to 2 hours for a 10000 mesh point, two-group case on the IBM 7090 for a fully converged flux and temperature solution.

An alternative three dimensional flux programme which allows more mesh points to be taken but does not allow explicitly for temperature effects takes about $2\frac{1}{2}$–3 hours on the IBM 7090 for a case having ~50000 mesh points and two neutron energy groups. It is still not clear at the time of writing how many times such a calculation must be repeated with revised temperature dependant data to get a satisfactorily converged flux and temperature solution.

APPENDIX 1

Typical equations solved by SKIP programme

(*a*) *The few-group diffusion equations*

$$-\text{div } D_i \text{ grad } \phi_i + \Sigma_i \phi_i = \underset{j \neq i}{\text{Sum}} (\Sigma^s_{ji} \phi_j) + \psi_i \{\text{Sum}_j (k_j \Sigma^a_j \phi_j) + S\}, \quad (1)$$

$$\text{where } \Sigma_i = \Sigma^a_i + (F_i + C_i + \sigma^x_i X) + \underset{j \neq i}{\text{Sum}} \Sigma^s_{ij} \quad (2)$$

and $1 \leqslant i, j \leqslant n$, $1 \leqslant n \leqslant 5$.

(*b*) *External boundary conditions*

At boundary B,

$$Di \frac{\partial \phi_i}{\partial m}\bigg| B = - \underset{j}{\text{Sum}} \{(r_{ij})\, \phi_j (B)\}, \quad (3)$$

where $m = x$, y, or z.

(*c*) *Xenon equation*

$$X = \frac{\Gamma \underset{i}{\text{Sum}} (\Sigma^f_i \phi_i)}{\lambda_x + \underset{i}{\text{Sum}} (\sigma^x_i \phi_i)} \quad (4)$$

(*d*) *Temperature dependence of nuclear properties*

$$k_j = (k_j)_0 \left\{1 + \kappa^{m_1}_j \bar{T}_m (1 + \kappa^{m_2}_j \bar{T}_m)\right\} \left\{1 + \kappa^f_j \left[(\bar{T}_f + 273.2)^{n1} - (273.2)^{n1}\right]\right\} \quad (5)$$

$$\text{and } \Sigma^a_i = (\Sigma^a_i)_0 \{1 + \alpha^a_i \bar{T}_m\}. \quad (6)$$

(*e*) *Heat transfer*

(*i*) *Fuel*

$$K_{f_2} (T_{f_2} - T_{f_1}) - K_{f_1} (T_{f_1} - T_{fs}) + (1 - b) H_f \underset{i}{\text{Sum}} \Sigma^f_i \phi_i = 0 \quad (7)$$

(*ii*) *Coolant*

$$W^{xy}_z \cdot P \cdot \frac{\partial T_c}{\partial z} = \frac{1}{\gamma_2} h_s (T_s - T_c) + h_m (T_{ms} - T_c) \quad (8)$$

(*iii*) *Can*

$$\frac{K_{fs}}{\gamma_1} (T_{fs} - T_s) - h_s (T_s - T_c) - Y \{(T_s + 273.2)^4 - (T_{ms} + 273.2)^4\} = 0 \quad (9)$$

Nomenclature used in equations

ϕ	= neutron flux (group suffixes i, j)
D	= diffusion coefficient
Σ	= macroscopic cross-section (s = scatter, a = absorption, f = fission)
k	= group multiplication constant

S = fixed neutron source term
n = number of neutron energy groups
r = term in $n \times n$ matrix boundary condition
F = absorption due to fixed absorbers
C = absorption due to moveable absorbers
X = xenon-135 concentration
Γ = total xenon yield per fission (direct and indirect)
λ_x = xenon-135 decay constant
σ_x = microscopic absorption cross-section for xenon-135
κ, n_1 = temperature coefficients on group multiplication constant
α = linear temperature coefficient on cross-sections
K_{f_1}, K_{f_2} = thermal conductance terms between fuel regions
T_{f_1}, T_{f_2} = temperatures in fuel regions
T_{fs} = temperature at fuel surface
b = fraction of total fuel heat generated in inner fuel region
H_f = heat generated in fuel per fission
W_z^{xy} = coolant flow rate at co-ordinate (x, y, z)
P = coolant specific heat
T_c = coolant temperature
T_s = temperature of fuel can
T_{ms} = temperature at moderator surface (channel wall)
h_s, h_m = convective heat transfer coefficients between coolant and fuel can and moderator surface respectively
K_{fs} = thermal conductance between fuel surface and can
γ_1, γ_2 = ratios of lengths can/fuel and channel/can
Y = coefficient of radiation heat transfer between can and moderator surface

REFERENCES

1. Prescott, R., Walsh, J., and Whiteley, A. B., *The SKIP three dimensional reactor computer programme*, CEGB Report CD/NS/10 (1963)
2. Enderby, J. A., *FTD2: A two dimensional flux and temperature distribution programme for thermal reactors*, UKAEA, TRG Report 46(R), HMSO, London (1961).
3. Curtis, A. R., Tyror, J. G., and Wrigley, H. E., *STAB: A kinetic, three dimensional one group digital computer programme*, UKAEA, AEEW–R77, HMSO, London (1961).
4. Varga, R. S., *Numerical solution of the two group diffusion equations in x–y geometry*, Inst. Radio Engrs. Trans. Nuclear Sci., *NS–4*, p. 52 (1957).
5. Cutts, B., Mummery, P. W., Syrett, J. J., and Tyror, J. G., *Graphite moderated thermal reactor calculations for Calder Hall*, Proceedings of the Second International Conference on the Peaceful Uses of Atomic Energy, P/15, Vol. 12, p. 612, United Nations (1958).
6. Buckler, A. N., and Macdougall, J. D., *A description of the TRACER–1 computational scheme*, UKAEA, Report AEEW–R305, HMSO, London (1963).
7. Buckler, A. N., and Tyror, J. G., *Representation of absorbers in finite difference diffusion codes*, UKAEA Report AEEW–R311, HMSO, London (1963).
8. Codd, J., and Rennie, C. A., *Two group theory of control rods in a thermal reactor*, UKAEA Report AERE R/R 818.
9. Carter, C., and Jarvis, R. J., Journal of Nucl. Energy, *15*, p. 113 (1961).
10. Brown, J., Whiteley, A. B., and Whitmarsh-Everiss, M. J., *Control, stability and protection of a gas-cooled graphite-moderated reactor*, P/179, Vol. 4, these proceedings.

ABSTRACT—RÉSUMÉ—АННОТАЦИЯ—RESUMEN

A/169 Royaume-Uni

Calcul de la distribution en trois dimensions spatiales de la puissance et de la température d'un réacteur

par A. B. Whiteley *et al.*

Le mémoire décrit la mise au point d'un important programme de calcul (SKIP) écrit pour la calculatrice IBM 7090 et servant à calculer la distribution en trois dimensions spatiales de la puissance et de la température dans un réacteur à l'état stationnaire.

La majeure partie des calculs se rapporte à la solution des équations de diffusion par groupes jusqu'à cinq groupes d'énergie sous forme non linéaire, c'est-à-dire avec effets explicites en rétroaction sur la réactivité, dus aux températures du matériau et à la concentration du xénon-135. Les équations de diffusion sont résolues par des méthodes des différences finies employant le schéma de sur-relaxation par blocs successifs, avec extrapolation Chebyshev des sources. Les équations auxiliaires définissant les températures et la concentration du xénon-135 sont résolues périodiquement; les coefficients dans les équations de diffusion sont ensuite évalués à nouveau et les matrices à différences finies sont modifiées en conséquence avant les répétitions ultérieures de flux. Le mémoire examine les raisons qui ont mené au choix des techniques numériques employées, et expose les méthodes et les problèmes de la programmation.

Deux nouvelles techniques ont été mises au point en vue d'accroître l'ampleur d'application des calculs de diffusion. Il s'agit tout d'abord d'une méthode servant à représenter des absorbeurs discrets (barres de commande) en n'importe quel point à l'intérieur d'un réseau à différences finies, et ensuite d'une méthode servant à superposer le calcul d'une structure fine du type source positive et source négative sur la distribution macroscopique des flux obtenue par calcul de la théorie de diffusion. Ces techniques (qui sont décrites de

manière quelque peu détaillée) ont été mises au point afin que l'on puisse se livrer à des études détaillées des réacteurs de puissance complets sans recourir à un nombre excessif de points du réseau à différences finies lorsqu'on résout l'équation de diffusion.

Le programme principal de diffusion ainsi que les programmes auxiliaires servant à calculer la structure fine des flux et l'information relative aux absorbeurs ont tous été écrits et éprouvés. Le programme de diffusion a accusé des rapidités satisfaisantes de convergence dans les cas aussi bien de deux groupes que de cinq groupes, et la durée des calculs est considérée comme étant raisonnable.

Le mémoire examine l'emploi futur auquel est destiné le programme aussi bien par le CEGB que par l'UKAEA, et expose l'extension du programme fondamental de diffusion à l'état stationnaire pour des états qui soient fonction du temps, c'est-à-dire pour l'étude des conditions transitoires dans le réacteur.

A/169 Соединенное Королевство

Расчет мощности реактора распределения температуры в трехмерном пространстве

А. Б. Уайтли *et al.*

В докладе обсуждаются вопросы составления программ (SKIP) для расчета на вычислительной машине IBM-7090 мощности реактора в устойчивом состоянии и распределения температуры в трехмерном пространстве.

Основная часть доклада посвящена решению диффузионных уравнений для пяти групп энергии в нелинейной форме, т. е. с учетом заметного эффекта обратной связи реактивности, обусловленной температурой материала и концентрацией Xe^{135}. Диффузионные уравнения решаются методом конечных разностей с использованием схемы последовательных затуханий и экстраполяцией источников по методу Чебышева. Приводится также решение вспомогательных уровней для определения температур и концентраций Xe^{135}; делается повторная оценка коэффициентов диффузионных уравнений и матрицы конечных разностей модифицируются в соответствии с вышеуказанной методикой с последующей итерацией потока. Обсуждаются причины выбора численной методики, а также указываются проблемы и методы программирования. Разработаны две новые методики, расширяющие область применения диффузионных расчетов. Во-первых, метод дискретных поглотителей (регулирующие стержни) для любой точки в пределах сетки конечной разности и, во-вторых, метод подгонки расчета тонкой структуры типа источник — поглотитель к макроскопическому распределению потока, полученному в результате диффузионных расчетов. Эти методы (которые в докладе довольно подробно описаны) разработаны с целью детального изучения полной мощности реакторов без использования большого числа точек сетки конечных разностей при решении диффузионного уравнения.

Были подготовлены и опробованы основная диффузионная программа и вспомогательные программы, предназначенные для расчета тонкой структуры потока и характеристик поглотителя. Диффузионная программа показала удовлетворительные скорости сходимости как в случае двухгрупповых, так и в случае пятигрупповых расчетов при приемлемом машинном времени.

Обсуждается использование этой программы в будущем как Центральным энергетическим управлением, так и Управлением по атомной энергии Великобритании; указывается также на расширение исследований диффузионной программы применительно к модели с временной зависимостью для изучения переходных процессов реакторов.

A/169 Reino Unido

Cálculos tridimensionales de distribuciones de potencia y temperatura en reactores nucleares

por A. B. Whiteley *et al.*

Este artículo describe el desarrollo de un gran programa de cálculo, SKIP, escrito para la calculadora IBM-7090 con el fin de estudiar distribuciones tridimensionales de potencia y temperatura en un reactor en estado estacionario.

La parte más importante del cálculo corresponde a la solución, para un máximo de cinco grupos, de las ecuaciones de difusión en forma no lineal, es decir, incluyendo explícitamente los efectos de realimentación debidos a temperaturas del material y a concentración del xenon-135. Las ecuaciones de difusión se resuelven mediante técnicas de diferencias finitas usando un esquema iterativo de super-relajación sucesiva puntual con extrapolación de Chebycheff para las fuentes. Se resuelven periódicamente las ecuaciones auxiliares que definen las temperaturas y la concentración de xenon-135; a continuación se recalculan los coeficientes de las ecuaciones de difusión y, de acuerdo con ellos, se modifican las matrices en diferencias finitas antes de proseguir con nuevas iteracciones de flujo. Se discuten las razones por las que se han elegido las técnicas numéricas empleadas y se especifican métodos y problemas de la programación.

Se han desarrollado dos nuevas técnicas para aumentar el campo de aplicabilidad de los cálculos de difusión. La primera es una forma de representar absorbentes discretos (barras de control) en cualquier punto de una malla de diferencias finitas, y la segunda es un método para superponer un cálculo de estructura

fina del tipo fuente-sumidero a la distribución macroscópica de flujo obtenida del cálculo en teoría de difusión. Estas técnicas (que se describen con cierto pormenor) se han desarrollado para poder hacer estudios detallados de reactores de potencia sin necesidad de usar un número excesivo de puntos en la malla de diferencias finitas al resolver la ecuación de difusión.

El programa principal de difusión y los programas auxiliares de cálculo de la estructura fina y para los datos del absorbente ya han sido codificados y comprobados. La rapidez de convergencia ha demostrado ser satisfactoria para dos y para cinco grupos y el tiempo de cálculo se considera razonable.

Se discute el probable uso futuro del programa por parte de CEGB y de UKAEA, así como la extensión a un modelo dependiente del tiempo para el estudio de transitorios del reactor.

Advancements in analytical methods and machine computations in reactor physics design

By E. L. Wachspress,* R. G. Luce,* J. J. Taylor** and G. J. Habetler***

Improved reactor design evidences the advances made in reactor physics analysis techniques. These advances have been stimulated by increased knowledge of microscopic cross-section data, improved numerical methods, and the availability of more versatile digital computers. A review of these developments since the last Geneva Conference is given.

A more fully developed few-group diffusion theory remains the primary nuclear design tool because of: (*a*) intrinsic simplicity, (*b*) wide applicability for calculating multi-dimensional neutron flux distributions and (*c*) the highly developed technology for numerical solution of the group-diffusion equations. Spatial heterogeneity factors and adjustment of group structure and constants from supplemental high order transport methods are incorporated to reduce inherent diffusion theory inaccuracies. This results in greater design precision.

The first section reviews the structure of the group diffusion equations and advances in numerical methods for solving these equations. The second section contains method improvements for obtaining spectral-averaged few-group constants and self-shielding factors, and other adjustments of diffusion equation constants. These provide increased design accuracy and analytical standards for assessment of the validity of design approximations. Since transport techniques predominate in this work, transport theory development is also reviewed herein.

These sections culminate in a model for prediction of the steady-state characteristics for a specific reactor configuration, while the third section summarizes a quasi-steady-state design procedure to estimate core depletion effects. Advances in depletion methods have occurred as a result of: (*a*) efficient calculation and incorporation in the few-group model of changes in spectra and spatial fine structure with core life; (*b*) improved synthesis of three-dimensional power distributions; and (*c*) digital computer automation of the depletion calculation procedure.

The final section discusses application of variational methods to formulate a theoretically sound and systematic method for combining the components of the calculational scheme into an over-all procedure allowing varying degrees of refinement.

* Knolls Atomic Power Laboratory, Schenectady, N.Y.
** Bettis Atomic Power Laboratory, Pittsburgh, Pennsylvania.
*** Rensselaer Polytechnic Institute, Troy, N.Y.

CORE SPATIAL DISTRIBUTIONS: THE DIFFUSION THEORY FORMALISM

Analytical model

The few-group diffusion theory representation, supported by auxiliary spectral and spatial calculations, has been subject to extensive comparison with critical experiments and analytical standards but still has remained satisfactory in concept for a variety of reactor types [1]. There have been many modifications in detail, particularly in auxiliary methods for estimating lattice parameters.

An adequate epithermal description can be obtained with essentially the same few-group structure, although change in the thermal neutron description has occurred. In the previous Conference summary [2], the thermal neutron description consisted of a single equivalent thermal diffusion group, with group constants determined by averaging over a single asymptotic spectrum. Advanced multi-region reactor designs with strong variations in thermal-neutron absorbing materials or in moderating materials (or their temperatures) require treatment of spatially varying thermal spectra.

A representation of space-dependent spectra within the diffusion theory formalism by a linear combination of asymptotic spectra (the "overlapping group" method) was developed by Calame *et al.* [3]. The coefficients of linear combination are determined by variational procedures. This technique results in equations of the same form as few-group diffusion theory. Calame [3,4] found that a wide range of spectral variation can be characterized by two infinite media spectra, one a Maxwellian and the other a hardened spectrum, characteristic of the region having the strongest absorption in the reactor. Buslik [5] found that the adjoint flux and source in the variational procedure can often be replaced by the flux and source themselves. Discrete few-group thermal descriptions, similar to the conventional discrete fast few-group schemes except for the addition of transfer from lower energy to higher energy groups (up-scattering), have also been developed [6,7]. However, a range of application similar to that covered by two overlapping groups requires four discrete groups, so that the

former method is more convenient calculationally and has wider use in design.

The adequacy of the few-group structure discussed above cannot be ascertained from the formulation itself since the approximations involved are either based on heuristic reasoning (choice of few groups or asymptotic spectra) or on mathematical processes such as the variational technique which have no rigorous criteria of accuracy. Thus an important parallel development has been required of spatially-dependent multi-group transport methods with which the adequacy and the detailed form of the few and overlapping group approximations can be determined. These methods have also been found useful in the computation of thermal lattice parameters and will be discussed in a subsequent section.

A variety of digital programmes have been developed to solve the group diffusion equations for use in nuclear design of reactors. Many have been produced in rectangular and polar one-dimensional geometries and in a variety of two-dimensional geometries (rectangular, cylindrical, and hexagonal) and some have been written for three-dimensional rectangular geometry.

Numerical methods

Development has continued on methods of solution of the multi-dimensional group diffusion equations in both the formulation of difference equations and in their numerical solution.

Difference equations

Discretization of the continuous group diffusion equation may be accomplished by a variety of techniques. Conventional finite difference methods are most often used to obtain equations which couple each grid point to its neighbours. Methods based on eigenfunction expansions have been applied by Garabedian [8] to some simple configurations, but are not suitable for complex reactor mock-ups.

Design interest in reactor geometries not adequately represented by rectangular or cylindrical co-ordinates led to a formulation with a uniform triangular mesh [9]. For some applications, restriction to uniform spacing resulted in a need for an excessive number of grid points. To reduce the number of points, the Ritz variational method as generalized by MacNeal [10] was applied by Kellogg to derive difference equations for a programme [11] allowing a non-uniform triangular mesh and retaining a periodic boundary condition [12] needed for design application. The seven-point difference equations in these triangular mesh programmes retain properties which enable solution by iterative methods similar to those employed for rectangular meshes [13–16].

Numerical solution of the discrete group-diffusion equations

Fractional iteration

Few-group one-dimensional and synthesized three-dimensional problems are solved by the method of fractional iteration [17, 18]. Solution of matrix three-term-linear systems by Gaussian elimination replaces the inner iteration of detailed two- and three-dimensional computations. The fission source iteration converges rapidly to the mode with eigenvalue closest to an estimated value. This enables computation of higher modes which may be used in the study of transients.

Unfortunately, solution for the group fluxes simultaneously by iterative methods has limited applicability because of the detrimental effect on inner-iteration convergence as the estimated eigenvalue approaches a true eigenvalue [19].

Inner iteration

Two basic inner iteration procedures have been widely used for solving the group diffusion equations; successive overrelaxation (SOR) and alternating-direction-implicit (ADI) iteration.

The discrete diffusion equation for a group may be written as the matrix equation;

$$A\vec{\phi}=\vec{k} \tag{1}$$

where A is a symmetric square matrix containing the (real) difference equations coefficients and $\vec{k}$ is a known non-zero vector representing the source of neutrons by fissioning and scattering. For application of a variety of iterative techniques, the matrix A is expressed in the form:

$$A=P-(R+R^T) \tag{2}$$

where P is a block diagonal matrix with diagonal blocks, P_i, such that;

$$P_i\vec{x_i}=\vec{b_i} \tag{3}$$

may be easily solved for $\vec{x_i}$ when given $\vec{b_i}$, and R is a lower triangular matrix with transpose R^T. SOR is defined by;

$$(P-\omega R)\vec{\phi}^{(m)}=(1-\omega)P\vec{\phi}^{(m-1)}+\omega R^T\vec{\phi}^{(m-1)}+\omega\vec{k} \tag{4}$$

where ω is a scalar called the "overrelaxation factor". Various block relaxation methods can be identified, depending on choice of P and the associated difficulty of solving (3). Methods are available for improving all points on a mesh line simultaneously with computation time about the same as for point relaxation [16,20]. Simultaneous solution for all points on two adjacent mesh lines [21] requires only about 20% more computation time per iteration than point relaxation. More rapid convergence of block relaxation often yields a reduction in total computation time [15].

Hageman and Varga have shown that once a particular partitioning of A has been decided upon the convergence of the iterative scheme can be improved upon by reduction of the iteration matrix to two uncoupled lower order matrix equations [14]. Table 1 gives estimates of the relative asymptotic convergence rates of the inner iterations for these methods, derived

Table 1. Asymptotic convergence rates of inner iterations

Iteration method	Est. convergence rate	Reference
Point SOR	$2h$	[14]
Single line SOR	$2\sqrt{(2)}\,h$	[25]
2-line SOR	$4h$	[23]
Cyclically reduced 3-line SOR	$5.5h$	[24]

for the Dirichlet problem on the unit square with small uniform mesh spacing, h.

For application of ADI iteration [22], the matrix of coefficients of the group difference equation is split into two components: $A = H + V$. The matrix relating the error vector after n iterations to the initial error vector is;

$$T_n = \prod_{k=1}^{n} (V+\omega_{kV}I)^{-1}(H-\omega_{kV}I)(H+\omega_{kH}I)^{-1}(V-\omega_{kH}I),$$

where I is the identity matrix and $\{\omega_{kV}, \omega_{kH}\}$ are scalars chosen to enhance convergence.

Advances have been made in the analysis of the homogeneous rectangular problem (the so-called "model problem") for which H and V commute. Generalization of the ADI scheme proposed by Peaceman and Rachford to permit $\omega_{kH} \neq \omega_{kV}$ [23] led to the solution by W. B. Jordan to the minimax problem;

$$\min_{\{\omega\}} 0 < a \leq \lambda(H) \leq b \; 0 < c \leq \gamma(V) \leq d \left| \prod_{k=1}^{n} \frac{(\lambda-\omega_{kV})(\gamma-\omega_{kH})}{(\lambda+\omega_{kH})(\gamma+\omega_{kV})} \right|$$

by application of the theory of modular transformations of elliptic functions.

For a homogeneous rectangle, the convergence rate of the Peaceman-Rachford method varies as $-c/\ln h$ where c is of order magnitude unity [23]. This method is thus considerably more efficient than SOR for solving homogeneous problems with fine grids. For the general neutron diffusion problem, however, the model problem convergence rate is not realized and care must be exercised in choosing effective iteration parameters [24]. A convergence proof has been obtained by Guilinger [25], bounding the number of iterations needed to approximate a finite difference solution to a given accuracy independent of the size of the mesh increments.

A compound iteration discussed by D'Yakonov [26] and amplified in [23] enables rigorous application of model-problem theory to the general group-diffusion equations. This compound iteration seems less suited for neutron diffusion computations than direct application of ADI with model-problem parameters. A theorem due to Pearcy [27] establishes convergence with this parameter choice even when H and V do not commute. Numerical studies indicate that this is an efficient iteration procedure.

Other variants of ADI iteration have been developed [28–30] in an attempt to increase the generality of application of the ADI technique. General convergence proofs comparable to Pearcy's have been given, but numerical results are limited and these methods have not yet been applied to neutron diffusion problems.

Algorithms for generating useful iteration parameters for non-singular matrices H and V have been extended by Douglas and Pearcy to the singular case [31], and these results have been applied to a digital programme for solution of the two-dimensional equations for heat conduction [32] which are a special case of the two-dimensional neutron diffusion equations.

Outer iteration and inner-outer strategy

The outer (fission-neutron source) iteration and its relationship to the inner (group flux) iteration has been studied intensively [13, 19, 33], but its complexity is such that convergence characteristics are not always predictable. A more satisfactory theoretical basis has been developed for flux extrapolation than for fission source extrapolation in the outer iteration [34, 35].

Chebyshev extrapolation in the outer iteration is less effective when the inner iteration is terminated before a significant error reduction is achieved. Poor convergence of the inner iteration leads to complex eigenvalues in the matrix relating successive fission source distributions, and convergence of the outer iteration is adversely affected by these complex eigenvalues. Computer characteristics play a decisive role in governing iteration strategy. Problems for which the inner iteration can be contained in fast memory are often solved most efficiently by imposing stringent error reduction requirements on the inner iteration. This enables more effective Chebyshev extrapolation of the outer iteration, thereby reducing the number of relatively inefficient outer iterations. When the inner iteration is not memory contained, an effective strategy is to perform relatively few inner iterations with restricted extrapolation of the outer iteration.

AUXILIARY COMPUTATIONS AND TRANSPORT THEORY

Development has continued of more accurate methods for predicting detailed spatial and spectral effects which can then be incorporated into the diffusion theory formalism. Accurate methods are also required to provide "standard" calculations to assist in assessing the validity of the simpler design methods. Thus, effort has continued in the development of calculational methods in transport theory proper which are theoretically capable of yielding any desired accuracy. The ensuing discussion briefly enumerates techniques applied in auxiliary calculations to diffusion theory and then reviews recent developments in application of transport theory.

Auxiliary computations

Thermal neutron description

Recognition of the need to account for spatial variations in the thermal spectra has led to the use of thermal multi-group transport methods in auxiliary

"fine structure" calculations. It is commonly assumed in these multi-thermal-group models that the slowing down source into the thermal energy range (the upper boundary of which ranges between 0.5 and 1 eV) is isotropic with a spectrum independent of the epithermal flux spectrum and of position. The assumption of space-energy separability of the source has been justified only for the case in which the moderator consists of free protons. A relaxation of this separability assumption is found in a Monte Carlo programme [36] which uses Nelkin's kernels [37] and associated epithermal dependent sources.

The various multi-group methods can be characterized by their treatment of the angular variable. Spherical harmonic expansion has been applied typically up to the P_3 approximation and including the double-P approximation [38,39]. Discrete ordinate methods, whose equivalence to the spherical harmonic expansion has been shown by Gast [40] and Lee [41] are also used most generally in the form of the S_n method [42,43] and its associated digital programmes [39] Honeck [44,45] and Judge [46] have developed solutions to the integral transport equation with limitations typically to a linearly anisotropic scattering kernel. Multi-thermal-group Monte Carlo methods have also been developed [36,47,48].

Since the primary transport effects in these fine structure problems are in the absorber itself, it is natural to use transport theory only in the absorber, while retaining an approximate approach in the scattering environment surrounding the absorber. The two solutions must then be matched at the boundary since different angular dependencies will occur on each side. A class of methods has been developed from this approach, of which blackness theory, elaborated by Maynard [49], the "thin-region" approach [50], and the ABH and related methods [51,52] are examples. Fukai [53] has compared several of these techniques with exact and integral transport methods.

The results of these and other transport methods reviewed in a later section are incorporated in the group diffusion theory programmes by adjusting the thermal group-constants (e.g., disadvantage factors). There are various procedures and, except possibly for the calculation of disadvantage factors in uniformly loaded cores, they must be developed intuitively to handle each specific class of design problems (see Ref. [7], Chapter 5 for some examples). Another difficulty with this general technique is that the heterogeneity is calculated in a cell for which boundary conditions of zero flux, zero gradient [54], or periodicity are set. Such conditions are not realized in many high performance reactors and a satisfactory method has not yet been developed to treat more general cell boundary conditions.

Neutron slowing down and resonance capture

Epithermal few-group constants are still principally determined by averaging over multi-group spectra obtained by the space-independent methods of Greuling and Goertzel [55], Selengut [56], and Hellens [57]. Improved digital programmes [58–63] to perform these calculations have been written which incorporate more accurate and detailed cross-section data, a wider range of compositions and geometry, and more sophisticated methods of incorporating resonance self-shielding. One-dimensional space-dependent multi-group P_1 and P_3 methods [64,65], discrete ordinate techniques [66], and Monte Carlo methods [48,67] have been developed mainly to assess the accuracy of these approximations. This work has motivated studies to improve the description of heavy element scattering and more accurate treatment of resonances which do not initiate numerical oscillations in the multi-group calculations.

The increased knowledge of resonance and epithermal cross-section data has stimulated advances in the accuracy of auxiliary heterogeneous neutron capture calculations. Computation of resonance capture of uranium and thorium has been placed on a firmer basis and the range of validity of approximate resonance capture formulae has been investigated (e.g., the work of Nordheim [68], Chernick [69], Bell [70], Dresner [71], Goldstein and Cohen [72], and Drawbaugh [73]). Attention has been directed to the heterogeneous nature of epithermal absorption which is not characterized by widely-spaced resonances and may also have a large $1/v$ contribution. Goldsmith [74] has developed few-group blackness theory methods which treat this problem in slab geometry and also include the effects of small amounts of moderator in the absorbing material. Similarly, Darr and Lubert applied the energy-dependent thin region theory described in [50] to obtain effective epithermal cross-sections for high-absorption regions for use in [75]. Many digital programmes are available to carry out resonance and epithermal capture calculations [68,76,77].

Transport theory

Investigations have continued on methods for solving higher order approximations to the transport equation using techniques developed for diffusion approximations. The monoenergetic one-dimensional P_l or double P_l equations (up to P_7 or double P_3) have been transformed by Gelbard into coupled second order equations similar in form to the few-group diffusion equations [78]. These may be solved using the existing programmes and a Gauss-Seidel iteration technique. The process converges quickly and the rate of convergence is not as sensitive to the parameters of the problem as it is for programmes employing methods of discrete ordinates [79].

Methods have been introduced to avoid iteration among the various P_l components. The first order equations obtained from the P_l approach can be considered simultaneously and auxiliary variables introduced to create a set of first order equations that are stable and can be solved numerically by non-iterative techniques [80]. This is equivalent to the manner in which each of the group-diffusion equations is solved in currently available one-dimensional diffusion programmes.

Besides the spherical harmonics methods, discrete ordinates methods have continued in extensive use. Here too there have been applications of the iterative techniques developed for use with the diffusion approximation. Successive overrelaxation [81–83] and Chebyshev iteration [84] have been used with limited success. Alternating direction methods have also been investigated [41].

Carlson's S_n method and its variations is now in use at many installations. Of particular importance are the simpler discrete S_n methods, introduced when the earlier S_n methods gave unrealistic flux oscillation in some problems [85]. These methods are extensions of the Wick-Chandrasekhar discrete ordinates methods. Their usefulness lies in the fact that they can be applied, quite readily, to the general problem of eigenvalue and source shape calculation in geometrically complicated reactors [86]. There have been various attempts, by means of different averaging procedures for deriving difference equations, to obtain better accuracy, comparable to earlier S_n accuracy, in some problems [87].

A parallel to Gelbard's method for P_l approximations, is an iterative procedure which involves alternating between diffusion and S_n calculations. It had been noticed by Carlson that the one-dimensional S_n difference equations could be written in such a way that by setting a few terms equal to zero, the diffusion difference equations would result [88]. This led to the possibility of iterating between the diffusion and the S_n equations so as to obtain the accuracy of the S_n approach and some of the speed of the diffusion equation. This is attractive in one-dimensional calculations where the equations are solved using "forward-backward" methods. Note that in this method ordinary diffusion theory is numerically imbedded in transport theory. One-dimensional S_4 calculations can be speeded up by a factor of as much as two to four by this device. A series of two-dimensional S_4 calculations were performed for a fast reactor [85] and the results were satisfactory [89].

Case's "singular eigenfunction method" for slabs [90] based on the singular integral equations theory of Muskhelishvilli [91] has led to a series of new, exact results for a variety of transport problems in slabs [92] and in spheres [93]. Besides providing standards of comparison, these results yield new families of solutions that may be employed in finding the solution to more difficult problems using the synthetic method [94].

One method that may be used for obtaining "exact" answers to complicated transport problems is Monte Carlo. An increase has occurred in its use for multi-dimensional multi-energy thermal neutron capture rate calculations as a result of improved mathematical techniques and faster digital computers. Among the theoretical advances leading to increased speed of computation are the following:

(*a*) Improved choices of unbiased estimators of capture rates in prescribed regions have been devised [95,96], thus reducing the number of histories required for a prescribed variance. One fruitful approach has been not to do any part of a calculation using random choices that can be done analytically by using the expected value of a random variable in place of a sample value. In several reactor physics Monte Carlo programmes, this approach has resulted in the choice of the track length estimator instead of the direct sample estimator. This results in a reduction in variance by as much as twenty or more for some typical thermal absorber problems. The validity of this approach, first suggested by Goertzel, has been established by Spanier [95] in a more general setting.

(*b*) Reductions in computations per history have been obtained by more rapid methods of generating random numbers [48] with both uniform and non-uniform distributions and by storing random numbers and other random variables in advance in the digital machine memory rather than generating them as needed.

(*c*) Maynard [97] has developed a technique, particularly useful for thermal absorber problems, based on the reciprocity theorem. A drastic reduction of the variance is obtained in computation of the capture probability in a single small region immersed in a large source region. To compute the capture probability in the small region, one solves an auxiliary (reciprocal) adjoint problem with unit source density in the small region and zero source elsewhere. A simple analytic relationship yields the solution to the original problem from that of the much more easily solved adjoint problem.

The use of Monte Carlo in criticality calculations has not been as widespread (but see, for example, Refs. [98–100]). Straightforward applications of the usual sampling techniques employed in the source-given problems results in excessive computational times. However, conditional Monte Carlo methods employed in source-given problems [101] have been applied to eigenvalue calculations [102] and it is hoped that such techniques may provide solutions to problems not susceptible to analysis by other means. A Monte Carlo programme has been developed by Rief [103] for evaluating fast fission effects.

DEPLETION METHODS

Lifetime behaviour of a core is not as amenable to investigation by critical experiments as the undepleted configuration, and is, therefore, subjected to extensive analysis. Computational methods are often verified by application to operating or depleted reactors for which data are available. The design of long life reactors with good fertile material conversion properties depends on the development of accurate and practical methods for predicting life-time behaviour. The slow rate of change of depletion effects permits a quasi-steady-state approach so that the techniques discussed in other sections can be applied.

A crucial step in a depletion study is the computation of time dependent number densities. The calculation of isotopic depletion requires accurate knowledge of cross sections and decay chains of heavy elements

burnable absorbers, and fission products. Some general techniques for obtaining reliable parameters have been described by Garrison and Roos [104]. The work of Greenhow and Hansen [105], Nephew [106], England [107], and Wikner [108] has refined the treatment of fission product absorption by describing the individual isotopes and their decay chains instead of using one gross absorption parameter. Nonlinearity of depletion equations coupled with complex space-energy effects necessitates several approximations in time integrations from which number densities are computed. For example, it is customary to assume either a constant flux or fission distribution during each time step. Rapid computation of fluxes enables shorter time steps, thereby reducing errors introduced by such assumptions.

Even with the high speed digital computers and advanced numerical techniques currently available, three-dimensional calculations are sufficiently expensive that they are used only as standards. Attention has focused on performing life studies by synthesizing three-dimensional solutions from lower dimensional results. An advance has been made over previous synthesis techniques [109]. Kaplan [110] has described how flux shapes from a preliminary life study with large time steps may be used as trial functions for a more refined computation based on synthesis methods discussed in [111] and [112]. Another approach has been applied to the depletion system described in [75] using the multichannel synthesis method of [113].

Accuracy has been improved by a more detailed treatment of changes in neutron energy spectrum and self-shielding during life studies. Although in principle the quasi-steady-state nature of depletion permits this problem to be handled by repeating the basic procedures used in normal steady-state calculations, this direct approach can lead to excessive digital calculation time. Two simplifications have been introduced: (*a*) computationally rapid approximations have been developed to compute group constant and self-shielding factor changes at frequent intervals through core life; and (*b*) automatic methods have been devised for reinserting these changes in the depletion programmes. Examples of the former are curve fitting and tabular extrapolation procedures which choose appropriate group constants or self-shielding factors from a set of calculations done at the start of the depletion programme over the expected range of depleted compositions. Automatic methods of reintroducing certain of the auxiliary calculations of the section on auxiliary computations and transport theory are required when spatial effects cannot be accurately represented by pre-computed tabular data or sufficiently simple auxiliary calculations.

VARIATIONAL METHODS

Theory [114]

Variational techniques provide a systematic means for reducing the Boltzmann equation to approximations which are computationally more convenient. The theory may be developed for each quantity of interest rather than for the entire state of the system. One may impose general conditions of insensitivity to approximation errors and derive an explicit procedure for constructing a variational principle to estimate the desired quantity [115]. If the theory has been stated in differential equation form, information about the system environment yields boundary terms which remove the usual restriction that trial functions satisfy boundary and continuity equations. Conversely, requiring the resulting functional to be stationary under arbitrary variations of its arguments implies not only the original direct and adjoint equations, but the boundary and continuity conditions as well.

Computational complexity results from irregular behaviour of functions, the presence of many independent variables, or interaction between parts of a problem each of which could be solved in isolation. These factors lead to the following four classes of trial functions:

(*a*) *Additive Approximations.* If the trial function is written as the exact solution to a simplified problem plus a remainder term, a generalization of conventional perturbation theory is obtained from both source-free and inhomogeneous systems. The use of a linear combination of several functions leads to a generalized interpolation procedure which allows a description of the system over a wide range in terms of a small number of detailed calculation, e.g., the computation of group constants [4].

(*b*) *Multiplicative Approximations.* If several independent variables are involved, the trial function may be approximated by a product of functions each depending on one or more variables, or by sums of such products [116]. The result is a set of equations which must be solved simultaneously, but which is simpler since each equation involves fewer independent variables. If the form of all the functions except one is specified, the iterations required for self-consistency can be avoided. Applications of this approach are found in the "overlapping-group" approximations [3], spherical harmonics and other polynomial expansion methods [116, 117] for solving the transport equation, simplified formulations of the space dependent kinetic equations [118, 119], and refined flux synthesis methods [110, 112].

(*c*) *Moment Approximations.* If the solution is expected to vary smoothly over the range of the kernel defining a theory in integral equation form, it is reasonable to expand the trial function in a truncated power series in one or more of its arguments. The effect of this is to replace the integral equation by a low-order differential equation, whose coefficients are the moments of the adjoint kernel. For an arbitrary linear equation, a similar expansion of the adjoint trial function, leaving the coefficients to be determined, leads to the requirement that the parameters in the approximate solution be chosen by matching the low-order moments of the equation [120].

(*d*) *Subsystem Approximations.* It is often convenient to divide a complicated system into several

components and concentrate on their interaction while suppressing details of the behaviour within each subsystem. An appropriate trial function is then a linear combination of functions, each one of which vanishes outside its corresponding region. By considering the interior and the boundary of a medium as separate regions, and choosing as a trial function the exact solution within the medium, complicated boundary effects can be taken into account. This approach may be applied to incorporate transport effects within the framework of diffusion theory [116, 121–123].

Application of variational methods to flux synthesis

Reactor design studies require simple but accurate computational models for complex configurations. Three-dimensional calculations are essential but detailed mock-ups are often too cumbersome for design studies. Synthesis computations use results of lower dimensional calculations (fluxes for lines or planes), as trial functions for a variational formulation of higher dimensional problems. The expression of stationarity of a functional with respect to arbitrary coefficients of combination of these trial functions yields exactly as many equations as there are unknowns. These synthesis computations provide a transition from crude to fine reactor mock-ups and thus furnish a means for balancing accuracy with complexity. Core life studies and transient analysis can be performed with the synthesis model, and a judicious choice of trial functions often yields acceptable results without excessive computational effort. The method of Galerkin, in which the adjoint fluxes are chosen to be the same as the direct fluxes, has given accuracy comparable to other methods requiring additional computation for determining adjoint trial functions [5].

Seemingly diverse synthesis schemes can be derived from a single variational principle by various choices of trial functions. For conventional variational formulations based on a functional with second order derivatives [112], the trial functions must be continuous. The multichannel synthesis approach [113] requires discontinuous trial functions and was not initially based upon variational methods for this reason. Selengut's variational formulation in terms of coupled first order equations admits discontinuous trial functions and thus provides a basis for a multichannel variational synthesis computation. Any of the existing synthesis models can be obtained with this variational technique, and more versatile synthesis models are currently being explored.

REFERENCES

1. Hicks, D., US Atomic Energy Comm. reports AEEW-R-64 (1961) and AEEW-R-249 (1962).
2. Gelbard, E. M. *et al.*, *The Role of Digital Computers in the Design of Water Moderated Reactors*, Proceedings of the Second International Conference on the Peaceful Uses of Atomic Energy, P/1843, Vol. 16, p. 473, United Nations (1958).
3. Calame, G. P., and Federighi, F. D., *A Variational Procedure for Determining Spatially Dependent Thermal Spectra*, Nuclear Sci. Eng., *10*, 190–201 (1961).
4. Calame, G. P., Federighi, F. D., and Ombrellaro, P. A., *A Two-Mode Variational Procedure for Calculating Thermal Diffusion Theory Parameters*, Nuclear Sci. Eng., *10*, 31 (1961).
5. Buslik, A. J., *The Description of the Thermal Neutron Spatially Dependent Spectrum by Means of Variational Principles*, US Atomic Energy Comm. report WAPD-BT-25 (Bettis Technical Review, Vol. 4), pp. 1–24 (May 1962).
6. Cantwell, R. M., *MO-176, A FORTRAN Program to Solve Several P-Approximations to the Few Group Neutron Transport Equation in Slab Geometry*, US Atomic Energy Comm. report WAPD-TM-320 (April 1962).
7. Radkowsky, A., *Naval Reactor Physics Handbook*, Vol. 1, Chapter 3, Section 3.7c.
8. Garabedian, H. L., and Thomas, D. H., *An Analytic Approach to Two-Dimensional Reactor Theory*, Nuc. Sci. Eng., *14*, 266–271 (1962).
9. Fletcher, J. L. *et al.*, *FLEER, A Two-Dimensional Triangular Mesh Diffusion Program for the IBM-704*, US Atomic Energy Comm. report KAPL-2086 (May 1960).
10. MacNeal, R. H., *An Asymmetrical Finite Difference Network*, Quart. of Appl. Math., *12*, 295–310 (1953).
11. Cadwell, W. R. *et al.*, *PDQ-6* (to be published).
12. Gonzales, A. A., and Ruth, B. H., *A Method of Numerical Solution of the Neutron Diffusion Equations in Hexagonal Geometry with a Variable Spatial Mesh*, Trans. ANS (November 1963).
13. Hageman, L. A., *Numerical Methods and Techniques Used in the Two-Dimensional Neutron-Diffusion Program PDQ-5*, US Atomic Energy Comm. report WAPD-TM-364 (February 1963).
14. Hageman, L. A., and Varga, R. S., *Block Iterative Methods for Cyclically Reduced Matrix Equations*, US Atomic Energy Comm. report WAPD-T-1643, Numerische Mathematik (to be published).
15. Varga, R. S., *Matrix Iterative Analysis*, Prentice Hall, New York (1962).
16. Varga, R. S., *Factorization and Normalized Methods in Boundary Problems in Differential Equations*, University of Wisconsin Press, Madison, Wisconsin (1960).
17. Wachspress, E. L., *A Numerical Technique for Solving Group Diffusion Equations*, Nuclear Sci. Eng., *8*, 164–170.
18. Wielandt, H., *Bestimmung Höherer Eigenwerte Durch Gebrochene Iteration*, Bericht der Aerodynamischen Versuchsanstalt Göttingen report 44/J/37, p. 290 (1944).
19. Wachspress, E. L., Proc. of IFIP Congress (Munich 1962).
20. Arms, R. J., *et al.*, *A Method of Block Iteration*, J. Soc. Ind. Appl. Math., *4*, 220–229 (1956).
21. Cadwell, W. R., *PDQ-3, A Program for the Neutron Diffusion Equations in Two Dimensions on the IBM-704*, US Atomic Energy Comm. report WAPD-TM-179 (May 1960).
22. Peaceman, D. W., and Rachford, H. H., *The Numerical Solution of Parabolic and Elliptic Differential Equations*, J. Soc. Ind. Appl. Math., *3* (1) (1955).
23. Wachspress, E. L., *Extended Application of ADI Iteration Model Problem Theory*, J. Soc. Ind. Appl. Math., *11*, 994 (1963).
24. Wachspress, E. L., and Habetler, G. J., *An Alternating Direction Implicit Technique*, J. Soc. Ind. Appl. Math., *8*, 403–424 (1960).
25. Guilinger, W. H. Jr., *The Peaceman-Rachford Method for Small Mesh Increments*, J. Math. Anal. and Appl. (to be published).

26. D'Yakonov, E. G., *An Iteration Method for Solving Systems of Finite Difference Equations*, Trans. ANS, *2* (3), 647 (May 1961).
27. Pearcy, C., Numerische Math., *4*, 172–176.
28. Kellogg, R. B., *Another Alternating-Direction-Implicit Method*, J. Soc. Ind. Appl. Math., *11*, 976–979 (1963).
29. Douglas, J. Jr., *et al.*, *Alternating Direction Iteration Methods for N Space Variables*, Math. of Computation, *17* (83), 279–282 (July 1963).
30. D'Yakonov, E. G., *On Some Difference Schemes for Solutions of Boundary Problems*, Z. Vyghisl. Mat. Mat. Fiz., *2*, 57–79 (1962).
31. Douglas, J. Jr., and Pearcy, C., *On the Convergence of Alternating Direction Procedures in the Presence of Singular Operators*, Numerische Math., *5*, 175–184 (1963).
32. Kellogg, R. B., and Spanier, J., *Alternating Direction Solutions of Heat Conduction Problems with some Neumann Boundary Conditions*, US Atomic Energy Comm. report (Bettis Technical Review, to be published).
33. Tobias, J., Vondy, D. R., and Fowler, T. B., Nuclear Sci. Eng., *15*, 98 (1963).
34. Hageman, L. A. (to be published).
35. Wachspress, E. L., *Solution of Linear Systems by Iteration*, Prentice Hall (to be published).
36. Habetler, G. J., Pfeiffer, R. A., and Tuecke, J. E., *DRAM, A Monte Carlo Program for the Calculation of Capture Probabilities*, US Atomic Energy Comm. report KAPL-3013.
37. Nelkin, M. S., *Scattering of Slow Neutrons by Water*, Phys. Rev., *119*, 741 (1960).
38. Bohl, H., *et al.*, *SLOP-1, A Thermal Multigroup Program for the IBM-704*, US Atomic Energy Comm. report WAPD-TM-188 (October 1960).
39. Dawson, C. W., *Thermal Energy Transport Code TET*, David Taylor Model Basin report 1613 (April 1962).
40. Gast, R. C., *On the Equivalence of Spherical Harmonics Method and the Discrete Ordinate Method using Gauss Quadrature for the Boltzman Equation*, US Atomic Energy Comm. report WAPD-TM-118 (April 1958).
41. Lee, C., *The Discrete S_n Approximation to Transport Theory*, US Atomic Energy Comm. report LA-2595 (1960).
42. Campise, A. V., *Accuracy of the S_n Code in Cell Calculations*, Nuclear Sci. Eng., *7*, 104 (1960).
43. Meneghetti, D., *Discrete Ordinate Quadratures for Thin Slab Cells*, Nuclear Sci. Eng., *14*, 295 (1962).
44. Honeck, H., *THERMOS, A Thermalization Transport Theory Code for Reactor Lattice Calculations*, US Atomic Energy Comm. report BNL-5826 (1961).
45. Honeck, H., and Takahashi, H., *The Angular Dependence of Thermal Neutron Spectra in Lattices*, Nuclear Sci. Eng., *15*, 115–123 (1963).
46. Judge, F. D., *Variational Methods in the Calculation of Reactor Neutron Flux Density*, US Atomic Energy Comm. report KAPL-2151 (February 1961).
47. Gelbard, E. M., *et al.*, *MARC, A Multigroup Monte Carlo Program for the Calculation of Capture Probabilities*, UN Atomic Energy Comm. report WAPD-TM-273 (May 1962).
48. Martino, M. A., and Stone, W., *TRAM, A Monte Carlo Thermal Neutron Code for the IBM-704*, US Atomic Energy Comm. report KAPL-2039.
49. Maynard, C. W., *Blackness Theory and Coefficients for Slab Geometry*, US Atomic Energy Comm. report WAPD-TM-168 (May 1959).
50. Wachspress, E. L., Nuclear Sci. Eng., *3*, 186–200 (1958)
51. Amouyal, A., *et al.*, *Nouvelle méthode de détermination du facteur d'utilisation thermique d'une cellule*, J. Nuclear Energy, *6*, 79 (1957).
52. Theys, M., *Integral Transport Theory of Thermal Utilization Factor in Infinite Slab Geometry*, Nuclear Sci. Eng., *7*, 58 (1960).
53. Fukai, Y., *Comparison of Flux Ratio Calculations in Lattices by Integral Transport Theory*, Nuclear Sci. Eng., *13*, 345–354 (1962).
54. Clendenin, W. W., *Effect of Zero Gradient Boundary Conditions on Cell Calculations in Cylindrical Geometry*, Nuclear Sci. Eng., *14*, 103–104 (1962).
55. Geortzel, G., and Grueling, E., *An Approximate Method for Treating Neutron Slowing Down*, Nuclear Sci. Eng., *7*, 69 (1960).
56. Selengut, D. S., *Critical Mass Calculations for Bare Hydrogen Moderated Reactors by Means of Transport Theory*, US Atomic Energy Comm. report APEX-121 (1952).
57. Hellens, R. L., *Neutron Slowing Down in Group Diffusion Theory*, US Atomic Energy Comm. report WAPD-114 (1956).
58. Bohl, H., and Hemphill, A. P., *MUFT-5, A Fast Neutron Spectrum Program for the Philco-2000*, US Atomic Energy Comm. report WAPD-TM-218 (February 1961).
59. Joanou, G. D., and Dudek, J. S., *GAM-1, A Consistent P_1 Multigroup Code for the Calculation of Fast Neutron Spectra and Multigroup Constants*, US Atomic Energy Comm. report GA-1850 (1961).
60. McGoff, D. J., *FORM, A Fourier Transform Fast Spectrum Code for the IBM-709*, US Atomic Energy Comm. report NAA-SS-Memo-5766 (September 1960).
61. Isegaris, M. E., *AGS-7090 Program for the Calculation of Average Group Cross Section*, US Atomic Energy Comm. report ORNL-TM-512.
62. Cooper, R. S., *A Code for Reducing Many Group Cross Sections to Few Groups*, US Atomic Energy Comm. report LAMS-2747 (October 1962).
63. de Coulon, G. A. G., *et al.*, *Spectral Shift Control Reactor Basic Physics Program, NPG Computer Program Report*, US Atomic Energy Comm. report BAW-1230, Part 2 (December 1960).
64. Bohl, H., *et al.*, *P1MG, A One-Dimensional Multigroup P_1 Code for the IBM-704*, US Atomic Energy Comm. report WAPD-TM-135 (July 1959).
65. Bohl, H., *et al.*, *P3MG-1, A One-Dimensional Multigroup P_3 Program for the Philco-2000*, US Atomic Energy Comm. report WAPD-TM-272 (1963).
66. Bareiss, E. H., *Multigroup Transport Code RDR-5*, David Taylor Model Basin report 1450 (December 1960).
67. Amster, H. J., *et al.*, *EURIPUS-3 and DAEDALUS, Monte Carlo Density Codes for the IBM-704*, US Atomic Energy Comm. report WAPD-TM-205 (February 1960).
68. Nordheim, L. W., *The Theory of Resonance Absorption*, Proceedings of Symposium on Appl. Math., Vol. 2, Nuclear Reactor Theory (1961), and US Atomic Energy Comm. report GA-2527 (1961).
69. Chernick, J., and Vernon, A. R., *Some Refinements in the Calculation of Resonance Integrals*, Nuclear Sci. Eng., *4*, 649 (1958) and *Calculation of the Effective Resonance Integral of ^{238}U*, Nuclear Sci. and Eng., 7, 252 (1960).
70. Bell, G. I., *A Simple Treatment for Effective Resonance Absorption Cross Sections in Dense Lattices*, Nuclear Sci. Eng., *5*, 139 (1959).
71. Dresner, L., *Resonance Absorption in Nuclear Reactor*, Pergamon Press (1960).
72. Goldstein, R., and Cohen, E. R., *Theory of Resonance Absorption of Neutrons*, Nuclear Sci. Eng., *13*, 132 (1962).
73. Drawbaugh, D. W., *Resonance Absorption in Water Moderated Lattices*, CEND 104 (June 1960).
74. Goldsmith, M., *Epithermal Absorption in Slab Lattices*, Nuclear Sci. Eng., *15*, 382–387 (1963).

75. Archibald, J. A. Jr., and Teaford, H. L., *KARE, A System of Diffusion Theory Programs for the Philco-2000*, US Atomic Energy Comm. report KAPL-2165-1 (November 1962).
76. Dawson, P., *et al.*, *Multi-Region Lattice Studies*, US Atomic Energy Comm. report WCAP-1434 (1961).
77. Candelore, N. R., and Gast, R. C., *RECAP-I, A Monte Carlo Program for Estimating Epithermal Capture Rates in Slabs*, US Atomic Energy Comm. report WAPD-TM-407 (1963).
78. Anderson, B., *et al.*, *FLIP, An IBM-704 Code to Solve the P_l and Double P_l Equations in Slab Geometry*, US Atomic Energy Comm. report WAPD-TM-134 (March 1959).
79. Bareiss, E. H., *A Survey and Classification of Transport Theory Calculation Techniques*, Proceedings of the Second International Conference on the Peaceful Uses of Atomic Energy, P/639, Vol. 16, p. 503, United Nations (1958).
80. Schmidt, E., US Atomic Energy Comm. report WAPD-T-1577 (1963).
81. Blue, E., and Flatt, H. P., *Convergence of the S_n Method for Thermal Systems*, Nuclear Sci. Eng., *7*, 127 (1960).
82. Bennett, J. H., *Accelerating Convergence of Discrete Ordinates Methods*, Nuclear Sci. Eng. (October 1963).
83. Hageman, L. A., *On a Numerical Approximation to the Solution of the One-Dimensional One-Velocity Transport Equation with Isotropic Scattering*, US Atomic Energy Comm. report WAPD-T-706 (1959).
84. Alexander, J. H., and Johnson, M. L., *S_n1 Cylindrical Cell, N Regions*, US Atomic Energy Comm. report GA-360 (1959).
85. Carlson, B., *et al.*, *The DSN and TDC Neutron Transport Codes*, US Atomic Energy Comm. report LAMS-2346 (February 1960).
86. Carlson, B., *Numerical Solution of Neutron Transport Problems*, Proc. of Symposium in Appl. Math., Vol. 2, Amer. Math. Soc. (1961).
87. Carlson, B., *Difference Equations in Neutron Transport Theory*, Trans. ANS, *6* (1) (1963).
88. Alder, B., *et al.*, *The Numerical Theory of Neutron Transport in Methods in Computational Physics*, Vol. 1, Academic Press (1963).
89. Best, G. H., Carmichael, B. M., and Labauve, R. Jr., *Two-Dimensional Calculations for LAMPRE 1*, Trans. ANS, *6* (1) (1963).
90. Case, K. M., *Elementary Solutions of the Transport Equation and their Applications*, Ann. Phys., *9* (1) (1960).
91. Muskhelishvilli, N. L., *Singular Integral Equations*, Noordhoff, Gröningen (1953).
92. Mika, J. R., *Neutron Transport with Anisotropic Scattering*, Nuclear Sci. Eng., *11*, 415 (1961).
93. Leonard, A., *A Transport Theoretical Method for a Class of Problems in Spherical Geometry*, Trans. ANS, *6* (1) (1963).
94. Kopp, H. J., *Synthetic Method Solution of the Transport Equation*, Nuclear Sci. Eng., *17*, 65–74 (1963).
95. Spanier, J., *Monte Carlo Methods and their Application to Neutron Transport Problems*, US Atomic Energy Comm. report WAPD-195 (July 1959).
96. Halperin, M., *Almost Linearly Optimum Combination of Unbiased Estimates*, US Atomic Energy Comm. report KAPL-2068 (January 1960).
97. Maynard, C. W., Nuclear Sci. Eng., *10*, 97–101 (1961).
98. Goad, W., and Johnston, R., *A Monte Carlo Method for Criticality Problems*, Nuclear Sci. Eng., *5*, 371 (1959).
99. Parker, J. B., and Woodcock, E. R., *Monte Carlo Criticality Calculations*, Progress in Nuclear Energy, Series IV, *4*, 435–457 (1961).
100. Bouquet, G., *et al.*, *Emploi de la méthode de Monte-Carlo pour la détermination du volume critique d'un cylindre*, Compte rendu, *246*, 1382–4 (1958).
101. Drawbaugh, D. W., *On the Solution of Transport Problems by Conditional Monte Carlo*, Nuclear Sci. Eng., *9*, 185 (1961).
102. Drawbaugh, D. W., *et al.*, *Criticality and Flux by Iteration using Conditional Monte Carlo*, Trans. ANS, *4*, (1961).
103. Rief, H., *The Fast Effect in Uranium and Beryllium Systems*, Nuclear Sci. Eng., *10*, 83 (1961).
104. Garrison, J. D., and Roos, B. W., *Fission Product Capture Cross Sections*, Nuclear Sci. Eng., *12*, 115–134 (1962).
105. Greenhow, C. R., and Hansen, E. C., *Thermal and Resonance Fission Product Poisoning for ^{235}U Systems*, US Atomic Energy Comm. report KAPL-2172 (October 1962).
106. Nephew, E. A., *Thermal and Resonance Absorption Cross Sections of the ^{233}U, ^{235}U and ^{239}Pu Fission Products*, US Atomic Energy Comm. report ORNL-2869 (March 1960).
107. England, T. R., *CINDER, A One Point Depletion and Fission Product Program*, US Atomic Energy Comm. report WAPD-TM-334 (August 1962).
108. Wikner, N. S., and Jaye, S., *US Atomic Energy Comm.* report GA-2113 (1961).
109. Pfeifer, C. J., and Urbanus, F., *A One-Dimensional Few Group Synthesis Nuclear Reactor Depletion Program for the Philco-2000 Computer*, US Atomic Energy Comm. report WAPD-TM-228 (October 1961).
110. Kaplan, S., Marlowe, O. J., and Bewick, J., *Application of Synthesis Techniques to Problems Involving Time Dependence*, Nuclear Sci. and Eng., *18*, 163–176 (1964).
111. Kaplan, S., *et al.*, US Atomic Energy Comm. report WAPD-TM-377 (December 1963).
112. Kaplan, S., *Some New Methods of Flux Synthesis*, Nuclear Sci. and Eng., *13*, 22–31 (1962).
113. Wachspress, E. L., Burgess, R. D., and Baron, S., Nuclear Sci. Eng., *12*, 381 (1962).
114. Selengut, D. S., *The Construction of Approximate Theories by Variational Methods*, Trans. ANS, *5*, 413 (1962).
115. Selengut, D. S., *On the Derivation of a Variational Principle for Linear Systems*, Nuclear Sci. Eng., *17*, 310 (1963).
116. Selengut, D. S., US Atomic Energy Comm. report HW-59126 (1959), Nuclear Physics Research Quarterly Report for October–December 1958.
117. Pomraning, G. C., *Variational Boundary Conditions for the Spherical Harmonics Approximation to the Neutron Transport Equation*, Nuclear Sci. Eng. (to be published).
118. Lewins, J. J. Nuclear Energy, *A12*, 180 (1960).
119. Dougherty, D., and Shen, C., *The Space-Time Neutron Kinetic Equations Obtained by the Semi-Direct Variational Method*, Nuclear Sci. Eng., *13*, 141 (1962).
120. Selengut, D. S., *Neutron Physics*, edited by Yeater, M., Academic Press (1962).
121. Pomraning, G. C., *A New Asymptotic Diffusion Theory*, Trans. ANS, *6* (2), 226 (1963).
122. Pomraning, G. C., *Reduction of Transport Theory to Multigroup Diffusion Theory*, Trans. ANS, *6* (2), 228 (1963).
123. Selengut, D. S., *Transport Corrections to Diffusion Theory*, Trans. ANS, *5*, 140 (1962).

ABSTRACT—RÉSUMÉ—АННОТАЦИЯ—RESUMEN

A/263 Etats-Unis d'Amérique

Progrès des méthodes analytiques et des calculs électroniques dans la physique des réacteurs appliquée aux projets

par E. L. Wachspress *et al.*

Les méthodes analytiques en physique des réacteurs évoluent sans cesse; l'amélioration continue des filières de réacteurs en est la meilleure preuve. Cette évolution a été stimulée par une connaissance plus approfondie des sections efficaces microscopiques, le perfectionnement des méthodes numériques et la mise en service de calculateurs numériques présentant des possibilités plus variées. Les auteurs du mémoire passent en revue les progrès accomplis depuis la deuxième Conférence de Genève sur l'utilisation de l'énergie atomique à des fins pacifiques.

Une théorie de la diffusion à un petit nombre de groupes développée de façon plus complète continue à jouer le rôle essentiel dans le calcul des réacteurs, pour les raisons suivantes: *a*) elle est intrinsèquement très simple; *b*) elle a un grand champ d'application pour le calcul des distributions des flux de neutrons à plusieurs dimensions; et *c*) on a élaboré des techniques très perfectionnées pour la solution numérique des équations de la diffusion à plusieurs groupes. On a introduit des facteurs d'hétérogénéité spatiale et des ajustements de la structure des groupes et des constantes, résultant de méthodes auxiliaires de transport d'ordre supérieur, pour réduire les inexactitudes inhérentes à la théorie de la diffusion. Il en résulte une plus grande précision des projets.

La première section examine la structure des équations de la diffusion à plusieurs groupes et les progrès faits dans les méthodes numériques de résolution de ces équations. La deuxième section expose les améliorations apportées aux méthodes permettant d'obtenir la moyenne sur le spectre des constantes pour un petit nombre de groupes et des facteurs d'autoprotection, et de faire d'autres ajustements des constantes de l'équation de diffusion. Ces améliorations permettent d'augmenter la précision des projets et fournissent des normes analytiques pour évaluer la validité des approximations faites dans l'établissement de ces projets. Comme il s'agit surtout dans ce travail de techniques de transport, l'amélioration de la théorie du transport est aussi passée en revue.

Ces sections terminent en donnant un modèle pour prévoir les caractéristiques à l'état stationnaire d'une configuration de réacteur donnée; la troisième section indique brièvement une méthode pour l'état quasi stationnaire permettant d'estimer les effets de l'appauvrissement du cœur. Les progrès qui ont été faits dans les méthodes concernant l'appauvrissement résultent: *a*) de l'efficacité des calculs et de l'incorporation dans le modèle à petit nombre de groupes des changements que présentent le spectre et la structure fine spatiale au cours de l'existence utile du cœur; *b*) de l'amélioration de la synthèse des distributions de puissance dans trois dimensions; et *c*) de l'automatisation au moyen de calculateurs numériques des méthodes de calcul de l'appauvrissement.

On discute à la fin du mémoire l'application de méthodes variationnelles en vue de formuler une méthode systématique et bien fondée au point de vue théorique pour combiner les éléments du plan de calcul en une méthode générale permettant plusieurs degrés de perfectionnement.

A/263 США

Успехи в развитии аналитических методов и применении вычислительных машин при физическом проектировании реакторов

Э. Л. Вакспресс *et al.*

Непрерывный прогресс при проектировании реакторов является несомненным доказательством успешного применения аналитических методов при исследовании физики реакторов. Этому способствовало накопление данных о микроскопических сечениях, улучшение численных методов и наличие более универсальных счетно-решающих устройств. В докладе сделан обзор достижений в этой области, полученных со времени Второй Женевской конференции.

Основным теоретическим методом, применяемым при проектировании реакторов, остается более полно развитая малогрупповая теория диффузии. Это обстоятельство объясняется следующими причинами: *a*) простота, присущая этой теории; *b*) применимость ее для многомерного расчета распределений потоков нейтронов и *c*) хорошо разработанная методика численного решения групповых уравнений диффузии. Для уменьшения неточностей свойственных теории диффузии, на основании дополнительных методов переноса высшего порядка, учитываются коэффициенты пространственной гетерогенности и уточнение групповой структуры и используемых констант. Все это приводит к увеличению точности, достигаемой при проектировании.

В первой части доклада содержится обзор как структуры групповых уравнений диффузии, так и успехов, достигнутых в методах численного решения этих уравнений. Во второй части описываются усовершенствования метода получения малогрупповых констант, усредненных по спектру, и коэффициентов самоэкра-

нирования; рассматривается также уточнение констант уравнений диффузии. Эти усовершенствования обеспечивают увеличение точности, достигаемой при проектировании, и дают определение некоторых критериев для оценки справедливости приближений, используемых в проекте Поскольку в этой работе преобладающими являются методы переноса, в ней также содержится обзор развития теории переноса.

Эти разделы заканчиваются описанием модели для предсказания стационарных характеристик реактора со специфичной конфигурацией. В третьей части делается обзор метода расчета квазистационарного состояния, необходимого для оценки влияния истощения активной зоны. Успехи, достигнутые в методах расчета истощения, основаны на следующих факторах: *a*) достаточно точный расчет и учет в малогрупповой модели спектральных и пространственных изменений потока нейтронов в течение жизни активной зоны; *b*) уточненный синтез трехмерного распределения мощности; и *c*) автоматизация цифровых вычислительных машин при расчетах истощения.

Обсуждается также вопрос о применении вариационных методов для формулировки теоретической основы статистического метода, объединяющего все компоненты расчетной схемы в единый общий процесс, обеспечивающий в соответствии с конкретными условиями требуемую степень точности.

A/263 Estados Unidos de América 1964

Progresos de los métodos analíticos y de los cálculos con máquinas en el diseño físico de reactores

por E. L. Wachspress et *al.*

Los continuos avances en el diseño de reactores son prueba de los progresos experimentados en las técnicas del análisis de la física de reactores. Estos progresos han sido estimulados por el creciente conocimiento de secciones eficaces microscópicas, por la mejora de los métodos numéricos y por la disponibilidad de calculadoras digitales de características más versátiles. En esta memoria se revisan los progresos realizados desde la última conferencia de Ginebra.

La teoría de difusión con pocos grupos ha conservado un papel dominante en el análisis de reactores debido: *a*) a su intrínseca simplicidad, *b*) a su amplia aplicación al cálculo multidimensional de distribuciones de flujos, y *c*) al gran desarrollo de las técnicas de resolución numérica de las ecuaciones de difusión en varios grupos. Para disminuir las inexactitudes propias de la teoría de difusión se añaden coeficientes de heterogeneidad espacial y se ajustan la estructura y las constantes de los grupos utilizando métodos suplementarios de teoría de transporte de grado superior. Así se gana en precisión de diseño.

La primera sección repasa la estructura de las ecuaciones de difusión con grupos y los progresos de los métodos numéricos de solución de esas ecuaciones. La segunda sección se ocupa de cómo se han mejorado los métodos de obtención de las constantes de teoría de pocos grupos ponderadas por espectro y de los coeficientes de autoapantallamiento, así como de otros ajustes de las constantes de la ecuación de difusión. Con ellos se aumenta más y más la precisión y se obtienen criterios analíticos para juzgar de la validez de las aproximaciones de diseño. Como aquí predominan las técnicas de transporte, aquí también se repasa el progreso efectuado en teoría de transporte.

Estas secciones se coronan con un modelo para predecir las características estacionarias de una configuración de reactor concreta, mientras que la tercera sección resume un procedimiento de diseño para estado casi-estacionario que calcula los efectos de empobrecimiento del núcleo. Los progresos en los métodos que tienen en cuenta este empobrecimiento se deben: *a*) a la eficacia del cálculo y a que se han incorporado al modelo de pocos grupos los cambios de espectro y de estructura fina espacial que ocurren al envejecer el núcleo, *b*) a que se ha mejorado la síntesis de las distribuciones tridimensionales de potencia, y *c*) a que el método de cálculo del empobrecimiento, por máquinas digitales, es ahora automático.

Finalmente se discute la aplicación de métodos variacionales a la formulación de un método sistemático y teóricamente firme para combinar los componentes del esquema de cálculo en un procedimiento general que permita distintos grados de refinamiento.

Расчеты спектров медленных нейтронов

Г. И. Марчук, Г. А. Илясова, В. Н. Морозов, В. В. Смелов, В. А. Ходаков

В проблеме термализации нейтронов можно выделить три наиболее существенных аспекта, а именно: построение теоретических моделей взаимодействия нейтронов с веществом и получение соответствующих физических констант, необходимых для расчета; разработка вычислительных алгоритмов, позволяющих с необходимой точностью получать решение математической задачи, и, наконец, проблема интерпретации экспериментальных данных по измерению спектральных характеристик потока медленных нейтронов. В настоящем докладе будут рассмотрены вопросы, связанные в основном со вторым аспектом проблемы.

Постановка задачи о рассеянии медленных нейтронов принадлежит Гурвитцу и Когену [1, 2]. Наиболее полно эта задача решена в рамках теоретической модели рассеяния нейтронов на ядрах одноатомного газа [1-4]. В последние годы отчетливо выяснилась необходимость более глубокого физического анализа механизма рассеяния нейтронов в веществе с учетом молекулярных и кристаллических связей. Результаты этих исследований широко представлены в материалах Брукхейвенской конференции по термализации нейтронов [5].

Отметим далее, что в последние годы получены существенные результаты также в области экспериментального исследования проблемы термализации нейтронов [5-7]. Эти исследования позволяют проводить тщательное сопоставление экспериментальных данных с соответствующими результатами теоретических расчетов, выполненных на основе различных физических моделей. Следует отметить, что по мере углубления наших знаний о физических процессах, происходящих в ядерных реакторах, появляется настоятельная необходимость в развитии все более совершенных и точных методов решения уравнения переноса нейтронов.

Особенность проблемы расчета распределения тепловых нейтронов состоит в том, что медленные нейтроны не только теряют, но и приобретают энергию, ввиду чего интегральный оператор в уравнении переноса оказывается оператором Фредгольма. Решение этого уравнения может быть выполнено в рамках P_n-приближений метода сферических гармоник, S_n-методом, методом характеристик, методом Монте-Карло и др. [8-15].

Ниже представлен обзор некоторых математических методов решения уравнения переноса, дано их сопоставление между собой и сравнение с экспериментальными данными [6-7]. Особое внимание уделено вопросу получения угловых распределений потока нейтронов в ячейке реактора.

1. РАСЧЕТ ПОТОКА И ЦЕННОСТИ НЕЙТРОНОВ МЕТОДОМ СФЕРИЧЕСКИХ ГАРМОНИК

Стационарный поток медленных нейтронов φ в цилиндрической ячейке может быть описан следующим интегро-дифференциальным уравнением переноса:

$$\sin\theta\left(\cos\psi\frac{\partial\varphi}{\partial r}-\frac{\sin\psi}{r}\frac{\partial\varphi}{\partial\psi}+\right.$$

$$\left.+\alpha(r,v)\right)\varphi(r,v,\theta,\psi)-\int_0^{v_{\text{гр}}}dv'\int d\Omega'\times \qquad (1)$$

$$\times\alpha_s(r;v'\to v,\vec{\Omega}'\to\vec{\Omega})\varphi(r,v',\theta',\psi')=q(r,v),$$

где $\alpha_s(r;v'\to v,\vec{\Omega}'\to\vec{\Omega})$ — дифференциальное сечение рассеяния; $\alpha(r,v)\equiv\alpha_s(r,v)+\alpha_a(r,v)$ — полное сечение; θ и ψ — широтный и азимутальный углы (рис. 1).

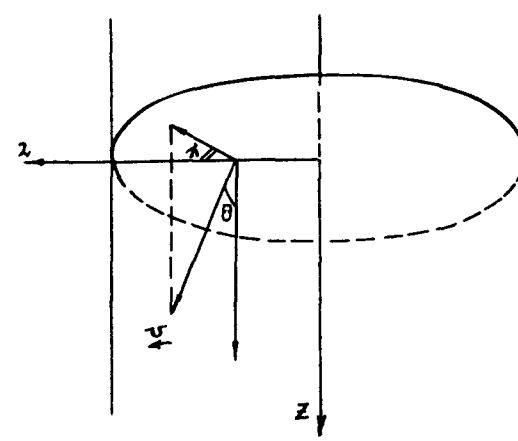

Рис. 1. Схема для расчета направления скоростей

Функцию $\varphi(r,v,\theta,\psi)$ представим в виде

$$\varphi(r,v,\theta,\psi)=\varrho(v)\nu(r,v,\theta,\psi), \qquad (2)$$

где $\varrho(v)$ выбирается с таким расчетом, чтобы наиболее полно учесть характер изменения потока нейтронов $\varphi(r, v, \theta, \psi)$ по переменной v. В качестве функции $\varrho(v)$ при расчете использовался энергетический спектр формально гомогенизованной ячейки. Из сказанного следует, что функция $\nu(r, v, \theta, \psi)$ должна быть слабо зависящей от скорости v во всей области термализации $0 < v < v_{\text{гр}}$.

Область $0 < v < v_{\text{гр}}$ разобьем на m интервалов $v_j < v < v_{j+1}$ $(j = 1, 2, \ldots, m)$. В пределах каждой из энергетических групп $v_j < v < v_{j+1}$ функцию $\nu(r, v, \theta, \psi)$ можно приближенно считать не зависящей от скорости нейтрона. Тогда, подставляя соотношение (2) в уравнении (1) и интегрируя последнее в пределах каждой из групп, получим следующую систему уравнений:

$$\sin\theta\left(\cos\psi\frac{\partial\varphi^{(j)}}{\partial r}-\frac{\sin\psi}{r}\frac{\partial\varphi^{(j)}}{\partial\psi}\right)+ \\ +\alpha^{(j)}(r)\varphi^{(j)}(r,\theta,\psi)- \\ -\sum_{l=1}^{m}\varphi^{(l)}(r,\theta',\psi')\,a_s^{l\to j}(r,\vec{\Omega}'\to\vec{\Omega})\,d\Omega'=q^{(j)}(r), \tag{1a}$$

где

$$\varphi^{(j)}(r,\theta,\psi)=\int_{v_j}^{v_{j+1}}\varphi(r,v,\theta,\psi)\,dv;$$

$$q^{(j)}(r)=\int_{v_j}^{v_{j+1}}q(r,v)\,dv;$$

$$\alpha^{(j)}(r)=\frac{1}{\varrho^j}\int_{v_j}^{v_{j+1}}\alpha(r)\varrho(v)\,dv;\quad \varrho_j=\int_{v_j}^{v_{j+1}}\varrho(v)\,dv;$$

$$a_s^{l\to j}(r,\vec{\Omega}'\to\vec{\Omega})= \\ =\frac{1}{\varrho_l}\int_{v_l}^{v_{l+1}}\varrho(v')\,dv'\int_{v_j}^{v_{j+1}}\alpha_s(r;v'\to v,\vec{\Omega}'\to\vec{\Omega})\,dv.$$

Функцию $a_s^{l\to j}(r,\vec{\Omega}'\to\vec{\Omega})$ разложим в ряд по полиномам Лежандра

$$a_s^{l\to j}(r,\vec{\Omega}'\to\vec{\Omega})=\frac{1}{2\pi}\sum_{n=0}^{\infty}\frac{2n+1}{2}\alpha_n^{l\to j}(r)\,P_n(\mu_0) \tag{3}$$

($\mu_0=\cos(\vec{\Omega},\vec{\Omega}')$), а нейтронный поток $\varphi^{(j)}$ — по сферическим функциям

$$\varphi^j(r,\theta,\psi)=\frac{1}{2\pi}\sum_{n=0}^{\infty}\frac{2n+1}{2}\Phi_{n0}^{(j)}(r)\,P_n(\cos\theta)+ \\ +\frac{1}{2\pi}\sum_{n=1}^{\infty}\sum_{m=1}^{n}(2n+1)\frac{(n-m)!}{(n+m)!}\times \\ \times\Phi_{nm}^{(j)}(r)\cos m\psi P_n^{(m)}(\cos\theta), \tag{4}$$

P_3-приближение соответствует допущению, что все $\Phi_{nm}^{(j)}(r)$ с $n\geqslant 4$ равны нулю. Поскольку функция рассеяния $\alpha_s^{l\to j}(r,\vec{\Omega}'\to\vec{\Omega})$ не зависит ни от поглощающих свойств среды, ни от ее размеров, то в разложении (3) можно ограничиться определенным числом слагаемых, не связывая это с порядком приближения. Для практических целей в разложении (3) можно ограничиться двумя слагаемыми. В результате в каждой энергетической группе получим систему из шести дифференциальных уравнений для функций $\Phi_{nm}^{j}(r)$, которая в матричной форме имеет вид *

$$a_0\frac{dI}{dr}+\frac{1}{r}T_0I+\Sigma_0\Phi=S_0; \\ a_1\frac{d\Phi}{dr}+\frac{1}{r}T_1\Phi+\Sigma_1I=3S_1, \tag{5}$$

где

$$\Phi=\begin{vmatrix}\Phi_{00}\\ \Phi_{20}\\ \Phi_{22}\end{vmatrix},\quad I=\begin{vmatrix}\Phi_{11}\\ \Phi_{31}\\ \Phi_{33}\end{vmatrix},\quad S_0=\begin{vmatrix}S_{00}\\ 0\\ 0\end{vmatrix},\quad S_1=\begin{vmatrix}S_{11}\\ 0\\ 0\end{vmatrix};$$

$$S_{00}^{(j)}(r)=4\pi q^{(j)}(r)+(1-\delta_{jl})\sum_{l=1}^{m}\Phi_{00}^{(l)}(r)\,\alpha_0^{l\to j}(r);$$

$$S_{11}^{(j)}(r)=(1-\delta_{jl})\sum_{l=1}^{m}\Phi_{11}^{(l)}(r)\,\alpha_1^{l\to j}(r);$$

a_0, a_1, T_0, T_1, Σ_0, Σ_1 — некоторые матричные коэффициенты [10, 16].

Исключая из системы (5) вектор I, получим уравнение

$$D\frac{d^2\Phi}{dr^2}+\frac{1}{r}K\frac{d\Phi}{dr}-\left(3\sigma_1\Sigma_0+\frac{1}{r^2}\Lambda\right)\Phi= \\ =-3\sigma_1S_0+3V\left(\frac{dS_1}{dr}+\frac{1}{r}S_1\right)-\frac{6}{r}WS. \tag{6}$$

В уравнении (6): Σ_0, Λ — диагональные матрицы,

$$\Sigma_0=[\sigma_0,\ 5\alpha,\ 5\alpha/6],\quad \Lambda=[0,\ 0,\ 4h];$$

$$D=\begin{bmatrix}1 & -1 & 1/2\\ -1 & f & -g/2\\ 1 & -g & h\end{bmatrix};$$

$$k=\begin{bmatrix}1 & -1 & 3/2\\ -1 & f & -3g/2\\ -1 & g & h\end{bmatrix};$$

$$V=\begin{bmatrix}1 & 0 & 0\\ -1 & 0 & 0\\ 1 & 0 & 0\end{bmatrix};\quad W=\begin{bmatrix}0 & 0 & 0\\ 0 & 0 & 0\\ 1 & 0 & 0\end{bmatrix},$$

причем $\sigma_0^{(j)}=\alpha^{(j)}-\alpha_0^{j\to j}$; $\sigma_1^{(j)}=\alpha_1^{(j)}-\alpha_1^{j\to j}$;

$$f=1+\frac{18}{7}\frac{\sigma_1}{\alpha};\quad g=1+\frac{3}{7}\frac{\sigma_1}{\alpha};\quad h=\frac{1}{2}+\frac{4}{7}\frac{\sigma_1}{\alpha}.$$

Уравнения (6) дополняются матричными граничными условиями, обеспечивающими сим-

* Ради простоты индекс номера группы опущен.

метрию нейтронного потока в центре ячейки и условие отражения на ее границе [10, 16].

Решение системы (6) осуществляется методом итераций по группам. Согласно методу Зейделя, который был использован в процессе итерирования, функции $S_{00}^{(j)}$ и $S_{11}^{(j)}$ в n-й итерации вычисляются по следующей схеме:

$$S_{00,\,n}^{(j)} = 4\pi q^{(j)}(r) + \sum_{l<j} \Phi_{00,\,n-1}^{(l)} \alpha_0^{l\to j} + \sum_{l>j} \Phi_{00,\,n}^{(l)} \alpha_0^{l\to j}.$$

Решение многогрупповой задачи (6) должно удовлетворять соотношению баланса нейтронов

$$\sum_{j=1}^{m} \int_0^{R_{\text{гр}}} \alpha_a^{(j)} \Phi_{00}^{(j)}(r)\, r\, dr = \sum_{j=1}^{m} \int_0^{R_{\text{гр}}} Q_{00}^{(j)}(r)\, r\, dr. \qquad (7)$$

Если итерационный процесс не закончен, балансное соотношение (7) не выполняется. Добиваясь выполнения балансного равенства (7) в процессе итерирования, можно значительно ускорить сходимость процесса [17]. В настоящей работе это осуществлялось перенормировкой источников.

Каждое одногрупповое уравнение системы (6) решается методом матричной факторизации [18].

Получаемые в результате решения задачи функции $\Phi_{00}^{(j)}(r) = \int \Phi^{(j)}(r, \theta, \psi)\, d\Omega$ могут быть использованы для вычисления эффективных тепловых констант, необходимых для дальнейших расчетов критических параметров реакторов. В ряде случаев, однако, возникает необходимость знать угловую зависимость нейтронного потока $\varphi^{(j)}(r, \theta, \psi)$. В различных экспериментах по изучению спектров тепловых нейтронов выводятся нейтронные пучки определенных направлений. Формула (4) позволяет осуществить расчет нейтронных потоков в любом заданном направлении. Приведем расчетные формулы для потоков нейтронов, имеющих различные направления скорости (см. рис. 1):

$$\varphi^{(j)}(r,\ \theta = 0) = \frac{1}{4\pi}\left[\Phi_{00}^{(j)}(r) + 5\,\Phi_{20}^{(j)}(r)\right];$$

$$\varphi^{(j)}\left(r, \theta = \frac{\pi}{2},\ \psi = \frac{\pi}{2}\right) = \frac{1}{4\pi}\left[\Phi_{00}^{(j)}(r) - \frac{5}{2}\Phi_{20}^{(j)}(r) - \frac{5}{4}\Phi_{22}^{(j)}(r)\right];$$

$$\varphi^{(j)}\left(r, \theta = \frac{\pi}{2},\ \psi = \begin{cases} 0 \\ \pi \end{cases}\right) = \frac{1}{4\pi}\left[\Phi_{00}^{(j)}(r) - \frac{5}{2}\Phi_{20}^{(j)}(r) + \frac{5}{4}\Phi_{22}^{j}(r) \pm \right. \qquad (8)$$

$$\left. \pm \left(3\Phi_{11}^{(j)}(r) - \frac{7}{4}\Phi_{31}^{(j)}(r) + \frac{7}{24}\Phi_{33}^{(j)}(r)\right)\right]$$

Наряду с потоком нейтронов $\varphi(r, v, \theta, \psi)$ представляет интерес функция ценности нейтрона $\varphi^*(r, v, \theta, \psi)$ относительно какого-либо процесса. Можно говорить, например, о ценности нейтрона относительно поглощения в блоке и т. п. [18-20].

Функция ценности является решением сопряженного уравнения, которое в многогрупповом представлении имеет вид

$$\sin\theta\left(\cos\psi\,\frac{\partial\varphi^{*(j)}}{\partial r} - \frac{\sin\psi}{r}\,\frac{\partial\varphi^{*(j)}}{\partial\psi}\right) + \alpha^{(j)}(r)\,\varphi^{*(j)}(r, \theta, \psi) - \sum_{l=1}^{m}\int \varphi^{*(l)}(r, \theta', \psi') \times \alpha_s^{j\to l}(r, \vec{\Omega}\to\vec{\Omega}')\, d\Omega' = q^{*(j)}(r, \theta, \psi). \qquad (9)$$

Конкретный вид правой части уравнения (9) диктуется тем физическим процессом, относительно которого определяется функция ценности. В частности, для вычисления ценности нейтронов относительно захвата в блоке в системе (9) нужно положить

$$q^{*(j)}(r, \theta, \psi) \equiv \begin{cases} \alpha_a^{(j)}(r) & \text{в блоке,} \\ 0 & \text{вне блока.} \end{cases}$$

Решение системы (9) осуществляется теми же методами, что и системы (1а).

Функция ценности нейтрона в сочетании с функцией распределения нейтронного потока находит широкое применение в теории возмущений [18, 21].

2. РАСЧЕТ ПОТОКА НЕЙТРОНОВ S_n-МЕТОДОМ

Для расчета потока тепловых нейтронов в ячейке реактора с успехом может быть использован S_n-метод, предложенный Карлсоном [12, 13]. Здесь мы остановимся на применении метода к многогрупповой системе (1а), причем анизотропию рассеяния будем учитывать в транспортном приближении.

Решение соответствующей системы уравнений с условиями отражения на границе ячейки осуществляется с помощью итерационного процесса, включающего итерации трех видов: итерации неупругих переходов, итерации упругих столкновений и итерации граничных условий. Итерируемое уравнение имеет следующий вид:

$$\sqrt{1-\gamma^2}\cos\psi\,\frac{\partial\varphi_{s,\,t,\,r}^{(j)}}{\partial r} - \sqrt{1-\gamma^2}\,\frac{\sin\psi}{r}\,\frac{\partial\varphi_{s,\,t,\,r}^{(j)}}{\partial\psi} + \alpha_{tr}^{(j)}(r)\,\varphi_{s,\,t,\,r}^{(j)} = Q_{s,\,t}^{(j)}(r), \qquad (10)$$

где j — номер энергетической группы ($j = 1, 2, \ldots, m$), $\gamma = \cos\theta$,

$$Q_{s,\,t}^{(j)}(r) = \beta^{j\to j}(r)\, N_{s,\,t-1}^{(j)}(r) + Q_s^{(j)}(r); \qquad (11)$$

$$Q_s^{(j)}(r) = \sum_{l\neq j}^{m} \beta^{l\to j}(r)\, N_{s-1}^{(l)}(r) + q^{(j)}(r); \qquad (12)$$

$$N^{(j)}(r)=\frac{1}{\pi}\int_0^{\pi}d\psi\int_0^{1}\varphi^{(j)}(r,\psi,\gamma)\,d\gamma; \quad (13)$$

$$\alpha_{tr}^{(j)}(r)=\sum_{l=1}^{m}\beta^{j\to l}(r)+\alpha^{(j)}(r); \quad (14)$$

$$\beta^{l\to j}(r)=\alpha_0^{l\to j}(r)\,(l\neq j);$$
$$\beta^{l\to j}(r)=\alpha_0^{l\to j}(r)-\alpha_1^{l\to l}(r)\quad (l=j). \quad (15)$$

Функции $\alpha_{tr}^{(j)}(r)$ и $\beta^{l\to j}(r)$ кусочнопостоянны, $q^{(j)}(r)$ — линейная функция на интервалах, ограниченных узловыми точками переменной r.

Итерация неупругих переходов с номером s заключается в последовательном решении уравнений (10) для всех j с функциями $Q_s^{(j)}(r)$, известными из предыдущей итерации неупругих переходов. Итерация упругих столкновений с номером t представляет собой решение уравнения системы (10) для данного j с функцией $N_{s,t-1}^{(j)}(r)$, найденной в предыдущей итерации упругих столкновений. В результате всех итераций упругих столкновений определяется функция $N_s^{(j)}(r)$. И, наконец, с помощью итераций граничных условий определяется функция $\varphi_{s,t}^{(j)}$, удовлетворяющая краевым условиям отражения: $\varphi^{(j)}(R_{\text{гр}},\psi,\gamma)=\varphi^{(j)}(R_{\text{гр}},\pi-\psi,\gamma)$. При итерации граничных условий с номером r на внешней границе ячейки ставится условие

$$\varphi_{s,t,r}^{(j)}(R_{\text{гр}},\psi,\gamma)=$$
$$=\frac{1}{2}\left[\varphi_{s,t,r-1}^{(j)}(R_{\text{гр}},\gamma,\psi)+\varphi_{s,t,r-1}^{(j)}(R_{\text{гр}},\pi-\psi,\gamma)\right] \quad (16)$$

для всех $\pi/2<\psi\leqslant\pi$.

Расчетные формулы S_n-метода, необходимые для решения итерируемых уравнений (10), были получены нами по общей для всех видов геометрии схеме, изложенной в работе [14]. Полученные по этим формулам приближенные решения многогрупповой системы удовлетворяют условию баланса нейтронов. В соответствии с этой схемой область изменения переменных r, ψ и γ покрывается сетью узловых точек (r_k,ψ_i,γ_p). Узловые точки γ_p на интервале $[0,1]$ выбираются соответствующими квадратурной формуле Гаусса; узловые точки ψ_i на интервале $[0,\pi]$ выбираются равноотстоящими друг от друга с шагом π/n (число n соответствует S_n-приближению); узловые точки r_k на интервале $[0,R_{\text{гр}}]$ выбираются произвольно с тем лишь условием, чтобы среди них были точки разрыва функций $\alpha_{tr}^{(j)}(r)$, $\beta^{l\to j}(r)$ и $q^{(j)}(r)$.

В предположении линейной зависимости $\varphi^{(j)}$ от ψ и r на интервалах $[\psi_{i-1},\psi_i]$ и $[r_{k-1},r_k]$ к уравнениям системы (10) при значениях $\gamma=\gamma_p$ последовательно применяются интегральные операторы

$$\frac{2n}{\pi}\int_{\psi_{i-1}}^{\psi_i}d\psi \text{ и } \int_{r_{k-1}}^{r_k}r\,dr.$$

В результате получаем алгебраические уравнения, связывающие между собой значения $\varphi^{(j)}$ в узловых точках. Дополняя эту систему уравнениями, получаемыми после подстановки в (10) значения $\psi=\pi$ с последующим применением оператора

$$\int_{r_{k-1}}^{r_k}r\,dr,$$

мы получаем полную систему уравнений, из которой значения $\varphi^{(j)}(r_k,\psi_r,\gamma_\rho)$ находятся по рекуррентным формулам.

Непосредственное осуществление определенных выше итерационных процессов требует очень большого числа итераций. Для сокращения числа итераций мы использовали соответствующие формулы ускорения сходимости итерационных процессов.

Ускорение сходимости процесса итераций граничных условий осуществлялось путем экстраполяции итерационных изменений величин $\varphi_{s,t,r}^{(j)}(R_{\text{гр}},\psi_i,\gamma_p)$ $(i=1,2,\ldots,n/2-1)$ на бесконечное число итераций r (метод Люстерника [24]).

Ускорение сходимости процесса итераций упругих столкновений проводилось по методу оценки итерационных отклонений [14,25]. Идея этого метода заключается в приближенном определении отклонения итерируемой функции от искомого точного решения уравнения по ее изменению в результате одной итерации. Соответствующие формулы в нашем случае могут быть получены следующим образом. Функция $\varphi_s^j(r,\psi,\gamma)$, являющаяся решением уравнения (10) при определенном $Q_s^{(j)}(r)$, может быть представлена в виде

$$\varphi_s^{(j)}(r,\psi,\gamma)=\varphi_{s,t}^{j}(r,\psi,\gamma)-\Delta\varphi_{s,t}^{(j)}(r,\psi,\gamma), \quad (17)$$

где $\Delta\varphi_{s,t}^{(j)}(r,\psi,\gamma)$ — итерационное отклонение, соответствующее итерации с номером t. Интегрируя (17) по ψ и γ, получаем

$$N_s^{(j)}(r)=N_{s,t}^{(j)}(r)-\Delta N_{s,t}^{(j)}(r), \quad (18)$$

где

$$\Delta N_{s,t}^{(j)}(r)=\frac{1}{\pi}\int_0^{\pi}d\psi\int_0^{1}\Delta\varphi_{s,t}^{(j)}(r,\psi,\gamma)\,d\gamma. \quad (19)$$

Используя (17) и (18), из итерируемого уравнения (10) получаем соотношение

$$\sqrt{1-\gamma^2}\cos\psi\frac{\partial\Delta\varphi_{s,t}^{(j)}}{\partial r}-\sqrt{1-\gamma^2}\frac{\sin\psi}{r}\frac{\partial\Delta\varphi_{s,t}^{(i)}}{\partial\psi}+$$
$$+\alpha_{tr}^{(j)}(r)\,\Delta\varphi_{s,t}^{(j)}=\beta^{j\to j}(r)\,\Delta N_{s,t-1}^{(j)}, \quad (20)$$

откуда следует уравнение для итерационного отклонения $\Delta\varphi_{s,t}^{(j)}$:

$$\sqrt{1-\gamma^2}\cos\psi\frac{\partial\Delta\varphi_{s,t}^{(j)}}{\partial r}-\sqrt{1-\gamma^2}\frac{\sin\psi}{r}\frac{\partial\Delta\varphi_{s,t}^{(j)}}{\partial\psi}+$$
$$+\alpha_{tr}^{(j)}(r)\Delta\varphi_{s,t}^{(j)}=\beta^{j\to j}(r)\Delta N_{s,t}^{(j)}+\Delta q_{s,t}^{(j)}(r), \quad (21)$$

где

$$\Delta q_{s,t}^{(j)}(r)=\beta^{j\to j}(r)[N_{s,t-1}(r)-N_{s,t}(r)]. \quad (22)$$

Краевые условия для этого уравнения сохраняют прежний вид условий отражения.

Следующий шаг состоит в оценке величины итерационного отклонения $\Delta N_{s,t}^{(j)}$ или, другими словами, в приближенном решении уравнения итерационной поправки (21). Используя то обстоятельство, что по мере приближения $\varphi_{s,t}^{(j)}$ к точному решению $\varphi_s^{(j)}(r)$ функция $\Delta\varphi_{s,t}^{(j)}$ стремится к нулю и становится все более гладкой, мы полагаем приближенно $\Delta N_{s,t}^{(j)}(r)=\Delta\varphi_{s,t}(r,\psi,\gamma)$ и получаем уравнение для оценки итерационного отклонения $\Delta\tilde{\varphi}_{s,t}^{(j)}(r,\psi,\gamma)$

$$\sqrt{1-\gamma^2}\cos\psi\frac{\partial\Delta\tilde{\varphi}_{s,t}^{(j)}}{\partial r}-\sqrt{1-\gamma^2}\frac{\sin\psi}{r}\frac{\partial\Delta\tilde{\varphi}_{s,t}^{(j)}}{\partial\psi}+$$
$$+\alpha_{tr}^{(j)}\Delta\tilde{\varphi}_{s,t}^{(j)}=\Delta q_{s,t}^{(j)}(r). \quad (23)$$

Решение этого уравнения не требует проведения йтераций упругих столкновений. Получаемая приближенная функция среднего потока

$$\tilde{N}_{s,t}^{(j)}(r)=N_{s,t}^{(j)}(r)-\Delta\tilde{N}_{s,t}^{(j)}(r), \quad (24)$$

где

$$\Delta\tilde{N}_{s,t}^{(j)}(r)=\frac{1}{\pi}\int_0^{\pi}d\psi\int_0^{1}\Delta\tilde{\varphi}_{s,t}^{(j)}(r,\psi,\gamma)\,d\gamma, \quad (25)$$

используется затем в качестве нового приближения в итерируемом уравнении (10) и весь процесс итерирования и введения итерационных поправок продолжается до тех пор, пока отношение $\Delta\tilde{N}_{s,t}^{(j)}/\tilde{N}_{s,t}^{(j)}$ при всех r не станет меньше определенного заданного числа ε.

Так как функция $\Delta\tilde{\varphi}_{s,t}^{(i)}$ дает лишь приближенную величину итерационного отклонения $\varphi_{s,t}^{(j)}$ от точного решения $\varphi_s^{(j)}$, то в целях сокращения вычислительной работы ее следует определять в более низких приближениях по сравнению с приближениями, используемыми при вычислении самой функции $\varphi_{s,t}^{(j)}$.

В тех случаях, когда условия, необходимые для введения поправки по формуле (24), не выполнялись, ускорение сходимости процесса итераций упругих столкновений осуществлялось путем умножения итерируемой функции на балансный нормировочный множитель [14]. Такое же ускорение сходимости применялось и к процессу итераций неупругих переходов.

3. РАСЧЕТ ПОТОКА НЕЙТРОНОВ МЕТОДОМ МОНТЕ-КАРЛО

Блуждание нейтрона в ячейке моделируется с помощью цифровой ЭВМ на основе вероятностных характеристик нейтронно-ядерных взаимодействий и геометрической структуры ячейки. На границе ячейки нейтрон зеркально отражается без изменения скорости. Источник в области термализации строится в предположении, что для скоростей $V>V_{\text{гр}}$ рассеяние нейтрона (упругое и сферически симметричное в системе центра масс) происходит на неподвижных свободных ядрах; спектр нейтронов выше $V_{\text{гр}}$—фермиевский. Все вероятностные характеристики взаимодействия нейтрона с веществом можно задавать таблицами, однако для этого требуется большой объем оперативной памяти машины.

В случае газовой модели замедлителя процесс рассеяния нейтрона на ядрах определенного сорта можно моделировать в следующем порядке. Разыгрывается абсолютное значение V_0 скорости ядра, с которым сталкивается нейтрон. Для этого решается относительно V_0 уравнение

$$K=\frac{\begin{cases}\frac{1}{\beta^2}\varphi_4(\gamma)+3\varphi_2(\gamma), & \gamma\leqslant\beta\\ \frac{1}{\beta^2}\varphi_4(\gamma)+3\varphi_2(\beta)+\frac{3}{\beta}[\varphi_3(\gamma)-\varphi_3(\beta)]+ & \\ \quad+\beta[\varphi_1(\gamma)-\varphi_1(\beta)], & \gamma>\beta\end{cases}}{\frac{1}{\beta^2}\varphi_4(\beta)+3\varphi_2(\beta)+\frac{3}{\beta}\left[\frac{1}{2}-\varphi_3(\beta)\right]+\beta\left[\frac{1}{2}-\varphi_1(\beta)\right]},$$

где $\beta=V/V_{\text{т}}$; $\gamma=V_0/V_{\text{т}}$; V—скорость нейтрона; $V_{\text{т}}$—наиболее вероятная скорость ядра при температуре T°K; K—случайное число, $0<K<1$; $\varphi_n(z)=\int_0^z t^n e^{-t^2}dt$. Функции $\varphi_n(z)$ вычисляются заранее.

Далее разыгрывается угол θ между направлениями движения нейтрона и ядра-мишени.

$$\cos\theta=\frac{1}{2\alpha}\{1+\alpha^2-[K(1+\alpha)^3+$$
$$+(1-K)|1-\alpha|^3]^{2/3}\},$$

где $\alpha=V_0/V$; K—случайное число. Второй угловой параметр находится из условия равноправия азимутальных направлений. По известным скоростям $\vec{V}$, $\vec{V}_0$ нейтрона и ядра вычисляется скорость рассеянного нейтрона

$$\vec{V}'=\frac{1}{M+1}[\vec{V}+M\vec{V}_0+M|\vec{V}-\vec{V}_0|\cdot\vec{e}].$$

Здесь $\vec{e}$—случайный изотропный единичный вектор.

Известно большое число способов накопления информации о потоке в процессе блуждания нейтрона [25]. Обычно в замедлителе спектр фор-

мируется быстро. Затруднения вызывают малые по объему и сильно поглощающие участки. Вычисление потока в любой части ячейки заметно ускоряется, если учитывать вклад от каждого столкновения, в результате которого возможный путь рассеянного нейтрона пересекает ее объем.

В ячейках с большим преобладанием объема замедлителя можно существенно ускорять вычисления, заменяя удаленные от блока участки замедлителя соответствующими поверхностными источниками. Характеристики источников (спектр, угловое распределение и др.) вычисляются предварительно. В одномерных ячейках это достигается особенно просто. Таким способом рассчитывалась уран-графитовая ячейка (см. таблицу).

Для достижения практически приемлемой точности расчета, как правило, достаточно 70—100 тысяч столкновений. В расчетах, результаты которых представлены на рис. 12 и 13, разыгрывалось немного более 100 000 столкновений.

Спектр в графите (рис. 13, *б*) дополнительно уточнялся. Ниже приводятся приближенные значения стандартных погрешностей некоторых характеристик вычисленных потоков.

В расчетах использовался трехкомандный датчик псевдослучайных чисел известного типа: $X_{n+1} \equiv PX_n \pmod M$. Мы брали $P = 5^5$, $M = 2^{24}$, $X_0 = 1$ или $X_0 = 3$. Датчик проверялся вычислением спектра Максвелла в ячейке без поглощения, а также по критериям Колмогорова χ^2, ω^2 при различных объемах выборок. Результаты удовлетворительные.

Функции плотности, полученные статистическим методом, полезно сглаживать. Оправдывает себя следующий прием [26]. Рассматривается эмпирическая функция распределения вероятности $F(X)$, соответствующая вычисленной функции плотности. В узловой точке X_k, $k = s$, $s+1$, ..., $n-s$, $n+1$ — общее число узлов, $F(X_k)$ заменяется значением $P(X_k)$, $P(X)$ — полином определенной степени, минимизирующий величину

$$\sum_{i=-s}^{s} [F(X_{k+i}) - P(X_{k+i})]^2.$$

Сглаженная функция плотности получается из построенной таким образом более гладкой функции распределения дифференцированием. Мы пользовались полиномами пятой степени при $s = 8$ ($n = 80$).

4. РЕЗУЛЬТАТЫ РАСЧЕТОВ

Описанные выше методы использовались для расчета пространственно-энергетического распределения медленных нейтронов в ячейках уран-водной и уран-графитовой решеток, экспериментально изученных Мостовым и др. [6, 7].

Уран-водная сборка представляет собой систему блоков природного урана диаметром 3,5 *см*, расположенных в узлах треугольной решетки с шагом 5,5 *см*. Уран-графитовая сборка состоит из таких же урановых блоков, расположенных в узлах квадратной решетки с шагом 20 *см*. В экспериментах урановые блоки отделены от замедлителя алюминиевой прослойкой. При расчетах экспериментальные шестиугольная и квадратная ячейки были заменены эквивалентными круговыми трехзонными ячейками.

Переходим к описанию расчетов ячеек в P_3-приближении. Расчет потока медленных нейтронов проводился в энергетической области $0 < E < E_{гр} = 0{,}67$ *эв*, в 15-групповом приближении. Источники тепловых нейтронов, обусловленные замедлением, рассчитывались в предположении, что при $E > E_{гр}$ спектр нейтронов является фермиевским, а молекулярные и кристаллические связи при $E > E_{гр}$ несущественны. В области $0 < E < E_{гр}$ неупругие молекулярные рассеяния и взаимодействия нейтронов с кристаллической решеткой учитывались на основе работ Турчина [22, 23].

Для делящихся изотопов учитывалось отклонение сечения захвата от закона $\overline{1/V}$.

Ячейка	Зона	Стандартная погрешность, %						
		полного потока	полного поглощения	потока* при изменениях X в интервале				
				0—1	1—2	2—3	3—4	4—8
Уран-водная	Блок	0,89	0,83	2,2	1,4	2,4	5,9	3,6
	Замедлитель	0,14	0,36	0,94	0,55	1,1	2,3	2,1
Уран-графитовая	Блок	0,79	0,89	2,9	1,3	1,9	2,4	3,5

* $X = V/\sqrt{2kT_0}$, $T_0 = 300°$ К.

На рис. 2 и 3 приводятся пространственные распределения среднего потока тепловых нейтронов

$$\Phi_{00}(r) = \frac{1}{4\pi} \int_0^{V_{гр}} dV \int \varphi(r, V, \theta, \psi)\, d\Omega,$$

а также направленных потоков (см. работу [8])

$$\Phi_{\parallel}(r) = \int_0^{V_{гр}} \varphi(r, V, \theta = 0)\, dV;$$

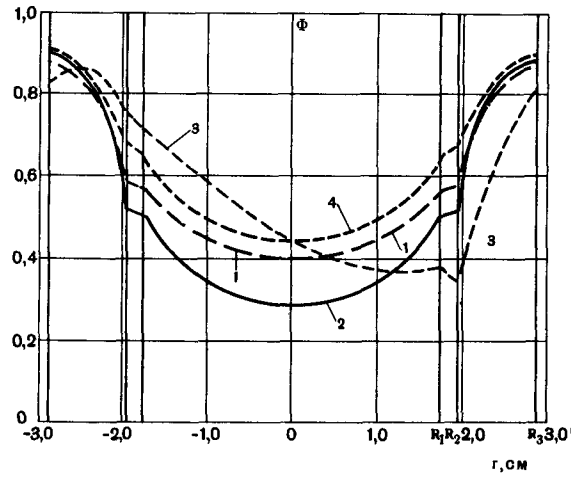

Рис. 2. Пространственное распределение тепловых нейтронов в уран-водной ячейке (T=323° К):

$1-\Phi_{00}(r)$; $2-\Phi_{\parallel}(r)$; $3-\begin{cases}\Phi_{\perp}^{(0)}(r)\,(r>0)\\ \Phi_{\perp}^{(\pi)}(r)\,(r<0)\end{cases}$; $4-\Phi_{\perp}^{(\pi/2)}(r)$

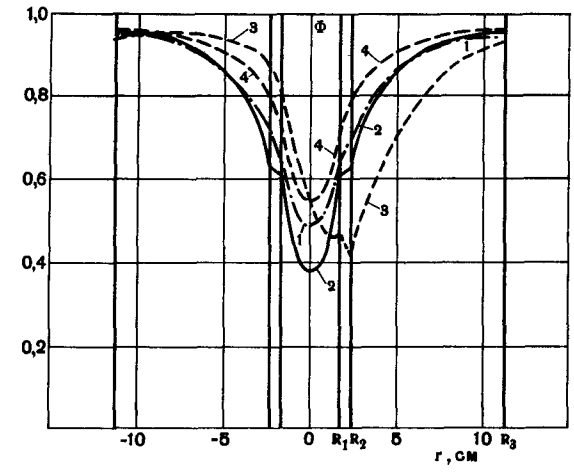

Рис. 3. Пространственное распределение тепловых нейтронов в уран-графитовой ячейке (T=523° К):

$1-\Phi_{00}(r)$; $2-\Phi_{\parallel}(r)$; $3-\begin{cases}\Phi_{\perp}^{(0)}(r)\;(r>0)\\ \Phi_{\perp}^{(\pi)}(r)\;(r<0)\end{cases}$; $4-\Phi_{\perp}^{(\pi/2)}(r)$

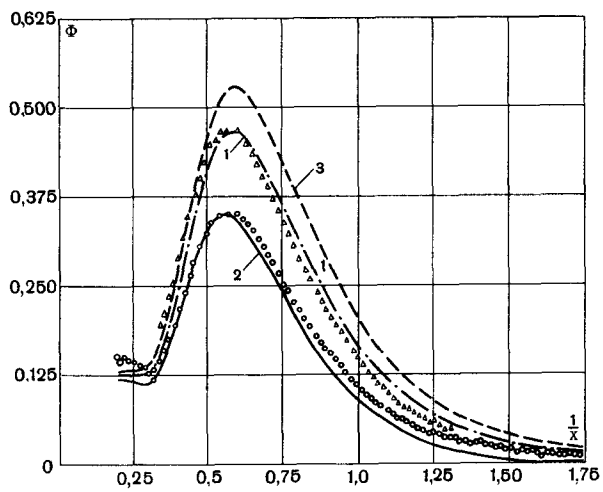

Рис. 4. Энергетическое распределение тепловых нейтронов в центре уран-водной ячейки (T=323° К):

$1-\frac{1}{4\pi}\int V\varphi\,(r=0, V, \theta)\,d\Omega$; $2-V\varphi\,(r=0, V, \theta=0)$;

$3-V\varphi\left(r=0, V, \theta=\frac{\pi}{2}\right)$; ○—экспериментальный спектр, нормированный на максимум кривой *2*; △—тот же спектр, нормированный на максимум кривой *1*

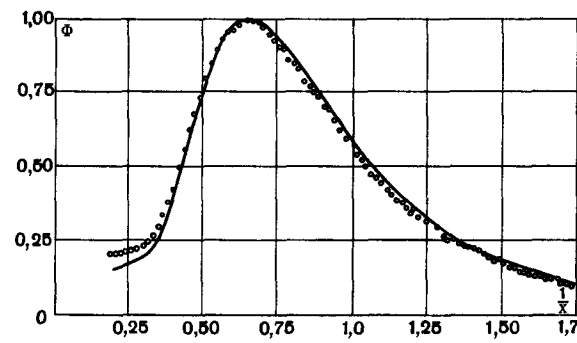

Рис. 5. Энергетический спектр тепловых нейтронов на границе уран-водной ячейки (T=323° К):

——— —расчетная кривая; ○—эксперимент

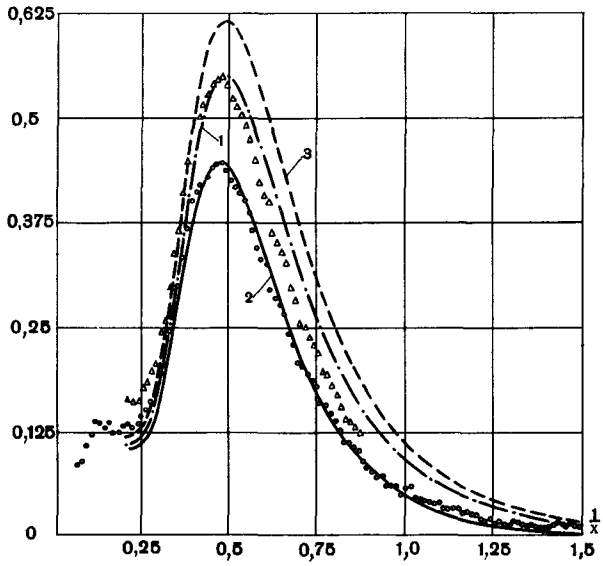

Рис. 6. Энергетическое распределение тепловых нейтронов в центре уран-графитовой ячейки (T=523° К):

$1-\frac{1}{4\pi}\int V\varphi\,(r=0,\ V,\ \theta)\,d\Omega$; $2-V\varphi\,(r=0,\ V,\ \theta=0)$; $3-V\varphi\,(r=0,\ V,\ \theta=\pi/2)$; ○—экспериментальный спектр, нормированный на максимум кривой *2*; △—тот же спектр, нормированный на максимум кривой *1*

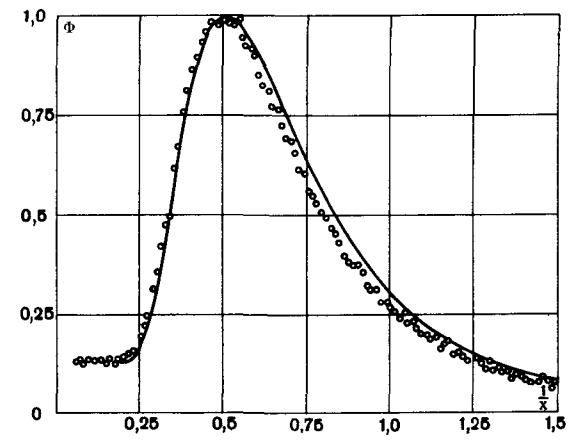

Рис. 7. Энергетический спектр тепловых нейтронов на границе уран-графитовой ячейки (T=523° К):

——— —расчетная кривая; ○—эксперимент

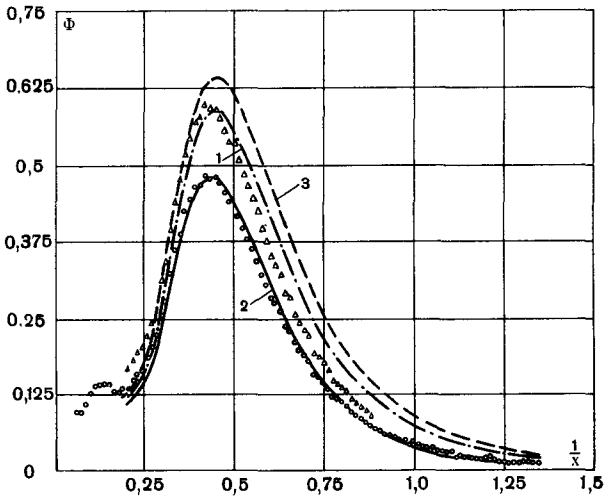

Рис. 8. Энергетическое распределение тепловых нейтронов в центре уран-графитовой ячейки (T=613° К):

$1-\frac{1}{4\pi}\int V\varphi\,(r=0,\ V,\ \theta)\,d\Omega$; $2-V\varphi\,(r=0,\ V,\ \theta=0)$; $3-V\varphi\,(r=0,\ V,\ \theta=\pi/2)$; ○—экспериментальный спектр, нормированный на максимум кривой *2*; △—тот же спектр, нормированный на максимум кривой *1*

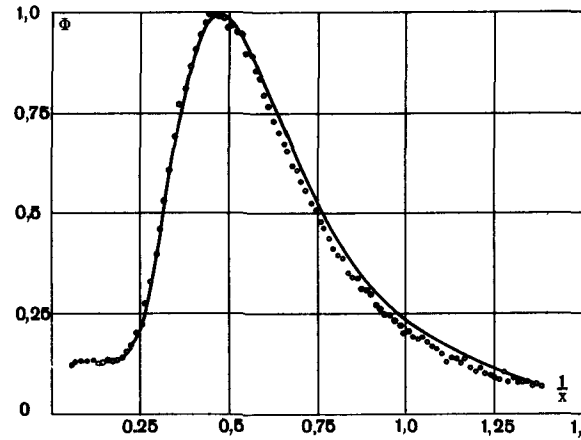

Рис. 9. Энергетический спектр тепловых нейтронов на границе уран-графитовой ячейки (T=613° К):

——— —расчетная кривая; ○—эксперимент

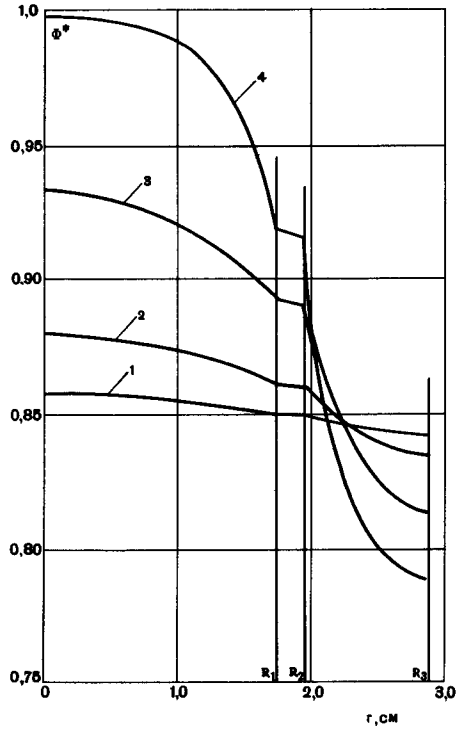

Рис. 10. Пространственное распределение функции ценности нейтрона (относительно захвата в блоке) в уран-водной ячейке:

1 — Ф* (r, $E = 0{,}6$ *эв*); *2* — Ф* (r, $E = 0{,}17$ *эв*); *3* — Ф* (r, $E = 0{,}028$ *эв*); *4* — Ф* (r, $E = 0{,}0006$ *эв*)

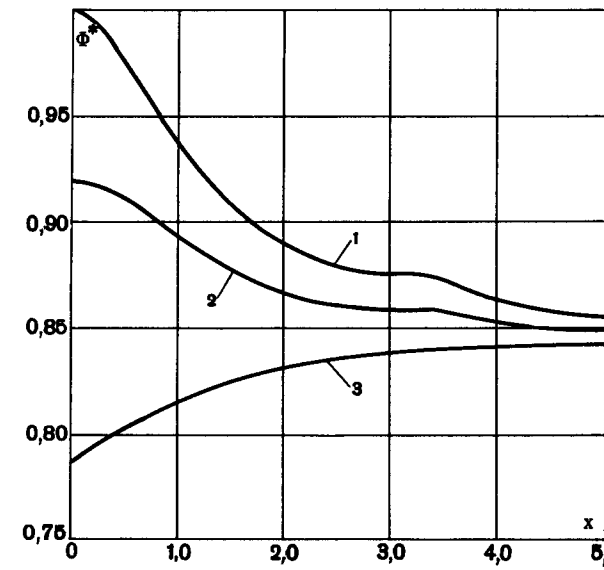

Рис. 11. Энергетическая зависимость функции ценности нейтрона (относительно захвата в блоке) в уран-водной ячейке:

1 — в центре блока; *2* — на границе блока; *3* — на границе ячейки

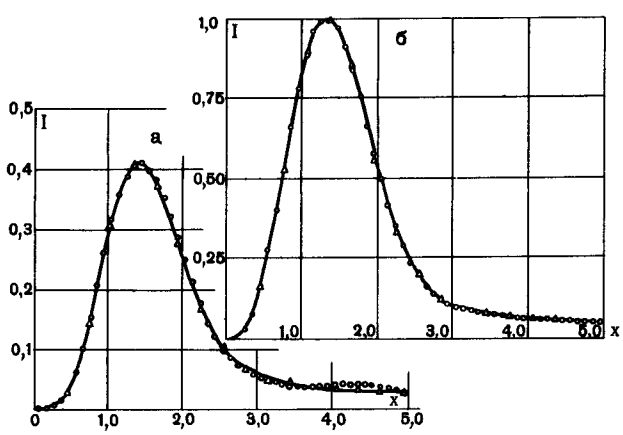

Рис. 12. Сопоставление энергетических спектров нейтронов в уран-водной ячейке, рассчитанных различными методами ($T = 323°$ K)

а — спектр нейтронов в объеме блока; *б* — спектр нейтронов в объеме замедлителя; —— — расчет методом сферических гармоник (P_3-приближение, 15 групп); △ — расчет S_n-методом (S_8-приближение, 10 групп); ○ — расчет методом Монте-Карло

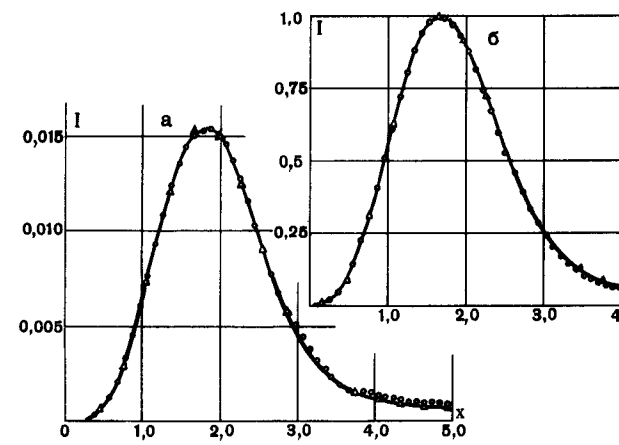

Рис. 13. Сопоставление энергетических спектров нейтронов в уран-графитовой ячейке, рассчитанных различными методами ($T = 523°$ K)

а — спектр нейтронов в объеме блока; *б* — спектр нейтронов в объеме замедлителя; ——— — расчет методом сферических гармоник (P_3-приближение, 15 групп); △ — расчет S_n-методом (S_8-приближение, 10 групп); ○ — расчет методом Монте-Карло

$$\Phi_{\perp}^{0}(r)=\int_{0}^{V_{\text{гр}}}\varphi\left(r,\ V,\ \theta=\frac{\pi}{2},\ \psi=0\right)dV;$$

$$\Phi_{\perp}^{\left(\frac{\pi}{2}\right)}(r)=\int_{0}^{V_{\text{гр}}}\varphi\left(r,\ V,\ \theta=\frac{\pi}{2},\ \psi=\frac{\pi}{2}\right)dV;$$

$$\Phi_{\perp}^{(\pi)}(r)=\int_{0}^{V_{\text{гр}}}\varphi\left(r,\ V,\ \theta=\frac{\pi}{2},\psi=\pi\right)dV.$$

Из рис. 2 и 3 видно, что поток нейтронов $\Phi_{\parallel}(r)$ (скорости нейтронов направлены параллельно оси ячейки) в блоке уменьшается значительно быстрее, чем средний поток $\Phi_{00}(r)$. Физически это следует из того, что нейтроны, движущиеся в блоке вдоль его оси, захватываются с большей вероятностью, чем нейтроны других направлений. По мере удаления от блока $\Phi_{\parallel}(r)$ становится больше $\Phi_{00}(r)$, что также легко объясняется физически.

Остановимся подробнее на кривой *3* (см. рис. 2 и 3). Она описывает пучок нейтронов, движущихся по диаметру ячейки. Левая ветвь кривой ($r<0$) описывает нейтроны, движущиеся к оси ячейки, $\Phi_{\perp}^{(\pi)}(r)$. Правая ветвь ($r>0$) соответствует нейтронам, движущимся от оси ячейки, $\Phi_{\perp}^{0}(r)$. Этот пучок на большей части своего пути в блоке в результате захвата теряет больше нейтронов, чем приобретает из других пучков за счет рассеяния. Этому соответствует монотонный характер кривой *3* в блоке. Нарушение монотонности пучка на выходе из блока связано с общим увеличением плотности нейтронов вблизи границы блока. Пересекая алюминиевую прослойку, пучок $\Phi_{\perp}^{(\varphi)}(r)$ не претерпевает существенных изменений за счет поглощения и рассеяния, и резкий спад кривой *3* в прослойке обусловлен геометрией прослойки.

Кривая *4* (см. рис. 2 и 3) представляет собой распределение по диаметру ячейки тех нейтронов, скорости которых перпендикулярны осевому сечению ячейки, $\Phi_{\perp}^{(\pi/2)}(r)$. Очевидно, что при $r=0$ $\Phi_{\perp}^{(\varphi)}(0)=\Phi_{\perp}^{\pi/2}(0)=\Phi_{\perp}^{\pi}(0)$.

Переходим к анализу энергетических спектров тепловых нейтронов в ячейках (рис. 4—9). На горизонтальной оси откладываются значения переменной $1/X\,(X=V/\sqrt{2kT},\ T=300^{\circ}K)$. На вертикальной оси откладывается значение плотности нейтронов $n\,(1/V)\equiv V^{2}n(V)\equiv V\varphi(V)$. На рис. 4, 6, 8 представлены спектры нейтронов в центре ячейки. Кривая *1* представляет собой усредненное по углам энергетическое распределение нейтронов $\frac{1}{4\pi}\int V\varphi(r=0,V,\theta)\,d\Omega$. Кривая *2* соответствует энергетическому распределению нейтронного пучка вдоль оси ячейки $V\varphi(r=0,\ V,\ \theta=0)$, а кривая *3* дает спектр нейтронного пучка, перпендикулярного оси ячейки $V\varphi(r=0,\ V,\ \theta=\pi/2)$.

Из физических соображений следует, что спектр *2* должен быть более жестким по сравнению с глобальным спектром *1*, а спектр *3* — более мягким, что и подтверждается расчетом. Приведенные спектры сравниваются с экспериментально измеренными [7]. Методика эксперимента была такова, что выведенные из блоков пучки состояли преимущественно из нейтронов, скорости которых направлены вдоль оси ячейки. Естественно поэтому экспериментальные спектры сопоставлять с функциями $V\varphi(r=0,\ V,\theta=0)$. Однако следует ожидать, что экспериментальный спектр окажется несколько мягче соответствующего теоретического, так как выводимый нейтронный пучок частично «разбавлен» нейтронами других направлений. В уран-водной ячейке этот прогноз подтверждается расчетом. В уран-графитовых ячейках данный эффект завуалирован заметным смягчением расчетного спектра в замедлителе по сравнению с экспериментом. Причина этого смягчения пока не ясна. Сравнение того же экспериментального спектра с глобальным $\frac{1}{4\pi}\int V\varphi(r=0,\ V,\ \theta,\ \psi)\,d\Omega$ показывает, что экспериментальный спектр более жесткий.

На рис. 5, 7, 9 приводятся сопоставления теоретических и экспериментальных спектров на границе ячейки. Расчеты показывают, что поток нейтронов на границе ячейки является практически изотропным.

На рис. 10, 11 дано пространственное и энергетическое распределение ценности нейтронов по отношению к поглощению в блоке для уран-водной ячейки. Наличие максимумов на кривых *1* и *2* (см. рис. 11) в интервале $3{,}0<X<4{,}0$ вызвано резонансом в сечении поглощения U^{235}.

Представляет интерес выяснить согласованность трех описанных выше методов. С этой целью каждым из методов были рассчитаны потоки тепловых нейтронов в уран-водной и уран-графитовой ячейках. Расчеты были проведены на основе газовой модели, так как в этом случае по методу Монте-Карло индикатриса рассеяния разыгрывается полностью. Результаты расчетов приведены на рис. 12 и 13. Взаимная привязка спектров, рассчитанных различными методами, производилась по максимуму отдельно в блоке и в замедлителе. Приведенные спектры в основном согласуются между собой в пределах погрешностей методов.

В заключение считаем приятным долгом выразить благодарность В. И. Мостовому и В. С. Дикареву за интерес к данной работе и полезные обсуждения в процессе ее выполнения.

ЛИТЕРАТУРА

1. H. Hurwitz, M. S. Nelkin, G. I. Habetler. Nucl. Sci. and Eng., *1*, 280 (1956).
2. Е. Коген. В сб. «Экспериментальные реакторы и физика реакторов», М., ГИТТЛ, 1956, стр. 257.

3. E. Gohen. Nucl. Sci. and Eng., *2*, 227 (1957).
4. М. В. Казарновский и др. Труды Второй международной конференции по мирному использованию атомной энергии, Женева, 1958, P/2148.
5. Proceedings of the Brookhaven conference on neutron thermalization, *1—4* (1962).
6. В. И. Мостовой и др. Атомная энергия, *13*, 547 (1962).
7. В. И. Мостовой, В. С. Дикарев и др. наст. издание, P/367.
8. Г. А. Бать, Е. А. Григорьева и др., наст. издание, P/373.
9. В. С. Владимиров. Вычислительная математика, *3*, 3 (1958).
10. Г. И. Марчук и др. Атомная энергия, *13*, 534 (1962).
11. Л. В. Майоров, М. С. Юдкевич. Атомная энергия, *13*, 563 (1962).
12. B. G. Carlson. Los Alamos Scientific Laboratory, report La 1891 (1955).
13. Б. Карлсон, Дж. Белл. Труды Второй международной конференции по мирному использованию атомной энергии, Женева, 1958, P/2386.
14. В. Н. Морозов, В сб. «Теория и методы расчета ядерных реакторов». М., Атомиздат, 1962, стр. 91.
15. А. Д. Галанин. Теория ядерных реакторов на тепловых нейтронах. М., Атомиздат, 1957.
16. Г. И. Марчук и др. Proceedings of the Brookhaven conference on neutron thermalization, *2* (1962).
17. H. Takahashi. Nucl. Sci. and Eng., in press.
18. Г. И. Марчук. Методы расчета ядерных реакторов. М., Атомиздат, 1961.
19. Л. Н. Усачев В сб. «Ядерные реакторы и физика реакторов». М., Изд-во АН СССР, 1955, стр. 251.
20. Г. И. Марчук, В. В. Орлов. В сб. «Нейтронная физика», 1961, стр. 30.
21. С. Глесстон, М. Эдлунд. Основы теории ядерных реакторов. М., ИЛ, 1954.
22. В. Ф. Турчин. Proc. of Symposium, Vienna, 259 (1960).
23. В. Ф. Турчин. Медленные нейтроны. М., Атомиздат, 1963.
24. Л. А. Люстерник. Труды Математического института АН СССР. М., Изд-во АН СССР, 1947, стр. 49.
25. Н. П. Бусиенко и др. Метод статистических испытаний. М., Физматгиз, 1962.
26. К. Ланцош. Практические методы прикладного анализа. М., Физматгиз, 1961.

ABSTRACT—RÉSUMÉ—АННОТАЦИЯ—RESUMEN

A/365 USSR

Calculation of slow neutron spectra

By G. I. Marchuk *et al.*

The paper reviews the methods of calculation of slow neutron spectra. A multi-group kinetic equation is given for the flux and importance of neutrons. Methods have been devised whereby the slow neutron spectra can be calculated using the spherical harmonic method, the Carlson method and the Monte Carlo method. A comparative analysis is made of calculations of the neutron spectra by these different methods. Angular distributions of the neutron flux are also given. Calculated results are compared with the experimental data obtained in the I. V. Kurchatov Atomic Energy Institute.

A/365 URSS

Calcul des spectres de neutrons lents

par G. I. Marchuck *et al.*

Le mémoire expose les méthodes de calcul des spectres de neutrons lents. Une équation cinétique multigroupe est construite pour le flux et la valeur des neutrons. Le calcul des spectres de neutrons lents est basé sur la méthode des harmoniques sphériques, la méthode de Carlson et celle de Monte-Carlo. Les résultats des calculs effectués par les différentes méthodes sont confrontés. On donne les répartitions angulaires du flux de neutrons. Les résultats des calculs sont comparés aux données expérimentales obtenues à l'Institut I. V. Kourtchatov.

A/365 URSS

Cálculo de espectros de neutrones lentos

por G. I. Marchuk *et al.*

En este documento se resumen los métodos para el cálculo de espectros de neutrones lentos. Se establecen las ecuaciones de transporte para varios grupos energéticos, para el flujo y para la importancia de los neutrones. Se desarrollan métodos para el cálculo de espectros de neutrones lentos basados en el método de los armónicos esféricos, en el de Carlson y en el de Monte Carlo. Se comparan los resultados de los cálculos de espectros neutrónicos realizados siguiendo los diferentes métodos. Se dan las distribuciones angulares del flujo neutrónico. Los resultados calculados se comparan con los datos experimentales obtenidos en el Institut Atomnoi Energuii «I. V. Kurchatov».

New aspects in the application of collision probabilities in reactor theory

By H. Märkl*

Collision probability methods are gaining more and more importance as a useful and practical tool in reactor theory. At the SSW Reactor Department, various computational methods involving the use of collision probabilities have been developed with the objective of basing the heterogeneous lattice calculations on a common collision probability concept.

(*a*) Starting from the integral transport equation, a set of N coupled integral equations is derived by subdividing the unit cell into N regions and introducing first-flight collision probabilities.

By treating the integral expressions in an approximate manner, the Wilkins thermalization theory for homogeneous media is extended to heterogeneous media. The resulting theory is reduced to a form which lends itself readily to numerical solution.

Similarly, on applying this collision probability concept to the fast and epithermal energy region, the slowing-down theories known as Greuling-Goertzel, Selengut-Goertzel and Fermi-Age approximations can be generalized to heterogeneous lattice cells.

(*b*) An alternate method of formulating neutron balance equations for a heterogeneous medium applies the concept of multiple collision probabilities (successive generations) in connection with neutron currents at the zone interfaces. This procedure is formulated in a general manner for L energy groups and N zones. It is applied to the calculation of the fast fission effect taking into account backscattering and fast interaction. Amouyal's and Benoist's method for computing the thermal utilization factor is included in the general method as a particular case.

(*c*) The practical applicability of the collision probability procedures depends decisively on the availability of methods adequate for calculating these collision probabilities to a fair degree of accuracy and with a tolerable amount of computational work. Simplified methods for calculating these quantities are described and discussed with regard to their accuracy.

METHODS INVOLVING FIRST-FLIGHT COLLISION PROBABILITIES

Transition from the general integral transport equation to a set of coupled integral equations

The energy dependent angular neutron flux $\phi(\vec{r},E,\vec{\Omega})$ can be described by the following integral equation [1]:

$$\phi(\vec{r},E,\vec{\Omega}) = \int_0^\infty \mathrm{d}R\, S(\vec{r}-R\vec{\Omega},E,\vec{\Omega}) \exp\left[-\int_0^R \mathrm{d}R'\Sigma(\vec{r}-R'\vec{\Omega},E)\right] \quad (1)$$

$S(\vec{r},E,\vec{\Omega})$ denotes the total source density depending on the space variable $\vec{r}$, the energy E and the solid angle $\vec{\Omega}$. In the general case it is composed of a scattering, a fission and an external source term and thus itself depends on the neutron flux.

With the definitions

$$\phi(\vec{r},E) = \int_{4\pi} \phi(\vec{r},E,\vec{\Omega})\mathrm{d}\Omega;\ \bar{\phi}_n(E) = \frac{1}{V_n}\int_{V_n} \phi(\vec{r},E)\mathrm{d}\vec{r} \quad (2)$$

and the relationships $\vec{r}' = \vec{r} - R\vec{\Omega}$; $\mathrm{d}\vec{r}' = |\vec{r}-\vec{r}'|^2 \mathrm{d}R\mathrm{d}\Omega$ integration of (1) over $\vec{r}$ and $\vec{\Omega}$ yields:

$$\int_{V_n}\mathrm{d}\vec{r}\int_{4\pi}\mathrm{d}\Omega\phi(\vec{r},E,\vec{\Omega}) = V_n\bar{\phi}_n(E)$$

$$= \int_{V_n}\mathrm{d}\vec{r}\int \frac{\mathrm{d}\vec{r}'}{|\vec{r}-\vec{r}'|^2} e^{-\tau(\vec{r}',\vec{r},E)} S\left(\vec{r}',E,\frac{\vec{r}-\vec{r}'}{|\vec{r}-\vec{r}'|}\right) \quad (3)$$

$\tau(\vec{r}',\vec{r},E)$ is the "optical distance" between the two points $\vec{r}'$ and $\vec{r}$ for neutrons of energy E.

The following considerations pertain to an infinity extended periodic lattice composed of uniform lattice cells. The lattice cell is allowed to consist of N partial volumes V_m' $(m = 1, 2, \ldots N)$ for which the nuclear cross sections are assumed to be spatially constant:

$$\Sigma(\vec{r},E) = \Sigma_m(E) \text{ for } \vec{r}\in V_m'$$

Combining the equivalent partial volumes V_m' of the different cells to a volume V_m representative of the m-th region, the integration over $\vec{r}'$ in (3) can be decomposed into a sum of integrals extended over the N partial volumes V_m. Defining $S(\vec{r},E)$ and $\bar{S}_m(E)$ analogous to (2) we finally obtain the neutron balance equations:

$$V_n\Sigma_n(E)\bar{\phi}_n(E) = \sum_{m=1}^{N} V_m P_{mn}(E)\bar{S}_m(E);$$
$$n = 1, 2, \ldots N; \quad (4)$$

with the abbreviation:

$$P_{mn}(E) = \frac{\int_{V_n}\mathrm{d}\vec{r}\Sigma_n(E)\int_{V_m}\frac{\mathrm{d}\vec{r}'}{|\vec{r}-\vec{r}'|^2} e^{-\tau(\vec{r}',\vec{r},E)} S\left(\vec{r}',E,\frac{\vec{r}-\vec{r}'}{|\vec{r}-\vec{r}'|}\right)}{\int_{V_m}\mathrm{d}\vec{r}'\int_{4\pi}\mathrm{d}\Omega S(\vec{r}',E,\vec{\Omega})} \quad (5)$$

* Abt. Reaktor-Entwicklung, Siemens-Schuckertwerke AG, Erlangen (Germany).

$P_{mn}(E)$ denotes the probability for a neutron of energy E generated in region m with the spatial and angular source density $S(\vec{r}',E,\vec{\Omega})$ to suffer its first collision in region n. The computability of these collision probabilities requires the knowledge of the space and angular dependence of the source. Usually we lack this knowledge, since the source S generally depends itself on the flux which is to be determined. For practical applications, it is therefore necessary to make adequate simplifying assumptions with regard to the spatial and angular distribution of the source.

(*a*) The simplest assumption concerning the angular distribution of the source neutrons is that of isotropy: $S(\vec{r},E,\vec{\Omega}) = \frac{1}{4\pi} S(\vec{r},E)$. Fission sources practically meet this requirement exactly; slowing-down or scattering sources, however, require the validity of isotropic scattering in the laboratory system in order that the above assumption holds.

(*b*) The simplest assumption with regard to the spatial distribution of the source neutrons is that of spatial constancy in each region m:

$$S(\vec{r},E) = \bar{S}_m(E) \text{ for } \vec{r} \in V_m$$

This condition holds the better, the smaller the dimensions of the partial volumes.

With the conditions (*a*) and (*b*), which in the following are always assumed to be fulfilled, (5) is reduced to the simplified expression:

$$P_{mn}(E) = \frac{\int_{V_n} d\vec{r} \Sigma_n(E) \int_{V_m} \frac{d\vec{r}'}{4\pi |\vec{r}-\vec{r}'|^2} e^{-\tau(\vec{r}',\vec{r},E)}}{V_m} \quad (6)$$

(*c*) Furthermore, we assume the infinitely extended periodic lattice to be adequately represented by an ideally reflecting Seitz-Wigner cell. Hence, allowance has to be made for neutron reflexions at the cell boundary when calculating the collision probabilities. In case the cell dimensions are not large as compared to the mean free path of a neutron, this approximation may lead to a certain inaccuracy which, however, can be ruled out by relatively simple corrections [2].

As can easily be shown by use of symmetry properties of the integrand in (6), the assumptions (*a*) and (*b*) suffice for the following reciprocity theorem to be valid:

$$\Sigma_n(E) V_n P_{nm}(E) = \Sigma_m(E) V_m P_{mn}(E) \quad (7)$$

Application to thermal neutron spectrum calculations in heterogeneous media

In two previous publications [3,4] the author has derived a generalization of the Wilkins theory by extending it to heterogeneous media making use of first-flight collision probabilities.

The Wilkins model in its original form, however, does not give an adequate description for materials and energies where binding effects play a role. According to a suggestion of Horowitz, the latter can be approximately accounted for by allowing the slowing-down power to be a function of energy [5].

In the following, the theory is briefly described using the more general Horowitz model.

The derivations start from the set of integral equations (4), where the source densities $\bar{S}_m(E)$ are to be interpreted as scattering sources. Hence:

$$V_n \Sigma_n(E) \phi_n(E) = \sum_{m=1}^{N} V_m P_{mn}(E) \int_0^\infty \Sigma_{sm}(E' \to E;\, T_m) \phi m(E') dE' \quad (8)$$

The medium considered is thought to be composed of N coaxial annular zones.

The modified (Horowitz) heavy gas approximation consists of the following replacement:

$$\int_0^\infty \Sigma_{sm}(E' \to E;\, T_m) \phi_m(E') dE' \to \xi_m \Sigma_{sm0} \frac{d}{dE} \left\{ g_m(E) \left[EkT_m \frac{d\phi_m(E)}{dE} + (E - kT_m)\phi_m(E) \right] \right\} + \Sigma_{sm}(E)\phi_m(E) \quad (9)$$

T_m is the average temperature (°K) of the m-th zone. Σ_{sm0} denotes the average macroscopic free atom scattering cross section of the m-th zone. $g_m(E)$ is a suitable function of energy determined by the moderating properties of the medium and the particular problem. However, for a large class of reactor problems $g_m(E)$ is independent of leakage and absorption and can be obtained from the neutron scattering law [5]. In the following derivations $g_m(E)$ will be assumed to be known and to have a first and second order derivative.

The Wilkins approximation is given by the special case $g_m(E) \equiv 1$. Substituting (9) into (8) yields

$$V_n[\Sigma_{an}(E) + \Sigma_{sn}(E)]\phi_n(E) = \sum_{m=1}^{N} V_m P_{mn}(E) \left\{ \xi_m \Sigma_{sm0} \frac{d}{dE} \left[g_m(E) \left(kT_m E \frac{d\phi_m(E)}{dE} + (E - kT_m)\phi_m(E) \right) \right] + \Sigma_{sm}(E)\phi_m(E) \right\} \quad (10)$$

$$n = 1, 2, \ldots, N;\ 0 \leq E \leq E_0;\ +$$

To obtain a unique solution of (10), it is necessary to impose 2 N suitable boundary conditions upon the fluxes $\phi_n(E)$. It is convenient to choose:

$$\phi_n(0) = 0;\ \phi_n(E_0) = \frac{c_n}{E_0}\left(1 + \frac{2kT_n}{E_0}\right);\ n = 1, 2, \ldots, N$$

where c_n is a suitably chosen constant associated with the average slowing-down flux in the n-th zone.

The relatively complicated set of differential equations (10) can be simplified appreciably by performing the following operations:

Equations (10) are at first looked upon as an ordinary linear set of equations for the differential expressions in the brackets { }. Provided that the collision probability determinant

$$(\mathscr{K}(E)) = \begin{vmatrix} P_{11} \ldots . P_{N1} \\ \vdots \quad \vdots \\ P_{1N} \ldots P_{NN} \end{vmatrix}$$

does not vanish, (10) can be solved for the "unknowns" { }.

The functions $\phi_n(E)$ are subjected to the following transformation:

$$\phi_n(E) = \bar{\psi}_n(E) \frac{\exp\left(-\frac{E}{2kT_n}\right)}{\sqrt{g_n(E)}} \tag{11}$$

Hence the following set of differential equations is finally obtained:

$$kT_n \frac{d^2\bar{\psi}_n(E)}{dE^2} - f_n(E)\bar{\psi}_n(E) + \sum_{\substack{m=1 \\ m\neq n}}^{N} f_{mn}(E)\bar{\psi}_m(E) = 0;\ n = 1, 2, \ldots, N \tag{12}$$

$$0 < \epsilon \leqq E \leqq E_0$$

subject to the boundary conditions

$$\bar{\psi}_n(\epsilon) - \epsilon\left[1 + \frac{\epsilon}{2}\left(\frac{1}{kT_n} + \frac{g_n'(\epsilon)}{g_n(\epsilon)}\right)\right]^{-1} \cdot \frac{d\bar{\psi}_n(\epsilon)}{dE} = 0$$

$$\bar{\psi}_n(E_0) = \frac{c_n}{E_0}\left(1 + \frac{2kT_n}{E_0}\right)\sqrt{g_n(E_0)}\exp\left(\frac{E_0}{2kT_n}\right) \tag{13}$$

Herein ϵ is a very small positive quantity ($\approx 1 \times 10^{-3}$). The first of these boundary conditions is equivalent to $\phi_n(\epsilon) - \epsilon\phi_n'(\epsilon) = 0$ which has to be used in place of $\phi_n(0) = 0$, since the coefficients $f_n(E)$ and $F_{mn}(E)$ exhibit singularities at $E = 0$.

$$f_n(E) = \frac{1}{4kT_n} - \frac{1}{E}\left(1 + \frac{\Sigma_{sn}(E)}{\Sigma_{sn0}\xi_n g_n(E)}\right) + \frac{(\Sigma_{an}(E) + \Sigma_{sn}(E))A_{nn}(E)}{(\mathscr{K}(E))\xi_n\Sigma_{sn0}Eg_n(E)} - \frac{kT_n}{4}\frac{(g_n'(E))^2}{(g_n(E))^2} - \frac{g_n'(E)}{g_n(E)}\left(\frac{1}{2} - \frac{kT_n}{E}\right) + \frac{kT_n}{2}\frac{g_n''(E)}{g_n(E)};$$

$$f_{mn}(E) = (-1)^{n+m+1}\frac{(\Sigma_{an}(E) + \Sigma_{sn}(E))}{(\mathscr{K}(E))\xi_n\Sigma_{sn0}Eg_n(E)} \frac{P_{nm}(E)}{P_{mn}(E)} A_{mn}(E)\sqrt{\frac{g_n(E)}{g_m(E)}}\exp\left[\frac{E}{2}\left(\frac{1}{kT_n} - \frac{1}{kT_m}\right)\right] \tag{14}$$

$A_{mn}(E)$ is that determinant which is obtained from $(\mathscr{K}(E))$ by cancelling the m-th row and the n-th column, i.e., the complement of $P_{nm}(E)$.

It is evident that (12) is in the form of multigroup diffusion equations with the space variable exchanged for the energy variable. Hence, subdivision of the cell into N spatial zones leads formally (and only formally) to N-group diffusion equations. Note that the transfer matrix $f_{mn}(E)$ does not represent a triangular matrix.

The advantage achieved by the formulation (12) is evident: provided that a suitable one-dimensional multigroup programme is available, it can be used directly to solve our thermalization problem, although the latter is entirely different in its nature from a multigroup problem.

Our computer code SUPERMUNGO, a generalized version of our one-dimensional multigroup-code MUNGO, programmed for the Siemens DVA 2002, has just the virtues required to solve the equations (12).

The method described forms the basis of the thermalization code THERMOPYL [6] programmed for the Siemens DVA 2002. The programme can treat up to 10 spatial zones and more than 110 energy points, depending on the number of zones. The computer time required is relatively short: a three-zone case with 110 energy points requires 15 minutes. For more than three zones, the computer time increases approximately proportional to the square of the number of zones (DVA 2002 computing times: addition 450 μs; subtraction 450 μs; multiplication 1440 μs; division 3240 μs). As an example, Fig. 1 shows the result of a 7-region treatment (3 fuel regions, 1 zone for the pressure and calandria tube and 3 moderator regions) of a 19-element CANDU-type lattice cell with D_2O coolant and moderator at ambient temperature (23 °C). In Fig. 1b the average neutron spectra in the seven zones are plotted versus energy. Fig. 1c shows the ^{239}Pu: ^{235}U fission ratios in the different zones in comparison with the corresponding experimental results [7].

Application to fast and epithermal neutron spectrum calculations in heterogeneous media

In the epithermal energy region, the integral Equation (4) to be solved takes the form:

$$V_n[\Sigma_{an}(u) + \Sigma_{sn}(u)]\phi_n(u) = \sum_{m=1}^{N} V_m P_{mn}(u) \sum_{k=1}^{N_m} \bar{S}_m^{(k)}(u) \tag{15}$$

where u denotes the neutron lethargy, and $\sum_{k=1}^{N_m} \bar{S}_m^{(k)}(u)$ represents $\bar{S}_m(u)$.

Each zone n is allowed to contain N_n different nuclides. (In the presentation which follows, a superscript k refers to the nuclide, a subscript m denotes the zone; other symbols have their usual meaning.) $\bar{S}_n^{(k)}(u)$ is the neutron source term resulting from reactions with the k-th nuclide of the n-th zone. For the sake of simplicity, this source term is assumed to involve only elastically scattered neutrons:

$$\bar{S}_n^{(k)}(u) = \int_0^{\ln\frac{1}{\alpha_k}} \Sigma_{sn}^{(k)}(u-t)\phi_n(u-t)w_{el}^{(k)}(t)\,dt;$$

$$w_{el}^{(k)}(t) = \frac{e^{-t}}{1-\alpha_k}; \tag{16}$$

By Taylor series expansion of the integrand in (16), analogous to the homogeneous case [8], the integral source term $\bar{S}_m(u)$ can be replaced by a first order differential expression:

$$\bar{S}_n(u) = \sum_{k=1}^{Nn} \bar{S}_n^{(k)}(u) = \sum_{k=1}^{Nn} (\Sigma_{sn}^{(k)}(u))\phi_n(u) - \frac{d}{du}\sum_{k=1}^{Nn} q_n^{(k)}(u) \tag{17}$$

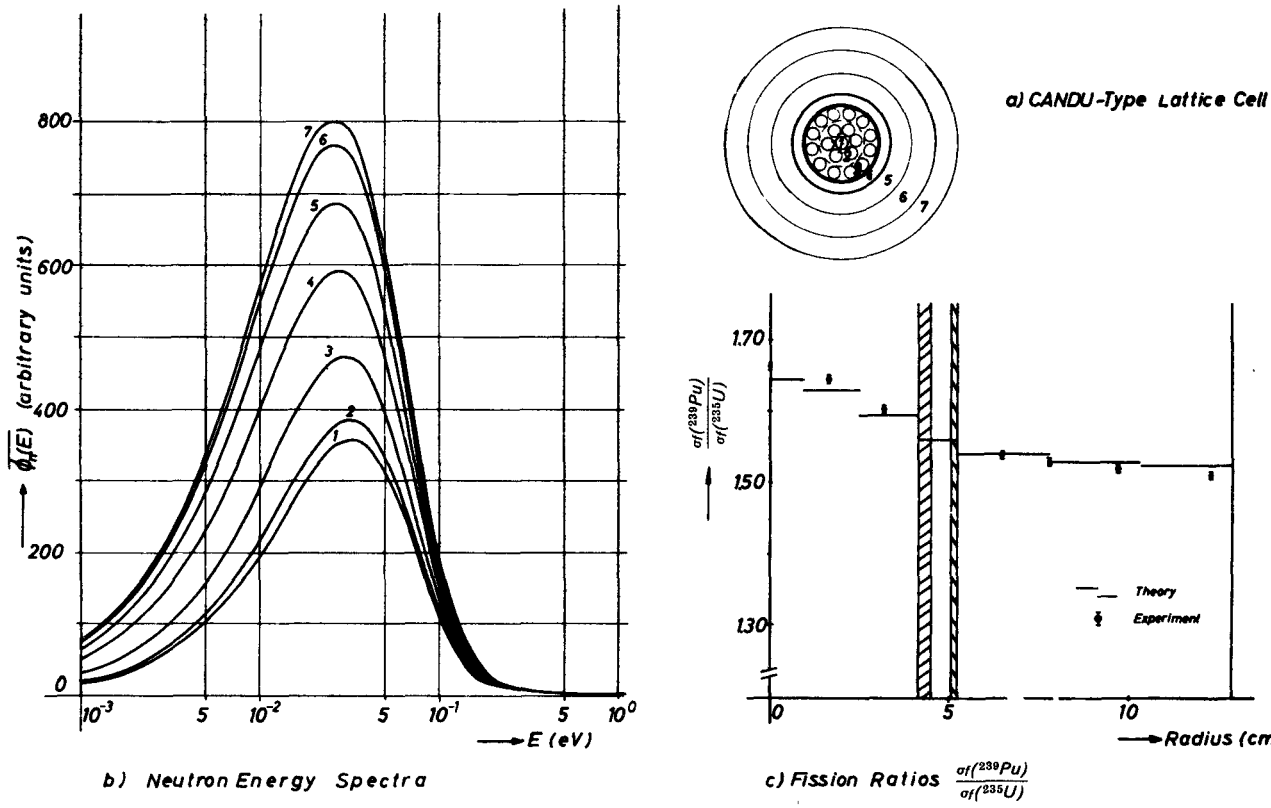

Figure 1. Thermal neutron energy spectrum in seven different zones of a 19-element CANDU-type lattice cell

where $q_n^{(k)}(u)$, the component of the slowing down density which results from neutron scatterings with nuclides k of the n-th zone, is described to a first order approximation by the following differential equation:

$$\gamma^{(k)} \frac{dq_n^{(k)}(u)}{du} + q_n^{(k)}(u) = \xi^{(k)} \Sigma_{sn}^{(k)}(u) \bar{\phi} n(u) \qquad (18)$$

$$k = 1, 2, \ldots, N_n; \; n = 1, 2, \ldots, N.$$

$\gamma^{(k)}$ is the so-called Greuling-Goertzel coefficient, i.e., the second moment of the slowing-down kernel, divided by two times the average lethargy decrement $\xi^{(k)}$:

$$\gamma^{(k)} = 1 - \frac{\alpha_k (\ln \alpha_k)^2}{2\xi^{(k)}(1-\alpha_k)} \qquad (19)$$

With (17), Eqs. (15) and (16) represent a set of $M = N + \sum_{m=1}^{N} N_m$ first order differential equations for the M unknown functions $\bar{\phi}_n(u)$, $q_n^{(k)}(u)$: $k = 1, 2, \ldots, N_n$; $n = 1, 2, \ldots, N$. The method described is to be considered a generalization to heterogeneous lattice cells of the Greuling-Goertzel method. The slowing-down methods for homogeneous media known as "Fermi-Age" and "Selengut-Goertzel" approximations can be readily extended to heterogeneous media with the above formalism.

The Fermi-Age approximation for a heterogeneous lattice cell results from the above Greuling-Goertzel Eqs. (15) and (18) by putting $\gamma^{(k)} = 0$ for each k, and combining all contributions to the slowing-down density resulting from the different nuclides of a zone to one term $q_n(u)$:

$$q_n(u) = \sum_{k=1}^{Nn} q_n^{(k)}(u) = \sum_{k=1}^{Nn} \xi^{(k)} \Sigma_{sn}^{(k)}(u) \bar{\phi}_n(u)$$

The Selengut-Goertzel approximation is obtained by splitting the slowing-down density $q_n(u) = \sum_{k=1}^{N_n} q_n^{(k)}(u)$ into two terms. One term is associated with hydrogen H, the other term accounts for slowing down by the other nuclides of region n. The hydrogen term is described rigorously by relation (18) with $\gamma^{(H)} = \xi^{(H)} = 1$. The other term associated with the rest of the nuclides in region n is subjected to the above Fermi-Age relation ($\gamma^{(k)} = 0$).

In principle, the differential equations involved in the above theory can be solved by means of a finite difference method; however, this problem will not be dealt with in any detail.

For the following special case, an explicit solution to the differential equations can be obtained: we consider a lattice cell consisting of two zones only, one of which (with subscript 1) meets the requirements of the so-called "infinite absorber" (IA) approximation whereas no restrictions are imposed with regard to the other (= moderator) zone (subscript 2).

The differential equations to be solved in this case are (for energies below the fission spectrum):

$$V_1[\Sigma_{a1}(u)+\Sigma_{s1}(u)]\bar{\phi}_1(u)=V_1P_{11}(u)\Sigma_{s1}(u)\bar{\phi}_1(u)+V_2P_{21}(u)\left\{\Sigma_{s2}(u)\bar{\phi}_2(u)-\frac{dq_2(u)}{du}\right\}$$

$$V_2[\Sigma_{a2}(u)+\Sigma_{s2}(u)]\bar{\phi}_2(u)=V_1P_{12}(u)\Sigma_{s1}(u)\bar{\phi}_1(u)+V_2P_{22}(u)\left\{\Sigma_{s2}(u)\bar{\phi}_2(u)-\frac{dq_2(u)}{du}\right\}$$

$$\gamma^{(2)}\frac{dq_2(u)}{du}+q_2(u)=\xi^{(2)}\Sigma_{s2}(u)\bar{\phi}_2(u) \qquad (20)$$

After some algebra, the following solution is obtained:

$$q_2(u)=q_2(u_0)\exp\left\{-\int_{u0}^{u}\frac{\Sigma_{a2}{}^{eff}(u')du'}{\xi^{(2)}\Sigma_{s2}(u')+\gamma^{(2)}\Sigma_{a2}{}^{eff}(u')}\right\}$$

$$\bar{\phi}_1(u)=\frac{P_{12}(u)\{\Sigma_{a1}(u)+\Sigma_{s1}(u)\}}{P_{12}(u)\Sigma_{s1}(u)+P_{22}(u)\Sigma_{a1}(u)}\cdot\frac{q_2(u)}{\xi^{(2)}\Sigma_{s2}(u)+\gamma^{(2)}\Sigma_{a2}{}^{eff}(u)}$$

$$\bar{\phi}_2(u)=\frac{1}{\xi^{(2)}\Sigma_{s2}(u)+\gamma^{(2)}\Sigma_{a2}{}^{eff}(u)}\cdot q_2(u) \qquad (21)$$

It is easily seen that by introducing the effective absorption cross section

$$\Sigma_{a2}{}^{eff}(u)=\frac{\Sigma_{a1}(u)\Sigma_{s2}(u)P_{21}(u)+\Sigma_{a2}(u)[\Sigma_{a1}(u)+\Sigma_{s1}(u)P_{12}(u)]}{P_{12}(u)\Sigma_{s1}(u)+P_{22}(u)\Sigma_{a1}(u)} \qquad (22)$$

q_2 takes the same form as in the corresponding homogeneous case [9].

METHODS INVOLVING MULTIPLE COLLISION PROBABILITIES

Derivations from integral transport theory

The basic principle underlying the multiple collision probability method is again the integral transport Eq. (1). If applied to a radially symmetrical annular region with volume V and outer (inner) surface area $So(Si)$, the neutron flux distribution within V can be written in the following way:

$$\phi(\vec{r})=\int_V\frac{d\vec{r}'}{4\pi|\vec{r}-\vec{r}'|^2}e^{-\Sigma_t|\vec{r}-\vec{r}'|}\Sigma_s\phi(\vec{r}')+\psi_0{}^V(\vec{r})+\psi_0{}^{So}(\vec{r})+\psi_0{}^{Si}(\vec{r}) \qquad (23)$$

where we have assumed isotropic scattering in the laboratory system and spatially constant cross sections in V. (For simplicity we restrict our derivations here to monoenergetic neutrons.) $\psi_0{}^V(\vec{r})$ gives the direct contribution to $\phi(\vec{r})$ due to a volume source $Q(\vec{r})$:

$$\psi_0{}^V(\vec{r})=\int_V\frac{d\vec{r}'}{4\pi|\vec{r}-\vec{r}'|^2}e^{-\Sigma_t|\vec{r}-\vec{r}'|}Q(\vec{r}') \qquad (24)$$

Similarly, $\psi_0{}^{So}(\vec{r})$ and $\psi_0{}^{Si}(\vec{r})$ give the direct contributions to $\phi(\vec{r})$ due to neutron incurrent densities $j(\vec{\Omega})$ at the outer and inner surface, respectively, e.g.

$$\psi_0{}^{So}(\vec{r})=\int\frac{d_{So}}{|\vec{r}-\vec{r}_{So}|^2}j\left(\frac{\vec{r}-\vec{r}_{So}}{|\vec{r}-\vec{r}_{So}|}\right)e^{-\Sigma_t|\vec{r}-\vec{r}_{So}|} \qquad (25)$$

The integral Eq. (23) can be solved by a Neumann series expansion [10] of the form:

$$\phi(\vec{r})=\sum_{n=0}^{\infty}\psi_n{}^V(\vec{r})+\sum_{n=0}^{\infty}\psi_n{}^{So}(\vec{r})+\sum_{n=0}^{\infty}\psi_n{}^{Si}(\vec{r}) \qquad (26)$$

with

$$\psi_n{}^x(\vec{r})=\Sigma_s\int_V\frac{d\vec{r}'}{4\pi|\vec{r}-\vec{r}'|^2}e^{-\Sigma_t|\vec{r}-\vec{r}'|}\psi_{n-1}{}^x(\vec{r}');\quad (n>0;\ x:\ V,So,Si) \qquad (27)$$

Upon integrating (26) over V we obtain after some algebra

$$C=\Sigma_tV\bar{\phi}=P_1{}^{VV}\left\{1+\sum_{j=2}^{\infty}\left(\frac{\Sigma_s}{\Sigma_t}\right)^{j-1}P_2{}^{VV}.P_3{}^{VV}\ldots P_j{}^{VV}\right\}.\int_V Q(\vec{r})d\vec{r}+P_1{}^{SoV}\left\{1+\sum_{j=2}^{\infty}\left(\frac{\Sigma_s}{\Sigma_t}\right)^{j-1}P_2{}^{SoV}.P_3{}^{SoV}\ldots P_j{}^{SoV}\right\}.\int_{So}\frac{j_{So}(\vec{\Omega})d\Omega}{2\pi}+P_1{}^{SiV}\left\{1+\sum_{j=2}^{\infty}\left(\frac{\Sigma_s}{\Sigma_t}\right)^{j-1}P_2{}^{SiV}.P_3{}^{SiV}\ldots P_j{}^{SiV}\right\}.\int_{Si}\frac{j_{Si}(\vec{\Omega})d\Omega}{2\pi} \qquad (28)$$

with $P_{j+1}{}^{VV(SV)}=\dfrac{\int_V\psi j^{V(S)}(\vec{r})d\vec{r}}{\frac{\Sigma_s}{\Sigma_t}\int_V\psi_{j-1}{}^{V(S)}(\vec{r})d\vec{r}}$ being the probability that a neutron from the volume (surface) source which has suffered j collisions in V will suffer at least one more collision therein. In the analysis which follows, two further simplifying assumptions are made:

(*a*) the spatial source distribution of the collided neutrons of any generation j be constant; thus the series appearing in (28) can be easily summed as shown under "Multiple collision probabilities";

(*b*) the angular direction of neutrons entering a surface be cosine distributed; by means of this assumption on $j(\vec{\Omega})$, the different spatial zones can be decoupled.

General formulation of the method

The foregoing considerations are now applied to a Seitz-Wigner cell with reflecting boundaries, consisting of N coaxial annular regions. The total energy range is assumed to be subdivided into L suitably chosen energy groups. The group cross sections involved are presumed to be known. The following notation is used:

$V_n(S_n)$ = volume (outer surface) of region n per unit length

$q_n{}^j$ = suitably normalized average source density for group-j neutrons in region n. $Q_n{}^j=q_n{}^j.V_n$.

$j_n{}^{j\pm}$ = group-j neutron current density through S_n in outward(+) and inward(−) direction, respectively. $J_n{}^{j\pm} = j_n{}^{j\pm}.S_n$.

$\tau_n{}^j$ = mean number of secondary neutrons of group j per collision of a group-j neutron in region n.

Where the symbols $W_n{}^{jxy}$ are used, the subscript n denotes the zone number, the first superscript j refers to the energy group, whereas the two subsequent superscripts x y indicate the process $x \to y$ "v" "i" and "o" stand for "volume", "inner" and "outer", respectively, E.g.

$W_n{}^{jVV}$ = number of collisions caused by group j neutrons in region n per group j neutron born in this region.

$W_n{}^{jVi}$ = number of group j neutrons leaving the n-th region through the inner boundary per group j neutron born in region n.

$W_n{}^{jio}$ = number of group j neutrons leaving the n-th region through the outer boundary per group j neutron injected into this region through the inner boundary.

The symbols $W_n{}^{jiV}$, $W_n{}^{joV}$, $W_n{}^{jVo}$, $W_n{}^{joi}$, $W_n{}^{jii}$, $W_n{}^{joo}$ are to be interpreted in an analogous way.

All these definitions are based on the assumptions that the boundaries of the region n are black to neutrons leaving this region.

The important quantities to be determined are the collision rates $C_n{}^j$=number of group j neutron collisions in region n per primary source neutron in the cell.

By means of the above definitions these collision rates can be computed according to (28)

$$C_n{}^j = Q_n{}^j W_n{}^{jVV} + J_{n-1}{}^{j+} W_n{}^{jiV} + J_n{}^{j-} W_n{}^{joV} \tag{29}$$

with

$$J_n{}^{j+} = Q_n{}^j W_n{}^{jVo} + J_{n-1}{}^{j+} W_n{}^{jio} + J_n{}^{j-} W_n{}^{joo}$$
$$J_{n-1}{}^{j-} = Q_n{}^j W_n{}^{jVi} + J_n{}^{j-} W_n{}^{joi} + J_{n-1}{}^{j+} W_n{}^{jii} \tag{30}$$

the two Eqs. (30) can be represented in a simpler form by the following matrix recurrence relation [11]

$$\vec{J}_n{}^j = M_n{}^j \,.\, \vec{J}_{n-1}{}^j + \vec{Q}_n{}^{j*} \tag{31}$$

with the vectors

$$\vec{J}_n{}^j = \begin{pmatrix} J_n{}^{j-} \\ J_n{}^{j\pm} \end{pmatrix}; \quad \vec{Q}_n{}^{j*} = Q_n{}^j \begin{pmatrix} -\dfrac{W_n{}^{jVi}}{W_n{}^{joi}} \\ W_n{}^{jVo} - \dfrac{W_n{}^{jVi} . W_n{}^{joo}}{W_n{}^{joi}} \end{pmatrix} \tag{32}$$

$$M_n{}^j = \begin{pmatrix} \dfrac{1}{W_n{}^{joi}}, & -\dfrac{W_n{}^{jii}}{W_n{}^{joi}} \\ \dfrac{W_n{}^{joo}}{W_n{}^{joi}}, & W_n{}^{jio} - \dfrac{W_n{}^{jii} \,.\, W_n{}^{joo}}{W_n{}^{joi}} \end{pmatrix} \tag{33}$$

Eqs. (29) to (33) hold for $n = 2, 3, \ldots N$.

For $n = 1$ the equivalent relations are:

$$C_1{}^j = Q_1{}^j W_1{}^{jVV} + J_1{}^{j-} W_1{}^{joV} \tag{34}$$

$$\vec{J}_1{}^j = J_1{}^{j-} \begin{pmatrix} 1 \\ W_1{}^{joo} \end{pmatrix} + Q_1{}^j \begin{pmatrix} 0 \\ W_1{}^{jVo} \end{pmatrix} \tag{35}$$

Applying the recurrence relationship (31) repeatedly, we obtain:

$$\vec{J}_N{}^j = M_{N2}{}^j \begin{pmatrix} 1 \\ W_1{}^{joo} \end{pmatrix} J_1{}^{j-} + \vec{S}_N{}^j \tag{36}$$

where we have used the abbreviations:

$$M_{Nk}{}^j = M_N{}^j \,.\, M_{N-1}{}^j \ldots M_k{}^j; \quad M_{NN}{}^j = M_N{}^j;$$

$$\vec{S}_N{}^j = \sum_{K=3}^{N} M_{Nk}{}^j \vec{Q}_{k-1}{}^{j*} + \vec{Q}_N{}^{j*} + M_{N2}{}^j \begin{pmatrix} 0 \\ W_1{}^{jVo} \end{pmatrix} Q_1{}^j \tag{37}$$

For each energy group j, (36) represents a coupled set of two linear equations for the three unknowns $J_N{}^{j+}, J_N{}^{j-}, J_1{}^{j-}$. In order to obtain a unique solution we have to add another equation; this will have to be a linear correlation between the two boundary currents $J_N{}^{j+}$ and $J_N{}^{j-}$:

$$J_N{}^{j-} = r J_N{}^{j+} + s \tag{38}$$

$r = 1$, $s = 0$ gives the usual cell boundary condition for a vanishing net current. $r < 1$, $s = 0$ would mean that there is a net outleakage of neutrons from the cell.

With (36) and (38), all the neutron currents at the zone interfaces needed to calculate the collision rates $C_N{}^j$ can be determined, provided that the collision probabilities $W_N{}^{jxy}$ are known. Methods for computing these quantities have already been given.

Application to the fast fission effect

The theory described in the preceding chapter can be directly applied to the calculation of the fast fission effect in heterogeneous media. Backscattering and fast interaction effects can be properly taken into account. (For a detailed description of this procedure, see [12].)

The sources relevant to this case are given by the expressions ($L = 2$):

$Q_n{}^1 = Q_n{}^{th} \,.\, f_n{}^1$;

$$Q_n{}^2 = Q_n{}^{th} \,.\, f_n{}^2 + C_n{}^1 \frac{\Sigma_n{}^{12} + \nu_n{}^1 f_n{}^2 \Sigma_{fn}{}^1}{\Sigma_{tn}{}^1} \tag{39}$$

where $Q_N{}^{th}$ denotes the thermal fission source ($= V_n \nu_n{}^{th} \Sigma_{fn}{}^{th} \phi_n{}^{th}$) and $f_n{}^{j*}$ stands for the fraction of the normalized fission spectrum in group j. $\Sigma_n{}^{ij}$ is the macroscopic energy transfer cross section from group i to group j and $\Sigma_{tn}{}^1 (\Sigma_{fn}{}^1)$ denotes the macroscopic total (fission) cross section for group 1 neutrons. The total thermal fission source of the cell is normalized as follows:

$$Q^{th} = \sum_{n=1}^{N} Q_n{}^{th} = 1 \tag{40}$$

The fast fission ratio for the n-th zone is obviously given by the relation

* Group $j = 1$ is defined as the ^{238}U fast fission energy region.

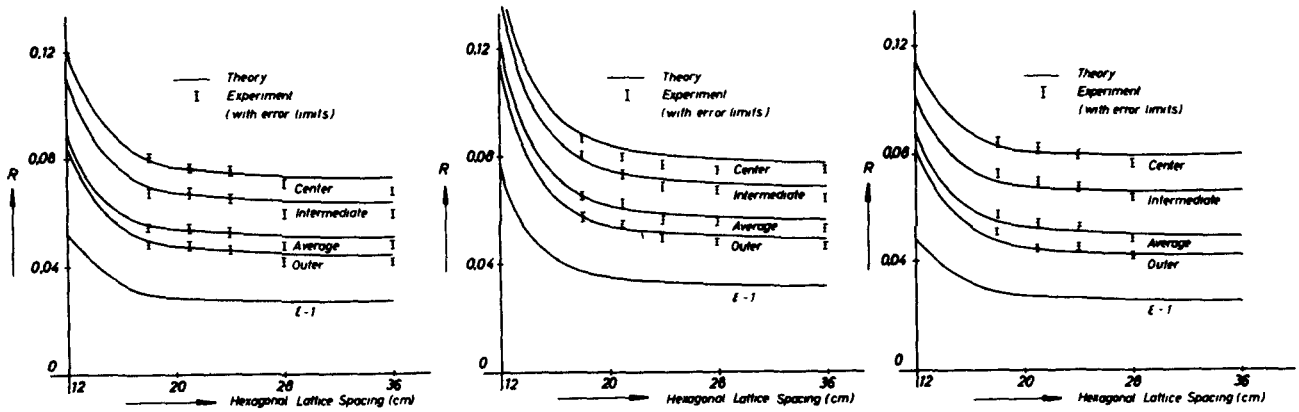

Figure 2. Fast fission ratios in the three rings of a 19-element CANDU-type cluster as a function of lattice pitch

$$R_n = \nu_n{}^{th} \frac{\frac{\Sigma_{fn}{}^1}{\Sigma_{tn}} \cdot C_n{}^1}{Q_n{}^{th}} \tag{41}$$

The average fast fission ratio for the total fuel assembly is

$$R = \frac{1}{\sum_{n=1}^{N} \frac{Q_n{}^{th}}{\nu_n{}^{th}}} \sum_{n=1}^{N} \frac{Q_n{}^{th}}{\nu_n{}^{th}} \cdot R_n \tag{42}$$

which, in case the neutron fission yield $\nu_n{}^{th}$ does not vary from zone to zone, reduces to

$$R = \sum_{n=1}^{N} Q_n{}^{th} \cdot R_n \tag{43}$$

If the fuel element is made up of rod clusters rather than annular fuel zones, the error arising through homogenization has to be corrected by applying the Pershagen prescription [13].

The theory outlined above has been checked against experiments performed by Bigham *et al.* [14], on CANDU-type fuel clusters with different coolants and covering a range of lattice pitches from 18 to 36 cm.

Fig. 2 shows the theoretically obtained fast fission ratios for a 19-element CANDU-type fuel cluster with different coolants in comparison with the measured data. The agreement between theory and experiment is found to be quite satisfactory. Note that the fast fission ratios are pitch-dependent due to the interaction effect between neighbouring clusters.

In a similar way, this theory can be applied to the calculation of the resonance escape probability of a widely spaced lattice in order to account for the so-called advantage factor.

Application to thermal utilization calculations

The well known one-group collision probability method for calculating the thermal utilization factor in a heterogeneous lattice cell, developed by Amouyal and Benoist [15] and extended by A. Müller [11], represents a special case of the general procedure derived in the section headed "General formulation of the method", differing from the latter only by a special diffusion theory treatment of the outermost (=moderator) region.

With the above terminology, f_n, the thermal utilization of the n-th zone, can be written as follows:

$$f_n = \frac{1}{\sum_{m=1}^{N} \frac{\Sigma_{am}{}^{th}}{\Sigma_{tm}{}^{th}} C_m{}^{th}} \cdot \frac{\Sigma_{an}{}^{th}}{\Sigma_{tn}{}^{th}} \cdot C_n{}^{th} \tag{44}$$

If the moderator is subdivided into sufficiently numerous zones, the theory as previously presented can be used directly to determine f_n. In most cases, however, it is convenient to treat the moderator in a diffusion theory way as suggested by Amouyal and Benoist.

In order to reduce both versions to a common basis, the outermost cell region N is dealt with separately in any of the two cases. In place of (36), we write

$$\vec{J}_{N-1}{}^{th} = M_{N-1,2}{}^{th} \left(\frac{1}{W_1{}^{th\,oo}} \right) J_1{}^{th-} + \vec{S}_{N-1}{}^{th} \tag{45}$$

This is a set of two equations for the three unknowns $J_{N-1}{}^{th-}$, $J_{N-1}{}^{th+}$, $J_1{}^{th-}$. The cell boundary condition

$$J_N{}^{th-} = r J_N{}^{th+} \tag{46}$$

used above as a third equation, is equivalent to

$$J_{N-1}{}^{th-} = Q_N{}^{th} \tilde{W}_N{}^{thVi} + J_{N-1}{}^{th+} \cdot \tilde{W}_N{}^{thii} \tag{47}$$

as can be shown by substituting (46) into (30), where we have put:

$$\tilde{W}_N{}^{thVi} = W_N{}^{thVi} + \frac{r \cdot W_N{}^{thVo} \cdot W_N{}^{thoi}}{1 - r \cdot W_N{}^{thoo}}$$

$$\tilde{W}_N{}^{thii} = W_N{}^{thii} + \frac{r \cdot W_N{}^{thio} \cdot W_N{}^{thoi}}{1 - r \cdot W_N{}^{thoo}} \tag{48}$$

$\tilde{W}_N{}^{thVi}$ is the probability for a thermal neutron born in V_N of finally leaving this region through the inner boundary taking proper account of the boundary condition (46). $\tilde{W}_N{}^{thii}$ is defined in an analogous way.

If diffusion theory is used for the outermost (=moderator) region, relations (48) have just to be replaced by equivalent expressions obtained from diffusion theory. The way this can be achieved be-

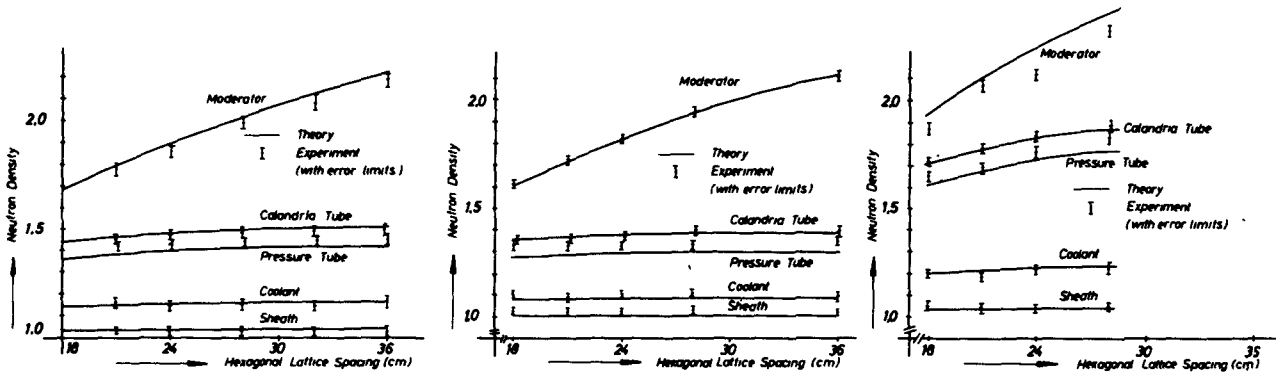

Figure 3. Neutron density fine structure of a 19-element CANDU-type lattice cell as a function of lattice pitch

comes plain by applying the balance equation

$$(J_{n-1}{}^{th-} - J_{n-1}{}^{th+}) + (J_n{}^{th+} - J_n{}^{th-}) + \underbrace{\frac{\Sigma_{an}{}^{th}}{\Sigma_{tn}{}^{th}} \cdot C_n{}^{th}}_{A_n{}^{th}} = Q_n{}^{th} \tag{49}$$

to the outermost region ($n = N$). According to the definition of $\tilde{W}_N{}^{thVi}$ only those neutrons have to be taken into account which originated in V_N and which leave this region for the first time (i.e. $J_{N-1}{}^{th+} = 0$). For $r = 1$ we get:

$$\tilde{W}_N{}^{thVi}\,(\text{Diff.}) = \frac{J_{N-1}{}^{th-}}{Q_N{}^{th}} = 1 - \frac{A_N{}^{th}}{Q_N{}^{th}} = \left(1 + K_N{}^2 R_N{}^2 \cdot C + \lambda \frac{V_N}{S_{N-1}} \frac{K_N{}^2}{\Sigma_{tr} N^{th}}\right)^{-1} \tag{50}$$

where λ and C are given in [15].

Similarly $\tilde{W}_N{}^{thii}$(Diff.) can be computed as the diffusion theory albedo:

$$\tilde{W}_N{}^{thii}(\text{Diff.}) = \left(1 + 4\Sigma_{aN}{}^{th} \frac{V_N}{S_{N-1}}\right)^{-1} \tag{51}$$

The practicability of the theory is demonstrated by its application to a 19-rod CANDU-type fuel element with different coolants, covering a range of lattice pitches from 18 to 36 cm. Fig. 3 shows the theoretical flux ratios in comparison with the experimental values obtained by Green and Bigham [14]. The hyperfine structure of the cluster has been determined by means of a micro-cell calculation.

METHODS FOR COMPUTING COLLISION PROBABILITIES

First-flight collision probabilities

The following considerations are restricted to N-region cells in cylindrical geometry; for slag geometry, the collision probabilities P_{mn} can be represented explicitly in terms of E_3-exponential integrals.

The calculation of collision probabilities P_{mn} for cylindrical geometry is known to involve rather complex numerical integrations. A. Müller [16], however, was able to reduce the problem to a single integral of the form

$$P_{mn} = \frac{2}{\pi(R_m{}^2 - R_{m-1}{}^2)\Sigma_{tm}} \int_0^{Rm} f(r)\,\mathrm{d}r \tag{52}$$

where $f(r)$ is a sum of K_{i3}-functions involving complicated arguments. A numerical integration of (52), though on principle no problem, is found to be rather time-consuming.

The computing time can be considerably reduced by requiring that the neutrons cross each zone boundary with an angular distribution proportional to the cosine of the angle between the direction of flight and the direction normal to the surface. With this assumption, the collision probabilities P_{mn}, according to A. Müller [17], can be represented in a relatively simple way as a function of two quantities $P_n{}^{Vi}$ and $P_n{}^{Vo}$ which denote the probability for a neutron arising in zone n with a uniform and isotropic source density to leave this zone without a collision in inward and outward direction, respectively. We obtain:

$$P_{mn} \underset{(m<n)}{=} P_m{}^{Vo} \frac{P_n{}^{iV} + P_n{}^{io} \cdot Q_{n+1}{}^{ii} \cdot Q_n{}^{oV}}{1 - P_n{}^{io} \cdot Q_{n+1}{}^{ii} \cdot Q_n{}^{oi} \cdot Q_{n-1}{}^{oo}} \begin{cases} 1 & \text{for } m = n-1 \\ \prod_{k=m+1}^{n-1} P_k{}^{io} & \text{for } m < n-1 \end{cases} \tag{53}$$

with

$$P_n{}^{iV} = \frac{4V_n}{S_{n-1}} \Sigma_{tn} P_n{}^{Vi}; \quad P_n{}^{oV} = \frac{4V_n}{S_n} \Sigma_{tn} P_n{}^{Vo};$$

$$P_n{}^{io} = 1 - P_n{}^{iV} \quad ; \quad P_n{}^{oi} = \frac{S_{n-1}}{S_n} \cdot P_n{}^{io} \tag{54}$$

$$P_n{}^{oo} = 1 - P_n{}^{oi} - P_n{}^{oV}; \quad P_n{}^{VV} = 1 - P_n{}^{Vi} - P_n{}^{Vo};$$

$$Q_n{}^{oo} = P_n{}^{oo} + \sum_{k=1}^{n-1} P_k{}^{oo} \prod_{l=k+1}^{n} P_e{}^{oi} \cdot P_e{}^{io};$$

$$Q_N{}^{oi} = P_N{}^{oi}\,(1 - P_N{}^{oo})^{-1};$$

$$Q_{N-1}{}^{oi} = P_{N-1}{}^{oi}\,(1 - P_{N-1}{}^{oo} \cdot P_N{}^{io} \cdot Q_N{}^{oi})^{-1};$$

$$Q_{N-2}{}^{oi} = P_{N-2}{}^{oi}\,(1 - P_{N-2}{}^{oo} \cdot P_{N-1}{}^{io} \cdot P_N{}^{io} \cdot Q_N{}^{oi} \cdot Q_{N-1}{}^{oi})^{-1}; \quad Q_{N+1}{}^{ii} = 1;$$

$$Q_n{}^{oi} = P_n{}^{oi}\,(1 - P_n{}^{oo} \prod_{k=n+1}^{N} P_k{}^{io}\, Q_k{}^{oi})^{-1};$$

$$Q_n{}^{oV} = P_n{}^{oV} \frac{Q_n{}^{oi}}{P_n{}^{oi}}; \quad Q_n{}^{ii} = \prod_{k=n}^{N} P_k{}^{io} \cdot Q_k{}^{oi}; \tag{55}$$

For $m>n$ P_{mn} is determined from P_{nm} by the reciprocity theorem (7). Furthermore:

$$P_{nn}=1-\sum_{\substack{m=1\\m\neq n}}^{N} P_{nm} \tag{56}$$

Hence, the problem reduces to the calculation of $P_n^{V\mathrm{i}}$ and $P_n^{V\mathrm{o}}$:

$$P_n^{V\mathrm{i}}(x_n,k_n)=\frac{2}{\pi x_n(1+k_n)}\int_0^{kn} \mathrm{d}t\left[\frac{\pi}{4}-K_{i3}\left(\frac{x_n}{1-k_n}(\sqrt{(1-t^2)}-\sqrt{(k_n^2-t^2)})\right)\right]$$

$$P_n^{V\mathrm{o}}(x_n,k_n)=P_n^{V\mathrm{i}}(x_n,k_n)+\frac{2}{\pi x_n(1+k_n)}\int_{kn}^{1} \mathrm{d}t\left[\frac{\pi}{4}-K_{i3}\left(\frac{2x_n}{1-k_n}\sqrt{(1-t^2)}\right)\right] \tag{57}$$

According to a method of J. M. Kennedy [12] these two probabilities can be calculated to a high degree of accuracy by simply interpolating between the two limiting cases of a solid cylinder ($k=0$) and a slab ($k=1$) resulting in a representation in terms of two parameters

$$x_n=\Sigma_{tn}(R_n-R_{n-1});\ k_n=\frac{R_{n-1}}{R_n}$$

The practicability of formula (53) is illustrated by the following sample comparison:
For a three-region cell with $R_1=4{,}85$ cm; $R_2=5{,}18$ cm; $R_3=14{,}31$ cm; $\Sigma_{t1}=0.74878$ cm^{-1}; $\Sigma_{t2}=0.37117$ cm^{-1}; $\Sigma_{t3}=0.68461$ cm^{-1}
we obtain (the first figures represent exact values; the figures in brackets were obtained with formula (53); Δ denotes the percentage error):

$P_{11}=0.86443(0.86446;\ \Delta=0.00)$
$P_{12}=0.02494(0.02524;\ \Delta=+1.20)$
$P_{13}=0.11063(0.11030;\ \Delta=-0.30)$
$P_{21}=0.35749(0.36188;\ \Delta=+1.23)$
$P_{22}=0.18227(0.18547;\ \Delta=+1.76)$
$P_{23}=0.46024(0.45265;\ \Delta=-1.65)$
$P_{31}=0.01600(0.01595;\ \Delta=-0.31)$
$P_{32}=0.00464(0.00456;\ \Delta=-1.72)$
$P_{33}=0.97936(0.97949;\ \Delta=+0.01)$

Multiple collision probabilities

The probabilities W_n^{jxy} occuring in the chapter entitled "Methods involving multiple collision probabilities", recalling the simplifying assumption introduced previously and making use of relations (54). One obtains:

$W_n^{jVV}=D_n^j\,.\,P_n^{jVV}$; $W_n^{jiV}=D_n^jP_n^{jiV}$;
$W_n^{joV}=D_n^jP_n^{joV}$; $W_n^{jV\mathrm{o}}=D_n^jP_n^{jV\mathrm{o}}$;
$W_n^{ji\mathrm{o}}=P_n^{ji\mathrm{o}}+D_n^jP_n^{jiV}\tau_n^jP_n^{jV\mathrm{o}}$;
$W_n^{joo}=P_n^{joo}+D_n^jP_n^{joV}\tau_n^jP_n^{jV\mathrm{o}}$; $W_n^{jV\mathrm{i}}=D_n^jP_n^{jV\mathrm{i}}$;
$W_n^{joi}=P_n^{joi}+D_n^jP_n^{joV}\tau_n^jP_n^{jV\mathrm{i}}$;
$W_n^{jii}=D_n^jP_n^{jiV}\tau_n^jP_n^{jV\mathrm{i}}$;

with $D_n^j=(1-\tau_n^jP_n^{jVV})^{-1}$ and τ_n^j as previously explained.

The valuable programming work performed by H. Raum is gratefully acknowledged.

REFERENCES

1. Case, K. M., *et al., Introduction to the Theory of Neutron Diffusion*, Vol. 1, Los Alamos, New Mexico (June 1953).
2. Honeck, H. C., Trans. American Nuclear Society, *5*, 350 (1962).
3. Märkl, H., Nukleonik, *4*, 39–45 (1962).
4. Märkl, H., C.N.A. Conference on D_2O-Reactors, Ottawa (May 1962).
5. Power Reactor Technology, *6*, No. 4, 39 (1963).
6. Märkl, H., and Raum, H., unpublished.
7. Bigham, C. B., *et al.*, Atomic Energy of Canada Ltd. report AECL-1350.
8. Greuling, E., *et al.*, US Atomic Energy Comm. report NDA10-96.
9. Meghreblian, R. V., and Holmes, D. K., *Reactor Analysis*, 104, McGraw-Hill Series in Nuclear Engineering, New York-Toronto-London (1960).
10. Stuart, G. W., Nuclear Sci. Eng., *2*, 617–625 (1957).
11. Müller, A., and Linnartz, E., Nukleonik, *5*, 23–27 (1963).
12. Märkl, H., and Fowler, A. G., Nukleonik, *6*, 39–51 (1964).
13. Pershagen, B., *et al.*, Proceedings of the Second International Conference on the Peaceful Uses of Atomic Energy, P/151, Vol. 12, p. 341, United Nations (1958).
14. Green, R. E., and Bigham, C. B., Atomic Energy of Canada Ltd. report AECL-1814, (1963).
15. Amouyal, A., and Benoist, P., Rapport, CEA-571 (1956).
16. Müller, A., Nukleonik, *4*, 53–56 (1962).
17. Müller, A., unpublished.

ABSTRACT—RÉSUMÉ—АННОТАЦИЯ—RESUMEN

A/640 République fédérale d'Allemagne

Aspects nouveaux de l'application des probabilités de collision dans la théorie des réacteurs

par H. Märkl

Les méthodes relatives à l'application des probabilités de collision prennent de plus en plus d'importance comme outils pratiques et utiles de la théorie des réacteurs. Au département des réacteurs de la Société Siemens-Schuckertwerke, diverses méthodes de calcul relatives à l'application des probabilités de collision ont été mises au point en vue de baser le calcul des réseaux hétérogènes sur une conception commune des probabilités de collision.

a) En partant de l'équation intégrale de transport, on obtient un système de N équations intégrales couplées en divisant la cellule élémentaire en N zones et en introduisant les probabilités de collision du premier trajet.

En traitant les expressions intégrales par approximation, on étend aux milieux hétérogènes la théorie de la thermalisation dans les milieux homogènes de Wilkins. La théorie résultante est réduite à une forme aisément utilisable pour une solution numérique.

De façon similaire, en appliquant cette conception des probabilités de collision au domaine des neutrons rapides et épithermiques, les méthodes de calcul de ralentissement connues comme approximations de Greuling-Goertzel, de Selengut-Goertzel et de l'âge de Fermi peuvent être aisément généralisées pour les cellules de réseaux hétérogènes.

b) Une autre méthode de formulation des équations du bilan de neutrons dans le cas d'un milieu hétérogène applique la conception des probabilités de collision multiples (générations successives) aux courants de neutrons aux interfaces des zones. Cette méthode est formulée d'une manière générale pour L groupes d'énergie et N zones. Elle est appliquée au calcul de l'effet de fission rapide en tenant compte de la rétrodiffusion et des effets d'interaction rapide. La méthode générale comprend comme cas particulier la méthode d'Amouyal et Benoist pour le calcul du facteur d'utilisation thermique.

c) La possibilité pratique d'application de toutes les méthodes relatives aux probabilités de collision dépend essentiellement de l'existence de méthodes convenables pour le calcul de ces probabilités de collision avec une précision suffisante et un volume de calcul acceptable. Des méthodes simplifiées pour le calcul de ces grandeurs sont examinées et jugées du point de vue de leur précision.

A/640 ФРГ

Новые аспекты применения вероятности соударения в теории реакторов

Х. Мэркль

Методы вероятности соударений приобретают все большее значение как полезное и практическое средство в теории реакторов.
В реакторном отделе фирмы «Сименс» было разработано несколько методов расчета, включая использование вероятности соударений. Задачей исследований было обосновать программы расчетов решетки на основе концепции вероятности соударений.

a) Начиная с интегрального уравнения переноса, описывающего нейтронный поток как функцию пространства и энергии, получена система N связанных интегральных уравнений путем деления единичной ячейки на N областей и введения вероятностей столкновения нейтронов при первом пролете. Путем аппроксимации интегральных выражений для гомогенной среды, полученных на основе известной теории термализации Уилкинса, эту теорию можно распространить на гетерогенную среду. Полученная теория сводится к форме, которая легко доступна для численного решения. Метод применим для некоторых случаев, представляющих практический интерес.

Аналогичным образом путем применения изложенной выше концепции к области энергий быстрых и эпитепловых нейтронов расчетные методы замедления, известные как аппроксимации Грюлинга — Гертцеля, Зеленгута — Гертцеля и Ферми-возрастная, могут быть легко обобщены для ячеек гетерогенной решетки.

b) В другом методе формулирования уравнений баланса нейтронов для гетерогенной среды применена концепция вероятностей многократных соударений (последовательных поколений) в сочетании с нейтронными токами на границах зон. Эта процедура сформулирована в общем виде для L энергетических групп и N зон. Этот метод может быть применен для расчета эффекта деления на быстрых нейтронах с учетом обратного рассеяния и эффектов взаимодействия быстрых нейтронов. Метод Амуяла и Бенуаста для расчета коэффициента теплового использования включен в общий метод как частный случай.

Практическая применимость всех названных методов с использованием вероятностей соударений существенным образом зависит от наличия методов, пригодных для вычисления этих вероятностей соударений с разумной точностью. Описаны упрощенные методы расчета этих величин и обсуждается их точность.

A/640 República Federal de Alemania

Nuevos aspectos en la aplicación de las probabilidades de choque en la teoría de reactores

por H. Märkl

Cada vez es más importante el papel de los métodos de probabilidades de choque en el campo de teoría de reactores como herramientas útiles y prácticas. El Departamento de Reactores de Siemens-Schuckertwerke ha desarrollado varios métodos de cálculo que implican el empleo de probabilidades de choque, con el fin de basar el programa de cálculo de redes en un concepto corriente de probabilidad de choque.

a) Partiendo de la ecuación integral de transporte se obtiene un conjunto de N ecuaciones integrales acopladas subdividiendo la celda unitaria en N regiones e introduciendo probabilidades de choque en un primer recorrido.

Tratando las expresiones integrales de modo aproximado, la teoría de termalización de Wilkins para medios homogéneos se amplía a medios heterogéneos. La teoría resultante se reduce a una forma que permite obtener fácilmente una solución numérica.

Análogamente, al aplicar la idea anterior a la región de energías de neutrones rápidos y epitérmicos, los métodos de cálculo de moderación conocidos por aproximaciones de Greuling-Goertzel, de Selengut-Goertzel y de edad de Fermi pueden generalizarse para celdas de redes heterogéneas.

b) Otro método de formular las ecuaciones de equilibrio neutrónico para un medio heterogéneo emplea la idea de probabilidad de choques múltiples (generaciones sucesivas) en relación con las corrientes neutrónicas en las superficies de separación de zonas. Este procedimiento se establece de manera general para L grupos de energía y N zonas. Se aplica el cálculo del efecto de fisión rápida, teniendo en cuenta la retrodispersión y la interacción rápida. El método de cálculo del factor de utilización térmica de Amouyal y Benoist se incluye como un caso particular.

c) La aplicabilidad práctica de todos los métodos que emplean probabilidades de choque depende esencialmente de la disponibilidad de métodos adecuados para calcular estas probabilidades de choque con una precisión aceptable y mediante un trabajo de cálculo admisible. Métodos simplificados para calcular estas magnitudes son examinados y discutidos desde el punto de vista de su precisión.

Statistical theory of neutron chain reactions

By L. Pál*

The customary theory of nuclear reactors is based on the Boltzmann equation, well-known from the kinetic theory of gases. The Boltzmann equation yields the average neutron density for any time, depending on the space co-ordinates and neutron energy, but does not give any information on the fluctuations of the neutron density in multiplying systems. In some cases (critical assemblies, pulsed reactors), however, these fluctuations may become appreciable, when a probabilistic approach to the problem of neutron multiplication is warranted.

FUNDAMENTAL RELATIONS

In order to ensure a simple boundary condition, the consideration will be restricted to multiplying systems of convex geometry, implying that the neutrons, once having left the system, will never return there.

We consider first the multiplication of a single neutron. Let us assume that the reactor at time $t < t_0$ does not contain any free neutrons. At the point $P_{r_0}^{\rightarrow}$ of the reactor V_R, a neutron of energy E_0 with velocity unit vector $\vec{\Omega}_0$ is injected at time t_0. This neutron, which may be called the "triggering" neutron, when first colliding with nuclei of the multiplying system, may cause fission, can be scattered or captured. The neutrons released in the first collision may initiate new branches of the chain reaction, so, because of this repeated multiplication process, the injected neutron will have precisely m descendants at time $t > t_0$ with a certain probability. The number m generally obeys a distribution law with a large variance due to fluctuations in the number of neutrons produced per fission and also in the branch lengths.

The theoretical task is the determination of the probability for finding at time $t > t_0$, in a volume $V_r^{\rightarrow}$ of the reactor V_R, m neutrons with energies below E, with directions of velocity within a cone of angle $\Omega_{\Omega}^{\rightarrow}$ around the unit vector $\vec{\Omega}$, when, at the point $P_{r_0}^{\rightarrow}$ of the neutron free reactor, a neutron of energy E_0 and direction of velocity $\vec{\Omega}_0$ had been injected at time t_0. Denote by

$$p[t_0,\vec{u}_0;\ t,m(\vec{s})] \tag{1}$$

this probability, where for the sake of simplicity the notations

$$\vec{u}_0=(\vec{r}_0,\vec{\Omega}_0,E_0) \text{ and } \vec{s}=(V_r^{\rightarrow},\Omega_{\Omega}^{\rightarrow},E) \tag{2}$$

have been used. The vector $\vec{u}_0$ characterizes the type of the injected neutron, while the vector $\vec{s}$ selects a class for the neutrons produced in the chain reaction. The probability distribution function $p[t_0,\vec{u}_0;\ t,m(\vec{s})]$ at time $t=t_0$ is given by

$$\lim_{t\to t_0} p\ [t_0,\vec{u}_0;\ t,m(\vec{s})]=\Delta(\vec{u}_0,\vec{s}), \tag{3}$$

where

$$\Delta(\vec{u}_0,\vec{s})=\begin{cases}1, \text{ if } \vec{u}_0\in\vec{s}\\ 0, \text{ if } \vec{u}_0\notin\vec{s}.\end{cases} \tag{4}$$

The function $\Delta(\vec{u}_0,\vec{s})$ can be written more explicitly as follows:

$$\Delta(\vec{u}_0,\vec{s})=\Delta(P_{r_0}^{\rightarrow},V_r^{\rightarrow})\Delta(\vec{\Omega}_0,\Omega_{\Omega}^{\rightarrow})\Delta(E_0,E). \tag{5}$$

The reactor is assumed to contain r kinds of atomic nuclei. Denote by $N_1(t_0,\vec{r}_0),\ldots,N_r(t_0,\vec{r}_0)$ the densities of nuclei at time t_0 and at the point $P_{r_0}^{\rightarrow}$. These densities, of course, can be considered as independent of time in a number of cases. Denote further by σ_{jf}, σ_{js} and σ_{jc} $(j=1,\ldots,r)$ the microscopic integral cross sections for fission, scattering and capture respectively while the corresponding macroscopic cross sections are expressed as

$$Q_{jf}=N_j(t_0,\vec{r}_0)\sigma_{jf}(E_0),\ Q_{js}=N_j(t_0,\vec{r}_0)\sigma_{js}(E_0),$$
$$Q_{jc}=N_j(t_0,\vec{r}_0)\sigma_{jc}(E_0). \tag{6}$$

The total cross section is evidently

$$Q_0=\sum_{j=1}^{r}(Q_{jf}+Q_{js}+Q_{jc}). \tag{7}$$

Since the fluctuations of the neutron density are closely related to the fission process we require the probability distribution function for the number of fission neutrons and fragments. Denote by $f_j(E_0;k_0,k_1,\ldots,k_l)$ the probability that in the fission of a type j nucleus k_0 prompt neutrons and $k_1,\ldots,k_l$ fission fragments emitting delayed neutrons are produced after the capture of a neutron with energy E_0. The fission fragments of the type i emit the delayed neutrons of the group i. Since each of the neutron-active fission fragments emits only one delayed neutron the number of delayed neutrons of the group i is the same as the number of i type fission fragments.

Introducing the generating function for the distribution $f_j(E_0,\vec{k})$ in the form

* Central Research Institute for Physics, Budapest.

$$q_j(E_0,\vec{x}) = \sum_{\vec{k}} e^{i\vec{k}\vec{x}} f_j(E_0,\vec{k}) \tag{8}$$

the derivates

$$\left[\frac{\partial q_j(E_0,\vec{x})}{\partial x_l}\right]_{\vec{x}=0} = \nu_{jl}(E_0) \tag{9}$$

and

$$\left[\frac{\partial^2 q_j(E_0,-\vec{x})}{\partial x_l \partial x_{l'}}\right]_{\vec{x}=0} = \nu_{jll'}(E_0) \tag{10}$$

can be used to express both the first and second moments of the number of prompt and delayed neutrons. The energy and velocity direction distribution of the prompt and delayed neutrons are described by the functions

$$R_{j0}^{(t)}(\vec{\Omega}_0,E_0;\vec{\Omega}',E') \text{ and } R_{jl}^{(t)}(\vec{\Omega}_0,E_0;\vec{\Omega}',E').$$

Thus, $R_{jl}^{(t)}(\vec{\Omega}_0,E_0;\vec{\Omega}',E')\mathrm{d}\vec{\Omega}'\mathrm{d}E'$ $(i=0,1,\ldots,l)$ is the probability that the energy of a fission neutron is inside the energy interval $(E',E'+\mathrm{d}E')$ and its direction of velocity is inside the elementary cone $\mathrm{d}\vec{\Omega}'$ provided the energy of the captured neutrons was E_0, and its direction of velocity $\vec{\Omega}_0$. It may be noted that the functions $R_{jl}^{(t)}(\vec{\Omega}_0,E_0,\vec{\Omega}',E')$ $(i=0,1,\ldots,l)$ are almost independent of the variables E_0 and $\vec{\Omega}_0$.

In order to describe the neutron scattering, the density function $R_j^{(s)}(\vec{\Omega}_0,E_0,\vec{\Omega}',E')$ is introduced, $R_j^{(s)}(\vec{\Omega}_0,E_0;\vec{\Omega}',E')\mathrm{d}\vec{\Omega}'\mathrm{d}E'$ being the probability that the energy of the neutron scattered on a nucleus of type j is within the energy interval $(E',E'+\mathrm{d}E')$ and its direction of velocity in the elementary cone $\mathrm{d}\vec{\Omega}'$, provided that before the scattering the energy of the incoming neutron was E_0 and its velocity direction $\vec{\Omega}_0$.

These definitions, as given above, are used in the subsequent calculations.

DETERMINATION OF THE DISTRIBUTION FUNCTION

The distribution function shall be determined by the so-called "first collision method". Let us follow the history of the neutron injected at time t_0 and point $\vec{P}_{r_0}$ of the reactor. In the time interval (t_0,t) the neutron may or may not suffer a collision. In the former case the first collision results either in fission, scattering or capture. From this it is evident that the probability $p[t_0,\vec{u}_0;t,m(\vec{s})]$ is the sum of the probabilities of four mutually excluding events, i.e.

$$p = p_0 + p_t + p_s + p_c. \tag{11}$$

Here p_0 gives the probability that the injected neutron of type $\vec{u}_0$ does not suffer collision in the time interval (t_0,t) and at time $t > t_0, m(\vec{s})$ neutrons are present in the reactor. p_t gives the probability that the first collision of the injected neutron of type $\vec{u}_0$ results in fission in the time interval (t_0,t) and for times $t > t_0, m(\vec{s})$ neutrons are present. The probabilities p_s and p_c can be defined analogously.

First of all let us determine the probability denoted by $T(t_0,\vec{u}_0,t)$ that the neutron injected at time t_0 and point $\vec{P}_{r_0}$ of the reactor does suffer no collision in the time interval (t_0,t). The function $T(t_0,\vec{u}_0,t)$ must have the following property:

$$T(t_0,\vec{u}_0,t) = T(t_0,\vec{u}_0,t')T(t',\vec{u}',t), \quad (t_0 \leq t' \leq t), \tag{12}$$

where

$$\vec{u}' = \{\vec{r}_0 + v_0(t'-t_0)\vec{\Omega}_0,\vec{\Omega}_0,E_0\}.$$

Considering that

$$\lim_{t\to t_0} T(t_0,\vec{u}_0,t) = 1,$$

we find

$$T(t_0,\vec{u}_0,t) = \exp\left\{-v_0\int_{t_0}^{t} Q_0 [t',\vec{r}_0 + v_0(t'-t_0)\vec{\Omega}_0,E_0]\mathrm{d}t'\right\}. \tag{13}$$

The determination of the probability $p_0[t_0,\vec{u}_0;t,m(\vec{s})]$ does not present any difficulties. Simple considerations show that

$$p_0 = T(t_0,\vec{u}_0,t)[\delta_{0m} + (\delta_{1m} - \delta_{0m})\Delta(\vec{u},\vec{s})], \tag{14}$$

where

$$\vec{u} = \{\vec{r}_0 + v_0(t-t_0)\vec{\Omega}_0,\vec{\Omega}_0,E_0\} \text{ and } m = m(\vec{s}).$$

The determination of the probability $p_t[t_0,\vec{u}_0;t,m(\vec{s})]$ is somewhat more involved. In this case the injected neutron does not collide in $(t_0,t')t' \leq t$ while in $(t',t'+\mathrm{d}t')$ causes a fission of a nucleus of type j, resulting in k_0 prompt neutrons and $k_1,\ldots,k_l$ neutron active fission fragments. The prompt and delayed neutrons are similar starting points of the chain reaction as the first, triggering neutron.

Let us denote by $k_{j0}[k_0,t',\vec{u}';t,m_0(\vec{s})]$ the probability that, at time $t, m(\vec{s})$ neutrons are in the reactor, provided that k_0 prompt neutrons were produced in the fission of a j type nucleus by a neutron of type $\vec{u}'$ at time $t' \leq t$. Similarly $k_{jl}[k_l,t',\vec{u}';t,m_l(\vec{s})]$ is the probability that $m_l(\vec{s})$ neutrons are present in the reactor at time t when k_l neutron active fission fragments were produced in a similar fission act.

In the terms of these probabilities we have

$$p_t = v_0\int_{t_0}^{t} T(t_0,\vec{u}_0,t')\left\{\sum_{j=1}^{r} Q_{jl}(t',r',E_0)\sum_{\vec{k}} f_j(E_0,\vec{k}) \times \sum_{m_0+m_1+\ldots+m_l=m} \prod_{i=1}^{l} k_{jl}[k_l,t',\vec{u}';t,m_l(\vec{s})]\right\}\mathrm{d}t', \tag{15}$$

where

$$\vec{r}' = \vec{r}_0 + v_0(t'-t_0)\vec{\Omega}_0.$$

It is easy to show that k_{j0} can be expressed by the probability p, since each of the k_0 prompt neutrons

initiates a chain reaction independent of one another. From this it is evident that

$$k_{j0}=\sum_{n_1+\ldots+n_{k0}=m_0}\prod_{i=1}^{k_0}\int R_{j0}^{(f)}(\vec{u}',\vec{u}'')p[t',\vec{u}'';t,n_i(\vec{s})]\mathrm{d}\vec{u}'', \tag{16}$$

where the following abbreviations are used:

$$R_{j0}^{(f)}(\vec{u}',\vec{u}'')=\delta(\vec{r}'-\vec{r}'')R_{j0}^{(f)}(\vec{\Omega}_0,E_0;\vec{\Omega}'',E''),$$

$$\mathrm{d}\vec{u}''=\mathrm{d}V_{\vec{r}''}\mathrm{d}\vec{\Omega}''\mathrm{d}E''.$$

In the course of the determination of k_{ji} use will be made of the probability $O_{ji}(t',\vec{u}';t,n_i)$ that at time $t,n_i(\vec{s})$ neutrons are present in the reactor, provided that the chain reaction was initiated in the interval (t',t) by the delayed neutron of an i type fission product.

It is not difficult to see that

$$O_{ji}=\lambda_{ji}\int_{t'}^{t}\mathrm{e}^{-\lambda_{ji}(t''-t')}\int R_{ji}^{(f)}(\vec{u}',\vec{u}'')p[t'',\vec{u}'';t,n_i(\vec{s})]\,\mathrm{d}\vec{u}''\mathrm{d}t'', \tag{17}$$

where

$$R_{ji}^{(f)}(\vec{u}',\vec{u}'')=\delta(\vec{r}'-\vec{r}'')R_{ji}^{(f)}(\vec{\Omega}_0,E_0,\vec{\Omega}'',E'').$$

Making use of Eq. (17), the probability k_{ji} can be brought into the following form:

$$k_{ji}=\sum_{k'_i=0}^{k_i}\binom{k_i}{k'_i}\mathrm{e}^{-\lambda_{ji}(k_i-k'_i)(t-t')}\sum_{n_1+\ldots+n_{k'_i}=m_i}\prod_{i=0}^{k'_i}O_{ji}[t',\vec{u}';t,n_i(\vec{s})]. \tag{18}$$

The probability $p_s[t_0,\vec{u}_0;t,m(\vec{s})]$ can be readily obtained by assuming the injected $\vec{u}_0$ type neutron to be scattered in the first collision, since then

$$p_s=\nu_0\int_{t_0}^{t}T(t_0,\vec{u}_0,t')\{\sum_{j=1}^{r}Q_{js}(t',\vec{r}',E_0)\int R_j^{(s)}(\vec{u}',\vec{u}'')p[t',\vec{u}'';t,m(\vec{s})]\mathrm{d}\vec{u}''\}\mathrm{d}t', \tag{19}$$

where

$$R_j^{(s)}(\vec{u}',\vec{u}'')=\delta(\vec{r}'-\vec{r}'')R_j^{(s)}(\vec{\Omega}_0,E_0;\vec{\Omega}'',E'').$$

Finally, we formulate the probability p_c as

$$p_c=\nu_0\delta_{0m}\int_{t_0}^{t}T(t_0,\vec{u}_0,t')\{\sum_{j=1}^{r}Q_{jc}(t',\vec{r}',E_0)\}\mathrm{d}t'. \tag{20}$$

Equations (14), (15), (19) and (20) yield the equation to the distribution function.

THE GENERATING FUNCTION

For the sake of a more convenient formalism the generating function g of the distribution function p is introduced by the definition

$$g[t_0,\vec{u}_0;t,z(\vec{s})]=\sum_{m=0}^{\infty}\mathrm{e}^{m(\vec{s})z(\vec{s})}p[t_0,\vec{u}_0;t,m(\vec{s})]. \tag{21}$$

It can be shown that the generating function obeys the non-linear integral equation:

$$g[t_0,\vec{u}_0;t,z(\vec{s})]=T(t_0,\vec{u}_0,t)\{1+\Delta(\vec{u},\vec{s})[\mathrm{e}^{z(\vec{s})}-1]\}+\nu_0\sum_{j=1}^{r}\int_{t_0}^{t}T(t_0,\vec{u}_0,t')\times\{Q_{jc}(t',\vec{r}',E_0)+Q_{js}(t',\vec{r}',E_0)\int R_j^{(s)}(\vec{u}',\vec{u}'')g[t',\vec{u}'';t,z(\vec{s})]\mathrm{d}\vec{u}''+Q_{jt}(t',\vec{r}',E_0)q_j[E_0,\vec{x}_j(t',\vec{u}';z(\vec{s}))]\}\mathrm{d}t' \tag{22}$$

The components of the vector $\vec{x}_j=(x_{j0},x_{j1},\ldots,x_{jl})$ appearing in the argument of q_j are given by the relations

$$x_{j0}=\log\int R_{j0}^{(f)}(\vec{u}',\vec{u}'')g[t',\vec{u}'';t,z(\vec{s})]\mathrm{d}\vec{u}'' \tag{23}$$

and

$$x_{ji}=\log\{\mathrm{e}^{-\lambda_{ji}(t-t')}+\lambda_{ji}\int_{t'}^{t}\mathrm{e}^{-\lambda_{ji}(t''-t')}\int_{(i=1,\ldots,l)}R_{ji}^{(f)}(\vec{u}',\vec{u}'')g[t'',\vec{u}'';t,z(\vec{s})]\,\mathrm{d}\vec{u}''\mathrm{d}t''\} \tag{24}$$

The derivation of Eq. (22) with respect to t_0 leads to an integro-differential equation similar to the well known kinetic equation. Considering Eq. (12) we get

$$\frac{\partial g(t_0,\vec{u}_0;t,z)}{\partial t_0}+\hat{T}g(t_0,\vec{u}_0;t,z)+\nu_0\sum_{j=1}^{r}\{Q_{jc}+Q_{jt}q_j(E_0,\vec{x}_j]\}=0, \tag{25}$$

where $\hat{T}$ is the so-called transport operator defined by

$$\hat{T}g(t_0,\vec{u}_0;t,\vec{z})=-\nu_0Q_0(t_0,\vec{r}_0,E_0)g(t_0,\vec{u}_0;t,z)+\nu_0\vec{\Omega}_0\cdot\mathrm{grad}_{r_0}g(t_0,\vec{u}_0;t,z)+\nu_0\sum_{j=1}^{r}Q_{js}(t_0,\vec{r}_0,E_0)+\int R_j^{(s)}(\vec{u}_0,\vec{u}')g(t_0,\vec{u}';t,z)\,\mathrm{d}\vec{u}' \tag{26}$$

Now, we have to formulate the initial and the boundary conditions. The former is obtained from Eq. (22) as

$$\lim_{t\to t_0}g(t_0,\vec{u}_0;t,z)=1+\Delta(\vec{u}_0,\vec{s})(\mathrm{e}^z-1) \tag{27}$$

The boundary condition has to take account of the obvious fact that no chain process can be started by the neutron injected at a surface point of a convex reactor when the neutron velocity makes an acute angle with the outward pointing surface normal. Denoting by $\vec{\Omega}_S$ the outward pointing surface normal in the surface point $\vec{P}_{r_s}$, the boundary condition can be formulated in the following way:

$$\lim.\ g(t_0,\vec{u}_0;t,z)=1\ \text{if}\ (\vec{\Omega}_0\cdot\vec{\Omega}_S)>0. \tag{28}$$

It is apparent from Eq. (25) that the nature of the fluctuations in the neutron multiplication is governed essentially by the probability distribution function $f_j(E_0,\vec{k})$ the form of which can be obtained from the experimental data.

GENERALIZATIONS

Since the above considerations have been restricted to chain processes started by single neutrons of type $\vec{u}_0$,

for the study of practical cases chain processes started by random neutron injection must be investigated as well. The probability that in the interval (t_0,t) exactly k triggering neutrons are injected into the reactor can be expressed as

$$L_k(t_0,t)=\frac{1}{k!}\{\int_{t_0}^{t} i(t')\,dt'\}^k \exp\{-\int_{t_0}^{t} i(t')\,dt'\}, \quad (29)$$

where $i(t')$ is the neutron source intensity at time t'. The distribution of the injected neutrons with respect to type is given by the density function $F(\vec{u_0})$. Let us denote by $P[t_0,t,m(\vec{s})]$ the probability that $m(\vec{s})$ neutrons are present in the reactor at time t, provided that the injection of triggering neutrons has commenced in the time $t_0 \leq t$ and up to the time t_0 there was no free neutron in the system.

Supposing that in (t_0,t) exactly k neutrons had been injected into the reactor, the probability that the injection of any one of them falls into the interval $(t',t'+dt')$, is clearly

$$i(t')\,dt'/\int_{t_0}^{t} i(t')\,dt'.$$

In this manner we find

$$u[t_0,t,m(\vec{s})]=[\int_{t_0}^{t} i(t')\,dt']^{-1} \int_{t_0}^{t} i(t')\int F(\vec{u'})p[t',\vec{u'};t,m(\vec{s})]\,d\vec{u'}dt'. \quad (30)$$

This expression gives the probability that at time t, $m(\vec{s})$ neutrons are found in the reactor when a single triggering neutron had been injected in (t_0,t) into the system. With the help of Eq. (29) we get:

$$P[t_0,t,m(\vec{s})]=\sum_{k=0}^{\infty} L_k(t_0,t) \sum_{m_1+\ldots+m_k=m} \prod_{i=1}^{k} u[t_0,t,m_i(\vec{s})]. \quad (31)$$

Denoting the generating function of $P(t_0,t,m)$ by $G(t_0,t,z)$ Eq. (31) leads to

$$\log G[t_0,t,z(\vec{s})]=\int_{t_0}^{t} i(t')\{\int F(\vec{u'})g[t',\vec{u'};t,z(\vec{s})]\,d\vec{u'}-1\}\,dt'. \quad (32)$$

Defining now the average intensity as

$$i_0=\frac{1}{t-t_0}\int_{t_0}^{t} i(t')\,dt' \quad (33)$$

and putting $i_0(t')=i(t')/i_0$ (34)

Eq. (32) becomes

$$\log G[t_0,t,z(\vec{s})]=i_0\int_{t_0}^{t} i_0(t') \int F(\vec{u'})\{g[t',\vec{u'};t,z(\vec{s})]-1\}\,d\vec{u'}dt'. \quad (35)$$

If i_0 is large enough the central limit theorem can be applied to get the asymptotical form of the distribution function.

If

$$i_0(t')=\lim_{t'_0\to 0}\delta(t_0+t'_0-t') \quad (36)$$

then all triggering neutrons are injected at time t_0. In this case, that of the pulsed neutron injection, Eq. (35) is somewhat simpler:

$$\log G[t_0,t,z(\vec{s})]=i_0\int F(\vec{u_0})\{g[t_0,\vec{u_0};t,z(\vec{s})]-1\}\,d\vec{u_0}. \quad (37)$$

In a number of practical problems the distribution function

$$P[t_0,t,m_1(\vec{s_1}),m_2(\vec{s_2})] \quad (38)$$

is needed. Here the classes $\vec{s_1}=(\vec{V_{r_1}},\vec{\Omega_{\Omega_1}},E_1)$ and $\vec{s_2}=(\vec{V_{r_2}},\vec{\Omega_{\Omega_2}},E_2)$ are entirely different. Two classes are entirely different, when neither of their volume, solid angle and energy intervals contain any common points. With similar arguments as above, the generating function

$$G[t_0,t,z_1(\vec{s_1}),z_2(\vec{s_2})]=\sum_{m_1,m_2} \exp\{m_1(\vec{s_1})z_1(\vec{s_1}) +m_2(\vec{s_2})z_2(\vec{s_2})\}P[t_0,t,m_1(\vec{s_1}),m_2(\vec{s_2})] \quad (39)$$

leads to the equation

$$\log G(t_0,t,z_1,z_2)=i_0\int_{t_0}^{t} i_0(t') \int F(\vec{u'})\{g(t',\vec{u'};t,z_1,z_2)-1\}\,d\vec{u'}dt', \quad (40)$$

where $g(t',\vec{u'};t,z_1,z_2)$ satisfies an equation of the form (25). The initial condition is given by

$$\lim_{t\to t_0} g[t_0,\vec{u_0};t,z_1(\vec{s_1}),z_2(\vec{s_2})] =1+\Delta(\vec{u_0},\vec{s_1})[e^{z(\vec{s_1})}-1]+\Delta(\vec{u_0},\vec{s_2})[e^{z(\vec{s_2})}-1], \quad (41)$$

while the boundary condition is the same as expressed by Eq. (28).

Finally, we have to evaluate the probability $W(t_0,t_1,t,m)$ that a neutron detector placed into the multiplying system counts exactly m neutrons in the interval (t_0,t) provided the injection of triggering neutrons has commenced at time t_0. The time t_1, is an independent parameter characterizing the start of the counting. It is obvious that $t_1 \leq t$ and $t_0 \lesssim t_1$. We shall consider an absorption type detector, with probability $\epsilon(\vec{r_0},E_0)\,dt$ for detecting a neutron of energy E_0 at the point $P_{\vec{r_0}}$ in the interval $(t,t+dt)$. Without repeating the now familiar considerations the generating function

$$H(t_0,t_1,t,z)=\sum_{m=0}^{\infty} e^{mz}W(t_0,t_1,t,m)$$

can be written in the form

$$\log H(t_0,t_1,t,z)=i_0\int_{t_0}^{t} i_0(t') \int F(\vec{u'})\{h(t',\vec{u'},t_1;t,z)-1\}\,d\vec{u'}dt', \quad (42)$$

where

$$h(t',\vec{u}';t_1;t,z)=\sum_{m=0}^{\infty} e^{mz}w(t',\vec{u}',t_1;t,m).$$

The distribution function $w(t_0,\vec{u}_0,t_1;t,m)$ describes here the chain process started by a single neutron injected at time t_0. It can be readily seen that the generating function $h(t_0,\vec{u}_0,t_1;t,z)$ satisfies the equation

$$\frac{\partial h(t_0,\vec{u}_0,t_1;t,z)}{\partial t_0}+\hat{T}h(t_0,\vec{u}_0,t_1;t,z)+\nu_0 Q_c$$

$$+\nu_0 Q_c+\nu_0\sum_{j=1}^{r} Q_{jt}q_j[E_0,\vec{v}_j]+s(t_0,t_1,\vec{r}_0,E_0,z)=0, \quad (43)$$

where

$$s(t_0,t_1,\vec{r}_0,E_0,z)=\epsilon(\vec{r}_0,E_0)(e^z-1)\Delta(t_0-t_1) \quad (44)$$

and

$$\nu_0 Q_c=\epsilon+\nu_0\sum_{j=1}^{r} Q_{jc}.$$

The components of the vector $\vec{y}_j$ are defined by Eq. (23, 24) when g is replaced throughout by h. The initial condition for Eq. (43) is now:

$$\lim_{t\to t_0} h(t_0,\vec{u}_0,t_1;t,z)=1$$

while the boundary condition is the same as that for g.

It may be noted that for two detectors the generating function

$$H(t_0,t_1,t_2;t,z_1,z_2)=\sum_{m_1m_2} e^{m_1z_1+m_2z_2}$$

$$W(t_0,t_1,t_2;t,m_1,m_2) \quad (45)$$

can be derived in a form similar to Eq. (42) with the only difference that the singular term in the equation for $h(t_0,\vec{u}_0,t_1,t_2;t,z_1,z_2)$ differs from the expression (44) since

$$s(t_0,t_1,t_2,\vec{r}_0,E_0,z)=\epsilon_1(\vec{r}_0,E_0)(e^{z_1}-1)\Delta(t_0-t_1)$$

$$+\epsilon_2(\vec{r}_0,E_0)(e^{z_2}-1)\Delta(t_0-t_2) \quad (46)$$

while the initial and boundary conditions are unchanged.

MULTIGROUP DIFFUSION APPROXIMATION

To facilitate the application of the general equations, the considerations are now restricted to a simplified model of the process. The neutron energies are restricted to the interval (E_0,E_n). Dividing this into sub-intervals:

$$(E_0,E_1),(E_1,E_2),\ldots,(E_{n-1},E_n).$$

The neutrons with energies in the sub-interval (E_{k-1},E_k) are termed to be neutrons of the group k. Denoting by $\mathcal{G}_k(t)$ the number of neutrons of group k at time t in the volume $V_{\vec{r}}$ of the reactor V_R, it is obvious that the vector

$$\vec{\mathcal{G}}(t)=\{\mathcal{G}_1(t),\mathcal{G}_2(t),\ldots,\mathcal{G}_n(t)\}$$

completely describes the neutron distribution in the volume $V_{\vec{r}}$ with respect to energy groups. Now we have to determine the probability $p_k(t,\vec{r}_0,\vec{m})$ that $\vec{\mathcal{G}}(t)=\vec{m}$ with the assumption that at time $t=0$ and point $P_{\vec{r}_0}$ a neutron of group k has been injected into the neutron-free reactor.

In order to obtain the generating function g_k of the probability p_k, both the group cross sections and the transition probabilities have to be given. The macroscopic cross sections of j type nuclei for fission, scattering and capture in the case of k group neutrons are Q_{jtk}, Q_{jsk}, and Q_{jck}, respectively. By f_{jk} $(k_0,k_1,\ldots k_l)$ we define the probability that the fission of a nucleus of type j induced by a neutron of group k produces k_0 prompt neutrons and $k_1,\ldots,k_l$ fission fragments. $R_j^{(s)}(k,k')$ is the probability that a neutron of group k will be scattered by a j type nucleus into a group k', while $R_{jt}^{(f)}(k,k')$ gives the probability that the fission neutron is of group k' when the fission has been induced by a neutron of group k.

The motion of the neutron of group k is assumed to be governed by the elementary diffusion equation. Let us denote by $T_k(t,\vec{r}_0,\vec{r})\,dV_{\vec{r}}$ the probability that at time $t>0$ a neutron of group k, can be found in the volume $dV_{\vec{r}}$, if at time $t=0$ it has been at the point $P_{\vec{r}_0}$. This probability distribution function satisfies the equation

$$\frac{\partial T_k(t,\vec{r}_0,\vec{r})}{\partial t}=D_k\Delta_{\vec{r}_0}T_k(t,\vec{r}_0,\vec{r})=D_k\Delta_{\vec{r}}T_k(t,\vec{r}_0,\vec{r}), \quad (47)$$

where D_k is the diffusion coefficient for neutrons of group k. The initial and boundary conditions for Eq. (47) are given by

$$T_k(0,\vec{r}_0,\vec{r})=\delta(\vec{r}_0-\vec{r}) \quad (48)$$

and

$$\lim_{\vec{r}_0\to\vec{r}_S} T_k(t,\vec{r}_0,\vec{r})=\lim_{\vec{r}\to\vec{r}_S} T_k(t,\vec{r}_0,\vec{r})=0 \quad (49)$$

respectively. Here the vector $\vec{r}_S$ sweeps through the points $P_{\vec{r}_S}$ of the extrapolated reactor surface. By describing the motion of the k group neutrons with the function $T_k(t,\vec{r}_0,\vec{r})$, the anisotropy of the scattering has been ignored.

For the generating function

$$g_k(t,\vec{r}_0,\vec{z})=\sum_{\vec{m}} e^{\vec{m}\vec{z}}p_k(t,\vec{r}_0,\vec{m}) \quad (50)$$

we get with the now familiar reasoning

$$\frac{\partial g_k(t,\vec{r}_0\vec{z})}{\partial t}=\hat{T}_k g_k(t,\vec{r}_0,\vec{z})$$

$$+\nu_k\sum_{j=1}^{r}\{Q_{jck}+Q_{jtk}q_{jk}(\vec{x}_{jk})\}. \quad (51)$$

In the diffusion approximation the operator $\hat{T}_k$ has the form

$$\hat{T}_k g_k(t,\vec{r}_0,\vec{z}) = D_k \Delta_{\vec{r}_0 \to g}(t,\vec{r}_0,\vec{z}) + \nu_k \sum_{j=1}^{r} Q_{jsk} \sum_{k'=1}^{n} R_j^{(s)}(k,k') \times g_{k'}(t,\vec{r}_0,\vec{z}) - \nu_k Q_{0k} g_k(t,\vec{r}_0,\vec{z}) \quad (52)$$

where

$$Q_{0k} = \sum_{j=1}^{r} \{Q_{jck} + Q_{jsk} + Q_{jfk}\}.$$

The components of the vector $\vec{x}_{jk}$ are now given by

$$x_{jk0} = \log \left\{ \sum_{k'=1}^{n} R_{j0}^{(t)}(k,k') g_{k'}(t,\vec{r}_0,\vec{z}) \right\}, \quad (53)$$

$$x_{jki} = \log \{ e^{-\lambda_{ji} t} + \lambda_{ji} \sum_{k'=1}^{n} R_{ji}^{(t)}(k,k') \int_0^t e^{-\lambda_{ji} t'} g_{k'}(t-t',\vec{r}_0,\vec{z})\, dt' \}. \; (i = 1,2,\ldots,l) \quad (54)$$

The initial and boundary conditions can be easily given:

$$g_k(0,\vec{r}_0,\vec{z}) = 1 + \Delta(P_{\vec{r}_0}, V_{\vec{r}})(e^{z_k} - 1) \quad (55)$$

$$\lim_{\vec{r}_0 \to \vec{r}_S} g_k(t,\vec{r}_0,\vec{z}) = 1. \quad (56)$$

The generating function $G(t,\vec{z})$ of the distribution function $P(t,\vec{m})$ can be constructed from the function $g_k(t,\vec{r}_0,\vec{z})$ as follows:

$$\log G(t,\vec{z}) = i_0 \int_0^t i_0(t') \sum_{k=1}^{n} \int F_k(\vec{r}_0) \{ g_k(t-t',\vec{r}_0,\vec{z}) - 1 \}\, dV_{\vec{r}_0} dt'. \quad (57)$$

CONCLUSIONS

The general statistical theory of chain reactions permits the solution of a number of practically important problems. The theory was used to compute the fluctuations in the neutron yield of pulsed reactors. The fluctuations in the number of neutrons per pulse was shown to be strongly dependent on the number of triggering neutrons. The details of these calculations are to be found in Ref. [1].

Another use of the statistical method was to investigate the effect of delayed neutrons on the accuracy of prompt period measurements. For thermal neutrons the criteria for the applicability of the Rossi method were determined. The theory underlying the Moguilner method has been developed. It has been shown that this method is applicable for measuring the prompt period. According to this method the prompt period is calculated from the experimentally obtained probability of zero counting in a given time interval. The detailed theoretical discussion of this method is given in Ref. [2].

REFERENCES

1. Pál, L., and Németh, Gy., *Pile neutron research in physics*, IAEA, Vienna, 491 (1962).

2. Pál, L., Reactor Sci. Technol./J. Nucl. Energy, Parts A/B/, *17*, 395 (1963).

ABSTRACT—RÉSUMÉ—АННОТАЦИЯ—RESUMEN

A/652 Hongrie

Théorie statistique des réactions neutroniques en chaîne

par L. Pál

L'auteur a mis au point une théorie statistique des réactions en chaîne dans les réacteurs. Il a établi la fonction de distribution de probabilité pour le nombre de neutrons se trouvant dans un état donné, avec des hypothèses d'un caractère tout à fait général. A partir de cette fonction, on obtient l'équation fondamentale de la fonction génératrice, laquelle permet de calculer la valeur probable et la variance de la densité des neutrons. On établit des équations pour la fonction de distribution de probabilité du nombre de fissions et de neutrons comptés au cours d'une période donnée. On établit plusieurs théorèmes aux limites pour les fonctions génératrices. Ces théorèmes jouent un rôle important dans diverses applications de la théorie. On tient compte de l'approximation multigroupe dans le cadre de la théorie statistique.

A/652 Венгрия

Статистическая теория цепных реакций в ядерных реакторах

Л. Пал

Разработана статистическая теория цепных реакций в ядерных реакторах. Определяется функция распределения (ФР) числа нейтронов, находящихся в данном состоянии, при довольно общих предположениях. Из ФР выводится фундаментальное уравнение для производящей функции, которая позволяет получить линейное интегро-дифференциальное уравнение не только для средней нейтронной плотности, но и для ее дисперсии. Рассматриваются ФР числа делений и ФР числа нейтронов, зарегистрированных в определенном промежутке времени. Для предельных распределений доказываются некоторые теоремы, которые используются в приложениях. Развивается многогрупповое приближение в рамках статистической теории.

A/652 Hungría

Teoría estadística de las reacciones neutrónicas en cadena

por L. Pál

Se desarrolla una teoría estadística para reacciones en cadena en reactores nucleares. Basándose en hipótesis bastante generales, se deduce la función de distribución de la probabilidad del número de neutrones en un estado (PDF) De esta PDF se deduce la ecuación fundamental para la función generatriz, lo que permite calcular el valor esperado y su varianza para la densidad neutrónica. Se deducen ecuaciones para la PDF del número de fisiones y neutrones medidos por unidad de tiempo. Para las funciones generatrices se deducen varios teoremas de límites que tienen importancia en algunas aplicaciones. Se introduce la aproximación de multigrupo en el esquema de la teoría estadística.

A method for calculating collision probabilities in general cylindrical geometry and applications to flux distributions and Dancoff factors

By I. Carlvik*

The collision probability method for calculating neutron flux distributions is acquiring increasing attention, particularly for its application to reactor lattice cells. The characteristic feature of this method is the calculation of the collision probability matrix. Once this matrix has been obtained, or, in the case of more than one energy group, after the collision probability matrices and the scattering matrices have been obtained, the problem of solving the flux is reduced to the problem of solving a system of simultaneous linear equations.

Reactor lattice cells are often taken as cylindrical for computational purposes, and collision probability codes have been devised for the calculation of flux distributions in annular geometry, for example the spectrum programme THERMOS [1,2]. Several approximations of a physical nature have been proposed in order to facilitate the calculation of the collision probability matrix for an annular system [3,4,5,6,7]. Other approximations have been proposed for cluster geometry, e.g., the use of elementary cells [8].

The approach made in the present paper is to refrain from approximations of this kind, and to look for other methods to facilitate the calculation of the collision probabilities. It is shown how an efficient Gauss integration can be used in the annular case to the effect that quite accurate collision probabilities can be calculated in a rather short time. Two computer codes for calculating flux distributions in one group will be described briefly, FLURIG for the annular case and CLUCOP for the cluster case.

For the closely connected problem of calculating Dancoff factors approximation schemes similar to those for the flux distribution have been proposed [9,10,11]. The approach chosen for this work was to calculate tables of Dancoff factors using a direct method, and to try to approximate the tables with suitable functions. Hexagonal clusters containing 7, 19, and 37 rods and an infinite square lattice of circular rods were considered.

THE PHYSICAL MODEL

Consider a system consisting of a number of cylindrical homogeneous regions. The system is divided into another set of homogeneous regions which either coincide with or are subdivisions of the regions of the first set. A stationary case with a prescribed neutron source density, constant in each region, is considered. Only the one-group approximation is considered, the generalization to a multi-group model being obvious. Then the following equation is valid for each region

$$V_i\Sigma_i\bar{\phi}_i=\sum_j V_j(S_j+\Sigma_{sj}\bar{\phi}_j)P_{i,j} \qquad (1)$$

where V_i is the volume, Σ_i the total cross section, $\bar{\phi}_i$ the average neutron flux density, S_i the source density and Σ_{si} the scattering cross section of the i^{th} region. $P_{i,j}(P_{i\leftarrow j})$ is the probability that neutrons starting in region j will make their next collision in region i.

$P_{i,j}$ depends upon the spatial and angular distribution of the neutron flux in region j. The common version of the collision probability method replaces the correct $P_{i,j}$ with the corresponding quantity for a flat and isotropic source distribution. This is equivalent to making two assumptions:

(*a*) The scattering is isotropic. Usually the cross sections are transport corrected.

(*b*) Neutrons which are scattered in a region are distributed uniformly over the region before they start again.

BASIC PRINCIPLES

Fundamental equations for cylindrical geometry

It is appropriate to eliminate the axial co-ordinate from the beginning, and to study the system in the plane perpendicular to the axis. Then in a way the role of the exponential function is taken over by Bickley functions. This step has been used for many years.

First the probability will be determined, that neutrons from a line source, which are emitted isotropically in a small azimuthal angle element $d\alpha$, will travel so far without colliding that the projection of the path on the plane will be τ measured in optical units. With notations according to Fig. 1, the fraction of uncollided neutrons at τ in the solid angle element $\sin\theta\, d\theta\, d\alpha$ is $\exp\left(-\frac{\tau}{\sin\theta}\right)$. The desired probability is

* A.B. Atomenergi, Stockholm.

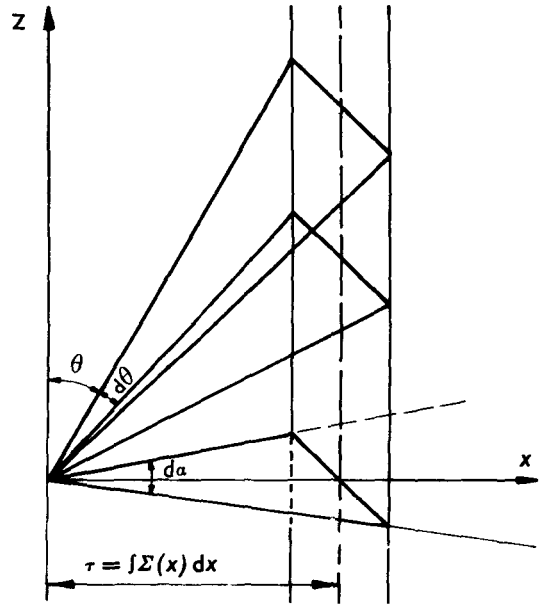

Figure 1. Elimination of the z co-ordinate in cylindrical geometry

obtained by integrating over θ and dividing by the total solid angle 2 dα

$$P(\tau)=\frac{1}{2\,\mathrm{d}\alpha}\int_{-\frac{\pi}{2}}^{+\frac{\pi}{2}}\exp\left(-\frac{\tau}{\sin\theta}\right)\sin\theta\,\mathrm{d}\theta\,\mathrm{d}\alpha=Ki_2(\tau) \quad (2)$$

The Ki_n-functions were defined by Bickley and Nayler [12] as

$$Ki_n(x)=\int_0^\infty \frac{\mathrm{e}^{-x\cosh u}}{\cosh^n u}\,\mathrm{d}u \quad (3)$$

Then the probability for neutrons starting uniformly and isotropically in a homogeneous cylindrical region to make their first collision in another such region will be derived.

The probability (Fig. 2) for neutrons starting along the line in region j inside dα to make the first collision in region i is

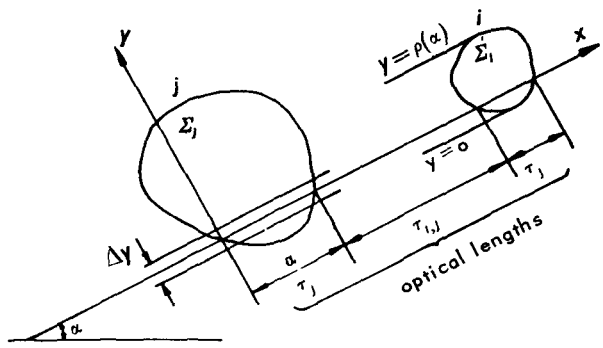

Figure 2. Calculation of collision probabilities in cylindrical geometry

$$P_{i,j}(a,y)=\frac{1}{a}\int_0^a[Ki_2(\Sigma_j(a-x)+\tau_{i,j})-Ki_2(\Sigma_j(a-x)+\tau_{i,j}+\tau_i)]\,\mathrm{d}x=\frac{1}{\Sigma_j a}[Ki_3(\tau_{i,j})-Ki_3(\tau_{i,j}+\tau_j)-Ki_3(\tau_{i,j}+\tau_i)+Ki_3(\tau_{i,j}+\tau_j+\tau_i)] \quad (4)$$

The total collision probability is obtained by multiplying this expression by the volume element $a\,\mathrm{d}y$ and the angular element dα, integrating over y and α (that is over those regions where the line crosses both bodies) and dividing the result by $2\pi V_j$. (V_j is the volume of body j).

$$\Sigma_j V_j P_{i,j}=\frac{1}{2\pi}\int\mathrm{d}\alpha\int\mathrm{d}y[Ki_3(\tau_{i,j})-Ki_3(\tau_{i,j}+\tau_j)-Ki_3(\tau_{i,j}+\tau_i)+Ki_3(\tau_{i,j}+\tau_j+\tau_i)] \quad (5)$$

Diagonal elements are given by a slightly different expression

$$\Sigma_i V_i P_{i,i}=\Sigma_i V_i-\frac{1}{2\pi}\int\mathrm{d}\alpha\int\mathrm{d}y[Ki_3(0)-Ki_3(\tau_i)] \quad (6)$$

The expression for $\Sigma_j V_j P_{i,j}$ is symmetric in i and j. Thus this derivation proves the reciprocity theorem for bodies of cylindrical geometry

$$\Sigma_j V_j P_{i,j}=\Sigma_i V_i P_{j,i} \quad (7)$$

Boundary conditions

The computer codes referred to in this paper use white boundary conditions at the cell boundary, that is all neutrons passing out over the cell boundary return with an angular distribution as if they came from a constant source distribution in a homogeneous half-space outside the boundary. This boundary condition is very easy to apply. After the $\Sigma_j V_j P_{i,j}$-matrix has been computed (assuming black boundary) the vector R_j defined as

$$R_j=\Sigma_j V_j-\sum_i \Sigma_j V_j P_{i,j} \quad (8)$$

is calculated. It is easy to show using the reciprocity theorem that

$$\Sigma_j V_j P_{i,j}^{\text{white}}=\Sigma_j V_j P_{i,j}^{\text{black}}+R_i R_j[\textstyle\sum_j R_j]^{-1} \quad (9)$$

The method of integration

For the numerical calculation of the ΣVP-matrix, sets of parallel lines are drawn across the system, all intersections with boundaries are determined and the segments of the lines lying in each region are measured. Then the segments are multiplied by their respective cross sections, the intersections are taken in pairs, the Ki_3-function for the optical distance between the points in each pair is computed and multiplied by the appropriate dy, and the results are added to the appropriate (generally 4) elements in the matrix. The Ki_3-routine used in the present work was derived by B. Tollander [13]. It uses polynomials of order 6 or

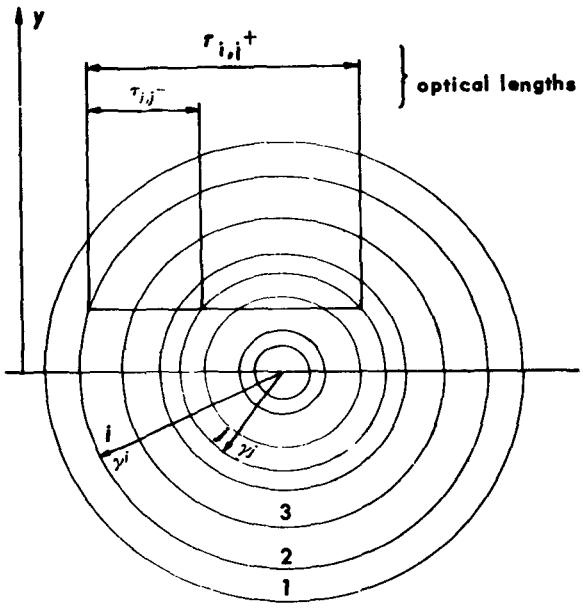

Figure 3. Calculation of collision probabilities in annular geometry

less in 6 regions of the argument and the maximum absolute error of the approximation is 3×10^{-5}.

APPLICATION TO ANNULAR GEOMETRY

In annular geometry no integration over the azimuthal angle is needed. It is also possible to use an efficient Gauss integration. The principles of a method which was used in a programme called "Flurig" will be described. Using the notations of Fig. 3 and applying the results of the preceding section one obtains using the Kronecker δ

$$\Sigma_j V_j P_{i,j} = \delta_{i,j}\Sigma_i V_i + 2\,[S_{i,j} - S_{i+1,j} - S_{i,j+1} + S_{i+1,j+1}] \quad (10)$$

$$S_{i,j} = \int_0^{\max(r_i, r_{i-1})} [Ki_3(\tau_{i,j}^-) - Ki_3(\tau_{i,j}^+)]\,dy \quad (11)$$

The integration over y in Eq. (11) is split up into elementary intervals from r_i to r_{i-1}. The integrands are either regular in the elementary intervals or they have a singularity of the type $Ki_3\,[f(y) + \sqrt{r_{i-1} - y}\,g(y)]$, where $f(y)$ and $g(y)$ are regular functions. $Ki_3(z)$ behaves as $z^3 \ln z$ in the vicinity of $z = 0$. Four different sets of Gauss constants were derived taking the type of singularity into account. Tests on various systems showed that a set based on the assumption that the integrands should be expandable in a power series of $\sqrt{r_{i-1} - y}$ was as good as more complicated sets based on logarithms. The Flurig code can use up to 5 Gauss points per interval but it has been found in practical calculations that 2 points per interval is usually sufficient.

Some computing times from a cell calculation with 20 regions are:

Number of Gauss points	Net computing time on Ferranti Mercury, seconds	Absolute difference in flux in % from 4-point calculation	
		Innermost region	Maximum in all other regions
1 . . .	35	2.5	0.7
2 . . .	53	0.7	0.2
4 . . .	90	—	—

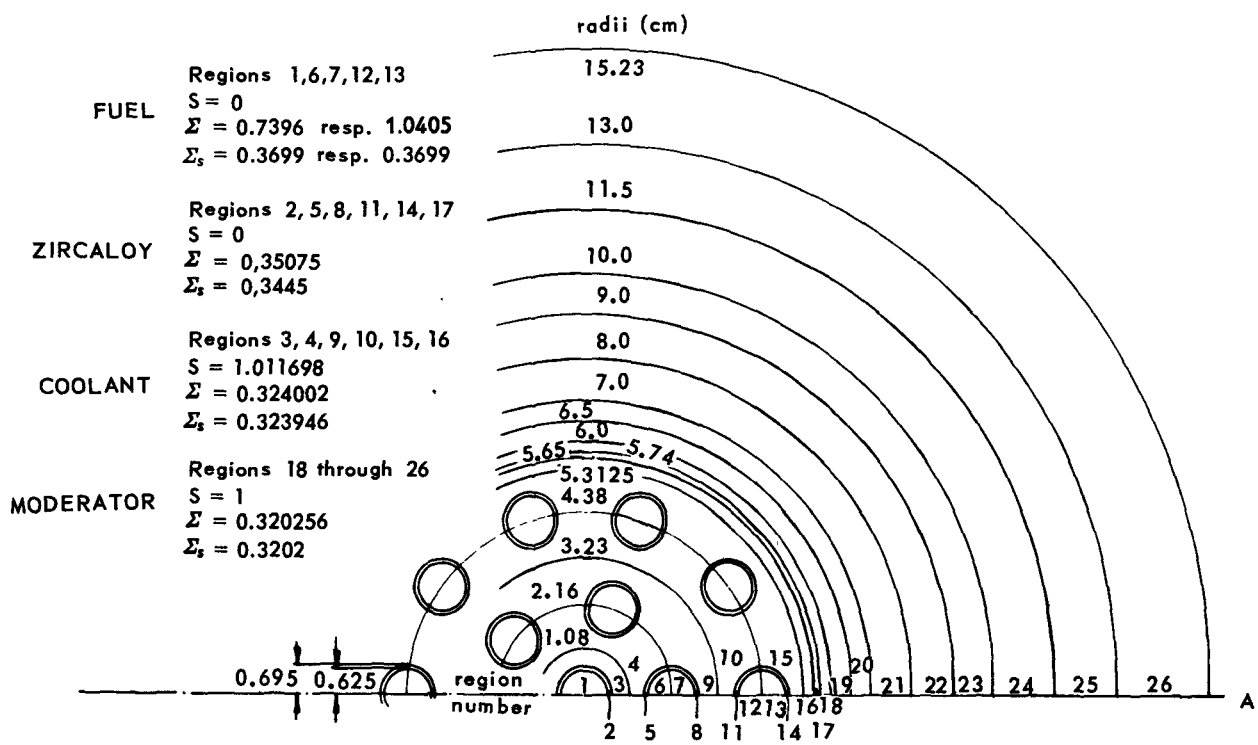

Figure 4. Cluster cell

These times compare favourably with times necessary for S_4-calculations on the same problem.

APPLICATION TO CLUSTER GEOMETRY

The basic principles given above were used for a programme Clucop, which calculates collision probabilities in one group for a cluster cell and calculates the flux distribution with a given source distribution.

The integration over the cluster region uses equidistant lines, and the Flurig-method is used in the part where only concentric annuli are involved. The speed and suitability of a programme of this kind depends to a large extent upon a clever choice of the geometrical variety allowed, and it was decided to use rather limited geometrical possibilities in the programme to guarantee its proper operation.

The geometry allowed consists of a number of concentric annuli and a number of circular fuel rods, equally spaced in circular rings. The rods consist of up to four concentric layers, and they may, together with the coolant, be divided further by the circle through the centres.

The efficiency of the programme will be illustrated by two flux calculations on the cell shown in Fig. 4. Numbers in the figure show how the regions were chosen. The fuel consists of PuO_2 mixed with natural UO_2, it is canned in zircaloy and there is a zircaloy shroud. D_2O is used as coolant and moderator.

Calculations were carried out for 1% and 2%Pu-enrichment, in both cases with 9.5%^{240}Pu.

The one-group flux distribution was first calculated with 17 lines over the cluster and 4 angles in the integration, and then repeated with 34 lines and 8 angles. The calculations took about one hour on Ferranti Mercury for each enrichment. The largest change in flux in any of the regions when the accuracy was improved was 3%. This is amazingly small with regard to the small number of lines and angles.

In Fig. 5 the calculated flux is shown along a radius crossing three fuel rods (A in Fig. 4). Also shown is a flux distribution obtained by homogenization of the fuel zone and using blackness technique. This method is believed to be about as accurate as an S_4-calculation in the homogenized zone.

One can expect heterogeneous effects to appear in fuel elements with very black fuel in open clusters, because in such cases the homogenization eliminates the possibility for the neutrons to penetrate into the cluster between the fuel rods. In these two cases the fuel rods are 0.93 and 1.31 mean free paths thick respectively. Most of the cross section in the fuel represents absorption. Figure 5 shows that the heterogeneous calculation does give a considerable flatter flux over the cluster.

MIGRATION AREA

The mean square distance to the first collision for neutrons starting in each region can be calculated in a similar way as the collision probabilities. The basic formula is the mean square distance, m^2, for neutrons starting uniformly from a line segment in a small

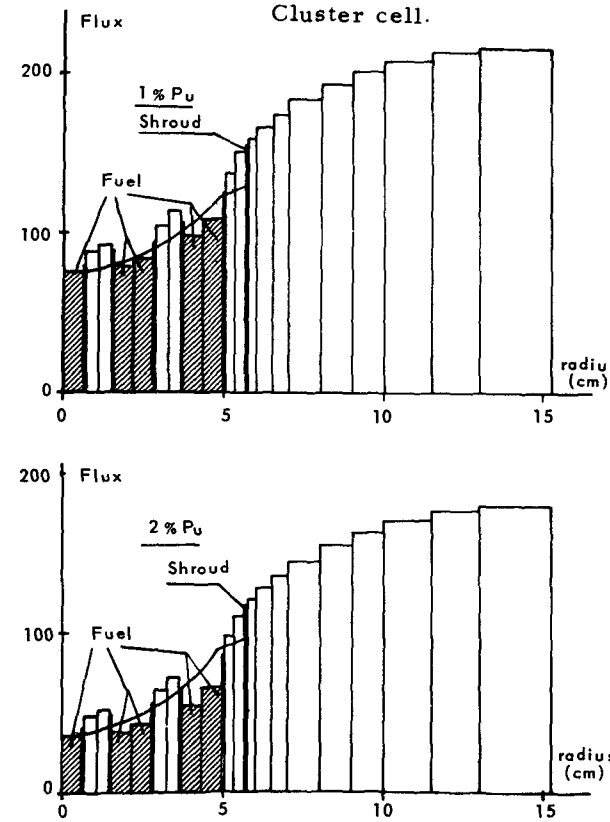

Figure 5. Calculated flux distributions in a cluster cell

azimuthal angular element with the projection of the direction parallel to the line segment. The derivation of the formula is straight forward

$$t_0 m^2 = 2\lambda_0 \left[\lambda_0 t_0 Ki_2(0) + \sum_n (\Delta\lambda)_n \{t_n Ki_2(\tau_n) - (t_n + t_0) Ki_2(\tau_n + \tau_0) + (\lambda_0 + \lambda^+_n + \lambda^-_n)\,[Ki_3(\tau_n) - Ki_3(\tau_n + \tau_0)]\} + \sum_m (\Delta t)_m \{t_m Ki_1(\tau_m) - (t_m + t_0) Ki_1(\tau_m + \tau_0) + \lambda_0\,[Ki_2(\tau_m) - Ki_2(\tau_m + \tau_0)]\}\right] \quad (12)$$

The mean square radial distance, m^2_r, is given by a similar expression. The only difference is that the order of all Ki-functions is increased by two.

The notations are given in Fig. 6. The first sum over n is taken over all boundaries that the neutrons cross between regions with different mean free path λ, and the second sum over m is taken over all empty regions. λ shall be made equal to 0 for an empty region in the first sum.

The mean square distance from birth to absorption is calculated by means of the formula

$$M^2 = \left[\sum_i V_i (S_i + \Sigma_{si}\bar{\phi}_i) m^2_i\right] \left[\sum_i V_i S_i\right]^{-1} \quad (13)$$

and an analogue formula for M^2_r. The corresponding axial mean square distance is obtained from

$$M^2_z = M^2 - M^2_r$$

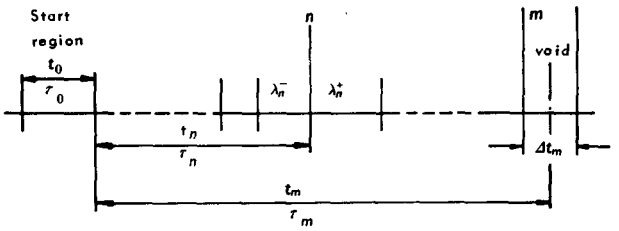

Figure 6. Calculation of the mean square distance to the first collision
$(\Delta\lambda)_n = \lambda_n^+ - \lambda^-_n$; t = true distance; τ = optical distance $= \int_0^t \Sigma(x)\,dx$

The axial leakage can be calculated from M^2_z, but the radial leakage cannot in general be obtained from a migration area, which is calculated from a rotational symmetric flux distribution.

THE DANCOFF-GINSBERG CORRECTION

General formulation

A closely related problem is the calculation of the Dancoff factor for correcting shadowed surfaces in the determination of resonance absorption. In the classical formulation one considers a black body immersed in an infinite homogeneous medium with constant source density, and the Dancoff factor measures how much the incurrent upon the surface of the body is reduced by shadowing from other black bodies.

Figure 2 is used also for this situation. A derivation similar to the one used for Eq. (4) gives that the incurrent on i in an azimuthal angular element $d\alpha$ on a surface element with projection dy perpendicular to α is proportional to

$$[Ki_3(0) - Ki_3(\tau_{i,j})]\,dy = \left[\frac{\pi}{4} - Ki_3(\tau_{i,j})\right] dy \qquad (14)$$

with the shadowing body j. Without shadowing the incurrent would be proportional to $\frac{\pi}{4}\,dy$.

The total incurrents on i in the two cases, I and I_o, are obtained by integrating over y and α. The integration over y goes from 0 to $p(\alpha)$. If the Dancoff factor is C, then $C = 1 - I/I_o$. Using

$$\int_0^{2\pi} d\alpha \int_0^{p(\alpha)} dy = 2S \qquad (15)$$

where S is the surface per unit length of the body i, one obtains

$$C = \frac{2}{\pi S}\int_0^{2\pi} d\alpha \int_0^{p(\alpha)} dy\; Ki_3\,[\tau(y,\alpha)] \qquad (16)$$

Dancoff factor for two parallel circular cylinders

The "classical" Dancoff problem is concerned with two parallel rods. Some values were computed in the basic work of Dancoff and Ginsburg [14]. Larger tables computed later [15] are included in the second edition of ANL-5800 [16]. A formula for a general case will be derived here from Eq. (16).

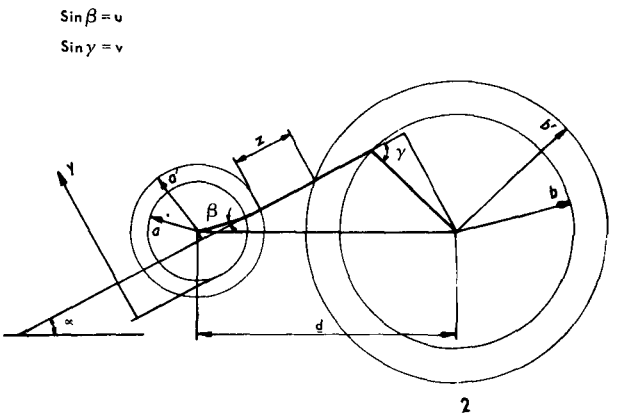

Figure 7. Calculations of the mean Dancoff factor for two parallel rods

Consider two parallel circular rods, 1 and 2, of different radii, each one surrounded by an airgap (Fig. 7). A transformation introduced in [15] used as the variables in the integration the sines of the angles between the projection of the neutron path and the radii in the circles to the points where the projection intersects the circles. The following equations can be derived from Fig. 7

$$y = a(1-u);\quad d\sin\alpha = au + bv;\quad d\cos\alpha = \sqrt{a'^2 - a^2u^2} + \sqrt{b'^2 - b^2v^2} + z \qquad (17), (18), (19)$$

Thus changing the variables of Eq. (16) and using $S = 2\pi a$

$$\frac{d(\alpha,y)}{d(u,v)} = \begin{vmatrix} a & b \\ -a & 0 \end{vmatrix} \frac{1}{d\cos\alpha} = ab\,[d^2 - (au+bv)^2]^{-\frac{1}{2}} \qquad (20)$$

$$C_1 = \frac{b}{\pi^2}\int_{-1}^{+1} du \int_{-1}^{+1} dv\; Ki_3(\tau)\,[d^2 - (au+bv)^2]^{-\frac{1}{2}} \qquad (21)$$

The optical length τ is obtained from Eqs. (18) and (19)

$$\tau = \Sigma z = \Sigma\,(\sqrt{d^2 - (au+bv)^2} - \sqrt{a'^2 - a^2u^2} - \sqrt{b'^2 - b^2v^2}) \qquad (22)$$

In the case of other rods between the two considered, the region of integration is reduced as shown in [15]. A computer programme ERIC by B. Almgren [17] uses this method for calculating the Dancoff factor for a cluster.

In the case of two touching rods the denominator in Eq. (21) is zero at the point $u = v = 1$ (and $= -1$). The pole is easily removed by subtracting (for $b' = b = a' = a$ and $d = 2a$)

$$\pi^{-2}\int_{-1}^{+1} du \int_{-1}^{+1} dv\; Ki_3(0)\,[4 - (u+v)^2]^{-\frac{1}{2}} = \frac{1}{2} - \frac{1}{\pi} \text{ from Eq. (21).}$$

The integrand will then be finite but many-valued at the points in question. A suitable average for numerical integration is

$$\Sigma a\,\pi^{-3}(\pi - A\pi + A \operatorname{arctg} A + B \operatorname{arctgh} B) = 0.0455\,\Sigma a\,\pi^{-2} \text{with } A = \sqrt{2\sqrt{2}+2} \text{ and } B = \sqrt{2\sqrt{2}-2}.$$

Table 1. Approximations to Dancoff factors for hexagonal clusters[a]

m, n	7 rods	19 rods	37 rods
0.0 . . .	0.74057	2.35506	4.85166
1.0 . . .	−1.60041	−6.32717	−9.94360
2.0 . . .	1.50271	5.17800	8.01494
3.0 . . .	−0.49098	−1.61964	−2.58422
4.0 . . .	0.04981	0.18188	0.30673
0.1 . . .	6.78138	6.30420	−12.09552
1.1 . . .	−1.77618	17.02403	33.53623
2.1 . . .	−3.11695	−15.41915	−24.90711
3.1 . . .	0.82980	2.79879	4.38837
0.2 . . .	−21.42712	−44.36990	17.65001
1.2 . . .	13.64425	−8.60321	−33.44073
2.2 . . .	0.31105	10.24963	18.09989
0.3 . . .	22.96655	83.42126	−18.40998
1.3 . . .	−8.25380	−1.28509	11.17206
0.4 . . .	−7.67455	−53.67943	11.48523

[a] (i) $C = \sum_{m+n \leq 4} a_{m,n} x^m y^{n+1}$
(ii) $0 \leq x \leq 1$
(iii) $0.2 \leq y \leq 0.5$
(iv) Maximum error probably < 0.01
(v) x = coolant cross section times lattice pitch
(vi) y = rod radius/lattice pitch

Table 2. The Dancoff factor for an infinite square lattice

x	y = 0.20	0.25	0.30	0.35	0.40	0.45	0.48	0.50
0.25	0.579	0.655	0.721	0.779	0.834	0.886	0.916	0.937
0.50	0.381	0.466	0.548	0.628	0.710	0.793	0.845	0.882
0.75	0.268	0.347	0.429	0.517	0.612	0.716	0.784	0.834
1.00	0.197	0.266	0.343	0.431	0.533	0.650	0.731	0.792
1.25	0.149	0.208	0.279	0.364	0.468	0.594	0.684	0.754
1.50	0.115	0.166	0.230	0.310	0.413	0.544	0.642	0.721
1.75	0.090	0.134	0.191	0.266	0.367	0.501	0.605	0.691
2.00	0.071	0.109	0.160	0.230	0.328	0.463	0.572	0.664
3.00	0.030	0.051	0.083	0.134	0.216	0.348	0.468	0.580
4.00	0.014	0.025	0.046	0.083	0.148	0.270	0.395	0.521
5.00	0.006	0.013	0.026	0.052	0.105	0.216	0.341	0.477
6.00	0.003	0.007	0.015	0.034	0.076	0.175	0.299	0.444

Dancoff factors for clusters and for an infinite square lattice

Two computer programmes for Dancoff factors were written, based on Eq. (16), Dancoff-2 for clusters of circular rods and Dancoff-4 for an infinite square lattice.

With rods of equal radii and no airgaps, the Dancoff factor is a function of two variables, and they were chosen as

x = coolant cross section times lattice pitch
y = the ratio rod radius to lattice pitch.

Calculations were performed for hexagonal clusters with 7, 19, and 37 rods and for an infinite square lattice. For the clusters the results were approximated by rational functions and the coefficients are given in Table 1. Dancoff factors for the square lattice are given in Table 2.

As an example of computing times, the calculation for the 19-rod cluster with 14 radii and 21 coolant cross sections took about 0.8 hours for an accuracy of about 3 times 10^{-3}.

CONCLUSION

The method of calculating flux distributions by means of collision probabilities is a powerful tool for one- and two-dimensional cylindrical systems, particularly when relatively small strongly heterogeneous systems are investigated. Because only the scalar flux is involved, it is often faster than other transport methods, which in principle solve for the total angular distribution.

A drawback is the necessary assumptions of the model, the assumption of regionwise flat sources of primary or secondary neutrons, and the assumption of isotropic scattering. The first restriction can be mitigated by a fine division in regions, but the second restriction is of a more fundamental nature. The application of the usual transport correction is the only possibility for taking anisotropic scattering into account. However, the same treatment is very often accepted also in calculations using methods where a more correct treatment of anisotropy is possible in principle.

It has been shown in examples that heterogeneous effects may be important in practical fuel elements so that homogenization in the usual way overestimates the flux variation. It is also important to see how this is coupled with spectral effects. There are plans for developing a code for spectrum calculations with the Clucop geometry.

ACKNOWLEDGEMENTS

The author is much obliged to Mr. B. Tollander, without whose fast routines for Bickley functions this work would have been difficult.

My thanks are also due to Dr. Leslie and his collaborators at Winfrith for an interesting discussion, where, among other things, the similarity of the British code PIJ and Clucop was established.

At last I want to thank members of the theoretical reactor physics section of AB Atomenergi for numerous valuable discussions and ideas.

REFERENCES

1. Honeck, H. C., Nuclear Sci. Eng., *8*, 193–202 (1960).
2. Honeck, H. C., Nuclear Sci. Eng., *18*, 49–68 (1964).
3. Bonalumi, R., Energia Nucleare, *8*, 326–336 (1961).
4. Hyslop, J., Reactor Science and Technology, *17*, 237–244 (1963).
5. Fukai, Y., Reactor Science and Technology, *17*, 115–120 (1963).
6. Jonsson, A., Reactor Science and Technology, *17*, 511–518 (1963).
7. Sauer, A., Nuclear Sci. Eng., *16*, 329–335 (1963).
8. Soodak, H. and Sullivan, R., NDA-2131-38 (1961).
9. Carlvik, I. and Pershagen, B., AB Atomenergi report (1957).

10. Fukai, Y., Nuclear Sci. Eng., *9*, 370–376 (1961).
11. Fukai, Y., J. Atomic Energy Society, Japan, *4*, 593–600 (1962).
12. Bickley, W. C. and Nayler, J., Phil. Mag., *20*, 343–347 (1935).
13. Tollander, B., private communication.
14. Dancoff, S. M. and Ginsburg, M., CP-2157 (1944).
15. Carlvik, I. and Pershagen, B., AB Atomenergi report, AE-16 (1959).
16. *Reactor Physics Constants*, USAEC Report, ANL-5800, Second Edition (1963).
17. Almgren, B. and Pörn, K., AB Atomenergi report (1963).

ABSTRACT—RÉSUMÉ—АННОТАЦИЯ—RESUMEN

A/681 Suède

Une méthode de calcul des probabilités de collision en géométrie cylindrique générale et ses applications aux répartitions de flux et facteurs de Dancoff

par I. Carlvik

La méthode des probabilités de collision pour le calcul des répartitions des flux de neutrons attire à l'heure actuelle une attention de plus en plus grande, surtout en raison de son application aux systèmes très hétérogènes relativement petits, par exemple les cellules élémentaires de réacteurs. Cette méthode est applicable aux systèmes dont la géométrie est assez compliquée. Etant donné qu'elle ignore la répartition angulaire du flux et se concentre sur la quantité intéressante, à savoir le flux scalaire, elle peut dans de nombreux cas entraîner des économies considérables du temps d'utilisation des calculatrices en comparaison avec diverses autres méthodes de résolution numérique de l'équation de transport. L'un des inconvénients évidents est que cette méthode présuppose généralement une diffusion isotropique et un flux constant par zones.

La caractéristique essentielle de cette méthode est le calcul des probabilités de collision. Les équations fondamentales de la géométrie cylindrique sont présentées dans ce mémoire et sont appliquées aux cellules à géométrie annulaire et aux cellules contenant un faisceau central de barres. Les intégrations nécessaires sont effectuées d'une manière différente de celle communément utilisée afin d'abréger le travail numérique. En particulier, dans le cas de la géométrie annulaire, il est possible de disposer l'intégration de manière à obtenir une intégration de Gauss efficace. Les constantes de Gauss sont choisies en tenant compte des irrégularités connues de l'expression à intégrer et en étudiant différents groupes de constantes possibles.

Des moments de la première distance de vol peuvent être calculés à peu près de la même manière que les probabilités de collision de neutrons provenant de chaque région. Cela permet de calculer les aires de diffusion axiale et radiale avec une répartition donnée des sources lorsque la répartition du flux a été résolue. Cette théorie est également présentée dans le mémoire.

Ces travaux ont abouti à plusieurs programmes de calculatrices et les résultats des calculs sont présentés. Étant donné que le problème étudié est le transport des neutrons, seuls les problèmes relatifs à un seul groupe d'énergie ont été étudiés jusqu'à présent. Cependant, rien ne s'oppose à l'emploi de cette méthode pour les calculs de groupes multiples.

Seule une condition limite blanche a été utilisée sur la limite de cellule tout au long des travaux exposés. La matrice de probabilité de collision est calculée pour une limite de cellule noire, et la matrice de limite blanche s'obtient par une correction simple.

Un problème du même ordre serait le calcul des facteurs de Dancoff. Dans le cas de la géométrie annulaire les facteurs de Dancoff peuvent être directement obtenus à partir des possibilités de collision. Les facteurs de Dancoff peuvent être obtenus de la même manière dans le cas de la géométrie des faisceaux, mais il serait plus adéquat d'utiliser un programme de calculatrice spécial. Dans ce mémoire il est présenté une théorie pour le calcul des facteurs de Dancoff dans la géométрie des faisceaux, et les résultats sont groupés dans des tableaux s'appliquant aux faisceaux ordinaires de 7, 19 et 37 barres.

A/681 Швеция

Метод вычисления вероятностей соударений в общей цилиндрической геометрии, применение этого метода к распределениям потока и коэффициенты Данкова

И. Карлвик

Метод вероятности соударений для расчета распределения нейтронного потока в настоящее время требует повышенного внимания, в частности, для применения его к сравнительно

небольшим сильно гетерогенным системам, например ячейкам решетки реактора. Этот метод может быть применен к системам с довольно сложной геометрией. Ввиду того что в этом методе пренебрегают угловым распределением потока, а основное внимание сосредоточивается на интересующей величине — скалярном потоке, он позволяет во многих случаях достичь значительной экономии времени для вычислений по сравнению с различными другими методами численного решения уравнения переноса. Очевидным недостатком этого метода является то, что в нем предполагается изотропное рассеяние и постоянный для определенных областей поток.

Основной особенностью метода является вычисление вероятностей соударений. В докладе представлены фундаментальные уравнения для цилиндрической геометрии в применении к ячейкам с кольцевой геометрией и к ячейкам, содержащим центральный пучок стержней. Проведено необходимое интегрирование способом, отличным от обычных, что позволяет сократить вычислительную работу. В частности, для кольцевой геометрии допускается провести интегрирование таким способом, что можно провести эффективное гауссово интегрирование. Гауссовы константы выбираются по отношению к известным нерегулярностям подынтегральной величины с различными возможными рядами исследуемых констант.

Моменты расстояния первого пролета можно вычислить почти таким же образом, как вероятности соударений нейтронов, образовавшихся в каждой области. Это позволяет вычислить площади аксиальной и радиальной диффузии для данного распределения источника, когда решено распределение потока. Эта теория также изложена в докладе.

Описываемая работа позволила создать несколько программ для вычислительных машин, и в докладе сообщаются результаты расчетов. Поскольку исследуется проблема переноса нейтронов, то до сих пор изучена задача только одной энергетической группы. Однако нет никаких возражений против использования этих методов в многогрупповых расчетах.

В ходе описанной в докладе работы для границ ячейки были использованы только белые граничные условия. Матрица вероятности соударений рассчитывалась для черной границы ячейки, а матрица белой границы была получена простой подгонкой.

Большое значение имеет проблема вычисления коэффициентов Данкова. В случае кольцевой геометрии коэффициенты Данкова можно получить непосредственно на основе вероятностей соударений. Коэффициенты Данкова можно определить таким же путем и для геометрии пучка, однако более правильно было бы использовать специальную программу вычислений. В этом докладе излагается теория вычисления коэффициентов Данкова для геометрии пучка и приводятся таблицы результатов, полученных для обычных пучков из 7, 19 и 37 стержней.

A/681 Suecia

Método para el cálculo de las probabilidades de colisión en geometría cilíndrica general, con aplicaciones a las distribuciones del flujo y a los coeficientes de Dancoff

por I. Carlvik

El empleo del método de las probabilidades de colisión en el cálculo de las distribuciones del flujo neutrónico está adquiriendo ahora una atención creciente, particularmente por sus aplicaciones a sistemas fuertemente heterogéneos y relativamente pequeños, por ejemplo las celdas de un reactor. Este método puede ser aplicado a sistemas con geometría bastante complicada. Debido al hecho de que este método ignora la distribución angular del flujo y se concentra en la magnitud que importa, en el flujo escalar, permite, en muchos casos, ahorrar una considerable cantidad de tiempo de cálculo, en comparación con otros métodos de resolución numérica de la ecuación de transporte. Un inconveniente obvio, es que este método generalmente considera la dispersión isotropa y el flujo constante en cada región.

La principal característica del método es el cálculo de las probabilidades de colisión. En este informe se presentan las ecuaciones fundamentales para geometría cilíndrica, y se aplican a celdas con geometría anular y a celdas con un haz central de barras. Las integraciones necesarias se efectúan de un modo diferente del comúnmente empleado, con objeto de reducir el cálculo numérico. Para geometría anular, por ejemplo, es posible preparar la integración de tal modo que se pueda aplicar eficazmente el método de integración de Gauss. Las constantes de Gauss se eligen teniendo en cuenta las irregularidades conocidas del integrando, investigándose diferentes conjuntos posibles de constantes.

Los momentos de las distancias recorridas en el primer vuelo pueden calcularse del mismo modo como se calculan las probabilidades de colisión de los neutrones originados en cada región. Esto permite calcular las áreas de difusión axil y radial para una distribución de fuente dada, cuando la distribución del flujo ha sido ya calculada. Esta teoría se presenta también en el informe.

Este trabajo ha originado diversos programas de cálculo, presentándose en este informe los resultados de los cálculos. Ya que el problema que se está investigando es el del transporte de neutrones, hasta ahora se han estudiado sólo problemas con un grupo energético. Sin embargo, nada impide el uso de estos métodos en cálculos con varios grupos.

En el estudio a que se refiere este informe, solamente se ha empleado una condición de contorno blanca en el borde de la celda. La matriz de probabili-

dad de colisión se ha calculado para un contorno negro de la celda, obteniéndose por un simple ajuste la matriz para contorno blanco.

Un problema que está estrechamente relacionado con los anteriores es el cálculo de los factores de Dancoff. En el caso de geometría anular, los factores de Dancoff pueden obtenerse directamente de las probabilidades de colisión. Para un haz de barras, los factores de Dancoff pueden obtenerse del mismo modo, pero sería más conveniente el uso de un programa especial. En este informe se presenta una teoría para el cálculo del factor de Dancoff en un haz de barras, y se dan tablas de los resultados para un haz ordinario de 7, 19 y 37 barras.

The heterogeneous method and its application

By T. Auerbach, G. Burnand and H. Soodak*

INTRODUCTION

Heterogeneous source-sink methods are well suited for calculating lattices that contain significant areas in which no cells with geometrically simple boundaries can be defined. Typical examples are substitution lattices, lattices containing control rods or channels, mixed lattices with two or more types of fuel element, cores containing zones of different lattice pitch for flux flattening, and small assemblies, where boundary effects are of importance.

The theory to be outlined was developed with D_2O-moderated systems in mind, but is not necessarily limited to this moderator. A correct treatment of the lattices mentioned above must obviously take their heterogeneous nature into account. It must also consider some important effects due to finite size and the existence of transition zones in substitution lattices, which will be discussed later.

The finite size of a system may be characterized by axial and radial bucklings, B_z and B_r. B_z will cause axial leakage in the moderator and streaming in voids. B_r will produce a flux asymmetry around the axis of an eccentric rod, resulting in radial leakage and streaming. This effect, which has been discussed by several authors [1–3], is of particular importance in lattices containing cluster elements.

A second effect associated with finite systems is the energy dependence of the extrapolated radius. It is quite negligible in large, reflected systems. However, in bare critical assemblies, and particularly in small exponential facilities, the effect may have important consequences for the evaluation of critical bucklings.

In the neighbourhood of boundaries the neutron spectrum will change as a function of position, causing a variation in resonance absorption essentially proportional to the relative change of resonance flux to thermal flux. This effect, which has been discussed by Naudet [4], is particularly important in the transition zone between test lattice and reference lattice of substitution experiments. A typical variation of resonance absorption, obtained from a heterogeneous two-group theory, is shown in Fig. 1. The effect of spectrum changes may be incorporated into the theory by expressing resonance absorption in terms of an absorption parameter at the surface of each fuel element (and not in terms of an over-all p), and by using a minimum of three energy groups (fast, resonance, and thermal). Three groups will still be insufficient to reproduce effects due to spectrum variations within the resonance range itself, but they will definitely improve results obtained from the oversimplified two-group treatment.

The heterogeneous theory to be described in this paper will have the following features:

(*a*) Diffusion theory is used throughout for calculating the flux in finite cylindrical systems with a single moderator in core and reflector.

(*b*) Three energy groups will be used, comprising a fast group, a resonance group, and a thermal group.

(*c*) The flux is expanded into a Fourier series in the azimuthal angle around each fuel element. The constant ("monopole") term describes absorption and production characteristics of the element. The sine and cosine terms ("dipoles") contain effects due to radial leakage and streaming as a result of radial buckling. Higher multipole terms describe higher order buckling effects and the influence of neighbouring elements. In actual practice, only monopole and dipole terms are needed.

(*d*) Boundary conditions at the surfaces of elements are specified in terms of absorption and production constants inversely proportional to the linear extrapolation length. In practice, only those for the monopole and dipole terms are needed, and these will be discussed. The effect of axial streaming will be considered in the monopole absorption constants.

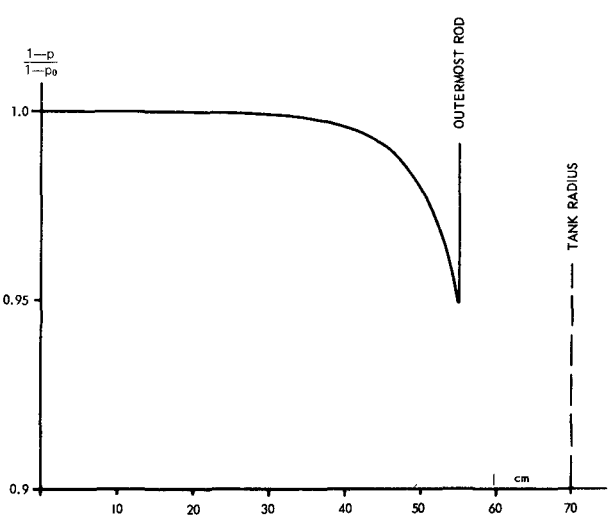

Figure 1. Radial variation $\frac{1-p}{1-p_0}$ in an exponential experiment.
$1-p_0$=value of resonance absorption at the centre

* Swiss Federal Institute for Reactor Research, Würenlingen, Switzerland.

(*e*) The fuel elements are treated as elements of finite radius.

(*f*) In each group the flux will go to zero at an extrapolated radius appropriately chosen for that group.

An important point to consider is the application of heterogeneous methods to the interpretation of experiment. The theory provides a detailed analysis of the flux fine structure, which may be used for direct comparison with the measured flux. In addition, the characteristic determinant provides a numerical value for one of the input parameters. Since most input parameters to a heterogeneous theory are quite different from the lattice-averaged constants of homogeneous methods, results of a heterogeneous calculation cannot be related directly to some familiar and measurable quantities like f, p, L^2, and, most important, B^2.

It is possible, nevertheless, to obtain these by use of the heterogeneous method. The quantities ϵ, p, and f are defined for an infinite lattice, whose heterogeneous treatment is much simpler than that of a finite lattice, because the so-called lattice sums can be reduced analytically to rapidly converging series. The results are closed expressions for ϵ, p, and f in terms of the absorption and production parameters mentioned under (*d*) above. The actual cell shape is correctly taken into account in these formulae, and it is of interest to compare results with those obtained from the circular cell approximation.

In the presence of buckling the flux is very well approximated (except near boundaries) by the Bloch solution, $\exp(i\vec{B}\cdot\vec{r})$, for an infinite periodic lattice, where $\vec{B}$ is a vector whose components in the axial and proper transverse directions are the square roots of the associated bucklings [5]. The lattice sums can again be performed, resulting in the well-known multigroup critical equation for a bare reactor, which relates B^2 to $k\infty$, k_{eff}, and the diffusion areas in each group. All quantities are expressed as formulae involving the absorption and production parameters mentioned above. If B_z differs from zero, ϵ, p, and f turn out to be slightly buckling dependent in this treatment, even after splitting off the non-leakage probability.

In actual practice, both finite and infinite theories will be needed for the interpretation of experiment. Consider, for example, the problem of finding the critical buckling in the test zone of a subcritical substitution lattice. Since some of the heterogeneous input parameters are as yet difficult to calculate from first principles, the finite theory will be used to fit one of them to the experiment. The quantity measured directly is the axial buckling. Hence, in a first step, the measured value of B_z is substituted into the finite heterogeneous theory, which solves the characteristic determinant by properly adjusting, say, the resonance absorption coefficient. Next, this value is substituted into the infinite heterogeneous expression for p mentioned in the preceding paragraphs. p, in turn, is substituted into the corresponding heterogeneous critical equation from which B^2 may be derived.

The sections to follow will outline the theory and its application in greater detail. The geometrical treatment will be given in the next section. Absorption and production constants will be discussed in the section on parameters, whilst the last section will deal with the infinite lattice sums. The theory has been coded for use on the CDC-1604 in Zürich.

Derivation of the flux

For practical purposes only three energy groups were chosen to represent the flux in the slowing-down and thermal regions. More groups may be included if desired, but owing to the great complexity of the theory three groups were felt to be a reasonable compromise.

Starting from the basic diffusion equations,

$$\begin{aligned}
&\nabla^2\Phi_1 - \kappa^2{}_1\Phi_1 = 0, && \text{(fast)}\\
&\nabla^2\Phi_2 - \kappa^2{}_2\Phi_2 + \frac{D_1}{D_2}\kappa^2{}_{12}\Phi_1 = 0, && \text{(resonance)}\\
&\nabla^2\Phi_3 - \kappa^2{}_3\Phi_3 + \frac{D_2}{D_3}\kappa^2{}_{23}\Phi_2 = 0, && \text{(thermal)} \qquad (1)
\end{aligned}$$

where

$$\kappa^2{}_1 = (\kappa^2{}_{12} + B^2{}_z),\ \kappa^2{}_2 = (\kappa^2{}_{23} + B^2{}_z),$$
$$\kappa^2{}_3 = (\kappa^2{}_{33} + B^2{}_z),\ \kappa^2{}_{pq} = \frac{\Sigma_{p\to q}}{D_p}, \qquad (2)$$

the flux in groups 1 to 3 may be written in the form,

$$\begin{aligned}
\Phi_1 &= \Phi_{11},\\
\Phi_2 &= c_{12}\Phi_{12} + \Phi_{22},\\
\Phi_3 &= c_{13}\Phi_{13} + c_{23}\Phi_{23} + \Phi_{33}, \qquad (3)
\end{aligned}$$

where

$$c_{12} = \frac{D_1\kappa^2{}_{12}}{D_2(\kappa^2{}_2 - \kappa^2{}_1)},\ c_{13} = \frac{D_1\kappa^2{}_{12}\kappa^2{}_{23}}{D_3(\kappa^2{}_2 - \kappa^2{}_1)(\kappa^2{}_3 - \kappa^2{}_1)},$$
$$c_{23} = \frac{D_2\kappa^2{}_{23}}{D_3(\kappa^2{}_3 - \kappa^2{}_2)}. \qquad (4)$$

Φ_{pp} is a solution of the homogeneous diffusion equation for group p, and Φ_{pq} is the same flux corrected for

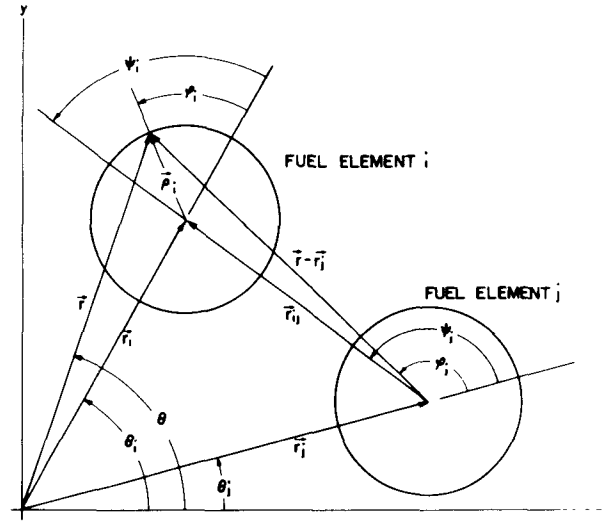

Figure 2. Lattice geometry

the extrapolated radius of group q. Since κ^2_p may become negative for large enough negative axial bucklings, flux expressions for both signs of κ^2_p will be included in the formulae below.

Figure 2 should be consulted to visualize the geometry. The flux at an arbitrary point $\vec{r}$ in the moderator consists of a sum of contributions from all rods j, given by the expression below:

$$\Phi_{pq}(\vec{r}) = \sum_{l=0}^{l=\infty} \Bigg\{ A^{(p)}{}_{lj} \Bigg[\frac{K_l}{Y_l}(\kappa_p|\vec{r}-\vec{r}_j|)\cos l\phi_j - \sum_{\nu=0}^{\infty} a_l{}^{(1)}_{\nu}(pq,j)\frac{I_\nu}{J_\nu}(\kappa_q r) f_\nu{}^{(1)}(\theta-\theta_j) - (1-\delta_{pq}) \sum_{\mu=1}^{q-p+1} \sum_{\nu=0}^{\infty} b^{\mu 1}{}_{l\nu}(pq,j)\frac{I_\nu}{J_\nu}(\kappa_{p+\mu-1} r) f_\nu{}^{(1)}(\theta-\theta_j) \Bigg] + B^{(p)}{}_{lj} \Bigg[\frac{K_l}{Y_l}(\kappa_p|\vec{r}-\vec{r}_j|)\sin l\phi_j - \sum_{\nu=0}^{\infty} a^{(2)}{}_{l\nu}(pq,j)\frac{I_\nu}{J_\nu}(\kappa_q r) f^{(2)}{}_\nu(\theta-\theta_j) - (1-\delta_{pq}) \sum_{\mu=1}^{q-p+1} \sum_{\nu=0}^{\infty} b^{\mu 2}{}_{l\nu}(pq,j)\frac{I_\nu}{J_\nu}(\kappa_{p+\mu-1} r) f^{(2)}{}_\nu(\theta-\theta_j) \Bigg] \Bigg\}, \quad (5)$$

where

$$a^{(k)}{}_{l\nu}(pq,j) = \epsilon_\nu \left\{ \frac{I_{\nu-l}}{J_{\nu-l}}(\kappa_p r_j) - (-1)^k{}_{(-1)^l} \frac{I_{\nu+l}}{J_{\nu+l}}(\kappa_p r_j) \right\} \frac{\dfrac{K_\nu}{Y_\nu}(\kappa_p R_q)}{\dfrac{I_\nu}{J_\nu}(\kappa_q R_q)},$$

$$b^{1k}{}_{l\nu}(pq,j) = a^{(k)}{}_{l\nu}(pp,j),$$

$$b^{2k}{}_{l\nu}(pq,j) = \frac{\kappa^2{}_3 - \kappa^2{}_{3+p-q}}{\kappa^2{}_3 - \kappa^2{}_2} \left\{ a^{(k)}{}_{l\nu}(p,p+1,j)\delta(2+p-q) - a^{(k)}{}_{l\nu}(pp,j) \frac{\dfrac{I_\nu}{J_\nu}(\kappa_p R_{p+1})}{\dfrac{I_\nu}{J_\nu}(\kappa_{p+1} R_{p+1})} \right\}$$

$$b^{3k}{}_{l\nu}(13,j) = -\left\{ a^{(k)}{}_{l\nu}(11,j) \frac{\dfrac{I_\nu}{J_\nu}(\kappa_1 R_3)}{\dfrac{I_\nu}{J_\nu}(\kappa_3 R_3)} + b^{2k}{}_{l\nu}(13,j) \frac{\dfrac{I_\nu}{J_\nu}(\kappa_2 R_3)}{\dfrac{I_\nu}{J_\nu}(\kappa_3 R_3)} \right\},$$

$f_\nu{}^{(1)}(\theta) = \cos\nu\theta$, $f^{(2)}{}_\nu(\theta) = \sin\nu\theta$,

$\delta_{pq} = 1$ if $p = q$ and zero otherwise,

$\delta(2+p-q) = 1$ if $2+p-q = 0$ and zero otherwise,

$\epsilon_\nu = \frac{1}{2}$ if $\nu = 0$ and 1 otherwise. (6)

R_q is the extrapolated radius for pure moderator in the q'th energy group. The upper Bessel functions apply when $\kappa^2 > 0$, the lower when $\kappa^2 < 0$.

The first coefficients of A_{lj} and B_{lj} in Eq. (5) are the infinite moderator contributions of the j'th element. The second coefficients are image terms which reduce the flux to zero at the extrapolated radius R_q. The third coefficients arise as a result of different extrapolated radii in groups p and q. They are small and go to zero at $r = R_q$.

The fuel is characterized by certain boundary conditions, which the moderator flux must satisfy at the surface of the i'th fuel element. This requires expanding Φ_{pq} around the circumference of the i'th element. The addition formulae below are used to evaluate the influence of the j'th element on the i'th element,

$$\frac{K_l}{Y_l}(\kappa|\vec{r}-\vec{r}_j|) f_l{}^{(n)}(\phi_j) = \frac{K_l}{Y_l}(\kappa\rho_i) f_l{}^{(n)}(\phi_i)\delta_{ij} + (1-\delta_{ij}) \sum_{m=-\infty}^{\infty} (-1)^m \frac{K_{l+m}}{Y_{l+m}}(\kappa r_{ij}) \frac{I_m}{J_m}(\kappa\rho_i) f_1{}^{(n)}(l\psi_j + m\psi_i - m\phi_i), \frac{I_\nu}{J_\nu}(\kappa r) f_\nu{}^{(n)}(\theta-\theta_j)$$

$$= \sum_{m=-8}^{\infty} (-1)m \frac{I_{\nu+m}}{J_{\nu+m}}(\kappa r_i) \frac{I_m}{J_m}(\kappa\rho_i) f_1{}^{(n)}(\nu\theta_{ij} - m\phi_i), \quad (7)$$

where

$$r_{ij} = |\vec{r}_i - \vec{r}_j|, \quad \theta_{ij} = \theta_i - \theta_j, \quad (8)$$

and ρ_i is the radius of the i'th element. The result of the expansion is,

$$\Phi_{pq}(\rho_i,\phi_i) = \sum_{m=0}^{\infty} [\Phi^{(1)}{}_{pq}(m,\rho_i)\cos m\phi_i + \Phi^{(2)}{}_{pq}(m,\rho_i)\sin m\phi_i], \quad (9)$$

where

$$\Phi^{(4)}{}_{pq}(m,\rho_i) = \sum_{\substack{l=0 \\ j}} \Bigg\{ A^{(p)}{}_{lj} \Bigg[\frac{K_l}{Y_l}(\kappa_p\rho_i)\delta_{lm}\delta_{ij} + \frac{I_m}{J_m}(\kappa_p\rho_i) H^{(1)}{}_{lm}(\kappa_p, ij) - \frac{I_m}{J_m}(\kappa_q\rho_i) G^{(pq,1)}{}_{lm}(ij,1) - h^{(pq,1)}(ij,1)_{lm} \Bigg] + B^{(p)}{}_{lj} \Bigg[\frac{I_m}{J_m}(\kappa_p\rho_i) H^{(3)}{}_{lm}(\kappa_p ij) - \frac{I_m}{J_m}(\kappa_q\rho_i) G^{(pq,3)}{}_{lm}(ij,2) - h^{(pq,3)}{}_{lm}(ij,2) \Bigg] \Bigg\},$$

$$\Phi^{(2)}{}_{pq}(m,\rho_i) = \sum_{\substack{l=0 \\ j}} \Bigg\{ A^{(p)}{}_{lj} \Bigg[\frac{I_m}{J_m}(\kappa_p\rho_i) H^{(2)}{}_{lm}(\kappa_p, ij) - \frac{I_m}{J_m}(\kappa_q\rho_i) G^{(pq,2)}{}_{lm}(ij,1) - h^{(pq,2)}{}_{lm}(ij,1) \Bigg] + B^{(p)}{}_{lj} \Bigg[\frac{K_l}{Y_l}(\kappa_p\rho_i)\delta_{lm}\delta_{ij} - \frac{I_m}{J_m}(\kappa_p\rho_i) H^{(4)}{}_{lm}(\kappa_p, ij) + \frac{I_m}{J_m}(\kappa_q\rho_i) G^{(pq,4)}{}_{lm}(ij,2) + h^{(pq,4)}{}_{lm}(ij,2) \Bigg] \Bigg\},$$

$$H^{(n)}{}_{lm}(\kappa_p,ij) = (-1)^m \epsilon_m (1-\delta_{ij}) \left\{ \frac{K_{l+m}}{Y_{l+m}} (\kappa_p r_{ij}) f_1{}^{(n)}(l\psi_j + m\psi_i) - (-1)^n {}_{(-1)}m \frac{K_{l-m}}{Y_{l-m}} (\kappa_p r_{ij}) f_1{}^{(n)}(l\psi_j - m\psi_i) \right\},$$

$$G^{(pq,n)}{}_{lm}(ij,k) = \sum_{\nu=0}^{\infty} a^{(k)}{}_{l\nu}(pq,j) i^{(n)}{}_{m\nu}(\kappa_q r_i, \theta_{ij}),$$

$$h^{(pq,n)}{}_{lm}(ij,k) = (1-\delta_{pq}) \sum_{\mu=1}^{q-p+1} \sum_{\nu=0}^{\infty} \frac{I_m}{J_M} (\kappa_{p+\mu-1}\rho_i) b^{\mu k}{}_{l\nu}(pq,j) i^{(n)}{}_{m\nu}(\kappa_{p+\mu-1} r_i, \theta_{ij}),$$

$$i^{(n)}{}_{m\nu}(k_q r_j, \theta_{ij}) = \epsilon_m \left\{ (-1)^m \frac{I_{\nu+m}}{J_{\nu+m}} (\kappa_q r_i) - (-1)^n \frac{I_{\nu-m}}{J_{\nu-m}} (\kappa_q r_i) \right\} f_\nu{}^{(n)}(\theta_{ij}),$$

$$f_\nu{}^{(1)}(\theta) = f_\nu{}^{(4)}(\theta) = \cos\nu\theta, \; f_\nu{}^{(2)}(\theta) = f_\nu{}^{(3)}(\theta) = \sin\nu\theta \tag{10}$$

At the surface of an element, absorption and production coefficients $\gamma_{pq}(m)$ are defined in each group and for each $\cos m\phi_i$ and $\sin m\phi_i$ term of the flux. For each such harmonic the three-group boundary conditions at ρ_i can be written in the form,

$$\frac{\mathrm{d}}{\mathrm{d}\rho_i} \Phi_1{}^{(n)}(m) = \gamma_{11}(m)\Phi_1{}^{(n)}(m) + \gamma_{12}(m)\Phi_2{}^{(n)}(m) + \gamma_{13}(m)\Phi_3{}^{(n)}(m),$$

$$\frac{\mathrm{d}}{\mathrm{d}\rho_i} \Phi_2{}^{(n)}(m) = \gamma_{21}(m)\Phi_1{}^{(n)}(m) + \gamma_{22}(m)\Phi_2{}^{(n)}(m),$$

$$\frac{\mathrm{d}}{\mathrm{d}\rho_i} \Phi_3{}^{(n)}(m) = \gamma_{32}(m)\Phi_2{}^{(n)}(m) + \gamma_{33}(m)\Phi_3{}^{(n)}(m), \tag{11}$$

where

$$\Phi_1{}^{(n)}(m) = \Phi_{11}{}^{(n)}(m,\rho_i), \tag{12a}$$

$$\Phi_2{}^{(n)}(m) = c_{12}\Phi_{12}{}^{(n)}(m,\rho_i) + \Phi_{22}{}^{(n)}(m,\rho_i), \tag{12b}$$

$$\Phi_3{}^{(n)}(m) = c_{13}\Phi_{13}{}^{(n)}(m,\rho_i) + c_{23}\Phi_{23}{}^{(n)}(m,\rho_i) + \Phi_{33}{}^{(n)}(m,\rho_i). \tag{12c}$$

The parameters have the following physical significance: γ_{11} and γ_{13} account for fast absorption, as well as for fast and thermal fission. γ_{12} accounts for resonance fission. γ_{21} is due to internal moderation from the fast group. γ_{22} is the resonance absorption parameter. γ_{32} is due to internal moderation from the resonance group, and γ_{33} accounts for thermal absorption. Note that $\gamma_{pq}(m)$ depends only on m and not on n, i.e., sine and cosine terms have the same γ's.

Boundary conditions (11) result in a set of homogeneous equations for the A's and B's, whose coefficient determinant is made to vanish by adjusting B_z or one of the γ's.

The parameters $\gamma(0)$ and $\gamma(1)$

Ideally, the $\gamma_{pq}(m)$ depend only on material properties of fuel and moderator and on fuel geometry. The use of $\gamma(m)$ assumes that asymptotic diffusion theory is valid in the moderator. This certainly is true for thermal neutrons, but for the fast and resonance groups it is definitely further from reality. It will nevertheless be considered true for all groups in order not to complicate the theory still further.

The most important parameters are $\gamma(0)$ and $\gamma(1)$, corresponding respectively to monopole and dipole terms. $\gamma(0)$ is the inverse of the usual linear extrapolation length at the surface of a cylinder. The presence of axial buckling in the fuel is accounted for by making $\gamma(0)$ depend on B_z. This dependence will change the flux ratios within the lattice cell, and as a result the factors ϵ, p, and f will remain buckling dependent even after separation of the non-leakage probability.

A number of methods exist for calculating $\gamma(0)$, provided the element consists of cylindrical zones. The most useful of these are the methods of Kushneriuk and McKay [6], or of Amouyal and Benoist [7], and the P_3-method. The dependence on axial buckling may be obtained from a knowledge of the total amount of axial leakage. Thus, for example, a knowledge of D_z leads to the knowledge of the buckling dependence of $\gamma(0)$. Work is in progress to obtain this dependence directly from P_3-theory.

The constant $\gamma(1)$ comes into play only under conditions of a transverse macroscopic flux gradient. It is related to the scattering or leakage properties of the fuel element, and thus to the transverse diffusion coefficient, D_r. Its value also determines the "dipole strength" induced in a given assembly by a macroscopic flux gradient. These relations can be determined exactly within the framework of asymptotic diffusion theory by applying lattice sum techniques.

The value of $\gamma(1)$ may be calculated in a number of ways:

(*a*) It can be determined by using the relationship between $\gamma(1)$ and D_r and evaluating D_r according to Behrens [8] or Benoist [9].

(*b*) The transport theoretical value of $\gamma(0)$ may be substituted into a formula derived from P_1-theory relating $\gamma(1)$ to $\gamma(0)$.

(*c*) P_3-theory may be used for a direct determination of $\gamma(1)$. This approach is presently being used in a programme employing P_3-theory in r-geometry to obtain the multizone flux and the linear extrapolation length to all orders in m.

(*d*) $\gamma(1)$ can also be obtained from a measurement on relative strengths of isotropic and dipole fluxes [3].

The γ's corresponding to higher values of m represent both higher effects of buckling and effects due to neighbouring elements. Both of these may be neglected in most practical applications of the theory.

The factors η, ϵ, p and f

As pointed out in the Introduction, cell averaged quantities can be obtained by performing the infinite lattice sums. With buckling present, pole and dipole terms must be included in the summation, leading to expressions for the group diffusion areas which take radial leakage from fuel elements into account. The indicated sums can be performed, but lead to very complicated formulae which will not be presented here.

Instead, the factors η, ϵ, p, and f will be derived for the case of no buckling.

For simplicity, a case will be considered in which there is no resonance fission ($\gamma_{12}=0$) and no moderation inside the fuel elements ($\gamma_{21}=\gamma_{32}=0$). Since there is no buckling, the dipole terms are zero and only monopole terms remain. All higher multipoles will be neglected. Under these conditions Eqs. (9) and (10) for an infinite regular lattice reduce to the simple expression,

$$\Phi_{pq}(\rho_i,\phi_i)=\Phi_{pp}(0,\rho_i)=A^{(p)}F_p(\rho_i), \tag{13}$$

where

$$F_p(\rho_i)=K_0(\kappa_p\rho_i)+S(\kappa_p)I_0(\kappa_p\rho_i),$$

$$S(\kappa_p)=\sum_{j=-\infty}^{\infty}(1-\delta_{ij})K_0(\kappa_p|\vec{r_i}-\vec{r_j}|). \tag{14}$$

Following the method of Galanin [5], Neumann [10] has shown that for a square lattice,

$$S(\kappa_p)=c+\ln\left(\frac{k}{2}\right)+\frac{\coth(\pi k)}{2k}\sum_{n=1}^{\infty}+\left[\left(\frac{1}{\sqrt{(n^2+k^2)}}-\frac{1}{n}\right)+\frac{\coth(\pi\sqrt{(n^2+k^2)-1}}{\sqrt{(n^2+k^2)}}\right], \tag{15}$$

where

$$c=0{,}57721\ldots=\text{Euler's constant},$$

$$k=\frac{\kappa a}{2\pi},$$

and a is the lattice pitch.

It will be noted that $F_p(\rho)$ has the same form as the flux in the circular cell approximation if $S(\kappa)$ is replaced by $S_c(\kappa)=K_1(\kappa R)/I_1(\kappa R)$, where R is the cell radius. If κ is large, the main contribution at ρ comes from $K_0(\kappa\rho)$, in which case an error in $S(\kappa)$ is not important. When κ is sufficiently small, the relative error between S_c and the correct S becomes small. Hence the equivalent cell approximation is expected to give nearly correct results in both limiting cases.

Boundary conditions (11) at $\rho_i=\rho$ now become,

$$\frac{d\Phi_1}{d\rho}=\gamma_{11}\Phi_1+\gamma_{13}\Phi_3, \tag{16a}$$

$$\frac{d\Phi_2}{d\rho}=\gamma_{22}\Phi_2, \tag{16b}$$

$$\frac{d\Phi_3}{d\rho}=\gamma_{33}\Phi_3, \tag{16c}$$

where γ_{pq} is understood to mean $\gamma_{pq}(0)$.

The most natural definition for $\eta\epsilon$ in the three-group framework is that

$\eta\epsilon=$ number of resonance neutrons produced per thermal neutron absorbed.

To calculate $\eta\epsilon$ one realizes first that the thermal absorption in fuel per cell is proportional to $D_3 d\Phi_3/d\rho$, and that the production of resonance neutrons per cell is the net fast current $-D_1 d\Phi_1/d\rho$. Thus,

$$\eta\epsilon=-D_1\frac{d\Phi_1}{d\rho}, \tag{17}$$

when the normalization is such that $D_3 d\Phi_3/d\rho=1$. Combining this with Eqs. (16c) and (16a) and writing $\Phi_1=A^{(1)}F_1(\rho)$ allows $A^{(1)}$ to be determined. When this is substituted into Eq. (17) the result is,

$$\eta\epsilon=\frac{\gamma_{13}D_1}{\gamma_{33}D_3}\frac{1}{\gamma_{11}\dfrac{F_1}{F_1'}-1}, \tag{18}$$

where $F'=dF/d\rho$.

The resonance absorption, $1-p$, is defined as the number of resonance neutrons absorbed per resonance neutron produced. The former is proportional to $D_2 d\Phi_2/d\rho$ and the latter is proportional to

$$-D_1 d\Phi_1/d\rho=-D_1A^{(1)}F_1'.$$

Thus

$$1-p=-\frac{D_2\dfrac{d\Phi_2}{d\rho}}{D_1A^{(1)}F_1'} \tag{19}$$

Using Eq. (12b), Φ_2 is expressed in terms of c_{12},$A^{(1)}F_1$, and $A^{(2)}F_2$. Substituting this into Eq. (16b) results in a relation between $A^{(1)}$ and $A^{(2)}$, which allows Φ_2 to be expressed in terms of $A^{(1)}$. This may be substituted into Eq. (19) with the result that

$$p=1-c_{12}\gamma_{22}\frac{D_2}{D_1}\frac{\dfrac{F_2}{F_2'}-\dfrac{F_1}{F_1'}}{1-\gamma_{22}\dfrac{F_2}{F_2'}} \tag{20}$$

Similarly, the thermal utilization f is the number of thermal absorptions in fuel per thermal neutron produced. Thus,

$$f=\frac{D_3\dfrac{d\Phi_3}{d\rho}}{-pD_1\dfrac{d\Phi_1}{d\rho}}. \tag{21}$$

Proceeding as before one finds,

$$f=\frac{D_3\gamma_{33}}{D_1p}\frac{c_{13}\left(1-\gamma_{22}\dfrac{F_2}{F'_2}\right)\left(\dfrac{F_3}{F'_3}-\dfrac{F_1}{F'_1}\right)-c_{12}c_{23}\left(1-\gamma_{22}\dfrac{F_1}{F'_1}\right)\left(\dfrac{F_3}{F'_3}-\dfrac{F_2}{F'_2}\right)}{\left(1-\gamma_{22}\dfrac{F_2}{F'_2}\right)\left(1-\gamma_{33}\dfrac{F_3}{F'_3}\right)} \tag{22}$$

The four factors may now be inserted into the usual three-group critical equation to determine the critical buckling. Such a procedure is not quite consistent, however, for a buckling will give rise to the dipole terms that were neglected in the present treatment. The error is not important if the leakage from a fuel element is small, as in the case of solid uranium rods. However, if the fuel is in the form of clusters, a more careful treatment, including dipole terms, will be required.

REFERENCES

1. Leslie, D. C., Reactor Sci. Technol., *16*, 1 (1962).
2. Galanin, A. D., Reactor Sci. Technol., *16*, 547 (1962).
3. Benoist, P., and Palmedo, P. F., IAEA Symposium on Exponential and Critical Experiments, Amsterdam (1963).
4. Naudet, R., EACRP-L-32.
5. Galanin, A. D., *The thermal coefficient in a heterogeneous reactor*, Proceedings of the First International Conference on the Peaceful Uses of Atomic Energy, P/666, Vol. 5, p. 477, United Nations (1956).
6. Kushneriuk, S. A., and McKay, C., Atomic Energy of Canada Ltd. report CRT-566.
7. Amouyal, A., and Benoist, P., CEA 571 (1956).
8. Behrens, D. J., Proc. Phys. Soc., *62*, 607 (1949).
9. Benoist, P., CEA-1354.
10. Neumann, H., U.S. Atomic Energy Comm. report HW-52048 (1957).

ABSTRACT—RÉSUMÉ—АННОТАЦИЯ—RESUMEN

A/690 Suisse

La méthode hétérogène et son application

par T. Auerbach *et al.*

Les méthodes hétérogènes pour le calcul des réseaux s'appliquent à des arrangements présentant des irrégularités qui ne peuvent être traitées par les méthodes homogènes habituelles. De telles irrégularités apparaissent lorsque des barres de contrôle sont insérées entre les éléments de combustible, dans les expériences de substitution ou même dans les réseaux complets contenant des zones où l'espacement des éléments de combustible diffère, comme c'est le cas pour la pile de Lucens.

Le traitement habituel, que ce soit en théorie à deux groupes ou en théorie de l'âge, avec représentation des éléments de combustible par des sources et des absorbeurs linéaires, est suffisant pour des réseaux où l'espacement des barres est grand par rapport à leur propre rayon. Les éléments en grappe proposés pour les piles de puissance modérées à l'eau lourde ne rentrent cependant pas dans cette catégorie et introduisent la complication supplémentaire du *streaming* axial et radial.

La méthode hétérogène a par conséquent été étendue en incorporant les points suivants:

a) Trois groupes d'énergie comprenant la région rapide, la région de résonance et la région thermique. Ces groupes sont nécessaires pour deux raisons. La première est de définir la bande d'énergie à l'intérieur de laquelle l'absorption par résonance a lieu. La seconde est d'introduire une zone tampon entre le groupe supérieur et le groupe thermique de façon à obtenir une source de neutrons thermiques suffisamment plate.

b) Le flux à la surface du combustible est exprimé sous forme de la somme d'un terme constant (monopôle) et d'un terme dipôle. Le terme constant décrit la caractéristique d'absorption de l'élément; le terme dipôle est nécessaire pour représenter convenablement les propriétés diffusantes du combustible ainsi que le *streaming* radial.

c) Les conditions limites à la surface du combustible sont exprimées en fonction des longueurs d'extrapolation à l'intérieur de celui-ci. La longueur d'extrapolation pour le terme monopôle est bien connue. Celle pour le dipôle est dérivée des valeurs calculées des coefficients radiaux de diffusion. Un travail est en cours pour obtenir celles-ci directement au moyen d'une théorie du transport.

d) Le *buckling* axial affecte dans une certaine mesure les longueurs d'extrapolation linéaire, spécialement en présence de cavités. Ces effets sont incorporés à la théorie afin de tenir compte du *streaming* axial.

e) Pour les éléments en grappe relativement grands, les dimensions finies des barres doivent être traitées d'une manière plus rigoureuse que celle qui consiste à supposer les éléments linéaires puis à corriger les résultats pour tenir compte de leur diamètre réel. La théorie présentée traite rigoureusement le diamètre fini des barres mais interrompt les séries obtenues après quelques termes.

La méthode est entièrement programmée en ALGOL et des résultats sont présentés.

A/690 Швейцария

Гетерогенный метод и его применение

Т. Ауэрбах *et al.*

Гетерогенные методы расчета решеток предназначаются для решеток, имеющих неправильности, которых нельзя избежать при обработке обычными гомогенными методами. Такие неправильности проявляются, когда регулирующие стержни вставляются между тепловыделяющими элементами, при экспериментах на замещение или даже в полных решетках, содержащих зоны с различным шагом между тепловыделяющими элементами, как это имеет место в реакторе в Люценсе.

Обычная обработка по двухгрупповой теории или теории возраста с представлением тепловыделяющих элементов источниками или линейными поглотителями является достаточной для решеток, у которых шаг между стержнями велик по сравнению с радиусом отдельного эле-

мента. Тепловыделяющие элементы в виде пучков, предложенные для энергетических реакторов с тяжеловодным замедлителем, не подходят к этой категории и вводят дополнительное осложнение: аксиальную и радиальную «утечки».

Гетерогенный метод был расширен путем введения следующих факторов:

a) Три группы энергий, охватывающие быструю, резонансную и тепловую области. Эти группы необходимы по двум причинам. Первая заключается в определении области энергий, внутри которой наблюдается резонансное поглощение. Вторая состоит в введении буферной зоны между высшей и тепловой группами для получения достаточного плоского источника тепловых нейтронов.

b) Поток на поверхности топлива выражается в виде суммы постоянного члена (монополия) и дипольного члена. Постоянный член описывает поглощающую способность элемента, дипольный член необходим, чтобы соответствующим образом представить рассеивающие свойства топлива, а также радиальную «утечку».

c) Граничные условия на поверхности тепловыделяющего элемента выражаются в зависимости от длин экстраполяции внутри тепловыделяющего элемента. Длина экстраполяции для монопольного члена хорошо известна. Длина экстраполяции для диполя получается из вычисленных радиальных коэффициентов рассеяния. Ведется работа для получения этих значений непосредственно с помощью теории переноса.

d) Аксиальный лапласиан влияет в некоторой степени на длины линейной экстраполяции особенно при наличии полостей. Эти влияния вводятся в теорию для учета аксиальной «утечки».

e) Для относительно больших элементов в виде пучков конечные размеры стержней должны обрабатываться с большей точностью, чем точность, которую дает предположение о линейных элементах, с последующей поправкой на их действительный диаметр. Представленная теория строго рассматривает конечный диаметр стержней, но прерывает ряды после нескольких членов.

Метод был полностью запрограммирован на ALGOL, и результаты представлены в докладе.

A/690 Suiza

El método heterogéneo y sus aplicaciones

por T. Auerbach *et al.*

Los métodos heterogéneos de cálculo de reticulados se aplican a disposiciones que presentan irregularidades imposibles de tratar por los métodos homogéneos habituales. Estas irregularidades aparecen al insertar barras de control entre los elementos combustibles, en los experimentos de sustitución e incluso en reticulados completos cuando los elementos combustibles no están uniformemente espaciados, como sucede en el reactor de Lucens.

El tratamiento habitual por la teoría de dos grupos o por la teoría de la edad, que representa los elementos combustibles por medio de fuentes y absorbentes lineales, es suficiente cuando la distancia entre las barras es grande en relación con su diámetro. Sin embargo, los conjuntos de elementos propuestos para los reactores de potencia moderados por agua pesada no entran en esta categoría y, además, introducen la complicación de la corriente rectilínea de neutrones (*streaming*) en los sentidos axial y radial.

Hay que aplicar, por consiguiente, el método heterogéneo teniendo en cuenta los siguientes factores:

a) Tres grupos energéticos que comprenden las regiones rápida, de resonancia y térmica, son necesarios por dos razones: para definir la banda de energía en cuyo interior tiene lugar la absorción por resonancia y para introducir una zona amortiguadora entre el grupo superior y el grupo térmico y obtener así una fuente de neutrones térmicos suficientemente plana.

b) El flujo en la superficie del combustible se expresa como la suma de un término constante (monopolar) y un término dipolar. El primero describe la característica de absorción del elemento mientras que el segundo es necesario para representar adecuadamente las propiedades de difusión del combustible y la corriente radial.

c) Las condiciones de contorno en la superficie del combustible se expresan en función de las longitudes de extrapolación en su interior. Para el término monopolar la longitud de extrapolación es bien conocida y para el dipolar se deriva de los valores calculados de los coeficientes de difusión radial. Se está trabajando para obtenerlas directamente por la teoría del transporte.

d) La laplaciana axil afecta hasta cierto punto a las longitudes de extrapolación lineal, especialmente en presencia de huecos por lo que su efecto se incorpora a la teoría para tener en cuenta la corriente axil.

e) Cuando se opera con haces de elementos relativamente grandes no es suficiente tratar las dimensiones finitas de las barras suponiendo elementos lineales e introduciendo un factor de corrección para tener en cuenta su diámetro real. La teoría que presentan los autores trata rigurosamente el diámetro finito de las barras, pero interrumpe las series obtenidas después de algunos términos.

Todo el método está programado en la clave ALGOL y el documento presenta los resultados obtenidos.

Dos esquemas de cálculo de reactores nucleares

por R. Ortiz, G. Velarde, R. Caro, J. L. de Francisco y A. Brú*

CÁLCULO DE CONSTANTES

En el primer esquema, el cálculo de las constantes nucleares para los diferentes grupos neutrónicos se efectúa siempre tomando como factor de peso el flujo neutrónico, bien en el intervalo de moderación, bien en la región térmica.

Cálculo de constantes rápidas

Se toma como intervalo de moderación el intervalo de 0,625 eV a 10 MeV. El número de grupos neutrónicos en el mismo puede ser uno, dos o tres, y las correspondientes constantes se obtienen promediando las secciones eficaces según el flujo $F_0(u)$ obtenido como solución de la ecuación de Boltzmann, en las aproximaciones P_1 o B_1, para una lámina homogénea infinita. La fuente exterior se supone isótropa. La densidad de moderación, q, que para el H es solución de

$$\frac{\partial q}{\partial u} + q = \Sigma_s F_0 \qquad (1)$$

para los demás elementos se ha tomada igual a

$$q = (\lambda \Sigma_a + \xi \Sigma_s) F_0 \qquad (2)$$

con $\lambda = \overline{\xi^2}/2\xi$. Aunque una nueva versión del programa ISLERO prevé la posibilidad de tratar por separado no sólo el hidrógeno, sino también el deuterio en la aproximación Greuling–Goertzel consistente, en los cálculos realizados hasta ahora la densidad de moderación se ha tomado en la forma (2). Generalmente se ha adoptado la aproximación B_1.

Las ecuaciones indicadas se resuelven numéricamente mediante los programas ISLERO-0 e ISLERO-1 [1]. El primero da los valores de las constantes macroscópicas promediadas para toda la celda o reactor y el segundo, además las constantes microscópicas, elemento por elemento. Los parámetros de entrada son las densidades atómicas de los diversos elementos, la laplaciana (que puede no ser la misma para todos los grupos en ISLERO-1) y el factor de autoblindaje, L, de los elementos que presenten resonancias. Este factor, al igual que $\nu^{25}{}_t$, se puede ajustar experimentalmente para cada tipo de reactor. En el caso del reactor DON (combustible en haces de 19 barras de UC refrigerado por un líquido orgánico, D_2O como moderador y Al y SAP como materiales estructurales), no se procedió a ajuste experimental ninguno para los cálculos preliminares. Para $\nu^{25}{}_t$ se adoptó el valor 2,43 [18], y el factor de autoblindaje se ha calculado de acuerdo con la fórmula dada en [2]. En cuanto a la integral de resonancia, se ha tomado

$$IR_T = IR_0 \left[1 + \left(a + b \frac{S_{ef}}{M} \right) (T^{\frac{1}{2}}{}_{(comb.)} - 17{,}1348) \right] \qquad (3)$$

con

$$IR_0 = A + B\,(S_{ef}/M + E)^{\frac{1}{2}} \qquad (4)$$

$$S_{ef} = S_g\,(1 - C) \qquad (5)$$

S_g es el área de la superficie geométrica y C el coeficiente de Dancoff-Ginsburg

$$C = \frac{2}{\pi L'} \int dL' \int \cos\beta\, K_{i3}\,(\Sigma_s \lambda)\, d\beta \qquad (6)$$

En (6), λ es la longitud de una cuerda entre dos puntos de la superficie del combustible situada dentro del moderador, β el ángulo que forma con la normal a la superficie dirigida hacia el moderador y L' el perímetro del combustible.

Los valores de los parámetros A, B, E, a y b se dan en la tabla 1. Para el caso de UC se emplearán las fórmulas de correlación de Vernon [3] partiendo del U metálico y del UO_2. Entre ambas correlaciones, se ha obtenido la siguiente correlación intermedia [4]

$$IR_0{}^{UC} = 3{,}64 + 25{,}87\,[(S_{ef}/M)^{UC}]^{\frac{1}{2}} \qquad (7)$$

En cuanto al valor de C, el cálculo numérico para el caso de dos barras ha sido efectuado por Carlvik y Pershagen [6]. Para un haz de barras se ha empleado la corrección de Fukai [7] y en el caso de una serie de anillos de combustible, el cálculo ha sido llevado a cabo por Velarde [8].

Tabla 1. Parámetros para las integrales de resonancia

Isótopo	Metal	UO_2	UC		
A . . .	2,95	4,15	4,15	2,81	3,64
B . . .	25,80	26,60	25,60	25,315	25,87
E . . .	0	0	− 0,02795	0,045293	0
$a \times 10^2$.	0,51	0,58	0,55	0,55	0,55
$b \times 10^2$.	0,50	0,50	0,50	0,50	0,50
Referencia.	[5]	[5]	[4]	[4]	[4]

Con la ayuda de programas preparados por T. Iglesias, F. Briones y M. R. Corella*.

* Junta de Energía Nuclear, Madrid.

Cálculo de constantes térmicas

Se toma como intervalo de termalización el comprendido entre 0 y 0,625 eV. Todos los neutrones térmicos se reunen en un mismo grupo (cf., sin embargo, más adelante), y las correspondientes constantes se determinan promediando respecto del flujo. Este resulta de la integración de la ecuación del transporte en su forma elemental, es decir, la que responde a las siguientes hipótesis simplificadoras: *a*) la termalización tiene lugar en un medio homogéneo, isótropo e infinito, corrigiéndose las fugas de neutrones mediante un término de la forma DB^2F_0; *b*) el medio dispersor es un gas monoatómico; *c*) la masa de los núcleos del gas es igual a la del neutrón en todo el intervalo 0–0,625 eV (espectro Wigner–Wilkins) o mucho mayor que la del neutrón en todo él (espectro Wilkins) o se comporta de la primera manera en un intervalo $E_c \leq E \leq E_0 = 0{,}625$ eV, y de la segunda en el intervalo complementario $O \leq E \leq E_c$. En estas condiciones, el problema se reduce a la integración de una ecuación diferencial de la forma

$$y''(E) = -H(E)\, y(E) \tag{8}$$

donde $H(E)$ es una función continua de E en todo el intervalo (O,E_0) en los dos primeros casos y presenta una discontinuidad de primera especie en E_c en el último caso. La solución $y(E)$ buscada es la que se anula en el origen y es continua, con derivada primera continua, en todo el intervalo (O,E_0). Como consecuencia, la densidad neutrónica $N(E)$ es continua en (O,E_0), pero su derivada primera presenta una discontinuidad de primera especie en E_c si en E_c es discontinua $H(E)$. Los programas PROMETEO-I, II y III [9–11] permiten la resolución numérica de (8), y con ello el cálculo del flujo $F_0(E)$, en los tres casos citados: espectro Wigner–Wilkins, espectro Wilkins o espectro Wilkins en (O,E_c) y Wigner-Wilkins, en (E_c,E_0). Los parámetros de entrada son las densidades atómicas de los diversos elementos, la laplaciana, la temperatura del moderador y el tipo de enlace molecular.

Regiones vacías

En el caso de estratos cilíndricos prácticamente vacíos (por ejemplo, regiones ocupadas por un gas cuyas secciones eficaces son muy pequeñas empleado como refrigerante o como aislante térmico en un reactor con moderador frío), en un modelo con varios grupos de neutrones y en la aproximación de difusión se puede considerar el vacío como un medio que sólo dispersa, caracterizado por las constantes $\Sigma_c = 0$, $\nu\Sigma_f = 0$ y un coeficiente D^v [12] dado por

$$D^v = \frac{r_{v-1}}{2\alpha} \ln \frac{r_v}{r_{v-1}} \simeq 1 \pm 0{,}2 \text{ para } 0{,}15 \leqslant \frac{r_{v-1}}{r_v} \leqslant 0{,}85 \tag{9}$$

donde $\alpha = 1 = (2/\pi)$ arcsen $(r_{v-1}/r_v) - (2/\pi)$ $(r_{v-1}/r_v) \times (1 - r_{v-1}/r_v)^{\frac{1}{2}}$ y r_v, r_{v-1} son los radios exterior e interior de la región vacía.

Estructura fina

La heterogeneidad de la región que contiene el haz de barras combustibles, con sus vainas, y el refrigerante se tiene en cuenta de la manera siguiente. En el grupo neutrónico para el que existen resonancias, la heterogeneidad interviene a través del área efectiva, S_{ef}. En el grupo térmico se obtienen los factores de desventaja aplicando la teoría de difusión monoenergética al refrigerante y la teoría de colisiones múltiples en la vaina y en el combustible. El enlace entre estos dos últimos modelos se efectúa por medio de la longitud extrapolada

$$\lambda\Sigma^r{}_{tr} = \frac{4}{3\beta} - H \tag{10}$$

en la cual $\Sigma^r{}_{tr}$ corresponde al refrigerante, β es la negrura de la vaina y del combustible y H es función de la corriente neutrónica en un medio infinito sin absorción [13,14].

Parámetros integrales de la celda

Una vez calculadas las constantes térmicas y rápidas de los $g \leq 4$ grupos neutrónicos para cada una de las regiones homogeneizadas de la celda, teniendo en cuenta los factores de desventaja debidos a la heterogeneidad de la región ocupada por el haz combustible, y caracterizadas las regiones vacías por un coeficiente de difusión efectivo (9), se obtiene aplicando la teoría de difusión con varios grupos neutrónicos, las g componentes del flujo, el factor de multiplicación k y la laplaciana material de la celda. Aun a sabiendas de que en muchos casos será conveniente emplear una aproximación mejor de la teoría del transporte, se han aplicado los programas EDIPO-I y II [15] al cálculo de las componentes del flujo en la celda. El programa EDIPO-I resuelve numéricamente en una dimensión las ecuaciones para varios grupos neutrónicos en la aproximación de difusión

$$\nabla D_i \nabla \phi_i - [D_i B^2{}_{\perp i} + \Sigma_{ai} + \sum_{j=i+1}^{j} \Sigma_{i\to j}]\phi_i + \sum_{j=1}^{i=1} \Sigma_{j\to i}\phi_j + \frac{1}{\lambda} X_i \sum_{j=1}^{g} (\nu\Sigma_f)_j \phi_j = 0 \tag{11}$$

para $g \leq 4$; 20 regiones y 199 puntos. Los resultados son las componentes ϕ_i del flujo y el valor propio $k_\infty = \lambda$. La laplaciana material, $B^2{}_m$, se calcula como la mayor de las raices de la ecuación secular asociada a (11) con $\lambda = 1$ [16]. El programa EDIPO-II resuelve un problema análogo al (11), con $g \leq 16$; 5 regiones y 49 puntos. En los tres últimos grupos (los tres de más bajas energías) se admite la posibilidad de dispersión regenerativa (*upscattering*), lo que permite emplearlo en un modelo con 3 grupos térmicos y $g-3$ grupos rápidos en el que los neutrones térmicos se tratan siguiendo en esencia, el método de Selengut.

Iteraciones sucesivas

En la primera iteración, para el cálculo de las constantes térmicas y rápidas, se parte, como se indicó, de

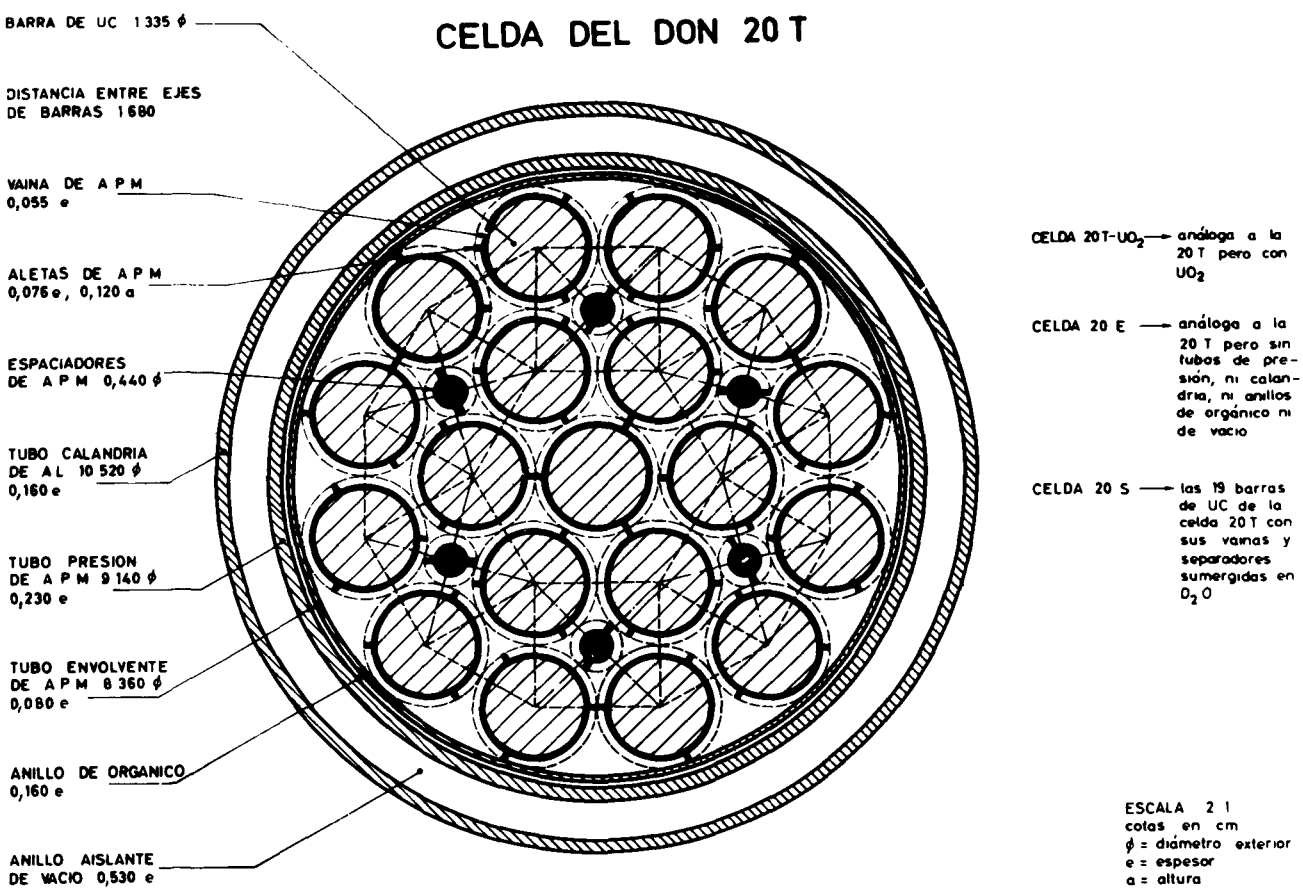

Figura 1

unas densidades atómicas ponderadas de acuerdo con los respectivos volúmenes. Al final, se obtienen las distribuciones en la celda de las g componentes del flujo. En las sucesivas iteraciones se parte de unas densidades atómicas pesadas con sus volúmenes y con el flujo resultante de la iteración anterior. El proceso se repite hasta obtener la convergencia deseada en el valor propio k o en el de la laplaciana material. En los cálculos de optimización se suele emplear una iteración solamente.

MÉTODO DE SÍNTESIS

Dada la capacidad, relativamente pequeña, de la calculadora UNIVAC USS-90, de que se dispone en la JEN, es difícil obtener con ella distribuciones de flujo bidimensionales. Con vistas a realizar cálculos de exploración, se preparó un programa para construir flujos sintéticos bidimensionales [17]. Se trata, en esencia, del llamado método ordinario de síntesis. Si $i=1, 2, \ldots, n$ es una región transversal y $\mu=1, 2, \ldots, g$ caracteriza al grupo μ-ésimo, con el programa EDIPO se determina la solución (general, no normalizada) de

$$\mathrm{div}_x\, D_\mu\, \mathrm{grad}_x\, \phi^i{}_\mu(x) - [\Sigma_{T\mu} + D_\mu B^2{}_{z\mu}(i)]\phi^i{}_\mu(x) + \sum_{\nu=1}^{\mu-1} \Sigma_{\nu\mu}\phi^i{}_\nu(x) + \frac{1}{\lambda_x} X_\mu \sum_{\nu=1}^{g} (\nu\Sigma_f)_\nu\, \phi^i{}_\nu(x) = 0 \quad (12)$$

que satisface las condiciones de contorno adecuadas y el correspondiente valor propio $\lambda_x(i)$. Hay que partir, claro está, de valores estimados de las g laplacianas $B^2{}_{z\mu}(i)$. Se procede entonces a un cálculo axil, determinando la solución de

$$\bar{D}^i{}_\mu\, Z''{}_\mu(z) - [\bar{\Sigma}^i{}_{T\mu} + \bar{D}^i{}_\mu\, B^2{}_{x\mu}(i)]\, Z_\mu(z) + \sum_{\nu=1}^{\mu-1} \bar{\Sigma}^i{}_{\nu\mu}\, Z_\nu + \frac{1}{\lambda_z} \sum_{\nu=1}^{g} \overline{X_\mu\, (\nu\Sigma_f)^i{}_\mu\, Z_\nu} = 0\,(i=1, 2, \ldots, n) \quad (13)$$

que satisface las condiciones de contorno adecuadas y el correspondiente valor propio λ_z. En (13), los promedios son de la forma

$$\bar{f}^i{}_\mu = \frac{\int_{(i)} \mathrm{d}x\, f_\mu(x)\, \phi^i{}_\mu(x)}{\int_{(i)} \mathrm{d}x\, \phi^i{}_\mu(x)} \quad (14)$$

y, además

$$\bar{D}^i{}_\mu\, B^2{}_{x\mu}(i) \int_{(i)} \phi^i{}_\mu(x)\mathrm{d}x = \sum_{\nu=1}^{g} \left[\bar{\Sigma}^i{}_{\nu\mu} + \frac{1}{\lambda_x} \overline{X_\mu(\nu\Sigma_f)^i{}_\nu}\right] \int_{(i)} \phi^i{}_\nu\, \mathrm{d}x - [\bar{\Sigma}^i{}_{T\mu} + \bar{D}^i{}_\mu\, B^2{}_{z\mu}(i)] \int_{(i)} \phi^i{}_\mu\, \mathrm{d}x \quad (15)$$

A partir de la solución de (13), se lleva a cabo una nueva sucesión de n cálculos transversales de acuerdo

Tabla 2. Laplacianas materiales calculadas y medidas[a]

Celda	Separación entre celdas con red: Exagonal (cm)	Separación entre celdas con red: Cuadrada (cm)	Pureza del D_2O, %	B^2_m, m^{-2}: Calculado	B^2_m, m^{-2}: Medido: Exp. JEN	B^2_m, m^{-2}: Medido: Aquilon II[a]
20 T . . .	21,59	20,092	99,75	1,23	$1,44 \pm 0,09$	
	24,13	22,456	99,75	1,85	$2,04 \pm 0,09$	
	26,67	24,819	99,75	2,02	$2,25 \pm 0,08$	
20 E . . .	20,417	19	99,50	3,74		4,08
	22,566	21	99,50	4,11		4,22
	25,789	24	99,50	3,98		3,94
20 S . . .	20,417	19	99,50	5,11		5,44
	22,566	21	99,50	5,64		5,84
	25,789	24	99,50	5,52		5,55
70F″7 . . .	20,417	19	99,50	5,24		
	22,566	21	99,50	5,44		
	25,789	24	99,20	5,13		
20T-UO_2 . .	26,67	24,819	99,75	1,05	$1,25 \pm 0,08$	

[a] Interpretado en la JEN por de Francisco [20].

con (12) y con las g laplacianas $B^2{}_{z\mu}(0)$ dadas por

$$D^i{}_\mu B^2{}_{z\mu}(i) \int_{z_{i-1}}^{z_i} Z_\mu(z)\,dz = \sum_{\nu=1}^{g} \left[\bar{\Sigma}^i{}_{\nu\mu} + \frac{1}{\lambda_x} \overline{X_\mu(\nu\Sigma_f)^i{}_\nu} \right] \int_{z_{i-1}}^{z_i} dz - [\bar{\Sigma}^i{}_{T\mu} + \bar{D}^i{}_\mu B^2{}_{x\mu}(i)] \int_{z_{i-1}}^{z_i} Z_\mu\,dz \quad (16)$$

El proceso se repite hasta conseguir que $\lambda_x(1) = \ldots = \lambda_x(n) = \lambda_z$, dentro de límites prefijados. La convergencia suele ser bastante rápida.

EXPERIMENTOS EN AQUILON-II Y EN LA JEN

El esquema de cálculo que precede se ha contrastado con los resultados de experimentos exponenciales realizados en la División de Física de la JEN y de experimentos de sustitución realizados en AQUILON-II. La celda empleada es la tipo 20 del reactor DON (fig. 1). En los experimentos exponenciales se emplearon las celdas completas (20T y 20T-UO_2) con el refrigerante orgánico y todos los tubos, empleando una red exagonal de pasos 8,5; 9,5 y 10,5 in. En los experimentos de sustitución se emplearon las celdas 20E y 20S en una red cuadrada de pasos 19; 21 y 24 cm con las celdas de referencia 70F″7 de UO_2 [19 y 20].

En la tabla 2 se dan los valores calculados y medidos de B^2, y en las figuras 2 y 3 se incluyen, además, los valores calculados de k.

Las diferentes configuraciones críticas del AQUILON-II (fig. 4, tabla 3) se calcularon teorícamente, cuyos resultados se dan en las tablas 4 y 5.

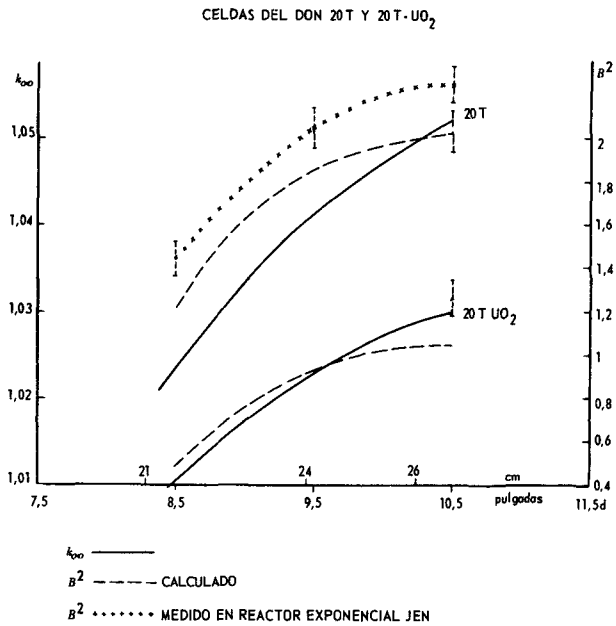

Figura 2

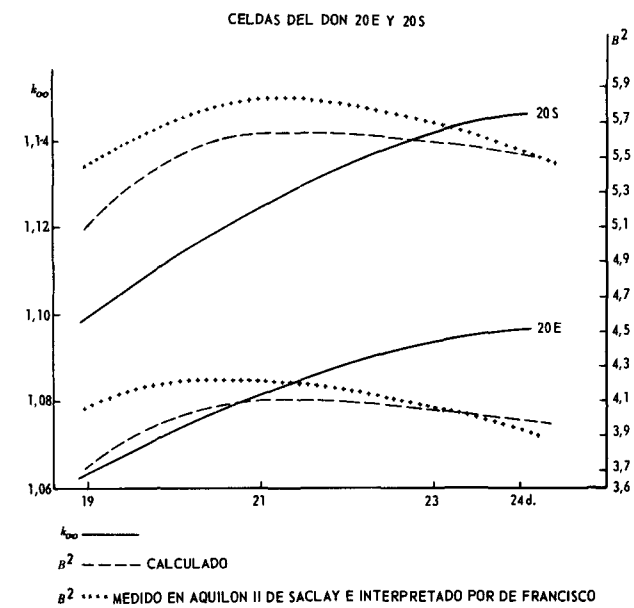

Figura 3

Tabla 3. Dimensiones del modelo geométrico de sustitución

Dimensiones radiales (Redes 20-S y 20-E)

Paso reticulado (cm)	OR_0 Número de elementos sustituidos 0	4	12	16	24	OR_1	OR_2	OR_3	OR_4
19	0	21,43	37,13	42,88	52,52	113,45	145	145,6	211,95
21	0	23,69	41,03	47,40	58,04	125,39	145	145,6	211,95
24	0	27,07	46,90	54,17	66,34	143,30	145	145,6	211,95

Dimensiones axiles

(Red 20-S)

Paso reticulado (cm)	OH_1 Número de elementos sustituidos 0	4	12	16	24	H_1H_2	H_2H_3	H_3H_4
19	148,80	148,38	147,97	147,71	147,44	7,5	1	71,95
21	141,44	140,81	139,41	138,94	137,87	7,5	1	71,95
24	147,45	146,36	144,31	143,52	141,99	7,5	1	71,95

(Red 20-E)

Paso reticulado (cm)	OH_0 Número de elementos sustituidos 0	4	12	10	24	H_0H_1	H_1H_2	H_2H_3	H_3H_4
19	$OH_1 = 148,74$	$OH_1 = 151,92$	7,74	11,46	19,16	151 (no) 0,4	7,5	1	71,95
21	$OH_1 = 141,96$	$OH_1 = 144,88$	$OH_1 = 150,8$	3,06	9,76	151 (no) 0,12	7,5	1	71,95
24	$OH_1 = 147,71$	$OH_1 = 151,31$	7,85	11,58	20,12	151 (no) 0,4	7,5	1	71,95

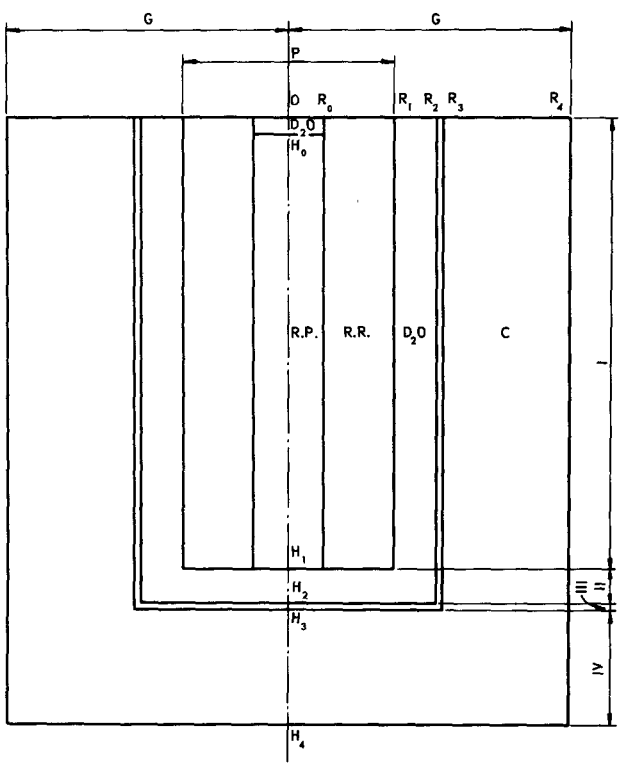

EXPERIENCIA AQUILON II

Figura 4

ESTÁTICA DE REACTORES RÁPIDOS

Cálculo de las constantes

El esquema de cálculo consta de dos programas, CAMPEADOR y EDIPO, ambos en teoría de difusión. El programa CAMPEADOR resuelve las ecuaciones para 16 grupos de neutrones en la aproximación de difusión y con las constantes recogidas por Yiftah, Okrent y Moldauer [21]. Determina primero las 16 componentes ϕ_i del flujo que obedecen al sistema

$$-D_iB^2{}_i\phi_i - \Sigma_{ai}\phi_i - \sum_{j=i+1}^{j=16} \Sigma_{i\to j}\phi_i + \sum_{k=1}^{k=i-1} \Sigma_{k\to i}\phi_k + \frac{X_i}{k_{ef}} \sum_{r=1}^{r=16} (\nu\Sigma_f)_r\phi_r = 0 \quad (17)$$

Tabla 4. Valores calculados de k_{ef} para los experimentos con la red 20-S

Número de barras sustituidas	Paso 19	Paso 21	Paso 24
0	0,991	0,996	0,999
4	0,990	0,994	0,999
12	0,989	0,995	0,998
16	0,989	0,995	0,998
24	0,988	0,996	0,998

Tabla 5. Valores de k_{ef} para los experimentos con la red 20-E

Número de barras sustituidas	Paso 19	Paso 21	Paso 24
0	0,991	0,996	1,000
4	0,991	0,995	1,000
12	0,991	0,996	1,001
16	0,992	0,996	1,002
24	0,992	0,998	1,003

y de la importancia, solución del sistema adjunto

$$-D_i B^2{}_i \phi^*{}_i - \Sigma_{ai}\,\phi^*{}_i - \sum_{j=i+1}^{j=16} \Sigma_{i\to j}\,\phi^*{}_i + \sum_{j=i+1}^{j=16} \Sigma_{i\to j}\,\phi^*{}_j + \frac{(\nu\Sigma_f)_i}{k_{ef}} \sum_{j=1}^{j=16} X_j\,\phi^*{}_j = 0 \quad (18)$$

Para ello se hace $\frac{1}{k_{ef}} \sum_{r=1}^{r=16} (\nu\Sigma_f)_r\ \phi_r = 1$ en (17) y $\frac{1}{k_{ef}} \sum_{j=1}^{j=16} X_j\,\phi^*{}_j = 1$ en (18), con lo que ambos sistemas se transforman en triangulares de muy fácil resolución.

A continuación, el programa condensa las constantes a cualquier número de grupos $g \leq 16$. Dicha condensación la efectúa con el espectro de flujos en la forma usual y con el producto del espectro de flujos por el de importancias. Permite calcular también el factor efectivo de multiplicación k_{ef} de sistemas desnudos según la fórmula

$$k_{ef} = \frac{\sum_{r=1}^{r=16} (\nu\Sigma_f)_r\,\phi_r}{\sum_{r=1}^{r=16} (D_r B^2 + \Sigma_{ar})\,\phi_r} \quad (19)$$

y la laplaciana crítica mediante un proceso de iteración sobre k_{ef}. Calcula así mismo el factor de multiplicación infinito k_∞, que corresponde a $B^2 = 0$.

Para el estudio de sistemas desnudos pequeños y muy concentrados, cabe la posibilidad en este programa de substituir el término de fugas de la teoría de difusión $B^2{}_j/3\Sigma_{trj}$ por el valor correspondiente de la solución asintótica de la ecuación de Boltzmann, $B_j/\text{arctg}\ (B_j/\Sigma_{trj}) - \Sigma_{trj}$, con lo cual se obtienen mejores valores para el espectro y la masa crítica.

Tabla 6.
Masas críticas, en kg de combustible (^{235}U, ^{233}Pu), de sistemas desnudos muy concentrados

Sistema	Ref.	Teoría de difusión	Solución asintótica (ec. de Boltzmann)	Valor experimental	Geometría
GODIVA .	3	63,5	41,1	48,7	Esfera
JEZEBEL .	3	29,7	12,5	16,22	Esfera

Contraste del esquema de cálculo

Este esquema de cálculo se ha aplicado a dos sistemas desnudos muy concentrados GODIVA y JEZEBEL [23] y a cuatro sistemas reflejados estudiados en la instalación para experimentos de criticidad ZPR-III [24,25]. Para los dos primeros se calculó la masa crítica según los dos procedimientos ya indicados, obteniéndose en difusión un resultado por exceso como era de esperar. Cuando el término de fugas es el dado por la solución asintótica de la ecuación de Boltzmann, el resultado es mejor, pero por defecto. Los resultados se dán en la tabla 6. Para los casos experimentados en ZPR-III, se condensaron las constantes a cuatros grupos con el espectro de flujos y con el producto de flujos e importancias, suponiendo un valor de la laplaciana independiente del grupo e igual a la laplaciana material. La reactividad y la distribución de flujos se obtuvieron a continuación por aplicación de EDIPO y de la técnica de síntesis explicada en el esquema expuesto para reactores térmicos. En algunos casos, de la distribución de flujos así obtenida se dedujo el valor de la laplaciana por grupos y se procedió a una nueva condensación con CAMPEADOR y a un nuevo cálculo de reactividad con el programa EDIPO.

Los resultados se presentan en la tabla 7. Los de la columna A están obtenidos por condensación con flujos. Los de la columna B por condensación con flujos e importancias.

Los resultados de las tablas 4 y 5 no se consideran suficientemente buenos para obtener la masa crítica. Se pretende mejorarlos mediante un cálculo de iteraciones sucesivas de las constantes de la celda y acaso ajustando los parámetros dejados libres a tal efecto. Las tablas 6 y 7 parecen indicar una situación similar; por otra parte es difícil llegar a conclusiones generales partiendo de los resultados de la tabla 6. La razón fundamental consiste en que deberían hacerse correcciones previas por la heterogeneidad de los elementos combustibles y el efecto de la región intermedia entre las dos mitades de la máquina ZPR-III.

EXPRESIONES DE AGRADECIMIENTO

Queremos agradecer a Atomics International la colaboración prestada en el cálculo de las constantes rápidas del elemento combustible tipo DON.

Tabla 7. Factor efectivo de multiplicación en sistemas críticos probados en ZPR-III

Número del sistema	Ref.	Geometría	A	B
6 C . . .	24	Cilindro	0,956	0,976
6 F . . .	24	Esfera	1,011	1,011
9	24	Cilindro	1,010	1,009
9 A . . .	24	Esfera	1,004	1,007

BIBLIOGRAFÍA

1. Briones, F., FTCR 4, informe interno, JEN (julio 1961).
2. Velarde, G., FTCR 24, informe interno, JEN (enero 1964).
3. Vernon, R., Nuc. Sci. Eng. *6*, 163 (agosto 1959).
4. Velarde, G., FTCR 23, informe interno, JEN (enero 1964).
5. Hellstrand, E., *et al.*, Nuc. Sc. Eng. *8*, 497 (1960).
6. Carlvik, I., y Pershagen, B., RFR 20 (febrero 1959).
7. Fukai, Y., Nuc. Sc. Eng. *9*, 370 (1961).
8. Velarde, G., Nuc. Sc. Eng. *15*, 1, 99 (1963).
9. Corella, M. R., e Iglesias, T., PROMETEO I (en prensa).
10. Corella, M. R., e Iglesias, T., PROMETEO II (en prensa).
11. Corella, M. R., e Iglesias, T., PROMETEO III (en prensa).
12. Velarde, G., Nuc. Sc. Eng. *13*, 2, 200 (1962).
13. McKay, C. D., NEI 143 (junio 1960).
14. Pershagen, B., y Carlvik, I., AEF 69.
15. Iglesias, T., FTCR 13, informe interno, JEN (marzo 1963).
16. Brú, A., FTCR 30, informe interno, JEN (1964).
17. Ortiz Fornaguera, R., e Iglesias, T., FTCR 32, informe interno, JEN (marzo 1964).
18. ANL-5800, segunda edición.
19. Bailly, J., *et al.*, DEP/EC/S 60-52 (junio 1960).
20. Rodríguez Mayquez, E., Francisco, J. L. de, y Olarte, F., *Estudio experimental de redes de carburo de uranio en agua pesada*, véanse las presentes Actas, P/743, Vol. 3.
21. Yiftah, S., *et al.*, *Fast Reactor Cross Sections*, Pergamon Press.
22. Caro, R., *CAMPEADOR, a Condensation Code for Fast Reactors*. EAES Symposium on Fast and Epithermal Spectra in Reactors, Harwell (diciembre 1963).
23. Loewenstein, W. B., y Okrent, K., *Física de reactores rápidos de potencia; informe sobre el estado del problema*, Actas de la segunda conferencia internacional sobre la utilización de la energía atómica con fines pacíficos, P/637, Vol. 6, pág. 323, Naciones Unidas (1958).
24. Long, J. K., *et al.*, *Estudios sobre reactores de potencia de neutrones rápidos con el ZPR-III*, Actas de la segunda conferencia international sobre la utilización de la energía atómica con fines pacíficos, P/598, Vol. 6, pág. 387, Naciones Unidas (1958).
25. Long, J. K., *et al.*, *Experimental Results on Large Dilute Fast Critical Systems with Metallic and Ceramic Fuels*, Physics of Fast and Intermediate Reactors, Vol. 1, pág. 271, IAEA, Viena (1962).

ABSTRACT—RÉSUMÉ—АННОТАЦИЯ—RESUMEN

A/742 Spain

Two schemes for nuclear reactor calculations

By R. Ortiz *et al.*

Two mathematical schemes for nuclear reactor calculations have been prepared at the Theoretical Physics and Reactor Calculations Division of the Junta de Energía Nuclear (JEN).

The tools for the first scheme are the following programmes, all coded at JEN for the UNIVAC USS-90 computer:

(*a*) ISLERO

This programme solves either the P_1 or B_1 approximation to the one-dimensional, multigroup slowing-down Boltzmann equation in an infinite homogeneous slab. The 54 energy groups range from 0.625 eV to 10 MeV. Few-group constants, to a maximum of three groups, are obtained by averaging over the flux spectrum. Input data are the isotopic composition, the geometric buckling and the self-shielding factor.

(*b*) PROMETEO-I, II and III

These programmes solve the differential equations, with spectra, for the Wigner-Wilkins and the Wilkins cases, and for a combination of the two. The thermal constants are averaged over the obtained flux spectrum. Input data are the isotopic composition, the geometric buckling, temperature and form of molecular binding.

(*c*) EDIPO-I and II

These programmes solve the one dimensional, several-group diffusion equations. EDIPO-I is a few-group (4 max.) programme, for a maximum of 20 regions and 199 mesh points. The corresponding values for EDIPO-II are, 16, 4 and 49, respectively. An interesting feature of the last programme is that it allows consideration of up-scattering in the last three groups. The conventional method of flux synthesis has been applied to synthesize two-dimensional fluxes by combining the results of one-dimensional problems. Isotopic composition in clusters follows from the thermal flux fine distribution according to the Pershagen-Carlvik approach. A generalized Selengut method has been developed by taking advantage of the possibility offered by EDIPO-II of having up-scattering in the three last energy groups. In this way interference phenomena between thermal spectra can be taken into consideration.

The whole theoretical scheme has been applied to the substitution experiments carried out in AQUILON II (Saclay) and to the exponential experiments carried out at the Physics Division of JEN, as a part of the DON Project Programme (a natural uranium carbide, heavy water, organic, reactor system), in all calculations the resonance self-shielding factor was left free as an adjustable parameter. Four-groups diffusion theory was used throughout.

The second scheme differs from the first essentially in that the weighting functions for averaging cross sections are not the flux spectra, but the product of importance and flux spectra. As a first step, the programme CAMPEADOR has been developed to be used on the USS-90 machine. This programme solves the multigroup (16 groups) diffusion equations and their adjoints for a finite or infinite homogeneous

medium. The condensation to a given number of groups ($\leq$16) takes place by averaging cross sections as said above. EDIPO-I and II are then used for reactivity and neutron flux distribution calculations. The scheme has been checked against experimental and theoretical results for fast neutron systems obtained from the referenced literature.

A/742 Espagne

Deux modèles de calcul de réacteurs nucléaires

par R. Ortiz et al.

La Division de physique théorique et de calcul des réacteurs de la Junta de Energía Nuclear (JEN) a mis au point deux schémas pour le calcul de réacteurs nucléaires.

Le premier se fonde sur les programmes suivants, tous préparés à la JEN pour l'ordinateur électronique UNIVAC USS-90:

a) ISLERO

Ce programme permet de résoudre l'équation de modération de Boltzmann, avec les approximations P_1 ou B_1 pour une plaque homogène infinie. Les 54 groupes énergétiques s'échelonnent de 10 MeV à 0,625 eV. Les constantes, réduites à trois groupes au maximum, sont obtenues en faisant une moyenne d'après le spectre du flux. Les données d'entrée sont: la composition isotopique, le laplacien géométrique et le facteur d'autoprotection.

b) PROMETEO-I, II et III

Ces programmes permettent de résoudre les équations différentielles de Wigner-Wilkins, de Wilkins ou une combinaison des deux. On obtient les constantes thermiques en faisant la moyenne d'après le spectre du flux ainsi calculé. Les données d'entrée sont: la composition isotopique, le laplacien géométrique, la température et le type de liaison moléculaire.

c) EDIPO-I et II

Ces programmes permettent de résoudre les équations unidimensionnelles de la diffusion de divers groupes de neutrons. EDIPO-I concerne les problèmes ayant au maximum quatre groupes, 20 régions et 199 points. Les valeurs correspondantes dans EDIPO-II sont respectivement 16, 5 et 49. Une caractéristique importante de ce dernier programme réside dans le fait qu'il permet d'envisager la dispersion avec un gain d'énergie dans les trois derniers groupes. On a appliqué la méthode habituelle de synthèse des flux à la synthèse des flux bidimensionnels à partir des résultats des problèmes de flux à une dimension. La composition isotopique dans les faisceaux est obtenue à partir de la distribution fine du flux de neutrons thermiques d'après la méthode Pershagen-Carlvik. On a mis au point une méthode de Selengut généralisée en tirant parti de la possibilité qu'offre EDIPO-II de traiter la dispersion avec un gain d'énergie. De cette façon, on peut tenir compte des phénomènes d'interférence des spectres des neutrons thermiques.

Les auteurs ont appliqué l'assemblage du schéma théorique aux expériences de substitution effectuées dans AQUILON-II (Saclay) et aux expériences exponentielles effectuées à la Division de physique de la JEN dans le cadre du programme relatif au projet DON concernant un réacteur à carbure d'uranium naturel, ralenti à l'eau lourde et refroidi par un fluide organique. Dans tous les calculs on a laissé libre, comme paramètre de réglage, le facteur d'autoprotection dans les résonances. On a utilisé dans tous les cas la théorie de diffusion à quatre groupes.

Le deuxième schéma diffère essentiellement du premier, en ce que les fonctions de pondération pour la moyenne des sections efficaces sont non pas les spectres de flux, mais les produits des spectres de flux par les fonctions d'importance. On a commencé par préparer le programme CAMPEADOR pour l'appareil USS-90. Ce programme permet de résoudre les équations de diffusion pour divers groupes et leurs compléments dans un milieu homogène fini ou infini. La réduction à un nombre donné de groupes $\leqslant$16 est obtenue en faisant la moyenne des sections efficaces de la façon indiquée ci-dessus. Un utilise ensuite EDIPO-I et II pour les calculs de réactivité et de distribution du flux. On a vérifié ce schéma par comparaison avec les résultats théoriques et expérimentaux relatifs aux systèmes à neutrons rapides décrits dans la littérature.

A/742 Испания

О двух численных методах расчета ядерных реакторов

Р. Ортиц et al.

В Отделении теоретической физики и расчета реакторов при Управлении по ядерной энергии были разработаны два метода расчета ядерных реакторов.

В основу первого метода положены описываемые ниже программы, которые были составлены Управлением по ядерной энергии для электронно-счетного устройства UNIVAC USS-90.

а) Программа ISLERO.

Эта программа дает возможность решать одномерное уравнение замедления Больтцмана в P_1- или B_1-приближениях для бесконечной гомогенной пластины. 54 энергетические группы перекрывают интервал от 0,625 *эв* до 10 *Мэв*. Малогрупповые константы не более чем для трех групп получаются усреднением по спектру потока нейтронов. Исходными данными являются изотопный состав, геометрический лапласиан и коэффициенты самоэкранировки.

b) Программы PROMETEO-I, PROMETEO-II и PROMETEO-III

Эти программы дают возможность решать

дифференциальные уравнения Вигнера — Вилкинса и Вилкинса или наложение обоих типов. Тепловые константы получают путем усреднения по рассчитанному спектру. Исходными данными являются изотопный состав, геометрический лапласиан, температура и тип молекулярных связей.

c) Программы EDIPO-I и EDIPO-II

При помощи этих программ можно решать одномерные уравнения диффузии для нескольких групп нейтронов. Программа EDIPO-I рассчитана на 4 или меньшее число групп, 20 зон и 199 точек. Соответствующие параметры для программы EDIPO-II равны 16, 5 и 49. Важной особенностью этой последней программы является то, что в трех последних группах она позволяет рассматривать рассеяние с повышением энергии. Исходя из результатов одномерных проблем, обычный метод синтеза потоков был применен для синтезирования двумерных потоков. Изотопный состав в кассете получался из тонкой структуры распределения потока тепловых нейтронов по методу Першагена — Карлвика. Для использования предоставляемой программой EDIPO-II возможности учета рассеяния с повышением энергии был разработан обобщенный метод Селенгута. Это позволяет учитывать явления интерференции тепловых спектров.

Все эти методы были применены для расчета экспериментов, проведенных на критической сборке AQUILÓN-II (в Сакле), а также к экспоненциальным экспериментам, проведенным в Физическом отделении Управления по ядерной энергии в качестве части проекта реактора DON на карбиде природного урана с тяжелой водой и органическим теплоносителем. При всех этих расчетах коэффициент резонансной самоэкранировки оставлялся в качестве свободного параметра, подлежащего подбору. Теория диффузии всегда применялась в четырехгрупповом приближении.

Второй метод отличается от первого главным образом тем, что коэффициентами взвешивания для усреднения эффективных сечений являются не спектры потоков, а произведения этих спектров потоков на величину ценности. В качестве первого шага была составлена программа CAMPEADOR для счетной машины USS-90. Эта программа позволяет решать многогрупповые уравнения диффузии и сопряженные уравнения в конечной или бесконечной гомогенной среде. Сведение до данного числа групп ($\leqslant 16$) производится путем усреднения эффективных сечений согласно указанному выше способу. Затем программы EDIPO-I и EDIPO-II используются для расчета реактивности и распределения потока. Этот метод был проверен путем сравнения с теоретическими и экспериментальными результатами для систем с быстрыми нейтронами по данным технической литературы.

Méthodes expérimentales de physique des réacteurs à neutrons thermiques

par D. Breton et P. Lafore*

Le CEA dispose d'un certain nombre de réacteurs expérimentaux de très faible puissance, sur lesquels sont effectuées des mesures de physique destinées à déterminer des constantes neutroniques particulières ou à s'assurer de la validité des formulaires utilisés dans les projets. Ces travaux sont exécutés sur: MARIUS, expérience critique modérée au graphite, à température ordinaire; CÉSAR, expérience critique modérée au graphite, à haute température; AQUILON, expérience critique modérée à l'eau lourde; ALIZÉ, expérience critique modérée à l'eau ordinaire; AZUR, expérience critique modérée à l'eau ordinaire; ALECTO, 1 et 2, expériences critiques homogènes; MINERVE, expérience critique spécialisée dans les mesures par oscillation. Des assemblages « sous-critiques » (C et BeO) sont également utilisés.

Par ailleurs, des mesures sont entreprises directement sur les réacteurs de puissance, au démarrage et au cours de leur évolution. Enfin, les mesures neutroniques nécessaires aux études de protection sont mises au point sur le réacteur TRITON. Ce texte fait le point des principales méthodes utilisées.

MÉTHODES GÉNÉRALES**

Mesures de distribution neutronique

Il s'agit essentiellement d'expériences classiques d'activation dans des réseaux.

En dehors de quelques cas où le rapport cadmium de l'or est mesuré pour étudier les conditions de mise en équilibre des spectres, il n'est jamais fait usage de rapport cadmium dans la détermination des distributions de densité neutronique. La plupart des mesures sont effectuées soit en utilisant des détecteurs ayant une loi de section efficace de capture voisine de $1/v$ qui ne nécessitent que de faibles corrections pour obtenir les densités neutroniques, soit le combustible lui-même (cas de l'uranium très enrichi) afin d'obtenir une mesure directe de la densité de puissance.

Mesures de densités neutroniques

Les détecteurs utilisés sont des disques, soit de manganèse-nickel ($e = 0{,}15$ mm, $\varnothing = 7$ ou 2 mm), soit de dysprosium métal pur ($e = 0{,}06$ mm, $\varnothing = 2$ ou 1 mm). Les flux intégrés nécessaires sont inférieurs à 10^{10}n/cm^2. Les mesures d'activité β^- sont effectuées sur des installations automatiques à photomultiplicateur équipées de huit têtes de lecture. Les intercalibrations sont effectuées sur des roues dans des flux thermiques. Des passages périodiques assurent des coefficients valables à mieux que 0,6 % (limite de confiance: 95 %). La mise en place des détecteurs dans les réseaux exige de grandes précautions. Pour les mesures de laplacien, il est fait usage de supports aluminium (eau lourde) ou plexiglas (eau légère). Pour des mesures plus délicates, les détecteurs sont positionnés sur des rubans de terphane (épaisseur: 0,01 mm) tendus entre des supports aluminium distants de quelques λ_t. Dans l'uranium, les détecteurs sont protégés par des disques d'aluminium ($e = 0{,}05$ mm).

La précision limite des mesures de laplacien est de l'ordre de 0,5 %; les difficultés proviennent essentiellement des mesures radiales (effets du réflecteur ou anisotropie radiale pour les réseaux à faible chargement).

Le rapport de la densité moyenne dans le combustible à la densité moyenne dans le modérateur est généralement mesuré avec une précision de l'ordre de 1 % pour l'eau lourde, où il est fait usage de la théorie Bailly du Bois pour évaluer l'intégrale sur une cellule carrée à partir de 2 mesures à 45 °C. Dans l'eau légère, pour des éléments type MTR, les mesures sont plus délicates et la précision souvent limitée à 2 %.

L'application de la théorie de Benoist [1] a permis la mesure du coefficient de diffusion radial dans les réseaux à eau lourde refroidis au gaz avec une précision de 2 %. La mesure s'effectue en déterminant le rapport D_r/λ_t lors de l'étude de la déformation anisotrope du flux autour d'une cellule placée dans un gradient macroscopique de flux.

Mesures de densité de puissance

Il s'agit de mesures relatives du taux de fission. Les valeurs sont souvent difficiles à interpréter, mais sont directement utilisables pour les problèmes thermiques. Effectuées avec des portions du combustible, ces mesures ne posent aucun problème de perturbation. Dans le cas de l'eau légère, où nos études ont porté sur des réseaux alliage aluminium-uranium à 90 % de ^{235}U, nous utilisons des plaquettes 15×2 mm^2 ou 5×5 mm^2 ($e = 1$ mm, 25 mg/cm^2 de ^{235}U) ajustées à

---

* Commissariat à l'énergie atomique.

** J. Bailly, Y. Girard, B. Sautiez.

0,96 mm près dans des emplacements prévus dans des plaques spéciales. Pour les réseaux eau lourde, nous utilisons, selon les cas, des disques ou aiguilles. Pour l'oxyde, les dimensions sont $e = 1$ mm, ou pour les aiguilles $\varnothing = 1$mm, $L = 15$ mm [2].

En dehors des cas spéciaux où il est fait usage d'un analyseur 400 canaux, des comptages sont effectués sur une installation automatique à photomultiplicateur comptant les γ d'énergie généralement supérieure à 400 keV. Un détecteur particulier pris comme moniteur passe périodiquement pour contrôler la correction de décroissance.

Pour l'uranium naturel, les efficacités différentes des fissions ^{235}U, ^{238}U conduisent à des incertitudes négligeables.

L'intercalibration est assurée par un comptage γ ayant un seuil à 120 keV (uranium enrichi) ou 60 keV (uranium naturel). Pour des détecteurs vierges ou ayant subi une irradiation depuis plus d'un mois, la précision accessible est meilleure que 1 %.

Dans le cas de l'eau légère sur des éléments du type MTR, l'intégration est résolue par ajustement sur deux directions d'une fonction $A + Be^{-x/L} + Ce^{-x/L}$, L étant la longueur de diffusion à l'intérieur d'un élément combustible. Après trois ou quatre expériences, on obtient en règle générale des valeurs dont les limites de confiance à 95 % sont évaluées à mieux de 0,8 %.

Autres mesures

Des mesures du facteur de conversion initial ont été effectuées sur le réacteur EDF1. Une série de mesures est également en cours sur toute une gamme de réseaux eau lourde uranium naturel du réacteur AQUILON ($\varnothing_U$: 29,2 et 44 mm; pas: 120 à 210 mm).

La technique de mesure des captures dans l'uranium 238 est celle des coïncidences $\gamma\gamma$ du neptunium 239. Des mesures comparatives sont effectuées entre la méthode qui consiste à utiliser un couple d'uranium appauvri (400 ppm) et d'uranium enrichi (U Al = 90 %) et la méthode utilisant un détecteur d'uranium naturel, pour laquelle des corrections de fission rapide sont nécessaires.

Ces mesures nécessitent un appareillage électronique stable et un rendement de détection uniforme entraînant l'utilisation de détecteurs en forme de secteur, de scintillateurs NaI(Tl) de gros diamètre.

MESURES CINÉTIQUES

Neutrons pulsés*

Etude des modérateurs graphite et oxyde de béryllium

a) *Graphite.*—Les paramètres de diffusion du graphite ont été déterminés par la méthode de la source pulsée de neutrons en mesurant la constante de décroissance sur 23 massifs de graphite de densité 1,619 dont les laplaciens variaient de 7 m^{-2} à 155 m^{-2} [3].

Les valeurs ajustées sont les suivantes, à la température de 20°C, $\overline{V\Sigma}_a = 75 \pm 3$ s^{-1}, $D_0 = 216{,}6 \pm 3\ 10^3$ $cm^2\ s^{-1}$, $C = 37{,}9 \pm 4\ 10^5$ $cm^4\ s^{-1}$, d'où, ramené à une densité de 1,6, $\lambda_t = 2{,}65 \pm 0{,}04$ cm.

Onze mesures ont été reprises à Grenoble par M. Lalande sur des massifs du même graphite (B^2 compris entre 7,7 m^{-2} et 16 m^{-2}), l'ajustement étant effectué sur les deux premiers termes après correction du terme en CB^4 en adoptant $C = 37{,}9$. Les valeurs obtenues confirment les précédentes: $\overline{V\Sigma}_a = 77 \pm 4\ s^{-1}$, $D_0 = 217{,}9 \pm 3\ 10^3$ $cm^2\ s^{-1}$. L'anisotropie du même graphite a été déterminée par mesure de α sur six massifs parallélépipédiques. On a trouvé: $D_\parallel / D_\perp = 1{,}017 \pm 0{,}008$. On a également mesuré le temps de vie dans divers massifs de graphite empoisonnés par des barres de cadmium de diamètre 3,31 cm réparties suivant un réseau de pas carré égal à 23 cm: $\overline{V\Sigma}_a = 972 \pm 50\ s^{-1}$.

b) *Oxyde de béryilium.*—Les mesures effectuées à ce jour portent sur 11 massifs dont les laplaciens s'échelonnent entre 15 m^{-2} et 38 m^{-2} (densité 2,96 à la température 21,5°C). Les mesures ont été corrigées du terme en CB^4 en adoptant $C = 40\ 10^{-4}$ $cm^4\ s^{-1}$ [4]. On en déduit: $\overline{V\Sigma}_a = 144{,}5 \pm 3\ s^{-1}$, $D_0 = 133 \pm 2\ 10^3 cm^2 s^{-1}$ et $\lambda_t = 1{,}60 \pm 0{,}03$ cm. Cette dernière valeur est à comparer à la dernière valeur expérimentale publiée par Zhezherun [4], $\lambda_t = 1{,}77 \pm 0{,}02$ cm; à la valeur théorique calculée par Bhandari [5], $\lambda_t = 1{,}58$, et à la valeur mesurée par la méthode de modulation [6], $\lambda_t = 1{,}76 \pm 0{,}05$ cm. Toutes ces valeurs sont données à la densité 2,96.

Milieux multiplicateurs

La technique des sources pulsées de neutrons appliquée aux expériences critiques donne des résultats intéressants. La constante de décroissance α est en effet fonction du temps de vie des neutrons dans le milieu, τ, et de l'écart à l'unité du facteur de multiplication $\Delta K = K_{eff} - 1$:

$$\alpha = \frac{\beta_{eff}}{\tau}\left[1 - \frac{K(1-\beta_{eff})}{\beta_{eff}}\right]$$

Il est donc possible de déterminer l'un de ces deux paramètres lorsque l'autre est connu. De nombreuses expériences ont été menées sur divers assemblages critiques [7–9], en particulier pour mesurer la valeur en réactivité de barres de sécurité. Les résultats ont été la plupart du temps comparés aux valeurs obtenues par d'autres méthodes (empoisonnement, variation du laplacien); cette comparaison a montré qu'il était pratiquement toujours nécessaire d'apporter des corrections calculées au temps de vie mesuré τ pour tenir compte des variations éventuelles des fuites ou de l'absorption.

De telles mesures ont par exemple été effectuées sur des réseaux modérés à l'eau légère [9] avec des plaques absorbantes ayant une antiréactivité comprise entre 2000 et 6300 pcm par cette méthode et par mesure de la concentration critique en bore. On a obtenu pour

* Y. Girard, J. Lalande, M. Sagot.

des plaques de cadmium: 5500 pcm par empoisonnement au bore, 5170 pcm par neutrons pulsés (β_{eff}/τ mesuré sur pile propre et non corrigé), 5540 pcm par neutrons pulsés (β_{eff}/τ mesuré sur pile avec absorbeurs).

On voit que l'absence de correction sur τ conduirait à une erreur de 7 % par défaut. Dans la gamme étudiée, on constate que α varie linéairement avec le titre critique (T_c), ce qui est très intéressant car il suffit de déterminer expérimentalement $\alpha = f(T_c)$ pour mesurer directement par interpolation la valeur d'un absorbant quelconque, quelle que soit sa nature (Cd, Sm, Ag–In–Cd).

La méthode des neutrons pulsés a été également utilisée pour déterminer un paramètre critique lorsque les dimensions de l'assemblage étaient insuffisantes pour atteindre la criticité. Si ρ est la réactivité de la pile, on a en effet:

$$\rho/\beta_{eff} = -A/B$$

A = contribution totale des neutrons prompts
B = contribution totale des neutrons retardés

En faisant plusieurs mesures de α à différentes hauteurs du niveau d'eau lourde dans AQUILON, on ajuste une relation harmonique entre α et H_e (hauteur extrapolée). Chaque mesure fournit une valeur de $\alpha_0 = \alpha/(1 + A/B)$ de laquelle on déduit $(H_e)_0$ hauteur critique extrapolée. L'antiréactivité du réacteur lors de ces mesures a varié de 400 pcm à 2500 pcm; la hauteur critique a été obtenue à 50 pcm près.

Fluctuations * [10, 11]

L'étude du coefficient de décroissance α de la population des neutrons prompts d'un réacteur peut être effectuée par la mesure des fluctuations en régime légèrement « sous-critique ». Plusieurs méthodes utilisant ces principes ont été mises en pratique sur les réacteurs homogènes PROSERPINE et ALECTO, principalement:

a) La méthode des variances réduites, consistant en la mesure de $Y = [(\overline{C})^2 - (\overline{C^2})]/\overline{C}$, C étant un nombre de neutrons comptés dans le réacteur pendant un intervalle de temps donné;

b) La méthode des probabilités, introduite par Mogilner, permettant d'atteindre Y par l'étude de la probabilité de compter zéro, un deux ... neutrons pendant un intervalle de temps donné.

Ces deux méthodes, qui permettent la détermination de α pour diverses réactivités, sont en bon accord avec la méthode des neutrons pulsés. Toutefois, le temps de mesure est plus long pour les premières.

Mesure des sections efficaces par la méthode d'oscillation **

Depuis plusieurs années, la méthode d'oscillation est utilisée pour la mesure des sections efficaces effectives; cependant, devant le besoin constant d'améliorer la précision, il a été nécessaire d'adapter les méthodes à chaque problème particulier pour en tirer le maximum d'efficacité. Des applications originales ont été développées pour obtenir, suivant la nature du matériau ou la section efficace à mesurer, des conditions de mesure permettant d'atteindre la précision maximale tout en rendant plus aisée l'interprétation des résultats en travaillant dans un spectre parfaitement connu.

Mesure des sections efficaces thermiques

La méthode d'oscillation de phase utilisée il y a plusieurs années par D. Breton [12] pour le contrôle de la pureté nucléaire des matériaux a été développée sur ZOÉ, pour mesurer les sections efficaces d'absorption thermique de corps peu capturants mais très diffusants. Elle permet d'effectuer des mesures précises dans un spectre thermique et atténue de façon très importante et d'un facteur connu l'effet de la diffusion [13].

On mesure la phase du signal fourni par un détecteur placé au voisinage de l'échantillon, qui est la résultante du signal correspondant à la variation locale de flux et du signal de réactivité. Pour des conditions d'oscillation déterminées on démontre que la variation de phase entre les signaux résultants produits par le support seul et par l'échantillon ayant des surfaces de capture ΔS_0 et de diffusion ΔS_d placé sur le même support peut s'exprimer par la relation:

$$\alpha = a\,[\Delta S_0 - (C/D)\Delta S_d].$$

En utilisant un support en graphite, le rapport C/D est voisin de 10^{-3}, rendant ainsi très faible l'effet de la diffusion.

Les échantillons sont comparés à des étalons de bore, pour lequel on adopte comme section efficace $\sigma_0 = 760{,}3 \pm 2$ barns à 2200 m/s.

Dans le tableau 1, les sections efficaces d'absorption à 2200 m/s mesurées sont comparées à celles publiées dans les deux éditions du BNL 325.

Tableau 1. Comparaison entre les sections efficaces d'absorption de quelques éléments

Eléments	Valeurs mesurées	BNL 325 (1958)	BNL 325 (1960)
Aluminium . .	229±3 mb	230±5	241±3
Magnésium .	64,2±1,5 mb	63±3	69±2
Fer	2,53±0,03 b	2,53±0,06	2,62±0,06
Cuivre . . .	3,74±0,04 b	3,77±0,03	3,85±0,03

Mesure des intégrales de résonances d'absorption

Les mesures sont effectuées au centre du cœur de MINERVE, réacteur à uranium très enrichi, modéré à l'eau légère, dans un spectre très riche en neutrons épithermiques sans filtre de cadmium [14]. On mesure par la méthode d'oscillation la section efficace effective, et, en retranchant la partie thermique, on en déduit l'intégrale de résonance.

La variation de réactivité produite par un échantillon contenant N noyaux s'écrit, pour la dilution

* C. Clouet d'Orval, R. Caizergues.
** J. C. Carré, R. Vidal.

infinie, la constante α caractérisant la dureté du spectre: $\Delta k = QN\dot{\sigma} = QN\,[g\sigma_0 + \alpha\hat{1}]$.

Les constantes Q et α sont déterminées par étalonnage respectivement avec des solutions de bore et d'or. Tous les échantillons sont en solution dans l'eau.

Pour déduire les valeurs correspondant à la dilution infinie, on extrapole les résultats obtenus avec des échantillons de différentes concentrations en adoptant les facteurs d'autoprotection calculés à l'aide du programme ZUT établi par Nordheim, et on vérifie que la loi théorique d'extrapolation confirme les résultats expérimentaux.

Dans le tableau 2, tous les résultats se rapportent à la teneur naturelle de l'élément. L'intégrale de résonance correspond à la dilution infinie et ne comprend que l'excès sur la partie en $1/v$. Elle est corrigée de la fonction de jonction pour la rapporter au spectre de référence en $1/E$ en adoptant le formalisme d'Horowitz–Tretiakoff [15]. Les valeurs sont comparées à celles calculées à partir des paramètres et à celles mesurées par Tattersall [16].

Tableau 2. Comparaison entre les valeurs mesurées et les valeurs calculées pour quelques éléments

Eléments	Valeurs mesurées	Valeurs calculées	Valeurs mesurées Tattersall [16]
Indium . .	3200±70	3010	3600±350
Hafnium . .	2080±50	1900	2850±350
Argent . .	670±20	730	810± 50
Cobalt . .	50± 5	45	
Césium . .	450±15	380	480± 80
Thorium . .	87± 4	87	106± 10

Pour les corps dont les paramètres de résonance sont les mieux connus, les valeurs mesurées sont en bon accord avec les valeurs calculées.

Mesures des sections efficaces effectives des matériaux fissiles

Une méthode originale a été développée pour mesurer par oscillation les sections efficaces effectives d'absorption et de production de neutrons dans un spectre bien défini [17]. Avec cette méthode, on compare les sections d'absorption par rapport au bore et les sections efficaces de production de neutrons par rapport à l'uranium 235.

Dans des spectres correspondant à des réseaux d'uranium naturel modérés à l'eau lourde ou au graphite, des mesures ont été effectuées avec des alliages d'uranium naturel et de plutonium et avec des échantillons irradiés pour étudier l'évolution de leurs propriétés neutroniques.

Les conditions de mesure actuellement utilisées permettent d'atteindre pour différents spectres les sections efficaces effectives d'absorption et de production avec une précision de 0,5 %, ce qui correspond à des variations de réactivité de $\Delta k/k = 0{,}7.10^{-7}$ et de densité locale de neutrons de $\Delta n/n = 0{,}3.10^{-5}$.

MESURES PAR EMPOISONNEMENT*

Dans une facilité critique, l'empoisonnement homogène du modérateur par dissolution d'un sel absorbant peut être utilisé comme intermédiaire de mesure, soit pour des études de réactivité à taille constante, soit pour des études de fuites à taille variable. Dans cette optique, nous avons utilisé l'acide borique dans l'eau légère et le sulfate de cadmium dans l'eau lourde.

Aspects technologiques

Divers problèmes technologiques ont retenu notre attention, l'un des plus importants étant celui du dosage.

Pour des concentrations en bore comprises entre 20 et 600 mg/l, l'acide borique est transformé en un complexe à fonction acide fort par le lévulose, complexe dosé ensuite par acidimétrie. Le dosage d'une solution inconnue s'effectue par comparaison à deux solutions de référence différant au plus de 20 %, titrées au préalable par gravimétrie avec une erreur inférieure à 0,15 %. Pour un seul dosage, on obtient par interpolation une incertitude de 0,4 % (confiance: 95 %). Cette valeur a été obtenue statistiquement sur un ensemble de 250 vérifications.

Pour le cadmium et des concentrations variant de 2 à 25 mg/l il s'agit en fait d'un dosage de traces. L'extraction du cadmium par une solution étalon de dithizone dans le chloroforme permet d'atteindre une précision de 0,6 à 1 %.

A ces problèmes on peut ajouter:

a) L'adsorption sur l'aluminium oxydé: question plus importante pour le bore que pour le cadmium (de l'ordre de 1 $\mu g/cm^2$), résolue par utilisation de vernis phénolique après oxydation anodique.

b) La récupération du cadmium dans l'eau lourde, effectuée facilement par un seul passage sur résines (teneur résiduelle: 0,05 ±0,05 mg/l).

c) La détermination de la section efficace du cadmium, dont une valeur effective est obtenue à 1 % près par oscillation comparée avec une solution de bore étalon dans une portion de réseau reconstitué dans le réacteur MINERVE.

Applications

Mesures de fuites neutroniques dans AQUILON [18]

Les mesures ont été faites avec du sulfate de cadmium en solution dans l'eau lourde sur deux réseaux, le premier utilisant des barres métalliques pleines à titre d'essai et de vérification, l'autre des grappes d'oxyde sous tube d'air. Chaque réseau a été étudié à deux pas. Les tailles critiques, titre en cadmium, indices de spectre et distribution en densité ont été mesurés. Les titres de cadmium ont varié entre 6,8 et 19,4 mg/l. L'équivalence entre la variation de capture du poison (de l'ordre de 3 % en réactivité) et la diminution des fuites permet une mesure absolue de la longueur de migration du réseau mais, compte tenu en

* J. Bailly, Y. Girard, P. Lourme.

particulier de l'incertitude sur la section effective du cadmium, la précision ne peut dépasser 3 %.

Mesures diverses dans l'eau légère (ALIZÉ)

L'utilisation de solutions de bore est systématique dans l'expérience ALIZÉ, qu'il s'agisse de masses critiques, d'effets d'absorbants ou de coefficient de température. L'idée directrice a été de permettre des études comparées sur des réseaux ayant des fuites rapides à peu près identiques et relativement faibles [19].

La meilleure illustration de cette technique est son emploi dans la mesure du coefficient de température. Dans la gamme de mesures de 20 à 95 °C, les différences de température entre deux points quelconques du cœur et du réflecteur restent inférieures à 0,2 °C, la reproductibilité des mesures passant de 0,5 pcm à 2 pcm. La précision d'un ajustement quadratique atteint 2 % sur le terme carré pour une variation d'environ 600 pcm. Les principales difficultés à surmonter ont été le dégazage des solutions par préchauffage et la stabilité des solutions, en minimisant les phénomènes de distillation.

ÉTUDES DE SPECTRES*

Dans le cadre des études concernant la thermalisation des neutrons, certaines techniques expérimentales ont été mises au point à Saclay, en vue de disposer de détecteurs particulièrement sensibles dans le domaine des énergies légèrement épithermiques. Un nombre important de mesures effectuées à l'aide de ces détecteurs a permis une exploration systématique de divers milieux fissiles: milieux homogènes modérés à l'eau légère, milieux hétérogènes modérés à l'eau lourde, au graphite.

Détecteurs choisis et techniques expérimentales

Choix des détecteurs

Il s'agit d'associer un corps présentant une résonance à un corps en $1/v$. Ainsi on a choisi: $^{239}Pu/^{235}U$, $^{176}Lu/Mn$, $^{115}In/Mn$.

Mode de détection

On a utilisé soit la fission, soit l'activation. La technique des chambres à fission nécessite des flux faibles et est d'une mise en œuvre rapide. Les détecteurs d'activation produisent des perturbations extrêmement faibles, mais nécessitent des flux relativement plus importants. Ils ont entre autres l'avantage de pouvoir être mis dans le combustible d'un réseau.

Chambres à fission: Cylindriques, d'un diamètre de 4 mm, d'une longueur de 23 mm, elles ont une sensibilité de l'ordre de 10^{-4} c/s dans un flux de 1 n/cm² s. Ces chambres contiennent des dépôts de plutonium ou d'uranium 235; elles ont des paliers suffisamment corrects pour que leur stabilité permette des mesures d'indices très précises (0,5 % par mesure).

Détecteurs d'activation: Les détecteurs fissiles sont découpés dans une feuille d'alliage d'aluminium. Les détecteurs au plutonium ont une densité superficielle de 2,5 mg/cm², ceux d'uranium (à 90 %) de 5 mg/cm². Le diamètre de ces détecteurs est de 7 mm ou de 29,2 mm. Les premiers sont gainés avec 0,05 mm d'aluminium, les seconds avec 0,1 mm. On compte l'activité γ des produits de fission au-dessus de 450 keV. Les détecteurs In et Mn sont comptés au-dessus de 208 keV, ceux au Lu au-dessus de 35 keV. Tous ces détecteurs nécessitent un flux intégré de 2.10^{12} n/cm².

Résultats expérimentaux

Milieux fissiles homogènes

Au moyen d'un couple de chambres plutonium–uranium à 90 %, placées au centre du réacteur critique homogène ALECTO, on a étudié la variation du rapport $Pu/^{235}U$ en fonction de la concentration de la solution. Le sel fissile dissous dans l'eau est soit du plutonium, soit de l'uranium à 90 %. Ces résultats de mesures, normalisés à un flux de Maxwell, ont été interprétés en utilisant les modèles de calcul mis au point à Saclay (fig. 1) [20].

Milieux hétérogènes

Des mesures peuvent être faites dans le modérateur et dans le combustible. Moyennant certaines hypothèses, elles peuvent être interprétées par des modèles analogues aux modèles homogènes, avec des modifications tenant compte de l'hétérogénéité.

Dans AQUILON (fig. 2, 3, 4), une série de mesures ponctuelles (modérateur et combustible) ainsi que quelques mesures intégrales (combustible) viennent d'être effectuées sur des réseaux d'éléments combustibles pleins ($\varnothing = 29{,}2$ mm) d'uranium naturel ou légèrement enrichi, en fonction du pas [21].

Dans les réacteurs à graphite, cette technique est maintenant systématique, et un grand nombre de réseaux ont été étudiés à MARIUS. Sur le réacteur EDF1, on a fait des mesures à 40 °C, 88 °C et 159 °C. Nous donnons dans le tableau 3 les résultats obtenus avec les couples Pu/U.

Tableau 3. Valeurs du rapport S_M/S_U [a] en fonction de la température

Températures	40 °C	88 °C	159 °C
$S_M/S_U = 41$			
R [b] ± 1 % . .	1,23	1,28	1,41
R calc. . . .	1,238	1,30	1,405
$S_M/S_U = 56$			
R ± 1 % . . .	1,17	1,235	1,33
R calc. . . .	1,185	1,242	1,342

a $S_M/S_U = \dfrac{\text{section modérateur}}{\text{section combustible}}$ b $R = \dfrac{(Pu/U)_{réseau}}{(Pu/U)_{colonne\ thermique}}$

ÉTUDES DE PROTECTION*

Il est nécessaire, pour les études de protection, de pouvoir prévoir certains effets dus aux neutrons

* J. Cherot, C. Clouet d'Orval, J. P. Frichet.

* J. Brisbois, M. Lott, J. Rastoin.

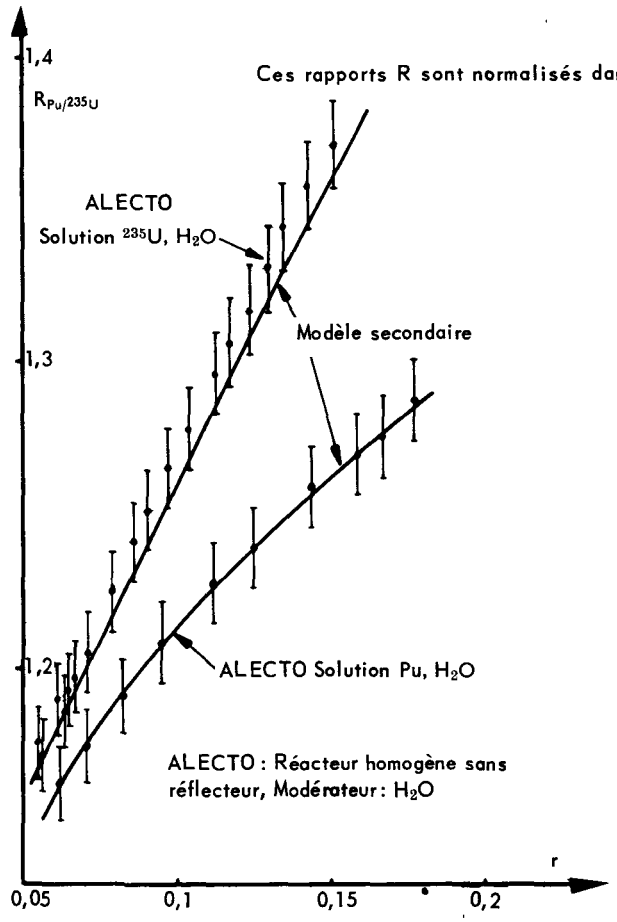

Figure 1. Indice de spectre

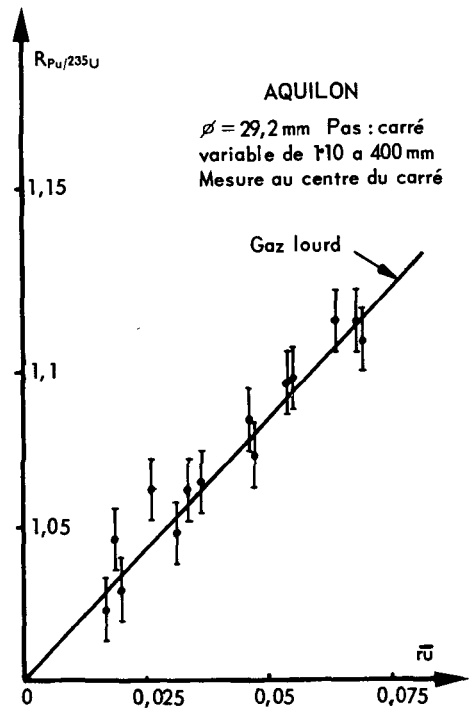

Figure 2. Indice de spectre

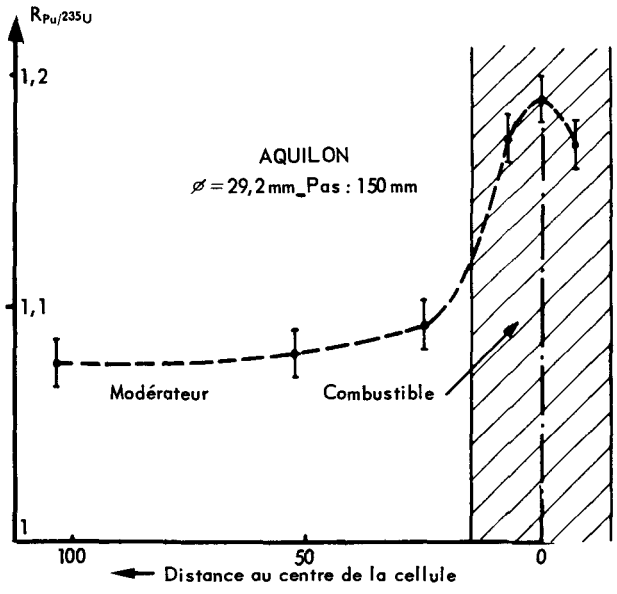

Figure 3. Indice de spectre

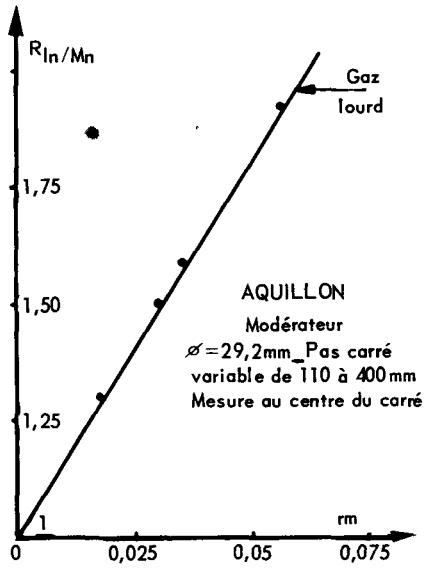

Figure 4. Indice de spectre

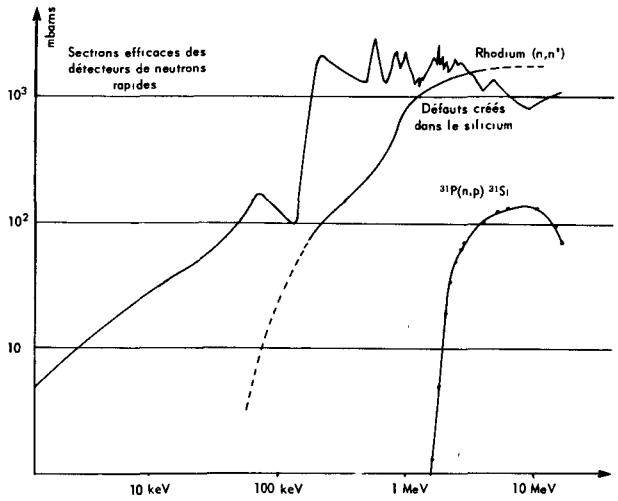

Figure 5. Détecteurs utilisés

rapides, par exemple les dommages sur les matériaux de structure, la dose biologique et l'activation des fluides de refroidissement.

Pour calculer ces effets, il faudrait connaître le spectre des neutrons et les sections efficaces différentielles de réaction. En pratique, étant donné les difficultés de détermination du spectre aussi bien par le calcul que par l'expérience, on utilise des détecteurs de neutrons dont la réponse est aussi voisine que possible de celle de l'effet cherché.

Ces mesures doivent répondre en outre à deux impératifs principaux. D'une part, il faut mesurer le flux en valeur absolue pour pouvoir relier les résultats à l'intensité des sources; d'autre part, il faut mesurer des flux d'intensité très différente (dans une gamme de 6 décades environ).

Principaux détecteurs utilisés

Pour les neutrons rapides, le détecteur de référence est le phosphore. Sa réponse caractérise les neutrons très rapides qui, dans la plupart des matériaux, sont les moniteurs de la propagation. La méthode d'étalonnage est basée sur la comparaison des activités du phosphore 32 et du silicium 31, qui sont des émetteurs β d'énergie voisine [22]. L'étalonnage absolu se fait au moyen d'une source étalon de neutrons thermiques, par l'intermédiaire des sections efficaces. Les détecteurs sont des disques de diamètre allant de 7 à 100 mm et d'épaisseur 2,5 mm. Ils permettent de mesurer des flux à partir de 10^3n/cm^2 s. Tous les autres détecteurs sont étalonnés par rapport au phosphore contre la plaque d'uranium naturel de NAIADE I, dont le spectre a été déterminé par le calcul.

Le rhodium est un détecteur particulièrement intéressant du fait du seuil bas (40 keV) de sa section efficace d'activation (nn'). On mesure son activité (rayons γ d'énergie 20 keV) avec un scintillateur NaI de 3 mm d'épaisseur. Le détecteur est utilisé sous forme de disque de 0,1 mm d'épaisseur et de 10 à 30 mm de diamètre. On peut mesurer des flux de l'ordre de 10^4n/cm^2 s.

Nous utilisons également un détecteur de dommages [23,24] constitué par une diode au silicium. Ce détecteur mesure des flux intégrés allant de 10^{10} à 10^{12} n/cm^2. On trouvera à la figure 5 les sections efficaces de ces trois détecteurs en fonction de l'énergie.

Pour ces trois types de détecteurs, les résultats sont donnés en flux de fission équivalents.

Nous utilisons pour les neutrons intermédiaires l'or et l'indium sous forme de dépôts ou de détecteurs épais [25].

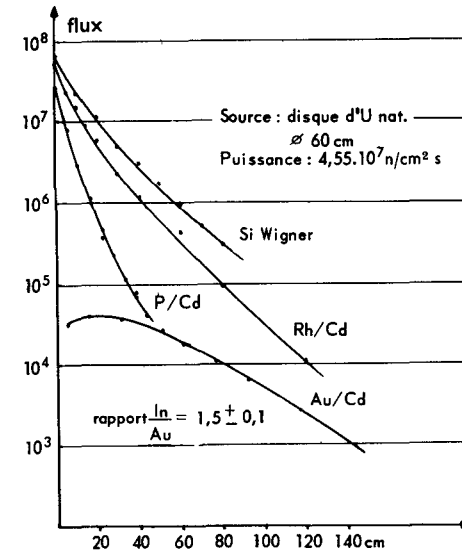

Figure 6. Atténuation du flux neutronique dans maquette de fer (2×2×2 m)

Quelques résultats expérimentaux [26]

Nous avons étudié la propagation des neutrons rapides dans un massif de fer de $2 \times 2 \times 2$ m placé dans le dispositif NAIADE I; la source de neutrons est constituée par une plaque d'uranium naturel de 2 cm d'épaisseur émettant 4,55 10^7 n/cm^2 s. Ces

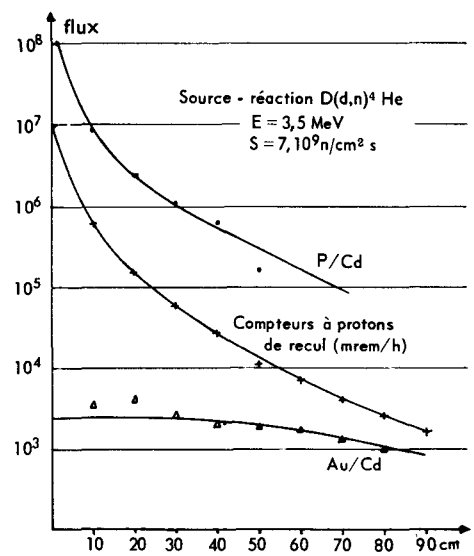

Figure 7. Atténuation du flux neutronique dans maquette de sodium

mesures ont été faites avec des détecteurs de phosphore, de rhodium, de silicium et d'or (fig. 6).

Nous avons également étudié la propagation des neutrons de 3,5 MeV dans un massif de sodium de $1,5 \times 1,5 \times 2,5$ m à l'aide d'un accélérateur dont la source est située au milieu du massif. Ces mesures ont été faites avec des détecteurs d'or, de phosphore et un dosimètre à protons de recul (fig. 7).

BIBLIOGRAPHIE

1. Boivineau, A., *et al.*, *Etudes de l'anisotropie de réseaux à eau lourde à réfrigerant gazeux*, Rapport CEA (à paraître).
2. Palmedo, P. F., Rapport CEA 2357 (1963).
3. Sagot, M., Tellier, H., Rapport CEA 2210 (1963).
4. Zhezherun, I. F., Atomn. Energ. SSSR, *14*, 2, pp. 193–199, 1963.
5. Bhandari, R. C., Kothari, L. S., Singwi, K. S., J. Nucl. Energy, *7*, 45, 1958.
6. Benoist, P., *et al.*, *Expériences critiques et sous-critiques sur réseaux U–Beo*, Actes de la deuxième Conférence internationale sur l'utilisation de l'énergie atomique à des fins pacifiques, P/1192, Vol. 6, p. 849, Nations Unies (1958).
7. Sagot, M., Tellier, H., Rapport CEA 2201 (1963).
8. Sagot, M., *et al.*, *Symposium Amsterdam*, AIEA Preprint SM 42/63 (1963).
9. Jacquemart, R., Rapport CEA 2376 (1963).
10. Bruna, J., *et al.*, Rapport CEA 2454 (1964).
11. Clouet d'Orval, C., *et al.*, Rapport CEA 1690 (1963).
12. Breton, D., Rapport CEA 400.
13. Carré, J. C., Vidal, R., Rapport CEA 2485 (1964).
14. Vidal, R., Rapport CEA 2486 (1964).
15. Horowitz, J., Tretiakoff, O., EANDC(E)14 (1960).
16. Tattersall, R. B., Reactor Sci. (J. Nucl. Energy, Part A), *12*, 32–46 (1960).
17. Tretiakoff, O., Vidal, R., Rapport CEA 2487 (1964).
18. Brettes, J., Ledanois, G., Rapport CEA 2483 (1964).
19. Bailly, J., *et al.*, Rapport CEA 2498 (1964).
20. Bruna, J., *et al.*, Rapport CEA 2455 (1964).
21. Frichet, J. P., Mougey, J., Sautiez, B., Rapport CEA 2482 (1964).
22. Brisbois, J., Lott, M., Manent, R., Rapport CEA 2491 (1964).
23. Lanore, J. C., Schuttler, R., C.R. Ac. Sci., *256*, 1264–1266 (1963).
24. Dulieu, P., Rastoin, J., *Les détecteurs de dommage dans le cadre des études de protection*, BIST, 82 (1964).
25. Brisbois, J., Fogagnolo, G., Rapport CEA 2162 (1962).
26. Brisbois, J., *et al.*, Rapport CEA 2492 (1964).

ABSTRACT—RÉSUMÉ—АННОТАЦИЯ—RESUMEN

A/102 France

Experimental methods in thermal reactor physics

By D. Breton and P. Lafore

This paper is a synthesis of various experimental methods in use with the reactors of the Commissariat à l'énergie atomique.

The main techniques used are mentioned and the difficulties encountered and the accuracy obtained are particularly dwelt upon. The application of these various methods to reactors in order to obtain specific results is also indicated. The paper consists of five parts:

General methods:

Macroscopic and microscopic flux distribution (anisotropy effect), power distribution, etc.

Kinetic measurements:

(*a*) Pulsed neutron technique: apparatus and accuracy; application to λ_t and to negative reactivity measurements; application to graphite, light water and beryllium oxide.

(*b*) Oscillation techniques: equipment and accuracy; application to the measurements of effective cross sections and resonance integrals.

Measurement by poisoning:

Description of methods for introducing and extracting the poison, difficulties encountered with light and heavy water, measurement of temperature coefficients and negative reactivity.

Spectral studies:

Choice and development of foils, problems of measurement, application to spectral measurements for thermalization studies, application to dosimetry.

Shielding studies:

The techniques and apparatus recently developed in this field are presented.

A/102 Франция

Экспериментальные методы в физике реакторов на тепловых нейтронах

Д. Бретон, П. Лафор

В настоящем докладе дается обзор различных экспериментальных методов, применяемых на реакторах Комиссариата по атомной энергии.

Описываются основные использованные методы, подчеркиваются трудности и приводятся полученные данные; указывается также на применение этих методов в реакторах с целью получения определенных результатов. Доклад состоит из 5 частей.

Общие методы

Макроскопические и микроскопические распределения потоков (эффекты анизотропии), распределения тепловыделения и т. д.

Кинетические измерения

a. Измерения при помощи импульсных нейтронных источников: аппаратура и ее точность; применение для измерения λ_t и антиреактивности; пример использования для исследования систем с графитом, обычной водой и BeO.

b. Измерения методом осцилляций: аппаратура и ее точность; использование для измерения эффективных сечений и резонансных интегралов.

Измерения отравления

Описание способов введения и удаления отравителей; трудности, возникающие при использовании обычной и тяжелой воды; измерения температурного коэффициента и коэффициента антиреактивности.

Изучение спектров

Выбор и применение фольг; трудности измерений; спектральные измерения для изучения термализации; использование в дозиметрии.

Изучение физики защиты

Описываются методы и аппаратура, которая недавно начала применяться в этой области.

A/102 Francia

Métodos experimentales de física de los reactores de neutrones térmicos

por D. Breton y P. Lafore

La memoria resume los diversos métodos experimentales que se aplican en los reactores del CEA.

Describe las principales técnicas empleadas e insiste particularmente sobre las dificultades de orden práctico y sobre la precisión alcanzada; indica también la aplicación de los diversos métodos en los reactores para obtener determinados resultados. Consta de cinco partes:

Métodos generales:

Distribución del flujo macroscópico y microscópico (efecto de anisotropía), distribución de potencia, etc.

Mediciones cinéticas:

a) Mediciones mediante neutrones pulsados: dispositivo empleado y precisión alcanzada, aplicación a las mediciones de λ_t y de la antirreactividad, aplicación al grafito, al agua ordinaria y al BeO.

b) Mediciones por oscilación: aparatos empleados y precisión alcanzada, aplicación a la medición de secciones eficaces efectivas y a las integrales de resonancia.

Mediciones por envenenamiento:

Descripción de los métodos de introducción y extracción del veneno, dificultades al emplear agua ligera y agua pesada, medición de los coeficientes de temperatura y antirreactividad.

Estudios de espectros:

Elección y construcción de los detectores, dificultades que presentan las mediciones, aplicación a las mediciones espectrales en el estudio de la termalización, aplicaciones dosimétricas.

Estudios de protección:

La memoria describe las técnicas y los aparatos recientemente perfeccionados.

Замедление нейтронов в водородсодержащих средах

Л. Н. Юрова, А. А. Поляков, С. Б. Степанов и Г. А. Алимов

Замедление быстрых нейтронов и процесс термализации в водородсодержащих средах довольно подробно изучались во многих работах [1-4].

Однако до сих пор нельзя сказать, что получено всестороннее решение проблемы. Например, многочисленные экспериментальные результаты исследования процесса замедления нейтронов в уран-водных средах до сих пор не согласуются с расчетными результатами; имеются ограниченные сведения о влиянии гетерогенности среды на замедление нейтронов; не достаточно изучена термализация нейтронов в различных водородсодержащих средах при высоких температурах. Поэтому накопление нового экспериментального материала представляет теоретический и практический интерес для понимания физики реакторов с водородным замедлителем.

В данной работе рассматриваются результаты экспериментального определения двух интегральных величин в различных средах: длины замедления быстрых нейтронов и коэффициента диффузии тепловых нейтронов.

I. ЗАМЕДЛЕНИЕ БЫСТРЫХ НЕЙТРОНОВ

Опыт по изучению замедления быстрых нейтронов в неразмножающих средах

Замедление быстрых нейтронов изучалось в водородсодержащих средах: легкой воде (H_2O), дифениле ($C_{12}H_{10}$), моноизопропилдифениле ($C_{15}H_{16}$), а также в средах: железо + вода, алюминий + вода, железо + дифенил и алюминий + дифенил.

Измерение пространственных распределений замедлившихся нейтронов проводилось в условиях «конечной среды». Под «конечной средой» понималась исследуемая среда ограниченного размера, окруженная бесконечным отражателем. Такая геометрия опыта позволила получать экспериментальные распределения замедлившихся нейтронов, соответствующие бесконечным средам, при использовании ограниченного количества исследуемых веществ. Аналогичный принцип измерений применяется при изучении физических параметров ограниченных по размерам размножающих сред, помещенных в критическую систему [5]

Для теоретического обоснования методики опыта и выбора размера системы использовался математический аппарат, изложенный в работе [6]. Как можно было ожидать, результаты расчета показали, что при цилиндрической геометрии исследуемой среды, помещенной в бесконечный отражатель, диаметр цилиндра должен быть не менее четырех длин замедления ($\sim 4L_s$).

Во всех экспериментах по исследованию замедления нейтронов в неразмножающих средах использовался цилиндр диаметром 41 и высотой 110 *см*, помещенный в бесконечный графитовый отражатель. Для экспериментального подтверждения выбранной геометрии были проделаны измерения пространственных распределений нейтронов от полоний-бериллиевого источника в дифенил-графитовом и дифенил-дифениловом отражателе. Измеренные распределения плотности замедлившихся до индиевого резонанса нейтронов в этих условиях оказались идентичными в пределах экспериментальных ошибок. Значения квадратов длин замедлений, вычисленные по этим распределениям, соответственно равны $102{,}3 \pm 3{,}5$ *см*^{2} для дифенил-графитового и $102{,}5 \pm 4{,}1$ *см*^{2} для дифенил-дифенилового отражателей [7].

При исследовании замедления быстрых нейтронов в металлводородных средах изучаемые системы состояли из замедлителя с равномерно расположенными в нем стерженьками из металла. Изучались две группы сред: квазигомогенные среды, в которых металлические стерженьки имели диаметр 10 *мм*, и гетерогенные среды с стержнями диаметром 40 *мм*.

Измерения проводились для нейтронов спектра деления U^{235} и нейтронов полоний-бериллиевого источника. Источником нейтронов деления являлся конвертер из металлического высокообогащенного урана, который помещался в тепловую колонну тяжеловодного реактора АН СССР.

Пространственные распределения измерялись индиевыми фольгами толщиной 90 *мг/см*^{2}, размеры которых выбирались, исходя из требований сохранения условия точечности источ-

Таблица 1

Среда	Источник нейтронов	V_v / $V_{зам}$	L_s^2, см² эксперимент L_s^2 (1,46 эв)	эксперимент L_s^2 (тепл.)	расчет L_s^2 (1,46 эв)	расчет L_s^2 (тепл.)
H_2O	Нейтроны деления U^{235}	—	26,7±1,0	—	27,3	—
$C_{12}H_{10}$		—	52,1±2,4	—	50,8	—
$C_{15}H_{16}$		—	43,2±1,8	—	43,4	—
$C_{15}H_{16}$—U_3O_8		0,07	—	51,4±1,5	—	52,1
		0,09	—	54,4±1,6	—	54,4
		0,12	—	57,2±1,9	—	57,8
		0,17	—	64,0±1,7	—	63,2
		0,22	—	73,3±2,3	—	69,8
$H_2O+U_3O_8$		0,07	—	35,5±1,4	—	33,1
		0,09	—	37,2±1,5	—	34,7
		0,17	—	43,1±2,3	—	41,1
H_2O	Ро+Be-источник	—	56,7±0,9	—	58,5±1,5 Работа[16]	—
$C_{12}H_{10}$		—	102,3±3,5	—	99,1	—

ника и детектора. В полученные значения активностей фольг вводились поправки, учитывающие, во-первых, вклад нейтронов с энергией выше первого резонансного уровня индия и, во-вторых, поправки, учитывающие толщину источника нейтронов деления. Все измеренные распределения[8-9] приводились к толщине источника, равной 0,3 *мм*. Квадраты длин замедления L_s^2 вычислялись из следующего соотношения:

$$L_s^2 = \frac{1}{6}\frac{\int_0^r A(r)\,r^4\,dr + \int_{r_0}^{\infty}\frac{ke^{-r/\lambda}}{r^2}\,r^4\,dr}{\int_0^{r_0} A(r)\,r^2\,dr + \int_{r_0}^{\infty}\frac{ke^{-r/\lambda}}{r^2}\,r^2\,dr}, \qquad (1)$$

где $A(r)$ — активность индиевых фольг; k,λ— константы, которые определялись из экспериментального распределения нейтронов для удаленной от источника области, где соблюдается линейный закон. Результаты значений квадратов длин замедления приведены в табл. 1 и 2 и на рис. 1 и 2.

Критический опыт по изучению замедления нейтронов

В критическом опыте изучалось замедление нейтронов в уран-водных и уран-моноизопропилдифениловых средах. На основании измерений утечки нейтронов, соответствующих различным геометриям активной зоны, определялись площади миграции нейтронов[10]. В эксперименте измерялись периоды удвоения мощности системы при изменении критической высоты активной зоны, по которым по формуле «обратных часов» рассчитывались значения реактивностей[11]. При этом учитывался вклад запаздывающих нейтронов различных энергетических групп в измеренные величины реактивностей. Для этого в формуле «обратных часов» вместо постоянных выходов запаздывающих нейтронов β_i использовались величины $\beta_i^{эфф}$, которые определялись следующим образом:

$$\beta_i^{эфф} = \frac{1+\varkappa^2 L_s^{мг\,2}}{1+\varkappa^2 L_{si}^{зап\,2}}, \qquad (2)$$

где $L_s^{мг2}$ — квадрат длины замедления мгновенных нейтронов деления; $L_{si}^{зап2}$ — квадрат длины замедления i-группы запаздывающих нейтронов; $\varkappa^2$ — материальный параметр.

На основании полученных значений реактивностей системы определялись отношения $\frac{M^2}{K_\infty}$ из соотношения

$$\frac{\partial\varrho}{\partial h} = -\frac{2\pi^2}{H^3 K_\infty} M^2, \qquad (3)$$

где H — критическая высота; h — превышение над критической высотой; K_∞ — коэффициент размножения нейтронов для бесконечной среды.

Необходимые для вычислений M^2 значения материального параметра были получены в критическом опыте из измерений аксиального и ра-

Таблица 2

Среда	Источник нейтронов	$V_{мет}/V_{зам}$		L_s^2 (1,46 эв), $см^2$	
				эксперимент	расчет
H_2O		—	—	56,7±0,9	58,5±1,5 Работа[16]
H_2O+Fe	Ро+Be-источник	1 : 3	Квазигомогенная среда	55,6±1,0	—
			Гетерогенная среда	63,1±1,2	—
		2 : 3	Квазигомогенная среда	53,1±1,4	—
			Гетерогенная среда	69,1±1,7	—
		1,42 : 1	Квазигомогенная среда	62,6±1,7	—
			Гетерогенная среда	77,7±1,8	—
H_2O+Al		1 : 3	Квазигомогенная среда	72,1±1,6	—
			Гетерогенная среда	79,6±2,1	—
$C_{12}H_{10}$		—	—	102,3±3,5	99,1
$C_{12}H_{10}+Fe$	Нейтроны деления U^{235}	1 : 3	Гетерогенная среда	75,0±4,4	68,5
$C_{12}H_{10}+Al$		1 : 4	Гетерогенная среда	87,8±2,3	79,9

диального распределений плотности нейтронов в активной зоне. Эти распределения измерялись медными фольгами.

Экспериментальная установка представляла реактор нулевой мощности. Активная зона реактора помещалась в шестигранном баке из нержавеющей стали со стороной шестигранника 50 *см*. Активная зона была окружена бесконечным боковым отражателем из замедлителя; верхний торцевой отражатель отсутствовал, а нижним торцевым отражателем являлось дно бака толщиной 15 *мм*. Тепловыделяющие элементы, представлявшие собой полые цилиндры из нержавеющей стали с засыпкой из U_3O_8 (размер внутренней трубы $9{,}0\times0{,}4$ *мм*, а размер внешней трубы $13{,}4\times0{,}2$ *мм*) размещались в дистанционирующих решетках из алюминия. Изменение шага решетки давало возможность исследовать замедление нейтронов в средах с различными отношениями объема горючего к объему жидкого замедлителя.

В результате обработки экспериментальных данных были получены значения площадей миграции нейтронов в средах, которые вследствие малости значений длины диффузии нейтронов в рассматриваемых размножающих средах $L\sim(1{,}5\div2{,}0)$ $см^2$ в пределах точности опыта не отличались от квадрата длины замедления нейтронов тепловой энергии.

Значение L_s^2 (тепл.) приведены в табл. 1.

Расчет квадрата длины замедления нейтронов методом моментов в многогрупповом приближении

Уравнение переноса нейтронов в многогрупповом приближении с учетом упругого и неупругого замедления может быть представлено в виде [12]

$$\partial\varphi_0^j+\Sigma_{ув}^j\varphi_0^j=\sum_{l=1}^{j-1}\Sigma_{in}^{l\to j}\varphi_0^l+\alpha_0^i\sum_{l=1}^{j-1}\beta_0^l\varphi_0^l+$$
$$+\left(\frac{\xi\Sigma_s}{\Delta u}\right)^{j-1}\varphi_0^{l-1}+\chi^j\delta(z)+\chi^j\sum_l\nu\Sigma_f^l\varphi_0^l;$$
$$\frac{1}{3}\frac{\partial\varphi_0^j}{\partial z}+\Sigma_1^j\varphi_1^j=\alpha_0^j\sum_{l=1}^{j-1}\beta_1^l\varphi_1^l, \qquad (4)$$

где $\sum_{ув}^j$ — групповые сечения увода нейтронов

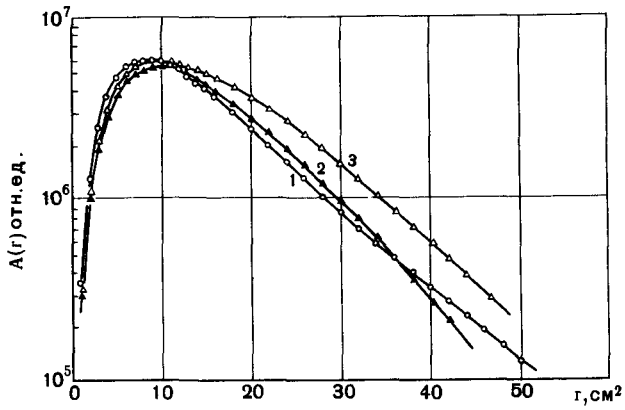

Рис. 1. Распределение потока нейтронов индиевого резонанса в трех средах:
1—вода; *2*—квазигомогенная среда Fe+H_2O; $V_{мет}:V_{зам}=2:3$; *3*—гетерогенная среда Fe+H_2O; $V_{мет}:V_{зам}=2:3$

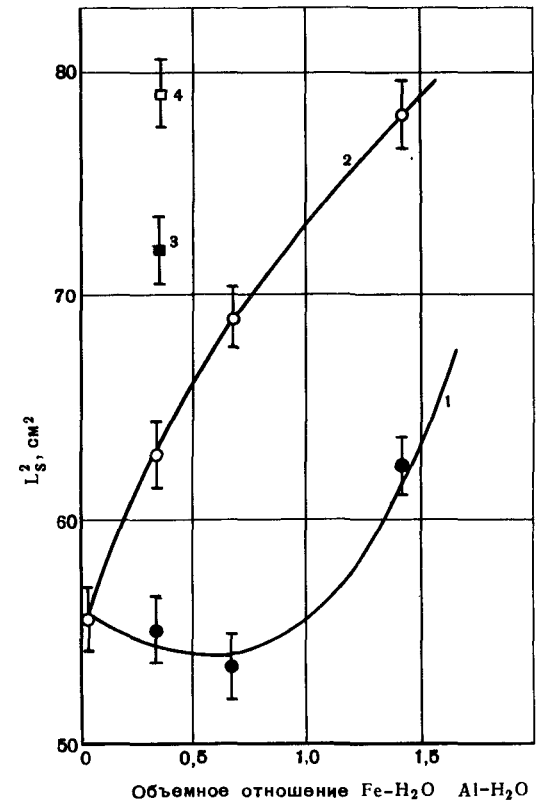

Рис. 2. Квадрат длины замедления нейтронов Po+Be-источника в металлводных средах:
1—квазигомогенная среда Fe+H_2O; *2*—гетерогенная среда Fe+H_2O; *3*—квазигомогенная среда Al+H_2O; *4*—гетерогенная среда Al+H_2O

из j-группы; $\sum_{in}^{l\to j}$ — групповые сечения неупругого рассеяния нейтронов из l-группы в j-группу; $\frac{\zeta\Sigma_s}{\Delta u}$ — групповые сечения замедления нейтронов на ядрах с $A>1$; χ^j — функция источника; φ_0^j, φ_1^j — интегральный (в пределах группы) поток и ток нейтронов; $\chi^s\sum_l \nu\sum_f^l \varphi_0^l$ — член, учитывающий размножение нейтронов в надтепловой области энергий;

$$\alpha_0^j=(1-e^{-\Delta u_j})\,e^{-u_{j-1}};$$

$$\beta_0^l=\frac{1-e^{-\Delta u_l}}{\Delta u_l}\,e^{u_l};$$

$$\alpha_1^j=\frac{2}{3}(1-e^{-3/2\Delta u_j})\,e^{-3/2u_{j-1}};$$

$$\beta_1^l=\frac{2}{3}\,\frac{1-e^{-3/2\Delta u_l}}{\Delta u_l}\,e^{3/2u_l}.$$

Резонансные эффекты в выражении (1) учитываются добавлением к сечениям увода следующей величины:

$$\delta\Sigma_c^j=\sum_{i=j-1}^{j}\varrho\frac{J_{эфф}}{\Delta u_j}. \qquad (5)$$

Если к системе (1) применить фурье-преобразование и затем произвести разложение в ряд по степеням p, то для определения квадрата длины замедления, получим систему связанных уравнений

$$\Sigma_{ув}^j\Phi_{00}^j=\sum_{l=1}^{j-1}\Sigma_{in}^{l\to j}\Phi_{00}^l+\alpha_0^j\sum_{l=1}^{j-1}\beta_0^l\Phi_{00}^l+$$
$$+\left(\frac{\xi\Sigma_s^1}{\Delta u}\right)^{j-1}\Phi_{02}^{j-1}+\chi^j;$$

$$\Sigma_1^j\Phi_{11}^j=\frac{1}{3}\Phi_{00}^j+\alpha_1^j\sum_{l=1}^{j-1}\beta_1^l\Phi_{11}^l;$$

$$\Sigma_{ув}^j\Phi_{02}^j=2\Phi_{11}^j+\sum_{l=1}^{j-1}\Sigma_{in}^{l\to j}\Phi_{02}^l+\alpha_0^j\sum_{l=1}^{j-1}\beta_{02}^l\Phi_{02}^l+$$
$$+\left(\frac{\xi\Sigma_s^1}{\Delta u}\right)^{j-1}\Phi_{02}^{j-1}+\chi^j\sum_l\nu\Sigma_f^l\Phi_{02}^l;$$

$$L_s^{2j}=\frac{\Phi_{02}^j}{2\Phi_{00}^j}. \qquad (6)$$

В выражении (6) Φ_{nl}^j являются пространственно-угловыми моментами функции распределения нейтронов j-группы в бесконечной среде с плоским изотропным источником.

Для численного расчета L_s^2 составлена программа на электронно-вычислительную маши-

ну [12-13]. Расчетные значения квадратов длин замедления нейтронов в водородсодержащих средах приведены в табл. 1 и 2.

Результаты измерений

Квазигомогенные среды. Результаты измерений и численного расчета значений L_s^2 для чистых замедлителей и квазигомогенных металло-водных сред приведены в табл. 1. Наблюдается хорошее согласие между экспериментальными и рассчитанными значениями, которое подтверждает, что существующие методики расчета замедления нейтронов, а также применяемые в расчетах системы многогрупповых констант правильно описывают процесс замедления нейтронов в водородсодержащих средах.

Гетерогенные среды. Результаты измерений замедления нейтронов в гетерогенных и квазигомогенных средах приведены в табл. 2 и на графиках рис. 1 и 2. Из рис. 2 видно, что наблюдается значительное различие в величинах L_s^2 при одинаковой концентрации металла в воде. Во всех случаях измеренные значения L_s^2 для гетерогенных сред намного превышают соответствующее значение для квазигомогенных сред. Аналогичная картина наблюдается и для сред дифенил + металл, для которых измеренные значения L_s^2 значительно больше расчетных, полученных по методике, применимой к гомогенным средам. Это различие объясняется резко выраженной анизотропией распределения нейтронов в гетерогенных системах. В более ранних работах [14-15] по изучению замедления быстрых нейтронов в металло-водных средах такой резкой анизотропии не наблюдалось, ввиду того что исследуемые среды фактически являлись квазигомогенными [16].

Полученные результаты, очевидно, представляют интерес при физическом расчете реакторов, активная зона которых имеет выраженную гетерогенность.

II. ДИФФУЗИЯ ТЕПЛОВЫХ НЕЙТРОНОВ

Методика эксперимента

Диффузия нейтронов в углеводородах (циклических и нециклических соединениях) изучалась в широком интервале температур среды (от плавления до кипения). Для исследования применялся метод импульсного нейтронного источника [17-20].

Распределение тепловых нейтронов в среде приближенно можно описать одногрупповым уравнением диффузии, в котором используются диффузионные константы, усредненные по спектру тепловых нейтронов

$$\overline{D(v)}\cdot\Delta n - \overline{\Sigma_a v}\cdot n = \frac{\partial n}{\partial t}, \qquad (7)$$

где $\overline{D(v)} = \frac{\overline{\lambda_{tr}(v)\cdot v}}{3}$ — коэффициент диффузии в бесконечной среде; $\overline{\Sigma_a v}$ — скорость поглощения нейтронов в бесконечной среде.

Для среды конечных размеров изменение плотности тепловых нейтронов во времени может быть описано суммой экспоненциально затухающих гармоник. По прошествии достаточно большого времени все гармоники затухают, кроме основной, и распределение нейтронов описывается законом $\sim e^{-\alpha t}$, где константа спада

$$\alpha = \overline{\Sigma_a v} + \overline{D(v)}\cdot\Omega - (C_D - C_T)\,\Omega^2, \qquad (8)$$

где Ω — геометрический параметр; C_D — коэффициент диффузионного охлаждения; C_T — недиффузионная поправка.

Описание эксперимента

Измерения проводились на циклотроне АН СССР. Установка представляла собой цилиндрический бак диаметром 30 *см*, экранированный слоем карбида бора толщиной 10 *мм* и кадмием толщиной 0,5 *мм*. Внутрь бака был введен кадмиевый поршень, перемещением которого можно было легко и просто менять геометрические размеры исследуемой среды. Под дном бака располагается блок счетчиков BF_3, экранированный от дна бака кадмиевой маской, форма которой определялась [17-20] функцией $rI_0\,(2{,}405\frac{r}{R})$. Маска уменьшала вклад высоких гармоник в распределение плотности нейтронов при больших значениях геометрических параметров. На боковой поверхности бака располагалась электрическая печь для нагрева среды. Внутрь бака была помещена термопара для контроля температуры, которая определялась с точностью $\pm$ 2° С.

Тарировка установки и контрольные опыты проводились на воде при температуре 21° С. Для определения эффекта взаимного расположения мишени циклотрона и установки проводились измерения на различных расстояниях и углах по отношению к мишени. Результаты оставались неизменными в пределах ошибки эксперимента. Вследствие близости водяной защиты и других рассеивателей от экспериментальной установки, а также довольно большого расстояния ее от мишени источник быстрых нейтронов был практически объемным.

Исследуемая жидкость нагревалась до высоких температур, поэтому минимальное расстояние от дна бака, на котором можно было располагать блок счетчиков, составляло 2 *см*. В связи с этим были измерены возможные искажения константы спада за счет различного времени прохождения расстояния от дна бака до счетчиков нейтронами разных энергий. Результаты исследования влияния пролетного расстояния на константу спада показали, что

начиная с $\Omega = 0{,}240\ см^{-2}$ влияние пролетного расстояния на константу спада незначительно. Измерения проводились для Ω не больше указанной величины.

Циклотрон работал в импульсном режиме с частотой следования импульсов 500 циклов и длительностью импульсов 6—8 *мксек*. Временной анализ спада потока тепловых нейтронов проводился временным 60-канальным анализатором, запуск которого был синхронизирован с запуском циклотрона. Задержка включения временного анализатора относительно импульса быстрых нейтронов колебалась в пределах 100—300 *мксек*. Ширина временного канала составляла 2—8 *мксек*. Дрожание временной шкалы не превышало 0,25 *мксек*.

Методика обработки результатов

Величины α, $\overline{\Sigma_a v}$, $\overline{D(v)}$, $(C_D - C_T)$ вычислялись методом наименьших квадратов. Зависимость коэффициента диффузии от температуры среды для всех исследованных веществ хорошо описывается законом

$$\frac{\varrho}{\varrho_0}\overline{D(v)}_T = AT^{a/2}, \tag{9}$$

где $\overline{D(v)}_T$ — коэффициент диффузии, усредненный по спектру тепловых нейтронов при температуре среды T; ϱ, ϱ_0 — плотность среды при данных температурах T, T_0; a — параметр, зависящий от структуры молекулы вещества.

Результаты обработки экспериментальных данных приведены в табл. 3.

Естественно предположить, что установившийся спектр нейтронов в бесконечной среде подчиняется распределению Максвелла

$$w(v)\,dv = A_0 e^{-\frac{v^2}{v_0^2}} v^2 dv,$$

где $v_0 = \sqrt{\frac{2T'k}{m}}$ — наиболее вероятная скорость нейтронов.

Строго говоря, спектр тепловых нейтронов подчиняется максвелловскому распределению лишь в непоглощающих средах. Однако, как показывает опыт, в случае слабого поглощения можно с большой степенью точности считать спектр максвелловским. Это позволяет без большой погрешности определить значения v_0, используя температуру среды в качестве параметра.

Тогда соотношение (9) можно переписать в виде

$$\frac{\varrho}{\varrho_0}\overline{D(v)}_T = Bv_{0T}^a \tag{10}$$

Коэффициент диффузии, усредненный по спектру Максвелла, можно записать в виде

$$\overline{D(v)} = \frac{\int_0^\infty e^{-\frac{v^2}{v_0^2}} v^2 D(v)\,dv}{\int_0^\infty e^{-\frac{v^2}{v_0^2}} v^2\,dv}. \tag{11}$$

Из уравнений (10) и (11) можно получить соотношения для определения дифференциального значения коэффициента диффузии нейтронов со скоростью v через значения коэффициента диффузии нейтронов для наиболее вероятной скорости v_0

$$D(v) = D(v_0)\left(\frac{v}{v_0}\right)^a; \tag{12}$$

$$D(v_0) = \frac{B}{m(a)}v_0^a, \tag{13}$$

где $m(a)$ — коэффициент усреднения функции, зависящей от вида спектра нейтронов и показателя степени a.

Усредненный коэффициент диффузии нейтронов по спектру Максвелла можно определить через дифференциальное значение коэффициента диффузии нейтронов для наиболее вероятной скорости

$$\overline{D(v)} = \frac{\int_0^\infty e^{-\frac{v^2}{v_0^2}} v^{2+a}\,dv}{v_0^a \int_0^\infty e^{-\frac{v^2}{v_0^2}} v^2\,dv} D(v_0) = m(a)\,D(v_0). \tag{14}$$

Из уравнения (13) можно получить зависимость транспортной длины от скорости нейтронов

$$\lambda_{tr}(v_0) = \frac{3B}{m(a)}v_0^{a-1} \tag{15}$$

и окончательно имеем

$$\overline{D(v)}_T = m(a)\,D(v_0)\left(\frac{v_T}{v_0}\right)^a; \tag{16}$$

$$\overline{\lambda_{tr}(v)}_T = m(a-1)\,\lambda_{tr}(v_0)\left(\frac{v_T}{v_0}\right)^{a-1}. \tag{16а}$$

Из вышеизложенного следует, что знание зависимости интегральной величины $\overline{D(v)}$ от температуры среды и знание вида спектра тепловых нейтронов позволяет получить из (14) дифференциальную величину $D(v)$, дифференциальное значение $\lambda_{tr}(v_0)$ — из соотношения

$$\lambda_{tr}(v_0) = \frac{\overline{3D(v)}}{m(a)\,v_0}. \tag{17}$$

Из (16) и (16а) следует

$$\overline{D(v)} = \frac{2}{\sqrt{\pi}}\,\frac{m(a)}{m(a-1)}\,\frac{\overline{\lambda_{tr}(v)}\,\bar{v}}{3}, \tag{18}$$

В связи с этим необходимо обратить внимание на то, что в литературе, например [17-20], применяется неточное соотношение для коэффициента диффузии

Таблица 3

Соединение	Химическая формула	t°,C	$\overline{\Sigma_a v}\cdot 10^{-4}$, сек$^{-1}$	$\overline{D(v)}\cdot 10^{-4}$, см$^2\cdot$сек$^{-1}$	$(C_D-C_T)\times 10^{-4}$, см$^4\cdot$сек$^{-1}$	ϱ, г$\cdot$см$^{-3}$	a	σ_{tr}^{H} (2200), барн
Бензол	C_6H_6	14	0,280±0,041	5,37±0,51	0,86±0,51	0,885	0,99±0,28	33,1±0,7
		27	0,252±0,021	5,24±0,21	0,16±0,47	0,871		
		34	0,248±0,019	5,66±0,36	1,26±0,38	0,863		
		38	0,248±0,017	6,27±0,41	2,92±0,91	0,859		
		52	0,283±0,042	6,09±0,59	3,42±1,70	0,845		
		71	0,310±0,031	6,13±0,33	2,34±0,83	0,824		
Дифенил	$C_{12}H_{10}$	123	0,280±0,011	7,70±0,08	8,20±0,50	0,955	1,35±0,05	32,5±0,3
		150	0,267±0,014	8,24±0,08	8,97±0,60	0,930		
		175	0,260±0,012	8,75±0,09	10,4±0,8	0,910		
		207	0,253±0,016	9,55±0,10	12,0±0,8	0,884		
		243	0,236±0,010	10,40±0,11	13,9±0,9	0,850		
Дифенилметан	$(C_6H_5)_2CH_2$	34	0,390±0,021	4,05±0,21	1,12±0,36	0,994	1,61±0,24	49,0±3,0
		110	0,386±0,017	5,35±0,23	2,62±0,82	0,936		
		160	0,411±0,028	6,80±0,30	4,9±1,2	0,897		
		230	0,433±0,026	6,95±0,33	3,5±1,7	0,842		
Даутерм[23]	$C_{12}H_{10}O_{0,735}$						1,90±0,08	46,5±1,5
Вода[17–20]	H_2O						1,91±0,02	44,0±0,08
Дифенилоксид	$(C_6H_5)_2O$	97	0,200±0,028	8,16±0,48	5,9±1,3	0,920	2,16±0,14	46,0±3,3
		110	0,243±0,019	9,87±0,61	7,6±2,0	0,908		
		175	0,230±0,017	10,48±0,84	8,6±1,9	0,845		
		204	0,200±0,030	13,52±1,14	13,9±2,9	0,816		
Газойль		24	0,482±0,020	3,23±0,21	2,2±0,6	0,842	2,44±0,09	61,3±3,1
		69	0,465±0,030	3,95±0,27	2,9±0,5	0,813		
		144	0,430±0,030	5,62±0,42	5,1±1,3	0,762		
Моноизопропилдифенил	$(C_6H_5)_2C_3H_7$	18	0,433±0,021	3,14±0,04	1,24±0,08	1,000	2,58±0,08	82,1±1,2
		85	0,417±0,018	4,51±0,06	3,08±0,20	0,950		
		144	0,401±0,019	5,81±0,06	5,04±0,30	0,900		
		197	0,380±0,015	7,01±0,08	6,91±0,41	0,852		
		243	0,356±0,014	8,17±0,08	8,70±0,52	0,821		
Анизол	$C_6H_5OCH_3$	18	0,351±0,031	4,10±0,32	2,3±0,8	0,995	2,94±0,19	86,7±5,8
		80	0,332±0,041	5,83±0,44	5,7±1,1	0,935		
		150	0,311±0,052	7,57±0,10	7,8±1,9	0,865		
Тетрадекан	$C_{14}H_{30}$	18	0,561±0,018	2,33±0,11	1,1±0,2	0,762	3,16±0,18	103,9±3,4
		76	0,533±0,011	3,19±0,16	2,0±0,4	0,724		
		160	0,427±0,014	5,33±0,21	4,2±1,0	0,668		
		248	0,360±0,013	7,00±0,22	6,8±2,0	0,598		

$$\overline{D(v)} = \frac{\overline{\lambda_{tr}(v)}\,\bar{v}}{3}. \qquad (19)$$

Получаемая из соотношения (19) $\overline{\lambda_{tr}(v)}$ не имеет определенного физического смысла.

Это же замечание относится к определению $\lambda_{tr}(v)$ из опытов по стационарной диффузии. В этом случае значение $\overline{L^2(v)}$ является усредненным по спектру тепловых нейтронов

$$\overline{L^2(v)} = \overline{TD(v)} = \overline{TD(v)} = m(a)\,TD(v_0) = \\ = T\frac{2}{\sqrt{\pi}}\frac{m(a)}{m(a-1)}\frac{\overline{\lambda_{tr}(v)}\,v}{3}. \qquad (20)$$

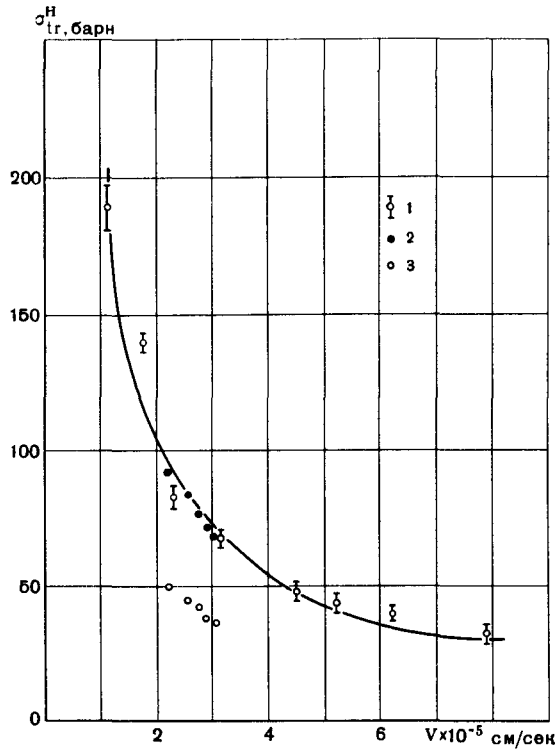

Рис. 3. Транспортное сечение рассеяния σ^{H}_{tr} на воде, полученное различными методами:

1 — дифференциальный опыт; *2* — интегральный опыт, полученный из соотношения (17); *3* — интегральный опыт, σ_{tr} получено из соотношения (19)

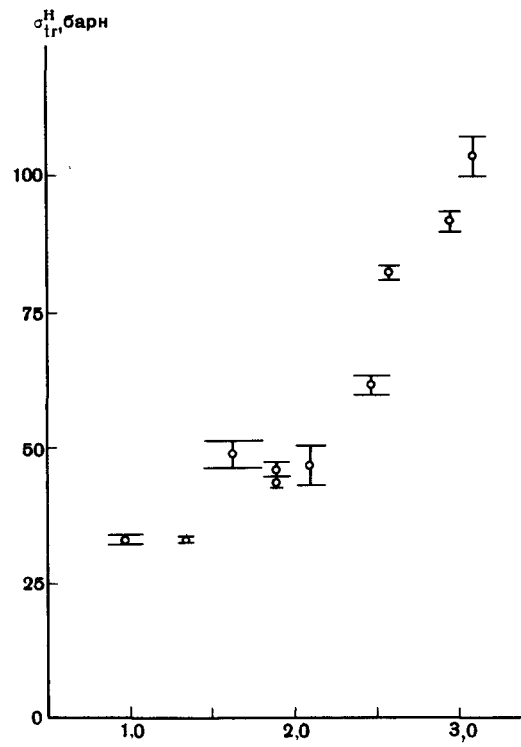

Рис. 4. Зависимость σ^{H}_{tr} от параметра a

Следовательно, для получения информации о значениях транспортной длины необходимо найти значение $m(a)$. Это можно сделать, если определить $\overline{L^2(v)}$ при различных температурах среды и результаты обработать вышеизложенным методом.

РЕЗУЛЬТАТЫ

Из полученных значений транспортной длины можно вычислить транспортное сечение рассеяния нейтронов на молекулу среды, усредненное по спектру нейтронов, а также в случае максвелловского распределения дифференциальное значение транспортного сечения рассеяния нейтронов молекулы среды. Из последнего можно вычислить транспортное сечение, приходящееся на один атом водорода, считая атомы углерода связанными.

Таким образом, можно определить как интегральные значения транспортного сечения рассеяния нейтронов на связанном водороде, так и дифференциальные сечения. Последние значения должны соответствовать величинам транспортного сечения, полученным из дифференциальных опытов.

Для подтверждения правильности методики обработки экспериментальных результатов было проведено сравнение значений транспортного сечения рассеяния нейтронов на молекулах среды, полученных как из интегральных, так и дифференциальных опытов. Сравнение было проведено для воды. Результаты интегрального опыта для воды (11) обрабатывались вышеизложенным методом [уравнение (17)].

Из дифференциальных опытов по рассеянию нейтронов различных энергий на воде были взяты значения $\cos\theta$ из доклада [21] и σ_s из ра-

боты [22]. Из статей [17-20] были получены σ_{tr} с использованием соотношения (17). Согласие в результатах хорошее. Кроме того, из статьи [19] были получены σ_{tr} с использованием соотношения (19). Эти значения σ_{tr} значительно отличаются от результатов дифференциального опыта. Различие порядка 40% (рис. 3).

В табл. 3 приведены значения параметра a и σ_{tr}^{H} на связанном водороде для исследованных веществ при температуре среды 18° С и данные по воде и даутерму [17-20, 23], обработанные вышеизложенным методом.

Транспортное сечение связанного водорода σ_{tr}^{H} меняется от 33 *барн* для $a \sim 1$ до 100 *барн* для $a \sim 3$, причем имеется целый спектр промежуточных значений (табл. 3, рис. 4), зависящих от структуры соединений.

Авторы выражают благодарность С. А. Гаврилову, И. Г. Морозову, Е. И. Инютину, Г. И. Сидорову, Б. М. Стасевичу, В. В. Окорокову, В. В. Долганову и В. А. Федоровичу за помощь в работе, а также В. П. Кочергину и А. Ф. Зажирко за проведение расчетов на электронно-вычислительной машине.

ЛИТЕРАТУРА

1. Х. Голдштейн, П. Цвейфел и Д. Фостер. Труды Второй международной конференции по мирному использованию атомной энергии, Женева, 1958, Р/2375.
2. Х. Каутс, Р. Шер, Дж. Браун, Клейн, С. Стейн, Р. Хелленс и Х. Арнольд. Труды Второй международной конференции по мирному использованию атомной энергии, Женева, 1958, Р/1841.
3. А. Мак-Рейнолдс, М. Нелкин, М. Розенблют и У. Уитмор. Труды Второй международной конференции по мирному использованию атомной энергии, Женева, 1958, Р/1540.
4. G. D. Joanov, A. J. Goodjahn and N. F. Wikner. Nucl. Sci. and Eng., *13*, 171-189 (1962).
5. Г. А. Столяров, Л. В. Комиссаров, В. П. Катков и Ю. В. Никольский. Сессия АН СССР по мирному использованию атомной энергии 1955 г. Изд-во АН СССР, Москва (1955).
6. А. Е. Глаубермани И. И. Тальянский. Атомная энергия, *3* (1957).
7. Л. Н. Юрова, А. А. Поляков, С. Б. Степанов и В. Б. Троянский. Нейтронная физика, Атомиздат, Москва (1960).
8. Л. Н. Юрова, А. А. Поляков и А. А. Игнатов, Атомная энергия, *12*, № 2 (1962).
9. Л. Н. Юрова, А. А. Поляков и А. А. Игнатов. Некоторые вопросы инженерной физики, Госатомиздат, Москва (1963).
10. Красик и Раковский. Материалы Международной конференции по мирному использованию атомной энергии, Женева, 1955, Р/601.
11. С. Глестон, М. Эдлунд. Основы теории ядерных реакторов, ИЛ, Москва (1954).
12. Г. И. Марчук. Методы расчета ядерных реакторов, Атомиздат, Москва (1961).
13. В. П. Кочергин и А. Ф. Зажирко. Программа расчета квадрата длины замедления нейтронов в гомогенных средах в многогрупповом приближении, препринт 557 ФЭИ СССР.
14. A. Munn and B. Pontecorvo. Can J. Res, A, *25*, 157-167 (1947).
15. M. Reier, M. F. Obenshaine and P. L. Hellens. Nucl. Sci. and Eng., *4*, 1-11 (1953).
16. G. D. Joanov, A. J. Goodjahn and N. F. Wikner. Nucl. Sci. and Eng., *13*, 171-189 (1962).
17. А. В. Антонов и др. Материалы Первой международной конференции по мирному использованию атомной энергии, Женева, 1955, Р/661.
18. G. F. von Dardel, Frans Royal. Inst. Techn, N 75, Stokholm (1954).
19. А. В. Антонов и др. Атомная энергия, *12*, № 1 (1962).
20. G. F. von Dardel, N. G. Sjöstrand, Phys. Rev., *96*, 1245 (1954).
21. В. И. Мостовой и др., наст. издание, Р/367.
22. Neutron cross section. Donald J. Hughes and Robert B. Shwartz. Brookhaven, National Laboratory, January 1 (1957).
23. M. Küchle, Nucleonics, 2, 131 (1960).

ABSTRACT—RÉSUMÉ—АННОТАЦИЯ—RESUMEN

A/356 USSR

Neutron moderation in hydrogenous media

By L. N. Yurova *et al.*

This paper deals with neutron moderation and diffusion in various hydrogenous media.

The first part of the paper describes the method of measuring neutron spatial distribution in "bonded" media and presents some results of experimental investigations of the spatial distribution of neutrons in various media.

The effect of the dimensions (width) of the neutron fission source and of the geometrical structure of the medium (heterogeneity) upon the neutron spatial distribution was determined for those neutrons which had been moderated down to 1.46 eV.

The second part of the paper presents the results of the thermal neutron diffusion measurements performed by the pulsed technique for a number of hydrogenous substances in a temperature range from the melting to the boiling points.

The diffusion coefficient was obtained in the form;

$$\overline{D(v)} = \text{const.}\ v^{a}$$

where a is the function of the molecular structure of the substance. The value of $\overline{D(v)}$ allows one to calculate the transport length and transport cross section per atom of bonded hydrogen.

It was found that the value of the transport cross section per atom of hydrogen strongly depends upon the molecular structure of the hydrogenous medium examined. For example, for monoisopropyldiphenyl $a = 2.58$ and $\sigma_{tr} = 86$ barns, and for diphenyl $a = 1.33$ and $\sigma_{tr} = 31$ barns.

A/356 URSS

Ralentissement des neutrons dans les milieux hydrogénés

par L. N. Yurova et *al.*

Le mémoire examine la question du ralentissement et de la diffusion des neutrons dans différents milieux hydrogénés.

Une première partie étudie les méthodes qui permettent de mesurer la distribution spatiale des neutrons dans les conditions d'un milieu « fini »; elle contient également les résultats de recherches expérimentales sur la distribution spatiale dans divers milieux. Les recherches ont notamment porté sur l'influence des dimensions (épaisseur) de la source des neutrons de fission et sur celle de la structure géométrique du milieu (hétérogénéité) sur la distribution spatiale des neutrons ralentis jusqu'à 1,46 eV.

Dans la deuxième partie du mémoire, les auteurs communiquent les résultats de mesures de la diffusion des neutrons thermiques effectuées par la méthode de la source pulsée pour plusieurs combinaisons hydrogénées, à des températures comprises entre la température de fusion et la température d'ébullition.

Pour le coefficient de diffusion, on a obtenu le rapport

$$\overline{D(v)} = \text{const. } v^a,$$

où a est fonction de la structure moléculaire de la substance. La valeur $\overline{D(v)}$ permet de calculer les longueurs et sections efficaces de transport pour un atome d'hydrogène lié.

Il a été établi que les différentes valeurs de la section efficace de transport correspondant à un atome d'hydrogène dépendent dans une large mesure de la structure moléculaire du milieu hydrogéné à étudier.

Ainsi, on a obtenu pour le monoisopropyldiphényle: $a = 2{,}58$, $\sigma_{tr} = 86$ barns; et, pour le diphényle: $a = 1{,}33$, $\sigma_{tr} = 31$ barns.

A/356 URSS

Moderación de los neutrones en los medios hidrogenados

por L. N. Yurova et *al.*

En el presente documento se estudian cuestiones relativas a la moderación y difusión de neutrones en diferentes medios hidrogenados.

En la primera sección se examina un método de medición de la distribución espacial de los neutrones en condiciones de medio «finito». Se presentan los resultados de una investigación experimental de la distribución espacial de los neutrones en diferentes medios. Se estudia la influencia de las dimensiones (del grosor) de la fuente de neutrones de fisión y de la estructura geométrica del medio (de la heterogeneidad) sobre la distribución espacial de los neutrones moderados hasta 1,46 eV.

En la segunda sección del documento se presentan los resultados de mediciones de la difusión de los neutrones térmicos, obtenidos por el método de impulsos, en toda una serie de compuestos hidrogenados para el intervalo de temperaturas desde la de fusión a la de ebullición.

Para el coeficiente de difusión se obtuvo la ley

$$\overline{D(v)} = \text{const. } v^a,$$

donde a depende de la estructura molecular de la sustancia. A partir del valor $\overline{D(v)}$ se calculan las longitudes y las secciones eficaces de transporte correspondientes a un átomo de hidrógeno ligado.

Se pudo establecer que los valores de la sección eficaz de transporte que corresponden a un átomo de hidrógeno depende fuertemente de la estructura molecular del medio hidrogenado investigado. Por ejemplo, para el monoisopropildifenilo so obtuvo $a = 2{,}58$ y $\sigma_{tr} = 86$ b; para el difenilo, $a = 1{,}33$ y $\sigma_{tr} = 31$ b.

Изучение термализации нейтронов в водородсодержащих средах

Е. Я. Доильницын, А. Г. Новиков, Г. А. Илясова, М. В. Панарин, В. В. Смелов, И. П. Стаханов, А. С. Степанов, А. И. Ступак (*)

Важнейшими водородсодержащими замедлителями нейтронов в реакторной технике в настоящее время являются вода и гидриды некоторых металлов. При термализации нейтронов в воде проявляются эффекты химической связи атомов и диффузия молекул жидкости.

При замедлении нейтронов в гидридах металлов обмен энергией между нейтроном и замедлителем идет порциями, определяемыми уровнями колебаний протона, жестко связанного с атомами металлов в решетке. Эти уровни могут проявляться в полных эффективных сечениях гидридов металлов [1].

В целях выяснения некоторых особенностей в формировании спектров тепловых нейтронов в этих средах были поставлены эксперименты по изучению термализации нейтронов в воде, гидриде лития и проведены измерения полных эффективных сечений гидрида лития, гидридов циркония с различным содержанием водорода. Результаты измерений сопоставляются с расчетами, учитывающими специфические особенности изучаемых замедлителей.

I. ТЕРМАЛИЗАЦИЯ НЕЙТРОНОВ В ВОДЕ И РАСТВОРАХ БОРНОЙ КИСЛОТЫ

При изучении термализации нейтронов в воде решались следующие вопросы:

1. Исследовался процесс формирования спектра тепловых нейтронов на различных расстояниях от источника.

2. Находилась длина релаксации температуры нейтронного газа непосредственно из эксперимента и проводился теоретический анализ наблюдаемых эффектов для условий данного опыта.

3. Определялось влияние концентрации поглотителя на формирование спектров тепловых нейтронов в бесконечной среде с равномерно распределенными источниками путем сравнения результатов измерений с расчетами по модели, учитывающей силы химической связи [2,3].

Экспериментальные данные, необходимые для решения поставленных задач, были получены посредством измерений пространственно-энергетических распределений тепловых нейтронов в воде, создаваемых сферическим источником, спектр которого в одном случае был близок к фермиевскому, а во втором представлял собой максвелловское распределение с $T = 760°$ К.

§ 1. Методика эксперимента

Измерение спектров тепловых нейтронов в воде на различных расстояниях от источника проводилось методом времени пролета. Использованная для этих целей установка схематически показана на рис. 1.

В бак цилиндрической формы диаметром 500 и высотой 600 *мм*, установленный вблизи защиты графито-водного энергетического реактора, заливалась дистиллированная вода. Коллимированный нейтронный пучок проходил по цилиндрической трубке ($d = 30$ *мм*) на свинцовый шар радиусом $r_0 = 20$ *мм*, расположенный в центре бака с водой. Этот шар, изотропно рассеивая падающие на него нейтроны, приблизительно имитировал сферический источник. Выводной канал, расположенный под углом 70° к направлению первичного пучка, представлял собой трубку прямоугольного сечения 15 × 30 *мм*. Распределение потока тепловых нейтронов вокруг шара, измеренное по активации индиевых индикаторов, лишь в прямом направлении обладало некоторой асимметрией (20%), которая в области расположения выводного канала уже полностью исчезала.

Спектры нейтронов, устанавливающиеся в воде, изучались с помощью механического селектора, описание которого можно найти в работе [4]. Разрешение прибора в этих измерениях составляло 40 *мксек/м*. Выводная трубка, механический прерыватель и детектор, будучи закреплены относительно друг друга, могли перемещаться вдоль направления выводимого пучка, что позволяло измерять спектры в воде на различных расстояниях от шара. Для их нормировки по амплитудам и введения поправки на градиент использовались данные, полученные с помощью индиевых индикаторов.

* Физико-энергетический институт, г. Обнинск.

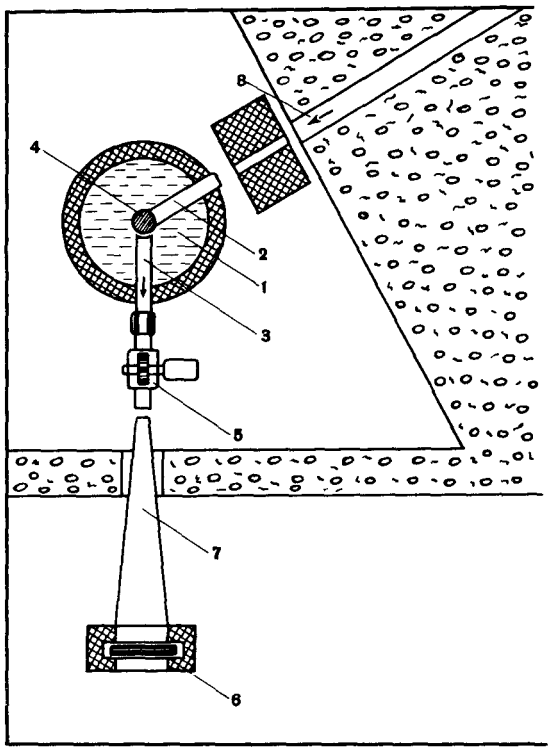

Рис. 1. Схема экспериментальной установки:
1—бак с водой; *2*—вводная трубка; *3*—выводная трубка; *4*—свинцовый шар; *5*—механический прерыватель; *6*—батарея из трех борных счетчиков; *7*—кадмиевая труба; *8*—пучок реактора

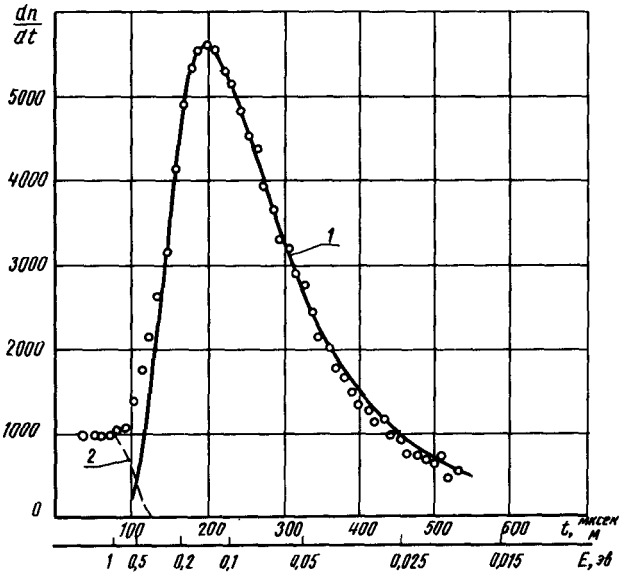

Рис. 2. Спектр источника:
1—максвелловское распределение с $T=760°$ К; *2*—пучок реактора перекрыт кадмиевым фильтром

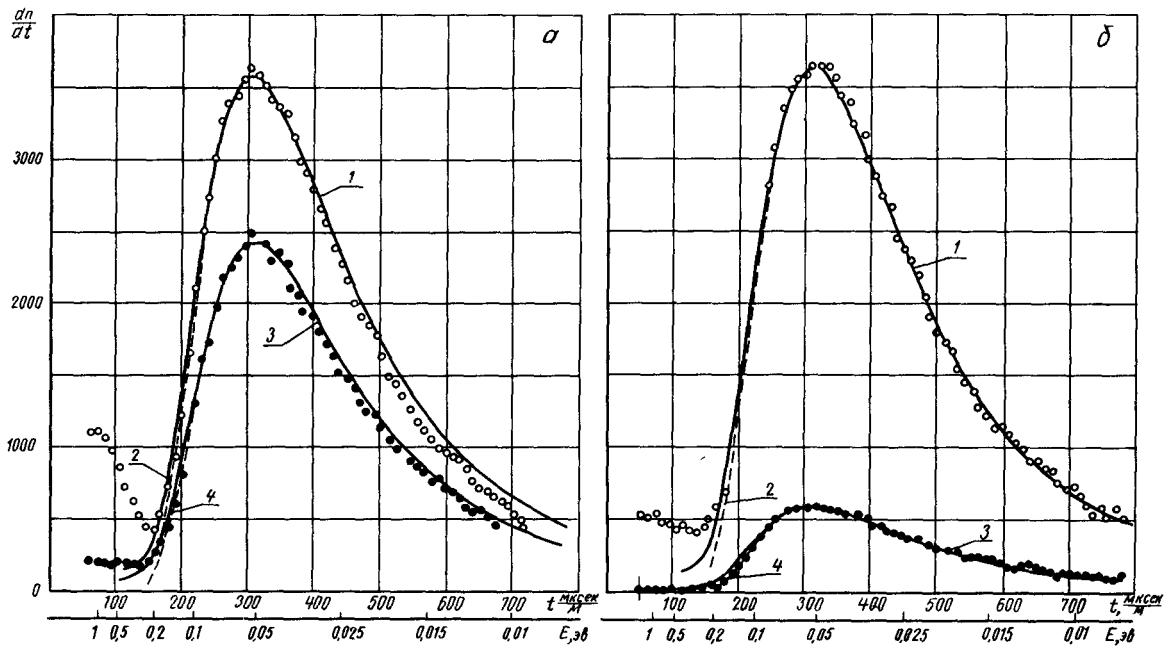

Рис. 3. Спектры нейтронов на различных расстояниях от источника с фермиевским распределением:
а—светлые кружки $r-r_0=0$; черные кружки $r-r_0=2$ *см*; *1*, *3*—расчет; *2*—максвелловское распределение с $T=312\pm10°$ К; *4*—максвелловское распределение с $T=309\pm10°$ К; *б*—светлые кружки $r-r_0=0{,}5$ *см*; черные кружки $r-r_0=6{,}5$ *см*; *1*, *3*—расчет; *2*—максвелловское распределение с $T=310\pm10°$ К; *4*—максвелловское распределение с $T=307\pm10°$ К

На всех приводимых ниже рисунках нейтронные спектры представлены в виде

$$\frac{dn}{dt} = f(t),$$

где $\frac{dn}{dt}$ — плотность нейтронов в единичном интервале пролетного времени; t — пролетное время, *мксек/м*.

Спектр источника, то есть спектр рассеиваемых шаром нейтронов, измеренный при отсутствии воды в баке, показан на рис. 2.

В воде измерения проведены на расстояниях от шара $r - r_0 = 0$; 5; 10; 20; 50; 65 *мм* (r — расстояние от центра шара до исследуемой точки). На каждом из указанных расстояний спектр измерялся дважды: без кадмиевого фильтра и с фильтром, помещаемым на входе пучка в бак. Экспериментальные кривые, снятые с фильтром в первичном пучке, представляют собой, как это видно из рис. 2, спектр нейтронов от источника с фермиевским распределением. Экспериментальная кривая, полученная на данном расстоянии как разность двух измерений (без фильтра и с фильтром в первичном пучке) представляет собой спектр нейтронов в воде, обусловленный действием тепловой компоненты пучка реактора, которая, как следует из рис. 2, близка к максвелловскому распределению с $T_н = 760°$ К.

§ 2. Спектры тепловых нейтронов от источника с фермиевским распределением

Пространственно-энергетическое распределение нейтронов от источника с фермиевским спектром показано на рис. 3. Во всех исследованных точках, включая и измерения вплотную к шару, тепловая область спектров удовлетворительно описывается максвелловскими распределениями с температурами, незначительно превышающими температуру среды, и в пределах экспериментальных ошибок, совпадающих между собой.

Результаты этого эксперимента сравнивались с расчетом пространственно-энергетического распределения тепловых нейтронов в воде, проведенном для сферической геометрии. Расчет выполнен в P_1-приближении в энергетической области $0 < E < 0{,}67$ *эв*, разбиваемой на 15 групп. Термализационные эффекты были учтены на основе работы Турчина [5]. При $E > 0{,}67$ *эв* (область источников) спектр нейтронов предполагался фермиевским, а в качестве пространственного распределения источников использовалась экспериментальная кривая, полученная с помощью индиевых индикаторов ($E = 1{,}46$ *эв*). Подробное изложение метода, использованного в данном расчете, можно найти в работах [3, 5].

Экспериментальные и расчетные кривые нормировались по максимуму распределения $\frac{dn}{dt}$. На рис. 3 видно, что результаты эксперимента и расчета согласуются достаточно хорошо, причем в тепловой области расчетные кривые практически совпадают с соответствующими максвелловскими распределениями. Таким образом, данные эксперимента и расчета позволяют сделать вывод, что при использовании источника с фермиевским спектром энергетическое распределение тепловых нейтронов в воде (в области $E < 0{,}15$ *эв*) не зависит от расстояния до источника и в любой точке среды может быть описано спектром тепловых нейтронов для бесконечной среды с распределенными источниками [3] (с точностью до небольшой поправки, связанной с влиянием локальной утечки, § 4).

§ 3. Спектры тепловых нейтронов от источника с температурой максвелловского распределения 760° К

Пространственно-энергетическое распределение нейтронов в воде, создаваемое источником, спектр которого представляет собой тепловую компоненту пучка реактора (разностные кривые), показано на рис. 4. Было установлено, что при $r - r_0 \geqslant 20$ *мм* экспериментальные кривые близки к максвелловскому распределению с $T_н = 304°$ К (температура, усредненная по измерениям на трех расстояниях: 20 *мм* — 303 ± 15° К; 50 *мм* — 306 ± 15° К; 65 *мм* — 302 ± 15° К). Следовательно, начиная с расстояния от шара 20 *мм*, спектр используемого нами источника в пределах точности эксперимента не влияет на характер энергетического распределения нейтронов.

В области $r - r_0 < 20$ *мм*, которую можно назвать переходной, измеренные распределения нейтронов носят существенно иной характер. Было проведено сопоставление этих кривых с расчетом, основанным на предположении, что процесс установления спектра среды идет через максвеллоподобные формы с температурой, зависящей от расстояния до источника. Кинетическое уравнение решалось методом Греда [6] путем разложения функции распределения нейтронов по симметризованным полиномам Эрмита. Параметр разложения, температура нейтронов T выбиралась таким образом, чтобы функция распределения достаточно хорошо аппроксимировалась двумя первыми членами

$$T = \frac{m}{3kn} S_p I_{ik}, \qquad (1)$$

где I_{ik} — второй момент функции распределения.

Интегрируя кинетическое уравнение по пространству скоростей, получаем систему уравнений для T, n (плотности нейтронов) и $\vec{I}$ (потока нейтронов)

$$\frac{\partial n}{\partial t} + \frac{\partial I_i}{\partial x_i} + \gamma n = 0;$$

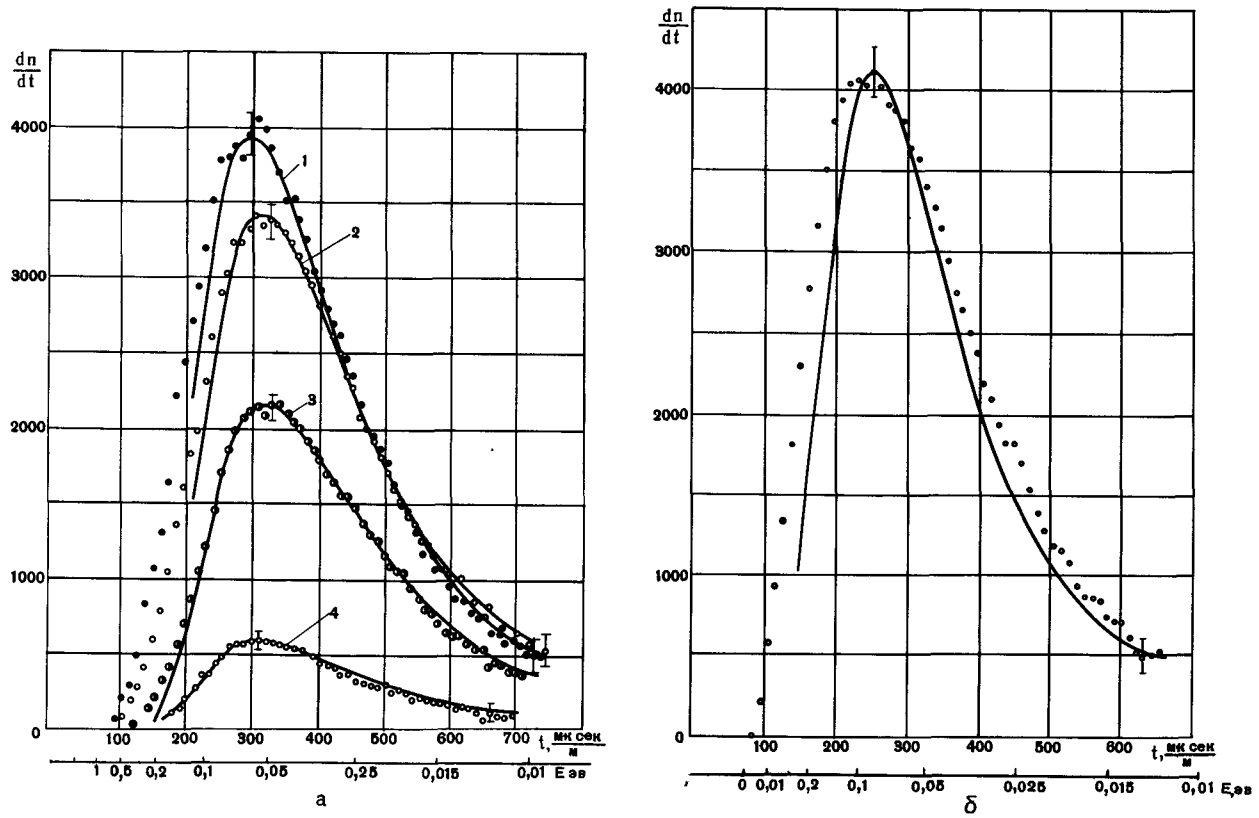

Рис. 4. Разностные спектры на различных расстояниях от источника:
а: *1* — $r - r_0 = 0{,}5$ *см*; $T_н = 360 \pm 18°$ K; *2* — $r - r_0 = 1$ *см*; $T_н = 317 \pm 15°$ K; *3* — $r - r_0 = 2$ *см*; $T_н = 303 \pm 15°$ K; *4* — $r - r_0 = 5$ *см*; $T_н = 306 \pm 15°$ K; *б* — $r - r_0 = 0$; $T_н = 500 \pm 30°$ K

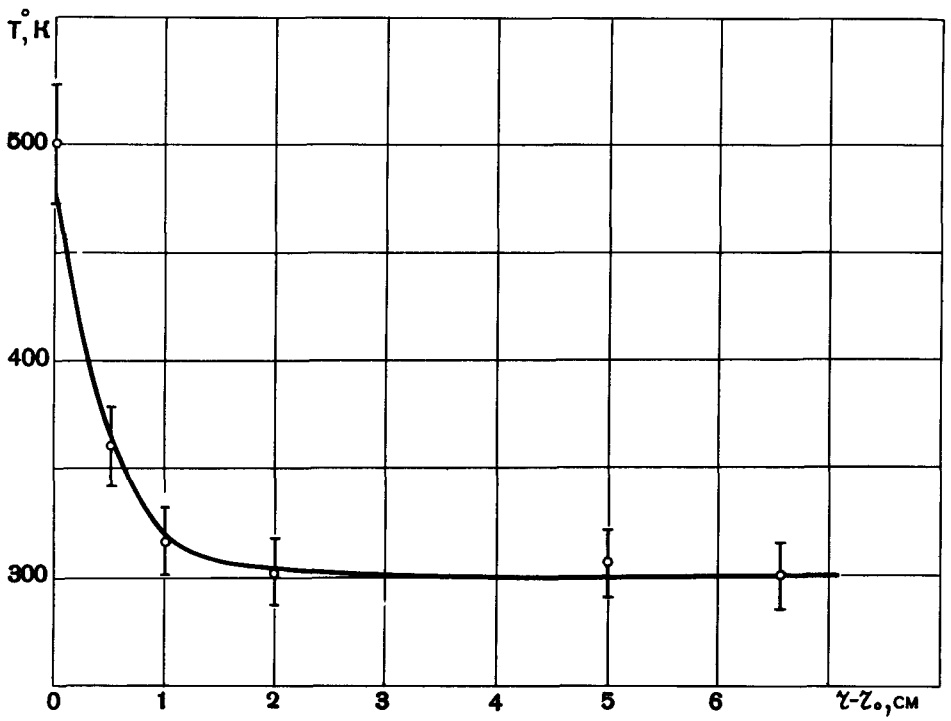

Рис. 5. Температура нейтронного газа T как функция расстояния $r - r_0$ от источника (точки—экспериментальные данные, кривая—расчет по формуле)

$$\frac{\partial nT}{\partial t}+\frac{5}{3}\frac{\partial}{\partial x_i}nI_i+\gamma nT=\frac{T-T'}{T'}nT\frac{1}{\tau}; \quad (2)$$

$$I_i=-\frac{k}{m}\frac{1}{\lambda}\frac{\partial nT}{\partial x_i},$$

где T' — температура среды; γ — коэффициент поглощения; m — масса нейтрона.

Кинетические коэффициенты λ и τ определены следующим образом:

$$\lambda=\frac{4}{3}\frac{1}{\sqrt{\pi}}n'\frac{1}{\beta}\int dx\,dx'\,e^{-x^2}[\sigma_0(x'\to x)x'^5-$$
$$-\sigma_1(x'\to x)xx'^4];$$
$$\frac{1}{\tau}=\frac{2}{3}\frac{1}{\sqrt{\pi}}n'\frac{1}{\beta}\int dx\,dx'\,e^{-x'^2}\times$$
$$\times(x^2-x'^2)x'^3\sigma_0(x'\to x), \quad (3)$$

где n' — плотность молекул среды; x — безразмерная скорость $\left(x=\beta v;\beta=\frac{m}{2kT'}\right)$; σ_0 и σ_1 — нулевой и первый моменты индикатрисы рассеяния.

Решение системы (2) для стационарного случая без поглощения и сферического источника с температурой T_0 дает [4]

$$|T'-T|=|T_0-T|\times$$
$$\times\exp\left\{-\frac{1}{L^2}\left[\frac{r^2-r_0^2}{2}+\frac{r^3-r_0^3}{3R}\right]\right\}, \quad (4)$$

где r_0 — радиус источника; R — радиус, характеризующий общие размеры системы; $L=\left(\frac{5}{3}\frac{\tau}{\lambda}\frac{kT'}{m}\right)^{1/2}$ — длина релаксации температуры нейтронного газа *.

Для сопоставления экспериментальных данных с этим расчетом разностные кривые, полученные на разных расстояниях от шара, следовало аппроксимировать максвелловскими распределениями. Их температура подбиралась таким образом, чтобы добиться наилучшего совпадения максвелловского распределения с правым скатом соответствующей разностной кривой. Этот способ определения температур вытекает из предположения, что если поток «горячих» нейтронов источника вызывает анизотропию функции распределения, то правый скат экспериментальной кривой является областью спектра, где эта анизотропия сказывается наиболее слабо. Температуры нейтронов, найденные таким образом, оказались равными: для $r-r_0=0$ $T=500\pm30°$ К; для $r-r_0=5$ *мм* $T=360\pm20°$ К; для $r-r_0=10$ *мм* $T=317\pm15°$ К (рис. 5).

Используя выражение (4) и температуры, полученные для различных расстояний, нашли, что $L=1\pm0{,}2$ *см*. Расчет длины релаксации нейтронной температуры на основе модели, предложенной в работе [2], дает для нашего случая величину $L=1{,}1$ *см*. Зависимость температуры нейтронов от расстояния до шара, рассчитанная по (4) с $L=1$ *см*, приведена на рис. 5.

Из рис. 4 следует, что аппроксимация разностных кривых максвелловскими распределениями может считаться удовлетворительной на расстояниях, где спектр близок к асимптотическому, но не пригодна для области, где близость источника вызывает заметную анизотропию функции распределения. Более точного описания формы экспериментальных кривых во всей переходной области можно добиться, представив их как суперпозицию спектра источника (максвелловское распределение с $T=750°$ К) и асимптотического спектра среды (максвелловское распределение с $T=300°$ К) с амплитудами, зависящими от координат. Подобный подход уже неоднократно использовался в ряде расчетных и экспериментальных работ, например [7,8]. Разложение разностных кривых на две такие составляющие показано на рис. 6.

Предполагалось, что на всех расстояниях от источника характер спектра при энергиях $\sim0{,}01$ *эв* полностью определяется максвелловским распределением с $T=300°$ К. Таким образом, оказывались найденными асимптотические составляющие. Вычитая их из разностных спектров, получили для всех трех расстояний (0; 5 и 10 *мм*) кривые, близкие по форме к максвелловскому распределению с $T=750°$ К, но различные по амплитудам. Плотности «горячей» и «холодной» компоненты, найденные в результате этого разложения как функции расстояния от источника, представлены на рис. 7.

Была предпринята попытка получить подобные кривые расчетным путем. Для этого функция распределения нейтронов представлялась в виде суперпозиции двух составляющих, каждая из которых зависила только от одной из температур. Использованная методика расчета не отличалась от изложенной выше [4].

Расчет был проведен для двух случаев: для среды без поглощения и при наличии слабого поглощения. Из рис. 7, на котором результаты этих расчетов сравниваются с экспериментом, видно, что на малых расстояниях трудно отдать предпочтение какой-либо из расчетных кривых. На больших расстояниях, однако, экспериментальные точки для плотности «холодных» нейтронов ближе к данным расчета, в котором учитывается поглощение.

---

* Для случая плоской задачи без поглощения распределение температуры нейтронов принимает вид

$$|T'-T|=|T_0-T|\exp\left\{-\frac{x}{L_x}\right\}$$

L_x связана с полученной выше длиной релаксации соотношением

$$L^2=L_xa,$$

где a — величина, характеризующая размер системы. При наличии поглощения a зависит от диффузионной длины.

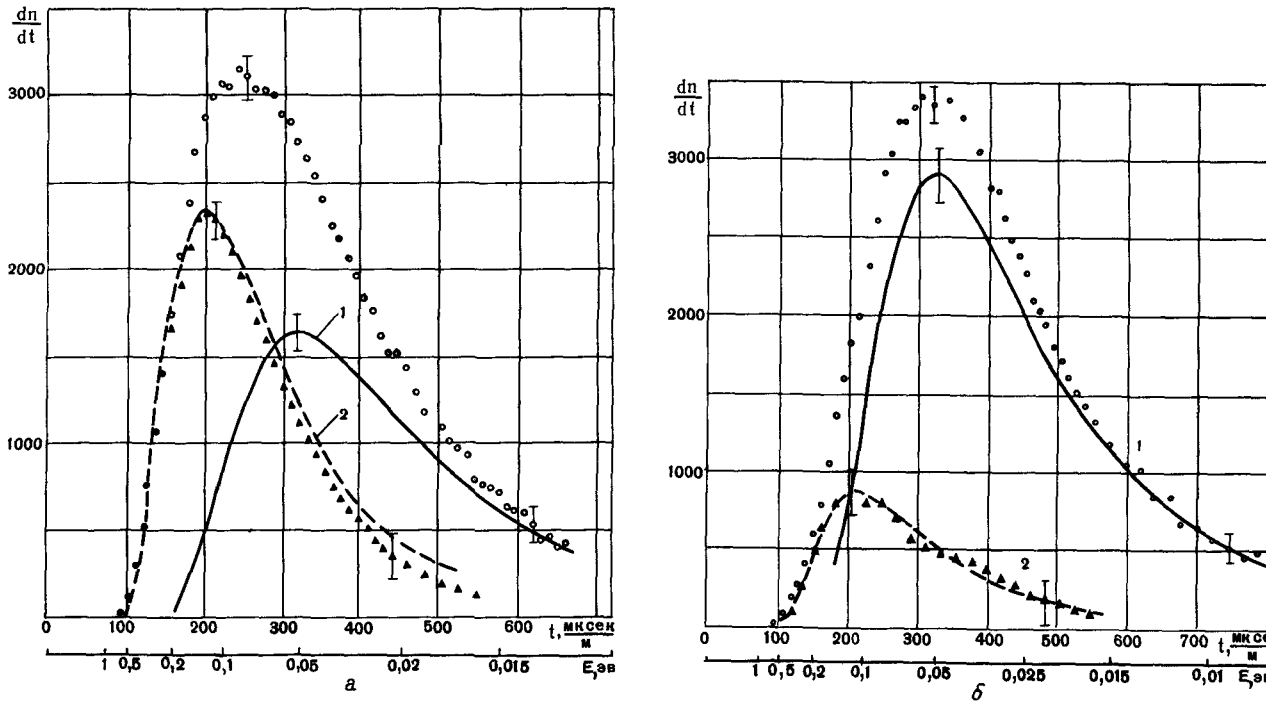

Рис. 6. Разложение разностных спектров на две составляющие:
а — $r - r_0 = 0$; *б* — $r - r_0 = 1$ *см*; *1* — максвелловское распределение с $T = 300°$ К; *2* — максвелловское распределение с $T = 750°$ К

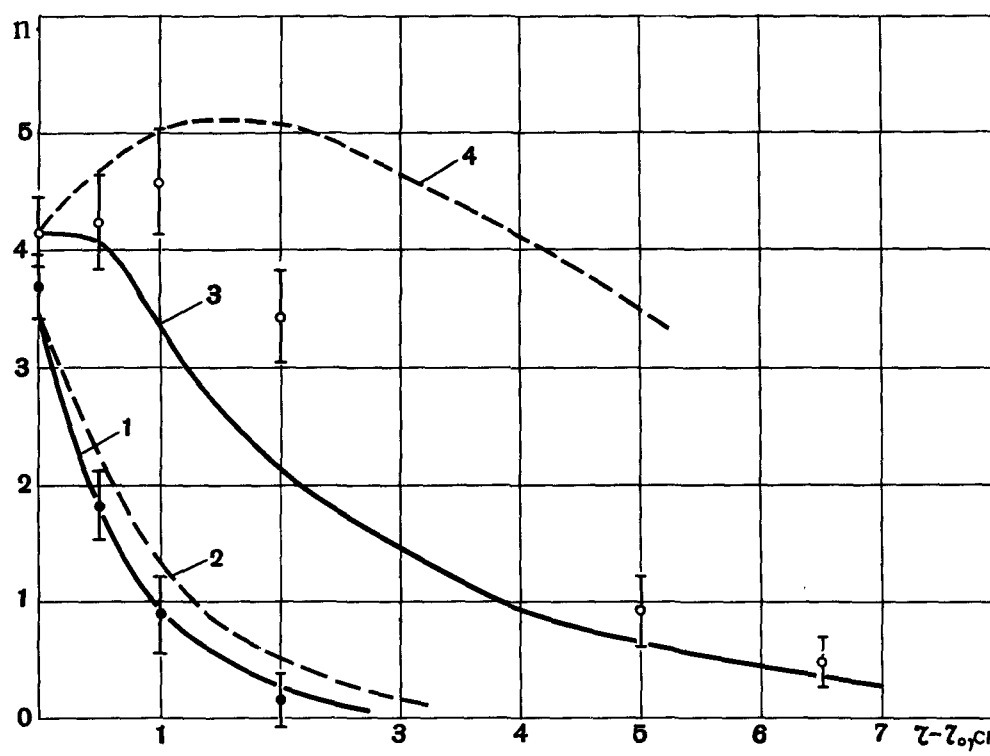

Рис. 7. Плотность нейтронов «горячего» и «холодного» спектра n как функция расстояния $r - r_0$ от источника.
«Горячий спектр»: черные точки — эксперимент; *1* — расчет с учетом слабого поглощения; *2* — расчет без учета поглощения; «холодный» спектр: светлые точки — эксперимент; *3* — то же, что и *1*; *4* — то же, что и *2*

§ 4. Спектры нейтронов в растворах борной кислоты

При измерении спектров тепловых нейтронов в растворах борной кислоты использовалась описанная выше экспериментальная установка. Пучок нейтронов из реактора на входе в бак был постоянно перекрыт кадмиевым фильтром, а торец выводного канала помещался над шаром, благодаря чему градиент скалярного потока в направлении вывода пучка был мал.

При сравнении полученных результатов с расчетами для бесконечной среды с равномерно распределенными источниками необходимо вводить поправку на локальную диффузионную утечку нейтронов. В области, близкой к источнику, эта поправка на первый взгляд представляется значительной. Однако характер распределения потока нейтронов, создаваемого спектром нашего источника, таков, что область вывода пучка ($r - r_0 \approx 1$ *см*) близка к точке перегиба кривой, описывающей распределение этого потока. Локальная утечка проявляется здесь как небольшое дополнительное поглощение ($\nabla^2\Phi < 0$), составляющее $\sim$15% от общего поглощения для чистой воды, и практически не сказывается на результатах измерений при введении дополнительного поглотителя.

Результаты измерений [9] и их сопоставление с расчетами, выполненными для бесконечной среды с равномерно распределенными источниками [3], представлены на рис. 8. При нанесении данных T_H/T_0 в функции концентрации поглотителя учтено дополнительное поглощение, связанное с локальной диффузионной утечкой. В тепловой области экспериментальные кривые удовлетворительно согласуются с расчетными спектрами, которые оказываются весьма близки к максвелловским распределениям с температурами, указанными на том же рисунке. Значения T_H/T_0 в зависимости от концентрации поглотителя в воде сравниваются на рис. 9 с расчетами, выполненными в работах [2,3] с учетом сил химической связи (кривые *1* и *2*) и по газовой модели (кривая *3*). Следует отметить, что результаты последних расчетов, изложенные в докладе, представленном на настоящую конференцию [2], лучше согласуются с нашими данными. Вся совокупность экспериментальных значений T_H/T_0 не может быть объяснена на основе газовой модели.

II. ИЗУЧЕНИЕ ЗАМЕДЛЯЮЩИХ СВОЙСТВ ГИДРИДОВ МЕТАЛЛОВ

§ 1. Полные эффективные сечения гидридов лития и циркония

Измерения полных эффективных сечений гидридов металлов производились с помощью механического селектора нейтронов, описанного в работах [10,11]. Веретенообразная форма щелей в роторе и использованная система синхронно вращающихся роторов обеспечивали пренебрежимо малый фон в измерениях на пролетной базе в 130 *м* при разрешении в тепловой области 3 *мксек/м*.

На рис. 10 приведен ход полного сечения рассеяния нейтронов на водороде, связанном в гидриде лития, по данным измерений полного сечения Li^7H в области от 0,02 до 2 *эв*. При энергии нейтронов выше 0,2 *эв* сечение рассеяния, полученное из экспериментов, следует закону [12,13].

$$\sigma_s = \sigma_0\left(1 + \frac{K_v}{3\mu E}\right), \qquad (5)$$

где K_v — средняя кинетическая энергия протона; μ — отношение массы протона к массе нейтрона; σ_0 — сечение рассеяния на свободном ядре.

Расчетные значения сечения рассеяния нейтронов гидридом лития, полученные в работе [2], с учетом уровней при 0,1; 0,13 *эв* и акустических колебаний удовлетворительно согласуются с экспериментальными данными. На рис. 10 нанесены пунктиром расчетные значения в области уровня при 0,1 *эв*, где имеется небольшое отличие от результатов эксперимента. Во всей остальной области имеет место хорошее согласие экспериментальных и расчетных данных.

Измерение полного эффективного сечения гидрида циркония проводилось для трех разновидностей гидрида с различным содержанием водорода. Результаты измерений показывают, что полные сечения гидридов циркония в пределах точности измерений (4%) совпадают между собой и с данными, опубликованными в работе [1]. Для исследованных разновидностей гидрида циркония не замечено смещения уровней возбужденных колебаний водорода в решетке. Сечение рассеяния нейтронов в области $E > 0{,}5$ *эв* описывается соотношением (5).

§ 2. Термализация нейтронов в гидриде лития-7

Исследование термализации нейтронов в гидриде лития-7 проводилось по методике, ранее описанной в этом докладе (§ 4). В этих опытах использовалась та же установка, идентичная геометрия и применялись аналогичные методы анализа экспериментальных данных. Сборка из гидрида лития была сделана в форме цилиндра диаметром $d = 430$ *мм* высотой $H = 520$ *мм* из дисков $d = 47$ *мм* и толщиной $H = 5$ *мм*. Диски из гидрида (в алюминиевых чехлах толщиной 0,1 *мм*) укладывались таким образом, чтобы уменьшить вылет нейтронов через щели сборки (в каждом слое гидрида диски соответственно смещены так, чтобы исключить утечку нейтронов без замедления). В центре сборки размещался свинцовый шар

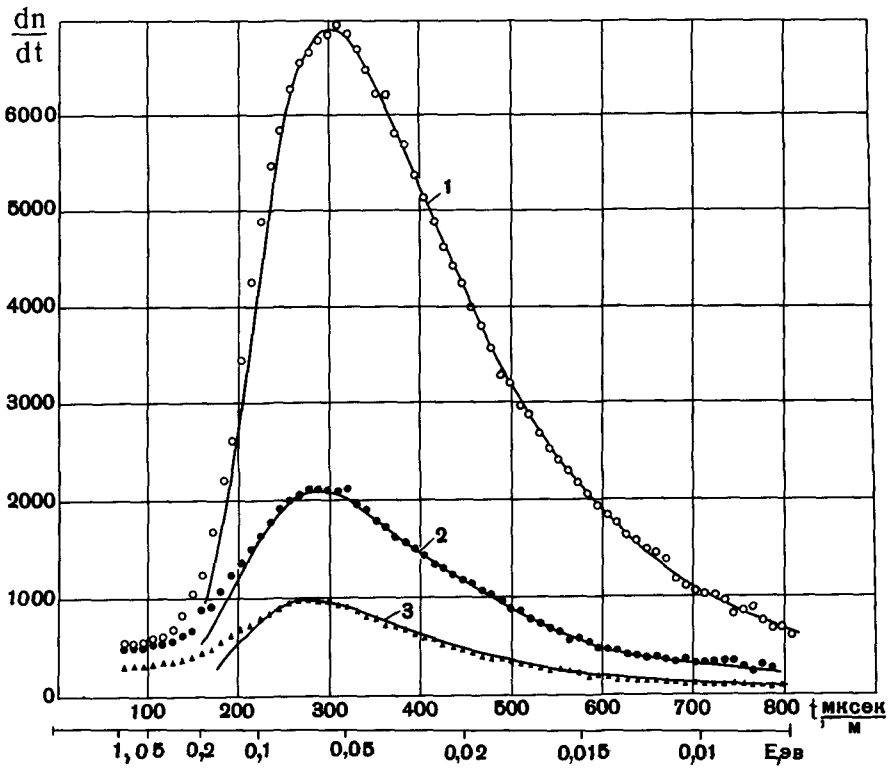

Рис. 8. Спектры тепловых нейтронов в растворе борной кислоты (температура воды $T_0 = 320 \pm 3°$ K) :
1 — чистая вода, $T_н = 330 \pm 15°$ K; *2* — $\sigma_c = 1{,}5$ *барн*, $T_н = 360 \pm 15°$ K; *3* — $\sigma_c = 2{,}9$ *барн*, $T_н = 380 \pm 15°$ K

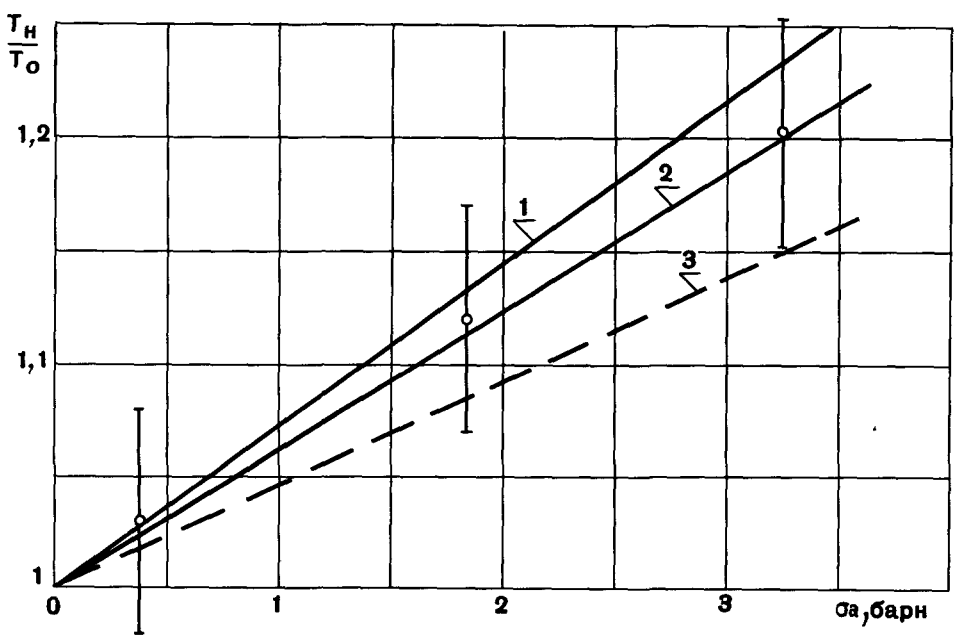

Рис. 9. Зависимость температуры нейтронного газа от концентрации поглотителя:
1 — расчет, взятый из работы [3]; *2* — расчет, проведенный в работе [2]; *3* — расчет на основе модели свободного водорода

диаметром 50 *мм*. По специальному каналу в сборке, имеющему в сечении квадрат со стороной 35 *мм*, на свинцовый шар проходил пучок нейтронов из реактора. На пути пучка, перед сборкой устанавливался кадмиевый фильтр. Пучок нейтронов выходил с торца канала над центром шара. Выводной канал представлял в сечении прямоугольник со сторонами 20 × 35 *мм*.

Результаты измерений плотности тепловых нейтронов приведены на рис. 11 в функции времени пролета, выраженном в *мксек/м*. Статистическая точность в определении $\frac{dn}{dt}$ составляла ~3%.

В первом приближении спектр тепловых нейтронов в гидриде лития-7 можно описать максвелловским распределением с температурой $T = 330 \pm 10°$ К. Сопоставление этих результатов с соответствующими измерениями

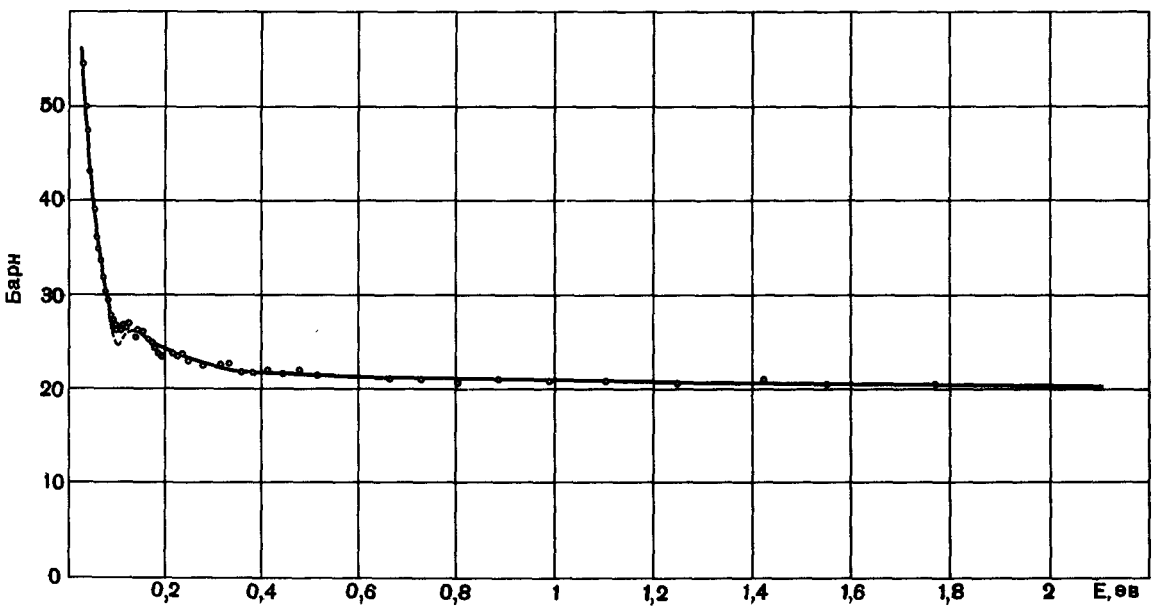

Рис. 10. Полное сечение гидрида лития

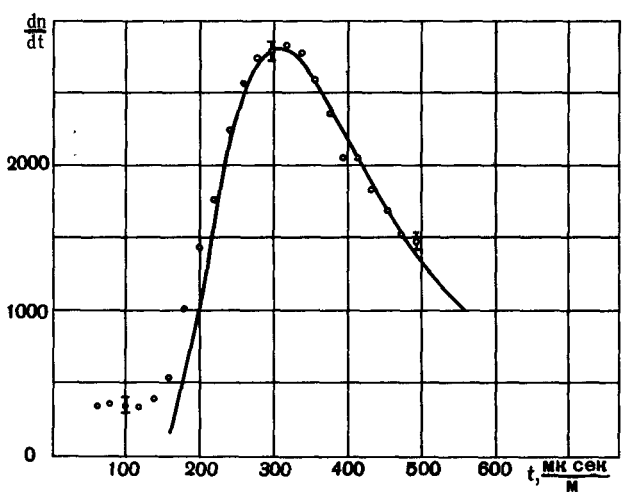

Рис. 11. Спектр тепловых нейтронов в Li^7H при $T_0 = 300°$ К

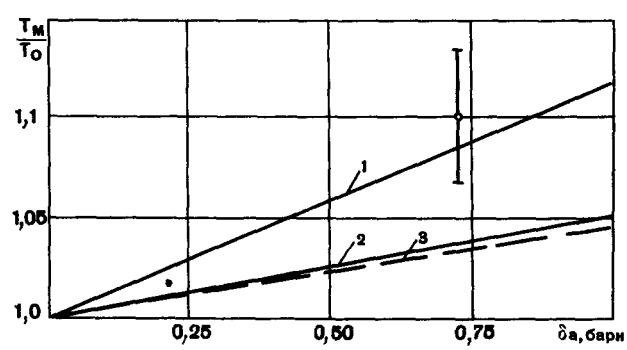

Рис. 12. Зависимость температуры нейтронного газа от концентрации поглотителя:
1—расчет, проведенный в работе [2] для Li^7H; *2*—расчет, проведенный в работе [3] для воды; *3*—расчет на основе модели свободного водорода; точка—экспериментальное значение T_H/T_0 для Li^7H

спектров в воде при той же температуре и равных поглощениях на атом водорода показывает, что спектр нейтронов, устанавливающийся в гидриде лития-7, более жесткий, чем в воде. На рис. 12 показано значение T_H/T_0, полученное в нашем эксперименте. Для сравнения на том же рисунке приведены кривые T_H/T_0, взятые нами из работы [2] для Li^7H (кривая *1*) и воды (кривая *2*). Кривая *3* рассчитана по модели свободного водорода. В отложенном по оси абсцисс поглощении нейтронов для Li^7H учтено эффективное сечение примеси $\sigma_a Li^6$,

Сравнение T_H/T_0 для гидрида лития-7 и воды показывает, что спектр тепловых нейтронов, устанавливающийся в гидриде, близок к спектру в воде, отравленной поглотителем по закону $1/v$, при поглощении в воде почти в два раза большем, чем в гидриде лития. По сравнению с распределением нейтронов, устанавливающимся в гидриде циркония при таком же поглощении [14], спектр тепловых нейтронов в гидриде лития-7 более мягкий.

ЗАКЛЮЧЕНИЕ

Проведенные опыты по изучению замедляющих свойств воды, гидридов лития-7 и циркония и сравнение с расчетами показывают, что наблюдаемые в экспериментах эффекты достаточно хорошо согласуются с расчетами, выполненными по соответствующим дифференциальным сечениям в работе [2].

Авторы выражают благодарность В. Ф. Турчину за полезные обсуждения.

ЛИТЕРАТУРА

1. A. W. Mc Reynolds, M. Nelkin, M. Rosenbluth and W. Whittemor. Труды Второй международной конференции по мирному использованию атомной энергии, Женева, 1958, P/1540.
2. Л. В. Майоров, В. Ф. Турчин и М. С. Юдкевич. Влияние химической связи на термализацию нейтронов, наст. издание, P/360.
3. Г. И. Марчук, В. Ф. Турчин, В. В. Смелов и Г. А. Илясова. Атомная энергия, *13*, 534 (1962).
4. Е. Я. Доильницын, А. Г. Новиков, И. П. Стаханов и А. С. Степанов. Атомная энергия, *15*, 255 (1963).
5. В. Ф. Турчин, Inelastic scattering of neutrons in solid and Liquids, International atomic energy agency; Vienna, 259 (1961).
6. H. Grad. Communs pure and appl. Math. z, 231 (1949).
7. D. S. Selengut. Nucl. Sci. and Eng., *9*, 1, 94 (1961).
8. R. Rennett, R. Neiman. Nucl. Sci. and Eng., *8*, 4 (1960).
9. Е. Я. Доильницын и А. Г. Новиков. Атомная энергия, *13*, 491 (1962).
10. В. В. Владимирский, В. В. Соколовский. Труды Второй международной конференции по мирному использованию атомной энергии, Женева, 1958, P/2041.
11. Е. Я. Доильницын, Л. П. Хамьянов и П. С. Клемышев. Материалы рабочего совещания по физике медленных нейтронов. ОИЯИ, Дубна, 1962, стр. 193.
12. J. Placzek. Phys. Rev., *86*, 377 (1952).
13. F. A. Messian. J. phys. rad., *12*, No. 6, 670 (1951).
14. R. B. Walton, J. R. Beyster, J. L. Wood and W. M. Lopez. Nucl. Sci. and Eng., *9* (1961).

ABSTRACT—RÉSUMÉ—АННОТАЦИЯ—RESUMEN

A/366 USSR

Neutron thermalization studies in hydrogenous media

By E. Y. Doilnitsyn *et al.*

This paper describes the investigation of thermal neutron spectra in water and hydrogenous media by means of the time-of-flight method.

Space and energy distribution of neutrons in water with a Fermi-spectrum source is presented.

Neutron spectra are measured in water poisoned by an absorber according to the $1/v$ law. The results are compared with the calculations for a gas model, taking into account the chemical binding forces.

The relaxation of a neutron-gas temperature in water has been studied.

Two approaches are considered, satisfactorily explaining the asymptotic spectrum for thermal neutrons.

A/366 URSS

Étude de la thermalisation des neutrons dans les milieux hydrogénés

par E. Y. Doilnitsyn *et al.*

Le mémoire décrit des études de spectres de neutrons thermiques d'après le temps de vol dans l'eau et dans les milieux hydrogénés.

On donne la distribution spatiale et énergétique dans l'eau des neutrons émis par une source à spectre de Fermi.

Les spectres de neutrons sont mesurés dans l'eau empoisonnée par un absorbeur suivant la loi $1/v$. Les résultats sont comparés aux calculs fondés sur un modèle de gaz, compte tenu des forces de liaison chimique dans l'eau.

On étudie la relaxation de la température du gaz neutronique dans l'eau. On examine deux conceptions permettant d'expliquer de facon satisfaisante l'exis-

tence d'un spectre asymptotique de neutrons thermiques.

A/366 URSS

Estudio de la termalización de neutrones en medios hidrogenados

por E. Y. Doilnitsyn *et al.*

En el informe se describen las investigaciones sobre espectros de neutrones térmicos, efectuadas por el método del tiempo de vuelo, en el agua y en medios hidrogenados.

Se presenta la distribución espacial y energética de los neutrones en el agua para una fuente con espectro de Fermi.

Se midieron los espectros neutrónicos en agua envenenada con un absorbente que sigue la ley $1/v$. Los resultados se comparan con cálculos relativos al modelo de gas y que tienen en cuenta el enlace químico en el agua.

Se estudió la relajación de la temperatura del gas neutrónico en el agua. Se consideraron dos enfoques que permiten explicar satisfactoriamente el proceso del establecimiento de un espectro asintótico de los neutrones térmicos.

Экспериментальные работы по термализации нейтронов

В. И. Мостовой, В. С. Дикарев, И. П. Еремеев, С. П. Ишмаев, И. П. Садиков, Ю. С. Салтыков, В. А. Тарабанько, А. А. Чернышов

ВВЕДЕНИЕ

Экспериментальные исследования по термализации нейтронов были начаты в Институте атомной энергии им. И. В. Курчатова в период физического обоснования проектов энергетических уран-водных реакторов. Как известно, физика этих реакторов существенным образом определяется характером пространственно-энергетического распределения тепловых и эпитепловых нейтронов [1]. Между тем расчет спектров нейтронов в гетерогенных уран-водных системах представлял в то время трудную проблему. Необходимо было не только разработать эффективные методы расчета, но и получить исходные данные по нейтронным сечениям, которые требуются для этих расчетов. Особенно трудной в экспериментальном и теоретическом отношении представлялась задача получения данных по дважды дифференциальному сечению рассеяния медленных нейтронов на воде. В связи с этим исследования по термализации были начаты с экспериментов по измерению пространственно-энергетического распределения нейтронов в уран-водных системах. Впоследствии такие измерения были проведены также и в гетерогенных системах урана с другими замедлителями, представляющими интерес для энергетических реакторов.

Результаты проведенных исследований позволили определить основные закономерности пространственно-энергетического распределения нейтронов в гетерогенных системах и выяснить влияние химической связи атомов замедлителя и поглощения на характер этого распределения. Они оказались также полезными при оценке точности приближенных методов решения кинетического уравнения для гетерогенных систем и проверки пригодности различных модельных представлений о характере обмена энергией между нейтроном и замедлителем в области энергий химической связи.

Для более глубокого изучения полученных закономерностей и выяснения роли поглощения и химической связи в процессах формирования спектров в различных системах программа исследований по термализации была существенно расширена. В настоящее время экспериментальные работы ведутся в трех основных направлениях, охватывающих наиболее интересные и существенные вопросы термализации:

1) изучение дважды дифференциальных сечений для замедлителей в тепловой области энергий нейтронов;

2) изучение спектров тепловых и эпитепловых нейтронов в различных размножающих и замедляющих средах;

3) изучение процесса установления теплового спектра нейтронов во времени.

Ниже приводятся результаты исследований по этим направлениям, полученные в последние годы, а также кратко описывается использованная экспериментальная методика.

ИЗМЕРЕНИЕ ДВАЖДЫ ДИФФЕРЕНЦИАЛЬНЫХ СЕЧЕНИЙ РАССЕЯНИЯ

Дважды дифференциальные сечения рассеяния $\sigma(E, E', \theta)$ были измерены для воды (H_2O) при T, равном 23 и 90° С, и моноизопропилдифенила ($C_{15}H_{16}$) при $T = 20°$ С.

Эксперименты по изучению дважды дифференциальных сечений производились на горизонтальном пучке тепловых нейтронов реактора ВВР-М Института физики АН УССР.

Методика измерений

Пульсирующий поток «монохроматических» нейтронов энергии E, падающих на образец замедлителя, выделялся из пучка тепловых нейтронов с помощью механического монохроматора с параболическими щелями (рис. 1). Разрешение монохроматора не зависело от скорости его вращения и составляло $\left(\frac{\Delta E}{E}\right)_{1/2} = 0{,}2$. Энергия нейтронов E', рассеянных от образца

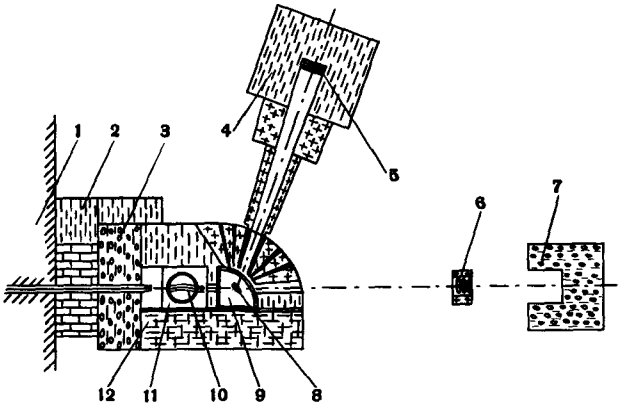

Рис. 1. Схема экспериментальной установки:
1—защита реактора ВВР-М; *2*—экспериментальный канал реактора; *3*—стационарная защита установки; *4*—подвижная защита детектора рассеянного пучка; *5*—детектор рассеянного пучка; *6*—монитор прямого пучка; *7*—ловушка; *8*—рассеиватель; *9*—камера рассеивателя; *10*—механический монохроматор; *11*—камера монохроматора; *12*—подвижная защита камер монохроматора и рассеивателя

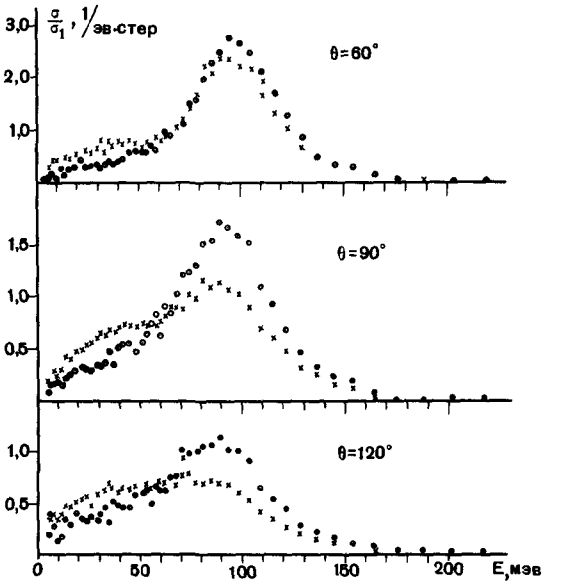

Рис. 2. Отношение дважды дифференциального сечения к сечению рассеяния на свободных атомах
$\sigma(E, E', \theta)-\sigma_f$ для H_2O и $C_{15}H_{16}$ $E=100$ *мэв*:
x—H_2O ($T=23°$ C), $R=18\%$; ●—$C_{15}H_{16}$ ($T=17°$ C) $R=18\%$

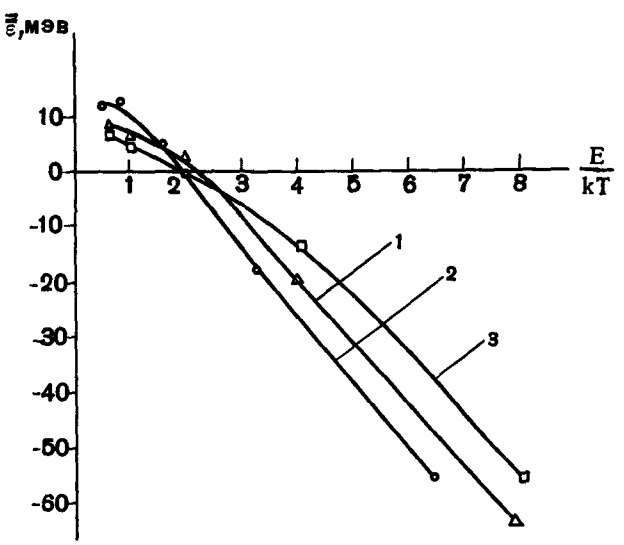

Рис. 3. Зависимость среднего изменения энергии при рассеянии от энергии падающих нейтронов:
1—H_2O, $T=23°$ C; *2*—H_2O, $T=90°$ C; *3*—$C_{15}H_{16}$, $T=17°$ C

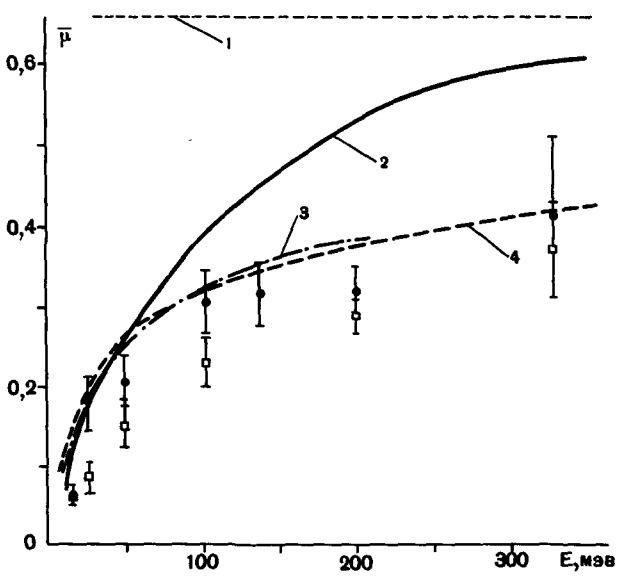

Рис. 4. Зависимость среднего косинуса угла рассеяния $\bar{\mu}$ от энергии падающих нейтронов E;
1—$\bar{\mu}(E)$ для покоящихся ядер с $M=1$; *2*—$\bar{\mu}(E)$ для газа[34] с $M_{эфф}=f(E)$; *3*—$\bar{\mu}(E)$, вычисленное в работе[7]; *4*—$\bar{\mu}(E)$, вычисленное по модели Нелкина[35]; ●—экспериментальные значения $\bar{\mu}(E)$ для H_2O ($T=296°$ K); □—экспериментальные значения $\bar{\mu}(E)$ для $C_{15}H_{16}$ ($T=290°$ K)

под углом θ, измерялась методом времени пролета с разрешением 10 ÷ 40 *мксек/м*. Рассеянные нейтроны регистрировались батареей BF_3-счетчиков, расположенной на пролетном расстоянии 2,74 *м*. Эффективные размеры детектора $30 \times 60 \times 10$ *см*. Установка позволяла вести измерения в следующих диапазонах изменения переменных:

$$E \text{ от } 5 \cdot 10^{-3} \text{ до } 0{,}5 \text{ эв},$$
$$E' \text{ от } 5 \cdot 10^{-3} \text{ до } 1{,}0 \text{ эв},$$
$$\theta \text{ от } 15 \text{ до } 120°.$$

Образцы, использованные в измерениях, рассеивали ~20% падающих нейтронов. Поправки к дважды дифференциальным сечениям на эффекты разрешения и многократного рассеяния не вводились, так как недостаточная точность и полнота экспериментальных данных не оправдывали соответствующей трудоемкой работы.

Результаты измерений

Характер изменения дважды дифференциального сечения $\sigma(E, E', \theta)$ иллюстрируется рис. 2.

Наряду с подобием в общих чертах дважды дифференциальные сечения рассеяния для воды и моноизопропилдифенила различаются в некоторых деталях, отражающих различие в динамике движения атомов водорода и молекул в этих жидкостях. По сравнению с водой величина пика квазиупругого рассеяния для моноизопропилдифенила больше, а ширина соответственно меньше почти для всех углов рассеяния и энергий нейтронов, падающих на образец. Эти данные могут свидетельствовать как о более жесткой связи водорода в моноизопропилдифениле, так и о меньшем коэффициенте диффузии молекул моноизопропилдифенила в жидкости. Последнее заключение является довольно естественным в связи со значительно большей массой молекулы $C_{15}H_{16}$ по сравнению с массой молекулы воды.

В области энергий неупругого рассеяния сечения для моноизопропилдифенила и воды близки по величине. Исключение составляет область $E - E' \simeq 60$ *мэв*, где отчетливо проявляется различие, связанное с возбуждением заторможенных вращений молекул воды.

По измеренным $\sigma(E, E', \theta)$ были вычислены среднее изменение энергии при рассеянии $\bar{\varepsilon}$ (рис. 3) и средний косинус угла рассеяния $\bar{\mu}$ (рис. 4). Видно, что термализующие свойства $C_{15}H_{16}$ несколько хуже, чем воды, а угловое распределение нейтронов при рассеянии более изотропно.

Данные, полученные для образца воды, нагретого до 90° С, показывают, что с повышением температуры пик квазиупругого рассеяния уширяется и уменьшается по амплитуде. Это можно качественно объяснить увеличением коэффициента диффузии и ослаблением межмолекулярных связей. С увеличением температуры увеличивается вероятность процессов рассеяния нейтронов с приобретением энергии.

Полная информация о полученных результатах измерений для воды и моноизопропилдифенила представлена в табл. 1 и 2 в виде закона рассеяния $S(\alpha, \beta)$, который отражает влияние характера связей и структуры самого замедлителя на сечение рассеяния [2]. Экспериментальные данные представлены также в виде обобщенных частотных спектров $P(\beta)$ (рис. 5), согласно Эгелстаффу и Скофилду [3, 4].

Обобщенный частотный спектр содержит в себе весьма ценную информацию о характере движения атомов в молекуле и молекул в жидкости. К сожалению, недостаточное разрешение и точность измерений не позволили выявить детальную структуру этих спектров. Однако даже довольно грубая картина обобщенного спектра, полученная для моноизопропилдифенила, указывает на его заметное отличие от вида спектра для воды. В воде при комнатной температуре вид обобщенного спектра определяется в основном взаимодействием нейтронов с заторможенным вращением молекул воды. Уровень заторможенного вращения довольно широкий и находится при энергии ~65 *мэв* (~2,5 β). С повышением температуры воды положение уровня смещается в сторону низких энергий, что качественно согласуется с результатами работ [5] и [6]. Физические причины температурного смещения уровня заторможенного вращения еще не изучены. Одной из возможных и естественных причин этого смещения может быть ослабление межмолекулярных связей при повышении температуры воды. Смещение уровня может быть также следствием более сложной его структуры, представляющей не только заторможенное вращение отдельной молекулы воды, но и другие виды движений [5].

В обобщенном частотном спектре моноизопропилдифенила, как видно из рис. 5, *в*, не наблюдается характерного для воды широкого уровня при $\beta \simeq 2{,}5$. В среднем энергия обобщенного частотного спектра в $C_{15}H_{16}$ меньше, чем в воде.

Полученный обобщенный частотный спектр $P(\beta)$ дает возможность вычислить $\sigma(E, E', \theta)$ для любых значений переменных. Такие вычисления проведены в работе [7] для воды при комнатной температуре. При вычислениях использовался вид спектра $P(\beta)$, приведенный на рис. 5, *а* и дополненный тремя дельта-функциями, отражающими известные внутримолекулярные колебания в воде. Результаты вычислений дважды дифференциальных сечений, а также средних характеристик рассеяния ($\bar{\mu}(E)$, ε, ε^2, $\bar{\xi}$) находятся в хорошем согласии с результатами данной работы.

Таблица 2. Закон рассеяния H_2O (T=23°C)

β	$S(\alpha,\beta)\times10^3$																						
0,25	α→	0,166	0,52	1,00	1,50																		
	S→	300±35	436±25	555 25	576 25																		
0,35		0,10	0,19	0,25	0,50	0,82	0,88	0,92	1,35	1,60	1,73	2,40	2,57										
		251 22	232 30	265 11	267 15	395 18	353 12	360 15	425 15	357 12	356 12	390 14	339 12										
0,45		0,12	0,23	0,28	0,48	0,85	0,89	1,15	1,65	1,72	2,45	2,54											
		140 15	184 50	223 12	236 30	250 20	247 12	220 40	275 9	304 12	290 9	304 12											
0,55		0,15	0,29	0,32	0,84	0,96	1,56	1,84	2,30	2,70													
		121 16	170 9	142 12	168 7	191 12	205 6	222 9	208 6	209 9													
0,65		0,17	0,20	0,35	0,44	0,50	0,80	1,04	1,43	1,68	1,95	2,10	2,76	2,87	3,30	4,10	4,90						
		78 11	135 23	141 10	112 7	128 5	110 8	142 12	148 6	165 4	159 10	139 9	161 7	167 12	162 2	129 6	154 4						
0,75		0,195	0,21	0,40	0,48	0,505	1,09	1,49	1,63	2,03	2,88	2,97	3,18	4,27	4,72								
		68 12	71 10	74 12	78 6	91 6	123 12	122 6	110 4	141 10	123 6	147 10	131 3	95 6	134 4								
0,85		0,22	0,435	0,52	1,15	1,60	2,12	3,08	4,56														
		64 10	45 12	66 5	104 10	85 4	127 8	112 2	122 4														
0,95		0,25	0,47	0,53	0,73	1,23	1,58	2,21	2,48	2,97	3,02	3,21	4,36	4,46	4,86	7,25							
		50 8	43 12	56 4	81 6	93 10	85 10	120 8	122 8	91 2	101 5	111 8	100 3	89 6	86 2	73 5							
1,10		0,31	0,56	0,59	0,80	0,99	1,32	1,68	1,53	2,36	2,60	2,82	3,17	3,48	4,15	4,06	4,90	6,88	7,50	10,28			
		51 8	50 4	62 5	59,3	76 4	77 6	77 4	55 3	82 5	114 3	73 2	76 4	84 4	83 2	71 9	69 2	60 2	64 2	46 2			
1,30		0,35	0,65	0,86	1,00	1,46	1,50	1,79	2,57	2,67	2,73	3,34	3,41	3,85	4,89	5,28	6,70	7,84	10,00				
		44 5	49 3	41 4	52 3	65 8	46 2	64 4	59 6	55 1	83 3	70·4	62 2	61 2	61 5	56 2	49 1	49 3	41 2				
1,50		0,40	0,73	0,80	0,91	1,02	1,48	1,56	1,92	2,40	2,71	2,83	3,33	3,40	3,53	3,86	5,14	5,45	6,48	8,06	9,62		
		39 5	45 4	34 5	39 4	36 3	30 3	47 8	52 4	43 2	55 6	72 3	46 2	50 2	58 4	63 6	51 4	49 2	45 1	44 3	38 1		
1,70		0,44	0,49	0,83	0,98	1,05	1,82	2,06	2,94	3,06	3,27	3,74											
		32 6	50 9	49 4	35 4	30 2	42 6	60 4	58 3	47 6	40 2	52 4											
1,90		0,50	0,59	0,94	1,04	1,08	1,97	2,23	3,06	3,20	3,26	3,98	4,55	5,73	5,80	6,10	8,55	8,99					
		37 5	29 9	42 4	32 3	24 2	34 6	44 4	53 3	33 2	39 6	42 4	42 5	38 3	37 2	34 1	34 3	30 1					
2,10		0,54	0,58	0,72	1,08	1,12	1,39	2,43	3,13	3,19	4,26	4,51	5,87	6,01	6,10	8,61	8,75	8,82	13,00				
		24 5	24 6	44 9	47 5	26 3	26 2	41 4	32 2	32 2	45 4	37 2	32 1	35 2	30 3	29 2	23 1	36 3	18 1				
2,30		0,60	0,66	1,15	1,18	1,21	1,42	2,14	3,08	3,33	3,49	4,44	4,84	5,68	6,22	8,28	8,55	9,12	12,67				
		15 6	32 5	28 9	27 2	20 4	25 2	42 6	32 2	45 2	42 5	33 26	52 5	31 1	29 2	28 1	18 1	32 2	16 2				
2,50		0,66	0,76	0,86	1,25	1,31	1,45	2,35	2,65	3,04	3,48	3,76	4,37	4,58	5,17	5,48	6,48	7,90	8,34	9,43	12,3		
		23 4	37 5	37 9	35 10	22 4	23 2	43 5	43 3	30 2	34 3	43 5	29 2	35 3	36 5	28 1	29 4	26 1	18 1	23 3	12 3		
2,70		0,72	0,90	1,36	1,42	1,49	1,99	2,59	3,01	3,66	4,07	4,31	5,27	5,55	6,62	6,71	7,53	8,17	9,77	12,0	12,95	19,3	
		16 3	35 5	26 2	21 4	19 2	20 1	25 5	29 2	29 3	33 5	27 3	26 1	42 5	17 1	24 2	26 1	18 1	27 3	14 2	11 1	7 1	
2,90		0,78	1,05	1,44	1,47	1,53	2,82	3,00	4,26	4,94	5,07	6,96	7,15	8,00	11,7								
		27 5	28 4	36 4	22 2	18 2	27 3	24 2	25 2	34 3	23 1	21 3	21 1	16 1	15 1								
3,10		0,79	0,89	1,54	1,60	1,63	1,83	2,03	2,97	3,00	3,85	4,20	4,42	4,88	5,97	6,55	6,70	6,99	7,75	10,13	11,3	12,73	18,91
		13 3	16 4	26 5	16 2	20 2	13 8	12 1	25 6	21 2	29 3	24 2	25 5	20 1	30 5	15 1	22 1	20 2	16 1	19 2	15 1	10 1	6 1
3,30		0,84	1,00	1,26	1,67	2,07	3,03	3,24	3,31	4,05	4,15	4,68	5,37	6,30	6,47	7,29	7,50	7,54	10,9	10,53	11,69	12,48	18,49	23,14	34,59
		7 3	16 5	37 10	21 2	12 1	20 2	24 2	12 1	24 3	23 1	18 1	22 3	20 1	12 1	18 2	20 3	15 1	15 1	21 2	5,9 0,4	8,8 0,5	6,6 0,7	2,5 0,2	1,0 0,2
3,50		0,93	1,08	1,73	2,05	2,10	3,08	4,12	4,48	5,90	6,37	7,38	10,60	12,21	18,0										
		11 2	16 5	16 1	19 4	9,7 1,0	17 3	15 1	19 1	11 1	13 1	14 1	14 2	8 1	5 1										
3,70		0,99	1,23	1,52	1,84	1,97	2,13	3,62	4,10	4,29	5,87	6,30	7,16	7,62	8,12	10,2	11,0	12,0	17,7						
		64 2	24 5	39 10	12 1	25 5	9 1	23 3	20 1	22 4	25 4	12 1	13 1	14 1	11 3	14 1	13 2	8 1	5 1						
3,90		1,39	1,97	4,08	6,95	9,82																	
		9 5	11 2	16 2	12 1	12 1																	
4,20		1,16	1,66	2,18	2,24	3,33	4,08	4,54	6,20	6,06	7,98	9,25	11,4	11,4	11,6	17,0	22,4	33,4					
		9 2	10 5	10 2	6 1	7 1	10 1	12 4	8 1	9 1	13 2	10 1	5 1	9 2	7 1	5 1	2,3 0,2	1,1 0,2					
4,60		1,33	2,35	3,36	4,83	6,08	8,38	11,1	11,2	11,9	16,3	21,7	32,3										
		6,1 1,7	6,2 0,7	4,8 0,6	14 4	8,5 0,6	9,0 2,0	3,6 0,2	6,6 0,3	7,2 2,1	4,5 0,3	2,0 0,1	1,0 0,1										
5,00		1,58	2,50	5,15	6,02	8,82	10,8	12,5	15,5														
		5,9 1,3	4,8 0,5	11 5	5,9 0,4	9 2	4,9 0,2	10 2	4,2 0,2														
5,40		1,83	2,73	3,43	5,95	10,3	10,9	14,8	21,1	31,3													
		5,6 1,3	5,1 1,6	3,1 0,6	4,2 0,5	4,3 0,2	2,8 0,2	3,6 0,2	1,5 0,1	1,0 0,1													
5,80		2,17	2,98	3,50	5,92	9,90	10,7	14,0	20,6	30,4													
		4,0 1,0	3,7 0,5	2,3 0,4	3,2 0,4	3,6 0,2	1,9 0,2	3,5 0,2	1,3 0,1	0,7 0,1													
6,20		2,62	3,60	5,95	9,50	10,6	13,1	20,1	29,6														
		4,3 1,0	1,6 0,4	3,2 0,4	2,8 0,2	1,5 0,2	3,0 0,2	1,0 0,1	0,8 0,1														
6,60		3,05	3,69	6,00	9,15	10,4	12,3	19,6	28,8														
		5,0 1,3	0,7 0,3	2,5 0,4	2,4 0,2	1,5 0,1	2,1 0,2	0,9 0,1	0,5 0,1														
7,00		3,78	6,17	8,73	11,6																		
		3,9 0,2	3,0 0,5	2,1 0,3	1,9 0,3																		
7,40	α→	3,85	10,3	19,1	27,9																		
	$S\times10^5$	69±2	10,6 7	69 5	53 6																		
7,80		4,02	10,16	18,55	26,94																		
		79,1 30	99,5 10	68,9 6	41,5 7																		
8,50		4,26	10,05	17,97	25,89																		
		46 13	82 5	50,3 3	34,3 3																		
9,50		4,85	9,94	16,88	23,83																		
		61,3 10	51,4 4	35,1 2	28 2																		
10,50		5,62	9,96	15,89	21,82																		
		35,7 7	39,6 3	27,4 2	22,3 2																		
11,50		6,89	10,25	14,84	19,45																		
		27 7	30,7 3	20 1	21 2																		

Таблица 1. Закон рассеяния H_2O ($T = 23°$ C)

β	$S(\alpha, \beta) \times 10^3$																													
0,25	α → 0,064	0,164	0,322	0,529	1,057	1,525																								
	S → 253±21	312 12	321 11	478 11	530 11	546 12																								
0,35	0,088	0,095	0,098	0,184	0,248	0,265	0,322	0,495	0,501	0,537	0,822	0,890	0,933	1,365	1,609	1,743	2,396	2,597												
	218 16	237 16	256 38	179 17	242 15	265 11	219 15	291 13	259 15	338 12	307 12	386 12	313 14	113 16	348 13	382 12	350 13	419 13												
0,45	0,113	0,116	0,214	0,276	0,279	0,339	0,484	0,529	0,542	0,853	0,858	0,881	1,222	1,652	1,715	2,447	2,945													
	158 16	139 15	106 26	177 10	175 10	164 23	207 21	226 10	213 10	202 20	257 10	248 11	252 25	279 10	252 11	312 11	247 11													
0,55	0,147	0,150	0,295	0,322	0,526	0,801	0,828	0,963	1,553	1,840	2,279	2,717																		
	115 14	91,5 14,2	110 9	124 9	146 8	151 9	168 8	164 9	204 8	193 9	234 10	210 10																		
0,65	0,171	0,175	0,181	0,207	0,334	0,364	0,439	0,497	0,536	0,656	0,799	0,865	1,035	1,420	1,447	1,677	1,951	2,072	2,760	2,867	1,010	3,289	4,100	4,900						
	103 10	92,3 7,6	79,6 18	46,9 18	67 10	99 11	90 7	121 6	117 10	122 11	100 9	122 7	132 10	118 7	136 9	151 6	172 11	138 10	125 8	158 12	147 6	164 6	122 8	151 6						
0,75	0,196	0,209	0,212	0,270	0,382	0,397	0,479	0,505	0,559	0,697	0,789	0,920	0,996	1,087	1,346	1,494	1,635	1,903	2,029	2,880	2,971	3,179	4,266	4,723						
	67,3 8,1	122 18	107 10	11,5 47,5	60 12	99 10	78,1 6,7	73,7 5,3	98 11	106 10	99 11	95 7	93,1 5,5	100 9	95,0 9	96,2 6,6	115 6	123 12	122 10	92,4 6,4	117 10	128 6	100 7	134 7						
0,85	0,222	0,241	0,435	0,435	0,519	0,591	0,745	0,790	0,989	1,147	1,273	1,602	1,755	2,109	3,083	3,091	4,564													
	50,2 8,2	80 16	74,8 9,4	69 22	46,0 5,0	119 20	82,9 8,6	70,8 18	82,7 5,9	99,1 8,9	121 18	85,2 5,8	97 21	95,6 8,6	108 6	95,6 9,1	107 7													
0,95	0,242	0,251	0,259	0,273	0,474	0,529	0,539	0,729	0,793	0,986	0,987	1,208	1,488	1,567	1,582	2,211	2,476	2,971	3,020	3,214	4,375	4,458	4,863	7,250						
	55,5 9,3	55,4 8,4	50,9 9,4	71 15	76,2 9,2	67,1 6,3	54,2 5,8	81,9 6,7	77,1 8,2	64,1 6,6	76,4 6,0	71,9 7,7	83,2 6,7	83,5 6,6	71,6 5,9	90,7 8,2	97,5 7,5	83,0 6,9	80,5 5,8	104 9	89,7 7,8	92,4 6,1	89,7 7,1	75,6 7,1						
1,10	0,286	0,295	0,310	0,315	0,341	0,557	0,575	0,585	0,789	0,888	0,990	0,990	1,058	1,275	1,530	1,573	1,677	2,070	2,380	2,595	2,835	3,169	3,437	3,480	4,139	4,661	5,064	6,280	7,532	10,28
	42,2 8,4	48,1 6,0	52,5 4,9	38,3 6,1	55,4 10,2	60,6 5,7	48,8 4,0	60,7 5,8	64,6 4,6	58,7 5,2	45,3 4,6	63,1 3,6	52,1 5,2	61,6 5,1	72 4	56,9 4,3	60,7 5,2	79,0 3,8	80,3 5,2	77,8 4,6	79,9 4,2	63,8 5,2	89,0 5,9	80,7 3,4	76,1 4,5	65,6 5,5	77,1 4,4	67,2 3,4	61,6 4,4	55,1 3,4
1,30	0,344	0,348	0,350	0,411	0,423	0,643	0,645	0,655	0,859	0,999	1,000	1,014	1,148	1,459	1,496	1,671	1,790	2,110	2,571	2,660	2,729	3,341	3,370	3,683	3,824	4,892	5,284	6,710	7,839	10,00
	45,1 8,2	19,6 7,9	23,0 3,2	24,8 6,4	43,4 13	43,7 3,9	51,7 7,5	39,5 5,4	44,2 5,6	68,4 7,3	40,4 2,3	41,4 3,6	53,2 5,0	50,9 6,5	54 4	38,0 5,4	48,9 4,8	62,8 2,5	65,1 6,6	52,8 3,7	49,2 5,7	59,6 4,8	54,7 2,4	13,4 7,5	51,6 4,4	65,6 5,2	46,7 5,6	56,9 2,3	43,7 5,6	47,3 2,2
1,50	0,390	0,391	0,413	0,523	0,760	0,735	0,758	0,914	1,020	1,072	1,131	1,244	1,479	1,617	1,746	1,916	2,030	2,461	2,790	2,829	3,330	3,443	3,529	3,963	5,142	5,445	6,480	8,061	9,640	
	14,7 3,1	23,1 7,7	42,2 8,0	58,5 9,0	31,9 5,4	42,2 5,0	38,7 4,7	29,5 4,6	30,4 2,2	34,4 5,3	40,8 4,3	46,5 4,8	41,9 5,1	49,3 4,3	38 5	38,5 4,4	38,3 2,1	46,9 5,1	61,7 4,4	46,6 5,1	43,4 2,2	57,1 6,3	47,1 4,4	49,1 4,6	49,8 4,9	53,3 5,4	41,7 2,1	39,4 5,4	33,9 2,1	
1,70	0,440	0,438	0,493	0,656	0,829	0,904	0,975	1,050	1,300	1,361	1,815	1,827	2,010	2,059	2,937	3,059	3,270	3,739	4,403	5,419	5,618	6,300	8,299	9,340						
	11,2 3,2	21,6 6,4	37,2 7,8	22 11	27,4 4,6	27,0 6,0	26,3 4,9	23,6 2,0	44,0 5,9	33,3 4,4	36,5 5,5	28,4 4,9	30,3 2,0	32,0 4,1	37 5	38,4 5,3	31,6 2,0	38,1 4,1	53,1 6,2	31,6 4,6	37,7 4,9	32,5 2,0	25,4 5,3	30,2 2,0						
1,90	0,495	0,500	0,592	0,759	0,943	1,018	1,044	1,080	1,429	1,500	-1,918	1,965	2,000	2,226	3,056	3,200	3,259	3,979	4,553	5,732	5,804	6,090	8,552	8,990						
	17,2 7,7	10,1 2,4	30,1 7,6	24 11	20,2 4,3	16,1 5,8	31,0 5,1	16,4 1,6	18,9 5,1	25,4 4,0	26,3 4,7	21,0 4,7	24,1 1,5	22,3 3,7	32 4	25,9 1,5	24,3 4,7	29,9 3,7	31,3 5,4	34,2 4,4	32,3 4,4	27,9 1,5	24,9 5,1	25,7 1,6						
2,10	0,559	0,580	0,715	1,082	1,129	1,122	1,665	2,000	2,019	2,425	3,130	3,186	4,260	5,870	6,005	6,095	8,610	8,824												
	19 8	15 3	38 7	29 4	18 2	19,3 4,9	21,4 3,9	20,6 1,9	25,4 4,6	24,6 3,7	23,7 1,9	22,8 4,0	21,1 3,5	19,2 1,7	24,4	22,3 4,0	24,2 2,0	19,8 5,1												
2,30	0,660	0,881	1,151	1,190	1,581	2,000	2,140	3,090	3,491	4,842	5,680	8,290																		
	5,6 2,5	54 11	17,9 5,6	14,4 1,4	15,9 5,0	17,5 1,4	22,6 4,7	19,4 1,3	20,4 4,4	36,7 5,5	21,3 1,4	18,6 1,6																		
2,50	0,770	0,861	1,080	1,246	1,250	1,313	1,762	1,858	2,030	2,347	2,654	3,040	3,760	4,578	5,173	5,480	6,502	7,920												
	6,0 2,6	19,2 7,5	37,7 1,1	13,6 4,2	9,7 1,5	10,8 5,3	24,8 5,3	21,3 3,9	13,2 1,4	20,6 4,5	23,6 3,7	14,0 1,4	21,6 4,5	16,4 3,3	13 5	16,1 1,3	15,0 3,6	19,1 1,6												
2,70	0,720	0,900	1,990	2,070	3,010	4,000	5,280	6,620	7,530	12,95	19,28																			
	12,9 2,1	6,6 2,4	17,3 1,3	10,4 1,2	12,1 1,1	13,1 1,2	11,6 1,2	14,9 1,4	11,8 1,0	11,8 1,0	10,1 1,0																			
2,90	1,035	1,050	1,440	2,082	2,130	2,219	3,000	4,940	5,070	6,961	7,150																			
	16,5 7,7	9,7 2,7	2,6 4,1	19,4 3,7	10,5 1,3	17,6 3,6	10,8 1,1	13,7 3,2	10,9 1,1	20,0 3,7	13,0 1,3																			
3,10	0,790	1,250	2,030	2,230	3,000	3,990	4,880	6,550	6,750	12,73	18,91																			
	6,3 1,9	8,1 3,0	13,9 1,3	10,0 1,5	13,1 1,3	10,5 1,1	11,1 1,2	11,2 1,1	12,6 1,5	8,1 1,0	6,0 1,0																			
3,30	0,840	1,020	2,070	2,350	3,030	3,310	3,980	4,670	6,310	6,470	6,950	11,69	12,48	18,49	23,14	34,59														
	7,9 1,7	12,8 1,9	13,2 1,1	13,1 1,6	9,8 1,5	13,8 1,0	8,2 1,0	9,6 1,2	13,2 1,5	8,2 1,0	10,7 0,8	5,1 0,6	7,3 0,9	5,7 0,9	2,8 0,5	2,5 0,6														
3,50	0,930	2,100	2,500	3,080	3,950	4,490	5,890	6,370	12,21	18,05																				
	5,0 1,6	10,9 1,0	11,3 2,3	7,7 1,7	5,4 0,9	6,9 1,7	10,9 2,3	8,4 0,9	8,7 0,9	6,3 0,9																				
3,70	0,990	2,130	3,940	6,300	12,00	17,70																								
	10,5 1,6	5,3 1,0	7,2 0,9	6,7 0,9	8,0 0,8	4,8 0,9																								
3,90	1,080	2,190	3,960	6,260	11,82	17,38																								
	4,7 1,7	6,2 1,0	5,2 0,9	5,6 0,9	4,4 0,8	5,4 0,9																								
4,20	1,130	1,200	2,270	3,330	3,960	6,180	6,830	11,38	11,53	16,87	22,38	33,38																		
	7,9 1,4	7,2 1,2	3,4 0,7	7,7 0,7	5,3 0,6	4,2 0,6	7,4 0,6	3,6 0,4	5,1 0,5	3,2 0,6	1,7 0,4	1,5 0,4																		
4,60	1,240	1,330	2,350	3,360	3,970	6,090	6,730	11,11	11,18	16,29	21,70	32,29																		
	4,4 1,1	4,3 1,1	4,3 0,6	4,5 0,6	4,3 0,6	4,0 0,6	4,6 0,4	3,0 0,4	4,5 0,5	4,1 0,6	1,0 0,3	1,6 0,4																		
5,00	1,570	2,520	4,040	6,020	10,78	15,55																								
	2,4 0,8	3,7 0,5	2,7 0,4	3,3 0,4	4,3 0,4	3,7 0,4																								
5,40	1,380	1,830	2,710	3,430	4,120	5,950	6,670	10,38	10,90	14,81	21,11	31,32																		
	3,5 0,9	3,9 0,9	3,7 0,5	2,6 0,5	2,6 0,5	2,9 0,4	3,4 0,4	3,2 0,4	1,6 0,3	3,2 0,4	0,9 0,2	0,9 0,3																		
5,80	1,530	2,980	3,500	4,260	5,920	6,630	9,950	10,71	13,97	20,65	30,41																			
	1,7 0,8	2,7 0,4	2,0 0,4	2,2 0,4	2,9 0,3	2,8 0,3	3,2 0,3	1,1 0,2	2,2 0,3	0,9 0,2	1,0 0,2																			
6,20	1,690	3,330	3,600	4,480	5,940	6,620	9,510	10,56	13,08	20,08	29,60																			
	2,0 0,7	2,7 0,5	1,8 0,3	1,5 0,4	2,7 0,4	1,7 0,2	2,2 0,3	0,9 0,2	2,1 0,4	0,6 0,2	0,9 0,2																			
6,60	3,700	4,710	6,010	9,160	12,32																									
	2,0 0,5	1,4 0,4	1,9 0,4	2,0 0,4	2,5 0,4																									
7,00	1,950	3,690	4,160	5,020	6,130	6,620	8,820	10,43	11,51	19,64	28,85																			
	2,0 0,6	1,3 0,6	1,1 0,3	2,7 0,5	2,0 0,4	1,3 0,2	2,7 0,4	0,6 0,2	1,6 0,4	0,7 0,2	0,8 0,2																			
7,40	2,090	3,850	4,540	5,280	6,250	6,640	8,590	10,28	10,93	19,06	27,85																			
	1,0 0,4	1,4 0,2	3,2 1,0	0,6 0,9	1,3 0,8	1,1 0,1	3,2 0,8	0,6 0,1	1,9 0,8	0,6 0,1	0,6 0,1																			
7,80	2,340	4,020	6,690	10,16	18,55	26,94																								
	1,1 0,5	1,1 0,2	0,8 0,2	0,4 0,1	0,8 0,1	0,6 0,2																								
8,50	2,750	4,320	6,800	10,04	17,86	25,54																								
	0,7 0,2	0,7 0,1	0,8 0,1	0,2 0,1	0,5 0,1	0,5 0,1																								
9,50	3,450	4,850	7,060	9,940	16,89	23,85																								
	0,7 0,2	0,4 0,1	0,4 0,1	0,20 0,04	0,26 0,04	0,33 0,05																								
10,5	4,440	5,620	7,510	9,970	15,91	21,85																								
	0,5 0,1	0,4 0,1	0,23 0,03	0,18 0,03	0,15 0,03	0,22 0,04																								
11,5	5,860	6,790	8,280	10,23	14,90	19,57																								
	0,4 0,1	0,29 0,04	0,14 0,03	0,14 0,03	0,16 0,03	0,23 0,03																								

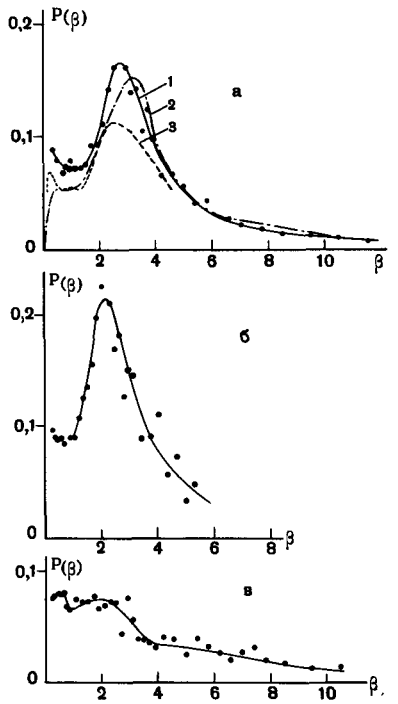

Рис. 5. *а* — спектры P (β) H_2O при $T=23°$ С: *1* — результат данной работы; *2* — измерения Эгелстаффа, Хейвуда и Торсона[5], Коттвица и Леонарда[33]; *3* — измерения Ларссона и Далборга[6]; *б* — спектр P (β) H_2O при $T=90°$ С; *в* — спектр P (β) $C_{15}H_{16}$ при $T=17°$ З

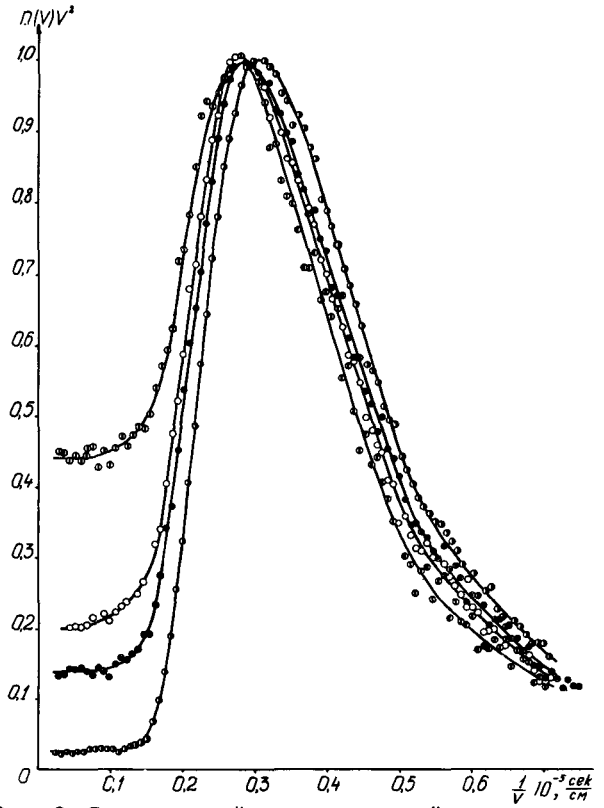

Рис. 6. Спектры нейтронов в чистой воде и воде, отравленной бором:

① — поглощение 4,83 $\frac{барн}{атом\ H}$; ○ — поглощение 2,25 $\frac{барн}{атом\ H}$; ⊙ — поглощение 1,50 $\frac{барн}{атом\ H}$; ◑ — поглощение 0,33 $\frac{барн}{атом\ H}$

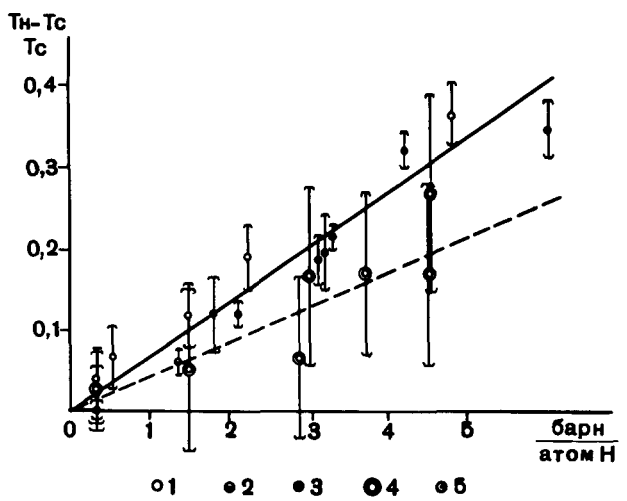

Рис. 7. Зависимость превышения температуры нейтронов над температурой среды от концентрации поглотителя:

○ — результаты данной работы; ◑ — результаты работы [12]; ◒ — результаты работы [15]; ⊙ — результаты работы [11]; ● — результаты работы [14]

ИЗМЕРЕНИЕ СТАЦИОНАРНЫХ СПЕКТРОВ НЕЙТРОНОВ В ЗАМЕДЛЯЮЩИХ И РАЗМНОЖАЮЩИХ СРЕДАХ

Методика измерений

Использованная методика измерений спектров нейтронов была подробно описана в работах [8, 9]. Она основана на выводе из изучаемой системы пучков нейтронов и измерении их спектра методом времени пролета с помощью механического прерывателя. Спектры нейтронов исследовались в воде с бором и в подкритических гетерогенных средах с блоками из естественного урана. В гетерогенных системах пучки выводились параллельно оси урановых блоков. Необходимая плотность нейтронов в изучаемых системах создавалась за счет облучения их широким пучком тепловых или быстрых (конвертированных из тепловых) нейтронов реактора ВВР-2.

Измеряемые спектры являлись спектрами векторного потока нейтронов в направлении

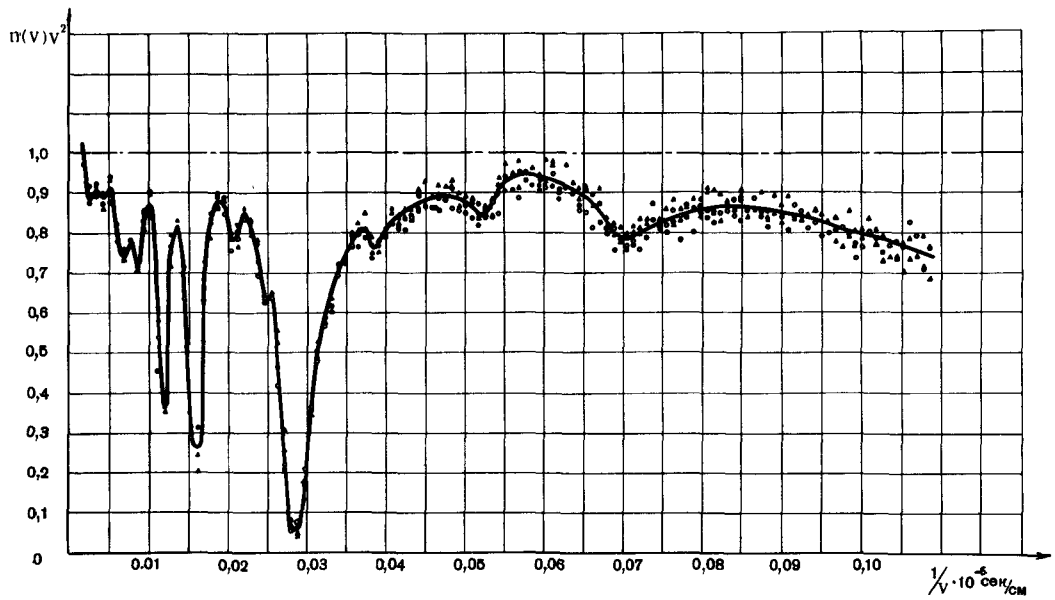

Рис. 8. Спектр замедляющихся нейтронов в уране уран-водной решетки с шагом 5,5 *см*

выведенного пучка. Этих измерений, вообще, недостаточно для получения наиболее интересного в практическом отношении спектра скалярного потока. Однако данные по спектрам нейтронов векторного потока, полученные в гомогенной среде для одного направления, позволяют легко вычислить в диффузионном приближении спектр скалярного потока.

Результаты измерений

а) Спектры нейтронов в чистой воде и воде, отравленной бором

На рис. 6 приведены спектры нейтронов, измеренные в чистой воде и воде, отравленной бором (бак размером $60 \times 60 \times 50$ *см*), на расстоянии 10,4 *см* от источника быстрых нейтронов. С увеличением концентрации бора происходит ужестчение спектра: максимум распределения тепловых нейтронов смещается в область больших энергий и его величина уменьшается по сравнению с потоком замедляющихся нейтронов.

Расчеты спектров нейтронов в воде, отравленной бором, с концентрациями, использованными в настоящем эксперименте, были проведены Марчуком и др. [10] с учетом химической связи водорода в воде и Лалетиным по газовой модели с массой, равной единице. Лучшее согласие с экспериментом дает расчет, учитывающий более реальную картину обмена энергией между нейтроном и замедлителем.

К настоящему времени выполнено много экспериментальных работ по изучению спектров нейтронов в чистой воде и воде, отравленной различными поглотителями [11-16]. Так как условия экспериментов в этих работах не совпадали по температурам и концентрациям, то одной из возможностей сравнения результатов различных работ является сравнение зависимости относительного превышения температуры нейтронного газа от концентрации поглотителя (рис. 7). На этом рисунке приведена хорошо известная зависимость

$$\frac{T_н - T_c}{T_c} = A\frac{\Sigma_a}{\xi\Sigma_s}$$

с коэффициентами $A = 1{,}84$ согласно модели газообразного замедлителя [17] и $A = 2{,}92$ согласно работе [10]. Хотя экспериментальные точки и имеют значительный разброс, однако видно, что значение коэффициента A, даваемое в работе [10], лучше согласуется с экспериментом.

б) Спектры нейтронов в уран-водных решетках

Были исследованы подкритические гетерогенные уран-водные системы, имеющие треугольную решетку с шагами 5,0; 5,5 и 6,0 *см*, и подкритическая гетерогенная система уранмоноизопропилдифенил с шагом 5,5 *см*. В решетках применялись блоки из естественного урана диаметром 3,5 *см*.

Результаты проведенных экспериментов были опубликованы ранее [8, 18]. Поэтому здесь приведем только основные выводы из этих экспериментов, которые сводятся к следующему. Спектр тепловых нейтронов в ячейке решетки как в горючем, так и в замедлителе заметно отличается от равновесного максвелловского распределения. В замедлителе спектр нейтронов может быть лишь приблизительно представлен максвелловским распределением, но с «температурой», значительно превышающей температуру среды. Основным фактором, определяющим спектр тепловых нейтронов в блоке,

является поглощение падающих из воды нейтронов. Как в горючем, так и в замедлителе спектр нейтронов мало меняется с пространственной координатой, и только на границе между горючим и замедлителем происходит резкое изменение спектра.

Спектр замедляющихся нейтронов в урановом блоке имеет ярко выраженную резонансную структуру, обусловленную поглощением нейтронов на уровнях U^{238} и U^{235}. На рис. 8 приведен спектр нейтронов в уране, измеренный с разрешением 1,2 *мксек/м* в решетке с шагом 5,5 *см* в области энергий выше 0,2 *эв*. Истинная форма спектра в области энергий выше 20 *эв* значительно искажена недостаточным разрешением селектора. Спектр в этой области в принципе может быть восстановлен с помощью метода, предложенного Тихоновым [19].

Заметим, что, вычисляя площадь между кривыми спектров в уране и замедлителе, можно получить величину резонансного поглощения нейтронов в блоке. Эта величина может быть получена для любого энергетического интервала. Спектр замедляющихся нейтронов в воде, измеренный с тем же разрешением, близок к спектру $1/E$ (рис. 9).

Результаты измерений спектров тепловых нейтронов в решетке уран-моноизопропилдифенил с шагом 5,5 *см* показывают, что основные закономерности пространственно-энергетического распределения нейтронов в решетке уран-моноизопропилдифенил те же, что и в уран-водных решетках. По своим термализующим свойствам моноизопропилдифенил мало отличается от воды. Решетка уран-моноизопропилдифенил эквивалентна водной решетке с меньшим шагом. Изучение температурной зависимости спектров нейтронов в решетке уран-моноизопропилдифенил позволяет сделать заключение, что замедляющая способность моноизопропилдифенила слабо меняется с температурой. Характер изменения спектра нейтронов в воде в зависимости от концентрации урана для изученных уран-водных решеток иллюстрируется качественно на рис. 10.

Спектры нейтронов в уран-водных решетках вычислялись рядом авторов на основе различных модельных представлений о характере обмена энергией между нейтроном и молекулой воды. Собрино и Кларк [20] произвели вычисление пространственно-энергетического распределения нейтронов на основе уравнения Вилкинса с учетом утечки $1/v$. Их расчет находится в хорошем согласии с результатами, полученными нами для уран-водной решетки с шагом 5,0 *см*. Хонек и Такахаши в работе [21] вычислили спектры векторного потока нейтронов в различных решетках. Расчеты недостаточно хорошо согласуются как с работой [22], так и с нашими измерениями для решеток с шагами 5 и 6 *см*.

В последнее время Марчуком, Смеловым и Илясовой [23] произведен расчет спектров векторного потока нейтронов в уран-водной решетке с шагом 5,5 *см*. Спектры нейтронов вычислялись в P_3-приближении с помощью функции рассеяния, предложенной Ван Хове. Дисперсия автокорреляционной функции получена на основе интерполяционных формул Турчина. Наблюдается хорошее согласие между расчетом и экспериментом для спектра в воде на границе ячейки [18]. Спектры нейтронов в воде на границе ячейки согласно расчетам практически не обнаруживают угловой анизотропии. В блоке спектры нейтронов векторного потока, вычисленные в параллельном и перпендикулярном оси блока направлениях, значительно различаются (рис. 11). Экспериментальные точки лежат между спектром, вычисленным в параллельном направлении, и спектром скалярного потока, ближе к последнему.

В работе Кемпбелла и др. [22] изучались спектры нейтронов в пучках, выведенных из уранового блока и воды в направлениях, параллельных и перпендикулярных оси блока. Была обнаружена сильная анизотропия спектра нейтронов как в блоке, так и в воде. Следует отметить, что результаты расчетов [23] дают значительно меньшую величину анизотропии спектра в блоке и практически не показывают анизотропии спектра в замедлителе для исследованных решеток.

в) Уран-графитовая решетка

Спектры нейтронов исследовались в ячейке подкритической уран-графитовой решетки типа Колдер Холл при различных температурах графита (шаг решетки 20 *см*, диаметр блоков из естественного урана 3,5 *см*). Подкритическая сборка имела размер 120 × 120 × 120 *см*. Урановые блоки, покрытые алюминием, находились в специальных каналах и изолировались от графита воздушным зазором. Объемные концентрации урана, графита, алюминия и воздуха составляли соответственно 0,096; 0,834; 0,021; 0,049. Нагрев сборки осуществлялся за счет ядерной мощности и электрических нагревателей, расположенных по боковым граням сборки. Различие между температурой графита в разных точках сборки было не более 20°, а в области измеряемой ячейки не более 10°.

Основные измерения спектров нейтронов были выполнены при температурах графита 523 и 613° К с разрешением 20 *мксек/м*. В качестве примера на рис. 12 и 13 приведены результаты измерений спектров нейтронов в центре блока и в графите на границе ячейки при температуре графита 613° К. На этих же рисунках приведены результаты расчетов, выполненных в работе [23]. Видно, что рассчитанный спектр удовлетворительно совпадает с экспериментальным. Анизотропия спектров в графите на границе ячейки по расчетам ничтожная, соответствующие спектры векторных потоков

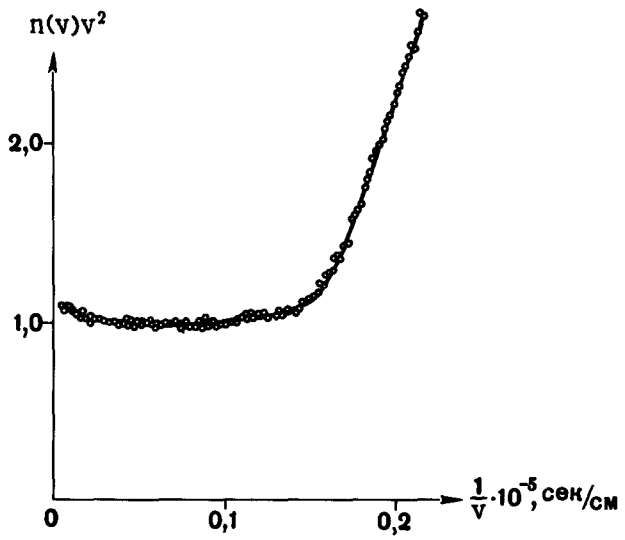

Рис. 9. Спектр замедляющихся нейтронов в воде уран-водной решетки с шагом 5,5 *см*

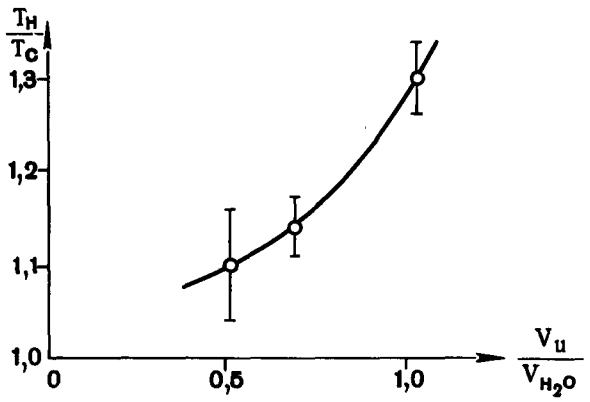

Рис. 10. Зависимость температуры нейтронов в воде уран-водных решеток от концентрации урана

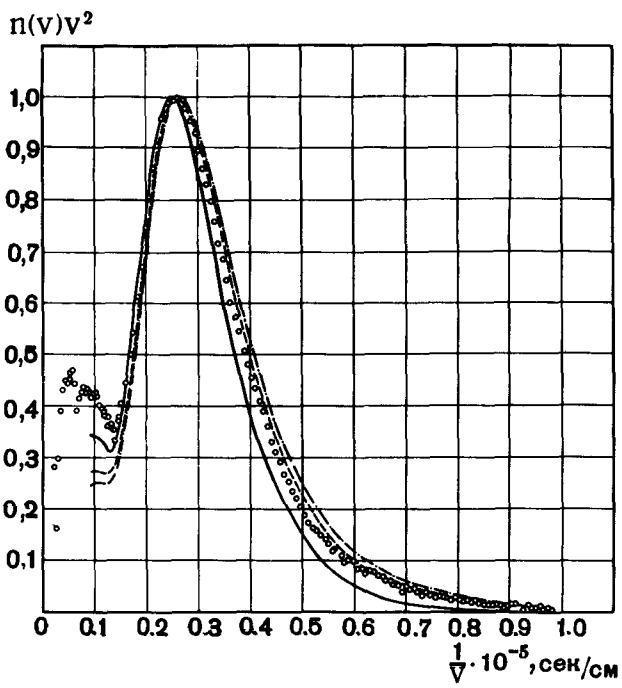

Рис. 11. Спектр нейтронов в уране уран-водной решетки с шагом 5,5 *см*; температура воды 323° К:
——спектр потока нейтронов в направлении оси блока; —·—спектр потока нейтронов в направлении, перпендикулярном оси блока; — — —спектр скалярного потока

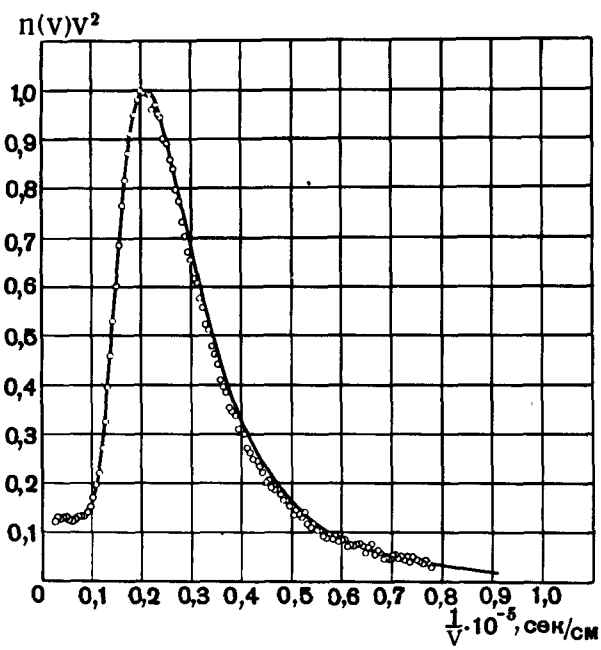

Рис. 12. Спектр нейтронов в графите на границе ячейки уран-графитовой решетки; температура графита 613° К:
○ — эксперимент; — расчет

в других направлениях совпадают с приведенной на рисунках кривой. В блоке анизотропия спектра значительна (рис. 13). Спектр нейтронов, вычисленный в направлении, параллельном оси уранового блока совпадает с измеренным спектром.

На рис. 14 приведена зависимость «температуры» нейтронов по ячейке. «Температуры» нейтронов, приведенные на рисунке, вычислялись из средней скорости, средней обратной скорости и наиболее вероятной скорости v_m в распределении $v^2 \cdot n(v)$ по формулам, связывающим эти величины и температуру для максвелловского распределения. Несовпадение «температур» по абсолютной величине связано с немаксвелловским характером спектра нейтронов в области усреднения 0,44—0,0086 *эв*. Спектр нейтронов в замедлителе, как и в случае уран-водной решетки, мало изменяется с координатой. В уране спектр нейтронов измерялся только в центре блока; однако можно полагать, что он так же, как и в случае уран-водной решетки, слабо изменяется по радиусу блока.

Спектры нейтронов в уран-графитовой решетке измерялись также Коутсом и Гейзером [24]. Решетка имела такой же шаг, как и использованная нами решетка, но отличалась диаметром блоков (2,95 *см*) и величиной воздушных зазоров вокруг блоков. В цитированной работе Коутса и Гейзера приводятся результаты измерений спектра нейтронов только в графите посередине между блоками при различных температурах графита.

ЭКСПЕРИМЕНТАЛЬНОЕ ИЗУЧЕНИЕ ПРОЦЕССА УСТАНОВЛЕНИЯ РАВНОВЕСНОГО ЭНЕРГЕТИЧЕСКОГО СПЕКТРА НЕЙТРОНОВ ВО ВРЕМЕНИ

Как известно, эффект химической связи заметно влияет на форму стационарного спектра тепловых нейтронов только при наличии достаточно сильного поглощения. Однако отравление системы (введение поглотителя) во многих случаях практически трудно осуществимо и связано со значительной потерей интенсивности измеряемого потока нейтронов. Изучение временного процесса установления равновесного спектра в чистом замедлителе позволяет получить не менее полную информацию о роли химической связи при термализации, чем в измерениях стационарных спектров. Однако при этом не требуется отравления системы. Следует отметить, что эти исследования, кроме того, непосредственно дают важные параметры, характеризующие процесс установления равновесного спектра во времени. Одним из таких параметров является время, необходимое для установления энергетического равновесия нейтронов со средой. До настоящего времени эксперименты по изучению нестационарных спектров нейтронов ограничивались работой Бернарда и др. [25]

Методика измерений

На рис. 15 изображено экспериментальное устройство, на котором проводится изучение процесса термализации нейтронов во времени. Пучок электронов из линейного ускорителя [26] с помощью магнитной системы отклоняется и фокусируется на свинцовую мишень, помещенную внутрь исследуемого замедлителя, создавая короткие вспышки быстрых нейтронов. Из замедлителя (через полость размером 10 × × 1 *см*) выводится пучок нейтронов и исследуется их энергетический спектр в различные моменты времени после вспышки быстрых нейтронов. Энергия измеряется методом времени пролета с помощью механического прерывателя, сфазированного с работой ускорителя. Прерыватель имеет две щели расходящегося профиля, что обеспечивает постоянство функции пропускания во всем исследуемом диапазоне энергий при минимальной длительности открытия щели 2,5 *мксек*. Нейтроны регистрируются пропорциональным BF_3-счетчиком, расположенным на пролетном расстоянии 4 *м*.

Особенностью в измерении нестационарного спектра является искажение спектра, возникающее при движении нейтронов от дна полости в замедлителе до прерывателя, которое должно учитываться при обработке экспериментальных результатов.

Результаты измерений

На рис. 16 показано изменение во времени энергетического распределения нейтронов, измеренное в бериллиевой призме размерами 60 × × 60 × 45 *см* ($B^2 \simeq 10^{-2}$). Диапазон исследованных времен от 30 до 2200 *мксек* охватывает практически всю область термализации нейтронов: от момента, когда начинают заметно сказываться межатомные связи и тепловое движение, до полного установления теплового равновесия нейтронного газа со средой. Видно, что через 300—400 *мксек* большая часть спектра со стороны больших энергий уже совпадает с максвелловским распределением при температуре среды. Дальнейшие, более медленные, изменения происходят только в области малых энергий и лишь спустя ~1500 *мксек* спектр становится полностью равновесным. На рис. 17 представлены спектры, измеренные в графитовой призме размером 60 × 60 × 45 *см* ($B^2 = 8{,}9 \cdot 10^{-3}$ *см*$^{-2}$). Измерения проведены примерно в том же интервале времен (30—2500 *мксек*), который в данном случае соответствует более широкому интервалу энергии. В отличие от бериллия асимптотические спектры в данном случае заметно отклоняются от максвелловского распределения с температурой среды.

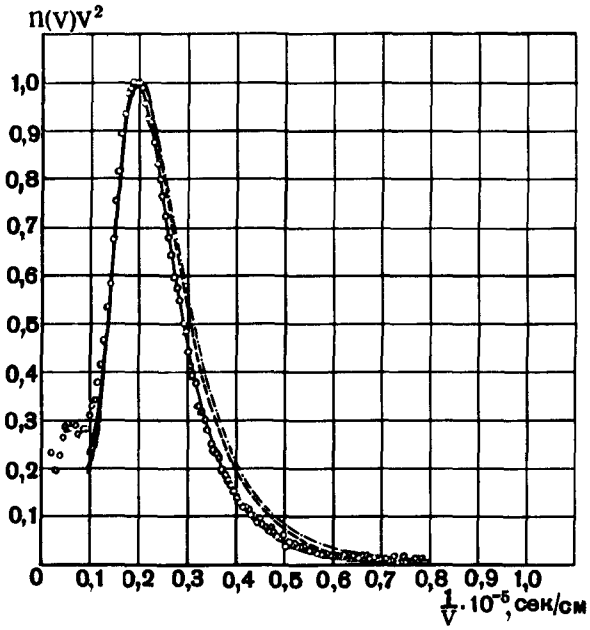

Рис. 13. Спектр нейтронов в уране уран-графитовой решетки; температура графита 614° К:
— спектр потока нейтронов в направлении оси блока; —·— спектр потока нейтронов в направлении, перпендикулярном оси блока; — — — спектр скалярного потока

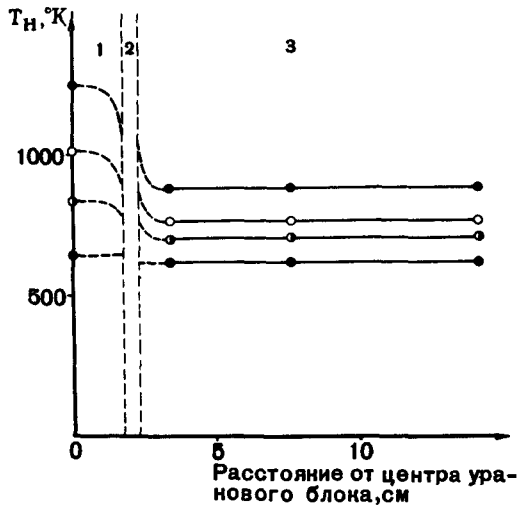

Рис. 14. Распределение «температуры» нейтронного газа по ячейке уран-графитовой решетки:
1 — блок; *2* — воздух и алюминий; *3* — графит;
○ — $T_n = \frac{\pi}{4} \cdot \frac{m(\bar{v})^2}{2k}$; ⊙ — $T_n = \frac{4}{\pi} \cdot \frac{m}{2k} \cdot 1 \Big/ \left(\frac{\bar{1}}{v}\right)^2$;
◑ — $T_n = \frac{mv_m^2}{4k}$; ● — температура среды

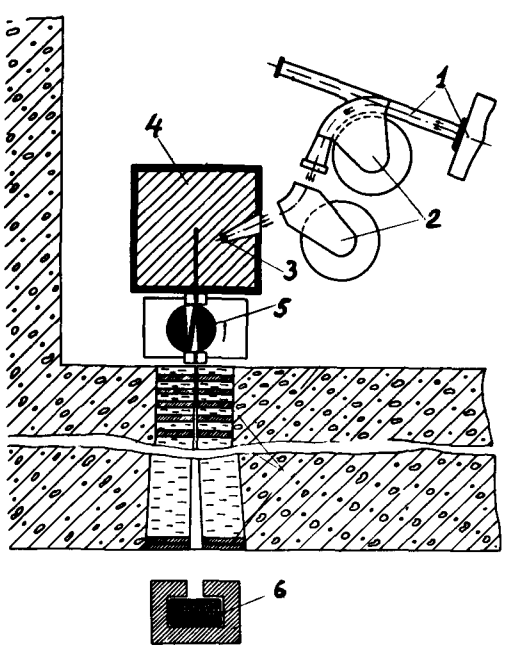

Рис. 15. Схема экспериментальной установки:
1 — вакуумная труба линейного ускорителя; *2* — отклоняющий и фокусирующий магниты; *3* — свинцовая мишень; *4* — призма из исследуемого материала; *5* — защита призмы (B_4C); *6* — механический прерыватель; *7* — биологическая защита бункера ускорителя; *8* — свинцовые диафрагмы; *9* — детектор нейтронов; *10* — защита детектора

Это проявление «диффузионного охлаждения» спектра, которое связано с большей величиной утечки из графитовой призмы данного размера. На следующем графике (рис. 18) представлено изменение во времени средней энергии нейтронов вычисленное по измеренным спектрам для бериллия и графита. Наклонные прямые изображают зависимость $\bar{E}(t)$ для свободных и покоящихся ядер бериллия и графита [27-28], пунктиром дан уровень $^3/_2\ kT$. На примере графита видно, что связь и тепловое движение атомов начинают заметно влиять на процесс замедления нейтронов уже при энергии $\simeq 1$ *эв*. В бериллии достигнутый предел по энергии заметно ниже, что связано с недостаточным разрешением по времени. По прошествии (1,5—2)10^3 *мксек* наступает практически полное равновесие между нейтронным газом и средой. При этом в бериллии равновесная температура равна температуре среды, а в графите, за счет диффузионного охлаждения,— несколько меньше. Следует заметить, что в аналогичных измерениях проделанных в Харуэлле [29] на графите в области от 300 до 1000 *мксек* получена зависимость $\bar{E}(t)$ подобная данной, однако абсолютные значения лежат систематически ниже. Скорость установления равновесного теплового спектра обычно характеризуют временем термализации τ_{th} полагая, что средняя энергия нейтронов приближается к своему равновесному значению по экспоненциальному закону:

$$\bar{E}(t) - E_p \sim \exp(-t/\tau_{th})$$

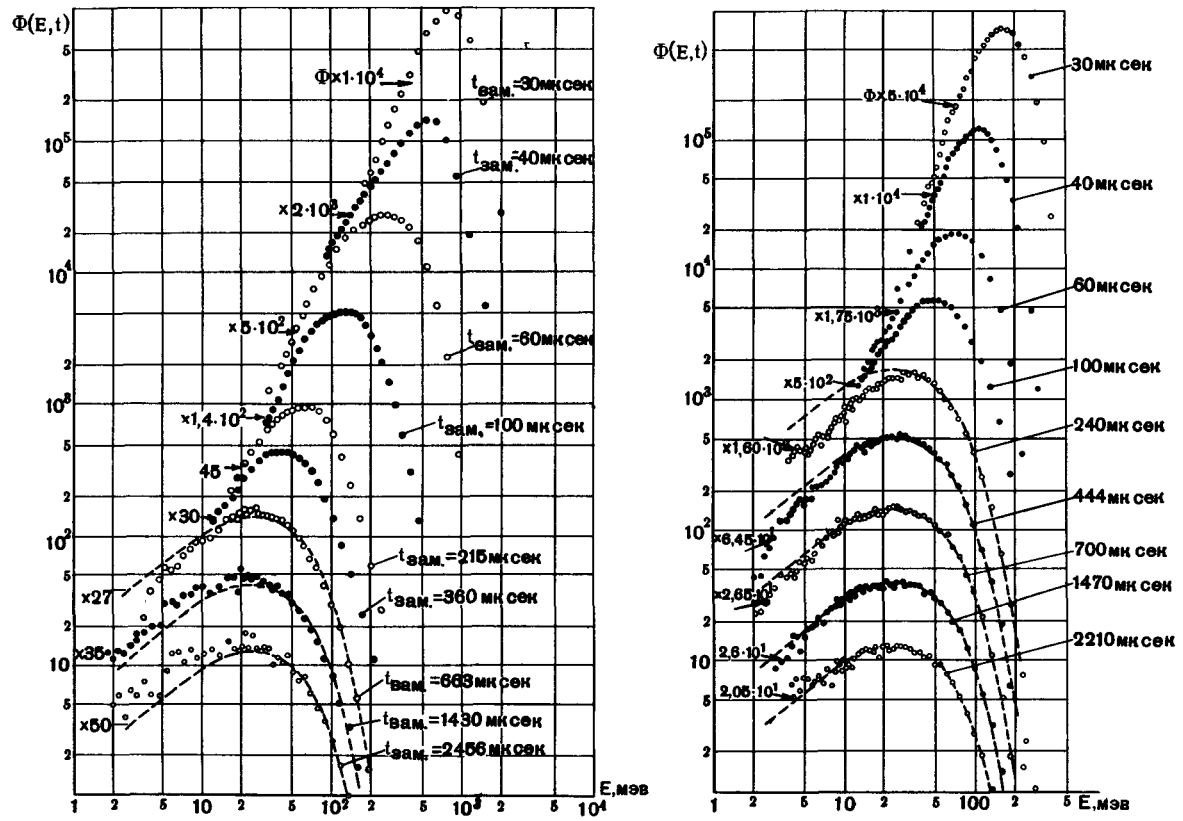

Рис. 16—17. Поток нейтронов Ф (E, t) в графите и бериллии
— — — спектр Максвелла $T=300°$ К

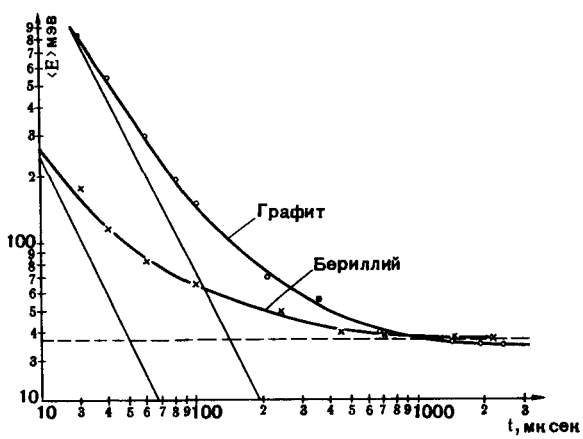

Рис. 18. Изменение средней энергии нейтронов во времени. Наклонными прямыми линиями представлены зависимости $\overline{E}=f(t)$ для графита и бериллия, вычисленные по модели свободных покоящихся ядер [28]

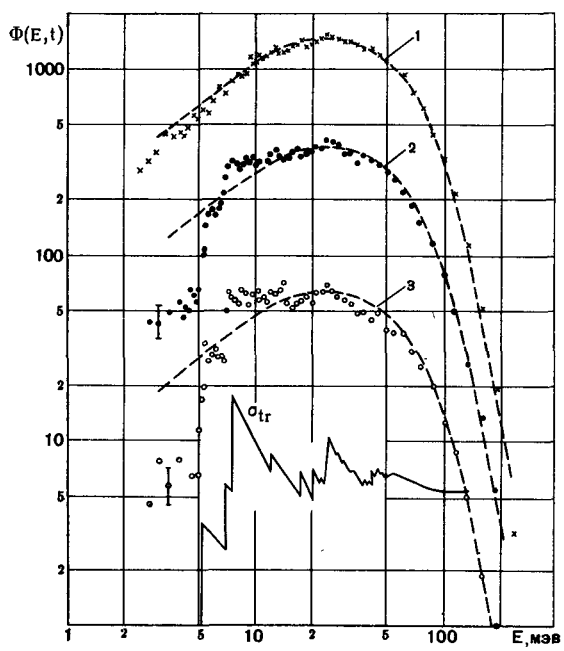

Рис. 19. Спектр нейтронов для $t=7000$ *мсек* в бериллиевых призмах разных размеров T
1—60×06×45 *см*, *2*—30×30×45 *см*, *3*—30×25×21 *см*
— — — спектр Максвелла $T=300°$ К

Анализ полученных кривых показывает, что такое простое описание зависимости $\overline{E}(t)$ справедливо, по-видимому, только для довольно узкой области изменения $\overline{E}$, когда его значение близко к E_p. Поэтому достаточно полно характеризовать процесс установления теплового равновесия одним параметром (τ_{th}) невозможно. Приближенно можно указать лишь время установления полного равновесия, которое составляет для бериллия около 1000 *мксек*, графита ~2000 *мксек*. Интересно отметить, что вычисления Пурохита [30], основанные на модели одноатомного тяжелого газа дают для этих времен значения значительно меньшие (~250 *мксек* для графита и ~150 *мксек* для бериллия). Это свидетельствует о сильном влиянии химической связи на скорость установления теплового равновесия нейтронов со средой.

Для того, чтобы более подробно исследовать влияние утечки нейтронов на форму равновесного спектра в кристаллическом замедлителе были проведены измерения спектров при больших временах замедления в бериллиевых призмах различных размеров. На рис. 19 представлены спектры близкие к асимптотическим ($t = 700$ *мксек*) для трех значений B^2 : $9{,}7\times$ $\times 10^{-3}$; $24{,}2\cdot 10^{-3}$ и $42{,}8\cdot 10^{-3}$. Для сопоставления там же приведена [31] зависимость $\sigma_{th}(E)$. Поскольку скорость утечки нейтронов определяется величиной $D = \frac{1}{3}\lambda_{th}\cdot v$, то наряду с «диффузионным охлаждением» спектра (преимущественная утечка быстрых нейтронов) должна наблюдаться зависимость формы спектра от изменения транспортного сечения с энергией. На графиках четко видно проявление этой зависимости. Подобные эффекты когерентного рассеяния наблюдались в аналогичных экспериментах на ренселлорском ускорителе [32] и в расчетной работе Иха [33], результаты которой в этом отношении весьма близки к представленным. Интересно отметить, что средняя энергия нейтронов для всех трех спектров оказывается одинаковой и равной ~39 *Мэв*. Отсутствие эффекта «охлаждения» можно объяснить как за счет сильной утечки холодных нейтронов ($E < 5$ *Мэв*), так и неполным установлением равновесия.

Результаты проведенных экспериментов содержат достаточно подробную информацию, которую можно использовать для проверки существующих методов расчета спектров термализирующихся нейтронов.

В докладе Майорова и др. [7] сообщается о создании программы, по которой в настоящее время проводятся подробные вычисления спектров нейтронов применительно к условиям данных опытов.

ЗАКЛЮЧЕНИЕ

Проведенные эксперименты не исчерпывают намеченной программы исследований, которая предусматривает детальное изучение более широкого круга замедлителей и размножающих систем и в большем интервале температур и энергий.

В настоящее время работы по термализации нейтронов продолжаются. Завершается создание новой многодетекторной установки для измерения дважды дифференциальных сечений с лучшей точностью и разрешением. Проводится изучение термализации нейтронов в средах при больших градиентах температур. Предполагается детально исследовать вопрос анизотропии спектра в гетерогенных средах. Будет изучен процесс установления равновесного спектра нейтронов в водородсодержащих замедлителях и др.

* * *

Изучение термализации нейтронов было начато в Институте атомной энергии по инициативе И. В. Курчатова. В дальнейшем эти работы получили развитие благодаря поддержке и постоянному интересу к ним академика А. П. Александрова.

ЛИТЕРАТУРА

1. И. В. Курчатов. Некоторые вопросы развития атомной энергетики в СССР, доклад в Харуэлле (1956).
2. P. A. Egelstaff. Symposium on inelastic scattering of neutrons in solids and liquids, Vienna (1960).
3. P. A. Egelstaff. Nucl. Sci. and Eng., *12*, 250 (1962).
4. P. A. Egelstaff, P. Schofield. Nucl. Sci. and Eng., *12*, 260 (1962).
5. P. A. Egelstaff, B. C. Haywood and I. M. Thorson. Symposium on inelastic scattering of neutrons in solids and liquids, Chalk River (1962).
6. K. E. Larsson, U. Dahlborg. Symposium on inelastic scattering of neutrons in solids and liquids, Chalk River (1962).
7. Л. В. Майоров, В. Ф. Турчин, М. С. Юдкевич. Влияние химической связи на термализацию нейтронов, наст. издание, Р/360.
8. В. И. Мостовой, В. С. Дикарев, М. Б. Егиазаров и Ю. С. Салтыков. Труды Второй международной конференции по мирному использованию атомной энергии, Женева, 1958, Р/2152.
9. В. С. Дикарев, М. Б. Егиазаров, В. И. Мостовой и Ю. С. Салтыков. Доклад в Дрездене (1960).
10. Г. И. Марчук, В. Ф. Турчин, В. В. Смелов, Г. А. Илясова. Атомная энергия, *13*, 6, 534 (1962).
11. Е. Я. Доильницын, А. Г. Новиков. Атомная энергия, *13*, 5, 491 (1962).
12. M. J. Poole. J. Nucl. Energy, *V*, 325 (1957).
13. R. B. Walton, J. R. Beyster, J. L. Wood, W. M. Lopez. Symposium on inelastic scattering of neutrons in solids and liquids, Vienna (1960).
14. J. R. Beyster, J. L. Wood, W. M. Lopez, R. B. Walton. Nucl. Sci. and Eng., *9*, 168 (1961).
15. K. Burkart, W. Reichardt. Proceedings of the Brookhaven conference on neutron thermalization (1962).
16. R. S. Stone, R. E. Slovacek. Nucl. Sci. and Eng., *6*, 466 (1959).

17. R. R. Goveyou, R. R. Bates, B. K. J. Osborne. J. Nucl. Energy, *11*, 3 (1956).
18. В. И. Мостовой, В. С. Дикарев, М. Б. Егиазаров и Ю. С. Салтыков. Атомная энергия, *13*, 6, 546 (1962).
19. А. Н. Тихонов. Докл. АН СССР, *149*, 529 (1963).
20. L. de Sobrino, M. Clark. Nucl. Sci. and Eng., *10*, 377 (1961).
21. H. C. Honeck, H. Takahashi. BNL-5924 (1962).
22. К. Кэмпбелл и др. Труды Второй международной конференции по мирному использованию атомной энергии, Женева, 1958. Избранные доклады иностранных ученых, т. II.
23. Г. И. Марчук, Г. А. Илясова, В. И. Морозов, В. В. Смелов и В. А. Ходаков. Расчеты спектров медленных нейтронов, наст. издание, P/365.
24. M. S. Coates, D. B. Gayther. AERE-R3829 (1961).
25. E. Barnard, N. A. Khan, M. J. Poole, J. H. Tait, R. C. F. McLatchie. Proceedings of the Brookhaven conference on neutron thermalisation (1962).
26. Р. М. Воронков, М. И. Певзнер и др. Атомная энергия, *13*, 4, 327 (1962).
27. И. Г. Дедькин, Э. П. Баталина. Атомная энергия, *10*, вып. 1, (1961).
28. J. Koppel, Nucl. Sci. and Eng., *8*, 157 (1960).
29. E. Barnard et al. Proceedings of the Brookhaven conference on neutron thermalisation (1962)
30. S. N. Purohit. Nucl. Sci. and Eng., *9*, 305 (1961).
31. R. S. Bhandari. Nucl. Energy, *6* 104 (1957)
32. R. R. Fullwood et al. Nucl. Sci and Eng., *18* 138 (1964)
33. S. S. Iha. J. Nucl. Energy, A, *12*, 89 (1960)
34. С. И. Дроздов, Д. Ф. Зарецкий, Л. П. Кудрин и Т. Х. Сидельников. Труды Второй международной конференции по мирному использованию атомной энергии, Женева, 1958.
35. M. D. Nelkin. Phys. Rev., *119*, 74 (1961).
36. D. A. Kottwits, B. F. Leonard. Symposium on inelastic scattering of neutrons in solids and liquids, Chalk River (1962).

ABSTRACT—RÉSUMÉ—АННОТАЦИЯ—RESUMEN

A/367 USSR

Experimental studies of neutron thermalization

By V. I. Mostovoy *et al.*

The paper reviews the experimental work on neutron thermalization which has been carried out in recent years in the Kurchatov Atomic Energy Institute. This work deals with the most interesting aspects of neutron thermalization which have practical importance, and is carried out along three lines.

1. Investigation of inelastic scattering of slow monochromatic neutrons on bound nuclei of the moderator.

In connection with this line of research the review gives the results of double differential scattering cross sections of slow monochromatic neutrons $\sigma(E, E', \theta)$ in hydrogen-containing moderators. A pulsed flux of monochromatic neutrons of energy E incident on the sample was separated from the horizontal beam of thermal neutrons of the VVR-M reactor (Physics Institute of the Academy of Sciences of the Ukranian SSR) with the aid of a mechanical monochromator. The resolution of the monochromator was independent of its speed of rotation and was equal to $\Delta E/E=0.2$. The energy E' of neutrons scattered from the sample at an angle θ was measured by the flight time method with a resolution of about 25 μs/m.

The double differential scattering cross sections were measured within the range of energies of the incident neutrons from 15 to 300 MeV at scattering angles from 15° to 120°. Certain data were obtained concerning the effect of the sample temperature on the double differential scattering cross section.

The comparative analysis of the cross sections and average characteristics of neutron scattering in water and monoisopropyldiphenyl ($C_{15}H_{16}$) shows that the chemical binding of the hydrogen in monoisopropyldiphenyl is stronger than in water and, accordingly, the neutron thermalization in monoisopropyldiphenyl proceeds at a slower rate.

The law of scattering $S(\alpha, \beta)$ and the generalized frequency spectrum for water and monoisopropyldiphenyl were obtained from the experimental data.

2. Investigation of the establishment of the thermal neutron spectrum in time in various moderators.

The establishment of the thermal neutron spectrum was studied with the aid of a pulsed neutron source and a mechanical chopper. Neutrons were produced on a target of a linear accelerator which operated in phase with the mechanical chopper. Neutron spectra were measured in beryllium and graphite at different time intervals after fast neutron burst. The resolution during measurements was 3 to 5 μs/m, the duration of the neutron pulse furnished by the mechanical chopper, 5 to 10 μs.

3. Investigation of thermal and slowing-down neutron spectra in homogeneous and heterogeneous media.

Microbeams of neutrons were extracted from the medium under investigation. The neutron spectra in the beams were studied with the aid of a mechanical chopper using the time-of-flight method. The resolution during the measurements of the thermal part of the spectrum was 10 to 25 μs/m, during the measurements of the slowing-down spectrum, 1.2 μs/m. Spectra of thermal neutrons in boron-poisoned water were studied at various boron concentrations.

A detailed investigation was made into the space-energy distribution of neutrons in the cells of subcritical lattices: uranium–water, uranium–monoisopropyldiphenyl, uranium–graphite.

The measurement results indicate that the thermal

neutron spectrum in water can be described by the Maxwell distribution with the temperature of the neutrons exceeding the temperature of the media. At the given temperature of the moderator the temperature rise of the neutrons is proportional to absorption.

The spectrum of thermal neutrons in the uranium block of a lattice and also in a moderator differs from equilibrium Maxwell distribution. The nature of the neutron spectrum abruptly changes at the boundary between uranium and moderator. Inside the block and the moderator, the neutron spectrum changes but little. A simple semi-empirical relation is given between the thermal neutron spectrum in the block and in the moderator. The spectrum of the slowing-down neutrons in the block has peculiar dips at energies corresponding to the known absorption levels of ^{238}U and ^{235}U.

A/367 URSS

Étude expérimentale de la thermalisation des neutrons

par V. I. Mostovoy *et al.*

Le mémoire présente les travaux expérimentaux sur la thermalisation des neutrons effectués au cours des dernières années à l'Institut de l'énergie atomique I.-V.-Kourtchatov. Ces travaux se rapportent aux questions les plus intéressantes et les plus importantes de la thermalisation des neutrons et sont menés dans trois directions.

1. Etude de la diffusion inélastique de neutrons lents monochromatiques sur les noyaux liés d'un modérateur.

Résultats des mesures de la section différentielle double de diffusion de neutrons monochromatiques lents, $\sigma(E, E', \theta)$, sur des modérateurs hydrogénés. Le flux pulsé de neutrons monochromatiques d'énergie E arrivant sur l'échantillon est séparé du faisceau horizontal de neutrons thermiques du réacteur VVR-M (Institut de physique de l'Académie des sciences de la RSS d'Ukraine) à l'aide d'un sélecteur mécanique. La résolution du sélecteur ne dépend pas de sa vitesse de rotation et est de $\Delta E/E = 0{,}2$. On a mesuré l'énergie E' des neutrons diffusés par l'échantillon sous l'angle θ par la méthode du temps de vol avec une résolution d'environ 25 μs/m.

On mesure les sections différentielles doubles dans une gamme d'énergie de 15 à 300 MeV des neutrons incidents sur l'échantillon et pour des angles de diffusion de 15° à 120°. On obtient quelques données sur l'influence de la température de l'échantillon sur la section différentielle double de diffusion.

La confrontation des sections et des caractéristiques moyennes de la diffusion des neutrons sur l'eau et le monoisopropyldiphényle ($C_{15}H_{16}$) montre que la liaison chimique de l'hydrogène dans le monoisopropyldiphényle est plus forte que dans l'eau et qu'en conséquence la thermalisation des neutrons dans le monoisopropyldiphényle est plus lente.

A partir des données expérimentales, on a obtenu la loi de diffusion $S(\alpha, \beta)$ et le spectre généralisé de fréquence $P(\beta)$ pour l'eau et le monoisopropyldiphényle.

2. Etude de la formation d'un spectre de neutrons thermiques dans le temps dans divers modérateurs.

On étudie la formation d'un spectre de neutrons thermiques à l'aide d'une source pulsée de neutrons et d'un sélecteur mécanique. On utilise comme source de neutrons la cible d'un accélérateur linéaire dont l'émission est en phase avec le sélecteur mécanique. On mesure les spectres de neutrons pour le béryllium et le graphite à différents moments après l'injection de neutrons rapides. La résolution dans les mesures est de 3 à 5 μs/m, la durée de l'impulsion neutronique donnée par le sélecteur mécanique étant de 5 à 10 μs.

3. Etude des spectres de neutrons thermiques et de neutrons ralentis en milieux homogènes et hétérogènes.

Des microfaisceaux de neutrons sont pris à la sortie du milieu étudié et on mesure les spectres à l'aide d'un sélecteur mécanique à temps de vol. La résolution des mesures de la partie thermique du spectre est de 10 à 25 μs/m, et celle des mesures du spectre de ralentissement de 1,2 μs/m. On étudie les spectres de neutrons thermiques dans l'eau empoisonnée par du bore, en fonction de la concentration du bore. On étudie en détail la distribution énergétique spatiale de neutrons dans des réseaux sous-critiques: uranium–eau, uranium–monoisopropyldiphényle, uranium–graphite.

Les résultats des mesures montrent que, lorsque l'absorption n'est pas grande, le spectre de neutrons thermiques dans l'eau peut être décrit par une distribution de Maxwell mais avec une température neutronique supérieure à celle du milieu. La différence, pour une température de modérateur donnée, est proportionnelle à l'absorption.

Le spectre de neutrons thermiques dans les barres d'uranium du réseau et dans le modérateur diffère d'une distribution de Maxwell à l'équilibre. Le spectre varie brusquement au passage de l'uranium au modérateur. Dans le barreau et le modérateur mêmes, il varie peu. On donne une fonction semi-empirique simple du spectre de neutrons thermiques dans le barreau par rapport au spectre de neutrons thermiques dans le modérateur. Le spectre de neutrons ralentis dans le barreau présente des creux caractéristiques aux énergies correspondant aux niveaux connus d'absorption de ^{238}U et de ^{235}U.

A/367 URSS

Trabajos experimentales sobre termalización de los neutrones

por V. I. Mostovoy *et al.*

En este documento se pasa revista a los trabajos experimentales sobre termalización de los neutrones realizados estos últimos años en el Institut Atomnoi Energuii, «I. V. Kurchatov». Estos trabajos se

refieren a las cuestiones más interesantes de termalización de los neutrones y de mayor importancia práctica y se llevaron a cabo en tres direcciones.

1. Estudio de la dispersión inelástica de neutrones lentos monoenergéticos por los núcleos ligados del moderador.

Respecto de estas investigaciones, se presentan aquí los resultados de mediciones de la sección eficaz diferencial de dispersión, por moderadores hidrogenados, de neutrones térmicos monoenergéticos, $\sigma(E,E',\theta)$. El flujo pulsádo de neutrones monoenergéticos de energía E que incide sobre la muestra se extraía de un haz horizontal de neutrones térmicos del reactor VVR-M (Instituto de Física de la Academia de Ciencias de la RSS de Ukrania) mediante un monocromador mecánico. La resolución de éste no dependía de su velocidad de rotación y era igual a $\Delta E/E = 0{,}2$. La energía E' de los neutrones dispersados por la muestra en la dirección θ se medía por tiempo de vuelo con una resolución $\sim$25 μs/m.

Las secciones eficaces diferenciales se midieron en un intervalo de energías de los neutrones incidentes sobre la muestra que iba de 15 a 300 MeV y en un intervalo angular de direcciones de dispersión de 15° a 120°.

Se obtuvieron algunos datos relativos a la influencia de la temperatura de la muestra sobre la sección eficaz diferencial.

La comparación de las secciones eficaces y de las características medias de dispersión neutrónica del agua y del monoisopropildifenilo ($C_{15}H_{16}$) indica que el enlace químico del hidrógeno en este último es más fuerte que en el agua y que, en consecuencia, la termalización de los neutrones en el monoisopropildifenilo tiene lugar más lentamente.

A partir de los datos experimentales se obtuvo la ley de dispersión $S(\alpha,\beta)$ y el espectro de frecuencia generalizado $P(\beta)$ para el agua y el monoisopropildifenilo.

2. Estudio del proceso de formación del espectro de los neutrones térmicos con el tiempo para diferentes moderadores.

El proceso de formación del espectro de los neutrones térmicos se estudió con ayuda de una fuente pulsante de neutrones y de un selector mecánico. Como fuente de neutrones se utilizó el blanco de un acelerador lineal cuya puesta en marcha está en fase con el selector mecánico. Se midieron los espectros neutrónicos para el berilio y el grafito en diferentes instantes después de la inyección de neutrones rápidos. La resolución en las mediciones era de 3–5 μs/m para una duración del impulso neutrónico, dado por el selector mecánico, de 5–10 μs.

3. Estudio de los espectros térmicos y de moderación de los neutrones en medios homogéneos y heterogéneos.

Del medio estudiado se extraían microhaces de neutrones. Los espectros neutrónicos en los haces se medían por tiempo de vuelo con ayuda de un selector mecánico. La resolución en la medida de la componente térmica del espectro era de 10 a 25 μs/m, y en la del espectro de moderación era de 1,2 μs/m. Se estudiaron los espectros de los neutrones térmicos en agua, envenenada con boro, como función de la concentración de boro. Se efectuó un estudio detallado de la distribución espacial y energética de los neutrones en celdas de redes subcríticas de: uranio–agua, uranio–monoisopropildifenilo, uranio–grafito.

Los resultados de las medidas muestran que el espectro de los neutrones térmicos en el agua puede representarse, cuando las absorciones no son muy grandes, por una distribución maxwelliana con una temperatura de los neutrones mayor que la del medio. Para una temperatura dada del moderador, dicho incremento de temperatura es proporcional a la absorción.

El espectro de los neutrones térmicos en un bloque de uranio de la red, y también en el moderador, difiere de la distribución maxwelliana de equilibrio. El espectro de los neutrones cambia bruscamente su caracter en la superficie de separación uranio–moderador. En el propio bloque y en el moderador, el espectro neutrónico varía poco. Se presenta una fórmula semiempírica que liga el espectro de los neutrones térmicos en el bloque con el espectro térmico en el moderador. El espectro de moderación de los neutrones en el bloque presenta depresiones características para las energías que corresponden a los conocidos niveles de absorción del ^{238}U y del ^{235}U.

Studies of neutron thermalization by a modified pulsed-source technique

By E. Friedman*

The pulsed neutron source technique has been extensively used in the past few years for measuring diffusion parameters of thermal neutrons in moderators [1,2]. The nonlinearity in the curve of the decay constant as a function of the geometrical buckling is partly due to transport corrections to the diffusion approximation [3,4] and partly due to the "diffusion cooling" effect, which is related to the transfer of energy between thermal neutrons and moderator. There are theoretical limitations that will be mentioned later which in certain cases prevent a reliable derivation of thermalization data from "diffusion cooling" measurements. In addition, there are large discrepancies between diffusion cooling coefficients obtained by different authors for the same moderator. These discrepancies are probably due to a dependence of the results on the shape of the moderator [5]. A new method for measuring neutron thermalization parameters that avoids the difficulties encountered in the diffusion cooling method has been proposed on theoretical grounds [6]. In the present work this method is demonstrated experimentally on H_2O.

THEORY

The diffusion equation for the flux in a moderator following a short pulse of fast neutrons, assuming time dependence $e^{-\lambda t}$ and taking into account only the fundamental mode with geometrical buckling B^2, is

$$\left[\Sigma_a(E)-\frac{\lambda}{v}+B^2D(E)\right]\phi(E) = \int_0^\infty dE'[\Sigma_s(E'\to E)\,\phi(E')-\Sigma_s(E\to E')\,\phi(E)] \quad (1)$$

where $\phi(E)$ is the flux per unit energy, $\Sigma_a(E)$ is the macroscopic absorption cross section, $D(E)$ is the energy dependent diffusion coefficient, and $\Sigma_s(E\to E')$ is the macroscopic cross section for scattering of neutron of energy E into a unit energy interval at E'. Substituting a Maxwellian flux,

$$M(E)=\frac{E}{T^2}e^{-E/T} \quad (2)$$

where the temperature of the moderator, T, is measured in energy units, the integral in equation (1) vanishes, as a result of the detailed balancing condition satisfied by $\Sigma_s(E\to E')$. If $\Sigma_a(E)+B^2D(E)$ is proportional to $1/v$, a Maxwellian flux is a solution of Eq. (1). We conclude that neutron removal processes that have a form of a/v do not distort the Maxwellian energy distribution. In all moderators of interest, $\Sigma_a(E)=\lambda a/v$, and so the non $1/v$ dependence of $D(E)$ is the reason for the dependence of $\phi(E)$ on B^2, and hence for the diffusion cooling effect.

A convenient method for dealing with Eq. (1) is to take an approximation [7,8,9]

$$\phi(E)=M(E)\sum_{i=0}^{L}a_iL_i^{(1)}(E/T) \quad (3)$$

The normalization used is

$$\int_0^\infty L_i^{(1)}(E/T)M(E)L_j^{(1)}(E/T)dE=\delta_{ij} \quad (4)$$

If we write

$$\lambda=\lambda_a+\frac{2v_0}{\sqrt{\pi}}B^2(D_{00}-C'B^2) \quad (5)$$

we obtain

$$C'=-\frac{\begin{vmatrix} 0 & t_{01} & t_{02} & \cdots & t_{0L} \\ t_{01} & \gamma_{11} & \gamma_{12} & \cdots & \gamma_{1L} \\ t_{02} & \gamma_{12} & & & \\ \cdot & \cdot & & & \\ \cdot & \cdot & & & \\ \cdot & \cdot & & & \\ t_{0L} & \gamma_{1L} & & & \gamma_{LL} \end{vmatrix}}{\begin{vmatrix} \gamma_{11} & \gamma_{12} & \cdots & \gamma_{1L} \\ \gamma_{12} & & & \\ \cdot & & & \\ \cdot & & & \\ \cdot & & & \\ \gamma_{1L} & & & \gamma_{LL} \end{vmatrix}} \quad (6)$$

where $v_0=\sqrt{2T/M_n}$ and M_n is the mass of a neutron. The neutron thermalization parameters are

$$\gamma_{ij}=\int_0^\infty\int_0^\infty dE\,dE'M(E)\Sigma_s(E\to E')[L_i^{(1)}(E/T)-L_i^{(1)}(E'/T)]\,L_j^{(1)}(E/T) \quad (7)$$

and

$$D_{ij}=\int_0^\infty L_i^{(1)}(E/T)\,M(E)D(E)\,L_j^{(1)}(E/T)dE \quad (8)$$

* Hebrew University of Jerusalem and Israel Atomic Energy Commission.

$$t_{0j} = D_{00} W_{0j} - D_{0j} \tag{9}$$

$$W_{0j} = \frac{2}{\sqrt{\pi}} (\sqrt{T/E})_{0j} \tag{10}$$

We notice that if $D(E) \sim 1/v$, the t_{0j} vanish identically, and $C' = 0$.

In addition to the difficulties of evaluating the transport correction to the diffusion approximation, which is required for deriving the diffusion cooling coefficient, and to the question of whether the geometrical buckling is the correct parameter describing the leakage of neutrons out of the system for the small systems used in such measurements, we notice here two more difficulties, namely:

(*a*) The functions $D(E)\,(=1/3\ \lambda t_{\mathrm{r}}(E))$ are not known to the accuracy required for evaluating t_{0j}

(*b*) only one independent measurement is possible for each moderator and so only one thermalization parameter can be derived.

In the new method of measuring thermalization parameters [6], we use non $1/v$ absorption instead of the leakage out of the system as the means for distorting the Maxwellian energy distribution. For an infinite system with an added "non $1/v$" strong absorber we have:

$$\lambda = \lambda_{\mathrm{a}} + N \frac{(\overline{\sigma_{\mathrm{a}}})}{(1/v)} = \lambda_{\mathrm{a}} + \frac{2v_0}{\sqrt{\pi}} N(\alpha + \beta N + \ldots) \tag{11}$$

where λ_{a} is the decay constant for the pure moderator (assuming $1/v$ absorption), N is the concentration (atoms/cm^3) of the added absorber and $\sigma_{\mathrm{a}}(E)$ is its absorption cross section. If $\sigma_{\mathrm{a}}(E)$ is much larger than the absorption cross section of the moderator in the thermal region, then N is very small compared to the density of the moderator atoms (for λ of the order λ_{a}) and we can develop the above averages in a power series in N. When the distortion of the Maxwellian spectrum is represented by a linear combination of Laguerre polynomials of order unity and degree i, one obtains, in analogy to Eq. (6)

$$\beta = \frac{\begin{vmatrix} 0 & S_{01} & S_{02} & \ldots & S_{0L} \\ S_{01} & \gamma_{11} & \gamma_{12} & & \gamma_{1L} \\ S_{02} & \gamma_{12} & & & \\ S_{0L} & \gamma_{1L} & & & \gamma_{LL} \end{vmatrix}}{\begin{vmatrix} \gamma_{11} & \gamma_{12} & & \gamma_{1L} \\ \gamma_{12} & & & \\ \gamma_{1L} & & & \gamma_{LL} \end{vmatrix}} \tag{12}$$

where L is the highest degree of polynomials taken in the approximation.

$$S_{0j} = (\sigma_{\mathrm{a}})_{00}\, W_{0j} - (\sigma_{\mathrm{a}})_{0j} \tag{13}$$

When the matrix γ is diagonal (as in the heavy gas model), the expression for β is

$$\beta = -\sum_{j=1}^{L} \frac{S^2_{0j}}{\gamma_{jj}} \tag{14}$$

Retaining linear terms in γ_{ij}/γ_{ii} one obtains,

$$\beta = -\frac{S^2_{01}}{\gamma_{11}} \left(1 - 2\frac{S_{02}}{S_{01}}\frac{\gamma_{12}}{\gamma_{22}} - 2\frac{S_{03}}{S_{01}}\frac{\gamma_{13}}{\gamma_{33}} - \ldots\right) - \frac{S^2_{02}}{\gamma_{22}} \left(1 - 2\frac{S_{03}}{S_{02}}\frac{\gamma_{23}}{\gamma_{33}} \ldots\right) - \frac{S^2_{03}}{\gamma_{33}} (1 - \ldots) - \tag{15}$$

For a finite system we have

$$\lambda = \lambda' + \frac{2v_0}{\sqrt{\pi}} N(\alpha'(B^2) + \beta'(B^2) N + \ldots) \tag{16}$$

where λ' is the decay constant in the finite system without added absorber. As suggested in [6], the parameter β for each absorber is obtained from measurements of $\beta'(\beta^2)$ for several values of B^2. The thermalization parameters are derived from β. The strong absorbers used are Cd, Sm, and Gd, and mixtures thereof. It is sufficient to calculate $(\sigma_{\mathrm{a}})_{0j}$ for these three elements only. Table 1 shows values obtained by numerical integration using a PHILCO 2000 computer

Table. 1. Calculated integrals for various absorbers

	T°C	$(\sigma_{\mathrm{a}})_{00}$ barns	$\frac{(\sigma_{\mathrm{a}})_{01}}{(\sigma_{\mathrm{a}})_{00}}$	$\frac{(\sigma_{\mathrm{a}})_{02}}{(\sigma_{\mathrm{a}})_{00}}$	$\frac{(\sigma_{\mathrm{a}})_{03}}{(\sigma_{\mathrm{a}})_{00}}$	$\frac{(\sigma_{\mathrm{a}})_{04}}{(\sigma_{\mathrm{a}})_{00}}$	$\frac{(\sigma_{\mathrm{a}})_{05}}{(\sigma_{\mathrm{a}})_{00}}$	$\frac{(\sigma_{\mathrm{a}})_{06}}{(\sigma_{\mathrm{a}})_{00}}$
Sm	20°	8266	−0.17103	−0.19668	0.04684	0.18302	0.17384	0.09062
	40°	8394	−0.14379	−0.22782	−0.00150	0.16000	0.18527	0.12267
	60°	8489	−0.11409	−0.24957	−0.04611	0.13125	0.18668	0.14715
	80°	8558	−0.08235	−0.26405	−0.08715	0.09850	0.17986	0.16420
	100°	8602	−0.04930	−0.27201	−0.12436	0.06353	0.16605	0.17403
Cd	20°	2964	−0.16498	0.14507	0.17578	0.04386	−0.02935	−0.01923
	40°	3016	−0.19629	0.11704	0.19330	0.06897	−0.02653	−0.03515
	60°	3072	−0.22070	0.08512	0.20378	0.09505	−0.01676	−0.04590
	80°	3130	−0.23930	0.05016	0.20799	0.12109	−0.000837	−0.05099
	100°	3191	−0.25259	0.01338	0.20526	0.14541	0.01974	−0.04983
Gd	20°	36188	0.47621	0.23417	0.13328	0.08945	0.06831	0.05673
	40°	34536	0.49200	0.24586	0.13983	0.09274	0.06984	0.05739
	60°	33061	0.50658	0.25728	0.14648	0.09628	0.07169	0.05823
	80°	31708	0.52053	0.26867	0.15336	0.10010	0.07367	0.05926
	100°	30412	0.53446	0.28042	0.16073	0.10427	0.07602	0.06053

$$\left((\sigma_a)_{0j} = \int_0^\infty L_0{}^{(1)}\left(\frac{E}{T}\right)\sigma_a(E)\frac{E}{T^2}e^{-E/T}L_j{}^{(1)}\left(\frac{E}{T}\right)dE\right.$$

where the normalization used is

$$\int_0^\infty L_i{}^{(1)}\left(\frac{E}{T}\right)\frac{E}{T^2}e^{-E/T}L_j{}^{(1)}\left(\frac{E}{T}\right)dE = \delta_{ij}\Big)$$

When we compare the present method to the diffusion cooling method, we note the following:

(*a*) Unlike t_{0j}, the S_{0j} may be calculated, since $\sigma_a(E)$ is a directly measured quantity while $D(E)$ is not;

(*b*) Measurements can be performed in systems large enough that terms containing B^4 can be neglected. Transport effects enter only into terms containing B^4 and higher terms [4] so that the diffusion equation may be used to describe the experiment;

(*c*) In this method the spectrum distorting mechanism is separated from the moderator itself, and we can perform independent experiments on the same moderator with different absorbers. If it were possible to describe a number of independent measurements by a smaller number of parameters γ_{ij}, one could compare these parameters to values calculated on the basis of some model of $\Sigma_s(E \to E')$.

For every function $f(E)$ that is smooth enough, the value of $(f_{00}W_{0j} - f_{0j})$ decreases monotonically for $j > J$, and thus only a limited number of terms contribute significantly in Eq. (14). It is therefore not possible to obtain an unlimited number of parameters γ_{ij}, but the number of parameters that are obtained should be sufficient for describing thermalization effects.

METHOD

The neutron source used in this work was a Texas Nuclear Neutron Generator, Model 9508 utilizing the T(d,n)^{4}He reaction at a bombardment energy of 150 keV. The pulsing system was a modified post-acceleration beam deflection, details of which are given elsewhere [10]. The relative background from the target (i.e. the ratio of neutron production during "off" position to that during "on") was about 3×10^{-5}. The water solutions studied were confined in cylindrical aluminium containers of diameter 200 mm. The detectors were NE-401 scintillators, 1½ in. in diameter, mounted on Phillips 53 AVP photomultipliers. These detectors are especially suitable for work where there is a high gamma radiation background and the N^{16} gamma rays from the water were rejected by the counting system. Small detectors were used in order to prevent time-of-flight distortions, which may occur when using detectors with dimensions of the order of 10 cm. The solution and the detectors were shielded by 35 mm of boric acid powder and 0.75 mm of cadmium. One of the difficulties in using the pulsed-source technique is in isolating the fundamental mode from the higher harmonic modes. By a suitable geometrical arrangement of the source and the detectors, one is able to suppress some of the harmonic modes. In the present experiment this is done as follows.

The symmetry axis of the source passes through the midpoint of the moderator and so the first axial mode is eliminated. The height of the water in the container is always less than 15 cm, thus the second axial mode has a short enough decay time. The radial modes are described by the functions $\cos(m\theta)J_m(k_n r)$. θ is measured with respect to the symmetry axis of the source. The first J_0 harmonic has the form $J_0(5.52\ r/R')$, where R' is the radius of the cylinder plus the extrapolation length. Since $J_0(2.405) = 0$, it is possible to eliminate the first J_0 harmonic by counting only neutrons emerging from the system at $r = (2.405/5.52)R'$. The J_1 modes are eliminated by using two detectors in parallel having the same efficiency for detecting thermal neutrons and detecting only neutrons emerging from the system at $\theta_1 = \pi/4$ and $\theta_2 = 5\pi/4$. For these angles, $\cos(2\theta) = 0$ and therefore the J_2 harmonics are eliminated. Because $\cos(3\theta_1) = -\cos(3\theta_2)$, the J_3 harmonics are eliminated. The J_4 harmonics are detected.

A cadmium sheet 0.75 mm thick was placed under the containers. Two holes were cut in the sheet along a diameter, at a radius $r = \frac{2.405}{5.52}R'$. This diameter was at an angle of 45° relative to the symmetry axis of the source. Two detectors were placed at the holes. Two separate power supplies were used, and the equality of the efficiencies of the detectors were checked daily.

The time dependence of the flux after a burst was studied using a 40-channel time analyser. The temperature during the measurements was (23 ± 0.6)°C.

The conventional method for obtaining the decay constant of the thermalized neutron flux in the fundamental mode is to fit by a least-squares method a straight line to the logarithms of the multi-channel readings (after correcting for dead time losses and subtracting the background). The sum of squares which has to be minimized is the sum of squares weighted by $1/\sigma_i^2$, where σ_i is the standard deviation of the ith measurement. The "goodness-of-fit" test may be made by calculating the value of the minimized sum of squares divided by the number of degrees of freedom (i.e., the number of channels used minus the number of calculated parameters). The smallest value of geometrical buckling (B^2) used was $B^2 = 0.096\ \text{cm}^{-2}$ and for that case the goodness-of-fit tests gave positive results only after a delay of 240 μs from the end of the burst. It was desirable to use also data obtained after shorter delays and to this end the method of analysis was changed. Two other methods were devised and both were found to be extremely useful.

The first method is based on the fact that we are interested not in the decay constant λ for each concentration of added absorber but only in $(\lambda - \lambda')$ where λ' is the decay constant for the same system without added absorbers (Eq. (10) of ref. [6]). We write the time dependence of the flux as

$$\phi'(t) = A'e^{-\lambda' t}(1 + \epsilon' e^{-\Delta\lambda \cdot t} + \ldots) \qquad (17)$$

for the pure moderator, and

$$\phi(t) = Ae^{-\lambda t}(1 + \epsilon e^{-\Delta\lambda \cdot t} + \ldots) \quad (18)$$

for the poisoned moderator, for some fixed value of B^2. ϵ' and ϵ represent the amplitudes of the first harmonic mode that can be detected. $\Delta\lambda$ is the difference between the decay constant for that mode and the decay constant for the fundamental one. We now consider the ratio

$$\frac{\phi(t)}{\phi'(t)} = \frac{A}{A'} e^{-(\lambda-\lambda')t}\{1 + (\epsilon - \epsilon')e^{-\Delta\lambda t} + \ldots\} \quad (19)$$

As the geometry in both measurements is the same, it is plausible that $|\epsilon - \epsilon'| \ll |\epsilon|$ and we can try to fit a straight line to the logarithms of the ratios of the corrected multi-channel readings, even after shorter delay times. Goodness-of-fit tests showed that it was thus possible to use data taken after as short a delay as 100 μs.

The second method that enables the use of relatively short delay times consists of fitting a sum of two exponentials to the data. In this case, the normal equations are no longer linear in the unknown parameters and it is necessary to iterate until convergence is obtained. In tens of cases that were tried using conventional least-squares techniques, no convergence was obtained. The difficulty lies in the highly nonorthogonal nature of the functions. Only by using a modified least-squares method was convergence possible. This modified method is described in the Appendix. The data taken after a delay of 100 μs were fitted by a sum of two exponentials. The goodness-of-fit criteria were fulfilled, the obtained $\Delta\lambda$ were in agreement with calculations based on the geometry of the detectors and $(\lambda - \lambda')$ obtained by this method were in agreement (within a standard error) with values obtained using the previous method.

Two sets of measurements were carried out for each absorber for three values of B^2 in the range 0.096 – 0.150 cm^{-2}. The highest concentration of added absorbers was such that $\lambda \approx 1.5\lambda'$. The analysis of data was carried out using a PHILCO 2000 computer.

RESULTS

The absorbers used were Sm, Cd, Gd and mixtures of Sm and Gd, and Sm and Cd. High purity chemicals (99.9%) were used. For Gd the parameter β is relatively small and the experimental accuracy is poor, so the measurements on Gd were used only as a check on the value of α. The results for four different absorbers are summarized in Table 2.

The results for Sm and Cd are in good agreement with those obtained by Meadows and Whalen [11].

Unfortunately, the experimental accuracy of the present measurements of β is of the order of the accuracy of diffusion cooling coefficients, though it was shown by Meadows and Whalen that it can be much higher. The accuracy in the present measurements is determined primarily by the accuracy of determination of the concentration of the water solutions under study. In the present work the concentrations were determined by adding to the system known amounts of highly concentrated solutions of absorbers, the concentrations of which were determined carefully. Although higher accuracies are obtainable, one can draw quantitative conclusions from the present results.

Table 2. Calculated and measured values of parameters $(\sigma_a)_{00}$, α and β using various absorbers in water

Absorber	$(\sigma_a)_{00}$ calculated (in barns)	α Measured (in barns)	β (in 10^{-17} barns × cm^2)
Sm	8285	8370 ± 70	−8.4 ±2.1
Cd	2973	2965 ± 21	−1.55 ±0.25
97.93%Sm + 2.07%Cd (atoms per cm^3) . . .	8850	8850 ± 30	−6.5 ±1.5
47.8%Sm + 52.2%Cd . . .	5510	5550 ± 50	−3.7 ±0.9
Gd	35900	35300 ± 300	—

When we use a least-squares method to represent the results in Table 2 by the equation

$$\beta_i = -\frac{S^2_{01}(i)}{\gamma_{11}}, \quad i = 1, \ldots 4$$

we obtain

$$\gamma_{11} = (0.210 \pm 0.026) \text{ cm}^{-1}$$

or (6.30±0.80) barns/H_2O. The sum of squares divided by the number of degrees of freedom is 1.27.

When we take the equation

$$\beta_i = -\frac{S^2_{01}(i)}{\gamma_{11}} - \frac{S^2_{02}(i)}{\gamma_{22}}, \quad i = 1, \ldots 4$$

we obtain $\gamma_{22} < 0$. It can be shown that $\gamma_{22} > 0$ by definition, so we discard this result.

If we take

$$\beta_i = -\frac{S^2_{01}(i)}{\gamma_{11}}\left(1 - 2\frac{S_{02}(i)}{S_{01}(i)}\right) - \frac{S^2_{02}(i)}{\gamma_{22}}, \quad i = 1, \ldots 4$$

we obtain reasonable results, but fitting 3 parameters to only 4 measurements does not give very reliable information. Therefore, using the first of the three equations discussed, we obtain the value:

$$\gamma_{11} = (0.210 \pm 0.026) \text{ cm}^{-1} \text{ for } H_2O \text{ at } 23\,^\circ\text{C}.$$

DISCUSSION

The above result may be compared with γ_{11} derived from diffusion cooling measurements on water. There are very large discrepancies between various authors regarding diffusion cooling coefficients in water, and the γ_{11} derived from these measurements lie in the range 0.4 to 0.8 cm^{-1}, which is in marked disagreement with the present results. In order to derive γ_{11} from the diffusion cooling coefficient one has to calculate the value of t_{01} and for H_2O it is calculated assuming $D(E) \sim E^{1/2}$. In order to examine whether the large discrepancy is due to the above assumption, we have calculated t_{01} by numerical integration of $D(E)$ using

the Radkowsky prescription [12] but the difference in value found for t_{01} was only 5%. The diffusion coefficient measured in the pulsed source technique is much lower than the value based on constant source measurements [2], the reason being that the geometrical buckling is probably not the correct parameter for representing the leakage from the system [13]. When the diffusion coefficient appears lower than its correct value, the value of the diffusion cooling coefficient is reduced also, and γ_{11} appears too high. This is only a rough qualitative argument.

A comparison is possible with calculated γ_{11} based on some model of the inelastic scattering of thermal neutrons in H_2O. We have taken the widely used Nelkin's model [14], and the results for 23 °C are given below (in units of cm^{-1}):

$\gamma_{11} = 0.855$
$\gamma_{12} = 0.0695$ $\gamma_{22} = 1.060$
$\gamma_{13} = 0.006$ $\gamma_{23} = 0.070$ $\gamma_{33} = 1.190$

These values are unexpected, in view of our measurements. The calculated values of β for the absorbers used, based on the above values of γ_{ij}, are small compared to the measured values. The possibility of large contributions from much higher polynomials is unlikely.

We tentatively conclude that Nelkin's model gives too high energy transfer moments, though the calculated scattering cross section by this model is in agreement with experiment. It can be shown in general from Wick's short collision time approximation [15] that the energy transfer moments are more sensitive to the details of the chemical binding of the scattering atoms than is the scattering cross section. The experimentally obtained γ_{11} is much lower than the value calculated using Nelkin's model. It seems that in the above calculation there is too high a contribution from the "hindered rotations" represented by a harmonic oscillator with a frequency ω, such that $\hbar\omega = 0.06$ eV. Very recently, there are some indications [16] that this frequency does not have the character of a harmonic oscillator and that energy transfers of $n\hbar\omega$ where $n > 1$ are not possible. The lack of agreement of results based on Nelkin's model deserves further attention.

We conclude that our method for measuring neutron thermalization parameters is feasible, at least for homogeneous systems. In cases where there is considerable coherent scattering of thermal neutrons, the function $D(E)$ is extremely complicated and the new method may serve as the only integral method for obtaining integral thermalization parameters.

It is possible that the present description of thermalization effects by a number of phenomenological parameters (like the γ_{ij}) can be utilized for the more elaborate problem of thermalization in heterogeneous systems [17].

ACKNOWLEDGEMENTS

The author wishes to thank Professor S. G. Cohen and Dr. G. Rakavy of the Hebrew University, Jerusalem, for helpful discussions.

APPENDIX

Least-squares fitting of a sum of two exponentials

By G. Rakavy* and E. Friedman

A method is described that enables a least-squares fitting of a sum of two exponentials to experimental data.

On trying to fit a linear combination of exponentials to a given series of results $f(t)$, for t_i, $i = 1, \ldots N$, where the coefficients of the combination and the decay constant are unknown, one very often finds that the usual least-squares method is inapplicable. The normal equations are not linear in the unknown parameters and one has to iterate the solution until convergence is obtained. Because of the nonorthogonal nature of the exponentials this is rarely achieved. We have used a modified method of least-squares fitting for the special case of a sum of two exponentials which avoids the difficulties usually encountered.

Given a set of experimental values $f(t)$ for t_i, $i = 1, \ldots N$, together with their standard deviations σ_i, one tries to fit it by an expression of the form

$$A_1 e^{-\lambda_1 t} + A_2 e^{-\lambda_2 t} \tag{A1}$$

In the conventional method, one tries to minimize the sum

$$Q = \sum_{i=1}^{N} \left(\frac{f(t_i) - A_1 e^{-\lambda_1 t_i} - A_2 e^{-\lambda_2 t_i}}{\sigma_i} \right)^2 \tag{A2}$$

with respect to A_1, A_2, λ_1, λ_2. In the modified method, as a first step the first N_1 experimental points are rejected and a straight line is fitted by least squares to $\log [f(t_i)]$ for $i > N_1$. When N_1 is chosen so that the goodness-of-fit criterion is fulfilled, one has initial values $A_1^{(0)}$ and $\lambda_1^{(0)}$ (denoting by λ_1 the smaller of the decay constants) together with standard deviations $\Delta A_1^{(0)}$ and $\Delta\lambda_1^{(0)}$.

The next step is to minimize the following sum

$$Q' = Q + \left(\frac{A_1 - A_1^{(0)}}{\Delta A_1^{(0)}} \right)^2 + \left(\frac{\lambda_1 - \lambda_1^{(0)}}{\Delta \lambda_1^{(0)}} \right)^2 \tag{A3}$$

with respect to A_1, A_2, λ_1, λ_2. This step is performed by iterations as in the conventional method. It seems that divergence problems cannot arise here, as Q' will increase when A_1 and λ_1 depart greatly from the values $A_1^{(0)}$ and $\lambda_1^{(0)}$, and so A_1 and λ_1 cannot diverge to unreasonable values as often happens in the conventional method. This step is a conventional least-squares fitting for A_1, A_2, λ_1, λ_2, except that we use the results of the first step as if they were separate experimental results.

The method may be regarded as follows: the problem is to fit a sum of two exponentials to a given set of experimental results. As this is not possible using the conventional method, we look for some additional information that can be utilized in avoiding the convergence difficulties. A possible source of additional information is a period-meter that can be used for

* Hebrew University of Jerusalem.

determining the long time behaviour of $f(t)$. In such a case we obtain $\lambda_1^{(0)} \pm \Delta\lambda_1^{(0)}$ for the smaller decay constant, and $A_1^{(0)} \pm \Delta A_1^{(0)}$ for the amplitude. The experimental values are $f(t_i) \pm \sigma_i$, $i = 1 \ldots N$, $A_1^{(0)} \pm \Delta A_1^{(0)}$ and $\lambda_1^{(0)} \pm \Delta\lambda_1^{(0)}$, and the sum of squares that has to be minimized is Q'. In the present method we actually do not use any additional information besides $f(t_i), i = 1 \ldots N$, but we use the long delay time part of the data in estimating the results of a possible additional measurement. The estimated values are used to prevent divergence of the parameters. It should be emphasized that no *a priori* information is used here, and that the smaller decay constant together with its amplitude are derived from a least-squares fitting to the whole experimental values rather than to the long delay time part.

About a hundred different cases have been tested numerically and a rapid convergence to meaningful results has been obtained in each case. The ratios of the decay constants in the cases that were tested were $2 < \lambda_2/\lambda_1 < 3$, and the ratios of the coefficients were $A_2/A_1 < 0.1$.

REFERENCES

1. Von Dardel, G., and Sjöstrand, N. G., Progr. in Nuclear Energy, Ser. I, *2*, 183 (1958).
2. Beckurts, K. H., Nuc. Instr. Methods, *11*, 144 (1961).
3. Sjöstrand, N. G., Arkiv Fysik, *15*, 147 (1959).
4. Nelkin, M., Nuc. Sci. Eng., *7*, 210 (1960).
5. Hall, R. S., Scott, S. A., and Walker, J., Proc. Phys. Soc. (London), *79*, 257 (1962).
6. Friedman, E., Nuc. Sci. Eng., *14*, 420 (1962). Part of the present results have also been submitted for publication.
7. Kazarnovsky, M. V., Stepanov, A. V., and Shapiro, F. L., Proceedings of the Second International Conference on the Peaceful Uses of Atomic Energy, P/2148, Vol. 16, p. 279, United Nations (1958).
8. Singwi, K. S., Arkiv Fysik, *16*, 385 (1960).
9. Purohit, S. N., Nuc. Sci. Eng., *9*, 157 (1961).
10. Friedman, E., and Gorni, S., Nuc. Instr. Methods, *23*, 155 (1963).
11. Meadows, J. W., and Whalen, J. F., Nuc. Sci. Eng., *9*, 132 (1961).
12. Reactor Physics Constants, USAEC Report ANL-5800, 121 (1958).
13. Lopez, W. M., and Beyster, J. R., Nuc. Sci. Eng., *12*, 190 (1962).
14. Nelkin, M., Phys. Rev., *119*, 741 (1960).
15. Wick, G. C., Phys. Rev., *94*, 1228 (1954).
16. Pelah, I., and Imry, J., Israel AEC Report IA-875 (1963).
17. Weiss, Z., Nukleonika, *6*, 243 (1961).

ABSTRACT—RÉSUMÉ—АННОТАЦИЯ—RESUMEN

A/509 Israël

Etudes sur la thermalisation des neutrons par une variante de la technique de la source pulsée

par E. Friedman

La technique classique de la source pulsée a été largement utilisée comme source d'information sur les processus de thermalisation des neutrons dans les dispositifs de modération. Cette information est déduite du « coefficient de refroidissement par diffusion » obtenu dans les expériences sur les sources pulsées. Il y a de grandes différences entre les résultats donnés par les différents auteurs, et une partie des limitations théoriques à l'utilisation des mesures de « refroidissement par diffusion » comme source de valeurs de thermalisation ont été formulées en 1958.

Une méthode nouvelle pour mesurer les paramètres de la thermalisation des neutrons qui avait été proposée pour des raisons théoriques fut vérifiée expérimentalement au cours du présent travail. La théorie en est étendue, et les résultats sont présentés dans une forme bien définie. L'expérimentation fut faite sur H_2O, parce que cette méthode, dans sa forme actuelle, est très convenable pour l'étude des systèmes homogènes dans lesquels de fort absorbeurs « non en $1/v$ » peuvent être dispersés.

Le montage expérimental est décrit et des détails sont donnés sur l'arrangement géométrique utilisé pour la suppression de quelques-uns des « modes harmoniques » plus élevés. Des détails sont donnés sur deux méthodes spéciales d'analyse des résultats expérimentaux. Ces méthodes permettent l'utilisation des données prises à des délais assez courts après l'explosion des neutrons rapides.

Les paramètres de thermalisation dans la formulation sont:

$$\gamma_{ij} = \int_0^\infty \int_0^\infty \frac{E}{T^2} e^{-E/T} \Sigma_s(E \to E') \left[L_i^{(1)}\left(\frac{E}{T}\right) - L_i^{(1)}\left(\frac{E'}{T}\right) \right] L_j^{(1)}\left(\frac{E}{T}\right) dE dE'$$

où T est la température du système en unités d'énergie, E est l'énergie d'un neutron, $\Sigma_s(E \to E')$ est la section efficace macroscopique pour la diffusion d'un neutron de l'énergie E dans un intervalle unité d'énergie à E', et $L_i^{(1)}\left(\frac{E}{T}\right)$ sont les polynomes associés de Laguerre de premier ordre et de degré i. Les résultats pour H_2O à 23 °C peuvent être représentés par $\gamma_{11} = (0{,}210 \pm 0{,}026)$ cm^{-1}. Ce résultat diffère d'une manière significative des résultats obtenus par les mesures par « refroidissement par diffusion », et des valeurs calculées sur la base du modèle de Nelkin pour H_2O. Ces différences sont discutées ainsi que la praticabilité de cette méthode pour l'étude des divers systèmes.

A/509 Израиль

Изучение термализации нейтронов с помощью модификации метода пульсирующего источника

Е. Фридман

Обычная импульсная методика была широко использована для получения информации о процессах термализации нейтронов в блоке замедлителя. В опытах с импульсным источником был определен коэффициент «диффузионного охлаждения». В результатах, приведенных различными авторами, имеются существенные различия, хотя еще в 1958 году были сформулированы некоторые теоретические ограничения в отношении использования измерений коэффициентов «диффузионного охлаждения» как источника данных о термализации.

В настоящей работе новый метод измерения параметров термализации нейтронов, предложенный на основании теоретических соображений, был проверен экспериментальным путем. Это дало возможность уточнить теорию и представить результаты в сжатой форме. Опыт проводился с водой, поскольку этот метод в его существующем виде очень хорошо подходит для изучения гомогенных систем, в которых могут быть диспергированы сильные «не $1/v$-поглотители».

Описывается экспериментальное устройство и приводятся конкретные данные по геометрическому решению, позволяющему устранить влияние ряда «высоких гармоник». Излагаются конкретные данные о двух специальных методах анализа экспериментальных результатов. Эти методы позволяют использовать данные, полученные за довольно короткие периоды времени после вспышки быстрых нейтронов.

Параметры термализации описываются формулой

$$\gamma_{ij} = \int_0^\infty \int_0^\infty \frac{E}{T^2} e^{-E/T} \Sigma_s (E \to E') \times$$

$$\times \left[L_i^{(1)}\left(\frac{E}{T}\right) - L_i^{(1)}\left(\frac{E'}{T}\right) \right] \cdot L_j^{(1)}\left(\frac{E}{T}\right) dE\, dE',$$

где T — температура системы в единицах энергии, E — энергия нейтрона, $\Sigma_s(E \to E')$ — макроскопическое эффективное сечение для рассеяния нейтрона с энергией E в единичный интервал при энергии E', а $L_i^{(1)}\left(\frac{E}{T}\right)$ — присоединенные полиномы Лагерра первого порядка степени i. Результаты для воды с температурой 23 °С могут быть представлены как $\gamma_{11} = (0{,}210 \pm 0{,}026)$ *см*$^{-1}$. Этот результат существенно отличается от результатов, полученных в измерениях коэффициентов «диффузионного охлаждения», и от значений, рассчитанных на основе модели Нелкина для воды. Обсуждаются как эти различия, так и практическое значение этого метода для изучения разных систем.

A/509 Israel

Estudios de termalización de neutrones con una técnica modificada de fuente pulsada

por E. Friedman

La técnica clásica de fuente pulsada se ha empleado ampliamente como fuente de información en los procesos de termalización de neutrones en medios moderadores. Esta información se deriva del coeficiente de « enfriamiento por difusión » obtenido en experiencias con fuente pulsada. Hay grandes discrepancias entre los resultados dados por distintos autores; algunas de las limitaciones teóricas del empleo de medidas de « enfriamiento por difusión » como fuente de datos de termalización fueron formuladas en 1958.

En este trabajo se ha comprobado experimentalmente un nuevo método para medidas de parámetros de termalización de neutrones cuyos fundamentos teóricos fueron ya propuestos. Se extiende la teoría y se presentan resultados en forma compacta. La experiencia se realizó con H_2O, ya que el método, en su forma actual, es más adecuado para el estudio de sistemas homogéneos en los que pueden dispersarse absorbentes que se aparten mucho de la ley $1/v$.

Se describe el equipo experimental y se dan detalles de la disposición geométrica empleada para eliminar algunos armónicos de orden superior. Se dan detalles de dos métodos especiales para el análisis de resultados experimentales. Estos métodos permiten emplear datos tomados con un retardo muy pequeño después del impulso de neutrones rápidos.

Los parámetros de termalización de neutrones en esta formulación son:

$$\gamma_{ij} = \int_0^\infty \int_0^\infty \frac{E}{T^2} e^{-E/T} \Sigma_s(E \to E') \left[L_i^{(1)}\left(\frac{E}{T}\right) - L_i^{(1)}\left(\frac{E'}{T}\right) \right] L_j^{(1)}\left(\frac{E}{T}\right) dE dE'$$

donde T es la temperature del sistema en unidades de energía, E es la energía de un neutrón, $\Sigma_s(E \to E')$ es la sección eficaz macroscópica de dispersión de un neutrón de energía E para pasar a un intervalo unidad de energía alrededor de E', y $L_i^{(1)}\left(\frac{E}{T}\right)$ son los polinomios asociados de Laguerre de orden uno y de grado i. Los resultados para H_2O a 23 °C pueden ser descritos por $\gamma_{11} = (0{,}210 \pm 0{,}026)$ cm^{-1}. Este resultado difiere significativamente de los resultados obtenidos por medidas de « enfriamiento por difusión » y de los valores calculados basándose en el modelo de Nelkin para H_2O. Se discuten estas discrepancias, así como la posibilidad de emplear este método para el estudio de sistemas diferentes.

Reactor physics research in United Kingdom universities

By W. Murgatroyd,* P. J. Grant,** N. S. Grassam,*** M. J. Harris,****
J. Walker***** and H. W. Wilson******

The paper outlines the reactor physics research carried out since the last Geneva Conference in the Universities of London (Imperial and Queen Mary Colleges), Birmingham, Manchester and Southampton, and at the Scottish Universities Research Reactor Centre.

Much of the effort has been devoted to studying the potentialities of measurements on sub-critical assemblies and on small amounts of pure moderator, using pulsed and steady source techniques. For example, one group has established criteria for the validity of control rod measurements in a graphite sub-critical assembly, another group is investigating the effect of size upon spectrum in light water/natural uranium lattices, and a third group is concerned with measurements on irregularly shaped and voided assemblies. One group is developing improved forms of reactor oscillator and investigating the use of correlation techniques in reactor diagnostics.

The work of most of these groups has been limited by the low neutron fluxes available at universities, a limitation which will be removed as the university reactors now authorized come into operation.

IMPERIAL COLLEGE (UNIVERSITY OF LONDON)

The Nuclear Power Group at Imperial College is part of the Mechanical Engineering Department and has been in existence since October 1957. Since then an increasing effort has been devoted to research and there are currently twelve research students engaged in reactor physics studies. Five of these are working for the Ph.D. degree and seven for the M.Sc.

Exponential assembly experiments

One of the major items of equipment provided in connexion with the diploma course was a graphite moderated natural uranium sub-critical assembly. Several research projects have been carried out with this; the most extensive and detailed has been a study of control-rod effectiveness. This work may be roughly divided into three stages:

1. Demonstration of the validity of the technique so that it may be used in place of a critical system to test theoretical predictions about control rod worth.
2. Investigation of the effect of the control rod environment on its effectiveness in order to explain discrepancies between theory and experiment.
3. Investigation of the interactions between control rods. The first two stages of this work have already been described [1,2] and will not be discussed here. The interaction effects between control rods were examined by measuring the worth of:
   (*a*) One control rod as a function of position in the stack.
   (*b*) Two or four control rods as a function of their separation when placed symmetrically in the stack.

The experiments were carried out both in fuelled and in unfuelled systems in order to separate the effects due to thermal and epithermal neutrons. The results were analysed on a two-group model using the normal method [3] modified to take account of the square outer boundary of the system.

If the control rod extrapolation lengths were determined from the single-rod experiments it was found that the theory satisfactorily predicted the behaviour of the two- or four-rod systems. Minor discrepancies were found for the unfuelled stack but these were attributed to the persistence of flux harmonics up to quite large distances from the source pedestal. A typical set of results is shown in Fig. 1.

Other work with the exponential stack has been the study of streaming effects in large air channels in fuelled and unfuelled systems and the use of variable width slab loadings of fuel to study reflector effects.

Slowing down of neutrons

Work is in progress on the slowing down of neutrons in various media. For this purpose a technique has been developed which shows some advantages in speed and sensitivity over conventional foil activation methods. It consists of detecting neutrons by a ^{6}Li glass scintillation counter covered with cadmium and measuring the change in count rate produced by additionally covering the scintillator with a suitable absorbing foil, for example indium. The method has so far been applied to the measurement of the age of neutrons from radioactive sources such as polonium–beryllium [4] but a 2 MeV electrostatic generator has

* Queen Mary College, University of London.
** Imperial College, University of London.
*** University of Southampton.
**** University of Manchester.
***** University of Birmingham.
****** Scottish Universities Research Reactor Centre.

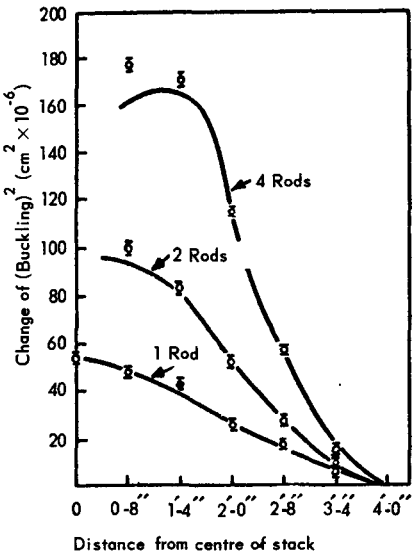

Figure 1. Buckling changes produced by one, two or four boron carbide control rods symmetrically placed in a graphite and natural-uranium sub-critical assembly

recently been installed and an extensive programme of slowing-down measurements is in hand.

Neutron diffusion

A programme of measurement of diffusion parameters by pulsed neutron methods has been started, using the electrostatic generator. Measurements of the diffusion length in water as a function of temperature have been carried out using an antimony–beryllium neutron source [5].

With the availability in July 1964 of the 100 kW London University research reactor CONSORT [6], a study will be made of the effects of temperature gradients and discontinuities upon neutron diffusion.

QUEEN MARY COLLEGE (UNIVERSITY OF LONDON)

The experimental nucleonics research at Queen Mary College has been centred around the uranium-water sub-critical assembly which was constructed in 1959. This assembly [7] consists of a 4 ft 6 in. cube aluminium core tank in which up to 4 tons of aluminium-clad natural uranium rods, 1.2 in. diameter and 43.25 in. long, are supported vertically by a series of lattice plates. Initially a 10 curie polonium–beryllium neutron source 2.5×10^7 n/s) was used to provide the neutron flux but later measurements have been made using a SAMES neutron generator (5×10^9 n/s) either as a pulsed or steady source.

The exponential measurements on a variety of lattices (V_m/V_n ranging from 1.7 to 3.2) using resonance and $1/v$ detectors have revealed a dependence of the measured value of the buckling upon the type of detector used [8]. The pulsed neutron technique has been used to determine the mean neutron lifetime in the assemblies by measuring the fundamental mode decay constant and using the value of k_{eff} obtained by the exponential experiments [9]. The pulsed neutron technique has also been used to measure the diffusion parameters of a number of hydrogenous moderators (Table 1).

The limited neutron flux available from the present sources does not permit a comprehensive assessment of reactor lattices, and to provide higher fluxes a critical assembly is being constructed in this laboratory and will be commissioned in July/August 1964. This critical assembly is of the Argonaut type and consists essentially of the core of the UTR 100 reactor, a thermal column and a stackable concrete block shield. By operating at power levels less than 10 watts active fuel handling remains possible and yet fluxes of 10^8 n/cm^2 s are available in the internal reflector. It is proposed to measure the lattice parameters of hydrogenous-moderated assemblies by substituting sub-assemblies for the internal reflector. A slow-neutron chopper has been designed for measuring the neutron spectrum by the time-of-flight technique.

A magnetically driven two-state reactivity perturber and associated control equipment have been constructed and digital correlation equipment has been designed. This will, in the first instance, be used in connexion with the critical assembly.

Table 1. Diffusion parameters of hydrogenous moderators

Rectangular geometry

Buckling ranges: 1. 0.06~0.39 cm^{-2} Pulse: Length 90 μs
2. 0.064~0.725 cm^{-2} Repetition rate 660 pulse/s
3. 0.064~0.657 cm^{-2}

No.	Moderator	Σav	Diffusion coefficient D	Diffusion cooling coefficient C	σaH	L
		s^{-1}	cm^2 s^{-1}	cm^4 s^{-1}	mb	cm
1	H_2O	4798 ± 21	35300 ± 230	4200 ± 1 500	327 ± 2 [c]	2.73 ± 0.03 [c]
2	$C_{28}H_{58}$ [a] (paraffin wax)	6164 ± 46	26800 ± 400	2500 ± 1 100	348 ± 4 [d]	2.11 ± 0.03 [d]
3	$(C_6H_5)_2\ C_6H_4$ [b] (terphenyl)	3220 ± 70	43700 ± 600	1870 ± 1 100	—	3.69 ± 0.06 [d]

[a] ρ: 0.905 mp 60~63 °C
[b] 97.8% $C_{18}H_{14}$ + 2.2% $C_{18}H_{10}$
[c] At 22 °C
[d] At 18 °C

Reactor noise measurements have been made on the JASON [10] and DAPHNE reactors at low power and on the PLUTO reactor at high power. This work has been backed up by digital and analogue simulation of reactor noise processes, and by theoretical studies of stochastic process in reactors [11].

Research is under way to develop a novel high intensity pulsed neutron source. This consists of an inverted magnetron ion accelerator with an outer cylindrical target. With a pulsed voltage of 200 kV a neutron output of 10^{11} neutrons per pulse is predicted for the T(d,n)^{4}He reaction. The source will be used for measuring the time variation in flux spectrum using the neutron chopper.

A novel type of reactor oscillator has been used on the reactor DAPHNE at Harwell. Pulses from a detector, placed within the reactor are counted by four separate pulse-counting channels during each of the four quadrants of motion of the reactor oscillator. Simple arithmetical operations on these four counts enable the amplitude and phase of the neutron flux oscillation at the detector to be determined. The advantages of the system are its accuracy, its ability to measure small signals, its freedom from the effects of slow drifts in reactor power.

Measurements were made on the reactor DAPHNE over a range of frequencies of 1 c/s to 10 c/s and show that a 3% amplitude of modulation could be measured within approximately 1/3% of this 3% and the phase angle could be measured to within approximately 2 minutes of arc. The measurements confirmed the existence of neutron wave effects in this reactor and also showed effects which, at the moment, are attributed to the heterogeneity of the reactor core and the asymmetry of the reactor oscillator.

UNIVERSITY OF MANCHESTER

Pulsed-source measurements

The thermal neutron absorption cross section of hydrogen has been determined by measuring the decay constants of a range of water sample sizes and extrapolating to find the decay constant, $v\Sigma_a$ at infinite size, or zero buckling. A range of low values of buckling, 0.08 to 0.30 cm^{-2}, was therefore used, rendering more accurate the extrapolation to zero buckling. The presence of high harmonics in the modes of decay was thus much more likely. Pulse decays were therefore followed at an array of points distributed axially and radially throughout the cylindrical water sample. Harmonic analysis then verified that the technique used in all subsequent measurements were such as clearly to isolate the fundamental mode decay.

A value was thus obtained for the 2200 m/s thermal neutron absorption cross section of hydrogen of 328 ± 4 mb, in good agreement with most previous results by whatever method. The 2200 m/s cross sections of chlorine, boron and cadmium were then measured by comparing the fundamental mode decays of solutions containing these elements with those of pure water.

The values obtained for chlorine, 32.84 ± 0.33 barns, and boron, 745 ± 10 barns, are in general agreement with the results of other workers and methods. Non $1/v$ absorbers, such as cadmium, pose a more difficult problem since they cause distortion of the thermal neutron spectrum. In this case the effective σ_a was determined at each of several cadmium solution concentrations. The zero concentration (no distortion) value of σ_a was thus found by extrapolation to be 2360 ± 30 barns at 2200 m/s. Santandrea *et al.* [12] have investigated the variation of system decay constant at various bucklings as a function of cadmium concentration. Their work indicates a $d\sigma_{eff}/dB^2_g$ of about -1100 barns cm^2 and hence a correction to the present result of $+85$ barns, giving excellent agreement with the BNL 325 average value of 2450 ± 50 barns.

It thus appears that for non $1/v$ absorbers, determination of the effective cross section at zero absorber concentration over a wide range of bucklings is required before an accurate result can be obtained.

In parallel with the above, and by similar multiple point measurements, a study has been made of the relative amplitude and separate decay constants of the harmonics present in a cylindrical tank of water somewhat larger than is usual in this type of study, so as to ensure a high harmonic content.

Only fundamental, second and third order harmonics were found to be significantly present but it was possible to measure their decay constants to within 2% accuracy. These, plotted on the usual α_{11}/B^2_{11} graph, fell on the same curve as the fundamental mode points.

This experiment will be extended so as to stimulate the production of large amplitude higher harmonics and improve detection and timing efficiency. It is then hoped to measure the decay constants, $\alpha_{l,m}$ at values of $B_{l,m}{}^2$ where diffusion cooling might be observed. It would be interesting to compare such results with α_{11}/B^2_{11} curves.

Uranium–water exponential

A programme of preliminary exponential measurements has been carried out on a water moderated subcritical assembly, fuelled with reject Calder elements with fins removed. The driving source has been either the tritiated target of the department's deuteron accelerator or four 1.5 curie Sb–Be units.

It is intended that this facility will play a part in the department's proposed research programme into the kinetic behaviour of water-moderated reactors. Voids formed by boiling have a shape and distribution depending strongly on the initial conditions and the method of heating. Void coefficients of reactivity depend on the void distribution, but for convenience have usually been measured with uniformly distributed voids. Preliminary work on this aspect of voidage will be carried out on the exponential, although at a later stage it may be necessary to use a reactor thermal column as a driving source, especially if, as is likely, fine structure studies are eventually envisaged.

Integral techniques

Effective neutron temperature in boric acid solutions at room temperature have been measured by spectrum measuring integral techniques. The results demonstrate the expected enhancement of neutron temperature and are being compared with theory and other measurements. A comprehensive study of the possibilities and limitations of the integral technique is being made with this work.

Joint reactor

The Manchester/Liverpool Universities' Joint Reactor Project at Risley, Lancs., due for completion in the spring of 1964, will greatly widen the scope of our experimental reactor physics investigations. The extra thermal neutron flux will lead to much more accurate exponential and flux fine structure experiments so that, for instance, the progressive substitution, zoned exponential method could be studied and applied to the investigation of voidage effects. Neutron spectrum studies by both integral and chopper techniques, and solid state studies using cold neutrons will also be facilitated by the higher fluxes. Neutron lifetime studies using the pulsed source, modulated source, noise analysis, "rod drop" and "source jerk" techniques are of particular interest.

UNIVERSITY OF SOUTHAMPTON

A nuclear engineering laboratory was set up in the Department of Mechanical Engineering in 1961. The main facility is a light water natural uranium subcritical assembly using 1.0 in.-diameter fuel rods arranged vertically on a pitch giving a 1.67 water to uranium ratio. Polonium–beryllium sources are used to supply neutrons.

During 1963, a 150 kV SAMES type J positive ion accelerator was coupled to the assembly so that neutrons may be produced by bombarding either deuterium or tritium targets with deuterons, giving a maximum fast neutron output of about 10^{10} n/s. The core is now surrounded by a water shield approximately 5 ft thick. For neutron detection apart from foils and gas counters, small ^{10}S and ^{6}Li phosphors coupled by 4 ft Perspex light guides to scintillation counters are now being used. With the facilities now fully installed and commissioned, research programmes as well as teaching and project work are under way. The research group is particularly interested in the pulsed neutron source technique for measuring the buckling of an assembly, and programmes of experiments to determine the effect of irregularities in the boundary shape of the core and the effect of voids in the core are in progress. The basis of the method is to determine the fundamental mode decay constant (α) of the thermal neutron flux following a burst of fast neutrons injected into a core, for a series of cores of simple geometric shape for which the buckling can be reliably calculated. The buckling of cores with irregular boundaries can then be deduced by the measurement of their decay constant (α). A high stability multi-channel analyser is now available for this experiment. A future research development is to use the accelerator for neutron activation analysis.

THE SCOTTISH RESEARCH REACTOR CENTRE

The Centre, which provides training and research facilities in the reactor field to the universities of Scotland and Northern Ireland (and also to other institutions) has only recently come into use, having been officially opened on the 13th November 1963, although occupation of the building took place two months previously. As a result, there is not yet a great deal to report, but work planned or being carried out in the neutron field will be described briefly below. The reactor itself is a 100 kW UTR-100 built by Advanced Technology Laboratories, and came into operation on 24 June 1963. The Centre includes laboratory, workshop, lecture, library and office accommodation.

Neutron diffraction

A semi-automatic neutron spectrometer of fairly low resolution (0.8° half angle at the sample, though this can be varied) is being set up mainly for crystal structure analysis by groups interested in this field in the Universities of Edinburgh, St. Andrew's and Glasgow. It may also be used for cross section and spectrum measurement.

Cold neutron studies

These will be carried out by a team from St. Andrew's University to investigate the structure of liquid helium and of crystals at low temperature.

Neutron focusing

The technique of neutron focusing by use of unhomogeneous magnetic fields suggested by Edinburgh University will be used to provide a highly polarized, partially monochromatic, focused neutron beam for neutron physics and cold neutron studies.

Fission

An investigation of the production of tritons is being carried out by a staff member of the Reactor Centre, in collaboration with Edinburgh University. It is hoped that results will be available by the time of the Conference. Further studies of the fission process by Centre staff are planned.

Reactor noise

Measurements of lifetime by reactor noise analysis are under way and, again, it is hoped that results will be available by September. The particular interest relates to the value of lifetime as a function of geometry and reactivity in the divided core design of the UTR-100 reactor.

Other experiments

Glasgow University and Reactor Centre Staff have started work on an investigation of the effects of radiation on molecules of biological interest by field ionization in-core mass spectrometry. Also well under way are a number of experiments using activation and tracer analysis in the fields of science, medicine and engineering.

UNIVERSITY OF BIRMINGHAM

Work in neutron and reactor physics has been in progress in the Physics Department at the University of Birmingham on an increasing scale since 1956, and has benefited considerably from close association with the large programmes in nuclear and accelerator physics, which were well established even at that time. The major experiments to date have been concerned with the application of the pulsed-source technique to pure moderators and to multiplying assemblies; some of the more recent results are summarized here. In addition, relevant experiments are now in progress on the inelastic scattering of very low energy neutrons (using the 5 MW HERALD reactor at AWRE, Aldermaston), and on fast neutron reactions such as the non-elastic processes in beryllium.

Pulsed-source measurements for neutrons in water, Dowtherm and graphite

Extrapolation lengths in water and Dowtherm

Pulsed-source measurements on neutrons in small volumes of water of different shapes have been reported already [13] and it was pointed out that uncertainties existed in the knowledge of extrapolation lengths. Extrapolation length measurements on pulsed systems have now been made for water and Dowtherm A (Thermex) at 20 °C [14]. The liquids were contained in cubic boxes of side 4 in. or 7 in. made from cadmium sheet bonded to aluminium [15]. The counts recorded by a small scintillator were corrected for the influence of the detector on the thermal neutron decay constant but a more refined procedure for correction perturbations is being developed; the effect of the detector light guide on the decay constant was shown experimentally to be negligible. Spatial harmonic analysis of flux plots was used to give the extrapolation lengths shown in Table 2, and the effect of flux distortion near the boundary was investigated by successive removal of the outer points.

Table 2. Extrapolation lengths for water and Dowtherm (20 °C)

Material	z-dimension physical cm	B_z^2 cm^{-2}	d_z cm
Water . . .	10.20	0.082	0.345 ± 0.015
	17.65	0.029	0.380 ± 0.04
Dowtherm . .	10.20	0.080	0.450 ± 0.02
	17.65	0.028	0.480 ± 0.03

Table 3. Asymptotic decay constants for graphite

Normalized to a density of 1.63 gcm^{-3}
Extrapolation length used: 1.85 cm

Block size in.	Buckling cm$^{-2} \times 10^{-3}$	Decay constant s^{-1}
$32 \times 32 \times 40$	3.63	817.0 ± 3.1
$32 \times 32 \times 32$	4 10	907.7 ± 3.3
$32 \times 32 \times 24$	5.10	1088.8 ± 6 5
$24 \times 24 \times 32$	6 09	1259.9 ± 3.1
$24 \times 24 \times 24$	7.09	1435.4 ± 5.1
$32 \times 24 \times 16$	8.76	1692.4 ± 7.2
$24 \times 24 \times 16$	9.75	1835.8 ± 9.4
$32 \times 16 \times 16$	11.42	2027.6 ± 20.8^a
		2019.7 ± 33.8^b
$24 \times 16 \times 16$	12.42	2131.8 ± 24.7^a
		2150.6 ± 27 0^b
$16 \times 16 \times 16$	15.08	2450 ± 100^a

[a] Measured with an external counter.
[b] Measured with an internal counter.

Thermalization measurements in graphite [16]

Rectangular parallel piped blocks of nuclear quality graphite up to 32 in. $\times$40 in. in size were assembled from sub-units and covered in cadmium sheet. Internal and external measurements were made on nuetrons supplied from a pulsed accelerator with pulse lengths from 500 μs to 1500 μs, and repetition periods from 6 to 12 milliseconds. A time analyser was used to measure the decay constants of the asymptotic energy and spatial distributions of neutrons in a range of graphite blocks. The time required for the neutrons to obtain an asymptotic energy distribution was determined by combining the analyser with the classical silver absorber technique in which counting rates are taken by a counter with and without a silver shield. The results made it apparent that long delays of 4 ms or more in the case of small bucklings are required to establish approximately asymptotic conditions and are therefore necessary before extraction of diffusion parameters from decay constants. The asymptotic decay constants for different bucklings are shown in Table 3 and have been normalized to a mean density of 1.63 gcm^{-3}; the densities of individual blocks varied by up to 4%.

The information in Table 3 can be used to give the coefficients in the relation between decay constant and buckling.

$$\lambda = \overline{\nu\Sigma_a} + \overline{D_0}B^2 - CB^4$$

and these are shown in Table 4 for different ranges of bucklings. The table gives results of the three term (up to B^4) analysis only.

Table 4. Diffusion parameters for graphite

B^2 cm$^{-2} \times 10^{-3}$	$\overline{\nu\Sigma_a}$ s^{-1}	D_0 cm^2 s$^{-1} \times 10^5$	C cm^4 s$^{-1} \times 10^6$
3.63 – 7.09	123 ± 57	1.98 ± 0.23	1.97 ± 2.16
3.63 – 9.75	75.7 ± 24.4	2.18 ± 0.08	3.86 ± 0.66
3.63 – 12.42	53.6 ± 19.6	2.26 ± 0.06	4.56 ± 0.47
3.63 – 15.08	55.4 ± 18.1	2.26 ± 0.06	4.51 ± 0.42

Pulsed-source measurements with a uranium–water sub-critical assembly

A sub-critical assembly of natural uranium bars in light water has been used with a pulsed source to provide decay constants as a function of buckling. Experimental results for four different lattice pitches have been given [17] and compared with calculations based on the four-group compression of the MUFT-SOFOCATE information, [18] and [19]. Time-dependent cadmium ratios were presented for the detector placed at a third harmonic node in one lattice to indicate the time required after the end of the neutron burst to establish an approximately equilibrium spectrum. Cadmium ratio measurements, analysed into spatial harmonics, have now been made at several points in a different lattice, 1.9 in. pitch, and the results are in broad agreement with those reported for the 1.71 in. pitch; there are small changes in the absolute values of the cadmium ratios but the behaviour with time is very similar. Decay constants for the 112 harmonics have also been added for some lattices to the curves of decay constant against buckling but no significant changes have been demanded in the curves given earlier.

Theoretical studies of neutron thermalization

Decay constants and energy spectra in pulsed systems

A numerical method has been used to solve the Boltzmann diffusion equation for a pulsed assembly. For the case of water at 20 °C both the gas kernel ($H=1$) and the effective width kernel [20] have been used and results have been obtained showing the variation of the fundamental and higher eigenvalues (decay constants) with the size of the system and the amount of non $1/v$ absorber. The corresponding energy spectra have also been calculated and the thermalization times were found to be 3.5 μs from the gas kernel and 4.1 μs from the effective model width. The fundamental decay constant is shown in Fig. 2 as a function of buckling for both models and compared with experimental results. P_3 solutions have recently been obtained and show that the differences between experiment and "effective width" theory, shown by Fig. 2 at high bucklings are largely due to the neglect of transport effects and not to limitations of the scattering kernel.

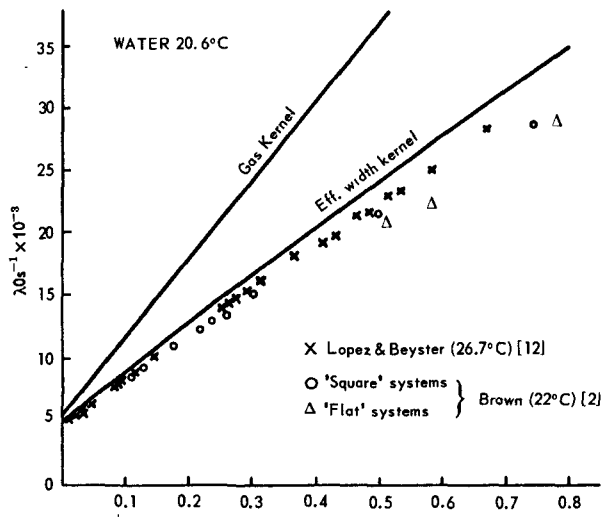

Figure 2. Decay constant-buckling relationship

Transport and energy behaviour near boundaries

The Milne problem [21] was solved in the two-group approximation using the method initially applied to the one-velocity problem by Case *et al.* [22]. The method was generalized to cover energy dependence using a degenerate series representation of the scattering kernel [23]. It was found that the solution could be approximately divided into asymptotic, rethermalization and transport terms although each have a certain interdependence. Numerical results have been obtained for beryllium to compare the diffusion theory and transport theory treatments.

ACKNOWLEDGEMENTS

The universities have been greatly assisted in developing research schools in reactor physics by the Department of Scientific and Industrial Research and the United Kingdom Atomic Energy Authority.

REFERENCES

1. James, C. G. and Till, C. E., Proc. Roy. Soc., *A269*, 66 (1963).
2. James, C. G. and Grant, P. J., IAEA Symposium on Exponential and Critical Experiments, Amsterdam (1963).
3. Codd, J. and Rennie, C. A., UKAEA report AEEW R/R 818 (1962).
4. Rathur, M. A. J. and Grant, P. J., Brit. J. Appl. Phys. (1964), (in press).
5. Besant, C. B. and Grant. P. J., Brit. J. Appl. Phys. (1964), (in press).
6. Kay, J. M., Grant, P. J., James, C. G. and Vaux, R., Conference on the Programming and Utilization of Research Reactors. IAEA (1961).
7. Murgatroyd, W., Mansfield, W. K. and Kim, J. M., *The Queen Mary College Uranium-Water Sub-Critical Assembly*, Nuclear Engineering (October 1959).
8. Mansfield, W. K. and Kim, J. M., *Exponential Experiments with Water and Natural Uranium Lattices*, IAEA Symposium on Exponential and Critical Experiments, Amsterdam (1963).
9. Kim, J. M., *Static and Dynamic Measurements of Uranium-Water Lattices*, Ph.D. Thesis, University of London. (To be published.)
10. Kemeny, L. G., *Random Fluctuations in a Nuclear Fission Reactor*, Nature, *189*, 130–131 (1961).
11. Kemeny, L. G. and Murgatroyd, W., *Stochiastic Models for Fission Reactors*, University of Florida Conference (November 1963).
12. Santandrea, E., *et al.*, Proceedings of the Second International Conference on the Peaceful Uses of Atomic Energy, P/1372, Vol. 16, p. 265, United Nations (1958).

13. Hall, R. S., Scott, S. A. and Walker, J., Proc. Phys. Soc., *79*, 257 (1962).
14. Brown, J. B. C., Ph.D. Thesis, University of Birmingham (1963).
15. Brown, J. B. C. and Hall, R. S., J. Sci. Instr., *38*, 381 (1961).
16. Serdula, K. J., Ph.D. Thesis, University of Birmingham (1963).
17. Gibson, I. H. and Walker, J., *Exponential and Critical Experiments*, Vol. 1, p. 469, IAEA, Vienna (1964)
18. Ombrellaro, P. A., USAEC report WAPD-TM-63.
19. Amster, H. J., USAEC report WAPD-TM-67.
20. Egelstaff, P., UKAEA report AERE NP/Gen. 29.
21. Davison, B., *Neutron Transport Theory*, Oxford University Press.
22. Case, K., De Hoffman, F. and Palczek, G., *Introduction to the Theory of Neutron Diffusion*, USAEC.
23. Corngold, N., Michael, P. and Wollman, W., Nuclear Sci. Eng., *15*, 13 (1963).
24. Lopez, W. M. and Beyster, J. R., Nuclear Sci. Eng., *12*, 190 (1962).

ABSTRACT—RÉSUMÉ—АННОТАЦИЯ—RESUMEN

A/564 Royaume-Uni

Recherches sur la physique des réacteurs dans les universités du Royaume-Uni

par W. Murgatroyd et *al.*

Le mémoire décrit brièvement les travaux effectués et les résultats obtenus jusqu'à présent dans les universités britanniques qui s'occupent d'une façon active des recherches sur la physique des réacteurs.

La validité de l'utilisation d'un ensemble exponentiel de graphite pour les mesures de barres de commande à la place d'un système critique a, à certains égards, été confirmée à l'Imperial College (Université de Londres). Il semble que si les longueurs d'extrapolations de barres de commande sont mesurées pour une seule barre, la théorie des groupes de deux barres prédit d'une facon satisfaisante le comportement d'ensembles à deux et quatre barres. A ce College, on poursuit les travaux sur le ralentissement de neutrons en utilisant un compteur à scintillations avec verre à lithium 6 couvert de cadmium. On effectue également des mesures des paramètres de diffusion par neutrons pulsés. Le nouveau réacteur CONSORT de 100 kW de l'Université de Londres permettra d'étudier les effets des gradients de température sur la diffusion neutronique.

Au Queen Mary College (Université de Londres), des mesures sur les réseaux uranium/eau, faites en utilisant la résonance et des détecteurs $1/v$, ont révélé que le laplacien mesuré varie selon le type de détecteur utilisé. On a mesuré la vie moyenne des neutrons dans les réseaux et les paramètres de diffusion dans divers systèmes hydrogénés, en utilisant des sources pulsées. Un réacteur critique de 10 W, conçu pour l'étude des systèmes hydrogénés, est en construction. Un nouvel oscillateur de réacteur de haute précision a été mis au point au College et est utilisé sur les réacteurs de Harwell. Des études expérimentales et théoriques sur l'utilisation de la théorie stochastique des réacteurs sont également en cours, et un oscillateur stochastique binaire a été construit.

Le groupe à l'Université de Manchester étudie l'utilisation des techniques à sources pulsées pour la mesure des paramètres de diffusion et des sections efficaces d'absorption, en apportant une attention particulière a l'analyse harmonique. Des mesures de spectres neutroniques sont effectuées sur un ensemble exponentiel à eau légère et uranium naturel et sur un assemblage important de graphite. Le groupe étudie également la cinétique des systèmes modérés à l'eau, utilisant des sources pulsées et des mesures à l'état stationnaire sur des ensembles sous vide. Le réacteur commun aux Universités de Manchester et de Liverpool sera utilisé pour ce travail.

A l'Université de Southampton, un laboratoire de génie nucléaire a été établi en 1961 au département « Mechanical Engineering ». Le principal outil de recherche est un ensemble sous-critique eau légère/uranium naturel, accouplé à un accélérateur d'ions positifs de 150 kV. Le groupe de recherche s'intéresse particulièrement à l'utilisation des techniques des sources pulsées pour la mesure du laplacien d'un cœur de forme irrégulière par comparaison avec celui d'un cœur simple.

En Ecosse, les recherches sur la physique des réacteurs se font au Scottish Research Reactor Centre, où l'équipement de base est un réacteur de recherche UTR-100 de 100 kW. Il est actuellement en fonctionnement. Le programme actuel de recherches comprend le développement des spectromètres pour les analyses de structure cristalline et la détermination du spectre neutronique.

A l'Université de Birmingham les principales expériences faites jusqu'ici concernent l'application de la technique des sources pulsées à des modérateurs purs et à des ensembles multiplicateurs. De plus, des expériences sont en cours sur la diffusion inélastique de neutrons à très faible énergie et sur les réactions où interviennent des neutrons rapides tels que les processus inélastiques qui se produisent dans le béryllium.

A/564 Соединенное Королевство

Исследования по реакторной физике в университетах Соединенного Королевства

Дж. Маргатройд *et al.*

В докладе кратко описывается работа, проводимая в тех британских университетах, кото-

рые активно занимаются исследованиями в области реакторной физики.

Возможность использования для измерений эффективности регулирующих стержней графитовых экспоненциальных сборок вместо критических систем была в некоторых отношениях подтверждена в Имперском колледже (Лондонский университет). Показано, что, если измерить длину экстраполяции регулирующих стержней для случая одного стержня, двухгрупповая теория дает возможность удовлетворительным образом рассчитать поведение сборок с двумя или четырьмя стержнями. В этом колледже проводится работа по замедлению нейтронов при использовании сцинтилляционного счетчика со стеклом из Li^6, покрытого кадмием. Измеряются также диффузионные параметры с помощью импульсной техники. Новый реактор CONSORT мощностью 100 *квт* при Лондонском университете откроет возможность изучить влияние температурных градиентов на диффузию нейтронов.

В Колледже королевы Марии (Лондонский университет) измерения на уран-водных решетках с использованием резонансных и $1/v$ детекторов показали зависимость измеренной величины лапласиана от типа используемого детектора. При помощи импульсных источников измерялись средняя продолжительность жизни нейтронов в этих решетках, а также диффузионные параметры в разных водородсодержащих системах. Строится критический реактор мощностью 10 *вт*, сконструированный для изучения водородсодержащих систем. В колледже был сконструирован новый тип точного реакторного осциллятора, который используется на реакторах в Харуэлле. Проводятся также теоретические и экспериментальные исследования по применению стохастической теории реакторов, для чего был постороен сдвоенный стохастический осциллятор.

Исследовательская группа при Манчестерском университете изучает применение импульсных источников для измерения параметров диффузии и сечений поглошения, уделяя особое внимание гармоническому анализу. Проводятся измерения нейтронных спектров на экспоненциальной сборке из природного урана и обычной воды, а также на большой графитовой сборке. Исследовательская группа изучает также кинетику систем с водяными замедлителями, используя для этого импульсную технику и стационарные измерения на сборках с пустотами. Проведению этой работы в большой мере будет способствовать сооружение реактора Манчестерского и Ливерпульского университетов.

При университете в Саутгемптоне на инженерно-механическом отделении в 1961 году была создана лаборатория по ядерной технике. Исследования проводятся в основном на подкритической сборке на природном уране с водой, а также на ускорителе положительно заряженных ионов на 150 *кв*. Исследовательская группа обращает особое внимание на применение методов пульсирующих источников для измерения лапласиана активных зон неправильной формы по сравнению с простыми формами.

В Шотландии исследования в области реакторной физики сосредоточены в Шотландском исследовательском реакторном центре, в котором основным оборудованием является исследовательский реактор UTR-100 мощностью 100 *квт*. Он уже введен в строй. Исследовательская программа включает разработку кристаллических спектрометров для анализа кристаллической структуры и определения спектров нейтронов.

В Бирмингамском университете проведенные до настоящего времени эксперименты касаются главным образом применения методики импульсных источников к чистым замедлителям и размножающим сборкам. Кроме того, проводятся эксперименты по неупругому рассеянию нейтронов очень малой энергии и реакций с быстрыми нейтронами, например неупругих процессов в бериллии.

A/564 Reino Unido

Investigación de la física de reactores en las Universidades del Reino Unido

por W. Murgatroyd et al.

Esta memoria describe someramente el trabajo que se está realizando y los resultados obtenidos hasta ahora en las Universidades británicas que se dedican activamente a la investigación de la física de reactores.

En el Imperial College de la Universidad de Londres se han confirmado algunos aspectos de la validez del empleo de una instalación exponencial, en lugar de una crítica, para medidas de la eficacia de barras de control. Si se miden las longitudes de extrapolación de una barra única, es posible, al parecer, predecir satisfactoriamente el comportamiento de sistemas de dos y cuatro barras mediante la teoría de dos grupos neutrónicos. En este centro se está investigando la moderación de neutrones mediante el uso de contadores de centelleo de ^6Li recubierto de cadmio. También se están llevando a cabo medidas de parámetros de difusión con técnicas de neutrones pulsados. El reactor CONSORT de 100 kW de la Universidad de Londres permitirá estudiar los efectos de los gradientes de temperatura sobre la difusión de neutrones.

En el Queen Mary College de la Universidad de Londres se han llevado a cabo medidas en redes de uranio-agua con detectores $1/v$ de resonancia que han puesto de manifiesto que la laplaciana medida depende del tipo de detector utilizado. Se han medido vidas

medias de los neutrones y parámetros de difusión en varios sistemas hidrogenados usando fuentes pulsantes. Está en construcción un reactor crítico de 10 W diseñado para el estudio de sistemas hidrogenados. Se ha desarrollado un nuevo tipo de oscilador que se usará en los reactores de Harwell. También se están llevando a cabo estudios teóricos y experimentales sobre la aplicación de la teoría estocástica de reactores.

El grupo de la Universidad de Manchester está estudiando la aplicación de técnicas de fuente pulsante a las medidas de parámetros de difusión y de secciones eficaces de absorción, prestando especial atención al análisis de armónicos. Se están haciendo medidas de espectros neutrónicos en un sistema exponencial de uranio natural y agua ligera y en un gran bloque de grafito. Este grupo también está estudiando la cinética de sistemas moderados por agua, con técnicas de fuente pulsante, y el estado estacionario en sistemas con huecos. El Manchester-Liverpool Joint Reactor contribuirá mucho a este trabajo.

En la Universidad de Southampton se estableció un laboratorio de ingeniería nuclear en 1961 dentro del Departamento de Ingeniería mecánica. La herramienta fundamental de investigación es un conjunto subcrítico de uranio natural-agua, acoplado a un acelerador de iones positivos de 150 kV. El grupo de investigación está particularmente interesado en la aplicación de técnicas de fuente pulsante a las medidas de laplacianas de un núcleo de forma irregular por comparación con otro de forma simple.

En Escocia, la investigación en física de reactores se realiza en el Scottish Research Reactor Centre, siendo su equipo básico, ya en funcionamiento, un reactor de investigación de 100 kW del tipo UTR-100. El programa actual de investigación comprende el desarrollo de un espectrómetro de cristal para la determinación de espectros neutrónicos y estudios de redes cristalinas.

En la Universidad de Birmingham, los experimentos más importantes, hasta ahora, han consistido en aplicar la técnica de la fuente pulsada a moderadores y a conjuntos subcríticos. Además, ahora se efectuan experimentos de importancia en la dispersión inelástica de neutrones de muy baja energía y en reacciones con neutrones rápidos, como los procesos inelásticos en el berilio.

Thermal neutron cross sections and diffusion parameters in several organic materials

By L. Pál, E. Kisdi-Koszó, L. Bod, Z. Szatmáry and I. Vizi*

In the past few years considerable effort has been put into measuring the influence of chemical binding on the scattering of slow neutrons in several organic materials. This is of practical importance, since the shape of the neutron spectrum might depend on the binding effect. The quantitative understanding of neutron thermalization requires a fairly good knowledge of the scattering law for slow neutrons in organic materials.

Unfortunately the determination of the scattering law needs the measurement of the double differential scattering cross section $\frac{d^2\sigma}{d\Omega d\omega}$. Up to now only a few measurements have been made because of the experimental difficulties.

In the calculations of the nuclear characteristics of reactors it is necessary to know the thermal neutron transport cross section of the moderator. In the diffusion approximation one obtains for the transport cross section:

$$\Sigma_{tr}(E) = \Sigma_t(E) - \mu(E)\Sigma_s(E),$$

where $\Sigma_t(E)$ is a macroscopic total cross section at energy E, $\Sigma_s(E)$ is the macroscopic scattering cross section at energy E, and $\mu(E)$ is the average cosine of the scattering angle at energy E. The cross sections Σ_t and Σ_s can be measured in a relatively simple way, but $\mu(E)$ necessitates the measurement of the differential scattering cross section $\frac{d\sigma}{d\Omega}$. To avoid the necessity of costly measurements of this quantity, Radkowsky [1] formulated a semi-empirical method of calculating the average transport cross section from the energy dependence of the integral scattering cross section. The aim of the present work is to show the usefulness of the Radkowsky method for calculations of the transport cross section in various organic materials. For this purpose we chose some hydrocarbons with different chemical structures, namely benzene, toluene, xylene, cyclohexane, n-hexane and diphenyl. In these materials we measured the energy dependence of the integral neutron cross section by the time-of-flight technique and the diffusion parameters by the pulsed neutron source method. From the integral cross section data, the average transport mean free path

$$\langle\lambda_{tr}\rangle = \frac{1}{\langle\Sigma_{tr}\rangle} \qquad (1)$$

was calculated by making use of the Radkowsky method. As a check of this method the calculated values were compared with the values measured directly by the pulsed method.

Measurement of the integral cross section

The energy dependence of the total neutron cross section was measured in the energy range from 0.001 to 0.1 eV. The collimated beam of neutrons from the reactor was chopped by a mechanical selector. The sample holder was preceded by a second collimator. The neutrons neither scattered nor absorbed in the sample were detected by a set of BF_3 counters coupled to a 128 channel time-analyser. The distance between the chopper and the detector was 4.7 m; the duration of the neutron pulse produced by the chopper was 126 μs and the total time resolution was 190 μs.

As a check of the apparatus the energy dependence of the total cross section in water was measured and the results were compared with the measurements of Melkonian [2] and Heinloth [3]. Present results are in good agreement with those obtained by them.

The energy dependence of the total cross section per hydrogen atom in benzene can be seen in Fig. 1. Kovner and Kolerov [4] and Boffi *et al.* [5] calculated the total cross section for benzene and their theoretical results are in good agreement with present experimental data. Figures 2–6 show the energy dependence of

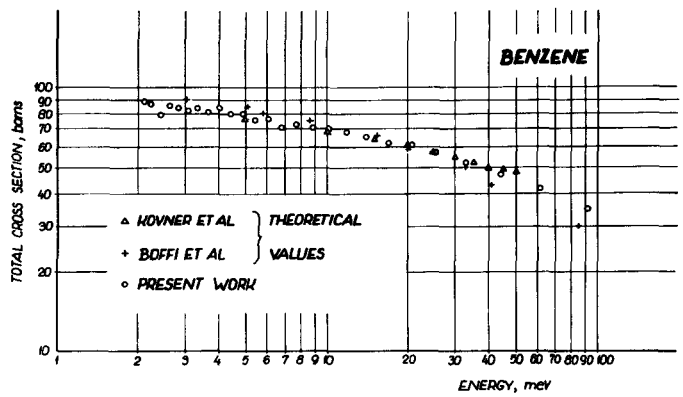

Figure 1. Energy dependence of the total neutron cross section per hydrogen atom bound in benzene

* Central Research Institute for Physics, Budapest.

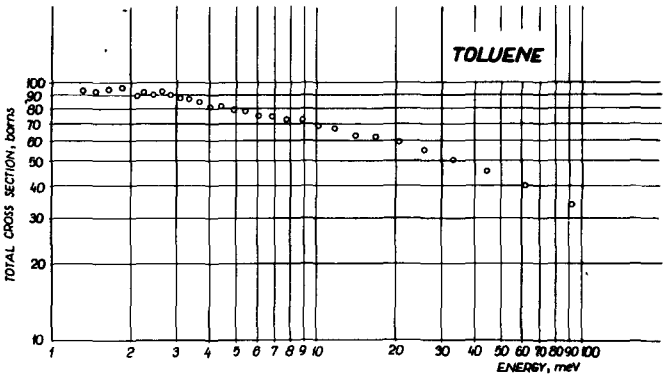

Figure 2. Energy dependence of the total neutron cross section per hydrogen atom bound in toluene

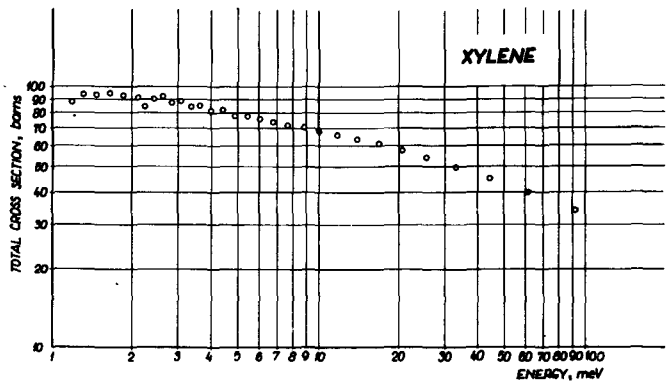

Figure 3. Energy dependence of the total neutron cross section per hydrogen atom bound in xylene

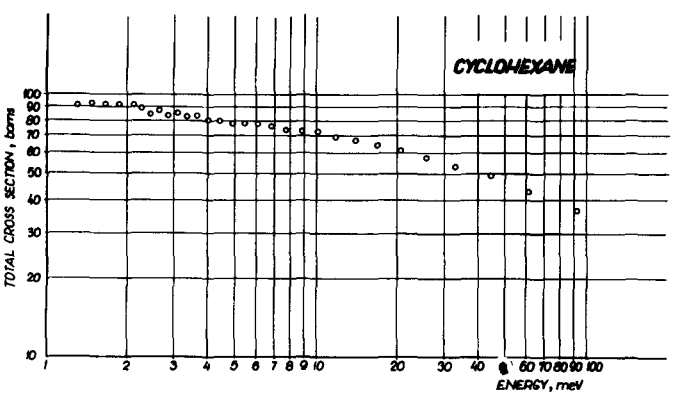

Figure 4. Energy dependence of the total neutron cross section per hydrogen atom bound in cyclohexane

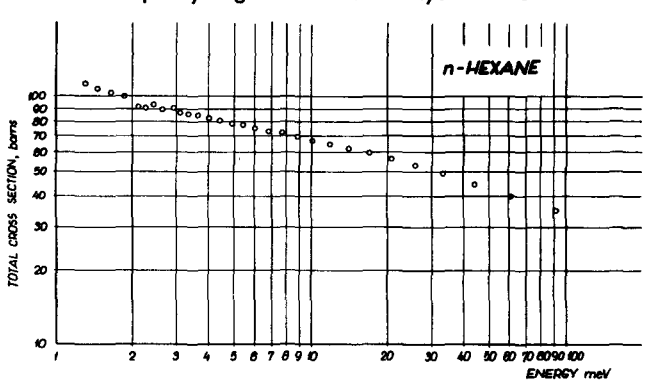

Figure 5. Energy dependence of the total neutron cross section per hydrogen atom bound in n-hexane

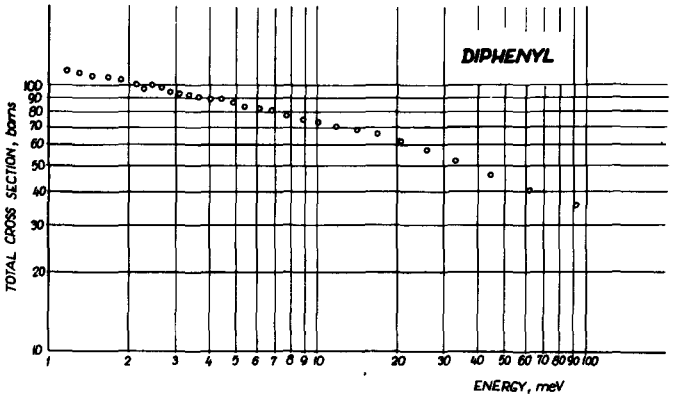

Figure 6. Energy dependence of the total neutron cross section per hydrogen atom bound in diphenyl

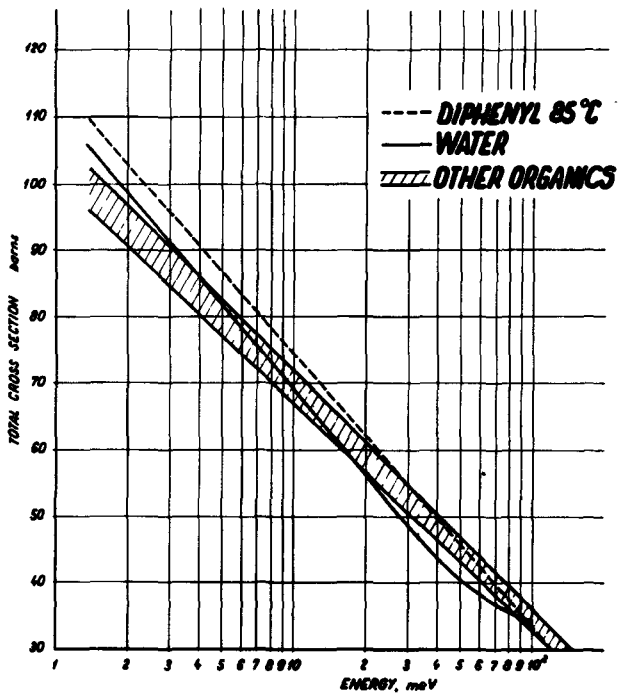

Figure 7. Schematic plot of the total neutron cross sections per hydrogen atom for water, benzene, toluene, xylene, cyclohexane, n-hexane and diphenyl

the total cross section in toluene, xylene, cyclohexane, n-hexane and diphenyl. For comparison all data are collected in Fig. 7. It is seen that below 0.01 eV the values of σ_t^H for diphenyl are definitely higher than those for the others since the temperature of the diphenyl sample was higher (85 °C).

Measurement of the diffusion parameters

The thermal neutron diffusion parameters were measured by pulsed source method. The principle of this method is quite simple: a burst of fast neutrons is injected into a moderating sample. After slowing down and thermalization of neutrons the decay constant α of the fundamental mode is measured at different bucklings B^2 of the moderating sample. The decay constant is given by the well known relation:

Table 1. Diffusion parameters of thermal neutrons measured by pulsed method

Material	$\langle \Sigma_a v \rangle$	$\frac{\langle \lambda_{tr} \rangle \langle \nu \rangle}{3}$	C	L	$N_H \langle \lambda_{tr} \rangle 10^{-21}$
Water 22°C . . .	4859±123	36533±1362	5939±3148	2.74±0.09	29.32±0.8
Benzene 22°C . .	2886±111	48649±1373	13869±3849	4.11±0.10	23.61±0.8
Toluene 22°C . .	3357± 80	44229± 847	9359±2007	3.63±0.06	23.97±0.8
Xylene 22°C . . .	3719± 66	41140± 648	11165±1415	3.32±0.04	24.11±0.8
Cyclohexane 22°C .	4925±103	29944±1382	5603±4185	2.47±0.06	23.91±0.8
n-Hexane 22°C . .	5046± 67	28818± 546	−927± 975	2.39±0.03	22.36±0.8
Diphenyl 85°C . .	2778± 72	59529±1534	20336±3632	4.63±0.08	25.03±0.8

N_H number of hydrogen atoms/cm³.

$$\alpha = \langle \Sigma_a v \rangle + \frac{\langle \lambda_{tr} \rangle \langle \nu \rangle}{3} B^2 - CB^4 \qquad (2)$$

where Σ_a and C are the macroscopic absorption cross section and the diffusion cooling coefficient respectively.

In present measurements the duration of the fast neutron burst was 20 μs. The fast neutrons were produced by a 200 kV Cockcroft-Walton generator in (d,t) reaction. The detector consisting of a sensitive thermal neutron scintillator and a Zeiss-60 type photomultiplier was placed in the middle of the moderator vessel bottom. The signals of the detector were recorded by a 24 channel time-analyser.

The decay constants were evaluated from the time-analyser data using the three parameter maximum likelihood estimation. The diffusion parameters were obtained by means of a weighted least square fit. Figure 8 is a plot of the decay constants as a function of buckling. The diffusion parameters obtained are listed in Table 1.

In the last column of Table 1, the $N_H \langle \lambda_{tr} \rangle$ values are given where N_H is the number of hydrogen atoms per cm³. It can be seen that they agree reasonably well within the statistical error except water. If the value found for diphenyl at 85°C is reduced to the temperature 22°C using the $T^{0.4}$ temperature dependence [6] it yields a better agreement. The comparison of these data shows that the difference in the molecular binding of the hydrogen atoms is very small in the hydrocarbons investigated.

Calculation of the transport mean free path

Scattering of neutrons on hydrogen in hydrocarbons is mostly incoherent. There are, therefore, no diffraction effects. In the laboratory system the average cosine of the scattering angle is given by:

$$\mu(E) = \frac{2}{3M}$$

where M is the number of mass units of the scattering atom. Because of the molecular binding effects, M can be considered to change with energy for low-energy neutrons, The energy dependent effective mass $M_{eff}(E)$ can be calculated using the Radkowsky method.

$$\frac{M_{eff}(E)}{1+M_{eff}(E)} = \sqrt{\frac{\sigma_s^H(E)}{80}} \qquad (3)$$

In case of hydrocarbons, the expression for the transport mean free path becomes:

$$[\lambda_{tr}(E)]^{-1} = N_H \sigma_{tr}^H(E) + N_c \sigma_{tr}^C(E) \qquad (4)$$

In the calculations for carbon, the following values were used:

$$\mu^C(E) = 1/18$$
$$\sigma_s^C = 4 \text{ b}$$
$$\sigma_a^C = 0$$

For hydrogen, the values of σ_a^H were calculated applying the $1/v$ law starting from the value

$$\sigma_a^H(0.025 \text{ eV}) = 331.5 \text{ mb}$$

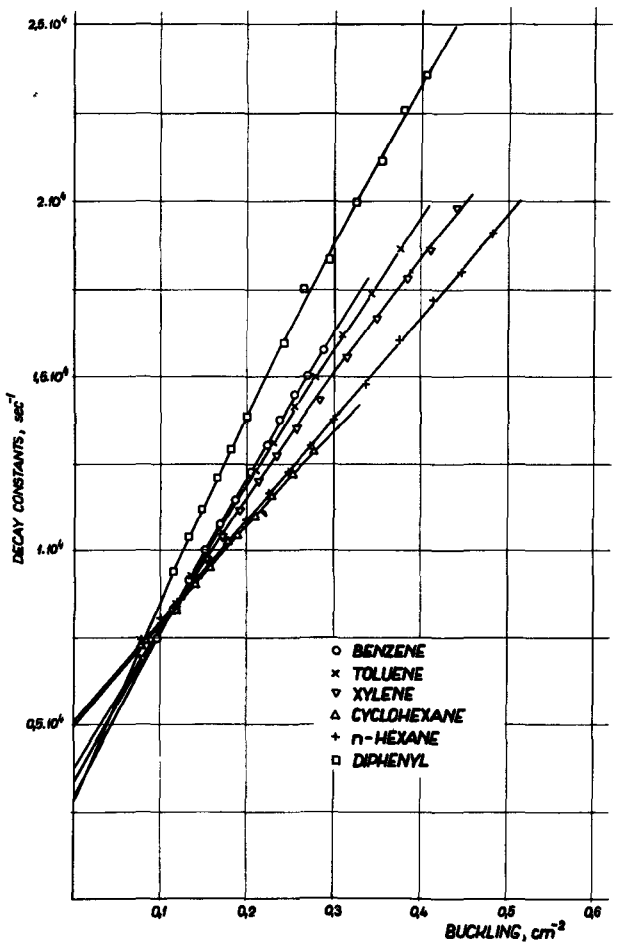

Figure 8. α vs. B_0^2 for benzene, toluene, xylene, cyclohexane, n-hexane and diphenyl

Table 2. Calculated and measured values of transport mean free path

Material	$\langle\lambda_{tr}\rangle$ (measured)	$\langle\lambda_{tr}\rangle$ (calculated)	$\langle\lambda_{tr}\rangle$ (from 1.3-butadiene)	Ratio of calculated and measured values
Water 22°C . . .	0.438±0.017	0.463		1.057
Benzene 22°C . . .	0.584±0.017	0.622	0.651	1.065
Toluene 22°C . . .	0.531±0.010	0.596	0.596	1.122
Xylene 22°C . . .	0.494±0.008	0.557	0.559	1.128
Cyclohexane 22°C . .	0.359±0.017	0.382	0.419	1.064
n-Hexane 22°C . .	0.346±0.007	0.437		1.263
Diphenyl 85°C . . .	0.654±0.017	0.706		1.080

Using these cross-section values and the Radkowsky method (3)$\lambda_{tr}(E)$ can be calculated from the measured $\sigma_t^H(E)$. The average value of the transport mean free path

$$\langle\lambda_{tr}\rangle = \frac{\int_0^\infty \lambda_{tr}(E)\phi_T(E)\mathrm{d}E}{\int_0^\infty \phi_T(E)\mathrm{d}E} \qquad (5)$$

was obtained by numerical integration. The energy distribution of neutrons was approximated by the usual Maxwellian distribution. The values of $\lambda_{tr}(E)$ had to be extrapolated to the high energy end of the Maxwellian distribution for lack of experimental points in that part of the spectrum. The contribution of this extrapolated energy region to the integral is rather small, thus the uncertainty introduced by the extrapolation can be neglected.

The results of the measurements and calculations are presented in Table 2. It contains also the values of $\langle\lambda_{tr}\rangle$ calculated from 1.3-butadiene cross-section data given by Petrie *et al.* [7].

Discussion

Present investigations show that the chemical binding plays the same role in each of the hydrocarbons considered. It should be noted, however, that in water the chemical binding shows a quite different behaviour.

The values of calculated mean free path are in fairly good agreement with those directly measured when the proper cross sections are used for the calculation. The agreement between the calculated and experimental values could be improved by substituting for the 80 b a somewhat lower value varying from material to material. Thus, the expression would loose its generality though the value of 80 b in the expression can be considered as the zero energy limit of the elastic scattering cross section only and does not reflect the general asymptotics of the integral cross section for low energies. For this reason, it was attempted to use, instead of 80 b, the values extrapolated from the measured cross-section data for low energies. The above agreement was spoilt by this procedure giving too high values for the transport mean free path. This is due to the inelastic part of the total scattering cross section. The 80 b used in the calculations seem to be a reasonable but theoretically not a rigorous value.

As a conclusion it should be emphasized that the Radkowsky method is to be considered rather as a useful tool, than as a theoretically rigorous treatment of neutron scattering in moderators.

REFERENCES

1. Radkowsky, A., U.S. Atomic Energy Comm. report ANL 4476, p. 89 (1950)
2. Melkonian, E., Phys. Rev., *76*, 1750 (1949)
3. Heinloth, K., Z. Physik, *163*, 218 (1961).
4. Kovner, M. A. and Kolerov, G. I., *Neutron Physics*, pp. 100–104 (Moscow 1961).
5. Boffi, V. C., Molinari, V. G. and Parks, D. E., *Inelastic Scattering of Neutrons in Solids and Liquids*, Vol. I., pp. 285–295, IAEA, Vienna (1963).
6. Küchle, M., Nukleonik, *2*, 131 (1960).
7. Petrie, C. D., Storm, M. L. and Zweifel, P. F., Nuclear Sci. Eng., *2*, 728 (1957).

ABSTRACT—RÉSUMÉ—АННОТАЦИЯ—RESUMEN

A/651 Hongrie

Sections efficaces et paramètres de diffusion des neutrons thermiques dans différentes matières organiques

par L. Pál *et al.*

Depuis quelques années, on s'efforce de mesurer l'influence de la liaison chimique sur la diffusion des neutrons lents dans différents liquides hydrogénés. Cette mesure a un grand intérêt du point de vue pratique, car la forme du spectre des neutrons dans les modérateurs hydrogénés dépend de l'effet de liaison. Pour déterminer les aspects quantitatifs de la thermalisation des neutrons, il est nécessaire de bien connaître la loi de diffusion des neutrons lents dans les liquides hydrogénés.

Malheureusement, la loi de diffusion est assez difficile à établir expérimentalement. La mesure de la section efficace totale est plus simple, mais ne donne pas d'indications aussi précises sur les caractéristiques du système de diffusion. Malgré cela, il peut être utile de connaître les sections efficaces totales pour calculer la section efficace de transport. On peut obtenir la section efficace de transport en fonction de la température à partir de la section efficace totale de diffusion, en utilisant la méthode de Radkowsky, qui est assez utile mais peu rigoureuse du point de vue théorique.

Les auteurs analysent en détail la méthode de Radkowsky, en prenant comme base les mesures des sections efficaces totales et des paramètres de diffusion dans différents liquides organiques: benzène, cyclohexane, *n*-hexane, toluène, xylène et diphényl. Les sections efficaces totales des neutrons en fonction de l'énergie ont été mesurées par la technique du temps de vol et calculées d'après la théorie de Zemach-Glauber. Les résultats des calculs concordent assez bien avec les résultats expérimentaux. Les paramètres de diffusion ont été établis à partir des mesures effectuées par la méthode de la source de neutrons pulsés. La section efficace de transport moyenne, obtenue à partir des mesures des sections efficaces, a été comparée aux résultats des mesures au moyen de la source pulsée. Il ressort de cette comparaison que les valeurs des sections efficaces de transport calculées par la méthode de Radkowsky concordent assez bien avec celles des mesures faites au moyen de la source pulsée.

Les auteurs ont également calculé les sections efficaces de transport d'après les données de $\sigma^{H}{}_{s}(E)$ pour le 1,3-butadiène, car Petric et ses collaborateurs ont proposé d'utiliser ces données pour calculer les sections efficaces de transport dans différents hydrocarbures. Malheureusement, les données fournies par 1,3-butadiène ne donnent pas de résultats satisfaisants; pour calculer la section efficace de transport moyenne, il apparaît donc nécessaire de connaître la section efficace en fonction de l'énergie.

En conclusion, il convient de souligner que la méthode de Radkowsky doit être considérée comme un instrument utile, et non comme une formule permettant de calculer de manière absolument rigoureuse la diffusion des neutrons dans les modérateurs.

A/651 Венгрия

Сечения рассеяния и параметры диффузии тепловых нейтронов в некоторых органических веществах

Л. Пал et al.

В последние годы значительные усилия были приложены для определения влияния химической связи на закон рассеяния в некоторых водородсодержащих жидкостях. Это важно и с практической точки зрения, так как вид нейтронного спектра в органических замедлителях также оказывается зависящим от эффекта химической связи. Поэтому количественное рассмотрение термализации нейтронов в этих замедлителях требует детального знания закона рассеяния.

К сожалению, определение закона рассеяния сопровождается большими экспериментальными трудностями. Измерение интегрального сечения проще, но зато оно менее чувствительно к деталям структуры рассеивающей системы. Несмотря на это, значение энергетической зависимости интегрального сечения может быть использовано. Для расчета транспортного сечения замедлителя температурная зависимость транспортного сечения может быть получена из интегрального сечения рассеяния с помощью метода Радковского, который весьма полезен для практических расчетов, хотя с теоретической точки зрения и нестрог.

В работе дается детальный анализ метода Радковского на основе измерений интегральных сечений и диффузионных параметров нейтронов в различных органических жидкостях (бензол, циклогексан, *n*-гексан, толуол, ксилол и дифенил). Энергетическая зависимость интегральных сечений рассеяния была измерена при помощи метода времени пролета и, кроме того, рассчитывалась на основе теории Земаха-Глаубера. Расчетные результаты хорошо согласуются с экспериментальными данными. Диффузионные характеристики определялись с помощью импульсного нейтронного источника. Усредненные транспортные сечения, полученные из интегральных сечений рассея-

ния, сравниваются с результатами непосредственных измерений. Сравнение показывает, что метод Радковского дает транспортные сечения, хорошо согласующиеся с данными измерений, выполненных по импульсной методике.

Транспортные сечения в исследуемых веществах вычислялись также на основе данных $\sigma_s^H(E)$ для 1,3-бутадиена. Использовать эти данные для определения Σ_{tr} в различных углеводах предложили Петри и др. К сожалению, эта методика не позволяет получить удовлетворительные результаты, так как для расчета транспортного сечения каждого углевода необходимо, по-видимому, знать его сечение в зависимости от энергии.

В заключение можно сделать вывод, что метод Радковского, хотя и не является теоретически обоснованным, имеет практическое значение для определения транспортного сечения в водородсодержащих замедлителях.

A/651 Hungría

Secciones eficaces y parámetros de difusión de neutrones térmicos en varias sustancias orgánicas

por L. Pál *et al.*

En los últimos años se han dedicado esfuerzos considerables a la determinación de la influencia del enlace químico sobre la dispersión de neutrones lentos en varios líquidos hidrogenados. Esta cuestión reviste importancia desde el punto de vista práctico porque la forma del espectro neutrónico en los moderadores de hidrógeno depende del efecto de enlace y porque, además, la interpretación cuantitativa de la moderación neutrónica en estos materiales exige un conocimiento detallado de la ley de dispersión de los neutrones lentos.

Por desgracia la determinación de la ley de dispersión encierra dificultades experimentales de bastante consideración; la medida de la sección eficaz integral de dispersión es más sencilla pero no es tan sensible a las particularidades del medio dispersivo, a pesar de lo cual su conocimiento puede tener importancia para calcular la sección eficaz de transporte. En efecto, esta última sección eficaz, cuyo valor depende de la temperatura, puede deducirse de la sección eficaz integral aplicando el método de Radkowsky, que es bastante útil aunque carece de rigor teórico.

La memoria presenta un análisis detallado del método de Radkowsky aplicado a las mediciones de la sección eficaz integral y del parámetro de difusión de varios líquidos orgánicos como el benceno, ciclohexano, *n*-hexano, tolueno, xileno y difenilo. La influencia de la energía sobre las secciones eficaces integrales se midió según la técnica de tiempo de vuelo y se calculó por la teoría de Zemach-Glauber; los valores calculados concuerdan satisfactoriamente con los resultados experimentales. Los parámetros de difusión se dedujeron de las medidas llevadas a cabo por el método de la fuente neutrónica pulsante y el valor de la sección eficaz media de transporte obtenido a partir de las determinaciones de sección eficaz integral se comparó con los resultados de la fuente pulsante. Los datos así obtenidos concuerdan satisfactoriamente con los valores calculados según el método de Radkowsky y los de la fuente pulsante.

También se calcularon secciones eficaces de transporte a partir de valores de la $\sigma^H{}_s(E)$ para el 1,3-butadieno, de acuerdo con Petric *et al.* quienes propusieron este cálculo para varios hidrocarburos. Los datos correspondientes al 1,3-butadieno no dan resultados satisfactorios, de donde se deduce la importancia de conocer la variación de la sección eficaz en función de la energía para cada uno de los hidrocarburos investigados, a fin de poder calcular el valor medio de la sección eficaz de transporte.

La memoria concluye subrayando la conveniencia de considerar el método de Radkowsky como medio de utilidad práctica, pero no como un tratamiento teórico de carácter riguroso de la dispersión de neutrones en un moderador.

A study on the diffusion length of thermal neutrons in terphenyl (Santowax — R) at temperatures up to 400°C

By S. Hohki, Y. Tsuji, T. Matsubara, T. Makaiyama and H. Tada*

It is well known that the temperature dependence of the diffusion length is important in relation to the neutron transport cross section as a basic reactor parameter because of the higher temperatures of modern reactors.

The diffusion length of thermal neutrons in various moderators containing hydrogen has been studied for a long time, especially theoretically. However, only a few experiments covering a wide temperature range have been reported, most experiments and calculations being at comparatively low or at spot temperatures, e.g., Wright and Frost [1], Rockey and Skolnik [2], Reier and de Juren [3], Csikai, Daroczy and Dede [4], Yurova [5] and Baumann [6]. This is due to experimental difficulties, such as using water at high temperatures. However, it appeared that a study of the deviations from the $1/v$ law due to molecular binding would be interesting at temperatures above 200 °C.

In this work, the temperature dependence of the diffusion length of thermal neutrons in terphenyl ($C_{18}H_{14}$) has been measured over the temperature range 200° to 400 °C, and from these results the transport cross section has also been studied. From comparing the results with calculated values, using $\sigma_s(E)$ from Brugger's experimental data on the scattering law for Santowax-R, it is clear that there are still problems arising from the assumption that the diffusion length varies as $(1/\rho)\sqrt{T}$ at temperatures above 300 °C.

Some of the experimental difficulties encountered in making the measurements were:

(*a*) maintaining a uniform temperature distribution during the experiments;

(*b*) assumptions about the neutron flux spectrum, including the epithermal spectrum;

(*c*) measurement of the neutron flux, that is, the development of gadolinium and dysprosium foils in view of the difficulty of using cadmium and indium foils at high temperatures.

EXPERIMENTAL ARRANGEMENT

All the components of the system used in these experiments are shown in Fig. 1.

It consists of a main organic loop and accessory loops, consisting of a nitrogen gas loop, an air loop, a cooling water loop and the cooling loop of the main circulating pump. Brief descriptions of the operating conditions are now given.

First, solid organic material was placed in the drain tank and all the components evacuated in order to replace the air in the system by nitrogen. Next the organic material was melted down in the drain tank at about 200 °C, then transferred to the pressure vessel through the circulating loop by pressurized nitrogen.

During experiments, the circulating pump and main heaters were operated to keep the organic temperature uniform and the vessel was pressurized with nitrogen to suppress bulk boiling.

The temperature of the organic liquid in the vessel was kept at 400 °C without difficulty.

All the pipes and valves of the loops were surrounded with sheathed wire heaters and thermal insulators to keep them at a temperature above the melting point of the organic material.

The distribution of thermal neutrons at various temperatures was measured in the pressure vessel by the foil method. A vertical section of the pressure vessel is shown in Fig. 2. In the experimental tubes of the vessel, the ceramic foils were fixed with aluminium foil holders.

The flow skirt in the vessel was used to maintain a constant level of the organic liquid and keep the temperature of the organic uniform in the measuring region.

The induction heating kept the vessel at a temperature close to 200 °C.

The temperature distribution in the vessel was measured with thermocouples at six different points. Good uniformity in the temperature distribution inside the flow skirt was confirmed.

The pressure vessel had a level controller, level gauges, a pressure gauge, a safety valve and an emergency valve. It was constructed of carbon steel and surrounded with thermal insulators and steel clad cadmium plates. An aluminium clad cadmium shutter was inserted between the vessel and the graphite pedestal for the control of epithermal neutrons.

The pressure vessel and the graphite pedestal were surrounded by a heavy concrete shield.

A polonium–beryllium neutron source of initial intensity 4.0×10^7 neutron/s was placed in the centre of the graphite pedestal.

* Research Division, Sumitomo Electric Industries Ltd., Osaka.

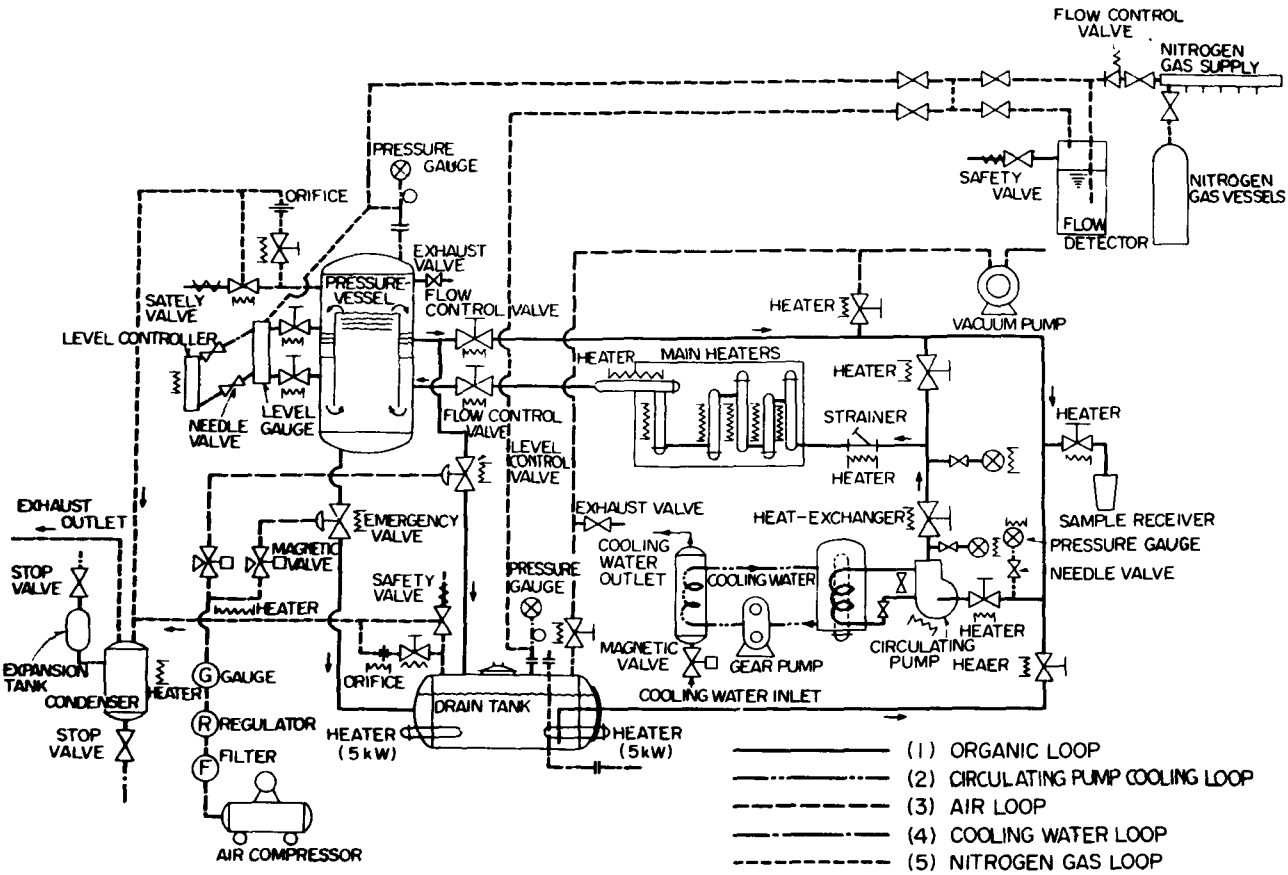

Figure 1. Organic circulating loop

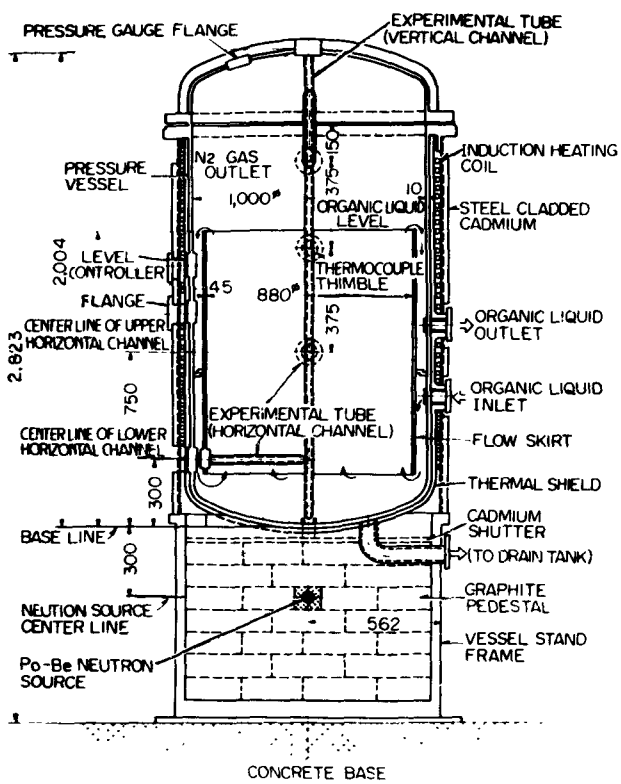

Figure 2. Pressure vessel for neutron diffusion experiments (vertical section), units in mm

Table 1. The composition of Santowax-R[a]

Biphenyl	o-Terphenyl	m-Terphenyl	p-Terphenyl	HBR
0.6%	11.4%	60.2%	27.2%	0.1%

[a] The sample was taken from liquid Santowax-R which had been kept at 200°C. for 24 hours.

The organic material used in the experiments was a mixture of terphenyl isomers ($C_{18}H_{14}$) that is known commercially as Santowax-R and was provided by the Monsanto Chemical Co. Its composition was checked by gas-chromatography and the analysis is shown in Table 1.

The yield of the high boiler residue (HBR) was very small during the present experiments. The density of Santowax-R was measured separately at every temperature with a pyknometer with bulk boiling suppressed by nitrogen.

THEORY OF THE METHOD

The diffusion of thermal neutrons in a source-free medium is expressed by the steady-state, one-group diffusion equation:

$$\nabla^2\phi(r) = \frac{1}{L^2}\phi(r) \qquad (1)$$

where $\phi(r)$ is the thermal neutron flux, and L is the

thermal diffusion length which is defined as:

$$L=\sqrt{\frac{\lambda_{tr}}{3\Sigma_a}} \tag{2}$$

with the macroscopic absorption cross section Σ_a and the transport mean free path λ_{tr} of the medium. In the case of cylindrical geometry and a circular symmetric source, Eq. (1) is solved in the form:

$$\phi(r,z)=\sum_{n=1} A_n J_0\left(\mu_n\frac{r}{R}\right)\exp\left[-z\sqrt{\frac{1}{L^2}+\left(\frac{\mu_n}{R}\right)^2}\right] \times\left\{1-\exp\left[-2(Z-z)\sqrt{\frac{1}{L^2}+\left(\frac{\mu_n}{R}\right)^2}\right]\right\} \tag{3}$$

where J_0 is the first kind Bessel function of the zeroth order and μ_n is the n-th zero point. Z and R are the extrapolated height and radius of the cylinder determined from the real height, Z_0 and radius R_0 of the cylinder and the extrapolation lengths. The Fourier-Bessels coefficients A_n are determined by the thermal flux distribution in the radial direction, $z=z_0$ and the orthogonal relation of the J_0 function:

$$A_n=\frac{1}{\frac{R^2}{2}\{J_1(\mu_n)\}^2}\frac{\exp\left[z_0\sqrt{\frac{1}{L^2}+\left(\frac{\mu_n}{R}\right)^2}\right]}{\left\{1-\exp\left[-2(Z-z_0)\sqrt{\frac{1}{L^2}+\left(\frac{\mu_n}{R}\right)^2}\right]\right\}} \times\int\phi(r,z_0)J_0\left(\mu_n\frac{r}{R}\right)rdr \tag{4}$$

If z is sufficiently large, the term exp $\left[-2(Z-z_0)\times\sqrt{\frac{1}{L^2}+\left(\frac{\mu_n}{R}\right)^2}\right]$ in Eq. (3) is negligible in comparison with unity and the flux distribution on the central axis, $\phi(0,z)$ is expressed in the simple form:

$$\phi(0,z)=A_1\,\mathrm{esp}\left\{-z\sqrt{\frac{1}{L^2}+\left(\frac{\mu_n}{R}\right)^2}\right\}K(0,z) \tag{5}$$

where $K(0,z)$ is a correction factor for the higher mode which has a value nearly equal to unity.

$$K(0,z)=1+\frac{A_2}{A_1}\exp\left[-z\left\{\sqrt{\frac{1}{L^2}+\left(\frac{\mu_2}{R}\right)^2}-\sqrt{\frac{1}{L^2}+\left(\frac{\mu_1}{R}\right)^2}\right\}\right]+\frac{A_3}{A_1}\exp\left[-z\left\{\sqrt{\frac{1}{L^2}+\left(\frac{\mu_3}{R}\right)^2}-\sqrt{\frac{1}{L^2}+\left(\frac{\mu_1}{R}\right)^2}\right\}\right]+\cdots. \tag{6}$$

The value L may be determined by the iteration method; A_n can be computed from the radial flux distribution at $Z=z_0$. The logarithmic axial flux distribution is plotted as a function of Z and a straight line is fitted by the method of least squares. With this slope, the first approximation L' is determined from the following relation:

$$\tan\alpha=\sqrt{\frac{1}{L'^2}+\left(\frac{\mu_1}{R}\right)^2} \tag{7}$$

Using the value L', the correction factor $K(0,z)$ can be obtained as a function of Z. Then L'', the second order approximation to L, can be determined as

$$\log\frac{\phi(0,z)}{K(0,z)}=\log A_1-z\sqrt{\frac{1}{L''^2}+\left(\frac{\mu_1}{R}\right)^2} \tag{8}$$

This iteration process goes on until the series L',L'',L''', $L^{(n)},\ldots$ converge into a constant value L.

MEASUREMENTS AND RESULTS

Measurements were performed in the pressure vessel previously described. The distribution of thermal neutrons was measured by the foil activation method using the experimental tubes in the vessel. Foils used in the experiments were binder-free Dy_2O_3 ceramic discs, 1.000 cm in diameter and 0.050 cm in thickness. Each foil was fixed in aluminium holders and activated in the vessel.

The induced activities were measured with a low background 2π-gas-flow counter. Besides corrections for the thermal expansion of foil holders and self-absorption of β-rays in the foils, additional correction factors for self-shielding and flux depression of each foil were calculated at each temperature by Bothe-Tittle's formula [7,8] which seemed applicable for the relatively thick foils. To evaluate the contribution of epithermal neutrons, duplicate runs were made with and without the cadmium shutter at each temperature and the epithermal neutron induced activity subtracted from the activity without the shutter.

The diffusion length of thermal neutrons was determined at seven different temperatures from 200° to 400 °C. The axial and radial distribution of the thermal (subcadmium) neutrons was plotted on semi-logarithmic graphs and typical data from the experiments are shown in Fig. 3. Because of the statistical fluctuation

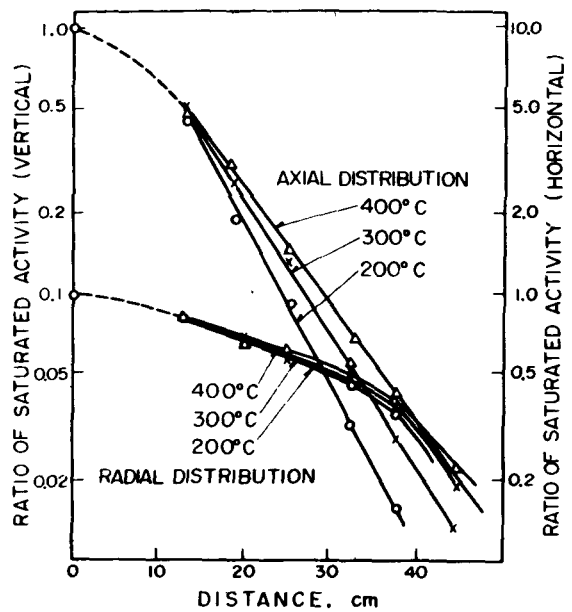

Figure 3. Axial and radial distribution of thermal neutrons in Santowax-R

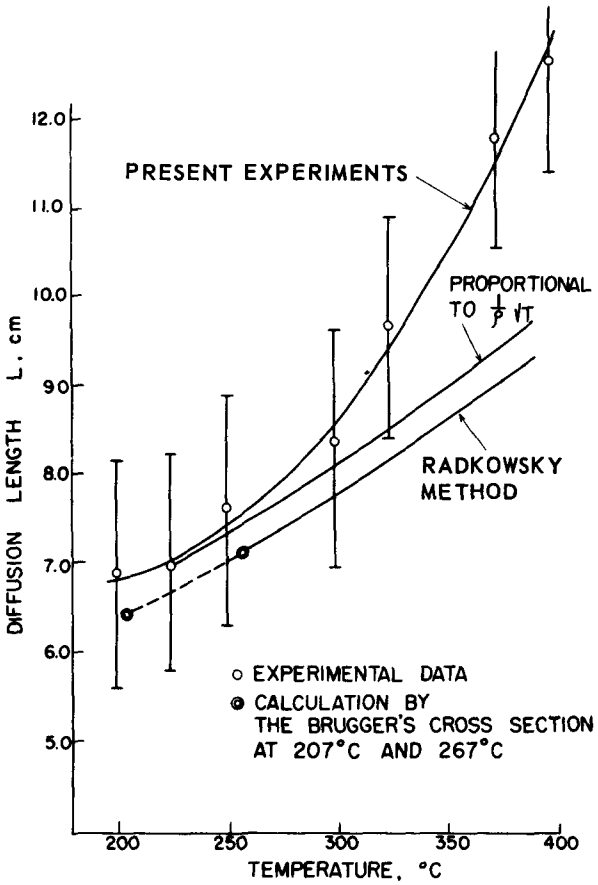

Figure 4. Diffusion length of thermal neutrons in Santowax-R

of the observed activity, the slopes of the axial distribution curves were determined by the least squares method. These data were substituted in Eq. (7) and the first approximation to the diffusion length L' calculated. Then, the higher harmonic correction factor $K(z,_0)$ was decided using the radial distribution data. Using this method the iteration calculation was made until convergence of the fit within the chosen degree of accuracy was obtained. In the experiments, the higher harmonic corrections were very small, less than a few per cent in every diffusion length.

All these calculations were carried out with the NEAC 2203 electronic computer, the capacity of which is comparable with an IBM 650.

The results of these corrections for the data are plotted in Fig. 4; the total probable error of the diffusion length is also shown.

DISCUSSION

The experimental values for the thermal diffusion length in Santowax-R were compared with the calculated values. In the expression of the thermal diffusion length:

$$L=\sqrt{\frac{\lambda_{tr}}{3\Sigma_a}}=\sqrt{\frac{1}{3\Sigma_{tr}\,.\,\Sigma_a}} \qquad (2')$$

Because the transport cross section σ_{tr} and the absorption cross section (σ_a) of Santowax-R are assumed to vary as $1/v$, the value of L should be proportional to $(1/\rho)\sqrt{T}$ where ρ and T are the density and temperature of the Santowax-R respectively and v is the neutron velocity which is in equibrium at the temperature of the Santowax-R.

Rockey and Skolnik [2] have verified that the theoretical $1/v$ law is in good agreement with the measured values in water at temperatures up to 296 °C. In order to compare this data with our experimental value, a curve proportional to $(1/\rho)\sqrt{T}$ is shown in Fig. 4. It is clear that there is still a problem in assuming that the diffusion length varies as $(1/\rho)\sqrt{T}$ at temperatures above 300 °C.

When calculating the diffusion length of thermal neutrons, it is difficult to estimate the scattering cross section $\sigma_s(E)$ for a hydrogen atom to include the effect of chemical binding. Thus an attempt was made to deduce the value of $\sigma_s(E)$ from Brugger's experimental data on the scattering law of Santowax-R [9]. Firstly, the value of σ_s (0.0252 eV) of Santowax-R was determined by subtracting the calculated value σ_a (0.0252 eV) from the total cross section σ_T (0.0252 eV) which was also measured by Brugger [9] assuming the $1/v$ law. Then the ratio of $\sigma_s(E)$ to σ_s (0.0252 eV) was calculated from the scattering law [9] and normalized to the previously determined value of σ_s (0.0252 eV). It was assumed that the value for $\sigma_s(E)$ of Santowax-R was similar to that of water in the energy region where experimental data were not obtained. Then, the macroscopic transport cross section of Santowax-R was calculated by the following formula:

$$\Sigma_{tr}^{C_{18}H_{14}}(E)=\sum_i N_i\{\sigma_T^i(E)-2\pi\int_{-1}^{1}\sigma_s^i(E,\cos\theta)\,.\cos\theta\times d(\cos\theta)\} \qquad (9)$$

where N_i,$\sigma_T^i(E)$ and $\cos\theta$ are, respectively, the number of atoms, microscopic total cross section and cosine of the scattering angle for the i-material.

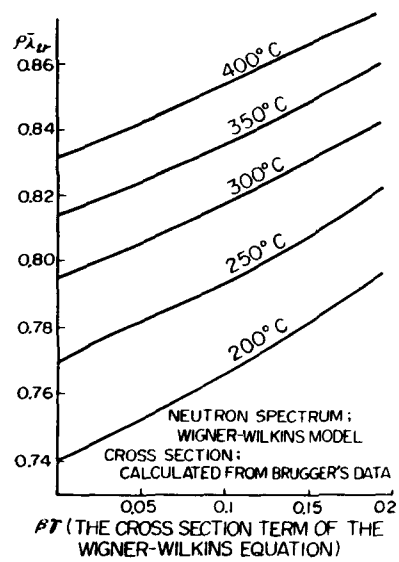

Figure 5. $\rho\lambda_{tr}$ of Santowax-R as a function of $\beta\gamma$ and temperature

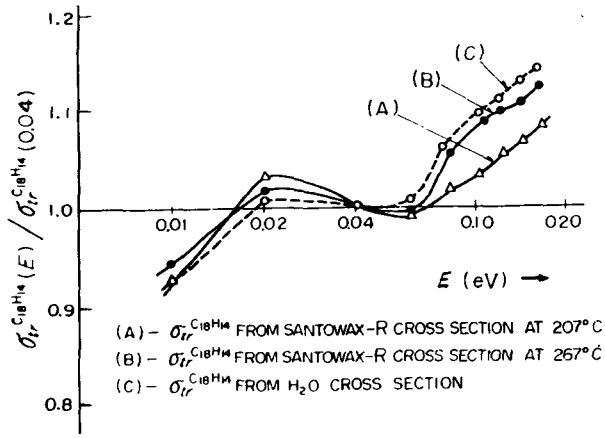

Figure 6. Deviation of transport cross section of Santowax-R from the 1/v law. The graphs were normalized to the data at 0.04 eV

The calculation of the average Σ_{tr} and Σ_a over a Wigner-Wilkins spectrum was made with a NEAC 2203 computer using a code translated from DONATE [10]. With this procedure, the value of L at 207° and 267 °C was calculated and is plotted in Fig. 4. Using the value of $\sigma_s(E)$ for Santowax-R at 267 °C, the extrapolated value $\rho\lambda_{tr}$ was calculated at the higher temperatures shown in Fig. 5. The effective mass of the bound hydrogen was obtained as described by Radkowsky [2]. The results of the calculations of the value of L made with the value of $\rho\lambda_{tr}$ are also shown in Fig. 4. The experimental values of L deviated considerably from the values calculated by the Radkowsky method at temperatures over 300 °C. This result might mean that the deviation of the transport cross section σ_{tr} from the $1/v$ law is considerable at temperatures over 300 °C. The deviations of the calculated values of $\sigma_{tr}^{H}(E)$ of Santowax-R and water are plotted in Fig. 6 where $\sigma_{tr}^{H}(E)$ of water was calculated using Melkonian's data [11]. It is difficult to determine any clear trend from these curves but it seems that the deviations of Santowax-R were relatively larger than those of water in the thermal region.

It was concluded from the experimental results that;

(*a*) the experimental values of L were proportional to $(1/\rho)\sqrt{T}$ at temperatures below 250 °C;

(*b*) the experimental values of L were somewhat larger than the theoretically expected values at high temperatures;

(*c*) the temperature dependence of the transport cross section could be substantial at temperatures over 300 °C.

ACKNOWLEDGEMENTS

We would like to express our gratitude to the staff of the Radiation Research Laboratory of the Sumitomo Atomic Energy Co., Ltd., for their assistance and to the members of the Atomic Energy Section of the Meidensha Electric Manufacturing Co. for their design and construction of the pressure vessel and other equipment.

REFERENCES

1. Wright, W. H., and Frost, H. T., US Atomic Energy Comm. report KAPL-M-WBV-2 (1956).
2. Rockey, K. S., and Skolnik, W., Nuclear Sci. Eng., *8*, 62 (1960).
3. Reier, M., and de Juren, J. A., Reactor Sci. Technol., *14*, 18 (1961).
4. Csikai, J., Daroczy, A., and Dede, K., *ibid.*, *15*, 204 (1961).
5. Yurova, L. N., *et al.*, Atomnaya Energ., *12*, 331 (1962).
6. Baumann, N. P., Nuclear Sci. Eng., *14*, 179 (1962).
7. Bothe, W., Z. Physik, *120*, 437 (1943).
8. Tittle, C. W., Nucleonics, *8* (6), 5 (1951).
9. Brugger, R. M., Phys. Rev., *126*, 29 (1962).
10. US Atomic Energy Comm. report WAPD-PM-45, DONATE code.
11. Melkonian, E., Phys. Rev., *76*, 1750 (1949).

ABSTRACT—RÉSUMÉ—АННОТАЦИЯ—RESUMEN

A/653 Japon

Etude sur la longueur de diffusion des neutrons thermiques dans le terphényle (Santowax-R) à des températures allant jusqu'à 400°C

par S. Hohki *et al.*

Il est bien connu que l'étude de la variation de la longueur de diffusion en fonction de la température est très importante pour les déterminations de la section efficace de transport des neutrons, qui est un paramètre fondamental du réacteur, en raison de l'élévation des températures utilisées dans les réacteurs modernes.

On a étudié depuis longtemps, surtout dans le domaine théorique, la longueur de diffusion des neutrons thermiques dans divers modérateurs contenant de l'hydrogène. Toutefois, on n'a publié qu'un petit nombre d'expériences faites dans un grand intervalle de température, la plupart des expériences et des calculs ayant été faits à des températures relativement basses ou isolées. Cela est dû à certaines difficultés qui se présentent, par exemple lorsque l'on utilise l'eau à haute température. Cependant, on a pensé qu'une étude des écarts par rapport à la loi $1/v$ dus à l'effet de la liaison moléculaire serait intéressante à des températures de plus de 200°C.

En conséquence, dans le présent travail la variation de la longueur de diffusion des neutrons thermiques en fonction de la température dans le terphényle ($C_{18}H_{14}$) a été mesurée de façon suivie dans l'intervalle de température de 200 à 400°C et la section efficace de transport étudiée d'après les résultats. En comparant les résultats avec les valeurs calculées, en faisant usage de $\sigma_S(E)$, d'après les données expérimentales de Brugger sur la loi de diffusion dans le Santowax-R, il est clair qu'il reste encore le problème que pose l'hypothèse selon laquelle la longueur de diffusion varie comme $(1/\rho)\sqrt{T}$ aux températures supérieures à 300°C.

Quelques-unes des difficultés expérimentales rencontrées en faisant les mesures ont été les suivantes:

a) Le maintien de l'uniformité de la distribution géométrique de température pendant les expériences;

b) L'obtention du spectre de flux souhaité, y compris les neutrons épithermiques;

c) La mesure du flux de neutrons, c'est-à-dire la mise au point de feuilles de gadolinium et de dysprosium, en raison de la difficulté que présente l'usage de cadmium et d'indium en feuilles aux températures élevées.

A/653 Япония

Исследование диффузионной длины тепловых нейтронов в терфениле (сантовакс-R) при высоких температурах до 400° С

С. Хоки *et al.*

Нет необходимости говорить о том, что в связи с использованием в современных реакторах высоких температур температурная зависимость диффузионной длины представляет собой весьма важный фактор, так как транспортное сечение является одним из основных параметров высокотемпературных реакторов.

Диффузионная длина тепловых нейтронов в различных замедлителях, содержащих водород, изучалась в течение долгого времени, особенно теоретически. Однако до настоящего времени было сообщено лишь о немногих экспериментах, выполненных в широком диапазоне температур, хотя опубликованы некоторые результаты экспериментов и расчетов для области сравнительно низких температур и для некоторых отдельных температурных точек. Это, по-видимому, объясняется техническими трудностями, например применением воды при высокой температуре.

Предполагается, однако, что вследствие действия молекулярной связи отклонение от закона $1/v$ при температурах выше 200° было бы значительным.

В данной работе температурная зависимость длины диффузии тепловых нейтронов в терфениле ($C_{18}H_{14}$) измерялась в широком диапазоне температур непрерывно с 200 до 400° С и в связи с этими результатами изучалось транспортное сечение. На основании сравнения экспериментальных данных с данными расчета, в котором $\sigma_S(E)$ определялось из экспериментальных данных Браггера относительно закона рассеяния в терфениле марки сантовакс-R, установлено, что справедливость предположения о том, что диффузионная длина при температурах выше 300° С изменяется по закону $\frac{1}{\varrho}\sqrt{T}$, весьма сомнительна. Можно полагать, что температурная зависимость диффузионной длины в горячей воде может быть получена из аналогии с данными настоящей работы.

В данном докладе указан также ряд технических проблем, которые возникли при проведении измерений в этих условиях:

a) Достижение равномерности геометрического распределения температур при проведении экспериментов.

b) Определение формы нейтронного потока,

в том числе эффекта надтепловых нейтронов.

c) Измерение потока нейтронов, а именно трудность использования кадмиевых и индиевых фольг из-за высокой температуры, и необходимость в связи с этим разработки техники использования гадолиниевых и диспрозиевых фольг.

A/653 Japón

Estudio de la longitud de difusión de los neutrones térmicos en el terfenilo (Santowax-R), hasta 400 °C

por S. Hohki *et al.*

Es sabido que la relación de dependencia entre la longitud de difusión y la temperatura reviste gran importancia en lo que atañe a la sección eficaz de transporte neutrónico, en su carácter de parámetro básico del reactor, y habida cuenta del aumento de temperatura que se registra en los reactores modernos.

La longitud de difusión de los neutrones térmicos en diversos moderadores hidrogenados se ha estudiado por largo tiempo, especialmente en sus aspectos teóricos. En cambio, sólo se han descrito contados experimentos efectuados en un amplio intervalo de valores de la temperatura, si bien se han publicado los resultados de algunos experimentos y cálculos correspondientes a temperaturas relativamente bajas o locales. Al parecer, la razón estaba en las dificultades técnicas, tales como las que derivan del empleo de agua a temperaturas elevadas. No obstante, se supone que, a temperaturas superiores a 200 °C, serían notables las desviaciones con respecto a la ley $1/v$ debidas al efecto del enlace molecular.

Los autores estudiaron la variación de la longitud de difusión de los neutrones térmicos en el terfenilo ($C_{18}H_{14}$) en función de la temperatura, entre los 200 °C y los 400 °C y analizaron las secciones eficaces de transporte teniendo en cuenta los resultados hallados. De la comparación de estos resultados con los valores calculados aplicando la $\sigma_s(E)$ deducida de los datos experimentales de Brugger sobre la ley de dispersión en el caso del Santowax-R, se desprende que sigue en pie el problema de si debe suponerse que la longitud de difusión varía en función de $(1/\rho)\sqrt{/T}$ a temperaturas superiores a 300 °C.

En la memoria se señalan también algunos problemas técnicos surgidos al efectuar las medidas en estas condiciones, a saber:

a) Uniformidad de la distribución espacial de la temperatura en el curso de los experimentos;

b) Configuración del flujo, incluso el efecto de los neutrones epitérmicos;

c) Dificultades que entraña la determinación del flujo neutrónico, con detectores de cadmio e indio a temperaturas tan elevadas y, por consiguiente, necesidad de recurrir a láminas de gadolinio y disprosio.

A study of fast-neutron transport in water with a pool-type reactor*

By M. S. Bokhari** and V. V. Verbinski***

A knowledge of the spatial, spectral and angular distributions of neutrons through the reactor shield is of interest particularly for shield design purposes and generally for a wide variety of experiments and instrument calibrations that require a neutron flux of known intensity and spectral shape. This paper reports spectral measurements of the fast-neutron angular flux at various positions and angles within the water shield of the Bulk Shielding Reactor 1 (BSR1) [1].

The geometry of the reactor core and its water shield is simple in that water acts as both reflector and shield. It should be relatively easy to reproduce this geometry in shielding calculations for a comparison with these measurements. An attempt has been made to compare the experimental results with the transport calculations embodied in the NIOBE (Numerical Integration of the Boltzmann Equation) code of Preiser *et al.* [2]. The NIOBE code handles only spherical geometry. Accordingly, one of the calculations was normalized to reproduce the measured source distribution along the centre line in the BSR1's horizontal mid-plane. This choice should provide a good comparison with measurements of forward-directed flux of the actual reactor, where the spectrometer views only a small central region of the BSR1, while the calculation should underestimate the angular flux at 40–50° by as much as a factor of 2 because the spherical source used for NIOBE has only about one-half of the volume of the BSR1.

Other rigorous techniques for calculating the spatial-spectral distribution such as Monte Carlo methods have not as yet been applied to the present work.

The experiments were carried out with the shielded-diode spectrometer described below. This spectrometer is especially suitable for spectral measurements of fast-reactor neutrons because of its unusual features such as reasonable counting rates behind thick shields, moderate energy resolution, and good discrimination against gamma pulses.

Experimental arrangement

The general arrangement of the reactor and the spectrometer in the Bulk Shielding Facility pool is shown in Fig. 1. The shielded-diode spectrometer was positioned in the horizontal mid-plane of the reactor and the data were obtained as a function of θ, the horizontal angle between the prolonged reactor centre line and the centre line of the spectrometer, and of r, the distance from the reactor face to the end of the air-filled spectrometer collimator. Sulphur pellets positioned 20 and 40 cm from the reactor face and 38 cm away from the prolonged reactor centre line were used to monitor the relative power of the reactor for various runs. The relative power level from one run to the other was thereby determined to an accuracy of about 2%.

Shielded-diode spectrometer

As shown in Fig. 1, the shielded-diode spectrometer essentially consists of a 580-μg/cm^2-thick ^{6}LiF layer which is supported in vacuum between two widely spaced silicon-gold surface-barrier diodes. To shield the diodes against intense gamma-ray fields and very fast neutrons, a lead shield and a tungsten-lined 18 in long lead collimator were used. By further shielding against thermal neutrons with ^{6}Li on all sides, the spectrometer was found to work satisfactorily for the fast-neutron directed-flux measurements above 1 MeV.

A neutron, after passing through the lead collimator, impinges on the ^{6}LiF layer and produces an alpha particle and a triton emitted in opposite directions in the centre-of-mass system. These charged particles share between them the energy of the incoming neutron plus 4.78 MeV, the Q value of the ^{6}Li(n,α)T reaction. Before electronically [3] summing up the pulses corresponding to the energy deposited in the diodes by the alpha-triton pair, a fast coincidence ($\approx$75 ns resolving time) was demanded between the individual pulses from the silicon-gold surface-barrier diodes.

Spectrometer response

The response of the shielded-diode spectrometer to monoenergetic neutrons was found to be linear, and the response function has been shown elsewhere [3] to be a Gaussian peak whose width at half-height, a measure of the resolution, is a function of the energy. The half width was 1.1% at 14 MeV, 8.2% at 3 MeV, and 18% for thermal neutrons. However, subjecting

---

* Work performed while first author was a visiting scientist at the Oak Ridge National Laboratory.

** Pakistan Atomic Energy Commission, Karachi.

*** Oak Ridge National Laboratory, Oak Ridge, Tennessee.

Research sponsored by the US Atomic Energy Commission under contract with the Union Carbide Corporation.

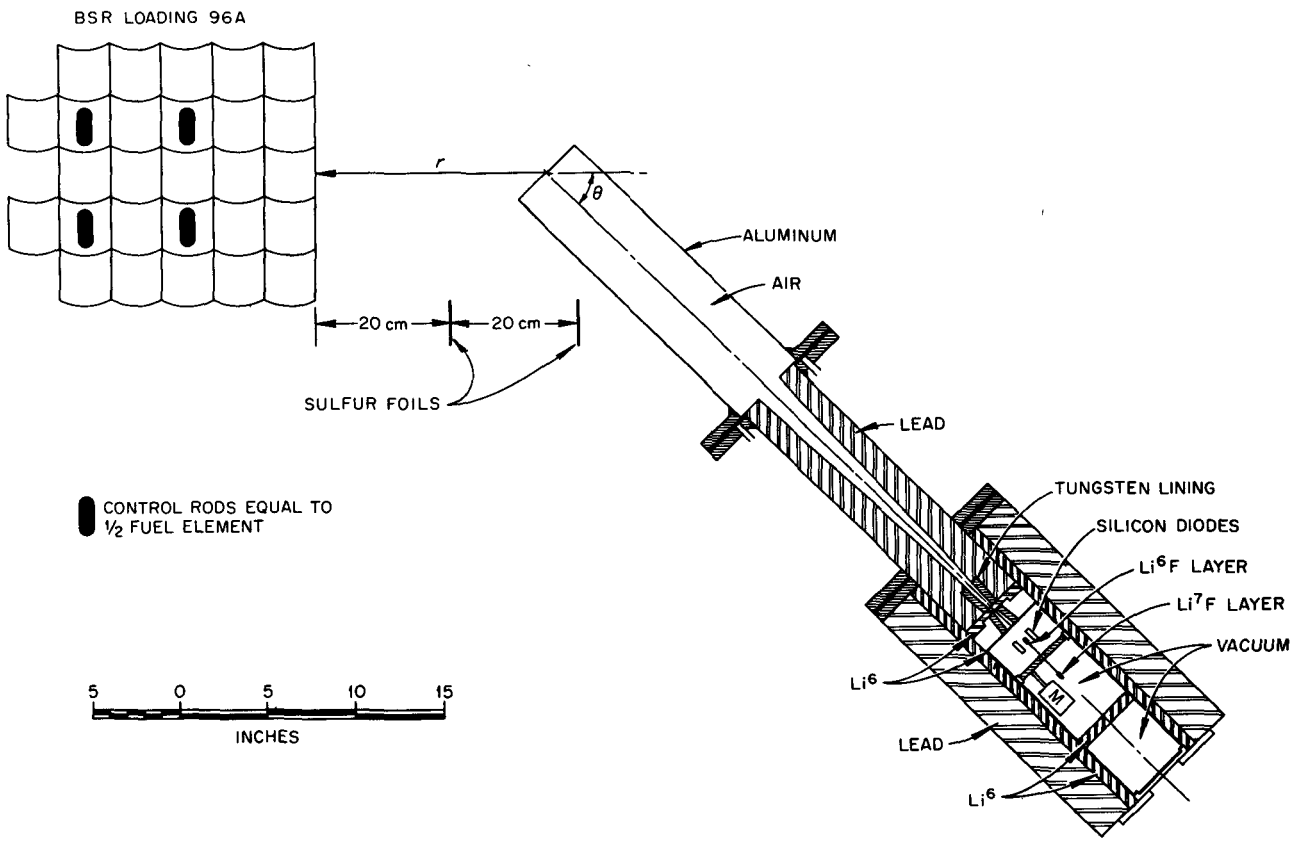

Figure 1. Experimental arrangement of BSR1 and shielded-diode spectrometer in the BSF pool

the instrument to intense gamma radiation results in both an increase in the width of the peak for monoenergetic neutrons and a channel shift that is a constant for all pulse heights (therefore a baseline shift). Both the width increase and the channel shift were measured by sending pulses from a pulse generator through the spectrometer pre-amplifiers in the actual operating environment. Both these effects were made negligible by selecting suitable levels of reactor power for each run [4].

Spectrometer efficiency

The spectrometer efficiency is taken as the count rate observed for a flux of 1 n/cm²s incident on the ^{6}LiF film. This efficiency depends on the differential-reaction cross section per steradian, the thickness of the ^{6}LiF film, and the geometry of the diode arrangement. If σ is the differential-reaction cross section per steradian, N the number of ^{6}Li nuclei, and ϖ the net average solid angle between the ^{6}LiF layer and the diodes, then efficiency ϵ is given by $N\varpi\sigma$. In obtaining ϖ, the alpha-triton coincidence requirement excludes those elements of solid angle in which only one particle strikes a diode. The value of ϵ was calculated and also experimentally determined to be $\approx 3.2\times10^{-3}$ and 3.5×10^{-3} ($\pm10\%$), respectively, for thermal neutrons. Both these values agree within 10%. Therefore, the efficiency calculated for MeV neutrons from the experimentally measured value for thermal neutrons is expected to be accurate to 10%, assuming an accurate knowledge of the ^{6}Li(n,α) differential cross section. Some assumptions regarding the differential-reaction cross section were required because of the lack of data in the neutron energy range from 2.15 MeV to 14 MeV. In particular, it was assumed that the differential cross section averaged about 90° in the centre-of-mass system could be reasonably represented by the total cross section reduced by a factor of 13.3 because this was found to be the case for energies up to 2.15 MeV and at 14 MeV. With this assumption the detection efficiency for fast neutrons was calculated.

The efficiency curve is shown in Fig. 2. Several independent checks of both the differential and the integral efficiency have been made. Figure 3 gives the

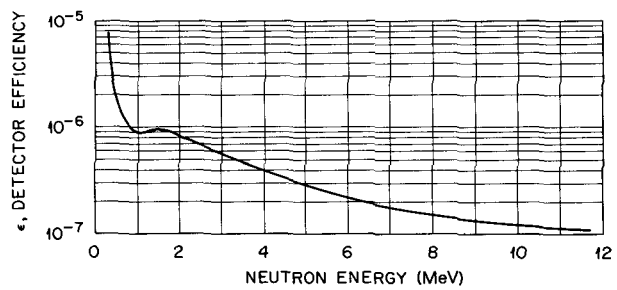

Figure 2. Shielded-diode spectrometer efficiency versus neutron energy

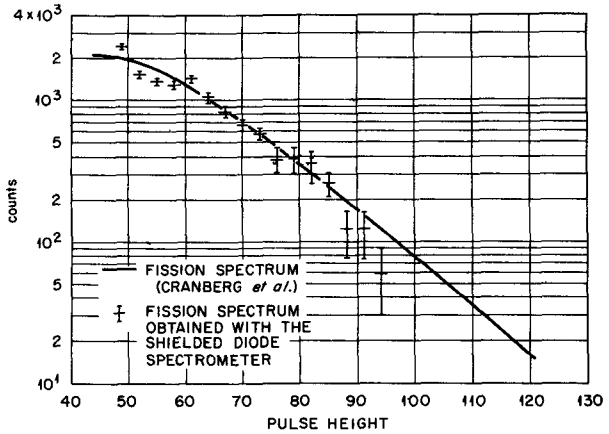

Figure 3. Uranium-235 fission spectrum obtained with shielded-diode spectrometer compared with spectrum measured by Cranberg *et al.*

fission spectrum [5] as measured with the spectrometer. A comparison with the measurements made by Cranberg *et al.* [6], also plotted in Fig. 3, shows reasonably good agreement within the statistical limits of the experiment. In Fig. 4 the spectrum at the BSR1 core-shield interface ($r=0$ and $\theta=0°$) has been compared with that measured at the same position with a proton-recoil telescope by Cochran and Henry [7]. The agreement in shape is excellent. The shielded-diode spectrometer data show a higher intensity of fast neutrons — for instance, 1.4×10^6 neutrons $cm^{-2}s^{-1}W^{-1}MeV^{-1}$ at 2 MeV compared with 1.22×10^6 neutrons $cm^{-2}s^{-1}W^{-1}MeV^{-1}$ for the proton-recoil-spectrometer data. The difference in absolute intensities measured with these two spectrometers is understood to be due to slightly different core loadings and the uncertainty in the reactor power for each of the two measurements. Data for the determination of absolute power of the BSR1 with the fuel configuration as shown in Fig. 1 have been collected and will be reported when analysed.

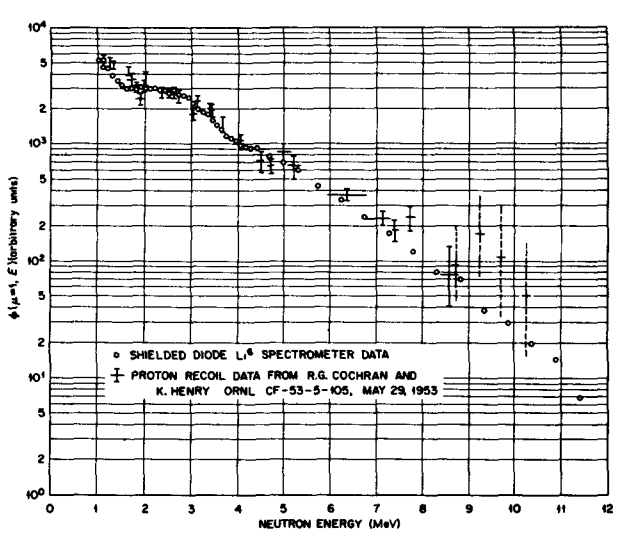

Figure 4. Comparison of BSR1 fast-neutron spectra measured with the shielded-diode spectrometer and with a recoil-proton telescope

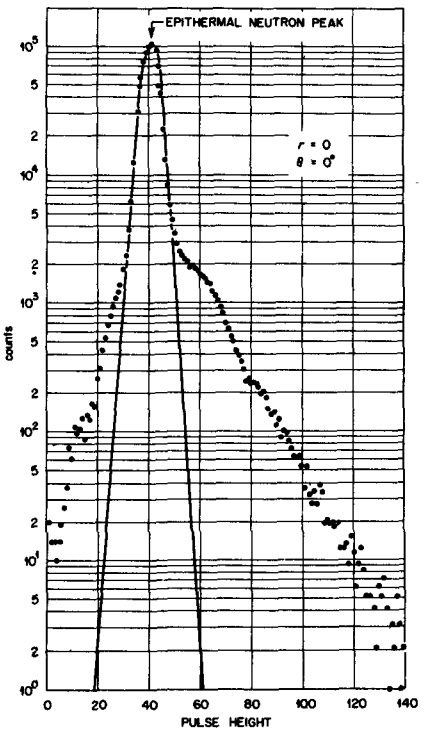

Figure 5. Pulse-height distribution of neutrons from the BSR1 at $r=0$ and $\theta=0°$

Data treatment

A typical pulse-height distribution for the spectrum at the core-shield interface is shown in Fig. 5. In this plot, background has been subtracted. At the end of each foreground run, the background was measured by replacing the ^{6}LiF film with a ^{7}Li film of almost identical size and mass. It has been shown [3] that measurement with ^{7}LiF accounts for the background arising from both the (n, charged-particle) reactions in the material of the diode and the competing reactions in ^{6}Li. By plugging the wedge-shaped collimator (Fig. 1) with water, it was also established that the background from the neutrons leaking through the sides was negligible.

As can be seen in Fig. 5, the peak due to epithermal neutrons extends to about 1 MeV. The subtraction of this peak, as shown by the solid line in Fig. 5, resulted in a large error in the data below 1 MeV while it had negligible effect on the data above 1 MeV. For this reason, only the data above 1 MeV have been reported here.

Transmission corrections for the presence of the 0.5 cm thick ^{6}Li shield in the neutron beam, the stainless-steel encapsulation of this ^{6}Li disc, and the aluminium window of the spectrometer were not applied to the data, since the effect of these corrections is to raise the spectrum at 5 MeV only about 5% relative to the 1 and 10 MeV points.

Results and discussion

The NIOBE transport calculations

Four types of radial-source distributions were

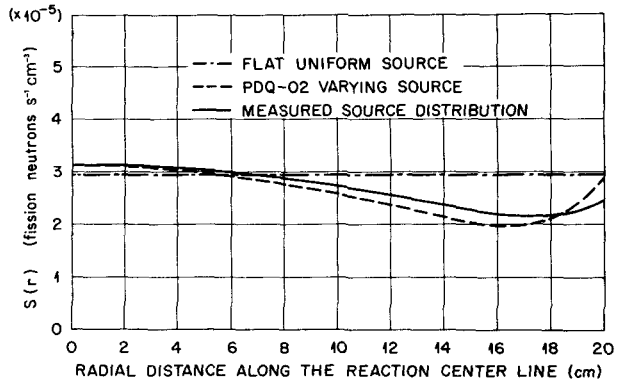

Figure 6. NIOBE source distribution versus radial distance

assumed for the spherically symmetric geometry of the NIOBE code. A 20 cm radius source region was used in each case. One of the source distributions was chosen to duplicate the measured flux at the face of the reactor, the results of which will be discussed later in the paper. For the other three cases, fission neutrons were distributed throughout the source region, which had a density equal to the average density of the water, aluminium and uranium in the BSR1 core. The three source distributions, shown in Fig. 6, are a flat distribution, a distribution calculated by the PDQ-2 code [8], and a distribution that was measured in the BSR1 mid-plane along the centre line. Each integrates to a total source strength of one fission neutron per second over the source region. A comparison of the NIOBE predictions of forward-directed angular flux, $\Phi(\mu = 0.989,r,E)$, is shown in Fig. 7 for the three cases. The spectral shape is seen to be quite insensitive to source distribution, and the intensity everywhere varies by only about 20% for the two extreme cases.

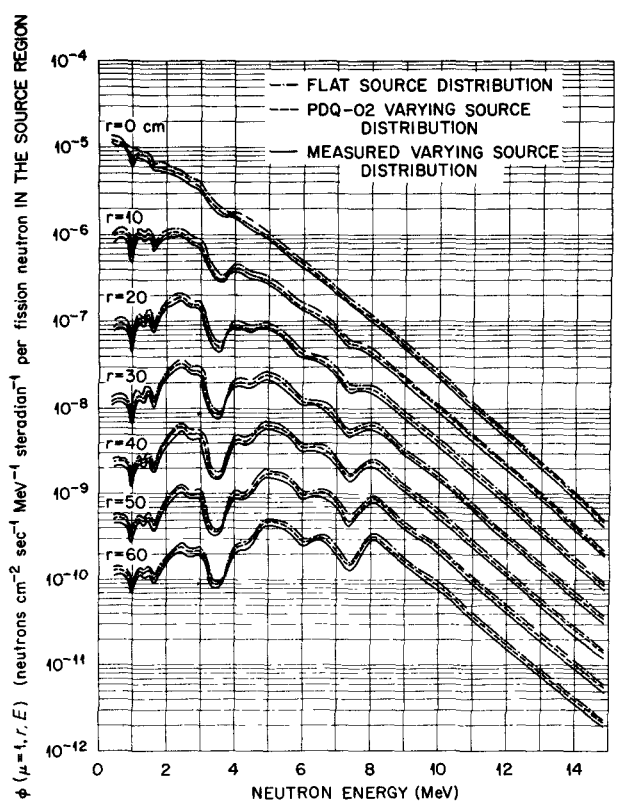

Figure 7. The NIOBE calculated values of $\Phi(\mu=0.989,r,E)$ with three source distributions shown in Fig. 6

Comparison with experiment

The calculation that utilized the source distribution measured along the BSR1 mid-plane centre line (Fig. 6) was chosen for comparison with experimental results for $\Phi(\mu=1,r,E)$, $\Phi(\mu=0.755,r,E)$, and $\Phi(\mu=0.617,r,E)$ in Figs. 8, 9 and 10, respectively. All the experimental data have been normalized to this source distribution by means of correlating the activity induced in the sulphur pellets placed at the standard location (Fig. 1) with the absolute fission rate measured with fission foils. These fission foils, in turn, had been calibrated by exposing them to the ORNL Standard Graphite Pile [9]. The measurements, therefore, represent the neutron flux obtained from the reactor whose source density along the reactor's mid-plane centre line is identical to that shown in Fig. 6, the source density used in the NIOBE calculation.

In Fig. 8, six measured spectra of forward-directed flux at $r=0$, 10, 20, 30, 40, and 50 cm are shown. These are harder than the calculated spectra. Otherwise, the over-all agreement in both shape and magnitude is everywhere within a factor of two, excluding the fine structure in the predicted spectral shape. The measured spectrum is consistently higher below 1.5 MeV, where the spectrometer is least reliable. The pronounced dips predicted by NIOBE at about 3.5 and 7.3 MeV arise from oxygen resonances in the water shield. Although this fine structure will be somewhat smeared by finite instrument resolution, the calculation should overestimate the resonance effect at 3.5 MeV, because the spherical geometry of NIOBE is more localized than the reactor. The highly forward

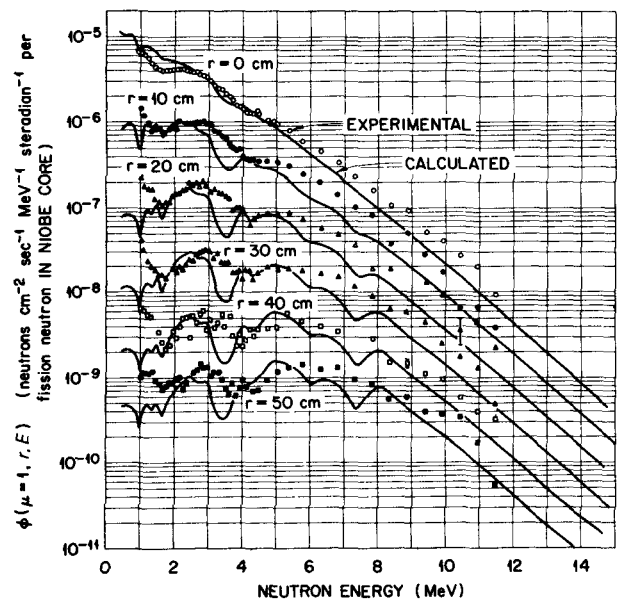

Figure 8. A comparison between measured and calculated values of $\Phi(\mu=1,r,E)$

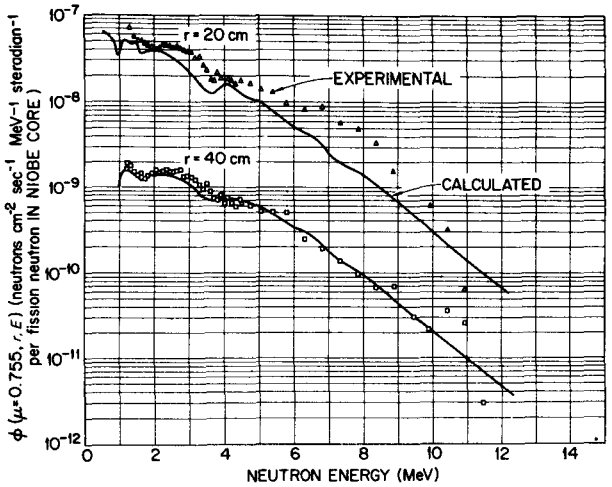

Figure 9. A comparison between measured and calculated values of $\Phi(\mu=0.755,r,E)$

scattering at 3.5 MeV [10] results in a strong dependence on the source geometry. In the limit of a very small source, the dips in the spectrum have been observed to be very pronounced in the high-resolution measurements of Verbinski *et al.* [11].

The angular flux measured at $\theta=40.5°$ ($\mu=0.755$) is compared with a NIOBE calculation in Fig. 9. The two show remarkably good agreement at $r=40$ cm. At $r=20$ cm, where the spectrometer is aimed at the edge of the reactor, the flux is considerably higher than that calculated for a spherical reactor where the edge of the reactor would be clearly out of view of the spectrometer.

For $\theta=51.8°$ ($\mu=0.617$) the measured spectra at $r=10$ and 20 cm (Fig. 10) show the effects of viewing the edge of the reactor in that the spectrum is considerably harder than the equilibrium spectra at $r=30$ and 40 cm, the flux is considerably higher than that calculated for a spherical reactor, and the spectral shape shows signs of the dips that characterize a 0° (forward leakage) spectrum. At greater distances, as with the 40.5° spectrum, both the spectral shape and intensity of the calculation reproduce the measured results reasonably well.

It should be noted that for directed fluxes at 40.5° ($r=40$ cm) and at 51° ($r=30$ and 40 cm) the calculated intensities should depend not so much on the absolute source strength along the reactor centre line as on the total power of the reactor. Therefore, since the volume of the spherical reactor in the calculation is less than half the volume of the BSR1 reactor, the NIOBE calculation appears to overestimate the angular flux at these angles.

In Fig. 11 the experimental results for forward-directed flux ($\theta=0$) are compared to a calculation in which both the spectrum and the intensity are forced to agree with experiment at the face of the reactor. The spectrum was forced by distributing a source which had a spectral shape identical to that measured at the face of the reactor throughout the volume of a non-scattering source region 20 cm in diameter. The intensity was "forced" by arbitrary normalization to

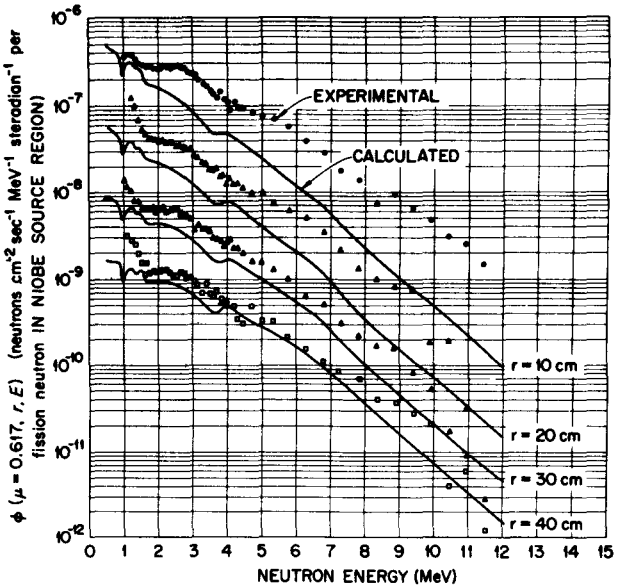

Figure 10. A comparison between measured and calculated values of $\Phi(\mu=0.617,r,E)$

that measured at the face of the reactor. The ratios of intensities calculated at the various depths have not been altered. While there is fairly good agreement in intensity and over-all spectral shape up to a 50-cm penetration in water, the measured spectrum appears to smooth out the peaks and dips of the calculated spectrum above 1.5 MeV.

ACKNOWLEDGEMENTS

The authors are indebted to Dr. F. C. Maienschein and Mr. E. P. Blizard for helpful discussions. M. S. Bokhari is grateful for the support received from the US State Department and the Pakistan Atomic Energy Commission.

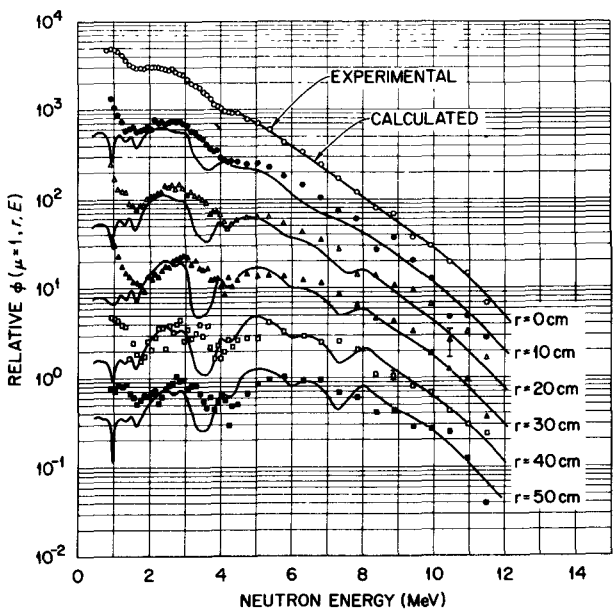

Figure 11. A comparison between measured $\Phi(\mu=1,r,E)$ and the calculated flux using spectrum at $r=0$, $\mu=1$ as NIOBE input

REFERENCES

1. Goldstein, H., *Fundamental Aspects of Reactor Shielding*, Addison-Wesley Publishing Co. Inc., Reading, Mass. (1959).
2. Preiser, S., *et al.*, *A Program for the Numerical Integration of the Boltzmann Transport Equation*, ARL Technical Report 60-314, US Department of Commerce, Washington, D.C. (December 1960).
3. Verbinski, V. V., Bokhari, M. S., and Todd, H. A., Neutron Physics Division Annual Progress Report. US Atomic Energy Comm. report ORNL-3499, Vol. I, 181–187 (August 1963).
4. Bokhari, M. S., Verbinski, V. V., and Kington, J. D., Neutron Physics Division Annual Progress Report, US Atomic Energy Comm. report ORNL-3499, Vol. I, 99 (August 1963).
5. Bokhari, M. S., Verbinski, V. V., and Todd, H. A., Neutron Physics Division Annual Progress Report. US Atomic Energy Comm. report ORNL-3499, Vol. I, 108 (August 1963).
6. Cranberg, L., *et al.*, Phys. Rev. *103*, 662 (1956).
7. Cochran, R. G., and Henry, K. M., *Fast-Neutron Spectra of the BSF Reactor*, US Atomic Energy Comm. report ORNL CF-53-5-105 (May 29 1953).
8. Bilodeau, G. G., *et al.*, PDQ – *An IBM-704 Code to Solve the Two-Dimensional Few-Group Neutron-Diffusion Equations*, US Atomic Energy Comm. report WAPD-TM-70 (August 1957).
9. Klema, E. D., *et al.*, *Recalibration of the X-10 Standard Graphite Pile*, US Atomic Energy Comm. report ORNL-1398 (October 1952).
10. Goldberg, M. D., *et al.*, *Angular Distributions in Neutron-Induced Reactions*, US Atomic Energy Comm. report BNL-400, Second Edition, Vol. I (October 1962).
11. Verbinski, V. V., *et al.*, Neutron Physics Division Annual Progress Report. US Atomic Energy Comm. report ORNL-3499, Vol. I, 114 (August 1963).

ABSTRACT—RÉSUMÉ—АННОТАЦИЯ—RESUMEN

A/670 Pakistan

Etude du transport des neutrons rapides dans l'eau dans un réacteur du type piscine

par M. S. Bokhari et V. V. Verbinski

On a mesuré les distributions spatiales, spectrales et angulaires de neutrons au-dessus de 1 MeV à l'intérieur du bouclier d'eau du réacteur dit « Bulk Shielding Reactor 1 ». On a fait varier la distance suivant des valeurs allant jusqu'à 50 cm le long de la normale à la paroi de l'enceinte du réacteur et jusqu'à 40 cm le long de droites faisant des angles de 51° et 40,5° avec la normale. Les données obtenues le long de la normale indiquent un durcissement du spectre et l'apparition d'une structure fine lorsque la distance augmente dans l'eau. Cette structure fine disparaît pratiquement et le spectre devient plus flou à 51° et 40,5°. Les résultats ont été comparés avec des calculs de transport faits en intégrant numériquement l'équation de transport de Boltzmann. L'accord général entre les calculs et l'expérience au-dessus de 1,5 MeV est raisonnablement bon; toutefois, les calculs indiquent des minimums plus prononcés pour les mesures à 0°. Ce désaccord a été attribué en partie à la différence entre la géométrie dans l'expérience et la géométrie utilisée dans le calcul pour la région de la source et à la limite finie de la résolution du spectromètre.

A/670 Пакистан

Изучение переноса быстрых нейтронов воде в реакторе погружного типа

М. С. Бокхари и В. В. Вербински

Были проведены измерения пространственного, спектрального и углового распределения нейтронов с энергией больше 1 *Мэв* в водяной защите реактора погружного типа. Расстояние изменялось до 50 *см* вдоль нормали к лицевой стороне реактора и до 40 *см* под углами 51 и 40,5° к нормали. Полученные вдоль нормали к лицевой поверхности реактора результаты показали, что с увеличением слоя воды спектр становится более жестким и появляется более тонкая структура. Эта тонкая структура спектра по существу исчезает, и спектр становится более мягким при 51 и 40,5°. Полученные экспериментальные данные сравниваются с результатами теоретических расчетов по теории переноса, и численно интегрируются Больцмановским уравнением переноса. Общее согласие между расчетными и экспериментальными данными для энергии выше 1,5 *Мэв* удовлетворительное, за исключением того, что расчеты предсказывают более сильный провал для измерений при 0°. Это расхождение можно частично объяснить различием в геометрии источника для расчета и экспериментов, а также конечной величиной разрешения спектрометра.

A/670 Pakistan

Estudio del transporte de neutrones rápidos mediante un reactor de piscina

por M. S. Bokhari y V. V. Verbinski

Se han medido las distribuciones neutrónicas espacial, espectral y angular en el blindaje de agua del Bulk Shielding Reactor 1 para energías superiores a 1 MeV. Se varió la distancia hasta 50 cm en dirección normal al reactor y hasta 40 cm en direcciones que forman 51° y 40,5° con la normal. A lo largo de la normal se observa un endurecimiento del espectro y que aparece estructura fina al aumentar la distancia en el agua. Esta estructura fina desaparece prácticamente y el espectro se reblandece a 51° y 40,5°. Se han comparado los resultados con cálculos que integran la ecuación de transporte de Boltzmann. Por encima de 1,5 MeV el acuerdo general entre cálculo y experimento es razonablemente bueno, excepto que los valles predichos por el cálculo a 0° son más pronunciados. Este desacuerdo se ha atribuido en parte a la diferencia entre las geometrías usadas en el cálculo y en la experiencia para la región de fuente y a la resolución finita del espectrómetro.

Desarrollo de la técnica de la fuente pulsada de neutrones en la Junta de Energía Nuclear

por F. Verdaguer, M. A. Vigón, F. Cordero, B. García-Castañer y E. R. Mayquez*

La utilidad de la técnica de la fuente pulsada de neutrones ha sido demostrada a lo largo de los últimos años a partir de los trabajos de von Dardel y Sjöstrand [1] en 1954. Con el fin de utilizar este método en nuestros laboratorios nuestro primer objetivo fué, en cuanto en la instrumentación se refiere, pulsar un acelerador Cockcroft-Walton de 600 kV para ser usado en medidas con medios moderadores, construyéndose otro de 150 kV, con mayor flexibilidad de montaje y traslado, para aplicarlo al estudio de medios multiplicativos. Se describen en este trabajo algunas características de estos aceleradores y las medidas efectuadas, o en curso, con ellos.

MEDIOS MODERADORES

Instrumentación

Se disponía de un acelerador de 600 kV tipo Cockcroft-Walton construído hace años en nuestros laboratorios. Consiste en tres etapas de aceleración, y se utiliza una fuente de iones de cátodo frío tipo Penning.

Los impulsos de neutrones se consiguen pulsando la fuente de iones con impulsos de forma sinusoidal con picos de corriente de 2A. Los picos de corriente de iones en el blanco son del orden de 200 μA. La anchura de los impulsos es variable entre 10 μs y 100 μs, y la frecuencia de repetición puede variar entre 500 y 2000 impulsos por segundo. El sistema de pulsar la fuente ha sido descrito en [2].

Se ha utilizado un analizador de tiempos de 9 canales cuyas características principales son las siguientes: los canales son contiguos con anchuras de 5, 20 y 50 μs. El instante de apertura del primer canal puede retardarse, respecto al impulso de sincronización recibido del acelerador, un intervalo de tiempo ajustable entre 0 y 800 μs. La sincronización entre el acelerador y el analizador de tiempos se consigue disparando al último con la señal producida en el blanco por la llegada de los iones, convenientemente modificada.

Como detectores se han utilizado contadores de F_3B con 96 % de B^{10} y presión del gas 120 cm Hg. Para probar la instrumentación y la puesta a punto de la técnica se midieron en primer lugar los parámetros de difusión del agua natural, obteniéndose los valores $(D\,v) = 35600 \pm 1100$ cm^2 s^{-1}, $c = 3000 \pm 1800$ cm^4 s^{-1} y $\lambda_0 = 4892 \pm 147$ s^{-1}, que están de acuerdo, dentro de los errores experimentales, con los resultados que figuran en la bibliografía.

Medida en soluciones de cadmio en agua natural

La relación existente entre el coeficiente de enfriamiento, c, y la transferencia cuadrática media de energía, o poder de termalización, M_2, hallada por primera vez por Nelkin [3], sugirió el estudio del efecto producido por una captura no $1/v$ sobre los parámetros de difusión del agua, y poder determinar así el valor de M_2 a partir de estos efectos.

Utilizando el método variacional usado por Nelkin para estudiar el efecto de enfriamiento superficial, es fácil demostrar que el valor de la constante de decrecimiento, λ, del modo fundamental en una disolución de cadmio en agua natural viene dada, en primera aproximación, o sea, para temperaturas de los neutrones que difieren poco de la del agua, por la siguiente expresión:

$$\lambda = \Sigma_0^{H_2O} v_0 + (\Sigma_{ef}^{Cd})_0 v_0 \left[g(T) - (\Sigma_{ef}^{Cd})_0 \frac{v_0 \pi^{\frac{1}{2}}}{v_T M_2} T^2 \times \left(\frac{d\,g(T)}{dT} \right)_T^2 \right] + (D\,v)_T B^2 \left[1 - 2 (\Sigma_{ef}^{Cd})_0 \frac{v_0 \pi^{\frac{1}{2}}}{v_T M_2} T \left(\frac{d\,g(T)}{dT} \right) \right] - \frac{\pi^{\frac{1}{2}} (D\,v)^2_T}{v_T M_2} B^4 \quad (1)$$

donde

$$(\Sigma_{ef}^{Cd})_T = (\Sigma_{ef}^{Cd})_0\, g(T) = \frac{\int_0^\infty \Sigma_c^{Cd}(E)\, M(E)\, dE}{v_0 \int_0^\infty (1/v)\, M(E)\, dE}$$

es la sección eficaz efectiva del cadmio a la temperatura T del medio, definida según Westcott [4], y donde $M(E)$ es la distribución maxweliana normalizada a la unidad,

$$(D\,v)_T = \frac{\int_0^\infty [D(E)v]\,(1/v)\, M(E)\, dE}{\int_0^\infty (1/v)\, M(E)\, dE}$$

* Junta de Energía Nuclear, Madrid.

es la constante de difusión en la temperatura T del medio, y los otros símbolos

v_0 $= 2{,}2 \cdot 10^5$ cm s^{-1}
v_T = velocidad más probable a la temperatura T
$\Sigma_0^{H_2O}$ = sección eficaz del agua para $v = v_0$
B^2 = laplaciana del modo fundamental

$$M_2 = \frac{1}{T^2}\int_0^\infty\int_0^\infty \Sigma(E \to E')\, M(E)\, (E - E')^2\, dE\, dE'$$

la transferencia cuadrática media de energía, o poder de termalización.

Friedman [5] llega a una expresión parecida desarrollando la perturbación producida sobre el espectro de neutrones por la presencia de la captura no $1/v$ y el tamaño finito del medio en polinomios de Laguerre y quedándose con el polinomio de primer orden.

Según la expresión (1), midiendo la constante de decrecimiento, λ, a distintas concentraciones de cadmio y los valores de la laplaciana, B^2, se puede evaluar el valor de M_2.

Las medidas se han efectuado con dos concentraciones de cadmio: 3,08 g/l y 1,59 g/l. Se escogieron estas concentraciones para obtener capturas el triple y el doble de la del agua natural.

Para eliminar los armónicos que acompañan al modo fundamental se ha utilizado el siguiente procedimiento: se han situado cuatro contadores de forma simétrica en el cero del primer armónico radial y de tal forma que el nivel máximo alcanzado por la disolución fuera igual a la longitud del volumen útil de los contadores. De esta forma, además del citado armónico, se eliminan, por integración, todos los impares axiales y se reducen a $1/(n+1)$ los pares axiales de orden n. Además, estando situados los contadores en el interior del medio, se aumentaba su velocidad de recuento, pudiendo aumentar el tiempo de retardo sin menoscabo de la estadística necesaria. En la Fig. 1 se presenta un esquema del montaje de la experiencia.

Con el fin de corregir por la perturbación producida por los contadores se efectuaron medidas sucesivas de λ con 4, 3, 2 y 1 contadores. En cada caso, los tubos no ocupados por el correspondiente contador se llenaron de disolución hasta el mismo nivel alcanzado en el resto del recipiente. En la Fig. 2 se presentan los valores así obtenidos para λ, en función del número de contadores para cada concentración y cada laplaciana. No observándose ninguna desviación de la linearidad, lo que demuestra que no existía perturbación mutua entre los contadores, era lícita la extrapolación a cero contador, obteniéndose así el valor de la constante de decrecimiento sin perturbar, correspondiente a cada concentración y laplaciana.

Los tiempos de retardo utilizados han estado comprendidos entre 200 μs y 300 μs, dependiendo del valor de la laplaciana. Por defecto de neutrones no pudo medirse a retardos mayores y para la mayor laplaciana,

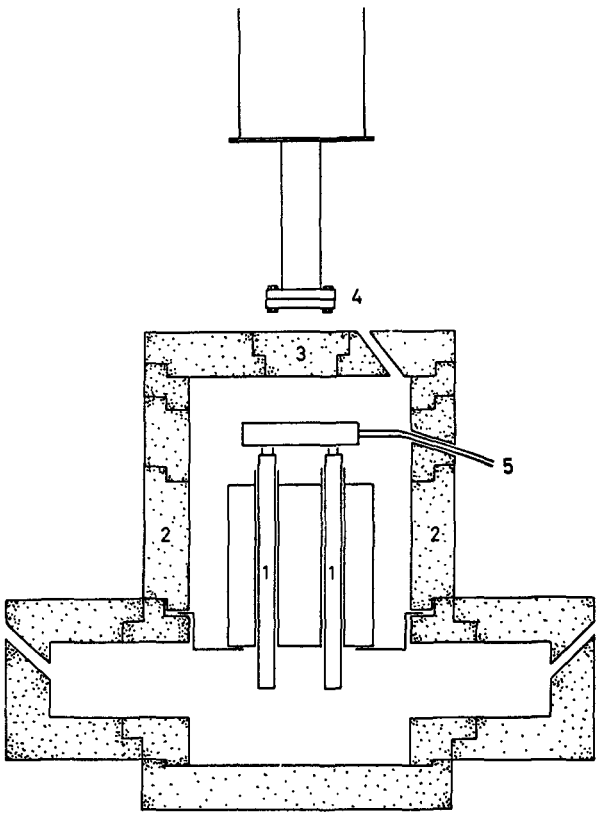

Figura 1. Esquema del montaje
1: Contadores; 2: Blindaje de óxido de boro; 3: Blindaje de carburo de boro; 4: Blanco; 5: Conexiones de los contadores

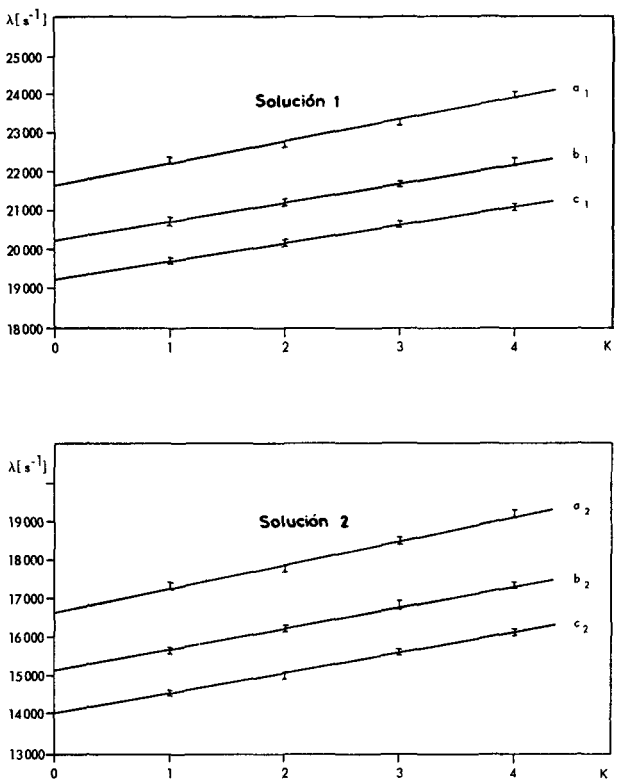

Figura 2. λ en función del número de contadores, en las soluciones 1 y 2
Las rectas a_1 y a_2 corresponden a $B^2 = 0{,}1571$ cm^{-2}; b_1 y b_2 a $B^2 = 0{,}1104$ cm^{-2}; c_1 y c_2 a $B^2 = 0{,}0846$ cm^{-2}

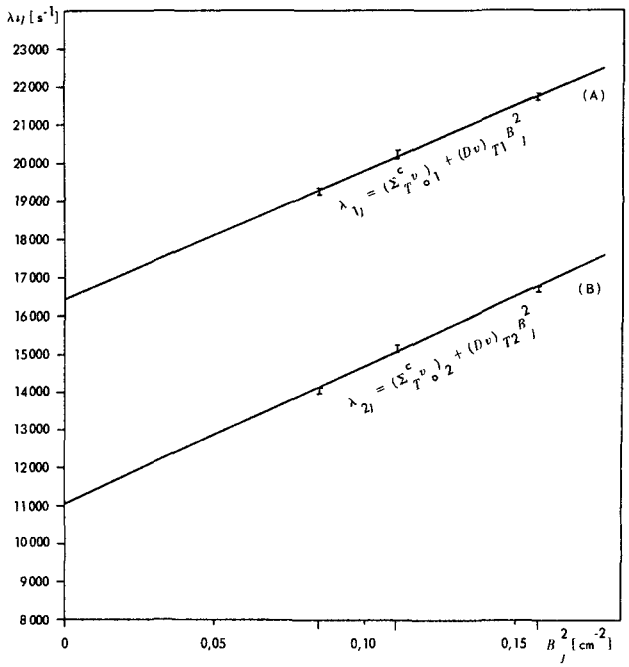

Figura 3. λ en función de B^2

$B^2 = 0{,}0846$ cm^{-2} se estimó, por cálculo, que a un retardo de 300 μs, la contribución de los armónicos en el primer canal era del orden de 1% del modo fundamental, dando lugar a una corrección sobre el valor de la constante de decrecimiento del orden de 0,2%.

Las medidas se efectuaron en tres laplacianas distintas. Para el cálculo de éstas se tomó como primer valor de prueba de la longitud extrapolada, $d_e = 0{,}33$ cm. Para corregir por el efecto de enfriamiento superficial se adoptó como valor de prueba del coeficiente de enfriamiento, $c = 3700$ cm^4 s^{-1}. En la Fig. 3 se presentan los valores de λ en función de B^2 y para las dos concentraciones. Las rectas se ajustaron por mínimos cuadrados según:

$$\lambda_{ij} = (\Sigma_T^c v_0)_i + (D\,v)_{Ti}\, B^2_j$$

obteniéndose los valores siguientes:

Concentración: 3,08 g/l (sol. 1)
$(\Sigma_T^c v_0)_1 = 16440 \pm 115$ s^{-1}
$(D\,v)_{T1} = 33807 \pm 1070$ cm^2 s^{-1}

Concentración: 1,59 g/l (sol. 2)
$(\Sigma_T^c v_0)_2 = 11073 \pm 97$ s^{-1}
$(D\,v)_{T2} = 36069 \pm 866$ cm^2 s^{-1}

Se dedujeron valores para M_2 y $(D\,v)_T$, identificando los resultados experimentales con las expresiones que figuran en (1). Para ello se ha utilizado el siguiente conjunto de valores:

$g(T) = 1{,}3281$ $T(\mathrm{d}\,g(T)/\mathrm{d}T)_T = 0{,}982$ de [4]

y

$(\Sigma_0^{H_2O} v_0)_1 = 4838 \pm 31$ s^{-1} $[(\Sigma_{ef}^{Cd})_0 v_0]_1 = 9020 \pm 54$ s^{-1}

$(\Sigma_0^{H_2O} v_0)_2 = 4851 \pm 31$ s^{-1} $[(\Sigma_{ef}^{Cd})_0 v_0]_2 = 4660 \pm 28$ s^{-1}

Tabla 1. Comparación de los valores de los parámetros de difusión, enfriamiento y termalización

Autor	$(D\,v)_T$ cm^2 s^{-1}	c cm^{-1} s^{-1}	M_2 cm^{-1}
Scott *et al.* (1954) . .	38500±800		
von Dardel *et al.* (1954)	36340±750	7300±1500	1,63±0,33
Antonov *et al.* (1955) .	35000±1000	4000±1000	2,76±0,69
Bracci *et al.* (1956) . .	34850±1100	3000±1000	3,66±1,20
Dio *et al.* (1958) . .	34450±600	3700±700	3,07±0,58
Küchle (1960) . . .	35400±700	4200±800	2,70±0,51
Lopez *et al.* (1962) . .	36892±400	5116±776	2,40±0,36
Reier (1961) . . .	37618±205		
Rocket *et al.* (1960) .	38800		
Este trabajo . . .	38411±910	8090±2400	1,65±0,49

calculados a partir de

σ^{Cd} (22 °C) = 3328 ± 20 b
σ^{H} (22 °C) = 329,3 ± 2,1 mb
$(N^H)_1 = 6{,}6788.10^{22}$ cm^{-3} $(N^{Cd})_1 = 1{,}636.10^{19}$ cm^{-3}
$(N^H)_2 = 6{,}6968.10^{22}$ cm^{-3} $(N^{Cd})_2 = 0{,}845.10^{19}$ cm^{-3}

Los valores obtenidos fueron $M_2 = 1{,}42$ cm^{-1} y $(D\,v)_T = 37864$ cm^2 s^{-1}. A estos corresponden valores de c y d_e mayores que los adoptados, con lo cual se operó iterativamente. Después de pocas iteraciones se alcanzó consistencia con los valores definitivos siguientes:

$$(D\,v)_T = 38411 \pm 910 \text{ cm}^2 \text{ s}^{-1}$$
$$M_2 = 1{,}46 \pm 0{,}43 \text{ cm}^{-1}$$

En la tabla 1 se presentan algunos de los datos publicados de $(D\,v)_T$ y c, y los valores correspondientes de M_2 calculados usando la expresión de Nelkin [3]. Para comparar nuestro valor de M_2, y el correspondiente de c, con los otros, aquél fué corregido por un factor 1,13 debido a la sustitución de $\pi^{\frac{1}{2}}$ por 2,004 en la expresión (1), tal como propone Nelkin.

Nuestro valor de $(D\,v)_T$ está de acuerdo con los obtenidos en volúmenes relativamente grandes, independientemente de si se ha utilizado fuente pulsada [6] o estacionaria [7,8] de neutrones. En cambio, es mayor que los obtenidos utilizando fuente pulsada con pequeña geometría [9–13] así como también el valor de c, excepto el publicado en [14]. Esta diferencia de valores podría ser quizá explicada suponiendo una subestimación del coeficiente del término B^6.

El valor de M_2 determinado en este trabajo es menor que los deducidos a partir de los valores de c publicados y que el calculado [3] suponiendo rotaciones completamente ligadas y traslación libre de moléculas de masa 18, ($M_2 = 2{,}27$ cm^{-1}). Según este resultado tendríamos que suponer que la masa aparente de las moléculas del agua es mayor de 18.

Usando las fórmulas presentadas en [3] que relacionan la masa $\overline{M}$ y el tiempo de termalización con M_2, se obtienen $\gamma^{-1} = 8{,}3 \pm 2{,}3$ μs y $\overline{M} = 26$. El valor de γ^{-1} está de acuerdo, dentro de los errores experimentales, con $\gamma^{-1} = 7$ μs, medido por von Dardel y Sjöstrand [14]. El valor de la masa: 26, es coherente, también dentro de los errores experimentales, con el de $\overline{M} = 23$, calculado suponiendo que el 43% de las

moléculas de agua, debido a su fuerte polaridad, están asociadas a pares, como se predice en la teoría fenomenológica de Eucken [15] sobre la estructura del agua. La existencia de complejos de moléculas también la han supuesto varios autores [16–18] para explicar la aparición de picos a baja energía en experimentos sobre la dispersión inelástica de neutrones fríos por el agua natural.

Refrigerantes orgánicos

Debido a la aplicación que tiene el Santowax-R como refrigerante orgánico en ciertos tipos de reactores de potencia era interesante medir sus parámetros de difusión.

El dispositivo experimental consistía en un recipiente cilíndrico que mediante resistencias arrolladas en su superficie permitía fundir y calentar el Santowax-R. La temperatura máxima era de 300°C. La existencia de la resistencia, así como del material aislante del calor que protegía a los contadores situados exteriormente produce un efecto equivalente a un reflector. Con el fin de asignar a este reflector un coeficiente de reflexión que permitiera corregir el valor de la longitud extrapolada a utilizar para el cálculo de la laplaciana, se efectuaron medidas previas, y con el mismo dispositivo, con Gilotherm a la temperatura ambiente.

Admitiendo los valores publicados sobre los parámetros de difusión [19,20] del Dowtherm, equivalente al Gilotherm, se calculó que el efecto del reflector era corregir la longitud extrapolada del medio por un factor igual a $1{,}8 \pm 0{,}2$.

Los resultados de la medidas efectuadas con Santowax-R están siendo tratados teniendo en cuenta la existencia de dicho reflector.

MEDIOS MULTIPLICATIVOS

La primera aplicación de la técnica de la fuente pulsada en medios multiplicativos va a ser el estudio del conjunto subcrítico de agua pesada, uranio natural y refrigerante orgánico descrito en el trabajo [21] presentado en esta conferencia y que expone las experiencias verificadas con fuente estacionaria de neutrones.

Para este fin se ha construído y está a punto de entrar en servicio un acelerador de 150 kV cuyas características se describen someramente a continuación: el sistema de vacío está formado por una bomba rotatoria de 12 m^3/h y una difusora de aceite de 2000 l/s. La presión final en el acelerador es de 1.10^{-6} torr y la presión máxima de trabajo es de 4.10^{-5} torr con un flujo máximo de 130 cm^3 atm/h de deuterio.

La fuente de iones es de tipo Penning con cátodo frío de uranio. La corriente máxima de descarga es de 5 A de pico y 50 mA de media. La tensión de mantenimiento del arco es de 650 V y la presión de trabajo de 3 a 5 10^{-3} torr. Se utilizan orificios de salida de 1 a 3 mm de diámetro. La anchura de los impulsos puede variarse desde 6 μs hasta varios milisegundos, y la frecuencia de repetición puede ser de 1 ó 2 por segundo a 2 kc/s.

El sistema extractor tiene geometría Pierce modificada ligeramente para mejorar la conductancia en vacío. Una lente electrostática de tres electrodos forma el sistema de enfoque y acelerador siendo desaceleradora la lente intermedia. En la Fig. 4 puede verse un esquema de este sistema. Las lentes son de gran abertura, siendo 22,5 cm el diámetro de la lente aceleradora.

En el blanco pueden obtenerse corrientes de

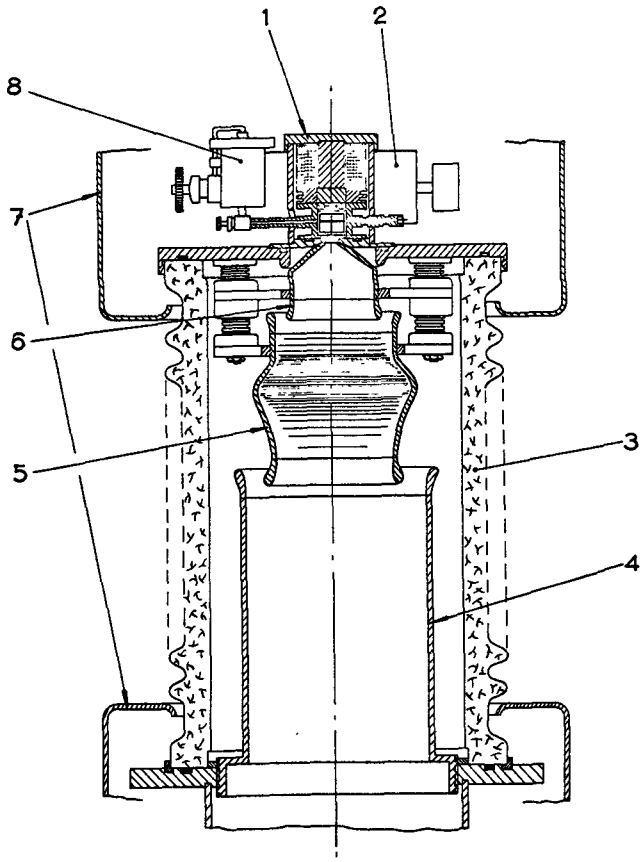

Figura 4. Sistema de extracción y enfoque del acelerador de 150 kV
1: Fuente de iones; 2: Refrigeración; 3: Aislante; 4: Electrodo acelerador; 5: Electrodo desacelerador; 6: Electrodo extractor; 7: Caperuzas antiefluvios; 8: Válvula de gas

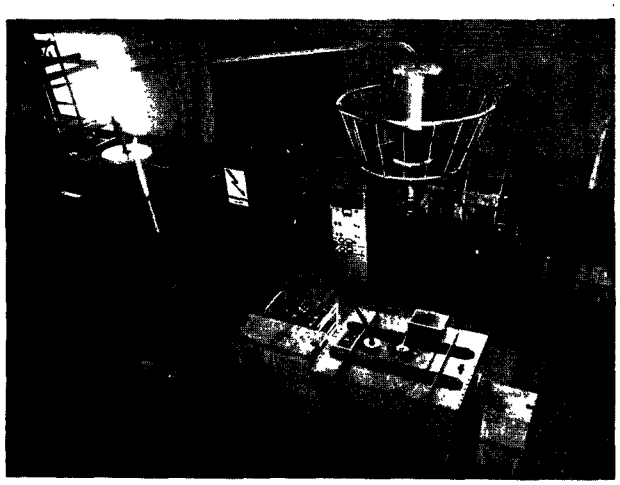

Figura 5. Vista general del acelerador de 150 kV

deuterones de 15 mA de pico a 150 kV, con diámetro del haz iónico de 3 cm. Se estima que el porcentaje de iones atómicos oscila entre 40% y 60%, según la intensidad de descarga en la fuente de iones.

En la Fig. 5 se presenta una fotografía del acelerador en su estado actual de montaje.

BIBLIOGRAFÍA

1. von Dardel, G. F., and Sjöstrand, N. G., Phys. Rev., *96*, 1245 (1954).
2. Cordero, F., Verdaguer, F., An. Real. Soc. Esp. Fís. y Quím., *58* (A), 85 (1962).
3. Nelkin, M., J. Nuclear Energy, *8*, 48 (1958).
4. Westcott, C. H., CRRP-787 (1958).
5. Friedman, E., Nucl. Sci. and Eng., *14*, 420 (1962).
6. Scott, F. R., Thomson, D. B., Wright, W., Phys. Rev., *95*, 582 (1954).
7. Reier, M., J. Nuclear Energy, Pts. A and B. Reactor Sci. and Technol., *14*, 186 (1961).
8. Rockey, K. S., Skolnik, W., Nucl. Sci. and Eng., *8*, 62 (1960).
9. Antonov, A. V., *et al.*, *Difusión de neutrones por el método de impulsos*, Actas de la primera conferencia internacional sobre la utilización de la energía atómica con fines pacíficos, P/661, Vol. 5, pág. 3, Naciones Unidas (1956).
10. Küchle, M., Nucl. Sci. and Eng., *8*, 88 (1960).
11. Dio, W. H., Schopper, E., Nuclear Phys., *6*, 175 (1958).
12. Lopez, W. M., Beyster, J. R., Nucl. Sci. and Eng., *12*, 190 (1962).
13. Bracci, A., Coceva, C., Il Nuovo Cimento, *4*, 59 (1956).
14. von Dardel, G. F., Sjöstrand, N. G., Progress in Nucl. Energy, Ser. I, Vol. II, 183 (1958).
15. Eucken, A., Akad. Wiss. Göttingen (Math. Phys. K1), *2*, 38 (1946).
16. Stiller, H. H., Danner, H. B., *Inelastic Scattering of Neutrons in Solids and Liquids*, p. 363, IAEA, Viena (1960).
17. Heinloth, K., Spinger, T., *Inelastic Scattering of Neutrons in Solids and Liquids*, pág. 323, IAEA, Viena (1960).
18. Larsson, K. E., Holmroyd, S., Otnes, K., *Inelastic Scattering of Neutrons in Solids and Liquids*, pág. 323, IAEA, Viena (1960).
19. Küchle, M., Nukleonik, *2*, 131 (1960).
20. Demanins, F., Rado, V., Vinci, F., CNEN-RT/FI (63) 22.
21. R. Mayquez, E., de Francisco, J. L., Olarte, F., *Estudio experimental de redes de carburo de uranio en agua pesada*, véanse las presentes Actas, P/743, Vol. 3.

ABSTRACT—RÉSUMÉ—АННОТАЦИЯ—RESUMEN

A/678 Spain

Development of the pulsed neutron source technique at the Junta de Energía Nuclear

By F. Verdaguer *et al.*

In this paper are presented some applications of the pulsed neutron source technique, the results obtained and the measurements in progress.

A 600 kV Cockcroft-Walton accelerator has been used as a neutron source, the neutron bursts being obtained by pulsing a Penning type ion source. The first measurements have been performed with a 9 channel time analyser.

First, the diffusion parameters of light water have been measured, the results agreeing with published data.

The connexion between the cooling effect coefficient c and the mean square energy transfer M_2 suggested the possibility of measuring M_2 through the perturbations which are produced on the capture and diffusion constant of non-$1/v$ capturing media. These media have been obtained by dissolving different amounts of cadmium in light water. The perturbations depend on the cadmium concentration, on the temperature dependence of the effective cross section of cadmium and on M_2. From measurements, a value of $M_2 = 1{,}65 \pm 0{,}49\ \text{cm}^{-1}$ has been deduced.

Previous results from measurements of the diffusion parameters of Santowax-R as a function of the temperature are also presented. To calibrate the experimental arrangement used, measurements have been performed in which Gilotherm was substituted for Santowax-R.

With regard to non-multiplying media, measurements are in progress to study the effect produced by a reflector on the mean life of neutrons in moderators.

In order to apply the pulsed neutron source technique to multiplying media, a 150 kV pulsed accelerator has been built and its description is given. The first measurements will be performed on a heavy-water moderated subcritical assembly with two different kinds of fuel elements.

A/678 Espagne

Progrès dans la technique de la source de neutrons pulsés à la Junta de Energía Nuclear

par F. Verdaguer *et al.*

Le mémoire décrit quelques applications de la technique de la source de neutrons pulsés et donne les résultats déjà obtenus, ainsi que les mesures en cours.

On utilise comme source de neutrons un accélérateur Cockcroft-Walton de 600 kV avec une source d'ions à impulsions du type Penning.

Pour les premières mesures, on a eu recours à un analyseur de temps à 9 canaux.

On a mesuré d'abord les paramètres de diffusion de l'eau légère, dont les valeurs concordent avec celles mentionnées dans la littérature.

La relation entre le coefficient de refroidissement c et le transfert moyen quadratique d'énergie M_2 a incité les auteurs à mesurer cette valeur à partir des perturbations de la capture et de la constante de diffusion d'un milieu dont la section efficace de capture n'obéit pas à la loi $1/v$. On a obtenu ce milieu en dissolvant dans de l'eau légère des quantités variables d'un composé du cadmium. Ces perturbations dépendent de la concentration en cadmium, de la variation de la section efficace effective du cadmium suivant la température des neutrons et de la valeur de M_2. On déduit des mesures effectuées que $M_2 = 1{,}65 \pm 0{,}49$ cm^{-1}.

Les auteurs indiquent également les résultats obtenus précédemment en mesurant les paramètres de diffusion de Santowax-R à diverses températures. Pour procéder à ces mesures, il a fallu étalonner le dispositif expérimental en remplaçant le Santowax-R par le Gilotherm.

En ce qui concerne les mesures de ce genre dans des milieux non multiplicateurs, on poursuit actuellement l'étude de l'effet que produit un réflecteur sur la vie moyenne des neutrons dans un milieu ralentisseur.

Afin d'appliquer la technique de la source pulsée à l'étude des propriétés des milieux multiplicateurs, on a construit un accélérateur pulsé de 150 kV. Les premières mesures seront faites dans un assemblage sous-critique modéré à l'eau lourde et avec deux types d'éléments combustibles.

A/678 Испания

Разработка способов применения импульсных источников нейтронов в Комиссии по атомной энергии

Ф. Вердагуер *et al.*

В настоящем докладе описываются некоторые способы применения импульсных источников нейтронов и сообщаются полученные результаты.

В качестве источника нейтронов используется ускоритель Кокрофта — Уолтона на 600 *кв*, оснащенный ионным источником типа Пеннинга и работающий в импульсном режиме.

В начальных измерениях применялся 9-канальный временной анализатор.

В первую очередь были измерены диффузионные параметры для обычной воды, причем полученные результаты совпали с имеющимися в литературе данными.

Соотношение между коэффициентом эффекта охлаждения c и средним квадратом величины передаваемой энергии M_2 наводит на мысль об определении последней величины из измерений возмущений в сечении захвата и в коэффициенте диффузии среды, сечение захвата которой не подчиняется закону $1/v$. Такая среда была получена путем растворения в обыкновенной воде различных количеств содержащего кадмий вещества. Возмущения зависят от концентрации кадмия, от изменений эффективного сечения захвата кадмия в зависимости от температуры нейтронов и от значения M_2. На основании произведенных измерений была найдена искомая величина: $M_2 = 1{,}65 \pm 0{,}49$ *см* $^{-1}$.

Приводятся также полученные ранее результаты измерения диффузионных параметров терфенила марки сантовакс-R при различных температурах. Для калибровки результатов сантовакс-R заменялся жилотермом.

Что касается проведения такого рода измерений в неразмножающих средах, то в настоящее время проводится изучение влияния наличия отражателя на среднее время жизни нейтронов в замедлителях.

В целях применения метода импульсного источника для изучения свойств размножающих сред разных составов был построен импульсный ускоритель на 150 *кв*, описание которого приведено в докладе. Первые измерения будут проведены на подкритической сборке с замедлителем из тяжелой воды, причем будут изучены два типа тепловыделяющих элементов.

Investigations into the moderating properties of water

By U. Dahlborg,* G. Grosshög,** K. E. Larsson,* E. Möller,*** S. N. Purohit*** and N. G. Sjöstrand**

In order to predict the neutron spectrum in a thermal reactor, one has to know how the neutrons interact with the moderator. Based on theoretical and experimental evidence, several scattering models have been proposed. In the present paper, a review is given of recent work performed in Sweden to test and improve the present models for neutron scattering in water. The work consists of differential neutron scattering experiments, integral time-dependent and stationary measurements as well as theoretical considerations.

PART 1

Cold neutron scattering experiments

(K. E. Larsson and U. Dahlborg)

During the last few years, some experiments on light and heavy water have been performed at the Stockholm reactor R1 by use of the cold neutron scattering technique [1–3]. A beryllium filtered neutron beam impinges upon a sample, and the energy distributions of the scattered neutrons are measured at some selected scattering angles by the slow chopper time-of-flight technique. In Fig. 1, the scattering pictures from H_2O at 275°K and 365°K are shown. It is seen that the scattered spectra divide into two parts, one inelastic part ranging from about 0.2 eV down to 0.005 eV and one quasi-elastic part for energies below 0.005 eV. It is immediately obvious by comparison with the neutron spectrum calculated according to the gas model (also shown in Fig. 1) that this model cannot at all describe the scattering picture. This fact seems to be generally true in the case of low energy neutrons scattered by a liquid.

The differential scattering cross section per atom may generally be written as [4]

$$\frac{d^2\sigma}{d\Omega d\omega} = \frac{a^2}{2\pi}\frac{k}{k_0}\int\int \exp[i(\vec{\kappa}\cdot\vec{r}-\omega t)]\cdot G(\vec{r},t)d\vec{r}dt \qquad (1)$$

where $G(\vec{r},t)$ is the generalized pair distribution function of the scattering medium which can be in the solid, liquid or gaseous state. $\vec{k}$ and $\vec{k}_o$ are the scattered and ingoing neutron wave vectors, $\hbar\vec{\kappa}$ is the momentum transfer, and $\hbar\omega$ the energy transfer. The function $G(\vec{r},t)$ can naturally be split up into a part $G_s(\vec{r},t)$, describing the correlation between positions of one and the same particle at different times, and a part $G_d(\vec{r},t)$ which refers to pairs of distinct particles. The G_s function gives rise to incoherent scattering and the G_d to coherent scattering. As the self part of the pair distribution function is much easier to handle mathematically, one normally omits the distinct part. This is justified in the case of scattering from light water, as the hydrogen nuclei scatter almost completely incoherently, but is not necessarily true for the case of heavy water, as up to 80 per cent of the deuterons scatter coherently. The incoherent differential scattering cross section for a solid can be rigorously derived in terms of the frequency spectrum of the normal modes. Similarly, in the case of a liquid the cross section can be expressed in terms of a generalized frequency distribution, which can be shown to be the velocity auto correlation function of the atoms in the liquid [5]. This function may be derived from experiments by two different methods, one according to Egelstaff *et al.* [6] and one according to Larsson *et al.*

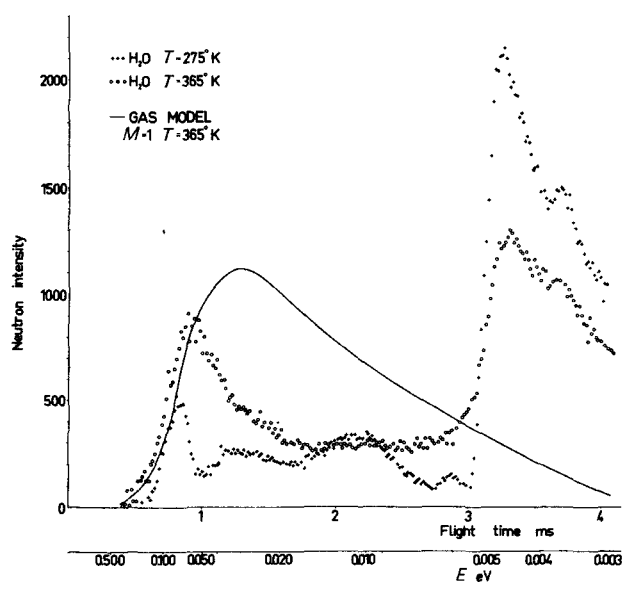

Figure 1. Examples of observed neutron spectra scattered from H_2O at two temperatures. For comparison the (mass=1) ideal gas model curve is shown as calculated for the highest temperature

* Royal Institute of Technology, Stockholm.
** Chalmers University of Technology, Göteborg.
*** AB Atomenergi, Studsvik.

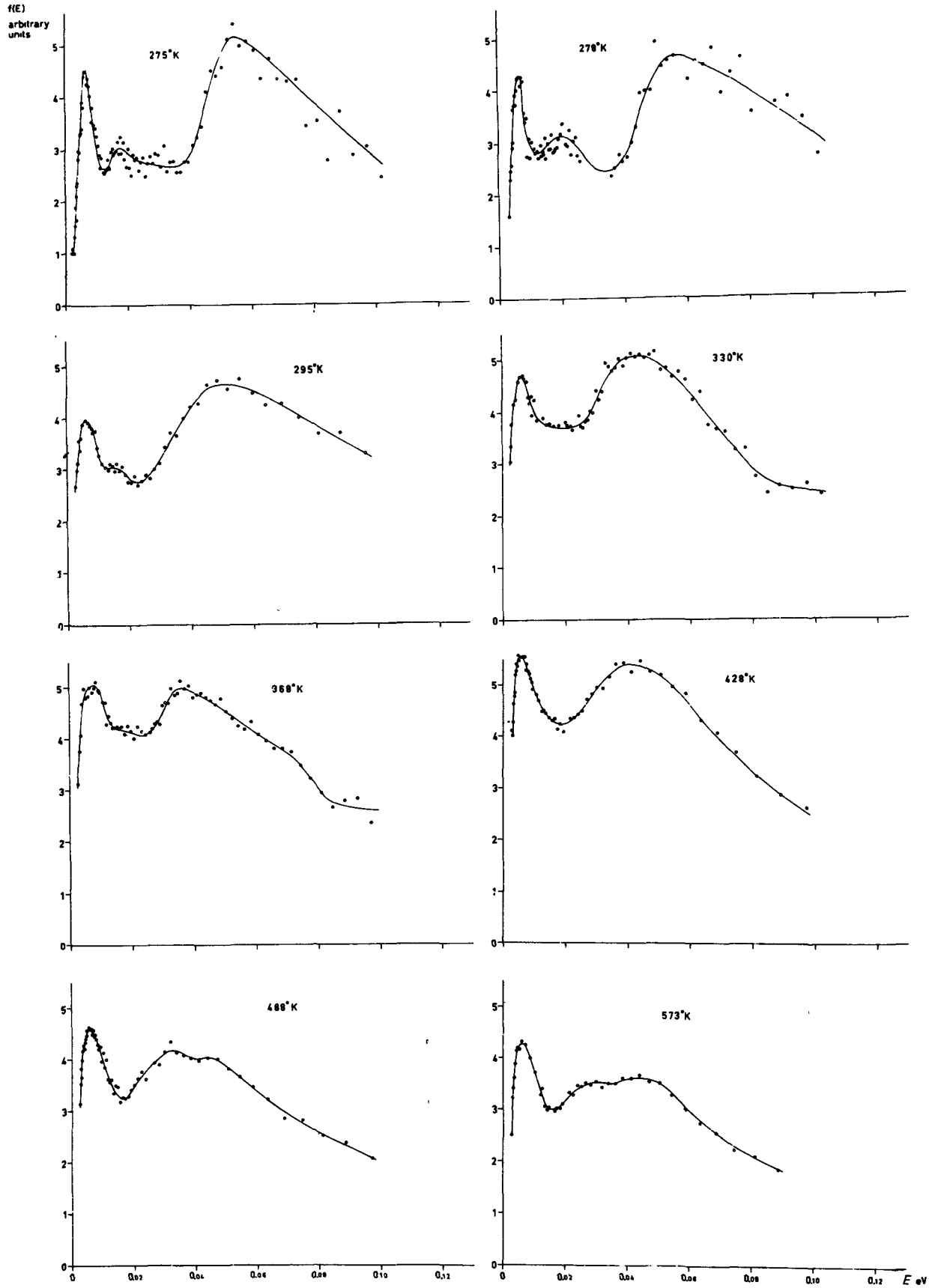

Figure 2. Frequency spectra for D_2O obtained at different temperatures

[2,3,7]. The two methods give on the whole the same result, but differences in the detailed structure of the obtained distributions may appear.

The justifications for the assumption that there exists a more or less pronounced vibrational spectrum in a liquid are many. From careful experimental studies of the broadening of the quasi-elastically scattered neutron spectrum it is possible to obtain relaxation times for the diffusive motions in liquids. Thus experiments on some hydrogenous liquids (H_2O and glycerine) have shown that the spectra of quasi-elastically scattered neutrons can be explained by a model of the atomic motions where the solid-like properties are predominant. From this model, and also directly from the uncertainty relation, relaxation times for the diffusive motions are obtained. This relaxation time seems to reach a saturation value, about 1×10^{-12} s, as the temperature is increased [7]. Thus, even close to the boiling point, any atomic or molecular, vibrational or rotational, motion with a period shorter than 10^{-12} seconds is defined and is existing although it must be more or less damped. It therefore seems reasonable to believe that a velocity spectrum or a frequency spectrum of these motions exists. We have derived such spectra on the basis of the formalism already developed for the phonons in a solid.

A strong support for this procedure is that the frequency spectra derived from the inelastically scattered neutron spectra in for instance D_2O just below and just above the melting point (Fig. 2) coincide almost exactly [2]. This means indeed that the internal motions do not differ to any appreciable amount in the solid and the liquid phase. Measurements at higher temperatures (Fig. 2) have shown that even for D_2O at 300 °C there exists a frequency spectrum with a rather well pronounced structure.

A rather intricate question in neutron spectra scattered from liquids is whether any coherent scattering is observed in the pattern or not. Coherent scattering could apparently be caused by the oxygen nuclei, the deuterons, and also to a small degree by the protons. One way to study this is to compare the frequency spectra for H_2O and D_2O just above the melting points [7]. If the high energy peak in H_2O, which is known to originate from the hindered rotation of the proton within the hydrogen bond, were shifted down in energy in the ratio $1:\sqrt{2}$, one should obtain the spectrum for D_2O very closely. The new H_2O spectrum obtained in this way is compared to the measured one for D_2O in Fig. 3. The two distributions are arbitrarily normalized to each other at about 0.055 eV. As can be seen the spectra differ in shape most markedly at about 0.02 eV at which energy the coherent scattering should be at its maximum. It thus seems that there exist coherent contributions in the observed patterns in cold neutron scattering from water. Recent measurements have, however, shown that only very weak coherent scattering from more complicated liquids such as glycerine seems to exist.

All the facts presented give strong support to the idea that there exists a spectrum of the internal

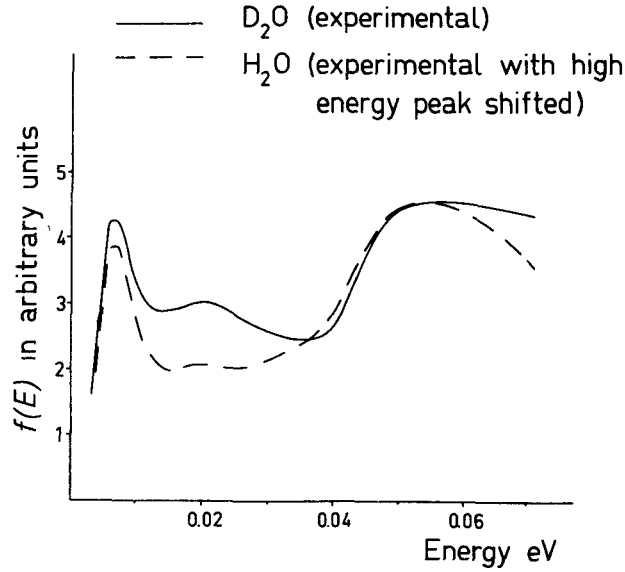

Figure 3. The frequency spectrum for H_2O at +2 °C with the high energy peak shifted down in energy in the ratio $1:\sqrt{2}$ compared to the measured frequency spectrum for D_2O at +5 °C

motions in water and that this spectrum can be derived, retaining the first term in the phonon expansion formula for the differential scattering cross section in the incoherent approximation given by [8],

$$\frac{d^2\sigma}{d\Omega d\omega} = a^2_{\text{inc}} \cdot \frac{k}{k_o} \cdot \exp\left(-\frac{\hbar\omega}{2k_BT} - 2W\right) \left[\frac{\hbar\kappa^2 f(\omega)}{4M\omega \sinh\frac{\hbar\omega}{2k_BT}} + \sum_{n=2}^{\infty} \frac{(2W)^n}{n!} \bar{G}_n(\omega)\right] \quad (2)$$

where $2W$ is the Debye-Waller factor, $f(\omega)$ is the frequency spectrum and the $\bar{G}_n$ denotes certain functions of the energy transfer $E=\hbar\omega$. If one includes the internal molecular vibrations at ~0.2 eV and ~0.4 eV it is possible to obtain a physically reliable expression for the scattering kernel. The use of very approximate models like the width model [9] is justified only by its ability to describe details of thermalization spectra but it has no physical significance as it exaggerates the importance of the diffusive part of the atomic motions. Likewise, the use of the gas model is only justified for neutron energies which are high compared to the energy transfer.

PART 2

Experimental investigation of time dependent slowing down

(E. Möller and N. G. Sjöstrand)

Principle of the experiment

Bursts of neutrons are produced in a large volume of water. In a chosen position, a pot is placed containing a weak solution of a substance with a known neutron capture cross section $\Sigma_a(E)$. The time and energy dependent neutron flux $\Phi(E,r,t)$ reacts with the capturing substance resulting in a time dependent reaction rate $R(t)$ given by

$$R(t) = \int_V \int_E \Phi(E,r,t)\Sigma_a(E)\mathrm{d}E\mathrm{d}V \qquad (3)$$

The integration is performed over the volume of the container. If the concentration of the capturing substance is low, the perturbing influence on the neutron spectrum is negligible, and the spectrum will be dependent on the neutron source energy and the scattering properties of the medium only. Knowing the properties of the source one may thus obtain information about the scattering laws by studying $R(t)$. The information depends on the cross section of the added substance, the spectrum indicator. A $1/v$ cross section results in a measurement of the time dependent neutron density. If the cross section deviates from the $1/v$ law, the time behaviour of certain energy regions is enhanced or suppressed. The near thermal region is of the greatest interest to study, since here the neutron scattering is a very complicated process and incompletely known. The most suitable spectrum indicators are cadmium (resonance energy 0.18 eV), samarium (0.098 eV) and gadolinium (0.03 eV). Silver has close to thermal energies a cross section which with good accuracy follows the $1/v$ law and may be used for neutron density measurements.

Experimental procedure

Neutrons with a mean energy of 1 MeV were produced by the ^{7}Li(p,n)^{7}Be reaction, the protons being delivered by the pulsed 5.5 MV van de Graaff accelerator in Studsvik. The absorption of the indicator solution reduced the lifetime of the thermal neutrons to 60μs. In order to avoid discontinuities in the medium, the whole volume was poisoned with boron to the same absorption. The capture gamma radiation from the spectrum indicator was detected by a scintillation counter with a plastic scintillator. The pulses from this were, after discrimination against capture gamma radiation of 2.2 MeV energy from hydrogen in the water, fed to a time analyser. Neutrons were produced every 250μs, and the measurements were made with time resolutions of 0.155 and 0.330μs. The position of the indicator was varied. Measurements were also made with indicator solution in the whole tank. The records of the measurements were corrected for dead-time, and the background was subtracted.

Experimental results and their interpretation

The results of the measurements at a distance of 9 cm from the source with a time resolution of 0.33μs are shown in Fig. 4. The maximum in the reaction rate curve is observed at 3.8 and 6.1μs for cadmium and samarium respectively. For gadolinium there is no pronounced peak. All the curves pass over into a smooth decay after 25–30μs. This is evidently the time for complete thermalization. Then an exponential decay follows, resulting from absorption and diffusion. The measurement with silver shows that the neutron density in the indicator pot decays exponentially from the first microsecond. The transients in the other curves have their origin in the energy changes

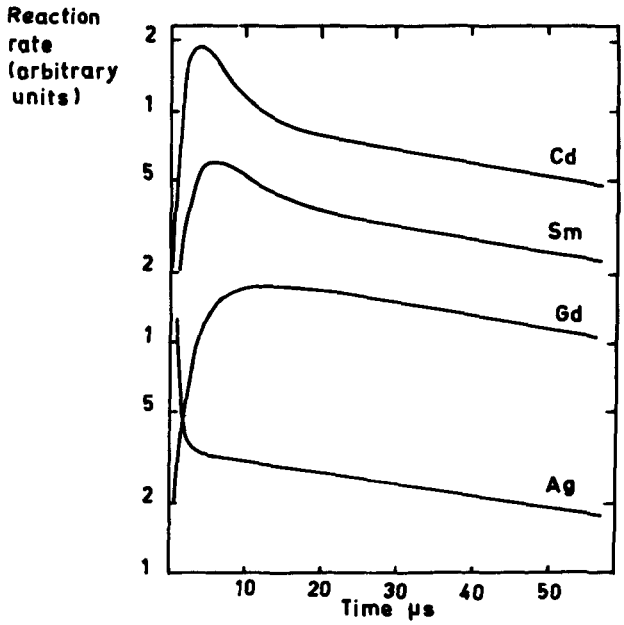

Figure 4. Measured reaction rate curves

during the thermalization. Figure 5 shows the same curves, but measured with a time resolution of 0.155μs and corrected for absorption. The curves have been normalized to the same final level after complete thermalization, and they have been found to represent the infinite medium. The basis for the theoretical curves in the same figure is given in part 4, where the results are also discussed.

The last stage of the thermalization has been described by von Dardel [10] as a cooling down Maxwell spectrum, the temperature of which is exponentially approaching the moderator temperature. The time constant, t_{th}, depends on the energy transfer during the scattering. Since the effective cross sections (g) for a Maxwell spectrum are linear functions of the temperature up to 250°C for cadmium and gadolinium, one obtains $g = g_{20} + k\exp(-t/t_{th})$. From the time 9$\mu$s, when all the neutrons are down in the near thermal region, the experimental curves yield, when analysed as a sum of a constant and an exponential,

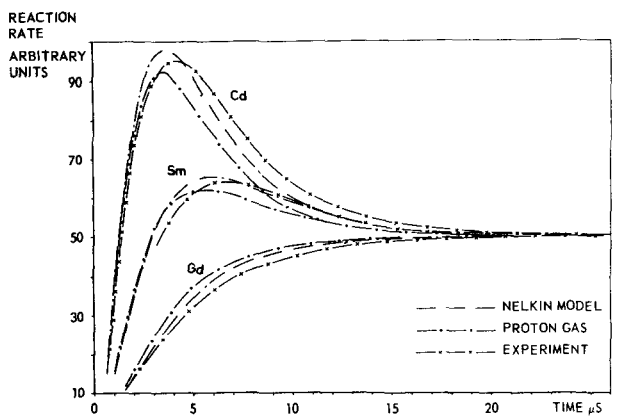

Figure 5. Reaction rate curves for cadmium, samarium and gadolinium corrected to zero absorption for water. All the curves are normalized at the final level

a thermalization time constant of $4.1 \pm 0.4 \mu s$. This value is lower than that predicted for the mass 18 gas model, but it is between the values expected for a proton gas and for Nelkins model (see part 4).

The slowing down time to a given energy cannot be found directly from the experimental curves. A measurement of this quantity requires an indicator cross section of $1/v$ shape with a sharp cut-off at a suitable energy. A cross section being a good approximation of the ideal is obtained by mixing cadmium and gadolinium in the atomic ratio 1:0.365. The experimental curve, in its shape, similar to the gadolinium curve but with a steeper slope in the beginning, can be obtained by adding in that ratio curves from the individual measurements, in Fig. 5, of the two indicators, after having normalized them to the same source strength and number of atoms. The slowing down time is found to be $2.7 \pm 0.4 \mu s$ for an energy of 0.2 eV. This result is discussed in part 3.

A more detailed report on these measurements will be given elsewhere [11]. The method has also been used to study transport effects in the time behaviour in the eV region and to investigate the thermalization in ice [12].

PART 3

Static measurement of the slowing down time

(G. Grosshög)

A neutron source which emits Q neutrons per second is placed in an infinite medium. If the total number of neutrons then present in the medium is N, the mean life time $\bar{t}$ of the total neutron population is N/Q. In the same way, if N_a is the number of neutrons in the medium having a velocity above v_c, the mean life time $\bar{t}_c$ of this part of the neutron population is N_a/Q. Thus we can write $\bar{t}/\bar{t}_c = R$, where R is the cut-off ratio of a $1/v$ detector, i.e., the ratio of the integrated counting rates observed with and without a filter having a cut-off at v_c. Neutrons are removed from the group having velocities above v_c through slowing down and absorption. Defining the slowing down time $\bar{t}_s$ as the average time a neutron spends from birth to reaching the cut-off velocity and assuming $1/v$ absorption in the medium we find

$$\bar{t}/\bar{t}_s = R - 1 \qquad (4)$$

Because $\bar{t}$ can be obtained easily from known cross sections it is possible to determine the slowing down time from a cut-off ratio measurement [13].

In the present experiment, cadmium and gadolinium were used in the form of cylindrical filters with thickness 600 and 150 mg/cm² respectively. A 100 mG Ra–Be neutron source was placed in the centre of a cylindrical aluminium tank (height 100 cm, diameter 90 cm) filled with water. The neutron distributions in the tank were measured with a small boron trifluoride proportional counter. Great care must be taken to eliminate the disturbance caused by the detector. The correction was determined both theoretically, using the P_1 approximation and experimentally by foil measurements in the vicinity of the detector. Good agreement was found between theory and experiment. The effect of leakage of thermal neutrons through the hole in the filters caused by the connection to the preamplifier was determined experimentally. Another correction was necessitated by the finite dimensions of the detector, which makes it average the neutron density differently, depending upon the shape of the distribution.

Using 330 ± 3 mb as the absorption cross section of hydrogen the slowing down times were determined as $\bar{t}_s = 2.47 \pm 0.11$ μs for gadolinium and $\bar{t}_s = 1.60 \pm 0.07$ μs for cadmium. The effective cut-off energies for the filters were taken from the tables of Stoughton and Halperin [14] to be 0.3 eV for the gadolinium and 0.5 eV for the cadmium filter. The uncertainty in these values is estimated to be less than 10 per cent.

In Fig. 6 various theoretical and experimental values are compared. The curve represents the relation $\bar{t}_s = 2l_s/v_c$ corresponding to slowing down in a gas of free protons at rest with a scattering mean free path $l_s = 0.75$ cm. The calculated points all lie below the curve, probably because of different primary data. The experimental points agree well with the curve down to an energy of 0.4 eV. At lower energies the deviations indicate that the assumed model is no longer valid, but that chemical binding and up-scattering are becoming important.

A detailed description of the experiment has been published in Arkiv för Fysik [15].

PART 4

Theoretical work on time dependent neutron thermalization

(S. N. Purohit)

Calculation procedure

Time-dependent neutron energy spectra have been obtained for free and bound proton models by the

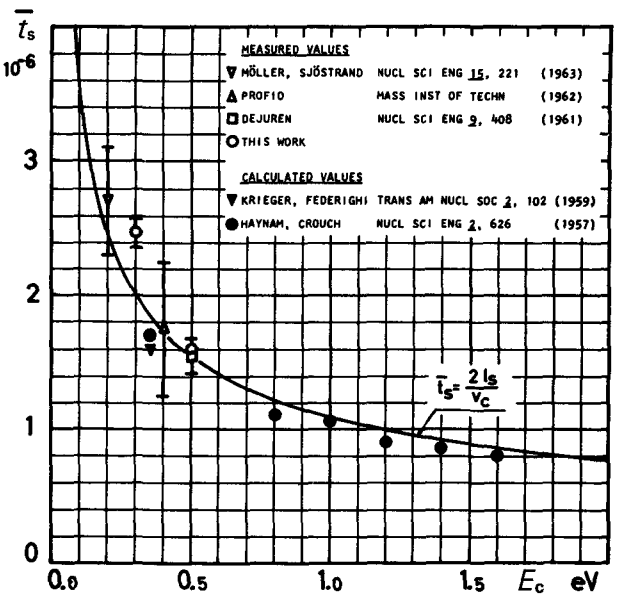

Figure 6. The slowing-down time as a function of neutron energy

same method as used for the heavy gas in a previous paper [16]. From these spectra reaction rates for the spectrum indicators used in the experiments have been calculated. The thermal neutron flux $\Phi(E,t)$ as a function of energy and time has been generated from the time dependent Boltzmann equation. The scattering integral was extended up to a thermal cut-off energy E_T. The source for neutrons with energies between zero and E_T was obtained from a source integral from energy E_T to the neutron source energy. It was calculated using the Ornstein-Uhlenbeck solution [17] for $\Phi(E,t)$ and the free proton gas scattering matrix with an effective temperature to characterize the binding. The numerical solution was undertaken by two multigroup programmes NEFLUDI and NEFLUDI-TDCS prepared by Mr. L. Persson in collaboration with Mr. K. Nyman for the Ferranti Mercury Computer. The programmes can handle a maximum number of 22 thermal groups. The NEFLUDI generated $\Phi(E,t)$ for a given thermal neutron scattering matrix for times greater than the initial time, 10^{-8}s. In the NEFLUDI-TDCS the thermal group cross sections are recalculated for a set of time points, using the calculated time and energy dependent neutron flux as the weighting factor. The programmes also calculate the reaction rates for specified neutron detectors.

The reaction rates for spectrum indicators

The reaction rates calculated with NEFLUDI-TDCS for the free proton gas and the bound proton model of Nelkin [18] along with the experimental results of Möller and Sjöstrand described in part 2 for cadmium, samarium and gadolinium detectors are shown in Fig. 5. The scattering matrix for the Nelkin model as given by Honeck's Gaker code [19] was used. All the curves are normalized so as to have the same asymptotic value 50. The free particle macroscopic scattering cross section $\Sigma_{s0} = 1.33$ cm^{-1} has been used in the present calculations. The following conclusions are drawn:

(*a*) The free proton gas model is inadequate to explain the experimental results in all the three cases. The deviation is large beyond 2.5 μs.

(*b*) Reaction rates for the bound proton model of Nelkin are in better agreement with the measured reaction rates than the proton gas model. Nevertheless, the disagreement still persists.

(*c*) The thermalization time constant values for the free proton gas and the Nelkin model are estimated to be equal to 3.5 μs and 4.7 μs respectively. These are consistent with the values obtained by the eigenvalue method. The experimental value of Möller and Sjöstrand given in Part 2 is equal to 4.1 ± 0.4 μs.

(*d*) The study of the reaction rate for cadmium may prove to be significant in the investigations of the details of the neutron scattering law in the energy region around the cadmium resonance of 0.178 eV.

The resolution of the difference between the results of Nelkin's model and experiments may be sought along two lines—by refining the present numerical calculations and by modifying the existing bound model.

Modification of the Nelkin model

The dynamics of atomic motions in the Nelkin model is represented by the free translation motion of the whole molecule plus the harmonic vibrations of four oscillators (three correspond to the intra-molecular vibrations of equal weight and the fourth represents hindered rotations). The generalized frequency spectrum discussed in part 1 for this model is represented by the following expression

$$f(\omega) = \frac{f_{\text{gas}}(\omega)}{M_{\text{molecule}}} + \sum_{i=1}^{4} \frac{\delta(\omega - \omega_i)}{M_i} \qquad (5)$$

Two modifications are proposed. First, the oscillator (delta function) representation of hindered rotations should be replaced by the distribution given by the cold neutron scattering experiments. As described in Part 1, Larsson and Dahlborg have derived the generalized frequency spectra for H_2O and D_2O for several temperatures. The modified bound model should therefore include the available information about the medium energy transfer modes (hindered rotations) and the low energy transfer modes (hindered translational and diffusive motions), as given by the experiments. This would ensure the correct estimation of Placzek's moments including the Debye-Waller factor.

Second, the realistic relative weight between one intra-molecular vibration and hindered rotations should be assigned. In the present Nelkin model, the use of the Sachs-Teller mass tensor concept is not rigorous. The exact theoretical and experimental estimates of the relative weight are not available. The theoretically least understood of all motions, hindered rotations, complicate the problem. On the other hand, the present neutron scattering experiments do not cover energy transfers of the magnitude of intra-molecular vibrations. Attempts have been made to obtain this parameter from the scattering law data [20]. The determination of the relative weight from the analysis of two integral experiments has also been

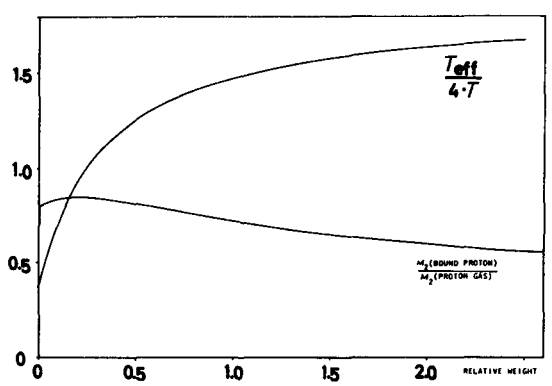

Figure 7. The ratio of M_2 (bound proton) to M_2 (proton gas) and the ratio of $T_{eff}/4T$ versus the relative weight between one intra-molecular vibration and hindered rotations

proposed in a study of the integral parameters of the neutron scattering law [21].

Integral parameters, such as M_2 (the second energy transfer moment weighted by the Maxwellian distribution) and the effective temperature T_{eff} (2/3 mean kinetic energy) are sensitive to the variation of the relative weight, as shown in Fig. 7. M_2 was obtained using the Doppler approximation by the method given in [21].

The thermalization time constant t_{th} versus T_{eff}/T for H_2O is shown in Fig. 8. t_{th} has been estimated using the L_1 approximation result [22] involving only M_2. There is always one point (from experiments) in this plot which is exact and corresponds to the real moderator. The point corresponding to the experimental results of Möller and Sjöstrand for $t_{\text{th}} = 4.1 \pm 0.4$ μs and of Poole *et al.* [23] for $T_{\text{eff}}/T = 3.9 \pm 0.4$ is also shown. From the analysis of the results presented here, one obtains an estimate of the relative weight between one intra-molecular vibration and hindered rotations equal to 0.222 (compared to 0.397 for the Nelkin model) assuming equal weight for three intra-molecular vibrations.

Further studies of time dependent thermal neutron energy spectra by varying the relative weight between the intra-molecular vibration and hindered rotations are being planned. A programme is in preparation for calculating the scattering matrices based upon the experimentally derived frequency spectra by Larsson and Dahlborg and also using the rigid hindered rotator model of Yip and Osborn [24].

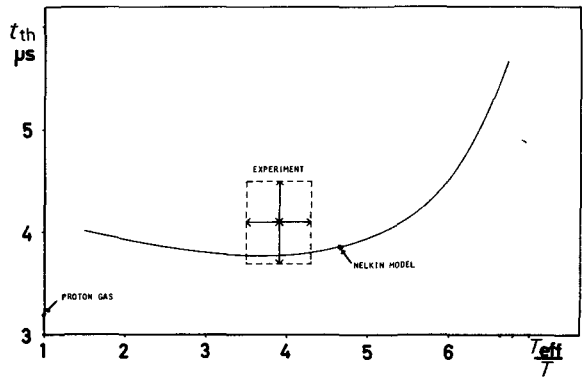

Figure 8. The variation of the thermalization time constant, t_{th}, with the effective temperature for H_2O obtained by varying the relative weight between one intra-molecular vibration and hindered rotations

REFERENCES

1. Larsson, K. E., Holmryd, S. and Otnes, K., Inelastic scattering of neutrons in solids and liquids, IAEA Vienna, 329 (1960).
2. Larsson, K. E. and Dahlborg, U., J. Nucl. Energy *16*, 81 (1962).
3. Larsson, K. E. and Dahlborg, U., Inelastic scattering of neutrons in solids and liquids, I, IAEA Vienna, 317 (1962).
4. van Hove, L., Phys. Rev. *95*, 249 (1954).
5. Rahman, A., Singwi, K. S. and Sjölander, A., Phys. Rev. *126*, 986 (1962).
6. Egelstaff, P. A., Inelastic scattering of neutrons in solids and liquids, IAEA Vienna, 25 (1960).
7. Larsson, K. E. and Dahlborg, U., to be published in Physica.
8. Sjölander, A., Ark. Fys. *14*, 315 (1958).
9. Leslie, D. C. and Terry, M. J., AEEW-R-250 (1963), also IAEA Report *20*, Tech. Report Series, 417 (1963).
10. von Dardel, G. F., Trans. Roy. Inst. Techn. Stockholm No. 75 (1954).
11. Möller, E. and Sjöstrand, N. G., Arkiv för Fysik, *27*, 501 (1964).
12. Möller, E., to be published in Arkiv för Fysik.
13. DeJuren, J. A., Nucl. Sci. Eng. *9*, 408 (1961).
14. Stoughton, R. W. and Halperin, J., ORNL-TM-236 (1962).
15. Grosshög, G., Ark. Fys. *27*, 215 (1964).
16. Purohit, S. N., Nucl. Sci. Eng. *9*, 305 (1961).
17. Ornstein, L. S., and Uhlenbeck, G. E., Physica *4*, 478 (1937)
18. Nelkin, M. S., Phys. Rev. *119*, 741 (1960).
19. Honeck, H., BNL 5826 (1961).
20. Beyster *et al.*, GA-3542 and GA-3853 (1962).
21. Purohit, S. N., *Integral parameters of the thermal neutron scattering law*, AE-154 (1964).
22. Purohit, S. N., Nucl. Sci. Eng. *9*, 157 (1961).
23. Poole, M. J., *et al.*, *Some measurements of thermal neutron spectra*, SM 42/18 (1963).
24. Yip, S. and Osborn, R. K., Phys. Rev. *130*, 1860 (1963).

ABSTRACT—RÉSUMÉ—АННОТАЦИЯ—RESUMEN

A/680 Suède

Recherches sur les propriétés modératrices de l'eau

par U. Dahlborg *et al.*

Le mémoire est consacré aux travaux de recherche effectués en Suède sur les propriétés modératrices de l'eau à l'aide de diverses méthodes expérimentales et théoriques.

La nature des mouvements atomiques dans l'eau légère et l'eau lourde a été étudiée à l'aide de spectromètres à temps de vol pour neutrons lents. Des distributions de fréquences généralisées ont été tirées des spectres de neutrons diffusés inélastiquement, déterminés par voie expérimentale, et il a été établi qu'elles existaient même à $+300\,°C$. Ce fait ainsi que la largeur du pic quasi élastique indiquent nettement que les molécules d'eau ont un comportement identique à celui des solides. Il est montré que le modèle de diffusion continue n'explique pas le comportement en largeur et que le modèle gazeux ne décrit pas les mouvements de translation des molécules d'eau. Il est établi que le pic quasi élastique est dans une grande mesure déterminé par le mouvement des protons dans les liaisons hydrogène.

Le comportement dans le temps des neutrons pendant le ralentissement et la thermalisation dans l'eau a été étudié à l'aide d'un générateur van de Graaff à pulsations. Des renseignements sur la variation, dans le temps, du spectre des neutrons ont été obtenus par sa réaction avec des indicateurs de spectres, la vitesse de réaction étant observée par la détection de rayons gamma de capture radiative. Des mesures ont été effectuées avec du cadmium, du gadolinium et du samarium comme indicateurs. On a obtenu un temps de ralentissement de $2{,}7 \pm 0{,}4$ μs à 0,2 eV. A partir de 9 μs après injection les résultats sont bien décrits par l'hypothèse du flux correspondant à une distribution de Maxwell se refroidissant à la température du modérateur avec une constante de temps de thermalisation de $4{,}1 \pm 0{,}4$ μs.

Les temps de ralentissement des neutrons Ra–Be dans l'eau aux énergies de coupure des filtres de cadmium et gadolinium ont été mesurés à l'aide d'une méthode stationnaire. Le temps de ralentissement est tiré du rapport des densités de neutrons intégrées mesurées dans un milieu de grandes dimensions à l'aide d'un détecteur $1/v$ avec ou sans les filtres en question. Les temps de ralentissement obtenus sont de $1{,}60 \pm 0{,}07$ et $2{,}47 \pm 0{,}11$ μs respectivement à des énergies de coupure de 0,5 et 0,3 eV.

Divers modèles théoriques pour le ralentissement des neutrons dans l'eau ont été comparés aux expériences intégrales. Une solution numérique de l'équation de Boltzmann pour le modèle du gaz de protons indique que la validité de ce modèle est limitée aux énergies supérieures à 0,4 eV. Le modèle de Nelkin est meilleur mais sa concordance avec les expériences n'est pas encore satisfaisante. Les possibilités d'amélioration basées sur les mesures différentielles détaillées font l'objet d'une discussion.

A/680 Швеция

Исследование замедляющих свойств воды

У. Дальборг *et al.*

В докладе дается обзор работ, проводимых в Швеции по исследованию замедляющих свойств воды различными экспериментальными и теоретическими методами.

Природа атомных движений в обычной и тяжелой воде была исследована при помощи спектрометров медленных нейтронов по методу времени пролета. Обобщенные распределения частот были выведены на основе экспериментально определенных спектров неупруго рассеиваемых нейтронов; установлено, что они существуют даже при $+300°$ С. Это обстоятельство, а также ширина квазиупругого пика свидетельствуют о ярко выраженном поведении молекул воды подобно твердому телу. Показано, что непрерывная диффузионная модель не объясняет поведения ширины и что газовая модель не описывает движений переноса молекул воды. Установлено, что квазиупругий пик в высшей степени определяется движением протонов в водородных связях.

Временное поведение нейтронов в процессе замедления и термализации в воде было изучено с использованием ускорителя Ван-де-Граафа в импульсном режиме. Информация по изменениям нейтронного спектра со временем была получена по их реакциям с индикаторами спектра; скорость реакции определяли путем детектирования излучения захвата. Были проведены измерения на кадмии, гадолинии и самарии в качестве инфикаторов. Время замедления до 0,2 *эв* составило $2{,}7 \pm 0{,}4$ *мксек*. От 9 *мксек* после инжекции результаты хорошо описываются предположением, что поток имеет максвелловское распределение замедления до температуры замедлителя с постоянной времени термализации порядка $4{,}1 \pm 0{,}4$ *мксек*.

Время замедления нейтронов радиево-бериллиевого источника в воде до пороговых энергий кадмиевых и гадолиниевых фильтров было измерено стационарным методом. Время замедления получают при помощи отношения интегральной плотности нейтронов, измеренной в большой среде детектором $1/v$ с указанными

фильтрами или без них. Было получено время замедления 1,60±0,07 *мксек* и 2,47±0,11 *мксек* до пороговых энергий 0,5 и 0,3 *эв* соответственно.

Различные теоретические модели замедления нейтронов в воде сравниваются с интегральными экспериментами. Численное решение больцмановского уравнения для модели протонного газа показывает, что пригодность этой модели ограничивается энергиями выше 0,4 *эв*. Модель Нелькина лучше, но согласие с экспериментом еще неудовлетворительное. Обсуждаются возможности усовершенствования, основанные на детальных дифференциальных измерениях.

A/680 Suecia

Estudio de las propiedades del agua como moderador

por U. Dahlborg *et al.*

Los autores reseñan los trabajos que se realizan en Suecia con el propósito de estudiar las propiedades moderadoras del agua mediante diversos métodos experimentales y teóricos.

Aplicando espectrómetros de tiempo de vuelo para neutrones lentos, se ha investigado la naturaleza de los movimientos atómicos en el agua ligera y en el agua pesada. De los espectros de dispersión inelástica de los neutrones, determinados experimentalmente, se han deducido las distribuciones de frecuencia generalizadas, comprobándose que persisten aún a los 300°C. Este hecho, unido a la amplitud del máximo cuasielástico, indica netamente que el comportamiento de las moléculas de agua es claramente parecido al de los sólidos. Se demuestra que el modelo de difusión continua no explica lo que ôcurre con las anchuras de banda y que el modelo gaseoso no describe los movimientos de traslación de las moléculas de agua. Se comprueba que el máximo cuasielástico depende en gran medida del movimiento de los protones en los enlaces de hidrógeno.

Mediante un generador van de Graaff pulsado, se estudió el comportamiento de los neutrones en función del tiempo durante la moderación y la termalización en el agua. Para obtener datos sobre la variación del espectro neutrónico en función del tiempo, se recurrió a la reacción con indicadores de espectro de cadmio, gadolinio y samario observándose la velocidad de reacción por medio de la detección de rayos gamma de captura. El tiempo de moderación hasta 0,2 eV obtenido fué de $2,7 \pm 0,4$ μs. A contar de los 9 μs después de la inyección, los resultados pueden formularse satisfactoriamente suponiendo que el flujo obedece a una distribución maxwelliana que va alcanzando la temperatura del moderador, con una constante de tiempo de termalización de $4,1 \pm 0,4$ μs.

Aplicando un método estacionario, se midió el tiempo de moderación de los neutrones de una fuente de Ra–Be, en agua, hasta las energías de corte de los filtros de cadmio y de gadolinio. El tiempo de moderación se deduce de la razón de las densidades neutrónicas integradas, determinadas en un medio de grandes dimensiones utilizando un detector $1/v$, sin y con el mencionado filtro. Los tiempos de moderación obtenidos son $1,60 \pm 0,07$ y $2,47 \pm 0,11$ μs, hasta las energías de corte de 0,5 y 0,3 eV, respectivamente.

Se compararon varios modelos teóricos de la moderación de los neutrones en el agua con los experimentos integrales. Una solución numérica de la ecuación de Boltzmann para el modelo de gas de protones demuestra que este modelo sólo es válido para energías superiores a 0,4 eV. El modelo de Nelkin es más correcto, pero todavía no concuerda satisfactoriamente con los resultados experimentales. Se discute la posibilidad de introducir mejoras sobre la base de mediciones diferenciales detalladas.

On the experimental region connecting diffusion length and pulsed neutron experiments

By K.-H. Joest and G. Memmert*

Integral properties of the theoretical scattering law of a moderator, such as diffusion and thermalization parameters, can easily be compared with the experimental values. The following possibilities exist:

(*a*) Measurement of the asymptotic decay constant of a neutron pulse for different bucklings establishes the function $\lambda(B^2)$;

(*b*) Measurement of the spatial attenuation coefficient as a function of poisoning establishes the function $\kappa^2(\nu\Sigma_a)$

The characteristic constants of the moderator can then be determined by

$$\nu D = D_0 = \left(\frac{d\lambda}{dB^2}\right)_{B^2=0} = \frac{1}{\left(\frac{d\kappa^2}{d(\nu\Sigma_a)}\right)_{\nu\Sigma_a=(\nu\Sigma_a)^0}}$$

$$C = -\frac{1}{2}\left(\frac{d^2\lambda}{dB^4}\right)_{B^2=0} = -\frac{1}{2}\frac{1}{D_0^3}\left(\frac{d^2\kappa^2}{d(\nu\Sigma_a)^2}\right)_{\nu\Sigma_a=(\nu\Sigma_a)^0}$$

According to H. C. Honeck [1], the results of the two experiments can be expressed in one diagram with

$$k^2 = \begin{cases} \kappa^2 & \text{if } k^2 > 0 \\ -B^2 & \text{if } k^2 < 0 \end{cases}$$

as abscissa, having the decay constant, λ for positive ordinate and poisoning, $\nu\Sigma_a - (\nu\Sigma_a)^0$, as negative ordinate. In that representation, one part of the curve between $-\kappa_{min}^2$ and 0 is not accessible with the above types of experiments because of the finite absorption $(\nu\Sigma_a)^0$ of the moderator itself. While arbitrary small B^2-values can be obtained by enlarging the moderator block, there is a minimum value for κ^2 given by

$$\kappa_{min}^2 = \frac{(\nu\Sigma_a)^0}{\nu D}$$

Higher values of κ^2 can be produced by poisoning techniques.

Consequently, an experimental gap is found in the region

$$\kappa_{min}^2 < -k^2 < 0$$

On the other hand, it is well known that a neutron flux decaying exponentially can be regarded as a stationary flux with the effective absorption $\nu\Sigma_a - \lambda$. This affords the possibility of effectively reducing absorption even to values below that of the moderator itself. A neutron flux decaying according to $e^{-\lambda_0 t}$ in a half-space can, therefore, be expected to have the asymptotic relaxation constant

$$\kappa = \sqrt{\frac{(\nu\Sigma_a)^0 - \lambda_0}{\nu D}}$$

The neutron flux would show the time variation $e^{-\lambda_0 t}$ imposed by the source, if $\lambda_0 < (\nu\Sigma_a)^0$, i.e., the decay of the source is slower than the decay process in the half-space far from the boundaries.

MATHEMATICAL TREATMENT OF NON-STATIONARY EXPONENTIAL EXPERIMENTS ACCORDING TO THE MONOENERGETIC DIFFUSION THEORY

The problem is treated unidimensionally of a source varying according to $e^{-\lambda_0 t}$ with time at the boundary of a moderator half-space. The spatial distribution of the source neutrons is then given by $e^{-\Sigma z}$ according to the first collision concept. Under these assumptions, the monoenergetic diffusion equation reads

$$\left\{\frac{\partial}{\partial t} + \nu\Sigma_a - \nu D\frac{\partial^2}{\partial z^2}\right\} N(z,t) = Q_0 e^{-\Sigma z - \lambda_0 t} \qquad (1)$$

List of symbols:

z	position
t	time
N	neutron density
$\overline{N}$	Laplace transform of N with respect to one variable
$\overline{\overline{N}}$	Laplace transform of N with respect to two variables
k	Laplace variable conjugated to z
s	Laplace variable conjugated to t
v	neutron velocity
Σ_a	macroscopic absorption cross section
Σ_s	macroscopic scattering cross section
$\Sigma = \Sigma_s + \Sigma_a$	total cross section
D	diffusion constant
Q_0	source intensity

* Interatom, Internationale Atomreaktorbau, GmbH, Bensberg.

Finite dimensions of the moderator in the x–y axis have to be included into Σ_a according to

$$\Sigma_a + (B_x^2 + B_y^2)D.$$

Taking into account the initial and boundary conditions

$$N(z,0) = 0; N(0,t) = d.\frac{\partial N}{\partial z}(0,t) \tag{2}$$

the Laplace transform with respect to z and t results in

$$\bar{\bar{N}}(k,s) = \int_0^\infty dt \int_0^\infty dz\, N(z,t)\, e^{-kz-st}$$

$$= \frac{\frac{Q_0}{(s+\lambda_0)(k+\Sigma)} - vD\bar{N}(0,s)[k+d^{-1}]}{s+v\Sigma_a - vDk^2} \tag{3}$$

When the Laplace inversion is made with respect to k, we have to pay attention to the compatibility condition of the boundary and initial values [2]

$$\bar{N}(0,s) = \frac{1}{vD}\frac{Q_0}{(s+\lambda_0)(k+\Sigma)(\kappa+d^{-1})} \tag{4}$$

for the singularity of Eq. (3) in the right-hand part of the complex k-plane

$$k_1 = \kappa = +\sqrt{\frac{(v\Sigma_a+s)}{vD}} \tag{5}$$

The result is given by the residues in $k_2 = -\kappa$ and $k_3 = -\Sigma$

$$\bar{N}(z,s) = \frac{Q_0}{vD}\frac{e^{-\kappa z}}{(s+\lambda_0)\,.\,2\kappa}\left[\frac{1}{\Sigma-\kappa} + \frac{\kappa - d^{-1}}{(\Sigma+\kappa)(\kappa+d^{-1})}\right] + Q_0\frac{e^{-\Sigma z}}{(s+\lambda_0)(s+v\Sigma_a - vD\Sigma^2)} \tag{6}$$

The Laplace inversion of (6) with respect to s in a closed form is possible only for a convolution representation of $N(z,t)$.

We therefore restrict the analysis to the calculation of the asymptotic representation for large t.

Let us assume a source with λ_0 such that $s_0 = -\lambda_0$ is the singularity with maximum real part compared to the other singularities of Eq. (6), then

$$\begin{aligned} s_1 &= -v\Sigma_a + vD\Sigma^2 \\ s_2 &= -v\Sigma_a + vDd^{-2} \\ s_3 &= -v\Sigma_a \end{aligned} \tag{7}$$

and we obtain

$$\bar{N}(z,s) = \frac{f(z,s)}{s+\lambda_0} \tag{8}$$

with $f(z,s)$ being a regular function in the neighbourhood of $s_0 = -\lambda_0$. Thus the asymptotic behaviour is given according to [3] by

$$N(z,t) \simeq e^{-\lambda_0 t}\,.\,f(z_1 - \lambda_0)$$

$$= \frac{Q_0}{2vD\kappa_0}e^{-\kappa_0 z - \lambda_0 t}\left[\frac{1}{\Sigma-\kappa_0} + \frac{\kappa_0 - d^{-1}}{(\Sigma+\kappa_0)(\kappa_0+d^{-1})}\right] + \frac{Q_0}{v\Sigma_a - \lambda_0 - vD\Sigma^2}e^{-\Sigma z - \lambda_0 t} \tag{9}$$

with

$$\kappa_0 = \sqrt{\frac{v\Sigma_a - \lambda_0}{vD}} \tag{10}$$

For small values of the effective absorption $v\Sigma_a - \lambda_0$ the relation

$$\kappa_0 \ll \Sigma$$

always applies. At some distance from the boundary and after the transients have died out, the variation of the neutron flux is characterized by $e^{-\kappa_0 z - \lambda_0 t}$.

The asymptotic decay of the neutron flux is determined by the decay constant of the source. The corresponding diffusion length $L_0 = \frac{1}{\kappa_0}$ is thereafter determined by λ_0 according to Eq. (5).

If it is possible to produce exponential sources suitable for non-stationary exponential experiments as described above, the experiments will show the following advantages in measuring the characteristic constants D_0, C, . . . of moderators.

(*a*) Poisoning can be simulated by neutron sources which increase exponentially with time according to $e^{+\lambda_0 t}$, and also by a source varying with $e^{i\omega t}$ [4].

(*b*) Depoisoning can be achieved by neutron sources which fall exponentially with time according to $e^{-\lambda_0 t}$.

Such experiments correspond to the region $0 < \kappa^2 < \kappa^2_{\min}$, which is not accessible with all other types of experiments as mentioned above.

Poisoning-variation by means of non-stationary exponential experiments can in some cases be faster and cheaper than real poisoning and provides a means of homogeneously poisoning even solid moderators.

According to Eq. (10), the time variation of the source is limited by $\lambda_0 < v\Sigma_a$. For $\lambda_0 > v\Sigma_a$ the squared relaxation constant κ_0^2 becomes negative, i.e., the value is really in the B^2-region. So, if the source falls too rapidly, a neutron pulse runs into the half-space.

The asymptotic behaviour discussed above is only valid for λ_0 when it is smaller than $v\Sigma_a - vD\Sigma^2$ and $v\Sigma_a - vDd^{-2}$ because the real part of the pole, $s_0 = -\lambda_0$, must be the greater.

TRANSPORT ANALYSIS OF THE ASYMPTOTIC EIGENVALUE EQUATION

The transport analysis results in modified transients and a modified equation for the eigenvalues. We are interested in the asymptotic state only and, therefore, we restrict treatment to the eigenvalue equation and its modifications according to the transport theory. In general, the methods adopted by H. C. Honeck [1] are

applicable with slight modifications even to the non-stationary exponential experiments. A short description is given below of the simultaneous treatment of the different experimental situations.

We consider the energy-dependent one-dimensional Boltzmann equation

$$\left\{\frac{\partial}{\partial t}+v(E)\mu\frac{\partial}{\partial z}+v(E)\left[\Sigma_a(E)+\Sigma_s(E)\right]\right\}N(E,z,\mu,t)=\int_0^\infty dE'\int_{-1}^{+1}d\mu' v(E')\Sigma_s\begin{pmatrix}E'\to E\\ \mu'\to\mu\end{pmatrix}N(E',z,\mu',t) \quad (11)$$

for an asymptotic state of the form

$$N(E,z,\mu,t)=N(E,k,\mu,s)\,e^{st+kz} \quad (12)$$

with a complex $k=\kappa+iB$.

In this way we can treat the three types of experiment envisaged:

	s	k
pulsed neutron experiments	$-\lambda$	iB_0
stationary exponential experiments	0	$-\kappa$
non-stationary experiments	$\pm\lambda_0$	$-\kappa$

The index 0 denotes those values which are fixed by the experimental conditions. Neutron wave experiments can be included by admitting complex s-values, for which the following representation is also valid.

For the asymptotic states we arrive at the eigenvalue equation

$$\{s+v(E)\mu k+v(E)\Sigma_a(E)\}N(E,k,\mu,s)=\int_0^\infty dE'\int_{-1}^{+1}d\mu' v(E')\Sigma_s\begin{pmatrix}E'\to E\\ \mu'\to\mu\end{pmatrix}N(E',k,\mu',s)-\Sigma_s(E)N(E,k,\mu,s) \quad (13)$$

With

$$J(E,k,\mu,s)=\int_0^\infty dE'\int_{-1}^{+1}d\mu' v(E')\Sigma_s\begin{pmatrix}E'\to E\\ \mu'\to\mu\end{pmatrix}N(E',k,\mu',s)$$

The corresponding system of integral equations in B_1-approximation is given by

$$s+v(E)[\Sigma_a(E)+\Sigma_s(E)]N_l(E,k,s)=\sum_{n=0}^{\infty}(2n+1)A_{ln}(E,k,s)J_n(E,k,s) \quad (14)$$

with

$$A_{ln}(E,k,s)=\frac{1}{2}\int_{-1}^{+1}\frac{P_l(\mu)P_n(\mu)}{1+\dfrac{v(E)\,.\,k}{s+v(E)[\Sigma_a(E)+\Sigma_s(E)]}\mu}\,d\mu \quad (15)$$

There are as many independent equations as the number of non-vanishing Legendre coefficients Σ_{sl} in the expansion of the scattering kernel. This system can be solved numerically according to an iteration method given in [1].

The coefficients $A_{ln}(\eta)$

$$\eta=-\frac{k}{\Sigma^*(E)}\text{ and }\Sigma^*(E)=\frac{s}{v(E)}+\Sigma_a(E)+\Sigma_s(E) \quad (16)$$

being symmetric in l and n being given by [5]

$$A_{ln}(\eta)=\frac{1}{\eta}Q_l\left(\frac{1}{\eta}\right)P_n\left(\frac{1}{\eta}\right) \quad (17)$$

with the first term:

$$A_{00}(\eta)=\frac{1}{\eta}\,\mathrm{ctgh}^{-1}\frac{1}{\eta}=\frac{1}{\eta}\tanh^{-1}\eta \quad (18)$$

For η being a real number and $s=0$, a numerical procedure was suggested by H. C. Honeck [1].

For isotropic scattering (B_0-approximation) there is only one integral equation

$$\{s+v(E)[\Sigma_a(E)+\Sigma_s(E)]\}N_0(E,k,s)=\frac{\tanh^{-1}\dfrac{k}{\Sigma^*(E)}}{\dfrac{k}{\Sigma^*(E)}}\int_0^\infty v(E')\Sigma_{s0}\,.\,.(E'\to E)N_0(E',k,s)dE' \quad (19)$$

for one of the three values λ, κ, B as an eigenvalue depending on which two of the parameters are fixed by the experiment.

If one admits complex s-values with a view to a source varying according to e^{iwt}, the neutron density function will be complex, too, which indicates a phase delay.

The integral equation is invariant with respect to a change of sign in k. Therefore, there is a k^2-dependence only. For experimentally reasonable states, either κ or B is equal to zero. It follows that the eigenvalue depends on $k^2=\kappa^2-B^2$. In general, we are interested in the dependence of $\lambda-v\Sigma_a$ on k^2. This corresponds to the diagram of states given by H. C. Honeck [1].

The series expansion for $k^2=-B^2<0$ has been treated by M. Nelkin [7] and the inverse expansion for $k^2=\kappa^2>0$ by H. C. Honeck [1]. For $v\Sigma_a-\lambda$ instead of $v\Sigma_a$ Honeck's expansion can be used for the non-stationary experiment.

In the monoenergetic model

$$N(E,k,s)=N_0(k,s)\,.\,\delta(E-E_0)$$

equation (19) can be expressed as follows

$$\frac{vk}{v\Sigma_s}=\tan g^{-1}\frac{vk}{s+v\Sigma_a+v\Sigma_s}=\frac{1}{2}\ln\frac{s+v\Sigma_a+v\Sigma_s+vk}{s+v\Sigma_a+v\Sigma_s-vk}$$

After some rearrangements, we find for the different types of experiments:

(*a*) pulsed neutron experiment:

$$s=-\lambda,\ k=iB$$

$$\lambda-v\Sigma_a=v\Sigma_s\left[1-\frac{vB}{v\Sigma_s}c+g\frac{vB}{v\Sigma_s}\right]=v\Sigma_s\sum\frac{2^{2n}}{(2n)!}\mathscr{L}_n\left(\frac{vB}{v\Sigma_s}\right)^2 \quad (21a)$$

with $\mathscr{L}_n$ being Bernoulli's numbers. The divergence at the slab-thickness $\frac{\pi}{B} = \frac{1}{\Sigma_s}$ occurs because there is no longer an asymptotic spatial distribution e^{iBz}

(*b*) non-stationary exponential experiment:

$$s = -\lambda_0,\ k = -\kappa$$

$$\lambda_0 - v\Sigma_a = v\Sigma_s\left[1 - \frac{v\kappa}{v\Sigma_s}\operatorname{ctgh}\frac{v\kappa}{v\Sigma_s}\right]$$

$$= v\Sigma_s \sum_n \frac{2^{2n}}{(2n)!}(-1)^{n-1}\mathscr{L}_n\left(\frac{v\kappa}{v\Sigma_s}\right)^{2n} \quad (21b)$$

(*c*) stationary exponential experiments.

For $\lambda_0 = 0$, we obtain the well-known equation

$$\frac{\kappa}{\Sigma_T} = \operatorname{tgh}\frac{\kappa}{\Sigma_s} \quad (21c)$$

The above equations determine the function

$$\lambda - v\Sigma_a = f(k^2)$$

for $k^2 = -B^2 < 0$ and $k^2 = \kappa^2 > 0$ according to the monoenergetic transport theory and isotropic scattering. There is no upper limit to the eigenvalues of λ and κ. For the energy dependent Boltzmann equation, the upper limit of the discrete eigenvalue spectrum is well known [1,6] to be

$$\lambda \leqq \min\ v(\Sigma_a + \Sigma_s)$$

$$\kappa \leqq \min\ (\Sigma_a + \Sigma_s)$$

To allow for these asymptotic values, the second derivative of $f(k^2)$ has to change its sign.

The influence of spectrum effects on the diffusion cooling constant, therefore, is generally larger and of opposite sign to the transport effects. The different behaviour of $f(k^2)$ depending on the theoretical approximation is shown in Fig. 1.

The authors intend to extend this work to multiplying media as done previously for pulsed neutron experiments [8].

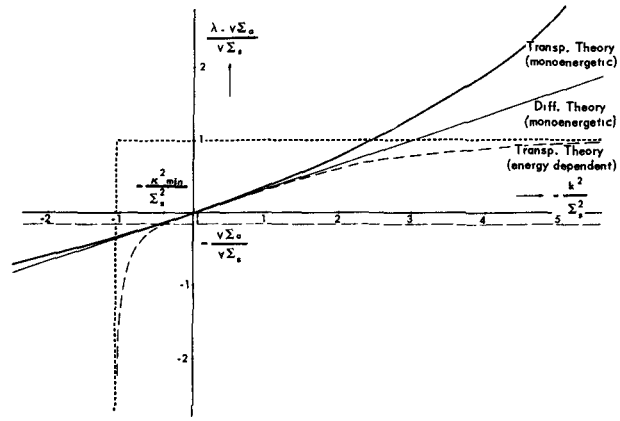

Figure 1. Schematic diagram of the function $\lambda - v\Sigma_a = f(k^2)$

REFERENCES

1. Honeck, H. C., USAEC report BNL 719 (C-32), Vol. IV, pp. 1186–1210 (1962).
2. Volker, D., and Doetsch, G., *Die Zweidimensionale Laplace-Transformation*, Verlag Birkhäuser, Basel (1950).
3. Doetsch, G., and Herschel, R., *Anleitung zum praktischen Gebrauch der Laplace-Transformation*, R. Oldenbourg, München (1956).
4. Perez, R. B., and Uhrig, R. E., Nuclear Sci. Eng., *17*, p. 90 (1963).
5. Hurwitz, H. Jr., and Zweifel, P. F., J. Appl. Phys., *26*, p. 923 (1955).
6. Corngold, N., Michael, P., and Wollmann, W., USAEC report BNL-719 (C-32), Vol. IV, pp. 1103–1131.
7. Nelkin, M., Nuclear Sci. Eng., *7*, 210 (1960).
8. Joest, K. H., Nukleonik, *6*, pp. 3–14 (1963).

ABSTRACT—RÉSUMÉ—АННОТАЦИЯ—RESUMEN

A/762 République fédérale d'Allemagne

Sur la région expérimentale reliant les mesures expérimentales de longueur de diffusion et les mesures expérimentales en neutrons pulsés

par K.-H. Joest et G. Memmert

Comme H. C. Honeck l'a remarqué, il y a un trou entre la région des mesures avec neutrons pulsés et la région des mesures de la longueur de relaxation, si elles sont décrites par $\lambda - v\Sigma_a$ en fonction de B^2. Cela est dû au fait qu'il n'y a pas d'absorption possible inférieure à celle du modérateur lui-même. Lorsqu'on considère des expériences exponentielles avec des sources croissantes avec le temps ou qui ne décroissent pas plus vite que $\exp(-v\Sigma_a \cdot t)$ on obtient une analogie complète entre les régions de B^2 et de $\kappa = -B^2$ sans aucun trou.

La variation exponentielle du flux en fonction du temps, qui est déterminée par la variation de la source en fonction du temps, est physiquement équivalente à un changement d'absorption du système. Spécialement, une décroissance en fonction du temps correspond à une réduction de l'absorption, de telle sorte que des absorptions effectives plus petites que $v\Sigma_a$ soient réalisables, ce qui est impossible avec des mesures stationnaires de la longueur de relaxation. L'accroissement de l'absorption peut être simulé par des sources croissant exponentiellement dans le temps. S'il est possible de réaliser une source exponentielle expérimentalement avec une exactitude suffisante, de telles expériences pourraient être moins chères et plus rapides que les expériences stationnaires avec changement de l'absorption.

La théorie des états asymptotiques donnés par $\exp(-\lambda t - \kappa z)$ a été traitée pour le cas monoénergétique et pour le cas d'une énergie dépendant de l'équation de Boltzmann.

Les états $\exp(-\lambda t - iBz)$ correspondant aux expériences en neutrons pulsés dans des milieux finis ont été inclus dans l'analyse pour montrer les relations étroites entre les deux types de théories asymptotiques.

A/762 ФРГ

Экспериментальное определение длины диффузии в области, где это не может быть выполнено ни стационарными, ни обычными импульсными методами

К. Джост и Г. Меммерт

Как было отмечено Хонеком, на графике зависимости $\lambda - v\Sigma_a$ от B^2 имеется разрыв между областью стационарных измерений длины диффузии и областью измерений с помощью импульсной техники. Это обусловлено тем обстоятельством, что поглощение не может быть меньше, чем поглощение в самом замедлителе. Однако если рассматривать возможность экспоненциальных экспериментов с источниками, интенсивность которых растет или падает со временем как $\exp(-v\Sigma_a \cdot t)$, то можно промерить всю область между B^2 и $\varkappa = -B^2$ без всякого разрыва.

Экспоненциальные временные колебания потока, обусловленные временными колебаниями источника, физически эквивалентны изменениям в поглощении системы. В частности, случай уменьшения интенсивности соответствует разотравлению системы, причем можно достичь состояния с эффективным поглощением меньше $v\Sigma_a$, что невозможно при стационарных измерениях длины диффузии. Увеличение отравления можно имитировать при помощи источников с экспоненциально увеличивающейся во времени интенсивностью. Если экспоненциальный источник может быть получен экспериментально с достаточной точностью, то такие эксперименты могут проводиться быстрее и дешевле, чем стационарные эксперименты с изменяющимся отравлением.

Теория асимптотических состояний вида $\exp[-\lambda t - \varkappa z]$ была рассмотрена как для моноэнергетического, так и для зависящего от энергии уравнения Больцмана. Состояния $\exp[-\lambda t - iBz]$, соответствующие импульсным экспериментам в конечной среде, были также включены в анализ, чтобы показать сильную связь между двумя видами асимптотических теорий.

A/762 República Federal de Alemania

Sobre la región experimental que une las experiencias pulsadas de neutrones y las de longitud de difusión

por K.-H. Joest y G. Memmert

De acuerdo con H. C. Honeck hay un claro entre la zona de medidas pulsadas de neutrones y medidas estacionarias de longitud de difusión, si se representan en el plano $\lambda - v\Sigma_a$ en función de B^2. Esto se debe al hecho de que no hay absorción posible que sea más pequeña que la del propio moderador. Si se considera la posibilidad de experimentos exponenciales con fuentes crecientes con el tiempo o que disminuyen más lentamente que $\exp(-v\Sigma_a \cdot t)$ puede establecerse

una analogía completa sin ningún claro entre la región de B^2 y de $\kappa = -B^2$.

La variación exponencial con el tiempo del flujo fijado por la variación temporal de la fuente es físicamente equivalente a un cambio en la absorción del sistema. Especialmente el estado de decrecimiento corresponde a una disminución del envenenamiento de forma que pueden conseguirse estados con absorción efectiva más pequeña que $v\Sigma_a$ que son imposibles en las medidas estacionarias de longitudes de difusión. El incremento en el envenenamiento podría simularse mediante fuentes que aumentasen exponencialmente con el tiempo. Si se pudiese conseguir experimentalmente una fuente exponencial con suficiente precisión, dichos experimentos serían más rápidos y más baratos que los experimentos estacionarios de variación del veneno.

La teoría de estados asintóticos de la forma $\exp(-\lambda t - \kappa z)$ ha sido tratada por la ecuación de Boltzmann dependiente de la energía y la monoenergética.

Los estados $\exp\{-\lambda t - iBz\}$, correspondientes a experimentos pulsados en medios finitos, han sido incluidos en el análisis con el fin de mostrar las fuertes relaciones existentes entre los dos tipos de teorías asintóticas.

On the determination of the diffusion constants of H_2O, polyphenyls, $ZrH_{1.92}$ and D_2O by neutron single-scattering experiments

By T. Springer,* C. Hofmeyr,** S. Kornbichler,** and H. D. Lemmel**

THEORY

For multigroup and other reactor calculations one needs the diffusion constant D as a function of neutron velocity v and moderator temperature T_m, that is

$$D(v,T_m) = 1/3\Sigma_s(1-\bar{\mu}) \tag{1}$$

$\Sigma_s(v,T_m)$ is the scattering cross section of the moderator, and $\bar{\mu}$ is the average cosine of the scattering angle θ:

$$\bar{\mu} = (1/\sigma_s)\int_{(4\pi)} \frac{d\sigma(\theta)}{d\Omega}\cos\theta d\Omega \tag{2}$$

$$\text{with } \sigma_s = \int_{(4\pi)} (d\sigma/d\Omega)d\Omega \tag{2a}$$

$d\sigma/d\Omega$ is the differential scattering cross section. It is related to the well-known scattering law $S(K,\omega)$ through

$$d\sigma(\theta)/d\Omega = \sigma_0 \int_0^\infty \sqrt{\frac{E'}{E}}\, S(K,\omega)dE' \tag{3}$$

where σ_0 is the bound scattering cross section, $\hbar\vec{K} = \hbar(\vec{k'} - \vec{k})$ with $K(E,E',\theta) = |\vec{K}|$, and $\hbar\omega = E' - E$ are the momentum and the energy transfer during scattering, respectively. Moreover, for flux calculations in the thermal group one needs the average diffusion constant $\langle Dv\rangle_{T_m}$ and the thermal diffusion length L as a function of the moderator temperature T_m. The average $\langle Dv\rangle_{T_m}$ has to be performed over the neutron spectrum which will be assumed to be a Maxwellian distribution of the density $N(v)$ with a temperature T_n, namely:

$$\langle Dv\rangle_{T_m} = \int_0^\infty N(v,T_n)vD(v,T_m)dv \Big/ \int_0^\infty N(v,T_n)dv \tag{4}$$

In the following, we put $T_n = T_m$, where T_m is the moderator temperature. In this work, measurements of the differential scattering cross section $d\sigma/d\Omega$ as a function of T_m and E have been made on different moderator materials. A "black" ^{6}LiI scintillation counter was used for the detection of the neutrons (Reinsch and Springer, 1961 [1]) which gives a nearly exact integration over all energies after scattering, E', as required by Eq. (3). From the measured $d\sigma/d\Omega$-curves, the quantities $\bar{\mu}$, $D(v)$ and $\langle Dv\rangle$ have been calculated.

Conventionally, the quantities $\langle Dv\rangle$ and L are directly obtained from "integral" experiments, which have been described by many authors (for example during the Brookhaven Conference 1962, e.g. [21], theory *cf.* [2]). In a *time* relaxation experiment, the neutron density is $n(z,t,v) = N(v)e^{-\alpha t + iBz}$; inserting this in the Boltzmann equation, one finds

$$\alpha = \Sigma_a v + B^2\langle Dv\rangle + \ldots \tag{5}$$

The relaxation time $1/\alpha$ is determined experimentally. B^2 is the buckling of the moderator vessel (here assumed one-dimensional, for simplicity). $\Sigma_a(v)$ is the moderator absorption cross section, which is assumed to be $1/v$. In a *space* relaxation experiment, one has $n(z,x,v) = N(v)e^{-\gamma z + iB_1^2 x}$. $1/\gamma$ is the experimental relaxation length along the z-axis with B_1^2 as the transverse buckling. In this case, the Boltzmann equation gives ($\alpha = 0$, $-\gamma^2$ for B^2)

$$\Sigma_a v + (B_1^2 - \gamma^2)\langle Dv\rangle + \ldots = 0$$

This is, for $\Sigma_a = \text{const}/v$, identical with

$$\gamma^2 - B^2 = \Sigma_a v/\langle Dv\rangle = \int_0^\infty \Sigma_a\phi dv \Big/ \int_0^\infty D\phi dv = L^{-2} \tag{6}$$

where $\phi(v)$ is the Maxwellian neutron flux, and L is the diffusion length.

The systematic errors in the evaluation of $\langle Dv\rangle$ from the relaxation experiments are well known, e.g., the difficulties in the determination of the bucklings because of the uncertainty in the extrapolation length, difficulties in fitting the function $\alpha(B)$, and the complication in the evaluation of the fundamental mode of a decay (*cf.* Beckurts [3]).

In our approach, there are no such sources for systematic errors in the evaluation of $D(v)$ and $\langle Dv\rangle$ and the experiments are less troublesome than the

* Institut für Neutronenphysik der Kernforschungsanlage, Jülich.
** Labor für Technische Physik der Technischen Hochschule, München.

integral measurements described before. Furthermore, our experiments have shown that $\bar{\mu}(E)$ is very insensitive to the moderator temperature, at least in the range $0° < T_m < 200°C$; therefore, one can easily calculate $\langle Dv \rangle$ as a function of temperature by means of Eq. (4) within a large temperature range.

Finally, the determination of $d\sigma/d\Omega$ allows a reliable check of the scattering law $S(K,\omega)$ by means of Eq. (3) as far as the "transport properties" of $S(K,\omega)$ are concerned (namely the θ-dependency). This was done earlier by Kiefhaber [4] according to Nelkin's theory [10] for H_2O (cf. also [5]).

On the other hand, $d\sigma/d\Omega$ evidently is not very sensitive to thermalization and moderation properties which can be studied better by pulsed experiments.

Several scattering experiments on H_2O, D_2O, diphenyl, terphenyl, benzene, and $ZrH_{1.92}$ will be reported here and compared, if possible, with integral data. A very detailed description of all these experiments will be published later (in *Nukleonik*) [13,16,8].

We do not claim that the determination of $\bar{\mu}$ and $D(E)$ from $d\sigma/d\Omega$ curves is an entirely new method. It was applied earlier, using boron counters as detectors [6] and by ourselves [1] with "black" ^{6}LiI counters. However, the possibility of finding the average diffusion constant $\langle Dv \rangle T_m$ as a function of T_m over a wide range by a few measurements only, its very good agreement with the integral data, and the useful information on the transport properties of $S(K,\omega)$ contained in $d\sigma/d\Omega$ itself justify drawing more attention to these investigations.

EXPERIMENTS

Monochromatic neutrons were obtained from a simple lead single crystal spectrometer. The neutrons were scattered from a thin sample sheet (transmission 0.7 . . . 0.9), either in reflexion or in transmission position. The scattered neutrons were detected at different angles by means of a ^{6}LiI counter. By using a single channel analyzer, a good gamma background suppression was achieved. For the water measurements at elevated temperatures, the sample container was surrounded by a cylindrical pressure vessel. It was filled with argon (having a rather small total cross section); thereby, the pressure in the sample container can be compensated and thin walls are possible in spite of the high sample pressure.

Great care had to be taken when determining background, especially during the pressurized sample experiments, because the background depends on the sample transmission itself. Therefore, it cannot be determined by simple sample-in-sample-out experiments. Double and multiple scattering corrections are necessary when the scattering probability in the sample $d\Sigma_s$ is larger than a few per cent. The correction curves given by Vineyard [7] (assuming isotropic scattering) are not sufficient for $d\Sigma_s > 0.2$ if the scattering is highly anisotropic. An improvement has been developed by Lemmel [8], which is briefly described in the appendix to this paper. From measurements with samples of widely differing thickness (up to $d\Sigma_s = 0.6$) the corrected results for $d\sigma/d\Omega$ were consistent within 3% for $20°K < \theta < 100°K$, and within about 8% at 160°K for the case of strongly anisotropic scattering on water. These results demonstrate that the background and multiple scattering corrections can be considered as reliable.

For the lowest energy under investigation, 0.022 eV, a correction for the second-order contamination of the beam was necessary. Its contribution in the incoming beam was determined by gold transmission experiments. The resulting scattering contribution was found from $d\sigma/d\Omega$ results at the fourfold energy. In future experiments it would be highly desirable to suppress the second-order neutrons by an auxiliary mechanical selector.

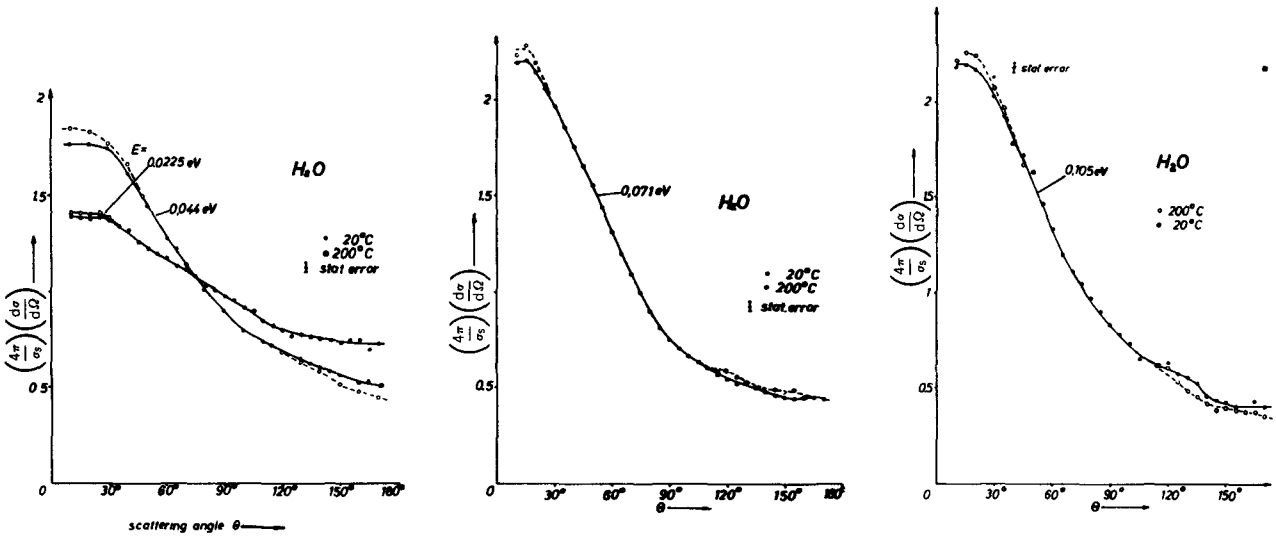

Figure 1(a, b, c). Experimental differential scattering cross section $d\sigma/d\Omega$ of ordinary water as a function of scattering angle θ at different neutron energies, E
Solid line: $T = 20°C$, dashed line: $T = 200°C$

RESULTS AND DISCUSSION

Light water

Results for scattering cross sections $d\sigma(\theta)/d\Omega$ are shown in Fig. 1. The ordinate is normalized by the integrated scattering cross section σ_s. It is rather striking that the curves are very insensitive to the sample temperature. As demonstrated [1] previously this is true even below the melting point. There is a kind of compensating action between the quasi-elastic and the inelastic scattering contribution: the first is a decreasing function of angle like a Gaussian distribution (a kind of Debye-Waller-factor) and the latter has a rather flat maximum at larger angles (see Brockhouse [9]). With increasing temperature, the average proton amplitude $\sqrt{u^2}$ increases and the Gaussian distribution becomes steeper. On the other hand, the inelastic contribution increases (being proportional to K^2u^2 in first order), making the scattering more pronounced at larger angles. This induces a sort of compensation effect, but we do not quantitatively understand why it is so complete. The curves do not show maxima from coherence as was observed previously in the solid phase of water [1].

From the curves in Fig. 1, the average cosine has been calculated by means of (1) and (2). The results are shown in Fig. 2. For comparison, experimental results from Reinsch and Springer [1], Whittemore and McReynolds [6], and calculations according to Nelkin's kernel [10] by Kiefhaber [4] are included.

From $\bar{\mu}(E)$, the average diffusion constant $\langle Dv \rangle$ was found by means of (4) as a function of moderator temperature T_m. The results are shown in Fig. 3 and compared with "integral" determinations by time and space relaxation experiments, and with theoretical calculations (see [4]). A number of room temperature data are represented in Table 1 (for a more detailed review see [3] and [19]).

There is good agreement between our values and most of the "integral" experiments. A small, but systematic discrepancy is observed between our data and those found from calculations by means of

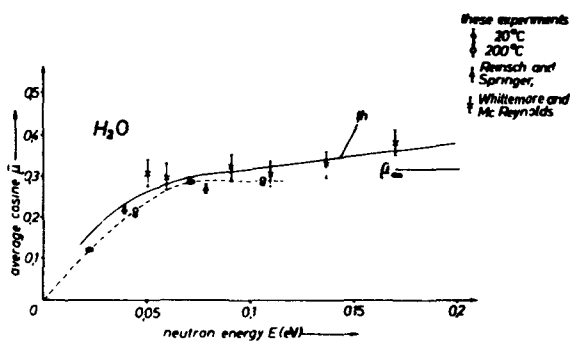

Figure 2. Average cosine of scattering angle $\bar{\mu}$ as a function of neutron energy for H_2O, as calculated from Fig. 1
● = 20 °C, O = 200 °C (error about ±0.007). ▲ Reinsch and Springer [1], 20 °C; × Whittemore and McReynolds [6] (room temperature). th: calculated by Kiefhaber [4] according to Nelkin's theory [10]. $\bar{\mu} = 2/3\ A_{eff}$ = asymptotic value with tensor mass $A_{eff} = 2.1$

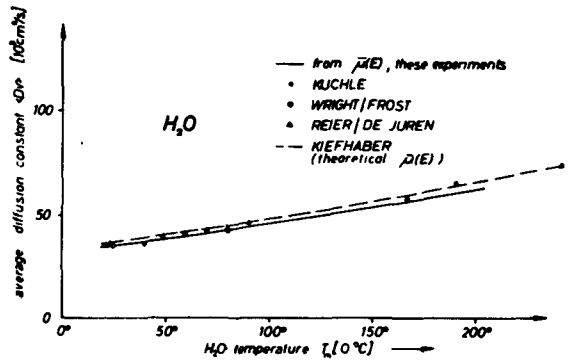

Figure 3. Average diffusion constant as a function of water temperature $T_m = T_n$, as calculated from experimental curve in Fig. 2 (solid line). Error about ±2 per cent
Dashed line: calculated from Kiefhaber's calculated $\bar{\mu}(E)$-curve. ● = Küchle [19], (time relaxation), O = Wright and Frost [31] (space relaxation and boron poisoning), Reier and De Juren [23] (calculated from the experimental diffusion length L)

Nelkin's kernel. This might be partly because this theory describes the hindered rotation of the H_2O-molecule by a single quantum energy instead of a broad rotation band. It should be mentioned that the

Table 1. Average diffusion constant $\langle Dv \rangle$ of H_2O at room temperature

Method and authors (Temp. °C)	$\langle Dy \rangle$ (10^5 cm²/s) Results		Extrapolated at 20 °C
Pulsed methods:			
Küchle, 1960 [19] (22 °C)	35.4	±0.7 (±0.4)	35.16±0.7
Antonow *et al.*, 1956 [20] (21 °C)	35.5	±1.0	35.4±1
Koppel and Lopez, 1962 [21] (average from different interpretations) (26.7 °C)	37.43	±0.37	36.63±0.37
Space relaxation and poisoning methods			
Beckurts and Klüber, 1958 [22] (room temperature)			35.5±1.1
Reier and De Juren, 1961 [23]	37.618±0.205		
corrected by Beckurts [3] (23 °C)	36.0		35.64
Starr and Koppel, 1962 [24] (21 °C)	35.8	±0.1	35.68±0.1
Baker and Wilkinson, 1958 [18] (average from 5 authors) (22 °C)	35.42	±0.37	35.18±0.37
This publication, from experimental $\bar{\mu}(E)$			
Average over Maxwell-spectrum ($Tn = Tm$) (20 °C)			35.30±0.30
Average over Beyster's experimental spectrum [25] (25 °C)	37.05	±0.30	36.45±0.30
Theory with $\bar{\mu}(E)$ from Nelkin's kernel			
Kiefhaber's calculated $\bar{\mu}(E)$ [4], average over Maxwell spectrum (20 °C)			38.10
Honeck [26] (room temperature)			37.46

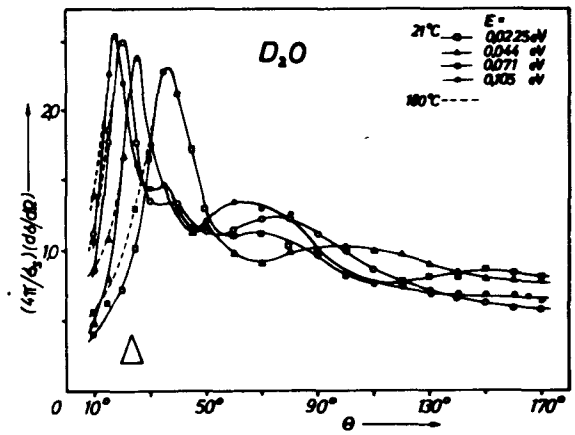

Figure 4. Experimental $d\sigma/d\Omega$ of heavy water, showing strong diffraction peaks, as a function of scattering angle θ at different neutron energies E
Solid line: $T = 21\,^{\circ}C$, dashed line: $T = 180\,^{\circ}C$

discrepancy cannot be due to the neglect of the hindrance of translational motion (cf. [5]).

From our results, the temperature coefficient of the diffusion constant at 20 °C is about

$$d\langle Dv\rangle/dT_m = 118\ cm^2/s\,^{\circ}C \text{ for } T_n = T_m$$

This value is mainly due to the change of density and to the shift of the spectrum. The change of the average cosine with temperature is very small (see above). Further, one finds

$$d\langle Dv\rangle/dT_n = 111\ cm^2/s\,^{\circ}C \text{ for } T_m = \text{const.}$$

Heavy water

The results for $d\sigma/d\Omega$ for D_2O are shown in Fig. 4. In this case, the influence of temperature on the cross section is also very small. The strong first, and the weaker second, maximum are due to interference effects. This is evident because the angles of the maxima, θ_1 and θ_2, agree with a relation

$$2k\sin\theta_i/2 = d_i (k = 2\pi/\lambda) \qquad (7)$$

with $d_1 = 2.02$ Å^{-1} and $d_2 = 3.8$Å^{-1}

If one assumes that the peak at $\theta = \theta_1$ is mainly due to elastical coherent scattering, it is obvious that $d\sigma(\theta)/d\Omega at \theta_1$ has the same value for all energies (in case of elastic scattering, $d\sigma/d\Omega$ depends on $(4\pi/\lambda)\sin(\theta/2)$ only). Therefore, the normalized experimental values $(4\pi d\sigma(\theta_i)/d\Omega)\sigma_s(E)^{-1}$ have to be proportional to

Table 2. The constancy of the peak values of $d\sigma/d\Omega$ with energy E [11]. ($\sigma_s(E)$ from [14])

E (eV)	$\frac{4\pi}{\sigma_s(E)}\frac{d\sigma}{d\Omega}$ (experimental) at $\theta = \theta_1$	$C/\sigma_s(E)$ (Arbitrary units)
0.0225 . . .	2.32	2.11
0.044 . . .	2.38	2.33
0.071 . . .	2.50	2.50
0.105 . . .	2.58	2.62

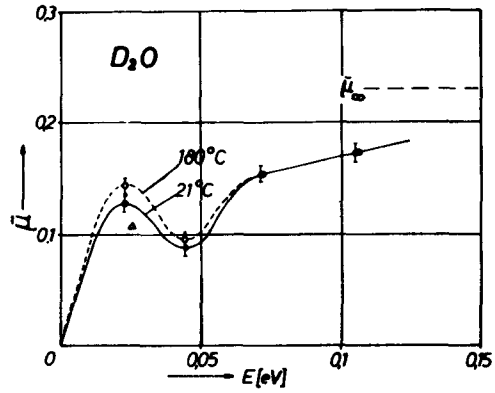

Figure 5. Average cosine as a function of E for D_2O, as calculated from Fig. 4; for higher energies, the low and high temperature points coincide. $\bar{\mu} = 2/3\, A_{eff}$

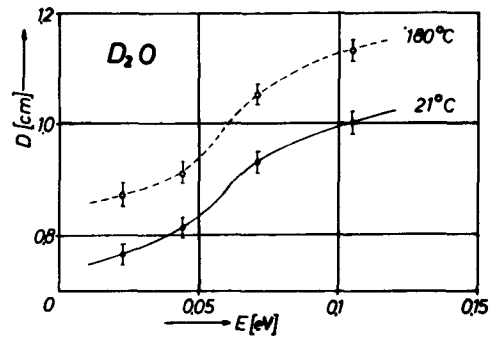

Figure 6. Diffusion constant $D(E)$ for D_2O

$C/\sigma_s(E)$, where C is a constant. This is true with reasonable accuracy (Table 2). This means that the intensity at the peaks contains mainly elastic and "nearly-elastic" scattering ($\hbar\omega \ll E$). Two prominent maxima have also been observed and discussed by Morgan and Warren [35] in their excellent X-ray study on water with

$$d_1 = 1.95\ \text{Å}^{-1},\ d_2 = 2.9\ \text{Å}^{-1}, \text{ and } d_3 = 4.3\ \text{Å}^{-1}$$

The positions of Morgan's and our first peak at about $d = 2.02$ Å^{-1} are in good agreement. Morgan's second peak is not resolved, and his third seems to correspond to our second. The very broad maximum at larger d_i ($\simeq 7$) of our curves might be due to scattering with rather large energy transfers. In a comparison of several points in Fig. 4 with Butler's theory [11, 12], good agreement has been obtained (cf. [13]). $\bar{\mu}$ and D as a function of E as calculated from $d\sigma/d\Omega$ are given in Figs. 5 and 6. The maximum and minimum are due to the shift of the interference peak with changing energy towards small angles.

Ramanna and Sarma [15] have investigated neutron spectra emerging from plane moderator surfaces. The "leakage function" defined in their work should be approximately proportional to the transport mean free path $\lambda_{tr} = 3\ D$. From their experiments, they found a maximum of λ_{tr} at 0.01 eV and a continuous decrease of λ_{tr} with increasing energy. This disagrees completely

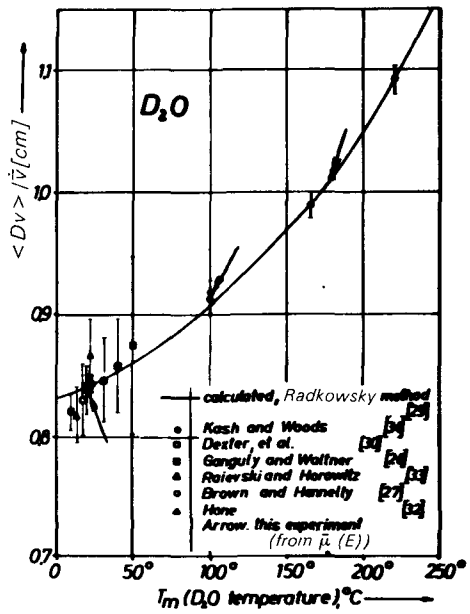

Figure 7. $\langle Dv \rangle / \bar{v}$ as a function of moderator temperature $T_m(\bar{v})$=average thermal velocity

● with arrows: Our experiments (average of Fig. 6 over a Maxwellian density distribution with $T_n = T_m$). The other experimental points and the theoretical curve were transferred from a figure published by Brown and Hennelly [27]

with our direct determination in Fig. 6. The Maxwellian average $\langle Dv \rangle$ is represented in Fig. 7 and Table 3 compared with "integral" measurements of other authors. In this case, also, there is rather good agreement, but one should remember that $\bar{\mu}(E)$ is not a monotonic function of E, and the curve has to be interpolated somewhat arbitrarily through the points in Fig. 6. Therefore, our values for $\langle Dv \rangle$ might include some systematic error which cannot be estimated. To avoid this, a smaller separation of the energy values would have been necessary in this instance. In further work, the method will be improved by interpolating the $d\sigma(\theta)/d\Omega$-curves of Fig. 4 drawn as a function of momentum K instead of the angle θ.

Table 3. Average diffusion constant $\langle Dv \rangle$ of D_2O at room temperature

Method and authors	$\langle Dv \rangle$ (10^5 cm²/s)
Space relaxation and boron poisoning method	
Kash and Woods [34]	2.09±0.03
Brown and Hennelly [27]. . . .	2.09±0.025
Pulsed source	
Ganguly and Waltner [28] . . .	2.08±0.05
Kussmaul and Meister [36] . . .	2.00±0.01
Theory	
Radkowsky [29]	2.10
From $\bar{\mu}$ (E) curve	
This experiment	2.09±0.02*

* Statistical errors only.

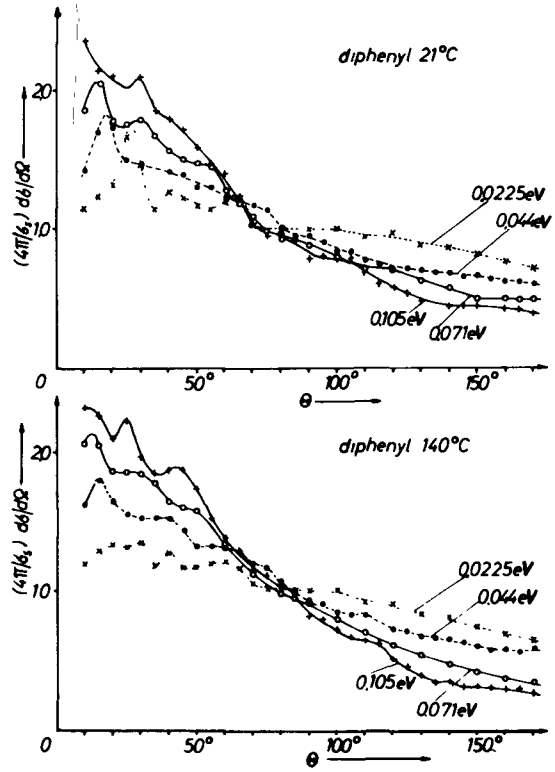

Figure 8. $d\sigma/d\Omega$ of diphenyl for different values of E

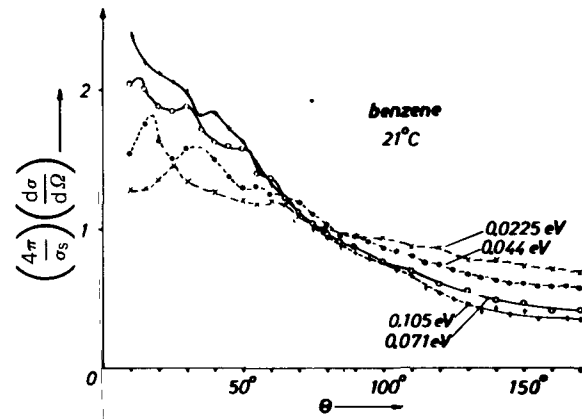

Figure 9. Differential scattering cross section of benzene for different energies

Benzene and polyphenyls

Several differential cross-section curves are shown in Figs. 8, 9 and 10 for diphenyl, benzene, and terphenyl at different energies and temperatures above and below the melting point. By various auxiliary experiments it has been demonstrated that the numerous peaks are not due to coherent scattering in the aluminium sample container. They result from C—C and C—H intra-molecular and partly inter-molecular scattering; the intra-molecular interferences can be identified by the fact that they have the same position in all these compounds both in the liquid and solid state. $\bar{\mu}(E)$ is given in Fig. 11. Fig. 12* shows that

* To avoid difficulties over the density, ρ,$\rho\langle Dv \rangle$ is plotted instead of $\langle Dv \rangle$.

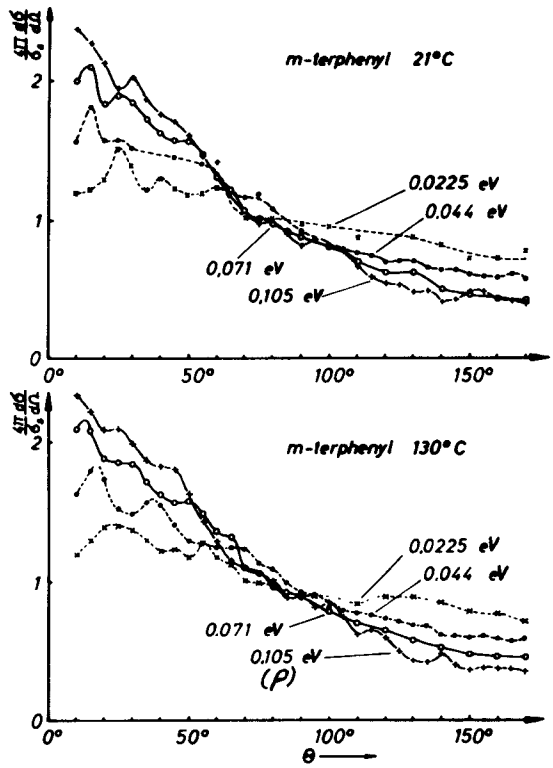

Figure 10. Differential scattering cross section of *m*-terphenyl (solid and liquid) for different energies. Curve at $E=0.105$ eV for p-terphenyl

there is good agreement between our $\langle Dv \rangle$-results and calculations [40], and with experiments by Brown [39], but there are considerable discrepancies with the results of other authors.

Zirconium hydride

Several differential scattering cross sections are presented in Fig. 13. Diffusion parameters have not yet been calculated. The average cosine $\bar{\mu}$ is compared with calculations of Memmert [37] in Fig. 14. The minimum is due to the increase of inelastic loss-scattering at 0.13 eV which makes scattering more isotropic.

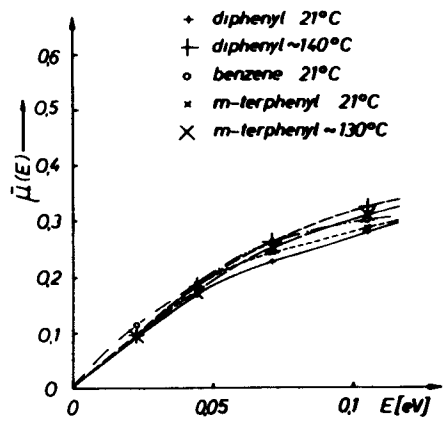

Figure 11. Average cosine of benzene and polyphenyls at different energies and temperatures, calculated from Fig. 10

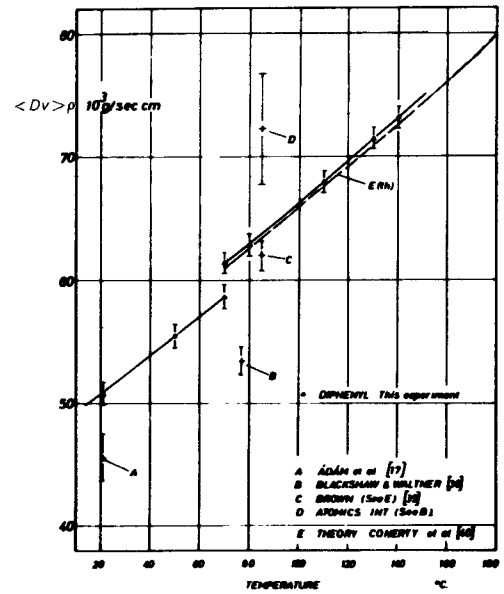

Figure 12. Average diffusion constants of diphenyl ρ = density (g/cm³), $\langle Dv \rangle \rho$ is shown instead of $\langle Dv \rangle$; solid line = our experiments

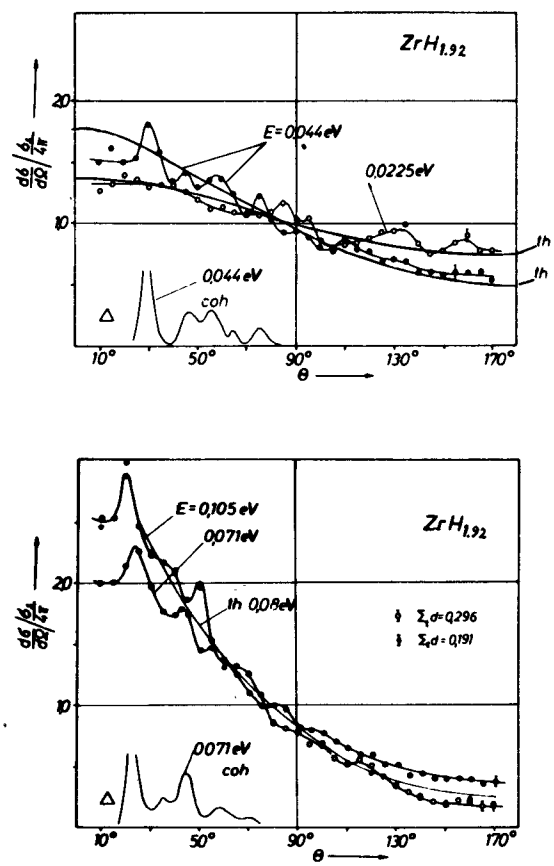

Figure 13. Differential scattering cross sections of zirconium hydride at room temperature
coh: calculated coherent contribution (arbitrary units). th: = incoherent approximation, according to Nelkin's calculus (by Memmert [37])

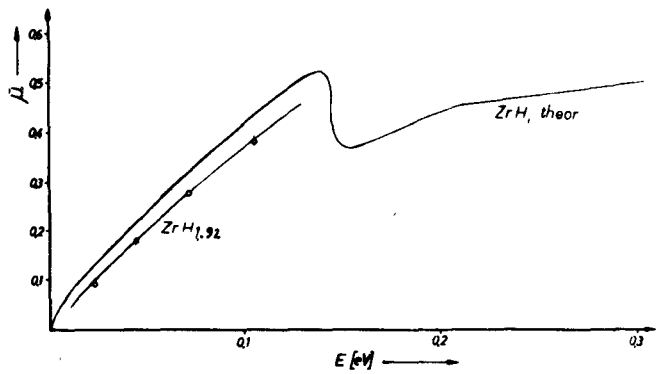

Figure 14. Average cosine of $ZrH_{1.92}$ ZrH, theor: calculated by Memmert (37)

CONCLUSION

Good agreement has been obtained between average diffusion parameters from integral experiments (time and space relaxation), and our values evaluated from differential scattering cross sections for H_2O, D_2O, and diphenyl. In the case of D_2O, there might be the possibility of a small systematic error because of the structure of the $\bar{\mu}(E)$-curve and the lack of sufficient experimental data. This might be improved by a more efficient interpolation method. Our $D(E)$-curves are important for multigroup diffusion calculations. Even if the extrapolation between our experimental points might not be completely correct with regard to D_2O, the curves will give good results because the *average* values of D are in good agreement with those from other experiments within a wide temperature range. Finally, the experimental $d\sigma/d\Omega$ curves are useful to check the transport properties of the scattering law and they allow a more detailed study of these properties than by using integral data.

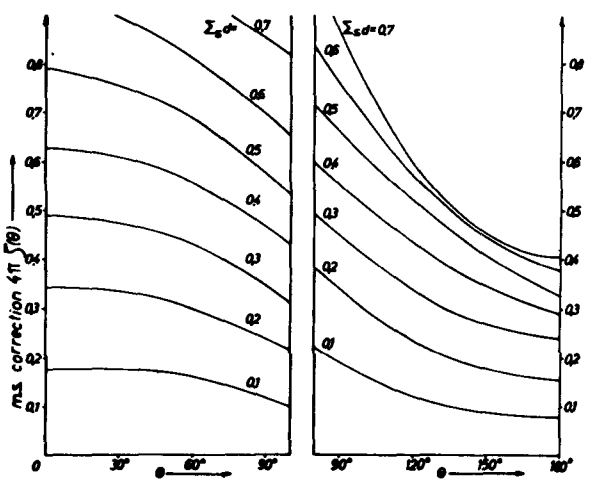

Figure 15. Typical multiple scattering correction curves $\zeta(\theta)$ for the determination of $d\sigma/d\Omega$ from a scattering experiment $\Sigma_s d$ = relative sample thickness (for a typical shape of the anisotropic $d\sigma/d\Omega$ curve, characterized by the parameters $a = 0.85$; $b = 1.40$; $c = 0.45$; $d = 0$)

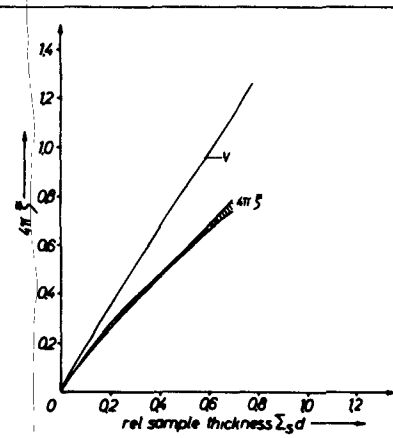

Figure 16. Average of ζ over solid angle as a function of relative sample thickness

The shaded region covers the range of the anisotropy parameters (b, c, d) which were applied for the differential scattering cross sections in Fig. 1*a*–1*c*. V = isotropic correction according to Vineyard [7]

ACKNOWLEDGEMENT

The authors are indebted to Professor H. Maier-Leibnitz for his steady interest in these investigations.

APPENDIX: MULTIPLE SCATTERING CORRECTIONS

In the work of Vineyard [7] isotropic scattering has been assumed throughout all scattering processes in the sample. In most cases, allowance has been made for anisotropy in our calculations for the first and second event, and isotropy has been assumed for third and higher order scattering events. To simplify calculations, the angular distribution has been expanded by $d\sigma/d\Omega = a + b\cos\theta + c\cos^2\theta + d\cos^3\theta$. The scattered intensity received by the counter is given by $Z_{exp} = P\left(\frac{K_d}{\sigma_s}\frac{d\sigma}{d\Omega} + K_m\right)$, P is a constant, K_m is the contribution of multiple scattering, and

$$K_d = \begin{cases} e^{-d\Sigma_s/\cos(\theta/2)}[d\Sigma_s/\cos(\theta/2)] & \text{("Transmission" arrangement of sample)} \\ (1/2)(1 - e^{2d\Sigma_s/\cos\left(\frac{\pi}{2} - \frac{\theta}{2}\right)}) & \text{("reflexion" arrangement)} \end{cases}$$

P can be eliminated by integrating Z over $d\Omega$ and using Eq. (2a). With $\zeta = K_m/K_d$ one finds that

$$\left(\frac{4\pi}{\sigma_s}\right)\frac{d\sigma}{d\Omega} = 4\pi Z_{exp}\frac{1 + \int_{(4\pi)}\zeta(\theta)d\Omega}{K_d\int_{(4\pi)} Z_{exp}(\theta)d\Omega} - 4\pi\zeta(\theta)$$

ζ has been numerically calculated for different $d\Sigma_s$ values and shapes (characterized by the choice of a, b, c, and d). A typical set of correction curves is shown in Fig. 15 for a scattering distribution which is about a factor of two more anisotropic than the steepest curve of Fig. 1.

Assuming the multiple scattering correction to be isotropic, the quantity $4\pi\zeta = \int_{4\pi}\zeta(\theta)d\Omega$ can be used as a rough first approximation. This is shown in Fig. 16.

The shaded region covers the range of the $d\sigma/d\Omega$ curves of Fig. 1. One can see that, on an average, the degree of anisotropy does not unduly influence the correction. For comparison, the simple isotropic correction of Vineyard [7], which is an overestimation is included.

REFERENCES

1. Reinsch, Ch., Z. Phys., *163*, 424 (1961); Reinsch, Ch., and Springer, T., Z. Naturforsch., *16a*, 112 (1961).
2. Nelkin, M. S., Nuclear Sci. Eng., *7*, 210 (1960).
3. Beckurts, K. H., USAEC report BNL-719, III, RE-1 (1962).
4. Kiefhaber, E., Nukleonik, *4*, 82 (1962).
5. Springer, T., USAEC report BNL-719, I, 54 (1962).
6. Whittemore, W. L., and McReynolds, A. W., Proceedings of Symposium on inelastic Scattering of Neutrons in Solids and Liquids, p. 511, IAEA, Vienna (1960).
7. Vineyard, G. H., Phys. Rev., *96*, 93 (1954).
8. Lemmel, H. D., to be published in Nukleonik (1965).
9. Brockhouse, B. N., Nuovo Cim., *9*, Suppl. 1, 45 (1958).
10. Nelkin, M. S., Phys. Rev., *119*, 741 (1960).
11. Butler, D., private communication.
12. Butler, D., Proc. Phys. Soc., *81*, 276 and 294 (1963).
13. Kornbichler, S., to be published in Nukleonik (1965).
14. Hughes, D. J., and Schwarz, R. B., USAEC report BNL-325 (1958).
15. Ramanna, R., and Sarma, N., Proceedings of Symposium on inelastic Scattering of Neutrons in Solids and Liquids, p. 631, IAEA, Vienna (1960).
16. Hofmeyr, Ch., to be published in Nukleonik (1965).
17. Adams, A., Bod. L., and Pál, L., Acta Phys., Hung. XIII, 25 (1961).
18. Baker, A. R., and Wilkinson, D. H., Phil. Mag., *3*, 647 (1958).
19. Küchle, M., Nukleonik, *2*, 131 (1960).
20. Antonow, A. V., Isakoff, A., Murin, I., Neupocoyev, B., Frank, L., Shapiro, F., and Shtranisch, I., Proceedings of the First International Conference on the Peaceful Uses of Atomic Energy, P/661, Vol. 5, pp. 3, 82, United Nations (1956).
21. Koppel, J. U., and Lopez, W. M., USAEC report BNL-719, III, 946 (1962).
22. Beckurts, K. H., and Klüber, O., Z. Naturforsch., *13a*, 822 (1958).
23. Reier, M., and De Juren, J. A., Reactor Sci. Technol., *14A*, 18 (1961).
24. Starr, E., and Koppel, J., Nuclear Sci. Eng., *14*, 224 (1962).
25. Beyster, J. R., Wood, J. L., Lopez, W. H., and Walton, R. B., Nuclear Sci. Eng., *9*, 168 (1961).
26. Honeck, H. C., USAEC report BNL-719, IV, 1186 (1962).
27. Brown, H. D., and Hennelly, E. J., USAEC report BNL-719, III, 879 (1962).
28. Ganguly, N. K., and Waltner, A. W., Trans. Am. Nucl. Soc., *4*, 282 (1961).
29. Radkowsky, A., USAEC report ANL-4476, 93 (1950).
30. Dexter, A. H., *et al.*, USAEC report ANL-4746, 14 (1951).
31. Wright, W. B., and Frost, R. T., USAEC report KAPL-M-WBW-2 (1956), cf. [18].
32. Hone, D. W., J. Nuclear Eng. A (Reactor Sci.), *11*, 34 (1959).
33. Raievski, V., and Horowitz, J., Proceedings of the First International Conference on the Peaceful Uses of Atomic Energy, P/360, Vol. 5, p. 42, United Nations (1956).
34. Kash, S. W., and Woods, D. C., Phys. Rev., *90*, 564 (1953).
35. Morgan, J., and Warren, B. E., J. Chem. Phys., *6*, 666 (1938).
36. Kussmaul, G., and Meister, H., Reactor Sci. Technol., *17*, 411 (1963).
37. Memmert, G., private communication.
38. Blackshaw, G. L., and Waltner, A. W., Reactor Sci. Technol., *17*, 341 (1963).
39. Brown, W. W., NAA-SR-MEMO-1706.
40. Conerty, M. C., Petrie, C. D., Storm, M. L., and Zweifel, P. F., USAEC report KAPL-1643.

ABSTRACT—RÉSUMÉ—АННОТАЦИЯ—RESUMEN

A/763 République fédérale d'Allemagne

Sur la détermination des constantes de diffusion de H_2O, de polyphényles, de $ZrH_{1,92}$ et de D_2O par des expériences de diffusion simple de neutrons

par T. Springer *et al.*

On détermine habituellement la constante de diffusion thermique moyenne $\langle Dv \rangle$ par des méthodes intégrales, c'est-à-dire en étudiant la relaxation de la densité neutronique dans le temps ou dans l'espace. Dans ce mémoire, on a utilisé une autre méthode: la mesure de la section efficace différentielle de diffusion $d\sigma(\theta)/d\Omega$ pour différentes énergies E des neutrons et différentes températures T de l'échantillon. On peut calculer la constante de diffusion $D(E,T)$ ainsi que $\langle Dv \rangle$ à partir des fonctions $d\sigma(\theta)/d\Omega$. On a trouvé que les sections efficaces de diffusion $d\sigma/d\Omega$ dépendent très peu de la température. Par suite, la grandeur $\langle Dv \rangle$ peut être calculée dans un domaine étendu de température à l'aide d'un nombre relativement faible de mesures de $d\sigma/d\Omega$. Un bon accord a été observé entre ces résultats sur $\langle Dv \rangle$ et les expériences plus classiques dans le cas de H_2O, de D_2O et du diphényle.

A/763 ФРГ

К вопросу об определении констант диффузии обычной и тяжелой воды в экспериментах по однократному рассеянию нейтронов

Т. Шпрингер *et al.*

Обычно средняя константа тепловой диффузии $\langle D_v \rangle$ определяется интегральными методами, а именно путем исследования релаксаций плотности нейтронов во времени или в пространстве. В этой работе был применен другой подход — путем измерения дифференциального эффективного сечения рассеяния $d\sigma(\theta)/d\Omega$ для различных энергий нейтронов E и температуры образца T. Из функций $d\sigma/d\Omega$ можно вычислить константы диффузии $D(E, T)$ и $\langle D_v \rangle$. Установлено, что эффективное сечение рассеяния $d\sigma/d\Omega$ очень малочувствительно к температуре. Следовательно, величину $\langle D_v \rangle$ можно вычислить в широком диапазоне температур при помощи сравнительно небольшого числа измерений $d\sigma/d\Omega$. Для обычной и тяжелой воды наблюдалось хорошее согласие между этими данными $\langle D_v \rangle$ и данными других, более обычных, экспериментов.

A/763 República Federal de Alemania

Determinación de las constantes de difusión del H_2O, polifenilos, $ZrH_{1,92}$ y del D_2O mediante experimentos de dispersión neutrónica simple

por T. Springer *et al.*

Por regla general, la constante media de difusión térmica $\langle Dv \rangle$ se viene determinando por métodos integrales, a saber, estudiando la relajación de la densidad neutrónica con el tiempo o en el espacio. En el presente trabajo, se enfoca el problema desde un punto de vista distinto: se mide la sección eficaz de dispersión diferencial $d\sigma(\theta)/d\Omega$ para distintas energías de los neutrones, E, y para diferentes temperaturas de la muestra, T. Entonces puede calcularse la constante de difusión $D(E,T)$ y $\langle Dv \rangle$ a partir de las funciones $d\sigma/d\Omega$. Se ha comprobado que las secciones eficaces de dispersión $d\sigma/d\Omega$ son escasamente afectadas por la temperatura. Por consiguiente, se puede calcular la magnitud $\langle Dv \rangle$, en un amplio intervalo de temperaturas realizando un número relativamente pequeño de mediciones de $d\sigma/d\Omega$. En el caso del H_2O, del D_2O y de difenilo, se ha podido observar que los datos obtenidos de este modo para $\langle Dv \rangle$ coinciden satisfactoriamente con los valores determinados con ayuda de experimentos de carácter corriente.

Neutron measurements inside reactors with semi-conductor counters

By V. Ajdačić, B. Lalović, M. Baručija and B. Petrović*

A method of absolute in-core measurement of high neutron fluxes inside reactors operating in the megawatt region is described. In this method a semi-conductor counter observes particles from neutron induced reactions in a target placed inside the reactor core through a long evacuated aluminium tube. The paper deals with factors which influenced the accuracy of the method and the possible use of the long-tube method for neutron flux measurements in advanced reactors with neutron fluxes of 10^{15}–10^{16} n/cm^2 s.

The possibility of using the ^{6}Li semi-conductor counter spectrometer for measuring fast neutron spectra inside the zero power reactor at Vinča has been investigated. Great difficulties associated with the high interference of thermal neutrons have been encountered. The thermal neutron interference is almost completely suppressed by a new detector–target arrangement, in which only those products of the ^{6}Li (n,α)T reactions whose mutual angle of emission is different from 180° are detected in coincidence. Resolution of the spectrometer as a function of the reactor power and correction factors of the spectrometer efficiency for various neutron energies are presented.

ABSOLUTE IN-CORE MEASUREMENTS OF HIGH NEUTRON FLUXES BY THE LONG-TUBE METHOD

Due to the lack of neutron counters which operate in high radiation fields, integral methods have been exclusively used for relative in-core measurements of high neutron fluxes (10^{12}–10^{15} n/cm^2 s). In addition, instead of direct absolute measurements of these fluxes, integral neutron fluxes determined by activation methods have been used.

In earlier papers describing the first counting method (the "long-tube" method which enables simple and direct measurements of high neutron fluxes inside the reactor core [1–3]), its application to relative measurements was dealt with. In this method, an evacuated aluminium tube six meters in length was inserted into the reactor core. A target made of fissile materials or light elements such as ^{6}Li or ^{10}B was placed at the bottom of the tube and a semi-conductor counter was mounted at the other end of the tube, outside the core, to detect fission fragments or charged particles coming from the target due to the neutron-induced nuclear reactions. It has been shown that high counting rates of the reaction products can be achieved with ^{235}U, ^{239}Pu, ^{6}Li and ^{10}B targets placed inside the reactor core.

To extend this method to absolute measurements of high neutron fluxes, it is necessary to consider all the factors defining the observed yields from the reactions. These factors include:

Flux depression. In view of the microgram quantities of the target material the flux depression caused by the target itself can be safely neglected. Other materials included only aluminium of $\sigma_a = 1$ barn purity. The aluminium tube was 0.5 mm thick in the vicinity of the target and 41 mm in diameter. An approximate calculation showed that the screening effect of the aluminium tube and the 50 micron thick targets supporting the aluminium foil placed at a distance of 15 cm from the bottom of the tube was less than 0.3%. After the tube was inserted into the 5 cm diameter air-filled channel in the core the change of the reactor reactivity was less than 5×10^{-5}

Number of atoms in the target. Enriched uranium obtained by electromagnetic separation was used as the target material. A mass-spectrometric analysis showed the following abundances in the material; 93.0 ± 0.05%^{235}U, 6.1%^{238}U and 0.9%^{234}U. The total quantity of the uranium in the target was determined gravimetrically and was 285 ± 4 μg.

Cross section. The Vinča 10 MW reactor is a well-moderated heavy water reactor. Therefore, Wescott's value for the thermal neutron cross section for the fission of ^{235}U ($\sigma_f = 550.4$ b) was used. The impurities ^{234}U and ^{238}U cannot contribute to the observed fission yields due to their high fission thresholds.

Scattering and absorption. Since a thin uranium target ($\sim$300 μg/cm^2) was used, the effects of self-absorption and self-scattering on the counting rate were estimated to be small. However, the scattering of fission fragments on the walls of the 6 m long aluminium tube was found to be the most serious difficulty in the absolute measurement of neutron fluxes [2]. The scattered fragments reaching the detector gave an unknown contribution to the counting rate and also distorted the fission spectrum, thus preventing the setting up of a correct discriminator level. An experiment in which

* Boris Kidrič Institute of Nuclear Sciences, Beograd-Vinča. The work was carried out under International Atomic Energy Agency contracts RB/179 and RB/130.

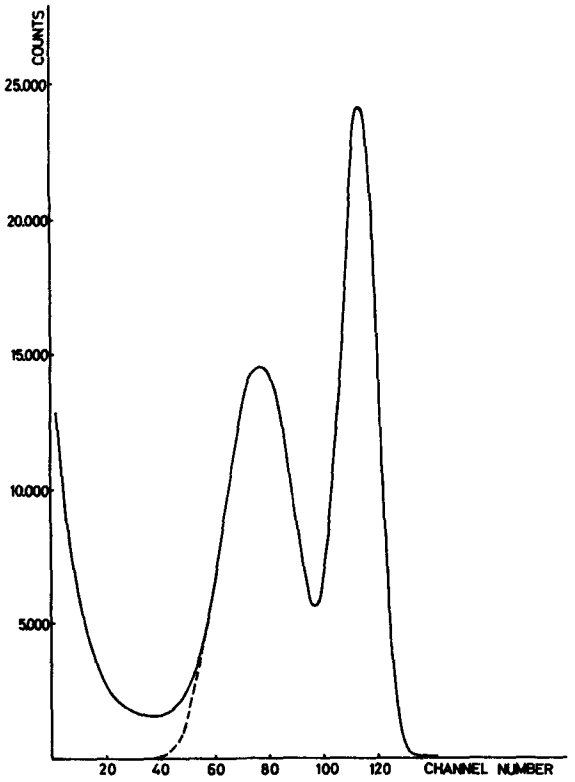

Figure 1. Fission-fragment spectrum at 6.5 mW power

the distance of the detector from the target was varied, showed that the counting rate did not follow a geometrical relationship because of the scattering effect. The effect of scattering on the counting rate was avoided by inserting a collimator, 1 cm in diameter, at a distance of 2 m from the target. Under these conditions the fission spectrum (Fig. 1) was almost identical to the spectrum obtained with the same target and the detector 5 cm apart, i.e., without scattering. As the measurements were made with a tube evacuated to a pressure lower than 10^{-3} mm Hg, the absorption and scattering of fission fragments in the residual gas were negligible.

Geometry. The geometrical efficiency of 2.644×10^{-8} was obtained with an effective detector area of 12.57 ± 0.25 mm^2, a target 12 mm in diameter, and a detector to target distance of 615 cm.

Absolute measurements of the thermal neutron fluxes were made in an air filled vertical channel VC-2 of the Vinča reactor operating at 6.5 MW. The value obtained for the thermal neutron flux was:

$$\phi = (3.47 \pm 0.13) \times 10^{13} \text{ n/cm}^2 \text{ s}$$

The estimated accuracy of about 4% results from the uncertainties in:

—number of ^{235}U atoms in the target (1.4%),
—fission cross section (1.8%),
—scattering of fission fragments (less than +2%),
—self-scattering, self-absorption, absorption (less than −2%),
—geometry (2%) and
—neutron flux instability and other factors (1.5%).

The statistical error was about 0.2%. The reproducibility of the results is 1%, as limited by the accuracy with which the same reactor power could be repeated and by the oscillations of the neutron flux at the point of measurement. It is interesting to note that by observing the changes of the counting rate we were able to notice very fine actions in the reactor system affecting the local neutron flux.

One of the disadvantages of this method when applied to higher neutron fluxes (10^{15}–10^{16} n/cm^2 s) for long time periods is that the burn-up of the high cross section target is appreciable. However, in the case of higher neutron fluxes use can be made of this fact for making absolute measurements since the counting rate as a function of time is given by:

$$A = GN_0\sigma\phi e^{-\sigma\phi t}$$

where G is the geometrical factor, N_0—number of atoms at time $t=0$, σ—reaction cross section, and ϕ—neutron flux. If the flux is constant the slope of the curve $\ln A$ *vs.* time is given by the value of the product $\sigma\phi$. Assuming that the reaction cross section is known, one can find the neutron flux simply by measuring the slope of this curve. For example, for a ^{10}B target and a thermal neutron flux of 10^{16} n/cm^2 s the half-time for the target burn-up is about 5 hours. A unique feature of this method of absolute measurement of neutron fluxes is that it is not necessary to know either the geometry of the experiment or the number of atoms in the target.

MEASUREMENT OF FAST NEUTRON SPECTRA INSIDE REACTORS WITH THE ^{6}Li SEMI-CONDUCTOR COUNTER SPECTROMETER

Two serious difficulties are encountered in the use of the ^{6}Li semi-conductor counter spectrometer for measurements of pile neutron spectra in well-moderated reactors. First, the resolution of the spectrometer is affected by the high level of gamma radiation inside the reactor [4]; this sets an upper limit to the reactor power at which measurements can be made. Second, the high flux of thermal neutrons which are detected in the spectrometer with an efficiency of about 4000 times that of fast neutrons, can seriously affect the low energy part of the fast neutron spectrum [5]. In addition to these problems, fast neutrons produce (n,p) and (n,α) reactions in silicon, which may result in a considerable background counting rate. They also cause radiation damage in the silicon monocrystal, which limits the life of the semiconductor counters to a total dose of about 10^{12} fast neutrons per cm^2.

To study the possibilities and limitations of this technique the fast neutron spectrum inside the Vinča heavy water zero power reactor was measured with a ^{6}Li sandwich-type spectrometer. Each counter in the spectrometer had a sensitive area of 75 mm^2, and the target consisted of 150 μg/cm^2 of ^{6}LiF evaporated onto a thin organic foil.

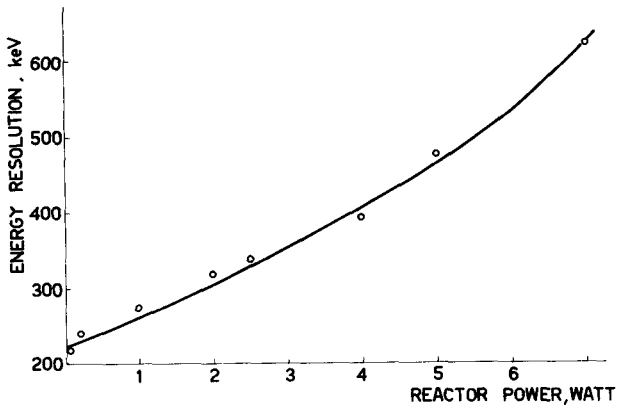

Figure 2. Energy resolution of the spectrometer *vs.* reactor power

To find suitable conditions for the measurements the change in energy resolution of the spectrometer was measured as a function of the reactor power. The energy resolution was found to be poorer as the reactor power increased (Fig. 2). This was probably caused by gamma radiation, since a similar loss in energy resolution was observed both with and without a boron and cadmium shield enclosing the detector chamber. Therefore, this effect imposes an upper limit to the reactor power at which neutron spectra can be measured. The charged particle energy spectrum obtained at the power of 2 W is shown in Fig. 3. The fast neutron spectrum can be derived by multiplying it by factors for neutron transmission in the shield and for the ^{6}Li (n,α)T cross section. In spite of using the boron (0.60 g/cm^2) and cadmium (0.43 g/cm^2) shield the

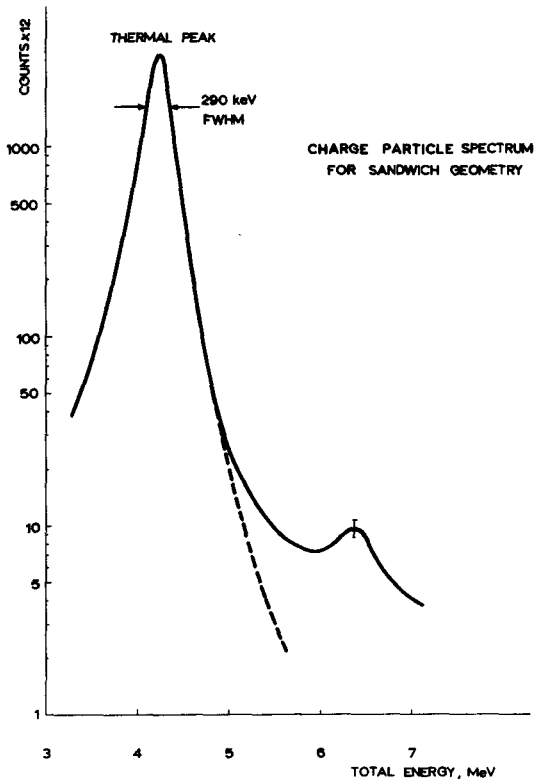

Figure 3. Coincidence sum spectrum of charged particles for sandwich geometry

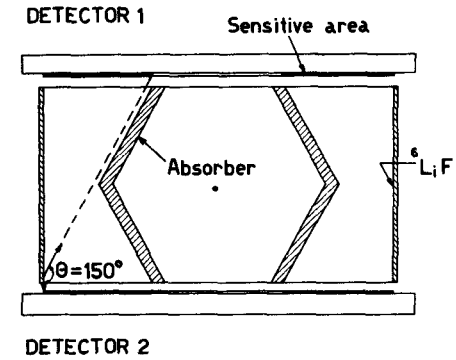

Figure 4. Cylinder geometry with an absorber placed between two counters having ring sensitive areas. Theta-minimum angle between triton and alpha particles for neutron energies up to 5 MeV

thermal neutron component, which was reduced by 66.4 times, was not suppressed to a sufficient degree and the data in the part of the spectrum below 1 MeV are uncertain. Hence, this thermal neutron interference is the main disadvantage of the ^{6}Li-semi-conductor counter spectrometer in the measurement of neutron spectra in well-moderated reactors.

It was attempted to overcome this difficulty by considering the fact that in the case of thermal neutron reactions the fragments (alphas and tritons) move in opposite directions, while in the case of fast neutron reactions they form angles other than 180°. These two types of reactions were distinguished by using a target in the form of a hollow cylinder with evaporated ^{6}LiF on its inner surface (Fig. 4). The dimensions of the cylinder were inner diameter 16 mm and length 10 mm. Two counters were placed at the opposite ends of the cylinder. In this way it was impossible for both coincident fragments travelling in opposite directions to reach the detectors. But if a neutron had an energy even as low as 100 keV, the mutual angle of the fragments differed from 180° by a value lying between 0° and 6° (Fig. 5) and both fragments could be detected. The efficiency of this geometrical arrangement is not the same for various neutron energies. The geometrical efficiency of the spectrometer for several neutron energies was calculated by the ZUSE digital computer, and is given in Fig. 6. The charged particle spectrum measured at 2 W for the same position of the

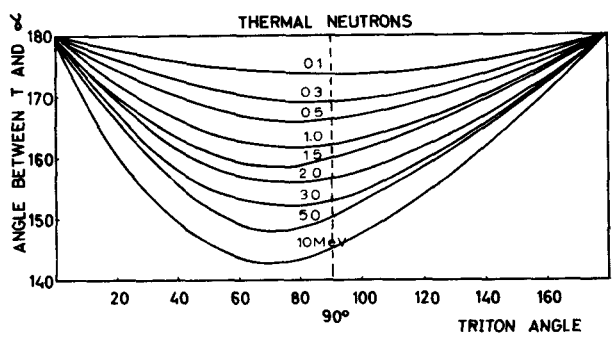

Figure 5. Dependance of the angle between triton and alpha particles on the angle of triton emission for various neutron energies

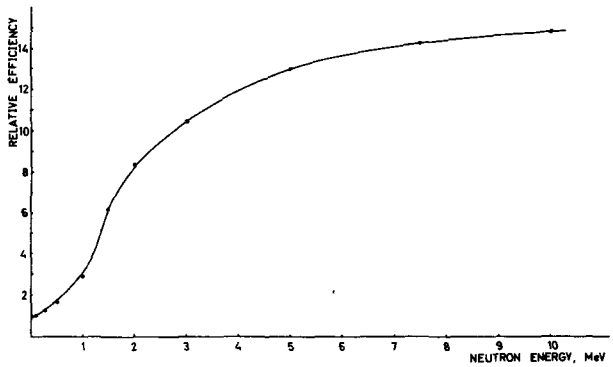

Figure 6. The relative geometrical efficiency of the spectrometer vs. neutron energy (in this calculation the isotropic angular distribution was assumed)

target inside the core as in the case of the plane target was similar to that obtained earlier [5]. The use of the absorber inside the cylinder improved the ratio of the true counting rate to background from 3:2 to 2:1.

In summary of this section it can be said that the ^{6}Li-semi-conductor counter spectrometer can be used for measuring fast neutron spectra inside reactors operating at a power of a few watts. However, such a spectrometer is not suitable for neutron spectra measurements in well-moderated reactors because of the high ^{6}Li (n,α)T thermal neutron cross section. The thermal neutron peak spreads over a substantial part of the spectrum and this is found to be a greater problem than the gamma-ray background. Hence, with this spectrometer and 1 microsecond electronics fast neutron spectra above 1 MeV can be measured in well-moderated reactors. Spectra below 1 MeV can be measured only in fast assemblies.

With the cylinder-target arrangement the difficulty of the thermal neutron interference can be overcome. However, the efficiency of this arrangement is lower than that of sandwich geometry, and this is the main disadvantage of the method.

ACKNOWLEDGEMENT

The authors wish to express their thanks to the members of the Scientific Institute of the "Atoms at Work" exhibition held in Belgrade in 1963 for their kind co-operation during the scattering experiments made on the exhibition Lockhead nuclear research reactor. The authors also thank the staff of the Vinča RA and RB reactors for their help during the experiments.

REFERENCES

1. Ajdačić, V., Kurepa, M., and Lalović, B., Nucleonics, *20* (2), 47 (February 1962).
2. Ajdačić, V., Azuma, R., and Fleming, W., *ibid.*, *21* (1), 60 (January 1963).
3. Ajdačić, V., and Lalović, B., *Neutron Dosimetry*, Vol. 1, p. 271, IAEA, Vienna (1963).
4. Nygaard, K., Electronique Nucléaire, p. 693, ENEA (Paris 1964).
5. Ajdačić, V., Lalović, B., and Petrović, B., *ibid.*, p. 181.

ABSTRACT—RÉSUMÉ—АННОТАЦИЯ—RESUMEN

A/858 Yougoslavie

Mesures du flux de neutrons dans les réacteurs à l'aide de compteurs à semi-conducteurs

par V. Ajdačić *et al.*

Des publications précédentes décrivant la première méthode de comptage (méthode du « tube long », qui permet de mesurer de façon simple et directe des flux élevés de neutrons dans le cœur d'un réacteur) ont traité de son application aux mesures relatives. Dans cette méthode, un tube d'aluminium sous vide, de 6 mètres de long, est introduit dans le cœur du réacteur. Une cible composée de matières fissiles, lithium 6 ou bore 10, est disposée au fond du tube. A l'autre extrémité du tube, à l'extérieur du cœur, on place un compteur à semi-conducteur pour détecter les fragments de fission ou les particules lourdes émises par la cible à la suite des réactions nucléaires provoquées par les neutrons. On a ainsi pu obtenir des taux de comptage élevés de produits de réactions neutroniques en plaçant dans le cœur du réacteur des cibles d'uranium 235, de plutonium 239, de lithium 6 et de bore 10.

Pour étendre cette méthode à la mesure absolue de flux élevés de neutrons, on a étudié les divers paramètres qui définissent le rendement observé des réactions. En ce qui concerne l'effet de la diffusion des particules, on a choisi avec beaucoup de soin la géométrie convenant le mieux à l'expérience (cible-collimateur-compteur).

On a réalisé, avec une cible d'uranium 235, des mesures absolues des flux de neutrons thermiques dans le réacteur modéré à l'eau lourde de Vinča, à une puissance de 6,5 MW. La précision de la méthode est estimée à 4 % environ.

On a également envisagé l'application de cette méthode à la mesure des flux de neutrons dans ces réacteurs de type avancé avec des flux très élevés de neutrons (10^{15}–10^{16} n/cm^2 s). Cette application utilise le fait que le taux de comptage pour une position donnée du détecteur décroît avec le temps à cause de l'épuisement de la cible de grande section efficace.

Les spectres de neutrons rapides dans le réacteur à eau lourde de puissance nulle de Vinča ont été mesurés avec des compteurs à semi-conducteurs et une cible de lithium 6. On a utilisé une nouvelle disposition détecteur-cible, seuls les produits de la réaction ^{6}Li(n,α)T dont l'angle d'émission est différent de 180° étant détectés par coïncidences. On supprime ainsi

presque complètement l'interférence des neutrons thermiques. On précise la résolution du spectromètre en fonction de la puissance du réacteur et les facteurs de correction du rendement du spectromètre pour diverses énergies de neutrons.

A/858 Югославия

Нейтронные измерения в реакторах с помощью полупроводниковых счетчиков

В. Айдачич *et al.*

В предварительных работах о первом счетном методе (метод «длинной трубки», с помощью которого осуществлено несложное прямое измерение интенсивных нейтронных потоков внутри активной зоны реактора) рассмотрены возможности его применения для относительных измерений. При использовании этого метода в активную зону реактора погружается эвакуированная алюминиевая трубка длиной 6 *м*. На дне этой трубки устанавливается мишень из делящегося вещества, Li^6 или B^{10}, а на другой ее конец, вне реактора, монтируется полупроводниковый счетчик. С помощью полупроводникового счетчика детектируются осколки деления или тяжелые частицы — продукты ядерных реакций нейтронов на мишени. Было показано, что с мишенями из U^{235}, Pb^{239}, Li^6 и B^{10}, установленными в активной зоне реактора, можно получить весьма большие скорости счета продуктов реакций.

Для того чтобы распространить этот метод и на абсолютные измерения сильных нейтронных потоков, были исследованы различные параметры, определяющие выход реакций. При этом основное внимание уделено выбору наиболее подходящей геометрии экспериментов (мишень — коллиматор — счетчик), позволяющей учесть эффект рассеяния частиц.

Используя мишень из U^{235}, определен поток тепловых нейтронов в активной зоне тяжеловодного реактора в Винче при мощности 6,5 *Мвт*. Точность метода, согласно оценкам, составляет около 4%.

Рассмотрена также перспектива использования того же метода в реакторе с более высоким нейтронным потоком (10^{15} — 10^{16} *нейтр/см*^{2}·*сек*) путем наблюдения за снижением скорости счета со временем, вызванным выгоранием вещества мишени с большим сечением.

Спектры быстрых нейтронов в реакторе нулевой мощности в Винче с тяжеловодным замедлителем измерялись с помощью полупроводниковых счетчиков мишенью из Li^6. При этом была использована геометрия системы счетчик — мишень, в которой детектировались (на совпадении) только те частицы из реакций Li^6 (n, α) T, угол между направлением движения которых отличался от 180°. Таким образом, влияние тепловых нейтронов почти полностью устранялось. В настоящей работе приводится энергетическое разрешение спектрометра как функция мощности реактора и поправочные множители эффективности спектрометра для различных энергий нейтронов.

A/858 Yugoslavia

Medidas neutrónicas en el interior de reactores usando detectores semiconductores

por V. Ajdačić *et al.*

En nuestros artículos previos, que describían el primer método de recuento, el método del « tubo largo », que permite medidas sencillas y directas de flujos elevados de neutrones dentro del núcleo del reactor, nos ocupábamos de su aplicación a medidas relativas. En este método se utiliza un tubo de aluminio de 6 metros de longitud en cuyo interior se ha hecho el vacío y que se introduce en el núcleo del reactor. Un blanco compuesto de materiales fisibles, ^6Li ó ^{10}B, se coloca en la parte inferior del tubo. En el otro extremo del tubo, que queda fuera del núcleo, se monta un detector semiconductor que detecta fragmentos de fisión o partículas pesadas que proceden del blanco debido a reacciones nucleares inducidas por los neutrones. De esta forma se demostró que pueden obtenerse ritmos elevados de recuento de los productos de reacción usando blancos de ^{235}U, ^{239}Pu, ^6Li y ^{10}B en el interior del núcleo del reactor.

Para extender este método a la medida absoluta de flujos elevados de neutrones, hemos medido, en el presente trabajo, parámetros que definen el rendimiento observado de las reacciones. Con relación al efecto de la dispersión de las partículas, se ha puesto un cuidado especial en elegir la geometría más conveniente para el experimento (blanco-colimador-detector).

Utilizando un blanco de ^{235}U se efectuaron medidas absolutas de flujos de neutrones térmicos en el reactor Vinča, moderado con agua pesada, operando a 6,5 MW. La precisión del método se estima en un 4% aproximadamente.

Se estudian posibles aplicaciones del método a la medida de flujos neutrónicos en reactores avanzados de flujo muy elevado (10^{15}–10^{16} n/cm^2 s). Esta aplicación se basa en el hecho de que el ritmo de recuento para una posición fija del detector disminuye con el tiempo, debido al agotamiento del blanco con alta sección-eficaz.

Con detectores semiconductores y un blanco de ^6Li se han medido espectros de neutrones rápidos en el interior del reactor de potencia cero y moderado con agua pesada, Vinča. Se ha empleado una nueva disposición detector-blanco, de modo que sólo se detectan

mediante un dispositivo de coincidencias aquellos productos de la reacción ^{6}Li (n,α)T cuyo ángulo relativo de emisión es diferente de 180°. De este modo se suprime casi completamente la interferencia de los neutrones térmicos. Se da la resolución del espectrómetro en función de la potencia del reactor y los factores de corrección de la eficiencia del espectrómetro para diferentes energías de los neutrones.

Neutron interactions with reactor materials

By E. R. Rae,* R. Batchelor,** P. A. Egelstaff* and A. T. G. Ferguson*

An important aim of reactor physics is the calculation from first principles of the behaviour of a reactor system, and the prediction of reaction rates, neutron fluxes and spectra as functions of position, time and temperature. Interest in this approach has grown rapidly in the UK since the 1958 Geneva Conference, and has been stimulated by the increasing availability of large digital computers. For thermal systems, these calculations required not only improved nuclear data in the thermal and epithermal regions, but also a detailed knowledge of the interaction of slow neutrons with fuel and moderator materials, which would permit calculation of the neutron spectrum in an assembly. Further confidence in the data and methods of calculation has been established by experimental measurements [1] of the neutron spectra in assemblies of particularly simple composition and shape.

This programme for thermal systems has now been under way for several years. Recently the widespread interest in large fast breeder reactors with relatively soft spectra has led to increasing demands for accurate neutron cross-section data throughout a wide neutron energy range, from fast fission neutrons right down to the resonance region. This latter region is of particular interest because of its influence on the temperature coefficients and stability of fast systems. Of the nuclear data measurements currently in progress, those in the thermal region and a part of the resonance region work are due to the requirements of thermal systems, but the fast neutron measurements and the bulk of the experiments in the resonance region arise out of the fast reactor programme.

In the thermal region the UKAEA programme includes a number of precision measurements on fuel materials which are still required to round off the set of parameters needed to allow calculations of reaction rates with a standard deviation of $\sim 1\%$. These consist of a careful study of the thermal fission cross section of ^{235}U, mass spectrometer measurements of α for ^{233}U, ^{235}U, ^{239}Pu, and ^{241}Pu and precision measurements of $\bar{\nu}$ for ^{233}U, ^{235}U and ^{239}Pu using the Boron Pile detector. The thermal region programme also includes studies of the scattering of slow neutrons by a range of moderator and fuel materials such as H_2O, D_2O, C, Be and UO_2. These studies, which consist of measurements of the angular distribution and spectra of the scattered neutrons, are made as a function of the temperature of the scatterer.

In the resonance region, a wide range of experiments is in progress. These include high resolution measurements of the total absorption cross section of ^{232}Th, ^{238}U, ^{233}U, ^{235}U, ^{239}Pu, and ^{241}Pu, of the fission cross section of ^{233}U, ^{235}U, ^{239}Pu and ^{241}Pu, of η (E) for ^{233}U, ^{235}U, and ^{239}Pu and of the capture cross section of ^{232}Th and ^{238}U. In addition to the work on fuel materials, capture cross section measurements are also in progress or planned on a number of structural and coolant materials such as iron and sodium.

Work in the fast neutron range (up to 14 MeV), in which electrostatic generators are used, includes inelastic scattering measurements on Fe, Na and K, and ^{238}U, and the determination of the capture cross section of ^{238}U, the fission cross section of ^{235}U and $\bar{\nu}(E)$ for ^{232}Th, ^{233}U, ^{234}U, ^{235}U, ^{238}U, ^{239}Pu, ^{240}Pu and ^{241}Pu.

It is impossible in a single paper to describe more than a small fraction of this programme, and consequently the neutron interactions of a small number of nuclides which are important to nearly all reactor systems are described here. In order to illustrate as many classes of materials as possible, the nuclides chosen are ^{235}U (fissile), ^{238}U (fertile), Fe (structural) and H_2O (moderator and coolant). The remaining sections of this paper review the measurements carried out on these materials at Harwell and Aldermaston.

URANIUM-235

Fission cross section and direct measurement of Eta

Two serious anomalies exist in the fission cross section data on ^{235}U. In the thermal region, the measurements of Bollinger and Saplakoglu [2,3] which appeared to employ one of the best experimental techniques, and which claimed an accuracy of 1%, were 4% higher than the accepted world value. In the resonance region, recent work by Bowman *et al.* [4] suggested that the normalization of previous measurements had been wrong by $\sim 20\%$. For these reasons, and in order to improve the quality of the available data in certain respects, the UKAEA has made measurements over a wide energy range.

In the thermal region Maslin has made a measurement similar to that of Bollinger and Saplakoglu, using the Aldermaston Fast Chopper. In this experiment both the neutron flux through a foil of ^{235}U and the

* UKAEA, Atomic Energy Research Establishment, Harwell, Berks.
** UKAEA, Atomic Weapons Research Establishment, Aldermaston, Berks.

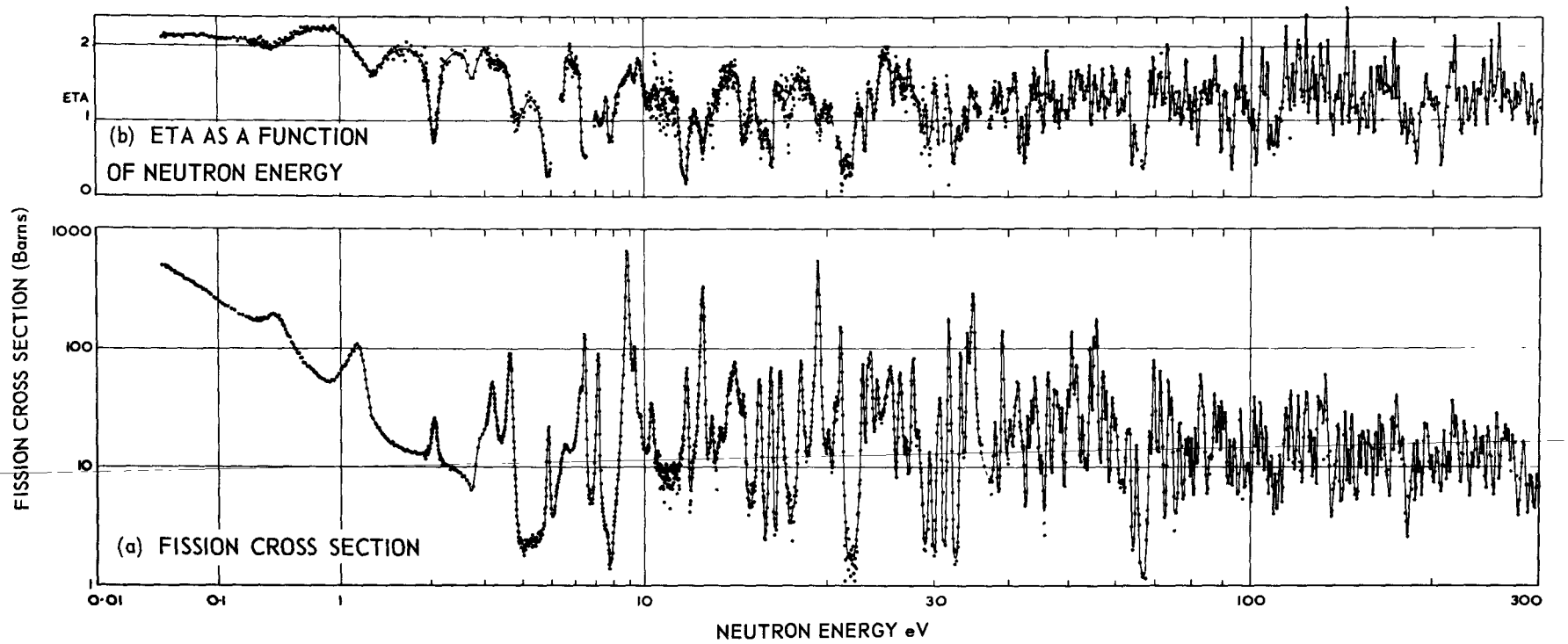

Figure 1. Neutron induced fission ^{235}U

number of fission events occurring in the foil (which is thick enough to be assayed by weighing) are measured absolutely using a coincidence technique. In particular the number of fissions occurring is determined by observing the fast fission neutrons with a set of liquid scintillator detectors employing pulse shape discrimination. The efficiency of this system is measured absolutely by a coincidence method involving the use of a ^{235}U fission chamber containing a thin (0.5, 0.14 and 0.1 mg/cm^2) ^{235}U foil placed back to back with the main foil (130 mg/cm^2).

The set of neutron counters does not subtend a 4π solid angle at the foil, and Maslin has found that the efficiency depends on the angle between the incident neutron beam and the set of counters. This can be understood since fission neutron emission is correlated with fragment direction and the lost fission events are predominantly those with fragments travelling in the plane of the foil. Measurements have been made at two angles and at each angle an extrapolation to zero foil thickness has been made. The preliminary value obtained for the fission cross section of ^{235}U at 2200 m/s is 574 ± 6 barns, a result in good agreement with the values suggested by Safford and Melkonian [5], Deruytter [6] and Bigham *et al.* [7].

In the resonance region, Brooks [8] has made a direct determination of $\eta(E)$ in the energy range from 0.04 to 300 eV using the Harwell Electron Linac (Neutron Project) time of flight spectrometers. In this measurement the fission neutron yield from a sample was again determined using liquid scintillators with pulse shape discrimination [9] while the absorption of neutrons in the same sample was obtained by applying a scattering correction to its measured transmission. Such an experiment was carried out for each of four samples of ^{235}U ranging in thickness from 0.001 to 0.02 atoms/barn and the time of flight resolution varied from 0.35 to 0.01 μs/m through the energy range. It will be readily observed that the raw data for this measurement yield, in addition to $\eta(E)$, the total and fission cross sections of ^{235}U, (the latter on the assumption that $\bar{\nu}$ is constant over the restricted neutron energy range involved). The final values of all three quantities, σ_f σ_T and η are obtained by taking a weighted mean of the values obtained from each of the four samples. The fission cross section and $\eta(E)$ are normalized by setting $\eta(E)$ near thermal energy to correspond to the value determined by Macklin *et al.* [10] at thermal energy.

Fig. 1(*a*) shows the fission cross section of ^{235}U from 0.04 to 300 eV. The present data are in good agreement with those of Shore and Sailor [11] to which previous higher energy measurements [12, 13] had been normalized; they do not support the contention of Bowman *et al.* [4] that this normalization was wrong by $\sim$20%. Fig. 1(*b*) shows the values of $\eta(E)$ over the same energy range.

In the fast neutron region, White, at Aldermaston, has measured the fission cross section of ^{235}U in the energy range 100 keV to 14 MeV. Painted and vacuum evaporated foils were used and were assayed by direct weighing, coulometry, spectrophotometry, alpha assay and back-to-back fission counting. As a result of these assays the mass of ^{235}U in the foils was considered to be known to $\sim$1%. Fission fragments were detected in a 2π ionization counter, and the correction for fragments lost in the foils was determined experimentally. Further corrections were made for the fission fragment angular distribution and for centre of mass effects.

The neutron flux was monitored at the lower energies by a hydrogen-filled proportional counter similar to that described by Skyrme *et al.* [14]. At higher energies a semi-conductor recoil counter similar to that described by Dearnaley and Whitehead [15] was used, the mass of the polythene radiator being determined by direct weighing. For both counters the recoil proton spectrum was calculated and compared with the observed spectrum [16]. The accuracy of this fitting was 1.5% to 2.5% depending on the neutron energy. At 14 MeV the flux was measured by the detection of the associated alpha particles at either 135° or 84° to the neutron beam. At all energies corrections (of a few per cent) were applied for neutron scattering in the targets and counters and for attenuation in the air.

The results of the measurements are shown in Table 1 together with the figures taken from Brookhaven report, BNL 325. It will be seen that the results of the present work while agreeing in shape with the BNL 325 curve, are systematically lower by about 5 per cent in the region 100–500 keV.

$\bar{\nu}$ measurement

Two independent experiments are being conducted to measure $\bar{\nu}_p$ the numbers of prompt neutrons emitted per fission. At Harwell, Colvin and Sowerby [17] have concentrated on obtaining absolute measurements of spontaneous and thermal neutron induced fission to high accuracy using the boron pile, and at Aldermaston, Mather, Moat and Fieldhouse [18] have used a large scintillator to obtain relative measurements over a wide energy range.

Colvin and Sowerby have measured the $\bar{\nu}_p$ values for the thermal fission of ^{233}U, ^{235}U, ^{239}Pu and ^{241}Pu and for fast fission of ^{235}U in the region 0.1 to 2.6 MeV relative to the values for the spontaneous fission of ^{240}Pu and ^{252}Cf, which they established absolutely.

The Aldermaston team find that $\bar{\nu}_p$ for ^{235}U can be represented by $\bar{\nu}_p(E) = 2.423 \pm 0.008 + 0.088\,(\pm 0.008)E$

Table 1. Measured fission cross section of ^{235}U

Energy MeV	Energy spread MeV	Cross section (Barns)	Error per cent	Cross section BNL 325 (Barns)
0.127	0.015	1.54	2.5	1.65
0.160	0.02	1.52	2.5	1.57
0.207	0.02	1.38	2.5	1.47
0.312	0.02	1.30	2.5	1.33
0.404	0.02	1.22	2.5	1.28
0.505	0.02	1.17	2.5	1.23
2.25	0.05	1.31	3.0	1.31
14.1	0.05	2.17	2.0	—

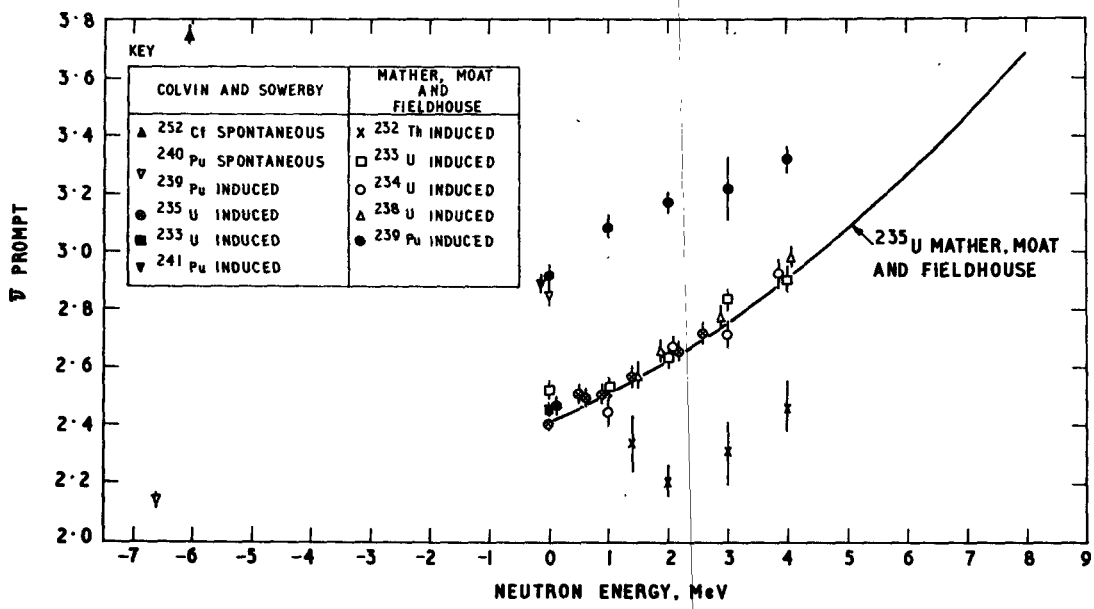

Figure 2. $\bar{\nu}_p$ as a function of neutron energy for a number of heavy nuclides

$+0.0088\ (\pm 0.0011)E^2$ and this curve is reproduced in Fig. 2, along with other recent data obtained at the two laboratories. The uranium data clearly show that $\bar{\nu}_p$ is very insensitive to N. It will be of considerable interest to see if this also holds for the Pu isotopes.

Neutron strength functions and absorption cross section of ^{235}U

A measurement and analysis of the total cross section of ^{235}U from 100 eV to 80 keV has recently been described by Uttley [19]. This work, carried out on the Harwell Electron Linac (Neutron Project) time of flight system, utilized the 120 metre flight path and the time of flight resolution was ~0.002 μs/m. Four metallic samples from 0.001 to 0.03 atoms per barn were employed which were thin enough to ensure accurate measurements of true average total cross section throughout the range.

The average cross section was analysed to obtain the s-wave potential scattering cross section and the s and p-wave strength functions (S_0 and S_1). The values obtained were 11.7 ± 0.1 b, $(1.02 \pm 0.03)10^{-4}$, and $(2{\cdot}0 \pm 0{\cdot}3)10^{-4}$ respectively. These results represent the first measurement of S_1 and by far the most accurate measurement of S_0 to date. The relatively high value of 2×10^{-4} for S_1 is in agreement with other recent determinations for heavy nuclides [20], and with recent theoretical estimates [21,22].

The average absorption cross section was also obtained from the total cross section data by subtracting the scattering cross section (potential scattering+ compound elastic contribution of 0.6 barn) and values are given in Table 2. Included also are data for the total cross section, fission cross section [12], capture cross section obtained by subtraction, and $\alpha = \sigma_0/\sigma_F$.

The errors quoted in α arise almost equally from uncertainties in the potential scattering and measured total cross section, and assume no error in the fission cross section.

The fluctuations in the observed total cross section have also been analysed and were found to be consistent with a Porter-Thomas distribution of reduced neutron widths, and a Wigner distribution in the level spacing.

URANIUM-238

Capture cross section

Neutron capture measurements have been made on ^{238}U in the energy range from a few eV to 14 MeV. At Harwell, Moxon and Rae have used one of the Electron Linac time of flight spectrometers in conjunction with detection of the prompt capture γ-rays [23], to measure the capture cross section from a few eV to 100 keV. The measurements are absolute below 100 eV but at higher energies the shape of the curve is normalized to that of the ^{10}B(n,α) curve in BNL 325. Hanna and Rose [24] at Harwell made activation measurements between 30 keV and 1 MeV, while at Aldermaston, Barry, White and Bunce have recently carried out a set of activation measurements between 0.12 and 7.6 MeV. In this experiment the ^{239}U formed on neutron capture was allowed to decay to ^{239}Np which was separated chemically and counted. The cross section was measured relative to the hydrogen scattering cross section. An activation measurement at 14 MeV was also made at Aldermaston by Perkin *et al.* [25].

The composite capture cross section curve obtained from all these measurements is shown in Fig. 3. It will be observed that from 300 keV upwards there is good agreement between the data of Hanna and Rose and of Barry *et al.* The Hanna and Rose point at 152 keV however, lies some 20% below the points of Barry *et al.* Moxon's data, on the other hand, are in good

Table 2. Average cross-section data for ^{235}U

Energy keV	Strength function $S_0(\times 10^4)$	$\langle\sigma_{n,A}\rangle$ Barns	$\langle\sigma_{n,f}\rangle$ Barns	$\langle\sigma_{n,\gamma}\rangle$ Barns	α
0.1–0.2	1.03±0.03	33.65±1.00	20.5	13.15	0.64±0.05
0.2–0.3	1.28±0.04	32.45±1.00	20.3	12.15	0.60±0.05
0.3–0.4	0.89±0.01	18.88±0.21	14.45	4.43	0.31±0.02
0.4–0.5	0.94±0.01	17.51±0.22	13.22	4.29	0.32±0.02
0.5–0.6	1.12±0.01	19.04±0.23	14.68	4.36	0.30±0.01
0.6–0.7	0.96±0.01	14.96±0.23	11.66	3.30	0.28±0.02
0.7–0.8	1.13±0.01	16.39±0.24	10.93	5.46	0.50±0.02
0.8–0.9	0.85±0.02	11.51±0.26	8.63	2.88	0.33±0.03
0.9–1.0	0.97±0.02	12.46±0.27	7.85	4.61	0.59±0.03
1.0–1.1	1.13±0.02	13.79±0.32	7.79	6.00	0.77±0.04
1.1–1.2	1.13±0.02	13.25±0.32	9.70	3.55	0.37±0.03
1.2–1.3	0.96±0.03	10.72±0.32	7.94	2.78	0.35±0.04
1.3–1.4	1.11±0.03	11.93±0.32	8.17	3.76	0.46±0.04
1.4–1.5	0.93±0.03	9.64±0.32	8.02	1.62	0.20±0.04
1.5–1.6	0.90±0.03	9.06±0.32	6.24	2.82	0.45±0.05
1.6–1.7	1.00±0.03	9.73±0.32	6.90	2.83	0.41±0.05
1.7–1.8	0.97±0.03	9.13±0.32	7.24	1.89	0.26±0.04
1.8–1.9	0.90±0.03	8.23±0.32	6.69	1.54	0.23±0.05
1.9–2.0	1.22±0.03	10.95±0.32	6.66	4.29	0.64±0.05
2.0–3.0		7.81±0.14	5.80	2.01	0.35±0.02
3.0–4.0		6.87±0.17	4.90	1.88	0.38±0.04
4.0–5.0		6.09±0.19	4.50	1.59	0.35±0.04
6.0–7.0		5.04±0.21	3.78	1.26	0.33±0.06
7.0–8.0		4.82±0.22	3.54	1.28	0.36±0.06
8.0–9.0		5.25±0.23	3.52	1.73	0.49±0.07
9.0–10.0		4.68±0.23	3.41	1.27	0.37±0.07

agreement with the Hanna and Rose point at 29 keV, and appear to support the low point at 152 keV. They are not, however, seriously inconsistent with the Barry data since the uncertainty in the $^{10}B(n,\alpha)$ cross sections to which they are normalized is large above 100 keV.

Elastic-inelastic scattering in ^{238}U

At Harwell the IBIS pulsed Van de Graaff has been used by Barnard, Ferguson, McMurray and Van Heerden [26] to make measurements of the elastic and inelastic cross sections between 75 keV neutron energy and 1400 keV using the neutron time of flight technique. Neutrons were produced by the reaction $^{7}Li(p,n)^{7}Be$, energy spread in the incident neutrons being 6–8 keV. A detector whose efficiency for 100 keV neutrons was ~40% of its maximum value [27] was used to detect the neutrons, its efficiency as a function of energy being determined with reference to the hydrogen cross section as is described in detail by Barnard *et al.* [27]. Cross sections were measured absolutely, by direct observation of the incident and scattered flux. Corrections are made for multiple scattering by a Monte Carlo method [28].

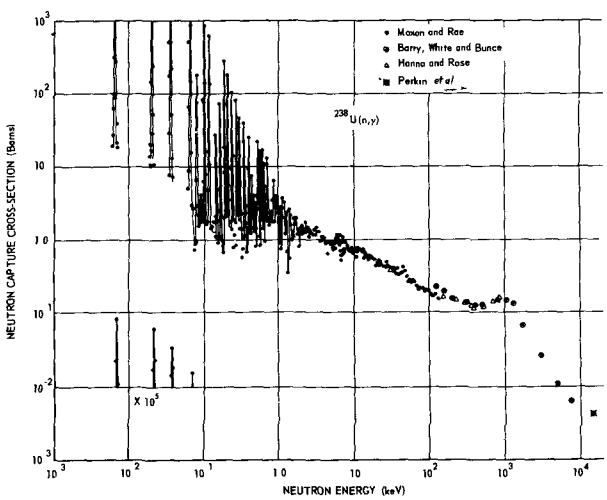

Figure 3. Capture cross section of ^{238}U

A typical time of flight spectrum obtained at an incident neutron energy of 1305 keV is shown in Fig. 4(*b*) and the levels observed are included in Fig. 4(*a*) where they are compared with those found by Coulomb excitation (Elbeck *et al.* [29]) and by Smith [30]. Inelastic scattering clearly excited levels in addition to the collective levels favoured by the Coulomb excitation but the remaining levels correspond well with those found in the latter process. Angular distributions of elastically scattered neutrons were measured at 75, 157, 250, 405 and 550 keV. The results at 550 keV agree to within 2 to 3% with those of Cranberg and Levin [31] and Smith [30]. Angular distributions of the inelastic neutron groups were measured at 157, 550, and 1305 keV. At 157 and 1305 keV all groups appeared to be isotropic within the errors of the experiment. However, a more detailed distribution at 550 keV confirmed threshold anisotropy found by Smith [30]. Differential cross sections at 90° for the excitation of the 45 keV level were measured at 107, 120,

(a) Level structure of ^{238}U

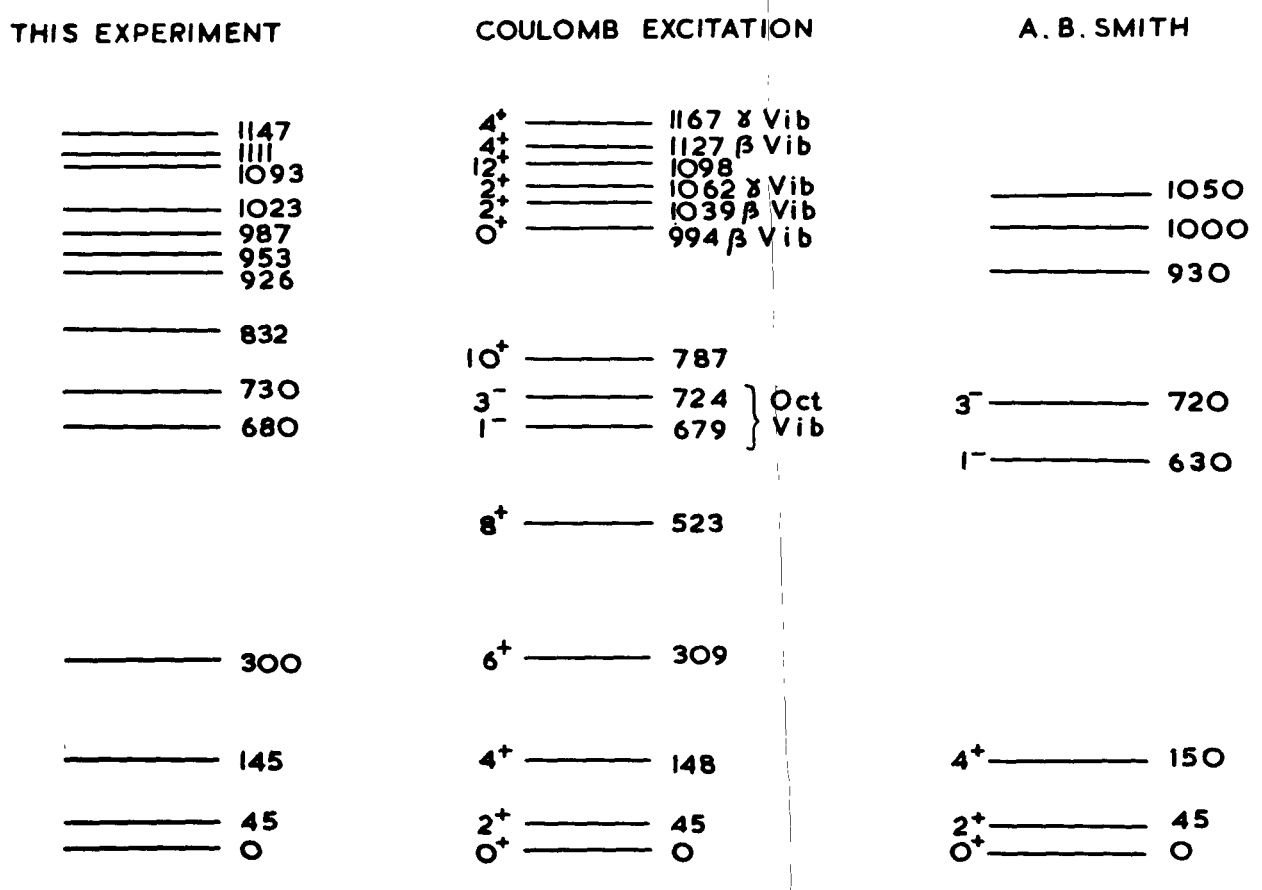

(b) Time of flight spectrum of scattered neutrons. Incident energy, 1305 keV

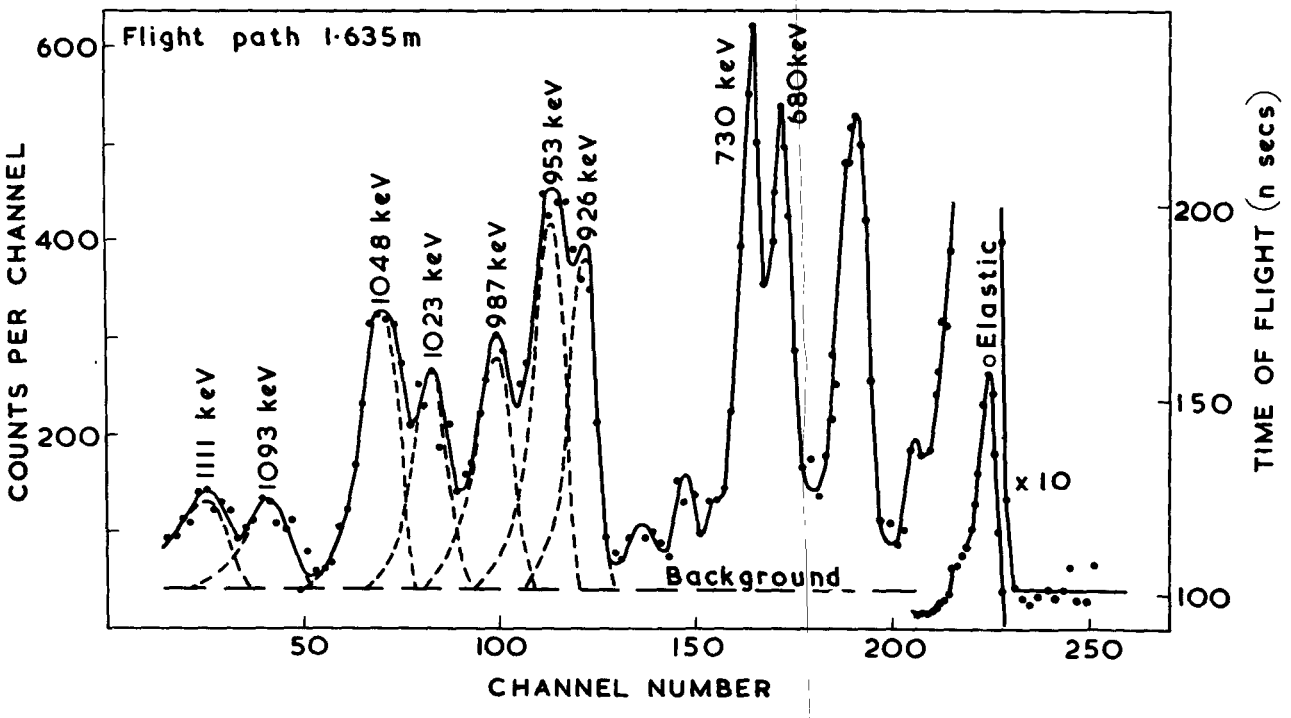

Figure 4. Neutron scattering by ^{238}U

Table 3. The inelastic cross sections of ^{238}U—differential cross sections at 90°

Level position	45 keV level	146 keV level		680 keV level	730 keV
E_n	$\frac{d\sigma}{d\Omega}$ mb/st.	$\frac{d\sigma}{d\Omega}$ mb/sr	E_n	$\frac{d\sigma}{d\Omega}$ mb/sr	$\frac{d\sigma}{d\Omega}$
107	40±10		800	19.8±2.6	
120	58±18		840	23.9±1.2	13.0±1.7
140	68±88		890	24.4±1.2	14.7±2
155	78±8		940	26.2±1.5	17.6±2
200	79±6		990	23.5±2	16.0±2
250	85±8		1090	26.6±2.5	18.3±4
405	106±7		1050	23.5±2.5	20.3±2
450	122±10	24±6	1099	23.5±2	21.0±1.5
550	125±5	23±3	1150	20.4	19.8±1
650	125±15		1240	17 ±1.5	16.5±1.5
720	—	30±5	1305	16.0±1.5	17.2±1.5
750	110±10	32±5			

Level position		832 keV	926 keV	953 keV	987 keV
	E_n	$\frac{d\sigma}{d\Omega}$	$\frac{d\sigma}{d\Omega}$	$\frac{d\sigma}{d\Omega}$	$\frac{d\sigma}{d\Omega}$
	1050	3.3 ±1.5	18.0±2	13.8±2	4.5±1.5
	1099	4.0 ±1.5	21.1±2	18 ±2	13.7±2
	1150	6.2 ±1.5	19.2±1.5	17.5±2	12.5±1.5
	1240	6.40±1.5	17.6±2	20.5±3	14.7±2
	1305	7.2 ±1.5	22.1±1.5	21.9±1.5	16.4±2

E_n	1023 keV	1048 keV	1093 keV	1111 keV	1147 keV
1050					
1099	13.7±2				
1150	12.5±1.5	15.7±2.5			
1240	14.7±1.6	19.7±2	9.9 ±2.5	6.8 ±2.5	4.05±2
1305	16.4±2	26.2±2	11.10±2	13.12±2.5	8.20±12

140, 157, 300, 350, 405, 450, 550, 650 and 720 keV, and cross sections for the 145 keV level between 450 and 750 keV. Cross sections for the levels between 680 and 1147 keV were measured at 50 keV intervals from ~80 keV above threshold to 1400 keV neutron energy. All of these results are shown in Table 3.

At AWRE Aldermaston measurements have been made by Batchelor, Towle and Gilboy of elastic and inelastic scattering from uranium of neutrons of 2 MeV, 3 MeV and 4.0 MeV, using the 6 MV Van de Graaff as described by Towle and Gilboy [32]. Neutrons were produced in the reaction T(p,n)^{3}He, with an energy spread ~100 keV. Absolute cross sections were obtained by comparison with scattering from hydrogen.

At 2 MeV, the elastic peak contains also inelastically scattered neutrons to the levels at 45, and 146 keV. The observed angular distribution for elastic neutrons agreed well with the results of Cranberg and Levin [33]. Underlying the scattered neutrons was a background due to fission neutrons. Assuming a fission spectrum given by $N(E)=kE^{\frac{1}{2}}\exp.(-0.75E)$ the observed fission spectrum at a higher energy than the elastic peak is extrapolated to lower energies beneath the elastic and inelastic neutrons. The inelastic neutrons were divided into two main groups (the 730 keV group) with bounds at 0.57 and 0.87 MeV and the 1.03 MeV group with boundaries at 0.87 and 1.38 MeV. The inelastic neutrons were found to be isotropic. The cross sections obtained at this energy are included in Table 4. At 3 MeV and 4 MeV incident neutron energy the only line structure in the secondary neutron spectrum is that of the "elastic" peaks. The remainder consisting of fission neutrons and an evaporation spectrum was assumed to have the form

$$N(E)=AE\exp(-E/a)+B\,E^{\frac{1}{2}}\exp(-0.75E)$$

where E=energy of the emitted neutron, and B was obtained from the known value of $\bar{\nu}\sigma_f$. The constants A and a were then chosen to give the best fit to the observed spectrum. The values found and the other cross sections etc., assumed are shown in Table 4. At 3 MeV incident energy, there is still a measurable cross section to levels near 1 MeV. An estimate of this cross section is $0.105\pm0.04b$. At 3 and 4 MeV the values found for a were 0.4 and 0.41 MeV respectively. At 3.0 MeV, the "elastic" peak includes inelastic scattering with energy loss less than 0.75 MeV while at 4.0 MeV it includes scattering with energy losses up to 1.5 MeV. At 4 MeV the angular distribution agrees with that of Walt and Beyster except at backward angles.

These results together with the earlier work referred to, now give a fairly detailed picture of elastic and inelastic scattering in ^{238}U up to an incident neutron energy of 4 MeV and should provide a sound basis for reactor calculations.

Table 4

Incident energy 2 MeV Parameter	Cross section (Barn)	Parameter	Incident energy 3 MeV	4 MeV
σ elastic	4.07 ±0.2	σ elastic	4.38 ±0.21	5.38±0.25
σ inel. (0.73 MeV Group)	0.285±0.03	σ total	7.80 ±0.21	7.84±0.21
		$\therefore\sigma$ non-elastic	3.42 ±0.30	2.46±0.32
σ inel. (1.03 MeV Group)	1.025±0.10	$\bar{\nu}$	2.76 ±0.03	2.95±0.03
σ nf	0.54	σ nf	0.56 ±0.02	0.56±0.02
σ nγ	0.05	σ nγ	0.02	0.02
		$\therefore\eta$	1.290±0.03	1.44±0.03
σ total	7.45	$\therefore\eta\sigma$ non-elastic	4.40 ±0.39	3.55±0.46
$\therefore\sigma$ soft	1.48 ±0.25	by direct observation $\eta\sigma$ non-elastic	4.22 ±0.30	3.78±0.25
		$\therefore$most consistent values are:		
		σ elastic	4.46	5.25
		σ non-elastic	3.34	2.59
		$\eta\sigma$ non-elastic	4.31	3.66
		η	1.290	1.413
		σ inelastic	2.76	2.03

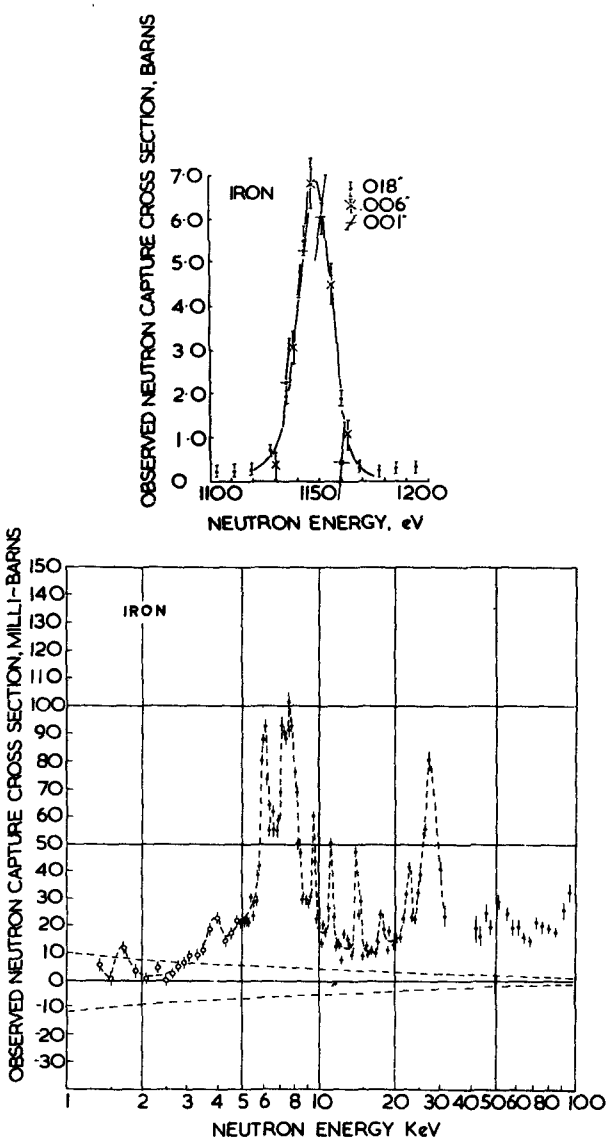

Figure 5. Capture cross section of iron

IRON

Capture cross section

The capture cross section of natural iron has been measured by Moxon at Harwell using the same equipment as was used for ^{238}U. Fig. 5 shows the cross section from 1 to 100 keV. The error bars represent the statistical uncertainty in the points, while the uncertainty in the zero position is shown by the dashed curves. The level at 1150 eV in ^{56}Fe [34,35] is clearly seen and its neutron width was estimated as 50 MeV. The cross section curve indicates the presence of several weak levels between 1 and 28 keV in addition to the two previously reported.

Neutron scattering and (n,n'γ)

The fast neutron time of flight spectrometer associated with the 6 MV Van de Graaff at Aldermaston has been used by Gilboy and Towle [32,36] to study neutron scattering by natural iron in the region 1 to 4 MeV. This study was similar to work previously carried out by these authors on sodium and aluminium.

Differential cross sections for elastic and inelastic scattering were measured at 0.98, 2.01, 3.01 and 3.99 MeV and excitation functions for scattering to levels at 0.845 and 2.085 MeV in ^{56}Fe and 1.409 MeV in ^{54}Fe were measured from 1.4 to 3.0 MeV.

Some of the integrated cross sections are shown in Fig. 6(*a*); and the data for the 0.845 MeV level show good agreement with previous measurements [34]. Fig. 6(*b*) also shows the angular distributions for elastic and inelastic scattering at 3.99 MeV; the symmetry of the inelastic distributions about 90° suggests that compound nucleus formation dominates at this energy. Consequently an attempt has been made to obtain information on level spins using Hauser-Feshbach theory. .

The elastic data were first fitted with optical model calculation using a Bjorklund-Fernbach potential [38]

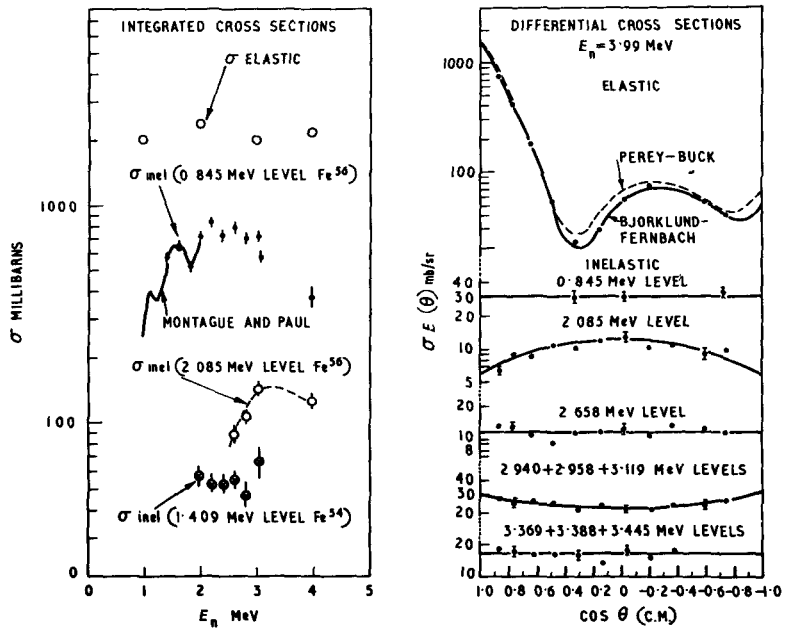

Figure 6. Neutron scattering by iron

(a) Integrated scattering cross section of iron; (b) Angular distributions of elastic and inelastic neutron scattering at 3.99 MeV

and the non-local potential of Perey and Buck [39]. After correcting the 3.99 MeV data for the presence of ^{54}Fe, the inelastic cross sections for ^{56}Fe were compared with the predictions of the theory of Hauser and Feshbach [40]. Transmission coefficients were derived from the two nuclear potentials which were used to fit the elastic data. The ^{56}Fe level spins which best fitted the data are 0.845 MeV(2), 2.085 MeV(4), 2.658 MeV(2 or 3), 2.958 MeV(2 or 3), 3.119 MeV(2), 3.369 MeV(3 or 4), 3.388 MeV(4 or 5) and 3.445 MeV(2). These assignments are relatively insensitive to the parities of the levels.

Perkin (Aldermaston) has used a three crystal pair spectrometer to measure the cross sections for emission of γ-rays from neutron interactions with Fe in the region 3.5 to 8.5 MeV. This work forms part of a survey of several materials of interest for reactor shielding calculations. The inset in Fig. 7 shows the experimental lay-out. The spectrometer gives a simple line shape for incident monoenergetic γ-rays and its γ-efficiency has been measured at 1.37, 2.76, 4.43 and 6.14 MeV. The absolute scale of the cross sections shown in Fig.7 was obtained by reference to the known cross sections for scattering to the first excited states of ^{12}C and ^{208}Pb [41]. Corrections have been made for neutron and γ-ray attenuation in the sample, and the background due to neutrons scattered by the sample. The solid lines in Fig.7 are theoretical curves [42] assuming that the level density of ^{56}Fe is given by $\rho(E)=B.\exp(aE)^{\frac{1}{2}}$ and that all γ-ray transitions are dipole. The experimental points follow the general shape of the theoretical distributions except at low energies where discrete structure is observed.

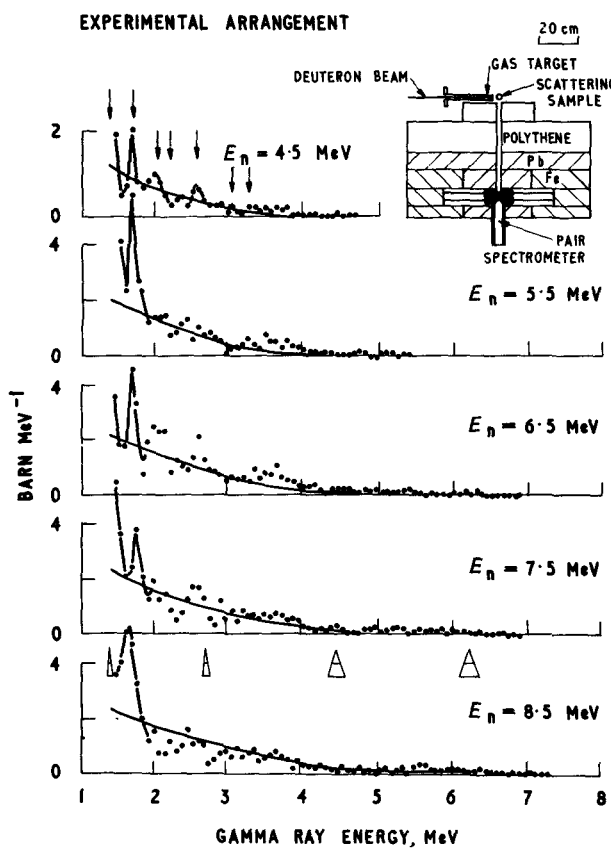

Figure 7. Spectra of gamma rays from neutron interactions with iron

WATER

Scattering of thermal neutrons

The earlier sections of this paper have discussed the slowing down of neutrons from several MeV to the region of 1 eV. Below 100 keV inelastic scattering is no longer important and the neutrons lose energy through the recoil of the scattering nucleus. In calculating this effect it is usual to assume isolated and stationary nuclei (the billiard ball model) but at sufficiently low neutron energies in a moderator this assumption is inadequate and both the dynamics and the structure of the sample modify its neutron scattering properties.

In a basic paper Van Hove [43] discussed the theory of neutron scattering in this limit, and he emphasized the importance of a function now called the scattering law. He shows that for isotropic samples only the magnitudes of the energy and momentum transferred are important in determining the cross section.

Van Hove's equation for the cross section is

$$\frac{d^2\sigma}{d\Omega dE} = <a^2> \left(\frac{E}{E_0}\right)^{\frac{1}{2}} S_1(Q,\omega)$$

$$\text{where } \hbar\omega = E_0 - E = \beta kT, \frac{\hbar^2 Q^2}{2m} = E_0 + E - 2(E_0 E)^{\frac{1}{2}}$$

$$\text{Cos}\theta = \frac{M}{m}\alpha kT$$

m is the neutron mass, M the nuclear mass and a the nuclear scattering length. S_1 is the "Scattering Law".

Egelstaff [44] has pointed out that this equation can usefully be modified to

$$\frac{d^2\sigma}{d\Omega dE} = \frac{\sigma_b}{4\pi kT}\left(\frac{E}{E_0}\right)^{\frac{1}{2}} \exp(-\beta/2)\, S(\alpha,\beta)$$

where σ_b is the bound atom scattering cross section and $S(\alpha,\beta)$ is the Egelstaff Scattering Law.

Measurements on the neutron scattering by moderating materials have been under way for several years at the NRU reactor at Chalk River, Canada (Egelstaff, Cocking and Alexander [45]). The moderators which have been studied include light and heavy water at room temperature and 150 °C, Be and BeO at room temperature, graphite at room temperature, 300 and 600 °C, and UO_2 at room temperature and 500 °C. In some cases, such as H_2O and graphite, earlier measurements (1959) on the equipment have been repeated more recently (1962) and agreement found which confirms their reliability. Due to shortage of space in this paper, we will discuss only the results on H_2O at room temperature and at 150 °C. These results have been reported by Haywood and Thorson [46,47] and a discussion of them has been given by Egelstaff, Haywood and Thorson [48]. They are shown in Figs. 8(*a*) and 8(*b*). Each line on the graphs is the "best" line through the experimental points.

It will be noticed that the scattering law has a low value for small values of α, rises to a maximum and then decreases at high α. The maximum corresponds to interactions in which the momentum transfer is of the same order of magnitude as the most probable momentum for the hydrogen atoms in water. Interactions for larger or smaller values of the momentum transfer are less probable. All the lines on these curves converge at high values of α. The point to which they converge indicates the beginning of the region where a "billiard ball" model is sufficiently accurate. The observed wide divergence between lines for different values of β is a measure of the departure of the actual scattering cross sections from those that would be predicted by this model.

The results may be compared with more sophisticated models, for example, the perfect gas, the Debye crystal model or Nelkin's [49] model of water. Comparison with the experimental data shows that the maxima in S of the perfect gas model are in the wrong place and the magnitudes are also incorrect. A comparison with the Debye model is more successful at large values of β. However, at the smaller values of β the Debye model curves are almost independent of β, and this is in marked contrast to the experimental results. The variation of the curves with β at low β demonstrates the existence of low energy modes of motion for hydrogen in water. It is perhaps to be expected that

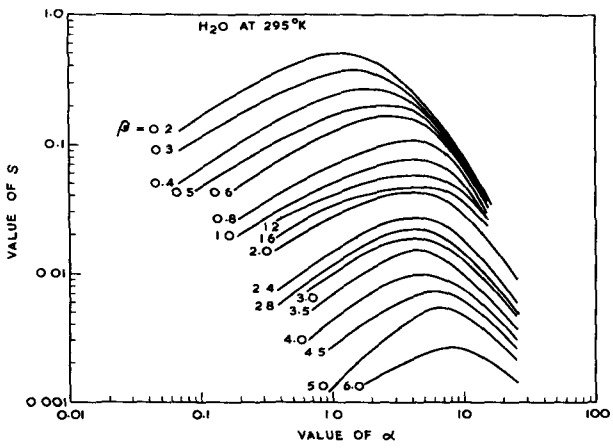

Figure 8(*a*) Scattering law for water, 295 °K

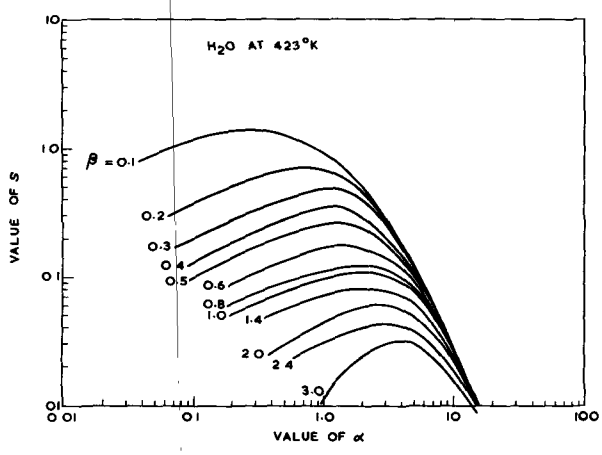

Figure 8(*b*) Scattering law for water, 423 °K

the Nelkin model of water comes closer to the results than the models previously discussed. However, there are also discrepancies in this case in both the magnitude and shape of the curves. A discussion of the significance of these discrepancies and of some possibilities for overcoming them has been given by Egelstaff, Haywood and Thorson [48].

The reasons for the search for a model are first that it is necessary to extrapolate the experimental results from the measured region to values of α and β not covered by the experiment, and secondly that since reactor physics quantities depend on certain averages over the scattering law it is convenient to use these average quantities in a model and determine them by fitting to the scattering law data. Some aspects of the use of these data for reactor physics calculations have been discussed in a companion paper by Story *et al.* [50].

REFERENCES

1. Poole, M. J., and Schofield, P., Proceedings of the IAEA Symposium on Exponential and Critical Experiments, Amsterdam (1963).
2. Bollinger, L. M., Saplakoglu, A., Coceva, C., Cote, R. E., and Thomas, G. E., Bull. A.P.S. II, *2*, 196 (1957).
3. Saplakoglu, A., Proceedings of the Second International Conference on the Peaceful Uses of Atomic Energy, P/1599, Vol. 16, p. 103, United Nations (1958).
4. Bowman, C. D., Auchampaugh, G. F., and Fultz, S. C., Phys. Rev., *130*, 1482 (1963).
5. Safford, G. J., and Melkonian, E., Phys. Rev., *113*, 1285 (1959).
6. Deruytter, A. J., Reactor Science and Technology, *15*, 165 (1961).
7. Bigham, C. B., Hanna, G. C., Tunnicliffe, P. R., Campion, P. J., Lounsbury, M., and Mackenzie, D. R., Proceedings of the Second Conference on the Peaceful Uses of Atomic Energy, P/204, Vol. 16, p.125, United Nations (1958).
8. Brooks, F. D., Proceedings of the Saclay Symposium on Neutron Time of Flight Methods, p. 131, EURATOM, Brussels (1961).
9. Brooks, F. D., Nucl. Instr., *4*, 151 (1959).
10. Macklin, R. L., de Saussure, G., Kingston, J. D., and Lyon, W. S., Nuclear Sci. Eng., *8*, 210.
11. Shore, F. J., and Sailor, V. L., Phys. Rev., *112*, 191 (1958).
12. Michaudon, A., Genin, R., Joly, R., and Vendryes, G., C.E.A. Report 1093, Saclay (1958).
13. Havens, W. W. jr., Melkonian, E., Rainwater, L. J., and Rosen, J. L., Phys. Rev., *116*, 1538 (1959).
14. Skryme, T. H. R., Tunnicliffe, P. R., and Ward, A. G., Rev. Sci. Inst., *23*, 204 (1952).
15. Dearnaley, G., and Whitehead, A. B., UKAEA report AERE-R3662 (1961).
16. Parker, J. B., White, P. H., and Webster, R. J., Nuc. Inst. and Methods, *23*, 61 (1963).
17. Colvin, D. W., and Sowerby, M. G., Proceedings of the Second International Conference on the Peaceful Uses of Atomic Energy, P/52, Vol. 16, p. 121, United Nations (1958)
18. Moat, A., Mather, D. S., and Fieldhouse, P., Proceedings of the IAEA Conference on Physics of Fast and Intermediate Reactors, Vol. 1, 139 (1962).
19. Uttley, C. A., UKAEA report AERE-M1272 (1963).
20. Lynn, J. E., Proc. Phys. Soc., *82*, 903 (1963).
21. Kreuger, T. K., and Margolis, B., Nuc. Phys., *28*, 578 (1961).
22. Buck, B., and Perey, F., Phys. Rev. Letters, *8*, 444 (1962).
23. Moxon, M. C., and Rae, E. R., Nuc. Inst. and Methods, *24*, 445 (1963).
24. Hanna, R. C., and Rose, B., J. Nuclear Energy, *8*, 197 (1959).
25. Perkin, J. L., O'Connor, L. P., and Coleman, R. F., Proc. Phys. Soc., *72*, 505 (1958).
26. Barnard, E., Ferguson, A. T. G., McMurray, R., and van Heerden, I. J., Paper to be submitted to Nuclear Physics.
27. Barnard, E., Ferguson, A. T. G., McMurray, R., van Heerden, I. J., and Adams, J. M., Paper to be submitted to Nuclear Inst. and Meth.
28. Parker, J. B., Towle, J. H., Sams, D., and Jones, P. G., Nuclear Inst. and Meth., *14*, 1 (1961).
29. Elbeck, B., Igo, G., Stephens, F. S. jr., and Diamond, R. M., UCRL-9566 (1960).
30. Smith, A. B., Nuclear Physics, *47*, 633 (1963).
31. Cranberg, L., and Levin, J. S., Phys. Rev., *109*, 2063 (1958).
32. Towle, J. H., and Gilboy, W. B., Nuclear Physics, *32*, 610 (1962).
33. Cranberg, L., and Levin, J. S., Phys. Rev., *103*, 343 (1956).
34. Isakov, A. I., Popov, Yu. P., and Shariro, F. L., J.E.T.P., *38*, 989 (1960).
35. Moore, J. A., Palevsky, H., and Chrien, R. E., Phys. Rev., *132*, 801 (1963).
36. Towle, J. H., and Gilboy, W. B., Nuclear Physics, *39*, 300 (1962).
37. Montague, J. H., and Paul, E. B., Nuclear Physics, *30*, 93 (1962).
38. Bjorklund, F., and Fernbach, S., Phys. Rev., *109*, 1295 (1958).
39. Perey, F., and Buck, B., Nuclear Physics, *32*, 353 (1962).
40. Hauser, W., and Feshbach, H., Phys. Rev., *87*, 366 (1952).
41. Hall, H. E., and Bonner, T. W., Nuclear Physics, *14*, 295 (1959).
42. Troubetzkoy, E. S., Phys. Rev., *122*, 212 (1961).
43. Van Hove, L., Phys. Rev., *95*, 249 (1954).
44. Egelstaff, P. A., UKAEA report AERE-R4019 (1959).
45. Egelstaff, P. A., Cocking, S. J., and Alexander T. K., Proceedings of the Chalk River Symposium on Inelastic Scattering of Neutrons in Solids and Liquids, IAEA, Vienna (1962).
46. Haywood, B. C., and Thorson, I. M., Proceedings of the BNL Conference on Neutron Thermalisation (1962).
47. Haywood, B. C., UKAEA report AERE-R4484 (1963).
48. Egelstaff, P. A., Haywood, B. C., and Thorson, I. M., Proceedings of the Chalk River Symposium on Inelastic Scattering of Neutrons in Solids and Liquids, IAEA, Vienna (1962).
49. Nelkin, M., Phys. Rev., *119*, 741 (1960).
50. Story, J. S., *et al.*, *Evaluation, Storage, and Processing of Nuclear Data for Reactor Calculations*, P/168, this volume.

ABSTRACT—RÉSUMÉ—АННОТАЦИЯ—RESUMEN

A/167 Royaume-Uni

Interactions neutroniques avec les matériaux pour réacteurs

par E. R. Rae *et al.*

Le programme de l'UKAEA de mesures des interactions neutroniques avec les matières fissiles, fertiles, modératrices, de refroidissement et de structure est exposé brièvement à la lumière des exigences de la physique des réacteurs. On résume dans la première partie les raisons de ces mesures et l'étendue du programme, tandis que le reste du mémoire est consacré à la description des travaux expérimentaux sur des exemples typiques de chacune des catégories mentionnées: uranium-235, uranium-238, fer et eau.

Le passage concernant l'uranium-235 décrit les mesures de la section efficace de fission dans différentes régions d'énergie neutronique depuis les énergies thermiques jusqu'à 14 MeV. On présente la variation des grandeurs $\bar{\nu}$ et η avec l'énergie neutronique, la première sur une vaste gamme d'énergie et la seconde dans la région de résonance. On donne également une détermination de la section efficace totale jusqu'à 80 keV, d'où on déduit les fonctions de forces d'ondes *s* et *p* et la section efficace d'absorption.

Le travail sur l'uranium-238 est illustré par des études de la section efficace de capture sur toute la gamme d'énergie depuis quelques eV jusqu'à 14 MeV et de la diffusion non élastique depuis le seuil jusqu'à 4 MeV. Les récentes améliorations de technique permettent la construction de schémas de niveaux d'énergie plus complets pour le noyau d'uranium-238.

La diffusion nucléaire non élastique dans le fer est également décrite pour la gamme d'énergie de 1 à 4 MeV et on donne les valeurs des paramètres du modèle optique qui correspondent le mieux aux données expérimentales. On présente les sections efficaces et les spectres pour l'émission des rayons gamma à la suite de diffusion non élastique et on discute brièvement la section efficace de capture au-dessous de 100 keV.

La dernière partie de l'exposé traite de la diffusion des neutrons thermiques par les noyaux liés. Les résultats des mesures ne contiennent pas les renseignements complets nécessaires pour les calculs de réacteur et doivent être complétés par des considérations théoriques basées sur des concepts choisis de façon appropriée concernant les matériaux de modération. On présente les données pour l'eau à des températures variées et on les compare avec plusieurs concepts théoriques.

A/167 Соединенное Королевство

Взаимодействия нейтронов с реакторными материалами

Э. Р. Рэй *et al.*

Кратко рассмотрена с точки зрения требований физики реакторов программа Управления по атомной энергии Великобритании по измерениям взаимодействий нейтронов с делящимися веществами, материалами для воспроизводства ядерного топлива, замедлителями, теплоносителями и конструкционными материалами. В первой части доклада изложены причины, побудившие провести то или иное измерение, и объем программы работ, а остальная часть доклада посвящена описанию экспериментальных работ на типичных материалах каждой названной категории, а именно взаимодействий с U^{235}, U^{238}, железом и водой.

В разделе, посвященном U^{235}, описаны измерения эффективного сечения деления для различных областей энергии нейтронов от тепловых энергий до 14 *Мэв*. Представлено изменение величин ν и η с энергией нейтронов, первой — в широкой области энергий и второй — в области резонансных энергий. Приведено также определение полного эффективного сечения до энергий 80 *кэв*, на основании чего выведены *s*- и *p*-волновые силовые функции и эффективные сечения поглощения.

Работы по U^{238} иллюстрируются изучением эффективного сечения захвата для области энергий от нескольких электронвольт до 14 *Мэв* и эффективного сечения упругого и неупругого рассеяния от пороговой энергии до 4 *Мэв*. Последние усовершенствования в методике позволяют построить значительно более полную схему энергетических уровней для ядра U^{238}.

Описано также неупругое рассеяние ядер в железе в области энергий от 1 до 4 *Мэв* и дана подгонка оптической модели на основе этих данных. Приведены эффективные сечения и спектры испускания гамма-излучения, сопровождающего неупругое рассеяние. Кратко рассмотрено эффективное сечение захвата в области энергии ниже 100 *кэв*.

В заключительном разделе доклада рассматривается рассеяние тепловых нейтронов связанными ядрами. Результаты измерений не содержат полной информации, необходимой для расчета реакторов, и должны быть дополнены теоретическими соображениями, основанными на соответствующим образом выбранных моделях материалов замедлителей. Представлены данные для воды при различных температу-

рах. Эти данные сравниваются с теоретическими моделями.

A/167 Reino Unido

Interacciones de los neutrones con los materiales de los reactores

por E. R. Rae *et al.*

Se examina brevemente, a la luz de las necesidades en materia de física de reactores, el programa que la UKAEA lleva a cabo en la esfera de las mediciones de las interacciones de los neutrones con los materiales fisionables, fértiles, moderadores, refrigerantes y estructurales. Las razones que inspiran estas mediciones y el alcance del programa se resumen en la primera parte; el resto de la memoria se dedica a la descripción de trabajos experimentales relativos a ejemplos típicos de cada una de las clases de materiales mencionadas, a saber, uranio-235, uranio-238, hierro y agua.

La parte relativa al uranio-235 describe la medición de la sección eficaz de fisión para varias energías neutrónicas comprendidas entre la región térmica y 14 MeV. Se indica la variación de las cantidades $\bar{\nu}$ y η en función de la energía neutrónica, la primera en un amplio intervalo energético, y la segunda en la región de resonancia. Se expone también la determinación de la sección eficaz total hasta 80 keV, de la que se deducen las intensidades de las ondas *s* y *p* y la sección eficaz de absorción.

Como ejemplo de los trabajos relativos al ^{238}U, cabe citar los estudios sobre la sección eficaz de captura en todo el intervalo de energía comprendido entre unos eV y 14 MeV, y sobre dispersión elástica e inelástica en el intervalo energía umbral—4 MeV. Los recientes perfeccionamientos técnicos permiten trazar esquemas de nivel de energía mucho más completos para el núcleo del ^{238}U.

También se estudia la dispersión inelástica nuclear en el hierro, en el intervalo de 1 a 4 MeV, ajustándose los datos según un modelo óptico. Se indican las secciones eficaces y los espectros correspondientes a la emisión de rayos gamma consecutiva a la dispersión inelástica, y se examina brevemente la sección eficaz de captura para energías inferiores a 100 keV.

La última parte de la memoria trata de la dispersión de neutrones térmicos por núcleos enlazados. Los resultados de la mediciones no proporcionan toda la información requerida para el cálculo de reactores y deben completarse con consideraciones de carácter teórico, basadas en modelos adecuadamente seleccionados de los materiales moderadores. Se indican los datos correspondientes al agua a diferentes temperaturas y se comparan con varios modelos teóricos.

Влияние химической связи на термализацию нейтронов

Л. В. Майоров, В. Ф. Турчин, М. С. Юдкевич *

При расчетах спектров тепловых нейтронов в реакторах необходимо учитывать, что химическая связь атомов замедлителя существенно влияет на сечения рассеяния нейтронов. Проблема учета влияния химических связей атомов в задачах теории реакторов в течение ряда лет решалась с помощью упрощенных моделей. В настоящее время в связи с развитием спектроскопии медленных нейтронов стало возможным получать экспериментальным путем необходимые данные о динамике связанных атомов вещества и, используя ранее развитые теоретические методы **, достаточно точно вычислять сечения рассеяния медленных нейтронов. Как известно, тонкая структура дифференциальных сечений слабо влияет на спектры медленных нейтронов, во всяком случае в рамках точности эксперимента. Поэтому для расчета спектров нейтронов в реакторах и анализа различных экспериментов, связанных с изучением взаимодействия медленных нейтронов с веществом, достаточно вычислять сечения в приближении, которое не претендует на описание тонкой структуры сечений, но дает правильные групповые константы при любом разумном выборе ширины группы. Мы исходим из общепринятого в настоящее время некогерентного гауссовского приближения, которое удовлетворяет этим требованиям.

Ниже описываются методы вычисления групповых констант медленных нейтронов и программы для вычислительных машин, которые в настоящее время используются для реакторных расчетов. Приводятся результаты расчетов сечений для некоторых замедлителей и анализируется влияние различных моделей на характеристики сечений, важные для описания термализации нейтронов. Для анализа влияния химических связей на термализацию нейтронов изучаются спектры нейтронов в бесконечных средах, ретермализация нейтронов и процесс установления спектров нейтронов со временем. Результаты расчетов сечений и спектров сравниваются с экспериментом, на основании чего можно делать заключение о применимости той или иной модели.

* Физико-энергетический институт, г. Обнинск.

** Систематическое изложение теорий рассеяния медленных нейтронов вместе с библиографией можно найти в работе [1].

ПРОГРАММА УПРАС

Для расчета многогрупповых дифференциальных сечений рассеяния медленных нейтронов была составлена программа УПРАС (универсальная программа расчета сечений), написанная на языке АЛГОЛ-60 и автоматически переведенная на конкретный машинный язык. По программе УПРАС вычисляется симметризованный закон рассеяния $\widetilde{S}(q, \varepsilon)$.

Могут быть учтены три модуса движения атома.

1. Акустические колебания с произвольным спектром. При малых q для вычисления закона рассеяния используется разложение по фононам, при больших q используются формулы, полученные Эгелстаффом и Скофилдом [2] с помощью метода наискорейшего спуска.

2. Оптические колебания с δ-образным спектром. (Оптические колебания со спектром конечной ширины могут быть учтены как акустические.)

3. Диффузионное движение с полушириной гауссиана, которая при $|t| \to \infty$ возрастает пропорционально $|t|$.

В общем случае закон рассеяния вычисляется как свертка законов рассеяния для различных модусов с произвольными весовыми коэффициентами.

По закону рассеяния вычисляются матрицы $\sigma(E_i \to E_j)$ и $\sigma_1(E_i \to E_j)$ нулевого и первого угловых моментов дважды дифференциального сечения. Матрицы могут иметь размерность 50×50. Вычисляются также интегральные характеристики сечений: σ_s, ξ, $\overline{\cos\theta}$ и др.

Кроме того, по программе УПРАС можно вычислить полные сечения $\sigma_t(E)$ и источники тепловых нейтронов, то есть полностью подготовить начальные данные для расчета спектров тепловых нейтронов.

ПРОГРАММА ПРАССИВ

Для проверки теоретических моделей динамики атомов на экспериментах по рассеянию медленных нейтронов была составлена программа ПРАССИВ (программа расчета сечений интегрированием по времени), по которой с помощью метода, совершенно отличного от опи-

санного выше, вычисляются в некогерентном гауссовом приближении дифференциальные сечения рассеяния нейтронов. В программе ПРАССИВ симметризованный закон рассеяния вычисляется непосредственно интегрированием по времени известного выражения для закона рассеяния как преобразования Фурье с введением под знак интеграла гауссовского обрезающего фактора $\exp\{-\delta^2 t^2/2\}$. Согласно свойству преобразования Фурье вычисленный таким образом закон рассеяния

$$\widetilde{S}'(q, \varepsilon) = \frac{1}{2\pi}\int_{-\infty}^{\infty} \exp\{-q\widetilde{\gamma}(t)\}\exp\{-\delta^2 t^2/2\}\cos \varepsilon t dt$$

отличается от истинного закона рассеяния $\widetilde{S}(q, \varepsilon)$ тем, что по аргументу ε он свернут с гауссианом ширины δ:

$$\widetilde{S}'(q, \varepsilon) = \int_{-\infty}^{\infty} \widetilde{S}(q, \varepsilon - \varepsilon')(2\pi\delta^2)^{-1/2}\exp\{-\varepsilon'^2/2\delta^2\},$$

однако именно такой «размазанный» закон рассеяния и проявляется в эксперименте. Величина δ, характеризующая разрешение экспериментальной установки, задается как некоторая функция начальной и конечной энергии E_0 и E (ибо в действительности δ сильно зависит от E_0 и E). Таким образом, введение обрезающего фактора не только делает возможным вычисление закона рассеяния простым интегрированием по времени, но также избавляет от необходимости введения поправок на разрешение.

При отсутствии диффузионного движения функция $\widetilde{\gamma}(t)$ вычисляется через спектр нормальных колебаний $g(\omega)$. Спектр может иметь любой вид, и наличие произвольного числа оптических колебаний не усложняет вычислений. При наличии диффузионного движения функция $\widetilde{\gamma}(t)$ вычисляется по интерполяционной формуле, предложенной ранее [1] (при малых t наличие диффузии меняет функцию $\gamma(t)$ незначительно).

По программе ПРАССИВ можно вычислять как дважды дифференциальные сечения, так и дифференциальные сечения $\sigma(E_0 \to E)$ и $\sigma_1(E_0 \to E)$, а также интегральные характеристики сечений. Она может быть использована для расчета групповых констант, если задать δ, не превышающее ширины группы.

ДИФФЕРЕНЦИАЛЬНЫЕ СЕЧЕНИЯ

Коротко охарактеризуем проблемы, возникающие при вычислении дифференциальных сечений для ряда важных замедлителей, и приведем некоторые результаты расчетов.

Вода. Спектр колебаний атома водорода в воде можно представить в виде суммы двух частей.

Первая (акустическая) включает акустические колебания и заторможенные вращательные колебания и простирается от нуля до $\sim 0{,}13$ *эв*. Вторая (оптическая) описывает колебания водородного атома в молекуле с характерными частотами 0,2 и 0,48 *эв*. Кригер и Нелкин [3] нашли вес акустической части спектра $A_a = 0{,}48$. Это значение и было принято нами для расчетов. Форма акустической части спектра определялась Ларссоном [4] по рассеянию холодных нейтронов и Эгелстаффом [5] и Мостовым и др. [6] из экспериментов с двойным спектрометром с помощью экстраполяционного метода, предложенного Эгелстаффом [7].

По программе ПРАССИВ вычислялись дифференциальные сечения $\sigma(E_0 \to E)$ при начальной энергии $E_0 = 0{,}102$ *эв* со спектрами Эгелстаффа и Ларссона и сравнивались с экспериментальными результатами Мостового (рис. 1). Из рисунка видно, что кривая, рассчитанная со спектром Эгелстаффа, хорошо согласуется с экспериментальными данными, поэтому в дальнейшем для расчетов термализации в воде использовался спектр Эгелстаффа.

Интегральные характеристики сечений гораздо менее чувствительны к форме акустического спектра, чем дифференциальные сечения, что можно видеть из рис. 2 и 3, на которых показаны средний косинус угла рассеяния $\cos\theta$ и средняя логарифмическая потеря энергии ξ. Теоретические кривые для обоих спектров хорошо согласуются с экспериментом.

Графит. Различные теоретические подходы при вычислении спектра нормальных колебаний графита дают различные результаты. Определение спектра нормальных колебаний из эксперимента по методу Эгелстаффа осложняется когерентными эффектами. Однако для реакторных расчетов достаточно модели, которая дает более или менее верные интегральные характеристики сечений рассеяния. Такой моделью, в частности, является модель Эгелстаффа [8]. По ней был проведен ряд расчетов для исследования термализации нейтронов в пространстве и времени, о которых будет сказано ниже. Кроме того, были рассчитаны сечения со спектром, предложенным Бэлдоком [9]. Их интегральные характеристики сравнивались с интегральными характеристиками сечений, рассчитанных по модели Эгелстаффа. Оказалось, что различия между ними невелики. В качестве примера на рис. 4 приводится средняя относительная потеря энергии по указанным моделям.

Бериллий. Высокая симметрия кристаллической решетки бериллия позволяет применять к ней дебаевскую модель со значением $\theta = 1000\ ^\circ$ K, найденным из теплоемкости. На рис. 5 в качестве иллюстрации работы по программе ПРАССИВ приведены дифференциальные сечения рассеяния на дебаевском кристалле с массой 9 при больших начальных энергиях, рассчитанные по этой программе. Температура T была выбрана равной θ. Кривые построены в масштабе начальной энергии нейтронов E_0. При $E_0 = 60\,\theta$ дифференциальное

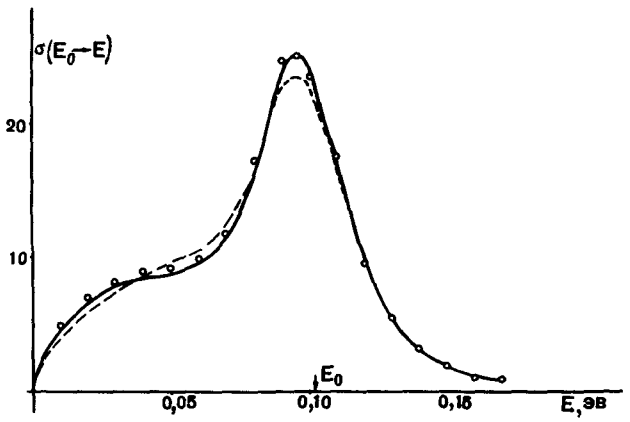

Рис. 1. Дифференциальное сечение рассеяния нейтронов в воде $\sigma(E_0 \leftarrow E)$ при $E_0 = 0{,}102$ *эв*. Сплошная кривая рассчитана со спектром Эгелстаффа [5], пунктирная — Ларссона [4]. Экспериментальные точки взяты из работы [6]

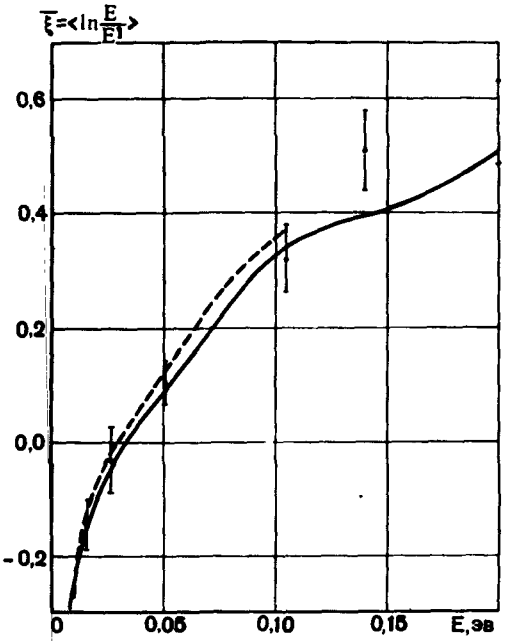

Рис. 2. Средняя логарифмическая потеря энергии нейтронов ξ в воде. Сплошная кривая рассчитана со спектром Эгелстаффа, пунктирная — Ларссона. Экспериментальные точки взяты из работы [6]

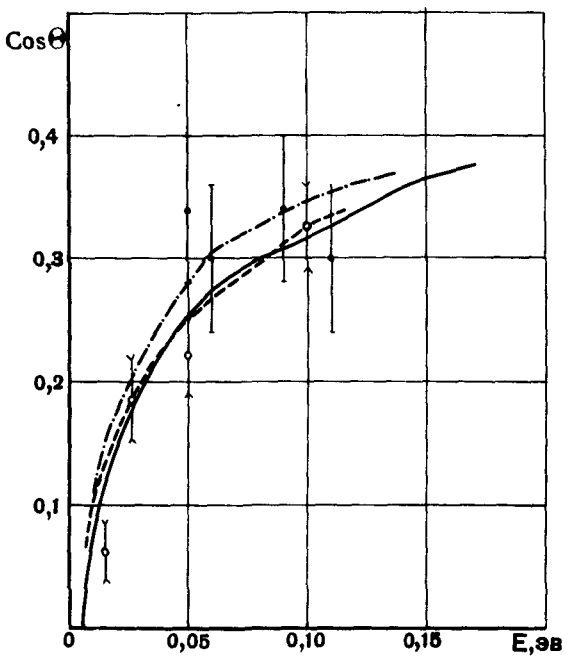

Рис. 3. Средний косинус угла рассеяния нейтронов в воде. Сплошная кривая рассчитана со спектром Эгелстаффа, пунктирная — Ларссона, штрих-пунктир — модель Нелкина. Экспериментальные точки из работы [6] (светлые кружки) и из работы [23] (темные кружки)

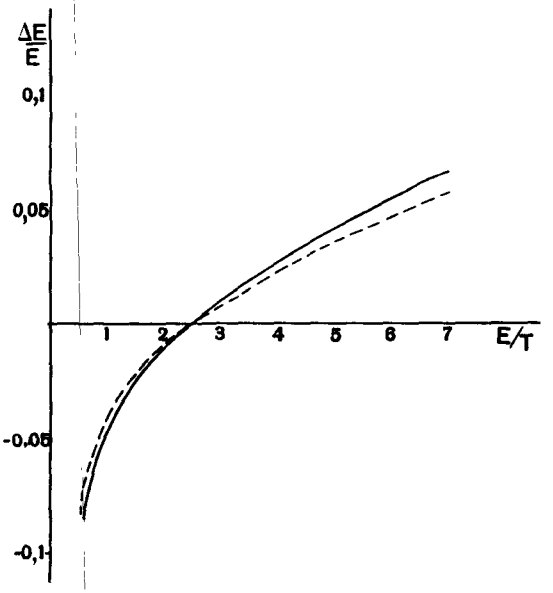

Рис. 4. Средняя относительная потеря энергии на графите со спектром эгелстаффа[8] (сплошная кривая) и Бэлдока[9] (пунктирная кривая)

сечение приближается к «столообразному» виду, характерному для рассеяния на свободном ядре.

Гидрид циркония. Спектр колебаний атома водорода в гидриде циркония состоит из оптической части со средней энергией $\sim 0{,}13$ *эв* и полушириной $\sim 0{,}025$ *эв* и акустической части с дебаевской температурой $\sim 0{,}02$ *эв* [10, 23]. Веса этих частей относятся как массы атомов Zr и H. С помощью программы ПРАССИВ можно уточнить спектр нормальных колебаний исследуемого вещества, если учитывать экспериментальные дважды дифференциальные сечения и действовать методом последовательных приближений. На рис. 6 показан спектр нейтронов с начальной энергией 0,020 *эв*, рассеянных под углом $\theta = 80°$, полученной группой Парфенова на двойном спектрометре медленных нейтронов, использующем импульсный быстрый реактор в Дубне [11], в сравнении с теоретической кривой, рассчитанной по программе ПРАССИВ после двукратного внесения поправки в спектр нормальных колебаний.

Гидрид лития. По данным работы [23] спектр нормальных колебаний атома водорода в гидриде лития принимался состоящим из двух оптических линий 0,10 и 0,13 *эв* с отношением весов 2 : 1 и акустической части с дебаевской температурой $\theta = 250°$ K и весом $M_H/(M_H + M_{Li}) = 0{,}125$. На рис. 7 показано полное сечение рассеяния на гидриде лития, рассчитанное по программе УПРАС в сравнении с экспериментальными данными Доильницына и др. [12]

СПЕКТРЫ В БЕСКОНЕЧНОЙ СРЕДЕ

Влияние химической связи на термализацию нейтронов можно оценить, исследуя, как меняются различные интегральные характеристики пространственных и временных спектров медленных нейтронов. В частности, одной из самых существенных термализационных характеристик вещества является температура нейтронного газа в бесконечной среде при не очень большом поглощении по закону $1/v$, когда спектр тепловых нейтронов можно описать как максвелловский.

Для трех водородсодержащих замедлителей: воды, гидрида циркония и гидрида лития, вычислялись спектры нейтронов в бесконечной среде ($T = 300°$ K), отравленной поглотителем по закону $1/v$ при нескольких значениях поглощения, в интервале до 10 *барн* на атом водорода. Спектры в воде и гидриде лития близки к максвелловским с некоторой температурой T_n. Спектры в гидриде циркония (рис. 8) существенно отличаются от максвелловских, однако по мягкой части спектра (до 0,1 *эв*) для них также были найдены эффективные температуры T_n. Чтобы представить зависимость температуры от поглощения, мы запишем ее в виде

$$T_n/T = 1 + \alpha\,(\sigma_a/\sigma_s),$$

где σ_a — сечение поглощения при $E = T$, а $\sigma_s = 20{,}4$ *барн* — сечение рассеяния на свободном водороде. Коэффициенту α можно придать смысл эффективной массы замедлителя: $\alpha = m_{ef}$, так как при рассеянии на одноатомном идеальном газе α примерно равна массе атома 13. На рис. 9 показана зависимость m_{ef} от σ_a для перечисленных замедлителей. Сильная зависимость m_{ef} от σ_a для гидрида циркония отражает тот факт, что механизм замедления для него сильно отличается от механизма замедления в тяжелом газе. Напротив, почти постоянное и близкое к единице значение m_{ef} для воды свидетельствует о том, что вода, как это неоднократно отмечалось в литературе, по своим замедляющим свойствам близка к свободным атомам водорода. Результаты расчета для воды и гидрида лития хорошо согласуются с экспериментальными данными [12, 14]

ДЛИНА РЕТЕРМАЛИЗАЦИИ

При вычислении пространственно-энергетического распределения медленных нейтронов в средах с большими градиентами температуры важно знать, на каком расстоянии от поверхности температурного разрыва устанавливается спектр, равновесный для среды с данной температурой. Это расстояние характеризуют так называемой длиной термализации, или ретермализации, L_{th}, которая определяется как показатель экспоненциального приближения температуры нейтронного газа T_n к равновесному значению

$$T_n(x) - T_n(\infty) = \text{const} \cdot \exp\{-x/L_{th}\},$$

где x — расстояние до плоскости температурного разрыва.

Длина ретермализации существенно зависит от химической связи атома замедлителя и служит важной характеристикой влияния этой связи. В качестве примера приведем результаты расчета пространственно-энергетического спектра нейтронов в двухзонном графитовом цилиндре. Его внутренняя зона радиусом $R = 40$ *см* имеет температуру 300° K. Внешняя зона радиусом 80 *см* имеет температуру 450° K. На рис. 10 показан ход температуры нейтронного газа по радиусу цилиндра, вычисленный по модели одноатомного газа ($M = 12$), и с сечениями, рассчитанными по программе УПРАС с модельным спектром Эгелстаффа [8]. Для одноатомного газа $L_{th} = 4{,}2$ *см*, для кристаллического графита $L_{th} = 6{,}9$ *см*. Так как длина термализации в одноатомном газе возрастает как $\sqrt{M}$, этот результат можно трактовать как возрастание эффективной массы графита вследствие химической связи до величины $m_{ef} \approx 32$.

Расчеты по ретермализации производились по программе T-2 (p — 1-приближение,

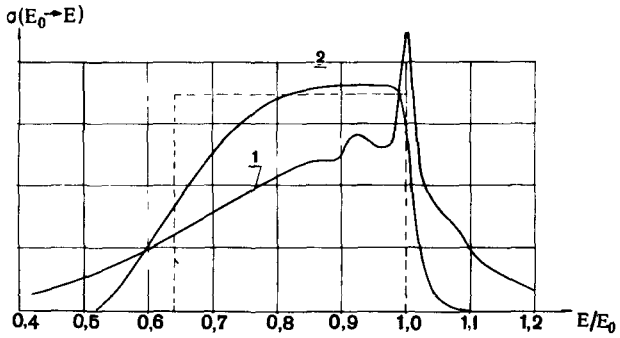

Рис. 5. Дифференциальное сечение σ $(B_0 \to E_0)$ рассеяния нейтронов на дебаевском кристалле с массой $M=9$:
1 — начальная энергия $E_0=10\,\theta$; *2* — начальная энергия $E_0=60\,\theta$

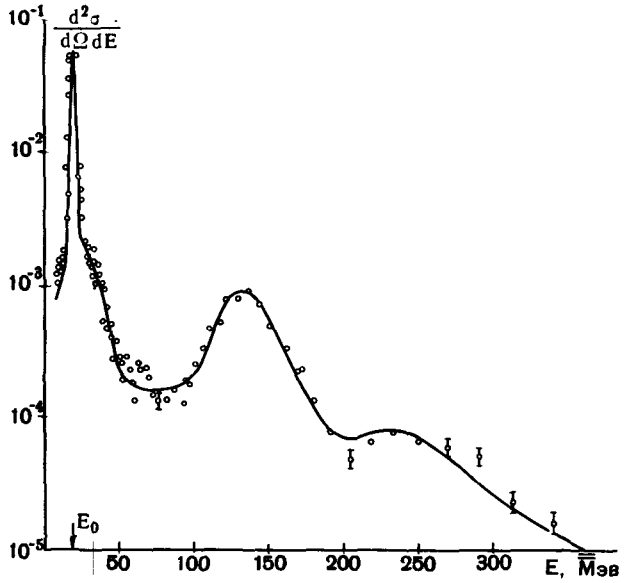

Рис. 6. Спектр нейтронов с начальной энергией 20 *Мэв*, рассеянных под углом $\theta=80°$ на гидриде циркония при температуре 760° К. Теоретическая кривая рассчитана по программе ПРАССИВ с учетом экспериментального разрешения

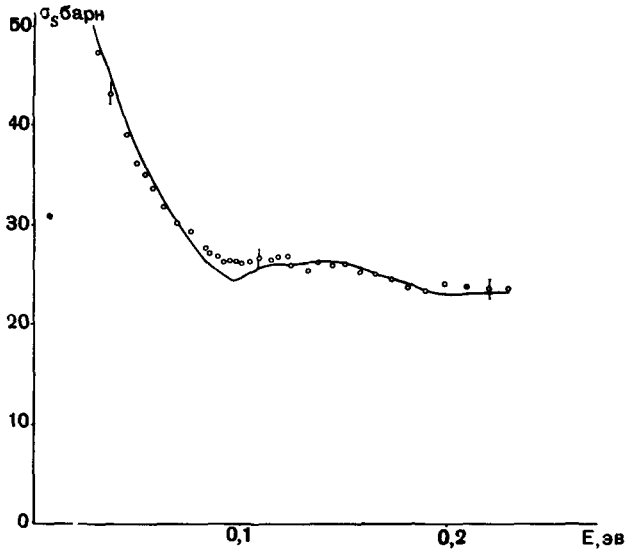

Рис. 7. Полное сечение рассеяния нейтронов на атоме водорода в гидриде лития

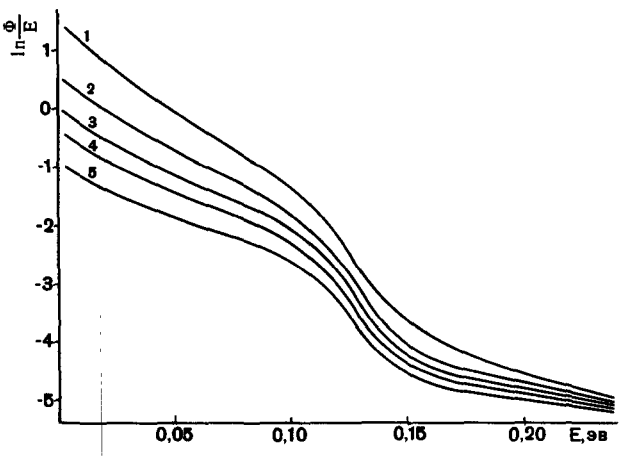

Рис. 8. Спектры нейтронов в бесконечной среде гидрида циркония при комнатной температуре с поглотителем по закону $1/v$.
Цифры у кривых означают сечение поглощения при $E=0{,}025$ *эв* в барнах на атом водорода

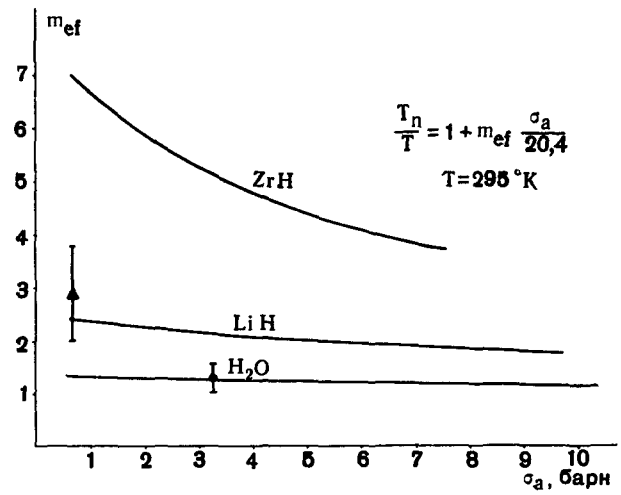

Рис. 9. Эффективная масса водорода в трех водород-содержащих замедлителях.
Кружком показано экспериментальное значение m_{ef} для воды из работы [14], треугольником — то же для гидрида лития [12]

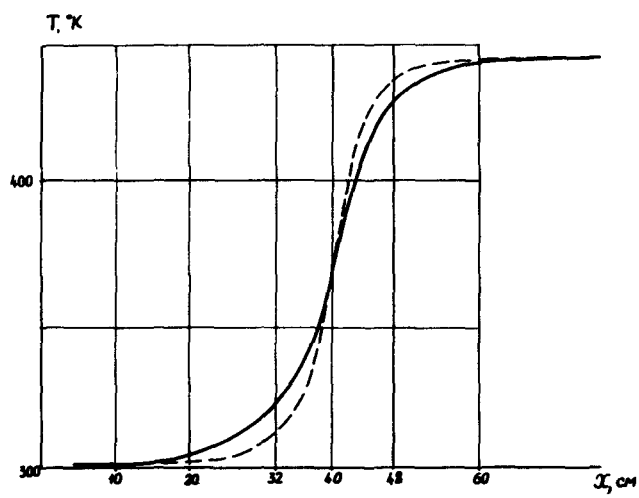

Рис. 10. Температура нейтронного газа в графитовом цилиндре.
Сплошная кривая рассчитана с учетом химической связи, пунктирная — по газовой модели

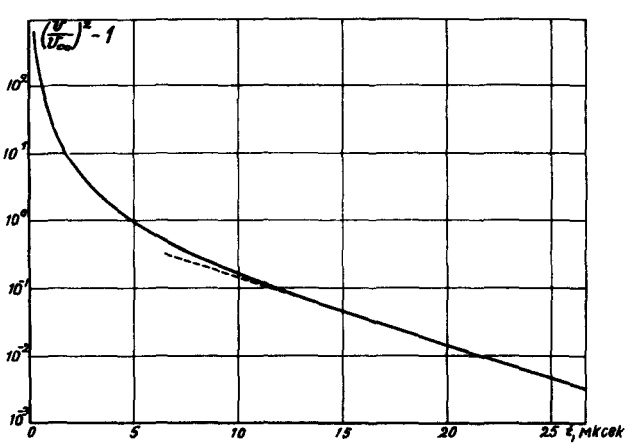

Рис. 11. Зависимость от времени средней скорости нейтронов импульсного источника в воде

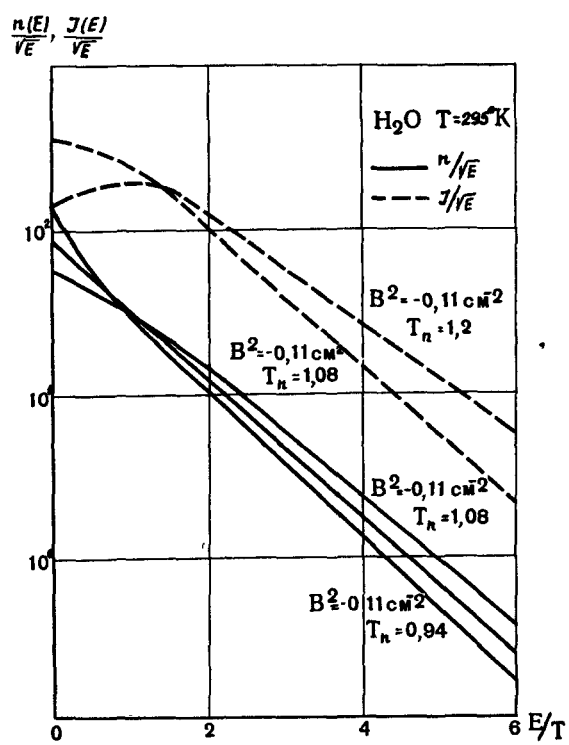

Рис. 12. Асимптотический спектр плотности и тока нейтронов в воде при различных B^2

40 групп, произвольные граничные условия и распределение источников).

ТЕРМАЛИЗАЦИЯ НЕЙТРОНОВ ОТ ИМПУЛЬСНОГО ИСТОЧНИКА

Большое количество информации о взаимодействии нейтронов с веществом дают эксперименты с импульсным источником нейтронов. Поэтому представляет интерес сравнение результатов экспериментов с расчетом. Для проведения подобного рода расчетов на языке АЛГОЛ-60 была написана программа расчета в p — 1-приближении термализации и диффузии нейтронов в ограниченной среде ТЕДИ (термализация и диффузия). Методом Рунге-Кутта решается система двух уравнений для плотности нейтронов $N(E, t)$ и тока $J(E, t)$ и производной $\partial J/\partial t$ не пренебрегается. Расчет ведется для пространственной гармоники с заданным B^2. Максимальное число групп по энергии равно 30.

На рис. 11 приведено изменение со временем средней скорости нейтронов в воде. Из графика видно, что через 12 *мксек* эффективная температура нейтронного газа T_n экспоненциально приближается к температуре среды

$$T_n - T = \text{const} \cdot \exp\{-t/t_{\text{th}}\},$$

где время термализации $t_{\text{th}} = 4{,}6$ *мксек*.

Для графита экспоненциальная зависимость начинается при 800 *мксек* и время термализации $t_{\text{th}} = 315$ *мксек* (плотность $\gamma = 1{,}6$ *г/см*^{3}).

Самостоятельный интерес имеет изучение асимптотических спектров нейтронов при больших временах, когда

$$N(E, t) = n(E)\, e^{-\alpha t}; \quad J(E, t) = I(E)\, e^{-\alpha t}.$$

Константа распада α в зависимости от B^2 измерялась для различных замедлителей многими авторами. Из этих измерений определяется коэффициент диффузии в бесконечной среде D_0 и коэффициент диффузионного охлаждения C. Как известно, рассмотрение задачи о стационарной диффузии нейтронов вдали от источника приводит к тому же уравнению, что и для асимптотического спектра в случае импульсного источника, но только с $B^2 < 0$. Измеряя квадрат диффузионной длины L^2 как функцию сечения поглощения σ_a, экспериментально определяют собственное число α как функцию B^2 (при отрицательных B^2). Поэтому асимптотические спектры и константа α рассчитывались по программе ТЕДИ как для $B^2 \geqslant 0$, так и для $B^2 < 0$.

На рис. 12 и 13 приведены спектры асимптотической плотности и тока нейтронов, рассчитанные для воды (см. рис. 12) и графита (см. рис. 13) при разных B^2. Для обоих замедлителей спектры плотности и тока значительно отличаются. Ясно виден эффект диффузионного охлаждения для $B^2 > 0$ и диффузионного нагревания для $B^2 < 0$. Интересно отметить, что $n(E)$ и $I(E)$ начиная с энергий $E \sim T$ описываются максвелловским распределением с температурой T_n, зависящей от B^2.

На рис. 14 приведен график $\alpha(B^2)$ для воды при температуре 295° К с сечениями, рассчитанными со спектром частот Эгелстаффа [5]. Там же приведены экспериментальные данные (импульсные измерения [15, 16] и эксперименты с отравлением [17]). Расчет и эксперимент с отравлением полностью согласуются. При положительных B^2 расчет хорошо согласуется с измерениями Лопеца и Бейстера [15] и несколько расходится с данными Антонова [16]. Та же картина наблюдается и при сравнении расчетов с экспериментами Кюхле [18] (на рис. 14 данные Кюхле не нанесены). Надо отметить, что эксперимент Лопеца и Бейстера проводился в геометрии параллелепипеда, в то время как эксперименты Антонова и Кюхле — в цилиндрической геометрии, где определение B^2 менее надежно. Расчетные значения параметров: $D_0 = 3{,}66 \cdot 10^4$ *см*^{2}*/сек*, $C = 3{,}08 \cdot 10^3$ *см*^{4}*/сек*.

Из сравнения расчета $\alpha(B^2)$ с экспериментом можно сделать вывод, что использование спектра частот Эгелстаффа приводит к правильному описанию термализации и диффузии нейтронов.

На рис. 15 приведено $\alpha(B^2)$ для графита при $T = 295°$ К. Сечения рассчитывались по программе УПРАС с модельным спектром Эгелстаффа [8]. Поскольку экспериментов с отравлением на графите не проводилось, на графике приведена только область $B^2 > 0$. Экспериментальные значения взяты из работ [19, 20]. При больших размерах системы согласие расчета с экспериментом хорошее, то есть расчетное значение коэффициента диффузии $D_0 = 2{,}12 \times 10^5$ *см*^{2}*/сек* совпадает с экспериментальным, при меньших размерах расчет дает завышенное значение α, что означает, что расчетное значение коэффициента диффузионного охлаждения $C = 1{,}95 \cdot 10^6$ *см*^{4}*/сек* несколько занижено.

ЗАКЛЮЧЕНИЕ

Благодаря интенсивной работе над проблемой термализации нейтронов, проводившейся в различных странах, к настоящему времени разработаны экспериментальные и теоретические методы, позволяющие получать дифференциальные сечения рассеяния нейтронов на химически связанных атомах и контролировать их путем сравнения с экспериментальными данными по нейтронным спектрам. В сочетании с существующими методами расчета спектров (см., например работу [21], а также доклад [22]) это дает возможность для любой системы рассчитать спектр медленных нейтронов и эффекты, связанные с его изменением.

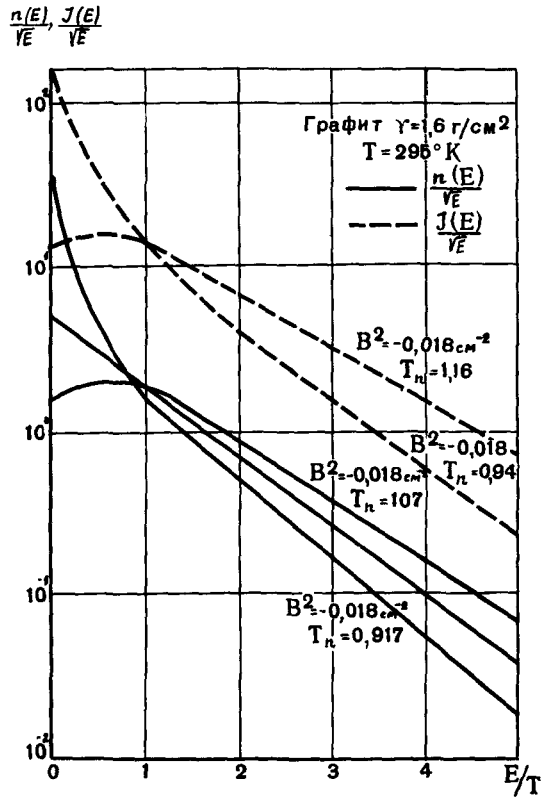

Рис. 13. Асимтотический спектр плотности и тока нейтронов в графите при разных B^2

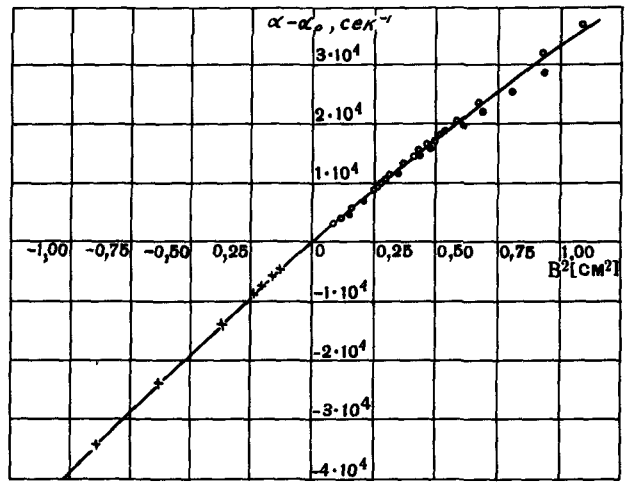

Рис. 14. Постоянная асимптотического спада плотности нейтронов для воды:
сплошная кривая — расчет; × — эксперимент [17]; ○ — эксперимент [15]; ● — эксперимент [16]

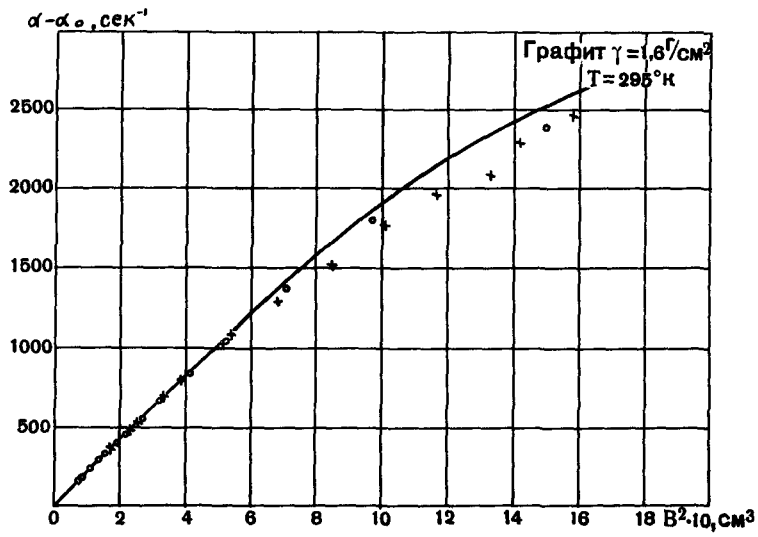

Рис. 15. Постоянная асимптотического спада плотности для графита:
сплошная кривая — расчет; × — эксперимент [19]; ○ — эксперимент [20]

ЛИТЕРАТУРА

1. В. Ф. Турчин. Медленные нейтроны. М., Госатомиздат, 1963.
2. P. A. Egelstaff, P. Schofield. Nucl. Sci. and Eng., *12*, 260 (1962).
3. T. J. Krieger, M. S. Nelkin. Phys. Rev., *106*, 290 (1957).
4. K. E. Larsson, U. J. Dahlborg. J. Nucl. Energy, *16*, 81 (1962).
5. P. A. Egelstaff et al. Inelastic scattering of neutrons in solids and liquids, vol. 1, Vienna, 1963, p. 343.
6. В. И. Мостовой и др., наст. издание, P/376.
7. P. A. Egelstaff. Nucl. Sci. and Eng., *12*, 250 (1962).
8. J. Macdougall. Brookhaven Conference on Neutron Thermalization, *1*, 1962, p. 121.
9. G. R. Baldock. Phil. Mag., *1*, 789 (1956).
10. А. Мак-Рейнольдс и др. Труды Второй международной конференции по мирному использованию атомной энергии, Женева, 1958, P/1540.
11. И. И. Бондаренко и др. Inelastic scattering of neutrons in solids and liquids, Vienna, *1*, 127 (1963).
12. Е. Я. Доильницын и др., наст. издание, P/366.
13. R. R. Goveyou et al. J. Nucl. Energy, *2*, 153 (1946).
14. Е. Я. Доильницын, А. Г. Новиков. Атомная энергия, *13*, 491 (1962).
15. W. M. Lopez, I. R. Beyster. Nucl. Sci. and Eng., *12*, 190 (1962).
16. А. В. Антонов. Исследования по ядерной физике, *XIV*, 147 (1962).
17. E. Starr, I. Koppel. Brookhaven Conference on Neutron Thermalization, 1962.
18. M. Kuchle. Nucleonik, *2*, 131 (1960).
19. E. Starr and G. A. Price, Brookhaven Conference on Neutron Thermalization, 1962.
20. D. Brune, J irlow. J. Nucl. Energy, Part A, B *17*, 349 (1963).
21. Г. И. Марчук. Методы расчета ядерных реакторов. М., Атомиздат, 1961.
22. Г. И. Марчук и др., наст. издание, P/655.
23. Inelastic scattering of neutrons in solids and liquids, Vienna, 1961.

ABSTRACT—RÉSUMÉ—АННОТАЦИЯ—RESUMEN

A/360 USSR

The effect of chemical binding on neutron thermalization

by L. V. Maiorov *et al.*

The paper discusses the effect of chemical binding on the integral and differential scattering characteristics and the formation of slow neutron spectra in the most important moderators (C, H_2O, Be, ZrH, LiH).

The differential scattering cross sections which are calculated with the aid of the UPRAS code, taking account of the acoustic, optical and diffusive motions of the atoms, are used for the analysis of the neutron spectra in heterogeneous media, media with a temperature gradient, and media with a pulsed source.

A/360 URSS

Influence de la liaison chimique sur la thermalisation des neutrons

par L. V. Maiorov et *al.*

Les auteurs étudient l'influence de la liaison chimique sur les caractéristiques intégrales et différentielles de la diffusion et sur la formation des spectres de neutrons lents dans les principaux ralentisseurs (C, H_2O, Be, ZrH, LiH).

Les sections efficaces différentielles de diffusion, que l'on calcule à l'aide du programme UPRAS, compte tenu des mouvements acoustiques et optiques et des mouvements de diffusion des atomes, sont utilisées pour l'analyse des spectres de neutrons dans des milieux homogènes, des milieux à gradients de température et des milieux à source pulsée.

A/360 URSS

Influencia del enlace químico sobre la termalización de los neutrones

por L. V. Maiorov *et al.*

Se estudia la influencia del enlace químico sobre las características integrales y diferenciales de la dispersión y sobre la formación de los espectros de los neutrones lentos en los moderadores más importantes (C, H_2O, Be, ZrH, LiH).

Las secciones eficaces de dispersión diferenciales, que se calculan con el programa UPRAS, teniendo en cuenta los movimientos acústicos, ópticos y de difusión de los átomos, se utilizan para analizar los espectros neutrónicos en medios homogéneos, en medios con gradiente de temperatura y en medios con fuente pulsante.

Analysis of integral data for few-group parameter evaluation of fast reactors

By G. Cecchini, U. Farinelli, A. Gandini and M. Salvatores*

The lack of many reliable nuclear data needed to evaluate fast reactor performance, in particular ^{233}U–Th systems, and the difficulties inherent in differential measurements suggest the exploitation of integral data obtainable in critical experiments in order to arrive at a final few-group cross-section set that is applicable to a certain range of systems. In the first part of this paper the requirements for calculating reactor performance are discussed; the applicability of a single few-group cross-section set to a broad range of reactors is then analysed. In the second part, integral experiments which can yield the required information are evaluated and a method of correlation for these results is developed. Various types of critical facilities (fast, coupled fast, coupled thermal-fast reactors) are finally compared on the basis of the precision obtainable from such measurements. In particular, some experiments which might give information on transport cross sections are examined.

FAST REACTOR SYSTEMS CONSIDERED

The choice of the reference systems for this study is consistent with a proposed Italian programme in this field, that is of sodium-cooled, paste fuel type reactors using U–Th oxides [1]; other fuels are considered for comparison and generality. However, the paste fuel concept appears in these calculations mainly as a lower fuel to sodium ratio than has usually been considered hitherto; thus the results are not limited to paste type fuelled reactors, since some present proposals for low density oxide fuel rods [2] lead to average compositions close to those considered here and heterogeneity is not taken into account. The reference systems studied are illustrated in Table 1. Calculations were carried out in spherical geometry by the RE-122 multigroup diffusion code of the Argonne National Laboratory. The sixteen group cross-section library of Yiftah, Okrent, Moldauer was used [3].

The volume fractions (VF) of fuel, coolant and structural materials in the various regions are the same for all systems, i.e.:

Core	VF-Fuel (oxide)	0.180
	VF-Na	0.667
	VF-Fe	0.153
Blanket	VF-ThO_2	0.537
	VF-Na	0.4306
	VF-Fe	0.0324
Reflector	VF-C	0.6
	VF-Na	0.4

ERRORS IN CALCULATION OF CRITICAL MASS AND CONVERSION RATIO

Errors may be introduced in the calculation of critical mass and conversion ratio from:

(*a*) schematization of the geometry of the system;
(*b*) homogenization of the various regions of the reactor;
(*c*) reduction of the cross sections to few-group constants;

* Comitato Nazionale per l'Energia Nucleare, Rome.

Table 1. Fast reactors studied

System	Core volume (litres)	Fuel	Fissile Fiss. + Fert. nuclei	Critical mass (kg)
1	400	$^{239}PuO_2$–$^{238}UO_2$	0.396	263
2	1500	$^{239}PuO_2$–$^{238}UO_2$	0.233	573
3	3000	$^{239}PuO_2$–$^{238}UO_2$	0.187	914
4	400	$^{233}UO_2$–ThO_2	0.387	250
5	800	$^{233}UO_2$–ThO_2	0.282	364
6	3000	$^{233}UO_2$–ThO_2	0.172	833
7	400	$^{235}UO_2$–ThO_2	0.673	430
8	800	$^{235}UO_2$–ThO_2	0.593	628
9	3000	$^{235}UO_2$–ThO_2	0.289	1428
10	800	$^{239}PuO_2$–$^{238}UO_2$	0.296	389

(*d*) use of approximations of transport theory (in the few-group scheme);
(*e*) errors that are present in the nuclear data before reduction to a few-group library.

In most cases, especially for large systems, (*e*) is at present the main source of uncertainty; this is particularly true when interest lies less in the absolute performance of the particular reactor than in the comparison of different systems, using for instance different fuels. When only relative performances are investigated, systematic errors (as may arise from the first four sources) may cancel out. A choice between two fuel cycles, which is largely based on considerations of neutron economy, is difficult on present knowledge and improved precision of the cross-section data for these fuel cycles is certainly desirable.

The relative importance of the various cross sections for the case considered here, may be explored by perturbation analysis [4]. We may thus set reasonable requirements for each nuclide, type of reaction and range of energy to be measured (by differential or integral techniques) so that the main contributions from the various cross sections to the uncertainty in the final results are of the same order of magnitude. A general criterion for the final precision required in the calculation of critical mass and conversion ratio is difficult to establish; one should compare the economic value of the information obtained, with the cost of carrying out the experiment.

In the following calculations, we have somewhat arbitrarily set an uncertainty requirement not greater than 2% in reactivity and 4% in conversion ratio. We feel that this goal represents a substantial improvement on the present situation (especially for U-Th oxide systems) and should allow a more reliable choice of a fuel cycle for a fast power reactor; at the same time, it seems that such figures are not unrealistic considering the type of integral experiments proposed in this work.

RANGE OF VALIDITY OF A FEW-GROUP SET WITH RESPECT TO GIVEN PRECISION REQUIREMENTS

It is well known that the reduction of nuclear data, given as continuous functions of energy, to a few-group constants for use in nuclear computational codes, generally introduces uncertainties in the calculated quantities. These uncertainties are larger if the system under consideration is characterized by a neutron spectrum that is very dissimilar from that used to weight the nuclear constants themselves and, of course, if the degree of coarseness of the energy subdivision is high. As a consequence, an energy group subdivision must be chosen which on the one hand involves only a few groups, in order to allow some calculational flexibility, and on the other hand is sufficiently detailed, so that the range of systems to which it is applicable within the specified precisions is broad enough to justify the integral experiments proposed for its evaluation. The problems to be solved are then:

(*a*) to see if a cross-section set exists with a reasonably small number of energy groups which is valid in the range of systems considered (e.g. ~20);
(*b*) if (*a*) is possible, to find a standard set by means of integral experiments, starting from a similar set chosen with best-value criteria.

To answer the first question, we have started considering an energy subdivision of 16 groups similar to that used in the YOM library. Such a subdivision seemed to match adequately the above-mentioned requirements of calculational flexibility and relative independence of the neutron spectra. Then using libraries with very high number of energy groups, fundamental mode calculations have been made for systems of the same compositions as the reference systems in order to calculate the equilibrium fine structure spectrum needed for the 16-group cross-section average. For this purpose, the ELMOE code of the Argonne National Laboratory has been employed. It uses a library of about 700 energy groups to account for the elastic scattering resonances of the light materials present in the system, such as Na, O, stainless steel. In addition, calculations were made with the GAM-I code of General Atomics, which uses a 40-group library to account for the effects of dilution on the capture and fission cross sections. Firstly, a very small dependence has been noticed in the 16-group scheme chosen of these latter quantities on the dilution and also on fuel materials (fissile and fertile) present. More precisely the deviations noticed among the different 16-group absorption and fission cross-section sets evaluated with perturbation calculations showed effects not larger than $0.1\,\%\Delta k/k$. The results obtained with the ELMOE code have similarly demonstrated that the deviations among the elastic removal and transport cross-section sets for the light materials are small for those systems where the volume fractions of the light elements are kept constant. In this case the corresponding reactivity effects are about $0.1\,\%\Delta k/k$. On the other hand there is a marked indication of deviations between the elastic removal and transport cross section obtained by averaging over a spectrum with a fine structure and the same types of cross section averaged over a coarse few-group spectrum. Reactivity effects are then of the order of $1\,\%\Delta k/k$ and this is consistent with the results obtained previously by others in a similar analysis [5].

We may conclude that a standard cross-section library exists with a number of groups less than or equal to 16, valid in the range of the reference systems considered in Table 1 (and probably valid outside the range to a certain extent), where the composition of the light elements is kept almost constant and only the fissile/fertile atoms ratio is varied. The fact that systems with different fissile and fertile materials are included in this range is particularly important as this means that the proposed integral experiments to determine the standard set do not need any particular quantity of ^{233}U (or Pu) but can be fuelled with ^{235}U and that the results obtained have a rather broad application.

DETERMINATION OF THE STANDARD SET BY MEANS OF INTEGRAL EXPERIMENTS

In order to determine the standard few-group cross-section set as described above, two different and possibly complementary approaches may be taken. One is the direct measurement of differential parameters, to be averaged into few-group constants, following *a priori* criteria derived from a sensitivity analysis. The considerable difficulties that exist in differential measurements of many important parameters suggest the second approach, namely to make use of the integral data obtained in critical experiments. The integral quantities to be measured are capture and fission rates and reactivity changes due to insertion of samples into the facility either in points of high flux gradient or where it is negligible so as to emphasize (or not as the case may be) the diffusion terms. Besides, spectra with different hardness must be chosen to emphasize the importance of the parameters at different points of the energy range of interest, within the limitations already defined for the validity of the standard set. The criteria to be applied to the analysis of these integral data are not uniquely defined because of the limited number of integral experiments and the difficulty of evaluating the precision of available data from which is derived the initial "best known" cross-section library to use in the theoretical-experimental correlations. A method has been developed which should allow a broad flexibility of use and represent a reasonable compromise between the need to reduce corrections to a minimum and to take care of the assumed absolute errors.

Let us suppose that H critical experiments are set up in a facility by generally changing size, geometry, and composition. In each of these critical experiments a series of measurements can be made of capture rates T_c^{hl}, fission rates T_f^{hl} and reactivity changes k^{hl} by insertion of samples of given materials in L significant positions of the facility. If it is assumed that the real and adjoint fluxes ϕ_i, ϕ_i^* are known precisely as well as the nuclear parameters σ_i (in a few-group energy subdivision where $i=1,2\ldots, N$), the experimental values can be interpreted in the following way (assuming the σ's as the volume integrated macroscopic cross sections of the sample):

$$T_c^{hl}=\sum_{i=1}^{N}\Phi_i^{hl}\sigma_{ci} \qquad T_f^{hl}=\sum_{i=1}^{N}\Phi_i^{hl}\sigma_{fi}$$

$$k^{hl}=\frac{1}{I^h}\left[\sum_{i=1}^{N}\nu_i\,\sigma_{fi}\,\Phi_i^{hl}\Phi_f^{*hl}-\sum_{i=1}^{N}\sigma_{fi}\Phi_i^{hl}\Phi_i^{*hl}\right.$$
$$-\sum_{i=1}^{N}\sigma_{ci}\Phi_i^{hl}\Phi_i^{*hl}+\sum_{i=1}^{N}\sum_{(j-i)=1}^{S(i)}(\sigma^{in}{}_{i\to j}+\sigma_i^{el}\beta_{i\to j})\Phi_i^{hl}$$
$$(\Phi_j^{*hl}-\Phi_i^{*hl})+\sum_{i=1}^{N}(\sigma_i^{el}+\sigma_{ci}+\sigma_{fi}$$
$$\left.+\sum_{(j-i)=1}^{S(i)}\sigma^{in}{}_{i\to j})3\,(D_i^{hl})^2\nabla\Phi_i^{hl}\nabla\Phi_i^{*hl}\right]$$

$$I^h=\int_V dV\sum_{i=1}^{N}\nu_i\,\Sigma_{fi}{}^h(r)\,\Phi_i{}^h(r)\Phi_f{}^{*h}(r) \qquad (1)$$

where $\Phi_f^{*hl}=\sum_{i=1}^{N}\Phi_i^{*hl}\chi_i$ (χ_i is the fission spectrum) and where we suppose groups broad enough so that [3]:

$$\beta_{i\to j}=\beta_{i\to(i+1)}=\frac{\xi_i\,\Phi(E_{i\min.})\;E_{i\min.}}{\Phi_i}$$

We are still considering here the case where ϕ and ϕ^* are precisely known, either by experiment or by calculation. This is not true in general but it is a starting point. If we substitute in (1) the values for σ that are now considered as best known (σ'), we obtain expressions similar to (1), where $(T_c^{hl})'$, $(T_f^{hl})'$ and $(k^{hl})'$ are now calculated values. We introduce now a set of "weighted corrections" δ_i and a set of α_i coefficients, so that:

$$\frac{\sigma_i-\sigma_i'}{\alpha_i}=\delta_i$$

The α_i values have been introduced to take into account the absolute error assumed for each parameter σ, and also to permit other sets of conditions to apply to the corrections. Subtracting now from expression (1) those parts relative to the computed quantities $(T_c^{hl})'$, $(T_f^{hl})'$ we obtain a set of equations which may be represented as follows when reduced to an implicit form:

$$\left.\begin{array}{l}\psi_1(\delta_1,\delta_2,\ldots,\delta_I)=A_1\\ \quad -a_{11}\delta_1-a_{12}\delta_2-\ldots-a_{1I}\delta_I=0\\ \psi_2(\delta_1,\delta_2,\ldots,\delta_I)=A_2\\ \quad -a_{21}\delta_1-a_{22}\delta_2-\ldots-a_{2I}\delta_I=0\\ \ldots\ldots\ldots\ldots\ldots\\ \psi_M(\delta_1,\delta_2,\ldots,\delta_I)=A_M\\ \quad -a_{M1}\delta_1-a_{M2}\delta_2-\ldots-a_{MI}\delta_I=0\end{array}\right\}\begin{array}{l}M=\text{Number of measurements}\\ I=\text{Number of unknown parameters}\end{array} \qquad (2)$$

where A_k and a_{ik} are given constants. Generally the inequality $M<I$ is valid and so further conditions have to be set in order to obtain a definite solution of system (2). In order to minimize the magnitude of the weighted corrections, δ's, that solution is chosen which minimizes the function:

$$E=\sum_{i=1}^{N}\sum_{(j-i)=1}^{S(i)}[(\delta_i{}^f)^2+(\delta_i{}^c)^2+(\delta_i{}^{nf})^2+(\delta_i{}^{el})^2$$
$$+(\delta_{i\to j})^2]=\sum_{i=1}^{I}\delta_i{}^2$$

The problem can be reduced to seeking the minimum of the function (3) under conditions (2). We also assume that the Jacobian characteristic of system (2) is equal to M. This means that the M values δ_{i1}, δ_{i2}, . . ., δ_{iM} can be assumed to be, without losing generality, $\delta_1,\delta_2,\ldots,\delta_M$ for which:

$$\frac{\partial(\psi_1,\psi_2,\ldots,\psi_M)}{\partial(\delta_1,\delta_2,\ldots,\delta_M)}\neq 0$$

This condition corresponds in our case to saying that the $\delta_k(k=1,2,\ldots,M)$ are linearly independent, that is $\|a_{ik}\|\neq 0$ $(i,k=1,2,\ldots,M)$. Introducing the Lagrangian multipliers λ_k, the search for the conditioned

Table 2. Example of σ's corrected consistently with given data

Group	True	σ_f ^{233}U. Wrong	Corrected	True	$(\nu\sigma_f)$ ^{233}U. Wrong	Corrected
1	1.64	1.75 ± 0.0525	1.7536	5.105	5.285 ± 0.158	5.3016
2	1.89	1.83 ± 0.0549	1.8526	5.233	4.491 ± 0.148	5.0294
3	1.95	1.89 ± 0.0567	1.9063	5.150	4.933 ± 0.148	4.9929
4	2.13	1.94 ± 0.0582	1.9826	5.475	4.986 ± 0.150	5.1351
5	2.38	2.24 ± 0.0672	2.2875	6.018	5.667 ± 0.170	5.8211
6	3.32	3.23 ± 0.2584	3.7297	8.302	8.107 ± 0.649	9.5715

minimum leads to values of δ_i which are linear combinations of the terms a_{ki}:

$$\delta_i = \frac{1}{2} \sum_{k=1}^{M} \lambda_k a_{ik}$$

where the λ_k values are given by the matrix expression:

$$\begin{vmatrix} \lambda_1 \\ \lambda_2 \\ \cdot\cdot \\ \lambda_M \end{vmatrix} = 2 \begin{vmatrix} b_{11} & b_{12} & \cdots & b_{1M} \\ b_{21} & b_{22} & \cdots & b_{2M} \\ \cdot & \cdot & \cdots & \cdot \\ b_{M1} & b_{M2} & \cdots & b_{MM} \end{vmatrix}^{-1} \begin{vmatrix} A_1 \\ A_2 \\ \cdot\cdot \\ A_M \end{vmatrix}$$

where

$$b_{ij} = \sum_{k=1}^{I} a_{ik} a_{jk}$$

The inversion of the matrix $\|b_{ij}\|$ is always possible under the assumed conditions. In case the initial real and adjoint fluxes, which account for the a_{ik} values, are incorrect, an iterative procedure may be adopted.

A small programme for the solution of equations (2) has been written for the IBM-1620 computer. The running time is of the order of a few minutes for most cases. To test the method with a simple numerical example, the critical configuration 51/03 of Table 9 has been considered. The experimental data relative to the central reaction rate and reactivity measurements have been replaced with computed ones starting from a given "true" cross-section library and the cross-section set to be corrected has been substituted by an arbitrary "wrong" set with given errors assumed for the α_i values. The results are given in Table 2. Even with the limitation of the amount of assumed data with respect to the assumed variables ($H=1$, $L=1$, $I=12$), all the cross sections σ_f with the exception for groups 1 and 6 have been corrected in the right way and by amounts reflecting well the criteria assumed for the method.

FAST, COUPLED-FAST AND COUPLED THERMAL-FAST FACILITIES CONSIDERED

The following criteria should be adopted in choosing the critical facility where the integral experiments have to be made:

(*a*) cost of the facility;
(*b*) safety of the system;
(*c*) flexibility and reproducibility;
(*d*) precision of measurement with respect to the more important quantities;
(*e*) possibility of using a simple theoretical method to correlate the experimental results.

We have reviewed and compared several facilities with respect to the last two criteria without making any specific optimization which might hinder the comparisons themselves. Three types of systems are considered: spherical fast systems (F), those with a fast driver, generally called coupled-fast systems (F–F) and those with a thermal driver, generally called coupled thermal-fast systems (T–F). In the test region the flux spectra of interest are obtained by a suitable composition and when there is a strong spectral difference between the driver and the test region a decoupler and, if necessary, a buffer are inserted. The critical facilities considered are described in Table 3 with their main characteristics. The calculation of critical compositions and fluxes have been made by means of the RE-122 code and the Yiftah, Okrent and Moldauer 16-group cross-section set. The facilities 7 and 8 are simply fast systems equivalent to those of the same number in Table 1. In systems 27 and 29 the test region is characterized by two different dilutions of ^{233}U corresponding to fast critical systems with cores of 800 and 3000 litres (systems 5 and 6 of Table 1). System 34 is a thermal-fast facility where the test region has no buffer and is fuelled with ^{235}U in a 800 litre critical core concentration. The thermal-fast systems 38 and 40 use ^{233}U as fuel for the test region with the same compositions as for systems 27 and 29, and are surrounded by a buffer with ^{235}U as fuel in a concentration corresponding to a critical 400 litre core. In all the thermal-fast systems a decoupler of 5 cm of metallic thorium separates the thermal from the fast zone. The composition of the thermal driver has been assumed to be similar to that used in the ECEL experiment of Atomics International.

Since the thermal-fast facilities considered for the central experiments do not seem to achieve a flux gradient sufficient for transport measurements, two other thermal-fast facilities have been considered for this kind of experiment. One is system 42 of Table 3 which is characterized by a cylindrical pancake geometry; it is formed by a thermal driver, 5 cm of thorium metal as decoupler, a fast test region of appropriate composition and a reflector of 30 cm of thorium oxide. The other is system 45 of spherical geometry similar to the other thermal-fast spherical facilities previously considered but with a central region, of 15 cm radius, filled with thorium metal.

Table 3. Facilities studied

System	Type of facility	Geometry	Outer radius (cm) Test region	Buffer	Driver	Fissile (test region)	Corresp.[a] critical volume (test region) litres	Fissile mass (test region) kg	Corresp.[a] critical volume (buffer) litres	Fissile mass (buffer) kg ^{235}U	Fissile mass (driver) kg ^{235}U
7	F	Sphere	45.7	—	—	^{235}U	400	436	—	—	—
8	F	Sphere	57.6	—	—	^{235}U	800	637	—	—	—
27	F–F	Sphere	17.3	—	57.6	^{233}U	800	10	—	—	613
29	F–F	Sphere	20.5	—	57.6	^{233}U	3000	10	—	—	626
34	T–F	Sphere	30.6	—	43.8	^{235}U	800	94.5	—	—	14.3
38	T–F	Sphere	17.3	30.6	43	^{233}U	800	10	400	106	13.4
40	T–F	Sphere	20.5	30.6	43.5	^{233}U	3000	10	400	90	14
42	T–F	Cylinder	H=26 R=35	—	H=72.34 R=35	^{235}U	800	78.8	—	—	3.2
45	T–F	Sphere	15	45	57.54	—	—	—	800	290	20.3
51	F	Sphere	21.2	—	—	^{235}U	40	109	—	—	—

[a] Critical volumes of the facilities in Table 1 corresponding to the same compositions of test region.

As an attempt to compromise between high performance and economy a highly compact fast facility is envisaged and represented here by system 51. In this the weight fractions of the light and heavy materials (in the latter case only ^{235}U) correspond to the reference systems of Table 1. In order to minimize the critical mass no fertile material is introduced and only high density materials are considered. Thus UO_2 is replaced with U metal and the corresponding oxygen requirement is provided by an appropriate quantity of sodium oxide which is much denser than sodium. Canned sodium and canned sodium oxide should be used in a facility of this kind, but in principle other high density materials might be considered.

SPECTRAL BEHAVIOUR IN THE FACILITIES

In order to study neutron spectra behaviour in the facilities considered, several reaction rate ratios have been computed in the test regions. The ratios relative to the thermal-fast and fast-fast facilities compare well with those relative to the corresponding reference systems and the differences do not seem important as far as the independence of the group parameters to spectrum is concerned. The situation is not so favourable for the compact fast facility 51. Here the 16-group elastic scattering and transport cross sections of light materials, weighted in a fine structure spectrum calculated with the ELMOE code, account for estimated errors around $1\%\Delta k/k$ if applied to the reference systems of Table 1.

No difficulties of this kind have been found for the fission and capture cross sections averaged in a neutron spectrum calculated with the GAM-1 code. As a consequence, if higher precisions are required, some intermediate facility with core volume of 100–200 litres might represent the optimum for high performance and economy or some finer group subdivision should be considered.

PRECISION OF THE CENTRAL REACTION RATE MEASUREMENTS

The precision of the measurements obtainable with a given facility depends upon three main factors:

(*a*) sensitivity of the instruments which are used in the experiment, for a given time of measurement and total power of the system (in other words, the influence of statistical noise);

(*b*) noise due to sources other than statistics (temperature and pressure fluctuations, mechanical vibrations, etc.);

(*c*) magnitude of the quantity to be measured.

With respect to the first two factors, for the central reaction rate measurements there appears to be no reason to prefer one type of facility to the others. However, with regard to the third factor, in Table 4 reaction rate values are normalized to equal total power and are reported for the various facilities. The values relative to the fast and fast-fast facilities are larger by factors of 2 to 8 when compared with those relative to the thermal-fast ones. Obviously these factors increase inversely with the core volume of the fast facilities themselves.

Table 4. Central reaction rates normalized to same power (arbitrary units)

System	Type of Facility	F(^{235}U)	F(^{233}U)	F(^{239}Pu)	F(^{240}Pu)	C(Th)	F(Th)	C(^{238}U)	F(^{242}Pu)
7	F	1328	2057	1585	500	185	16.7	155	483
8	F	985	1515	1132	309	144	9.65	122	299
27	F–F	1008	1545	1145	308	148	9.55	126	298
29	F–F	970	1475	1069	250	147.5	7.35	127	244
34	T–F	487	750	582	170	69	5.4	58.5	164
38	T–F	460	712	561	166	64.7	2.25	54.7	161
40	T–F	516	790	635	158	74.3	4.72	63.6	153
51	F	4250	6600	5250	—	550	71.0	450	—

Table 5. Central reactivity worths (10^{-8} $\Delta k/k$) per gram of material

System	Type of facility	Radius of perturbed zone (cm)	Sample	Reactivity worths				
				Total	Fission	Absorpt.	Transf.	Diff.
7	F	1.83	^{233}U	496.88	924.88	−433.48	5.45	0.022
			Th	−26.49	7.61	−40.165	6.04	0.024
			Fe	4.52	—	−4.11	8.59	0.034
8	F	2.30	^{233}U	381.29	714.33	−335.89	2.84	0.014
			Th	−24.08	4.68	−31.84	3.07	0.012
			Fe	1.26	—	−3.24	4.47	0.022
27	F–F	2.32	^{233}U	383.82	725.91	−345.18	3.09	0.015
			Th	−24.80	4.56	−32.90	3.54	0.014
			Fe	1.71	—	−3.32	5.00	0.025
29	F–F	2.05	^{233}U	349.47	652.63	−304.96	1.8	0.0024
			Th	−24.21	3.31	−29.50	1.98	0.0022
			Fe	−0.225	—	−2.96	2.73	0.0031
34	T–F	2.04	^{233}U	172.24	313.99	−142.67	0.916	0.0045
			Th	−9.83	2.29	−13.15	1.02	0.005
			Fe	0.232	—	1.33	1.56	0.0075
38	T–F	1.73	^{233}U	208.41	386.38	−179.69	1.71	0.0049
			Th	−11.54	2.89	−16.47	2.03	0.0045
			Fe	1.25	—	−1.69	2.92	0.0073
40	T–F	2.05	^{233}U	172.69	318.30	−146.33	0.724	0.0145
			Th	−10.61	1.94	−13.41	0.861	0.0135
			Fe	−0.055	—	−1.39	1.33	0.017
51	F	1.40	^{233}U	1913.56	3491.04	−1607.23	29.41	0.352
			Th	−73.65	37.00	−144.25	33.27	0.337
			Fe	31.41	—	−14.70	45.54	0.968

Table 6. Estimated weight (g) and volume (cm^3) of samples relative to a precision of the central reactivity measurements of 0.1% for fissile and 1% for non-fissile materials

System	Type of facility	^{233}U		Th		Fe	
		Weight (g)	Volume (cm^3)	Weight (g)	Volume (cm^3)	Weight (g)	Volume (cm^3)
7	F	20	1.1	38	3.3	220	28
8	F	26	1.4	42	3.6	790	101
27	F–F	26	1.4	42	3.6	585	74
29	F–F	29	1.6	41	3.5	4400	560
34	T–F	6	0.32	10	0.87	430	55
38	T–F	5	0.27	8.7	0.75	80	10.2
40	T–F	6	0.32	9.4	0.81	1800	230
51	F	5	0.27	14	1.2	32	4.1

PRECISION OF THE CENTRAL REACTIVITY MEASUREMENTS

Referring to the first factor of measurement precision introduced in the previous chapter, statistical evaluations have been made of reactor noise [6] in connexion with oscillation experiments in the two types of facilities. Under the same operating conditions, the sensitivity of the instruments is higher approximately by a factor of ten in the thermal-fast compared with the fast-fast facilities. This difference is due mainly to the poor flux detector efficiency in a fast neutron spectrum but if other experimental conditions are considered, it may change. For instance, it might be more realistic to set limitations on the specific power if fuel refabrication is considered. Then, the performance of the fast-fast facilities considered is improved by about a factor of 3. This performance might also be improved by surrounding the counters with a layer of moderating material (provided this does not perturb the flux in the test region). A comparison of different facilities in relation to the source of non-statistical noise is difficult, and involves detailed design considerations. As regards the magnitude of the signal, i.e., the amount of reactivity introduced by a given sample, some values are given in Table 5. The values relative to the fast-fast facilities are larger by a factor of 2 or 3 than those in the thermal-fast case; for the fast facility 51 results are larger by a factor of 10 or more for the light elements. Let us assign now an instrument sensitivity of $10^{-8}\Delta k/k$ to the reactivity measurements in the thermal-fast case (limit achieved in the ECEL experiment of Atomics International for a two hour oscillation experiment at 200 watts) and consequently a sensitivity of about $10^{-7}\Delta k/k$ for a fast-fast facility. Under those conditions and for the sake of comparison, the weight and dimensions of the samples to be used in the experiments were calculated (see Table 6) so that the measurements on the fissile elements have a 0.1% precision and those relative to the other materials have a 1% precision. Measurements relative to oxygen can be effected by using compact oxide samples, e.g., canned sodium oxide.

Table 7. Eccentric reactivity worth (10^{-8} $\Delta k/k$) per gram of material

System	Type of facility	Sample	Inner radius of perturbed zone (cm)	Outer radius of perturbed zone (cm)	Reactivity worth				
					Total	Fission	Absorpt.	Transf.	Diff.
8	F	Th	47.22	48.37	−3.384	1.101	−8.300	0.248	3.568
		Fe	47.22	48.37	5.511	—	−0.828	0.466	5.874
		Na	47.22	48.37	17.571	—	−0.908	3.016	15.463
		Th	52.98	54.13	−1.466	0.683	−5.715	−0.0443	3.610
		Fe	52.98	54.13	5.440	—	−0.567	0.0477	5.960
		Na	52.98	54.13	15.603	—	−0.714	0.689	15.629
42[a]	T–F	Th	$H_1 = 18.2$[b]	$H_2 = 19.07$[b]	−11.969	3.545	−19.505	0.632	3.359
		Fe	$H_1 = 18.2$[b]	$H_2 = 19.07$[b]	5.191	—	−1.926	1.124	5.994
		Na	$H_1 = 18.2$[b]	$H_2 = 19.07$[b]	17.405	—	−3.052	4.361	16.094
		Th	$H_1 = 21.67$[b]	$H_2 = 22.53$[b]	−15.101	4.225	−22.549	0.833	2.39
		Fe	$H_1 = 21.67$[b]	$H_2 = 22.53$[b]	3.437	—	−2.298	1.417	4.319
		Na	$H_1 = 21.67$[b]	$H_2 = 22.53$[b]	10.709	—	−4.574	3.974	11.309
51	F	Th	16.84	17.54	2.189	11.223	−52.165	5.699	37.433
		Fe	16.84	17.54	67.346	—	−5.305	8.916	63.734
		Na	16.84	17.54	201.528	—	−3.098	38.202	166.425
		Th	14.65	20.35	12.133	6.668	−36.205	1.346	40.322
		Fe	14.65	20.35	68.312	—	−3.686	3.219	68.779
		Na	14.65	20.35	189.559	—	−2.834	14.307	178.086

[a] Values have been multiplied by $2.113 = \dfrac{\int_0^R \phi(0,x)\,dr}{\int_0^R \phi(0,x) J_0^2\left(\dfrac{2.4048\, r}{R}\right) dr}$

[b] H_1 and H_2 indicate distance from boundary with outer ThO_2 reflector.

PRECISION OF THE ECCENTRIC REACTIVITY MEASUREMENTS

Transport cross sections are very important in fast reactor calculations in general. The integral experiments needed to evaluate these parameters require a sufficiently high flux gradient at the point where the samples are to be inserted. While these conditions are generally obtainable with the fast and fast-fast systems considered, this is not so in the thermal-fast spherical case. If a thermal-fast facility has to be utilized, a special geometry assembly must be worked out in some detail. We have considered for this purpose system 42, which exhibits a pancake geometry, and the spherical system 45, with a thorium metal sphere at the centre surrounded by a buffer. These facilities are compared with the 800 litre core facility 8. The results are given in Table 7 for different sample materials inserted in two different positions in the test regions.

The 45 facility has to be ruled out because an appreciable flux gradient is not obtainable in the thorium metal sphere. The solution with facility 42 seems rather interesting if we consider the relatively small quantity of sample materials necessary in the various cases in order to obtain transport reactivity worths affected by a statistical error of 1 %, as it can be seen in Table 8. On the other hand a disadvantage of a facility of this kind is the calculational difficulties introduced in the pancake geometry. The compact fast facility 51 allows a precision in the eccentric measurements comparable with that for system 42.

CRITICAL EXPERIMENTS

To exploit a critical facility in order to obtain the maximum information on the spectral behaviour of nuclear parameters, critical assemblies should be devised which, though keeping broadly the fine structure of the neutron spectrum, have different degrees of hardness (or softness) to emphasize different energy bands. To evaluate the extent to which this is permissible, systems 7 and 51 were studied for several configurations relative to various weight ratios of light materials and ^{235}U, from a factor of 0.5 to a factor of 2 with respect to the two reference facilities. ELMOE

Table 8. Estimated weight (g) and volume (cm^3) of samples relative to an uncertainty in the diffusion worth contribution of 1% for all materials

System	Type of facility	Th		Na		Fe	
		Wt (g)	Vol. (cm^3)	Wt (g)	Vol. (cm^3)	Wt (g)	Vol. (cm^3)
8–1	F	280	24.2	65	77	170	22
8–2	F	277	24.0	64	76	168	21
42–1	T–F	30	2.6	6.2	7.4	16.7	2.1
42–2	T–F	42	3.6	8.8	10.5	23.2	3.0
51–1	F	27	2.3	6.0	7.1	15.7	2.0
51–2	F	25	2.2	5.6	6.7	14.5	1.8

Table 9. Critical configurations of facilities N.7 and N.51

Critical configuration	% Increment of light materials	Critical radius (cm)	Critical mass ^{235}U (kg)	F^{Th}/F^{25}	F^{28}/F^{25}
7/01	−50	31.3	252	0.0165	0.0795
7/02	−20	40.4	361	0.0139	0.0673
7	—	45.7	436	0.0126	0.0615
7/03	+20	50.6	496	0.0115	0.0557
7/04	+50	57.4	589	0.0101	0.0493
7/05	+100	67.6	733	0.0085	0.0413
51/01	−50	14.4	64	0.0208	0.0993
51/02	−20	18.6	91	0.0179	0.0862
51	—	21.2	109	0.0167	0.0805
51/03	+20	23.3	125	0.0152	0.0733
51/04	+50	26.5	148	0.0136	0.0658
51/05	+100	31.2	185	0.0116	0.0561

code calculations for compositions within this range have indicated that the deviation of scattering and transport cross sections of light materials due to different dilutions account for reactivity effects of $0.5\%\Delta k/k$. Some characteristics and spectral indexes of these systems are reported in Table 9.

CONCLUSIONS

The following conclusions may be drawn from the results obtained.

(*a*) There exists a standard few-group (~20) cross-section library applicable to the whole range of systems shown in Table 1 and to the test region of the facility to be used for the experiments, which is valid within the precision specifications of 2 and 4% for reactivity and conversion ratio calculations. If higher precisions are required, higher energy subdivision and/or a narrower range of reference systems must be considered. The first condition involves an even more extensive set of experiments to span in detail the energy range.

(*b*) From a given set of integral measurements and starting from a "best value" cross-section library, it is possible to determine a unique set of parameters which accounts for all the experimental results so far obtained and satisfies the condition of reducing the corrections on the original "best value" set to a minimum, with some weighting of the absolute errors assumed for each nuclear parameter.

(*c*) Among the facilities considered in Table 3, the compact fast types seem to have some advantage over the thermal-fast systems, especially if the performance is normalized to the same power. The precision of the reactivity measurements is comparable enough, if a pancake geometry thermal-fast facility is considered for the eccentric reactivity measurements, but the compact fast systems show considerable advantages for higher reaction rate measurements and for the more simple interpretation of the results related to the eccentric reactivity measurements themselves.

ACKNOWLEDGEMENT

The authors wish to thank S. G. Carpenter and M. Marseguerra for their participation in the preliminary stage of this work.

REFERENCES

1. Ferretti, B., *et al.*, *Il Program. RAPTUS*, Not. CNEN, Anno 8, No. 7 (July 1962).
2. Okrent, D., *Breeding, Safety and Fuel Cycles*, 7th Nuclear Congress, Rome (June 1963).
3. Yiftah, S., Okrent, D., and Moldauer, P., *Fast Reactor Cross Sections*, Pergamon Press (1960).
4. Gandini, A., *Study of the Sensitivity of Calculation for Fast Reactors Fuelled with ^{239}Pu-^{238}U and ^{233}U-Th to Uncertainties in Nuclear Data*, USAEC report ANL-6608 (1962).
5. Hummel, H., and Rago, A., *An Accurate Treatment of Resonance Scattering in Light Elements in Fast Reactors*, Doc. SM-18/45, Vienna Conference (1961).
6. Brownrigg, W., and Littler, D., *Pile Modulation and Statistical Fluctuation in Piles*, UKAEA report AERE N/R 476 (1950).

ABSTRACT—RÉSUMÉ—АННОТАЦИЯ—RESUMEN

A/627 Italie

Analyse de données intégrales pour l'évaluation de paramètres à petit nombre de groupes des réacteurs rapides

par G. Cecchini *et al.*

Un problème sérieux dans l'évaluation de la performance des réacteurs rapides est le peu de confiance qu'on peut accorder aux valeurs des sections efficaces dont on dispose. Il s'agit, dans la plupart des cas, de valeurs déduites en prenant la moyenne des mesures différentielles obtenues par des procédés différents, dont les résultats ne sont très souvent pas cohérents, ou calculées à partir de modèles théoriques. Cette situation est particulièrement sérieuse pour les systèmes rapides qui emploient le cycle ^{233}U–Th. La difficulté qu'on rencontre dans la mesure différentielle de ces paramètres suggère l'exploitation de données intégrales obtenues dans un ensemble critique pour aboutir à une série à petit nombre de groupes applicable à tous les systèmes d'une certaine catégorie.

Dans la première partie du mémoire on analyse la possibilité d'appliquer une seule série de sections efficaces à petit nombre de groupes à une classe assez étendue de réacteurs. Cette applicabilité dépend évidemment du nombre des groupes et, pour cette raison, on a choisi une série à seize groupes, ce qui représente un nombre suffisant pour une bonne latitude d'emploi et en même temps n'est pas trop grand pour la majorité des codes nucléaires de diffusion ou de transport, à une ou deux dimensions. On fait successivement une analyse de plusieurs types d'ensembles critiques dont on fait une comparaison en ce qui concerne la représentation du spectre neutronique du système de référence dans la région étudiée et en ce qui concerne la précision des mesures. On considère des ensembles couplés thermiques-rapides et des ensembles rapides à plusieurs régions pour des mesures dans un flux à gradient nul aussi bien que pour des mesures de sections efficaces de transport. Ces dernières ont une très grande importance dans l'évaluation des réacteurs rapides. Dans les ensembles couplés thermiques-rapides le gradient de flux nécessaire aux mesures de transport peut être réalisé en principe ou par une expérience exponentielle centrale ou par une disposition en plaque. Enfin on décrit une méthode pour la réduction des données intégrales à des paramètres à petit nombre de groupes à partir d'une série optimisée obtenue par des mesures différentielles.

A/627 Италия

Анализ интегральных данных для оценки реакторов на быстрых нейтронах по методу малогрупповых параметров

Г. Чеккини *et al.*

При оценке характеристик реакторов на быстрых нейтронах возникает крайне серьезная проблема, связанная с отсутствием надежных данных в целом ряде важных ядерных процессов. Имеющиеся данные получаются путем разрозненных дифференциальных измерений или с помощью некоторых специальных моделей атомных ядер. Обычно системы ядерно-физических констант, полученные в различных лабораториях, значительно отличаются друг от друга. Это положение является особенно серьезным в отношении быстрых систем с циклом U^{233} — Th. В связи с трудностями, свойственными дифференциальным измерениям этих параметров, предлагается использовать некоторые интегральные данные, которые можно получить на критической сборке для составления окончательной малогрупповой системы, пригодной для расчета определенного круга систем.

В первой части этой работы содержится анализ применимости одной малогрупповой системы констант для широкого круга реакторов. Эта применимость зависит, конечно, от числа групп. Поэтому была выбрана 16-групповая система, которая является довольно стандартной малогрупповой системой, обладающей максимальным числом групп, приемлемым для проведения одно- или двумерных расчетов по диффузионной или транспортной теории. Затем рассматриваются несколько критических сборок и производится сопоставление их нейтронных спектров и точности измерений. Производится сравнение экспериментальных устройств, использующих в качестве источников системы на тепловых или на быстрых нейтронах. Эти устройства сравниваются как с точки зрения измерений градиента (в сборках нулевой мощности), так и с точки зрения измерения транспортных параметров, которые, по-видимому, имеют большое значение для расчета характеристик реакторов на быстрых нейтронах. В сборках на тепловых нейтронах градиент потока может быть получен или путем внутреннего экспоненциального эксперимента, или в геометрии, обратной геометрии конечной пластины. В заключение описывается метод преобразования интегральных данных в малогруп-

повые параметры, начиная с системы констант, считающейся лучшей.

A/627 Italia

Análisis de los datos integrales para la evaluación de parámetros de reactores rápidos con pocos grupos

por G. Cecchini et al.

Un problema fundamental que existe en el cálculo de reactores rápidos es la falta de confianza que ofrecen los datos existentes sobre secciones eficaces. Estos datos se obtienen generalmente promediando valores de medidas diferenciales realizadas en condiciones distintas, y con frecuencia proporcionan resultados poco coherentes, o a partir de modelos teóricos. Generalmente, la serie de secciones eficaces obtenidas por diversos laboratorios presentan discrepancias considerables. Esta situación es muy importante cuando se estudian reactores rápidos que utilizan el ciclo ^{233}U–Th. La dificultad inherente a las medidas diferenciales de estos parámetros, sugiere la utilización de datos integrales obtenidos en sistemas críticos en una teoría de pocos grupos aplicable a un determinado conjunto de sistemas.

En la primera parte de este trabajo se analiza la posibilidad de aplicar una sola serie de secciones eficaces correspondientes a una teoría de pocos grupos, a un número bastante amplio de reactores. La aplicabilidad depende evidentemente del número de grupos empleados y por esta razón se han tomado diez y seis grupos, que representa el número máximo de grupos que se pueden utilizar en los programas de cálculo que utilizan teoría de difusión en una o dos dimensiones o teoría de transporte. Se hace un análisis de diversos sistemas críticos realizando una comparación de los espectros neutrónicos en la zona que se estudia y de la precisión de las medidas. Se consideran sistemas térmico-rápidos y rápidos con varias regiones y se realizan medidas en un flujo de gradiente nulo así como medidas de secciones eficaces de transporte que tienen importancia para la evaluación de reactores rápidos. En los sistemas térmicos rápidos, el gradiente de flujo se puede conseguir mediante una experiencia exponencial central o por una geometría de lámina. Finalmente se describe un método para la reducción de los datos integrales a la forma de parámetros de pocos grupos partiendo de una serie que se supone representa el mejor valor, obtenido de datos diferenciales.

Multi-group constants from integral data

By M. Humi, J. J. Wagschal and Y. Yeivin*

The purpose of this paper is to demonstrate that, in principle, it is possible to derive multi-group constants from integral data rather than from sets of basic microscopic cross sections.

A G-group approximation in neutron transport calculations consists of replacing the correct, energy-dependent, Boltzmann equation by a set of G coupled equations

$$\vec{\Omega}.\nabla\psi_g+\alpha_g\psi_g=\frac{1}{4\pi\gamma}\sum_{g'=1}^{G}\beta_{gg'}\Phi_{g'},\ g=1,2,\ldots,G \quad (1)$$

where ψ_g and Φ_g respectively are the group angular and scalar fluxes and γ is the eigenvalue, which is related to the criticality constant. Isotropic scattering is assumed for simplicity. These equations involve $G(G+1)$ constant coefficients, the so-called group constants, for each space region (or zone) of the system considered. The determination of these constants is a rather delicate problem, and no completely satisfactory solution has so far been proposed. When anisotropic scattering is considered, the source terms, on the right hand side of Eq. (1), are modified, and involve even more constants.

The common practice in determining group constants is to start from a set of basic cross sections, and to average these over the energy groups using a proper weight function. However, with respect to the numerous sets of basic cross sections and related data which have been published, we may cite Parker [1], who lists these compilations and comments that "For hardly any material can the data be said to be complete, up to date and in satisfactory form". Furthermore, one is not sure what a "practical" weighting function should be. The usual averaging within the energy groups is flux averaging:

$$\sigma_g=\frac{\int_{E_1}^{E_2}\sigma(E)\Phi(E)\mathrm{d}E}{\int_{E_1}^{E_2}\Phi(E)\mathrm{d}E} \quad (2)$$

Here, $\Phi(E)$ is either a spatially averaged spectrum in a system typical of the kind of reactors in which one is interested, or a "universal" flux shape of the sort used by Yiftah *et al.* [2]. In the former case, one expects to be able to calculate reasonably well the system for which the flux is assumed to be known, but one does not know how accurate the "similar" systems calculation will be. In the latter case, not even for a very special system can one estimate how good the approximation will be. Besides, this artificial flux shape certainly fails in few-group calculations.

It should also be pointed out that, as shown by Marchuk [3], in order that any multi-group approximation should yield the correct eigenvalue, γ, of Eq. (1), the group constants must satisfy a certain condition. The constants derived according to Eq. (2) do not satisfy this condition. The averaging recommended by Marchuk is

$$\sigma_g=\frac{\int_{E_1}^{E_2}\sigma(E)\Phi^*(E)\Phi(E)\mathrm{d}E}{\int_{E_1}^{E_2}\Phi^*(E)\Phi(E)\mathrm{d}E} \quad (3)$$

which further complicates the situation, since now also an adjoint flux, $\Phi^*(E)$, must be determined.

Several attempts have been made to derive sets of "universal" group constants for multi-group calculations [4]. These have not been entirely successful, or at most their application is limited. Certainly one cannot expect to derive by these "conventional" methods reasonable constants for few-group calculations, applicable to a variety of systems. We therefore propose to discuss and illustrate a different approach, that of deriving the group constants from integral data.

The first requirements are to decide the purpose of the calculation and to define the quantities to be derived. Each such quantity forms a constraint on the manifold of possible sets of constants. If, for example, one is interested only in the eigenvalue (criticality), then clearly there are still many degrees of freedom available in the choice of constants.

The sets of possible constants for a certain system form a manifold in the appropriate hyperspace. In searching for a set of constants which will correctly describe several systems, one naturally selects a set in the intersection of the relevant manifolds, if such an intersection actually exists. As more constraints, in the sense mentioned above, are imposed on the sets, the manifolds shrink, but as long as they still intersect, it is possible to find a useful set for all the systems.

As an illustration of this integral-data approach, let us consider a very simple family of systems, namely that of critical uniform spherical shells of ^{235}U, and

* The Hebrew University of Jerusalem, Israel.

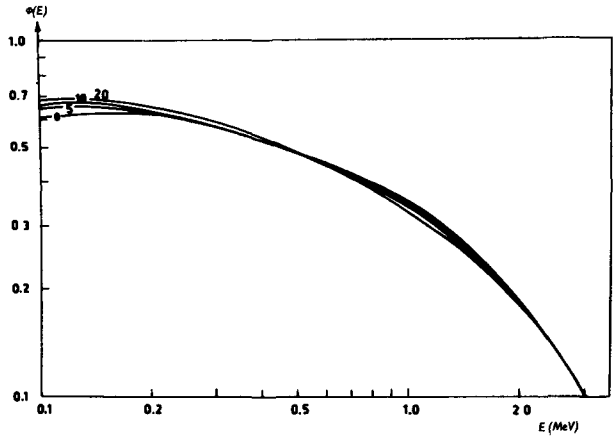

Figure 1. Intrinsic spectra of the four uniform shells of metallic ^{235}U

Numbers specifying curves are inner radii of shells (cm). The softening of the spectrum with increase in radius is clearly demonstrated. All spectra are normalized—$\int \Phi(E)dE = 1$

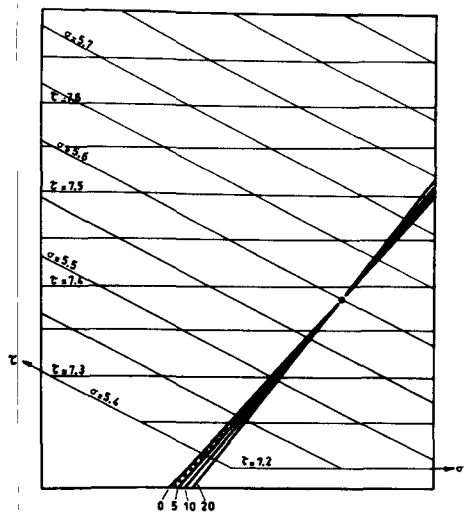

Figure 2. The curves $\tau = \tau(\sigma)$, characteristic of the four ^{235}U shells

Numbers specifying curves are inner radii of shells (cm). The dashed curve pertains to the critical sphere-and-shell, described in the text. In spite of the different geometry, resulting in a softer spectrum, this extra curve also passes through the intersection of the shell-curves

treat them in the one-group approximation. The equation describing these systems is then:

$$\vec{\Omega}.\nabla\psi + \alpha\psi = \frac{1}{4\pi\gamma}\beta\Phi \qquad (4)$$

with

$$\alpha = n\sigma,\ \beta = n\tau = n(\bar{\nu}\sigma_f + \sigma_s + \sigma_i) \qquad (5)$$

where σ, σ_f, σ_s and σ_i are the one-group total transport, fission, transport and inelastic scattering-microscopic cross sections, respectively, and n is the number-density of the medium. The constants we wish to derive are the pair σ and τ which should give the correct critical thicknesses for all shells.

Suppose now that the critical thickness of such a uniform shell is known. We can then find a curve in the plane (σ, τ), the locus of all pairs of values which, when inserted in Eq. (4) with the appropriate boundary conditions, result in a solution with $\gamma = 1$. Different values of σ correspond to different thicknesses of this shell, measured in mean-free-paths; but these will be compensated by the corresponding different values of τ, equivalent to different "infinite multiplication constants" of the medium (τ/σ is the average multiplication in a single collision).

When another system of the family, for which the critical thickness is also known, is considered, another curve $\tau = \tau(\sigma)$ can be obtained. If the two curves intersect, the co-ordinates σ_0 and τ_0 of the point of intersection give the true critical thicknesses of the two shells. On the other hand, the conventionally calculated one-group constants will differ for the two systems, since their spectra are different owing to their different geometries.

As integral data we have used the critical dimensions of a full sphere and of three shells of inner radii 5, 10, and 20 cm. These were obtained from 24-group-S_8 calculations, with group constants derived from the Aldermaston ^{235}U basic data [5], and with $n = 0.048 \times 10^{-24}$ cm, corresponding to the natural density of metallic uranium. A first set of constants was calculated using the fission spectrum as weighting function and using these constants the critical radius and the spatially averaged spectrum of the sphere were calculated. This spectrum was used to generate a new set of constants, and the procedure was repeated until convergence of spectrum and radius was established. The intrinsic spectrum of the sphere was used as the initial weighting function for the group constants for the first shell, and so on.

The critical outer radii of the four systems were calculated to within 10^{-3} cm, and are presented in Table 1. The systems' spectra shown in Fig. 1 demonstrate the softening of the spectra with increase in radius.

The curves $\tau = \tau(\sigma)$ for these systems were also calculated by an S_8 code and were found to be almost linear over a wide range of σ. In the range $5.5 \lesssim \sigma \lesssim 5.7$ the curves are almost coincidental and to an accuracy of one millibarn, they intersect at $\sigma = 5.6$ b, $\tau = 7.387$ b. The curves are presented in Fig. 2. Oblique co-ordinates were used to separate them graphically. The dashed curve corresponds to the critical system consisting of a sphere of radius 6.826 cm (which has half the mass of a full critical sphere) and a shell of inner and outer radii 11.826 and 14.986 cm. This curve also passes through the intersection point of the others, even though the spectrum of this system is much softer than the other spectra.

Table. 1 Critical radii (cm) used as integral data

Inner radius (cm)	0	5	10	20
Outer radius (cm)	8.627	10.402	14.502	23.946

Table 2. One-group constants calculated according to the conventional method

Inner radius of system (cm)	0	5	10	20
σ (barns) . . .	6.080	6.088	6.099	6.111
τ (barns) . . .	7.870	7.882	7.896	7.909

We may thus conclude that, with $\sigma = 5.6$ b and $\tau = 7.387$ b, one can correctly predict by one-group calculations critical dimensions of spherical shells, and probably of other ^{235}U systems, at any rate of systems with spherical symmetry. Since for the shells considered $\partial R/\partial\tau \approx 1.5$ cm/barn (at $\sigma \approx 5.6$ b) taking also into account the accuracy of our calculations, the expected accuracy of the predicted radii should be within $\pm 1\text{–}2 \times 10^{-3}$ cm.

We have also derived the one-group constants for each of the four systems, averaging the basic cross sections with their respective spectra. These are given in Table 2, and also shown in Fig. 3, which corresponds to Fig. 2 over a wider σ range.

In the case of the full sphere we have also derived the one-group constants according to Marchuk's method Eq. (3), obtaining $\sigma = 6.142$ and $\tau = 7.539$ b (see Fig. 3).

The results demonstrate how unreliable are the "conventional" formulae for deriving group constants for few-group calculations. Applying each of the pairs of constants in Table 2 gives quite wrong dimensions for spherical shells in general. Moreover, the correct dimensions of the systems with the intrinsic spectrum of which each pair was derived will not even be reproduced.

Having demonstrated the applicability of the integral-data approach to at any rate the very simple systems discussed above, further simple cases, such as two-zone spherical systems, and other one-zone systems of various geometries, are now being studied.

Also, following unpublished work of Friedman and Rakavy, an attempt is being made to develop a practical procedure for deriving group constants based on both basic microscopic cross-section data and integral data. An outline of this proposed procedure follows.

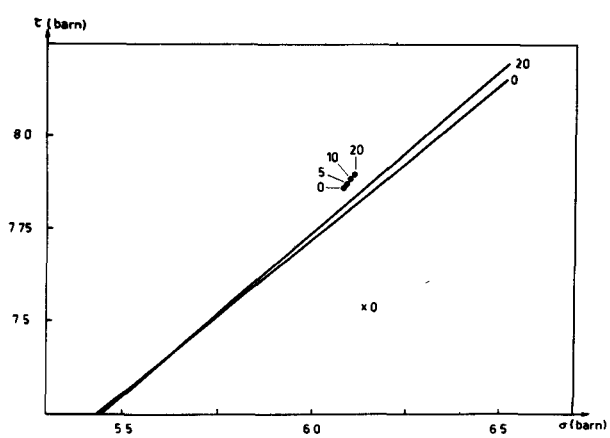

Figure 3. One-group constants derived from ^{235}U basic data of Buckingham et al.[5]

Numbers indicate the inner radii of shells (cm)
● indicates flux averaging
× indicates flux-adjoint, flux averaging

We start from a set of group constants calculated conventionally from basic cross-section data and their corresponding uncertainties (estimated from the experimental errors in cross-section measurements, etc.),

$$\alpha_n{}^{(\text{in})} \pm \delta_n \tag{6}$$

and from a set of experimental integral data, such as critical masses or dimensions, spectral indices, flux traverses, etc., pertaining to systems composed of the same materials as the systems to be considered, and the uncertainties corresponding to these quantities,

$$\gamma_i{}^{(\text{exp})} \pm \epsilon_i \tag{7}$$

The quantities we are looking for are the "true" group constants

$$\alpha_n = \alpha_n{}^{(\text{in})} + d_n \tag{8}$$

The corresponding "correct" integral quantities, calculated from these constants are,

$$\gamma_i = \gamma_i(\alpha_n) = \gamma_i{}^{(\text{exp})} + e_i \tag{9}$$

Changing variables, and denoting

$$x_n = \frac{d_n}{\delta_n},\ y_i = \frac{e_i}{\epsilon_i} \tag{10}$$

we now stipulate that the sum of squares

$$Q = \sum_n x_n{}^2 + \sum_i y_i{}^2 \tag{11}$$

is minimal for the correct d_n and e_i.

The y_i may be eliminated from Eq. (11) using

$$y_i = \frac{\gamma_i(\alpha_n) - \gamma_i{}^{(\text{exp})}}{\epsilon_i} = \frac{\gamma_i(\alpha_n{}^{(\text{in})}) - \gamma_i{}^{(\text{exp})}}{\epsilon_i} + \sum_n \frac{\delta_n}{\epsilon_i}\frac{\partial\gamma_i}{\partial\alpha_n} x_n \tag{12}$$

With Q now a function of the x_n only, the equations

$$\frac{\partial Q}{\partial x_n} = 0 \tag{13}$$

which will be of the form

$$\sum_n F_{mn} x_n = C_m, \tag{14}$$

are solved for the x_n; the desired group constants are obtained as

$$\alpha_n = \alpha_n{}^{(\text{in})} + d_n x_n \pm S_n \tag{15}$$

with

$$S_n = \sqrt{[(F^{-1})_{nn}\, Q/(\text{number of } \gamma_i)]}\,^{\frac{1}{2}} \tag{16}$$

REFERENCES

1. Parker, K., European–American Nuclear Data Commission (UK) report No. 26 "U" (1963).
2. Yiftah, S., *et al.*, *Fast reactor cross sections*, Pergamon, 103 (1960).
3. Marchuk, G. I., *Numerical methods for nuclear reactor calculations*, Consultants Bureau, 214 (1959).
4. Yiftah, S., *et al.*, *Fast reactor cross sections*, Pergamon, p. 6, for a partial list of other sets (1960).
5. Buckingham, B. R. S., *et al.*, UKAEA report AWRE 0-28/60 (1960).

ABSTRACT—RÉSUMÉ—АННОТАЦИЯ—RESUMEN

A/668 Israël

Constantes multigroupes déduites des données intégrales

par M. Humi et *al.*

L'approximation par G groupes dans les calculs du transport de neutrons consiste à remplacer l'équation de Boltzmann correcte, dépendante de l'énergie, par une série de G équations associées

$$\vec{\Omega}.\nabla\psi_g+\alpha_g\psi_g=\frac{1}{4\pi\gamma}\sum_{g'=1}^{G}\beta_{gg'}\Phi_{g'},\qquad g=1,2,\ldots G$$

où ψ_g et Φ_g sont respectivement le flux angulaire et le flux scalaire des groupes. Pour simplifier les choses, on suppose que la diffusion est isotrope. Ces équations comportent $G(G+1)$ coefficients constants, dont la détermination est en général un problème très délicat. Dans le cas d'une diffusion anisotrope, les termes de source sont modifiés et supposent un nombre plus grand de constantes.

Pour déterminer ces constantes, dites constantes de groupe, on commence d'habitude par rassembler une collection de sections efficaces fondamentales, dont on établit la moyenne pour chacun des groupes d'énergie au moyen de fonctions de pondération appropriées. Toutefois, il n'existe à ce jour aucune collection complète et satisfaisante de sections efficaces fondamentales et, par ailleurs, on n'est pas sûr de la fonction de pondération qu'il faut utiliser.

Plusieurs tentatives infructueuses ont été faites pour établir des collections de constantes de groupe « universelles » pour les calculs à un grand nombre de groupes. Evidemment, on ne peut pas espérer obtenir par ces méthodes « conventionnelles » des constantes valables pour des calculs à un nombre limité de groupes qui soient applicables à des systèmes divers.

En principe, on doit pouvoir tirer les constantes multigroupes des données intégrales plutôt que des sections efficaces fondamentales elles-mêmes. Le but du mémoire est d'illustrer et de discuter cette méthode.

Pour commencer, il faut fixer le but du calcul et bien définir les grandeurs à déterminer. Chacune de ces grandeurs impose une contrainte à l'ensemble de toutes les collections possibles de constantes. Si, par exemple, on s'intéresse seulement à la valeur propre (criticité), on a évidemment encore beaucoup de degrés de liberté dans le choix des constantes.

Les collections de constantes pour un système donné forment un ensemble dans l'hyperespace propre. Lorsqu'on cherche une collection de constantes valables pour plusieurs systèmes, il faut naturellement adopter une collection correspondant à l'intersection des ensembles pertinents, si une telle intersection existe. Au fur et à mesure que plus de contraintes, au sens indiqué ci-dessus, sont imposées aux collections de constantes, les ensembles se contractent. Tant qu'ils présentent encore une intersection, il sera possible de trouver une collection valable pour tous les systèmes.

Les auteurs ont appliqué cette méthode à plusieurs systèmes simples. Les constantes obtenues sont discutées et comparées avec les constantes correspondantes fournies par les méthodes classiques.

A/668 Израиль

Многогрупповые константы, полученные из интегральных данных

М. Хуми *et al.*

G-групповая аппроксимация в расчетах переноса нейтронов состоит в замене строгого, выражающего зависимость от энергии уравнения Больцмана рядом G-связанных уравнений:

$$\vec{\Omega}\,\triangle\,\psi_g+\alpha_g\psi_g=\frac{1}{4\pi\gamma}\sum_{g'=1}^{G}\beta_{gg'}\varphi_{g'};\ g=1,2,\ldots,G,$$

где ψ_g и φ_g — групповые угловой и скалярный потоки соответственно. Для простоты рассеяние принимается изотропным. Эти уравнения включают постоянные коэффициенты $G(G+1)$, определение которых обычно представляет собой весьма сложную проблему (если рассматривается анизотропное рассеяние, члены, определяющие источник, изменяют свой вид и включают больше постоянных).

При определении этих так называемых групповых констант обычно принято начинать с ряда основных эффективных сечений, которые затем усредняются с собственной весовой функцией по энергетическим группам. Однако до настоящего времени нет удовлетворительного полного набора основных эффективных сечений и, более того, нельзя быть уверенными в значениях весовых функций.

Было предпринято несколько безуспешных попыток определить ряд «универсальных» групповых констант для многогрупповых расчетов. Конечно, нельзя ожидать, что этими обычными методами удастся получить надежные константы для расчетов с небольшим числом групп, применимых к различным системам. В принципе можно будет определить многогрупповые константы скорее на основании интегральных данных, чем на основе действительных эффективных сечений. Задачей этого доклада являются иллюстрация и обсуждение этого подхода.

Вначале необходимо решить, какова задача расчета, и определить, какие необходимо вывести величины. Каждая такая величина представляет собой ограничение на совокупности

возможной группы констант. Если, например, интерес представляет только собственное значение (критичность), тогда имеется много степеней свободы в выборе констант.

Группа констант для определенной системы образует совокупность в собственном гиперпространстве. Подбирая группу констант, которая правильно описывала бы несколько систем, естественно необходимо сортировать ряд в пересечении соответствующих совокупностей, если такие пересечения действительно существуют. Поскольку больше ограничений в упомянутом смысле накладывается на наш ряд, совокупности будут сокращаться. А пока они пересекаются, можно найти хороший ряд для всех систем.

Этот метод применим к нескольким простым системам; полученные константы обсуждаются и сравниваются с константами, определенными обычными способами.

A/668 Israel

Constantes de multigrupos obtenidas de datos globales

por M. Humi *et al.*

La aproximación de G-grupos en los cálculos de transporte de neutrones consiste en sustituir la ecuación de Boltzmann correcta, dependiente de la energía, por una serie de G ecuaciones acopladas

$$\vec{\Omega}.\nabla\psi_g + \alpha_g\psi_g = \frac{1}{4\pi\gamma}\sum_{g'=1}^{G}\beta_{gg'}\Phi_{g'}, \qquad g = 1, 2, \ldots G$$

donde ψ_g y Φ_g son, respectivamente, los flujos angulares y escalares de los grupos. Para simplificar se supone que la dispersión es isotrópica. Estas ecuaciones llevan consigo $G(G+1)$ coeficientes constantes cuya determinación es en general un problema muy delicado. Cuando se considera dispersión anisotrópica se modifican los términos fuente y aparecen más constantes.

El procedimiento corriente para determinar estas constantes, llamadas constantes de grupo, es partir de una serie de secciones eficaces básicas de la cuales se obtiene una media ponderada, con un peso adecuado, sobre los grupos de energía. Sin embargo, no existe hasta la fecha una serie completa de secciones eficaces básicas y, además, no se está seguro de cual sea el peso adecuado.

Se hicieron varios intentos sin éxito para obtener constantes de grupo « universales » para los cálculos de multigrupos. Evidentemente, no se puede esperar obtener mediante estos métodos « convencionales » constantes aceptables para cálculos de menor número de grupos que sean aplicables a sistemas diversos. En principio sería posible obtener las constantes de multigrupo de los datos globales, más bien que de las secciones eficaces básicas reales. El fin de este trabajo es ilustrar y comentar este método.

En primer lugar debe determinarse cual es el fin del cálculo y deben definirse las magnitudes a determinar. Cada una de tales magnitudes constituye una restricción en el conjunto de las series posibles de constantes. Si, por ejemplo, sólo se tiene interés en el valor propio (criticidad), todavía se tiene, evidentemente, muchos grados de libertad en la elección de las constantes.

Las series de constantes para un sistema dado forman un conjunto en el hiperespacio adecuado. Al buscar una serie de constantes que describan correctamente varios sistemas, se escogería naturalmente una serie en la intersección de los conjuntos apropiados, si realmente existe tal intersección. Al imponer unas restricciones, en el sentido dicho anteriormente, a las series, los conjuntos se reducen y mientras continúen cortándose sería posible encontrar una serie adecuada para todos los sistemas.

Este método se aplica a varios sistemas sencillos y se comentan y comparan las constantes así obtenidas con las constantes obtenidas mediante procedimientos convencionales.

The temperature dependence of neutron inelastic scattering in heavy water

By N. Mateescu, H. Teutsch, V. Nahorniak, A. Diaconescu and P. Timis*

Slow neutron scattering experiments with liquids and solids have proved to be one of the best methods in the study of their structure and microdynamic properties, the experimental results for liquids leading toward the formulation of more and more improved theoretical models [1–3]. Besides this information, the determination of the double differential scattering cross section and the scattering laws for moderators, by this technique, is important for reactor design.

In this work, the scattering spectra of cold neutrons in heavy water in liquid and solid phases for different scattering angles have been determined. As experimental results, obtained in other laboratories on the scattering of thermal and sub-thermal neutrons by heavy water, are not conclusive and are inconsistent, the value of the diffusion coefficient was not calculated directly from experimental data but a value was taken similar to that for water. The possibility of calculating the diffusion coefficient from quasi-elastic scattering has been studied and both the scattering law and the molecular frequency distribution of the heavy water has been deduced.

EXPERIMENTAL METHOD

The filter method for the production of cold neutron beams has been used. In order to reduce the thermal and epithermal neutron background, a monocrystalline lead filter (70 mm thick) was added to the polycrystalline sintered beryllium filter (150 mm thick).

The filtered beam spectrum is shown in Fig. 1. It can be seen that the cut-off from 3.952 Å due to the (100) plane is incomplete and the intensity of the thermal neutrons is almost reduced to zero only by the cut-off of the (002) beryllium plane. The peaks which appear at longer wavelengths are due to aluminium and lead which are interposed in the beam.

The filtered beam was incident on the sample, around which an arm, provided with a neutron chopper and a battery of counters in a boron-glass shield, could turn from 0° to 90° with respect to the incident beam direction (Fig. 2).

The analysis of the scattered neutrons was achieved by the time-of-flight method. The chopper which had curved slits is described in [4]. The experiments were carried out using a 2.1 m path of flight and a rotation

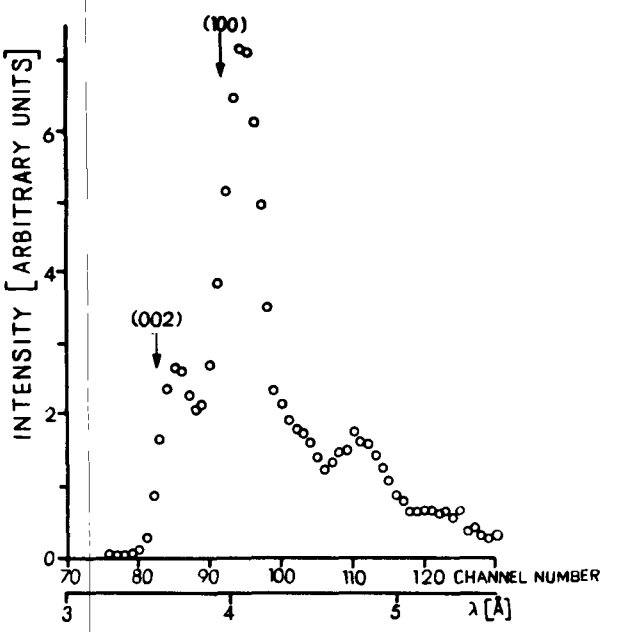

Figure 1. The spectrum of the filtered beam

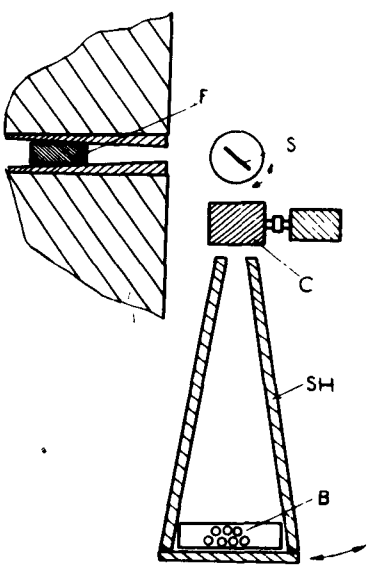

Figure 2. The time of flight spectrometer; F—filter; S—sample; C—chopper; SH—boron-glass shielding; B—detector battery

* Institute of Atomic Physics, Bucharest.

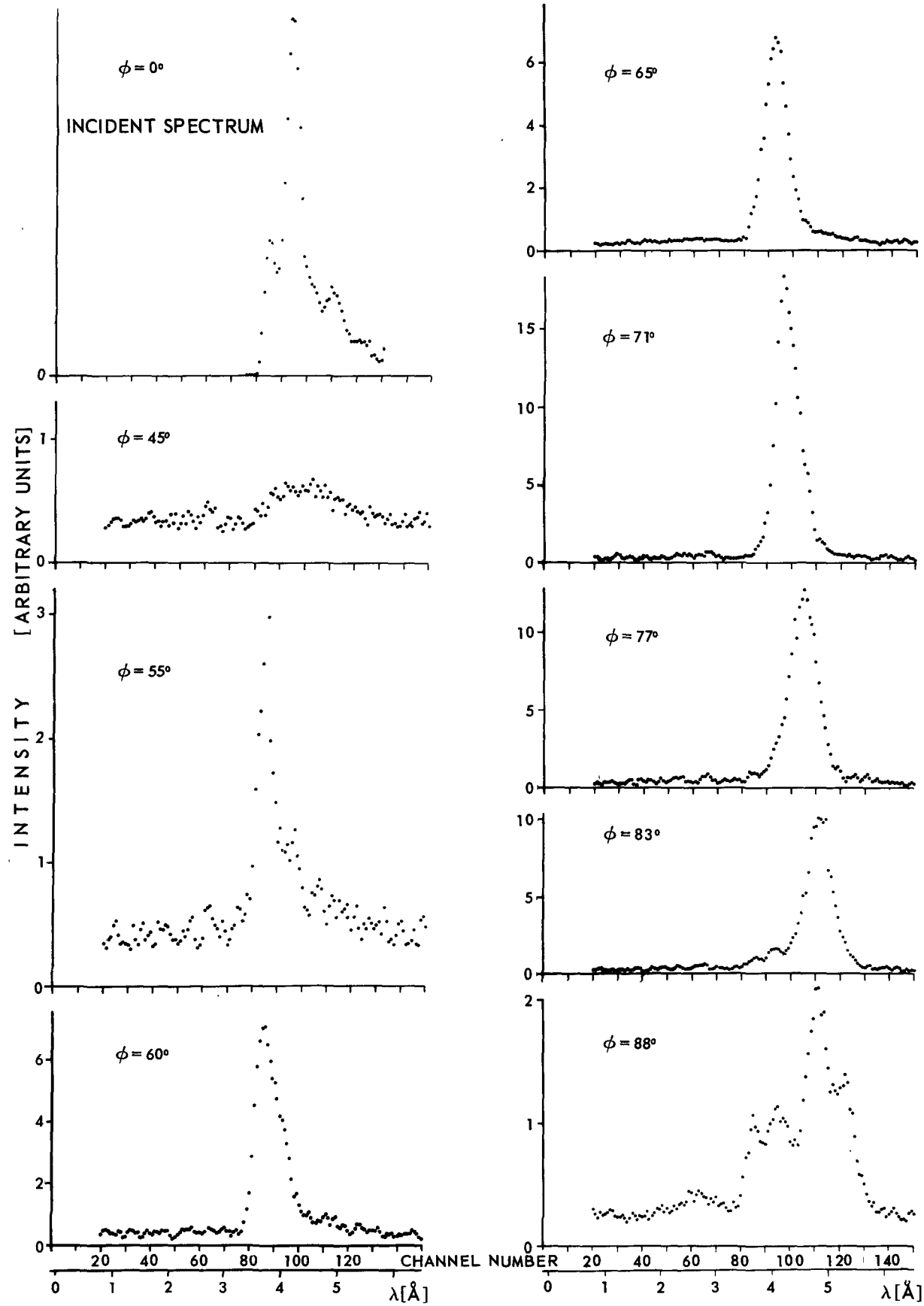

Figure 3. The spectra of neutrons scattered by heavy ice at —100°C for various scattering angles

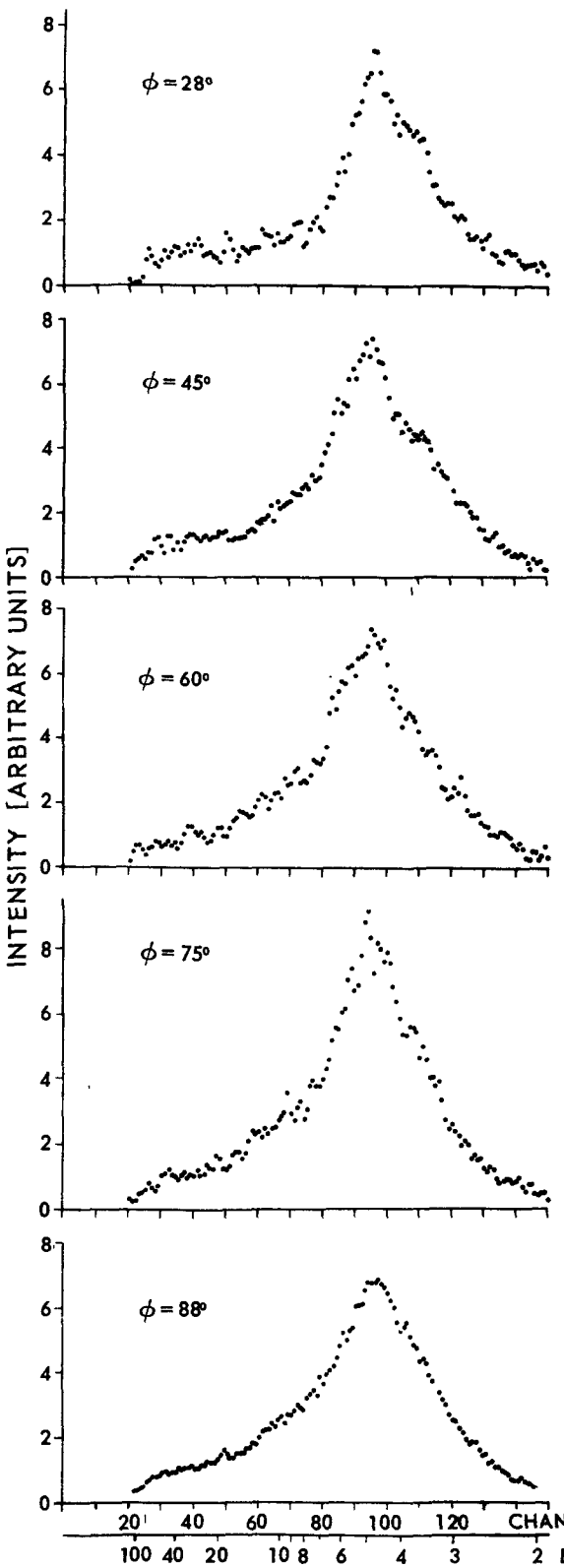

Figure 4. The spectra of neutrons scattered by heavy water at 24 °C for various scattering angles

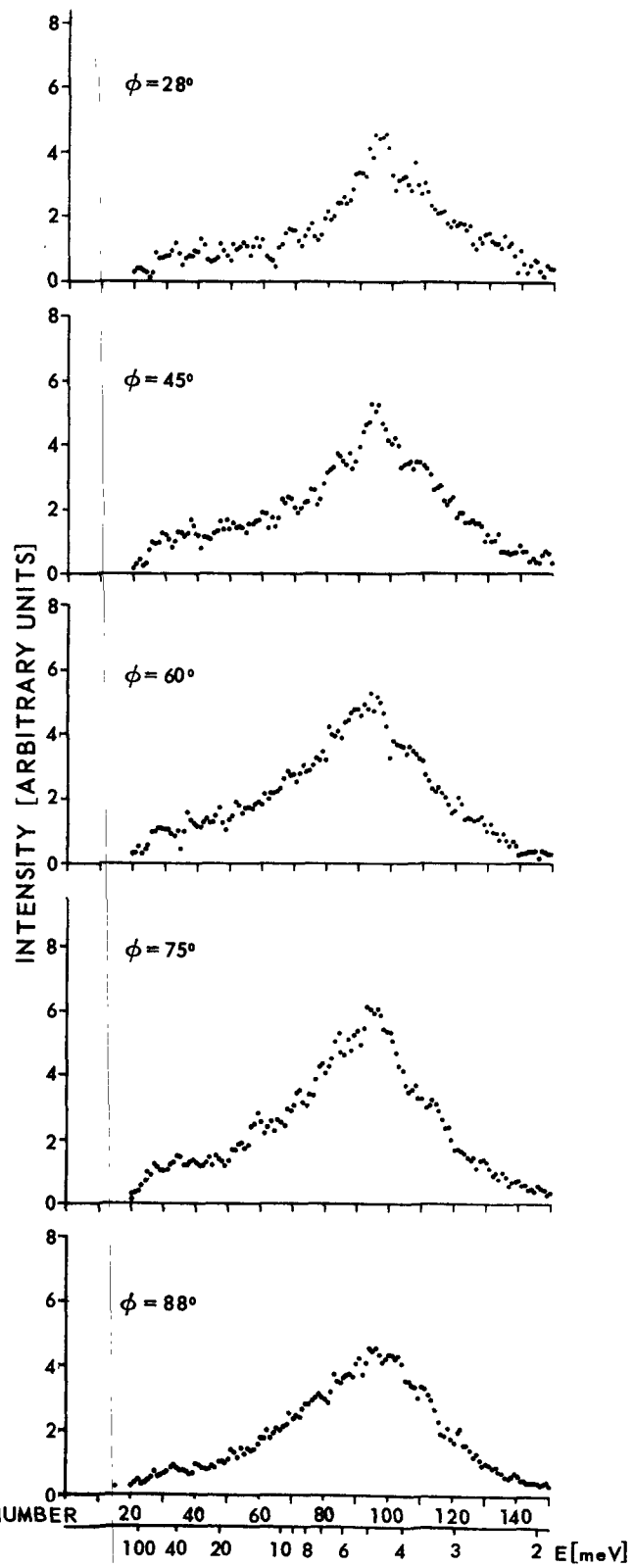

Figure 5. The spectra of neutrons scattered by heavy water at 73 °C for various scattering angles

speed of 4700 rpm maintained electronically constant with a precision of $\pm 0.5\%$ [5], which gives a maximum transmission at 4 Å [6]. The recording was done with a 400 channel analyser using a channel width of 23.4 μs. The time-of-flight resolution $\Delta t/t$ of the whole device was 3.5%.

In order to mount the solid and liquid samples in the neutron beam at the desired temperature and position, a special sample support was built through which circulated a thermostatically controlled cooling or heating agent, the temperature of the sample being measured with a thermocouple. The experiment was tested with a sample of heavy water of 2.4 mm thickness, for which the multiple scattering was negligible.

EXPERIMENTAL RESULTS

At −100°C the spectra of the scattered neutrons have been measured for 88°, 83°, 77°, 71°, 65°, 60°, 55° and 45° scattering angles (Fig. 3). For 24°C and 73°C the measurements have been carried out at the 88°, 75°, 60°, 45° and 28° scattering angles (Figs. 4 and 5). The spectra in Figs. 4 and 5 have been corrected for background and the scattering of cold neutrons by the support. They were then corrected for the following factors.

(*a*) The neutron scattering and selective absorption in air along the path from sample to counter, the cross section being taken from [7].

(*b*) The variation of the chopper transmission depending on the neutron energy, given in [8].

(*c*) The variation of counter efficiency, experimentally determined by measuring their transmission.

Figure 6 shows the spectrum for 24°C and a scattering angle of 88° corrected in this way.

Cold neutron scattering in heavy ice at −100°C

As can be seen in Fig. 3, the scattering spectrum by heavy ice at −100°C consists essentially of a prominent peak due to Bragg scattering whose position and intensity varies within the energy range of the incident spectrum, with the scattering angle. The method used to obtain such diffraction patterns using a polychromatic incident beam is described by Buras and Leciejewicz [9].

Plotting the peak position versus the scattering angle (Fig. 7) shows that the experimental points approximately lie on a straight line corresponding to a distance between the reflecting planes of $d = 3.63$ Å.

By identifying the planes able to give Bragg scattering [10] for the range of incident energies and scattering angles used in this work and by considering their integrated intensities [11] it can be seen that the scattered neutron spectrum is a result of the super position of effects of the (100), (002) and (101) planes (Fig. 7). Only in the case of the scattering spectrum at 88° can one resolve the difference between the effects of the three planes.

It can also be noticed that in the inelastic scattering region there is an increased intensity in the 10–12.5 meV range that could correspond to an energy transfer of 5.2–7.6 meV.

Quasi-elastic neutron scattering by heavy water at 24°C and 73°C

In the quasi-elastic scattering region the full-line width change due to molecular diffusion effects can be determined. According to the Vineyard theory [1], if we take into account the molecular motion in a continuous diffusion model;

$$\Delta E = 2\hbar K^2 D \tag{1}$$

where

D is the self-diffusion constant and

$K = \vec{k}_0 - \vec{k}$ is the wave-vector transfer.

Considering the "jump-diffusion" model suggested by Singwi and Sjölander [2], according to which a molecule performs an oscillatory motion for a certain mean time τ_0, then diffuses by continuous motion for a mean time τ_1, then repeats the process, for the case $\tau_0 \gg \tau_1$;

$$\Delta E = \frac{2\hbar}{\tau_0}\left(1 - \frac{e^{-2W}}{1 + \tau_0 K^2 D}\right) \tag{2}$$

where e^{-2W} is the Debye-Waller factor.

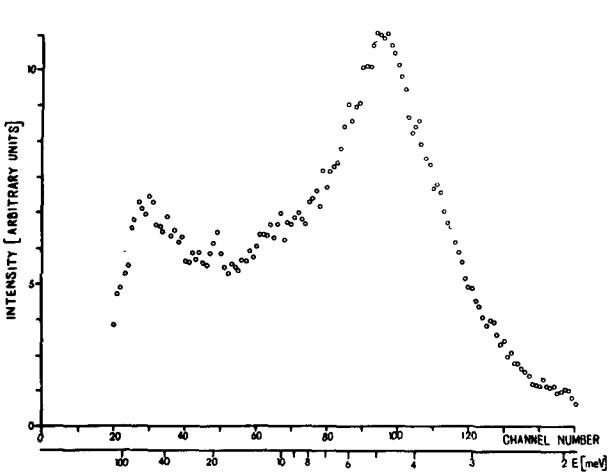

Figure 6. The spectrum of neutrons scattered at an angle of 88° at 24°C, after application of corrections

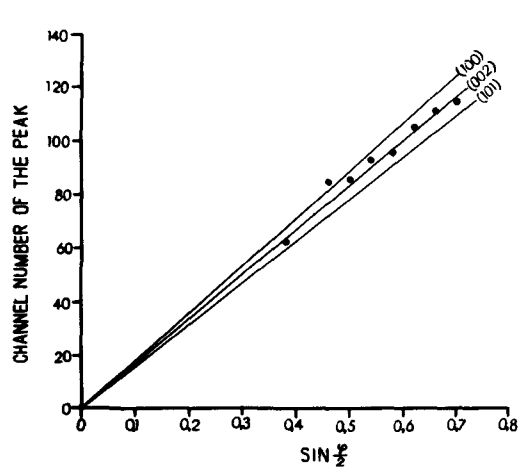

Figure 7. Peak position as a function of the scattering angle for scattering by heavy ice at —100°C

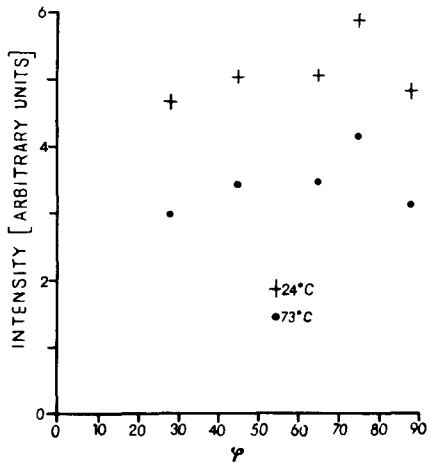

Figure 8. Variation of the peak height for quasi-elastic scattering (averaged on channels 91–100)

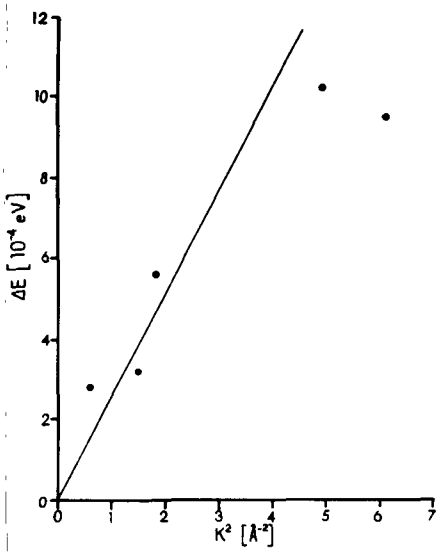

Figure 9. Variation of ΔE with K^2 for heavy water at 24 °C

The way of interpreting the quasi-elastic scattering requires clarification:

(*a*) The contribution of inelastic scattering must be subtracted from the corrected spectra. For this purpose the method indicated by Larsson *et al.* [12] was used.

(*b*) A discontinuity in the incident spectrum of a crystalline plane can be assimilated as a spectral line and its width Δt can be determined from the tangent projection on the abscissa axis at the point of inflexion of the cut-off [13, 14]. In the present incident spectrum there are two cut-offs, that are partially superposed on the scattered spectra. This implies separate treatment of the two cut-offs, i.e., after normalization of the curves with respect to the incident spectrum, the spectral line widths were deduced from the slope change of the two cut-offs and the change ΔE of these line widths due to diffusion relative to that of the incident beam was calculated.

(*c*) The quasi-elastic scattering range for different angles is influenced by the angular variation of neutron coherent scattering in heavy water. From the spectra shown in Fig. 4 and 5 it can be seen that this effect occurs in two ways:

(i) Evidently from the change of quasi-elastic peak intensity shown in Fig. 8 it can be deduced firstly that the angular change of coherent scattering is less pronounced than the change reported by Larsson (Ref. [12]; Fig. 11), and secondly that the influence of coherency is highest for a scattering angle of about 75°.

(ii) One can also see a variation of the ranges of the peaks of coherent scattering against the background of the quasi-elastic scattering spectrum.

For these reasons it was considered that an evaluation of the quasi-elastic peak slope couid be made only for scattering angles of 88°, 45° and 28° at 24 °C where better statistics (about 2000 counts per channel) were obtained.

In Fig. 9 ΔE is plotted against K^2 for heavy water at 24 °C. By calculating the value of D according to the Vineyard theory, from the points corresponding to small K^2 values;

$$D = (2.0 \pm 0.4) \times 10^{-5} \text{ cm}^2/\text{s}$$

As can be seen from Fig. 9, fitting all the experimental points to a linear law was not possible. Considering on the other hand the Singwi-Sjölander model, taking $D = 2 \times 10^{-5}$ cm²/s and $2W = 0.141$ K^2 [12], one obtains from the points corresponding to large K^2 values;

$$\tau_0 \approx 1.05 \times 10^{-12} \text{ s},$$

(if $\tau_1 = 0$)

From all the curves of Figs. 4 and 5 it can be seen that the broadening of the quasi-elastic peak with temperature increase is smaller than that predicted by theory. A decrease in the magnitude of quasi-elastic peak with temperature increase is also observed, but this is not as noticeable as that reported by Larsson (Ref. [14], Fig. 12).

Inelastic scattering of cold neutrons by heavy water at 24 °C and 73 °C

In order to obtain the frequency distribution from the experimental data, Van Hove's [15] and Egelstaff's [16] method was used according to which the scattering cross section of isotropic materials can be written as follows:

$$\frac{\mathrm{d}^2\sigma(E_1 \to E_2, \psi)}{\mathrm{d}\Omega \mathrm{d}E} = \frac{\sigma_b}{4\pi kT}\left(\frac{E_2}{E_1}\right)^{\frac{1}{2}} \mathrm{e}^{-\beta/2}\, S(\alpha, \beta) \qquad (3)$$

where

$$\alpha = \frac{m}{MkT}\left[E_1 + E_2 - 2\,(E_1 E_2)^{\frac{1}{2}} \cos\psi\right]$$

$$\beta = \frac{E_2 - E_1}{kT}$$

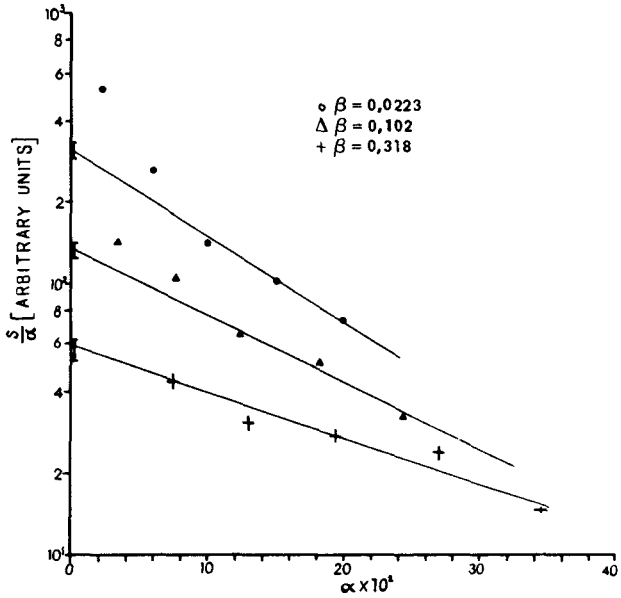

Figure 10. Variation of log (S/α) with respect to α for various values of β at a sample temperature of 24 °C

E_1 is the initial neutron energy (in our case we considered an energy $E_1 = 4.87$ meV),
E_2 is the final scattered neutron energy,
ψ is the scattering angle,
k is the Boltzmann's constant,
m is the mass of a neutron,
M is the mass of the principal scattering atom,
T is the absolute temperature of the sample,
σ_b is the bound cross section of the principal scattering atom.

The scattering law $S(\alpha,\beta)$ depends on the motion and distribution of the atoms in the scattering material and can be divided into two components corresponding to coherent and incoherent scattering;

$$S(\alpha,\beta) = S_s(\alpha,\beta) + \langle a \rangle^2 S_d(\alpha,\beta) \qquad (4)$$

where a is the scattering length of the bound atom $(4\pi\langle |a|^2\rangle = \sigma_b)$.

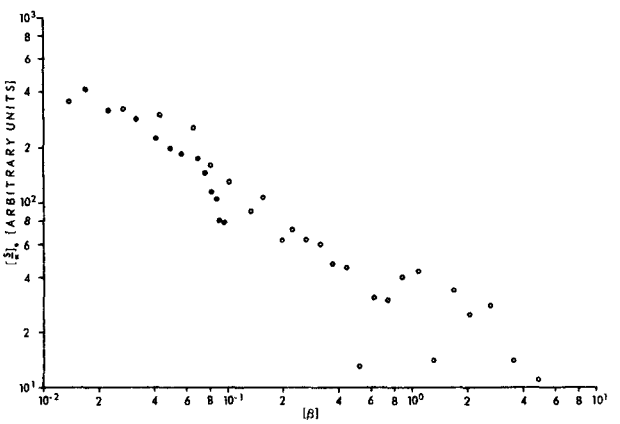

Figure 11. Function $(S/\alpha)_{\alpha\to 0}$ for heavy water at 24 °C. Full circles correspond to negative values of β

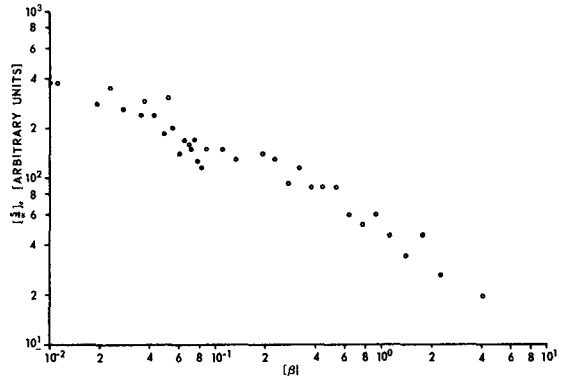

Figure 12. Function $(S/\alpha)_{\alpha\to 0}$ for heavy water at 73 °C. Full circles correspond to negative values of β

Information about the motions of the atoms in the scattering sample is contained in the generalized frequency spectrum function $p(\beta)$, introduced by Egelstaff [16–17];

$$p(\beta) = \beta^2 \lim \left(\frac{S_s(\alpha,\beta)}{\alpha}\right)_{\alpha\to 0} \qquad (5)$$

In the case of liquids $p(\beta)$ describes the spectrum of frequencies associated with translation, rotation and vibration motions. Egelstaff [16, 18, 19] has also shown that the separation of the interference component $S_d(\alpha,\beta)$ can be made as S_d is negligible for large values of α. Linear extrapolation of log S/α values in the range of large values of α to the region $\alpha\to 0$, therefore eliminates the interference effect.

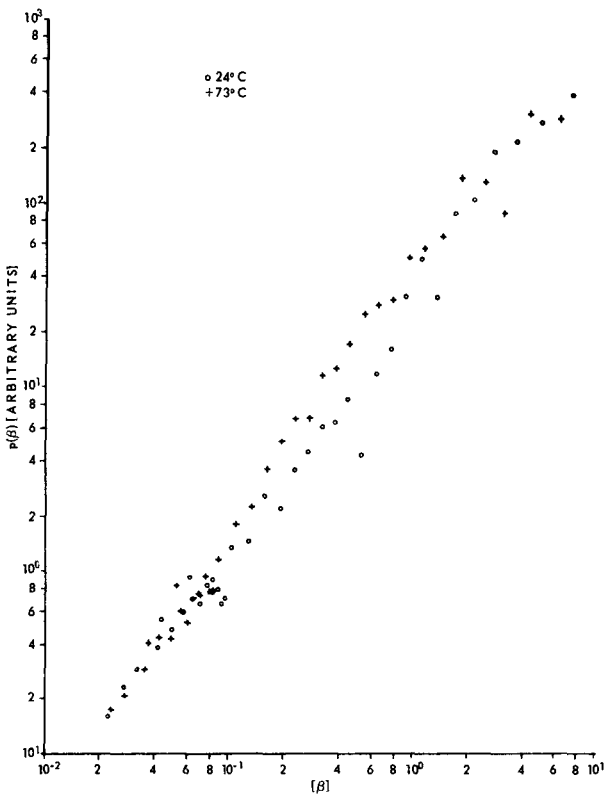

Figure 13. Function $p(\beta)$ for heavy water at 24 °C and 73 °C. Full circles correspond to negative values of β

In Fig. 10 some graphs of $\log(S/\alpha)$ *vs.* α for different values of β are shown, from which $(S/\alpha)_{\alpha\to 0}$ values have been deduced; the errors arising from extrapolation are also given. The β-values also are affected by errors arising from the method of choosing the incident neutron energy value; these are discussed by Larsson and Dahlborg [14]. In Fig. 11 and 12 $\log(S/\alpha)_{\alpha\to 0}$ is plotted against β. The slight displacement between negative β-values (full circles) and the positive β-values is also probably due to the choice of the incident energy value. The $(S/\alpha)_{\alpha\to 0}$ *vs.* β curves and the scattering curves (Figs. 4 and 5) provide evidence for the following levels:

(*a*) The peak for $\beta = 1.9$, corresponding to an energy transition of 48 meV, can be ascribed to the hindered rotation of a single molecule and was noticed at both temperatures. As expected, this energy level is lower than the corresponding one for water [20] by a factor $\cong\sqrt{2}$.

(*b*) The 25 meV transition corresponds to the 35 meV level for light water reported by us in a previous paper [21]. We found an energy level of 15 meV, which shifts slightly to higher energies at 73 °C, corresponding to the energy level for water at about 20 meV which was found by Hughes *et al.* [22], Larsson *et al.* [14] and by us [21] and ascribed to a hindered translation of the water molecule. We also noticed levels of 4.8 meV, 2.5 meV and $\cong 0.6$ meV that can be ascribed to a fine structure for heavy water. The values of these energy levels can be influenced by the value chosen for incident neutron energy.

In Fig. 13 the function $p(\beta)$ is represented for the two sample temperatures. Although the measurement was extended to very low values of β, one cannot observe any increase of $p(\beta)$ due to diffusion at either temperature for the points continue monotonically towards zero.

ACKNOWLEDGEMENTS

We take this opportunity to thank Dr. D. Bally for very interesting and fruitful discussions, Miss D. Pasculescu and Mr. Z. Gheorghiu for their kindness in calculating the contribution of different crystalline planes to neutron scattering by heavy ice and D. Hacman, A. Paulescu and D. Pasat for their assistance in operating the spectrometer.

REFERENCES

1. Vineyard, G. H., Phys. Rev., *110*, 999 (1958).
2. Singwi, K. S., and Sjölander, A., Phys. Rev., *119*, 863 (1960).
3. Egelstaff, P. A., Advances in Physics, *11*, 43, 203 (1962).
4. Teutsch, H., Mateescu, N., Pirlogea, P., Radulescu, C., Timis, P., and Vasiliu, V., Rev. Physique R.P. Roumaine, *6* (3), 411 (1961).
5. Timis, P., Studii si Cercetări de Fizică, *13* (1), 131 (1962).
6. Teutsch, H., Nuclear Instr. and Methods, *15*, 203 (1962).
7. Hughes, D. J., and Schwartz, R. B., U.S. Atomic Energy Comm. report BNL-325 (1958).
8. Teutsch, H., Nukleonik, *3* (1), 15 (1961).
9. Buras, B., and Leciejewicz, J., Nukleonik, *8* (1), 75 (1963).
10. Wyckoff, R. W. G., *The Structure of Crystals*, New York (1931).
11. Wollan, E. O., Davidson, V. L., and Shull, C. G., Phys. Rev., *75*, 1348 (1949).
12. Larsson, K. E., Holmryd, S., and Otnes, K., *Inelastic Scattering of Neutrons in Solids and Liquids*, Vol. 1, p. 329, IAEA, Vienna (1961).
13. Larsson, K. E., and Otnes, K., Arkiv Fys., *15*, 49 (1959).
14. Larsson, K. E., and Dahlborg, U., Ref. [12], p. 317.
15. Van Hove, L., Phys. Rev., *95*, 294 (1954).
16. Egelstaff, P. A., Ref. [12], p. 25.
17. Egelstaff, P. A., Nuclear Sci. Eng., *12*, 250 (1962).
18. Egelstaff, P. A., Ref. [12], p. 65.
19. Egelstaff, P. A., Nuclear Sci. Eng., *12*, 260 (1962).
20. Egelstaff, P. A., Haywood, B. C., and Thorson, I. M., Ref. [12], p. 343.
21. Teutsch, H., Mateescu, N., Nahorniak, V., Diaconescu, A., and Timis, P., Rev. Roumaine de Phys., *6–7* (1964).
22. Hughes, D. J., Palewski, H., Kley, V., and Tunkelo, E.. Phys. Rev., *119*, 872 (1960).

ABSTRACT—RÉSUMÉ—АННОТАЦИЯ—RESUMEN

A/673 Roumanie

Rôle de la température dans la diffusion inélastique des neutrons dans l'eau lourde

par N. Mateescu *et al.*

Les auteurs ont étudié la diffusion de neutrons lents dans l'eau lourde en utilisant la méthode de filtrage pour produire le faisceau de neutrons lents et la méthode du temps de vol pour analyser les spectres des neutrons diffusés.

En vue d'obtenir un rapport optimal entre neutrons lents et neutrons thermiques et épithermiques, les auteurs ont adopté un dispositif de filtrage constitué par un filtre polycristal au béryllium et par un monocristal au plomb.

On est parvenu à un pouvoir de résolution global de 3,5% pour le temps de vol en utilisant un sélecteur mécanique à fente courbe en régime de transmission optimal pour les neutrons de 4 Å.

Les mesures ont porté sur un angle de diffusion allant de 30 à 90°C, la température de l'échantillon variant entre −100°C et +80°C.

Les courbes obtenues ont été corrigées pour tenir compte du bruit de fond, de la transmission du sélecteur, de la diffusion et de l'absorption dans l'air ainsi que de l'efficacité du compteur.

On a déterminé les propriétés de diffusion de l'eau lourde en fonction de la température par l'analyse détaillée des maximums de diffusion quasi élastique.

Les résultats ont été comparés à des modèles théoriques — modèle de Vineyard (diffusion continue) et modèle de Singwi-Sjölander (diffusion discontinue) respectivement — ainsi qu'aux résultats expérimentaux obtenus dans d'autres laboratoires.

On a également détecté un niveau quantique qui se superpose aux maximums de dispersion quasi élastique; il est probablement dû à une structure fine du même ordre de grandeur que celle obtenue par Hughes *et al.* dans le cas de l'eau légère.

On a observé dans la région de diffusion inélastique une suite de maximums, qui ont été attribués aux niveaux de vibration dus à la rotation des molécules d'eau lourde.

Quand la température de la cible descend à −100°C, il se produit une modification importante des spectres de diffusion inélastique.

A/673 Румыния

Температурная зависимость неупругого рассеяния нейтронов в тяжелой воде

Н. Матееску *et al.*

Рассеяние холодных нейтронов в тяжелой воде исследовалось с помощью метода фильтра для получения пучка холодных нейтронов и метода времени пролета для анализа спектра рассеянных нейтронов.

Для достижения оптимального соотношения между интенсивностью холодных нейтронов и интенсивностью тепловых и надплетовых нейтронов было выбрано сочетание поликристаллического бериллиевого фильтра с монокристаллом свинца.

Использование прерывателя с кривыми щелями в режиме оптимального пропускания нейтронов с длиной волны 4 А обеспечило разрешение по времени пролета для нейтронов всех энергий, равное 3,5%.

Измерения охватывали интервал углов рассеяния от 30 до 90°, причем температура пробы менялась от −100° до +80° С.

В полученные результаты вводились поправки на фон, на пропускание прерывателя, на рассеяние и поглощение в воздухе и на эффективность счетчиков.

Из детального анализа максимумов квазиупругого рассеяния были получены рассеивающие свойства тяжелой воды в зависимости от температуры. Результаты сравниваются как с теоретическими моделями Вайнярда (непрерывная диффузия) и Сингви — Шеландера (скачкообразная диффузия), так и с экспериментальными результатами, полученными в других лабораториях.

Обнаружен также квантовый уровень, наложенный на квазиупругий пик и обусловленный, по-видимому, тонкой структурой, имеющей тот же порядок величины, что и замеченная для обычной воды Юзом и др.

В области неупругого рассеяния наблюдался ряд пиков, которые приписывались вращательным и колебательным уровням молекул тяжелой воды. При уменьшении температуры мишени до −100° С имеет место заметное изменение спектра неупругого рассеяния.

A/673 Rumania

Efecto de la temperatura sobre la dispersión inelástica de neutrones en agua pesada

por N. Mateescu *et al.*

Los autores estudiaron la dispersión de neutrones muy lentos, o fríos, en agua pesada aplicando la técnica de filtrado para producir el haz de neutrones y el método del tiempo de vuelo para el análisis del espectro de los neutrones dispersados.

A fin de obtener un valor óptimo de la relación entre neutrones fríos y neutrones térmicos y epitérmicos, se escogió un dispositivo filtrante constituido por un filtro policristalino de berilio y un monocristal de plomo.

El poder de resolución global del dispositivo de tiempo de vuelo, que alcanza a 3,5 por ciento, se logró recurriendo a un selector de rendija curva cuyo régimen de transmisión óptimo corresponde a neutrones de 4 Å.

Se efectuaron las mediciones dentro de un intervalo angular de 30° a 90°C y se varió la temperatura de la muestra desde -100 °C hasta $+80$ °C.

En las curvas obtenidas se introdujeron las correcciones correspondientes a fondo, transmisión del selector, dispersión y absorción en aire y rendimiento del cóntador.

Las propiedades de difusión del agua pesada en función de la temperatura se dedujeron del análisis detallado de los máximos de dispersión cuasielástica.

Se compararon los resultados obtenidos con los modelos teóricos, por ejemplo con el de Vineyard (difusión continua) y con el de Singwi-Sjölander (difusión intermitente), y también con los resultados experimentales comunicados por otros laboratorios.

Se descubrió también un nivel cuántico superpuesto al máximo cuasielástico que probablemente se debe a una estructurá fina del mismo orden de magnitud que la obtenida por Hughes *et al.* en el caso del agua ligera.

En la región de dispersión inelástica se observó una serie de máximos cuya presencia se atribuyó a los niveles vibratorios de rotación de las moléculas de agua pesada.

Al descender la temperatura de la muestra hasta -100 °C los espectros de dispersión inelástica se modifican apreciablemente.

Survey of nuclear data for reactor calculations

By C. H. Westcott,* K. Ekberg,* G. C. Hanna,** N. J. Pattenden*** and S. Sanatani*

The field of "Nuclear Data", comprising neutron cross sections and related quantities of importance in reactor design, which at the 1955 Geneva Conference was discussed openly for the first time, has made considerable progress since the last Geneva Conference in 1958. At both the earlier conferences many papers in this field were contributed, but on this occasion a single review paper has been requested for this area of activity. The increasingly specialized interests of those who measure such data, and the increasingly sophisticated techniques now used, can therefore be described only in barest outline, and this review will therefore be addressed more to the users of nuclear data than to those whose activities are the source of most of the data.

Nevertheless, something must be said of the scientific effort involved in these measurements and the development of techniques. This effort is very large and if the various requests for better nuclear data are to be met, it will have to continue for quite some time. In measurements at low neutron energies (e.g., thermal) increasing care is being taken, but our standards of what is acceptable have risen, and significant discrepancies in the data persist. In the resonance region of neutron energies, the very high intensity short pulses of neutrons obtainable from electron linear accelerators have had a very considerable effect on techniques, although the older techniques of choppers and crystal spectrometers continue to be useful, and pulsed cyclotrons remain a very competitive contributor. The subcritical uranium-235 booster at Harwell (fed by an electron linac) [1] is an interesting installation, while the Dubna pulsed reactor [2] provides a very interesting alternative system, although its rather long pulse-length is a disadvantage for this work, requiring correspondingly large flight-paths if a reasonable resolution is to be obtained.

At higher neutron energies Van de Graaff and other accelerators also contribute a steady succession of measurements, and for pulsed machines the "bunching magnet" and high-resolution time-of-flight techniques have developed so that the former gap between the low- and high-energy regions, where resolution was inadequate or measurements were lacking, is now rapidly disappearing. However, although attainable resolution has been greatly improved, much remains to be measured in the rather difficult region of energy around, say, 5 keV. For all energy ranges, detectors and electronic techniques have developed also in a parallel fashion. The newer solid-state detectors represent an interesting advance, but otherwise it is mainly in increased speed, and in reduced cost for the more complex systems; that advances have been made, 4096-channel analysers are now almost commonplace and the on-line use of small computers is increasing.

While some of the measurements serve mainly to provide data, some also serve to improve the fundamental understanding of nuclear physics. Thus as resonance data accumulate more is learned about nuclear behaviour, and measurements of inelastic scattering are now also detailed enough to contribute in the same way, as discussed in the next section. Many measurements whose authors are motivated primarily by the desire to discover more about the fundamental physics of nuclei also contribute to our pool of useful nuclear data.

The change since 1958 in the degree of detail available is most marked for total cross sections. For examples we chose ^{232}Th and ^{235}U. In 1958 the curve for ^{232}Th was quite featureless above 600 eV, and was evidently only approximate above 200 eV. Figure 1 (a, b) illustrates the results of some recent measurements [4] [5] near 250 eV and 2.3 keV respectively (in Fig. 1a the old curve [3] is shown dotted, in Fig. 1b it would have been simply a horizontal straight line). An interesting feature of the French measurements [4] of Fig. 1b is the use of a sample cooled to liquid-nitrogen temperature to reduce the Doppler-broadening effect. In Fig. 2 are shown similar curves [5] for ^{235}U. These examples are given simply to illustrate the effects of the techniques now available. The considerable effort involved in this research has certainly been influenced by the needs of reactor designers, but before a next generation of bigger and better devices is put into use the question must arise whether reactor physicists really need data as sophisticated as those now becoming available.

THE NEEDS OF REACTOR DESIGN

It appears worth while to consider in some detail what are the needs for nuclear data arising from

* International Atomic Energy Agency, Vienna, Austria.
** Atomic Energy of Canada Limited, Chalk River, Ontario, Canada.
*** Atomic Energy Research Establishment, Harwell, England.

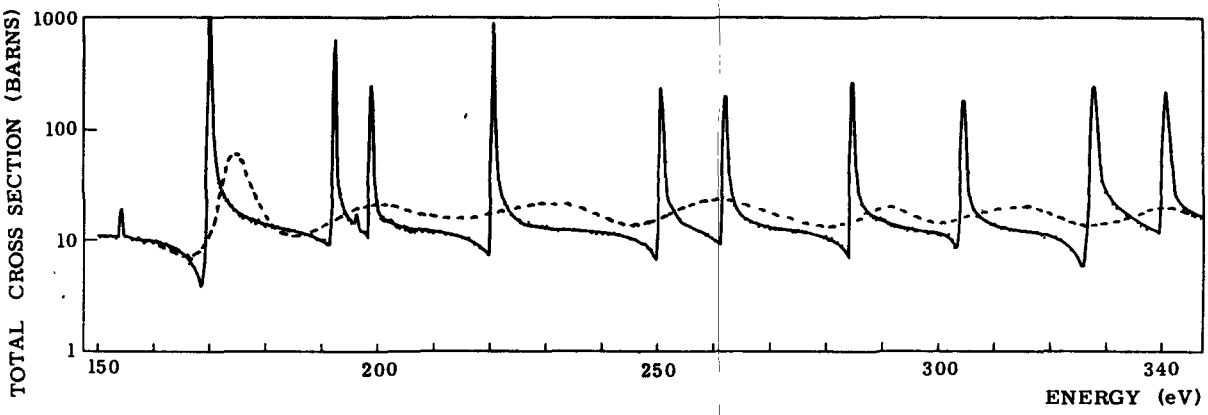

Figure 1a. The total neutron cross section of thorium-232
The dotted line is extracted from BNL-325

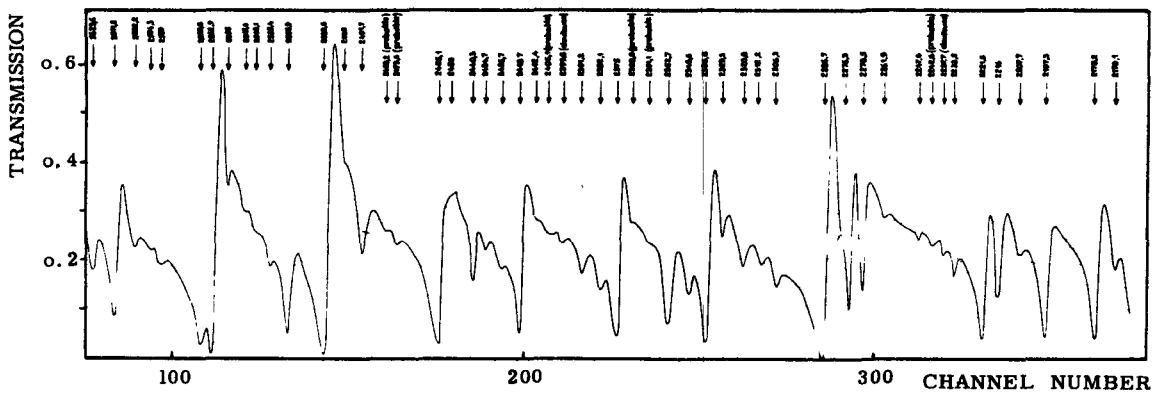

Figure 1b. Neutron transmission of thorium-232
The numbers at the arrows indicate the resonance energy in eV

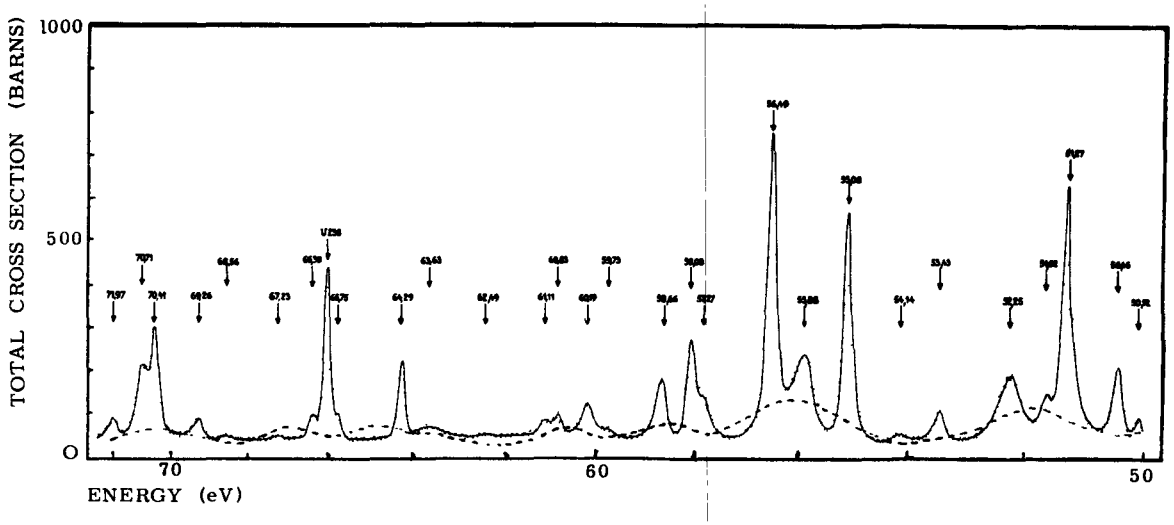

Figure 2. The total neutron cross section of ^{235}U
The dotted line is extracted from BNL-325

reactor design. In an ideal world the available data and calculational methods would enable a reactor (e.g., for a large power station) to be built without previously constructing a zero-power model or undertaking experimental subcritical lattice studies. At present this is far from being possible, except where the new plans closely resemble reactors already built; even for reactors now being completed predictions of the temperature coefficient or the reactivity life-time of the fuel may be quite appreciably in error. This situation is at least as much due to approximations and imperfections contained in the computing methods as in the nuclear data fed in. The scientific effort devoted to obtaining and understanding nuclear data is, as already stated, by no means small, even though that devoted to reactor codes and design is still considerably larger. Nevertheless, at present, the uncertainties associated with the approximations of calculational methods for reactor design are often the larger source of error.

However, the physicist who measures nuclear data is still rather frequently asked why near-perfect data cannot be made available, cross sections to, say, 0.25% accuracy, and the neutron yield per fission (ν) or the neutron yield per absorption (η) to 0.1%, perhaps. If this were easily achieved it would certainly be desirable, but the scientific resources to make this feasible within a few years in any but a few special cases just do not exist. In some studies of this point performed a few years ago for the European American Nuclear Data Committee, it was seen that requests for 0.5% or 0.25% accuracy for the more important constants were very difficult to meet, even for the simpler data, e.g., thermal cross sections (cf. the section below); in the resonance region even a 10% accuracy for $\sigma_T(E)$ on the steep side of a resonance would be a quite impossible request; resonance parameters to perhaps $\pm 5\%$ is at present the more realistic aim, while a determination of the average σ over a fairly wide energy range, or of a resonance integral, to 2 or 3% remains quite difficult.

Therefore, although period-reactivity and/or pile oscillator measurements near the critical condition may serve to determine the neutron reproduction constant, k, to 1 part in 10^4 or 10^5, calculations based on fundamental nuclear data may not be accurate even to 1 part in 10^3. Zero power experiments and similar studies are therefore normally needed when the critical configuration must be known accurately in advance.

If this were all, it might perhaps be concluded that efforts should now be concentrated on lattice studies and nuclear data work stopped, but in fact good basic data are also necessary for the better understanding of lattice experiments, as well as for studying temperature coefficients, fuel burn-up effects, etc. It is perhaps in the latter types of work that new data may be most useful. It is, for example, now much easier to improve the ^{241}Pu low-energy data than those for ^{235}U or ^{238}U, and this will of course improve burn-up predictions for natural uranium fuel. For temperature coefficient predictions, the resonance-region data needed are also not yet exhaustively studied and, with the higher experimental resolution now available, further improvements in data may still not be too difficult to achieve. However, in the resonance region other limitations arise; for the closely-spaced levels of the odd-mass-number isotopes of uranium and plutonium, Doppler broadening, added to only quite modest instrumental broadening, causes the levels to overlap at relatively low neutron energies, thus preventing further progress in data measurement. But already, in one case at least [6], reactor computations have been made in which parameters of imaginary levels are postulated on a random basis from the average level densities and strength functions measured in the resolved region, as a method of calculating the behaviour of reactor fuel isotopes in the overlap regions where the data cannot be measured.

At higher neutron energies, and primarily for fast reactors, there are other problems. The techniques for measuring neutron inelastic scattering or the spectrum of γ-rays resulting from this process (or from neutron capture) have now been developed in a number of laboratories, but the amount of detail which could be measured is large and quite a number of years will be needed before all the data desired will be available. In some cases, too, increased accuracy is desirable, and at least the more important data may need to be remeasured to achieve this.

Recent design studies of large fast power reactor systems have shown that the neutron energy spectrum is so degraded that a significant fraction of the number of fissions occurs at neutron energies as low as 100 eV. Therefore it is important to calculate the Doppler temperature coefficient of reactivity [7]. The nuclear data requirements for such calculations include the resonance parameters and their distributions to an accuracy of about 10% in the range 0.1 to 10 keV for the fissile and fertile materials. These requirements are almost impossible to meet completely, but some can be satisfied by techniques which are now starting to be used. In the case of ^{239}Pu, for example, measurements of individual parameters of about 200 resonances should give their statistical distributions to the required accuracy, and average measurements in the poor resolution region can provide independent data on s- and p-wave strength functions.

In some cases the complexity of the data can be reduced to more manageable proportions on the basis of a theoretical understanding of the processes occurring. Figure 4 of the paper (P/167) by Rae *et al.* for this conference [8] shows an interesting example of this, in which the inelastic scattering of neutrons by ^{238}U is interpreted in terms of a level scheme. A somewhat different use of theory in the case of the moderator scattering law work (fourth section of the same paper) is the reduction of the number of independent variables from three to two represented by the $S(\alpha,\beta)$ function of Egelstaff. In both cases the result is to reduce the extent of the numerical information to be presented, much as the use of resonance parameters does for data in the resonance region. There is also the role of theory, using as a basis the optical model of the

nucleus and other fundamental ideas, in filling the gaps of measured data in a more general way.

In summary, then, it can be said that the needs of reactor designers for nuclear data and the possibility of their being satisfied require a detailed study for particular cases and types of measurement, such as has been made by the European American Nuclear Data Committee. It is also true that as more sophisticated data become available (as for the moderator scattering law, for example), reactor computation methods may be revised and developed accordingly, so that the interaction is mutual. However, it would appear at the present time that elastic and inelastic scattering and neutron capture data for fast neutrons are important general fields where more measurements are desirable, as are detailed data for the resonance region. Structural and shielding materials, burnable poisons and fission products are among the nuclear species for which the data are important in addition, of course, to the fuel isotopes.

A PARTICULAR PROBLEM

Since limitations of space preclude more detailed studies of most types of nuclear data, this section of this paper is devoted to considering a few important values, where the quantity of data available is more manageable. The data thus selected for detailed study are the 2200 m/s neutron constants for the important fissile nuclides ^{233}U, ^{235}U, ^{239}Pu and ^{241}Pu, viz. σ_a, σ_f, ν, and related quantities like $\eta(=\nu\sigma_f/\sigma_a)$, $\sigma_\gamma(=\sigma_a - \sigma_f)$ and $\alpha(=\sigma_\gamma/\sigma_f)$. These quantities are frequently used for normalizing other results, as well as being of major importance in thermal reactors. They have been reviewed by several authors [9] in the last few years, some of whom obtained recommended values by a least-squares fitting process.

Since several more recent measurements now exist, and since some of the earlier fits contained unsatisfactory features, the Nuclear Data unit of the IAEA has undertaken a new critical review of these values, of which a fuller account will be published elsewhere.* A least-squares fit for three independent variables for each of the first three nuclides listed above has been performed, with the input data described below; for ^{241}Pu a subsequent fit using the output from the simultaneous fit for the other nuclides has been performed. The input data for this last nuclide are so meagre that they do not react significantly on the values for the other three nuclides.

The measurements considered in the present assessment are those yielding values of the quantities mentioned above, or combinations thereof (such as $(\eta - 1)\sigma_a$) for any of the four nuclides or the ratios between their values for two different nuclides from the four which we consider. The criterion for the acceptance of any value is that the measurement be adequately documented with, for example, statements of precautions or procedures about problems such as the assay or uniformity of the sample used. Similarly, for measurements using a Maxwellian or reactor neutron spectrum, an adequate characterization of the spectrum is expected. Generally publication in a journal is required, except for recent measurements where time would not have allowed this. Results contained only in laboratory reports are often given a lower weight, since it is felt that, by now, most worth-while experiments, except the most recent, should have been written up in detail adequate for publication. When this has not been done it may indicate that the authors lacked complete confidence in their work. The early work, performed before the general removal of secrecy classification (about 1955), suffers from the disadvantage that at that time, the work may not have been known to other workers so that possible criticisms could not be brought to the authors' notice; regrettably we must report that 80 per cent of the measurements made before 1955 have had to be totally rejected, for lack of information if for no other reason. Naturally, also, techniques have advanced greatly since this time, so the loss involved may not be serious.

In the least-squares fitting procedure, every measured value is taken as an input datum, with a stated error, which becomes the basis of the weighting of that value in all subsequent analysis. The statements of error therefore are fundamental, and the errors of all measurements must be properly assessed on a consistent basis; if a direct measurement of any quantity is more difficult than a determination based on separate measurements of other quantities, the errors assigned should bear out this fact. The bases on which authors have claimed their accuracy have therefore been restudied; in cases of incomplete documentation, the stated (or reassessed) errors have been increased (i.e., the values down-weighted) by a factor estimated to allow for the deficiency. A full discussion of the weights given and the references to the work considered will appear in the detailed report now in preparation. The weighted mean value for each quantity, with the error of the mean, is given in Table 1 (in brackets after each error is stated the number of measurements used). In some cases relative values for different isotopes are more accurately known than the absolute values; in such cases the ratios have been used as input as well as the absolute values, but care has been taken to choose weights accordingly, so as not to use any value twice in the least-squares work. Similarly, correlated errors which affect the values from several similar measurements have been allowed for in computing the error of the mean value of the quantity concerned, and therefore also in the weight used in the least-squares procedure. Care was also taken, for example, in converting σ_T values to σ_a, to allow for coherent scattering effects; rolled metal foils of different origin were treated as only partly correlated in that their atomic structure may have been similar but not identical.

* This will be published in 1965 in the *Atomic Energy Review*. It is now clear that the results will be slightly changed and the results in the *Atomic Energy Review* paper are to be considered as superseding the present results.

Table 1a. Input data for ^{233}U, ^{235}U and ^{239}Pu

Quantity	^{233}U Value	Error	N	^{235}U Value	Error	N	^{239}Pu Value	Error	N
σ_a	575.1	2.8	(8)	680.4	2.6	(8)	1006.8	6.1	(5)
σ_f	517.0	3.8	(4)	583.6	1.1	(6)	719.9	16.6	(2)
σ_γ	52.7	3.0	(1)	No value			271.0	7.9	(2)
α	0.0936	30	(4)	0.1733	20	(6)	0.3590	68	(2)
ν	2.4950	210	(2)	2.4320	143	(5)	2.8979	276	(2)
η	2.2935	85	(2)	2.0761	84	(2)	2.1400	150	(1)

Quantity	$^{233}U/^{235}U$ Ratio	Error	N	$^{239}Pu/^{235}U$ Ratio	Error	N	$^{239}Pu/^{233}U$ Ratio	Error	N
σ_f	0.9110	25	(1)	1.3073	70	(1)	1.4540	300	(1)
ν	1.0191	51	(4)	1.1817	77	(3)	1.1602	215	(2)
η	1.1069	58	(3)	1.0320	120	(1)	No value		
$\eta\sigma_a$	0.9434	172	(1)	1.4857	270	(1)	1.5714	286	(1)
$(\eta-1)\sigma_a$	1.0127	179	(4)	1.4948	323	(4)	1.4737	391	(2)

Table 1b. Input data for ^{241}Pu

Quantity	σ_f Value	Error	N	σ_γ Value	Error	N	α and η Value	Error	N
Absolute value	1377.2	25.7	(3)	350	90	(1)	No values		

Quantity	σ_f			ν			$\eta\sigma_a$		
Ratio to ^{235}U	1.6180	870	(1)	1.2120	109	(2)	No value		
Ratio to ^{239}Pu	1.3604	80	(3)	1.0519	113	(2)	1.3810	320	(1)
Mean of absolute values obtained from these ratios[a]	1014.1	7.0	(4)	2.9826	214	(4)	2963.8	70.8	(1)

Note: In all tables, values and errors for cross sections are in barns while all ratios are dimensionless and their errors are in units of 10^{-4}. N = number of measurements used to obtain the mean.

[a] To obtain these input values for ^{241}Pu the output of the fit for the other isotopes with g-factor-errors excluded was used; this avoids the double inclusion of the errors of the g-factors for σ_f and $\eta\sigma_a$ for the comparison nuclides.

One important problem in this work is the relative weight to be assigned to 2 200 m/s measurements using monokinetic neutrons to those made with Maxwellian neutron spectra. For a number of quantities (α for three of the isotopes, or the ratio of σ_f for ^{233}U to that for ^{235}U, for example), the most accurate values are those made with thermal or reactor neutron spectra. And although the aim of the present work is to obtain the values of the constants for 2 200 m/s neutrons, it is to be remembered that the most important uses of these numbers are for thermal reactor design, where the values in a Maxwellian spectrum are what is in fact needed. Even so-called "monokinetic" measurements in fact often involve averaging over a number of points on a curve to obtain an accurate spot-value, so that averaging over a Maxwellian spectrum may well be acceptable where the spectrum itself is really well known.

The effects of uncertainties in the spectrum are (or have been) included in the experimental errors, but earlier measurements of this type, especially in reactor spectra including a slowing-down flux, often have to be rejected because the knowledge of the spectrum used is inadequate. In the present work, the only down-weighting of Maxwellian spectrum values as against 2 200 m/s measurements was that corresponding to the error attributable to the g-factor [10] used in converting to 2 200 m/s values. The errors of g-factors were chosen by examining the spread of the values in a number of recent compilations, and for fission were taken to be as follows: for ^{233}U $\pm 0.2\%$, for ^{235}U or ^{239}Pu $\pm 0.12\%$, and for ^{241}Pu $\pm 0.3\%$. For σ_a, in view of the higher accuracy of the $\sigma(E)$ data, we assume the error of the g-factors for ^{233}U, ^{235}U and ^{239}Pu to be smaller by a factor 0.7 than for σ_f, while for $1+\alpha$ the two g-errors are added in quadrature, although we admit that some correlation of σ_a and σ_f values may exist.

Since the "best values" of thermal neutron nuclear data which we have obtained will often be needed to calculate values for Maxwellian spectra, we felt it worth while to carry out a least-squares fit without including the errors in the g-factors for the values measured with thermal spectra; we should perhaps for this purpose have also down-weighted values measured with monokinetic neutrons, but this was not in fact done. The results presented in Table 2 are from the fit with g-factor errors included; when these errors were

Table 2. Output of least-squares fit of 2200 m/s parameters for the four fissile nuclides

Quantity	^{233}U Value	Error	^{235}U Value	Error	^{239}Pu Value	Error	^{241}Pu Value	Error
σ_a . . .	574.8	1.8	678.4	1.9	1010.6	4.3	1376.1	24.7
σ_f . . .	525.5	1.6	577.5	1.6	745.9	3.3	1012.7	6.7
σ_γ . . .	49.3	1.2	100.9	1.0	264.7	3.2	363.5	25.4
α . . .	0.0938	23	0.1748	18	0.3548	47	0.3589	252
ν . . .	2.5073	76	2.4424	66	2.8759	120	2.9779	205
η . . .	2.2923	63	2.0790	55	2.1227	89	2.1913	439

Note: In all tables, values and errors for cross sections are in barns while all ratios are dimensionless and their errors are in units of 10^{-4}.

excluded and the weighting of the input data was thus changed, no significant change of the output values occurred. This shows that no serious systematic errors are likely to have been introduced by including Maxwellian spectra values as well as monokinetic ones in deducing a fit for 2200 m/s neutrons.

One point of interest is that our ground rules, when applied to pile-oscillator measurements of reactivity [giving the $(\eta - 1)\sigma_a$ ratios of Table 1], tended to lead to the rejection of most of these measurements for reasons of non-publication, insufficient documentation or of uncertainty of the reactor neutron spectrum used. However, recognizing that one of the main uses of the basic nuclear data is to predict criticality conditions and reactivity changes, some minor relaxations were made in applying the rules to this class of measurements. Examination of the result of the least-squares fit shows however that the $(\eta - 1)\sigma_a$ input in fact carried only a rather small weight in determining the output.

The results of the present work, presented in Table 2, do not differ greatly from those of the previous surveys, but one or two of the changes are probably significant, such as the increase of η for ^{239}Pu and the decrease of α and σ_a for the same nuclide. A slight downward trend for σ_a and σ_f for ^{235}U may also be noted, while the value of ν for this isotope shows a small but perhaps not significant increase.

OTHER RECENT ADVANCES

Space limitations do not permit a detailed survey of more than a few examples of recent advances of technique or knowledge. A great deal of work has been done on neutron scattering, both elastic and inelastic for fast neutrons as well as in thermal-inelastic scattering, but the brief mention already made must suffice to cover these subjects, important though they are for reactor technology. However, one area of interest is the development in the physics of fission since 1958 and the relation between this and such nuclear data as the variation of ν for ^{235}U with neutron energy, which is of course also quite important to the designer of fast reactors. Some years ago the measurements were not very exact and it merely seemed that ν increased roughly by 0.14 per MeV increase in neutron energy. Figure 3 shows the present situation [11], in which either a pair of straight lines, with a change of slope at 2 or 3 MeV, or a quadratic expression have been advanced as representing the phenomena. For ^{233}U or ^{239}Pu similar relationships have been proposed, one suggestion being that one relationship applies to all three nuclei with a simple displacement of the energy scale.

Studies of fission yields, and in particular the greater probability of symmetrical fission when the incident neutrons are fast rather than slow have now been supplemented by much more detailed information about the variation of ν or of the fragment kinetic energies with fission mode. The well-known work of Milton and Fraser [12], and other workers [13], mainly in the US, is complemented by detailed information from teams in the USSR, including recent work by Apalin *et al.* [14]; the tendency of ν to be anticorrelated with the fragment kinetic energy, observed in Apalin's earlier work [15], is complicated by channel effects [16]. Although it cannot be said that the physics of the process is yet fully understood, it is likely that the form of the variation of ν with neutron energy (Fig. 3) is correlated with such detailed effects and their further study should contribute both to an understanding of fundamental physics and a more complete source of nuclear data.

COMPILATION OF NUCLEAR DATA FOR REACTOR PURPOSES

We now turn to the compilation of nuclear data, mainly from the point of view of uses for reactor calculation. There are many types of compilations, ranging from the US Nuclear Data Sheets produced by Dr. Way's group to handbooks like ANL-5800 [17] or the Russian handbook [18], both of which are addressed specifically to reactor designers and both recently appeared in second editions. In between these extremes lies the well-known BNL-325 neutron cross-section compilation, and BNL-400, the angular distribution compilation. These contain a collection of numerical information, mostly deriving from published papers, relating to cross-section measurements of various kinds.

There are several difficulties which may not be generally realized in connexion with compilations like BNL-325. Firstly, the mass of data now available and its degree of detail make it increasingly difficult to put it all in a compilation; the use of the log-log scales which sufficed five years ago may now obscure the details of the measurements. In future, one may well have to file the original results, perhaps on magnetic

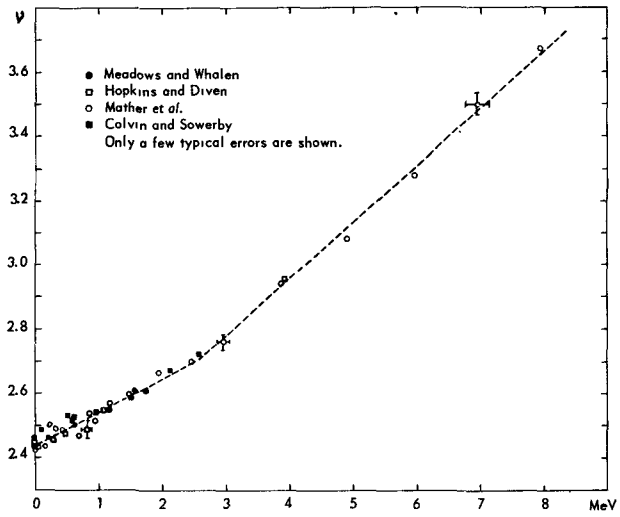

Figure 3. Neutron yield per fission of ^{235}U

The broken line is illustrative and is only fitted to the points by eye

tapes suitable for a digital computer, and only publish specimens of the data, perhaps as an index or catalogue of what is held in store. Other difficulties are connected with the need for critical judgement in choosing "best values" (as in our 2200 m/s case discussed above) or "best curves" (the latter are important for fissile and some other nuclei as leading to *g*-factors). The treatment of the original data may involve renormalization and other more complicated reinterpretation in some cases. At the higher energies (but still below a few keV for all but the lightest nuclides) Doppler and instrumental broadening are the cause of further complications so that plotting the original experimental results may be a quite inadequate presentation of our knowledge.

A rather different type of compilation exists, in which the experimental points are less in evidence, but which aims at producing more complete sets of data, evaluated for use in reactor calculations. This type includes many productions [19]. In such cases the evaluation leads to the choice of a unique "best" value of the quantity concerned for every neutron energy; where there are gaps in the measurements, values are deduced from theoretical considerations, or, if necessary, from informed guesses. Some files of this type are already in existence stored on computer magnetic tape, and an international exchange of such data is already in a rudimentary stage of operation. A more detailed discussion of this aspect of the work is contained in the paper by Story *et al.* for this conference [20].

Such data files are of general applicability, in that the σ (or η or other quantity) is given explicitly as a function of neutron energy. As such they can be internationally exchanged or compared. For most reactor calculations, however, a further preparation stage is needed, e.g., to produce a 16-group or a 26-group set of constants such as those of Yiftah, Okrent and Moldauer [21] or of Abagyan *et al.* [22]. Such sets are usually best produced locally to suit the requirements of a particular reactor calculation, or to the national standards of the country concerned; regrettably, there is as yet no internationally accepted set (or even a few acceptable alternatives) of multi-group specifications for this purpose. Equally, an evaluated set of data, if it could be internationally accepted, would be a good basis for producing compilations like ANL-5800, which includes quantities such as the effective resonance integral of fuel isotopes in various geometrical configurations (including self-shielding effects); if compilations of this type could be based on an agreed basic data file this would certainly be advantageous. This does not, of course, remove the requirement that results of experimental measurements should agree with the results so calculated, but this requirement is basic and represents no new factor.

There is therefore room for international collaboration in at least two aspects of this problem, viz., the selection of a uniform format (on cards or computer magnetic tape) for complete files of nuclear data, and the specification, if possible, of one or a few multi-group systems for use in reactor calculations. The latter is probably the more difficult to attain, but the activities of the ENEA compilation group at Saclay and the IAEA Nuclear Data Unit in Vienna may be able to help in such matters.

There are other possibilities for international collaboration at an earlier stage of the compiling process — for example where experimental results are analysed for the production of resonance parameters. Computer programmes for this type of work have been developed in several laboratories, but the problem of making a detailed interpretation of the results remote from the measuring location has not so far been seriously studied. Other such possibilities may also exist in other specialist fields, and with the increasing mechanization of data handling, these may become important. However, in all such operations, and in the choice of best values and evaluations generally, there is in the last resort no substitute for the critical judgement of the physicist working in the field.

To close this section, an example illustrating some of the problems which can arise in interpreting measurements seems worth discussion. The example we select concerns the fission cross section of ^{235}U in the 5–100 eV region, chosen not because it involves any particularly bad measurements, but because of the importance of ^{235}U and in order to illustrate what pitfalls can exist.

It is common practice for some types of measurement in one energy range to be normalized to a known (e.g., thermal) cross section by fitting to other results in an overlapping energy range. In 1963 a paper by Bowman *et al.* [23] appeared in which a remeasurement of σ_f for ^{235}U from 0.03 to 60 eV was interpreted as requiring 18% (downwards) renormalization of the generally accepted ^{235}U fission cross sections above 5 eV, including those from Saclay [24]. In a survey [25] of resonance integrals it was then claimed that the

$\int \sigma_f \frac{dE}{E}$ over the range 60–100 eV would be larger than $\int \sigma_a \frac{dE}{E}$ if the fission results were used without the renormalization proposed by Bowman, and this is clearly impossible, since $\int \sigma_\gamma \frac{dE}{E}$ would then have to be negative. While the situation does not yet satisfy everyone, it seems that both these conclusions may be in error. It now seems likely [26] that neutron scattering due to some rather appreciable quantities of aluminium in the beam in the Bowman experiment may have caused the valley levels of σ_f to be raised at the expense of the peaks of the resonance; in this case the Saclay normalization may remain correct. Then, to avoid the negative $\int \sigma_\gamma \frac{dE}{E}$, the total cross sections must be in error; it appears that another trouble arose here, in correcting for resolutions effects. It is well known that Doppler or instrumental broadening of a resonance should not change the area under a cross-section curve, but for the transmission of samples of finite thickness obtained under conditions of appreciable instrumental broadening of the resonances, a point-for-point transformation from the transmission to an apparent cross-section curve does not give the correct area under this curve. This is a rough analogy with the effect of Doppler broadening in reducing the self-shielding of fuel in thick fuel elements and thus raising the resonance integral, but the case is rather different and the present effect is due to averaging over the instrumental resolution.

Thus the compilation in BNL-325 of the results of the MTR work as $\sigma(E)$ curves can lead to errors in interpretation, and in this case this may well result in the deduced $\int \sigma_a \frac{dE}{E}$ value being too low. Thus a too naïve interpretation of the total cross-section measurements may have led to erroneous conclusions affecting σ_f also, and this is just the sort of thing which can too easily occur in compilation and should serve as a warning for the future. Especially if only deduced σ values (without the transmission data) are sent to a compilation centre, a later review of the problem is rendered difficult. As mechanized methods of handling large numbers of data-points from time-of-flight and similar experiments grow, it is this kind of danger which will most need to be guarded against.

ACKNOWLEDGEMENTS

The authors wish to thank the many correspondents who sent information to the IAEA in connexion with this summary, although it is regretted that much of their information could not be included in this paper. They also wish to thank C. B. Bigham, G. R. Keepin, D. W. Magnuson, and M. G. Sowerby for helpful discussions and Mrs. P. Attree for assistance in programming for the IBM 7040 computer used (located in the Vienna Technische Hochschule).

REFERENCES

1. Poole, M. J., and Wiblin, E. R., *The Design of a High-Intensity Pulsed Source using a Neutron Booster Target (F, S)*, Proceedings of the Second International Conference on the Peaceful Uses of Atomic Energy, P/59, Vol. 14, p. 266, United Nations (1958).
2. Blokhin, G. E., *et al.*, At. En., *10*, 437 (1961) and AEC translation 5734.
3. Hughes, D. J., and Schwartz, R. B., *Neutron Cross Sections*, BNL-325, 2nd Ed. (1958).
4. Private communication, Saclay (1964).
5. Uttley, C. A., and Jones, R. H., UKAEA report AERE M-1223 (1963).
6. Brissenden, R. J., and Durston, C., UKAEA report AEEW—M 429 (1964).
7. Codd, J., Beardwood, J. E., Leslie, D. C., and Sumner, H. M., *Studies of Resonance Absorption and the Doppler phenomenon for fast and thermal reactors*, P/172, this volume.
8. Rae, E., Batchelor, R., Egelstaff, P. A., and Ferguson, A. T. G., *Neutron Interactions with Reactor Materials*, P/167, this volume.
9. Evans, J. E., and Fluharty, R. G., Nuclear Sci. Eng., *8*, 66 (1960); Safford, G. J., and Havens, W. W., Nucleonics, *17*, No. 11, 134 (1959); Sjöstrand, N. G., and Story, J. S., UKAEA report AEEW—M 125 (1961); Sher, R., and Felberbaum, J., USAEC report BNL-722 (1962); Leonard, B. R., in *Neutron Physics*, p. 3, ed. Yeater, Academic Press, New York and London (1962).
10. Westcott, C. H., J. Nuclear Energy, *2*, 59 (1955), also USAEC report AECL-1101.
11. Hopkins, J. C., and Diven, B. C., Nuclear Physics, *48*, 443 (1963); Mather, D. S., *et al.*, Phys. Rev., *133*, B 1403 (1964); Colvin, D. W., and Sowerby, M. G., private communication; see also USAEC report ANL-6792, p. 11 (1963) and Rae *et al.*, (Reference 8); Meadows, J. W., and Whalen, J. F., Phys. Rev., *126*, 197 (1962); also a useful summary in Keepin, G. R., *Physics of Nuclear Kinetics*, Addison-Wesley, Reading, Mass. (1964).
12. Milton, J. C. D., and Fraser, J. S., Can. J. Phys., *40*, 1626 (1962).
13. Whetstone, S. L., Phys. Rev., *114*, 581 (1959); see also Bowman, C. D., *et al.*, *ibid.*, *129*, 2133 (1963); Nuclear Physics, *41*, 492 (1962) and *38*, 193 (1962).
14. Apalin, V. F., *et al.*, Zh.E.T.F., *46*, 1197 (1964); English translation Sov. JETP, *19*, 810 (1964).
15. Apalin, V. F., *et al.*, J. Nuclear Energy, *17*, 25 (1963), also AEC translation 6285 (1963) and JETP (English edition), *16*, 1451 (1963).
16. Blyumkina, Yu. A., *et al.*, Nuclear Physics, *52*, 648 (1964).
17. *Reactor Physics Constants*, USAEC report ANL-5800, pp. 850, xvii, 2nd Edition (1963).
18. Gordeev, I. V., *et al.*, *Yaderno-Fisicheskie Konstanti*, Atomizdat, Moscow (1963).
19. Schmidt, J. J., KFK-120 (1962); Liskien, H., and Paulsen, A., Euratom report EUR 119.e (1962–63); Parker, K., UKAEA reports AWRE 0-79/63 and 0-82/63; many others are listed in Parker, K., EANDC (UK) 26-U (1963).
20. Story, J. S., James, M. F., Kerr, W. M. M., Parker, K., Pull, I. C., and Schofield, P., *Evaluation, storage and processing of nuclear data for reactor calculations*, P/168, this volume.

21. Yiftah, S., Okrent, D., and Moldauer, P. A., *Fast Reactor Cross Sections*, Pergamon Press (1960).
22. Abagyan, L. P., *et al.*, *Group Constants*, Atomizdat, Moscow (1964).
23. Bowman, C. D., *et al.*, Phys. Rev., 130, 1482 (1963).
24. Michaudon, A., *et al.*, J. Phys. et Radium, *21*, 432 (1960).
25. Hanna, G. C., and Walker, W. H., EANDC (Can)-20.
26. Havens, W. W., and Melkonian, E., private communication (1964).

ABSTRACT—RÉSUMÉ—АННОТАЦИЯ—RESUMEN

A/717 AIEA

Etude des constantes nucléaires pour les calculs des réacteurs

par C. H. Westcott *et al.*

Depuis la Conférence de Genève de 1958, l'amélioration des méthodes de mesure a permis d'obtenir beaucoup plus de détails pour les valeurs des sections efficaces de noyaux importants en fonction de l'énergie des neutrons incidents. C'est notamment en ce qui concerne les techniques pour l'étude des neutrons rapides et la résolution dans la région de « résonance » que les progrès ont été les plus remarquables. Malgré ces améliorations, et la plus grande précision des données qui en résulte, il subsiste un certain nombre d'incertitudes et d'incompatibilités qui sont examinées dans le mémoire. Les auteurs examinent aussi brièvement dans quelle mesure on a besoin de données encore plus détaillées ou plus précises. A titre d'exemple, plusieurs grandeurs déterminées sont choisies, notamment les constantes relatives aux neutrons thermiques pour les noyaux fissiles d'uranium et de plutonium.

Le rassemblement et l'évaluation des constantes nucléaires et leur adaptation à des programmes spéciaux pour les calculs automatiques de réacteurs sont devenus des opérations extrêmement compliquées, et le mémoire traite succinctement du rôle que peut jouer l'AIEA dans ce domaine. Le mémoire passe en revue les sources d'information dont on dispose en la matière et les recueils de données déjà publiés, sous l'angle des efforts déployés pour les obtenir et de l'utilité qu'ils présentent pour certaines applications. L'évaluation critique des facteurs, à laquelle il faut procéder pour concilier les résultats divergents des mesures et interpréter certains effets inhérents aux techniques expérimentales utilisées, donne lieu à des difficultés particulières. Il arrive également, dans certains cas, que l'on ne dispose d'aucune donnée mesurée et qu'il faille recourir à la théorie pour obtenir certaines valeurs. On aboutit ainsi à une série de valeurs de la section efficace ou d'une autre grandeur pertinente en fonction de l'énergie neutronique; on peut alors tirer de ces données les valeurs moyennes ou autres valeurs dont on a besoin.

A/717 МАГАТЭ

Обзор ядерных констант для расчетов по ядерным реакторам

С. Х. Уэстнотт *et al.*

Со времени Женевской конференции 1958 года развитие методов измерений привело к значительному увеличению данных, имеющихся для констант по нейтронным эффективным сечениям важных изотопов, в зависимости от энергии падающих нейтронов. Стало более заметным усовершенствование методики измерений, в особенно для быстрых нейтронов, и увеличение разрешения в области резонансов. Несмотря на это и на одновременное накопление данных и увеличение их точности, остается ряд важных неточностей и несовпадений, которые будут рассмотрены в докладе. Кратко рассмотрена также степень необходимой дальнейшей детализации и уточнения данных. Для иллюстрации задачи выбраны некоторые величины, в частности константы для тепловых нейтронов по делящимся ядрам урана и плутония.

Подбор и оценка ядерных констант, их подготовка для использования в конкретных программах по расчету реакторов стали очень сложным процессом; в докладе кратко описана роль, которую может играть МАГАТЭ в выполнении этой работы. Рассмотрены источники информации в этой области и опубликованы тома подобранных данных с описанием усилий, затраченных на их подготовку и использование в частных случаях. Особые трудности касаются необходимости критического суждения при согласовании расходящихся измерений и интерпретации некоторых эффектов, связанных с использованием определенной экспериментальной методики. Имеются также случаи, когда нет измерений и когда для получения данных должна быть применена теория. Наконец, в результате получают ряд значений эффективных сечений или других величин в зависимости от энергии нейтронов; на основании этих значений можно определить среднее или другое необходимое значение.

A/717 OIEA

Estudio panorámico de datos nucleares para el cálculo de reactores

por C. H. Westcott *et al.*

Desde la Conferencia de Ginebra de 1958, el perfeccionamiento de los métodos de medición permitió obtener datos mucho más detallados acerca de las secciones eficaces para núclidos importantes, en función de la energía de los neutrones incidentes. Los progresos más notables se han registrado en lo concerniente a las técnicas para el estudio de los neutrones rápidos, así como en la resolución en la región de «resonancia». A pesar de estos adelantos y de la mayor precisión de los datos resultantes, subsiste cierto número de dudas y contradicciones que se examinan en la presente memoria. También se discute en la misma en qué medida se requieren datos aún más detallados o más precisos. A título de ejemplo, se han elegido ciertas magnitudes dignas de atención, especialmente las constantes relativas a los neutrones térmicos para los núclidos fisibles de uranio y plutonio.

La compilación y evaluación de los datos nucleares, y su adaptación a las claves de cómputo para un reactor determinado, se han convertido en operaciones sumamente complicadas, y los autores tratarán brevemente del papel que el Organismo puede desempeñar en esta esfera. Pasan revista a las fuentes de información disponibles sobre la materia y a las colecciones de datos ya publicadas, considerando los esfuerzos desplegados para reunirlos y la utilidad que presentan para determinadas aplicaciones. Destacan la necesidad de proceder con sentido crítico para conciliar resultados discrepantes e interpretar ciertos efectos inherentes a las técnicas experimentales utilizadas. En algunos casos no se cuenta con resultados de determinaciones experimentales y es preciso recurrir a la teoría para obtener ciertos valores numéricos. El resultado final consiste en una serie de valores de las secciones eficaces, u otras magnitudes pertinentes, presentados en función de la energía neutrónica; de estos grupos de datos es posible deducir los valores medios o de otra índole que sean necesarios.

New developments in reactor physics

Chairman: J. A. Goedkoop (Netherlands)

Paper P/261 (presented by G. I. Bell)

DISCUSSION

Sh. YIFTAH (Israel): Are there any measurable effects of polarization on neutron transport?

G. I. BELL (United States of America): Polarization effects are readily detectable in multiple scattering experiments. In a double scattering experiment, a neutron beam will acquire polarization perpendicular to the plane of first scattering. In the second scattering, a right-left asymmetry will be observed owing to the polarization, and this allows measurement of the polarization induced by the scattering.

With polarization, the transport theory actually involves four quantities (two complex amplitudes for scattering), which could be obtained by a triple scattering experiment, or alternatively by calculation.

Neutron transport in the >100 keV energy range depends on polarization, but since polarization cannot be turned on and off there is no easy way to separate the effects due to it.

Sh. YIFTAH (Israel): In neutron systems we are dealing statistically with very large neutron populations, so do you think polarization effects will have any importance for the calculations of these systems?

G. I. Bell (United States of America): In principle, the dependence of neutron transport on polarization is not related to the size of the neutron population. However, owing to the uncertainties in total cross sections, these refinements may not be of great practical significance.

E. V. ORLOV (USSR): The study of polarization effects in neutron transport processes, as dealt with in your paper, has assumed importance in recent years because experiments sometimes indicate an unexpectedly high degree of neutron polarization associated with scattering. A qualitative account of polarization effects on neutron reflection from various media has been given by P. S. Otstavnov.* Y. N. Kazachenkov and I subsequently formulated kinetic equations for flux density and spin, taking account of neutron polarization caused by spin-orbit interaction during scattering, and also diffusion approximations.

In connexion with Mr. Yiftah's first question, I should like to state that we have estimated changes in the neutron diffusion coefficient D due to polarization effects, using experimental data. For heavy nuclei and neutron energies about $E \approx 1$ MeV, $\delta D/D \approx -(1 \text{ to } 2)\%$; for Mg and Si nuclei and neutron energies about $E \approx 20$ keV, $\delta D/D \approx -(10 \text{ to } 20)\%$. An abstract of this work has been published in *Atomnaya Nauka i Tekhnika*. The difference in these values may be due to the change in sign of polarization for scattering at angles that correspond to the extremes in differential cross section. This may explain the decrease in the polarization correction for the neutrons with high orbital momentum.

G. I. BELL (United States of America): Your comments are very interesting, and the pronounced effect you mentioned surprises me. Perhaps I could at this juncture make a statement adding to the information contained in my paper.

Anisotropic scattering is now usually handled by expanding the scattering kernel (transference function) in a series of Legendre Polynomials in the scattering angle. For example, the new DTF code is a FORTRAN code using the discrete S_n (DSN) method which allows up to a ten-term Legendre expansion of the scattering kernel for slabs and spheres. Actually, for criticality calculations, a two-term expansion usually suffices, but for computing the penetration of γ-rays through thick regions, five or more terms have been used, and have given excellent agreement with Monte Carlo results.

As an example of such a comparison between S_n and Monte Carlo let us consider the results shown in Figure 1. A gamma source of 2 MeV was distributed in a spherical region of radius 7.74 cm containing uranium, iron and sodium. Outside this was mostly iron to a radius of 29.5 cm followed by 50 cm of graphite. The figure shows the gamma flux between 1 and 1.25 MeV as computed by the Monte Carlo SAGE code and the S_n DTF code with a P_5 expansion of the scattering kernel and double P_7 quadrature for the angular flux. In double P_7, 16 discrete gamma directions are used. We observe agreement between S_n and Monte Carlo results to within more or less the statistical uncertainty of the latter. A P_3 scattering expansion also gives fluxes which are indistinguishable from P_5 on this scale.

A series of calculations of slab critical thicknesses with anisotropic scattering has just been completed and provides a nice comparison of the results obtainable with two completely different methods. The calculations were done by Leonard, using the singular integral equation method, and by Lathrop, using the DTF code with the double P_7 quadrature scheme,

* Atomnaya Energia, *14*, 487, Moscow (1963).

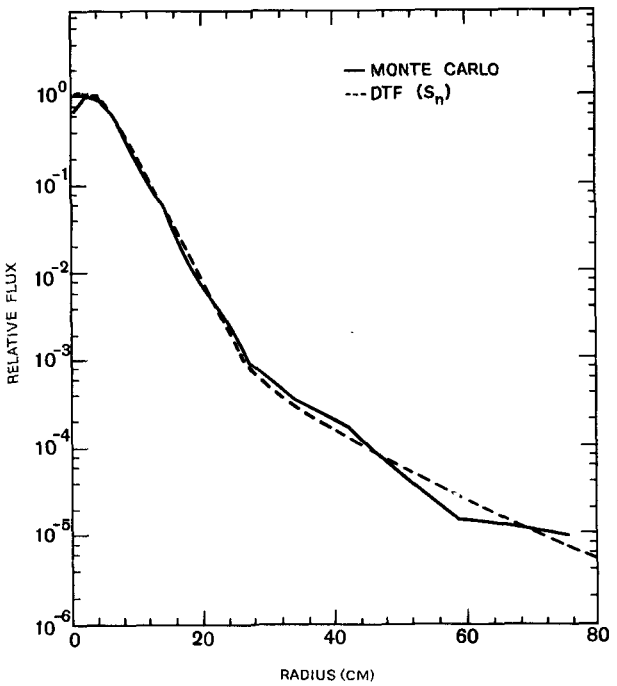

Figure 1

which for slabs is equivalent to a discrete ordinates method with 16 directions. One-velocity calculations were made with an anisotropic scattering function having the same angular dependence as elastic scattering from hydrogen. The transport equation for the problem can be written:

$$\mu \frac{\partial \psi(x,\mu)}{\partial x} + \psi(x,\mu) =$$

$$c' \int_{-1}^{1} \psi(x,\mu')\mathrm{d}\mu' + c \sum_{n=0}^{2} \frac{2n+1}{2} b_n \mathrm{P}_n(\mu) \int_{-1}^{1} \mathrm{P}_n(\mu')\psi(x,\mu')\mathrm{d}\mu'$$

where $b_0 = 1$, $b_1 = 2/3$, $b_2 = 1/4$

Thus, c' and c respectively are coefficients of the isotropic and the anisotropic parts of the scattering. We have retained only two terms in the scattering function. It will be observed that b_2 has only a rather small effect on the result, while for hydrogen $b_3 = 0$ and b_4 ($= -1/24$) may be ignored for present purposes.

In the singular integral theory a first approximation to the critical thickness is;

$$\tau_0 = \pi |\nu_0| - 2Z_0$$

where ν_0 is the discrete eigenvalue of the Boltzmann equation and Z_0 is the extrapolation distance appropriate to anisotropic scattering. This result is thus formally identical to end-point theory and is so labelled in Table 1. The iterative scheme may be written:

$$\tau_n = \pi |\nu_0| - 2Z_0 - R(\tau_{n-1})$$
$$n = 0,1, \ldots \text{ and } R(\tau_{-1}) = 0$$

Table 1. Slab critical half-thickness (mfp)

c	$P1_{DTF}$	$P1_{exact}$	$P1_{end\text{-}point}$	$P2_{DTF}$	$P2_{exact}$	$P2_{end\text{-}point}$
			$c + c' = 1.05$			
0.1	3.39225	3.39216	3.39216	3.39042	3.39032	3.39032
0.3	3.60356	3.60346	3.60346	3.59724	3.59714	3.59714
0.5	3.86368	3.86358	3.86358	3.85135	3.85126	3.85126
0.7	4.19568	4.19558	4.19558	4.17506	4.17495	4.17495
0.9	4.64212	4.64203	4.64203	4.60935	4.60927	4.60927
			$c + c' = 1.10$			
0.1	2.16524	2.16519	2.16525	2.16311	2.16306	2.16313
0.3	2.28290	2.28285	2.28291	2.27558	2.27553	2.27559
0.5	2.42452	2.42447	2.42452	2.41031	2.41026	2.41033
0.7	2.59999	2.59994	2.59998	2.57637	2.57632	2.57639
0.9	2.82629	2.82625	2.82628	2.78923	2.78917	2.78924
			$c + c' = 1.20$			
0.1	1.31521	1.31519	1.31567	1.31299	1.31296	1.31347
0.3	1.37256	1.37254	1.37308	1.36498	1.36496	1.36558
0.5	1.43939	1.43935	1.43997	1.42486	1.42484	1.42561
0.7	1.51884	1.51882	1.51948	1.49506	1.49505	1.49604
0.9	1.61576	1.61575	1.61646	1.57930	1.57929	1.58061
			$c + c' = 1.30$			
0.1	0.95354	0.95352	0.95473	0.95142	0.95140	0.95266
0.3	0.98811	0.98810	0.98955	0.98098	0.98096	0.98262
0.5	1.02747	1.02746	1.02922	1.01398	1.01399	1.01621
0.7	1.07292	1.07291	1.07507	1.05123	1.05127	1.05439
0.9	1.12636	1.12635	1.12903	1.09382	—	—
			$c + c' = 1.40$			
0.1	0.74726	0.74727	0.74930	0.74532	0.74529	0.74743
0.3	0.77031	0.77032	0.77288	0.76381	0.76378	0.76669
0.5	0.79607	0.79606	0.79936	0.78393	0.78396	0.78800
0.7	0.82519	0.82519	0.82948	0.80595	0.80610	0.81199
0.9	0.85853	0.85853	0.86424	0.83022	—	—

where R is a rather complicated functional of functions which satisfy Fredholm equations.

In Table 1, the critical half-thicknesses are given for various values of c and c'. The columns labelled P1 mean that only terms through $P_1(\mu)$ were included in the scattering function, while those labelled P2 included the $P_2(\mu)$ term also. The *exact* values are those found by Leonard by iteration starting from tne *end-point* values.

From the table we see that DTF(S_n) and exact values differ only in the fourth or fifth decimal. Such slight differences may not be meaningful. The end-point values are excellent until $c + c'$ becomes large, in agreement with experience for isotropic scattering. The effect of the $P_2(\mu)$ term is seen to be 1 to 3% for $c = 0.9$ and the effect is, of course, larger for small slabs where flux anisotropy is greater.

Computing times for the DTF programme and the iterative method were similar—about one minute per problem on the IBM 7094. The DTF programme is immediately applicable to more complicated multigroup-multiregion problems while the iterative method is not.

Finally, I would like to describe results from a study of the effects of polarization on neutron transport, which has just been made at Los Alamos by Dr. Walter Goad and myself. In conventional transport theory, a neutron is treated as a point particle which is completely described by its position and velocity. But in fact the neutron has a spin, and experiments, particularly in the last few years, have shown that the spin has a marked effect on neutron scattering from most nuclei at neutron energies greater than a hundred kilovolts or so. An unpolarized neutron beam (i.e., a beam with no preferred spin direction) will upon scattering (from an unpolarized target) become polarized (i.e., acquire a preferred spin direction) and this polarization will affect the next scattering. A new correlation is thus introduced between scatterings, and this will affect neutron transport. The polarization induced by the first scattering is typically tens of per cent for MeV neutrons, and the effect is explained by a spin-orbit term in the neutron-nucleus interaction energy.

We have formulated a transport theory for neutrons with spin where scattering is no longer described by a differential cross section, but by two complex scattering amplitudes and where the state of a neutron beam is specified not just by the neutron density but by the polarization vector (or spin density matrix) as well. For plane or spherically symmetrical geometry, where there is an axis of symmetry for neutron directions, it was found that the polarization vector will always be perpendicular to the plane containing the axis and the neutron direction. The neutron population can then be determined from two coupled scalar transport equations for the neutron density $\bar{n}$ and the density of polarization $\overline{np}$. If we assume that $\bar{n}(x,\theta) = n_0(x) + 3\cos\theta\, j(x)$, as in diffusion theory, then $\overline{np} \sim j(x) \sin\theta$. Here θ is the usual angle between the axis of symmetry and neutron direction. Furthermore, in this approximation, the effect of polarization on neutron transport is simply equivalent to an *increase* in the transport cross section. For the materials which we have examined the increase is not large, being typically of the order of 1% and thus less than experimental cross section uncertainties. We feel, however, that it is gratifying that we now have a sound reason for neglecting polarization effects, at least for most practical cases.

Paper P/263 (presented by R. G. Luce)

DISCUSSION

J. M. DÖDERLEIN (Norway): Can you advise us as to an efficient and convenient few-group two-dimensional diffusion theory computer code, written to 90 or 100 % in FORTRAN?

R. G. LUCE (United States of America): There are several. The one used in our laboratory is not entirely in FORTRAN: it is the KARE code. Others are completely in FORTRAN.

Paper P/717 (presented by C. H. Westcott)

DISCUSSION

J. CHERNICK (United States of America): Would you comment on the extent to which data from integral experiments, in particular the Mn bath experiments, have been used in arriving at your estimates of 2200 m/s nuclear data?

C. H. WESTCOTT (IAEA): Results from integral experiments were only included if published or drawn to the attention of our group and sufficiently documented: for instance, a description of the neutron spectrum adequate for direct and unambiguous interpretation in terms of 2200 m/s constants was necessary. The Oak Ridge Mn bath measurements were included in our study.

J. CHERNICK (United States of America): The results of recent critical experiments in the United Kingdom and the United States indicate that the 2200 m/s value of η for ^{239}Pu is somewhat less than your estimate of 2.123. Should not data of this type be factored into cross-section evaluation and included in your analysis?

C. H. WESTCOTT (IAEA): The Gwin and Magnusson criticality measurements were also included in our study, and I do not recall seeing more recent published work. However, I should add that the estimated errors of all measurements made with a Maxwellian spectrum were increased to allow for the estimated error of the g-factor used in converting the constants concerned to 2200 m/s values.

J. E. SANDERS (United Kingdom): In connexion with Dr. Chernick's comment on the η of ^{239}Pu I should like to say that United Kingdom experiments on ^{235}U and ^{239}Pu fuels in H_2O and graphite moderators support the higher value of η for ^{239}Pu suggested by Dr. Westcott's new survey. This conclusion is reached in paper P/165 by Askew and Sanders.*

* Vol. 3, these Proceedings.

J. CHERNICK (United States of America): Yes, but the British data reported in paper P/165 by Askew and Sanders suggest a 1 % increase in the value of η for ^{239}Pu which they had previously been using (2.088) and this leads to a value slightly under 2.11.

Paper P/73 (presented by M. Cadilhac)

DISCUSSION

J. R. BEYSTER (United States of America): My question concerns the range of applicability of your secondary model. After you have obtained a fit for the G and H functions, how do you know the range of temperature, degree of poisoning, types of resonance absorber and degree of leakage to which the fit will apply?

M. CADILHAC (France): A general study of the validity of the model has yet to be carried out. We have noted good agreement in certain carefully selected cases, which were sufficiently representative of normal situations to convince us that the model cannot be totally inadequate except in very exceptional cases. This is true, at any rate, during continuous operation, though we do not know whether the model can be used to deal with pulsed neutron problems.

Paper P/367 (presented by A. A. Chernishov)

DISCUSSION

J. R. BEYSTER (United States of America): How do you explain the disagreement between your experimental neutron spectra in uranium water lattices and the calculations of Honeck and Takahashi?* The latter calculations were based on a bound atom model for water with which much other neutron data agreed.

A. A. CHERNISHOV (USSR): I am afraid I cannot explain this divergence at the moment. However, I should point out that the results of the calculations you refer to are not in agreement with the experimental results obtained at Harwell either.

K. H. BECKURTS (Federal Republic of Germany): How do you extract the general frequency distribution $P(\beta)$ from the measured scattering law? Do you just extrapolate the two momentum transfers or do you use an iterative procedure?

A. A. CHERNISHOV (USSR): We get the $P(\beta)$ function very simply, if not very exactly, without using an iterative procedure or a computer. The form of $P(\beta)$ can be made more exact by calculating double differential cross sections from $P(\beta)$ (taking apparatus effects into account) and comparing the calculated results with measured cross sections. A programme of such calculations is described in paper P/360 by L. V. Maiorov *et al.*

K. H. BECKURTS (Federal Republic of Germany): Your time-dependent spectrum measurement is essentially the same as that done by M. J. Poole's group at Harwell. Have you compared the results?

A. A. CHERNISHOV (USSR): Yes. The comparison showed the Harwell values to be consistently lower, which indicates that there are certain systematic errors in the measurements.

D. BALLY (Romania): What must be the range of variation of the water diffusion coefficient to explain the widening of the quasi-elastic maximum with temperature as mentioned in your paper?

A. A. CHERNISHOV (USSR): As stated in the paper, the measurements were carried out with a relatively low resolution; the aim was to obtain information necessary for thermalization calculations, so no special analysis of quasi-elastic scattering was made. It can be seen from the curves that the widening never exceeds 10 %.

Paper P/858 (presented by V. Ajdačić)

DISCUSSION

E. P. BLIZARD (United States of America): I notice that you are concerned about (n,p) and (n,α) reactions in silicon in your spectrometer. Have you studied the advantages to be gained by using silicon isotopes such as silicon-30, for which these reactions would be much less important?

V. AJDAČIĆ (Yugoslavia): Our semi-conductor detectors are silicon monocrystals, and it would be very costly to make these out of single isotopes.

E. P. BLIZARD (United States of America): Do you not have trouble with the high flux leaving the long tube? Have you considered deflecting charged particles by magnets?

V. AJDAČIĆ (Yugoslavia): We used an electric field for deflecting electrons, but found that protons and alphas from neutron reactions on aluminium formed the major part of the background. Of course, it is not easy to deflect them and yet have a very simple method for high neutron flux measurements.

G. BEN-DAVID (Israel): What is the energy resolution of the ^{6}Li fast-neutron counter?

V. AJDAČIĆ (Yugoslavia): The resolution of the spectrometer was about 300 keV at a power of 2 watts. The resolution depends on the reactor power and the dependence is given in Fig. 2 of the paper.

Papers P/498 and P/705

There was no discussion of these papers.

GENERAL DISCUSSION

P. LO IZZO (Italy): The methods and cross sections used by reactor designers (in the water reactor field, at least) date back five to ten years. New methods are considerably better and new data are piling up, but reactor designers always need critical experiments to design a really new reactor. Simple methods are actually able to give us say 1 % error in k_{eff}—probably because certain large errors cancel each other—and if we substitute more precise values for cross sections or

* Ref. [21] of the paper.

a more sophisticated method for the calculation of a reactor parameter, we often get bigger errors. Could anybody comment on whether this is a general effect and whether there is any way to overcome it?

J. S. STORY (United Kingdom): With regard to Mr. Lo Izzo's comments, I think it is unfortunately true that, at first, more sophisticated methods of calculation all too often give results which agree less well with what is expected from integral measurements. Nevertheless, I believe one has to pursue the more sophisticated methods, as this can help to bring to light shortcomings in our understanding of reactor behaviour.

This view leads me to make a few remarks on the problems of evaluating nuclear cross-section data and processing these data to obtain multigroup data and other derived quantities for use in the sophisticated reactor neutron transport programmes. Dr. Westcott has briefly mentioned these questions in his paper (P/717) and they are also discussed in rather more detail in the United Kingdom paper (P/168).

During the last few years the quality and output of basic neutron cross section data have improved very greatly and the rate of output is still increasing. We are beginning to be faced with a veritable "population explosion" of new data. In conjunction with the advances in transport theory this is very gratifying, but it takes a great deal of hard work to get the data into the forms needed in transport theory programmes. We have considerable practical experience of this problem in the United Kingdom, and we find that it takes from two to six man-months to prepare a complete set of evaluated cross sections for a single nuclide or element; so to do this work for all the materials of interest for reactor physics, keeping the evaluations up to date as new data come along, will call for a very substantial effort.

We believe that a determined and persistent effort is called for in this field, and that international collaboration is urgently needed to ensure an adequate scale of effort.

Compte rendu de la séance 3. 1

Progrès en physique des réacteurs

Président: J. A. Goedkoop (Pays-Bas)

Mémoire P/261 (présenté par G. I. Bell)

DISCUSSION

Sh. YIFTAH (Israël): Existe-t-il des effets mesurables de la polarisation sur le transport des neutrons?

G. I. BELL (Etats-Unis d'Amérique): Des effets de polarisation sont facilement décelables dans des expériences de diffusion multiple. Dans une expérience de double diffusion, un faisceau de neutrons présentera une polarisation perpendiculaire au plan de la première diffusion. Dans la seconde diffusion, on observera une asymétrie droite – gauche due à la polarisation, et cela permet une mesure de la polarisation créée par la diffusion.

Avec la polarisation, en faït, la théorie du transport met en jeu quatre quantités (deux amplitudes complexes par diffusion), que l'on pourrait obtenir par une expérience de diffusion triple, ou encore par le calcul.

Le transport des neutrons dans un domaine d'énergies supérieures à 100 keV dépend de la polarisation, mais, comme cette polarisation ne peut pas être interrompue et rétablie, il n'y a pas de méthode simple pour en isoler les effets.

Sh. YIFTAH (Israël): Dans les systèmes de neutrons, on considère statistiquement de très grandes populations de neutrons; pensez-vous que les effets de polarisation auront de l'influence sur les calculs relatifs à ces systèmes?

G. I. BELL (Etats-Unis d'Amérique): En principe, l'effet de la polarisation sur le transport des neutrons est indépendant de la taille de la population de neutrons. Cependant, vu l'incertitude des sections efficaces totales, ces précisions n'ont peut-être guère de portée pratique.

E. V. ORLOV (URSS): L'étude des effets de polarisation dans les phénomènes de transport de neutrons, traités dans votre mémoire, a pris de l'importance ces dernières années, car parfois les expériences révèlent un degré inattendu et considérable de polarisation des neutrons liée à la diffusion. Une explication qualitative des effets de polarisation sur la réflexion de neutrons par divers milieux a été donnée par P. S. Otstavnov*. Y. N. Kazachenkov et moi-même avons écrit, depuis, les équations cinétiques pour la densité de flux et pour le spin, en tenant compte de la polarisation des neutrons due à l'interaction spin-orbite pendant la diffusion, et également des approximations de la diffusion.

A propos de la première question de M. Yiftah, je voudrais dire que nous avons évalué les modifications

* Atomnaya Energia, *14*, 487, Moscou (1963).

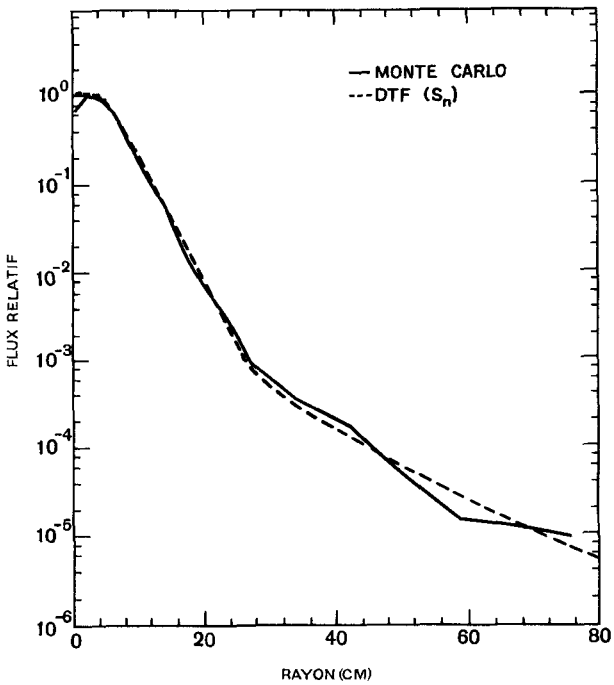

Figure 1

du coefficient de diffusion des neutrons D dues aux effets de polarisation, à partir de données expérimentales. Pour des noyaux lourds et des neutrons d'énergies E voisines de 1 MeV, $\delta D/D \approx -(1 \text{ à } 2)\%$; pour des noyaux de Mg et Si et des neutrons d'énergies E voisines de 20 keV, $\delta D/D \approx -(10 \text{ à } 20)\%$. Un résumé de ces travaux a paru dans *Atomnaya Nauka i Tekhnika*. L'écart entre ces valeurs peut provenir du changement de signe de la polarisation pour des angles de diffusion correspondant aux valeurs extrêmes de section efficace différentielle. Cela peut expliquer la diminution de la correction due à la polarisation pour des neutrons de moment orbital élevé.

G. I. Bell (Etats-Unis d'Amérique): Vos commentaires sont très intéressants, et l'importance de l'effet que vous signalez me surprend. A cette occasion je pourrais peut-être développer l'exposé fait dans mon mémoire.

La diffusion anisotrope se traite d'habitude aujourd'hui en développant le noyau de diffusion (fonction de transfert) en série de polynomes de Legendre selon l'angle de diffusion. Par exemple, le nouveau code DTF est un code FORTRAN utilisant la méthode S_n discrète (DSN) qui permet jusqu'à dix termes dans le développement de Legendre du noyau de diffusion pour des plaques et des sphères. En fait, les calculs de criticité se contentent en général de deux termes dans le développement, mais, pour les calculs de pénétration des rayons γ dans des milieux épais, on s'est servi de cinq termes au moins et on a trouvé un accord excellent avec les résultats obtenus par la méthode de Monte-Carlo.

Pour illustrer une telle comparaison entre S_n et la méthode de Monte-Carlo, considérons les résultats présentés à la figure 1. Une source γ de 2 MeV était distribuée dans une région sphérique de rayon 7,74 cm contenant de l'uranium, du fer et du sodium. L'extérieur était constitué principalement de fer jusque dans un rayon de 29,5 cm, suivi de 50 cm de graphite. La figure montre le flux gamma entre 1 et 1,25 MeV calculé en utilisant le code SAGE de Monte-Carlo et en utilisant le code S_n DTF avec un développement P_5 du noyau de diffusion et une intégration en double P_7 pour le flux angulaire. Dans le double P_7, on utilise 16 directions discrètes des gammas. On constate un accord des résultats de S_n et de la méthode de Monte-Carlo, à peu près dans les limites de l'incertitude statistique de cette dernière méthode. Un développement P_3 de la diffusion donne de même des flux qui ne se distinguent pas de ceux donnés par un P_5 à cette échelle.

Une série de calculs d'épaisseurs critiques pour des plaques avec diffusion anisotrope vient d'être terminée, et donne une bonne comparaison des résultats que l'on peut obtenir par deux méthodes entièrement distinctes. Les calculs ont été faits par Leonard suivant la méthode de l'équation intégrale singulière et par Lathrop au moyen du code DTF avec le modèle d'intégration en double P_7 qui équivaut pour des plaques à une méthode d'ordonnées discrètes à 16 directions.

Les calculs monocinétiques ont été faits avec une fonction de diffusion anisotrope ayant la même relation angulaire que la diffusion élastique de l'hydrogène. L'équation de transport du problème peut s'écrire:

$$\mu \frac{\partial \psi(x,\mu)}{\partial x} + \psi(x,\mu) =$$

$$c' \int_{-1}^{1} \psi(x,\mu')\mathrm{d}\mu' + c \sum_{n=0}^{2} \frac{2n+1}{2} b_n P_n(\mu) \int_{-1}^{1} P_n(\mu')\psi(x,\mu')\mathrm{d}\mu'$$

où $b_0 = 1$; $b_1 = 2/3$; $b_2 = 1/4$

Ainsi, c' et c sont les coefficients respectifs des parties isotrope et anisotrope de la diffusion. Nous n'avons gardé que deux termes dans la fonction de diffusion. On notera que b_2 n'a qu'un effet plutôt faible sur le résultat, et que, pour l'hydrogène, $b_3 = 0$ et $b_4 = -1/24$ peuvent être négligés dans le présent calcul.

La théorie de l'intégrale singulière donne pour première approximation de l'épaisseur critique:

$$\tau_0 = \pi |\nu_0| - 2Z_0$$

où ν_0 est la valeur propre discrète de l'équation de Boltzmann, et Z_0 la longueur d'extrapolation correspondant à la diffusion anisotrope. Ce résultat est donc d'une forme identique à la théorie du « point terminal » et c'est ainsi qu'on l'indique dans le tableau 1. Le modèle d'itération peut s'écrire:

$$\tau_n = \pi |\nu_0| - 2Z_0 - (R\tau_{n-1})$$
$$n = 0,1, \ldots \text{ et } R(\tau_{-1}) = 0$$

où R est une fonctionnelle assez compliquée satisfaisant les équations de Fredholm.

Tableau 1. Demi-épaisseurs critiques pour une plaque (lpm)

c	$P1_{DTF}$	$P1_{valeur\ exacte}$	$P1_{point\ terminal}$	$P2_{DTF}$	$P2_{valeur\ exacte}$	$P2_{point\ terminal}$
			$c+c'=1{,}05$			
0,1 . .	3,39225	3,39216	3,39216	3,39042	3,39032	3,39032
0,3 . .	3,60356	3,60346	3,60346	3,59724	3,59714	3,59714
0,5 . .	3,86368	3,86358	3,86358	3,85135	3,85126	3,85126
0,7 . .	4,19568	4,19558	4,19558	4,17506	4,17495	4,17495
0,9 . .	4,64212	4,64203	4,64203	4,60935	4,60927	4,60927
			$c+c'=1{,}10$			
0,1 . .	2,16524	2,16519	2,16525	2,16311	2,16306	2,16313
0,3 . .	2,28290	2,28285	2,28291	2,27558	2,27553	2,27559
0,5 . .	2,42452	2,42447	2,42452	2,41031	2,41026	2,41033
0,7 . .	2,59999	2,59994	2,59998	2,57637	2,57632	2,57639
0,9 . .	2,82629	2,82625	2,82628	2,78923	2,78917	2,78924
			$c+c'=1{,}20$			
0,1 . .	1,31521	1,31519	1,31567	1,31299	1,31296	1,31347
0,3 . .	1,37256	1,37254	1,37308	1,36498	1,36496	1,36558
0,5 . .	1,43939	1,43935	1,43997	1,42486	1,42484	1,42561
0,7 . .	1,51884	1,51882	1,51948	1,49506	1,49505	1,49604
0,9 . .	1,61576	1,61575	1,61646	1,57930	1,57929	1,58061
			$c+c'=1{,}30$			
0,1 . .	0,95354	0,95352	0,95473	0,95142	0,95140	0,95266
0,3 . .	0,98811	0,98810	0,98955	0,98098	0,98096	0,98262
0,5 . .	1,02747	1,02746	1,02922	1,01398	1,01399	1,01621
0,7 . .	1,07292	1,07291	1,07507	1,05123	1,05127	1,05439
0,9 . .	1,12636	1,12635	1,12903	1,09382	—	—
			$c+c'=1{,}40$			
0,1 . .	0,74726	0,74727	0,74930	0,74532	0,74529	0,74745
0,3 . .	0,77031	0,77032	0,77288	0,76381	0,76378	0,76669
0,5 . .	0,79607	0,79606	0,79936	0,78393	0,78396	0,78800
0,7 . .	0,82519	0,82519	0,82948	0,80595	0,80610	0,81199
0,9 . .	0,85853	0,85853	0,86424	0,83022	—	—

Les résultats figurent au tableau 1, qui donne les demi-épaisseurs critiques pour diverses valeurs de c et c'. Les colonnes marquées P1 signifient que seul le développement jusqu'a $P_1(\mu)$ est conservé dans la fonction de diffusion, alors que celles marquées P2 comprennent aussi les termes $P_2(\mu)$. Les valeurs *exactes* sont celles trouvées par Léonard par itération à partir des valeurs au point terminal.

Le tableau montre que les valeurs obtenues par DTF (S_n) ne diffèrent des valeurs exactes qu'à partir de la quatrième ou de la cinquième décimale. De si faibles différences ne peuvent être significatives. Les valeurs au point terminal sont excellentes tant que $c+c'$ n'est pas trop grand, et en accord avec les expériences pour la diffusion isotrope. L'influence du terme $P_2(\mu)$ est, comme on le voit, de un à trois pour cent pour $c=0{,}9$ et cette influence est, assurément, plus grande pour des plaques minces où l'anisotropie du flux est plus marquée.

La durée des calculs pour le programme DTF et pour la méthode d'itération était la même — de l'ordre d'une minute par problème sur IBM 7094. Le programme DTF s'applique dès maintenant à des problèmes plus complexes, à plusieurs groupes et à plusieurs régions, ce qui n'est pas le cas pour la méthode d'itération.

Pour terminer, je voudrais présenter des résultats d'une étude sur les effets de polarisation sur le transport des neutrons, qui vient d'être faite à Los Alamos par le Dr. Walter Goad et moi-même. Dans la théorie classique du transport, un neutron est considéré comme une particule ponctuelle, définie complètement par sa position et sa vitesse. Mais en fait le neutron possède un spin, et des expériences, surtout ces toutes dernières années, ont montré que le spin a une grande influence sur la diffusion des neutrons par la plupart des noyaux quand l'énergie des neutrons dépasse une centaine de kiloélectron-volts. Un faisceau de neutrons non polarisé (c'est-à-dire un faisceau sans orientation préférentielle de spin) après diffusion (par une cible non polarisée) va se polariser (c'est-à-dire acquiert une orientation préférentielle de spin), et cette polarisation modifiera la diffusion suivante. Une relation nouvelle s'établit donc entre les diffusions, ce qui modifie le transport des neutrons. La polarisation induite par la première diffusion vaut couramment plusieurs dizaines pour cent pour des neutrons de quelques MeV et l'effet s'explique par un terme spin-orbite dans l'énergie d'interaction neutron-noyau.

Nous avons formulé une théorie du transport pour neutrons avec spin, où la diffusion n'est plus caractérisée par une section efficace différentielle mais par deux amplitudes de diffusion complexes, et où un faisceau de neutrons n'est plus défini seulement par la densité des neutrons mais également par le vecteur de polarisation (ou matrice de densité de spin). En géométrie de symétrie plane ou sphérique, où il existe un axe de symétrie pour les directions des neutrons, on

a trouvé que le vecteur de polarisation est toujours perpendiculaire au plan contenant l'axe et la direction des neutrons. La population de neutrons peut alors se définir à partir d'un système de deux équations de transport scalaires pour la densité neutronique $\bar{n}$ et la densité de polarisation $\overline{np}$. Si l'on suppose $\bar{n}(x,\theta) = n_0(x) + 3\cos\theta j(x)$, comme dans la théorie de la diffusion, on a $\overline{np} \sim j(x) \sin\theta$. Ici θ est, comme d'habitude, l'angle entre l'axe de symétrie et la direction des neutrons. En outre, avec cette approximation, l'effet de la polarisation sur le transport des neutrons est équivalent à une simple augmentation de la section efficace de transport. Pour les matériaux que nous avons étudiés, cette augmentation est faible, couramment voisine de 1%, soit inférieure à la précision des mesures de sections efficaces. Cependant il est intéressant d'avoir maintenant une solide raison de négliger les effets de polarisation, au moins dans la plupart des applications.

Mémoire P/263 (présenté par R. G. Luce)

DISCUSSION

J. M. DÖDERLEIN (Norvège): Pourriez-vous nous indiquer un code efficace et pratique pour calculateurs, écrit de 90 à 100% en FORTRAN, pour une théorie de la diffusion à quelques groupes et à deux dimensions?

R. G. LUCE (Etats-Unis d'Amérique): Il y en a plusieurs. Celui qu'utilise notre laboratoire n'est pas entièrement en FORTRAN: c'est le code KARE. Les autres sont entièrement en FORTRAN.

Mémoire P/717 (présenté par C. H. Westcott)

DISCUSSION

J. CHERNICK (Etats-Unis d'Amérique): Voudriez-vous expliciter dans quelle mesure des données fournies par des expériences intégrales, en particulier par les expériences de bain de manganèse ont servi à établir vos évaluations des données nucléaires a 2200 m/s?

C. H. WESTCOTT (AIEA): Les résultats d'expériences intégrales n'ont été inclus que s'ils avaient été publiés, ou signalés à l'attention de notre équipe avec une documentation suffisante: par exemple, il nous fallait une définition du spectre de neutrons permettant une interprétation directe et sans ambiguïté en fonction de constantes à 2200 m/s. Les mesures de bain de manganèse d'Oak Ridge ont été incluses dans notre étude.

J. CHERNICK (Etats-Unis d'Amérique): Les résultats d'expériences critiques récentes au Royaume-Uni et aux Etats-Unis montrent que la valeur à 2200 m/s de η pour le plutonium 239 est un peu au-dessous de votre estimation de 2,123. Ne devrait-on pas tenir compte des données de ce genre dans l'évaluation des sections efficaces et les introduire dans votre analyse?

C. H. WESTCOTT (AIEA): Nous avons aussi inclus dans notre étude les mesures de criticité de Gwin et Magnusson, et je ne me rappelle pas avoir vu de travaux publiés plus récemment. Cependant je dois ajouter que les erreurs estimées sur toutes les mesures faites avec un spectre de Maxwell ont été majorées pour tenir compte de l'erreur estimée sur le facteur g utilisé pour ramener les constantes en question à leurs valeurs à 2200 m/s.

J. E. SANDERS (Royaume-Uni): A propos de la remarque du Dr Chernick sur la valeur de η du plutonium 239, je tiens à dire que des expériences faites au Royaume-Uni sur des combustibles d'uranium 235 et de plutonium 239 dans des modérateurs d'eau et de graphite viennent à l'appui de la valeur la plus élevée de η du plutonium 239, telle que la donne la nouvelle étude du Dr Westcott. C'est à cette conclusion qu'on aboutit dans le mémoire P/165 de Askew et Sanders*.

J. CHERNICK (Etats-Unis d'Amérique): Oui, mais les chiffres du Royaume-Uni rapportés dans le mémoire P/165 de Askew et Sanders proposent une majoration de 1% de la valeur de η du plutonium 239 utilisée auparavant (2,088), et cela conduit à une valeur légèrement inférieure à 2,11.

Mémoire P/73 (présenté par M. Cadilhac)

DISCUSSION

J. R. BEYSTER (Etats-Unis d'Amérique): Ma question porte sur le domaine d'applicabilité de votre modèle secondaire. Une fois obtenu l'ajustement pour les fonctions G et H, comment connaissez-vous le domaine de température, le degré d'empoisonnement, les types d'absorbants de résonance et le degré de fuites pour lesquels l'ajustement est valable?

M. CADILHAC (France): Une étude générale de la validité du modèle reste encore à faire. Nous avons observé un bon accord dans certains cas soigneusement choisis, qui étaient assez représentatifs du cas général pour nous donner la certitude que le modèle ne peut être mauvais sauf dans certains cas tout à fait exceptionnels. Cela est vrai, en tout cas, en continu, bien que nous ne sachions pas si le modèle peut servir à traiter des problèmes de neutrons pulsés.

Mémoire P/367 (présenté par A. A. Chernishov)

DISCUSSION

J. R. BEYSTER (Etats-Unis d'Amérique): Comment expliquez-vous le désaccord entre vos déterminations expérimentales de spectres de neutrons dans des réseaux uranium – eau et les calculs de Honeck et Takahashi**? Ces calculs partaient d'un modèle d'atome lié pour l'eau, modèle avec lequel bien d'autres données neutroniques sont en accord.

A. A. CHERNISHOV (URSS): Je crains de ne pouvoir expliquer ces divergences pour l'instant. Mais je dois

* Voir les présents Actes, vol. 3.

** Référence [21] dans le mémoire.

souligner que les résultats des calculs que vous invoquez ne sont pas non plus en accord avec les résultats d'expériences faites à Harwell.

K. H. BECKURTS (République fédérale d'Allemagne): Comment tirez-vous la distribution générale de fréquence $P(\beta)$ de la loi de diffusion établie par vos mesures? Extrapolez-vous simplement les deux transferts de moment, ou procédez-vous par itération?

A. A. CHERNISHOV (URSS): Nous obtenons la fonction $P(\beta)$ d'une manière très simple, sinon très exacte, sans itération ni calculateur. La forme de $P(\beta)$ peut être précisée en calculant des sections efficaces différentielles doubles à partir de $P(\beta)$ (en tenant compte des effets de l'appareillage) et en comparant les résultats des calculs aux sections efficaces mesurées. Un tel programme de calculs est décrit dans le mémoire P/360 par L. V. Maiorov *et al.*

K. H. BECKURTS (République fédérale d'Allemagne): Votre mesure de spectre en fonction du temps est la même dans son principe que celle faite par l'équipe de M. J. Poole à Harwell. Avez-vous confronté les résultats?

A. A. CHERNISHOV (URSS): Oui. La comparaison a montré que les chiffres de Harwell étaient tous plus faibles, et d'une manière cohérente, ce qui indique des erreurs systématiques dans les mesures.

D. BALLY (Roumanie): Quel doit être le domaine de variation du coefficient de diffusion de l'eau pour expliquer l'élargissement du maximum quasi élastique avec la température que vous indiquez dans votre travail?

A. A. CHERNISHOV (URSS): Comme on le dit dans le mémoire, les mesures étaient faites avec une résolution relativement faible. Le but était d'obtenir des renseignements nécessaires aux calculs de thermalisation; on n'a pas donc spécialement analysé la diffusion quasi élastique. On peut voir d'après les courbes que l'élargissement ne dépasse jamais 10 %.

Mémoire P/858 (présenté par V. Ajdačić)

DISCUSSION

E. P. BLIZARD (Etats-Unis d'Amérique): Je note votre préoccupation à propos de réactions n-p et n-α dans le silicium dans votre spectromètre. Avez-vous étudié les avantages qui peuvent être retirés de l'emploi d'isotopes du silicium, par exemple de silicium 30, pour lesquels ces réactions seraient beaucoup moins importantes?

V. AJDAČIĆ (Yougoslavie): Nos détecteurs semiconducteurs sont des monocristaux de silicium, et il serait très coûteux de les faire en isotopes uniques.

E. P. BLIZARD (Etats-Unis d'Amérique): N'avez-vous pas d'ennuis dus à ce que le flux élevé ne reste pas dans le tube sur toute sa longueur? Avez-vous envisagé la déflexion des particules chargées par des aimants?

V. AJDAČIĆ (Yougoslavie): Nous avons utilisé un champ électrique pour la déflexion des électrons, mais nous avons trouvé que les protons et les alphas issus de réactions des neutrons sur l'aluminium formaient l'essentiel du bruit de fond. Il n'est certainement pas facile de les dévier et d'avoir quand même une méthode très simple pour des mesures de flux élevés de neutrons.

G. BEN-DAVID (Israël): Quelle est la résolution en énergie du compteur à neutrons rapides au lithium 6?

V. AJDAČIĆ (Yougoslavie): La résolution du spectromètre était d'environ 300 keV à une puissance de 2 watts. La résolution dépend de la puissance du réacteur, et la relation est indiquée à la figure 2 du mémoire.

Mémoires P/498 et P/705

Ces mémoires n'ont pas été discutés.

DISCUSSION GÉNÉRALE

P. LO IZZO (Italie): Les méthodes et les sections efficaces utilisées dans les projets de réacteurs (au moins dans la catégorie des réacteurs à eau) remontent à cinq ou dix ans. Les nouvelles méthodes sont nettement meilleures et les données nouvelles s'accumulent, mais ceux qui calculent les réacteurs ont toujours besoin d'expériences critiques pour établir un projet de réacteur vraiment nouveau. Des méthodes simples sont en fait capables de nous donner une erreur de 1 %, par exemple, sur k_{eff} — sans doute parce que certaines erreurs importantes s'annulent mutuellement — et si, pour remplacer ces méthodes, nous prenons des valeurs plus précises des sections efficaces ou une méthode plus élaborée pour le calcul d'un paramètre du réacteur, nous obtenons souvent des erreurs plus grandes. Quelqu'un pourrait-il dire avec plus de détails s'il s'agit d'un effet général et s'il existe quelque moyen d'en venir à bout?

J. S. STORY (Royaume-Uni): En ce qui concerne les remarques de M. Lo Izzo, je crois malheureusement vrai que de prime abord les méthodes de calculs plus élaborées donnent toutes trop souvent des résultats en moins bon accord avec ce que l'on attend des mesures intégrales. Néanmoins, je crois qu'il faut persévérer dans les méthodes plus élaborées, car cela peut aider à mettre en lumière des lacunes dans notre compréhension du comportement des réacteurs.

Cette idée me conduit à quelques remarques sur les problèmes d'évaluation de sections efficaces de noyaux et de traitement de ces données pour en tirer des données pour les calculs à plusieurs groupes et d'autres grandeurs dérivées destinées aux programmes compliqués de transport des neutrons des réacteurs. Le Dr Westcott a mentionné brièvement ces questions dans son mémoire (P/717), et elles sont aussi discutées avec un peu plus de détail dans le mémoire (P/168), du Royaume-Uni.

Ces dernières années, la qualité et la production des données sur les sections efficaces neutroniques de base se sont beaucoup améliorées et le taux de production s'accroît encore. Nous commençons à nous trouver en

face d'une véritable « explosion démographique » de données nouvelles. En liaison avec les progrès de la théorie du transport, cela est très satisfaisant; mais il faut un long et difficile travail pour mettre les données sous la forme exigée par les programmes de la théorie du transport. Nous avons une grande expérience pratique de ce problème au Royaume-Uni, et nous trouvons qu'il faut entre deux et six hommes-mois pour préparer un jeu complet de sections efficaces calculées pour un seul noyau ou élément; ainsi, faire ce travail pour tous les matériaux intéressant la physique des réacteurs, en tenant à jour les résultats à mesure qu'arrivent de nouvelles données, exigera un très gros effort.

Nous croyons à la nécessité d'un effort résolu et persévérant dans ce domaine, et au besoin pressant d'une collaboration internationale pour assurer à cet effort une ampleur convenable.

Протокол заседания 3.I

Новые исследования в физике реакторов

Председатель: Дж. А. Гоедкоп (Нидерланды)

Доклад P/261 (представил Дж. И. Белл)

ДИСКУССИЯ

Ш. ИФТА (Израиль): Оказывает ли поляризация ощутимое влияние на перенос нейтронов?

Дж. И. БЕЛЛ (США): Поляризацию можно легко обнаружить в экспериментах с многократным рассеянием. При двойном рассеянии пучок нейтронов поляризуется под прямым углом к плоскости первого рассеяния. При втором рассеянии будет наблюдаться асимметрия правого-левого направлений, обусловленная поляризацией, что дает возможность измерить поляризацию, вызванную рассеянием.

При наличии поляризации теория переноса фактически включает четыре величины (две сложные амплитуды для рассеяния), которые могут быть получены при помощи экспериментов с тройным рассеянием или в противном случае расчетным путем.

Перенос нейтронов в диапазоне энергий > 100 *кэв* зависит от поляризации, а поскольку поляризацию нельзя «включить» или «отключить», нет легкого способа выделить производимое поляризацией действие.

Ш. ИФТА (Израиль): Поскольку в нейтронных системах мы имеем дело с очень большой статистической плотностью, не думаете ли Вы, что действие поляризации будет иметь какое-то значение при расчетах этих систем?

Дж. И. БЕЛЛ (США): В принципе зависимость переноса нейтронов от поляризации не связана с величиной плотности нейтронов. Однако в связи с неопределенностью в полных эффективных сечениях эти уточнения не могут иметь большого практического значения.

Е. В. ОРЛОВ (СССР): Изучение влияния поляризации на процессы переноса нейтронов, рассмотренное в Вашем докладе, за последнее время приобрело большое значение, поскольку иногда эксперименты дают неожиданно большую степень поляризации нейтронов, связанную с рассеянием. Количественная оценка влияния поляризации на отражение нейтронов от различных сред была сделана П. С. Отставновым *. Впоследствии Ю. Н. Казаченков и я сформулировали кинетические уравнения для плотности потока и спина, учитывая поляризацию нейтронов, вызванную спинорбитальным взаимодействием во время рассеяния, а также диффузионные приближения.

В связи с первым вопросом г-на Ифта я бы хотел заявить, что на основе экспериментальных данных мы вычислили изменения коэффициента диффузии нейтронов под действием поляризации. Для тяжелых ядер и энергий нейтронов $E \approx 1$ *Мэв* $\frac{\delta D}{D} = -(1 \div 2)\%$, для ядер магния и кремния при энергии нейтронов $E \approx 20$ *кэв* $\frac{\delta D}{D} \approx -(10 \div 20)\%$. Реферат этой работы опубликован в журнале «Атомная наука и техника». Разница в этих значениях может быть обусловлена изменением знака поляризации для рассеяния при углах, которые соответствуют экстремумам в дифференциальных сечениях. Этим можно объяснить уменьшение в поправке на поляризацию для нейтронов с большим орбитальным моментом.

Дж. И. БЕЛЛ (США): Ваши замечания весьма интересны, но тот эффект, о котором Вы говорили, удивляет меня. Возможно, при таком положении дел я смог бы сделать некоторое добавление к тем сведениям, которые содержатся в моем докладе.

Анизотропное рассеяние в настоящее время поддается обработке разложением ядра рассея-

* Атомная энергия, *14*. 487 (1963),

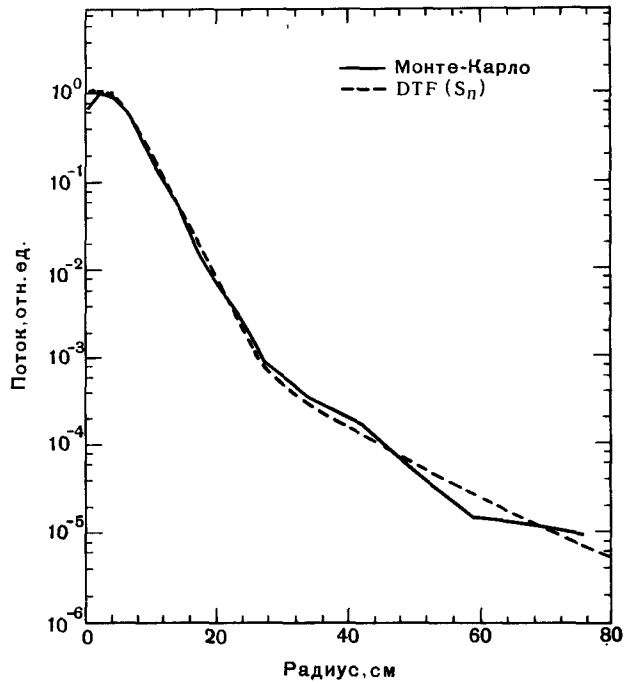

ния (передаточная функция) в ряд полиномов Лежандра при рассеянии под углом. Например, новая программа DTF является программой, основанной на языке FORTRAN, использующей дискретный метод S_n (DSN), который дает возможность разложить ядро рассеяния для пластин и сфер на полиномы Лежандра до десятого порядка. Фактически для расчетов критичности обычно достаточно разложение до второго порядка, но при расчетах прохождения γ-лучей через толстые слои использовалось разложение до пятого порядка или выше; полученные результаты хорошо согласуются с результатами, полученными методом Монте-Карло.

В качестве примера такого сравнения результатов, полученных методами S_n и Монте-Карло, давайте рассмотрим результаты, представленные на рис. 1. Источник γ-квантов с энергией 2 *Мэв* представляет собой сферическую область радиусом 7,74 *см*, содержащую уран, железо и натрий. Он окружен железной сферой радиусом 29,5 *см*, а затем графитовой радиусом 50 *см*. На рисунке показан поток γ-квантов в диапазоне энергий от 1 до 1.25 *Мэв*, вычисленный с использованием метода Монте-Карло и методом S_n с программой DTF, с разложением в P_5-приближении ядра рассеяния и квадратурной схемы в двойном P_7-приближении для углового потока. Мы видим, что результаты, полученные методом S_n и методом Монте-Карло, согласуются в пределах статистической точности последнего метода. Разложение на полиномы в P_3-приближении функции рассеяния также дает значения потоков, которые в этом масштабе не отличаются от результатов, полученных в P_5-приближении.

Только что закончена серия расчетов критической толщины пластины при анизотропном рассеянии, которые можно сравнить с результатами, полученными при помощи двух совершенно различных методов. Расчеты были выполнены Леонардом методом, использующим сингулярное интегральное уравнение переноса, и Латропом при помощи программы DTF с квадратурной схемой в двойном P_7-приближении, которая для пластин эквивалентна методу дискретных ординат с 16 направлениями. Расчеты в односкоростном приближении были выполнены с функцией анизотропного рассеяния, имеющего ту же угловую зависимость, как и упругое рассеяние на атомах водорода. Для этой задачи может быть записано уравнение переноса

$$\mu \frac{\partial \Psi(x, \mu)}{\partial x} + \Psi(x, \mu) = c' \int_{-1}^{1} \Psi(x, \mu')\, \partial\mu' + c \sum_{n=0}^{2} \frac{2n+1}{2} b_n P_n(\mu) \int_{-1}^{1} P_n(\mu')\, \Psi(x, \mu')\, d\mu',$$

где $b_0 = 1$; $b_1 = 2/3$; $b_2 = 1/4$.

Таким образом, c' и c являются коэффициентами соответственно изотропной и неизотропной частей рассеяния. Мы сохраним только два члена в функции рассеяния. Заметим, что b_2 оказывает незначительное влияние на результат, в то время как для водорода $b_3 = 0$, а b_4 (равным—1/24) можно для настоящих целей пренебречь.

В сингулярной интегральной теории переноса первое приближение при определении критической толщины составляет

$$\tau_0 = \pi [\nu_0] - 2Z_0,$$

где ν_0 — собственное дискретное значение уравнения Больцмана, а Z_0 — расстояние экстраполяции, соответствующее анизотропному рассеянию. Этот результат, таким образом, идентичен результатам по теории граничных точек, так он и обозначен в таблице. Итеративная схема может быть записана следующим образом:

$$\tau_n = \pi |\nu_0| - 2Z_0 - R(\tau_{n-1}),$$
$$n = 0, 1, \ldots; R(\tau_{-1}) = 0,$$

где R — довольно сложный функционал функций, которые удовлетворяют уравнению Фредхольма.

В табл. 1, приведены значения критической полутолщины для различных значений c и c'. Значок P_1 означает, что при разложении функции рассеяния использовались члены вплоть до $P_1(\mu)$, в то время как значок P_2 означает, что член $P_2(\mu)$ также включен. Точные значения — это значения, определенные Леонардом

Табл. 1. Критическая полутолщина пластины

c	P_1	$P_{1\text{точн}}$	$P_{1\text{гран. тчк}}$	$P_{2\text{DTF}}$	$P_{2\text{точн}}$	$P_{2\text{гран. тчк}}$
			$c+c'=1{,}05$			
0,1	3,39225	3,39216	3,39216	3,39042	3,39032	3,39032
0,3	3,60356	3,60346	3,60346	3,59724	3,59714	3,59714
0,5	3,86368	3,86358	3,86358	3,85135	3,85126	3,85126
0,7	4,19568	4,19558	4,19558	4,17506	3,17495	4,17495
0,9	4,64212	4,64203	4,64203	4,60935	4,60927	4,60927
			$c+c'=1{,}10$			
0,1	2,16524	2,16519	2,16525	2,16311	2,16306	2,16313
0,3	2,28290	2,28285	2,28291	2,27558	2,27553	2,27559
0,5	2,42452	2,42447	2,45452	2,41031	2,41026	2,41033
0,7	2,59999	2,59994	2,59998	2,57637	2,57632	2,57639
0,9	2,82629	2,82625	2,82628	2,78923	2,78917	2,78954
			$c+c'=1{,}20$			
0,1	1,31521	1,31519	1,31567	1,31299	1,31296	1,31347
0,3	1,37256	1,37254	1,37308	1,36498	1,36496	1,36558
0,5	1,43939	1,43935	1,43997	1,42486	1,42484	1,42561
0,7	1,51884	1,51882	1,51948	1,49506	1,49505	1,49604
0,9	1,61576	1,61575	1,61646	1,57930	1,57929	1,58061
			$c+c'=1{,}30$			
0,1	0,95354	0,95352	0,95473	0,95142	0,95140	0,95266
0,3	0,98811	0,98810	0,98955	0,98098	0,98096	0,98262
0,5	1,02747	1,02746	1,02922	1,01398	1,01339	1,01621
0,7	1,07292	1,07291	1,07507	1,05123	1,05127	1,05439
0,9	1,12636	1,12635	1,12903	1,09382	—	—
			$c+c'=1{,}40$			
0,1	0,74726	0,74727	0,74930	0,74532	0,74529	0,74743
0,3	0,77031	0,77032	0,77288	0,76381	0,76378	0,76669
0,5	0,79607	0,79606	0,79936	0,78393	0,78396	0,78800
0,7	0,82519	0,82519	0,82948	0,80595	0,80610	0,81199
0,9	0,85853	0,85853	0,86424	0,83022	—	—

итерацией, исходя из значений, полученных по теории граничных точек.

Из таблицы видно, что значения, полученные методом DTF(S_n), и точные значения отличаются только в четвертом или пятом десятичном знаке. Такие незначительные расхождения не могут иметь значения. Значения граничных точек удовлетворительны до тех пор, пока $c+c'$ не становится большим, что согласуется с результатами для изотропного рассеяния. Видно, что действие члена $P_2(\mu)$ составляет от одного до трех процентов для $c=0{,}9$; это действие, конечно, больше для небольших пластин, где анизотропия потока больше.

Время расчета по программе DTF и итеративным методом было одинаково — около 1 *мин* на решение задачи на машине IBM-7094. Программу DTF можно немедленно приложить к решению многогрупповых — многообластных проблем, а итеративный метод нельзя.

Наконец, мне бы хотелось рассказать о результатах исследований влияния поляризации на перенос нейтронов, проведенных д-ром В. Годом и мною в Лос-Аламосе. В обычной теории переноса нейтрон рассматривается как точечная частица, которая полностью описывается своим положением и скоростью. Но фактически нейтрон имеет спин, и эксперименты, проведенные особенно за последние несколько лет, показали, что спин заметно влияет на рассеяние нейтронов на различных ядрах при скорости нейтронов большей или около 100 *кэв*. Пучок неполяризованных нейтронов (то есть пучок нейтронов, спин которых не имеет предпочтительного направления) при рассеянии (на неполяризованной мишени) поляризуется (то есть приобретает предпочтительное направление спина), и эта поляризация будет влиять на следующее рассеяние. Таким образом, между рассеяниями проводится новая корреляция, и это будет влиять на перенос нейтронов. Поляризация, обусловленная первым рассеянием, составляет обычно десятки процентов для нейтронов с энергией порядка мегаэлектронвольт или выше, и это влияние объясняется спин-орбитальным членом в энергии итерации нейтрон—ядро.

Мы сформулировали теорию переноса для нейтронов со спином для случая, когда рассеяние больше не описывается дифференциальным сечением, а двумя сложными амплитудами рассеяния и когда состояние пучка нейтронов определяется не плотностью нейтронов, а вектором поляризации (или матрицей плотности спина). Для плоской или сферически симметричной геометрии, где есть ось симметрии для направлений распространения нейтронов, найдено, что вектор поляризации будет направлен всегда под прямым углом к плоскости, содержащей ось симметрии и вектор направления распространения нейтронов. Тогда можно определить плотность нейтронов из двух соединенных скалярных уравнений переноса для плотности нейтронов $\bar{n}$ и плотности поляризации $\bar{n}p$. Если допустить, что $\bar{n}(x, \theta) = \bar{n}_0(x) + 3\cos\theta\, j(x)$, как в теории диффузии, то $\bar{n}p \sim j(x)\sin\theta$. Здесь θ является обычным углом между осью симметрии и направлением распространения нейтронов. Кроме того, в этом приближении действие поляризации на перенос нейтронов равно увеличению сечения переноса. Для материалов, которые мы испытали, это увеличение небольшое, обычно порядка 1%, и, таким образом, меньше, чем неточности экспериментальных эффективных сечений. Однако мы чувствуем удовлетворение от того, что у нас теперь есть обоснованная причина пренебречь действием поляризации, по крайней мере в практических случаях.

Доклад P/263 (представил Р. Дж. Люс)

ДИСКУССИЯ

Дж. М. ДОДЕРЛАЙН (Норвегия): Не можете ли Вы нам посоветовать эффективную и удобную программу для расчетов на вычислительной машине с применением малогрупповой теории двухмерной диффузии, написанную на 90—100% на языке FORTRAN?

Р. Дж. ЛЮС (США): Таких программ несколько. Одна из них, которая применяется в нашей лаборатории, не полностью написана на языке FORTRAN: это программа KARE.

Другие программы полностью написаны на языке FORTRAN.

Доклад P/717 (представил С. Х. Уэсткотт)

ДИСКУССИЯ

Дж. ЧЕРНИК (США): Не объясните ли Вы, в какой мере данные, полученные в процессе интегральных экспериментов, и в частности в процессе экспериментов с марганцевыми ваннами, использовались при измерении данных для нейтронов со скоростью 2200 *м/сек*?

С. Х. УЭСТКОТТ (МАГАТЭ): Результаты интегральных экспериментов использовались только в том случае, если они опубликовывались или привлекали внимание нашей группы и были достаточно документированы. Например, было необходимо описать спектр нейтронов для прямого и ясного объяснения величин, соответствующих нейтронам со скоростью 2200 *м/сек*. В нашу работу включены результаты измерений в ваннах, проведенных в Окридже.

Дж. ЧЕРНИК (США): Результаты последних критических экспериментов в Англии и США говорят о том, что для нейтронов со скоростью 2200 *м/сек* значение η для Pu^{239} несколько меньше подсчитанного Вами значения 2,123. Не должны ли данные такого типа учитываться при оценке сечения захвата нейтронов и включаться в Ваш анализ?

С. Х. УЭСТКОТТ (МАГАТЭ): В нашу работу включены также результаты измерений критичности, проведенных Гвином и Магнуссоном, и я не припоминаю, что есть более новая опубликованная работа. Однако я должен добавить, что погрешности при всех измерениях максвелловского спектра увеличены за счет того, что сюда включена погрешность при вычислении g-фактора, применяемого при преобразовании постоянных величин для нейтронов со скоростью 2200 *м/сек*.

Дж. И. САНДЕРС (Великобритания): В связи с замечанием д-ра Черника относительно величины η для Pu^{239} мне бы хотелось отметить, что эксперименты, проведенные в Англии, для U^{235} и Pu^{239} и водяного и графитового замедлителей подтверждают более высокое значение η для Pu^{239}, предлагаемое д-ром Уэсткоттом в его последнем обзоре. Этот вывод сделан Аскью и Сандерсом в докладе P/165*.

Дж. ЧЕРНИК (США): Да, но данные, полученные в Англии, о которых Аскью и Сандерс сообщают в докладе P/165, предполагают увеличение значения η для Pu^{239} на 1%, которое они раньше и применяли (2,088), что в результате дает величину немного меньше, чем 2,11.

* Настоящее издание, т. 3

Доклад P/73 (представил М. Кадилак)

ДИСКУССИЯ

Дж. Р. БЕЙСТЕР (США): Мой вопрос касается применимости Вашей второй модели. После того как Вы подбираете значения для функций G и H, как Вы определяете диапазон температур, степень отравления, типы резонансного поглотителя и степень утечки, к которым будут применяться эти значения?

М. КАДИЛАК (Франция): Ценность модели все еще подлежит обобщенному изучению. Мы отметили наличие хорошего соответствия в известных тщательно подобранных случаях, которые являются довольно показательными для нормальных условий, чтобы мы могли убедиться в том, что эта модель не может оказаться плохой за очень редким исключением. Во всяком случае это справедливо для длительного периода работы, хотя мы и не знаем, может ли эта модель применяться для решения проблем, связанных с нейтронными импульсами.

Доклад P/367 (представил А. А. Чернышев)

ДИСКУССИЯ

Дж. Р. БЕЙСТЕР (США): Как Вы объясните несоответствие между спектрами нейтронов в уран-водных решетках, измеренными Вами экспериментально и с помощью расчетов, сделанных Хонеком и Такахаши [21]? Эти расчеты основаны на модели связанного атома для воды, и с ними согласуются многие другие данные.

А. А. ЧЕРНЫШЕВ (СССР): Боюсь, что в данный момент я не смогу объяснить это расхождение. Однако я должен указать на то, что результаты расчетов, на которые Вы ссылаетесь, не соответствуют экспериментальным результатам, полученным также и в Харуэлле.

К. Х. БЕКУРТС (ФРГ): Как Вы выводите распределение обобщенного частотного спектра $P(\beta)$ на основании закона рассеяния? Вы экстраполируете переносы двух импульсов или пользуетесь методом итераций?

А. А. ЧЕРНЫШЕВ (СССР): Мы весьма просто, но не очень точно, пользуемся функцией $P(\beta)$ и не прибегаем к методу итерации или к расчетам на вычислительной машине. Функции $P(\beta)$ можно придать более точную форму путем расчета дважды дифференциальных сечений из $P(\beta)$ (с учетом приборных эффектов) и путем сравнения этих расчетов с измеренными сечениями. Программа таких расчетов описывается Л. В. Майоровым и др. в докладе P/360.

К. Х. БЕКУРТС (ФРГ): Ваше измерение спектра в зависимости от времени в основном то же, что и проведенное группой Пула в Харуэлле. Вы сравнивали результаты?

А. А. ЧЕРНЫШЕВ (СССР): Да. Сравнение показало, что значения, полученные в Харуэлле, гораздо ниже. Это говорит о наличии определенных систематических погрешностей в измерениях.

Д. БАЛЛИ (Румыния): Каков должен быть диапазон изменения коэффициента диффузии для воды, чтобы объяснить уширение пика квазиупругого рассеяния с изменением температуры, как это упоминается в Вашем докладе?

А. А. ЧЕРНЫШЕВ (СССР): Как отмечается в докладе, измерения проводились при относительно низком разрешении; цель заключалась в получении данных, необходимых для расчета термализации. Поэтому квазиупругое рассеяние специально не анализировалось. Из кривых видно, что уширение никогда не превышало 10%.

Доклад P/858 (представил В. Айдачич)

ДИСКУССИЯ

Э. П. БЛИЗАРД (США): Я обратил внимание, что Вы интересуетесь реакциями (n,p) и (n,α) в кремнии при исследованиях на Вашем спектрометре. Изучили ли Вы преимущества, которые получаются при использовании изотопов кремния, таких как Si^{30}, для которых эти реакции были бы менее важными?

В. АЙДАЧИЧ (Югославия): В наших полупроводниковых детекторах используются монокристаллы кремния, и было бы очень дорого получать их из отдельных изотопов.

Э. П. БЛИЗАРД (США): Не имели ли Вы затруднений с сильным потоком, выходящим из длинной трубки? Рассматривали ли возможность отклонения заряженных частиц с помощью магнитов?

В. АЙДАЧИЧ (Югославия): Мы использовали для отклонения электронов электрическое поле, но установили, что протоны и α-частицы от нейтронных реакций на алюминии образовали большую часть фона. Конечно, их нелегко отклонить и, кроме того, нет очень простого метода измерений сильных нейтронных потоков.

Д. БЕН-ДАВИД (Израиль): Какой разрешающей способностью по энергии обладает счетчик быстрых нейтронов на Li^6?

В. АЙДАЧИЧ (Югославия): Разрешающая способность спектрометра составляет около 30 *кэв* при мощности 2 *вт*. Разрешающая способность зависит от мощности реактора. Эта зависимость приводится на рис. 2 доклада.

Доклад P/498 и доклад P/705

Дискуссии по этим докладам не было.

ОБЩАЯ ДИСКУССИЯ

П. ЛОИЦЦО (Италия): Методы и данные по сечениям, используемые проектировщиками реакторов (по крайней мере в области водяных реакторов), имеют 5—10-летнюю давность. Новые методы значительно лучше, и продолжают накапливаться новые данные, однако проектировщики реакторов всегда нуждаются в критических экспериментах для конструирования действительно нового реактора. Простые методы фактически могут дать погрешность в $k_{эфф}$ порядка 1%, вероятно, потому, что некоторые большие погрешности аннулируют друг друга, и если мы подставим более точные значения сечений или используем более усложненный метод расчета параметров реактора, то часто получаем большие погрешности. Может ли кто-нибудь объяснить, является ли это общим явлением и существует ли путь преодоления его?

Дж. С. СТОРИ (Соединенное Королевство): Относительно замечаний г-на Лоиццо мне хочется сказать, что, к сожалению, это действительно справедливо, что сначала все более усложненные методы расчета слишком часто дают результаты, плохо согласующиеся с результатами, ожидаемыми от интегральных измерений. Тем не менее я полагаю, что следует продолжать заниматься более усложненными методами, так как это может помочь восполнить недостаток в нашем понимании поведения реактора.

Эта точка зрения заставила меня сделать несколько замечаний по проблемам оценки данных по ядерным сечениям и обработки этих данных с целью получения многогрупповых данных и других производных величин для использования их в программах исследования переноса нейтронов в более сложных реакторах. Д-р Уэсткотт кратко упомянул об этих вопросах в своем докладе P/717; более подробно они также рассматриваются в докладе P/168, представленном Великобританией.

За последние несколько лет значительно улучшились качество и количество данных по основным нейтронным сечениям, и поток этих данных непрерывно растет. Мы начинаем сталкиваться с массовым поступлением новых данных. Так же как и успехи в теории переноса, это явление весьма отрадно, но получение данных в формах, необходимых для программ по теории переноса, требует проведения большого количества трудоемкой работы. В Великобритании накоплен значительный практический опыт по решению этой проблемы, и мы установили, что для подготовки полного комплекта подсчитанных сечений для одного изотопа или элемента требуется от двух до шести человекомесяцев. Таким образом, чтобы проделать эту работу по всем материалам, представляющим

интерес с точки зрения физики реактора, при обеспечении оценки на уровне современных требований по мере поступления новых данных потребуются значительные усилия.

Мы считаем, что в этой области необходимы решительные и настойчивые усилия, для обеспечения которых необходимо международное сотрудничество.

Acta de la sesión 3. 1

Adelantos en física de reactores

Presidente: J. A. Goedkoop (Países Bajos)

Documento P/261 (presentado por G. I. Bell)

DISCUSIÓN

Sh. YIFTAH (Israel): ¿ Da lugar la polarización a algún efecto medible sobre el transporte de neutrones?

G. I. BELL (Estados Unidos de América): Es fácil detectar efectos de polarización en experimentos de dispersión múltiple. En un experimento de dispersión doble, un haz de neutrones adquirirá una polarización perpendicular al plano de la primera dispersión. En la segunda dispersión so observará una asimetría entre derecha e izquierda que es consecuencia de la polarización y permite su medida. Cuando se tiene en cuenta la polarización, la teoría del transporte entraña cuatro magnitudes (dos amplitudes complejas de dispersión), que pueden obtenerse mediante un experimento de dispersión triple o por cálculo.

El transporte de neutrones en el intervalo de energías > 100 keV depende de la polarización pero, como ésta no puede ser manejada a voluntad, no resulta fácil separar su contribución.

Sh. YIFTAH (Israel): En sistemas de neutrones manejamos estadísticamente poblaciones muy numerosas, ¿cree usted, por lo tanto, que los efectos de polarización pueden tener importancia para los cálculos de estos sistemas?

G. I. BELL (Estados Unidos de América): En principio, la dependencia del transporte de neutrones respecto de la polarización no tiene que ver con el tamaño de la población de neutrones. Sin embargo, puede que estos refinamientos no sean de mucha importancia práctica debido a las incertidumbres en las secciones eficaces totales.

E. V. ORLOV (URSS): El estudio de los efectos de polarización sobre los procesos de transporte de neutrones, tal como aparece en su artículo, ha adquirido recientemente gran importancia ya que algunos experimentos indican, como resultado de la dispersión, un grado de polarización de los neutrones superior a lo esperado. P. S. Otstavnov * ha expuesto cualitativamente los efectos de polarización sobre la reflexión de neutrones en diferentes medios. Posteriormente Y. N. Kazachenkov y yo hemos formulado ecuaciones cinéticas en la aproximación de difusión para la densidad de flujo y de spin, teniendo en cuenta la polarización causada por la interacción spin-órbita durante la dispersión.

Con referencia a la primera pregunta del Sr. Yiftah, me gustaría indicar que, utilizando datos experimentales, hemos estimado los cambios en el coeficiente D de difusión de neutrones, debidos a efectos de polarización. Para núcleos pesados y energías neutrónicas E del orden de 1 MeV, $\delta D/D \approx -(1 \text{ a } 2)\%$; para núcleos de Mg y Si y energías neutrónicas de unos 20 keV, $\delta D/D \approx -(10 \text{ a } 20)\%$. Un resumen de este trabajo ha sido publicado en *Atomnaya Nauka i Tekhnika*. Las diferencias en estos valores pueden deberse al cambio de signo de la polarización para ángulos correspondientes a los valores extremos de la sección eficaz diferencial. Esto puede explicar la disminución en la corrección de polarización para neutrones de momento orbital elevado.

G. I. BELL (Estados Unidos de América): Sus comentarios son muy interesantes y me sorprende el fuerte efecto que usted ha mencionado. Quizás debería aprovechar la ocasión para añadir unos comentarios a la información contenida en mi artículo.

Usualmente la dispersión anisótropa se trata desarrollando el núcleo de dispersión (función de transferencia) en serie de polinomios de Legendre del ángulo de dispersión. Por ejemplo, el nuevo código DTF es un código FORTRAN que utiliza el método discreto S_n (DSN) y que para láminas y esferas permite un desarrollo de Legendre de hasta diez términos del núcleo de dispersión. Realmente son suficientes dos términos del desarrollo para cálculos de criticidad pero en cambio para calcular la penetración de rayos γ a través de grandes espesores se han usado cinco o más términos, obteniéndose excelente acuerdo con los resultados dados por el método de Monte Carlo. Como ejemplo de tal comparación entre los métodos S_n y de Monte Carlo, consideremos los resultados de la figura 1. Una fuente gamma de 2 MeV se distribuyó en

* Atomnaya Energia, *14*, 487, Moscú (1963).

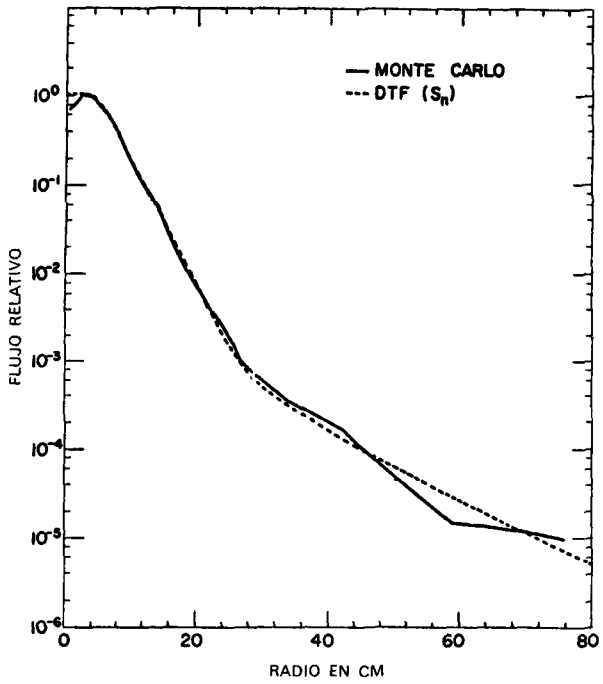

Figura 1

una región esférica de radio 7,74 cm que contenía uranio, hierro y sodio. Fuera de ella había principalmente hierro hasta un radio de 29,5 cm, seguido de 50 cm de grafito. La figura muestra el flujo gamma entre 1 y 1,25 MeV calculado mediante el código de Monte Carlo SAGE y mediante el código S_n DTF con un desarrollo P_5 del núcleo de dispersión y cuadratura P_7 doble para el flujo angular. Se utilizaron 16 direcciones discretas para las gammas en el P_7 doble. Se observa que la concordancia entre los resultados S_n y Monte Carlo cae dentro, más o menos, de la incertidumbre estadística de este último método. Un desarrollo P_3 da también flujos que son indistinguibles de los correspondientes a P_5.

Se acaba de terminar una serie de cálculos de espesores críticos de láminas con dispersión anisótropa que proporciona una comparación interesante de los resultados obtenibles con dos métodos completamente diferentes. Los cálculos fueron hechos por Leonard, quien usó el método de la ecuación integral singular, y por Lathrop utilizando el código DFT con el esquema de la cuadratura P_7 doble, que para láminas es equivalente a un método de ordenadas discretas con 16 direcciones. Los cálculos en la aproximación de velocidad constante, se efectuaron con una función de dispersión anisótropa que tenía la misma dependencia angular que la dispersión elástica en hidrógeno. La ecuación de transporte para el problema puede escribirse:

$$\mu \frac{\partial \psi(x,\mu)}{\partial x} + \psi(x,\mu) =$$

$$c' \int_{-1}^{1} \psi(x,\mu')\mathrm{d}\mu' + c \sum_{n=0}^{2} \frac{2n+1}{2} b_n P_n(\mu) \int_{-1}^{1} P_n(\mu')\psi(x,\mu')\mathrm{d}\mu'$$

donde $b_0 = 1$, $b_1 = 2/3$, $b_2 = 1/4$.

Así pues, c' y c son, respectivamente, los coeficientes de la partes isótropa y anisótropa de la dispersión. Hemos conservado solamente dos términos en la función de dispersión. Se notará que b_2 tiene un efecto relativamente pequeño sobre el resultado, mientras que para hidrógeno b_3 y b_4 (que valen: cero y $-1/24$, respectivamente) pueden ignorarse para nuestro propósito.

En la teoría de la integral singular, una primera aproximación para el espesor crítico es

$$\tau_0 = \pi |\nu_0| - 2Z_0$$

donde ν_0 es el autovalor discreto de la ecuación de Boltzmann y Z_0 es la distancia extrapolada correspondiente a dispersión anisótropa. Este resultado es, por tanto, formalmente idéntico al de la teoría del punto límite y se designa de este modo en la tabla 1. El esquema iterativo puede escribirse

$$\tau_n = \pi |\nu_0| - 2Z_0 - R(\tau_{n-1})$$
$$n = 0,1, \ldots, \text{y } R(\tau_{-1}) = 0$$

donde R es una funcional relativamente complicada de funciones que satisfacen ecuaciones de Fredholm.

En la tabla 1 se dan los semiespesores críticos para diferentes valores de c y c'. En las columnas encabezadas con P1 sólo se incluyeron en la función de dispersión los términos hasta el $P_1(\mu)$ mientras que en las encabezadas con P2 se incluyó tambien el término $P_2(\mu)$. Los valores exactos son los que obtuvo Leonard mediante iteración a partir de los valores del método del punto límite.

En la tabla se ve que los valores DFT (S_n) y los exactos difieren sólo en la cuarta o quinta cifra decimal. Puede que diferencias tan pequeñas no sean significativas. Los valores del método del punto límite son excelentes hasta que $c + c'$ se hace grande, de acuerdo con las experiencias de dispersión isótropa. Se ve que el efecto del término $P_2(\mu)$ es de uno a tres por ciento para $c = 0,9$ y naturalmente mayor para láminas delgadas en las que la anisotropía del flujo es mayor.

Los tiempos de cálculo para el programa DTF y para el método iterativo fueron similares (alrededor de un minuto para cada problema en la IBM 7094). El programa DTF es inmediatamente aplicable a problemas más complicados con múltiples regiones y grupos, mientras que el método iterativo no lo es.

Para terminar, me gustaría describir los resultados de un estudio de los efectos de polarización sobre el transporte de neutrones que acabamos de realizar en Los Alamos el Dr. Walter Goad y yo. En la teoría de transporte convencional, un neutrón se trata como una partícula puntual que queda completamente descrita por su posición y velocidad. En realidad el neutrón tiene spin y la experiencia (especialmente en los últimos años) ha demostrado que tiene una influencia notable sobre la dispersión de neutrones por la mayoría de los núcleos a energías mayores que cien keV aproximadamente. Un haz de neutrones no polarizado (es decir: sin dirección preferente del spin) emergerá polarizado (es decir: su spin adquirirá una dirección

Tabla 1. Semiespesores críticos para láminas (mfp)

c	$P1_{DTF}$	$P1_{exacto}$	$P1_{punto\ límite}$	$P2_{DTF}$	$P2_{exacto}$	$P2_{punto\ límite}$
			$c+c'=1{,}05$			
0,1 . .	3,39225	3,39216	3,39216	3,39042	3,39032	3,39032
0,3 . .	3,60356	3,60346	3,60346	3,59724	3,59714	3,59714
0,5 . .	3,86368	3,86358	3,86358	3,85135	3,85126	3,85126
0,7 . .	4,19568	4,19558	4,19558	4,17506	4,17495	4,17495
0,9 . .	4,64212	4,64203	4,64203	4,60935	4,60927	4,60927
			$c+c'=1{,}10$			
0,1 . .	2,16524	2,16519	2,16525	2,16311	2,16306	2,16313
0,3 . .	2,28290	2,28285	2,28291	2,27558	2,27553	2,27559
0,5 . .	2,42452	2,42447	2,42452	2,41031	2,41026	2,41033
0,7 . .	2,59999	2,59994	2,59998	2,57637	2,57632	2,57639
0,9 . .	2,82629	2,82625	2,82628	2,78923	2,78917	2,78924
			$c+c'=1{,}20$			
0,1 . .	1,31521	1,31519	1,31567	1.31299	1,31296	1,31347
0,3 . .	1,37256	1,37254	1,37308	1,36498	1,36496	1,36558
0,5 . .	1,43939	1,43935	1,43997	1,42486	1,42484	1,42561
0,7 . .	1,51884	1,51882	1,51948	1,49506	1,49505	1,49604
0,9 . .	1,61576	1,61575	1,61646	1,57930	1,57929	1,58061
			$c+c'=1{,}30$			
0,1 . .	0,95354	0,95352	0,95473	0,95142	0,95140	0,95266
0,3 . .	0,98811	0,98810	0,98955	0,98098	0,98096	0,98262
0,5 . .	1,02747	1,02746	1,02922	1,01398	1,01399	1,01621
0,7 . .	1,07292	1,07291	1,07507	1,05123	1,05127	1,05439
0,9 . .	1,12636	1,12635	1,12903	1,09382	—	—
			$c+c'=1{,}40$			
0,1 . .	0,74726	0,74727	0,74930	0,74532	0,74529	0,74743
0,3 . .	0,77031	0,77032	0,77288	0,76381	0,76378	0,76669
0,5 . .	0,79607	0,79606	0,79936	0,78393	0,78396	0,78800
0,7 . .	0,82519	0,82519	0,82948	0,80595	0,80610	0,81199
0,9 . .	0,85853	0,85853	0,86424	0,83022	—	—

preferente) de una dispersión por un blanco no polarizado y esa polarización afectará la dispersión siguiente. Se introduce así una nueva correlación entre dispersiones que debe afectar el transporte de neutrones. La polarización inducida por la primera dispersión es, en casos típicos, de decenas de tantos por ciento para neutrones con energías del orden del MeV y el efecto se explica mediante un término spin-órbita en la energía de interacción del neutrón con el núcleo.

Hemos formulado una teoría de transporte para neutrones con spin donde la dispersión ya no se describe por una sección eficaz diferencial sino por dos amplitudes de dispersión complejas y donde el estado del haz de neutrones se especifica no sólo por la densidad de neutrones sino tambien por el vector de polarización (o matriz densidad de spin). Para geometría plana o con simetría esférica, donde hay un eje de simetría para las direcciones de los neutrones, se encontró que el vector polarización es siempre perpendicular al plano que contiene el eje y la dirección del neutrón. La población de neutrones puede determinarse a partir de dos ecuaciones escalares de transporte acopladas para la densidad $\bar{n}$ de neutrones y la densidad de polarización $\overline{np}$. Si admitimos que $\bar{n}(x,\theta)=n_0(x)+3\cos\theta\, j(x)$ como en teoría de difusión, entonces $\overline{np}\sim j(x)$ sin θ. Como siempre, θ es el ángulo entre el eje de simetría y la dirección del neutrón. Por otra parte en esta aproximación, el efecto de la polarización sobre el transporte de neutrones equivale simplemente a un incremento en la sección eficaz de transporte. Para los materiales que hemos examinado el incremento no es grande, siendo en casos típicos del orden de 1 %, y por tanto inferior a la incertidumbre en los valores experimentales de las secciones eficaces. Sin embargo creemos que es satisfactorio el disponer ahora de una razón sólida para despreciar efectos de polarización, al menos en la mayoría de los casos prácticos.

Documento P/263 (presentado por R. G. Luce)

DISCUSIÓN

J. M. Döderlein (Noruega): ¿Puede usted aconsejarnos sobre un código de cálculo cómodo y eficiente en teoría de difusión bidimensional empleando unos pocos grupos y que esté escrito un 90 o un 100 % en lenguaje FORTRAN?

R. G. Luce (Estados Unidos de América): Hay varios. El usado en nuestro laboratorio no está enteramente en lenguaje FORTRAN; es el código KARE. Otros están completamente en FORTRAN.

Documento P/717 (presentado por C. H. Westcott)

DISCUSIÓN

J. CHERNICK (Estados Unidos de América): ¿Querría usted indicar hasta qué punto se han utilizado datos de experimentos integrales y en particular los del baño de Mn para llegar a sus estimaciones de datos nucleares a 2200 m/s?

C. H. WESTCOTT (OIEA): Se incluyeron solamente los resultados de experimentos integrales que habían sido publicados o presentados a la atención de nuestro grupo y suficientemente documentados; por ejemplo, era necesaria una descripción del espectro que permitiese una interpretación directa y sin ambigüedad en términos de constantes a 2200 m/s. Las medidas en baños de Mn de Oak Ridge fueron incluídas en nuestro estudio.

J. CHERNICK (Estados Unidos de América): Los resultados de experimentos críticos recientes en el Reino Unido y en los Estados Unidos indican que el valor de η para ^{239}Pu es algo menor que su estimación de 2,123. ¿No deberían utilizarse datos de este tipo en la evaluación de las secciones eficaces y ser incluidos en su análisis?

C. H. WESTCOTT (OIEA): Las medidas de criticidad de Gwin y Magnusson también se incluyeron en nuestro estudio y yo no recuerdo ningún trabajo publicado más recientemente. Sin embargo debo añadir que los errores estimados de todas las medidas efectuadas con un espectro maxwelliano se incrementaron para incluir el error estimado del factor g utilizado para convertir las constantes correspondientes en los valores a 2200 m/s.

J. E. SANDERS (Reino Unido): Con referencia al comentario del Dr. Chernick sobre la η del ^{239}Pu me gustaría indicar que los experimentos en el Reino Unido sobre combustibles de ^{235}U y ^{239}Pu en moderadores de H_2O y grafito apoyan el valor más alto de η para ^{239}Pu sugerido por la nueva revisión del Dr. Westcott. A esta conclusión se llega en el documento P/165 de Askew y Sanders *.

J. CHERNICK (Estados Unidos de América): Sí, pero los datos británicos publicados en el documento P/165 de Askew y Sanders sugieren un incremento de 1 % en el valor de η para ^{239}Pu que ellos habían estado utilizando previamente (2,088) y esto conduce a un valor ligeramente inferior a 2,11.

Documento P/73 (presentado por M. Cadilhac)

DISCUSIÓN

J. R. BEYSTER (Estados Unidos de América): Mi pregunta se refiere al margen de aplicabilidad de su modelo secundario. Una vez que usted ha obtenido un ajuste para las funciones G y H, ¿cómo conoce el intervalo de temperatura, el grado de envenenamiento, los tipos de absorbente de resonancia y el grado de escape a los que se aplicará dicho ajuste?

M. CADILHAC (Francia): Todavía está sin hacer el estudio general de la validez del modelo. Hemos observado una buena concordancia en ciertos casos cuidadosamente seleccionados, que eran suficientemente representativos en situaciones normales para convencernos de que el modelo no puede ir del todo mal excepto en casos muy excepcionales. De todos modos esto es cierto para régimen estacionario pero no sabemos si el modelo se puede usar en problemas con fuentes pulsadas de neutrones.

Documento P/367 (presentado por A. A. Chernishov)

DISCUSIÓN

J. R. BEYSTER (Estados Unidos de América): ¿Cómo explica usted la discrepancia entre sus espectros experimentales de neutrones en redes de agua y uranio y los cálculos de Honeck y Takahashi*? Los cálculos de estos últimos autores se basan en un modelo de átomos ligados para el agua, con el que están de acuerdo muchos otros datos de neutrones.

A. A. CHERNISHOV (URSS): Creo que no puedo explicar esta discrepancia por ahora. Sin embargo, debo hacer notar que los resultados de los cálculos a que usted se refiere tampoco están de acuerdo con los resultados experimentales obtenidos en Harwell.

K. H. BECKURTS (República Federal de Alemania): ¿Cómo obtiene usted la distribución general de frecuencias $P(\beta)$ a partir de la ley de dispersión medida? ¿Extrapola simplemente las dos transferencias de momento o utiliza un procedimiento iterativo?

A. A. CHERNISHOV (URSS): Obtenemos la función $P(\beta)$ muy simple, aunque no muy exactamente, sin usar un método iterativo ni una calculadora. La forma de $P(\beta)$ se puede hacer más exacta calculando a partir de ella secciones eficaces diferenciales dobles (teniendo en cuenta efectos instrumentales) y comparando los resultados del cálculo con las secciones eficaces medidas. En el documento P/360 de L. V. Maiorov *et al.* se describe un programa de tales cálculos.

K. H. BECKURTS (República Federal de Alemania): Su medida del espectro dependiente del tiempo es esencialmente la misma que la efectuada por el grupo de M. J. Poole en Harwell. ¿Ha comparado usted los resultados?

A. A. CHERNISHOV (URSS): Sí. La comparación ha demostrado que los valores de Harwell son sistemáticamente inferiores, lo que indica que hay ciertos errores sistemáticos en las medidas.

D. BALLY (Rumania): ¿Cual debe ser el intervalo de variación del coeficiente de difusión del agua para explicar el ensanchamiento del máximo cuasi-elástico con la temperatura que usted menciona en su artículo?

* Estas Actas, vol. 3.

* Referencia [21] del documento.

A. A. CHERNISHOV (URSS): Como se indica en el documento, las medidas se efectuaron con una resolución relativamente baja; el propósito fué obtener información necesaria para cálculos de termalización, de modo que no se hizo ningún análisis especial de la dispersión cuasi-elástica. De las curvas se deduce que el ensanchamiento nunca excedía de 10 %.

Documento P/858 (presentado por V. Ajdačić)

DISCUSIÓN

E. P. BLIZARD (Estados Unidos de América): Observo que usted tiene el problema de las reacciones (n,p) y (n,α) en silicio con su espectrómetro. ¿Ha estudiado las ventajas que se derivarían de utilizar isotopos del silicio tales como el silicio-30 para los cuales esas reacciones serían mucho menos importantes?

V. AJDAČIĆ (Yugoslavia): Nuestros detectores semiconductores son monocristales de silicio y resultaría muy caro obtenerlos de un solo isotopo.

E. P. BLIZARD (Estados Unidos de América): ¿Tiene usted problemas con el alto flujo que sale del tubo largo? ¿Ha considerado la posibilidad de desviar las partículas cargadas mediante imanes?

V. AJDAČIĆ (Yugoslavia): Utilizábamos un campo eléctrico para desviar los electrones pero encontramos que los protones y partículas α de las reacciones de neutrones con aluminio constituían la mayor parte del fondo. Naturalmente, no es fácil desviarlas y al mismo tiempo disponer de un método muy sencillo para medidas de flujos elevados de neutrones.

G. BEN-DAVID (Israel): ¿Cuál es la resolución de su detector de ^{6}Li para neutrones rápidos?

V. AJDAČIĆ (Yugoslavia): La resolución del espectrómetro era de unos 300 keV a una potencia de 2 vatios. La resolución depende de la potencia del reactor tal como se indica en la figura 2 del documento.

Documentos P/498 y P/705

No hubo discusión sobre estos documentos.

DISCUSIÓN GENERAL

P. LO IZZO (Italia): Los métodos y secciones eficaces utilizadas por los diseñadores de reactores (al menos en el campo de los reactores de agua) datan de hace cinco a diez años. Los métodos nuevos son considerablemente mejores y nuevos datos se están ya acumulando, pero los diseñadores de reactores necesitan siempre experiencias críticas para diseñar un reactor realmente nuevo. Los métodos sencillos son realmente capaces de darnos por ejemplo un error de 1 % en k_{ef} (probablemente debido a que ciertos errores grandes se cancelan entre sí) y si utilizamos valores más precisos para el cálculo de un parámetro de un reactor, obtenemos a menudo errores mayores. ¿Podría alguien hacer un comentario sobre si este es un efecto general o si hay algún modo de evitarlo?

J. S. STORY (Reino Unido): En relación con los comentarios del Sr. Lo Izzo, creo que desgraciadamente es verdad que en un principio, métodos más elaborados de cálculo dan muy a menudo resultados que concuerdan menos bien de lo que cabría esperar de medidas integrales. Sin embargo, creo que se deben seguir los métodos más elaborados puesto que nos pueden ayudar a poner en claro deficiencias en nuestro conocimiento del comportamiento de un reactor.

Esta situación me lleva a hacer unas pocas sugerencias sobre el problema de evaluar datos de secciones eficaces nucleares y de tratar estos datos para obtener parámetros de multigrupos y otras magnitudes derivadas para su uso en programas elaborados de transporte de neutrones en un reactor. El Dr. Westcott ha mencionado brevemente estas cuestiones en su documento (P/717) y son también analizadas con más detalle en el documento del Reino Unido P/168.

Durante los últimos años la calidad y el número de datos básicos de secciones eficaces ha mejorado considerablemente y su ritmo de aparición es aún creciente. Estamos empezando a hacer frente a una verdadera « explosión de población » en cuanto a nuevos datos. Esto, junto con los avances en teoría de transporte, es muy satisfactorio pero exige mucho trabajo para expresar los datos en la forma necesaria para los programas de cálculo en esa teoría. En el Reino Unido tenemos una experiencia práctica considerable en este problema y hemos encontrado que preparar la evaluación de una serie completa de secciones eficaces para un solo núcleo o elemento, supone de 2 a 6 meses – hombre; en estas condiciones, el llevar a cabo este trabajo para todos los materiales de interés en física de reactores y mantenerlo al día según van llegando los nuevos datos representará un esfuerzo enorme.

Creemos que se requiere un esfuerzo decidido y continuado en este campo y que se necesita urgentemente una colaboración internacional para asegurar un ritmo de esfuerzo adecuado.

List of Volumes

PEACEFUL USES OF ATOMIC ENERGY

Proceedings of the Third International Conference held at Geneva, 31 August-9 September 1964

The full list of the sixteen volumes comprising the multilingual edition of the Proceedings is given below. The sessional titles are included to show the main subjects dealt with in each individual volume.

Volume 1

Progress in Atomic Energy

Programme of the Conference

A Opening of the Conference

B New Economic Data. Energy Needs in Coming Years and the Role of Nuclear Power in Meeting these Needs

1.6 Technical and Economic Aspects of the Use of Nuclear Power

C International Collaboration in Nuclear Reactor Projects, including Developments of Major Co-operative Installations

H Closing of the Conference

Evening Lecture

Scientific Exhibition

Volume 2

Reactor Physics

3.1 New Developments in Reactor Physics

Volume 3

Reactor Studies and Performance

3.2 Lattice Studies and Critical Experiments

3.3 Reactor Performance

Volume 4

Reactor Control

3.4 Reactor Kinetics

3.5 Reactor Control and Shielding

Volume 5

Nuclear Reactors — I. Gas-cooled and Water-cooled Reactors

1.1 Gas-cooled and Graphite-moderated Reactors

1.2 Light-water Reactors

1.3 Heavy-water and Organic Reactors

Volume 6

Nuclear Reactors — II. Fast Reactors and Advanced Concepts

1.4 Fast Reactor Physics and Breeders

1.5 Superheating and Advanced Concepts

1.7 Reactors of Special Applications. Future Developments

Volume 7

Research and Testing Reactors

D Research Reactors

1.9 High Flux Reactors for Material Testing

1.8 Very High Flux Reactors, Construction and Uses

Volume 8

Reactor Engineering and Equipment

1.10 Heat Transfer

1.11 Hydraulic Problems of Reactor Engineering

3.7 Reactor Plant Equipment

Volume 9

Reactor Materials

2.8 Structural Materials

2.9 Structural and Control Materials and Moderators

2.4 Corrosion Studies. Non-destructive Testing

Volume 10

Nuclear Fuels — 1. Fabrication and Reprocessing

2.3 Fuel Element Fabrication and Experience

2.6 Fuel Reprocessing, Part I

2.7 Fuel Reprocessing, Part II

Volume 11

Nuclear Fuels — II. Types and Economics

2.5 Economics of the Fuel Cycle

2.1 Metallic and Various Fuels

2.2 Ceramic Fuels

Volume 12

Nuclear Fuels — III. Raw Materials

2.11 Resources and Requirements

2.12 Prospecting Techniques and Recovery from Ores

2.10 Isotope Separation

Volume 13

Nuclear Safety

3.9 Nuclear Safety Research

3.8 Chemical Processing Plant Safety; Fuel Transport

3.6 Reactor Safety; Location and Containment; Reactor Tests

Volume 14

Environmental Aspects of Atomic Energy and Waste Management

3.10 Safety Aspects of Large-scale Use of Atomic Energy. Measurement and Limitation of Exposure in Radiation Emergencies

3.11 Radioactive Waste Management

Volume 15

Special Aspects of Nuclear Energy and Isotope Applications

E Controlled Nuclear Fusion

4.1 Direct Conversion of Heat to Electricity

F Applications of Isotopes and Radiation Sources in the Physical Sciences

G Applications of Isotopes and Radiation Sources in the Life Sciences

4.2 Miscellaneous Applications of Atomic Energy

Volume 16

List of Papers and Indexes

List of Papers

Author Index

Country Index

Sessional Index